Synthesis and reactivity of succinylthioimidazolium salts:

A unified strategy for the preparation of thioethers

Dissertation

zur Erlangung des mathematisch-naturwissenschaftlichen Doktorgrades

„Doctor rerum naturalium“

der Georg-August-Universität Göttingen

im Promotionsprogramm der

Georg-August University School of Science (GAUSS)

vorgelegt von

Marvin Jeldrik Böhm

aus Rodewald

Göttingen, 2020

Betreuungsausschuss:

Prof. Dr. Manuel Alcarazo (Institut für Organische und Biomolekulare Chemie, Tammannstr. 2, 37077 Göttingen)

Prof. Dr. Lutz Ackermann (Institut für Organische und Biomolekulare Chemie, Tammannstr. 2, 37077 Göttingen)

Mitglieder der Prüfungskommission

Referent: Prof. Dr. Manuel Alcarazo (Institut für Organische und Biomolekulare Chemie, Tammannstr. 2, 37077 Göttingen)

Korreferent: Prof. Dr. Lutz Ackermann (Institut für Anorganische Chemie, Tammannstr. 2, 37077 Göttingen)

Weitere Mitglieder der Prüfungskommission:

Prof. Dr. Dietmar Stalke (Institut für Anorganische Chemie, Tammannstr. 4, 37077 Göttingen)

Prof. Dr. Konrad Koszinowski (Institut für Organische und Biomolekulare Chemie, Tammannstr. 2, 37077 Göttingen)

Jun.-Prof. Dr. Johannes C. L. Walker (Institut für Organische und Biomolekulare Chemie, Tammannstr. 2, 37077 Göttingen)

Dr. Holm Frauendorf (Institut für Organische und Biomolekulare Chemie, Tammannstr. 2, 37077 Göttingen)

Tag der mündlichen Prüfung: 14.12.2020

I hereby declare, that this dissertation has been written independently and with no sources or aids other than those quoted. The parts performed by project collaborators have been clearly indicated.

_____

Marvin J. Böhm

Die Naturwissenschaften braucht der Mensch zum Erkennen, den Glauben zum Handeln.

Max Planck

Abbreviation

ATI	Arylthioindole derivative
°C	Degree Celsius
^{18}F	Fluorine-18
Å	Ångstrom (10^{-10}m)
ACM	Alkyne cross metathesis
Ar	Generic arene
Bn	Benzyl
Bpin	(Pinacolato)diboron
BTBT	Benzothieno[3,2-*b*]benzothiophene
BuLi	Butyllithium
Bz	Benzoyl
cald.	Calculated
cat.	Catalytic
CF_3	Trifluoromethyl group
CFL	Compact Fluorescent Lamps
CuTC	Copper(I) thiophene-2-carboxylate
DABCO	1,4-diazabicyclo[2.2.2]octane
DBU	1,8-Diazabicyclo(5.4.0)undec-7-ene
DCDMH	1,3-Dichloro-5,5-dimethylhydantoin
DCE	1,2-Dichloroethane
DCM	Dichloromethane
DDQ	2,3-Dichloro-5,6-dicyano-1,4-benzoquinone
dil.	Diluted
DIPEA	*N,N*-Diisopropylethylamine
DMF	*N,N*-Dimethylformamide
DMSO	Dimethylsulfoxide
DNTT	Dinaphtho[2,3-*b*:20,30-*f*]thieno[3,2-*b*]thiophene
dppf	1,1'-Bis(diphenylphosphino)ferrocene
EDA	Electron donor-acceptor
EDTA	Ethylenediaminetetraacetate
ee%	Enatiomeric excess
EI	Electron Ionisation
EMA	European Medicine Agency
equiv.	Equivalents
ESI-MS	Electrospray Ionisation Mass Spectrometry
et al.	Et alia
EtOAc	Ethyl acetate
EtOH	Ethanol

EWG	Electron withdrawing group
fac	Facial
fcc	Flash column chromatography
FDA	Food and Drug Administration
g	Gram
GC-MS	Gas Chromotography Mass Spectrometry
glyme	Dimethoxyethane
HEP	Huynh´s electronic parameter
HFIP	Hexafluoroisopropanol
HOMO	Highest occupied molecular orbital
HRMS	High Resolution Mass Spectrometry
hυ	Light irradiation
i	*ipso*
i-Pr	*iso*-Propyl
IR	Infrared spectroscopy
J	Coupling constant
K	Kelvin
KHMDS	Potassium hexamethyldisilazide
L	Ligand
LG	Leaving group
LiHMDS	Lithium hexamethyldisilazide
LUMO	Lowest unoccupied molecular oribtal
m-	*meta*-
M	Metal
M	Molar (Mol dm^{-3})
*m*CPBA	*meta*-Chloroperoxybenzoic acid
MeCN	Acetonitrile
min	Minute
MS	Molecular sieves
NCS	*N*-Chlorosuccinimide
NEt_3	Triethylamine
n-Hex	*n*-Hexane
NMR	Nuclear Magnetic Resonance
Nu	Nucleophile
o-	*ortho*-
OFET	Organic field-effect transistors
OLED	Organic light-emitting diode
o/n	Overnight
OTFT	Organic thin-film transistor
p-	*para*-
Ph	Phenyl
PIDA	Phenyliodine(III) diacetate
ppm	Parts per million

PPS	Polyphenylene sulfide
Pr	Propyl
P.T.	Proton transfer
PTSA	*para*-Toluenesulfonic acid
q	Quartet (NMR)
Quant.	Quantitative
QSAR	Quantitative structure activity relationships
R	Generic substituent
rt	Room temperature
s	Second
s	Singlet (NMR)
SET	Single-electron transfer
S_N	Nucleophilic substitution
T	Temperature
t	Time
t	Triplet (NMR)
t-Am	*tert*-Amyl
TBDMS	*tert*-Butyldimethylsilyl
t-Bu	*tert*-Butyl
TEA	Triethylamine
Tf	Trifluoromethanesulfonyl
Tf_2O	Trifluoromethanesulfonic anhydride
TFA	Trifluoroacetic acid
THF	Tetrahydrofurane
TM	Transition metal
TMS	Trimethylsilyl
TMTU	Tetramethylthiourea
Tol	Tolyl
UV	Ultra violett
Vis	Visible light
X	Generic heteroatom
X-ray	X-ray crystallography
Y	Generic substituent
Z	Generic heteroatom
δ	Chemical shift
λ	Wavelength

Table of Contents

1 Introduction to thioethers

Sulfur is one of the main group elements on our planet with a natural abundance of (0.46±0.15)w%.[1] In its most common allotropic form sulfur is a yellow powder and exhibits a cyclic S_8 structure. Apart of the cyclic S_8 form, several smaller and larger ring allotropes of S_n with n = 6 to 20 have been isolated. Aside from its natural occurrence as the pure element, sulfur is also forming inorganic salts like sulfides, sulfates, or sulfites.[2] Moreover, sulfur plays an important role in the field of organic chemistry and biochemistry.[2] In this regard various sulfur-containing functional groups with different oxidation states of the sulfur atom, e.g. thiols (+II), disulfides (+I), sulfoxides (+IV) and sulfones (+VI) and thioethers (+II), are known (Figure 1).

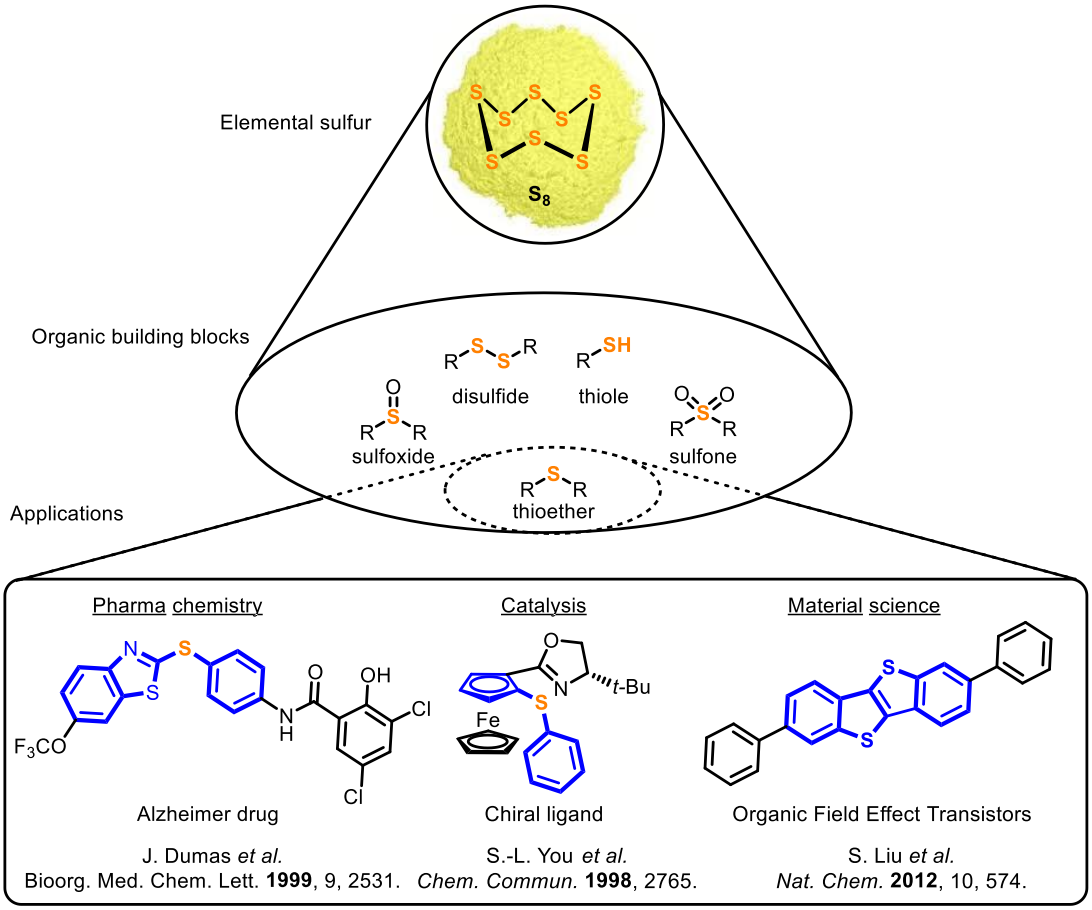

Figure 1: Sulfur as a crucial element and its application as thioethers in various fields of research.[3]

Especially aryl thioethers are predominantly important representatives of sulfur containing functional groups in organic chemistry because of their appearance in key scaffolds of pharmaceutical important compounds, natural products, in the field of material science as well as in the field of ligand design (see Chapter 1.2).

Additionally, aryl thioethers, also known as aryl sulfides, are a versatile synthetic platforms because they can be easily converted in a variety of other functional groups and find also applications as directing groups in chemistry of C–H functionalization (see Chapter 1.3).

Due to the significant importance of this compound class, this work will focus on the development of a transition metal free and highly modular protocol for the synthesis of a wide range of different unsymmetrically substituted aryl thioethers. Furthermore, the developed concept will be used to access further sulfur-containing compounds as (arylthio)sulfonamides.

1.1 General structure of thioethers

Thioethers are functional groups in which two carbon-based residues are bridged by a sulfur atom (Figure 2). The sulfur atom possesses two additional free electron pairs which causes an average bond angle (∢ (R^1–S–R^2)) of 103°.[4] Compared to ethers, the lower degree of hybridization of the sulfur atoms compared to the oxygen analogue results in a higher p-character of the involved sulfur orbital of the R–S σ-bond. Therefore, the average ∢ (R^1;S;R^2) angle in thioethers with two aryl substituents is smaller than the ∢ (R^1–O–R^2) angle in the corresponding ethers (118°).[4] As the free electron pairs of thioethers are more diffuse and their highest occupied molecular orbital (HOMO) are above those of the corresponding ether electron pairs, they behave as weaker nucleophiles and can react as soft Lewis bases according to the HSAB concept.[5]

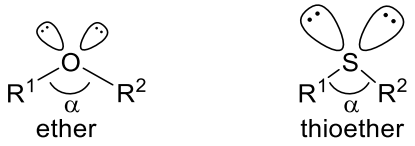

Figure 2: General structure of thioethers.

Due to its free electron pairs, thioethers can coordinate metals and act as potent directing groups in the field of catalysis (see Chapter 1.3.1.4). The rising number of applications of compounds with a thioether moiety in the fields of pharmaceutical chemistry and material science are leading to an increasing interest in the development of new synthetic protocols for the synthesis of this ubiquitous core structure. Starting from simple substitution reactions up to transition metal catalyzed cross-coupling reactions and versatile transition metal free protocols, a variety of synthetic strategies are already known (compare Chapter 1.4).

The reactivity and application of thioethers and different approaches towards their preparation will be summarized and further discussed in this chapter.

1.2 Relevance of aryl thioethers

The structural motif of aryl thioethers is omnipresent in molecules with many different applications. Various aryl sulfides show useful biological activities and are applied in medicinal chemistry. Additionally, they are important building blocks in functional materials like transistors. For applications in the field of catalysis, aryl sulfides are reported as ligands in the catalysis of several reactions.

1.2.1 Medicinal chemistry and natural products

As recently reviewed by M. Feng *et al*., sulfur-containing molecules, represented by over 362 sulfur compounds approved by the FDA in 2016,[6] are of extreme importance in medicinal chemistry. Apart from sulfonamides and sulfones which can be easily obtained by oxidation of sulfides (see Chapter 1.3.1.1), sulfides are one of the most dominant sulfur scaffold in this area.[7]

One of the earliest approved drugs for the treatment of schizophrenia and major depressive disorder, bearing a diaryl sulfide scaffold in its dibenzothiazine backbone, is Prochlorperazine (**1**), which is commercially available since 1956 under the trade name Compazine (Figure 3).[6] It has been demonstrated, that derivatives of Prochlorperazine can also be used for the treatment of meningitis.[8] Several other Prochlorperazine-based anti-psychotic drugs were developed by modification of the *N*-attached alkyl chain or the substitution pattern on the internal diaryl sulfide core. For these derivatives, the risk of adverse drug reactions, such as dizziness, was dramatically reduced.[9] Besides the anti-psychotic activity of diaryl sulfide-based molecules, also sulfides with the potential to treat neurodegenerative diseases like Alzheimer are known in literature. As presented by J. Dumas *et al*., diaryl sulfide **2** has a high activity for the inhibition of Cathepsin D (IC_{50} = 1.7 µM) (Figure 3).[10] This enzyme cleaves amyloid precursor proteins in neurons, and the obtained protein fragments are known to form amyloid plaques which are attached to neurons in Alzheimer affected brains.

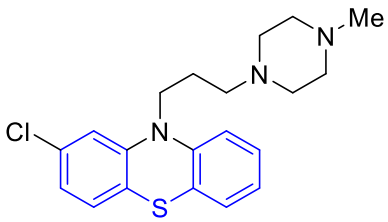

Anti-psychotic
Prochlorperazine
1

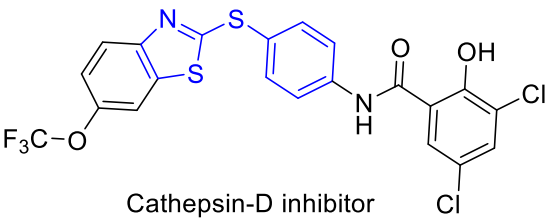

Cathepsin-D inhibitor
2

Figure 3: Pharmacologically relevant molecules bearing diaryl sulfide motifs like an anti-psychotic drug Prochlorperazine (**1**),[6] or Cathepson D-inhibitor **2**, which can potentially prevent the formation of plaques in Alzheimer infected brains.[10]

Additionally, arylthioindole derivatives (ATIs) are known to inhibit the polymerization of tubulin; this makes them potent candidates in the treatment of various cancer diseases.[11] Detailed analysis of the structure-activity relationship of ATIs and variation of the substitution pattern resulted in the synthesis of compound **3,** which is one of the most efficient inhibitors of the tubulin polymerization (Figure 4). The potential of ATIs for the treatment of cancer was additionally substantiated by molecular docking studies as well as inhibition tests with human breast carcinoma cells.[11,12] Alternative potential application of ATIs lie in the field of asthma treatment, as some ATI derivatives are potent inhibitors of 5-lipoxygenase, which plays a key role in the allergy-induced asthma.[13] Also infection with *Streptococcus pneumoniae* could be potentially treated with ATI derivative **4**, as demonstrated by the studies of S. S. Khandekar and coworkers.[14] The authors demonstrated the ability of indole derivative **4** to inhibit the important protein synthase III (FabH) of *Streptococcus pneumoniae* as well as of *E. Coli* and *H. influenza*. This shows the high antibiological potential of ATIs. Further ATIs may have therapeutic value for the curing of obesity.[15]

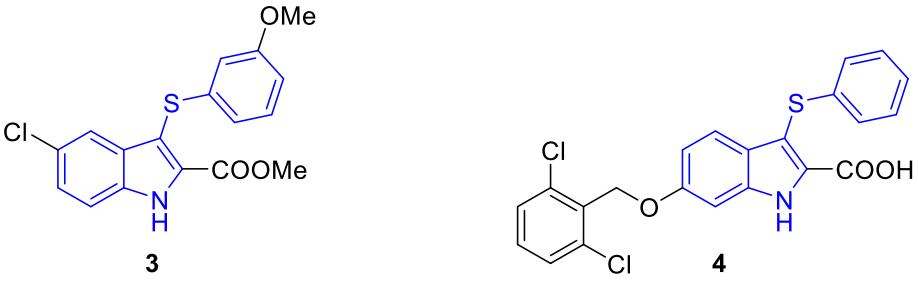

Figure 4: 3-Arylthioindole derivatives which can potentially inhibit cancer growth by blocking the tubulin polymerization (**3**)[11] or which have antimicrobial properties (**4**).[14]

The protein tyrosine phosphatase SHP2, which is an oncoprotein and associated with several different leukemia types, can be sufficiently inhibited with compounds containing thioether motifs like **5** and **6** (Figure 5). Even if the exact role of SHP2 is not fully understood yet, an interdisciplinary team around M. J. LaMarche and coworkers from Novartis Pharmaceutical has recently shown that **5** and **6** can efficiently inhibit SHP2. The exact pharmacokinetic was studied in mice models bearing subcutaneously implanted tumor cells and was accompanied by X-ray crystallography studies of **6** in the active pocket of SHP2.[16]

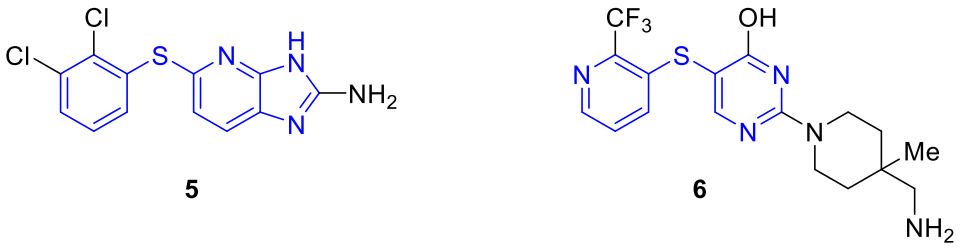

Figure 5: Selective SHP2 inhibitors for the potential treatment of different cancer diseases as reported by M. J. LaMarche and coworkers.[16]

Besides the previously presented fields of application diaryl, sulfides have also shown excellent anti-inflammatory behaviors, as shown by an extensive compound screening of G. Liu and coworkers.[17] Binding studies revealed the importance of the diaryl sulfide core with an anilino moiety in the structure of **7** to suppress a main pathway in the biochemical cascade of inflammations (Figure 6).

Additionally, diaryl sulfides like **8** have a valuable impact for the potential treatment of parasitic infections (Figure 6). As evaluated by K. T. Douglas and coworkers, 2-amino-4-chlorophenyl phenyl sulfides like **8** are versatile molecules with anti-trypanosomal, anti-leishmanial, and anti-malarial properties.[18]

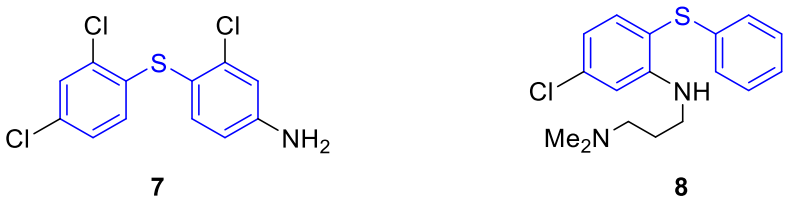

Figure 6: Diaryl sulfides derived drug targets with anti-inflammatory (**7**)[17] and anti-parasitic (**8**)[18] activity.

Another family of compounds with high pharmacological significance are those containing a trifluoromethylthio group which has the highest Hansch constant of all functional groups (π_R = 1.44). The Hansch constant describes the contribution of a substituent to the lipophilicity of the molecule based on quantitative structure activity relationships (QSAR).[19] A high lipophilicity enables fast adsorption and increased bioavailability of medicinal target compounds. Examples for those relevant trifluoromethylthio ethers are Tiflorex (**9**) and Toltrazuril (10) (Figure 7). Tiflorex is a stimulant amphetamine derivative and is used as anorectic drug for the treatment of obesity.[20,21] Toltrazuril is a coccidiostatic (antiprotozoal) agent to cure animals of coccidia parasite infections and is traded under the name Baycox or Vecoxan.[22]

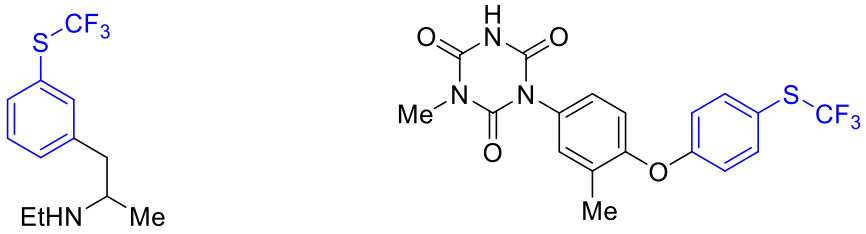

Figure 7: Examples of pharmaceutically relevant trifluoromethyl aryl thioethers: Tiflorex (**9**), an amphetamine derivative for the suppression of appetite,[20,21] and Toltrazuril (**10**), a drug for the treatment of coccidia infections.[22]

Several natural products have an aryl thioether scaffold. Chuangxinmycin (**11**) is a cyclic aryl thioether which can be isolated from *Actinoplanes tsinanensis n. sp.* and exhibits antibiotic activity against several Gram-positive and Gram-negative bacteria like infections with *Escherichia coli* and *Shigella dysenteriae* (Figure 8).[23] The methyl aryl thioether Roseochelin B (**12**) is an algacidal regulator in the algal-bacterial symbiose of haptophyte *Emiliania huxleyi* and several marine *Roseobacter* clades. The compound regulates the growth of the algae (Figure 8).[24]

A further natural product featuring a aryl thioether functionality is Collismycin A (**13**) which was initially isolated by S. Gomi and coworkers from the bacterium *Streptomyces sp* in 1994 (Figure 8).[25] In addition to its originally reported activity against fungi, Gram-positive and Gram negative bacteria, Collismycin A shows protective properties against oxidative stress which makes it a potentially useful compound for the treatment of neurodegenerative diseases.[26]

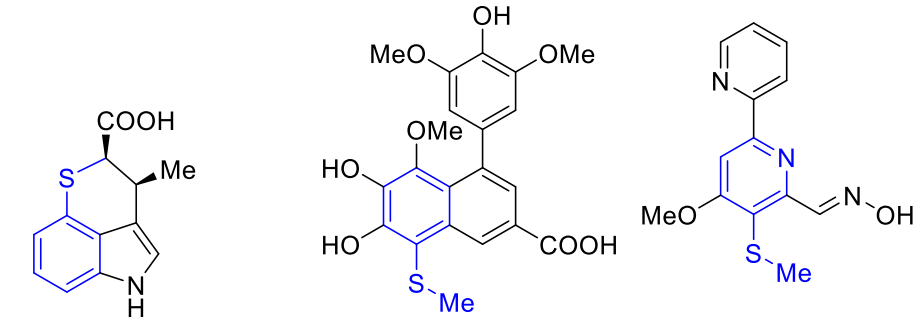

Figure 8: Natural products which contain aryl thioether moiety in their core structures.

1.2.2 Material science

Aryl sulfides are widely used in the field of material science especially as organic thin-film transistors (OTFTs) or in the polymer chemistry.

Organic transistors have huge advantages compared to their inorganic counterparts, as they are employable in flexible electronic applications.[27] Examples of those functional materials are derivatives of benzothieno[3,2-*b*]benzothiophene (BTBT, **14**) and dinaphtho[2,3-*b*:20,30-*f*]thieno[3,2-*b*]thiophene (DNTT, **15**) (Figure 9). In general, modified DDNTs have significantly smaller contact resistances and larger charge-carrier motilities than pentacene, which can also be used as an organic semiconductor.[28] BTBT derivatives with 2,7-diphenyl substitution pattern are of additional value for organic field-effect transistors (OFET) because of their high stability in operation as well as during storage.[29] The electronic properties of BTBTs can be modulated by substitution of the core with pentafluorophenyl groups to expand the optical band gap.[30]

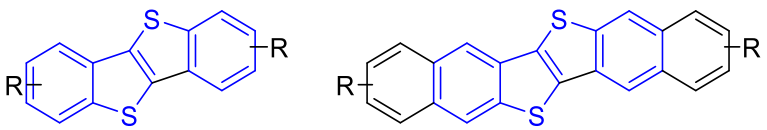

BTBT **14** DNTT **15**

Figure 9: BTBT and DNTT as examples of benzothiophene-containing motifs which can be utilized as organic thin-film transistors.

Apart from aryl sulfides with low molecular weight, compounds with a high molar mass can exhibit useful properties and are used as versatile materials in industrial contexts. An excellent example is polyphenylene sulfide (PPS, **16**), a high-performance polymer with high thermal stability which also features a high chemical stability and was originally developed by Phillips Petroleum Company (Figure 10).[31] PPS is used for coating and for precision mechanical parts. Especially because of the high melting temperature (285 °C) and decomposition temperature of 450 °C PPS is known as a robust and useful material for manifold applications.[32]

These supreme properties of PPS can be further boosted by the introduction of fluoro functionalities, as recently reported by the group of J. L. Hedrick.[33] Their presented synthesis of fluorinated poly(aryl thioethers), resulted in a series of different polymers like **17** (Figure 10). Latest trends in the synthesis and application of PPS have been summarized in a review by F. Bakir and coworkers.[34]

A. Shockravi *et al*. demonstrated the applicability of diaryl backbones in the synthesis of various polyamide like compound **18** (Figure 10).[35] The obtained sulfide-based polyamides

are soluble in polar organic solvents and thermally stable. Additionally, diaryl sulfides-containing polyamides, polyesters and polybenzimidazoles have been reported in literature.[36] A broad overview of sulfur compounds in polymer and material science can be found in a recently published review of P. Theato and coworkers.[37]

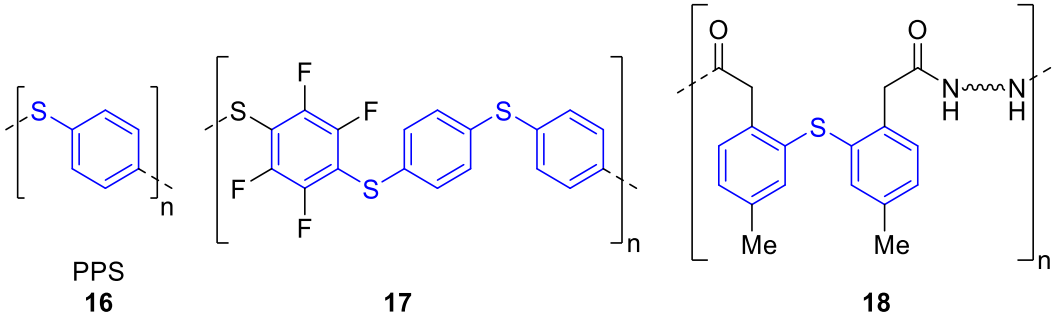

PPS **16** **17** **18**

Figure 10: Different diaryl thioethers-containing polymers like PPS (**16**), fluorinated PPS derivatives (**17**) and polyamide species **18**.

Also, the electronic properties of diaryl sulfides were used in the field of organic light-emitting diodes (OLEDs). As reported by L.-S. Liao, J. Fan and coworkers, the introduction of diaryl sulfide-containing substituents at the 3,3'-position of 9,9'-bicarbazoles resulted in improved photoelectrical properties like a low-lying energy level of the triplet state and appropriate HOMO/LUMO energy levels.[38] Compound **19** was tested as a host material in red- and green-emitting OLEDs and exhibited good thermal stabilities and a strong absorption band at 292 nm (Figure 11). Finally, diaryl sulfides like the fluorine-substituted tetrakis(arylthio)benzene **20** can be used as organic luminophores. They have a unique singlet and triplet emission properties that can be controlled by deformation of their C–S bonds (Figure 11). The different degrees of deformation in the solid state of **20** depend on the nature of the solvent molecules incorporated in the crystal. This allows the synthesis of materials with distinct photoluminescence properties. A high conformational distortion of C–S bonds leads to an increased fluorescence of the compounds, whereas nearly undistorted C–S bonds resulted in dominant phosphorescence ability of the material.[39]

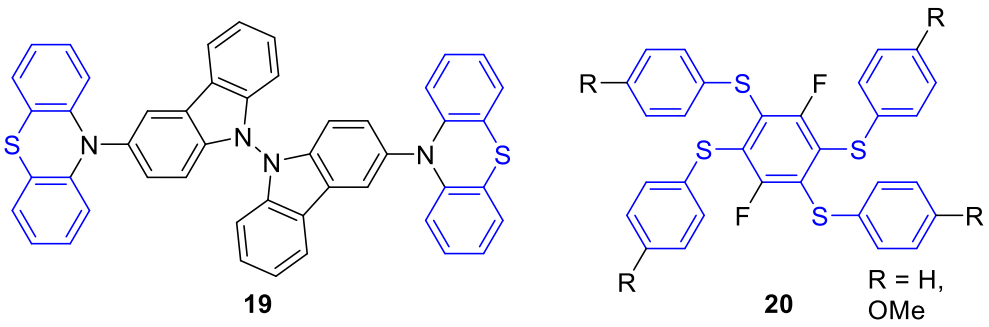

Figure 11: Functional diaryl sulfide-based materials with optical properties. **19** can be used as host materials in OLEDs,[38] and **20** exhibits strong fluorescence photoluminescence properties depending from the C–S bond distortion.[39]

1.2.3 Use in ligand design and catalysis

Several organocatalysts as well as ligands for transition metal catalysis possess an aryl sulfide unit in their core structure. One of the early examples of chiral thioethers-based ligands was reported by J. M. J. Williams and coworkers in 1993.[40] The authors presented a bidentate ligand **21** which combines a coordinating chiral oxazoline group with an auxiliary sulfur donor. Thus, catalyst **21** was employed in the enantioselective palladium-catalyzed allylic substitution in 1,3-diphenylprop-2-enyl acetate to give the nearly pure *S*-enantiomer (*ee*% > 96%) in excellent yield (Scheme 1). Additionally, the authors could demonstrate that the diaryl sulfide moiety in catalyst **21** plays a crucial role for the enantioselectivity of the reaction. This principle was further explored by L.-X. Dai *et al.* who presented the chiral (2-phenyllthioferrocenyl)oxazoline **22** as a catalyst.[41] In comparison with **21**, this catalyst was able to shorten the reaction time to 5 h with an equal loading of the palladium catalyst.

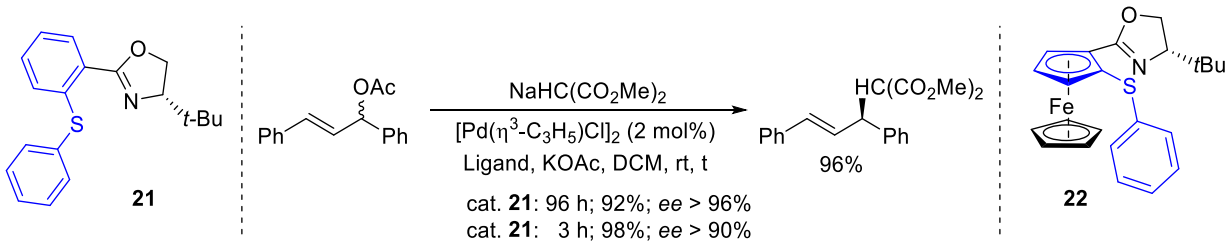

Scheme 1: Palladium-catalyzed allylic substitution in 1,3-diphenylprop-2-enyl acetate utilizing chiral aryl sulfide-based ligands **21** and **22**.[40],[41]

Another ferrocene-derived ligand with a sulfide functionality is the already well-established Fesulphos ligand (**23**), which was initially reported by J. C. Carretero and coworkers (Figure 12).[42] Fesulphos can easily be prepared from ferrocene and commercially available (*R*)-*S*-*tert*-butyl *tert*-butanethiosulfinate via a short four-step and high yielding synthesis and has proven to be an ideal chiral ligand for several palladium catalyzed transformations. Apart from

palladium-catalyzed allylic substitution reaction[42], several other transformation were enabled by transition metal complexes of this sulfenylphosphinoferrocene derivative. In this regard, palladium-catalyzed alkylative ring opening reactions of oxabicyclic alkenes[43] or the copper-catalyzed aza-Diels-Alder reaction between *N*-sulfonylaldimines and Danishefsky's-type dienes have to be mentioned.[44]

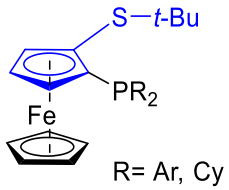

23

Figure 12: Fesulphos (**23**), 1-sulfenyl-2-phosphinoferrocenes – versatile ligands presented by J. C. Carretero and coworkers.[42]

In 2019, A. K. Singh *et al.* presented the novel palladium catalyst **24** for the transfer hydrogenation of aldehydes and ketones employing 2-propanol as a hydrogen source (heme 2).[45] The utilization of the monoanionic [*S*,*N*,*C*]-tridentate ligand in the complex **24** enabled the hydrogenation of several electron-rich and electron-poor benzaldehyde derivatives, alkyl aldehydes and ketones in up to 85% yields. Most of the desired alcohols were even obtained with an extremely low catalyst loading of 0.05 mol%. Rhodium complexes of the same ligand were also employed in the *N*-alkylation of aniline with benzyl alcohol.

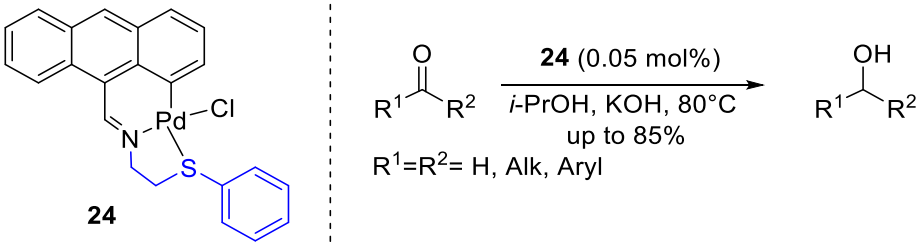

heme 2: Pd-catalyzed transfer hydrogenation of carbonyl groups employing an aryl sulfide-containing ligand scaffold, as presented by A. K. Singh *et al.*[45]

Aryl thioethers-derived [*S*,*O*]-bidentate ligands were also used in the C-H olefination of arenes (Scheme 3). As M. Á. Fernández-Ibáñez and coworkers demonstrated, the palladium complex of [*S*,*O*]-ligand **25** has unique properties and can be used for Fujiwara-Moritani olefination (dehydrogenative Heck reactions).[46] Usage of ligand **25** resulted in a high selectivity towards the olefination of substituted arenes. Furthermore, it enabled the late stage functionalization of pharmaceutically relevant compounds like Naproxen, a nonsteroidal anti-inflammatory drug. The palladium complex of **25** has also been used for the acetoxylation of arenes with

phenyliodine(III) diacetate (PIDA) as an oxidant and could additionally be utilized in the allylation reaction of arenes with allylbenzene. In the latter case, silver acetate acted as an oxidant. Recently, the substrate scope of the olefination protocol was extended to thiophene derivatives, as reported by the Fernández-Ibánez group as well.[47]

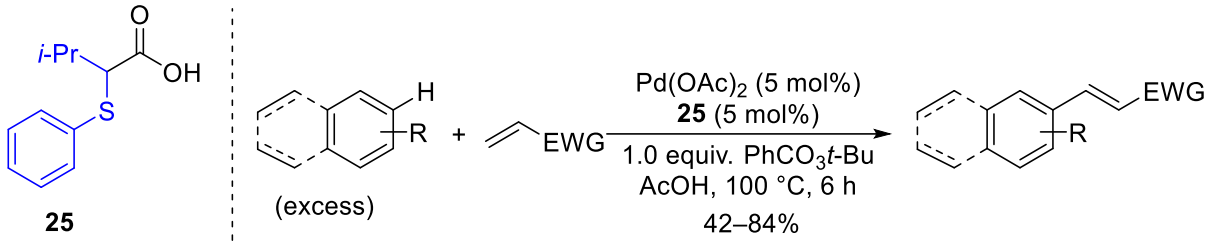

Scheme 3: Aryl sulfide ligand **25** in Pd-catalyzed C-H functionalization reactions of arenes and thiophenes, as reported by M. Á. Fernández-Ibáñez and coworkers.[46,47]

Diaryl sulfide-based ligands are also employed in the catalytical alkane transfer dehydrogenation, as was demonstrated by the group of A. S. Goldmann in 2019 (Scheme 4).[48] The presented ruthenium pincher complex **26** featuring a [*P*,*S*,*P*]-tridentate ligand is able to catalyze the transfer dehydrogenation of cyclooctane with turnover frequencies up to ca. 1 s^{-1} at 150 °C and 0.2 s^{-1} at 120 °C. This is more efficient than with a similar iridium [*P*,*C*,*P*]-complex. Interestingly, in the solid state the complex **26** exhibits a bowl-like structure, whereas the corresponding [*P*,*S*,*P*] analog possess an approximately planar configuration. The authors suggested that this structural change is caused by the higher degree of sp^2 hybridization of oxygen compared to sulfur. Presumably, the free electron pairs of the softer sulfur Lewis base coordinates the weak Lewis acid Ru(0) better than the harder oxygen donor. Additionally, the coordinative Ru–S bond is longer than the analogous Ru–O bond.

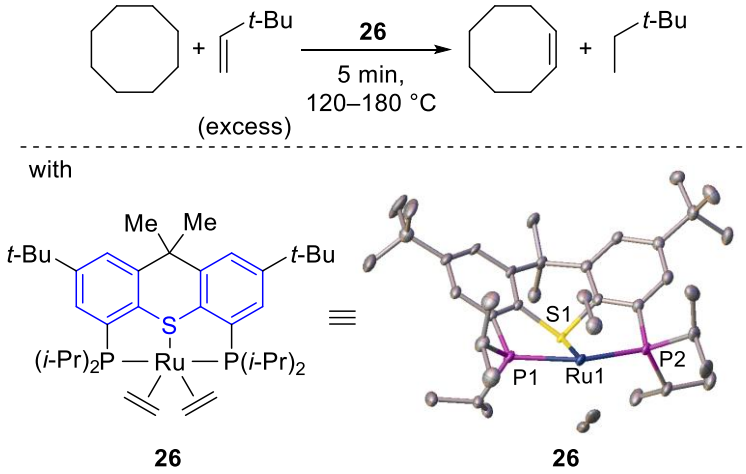

Scheme 4: Alkane transfer dehydrogenation catalyzed by the complex **26** with a diaryl sulfide backbone, as reported by the group of A. S. Goldmann.[48]

Apart from the application of [*S*,*N*,*C*]- and [*P*,*S*,*P*]-tridentate pincer ligands discussed above, further catalytically active complexes with ligands possessing the aryl sulfide-containing scaffolds have been reported.[49] Their chemistry as well as the applications of aryl sulfide-containing ligand, including the chiral ones, have been recently reviewed.[50]

Thioesters themselves can act as chiral catalysts, as demonstrated unprecedentedly by X. Zhao and coworker (Scheme 5).[51] In the presented chlorination and desymmetrization protocol, benzyl-tethered diolefins were enantioselectively cyclized, resulting in the formation of two quaternary and one tertiary stereo centers. The induction of chirality resulted from the utilization of **27** as organocatalyst. It has been suggested that intermediate **28** is formed *in situ* from **27** by chlorination with 1,3-dichloro-5,5-dimethylhydantoin (DCDMH). As a result, **28** acts as an active chiral chlorinating reagent.

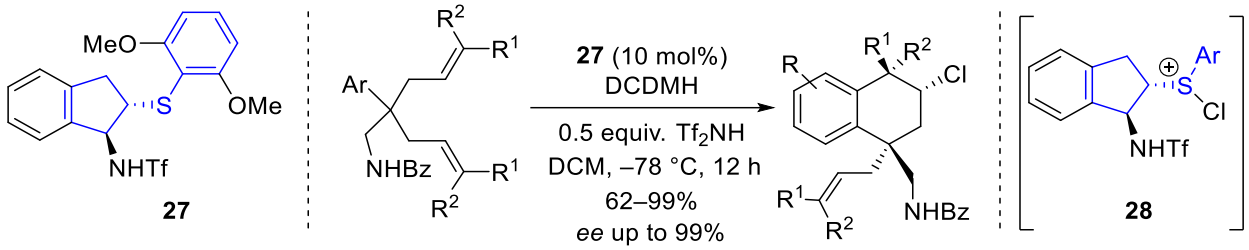

Scheme 5: Action of the sulfide **27** as a chiral catalyst for desymmetrizing enantioselective chlorination via formation of intermediate **28**, as reported by X. Zhao and coworkers.[51]

The cyclic aryl thioethers themselves can also be utilized as catalysts, as recently reported by the group of Y. Huang (Scheme 6).[52] The authors reported on the transition metal-free Suzuki coupling reaction of arylboronic acids with benzyl chlorides. The reaction mechanism involves the initial formation of a sulfonium salt from catalyst **29** and the benzyl chloride. This salt subsequently reacts with a base affording the corresponding sulfur ylide. The latter forms a boron "ate" complex with the boronic acid. Through the subsequent 1,2-aryllate shift, a new carbon-carbon bond is formed and the catalyst is regenerated. Under these conditions, the protodeboration results in the formation of the desired coupling product.

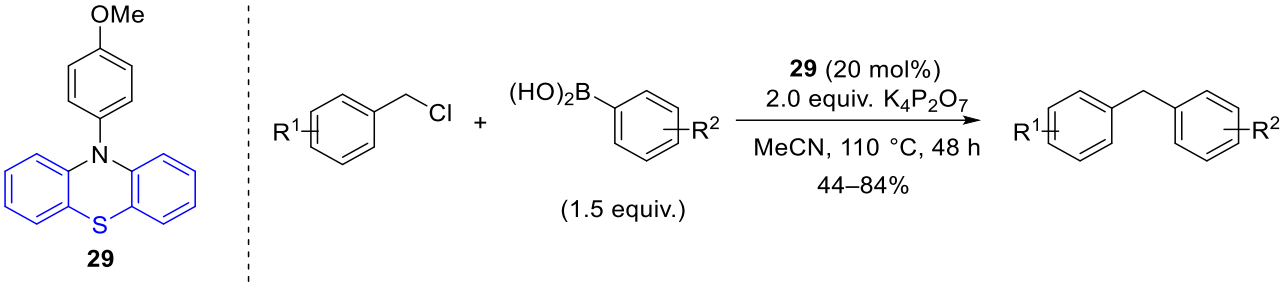

Scheme 6: Employment of **29** as a catalyst in the transition metal-free Suzuki couplings of aryl boronic acids and benzyl chlorides, as presented by the group of Y. Huang.[52]

1.3 Reactivity of aryl thioethers

Aryl thioethers can be used for several chemical transformations, as they can be converted into other sulfur-containing functional groups such as sulfoxides and sulfones. Additionally, thioethers can also be applied as leaving or directing groups in the modern organic chemistry. Also they are precursors for the formation of sulfur-carbon bonds as well as carbon-E bonds (E = N, P, B, C) by transition metal catalysis (Figure 13). The chapter will highlight recent developments is this area and will give insights into the full synthetic potential of thioethers by discussing representative literature examples.

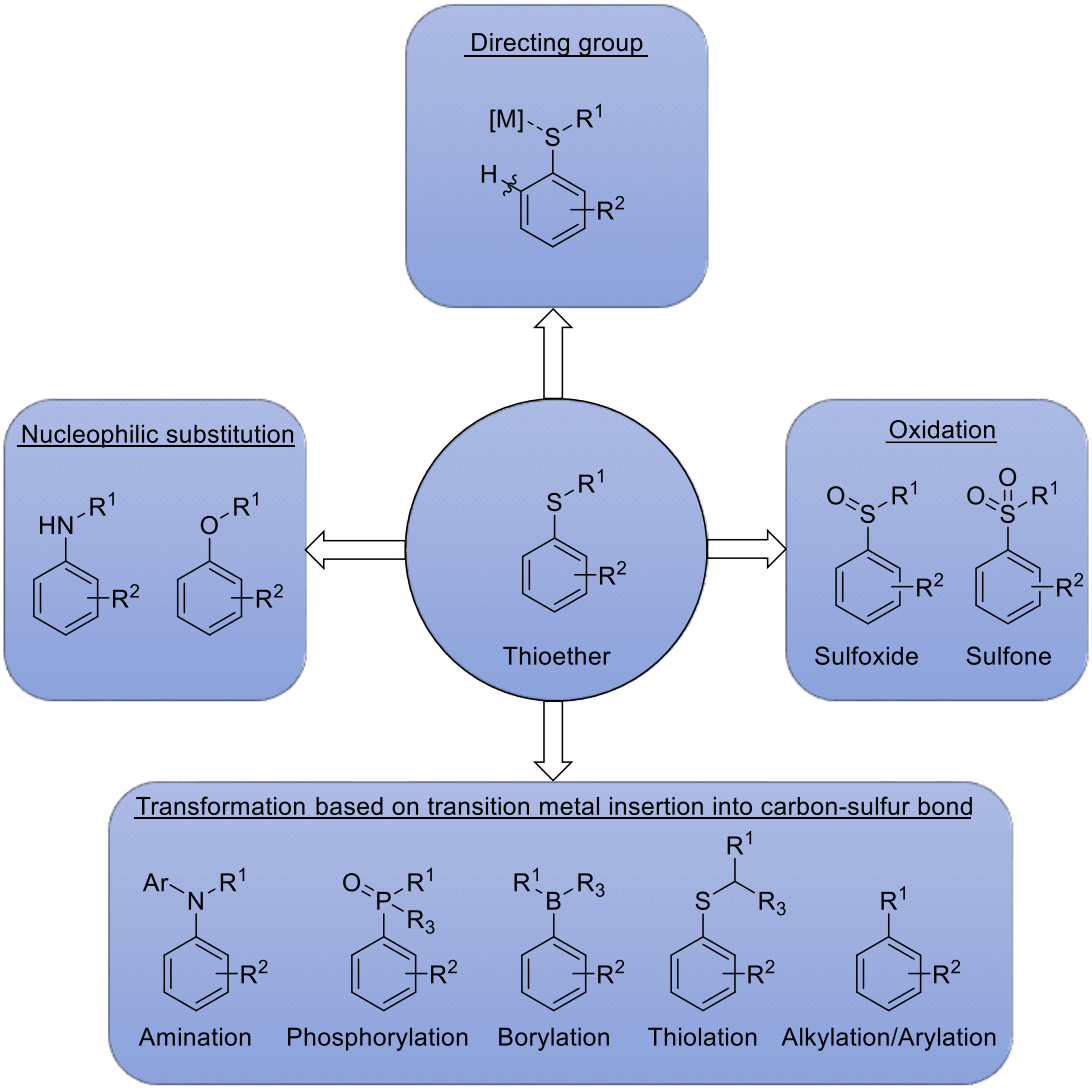

Figure 13: Aryl thioethers as valuable platforms for the formation of various functional groups.

1.3.1.1 Oxidation

The derivatization of thioethers **30** by oxidation gives access to racemic sulfoxides **31** and sulfones **32** (Scheme 7) and is one of the oldest transformations of thioethers, as already C. Märker described by the synthesis of dibenzyl sulfoxide from dibenzyl sulfide in 1865.[53]

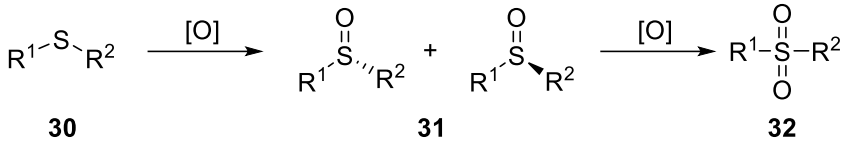

Scheme 7: Stepwise oxidation of thioethers **30** to sulfoxides **31** and sulfones **32**.

Traditionally, strong oxidants are employed in the synthesis of sulfones. Among them, for example, potassium permanganate,[54] elemental bromine,[55] sodium bromate,[56] ozone,[57] hydrogen persulfate,[58] and hydrogen peroxide combined with several catalysts *e.g.* tantalum carbide,[59] sodium tungstate,[60] Mo(IV) catalysts,[61] methyltrioxorhenium,[62] borax[63] and further polymer immobilized systems.[64] Organocatalytical approaches have also been published recently. Accordingly, the group of C. G. Kokotos studied the catalytic activity of 2,2,2-trifluoroacetophenone in the oxidation of several different thioethers (Scheme 8).[65] On the other hand, M. Jereb showed that oxidation with aqueous hydrogen peroxide can proceed also without additional solvents and catalysts.[66]

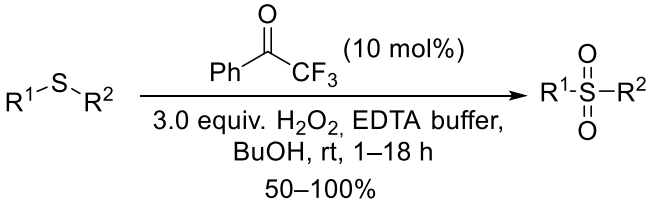

Scheme 8: Organocatalytic oxidation of thioethers to sulfones with hydrogen peroxide as an oxidant, as presented by C. G. Kokotos and coworkers. [65]

The drawback of the most harsh oxidation conditions is their reduced tolerance towards numerous functional groups of the substrate molecules. Therefore, several other research groups have developed milder protocols which use *m*-chloroperbenzoic acid (*m*CPBA)[67] or periodic acid[68] as an oxidant. The mild conditions allow the late stage oxidation of sulfides in pharmaceutically relevant compounds, as described by R. J. Griffin, B. T. Golding *et al*.[67]

The synthesis of sulfoxides can be achieved in most cases by using equimolar amounts or a slight excess of the oxidant. For example, in the protocol of C. G. Kokotos (see Scheme 8) the

usage of 1.5 instead of three equivalents hydrogen peroxide resulted in the selective formation of the sulfoxide.[65] Additionally, the utilization of triflic anhydride (0.5 equiv.) can prevent the overoxidation by an excess of oxidant, as reported by M. M. Khodaei, K. Bahrami *et al.*[69] An alternative approach to avoid the overoxidized side-products is the decreasing of the reaction temperature. In some other protocols the usage of a small excesses of bromine for the selective oxidation of thioethers have been reported.[70]

In the borax-catalyzed oxidation of sulfides with hydrogen peroxide, the selective formation of sulfoxides can be enabled by adjusting the pH-value of the reaction mixture (Scheme 9).[63] Thus, under basic conditions the formation of diperoxoborates $(HO)_2B–(OOH)_2$ favors the formation of the sulfones, as proposed by the authors. In contrast to this, under neutral condition the less active peroxoboric acid $(HO)_2BOOH$ is formed predominantly and gives mainly the desired sulfoxide.

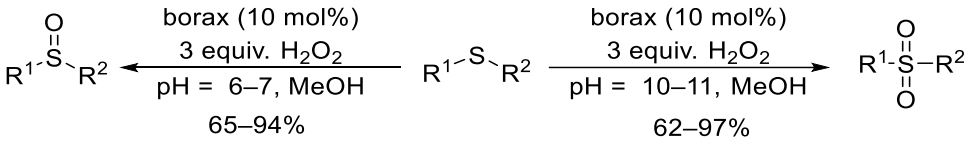

Scheme 9: pH-Controlled selective oxidation of organic sulfides with hydrogen peroxide as an oxidant.[63]

In recent years, special attention has been paid to the development of protocols for the stereoselective oxidation of sulfides due to the fundamental impact of enantiopure sulfoxides on several research areas. Chiral sulfoxides can be used as ligands for asymmetric catalysis as recently reviewed by B. M. Trost *et al*.[71]

Also medicinal chemistry benefits from these efforts because of the high potential of chiral sulfoxides in the treatment of various diseases. In this respect, specialized protocols for the synthesis of proton pump inhibitors like esomeprazole (**34**) have been developed utilizing chiral Schiff bases for the stereoselective oxidation of thioethers (Scheme 10).[72] Additionally, approaches towards the biocatalytical enantioselective oxidation of pyrmetazole (**33**), the precursor of esomeprazole, by a wild-type Baeyer-Villiger monooxygenase have been reported in literature.[73]

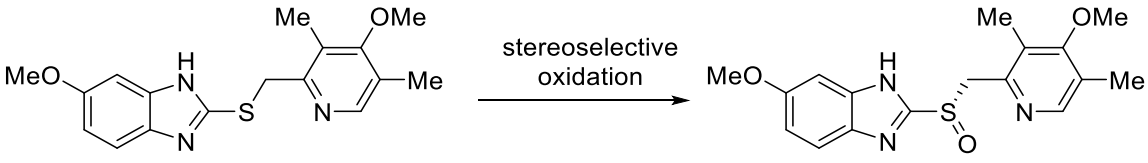

pyrmetazole **33** esomeprazole **34**

Scheme 10: Stereoselective synthesis of esomeprazole (**34**) from pyrmetazole (**33**) using chemical[72] or biochemical[73] oxidation protocols.

Further methodologies for the oxidative synthesis of sulfoxides and sulfones have been recently reviewed by R. V. Kupwade.[74]

1.3.1.2 Transformations based on transition metal insertion in C_{Ar}–SR bond

In the recent decade, several transition metal-catalyzed conversions of thioethers into a variety of functional groups have been reported in literature. In this regard, the development of protocols for *ipso*-borylation, *ipso*-phosphorylation, *ipso*-amination and *ipso*-thioalkylation has expanded the range of synthetic tools for organic chemists. Furthermore, protocol for the arylation of thioethers, also known as *Liebeskind-Strogl* reaction, has been reported as well. The utilization of robust and stable thioether C–S bonds as levers for these reactions is desirable as a useful alternative to other cross-coupling reactions, in which aryl halides and pseudohalides are mainly used as precursors.

i-Borylation of thioethers (C–S to C–B conversion)

In 2016, the group of T. Hosoya reported the *ipso*-borylation of alkyl thioarenes *via* rhodium-catalyzed cleavage of the sulfur-carbon bond (Scheme 11).[75] Their protocol allowed the synthesis of aryl pinacolboronates from alkyl and aryl sulfides in the presence of functional groups like acetates, tosylates and protected alcohols. Bis(pinacolato)diborane $(Bpin)_2$ was used as a boron-containing precursor without an additional base. To achieve high yields, the catalyst has to be pre-activated by heating the rhodium precatalyst in the presence of the ligand and bis(pinacolato)diborane before adding the alkyl thioethers to the reaction mixture.

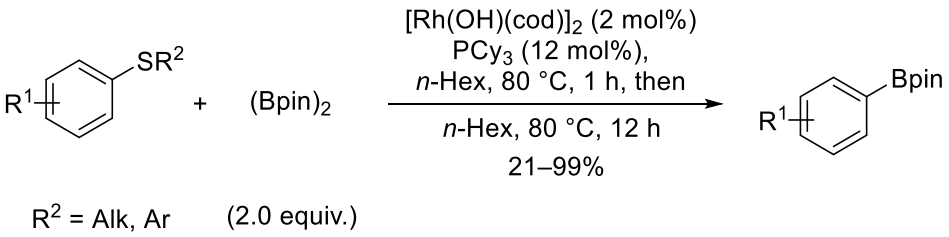

Scheme 11: Rh-catalyzed *ipso*-borylation of thioethers, as reported by T. Hosoya and coworkers.[75]

i-Phosphorylation of thioethers (C–SR to C–P conversion)

Recently, the first *ipso*-phosphinylation of aryl thioethers was presented by the groups of T. Chen, S.-F. Yin and L.-B. Han (Scheme 12).[76] By utilization of a commercially available nickel catalyst the authors were able to synthesize triaryl and dialkyl aryl phosphine oxides from aryl thioethers and secondary phosphine oxides with low catalyst loading down to 0.1 mol%. Electron-rich as well as electron-withdrawing substituents were tolerated. This versatile protocol allowed the synthesis of several organophosphorus compounds in gram scale. The formation of the desired C–P bond was also possible by utilization of methylsulfoxide and methylsulfones as starting materials.

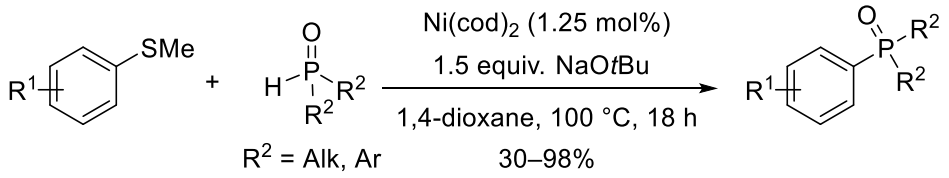

Scheme 12: C**–**S/P**–**H cross-coupling of aryl sulfides with secondary phosphinoxides, as reported by T. Chen, S.-F. Yin and L.-B. Han with coworkers.[76]

i-Amination of thioethers (C–SR to C–N conversion)

One of the first transition metal-catalyzed synthesis of diarylamines by replacing of C–S bonds with C-N ones was presented by K. Murakami, H. Yorimitsu and coworkers (Scheme 13).[77] The authors utilized a bulky NHC-derived palladium catalyst (SingaCycle-A3) with potassium hexamethyldisilazide (KHMDS) in the amination of aryl sulfides with substituted anilines. Previously, similar transformations were known only for the oxygen analogues upon cleavage of the C–O bonds.[78] The high reactivity of the used SingaCycle-A3 (**35**) complex also allowed the amination of bulky *ortho*-substituted aryl sulfides. The protocol enabled the conversion of several different alkyl and aryl thioethers into their aminated derivatives and was highly selective, as only secondary anilines were obtained by the transformation.

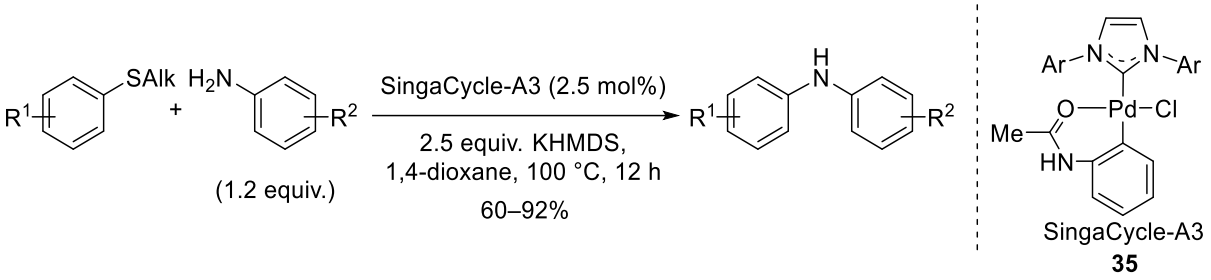

Scheme 13: Pd-catalyzed amination of aryl thioethers with anilines, as reported by K. Murakami, H. Yorimitsu and coworkers.[77]

In a consecutive publication, the group of H. Yorimitsu extended the protocol towards the amination of aryl sulfides with primary and secondary aliphatic amines.[79] The optimized reaction conditions utilizing the structurally similar catalyst SingaCycle-A1 (structure see below in Scheme 14) allowed also the amination with alkyl aryl amines, which was not reported in their previous publication.

i-Thioalkylation of thioethers (C–S to C–S conversion):

While alkene and alkyne metathesis are well established transformations in the field of organic synthesis and material science,[80,81] protocols for carbon-sulfur bond metathesis are rare in the literature. The first example in this nearly untapped area of research was presented by B. Morandi and coworkers in 2017 (Scheme 14).[82] They reported on the palladium-catalyzed carbon-sulfur bond metathesis by reversible arylation of several alkyl aryl sulfides, with a low catalyst loading of 0.4 mol%. Especially, methyl thioethers could be easily transferred into the envisaged alkyl aryl sulfides by reaction with thiolates, which were *in situ* generated by deprotonation of the thiol with an excess of lithium hexamethyldisilazane (LiHMDS). The driving force of the metathesis is the formation of nearly insoluble lithium methanethiolate. The authors examined a broad scope of arene- and heteroarene-derived methyl thioethers as substrates as well as different alkyl thiols as reactants. The reaction afforded the products in good to excellent yields and tolerated several functionalities, e.g. protected alcohols, aldehydes and nitrile groups.

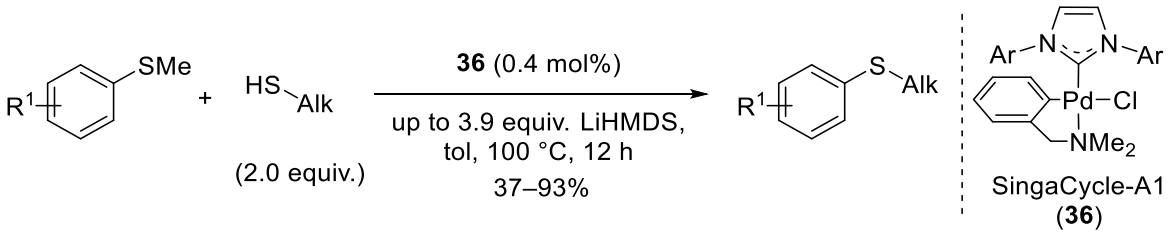

Scheme 14: Sulfur-carbon bond metathesis reaction for the synthesis of various alkyl aryl thioethers, as presented by B. Morandi and coworkers.[82]

i-Alkylation/Arylation of thioethers (C–SR to C–C conversion)

In 2002, L. S. Liebeskind and J. Srogl reported the first cross-coupling of boronic acid with heteroaromatic thioether for the formation of carbon-carbon bonds under mild conditions (Scheme 15).[83] The Pd-catalyzed, CuTC-mediated [copper(I) thiophene-2-carboxylate (**37**)] cross-coupling reaction allowed the synthesis of several variously functionalized diaryl substrates. However, the reaction was limited to application of electron-deficient thioethers. Apart from diaryl sulfides, also alkyl aryl sulfides were used as reactants.

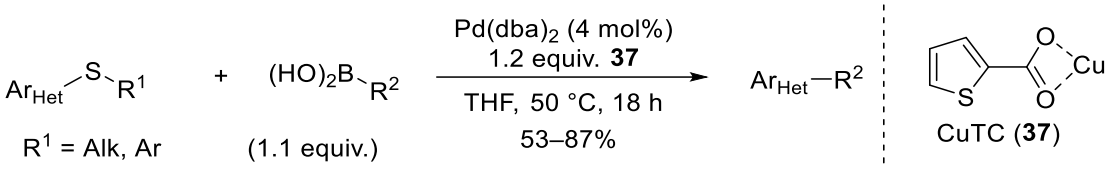

Scheme 15 Liebeskind-Srogl cross-coupling of aromatic thioethers with boronic acids using CuTC as a mediator and thiolate scavenger.[83]

The reported protocol is based on their previously developed cross-coupling reaction with thiol esters as electrophilic reagents, also known as the first generation Liebeskind-Srogl cross-coupling reaction. The latter can be used for the synthesis of unsymmetrical diaryl ketones.[84] In subsequently modified procedures, the boronic acid was replaced by aryl stannanes[85], siloxanes[86] and Grignard reagents[87] as well as organozincates[88] under transition metal catalysis. The orthogonality of the Liebeskind-Srogl-like cross-coupling compared to classical cross-coupling protocols was demonstrated by the group of M. C. Willis. They reported on the Rh-catalyzed coupling of boronic acids and aryl methyl sulfides in the presence of aryl halides and alkyl iodide residues.[89]

The applications along with the detailed mechanistic evaluation of the Libeskind-Srogl reaction have been recently reviewed.[90]

In 2019, J. Cornella and coworkers reported a protocol for the reductive Ni-catalyzed alkylation of heterocyclic aryl sulfides with primary and secondary alkyl bromides as well as aryl bromides (Scheme 16),[91] reminiscent to the Liebeskind-Srogl coupling. The use of electron-rich ligands like 1,1'-bis(diphenylphosphino)ferrocene (dppf) in the nickel-catalyzed activation of the strong thioether bond facilitated the formation of new C-C bonds. As a reducing agent, inexpensive elemental zinc was employed. The authors demonstrated the versatility of the presented methodology by a broad scope of different (hetero)cyclic frameworks and alkyl bromides.

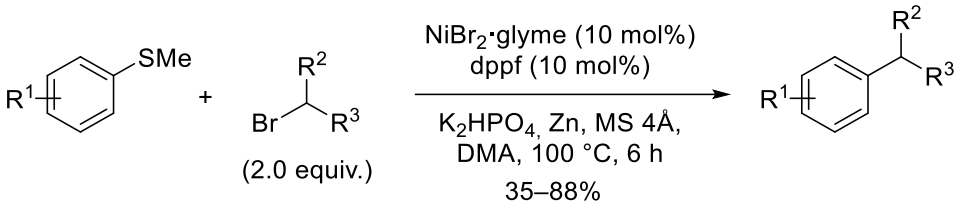

Scheme 16: Ni-catalyzed alkylation of (hetero)cycles by reductive cleavage of methyl thioethers, as reported by J. Cornella and coworkers.[91]

Apart from pre-functionalized arenes and alkanes like boronic acids or bromides, also un-functionalized heteroarenes can be used in C-C coupling reactions with thioethers through a C–H bond activation step. Z.-X. Wang *et al.* demonstrated that electron-poor and -rich aryl thioethers react with unactivated azole and thiazole derivatives in a Pd-catalyzed coupling reaction (Scheme 17).[92] The authors extended the transformation to aryl selenides and demonstrated the broad functional group tolerance of their protocol. Other transition metal-catalyzed C–C bond formations, which proceed *via* C–S bond cleavage, have been recently reviewed as well.[93]

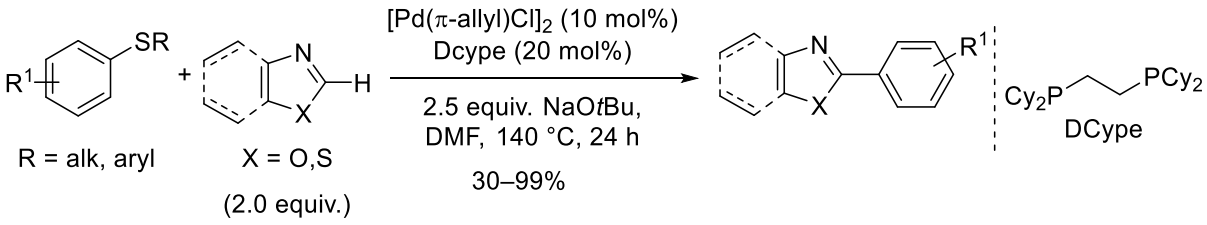

Scheme 17: Pd-catalyzed C-C bond formation via C-H/C-S activation of thioethers and hetero arenes, as reported by Z.-X. Wang *et al.*[92]

1.3.1.3 Nucleophilic substitution ($S_{N,Ar}$)

Electron-poor aryl alkyl thioethers decorated with a nitrile substituent on the aryl moiety react with anilines or alkyl alcohols to form the corresponding diarylated aniline or ether derivatives. As presented by W. Zhao, X.-Q. Wang *et al.*, such substitution of the alkyl thioethers allowed the transition metal-free synthesis with a broad scope of substrates, tolerating a plethora of functional groups (Scheme 18).[94] The protocol was further extended to secondary amines, thus providing access to tertiary substituted aniline derivatives. Mechanistic investigations showed that the reaction proceeded *via* a radical-free nucleophilic substitution pathway. Accordingly, the *in situ* generated alkylthiolate could be captured by addition of benzyl bromide after the reaction was completed. The methodology was used for the functionalization of several pharmaceutically relevant compounds and could be scaled up to 20 mmol.

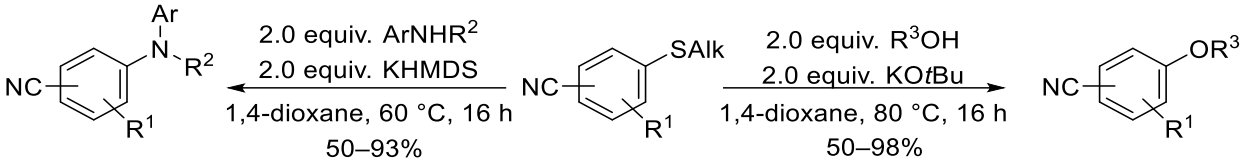

Scheme 18: The transition metal-free nucleophilic amination and etherification of cyanoaryl alkyl thioethers, as presented by W. Zhao, X.-Q. Wang *et al.*[94]

The general mechanism and the kinetic of the nucleophilic attack of amines on electron-poor aryl thioethers with a special focus on the intermediate Meisenheimer complex was described by M. R. Crampton *et al*. in 1993.[95]

1.3.1.4 Directing group

Apart from substitutive and conversional transformations of thioethers groups, considerable attention was recently paid to their ability to act as a directing group in transition metal-catalyzed C–H activation reactions of (hetero)arenes.

In 2012, Y. Zhang and coworkers reported one of the first aryl thioethers-directed Fujiwara-Moritani olefination[47b] (Scheme 19).[96] The reported palladium-catalyzed reaction gave access to a variety of substituted cinnamic esters **38**. Furthermore, it was demonstrated that the presence of a thioether group is crucial for the C–H alkenylation, whereas the corresponding sulfoxide, sulfone and ether analogs were not reacting. The yield of the reaction was moderate to good and almost independent on the nature of the thioether (R^2 = Alk, Ar, Bn).

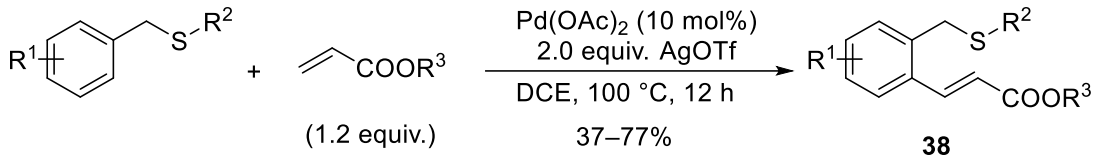

Scheme 19: Thioether-directed alkenylation of arenes, as presented by Y. Zhang and coworkers.[96]

One year later, in 2013, this concept was utilized by Z.-J- Shi group in an optimized protocol using a rhodium catalyst instead of palladium acetate. With copper acetate as an additional oxidant it was also possible to conduct the alkenylation of arenes with acryl amides and styrene derivatives. Additionally, it has been shown that, depending on the choice of solvent, the reaction selectively lead to the mono- or dialkenylated products.[97]

To enable the access to higher substituted alkene derivatives, E. P. Urriolabeitia *et al*. used microwave-assisted within 30 min hydroarylation of unsymmetrically substituted alkynes with thioether of the general structure **39** (Scheme 20, **A**).[98]

Related thioether derivatives **40** can also be acylated with α-oxocarboxylic acids under palladium catalysis, as presented by C. Kuang *et al.* (Scheme 20, **B**).[99] The coordinating abilities of the thioethers enabled the palladium-catalyzed regioselective monoacylation of **40** in good yields and gave access to several unsymmetrical diaryl ketones.

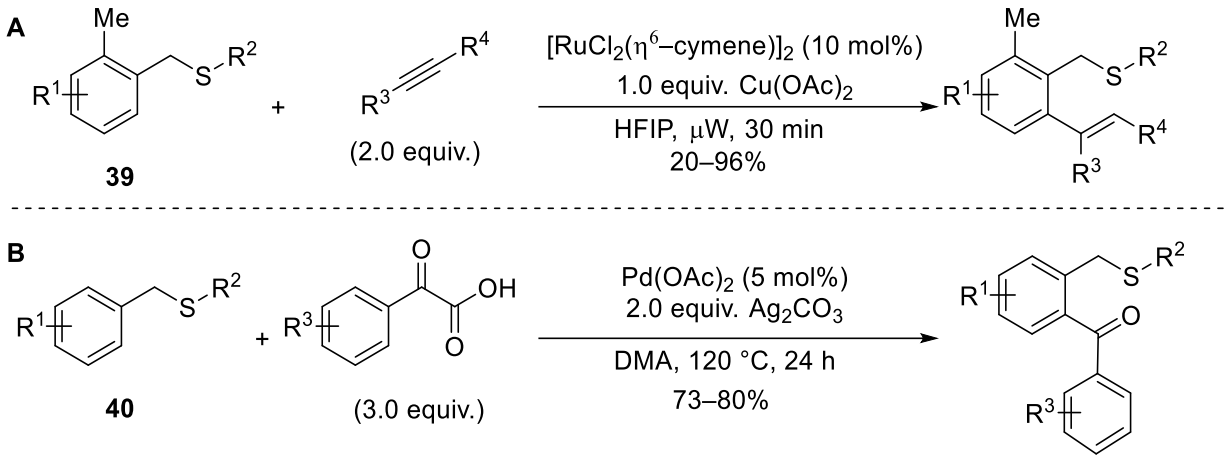

Scheme 20: **A:** Ru-catalyzed alkenylation of arenes with alkynes, as presented by E. P. Urriolabeitia *et al*.;[98]
B: Thioether-directed *ortho*-acylation of thioethers.[99]

An additional example of the directing ability of thioethers was presented by the group of M. Miura, who reported the rhodium-catalyzed selective C–H alkenylation of 3-alkyl(aryl)thioindoles at C4 position with a commercially available Rh catalyst (Scheme 21).[100] The coordination of the catalyst enabled a regioselective *trans*-alkenylation of several different thioethers with electron-rich and electron-poor alkenes. Very recent the group of M. Miura reported the direct on C4-selective acylation catalyed by an iridium catalyst.[101]

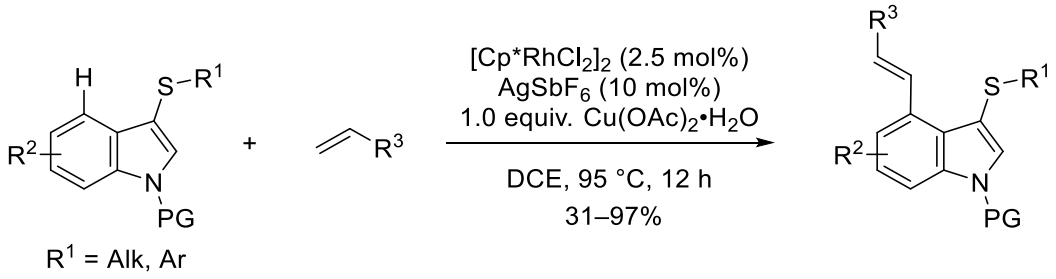

Scheme 21: Thioether-directed C**–**H functionalization of indole derivatives, as presented by M. Miura and coworkers.[100]

In a subsequent publication, the authors expanded the scope of the thioethers-directed alkenylation towards naphthyl sulfides and were able to obtain higher substituted naphthyl alkenes by hydroarylation of internal alkynes (Scheme 22).[102] The presented *peri*-selective C–H activation protocol was also extended to the arylation of naphthalene and anthracene

derivatives.[103] Additionally, the double C–H arylation of anthracenes by usage of two equivalents boronates was reported as well, however, in lower yield (19–43%).

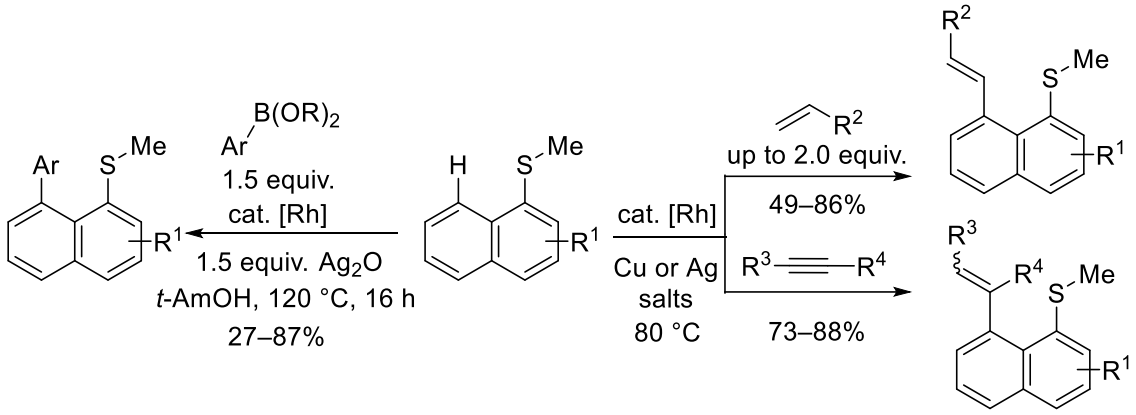

Scheme 22: Rhodium-catalyzed thioethers-directed *peri*-selective arylation[103] and alkenylation[102] reactions, as presented by the group of M. Miura.

1.4 Synthesis of aryl thioethers

Since aryl sulfide-containing core structures are of tremendous importance in several areas of organic synthesis (see previous Chapter), numerous synthetic protocols were developed for the design of this distinct structural motif.

In addition to the classical Williamson-type thioether synthesis,[104] which consists in nucleophilic substitution on an alkyl halide with an aryl thiolate following a consecutive (S_N1) or concerted (S_N2) pathway (see Scheme 23), several new methodologies to sulfenylate arenes, with or without previous pre-functionalization, were elaborated over the past decades.

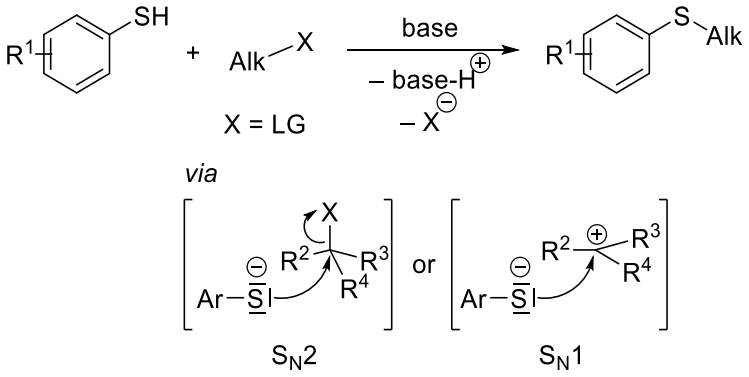

Scheme 23: Classical Williamson-type thioether synthesis of alkyl aryl sulfides by nucleophilic substitution on a alkyl halide with an aryl thiolate.

In general, these approaches can be divided into two general categories: transition metal-based protocols and transition metal-free approaches. Traditional developments as well as recent results of both approaches will be discussed in this Chapter.

1.4.1 Transition metal-based protocols

The transition metal (TM)-catalyzed formation of C–S bonds has received significant attention in recent decades and changed the face of modern organic synthesis. Several different 3d-, 4d- and 5d-metalcomplexes have shown significant reactivity in the preparation of aryl sulfides from pre-functionalized arenes with sulfur-containing precursors (Scheme 24, **A**). In these cases, the sulfur-containing moiety can be viewed as nucleophilic sulfur building block since it formally substitutes a negatively charged leaving group X.

In recent years, various protocols have been reported for the formation of a C–S bond *via* C–H functionalization, which allow a more atom economical synthesis of thioethers (Scheme 24, **B**). In most of these cases, the utilized sulfur-containing precursor shows an electrophilic character in the reaction mechanism. Additionally, sulfur-based radical reaction pathways have been elaborated, especially in the cases of photocatalytically- or electrochemically-induced transformations

The following Chapter will discuss selected examples of the TM-catalyzed aryl sulfide synthesis. It is divided into Subchapters depending on the utilized metal. Various aspects of TM-catalyzed C–S bond formation reactions has been reviewed by several authors.[105]

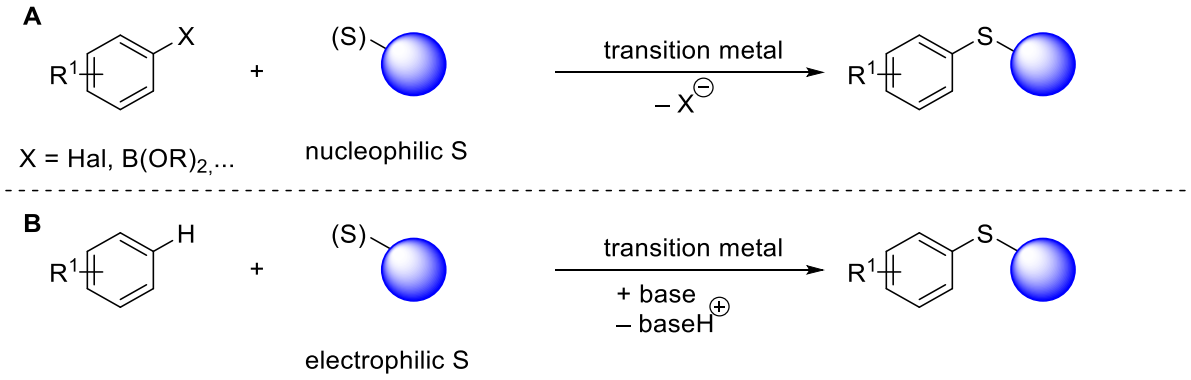

Scheme 24: Concept of transition metal-catalyzed synthesis of aryl sulfides by (**A**) cross-coupling of pre-functionalized arenes with sulfur-containing precursors or (**B**) by C**–**H thiolation of arenes.

1.4.1.1 Palladium-based transformations

One of the first palladium-catalyzed formations of aryl sulfides was reported by T. Migita *et al.* in 1978 (Scheme 25).[106,107] The authors demonstrated the ability of tetrakis(triphenylphosphine) palladium(0) to catalyze the cross-coupling reaction of aryl halides with aryl and alkyl thiolates which resulted in the formation of diaryl sulfides. Based on this initial result, the field of palladium-catalyzed aryl sulfide synthesis has been extended by several research groups.

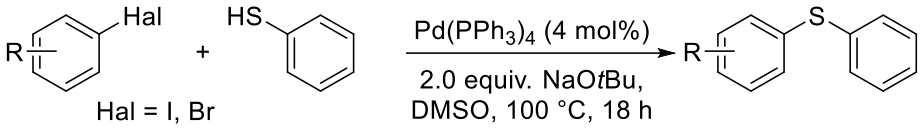

Scheme 25: Early example of palladium-catalyzed formation of diaryl sulfides, as reported by T. Migita *et al.*[106]

The sequence of elementary steps in the classical cross-coupling of iodo-, bromo- and chloroarenes or arly triflates with thiols (Table 1, Entries 1–6) have been evaluated by detailed kinetic and mechanistic investigations by J. F. Hartwig and coworker[108] as well as by J. M. Campagne, A. Jutand *et al*.[109] Aryl hydrazines and aromatic carbonic acids (Table 1, Entries 7&8) can also be transformed into the corresponding aryl sulfides by an oxidative cross-coupling with oxygen or silver(I) salts as oxidizing reagents.[110–112] Apart of thiols, also further sulfur-containing substrates can be utilized in palladium-mediated C–S bond-forming reactions. (Table 1, Entries 9–13). Palladium-catalyzed cross-couplings of aryl halides with thiols can even proceed with extremely low catalyst loadings of down to 0.01 mol%, thus showing the high potential of this approach.[113]

Table 1: Representative examples of palladium-catalyzed cross-coupling reactions for the synthesis of aryl sulfides.

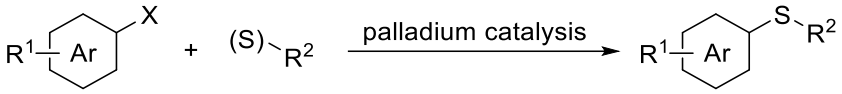

Entry	X	(S)	R	Reference
1	I	SH	Alkyl	[114]
2	Br	SH	Alkyl, Aryl	[115]
3	Br	SH	Alkyl, Aryl, Silyl	[116]
4	Br	SH	Silyl	[113]
5	Cl	SH	Alkyl, Aryl, Silyl	[117]
6	OTf	SH	Alkyl	[118]
7	$NHNH_2$	SH	Aryl	[110]
8	COOH	SH	Alkyl, Aryl	[111,112]
9	I	S-BBN	Aryl	[119]
10	Br	SSR	Aryl	[120]
11	$Si(OEt)_3$	SSO_3Na	Aryl	[121]
12	Br	SBn	Aryl	[122]
13	Br	S-TIPS	Aryl	[123]

Due to the high value of trifluoromethyl thioethers in medicinal chemistry (compare Chapter 1.2.2), several synthetically oriented groups have invested great efforts to develop protocols for the trifluoromethylthiolation of arenes. In this regard, it has been reported that a series of palladium-catalyzed cross-couplings of aryl halides with trifluoromethyl thiolate provide access to a variety of different trifluoromethyl thioethers. Accordingly, different M–S–CF_3 salts (like $AgSCF_3$, Me_4NSCF_3) were employed.[124,125] A recent example of these protocols was published by F. Schoenebeck and coworkers, who presented the trifluoromethylthiolation of aryl iodides and bromides with a palladium(I) catalyst **41** (Scheme 26).[124] The recyclable and bench-stable catalyst **41** enabled the functionalization of aryl and heteroaryl halides and tolerated several functional groups in the substrate.

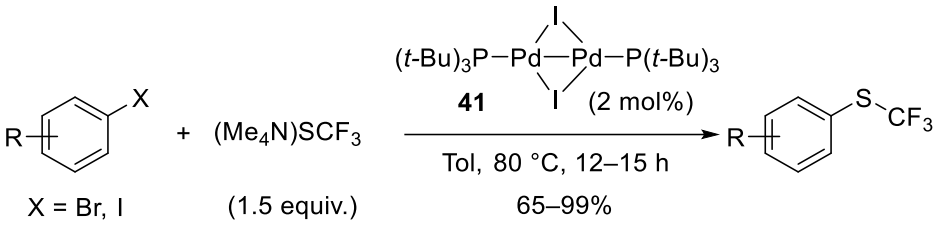

Scheme 26: Palladium-catalyzed synthesis of trifluoromethyl thioethers, as presented by the group of F. Schoenebeck.[124]

In the past few years, special attention has been paid also to the development of palladium-catalyzed C–H thiolation of arenes and heteroarenes bearing different directing groups, such as pyridine moieties.[126] In 2015, F. Glorius and coworkers reported on the C–H sulfenylation of several heteroarenes like thiophenes, pyrroles and furanes with diarylsulfides as sulfenylation reagent (Scheme 27, **A**).[127] This complemented the results of P. Anbarasan and colleague, who performed C–H thiolation of unactivated phenyl derivatives by usage of *N*-(arylthio)succinimides as electrophilic sulfur reagent (Scheme 27, **B**).[128] The both presented protocols did not require additional oxidants and allowed the synthesis of several diaryl sulfides.

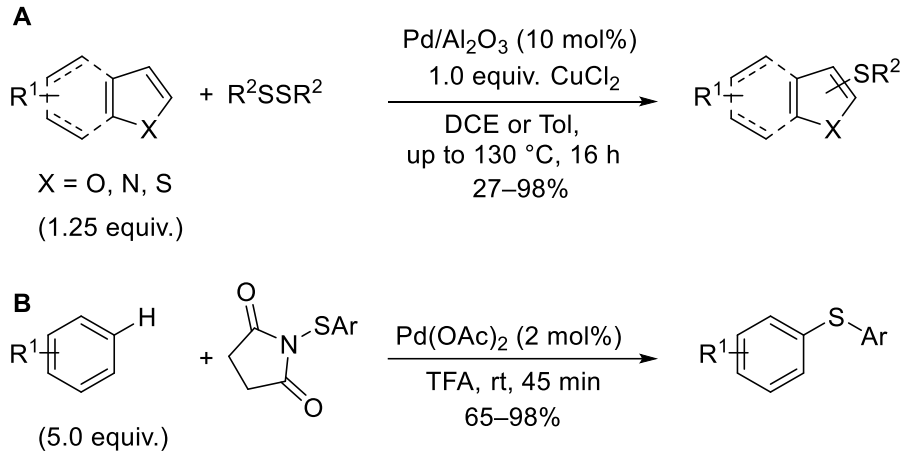

Scheme 27: Pd-catalyzed C-H sulfenylation protocols for the functionalization of unactivated (**A**) heteroarenes[127] and (**B**) arenes.[128]

Additionally, the group of M. Beller demonstrated, that arylsulfonyl cyanides can be used as precursors for the thioarylation of electron-rich arenes in the presence of palladium catalysts.[129]

1.4.1.2 Nickel-based transformations

Nickel is an abundant and inexpensive transition metal which is also known for the ability to enable the formation of aryl sulfides applying the general cross-coupling approach shown above in Scheme 24. The history of nickel-catalyzed aryl sulfide synthesis started in 1982 with a protocol of H. J. Cristau and coworkers, who reported the arylation of arenethiolates with aryl bromides in the presence of a nickel catalyst from $NiBr_2$ and a bidentate [*P*,*P*]-ligand under very harsh reaction conditions (200 °C) (Scheme 28).[130]

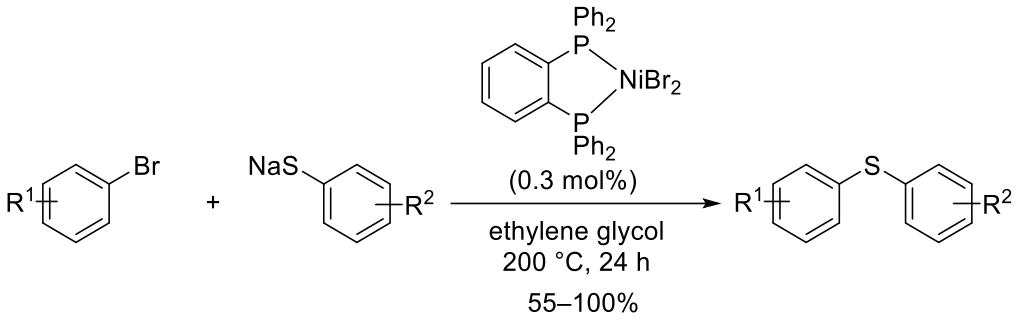

Scheme 28: Nickel-catalyzed thioarylation of aryl bromides at elevated temperatures, as reported by H. J. Cristau and coworkers.[130]

Based on this result, several thiolations of halogenated arenes utilizing aryl thiols, thiolates and aryldisulfides as nucleophilic sulfur reagents have been reported in the literature. Representative examples of these reactions are given in Table 2.

Table 2: Representative examples of nickel-catalyzed cross-coupling reactions for the synthesis of aryl sulfides.

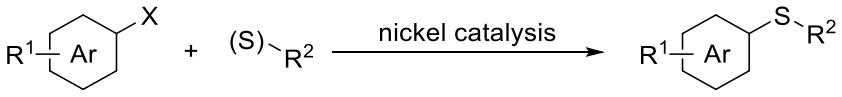

Entry	X	(S)	R	Reference
1	I	SSR	Alkyl, Aryl	[131]
2	I	SH	Alkyl, (hetero) aryl	[132]
3	Br	SH	Alkyl, Aryl	[133]
4	Cl	SH	Alkyl, (hetero)aryl	[134]
5	OMs	SNa	Aryl	[135]
6	Cl, Br, I	SH	Alkyl, Aryl	[136]

In the case of disulfides as precursors, overstoichiometric amounts of zinc powder are commonly used to reduce the employed Ni(II) pre-catalyst to a Ni(0) species. The latter inserts

into the sulfur-sulfur bond of the disulfide and enables the reductive elimination of the envisaged aryl sulfide with a formation of the new desired carbon-sulfur bond.[137]

Almost all traditional nickel-catalyzed C–S-forming cross-couplings require harsh conditions like elevated temperatures (for an exceptional case see the work of N. D. Paul's team[138]). Therefore, the development of mild coupling conditions was targeted by several groups. Very recently, nickel-catalyzed electrochemical thiolations of aryl halides have been reported. This new approach enables the desired C–S bond formation at room temperature (Scheme 29). Y. Wang *et al.*[139] presented detailed electrochemical studies on the thioarylation of aryl iodide derivatives, whereas, the group of T.-S. Mei was able to utilize aryl bromides and chlorides as substrates with the same catalytic system.[140] Both protocols allowed the synthesis of heteroaryl sulfides and both groups proposed an initial anodic oxidation of the thiol as a key step of the catalytical cycle to generate a thiyl radical as the reactive species.

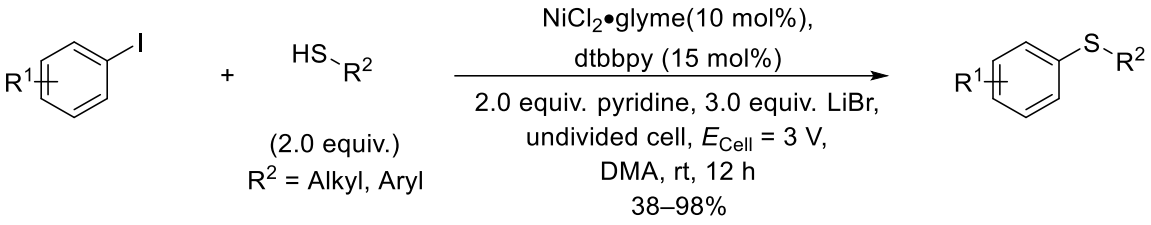

Scheme 29: Electrocatalytical synthesis of aryl sulfides, as reported by Y. Wang *et al.*[139]

Alkyl aryl sulfides can also be synthesized in a complementary fashion by utilization of aryl thiosulfonate and unactivated alkyl bromides. In this regard, a nickel-catalyzed reductive thiolation protocol has been reported in a collaborative publication of the L. Ackermann and S.-J. Ji groups, presenting an elegant and versatile catalytic method for the preparation of highly functionalized alkyl aryl sulfides under mild conditions (no base, 30 °C).[141] The authors were able to extend their newly elaborated protocol towards the synthesis of dialkyl sulfides as well as selenides.

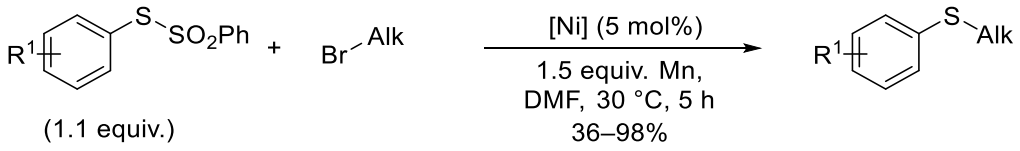

Scheme 30: Versatile nickel-catalyzed reductive chalcogenation of unactivated alkyl bromides with thiosulfonates, as reported by the L. Ackermann and S.-J. Ji groups.[141]

In contrast to the previously published protocols utilizing pre-functionalized arenes, L. Ackermann and colleagues circumvent this disadvantage by reporting the first Ni-catalyzed directed C–H chalcogenation of anilines with pyrimidyl as a directing group (Scheme 31).[142] The procedure did not require pre-functionalized substrates like halides and permited the selective *ortho*-thiolation with diaryldisulfides. By oxidation of the *in situ* generated aryl thiolate to aryl disulfide through addition of manganese oxide, the disulfide loading could be reduced to 1.2 equivalents. This new C–H activation protocol enables a more step-economical synthesis of the target molecules avoiding complex pre-functionalization of substrates. The catalytic cycle involves the formation of a sulfur-centered radical.

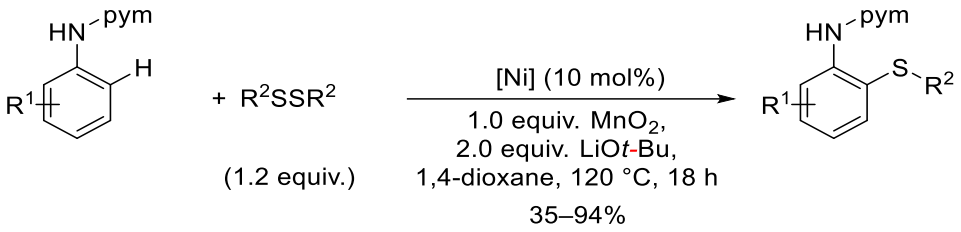

Scheme 31: Nickel-catalyzed C-H thiolation of protected anilines, as reported by the group of L. Ackermann.[142]

1.4.1.3 Copper-based transformations

Extensive work in the area of copper-catalyzed C–S bond-forming reactions has resulted in a significant progress in the synthesis of aryl sulfides. The use of copper catalysts is desirable due to the low price of the metal (~$0.01 per gram) and its relatively low toxicity. The general strategy relies upon the coupling of aryl iodides with thiols, which follows the concept of the copper-mediated Ullmann-type chemistry. In some cases (Entry 1, Table 3) expensive phosphazene-bases or high catalysts loading (up to 20 mol%) are required.[143] G. C. Fu, J. C. Peters and coworkers extended the reactant scope to aryl bromides by photoinduced, copper-catalyzed cross-couplings *via* single electron transfer (SET) under mild conditions (0 °C) (Entry 3, Table 3).[144,145] A few couplings of aryl chlorides with aryl thiols at elevated temperatures and long reaction times (135 °C, 24 h) are reported in the literature as well.[146] The mechanism of these Ullmann-type coupling reactions, either radical or via an oxidative addition, depends on the structure of a substrate and the reaction conditions and still remains a topic of current investigations.[147]

Apart from aryl halides, also boronic acids and boronic esters can be arylthiolated by a variation of the Chan-Lam reaction with different sulfur precursors (Entries 5–14, Table 3).[148] While most of the Chan-Lam like protocols with thiols or disulfides (Entries 5–8, Table 3) as S-reagents require elevated temperature, some processes for the S-arylation of boronic acids with thiols proceed at room temperature.[149] Also sulfothioates (Entry 9), thiosulfonates (Entries 10 & 11), sulfonylhydrazines (Entry 12) and *N*-thioimides (Entry 13) can be utilized as precursors. The potential of copper-mediated cross-coupling reactions of Chan-Lam type was simultaneously demonstrated by the groups of Q. Shen and M. Rueping, who extended the methodology towards the synthesis of trifluoromethyl thioethers with *N*-(trifluoromethylthio)phthalimide as a trifluoromethyl thiolating reagent (Entry 14, Table 3).[150,151]

As reported by J. M. Hoover *et al*., (hetero)aromatic carboxylic acids can be used as starting materials in the copper-catalyzed synthesis of diaryl sulfides. This aerobic - decarboxylative thiolation uses molecular oxygen as an oxidant and (hetero)aryl thiols as reactants (Entry 15, Table 3).[152]

Table 3: Representative examples of copper-catalyzed cross-coupling reactions for the synthesis of aryl sulfides.

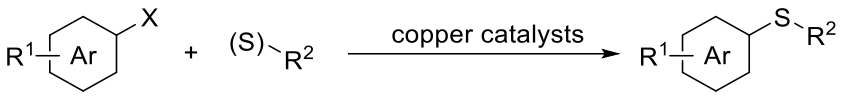

Entry	X	Ar	(S)	R	Reference
1	I	Arene	SH	Aryl	[143,153]
2	I	Arene	SH	Aryl, Alkyl	[154]
3	Br	Arene	SH	Aryl	[144]
4	Cl	Arene	SH	Aryl	[146]
5	$B(OH)_2$	Arene	SH	Alkyl	[155]
6	$B(OH)_2$	Arene	SSR	Alkyl, Alkenyl, Aryl	[156]
7	$B(OH)_2$	Arene	SSR	(hetero)Aryl	[157]
8	Bpin	(hetero-)arene	SSR	Aryl	[158]
9	$B(OH)_2$	Arene	SSO_3Na	(hetero)Aryl	[159]
10	$B(OH)_2$	Arene	SSO_2R	Alkyl, (hetero)Aryl	[160]
11	Bpin	Alkenyl, (hetero-)arene	SSO_2R	Alkyl, (hetero)Aryl	[161]
12	$B(OH)_2$	Arene	SO_2NHNH_2	Alkyl, Aryl	[162]
13	$B(OH)_2$	Arene	S-Suc	Alkenyl, Aryl	[163]
14	$B(OH)_2$	Arene	S-Pht	CF_3	[150,151]
15	COOH	(hetero-)arene	SH	(hetero)Aryl	[152]

Additionally, a straightforward synthetic protocol for the copper-catalyzed electrophilic trifluoromethylthiolation of boronic acids with a benziodoxol reagent was reported by L. Lu, Q. Shen *et al.*[164] The presented methodology allowed the synthesis of several trifluoromethyl aryl sulfides in good to excellent yields.

Apart from aryl halides, aryl boronic and carbonic acids as well as selected unfunctionalized aromatic systems can be arylthiolated in a copper-mediated fashion. Those C–H functionalization reactions use diaryldisulfides as sulfur-containing precursors and have been reported for arenes with[165] or without[166] additional directing groups as well as for hetero-cyclic systems.[167] These transformations need an additional oxidant like *e.g.* oxygen or persulfates and involve radical sulfur species in the catalytic cycle.

1.4.1.4 Iron-based transformations

In the last two decades, iron-catalyzed transformations have been elaborated to replace expensive and toxic transition metals in organic synthesis. As reviewed by H.-J. Knölker and coworker, iron catalysis is an fastly growing research topic with promising potential and versatile applications in laboratory as well as in chemistry on industrial scale.[168] Several sulfenylation protocols for pre- and un-functionalized arenes are reported in the field of iron-mediated aryl sulfide synthesis.

The cross-coupling reaction of aryl iodides with thiols is described for the synthesis of diaryl sulfides and alkyl aryl sulfides with different substitution patterns (Entries 1–2, Table 4). In a subsequent publication, the group of C. Bolm discussed the influence of transition metal contaminations [mainly copper(I)oxide] in iron(III)chloride on the yield of the diaryl sulfide and concluded that in certain cases Cu_2O can significantly affect the result of the reaction.[169] Further procedures with simple iron(III)chloride as a pre-catalyst based on the initially reported protocol of C. Bolm and coworkers have been reported by C.-F. Lee and coworkers.[169]

As demonstrated by T. G. Abi, G. Anilkumar *et al.*, the substrate scope can be extended from aryl iodides to bromides and chlorides (Entry 3, Table 4). Nevertheless, iodides are substrate of choice for this kind of transformation.

Table 4: Representative examples of iron-catalyzed cross-coupling reactions for the synthesis of aryl sulfides.

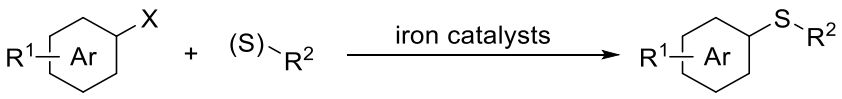

Entry	X	Ar	(S)	R	Reference
1	I	(hetero-)arene, Alkyl	SH	(hetero)Aryl Alykl	[168,169]
2	I	Arene	SH	Aryl, Alkyl	[170]
3	I, Br, Cl	Arene	SH	Aryl	[171]

In contrast to pre-functionalized arenes, also unfunctionalized and electron-rich (hetero)arenes can be efficiently converted into the corresponding thioethers by iron-catalyzed transformations. Accordingly, the group of J. Yadav reported on iron(III)-catalyzed direct thiolation of indole derivatives with (hetero)aryl thiols at elevated temperature (Scheme 32).[172]

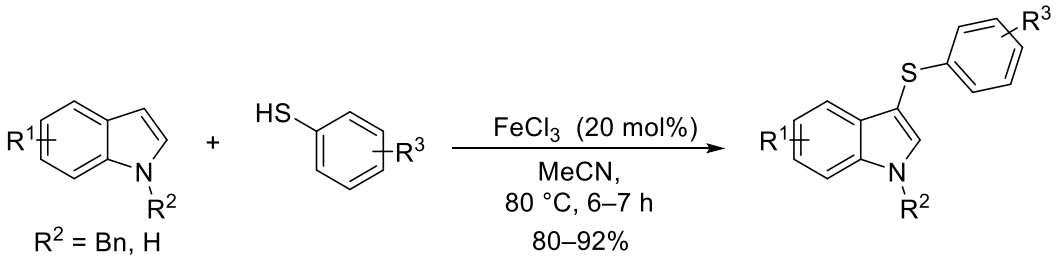

Scheme 32: Iron-catalyzed sulfenylation of indole derivatives, as presented by J. Yadav and coworkers.[172]

In 2014, X.-G. Zhang, J.-H. Li and coworkers extended the scope of the sulfenylation protocol to electron-rich aniline derivatives (Scheme 33).[173] In their procedure, equimolar amounts of diaryldisulfides and additional catalytical amounts of iodine (10 mol%) are used. Furthermore, iron (III)chloride has been replaced by iron(III)fluoride for the efficient synthesis of several diarylsulfides. The authors postulate the *in situ* formation of sulfenyl iodide as the reactive species but did not present any experimental support of this idea.

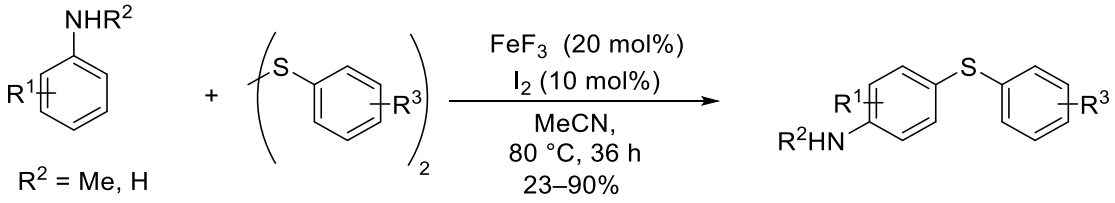

Scheme 33: Synthesis of 4-chalcogensubstituted arylamines, as described by X.-G. Zhang, J.-H. Li and coworkers.[173]

Since the yield of the reported iron-catalyzed transformations might be significantly affected by trace quantities of other transition metals, these protocols may lack in reproducibility.

1.4.1.5 Miscellaneous transition metal-based transformations

In addition to protocols based on palladium, copper, nickel, and iron, complexes of other 3d and 4d metals are also known to be useful catalysts in the synthesis of aryl sulfides.

From the family of 3d metals, manganese-,[174]; cobalt-[175] and zinc-derived catalysts[176] have been applied for the synthesis of aryl sulfides. Further representatives of 4d metal derivatives with catalytic activity in the synthesis of diaryl sulfides are for example rhodium-based systems. As reported by various authors, rhodium(III) catalysts can be utilized for the sulfenylation of unactivated arenes with diaryldisulfides.[177,178] In such cases, the directed sulfenylation of arene C–H bonds requires the addition of an external oxidant like silver(I) salts to increase both the conversion and the yield. In some cases the over-stoichiometric use of the disulfide as well as high temperatures (130 °C) were necessary.[177] Remarkably, selective rhodium-catalyzed substitution reactions of aryl fluorides with disulfides and the cross-coupling of boronic acids with *S*-aryl thiosulfonates have been reported.[179] Some other 4d metals like silver were utilized in the synthesis of aryl sulfides as well.[180]

1.4.1.6 Photomediated approaches

Recently, the utilization of photoredox catalysts for the preparation of aryl thioethers has become an emerging field in catalysis. Apart from organic photocatalysts (see mainly Chapter 1.4.2.1), 4d and 5d transition metal complexes of ruthenium and iridium have been reported to be useful in the synthesis of aryl sulfides.

In 2018, A. Polyzos *et al.* utilized $Ir(ppy)_3$ for the photoredox-catalyzed thiolation of (hetero)aryl iodides at room temperature (Scheme 34).[181] The reaction tolerated several functional groups and provided the desired aryl thioethers in good to excellent yields. The reported transformation was compatible with a wide range of aryl, heteroaryl and vinyl iodides but was limited to dialkyl disulfides as precursors. Moreover, the latter must be used in a large excess. This makes this aryl radical-controlled protocol less economical for industrial purposes compared to previously reported procedures.

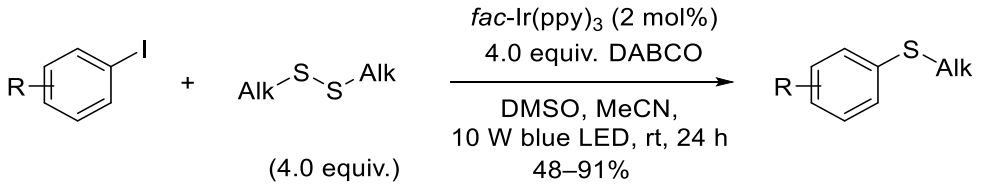

Scheme 34: Application of visible light-induced photoredox catalysis for the synthesis of alkyl sulfides, as reported by A. Polyzos *et al.*[181]

One year before, H. Fu *et al.* already reported on the similar synthesis of diaryl sulfides from aryl thiols.[182,183] The procedure allowed the selective sulfenylation of aryl iodides, bromides and chlorides and was even extendable to heteroaryl iodides and bromides as well as to aryl fluorides bearing electron-withdrawing groups.

The authors propose a SET-based[181b] oxidation of the thiolate by the excited Ir(III) photocatalyst forming the sulfenyl radical and the reactive Ir(II) species, which can reduce the aryl halides substrate to the corresponding radical anion. The latter undergoes a nucleophilic substitution with a thiolate, whereby the desired carbon-sulfur bond is formed and the halide anion is released. The initially formed sulfur-centered radical oxidizes the finally obtained sulfur-centered radical anion of the formed diaryl sulfide, and the desired product is obtained.

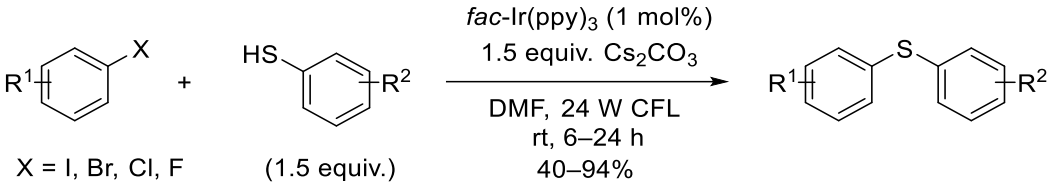

Scheme 35: Photocatalytical synthesis of diaryl sulfides from aryl halides and thiols.[182]

Additionally, examples of thioetherification *via* dual photoredox/nickel catalysis have been reported in literature.[184]

The full potential of photocatalysts for the formation of sulfur–carbon bonds has been summarized recently in a review by A. Wimmer and B. König.[185]

1.4.2 Transition metal-free protocols

Apart from transition metal-catalyzed reactions, several transition metal-free approaches have been reported in the literature. These methodologies have the advantage, that they do not provoke the risk of toxic heavy metal contaminations of the desired products. This is of particular interest in the final steps of the synthesis of pharmaceutically active compounds.

Regulatory standards of the Food and Drug Administration (FDA) as well as the ICH guidelines on elemental impurities of the European Medicine Agency (EMA) claim very low metal concentration, especially for elements like Co, Pd, Rh and Ru.[186]

From a historical point of view, the transition metal-free synthesis of aryl sulfides has been already realized in the first half of the last century through nucleophilic aromatic substitution reactions (S_NAr) of aryl thiolates with electron-poor arenes, like nitrobenzene derivatives (Scheme 36).[187] The mechanism of this reaction involves a two-step addition-elimination sequence with a non-aromatic intermediate Meisenheimer complex **42**. By elimination of the leaving group (LG), the aromaticity of the system is regenerated and the final diaryl sulfide is released. Depending from the substitution pattern on the arenes, a concerted mechanism is proposed as well. Detailed studies on the influence of substituents have been recently reported by E. N. Jacobsen and coworkers.[188]

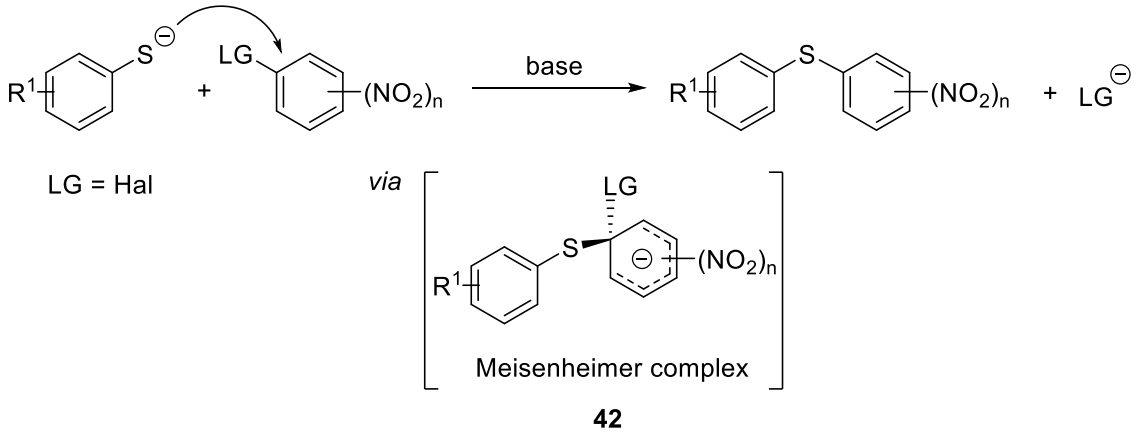

Scheme 36: Concept of nucleophilic aromatic substitution reactions for the synthesis of aryl sulfides.

An alternative, traditional transition metal-free protocol for the synthesis of diaryl sulfides is the Stadler-Ziegler reaction, which utilizes aniline-derived aryl diazonium salts **43** and thiolates (Scheme 37).[189] The desired C–S bond is formed under evolution of equimolar amounts of nitrogen and involves the formation of very active radical intermediates which can lead to the formation of by-products. The other drawbacks of this protocol are its multi-step synthetic chain starting from aniline precursors and, more importantly, the potentially explosive nature of the diazonium salts.

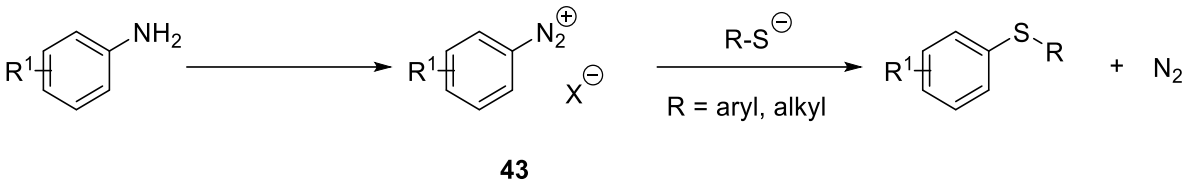

43

Scheme 37: Stadler-Ziegler reaction for the synthesis of aryl sulfides following a radical mechanism.

One strategy for reducing the risk of this transformation is to generate the diazonium species *in situ* and their subsequent reaction with the thiolate, as proposed by C.-F. Lee *et al.*[190] Due to the restrictive requirements for the nature of the substrates and the resulting limitation of the accessible structure motifs, the development of novel transition metal-free protocols is a desirable aim in modern organic synthesis. In recent decades, many groups have invested huge effort on the elaboration of general protocols for the metal-free synthesis of aryl sulfides because of their tremendous impact in different research fields (compare Chapter 1.2). In this Chapter, modern transition metal-free protocols for the synthesis of aryl sulfides will be discussed. Starting with new developments in the radical-controlled sulfenylation reaction, which demonstrate broader applicability than the historical Stadler-Ziegler reaction, new strategies for the sulfenylation of arenes with nucleophilic sulfur reagents will also be discussed in selected examples.

Since the nucleophilic sulfenylation methodologies require the pre-functionalization of the arene before the sulfenylation step and most radical-driven approaches tend to form by-products, alternative electrophilic sulfenylation reagents were developed in recent decades. In this way, the disadvantage of pre-functionalization could be overcome and a more atom-economical synthesis of aryl sulfides could be made possible. This new strategy will be discussed in Subchapter 1.4.2.3.

1.4.2.1 Radical sulfenylation reactions

A. P. Antonchick and coworkers reported the ability of nitrosoniums ions to catalyze the carbon–sulfur bond formation via C–H/S–H cross-dehydrogenative coupling of thiols with phenol and indole derivatives (Scheme 38).[191] In this reaction ambient O_2 serves as a terminal oxidant for the regeneration of the catalytically active nitrosonium ion. The reaction was carried out in hexafluoroisopropanol (HFIP) which enables a sufficient stabilization of the reactive thiyl radical intermediates.

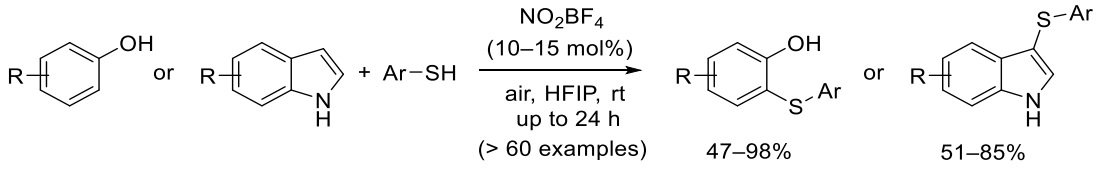

Scheme 38: Nitrosonium-catalyzed coupling of phenols or indoles with aryl thiols, as reported by A. P. Antonchick and coworkers.[191]

Another radical-based sulfenylation has been presented by the group of A. Lei who utilized 2,3-dichloro-5,6-dicyano-1,4-benzoquinone (DDQ) as an oxidant for the radical-recombinative cross-coupling of electron-rich arenes and aryl thiols (Scheme 39).[192] The reaction of thiyl radicals **44** with an *in situ* generated arene radical resulted in the formation of several unsymmetrical aryl thioethers. The authors substantiated their proposed mechanism by identifying all postulated radical intermediates by means of radical trapping experiments and identified the SET-based formation of an aryl radical cation as the rate-determining step.

Scheme 39: DDQ-controlled selective radical-radical cross-coupling of thiols with electron-rich arenes, as reported by the group of A. Lei[192]

Recently, visible light-promoted radical-based transformations for the formation of diarylsulfides were published by several groups.

X. Jiang *et al.* presented a protocol which allows the sulfenylation of diaryliodonium salts **45** with organic thiosulfates. The reaction is promoted by blue LED radiation with Eosin Y (**46**) as a photatalyst (Scheme 40).[193] The procedure allowed the synthesis of several diaryl sulfides and alkylaryl sulfides in moderate to excellent yields in gram-scale from commercially available thiosulfate salts as staring materials. Mechanistic studies of X. Jiang *et al.* revealed that the first step of the reaction is a single electron transfer (SET)[181b] of the photoexcited Eosin Y to the aryliodonium species which subsequent formation of an aryl radical. Afterwards, the radical reacts with the thiosulfate to form the desired new sulfur-carbon bond and a sulfite as a leaving group. Finally, the obtained diaryl sulfide radical is reduced by the initially generated $EY^{+\cdot}$ to regenerate the photocatalyst.

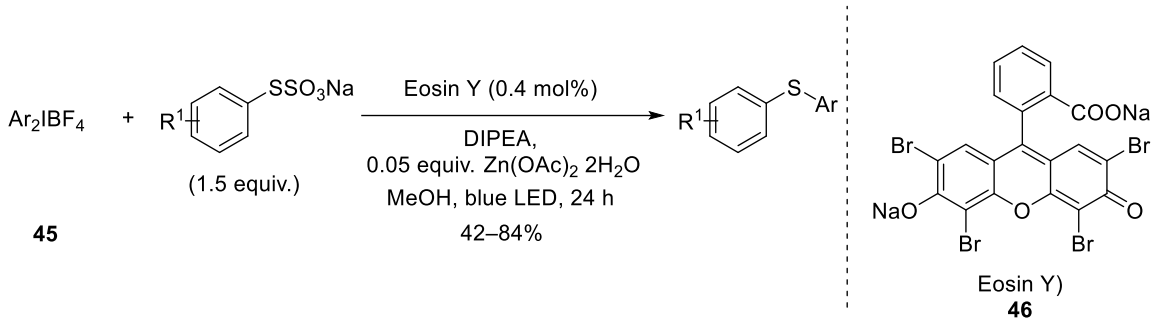

Scheme 40: Eosin Y-promoted photocatalytic reaction of thiosulfate salts with diaryl iodonium salts for the synthesis of diaryl sulfides, as presented by X. Jiang *et al.*[193]

An additional methodology for the photocatalytical formation of diarylsulfides was reported by A. Hajra *et al.*[194] The authors published a light-mediated oxidative coupling of arlylhydrazines with thiols. The transformation was photocatalyzed by rose bengal (**47**) and used air as an oxidant (Scheme 41). This allowed the synthesis of up to 33 unsymmetrical diaryl sulfides and aryl heteroaryl sulfides with electron-withdrawing as well as electron-donating substituents but did not tolerate proton-donating functional groups, e. g. alcohols and amines. In addition, the transformation was successfully extended towards selenides. The radical mechanism was proposed for the reaction: by stepwise oxidation of the arlylhydrazine, an arylradical is generated under evolution of gaseous N_2. Based on radical-trapping experiments it was proposed that the aryl radical reacts with the *in situ* generated aryl disulfide under formation of the desired diaryl sulfide and liberation of a thiyl radical.

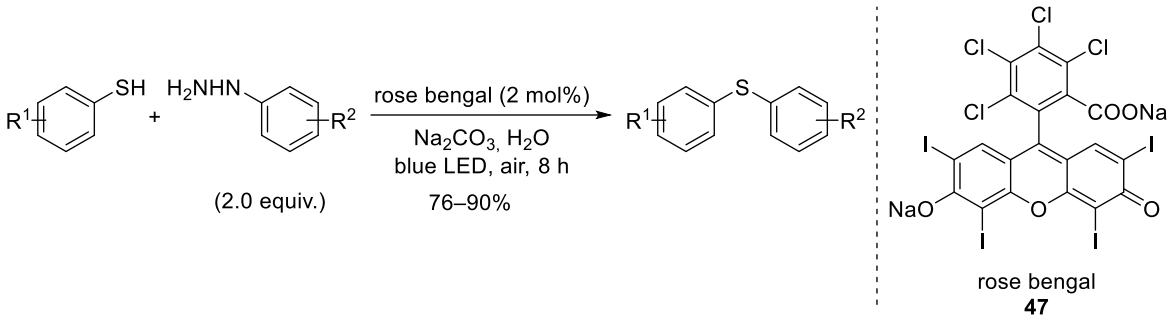

Scheme 41: Rose bengal (**47**)-catalyzed oxidative coupling of phenyl hydrazines and thiols in the synthesis of unsymmetrical diarylsulfides presented by A. Hajra *et al.*[194]

Recently, M. Miyake and coworkers designed a photo-catalyst-free protocol using simple aryl halides (X = I, Br, Cl) and thiols for the synthesis of unsymmetrical diarylsulfides (Scheme 42, **A**). Based on detailed DFT-studies the authors proposed a photoinduced intermolecular charge transfer process within the electron donor-acceptor (EDA) complex between the aryl halide and the thiolate (see Scheme 42 , **B**), followed by the radical combination of the aryl radical with the thiyl radical. This highly atom-economical reaction was scalable up to 50 mmol and allowed the late stage functionalization of pharmaceutically relevant compounds. Since the formation of a sufficient EDA complex with suitable geometry and energy of the HOMO of the thiolate and the LUMO of the aryl halide is crucial for the reaction to take place, neither arylheteroaryl sulfides, nor arylalkyl sulfides were accessible by this protocol.

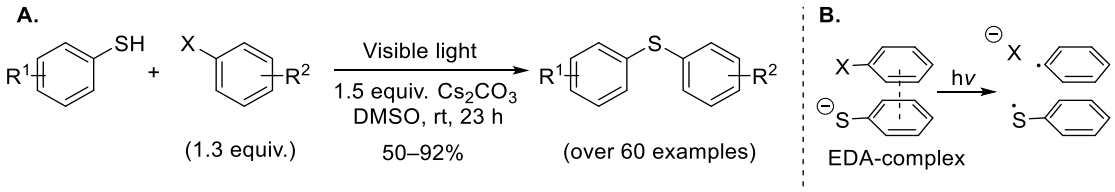

Scheme 42: Transition metal-free visible light-promoted synthesis of diarylsulfides presented by M. Miyake and coworkers.[195]

The utilization of visible light as an energy source is a fundamental improvement of previously reported protocols, which used UV radiation and liquid ammonia as a solvent for the formation of the radicals. Due to the high energy radiation, the applicability of this methodology was limited to rather simple diarylsulfides.[196]

Further applications of sulfur radicals in the area of organic chemistry have been recently reviewed by R. S. Glass.[197]

1.4.2.2 Nucleophilic sulfenylation reactions

As mentioned above (see Scheme 36), in a nucleophilic sulfenylation reaction, the sulfur in a sulfenylation reagent is formally negatively charged and reacts with a pre-functionalized electrophilic arene. Typical electrophiles for this purpose are, for example, aryl halides.

Alternatively, diaryliodonium salts can also be sulfenylated in this fashion by thiols or alkyl thioethers. As reported by M. S. Sanford *et al.*, several different diaryliodonium salts **48** form new sulfur-carbon bonds with alkyl/aryl thiols or alkyl thioethers (Scheme 43, **A**).[198] The authors proposed a mechanism based on the oxidative formation of sulfonium intermediate **49** (Scheme 43, **B**). Subsequently, the intermediate undergoes a nucleophilic substitution with residual trifluoroacetate, and the desired aryl thioethers is formed under release of trifluroacetic acid (**50**, R = H). The disadvantage of this protocol is the formation of stoichiometric amounts of aryl iodides as a by-product. Furthermore, in cases where alkyl thioethers (R = Me or Bu) are used as sulfur-containing precursors, the desired aryl thioether is formed along with trifluroacetate ester (R = Alkyl) as a side product.

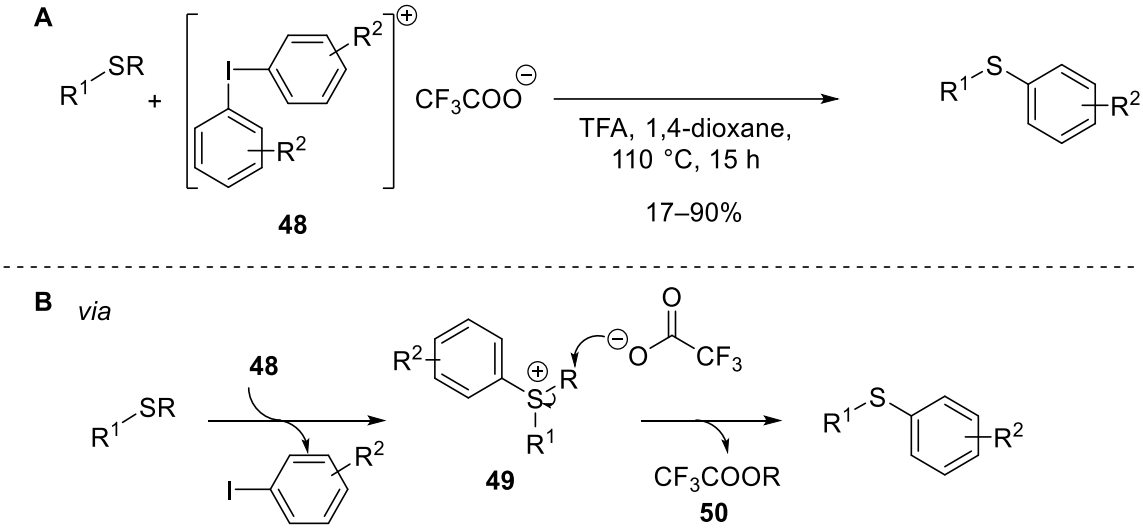

Scheme 43: **A**: Diaryliodonium salt-promoted formation of aryl sulfides reported by M. S. Sanford *et al.*; **B**: Proposed mechanism of the transformation.[198]

Electrophilic diaryliodonium salts can also be generated *in situ*, as presented by J. A. Campbell *et al*.[199] (Scheme 44). The authors activated electron-rich (hetero)arene substrates with phenyliodine(III) bis(trifluoroacetate) (PIFA) to generate a (hetero)diaryliodonium intermediate **51** which undergoes C–S bond formation with thiols in the same fashion as described by M. S. Sanford *et al.*[198]. The reaction shows a high functional group tolerance, however, required an excess of PIFA for the initial activation of the heteroarene and was limited to indoles.

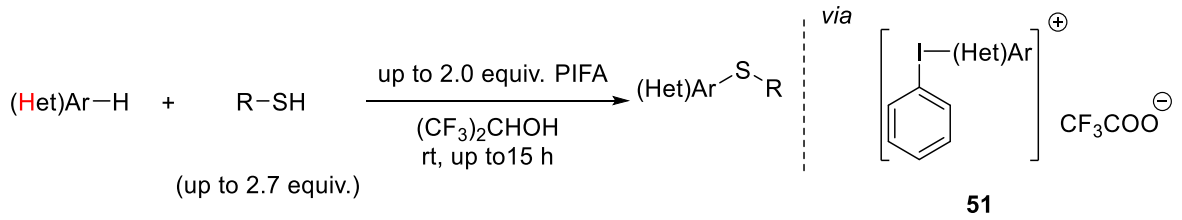

Scheme 44: Concept of the PIFA-mediated sulfenylation of electron-rich (hetero)arenes like indole derivatives.[199]

1.4.2.3 Electrophilic sulfenylation reactions

An efficient way to activate and functionalize electron-rich (hetero)arenes or carbanions is the usage of Lewis-acidic, electrophilic sulfenylation reagents. Such sulfur-based electrophilic reagents as **52** can be envisaged by attaching a strong electron-withdrawing group (EWG) onto the sulfur atom. This results in an inversion of its polarity (Figure 14).

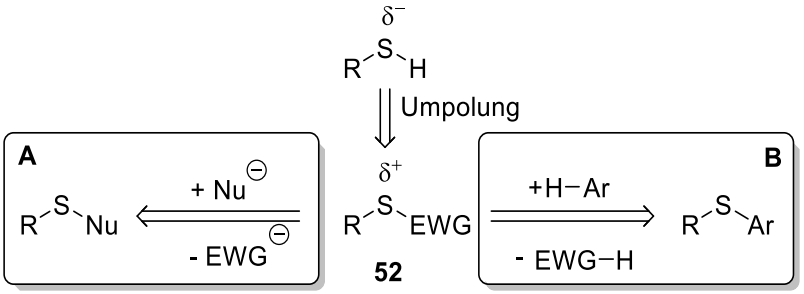

Figure 14: Concept of Umpolung to invert the electronic character of a thiol into an electrophilic sulfur reagent and the reaction with carbonucleophile (**A**) or an electron-rich arene (**B**).

As a result of the Umpolung, the sulfur reagent **52** can either react with strong carbon nucleophiles e.g. a Grignard reagent (Figure 14, pathway **A**) or undergo an electrophilic aromatic substitution reaction (S_EAr) with mainly electron-rich arenes to form a new carbon-sulfur bond (Figure 14, pathway **B**).

An example of the reaction of a carbon-nucleophiles with such an electrophilic sulfenylation reagent has been published by C.-F. Lee *et al.* (Scheme 45).[200] The transformation is based on the *in situ* generation of sulfenyl chloride **52** with EWG = Cl, which is formed in the reaction of the corresponding thiol with *N*-chlorosuccinimide (NCS). By subsequent reaction of **52** with a Grignard reagent a new carbon-sulfur bond is formed. The protocol gave access to a broad range of different aryl thioethers, but the functional group tolerance is limited due to the utilization of the highly reactive Grignard reagent at ambient temperature.

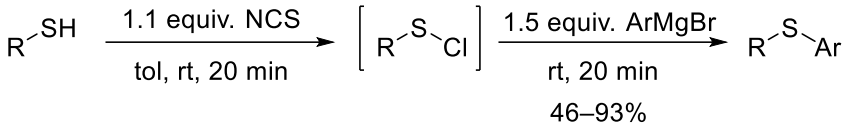

Scheme 45: One-pot synthesis of aryl sulfides by *in situ* formation of sulfenyl chloride its and subsequent reaction with a Grignard reagent, as presented by C.-F. Lee *et al*.[200]

Apart from sulfenyl chlorides (**52**, EWG = Cl), sulfenyl thiocyanates (**52**, EWG = CN) can also react in similar fashion with these strong carbon nucleophiles. For example, sulfenyl pyrroles have been synthesized in this way from 2-(thiocyanato)pyrrole derivatives and Grignard reagents, albeit in low yields.[201]

In this Subchapter further different electrophilic sulfur reagents for the electrophilic sulfenylation of (hetero)arenes will be discussed based on thenature of the sulfur-containing starting materials. Additionally, further versatile applications of these electrophilic sulfenylation reagents will be highlighted in selected examples.

N-(Alkyl/arylthio)succinimides

The succinimide group possesses suitable electron-withdrawing abilities for the Umpolung of thiols, as it was demonstrated by J. Cossy and coworkers (Scheme 46). The authors showed that *N*-(arylthio)- and *N*-(alkylthio)succinimides **53** can be used as sulfenylating reagents in the reaction with (hetero)arenes. By addition of an excess of trifluoroacetic acid (TFA) to *N*-thiosuccinimides it was possible to convert several arenes[202] and indole derivatives[203] into the corresponding unsymmetrical thioethers. Due to the strong acidic conditions the functional group tolerance of this protocol was limited. Additionally, a general drawback of this methodology is that each *N*-(alkyl/arylthio)succinimide has to be synthesized separately from the corresponding thiol, sulfuryl chloride and succinimide.

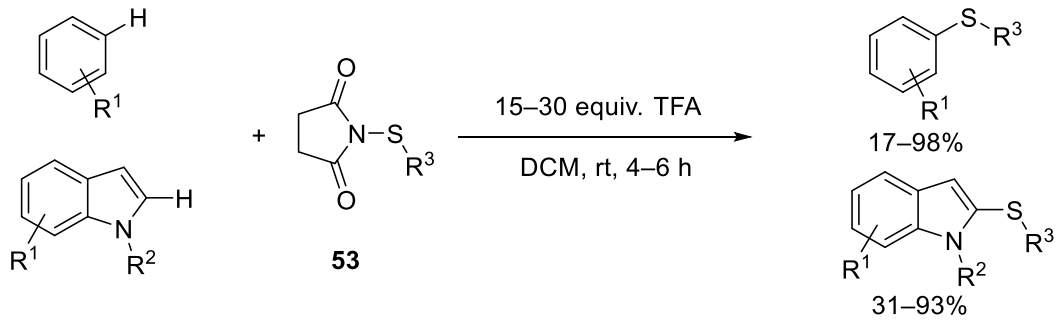

Scheme 46: Synthesis of unsymmetrical thioethers with *N*-(arylthio)- and *N*-(alkylthio)succinimides from corresponding arenes[202] and indoles.[203]

Further studies on *N*-(arylthio)succinimides-based systems were conducted by J. L. Gustafson *et al.*[204] who could further improve the protocol by lowering the TFA loading to 10 mol% and using bis(*p*-methoxyphenyl) selenide (**54**) as an organocatalyst (Scheme 47). The authors proposed that the reaction reported by *J. Cossy* and coworkers proceeds by an autocatalytic mechanism whereby already formed thioethers **55** aggregated with residual protonated *N*-(arylthio)succinimides. The obtained activated species **56** can easily react with arene substrates to give an additional molecule of the desired product **55**. The formation of **56** is very slow and gives low yields in cases where the *N*-(arylthio)succinimides features an electron-poor arene R^1.

In those cases (e.g. R^1 = *p*-phenylazide), the addition of organocatalyst **54** can increase the yield of the desired unsymmetrically substituted thioethers by a factor up to 11, since the reaction pathway via intermediate **57** is favored. Due to the utilization of **54** J. L. Gustafson *et al.* could use an equimolar amount of TFA or 10 mol% of TfOH which makes the reaction more atom-economical compared to previous reaction conditions. Additionally, the authors expanded the scope of their elaborated protocol by using *N*-(trifluoromethylthio)saccharine to enable access to different trifluoromethylthiolated products.

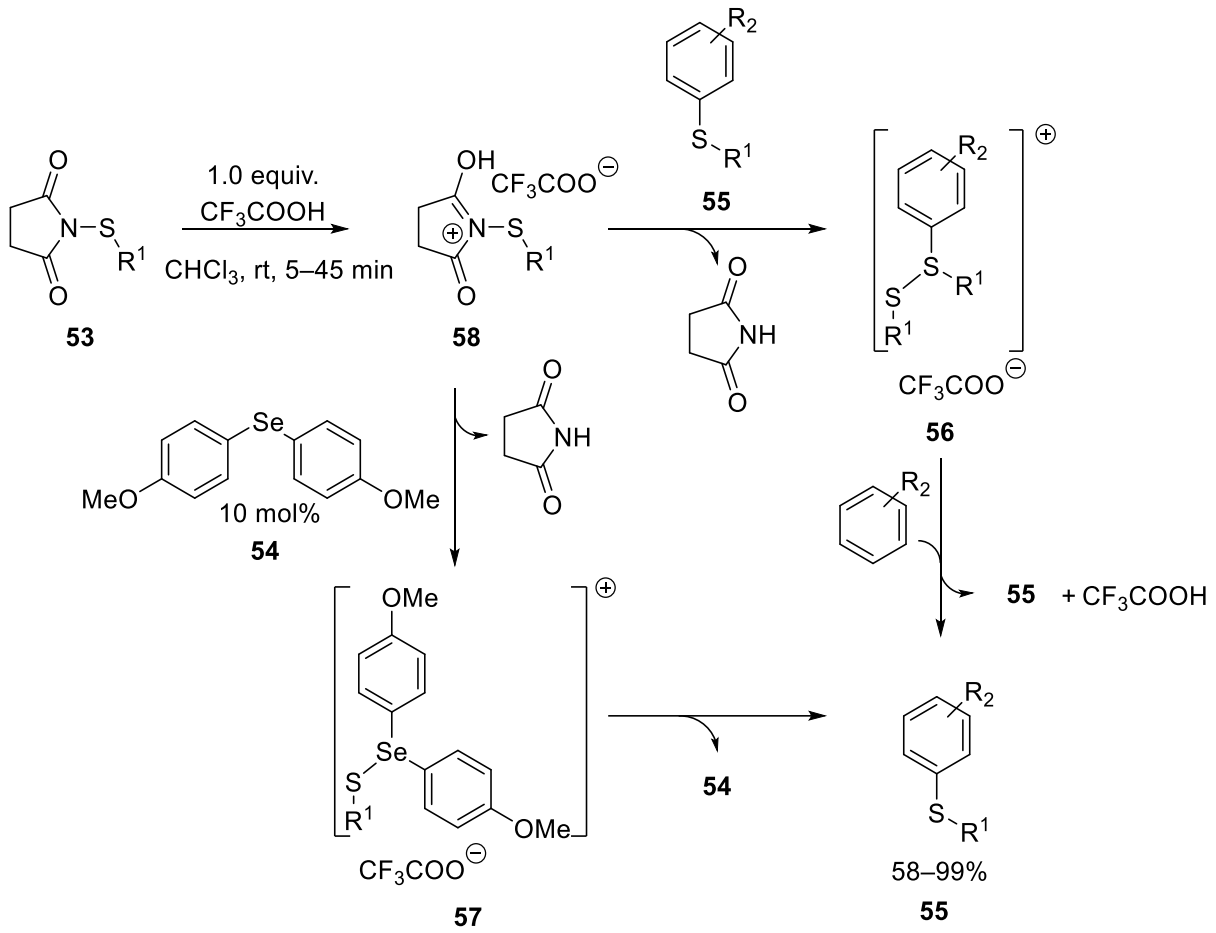

Scheme 47: Mechanistical and catalytical studies on the *N*-(arylthio)succinimides-based sulfenilation with additional improvements of the protocol by using organocatalyst **54**.[204]

Apart from selenide **54,** J. L. Gustafson *et al.* showed that conjugate thiourea-based Lewis base-Brønsted acid catalysts **59** can facilitate the activation of *N*-(arylthio)succinimides for the sulfenylation of indole and pyrrole derivatives (Scheme 48).[205] Due to the high molecular weight and complicated synthesis of the thiourea the employment of this methodology on industrial scale is debatable.

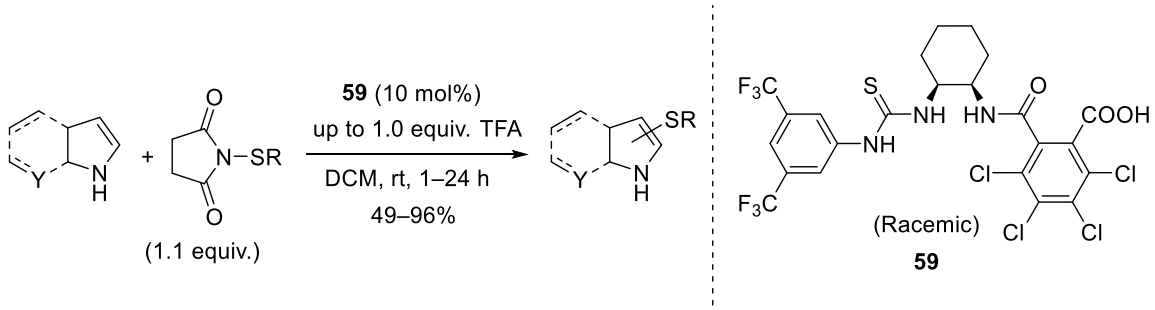

Scheme 48: Application of thiourea **59** as a catalyst for the formation of unsymmetrical thioethers in the alternative protocol of J. L. Gustafson *et al.*.[205]

Furthermore, catalyst- and acid-free protocols avoiding contaminations from transition metals have been reported by H. Fu *et al.* for the arylthiolation of aniline derivatives with *N*-(arylthio)succinimides.[206] However, this reaction demands more harsh reaction conditions such as elevated temperature (100 °C) and longer reaction times (up to 30 h). This results in the formation of diarylthiolated side-products

N-(alkyl/arylthio)phthalimides

Besides *N*-(arylthio)- and *N*-(alkylthio)succinimides, the corresponding phthalimides can react in a similar fashion with electron-rich arenes and heteroarenes.

As reported by A. Thompson *et al.*, several pyrroles can be transformed into their 2-sulfenyl derivatives by reaction with different thiophthalimide reagents **60** (Scheme 49; R^2 = alkyl, aryl).[207] The authors demonstrated that (semi)catalytic amounts of a Lewis acid like $MgBr_2$ are crucial for the selective formation of the desired C-S bond in an electrophilic aromatic substitution reaction.

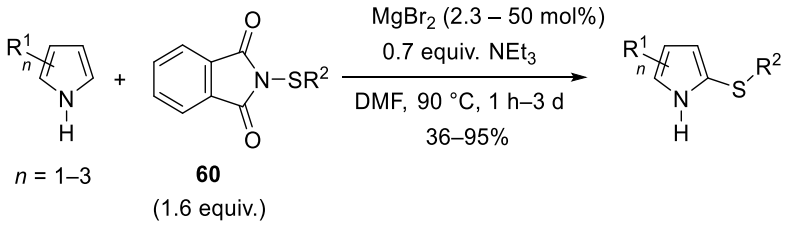

Scheme 49: Reaction of pyrroles with *N*-(alkyl/aryl)succinimides presented by A. Thompson *et al.* [207]

Apart from $MgBr_2$ other Lewis acids like $AlCl_3$[208], $TiCl_4$[208] , BF_3•Et_2O[209], $CeCl_3$ 7•H_2O[210] or anhydrous $CeCl_3$[211] have been reported to catalyze the formation of unsymmetrical diarylsulfides from *N*-(alkyl/arylthio)succinimides or -phthalimides and (hetero)arenes.

In 2015, F. Glorius and coworkers extended the phthalimide-based protocol towards the synthesis of trifluoromethylthioethers of pyrroles, indoles and further electron-rich *N*-hetero-arenes (Scheme 50).[212] Additionally, the methodology allows the late-stage functionalization of pharmaceutically relevant compounds.

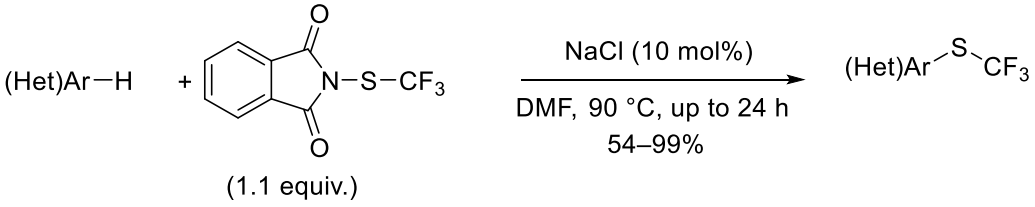

Scheme 50: Extension of phthalimide-based protocol to trifluoromethylthiolation of (hetero)arenes, as presented by F. Glorius and coworkers.[212]

In the same year, L. Lu, Q. Shen *et al.* reported a similar phthalimide-based reagent for difluorothiomethylation reactions. Its reaction with electron-rich (hetero)arenes proceeded at 80–120 °C in DCE and required addition of overstoichiometric amounts of trimethylsilyl chloride, affording a variety of difluorothiomethylated compounds.[213]

The conspicuous electrophilicity of *N*-(arylthio)succinimides and -phthalimides can also be used for the activation of alkenes in the process of aryl thioether formation. S. E. Denmark and coworkers reported an enantioselective sulfenocyclization of polyenes (Scheme 51).[214] The transformation proceeded with participation of selenocatalyst **61** and was extendable to geranylphenoles. The highest diasteriomeric ratio of up to 93:7 was obtained in hexafluoroisopropyl alcohol (HFIP) as a solvent. Additionally, the enantioselective syntheses of (+)-ferruginol (**62**) and (+)-hinokiol (**63**) along this path showed the value of the presented methodology.

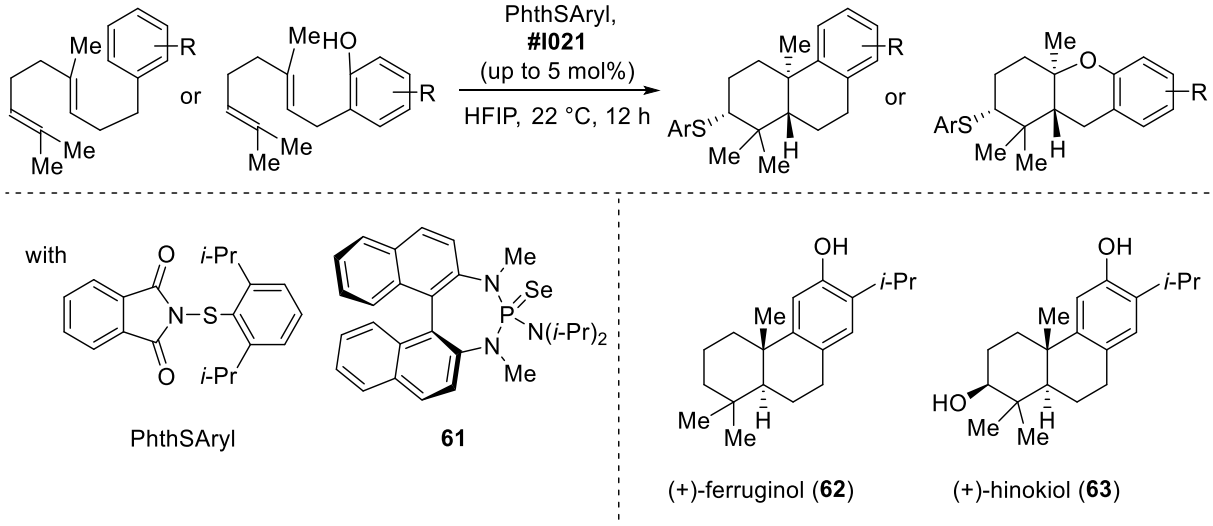

Scheme 51: Enantioselective sulfenocyclization with *N*-(arylthio)phthalimide (PhthSAryl) employing selenocatalyst **61**.[214]

Furthermore, *N*-(arylthio)succinimides and alcohols can be used for the oxysulfenylation of alkenes like styrenes. H. Fu *et al.* reported on the selective functionalization of activated and deactivated styrene derivatives (Scheme 52). The authors proposed the participation of carbocation intermediate **64**, which can further react with an alcohol.[215]

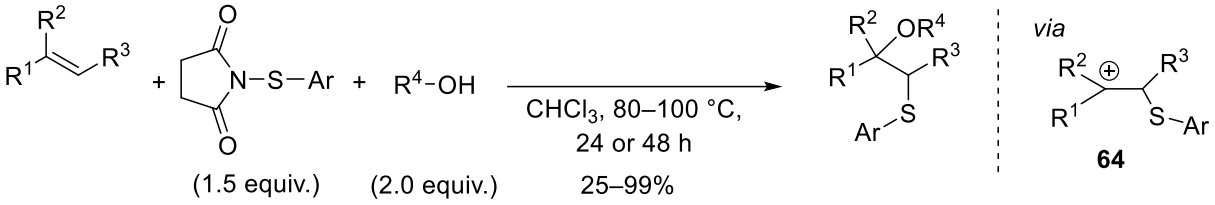

Scheme 52: Oxysulfenylation of alkenes by *N*-(arylthio)succinimides in the presence of an alcohol, as reported by H. Fu *et al.*[215]

In situ generation of sulfenyl chlorides and iodides from thiols

Apart from thiosuccinimides and thiophthalimides, also sulfenyl halides can be used for the sulfenylation of arenes following an electrophilic aromatic substitution (S_EAr) pathway due to the high electronegativity of halides, as mentioned in the beginning of the Chapter. In many cases the sulfenyl halides are generated *in situ* because of their high reactivity and instability.

An example of the *in situ* formation of sulfenyl chloride was published by K. M. Schlosser *et al.* (Scheme 53).[216] In the protocol they presented, the activation of the thiol was achieved by *N*-chlorosuccinimide (NCS). The obtained sulfenyl chloride (**65**) reacted under mild conditions with a wide range of indoles tolerating several other functionalities. The methodology was further expanded by S. Adimurthy and coworkers towards the regioselective sulfenylation of imidazoheterocycles at room temperature.[217]

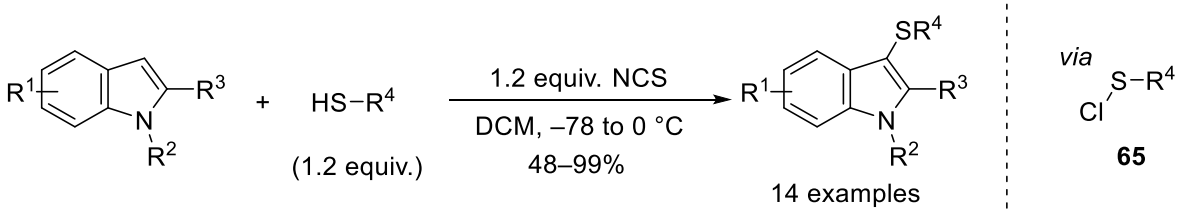

Scheme 53: Procedure for the 3-sulfenylation of indole elaborated by K. M. Schlosser *et al.*[216]

One of the major disadvantages of the utilization of sulfenyl chlorides is their uncontrolled reactivity. Sulfenyl chlorides are known to undergo multifold addition reactions with electron-rich heteroarenes. The mechanism of the twofold sulfenylation of indoles was studied in detail by R. Hamel.[218]

In contrast to this, *in situ* generated aryl sulfenyl iodides can overcome these limitations, as they exhibit much milder reaction behavior. As reported by R. K. Peddinti *et al.,*[219] the dehydrogenative coupling of *in situ* generated from thiols sulfenyl iodides with electron-rich arenes like aniline, methoxy- or hydroxyl-substituted arenes as well as hydroxylcoumarines gives only the desired monothiolated products (Scheme 54).[219] The authors proposed a catalytic cycle, in which the formed hydroiodic acid is oxidized by DMSO to regenerate iodine with the release of water and dimethylsulfide.

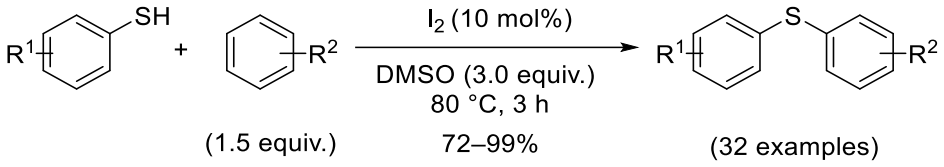

Scheme 54: Iodine-catalyzed cross-coupling of thiols with electron-rich arenes presented by R. K. Peddinti *et al.*[219]

In situ generation of sulfenyl iodides from diarylsulfides

Very similar, but disulfide-based iodine-catalyzed sulfenylations of indoles via *in situ* generation of sulfenyl iodides and utilizing DMSO as a co-oxidant are described in the literature.[220][221] Although the latter protocol, reported by the group of A. L. Braga, allowed the sulfenylation of indole derivatives, it revealed poor functional group tolerance, essentially limited to methoxy- and bromoindoles (Scheme 55, **A**).[221] Again, in the proposed mechanism DMSO oxidizes the *in situ* generated hydroiodic acid to iodine (Scheme 55, **B**).

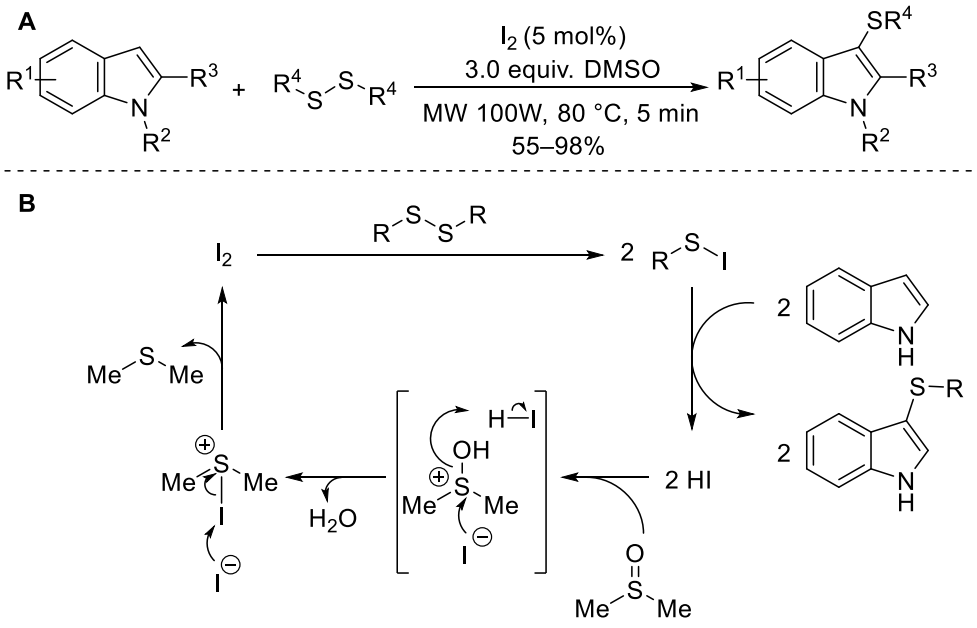

Scheme 55: **A**: 3-Sulfenylation of indole derivatives as presented by L. Braga and coworkers; **B**: proposed mechanism.[221]

Apart from the presented electrophilic sulfenylation pathways based on sulfenyl iodide, diaryldisulfides can also react with electron-rich hetero arenes to give access to various aryl sulfides. In this case iodate is the catalyst of choice, as reported by A. L. Braga and coworkers in a consecutive publication (Scheme 56, **A**).[222] The authors proposed the initial activation of heteroarene by the iodate anion furnishing intermediate **66** followed by intramolecular proton transfer and release of a hydroxide anion (Scheme 56, **B**). Subsequently, the nucleophilic attack on the disulfide liberates an aryl thiolate and leads to the formation of the desired C–S bond in the intermediate **67**. Nucleophilic attack of hydroxide on the latter regenerates the iodate anion.

The generated thiolate is oxidized by air to give disulfide RSSR which then can react again as discussed above. The methodology was furthermore extended to diaryldiselenides giving access to electron-rich seleno-ethers.

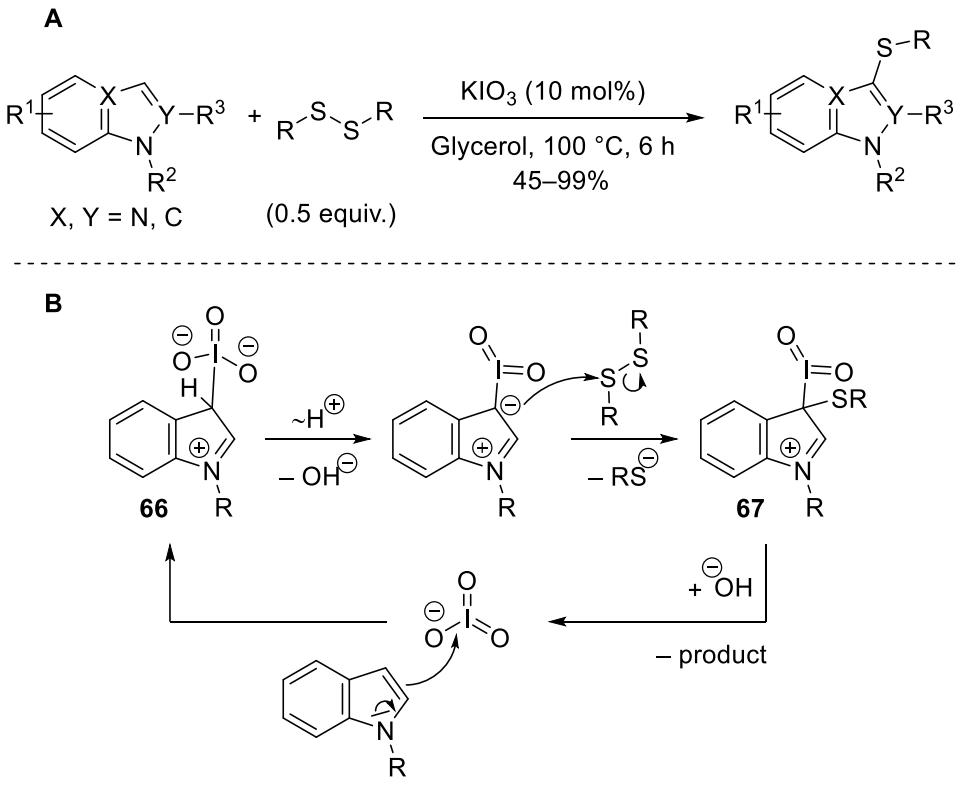

Scheme 56: Direct C-H sulfenylation of indoles and imidazo-pyridines with disulfide in an iodate-catalyzed fashion as presented by A. L. Braga and coworkers.[222]

In several previously published protocols, the same reaction was carried out with electron-rich (hetero)arenes applying one equivalent of disulfide and additional base at elevated temperature under an inert atmosphere (Scheme 57).[223,224] The drawback of this historical approach was the non atom-economical formation of equimolar amounts of aryl thiolate as a by-product.

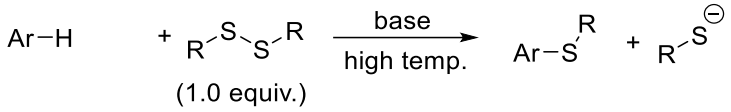

Scheme 57: General concept of former disulfide-based sulfenylation resulting in the release of equimolar amounts of thiolate as side-product.[223,224]

In situ generation of sulfenyl chlorides from arylsulfonyl chlorides

Apart from the already discussed approaches, sulfenyl chlorides can be generated *in situ* by reduction of arylsulfonyl chlorides with triphenylphosphine. This methodology allows the synthesis of di(hetero)aryl sulfides from electron-rich (hetero)arenes as indolizines, indoles and trimethoxybenzene (Scheme 58). Results of J. You *et al.* demonstrated that triphenylphosphine is superior to other reducing agents like TMSCl or $P(OEt)_3$, as it led to the highest yields of the arylsulfide.[225] This protocol based on previous work by K. B Sharpless and coworker who showed, that more expensive trimethyl phosphite $(MeO)_3P$ can be used for the reduction of sulfonyl chlorides as well.[226]

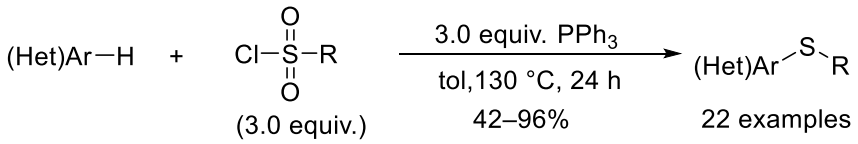

Scheme 58: Synthesis of diarylsulfides from arylsulfonyl chlorides via *in situ* reduction of the latter with PPh_3, as presented by J. You *et al.*[225]

On the other hand, the work of J. You *et al.* was inspired also by the studies of M. Raban *et al.* who performed detailed investigations on the reactions of arenesulfenyl chlorides with phosphines already in the early 1980.[227]

Furthermore, A. T. Radosevich *et al.* designed a protocol for organophosphorus-catalyzed deoxygenation of sulfonyl chlorides which uses phenylsilane as a reducing agent (Scheme 59).[228] Mechanistic investigations indicate that the phosphacyclic catalyst **68** is involved in the reaction of the *in situ* generated sulfenyl chloride with the electron-rich heteroarenes. The catalytic desoxygenative O-atom transfer resulted in the formation of the reactive sulfenyl

chloride. Unfortunately, the scope of this reaction was limited to indoles. Notwithstanding, the authors demonstrated that the methodology also enables the trifluoromethylthiolation, perfluoroalkylthiolation and alkylthiolation of indoles.

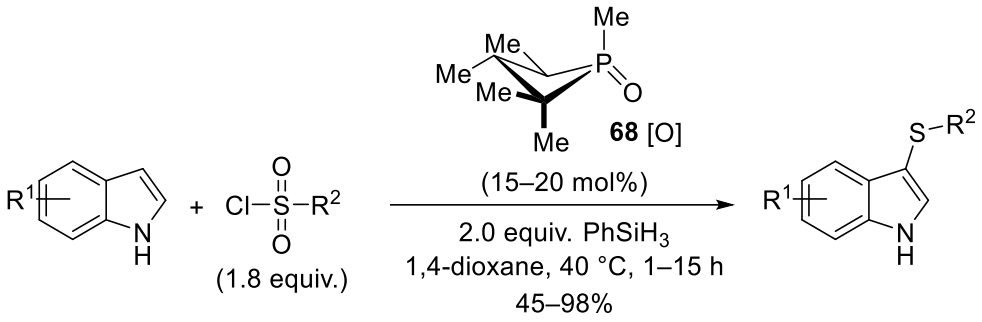

Scheme 59: Organocatalytic sulfenylation of indole derivatives using sulfonyl chlorides as sulfur-containing precursor and phenylsilane as reductant.[228]

In situ generation of sulfenyl iodides from sulfonyl hydrazines

Several transition metal-free C-H thioarylations using sulfonyl hydrazines have been recently published. The majority of the reported procedures used iodine as a catalyst to generate the reactive species. Interestingly, S.-K. Tian *et al.* postulated the participation of intermediates **69** and generated from this sulfenyl iodide **70**: the both can react with such electron-rich heteroarenes as indole derivatives (Scheme 60).[229] In contrast, R. Yan, G. Huang and coworkers presented a mechanism mainly based on sulfenyl iodide **70** as a sole reactive species (Scheme 60).[230] In both protocols harsh conditions (THF, 100 °C[230] or EtOH, 70 °C[229]) were required to transform indole derivatives[229,231] or naphthols/naphthylamines[230] into the desired thioethers. Additionally, these reactions were limited to a very narrow substrate scope but gave the desired products in good to excellent yields. On the other hand, electron-poor sulfonyl hydrazines could not be utilized, and the envisaged products were obtained only as traces.

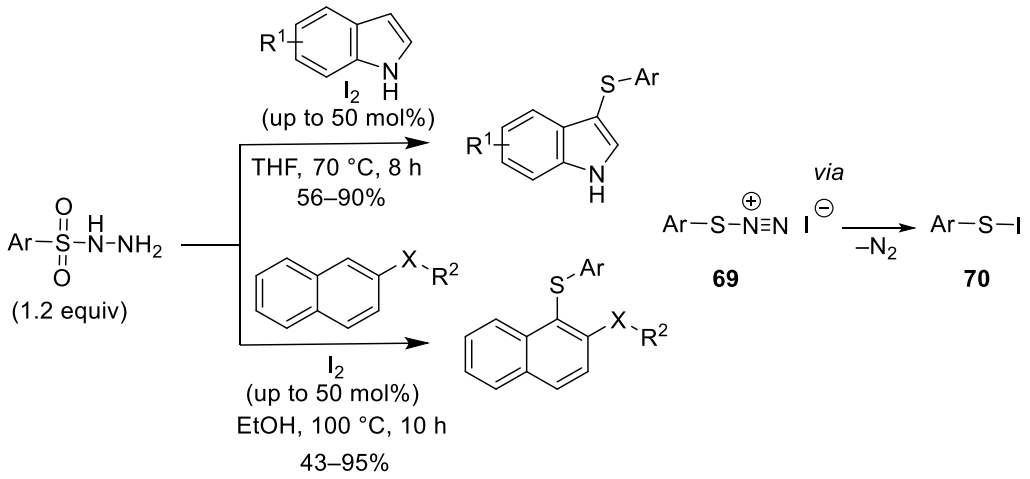

Scheme 60: Iodine-catalyzed sulfenylation of indole derivatives[229] and naphthols/naphthylamines[230] (X = O, NH) using sulfonyl hydrazine as a precursor.

The scope of arenes was further extended to benzo[*b*]furanes by X. Zhao, K. Lu and coworkers.[232] In their protocol, heating in 1,4-dioxane at 120 °C was necessary for the conversion of different furane derivatives into the corresponding thioethers.

Sulfenyl iodides **70** are also capable to activate alkenes and alkynes. This was shown by S.-K. Tian *et al.* who presented the oxysulfenylation of alkenes with sulfenyl hydrazine in the presence of catalytical amounts of iodine (Scheme 61).[233] The authors postulated nucleophilic ring opening of the thiiranium intermediate **71** with the participating alcohol as a key mechanistic step. This reaction gave access to several β-alkoxy aryl/alkyl sulfides starting from alkyl or aryl sulfenyl hydrazines.

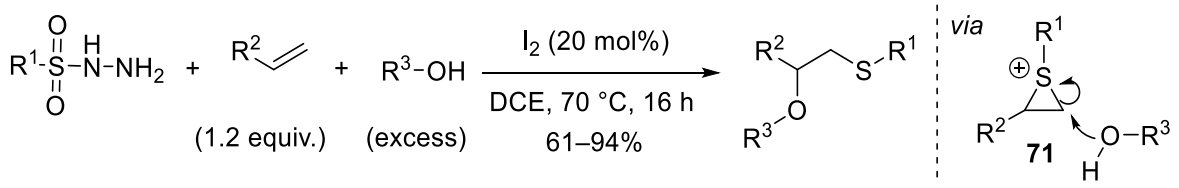

Scheme 61: Three-component oxysulfenylation reaction of alkenes presented by S.-K. Tian *et al.*[233]

Furthermore, X. Zhao, K. Lu *et al.* activated the alkyne moieties upon electrophilic cyclization of 2-alkynylphenol derivatives with *in situ* generated thiodiazonium iodide **69**.[232] The formation of the latter was also catalyzed with iodine. *para*-Toluenesulfonic acid (PTSA) was added to

obtain the desired 3-arylthio benzo[*b*]furans in moderate to good yield, and the reaction did not require inert conditions.

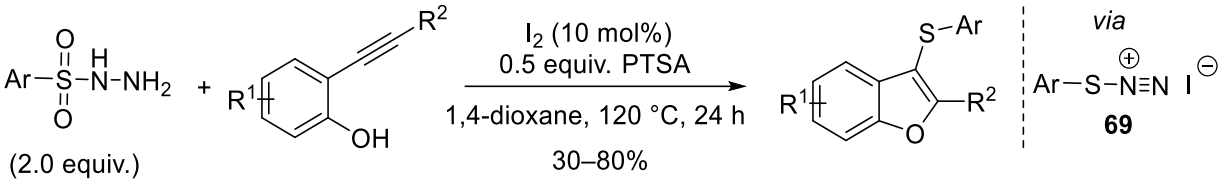

Scheme 62: Oxysulfenylation of akynes with an internal alcohol and sulfenyl hydrazine as a sulfur precursor presented by X. Zhao, K. Lu *et al.*[232]

<u>*In situ* generation of sulfenyl iodides from S-arylthiosulfates:</u>

An alternative sulfur sources for the iodine-catalyzed synthesis of 3-thioindoles are S-arylthiosulfates (Bunte salts). Bunte salts are commercially available and easy to handle. The protocol of T. Zhang, M. Luo *et al.* utilizes a catalytic amount of iodine for the *in situ* generation of sulfenyl iodides **70** which react with certain indole derivatives (Scheme 63).[234] The authors used DMSO as a solvent and also as an oxidizing agent for iodine regeneration the catalytic cycle.

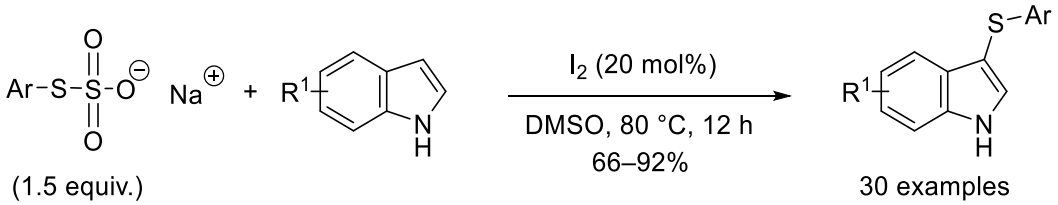

Scheme 63: Bunte salts as a sulfur source for the C3-sulfenylation of indole derivatives, as presented by T. Zhang, M. Luo *et al.*[234]

In situ generation of sulfenyl iodides from sulfinates

Under catalysis with iodine, sulfenyl iodides **70** can also be generated *in situ* from sulfinates, which are easy-to-handle salts. As presented by G.-J. Deng *et al.* (Scheme 64, **A**), upon treatment with the sulfinate/I_2/DMSO system indoles were converted into the corresponding 3-sulfenylated derivatives in 39–93% yield.[235] Diethyl phosphite was used as an additive in the initial step to generate diaryl disulfide, which then was converted with elemental iodine to form the reactive sulfenyl iodide. The subsequent reaction with indoles resulted in the formation of the desired sulfides. Due to the iodine-mediated *in situ* formation of sulfenyl iodide, the process resulted in selective monosulfenylation, whereas control experiments with disulfide as a starting material lead to the formation of twice sulfenylated by-products. Based on their initial observations, in the subsequent publication F. Xiao, Y. Liu, G.-J. Deng *et al.* described the chemoselective cross-coupling of thus generated sulfenyl iodides **70** with different phenols for the synthesis of alkylaryl sulfides and diaryl sulfides in water (Scheme 64, **B**).[236] In the case of electron-rich aryl sulfinates the products were obtained in lower yields. As for the reactions discussed above, the authors proposed a mechanism involving sulfenyl iodide **70** as the reactive intermediate.

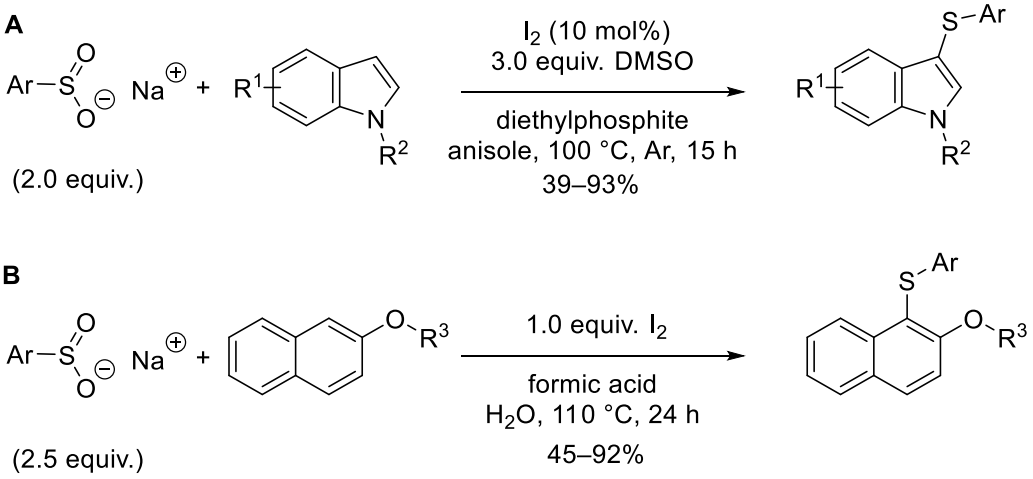

Scheme 64: Sulfenylation of indoles[235] (**A**) and of phenol derivatives[236] (**B**) using sulfinate salts as sulfur-containing precursors and iodine at elevated temperatures.

Furthermore, iodine/triphenylphosphine-mediated protocol for the sulfenylation of indols[237] as well as method in which the sulfinate salts were replaced with free sulfinic acid[238] have been published.

Quinone O,S-monoacetals

The unusual sulfenylation reagent **72**, bearing a highly active quinone O,S-monoacetal moiety, was presented by Y. Kita *et al.* (Scheme 65).[239] In their communication, **72** was activated by TMSOTf and caused sulfenylation of different electron-rich arenes and heteroarenes like indols, dimethoxybenzene derivatives and 2-methoxynaphtalene as well as thiophenes and furans. As the methodology was limited to the transfer of pentafluorophenylthio groups, only corresponding thioethers were accessible. The authors suggested that the driving force of the reaction was the aromatization of the quinone.

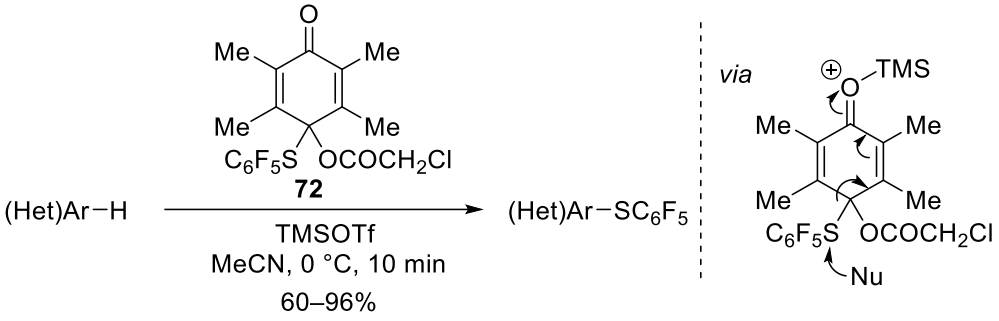

Scheme 65: Quinone-based sulfenylation reagent presented by Y. Kita *et al.*[239]

In situ generation of sulfonium salts from sulfoxides

As reviewed by V. G. Nenaidenko *et al*.[240,241] and recently by M. Alcarazo *et al.,*[240,241] sulfonium salts are a valuable compound class with several new synthetic capabilities, which can be utilized as electrophilic sulfenation reagents. In 2016, D. J. Procter and coworkers reported the first protocol for the synthesis of electrophilic sulfenylation reagents starting from sulfoxides (Scheme 66).[242] Hereby, the direct C–H thioarylation of unfunctionalized arenes was achieved by activation of arylsulfoxide **73** with trifluoromethanesulfonic anhydride (Tf_2O) to form the electrophilic sulfur species **74** which reacts with different arenes. The scope of the reaction included electron neutral benzene derivatives such as toluene as well as several hetero arenes. Due to the activation of the sulfoxide by Tf_2O, protic functional groups like alcohols, thiols and primary amines were not tolerated by the protocol.

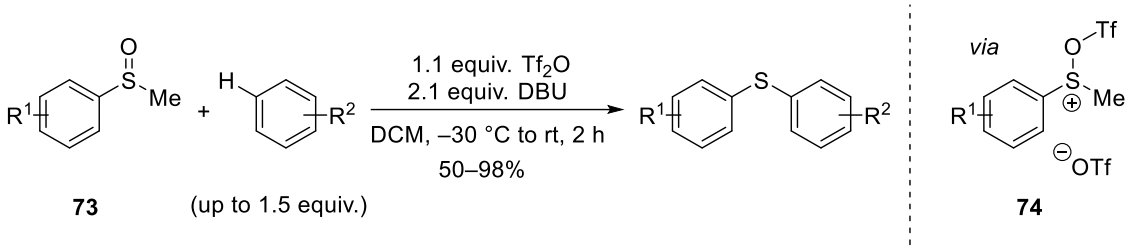

Scheme 66: Sulfonium triflate **74**-based protocol for the synthesis of diarylsulfides from aryl sulfoxides and arenes without any further pre-functionalization.[242]

A similar reagent was recently used by H. Du, J. Xu, P. Li *et al.* for the electrophilic cyclization of aryl substituted internal alkynes (Scheme 67, **A**).[243] Similar to the protocol of D. J. Procter and coworkers,[242] H. Du, J. Xu, P. Li *et al.* used a nitrogen base for the nucleophilic substitution in intermediate **75** which resulted in release of the final sulfide (Scheme 67, **B**).

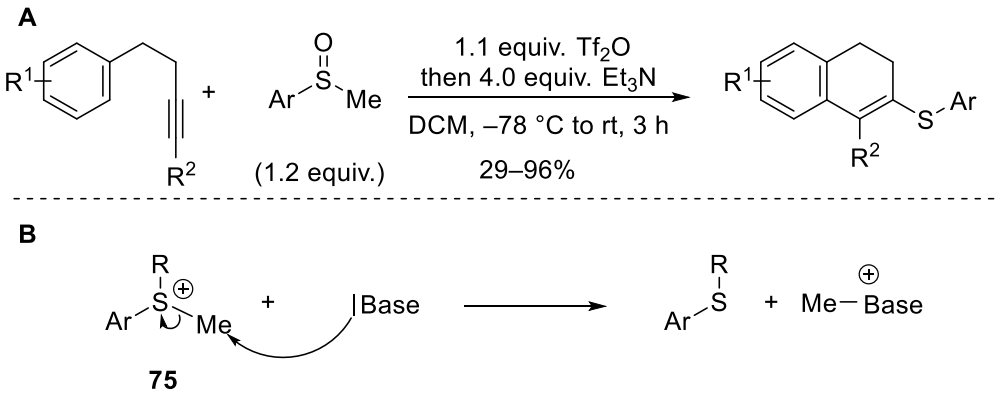

Scheme 67: **A**: Electrophilic cyclization initialized by *in situ* generated sulfonium triflates presented by H. Du, J. Xu, P. Li *et al.*[243]; **B**: Base-promoted release of the aryl sulfide.

2 Design of the project

2.1 State of the art

2.1.1 Thioimidazolium reagents from the Alcarazo group

As recently published by M. Alcarazo and coworkers, imidazoline-2-thione derivatives are a powerful platform for the synthesis of new electrophilic group-transfer reagents. In 2015, M. Alcarazo, G. Talavera *et al.* reported the synthesis and application of imidazolium based reagents **76** and **77** for the electrophilic cyanation and alkynylation of several nucleophiles (Scheme 68).[244] The transfer of the $[CN]^+$ to unfunctionalized (hetero)arenes was catalyzed by substoichiometric amounts of $BF_3{\cdot}Et_2O$. In case of S-, C- or N-centered nucleophiles equimolar amounts of Hünig base were required. The alkynylation of thiols or carbanions with a $[C{\equiv}CR]^+$ synthon derived from reagent **77** illustrated the high potential of imidazolium sulfuranes for the Umpolung of functional groups. Additional work by M. Alcarazo, A. Barrado *et al.* reported on the chlorocyanation of alkynes with **76** in the presence of BCl_3.[245]

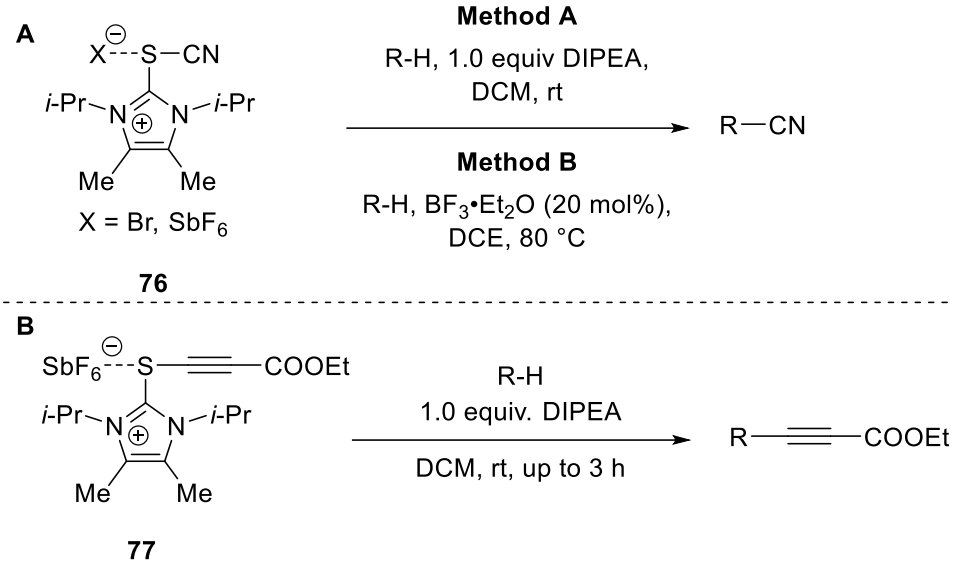

Scheme 68: Electrophilic cyanation (**A**) and alkynylation (**B**) utilizing imidazolium based reagent **76** and **77** as presented by M. Alcarazo *et al.*[244]

In a subsequent publication, M. Alcarazo and coworkers presented a series of distinct alkynylthioimidazolium salts **80** which can be utilized for the electrophilic thioalkynylation of C-centered nucleophiles. The synthesis of this versatile reagents follows a two-step protocol. After initial bromination of imidazoline-2-thione **78** with elemental bromine, one bromide atom of the obtained dibromo(imidazolium)sulfurane **79** is substituted by an alkynyl residue upon treatment with organozincates (Scheme 69, **A**).[246] The authors reported that the well characterized salts **80** allow an easy access to dialkynyl sulfides and aryl alkynyl sulfides as well as alkyl alkynyl sulfides by reaction with Grignard reagents. During the electrophilic attack of the latter on the thioalkynyl moiety of the reagent, an imidazole carbene **81** is released as a leaving group and a formal RS^+ synthon is transferred (Scheme 69, **B**). Additionally, Alcarazo *et al*. were able to extend the protocol towards alkynyl seleno ethers.

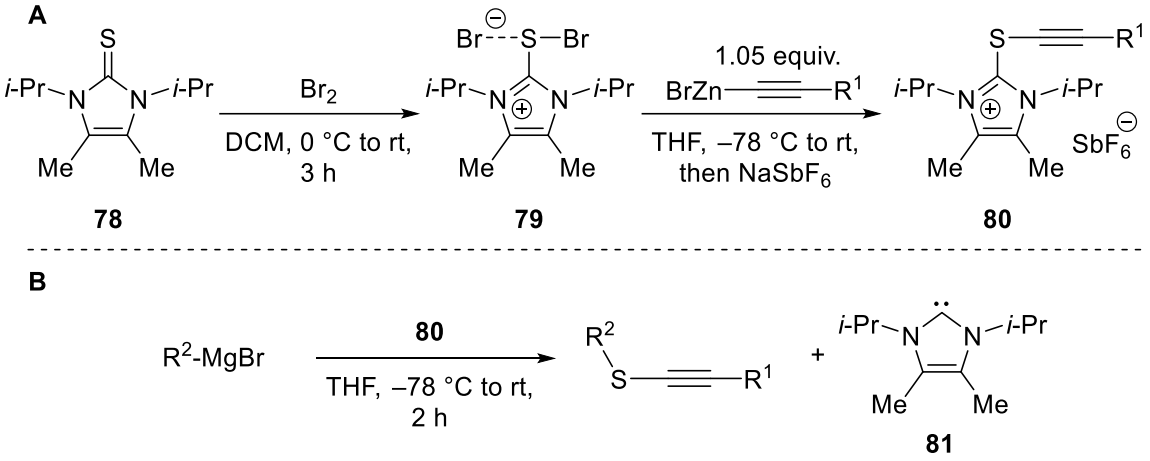

Scheme 69: Electrophilic thioalkynylation of Grignard reagents with alkynylthioimidazolium salts recently presented by M. Alcarazo, J. Peňa *et al*.[246]; **A**: Synthesis of thioalkynylation reagent **80**; **B**: Thiosulfenylation of C-centered nucleophiles.

2.1.2 Thiourea derivatives as sulfur-containing precursors

As recently reported by the group of W. Yi *et al.*, the C–H activation of electron-rich (hetero)arenes by iodinated thiourea is a useful methodology for the formation of carbon-sulfur bonds in difluoromethylthiolation reactions.[247] The cationic sulfides **82** obtained from thiourea or imidazolium analogues can undergo hydrolysis or aminolysis upon heating with a base (e. g. $NaOH/H_2O$, 90 °C; K_2CO_3/H_2O, 80 °C or Na_2CO_3/wet PEG 200, 120 °C) to afford the corresponding (hetero)aryl thiolates (Scheme 70).[248,249]

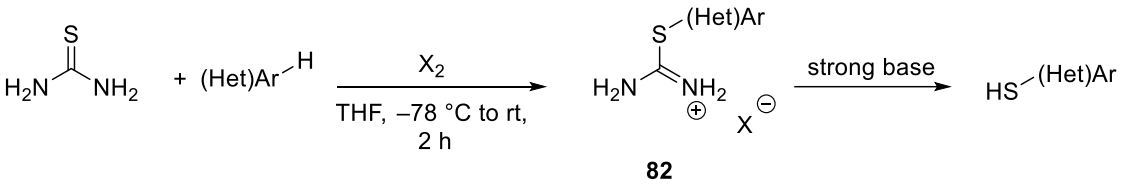

Scheme 70: Thiolation of electron-rich (hetero)arenes with TMTU as sulfur-containing precursor

Surprisingly, no study on the corresponding initial C–H activation of (hetero)arenes with halogenated imidazole-2-thiones has been reported to date, even if the electronic structure of those (dihalo)imidazothions has been already discussed in detail in the literature.[250] The only published methodologies for the synthesis of analogous to **82** arylthioimidazolium salts **83** are based on the alkylation of imidazole thioethers by strong alkylation reagents like alkyl iodides,[248,251] by reaction of a imidazole carbene with a diaryldisulfide[252] or by treatment of 2-chlorimidazolium salts with thiolates (Scheme 71).[253] However, compounds **83** were never used for the synthesis of unsymmetrical thioethers.

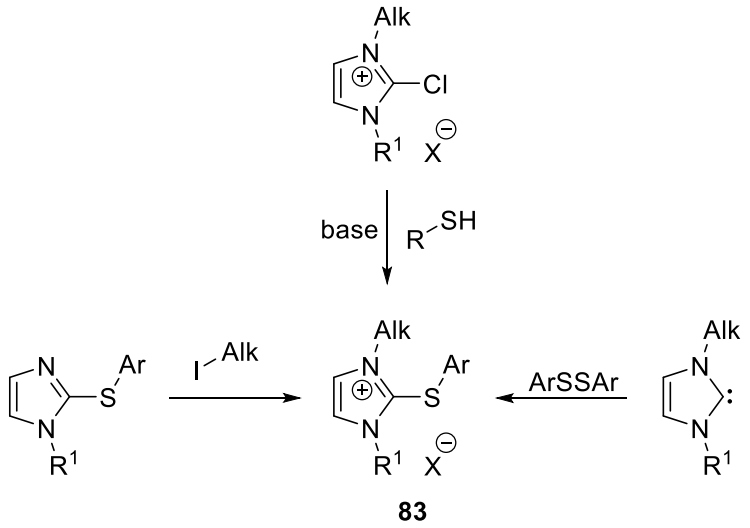

Scheme 71: Known protocols for the synthesis of arylthioimidazolium salts **83**.

2.2 Project aim

The aim of the project is the development of a modular and transition metal-free protocol for the straightforward synthesis of un-symmetrical aryl sulfides based on the reaction of two nucleophiles a sulfur-containing reagent (Scheme 72). These reagents can then be considered as a $[S]^{2+}$ synthetic equivalents. This is of special interest, because nearly all previously reported C–H sulfenylation procedures require the synthesis of a new reagent for each electrophilic $[R–S]^{+}$ transfer starting from a reactant already containing sulfur. Additionally, with most of the reported sulfenylation strategies only aryl sulfides of electron-rich arenes were accessible. Therefore, the development of a $[S^{2+}]$ synthon fills the gap in the toolbox of organic chemists.[254]

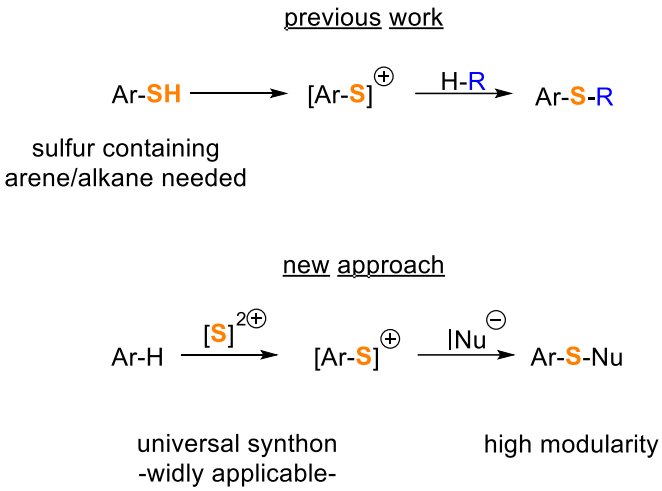

Scheme 72: New approach for the synthesis of aryl sulfides.

The first part of the project will focus on the synthesis towards an electrophilic S^{2+}-containing sulfur reagent which can activate arenes and heteroarenes. Hereby the electrophilic character of the sulfur will be targeted by attaching a strong electron-withdrawing group (EWG) on the sulfur atom in analogy to the electrophilic sulfenylation protocols reviewed above (Scheme 73; compare Chapter 1.4.2.3). Ideally, the EWG in the reagent **84** also can act as an internal base and capture the released from the arene proton during the first electrophilic sulfenylation step.

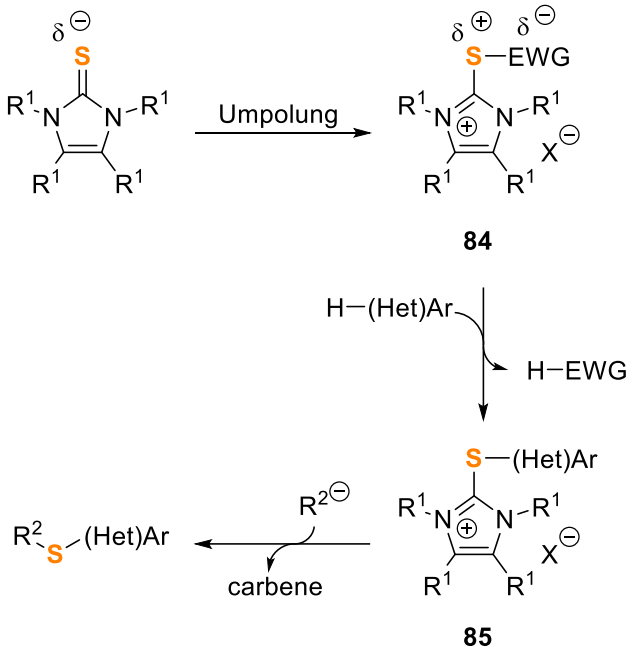

Scheme 73: Proposed reactivity of thioimidazolium salts **85** as a potential intermediate in the modular synthesis of unsymmetrical diaryl sulfides.

As presented in Chapter 2.1.2, the C–H activation of electron-rich heteroarenes with *in situ* oxidized thioureas is possible from the conceptual point of view. Afterwards, suitable conditions of the sulfenylation step will be examined and different sulfur containing precursors will be screened for the sulfenylating reagent synthesis, with a special focus on imidazole-2-thiones to get access to the general structure **85**. In a second consecutive step, the ability of the obtained thioimidazolium salts **85** to form new carbon-sulfur bonds with carbon-centered nucleophiles like Grignard reagents will be investigated in continuation to former results of M. Alcarazo, J. Peňa *et al*. (Scheme 69, **B**). Additionally, the methodology will be extended towards the synthesis of unsymmetrical diaryl selenides and arylimidazole-containing thioethers.

The synthetic utility of the developed protocols will be verified by the functionalization of pharmaceutically active compounds like the first-generation antihistamine Phenbenzamine (**86**). Additionally, the synthesis of the precursor **87** of an active tubulin inhibitor as well as the subsequent double sulfenylation of pyrrole derivatives **88** (Figure 15) will demonstrate the versatility of the developed protocol.

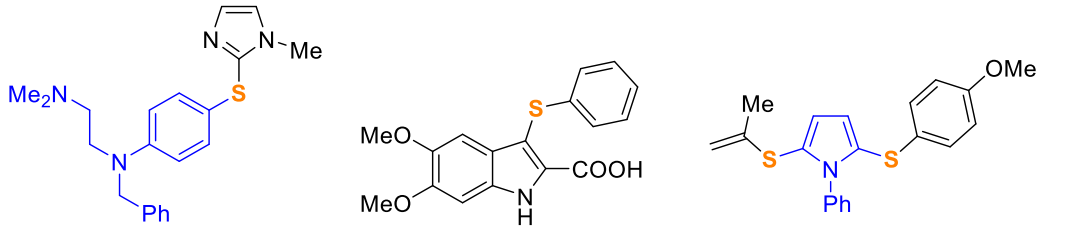

Sulfenylated Phenbenzamine (**86**) | drug precursor (**87**) | Double-sulfenylated *N*-phenyl pyrrole (**88**)

Figure 15: Potential targets for the desirable sulfenylation protocols.

Due to the importance of sulfinimide in medical chemistry,[255] a later side project will focus on the synthesis of potential thiosulfinimide transfer reagents which can react e. g. with carbon-centered nucleophiles. Therefore, representative compound of the general structure **89** will be synthesized, and the reactivity of these compounds will be further investigated (Scheme 74).

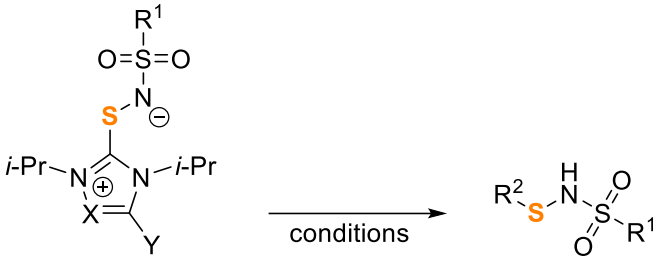

89

Scheme 74: Zwitterion **89** as a potential reagent for the transfer of thiosulfinimide groups.

3 Results and discussion

The need for the elaboration of a selective electrophilic sulfenylation protocol by introduction of a general applicable S^{2+} synthon in organic frameworks as well as the state of the art sulfenylation approaches were discussed in the former Chapters. As explained, no protocol for the selective introduction of a general applicable S^{2+} synthon is known so far. Since multiple sulfenylation protocols require the sulfur atom to be already present in the $[RS]^+$ sulfenylating reagent, each of these sulfenylation reagent must be prepared separately in advance for each R.

3.1 Synthesis of different thioimidazolium reagents

Based on the experience of the Alcarazo group with thioimidazolium-based transfer reagents, a series of potential electrophilic sulfenylating reagents will be synthesized by attaching different electron withdrawing group on the sulfur of the imidazole-2-thione (Scheme 75).

Since the electron-withdrawing group should act as an internal base in the sulfenylation step, *N*-basic residues like phthalimide (**90**), succinimide (**91**) and pyrrolidinone (**92**) were chosen as potential candidates for the EWG in **84**. The strategy seems to be very promising because most of these groups have already been used in traditional sulfenylation approaches (compare Chapter 1.4.2.3).

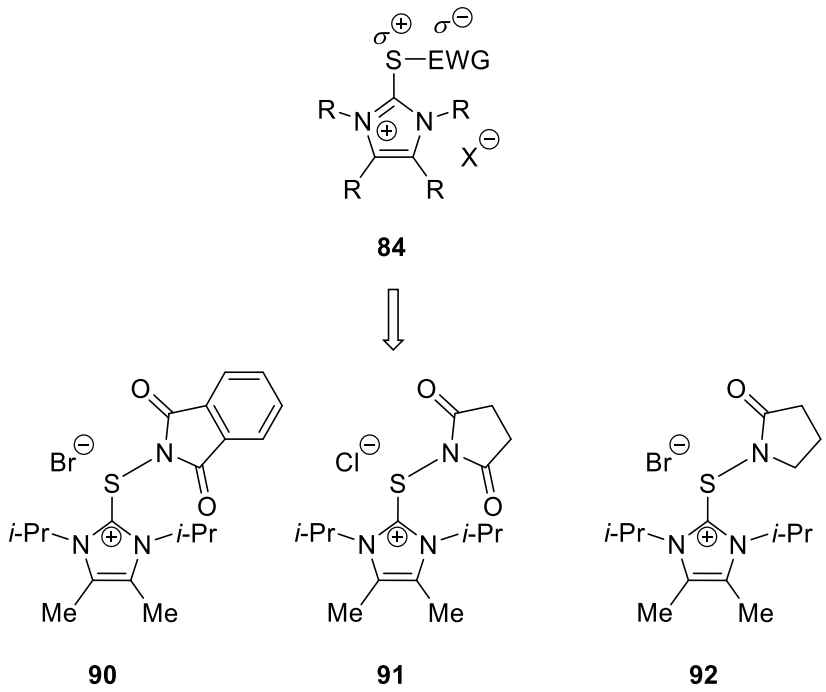

Scheme 75: Envisaged reagents **90**, **91** and **92** for the activation of electron-rich (hetero)arenes.

3.1.1 Synthesis of phthalimidylthioimidazolium bromide

The phthalimide-containing potential sulfenylating reagent **90** was synthesized from the imidazolthione backbone **78** which was obtained in a condensation reaction of acetoin and 1,3-diisopropylthiourea (Scheme 76). The bromination of **78** according to the published procedure[242] gave access to dibromide **79** in excellent yields. In a final step, the desired imidazolium reagent **90** was obtained by reaction of **79** with potassium phthalimide in 23% overall yield.

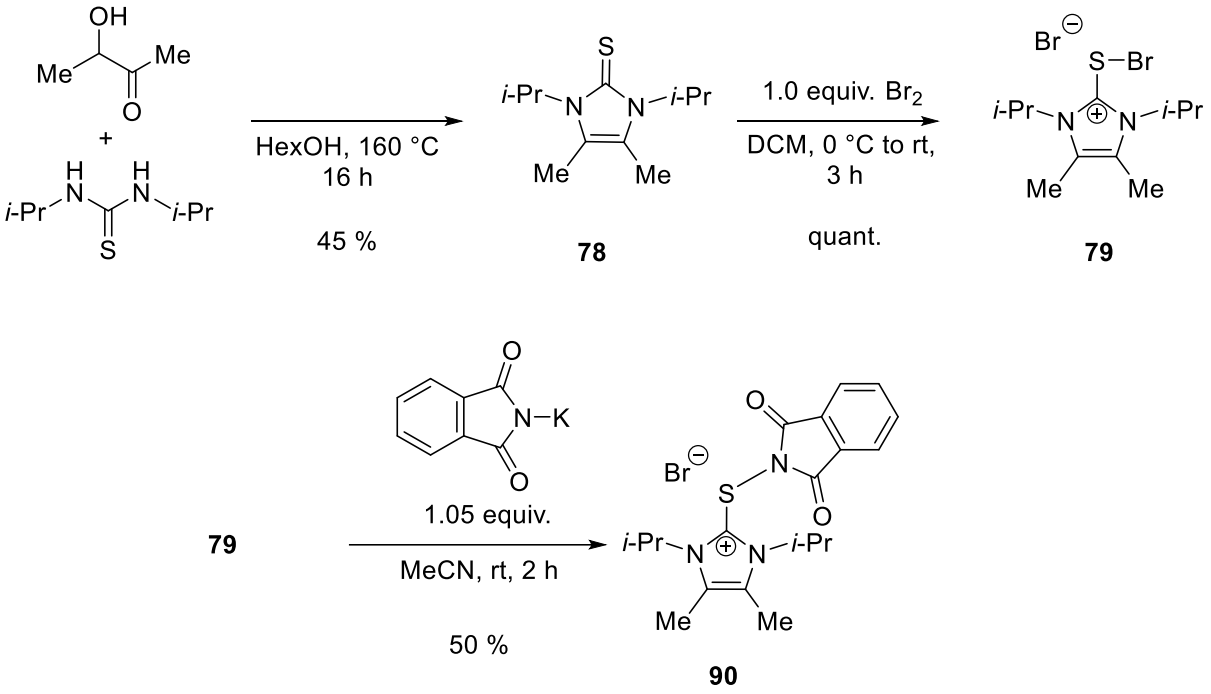

Scheme 76: Synthesis of a new potential sulfenylating reagent **90**.

Single crystals of **90** suitable for X-ray diffraction analysis were obtained by slow diffusion of pentane into an acetonitrile solution of **90** under inert conditions since compound **90** hydrolyses within a short period under ambient conditions.

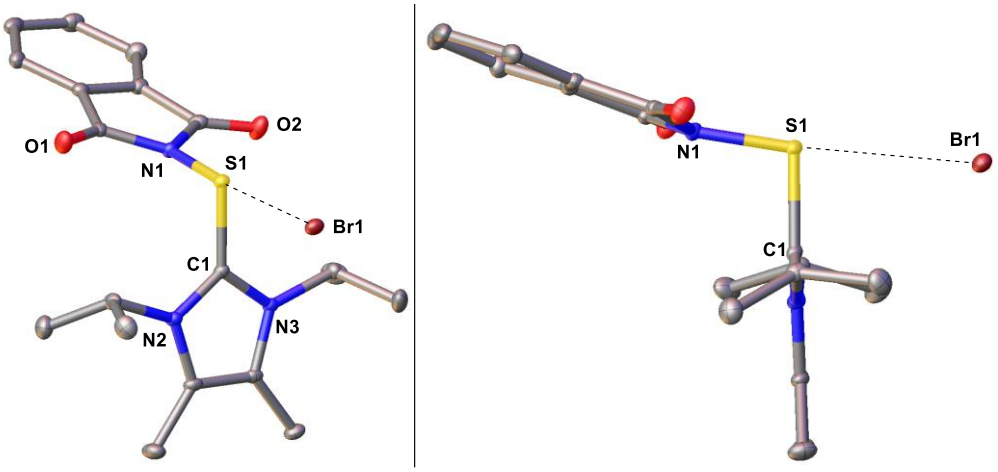

Figure 16: Molecular structure of compound **90** × MeCN. Thermal ellipsoids at 50% probability. Hydrogen atoms and MeCN molecules are omitted for clarity. Selected bond lengths, distances and angles: S1–C1 1.7584(15) Å, N1–S1 1.7137(13) Å, S1–Br1 3.177(8) Å, N1–S1–Br1 175.10(7)°, C1–S1–Br1 85.08(3)°, N1–S1–Br1 99.51(17)°.

In the solid state **90** exhibits a slightly distorted T-shaped conformation with a nearly linear N1–S1–Br1 axis (N1–S1–Br1 angle 175.1°) (Figure 16) which can be understood as a directed σ-hole interaction of the bromide anion and the partly polarized sulfur atom. Due to the potential Coulomb attraction between the positively charged imidazolium moiety and the negatively charged bromide anion the N1–S1–Br1 axis is slightly tilted resulting in a large N1–S1–C1 angle of 99.5° and a smaller C1–S1–Br1 angle of 85.1°. The C1–S1 bond is elongated by 0.068 Å compared to the non-oxidized imidazole-2-thione **78** [1.690(5) Å] due to the partial loss of the double bond character.[256] This can be rationalized by a weaker π back-donation of the less electron-rich sulfur into the unpopulated p-orbital of the carbene-C in the reagent **90** (Scheme 77).[257]

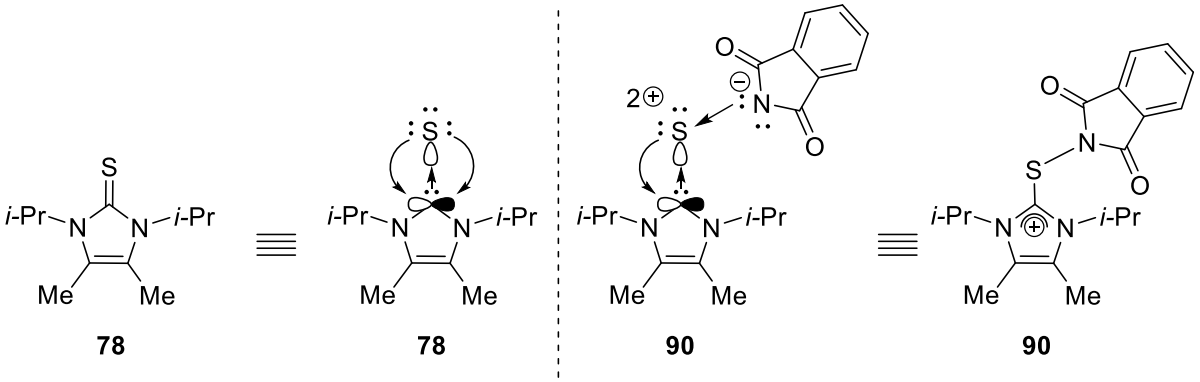

Scheme 77: Molecular orbitals of thione **78** and reagent **90**.

As expected, the N1–S1 bond length of 1.7137(13) Å is in line with a typical sulfur-nitrogen single bond[258] whereas the short S1–Br1 distance of 3.177(4) Å is significantly less (15%) than the sum of the S–Br van-der-Waals radii (3.7 Å)[259].

An explanation for this observation is the donation of electrons from the bromide anion into the anti-bonding S1–N1 orbital, commonly described in the literature as charge-assisted chalcogen bonds.[260] This observation is in accordance with the envisaged high electrophilic character of the sulfur atom in **90** and is frequently observed in other cationic sulfur reagents synthesized by the Alcarazo group.[261–263]

3.1.2 Synthesis of succinylthioimidazolium chloride 91

Compared to phthalimidylthioimidazolium bromide **90**, the succinyl analogue was accessible directly from imidazole-2-thione **78** by treatment with *N*-chlorosuccinimide (NCS) in DCE at room temperature (Scheme 78). Succinylthioimidazolium chloride **91** was quantitatively obtained as a moisture-sensitive yellow powder which readily hydrolyses when exposed to ambient conditions furnishing a brown oil.

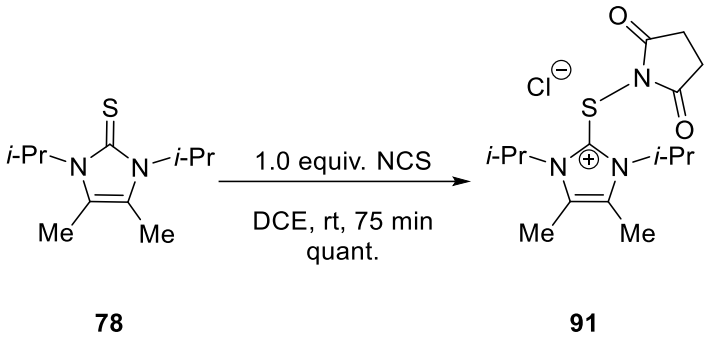

78 **91**

Scheme 78: Synthesis of succinylthioimidazolium chloride **91**.

The structural identity of **91** was confirmed by X-ray diffraction (Figure 17). Appropriate single crystals were obtained by slow diffusion of pentane into a concentrated solution of **91** in dichloromethane at room temperature. Similar to **90**, **91** also exhibits a slightly disturbed T-shaped conformation with a nearly linear N1–S1–Cl1 axis. The N1–S1 [1.724(9) Å)] and C1–S1 bond lengths of **91** [C1–S1: 1.7486(10) Å] are similar to those found in **90**.

In analogy to **90**, the sulfur-halogen distance S1–Cl1 in **91** [3.024(4) Å] is significantly shorter (16%) than the sum of the S and Cl van-der-Waals radii (3.6 Å).[259]

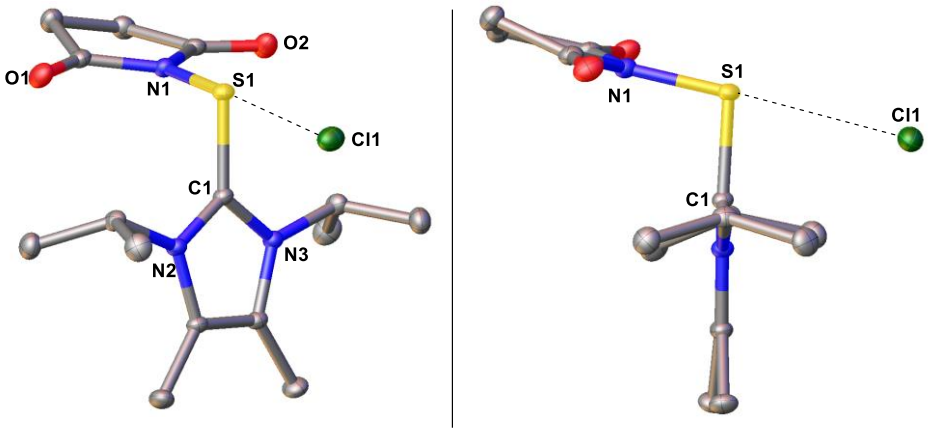

Figure 17: Molecular structure of compound **91** in the crystal. Thermal ellipsoids at 50% probability, hydrogen atoms are omitted for clarity. Selected bond lengths, distances and angles: S1–C1 1.7486(10) Å, N1–S1 1.7181(9) Å, S1–Cl1 3.0311(4) Å, N1–S1–Cl1 177.99(3)°, C1–S1–Cl1 78.62(3)°, N1–S1–C1 100.0(4)°.

It was assumed that the coordination of the chloride anion to the electrophilic sulfur atom could potentially reduce the reactivity of the reagent by blocking the electrophilic sulfur center. In the case of a reaction of **91** with nucleophiles like electron-rich arenes, the chloride may inhibit the reaction because it interacts significantly with the sulfur and must be displaced before the activation step of the arene. A weakly coordinating anion like hexafluoroantimonate would potentially be less competitive with the putative nucleophiles. Therefore, the hexafluoroantimonate **93** was synthesized by anion exchange of **91** with $NaSbF_6$ (Scheme 79).

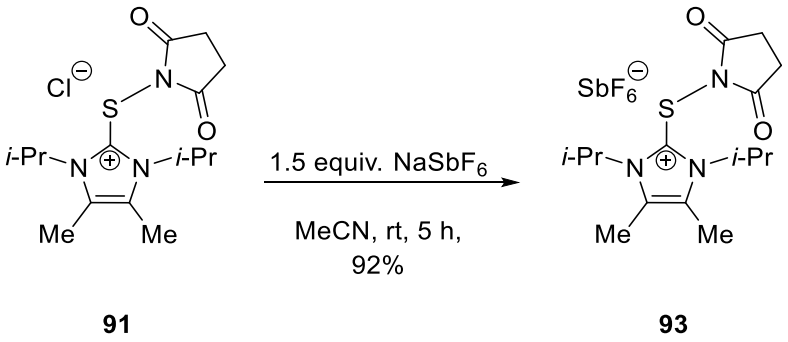

Scheme 79: Synthesis of succinylthioimidazolium hexafluoroantimonate **91**.

3.1.3 Synthesis of pyrrolidinylthioimidazolium bromide 92

Similar to **90**, the pyrrolidinyl derivative **92** was accessible from dibromide **79** (Scheme 80). The reaction of **79** with trimethylsilyl-2-pyrrolidinone gave access to the desired reagent **92** in excellent yield.

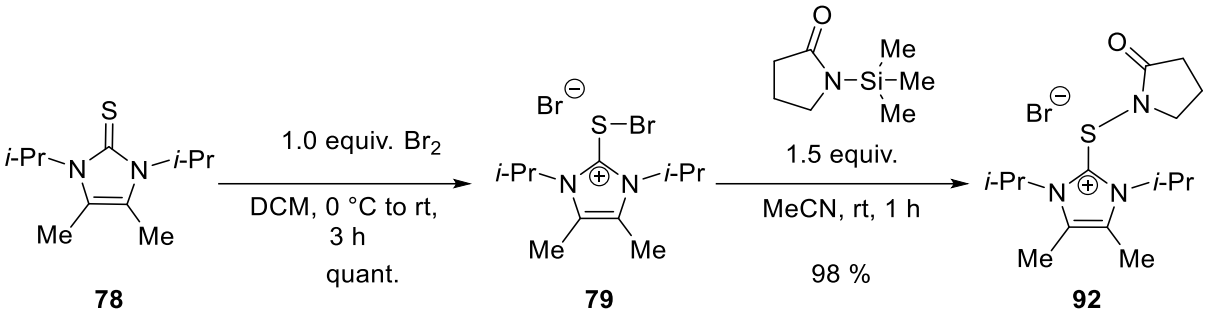

Scheme 80: Synthesis of pyrrolidinylthioimidazolium bromide **92**.

All diffusion-based attempts to grow suitable single crystals of compound **92** for X-ray diffraction experiments failed. After several unsuccessful attempts like the testing different solvent mixtures and temperature, the tetramethylimidazole-2-thione-derived analog **94** was synthesized, because the less sterically demanding methyl substituents on nitrogen atoms in the **95** backbone may favor the formation of more readily crystallizing solids (Scheme 81).

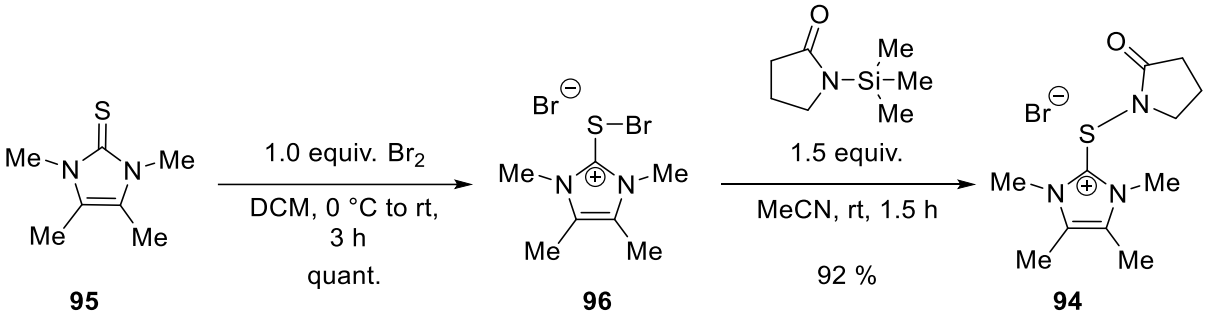

Scheme 81: Synthesis of pyrrolidinylthioimidazolium bromide **94**.

After successful crystallization of **94** by slow diffusion of pentane into a saturated dichloromethane solution, X-ray diffraction analysis of the obtained single crystals confirmed the expected connectivity (Figure 18). Therefore, it is assumed that observed sulfur nitrogen bond connectivity in **94** of is the same as in **92**.

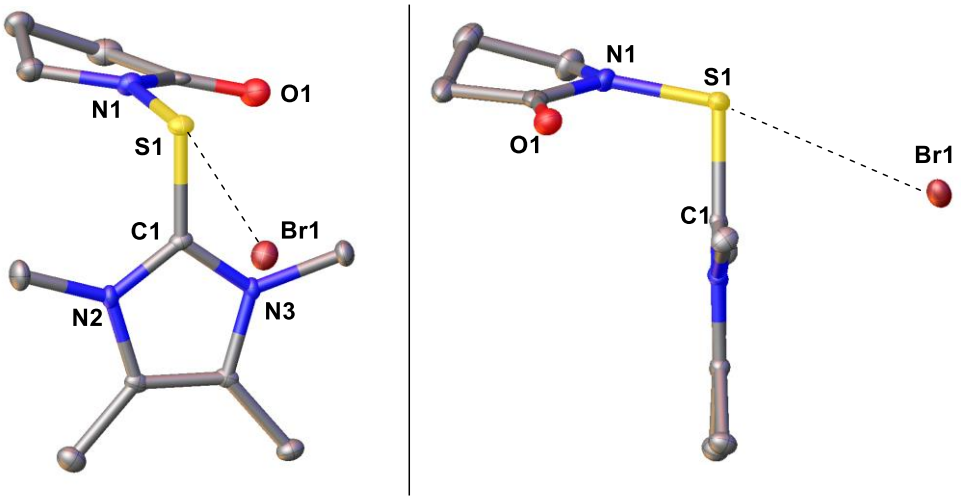

Figure 18: Molecular structure of compound **94** in the crystal. Thermal ellipsoids at 50% probability, hydrogen atoms are omitted for clarity. Selected bond lengths, distances and angles: S1–C1 1.749(3) Å, N1–S1 1.699(3) Å, S1–Br1 3.476 Å, N1–S1–Br1 167.06°, C1–S1–Br1 66.88°, N1–S1–C1 100.77(14)°.

Compared to **90** and **91**, the anion C1–S1–Hal angle in **94** is smaller, most likely due to the lower steric demand of the methyl groups in comparison to *iso*-propyl substituents.

This results into a weaker σ-hole interaction of the bromide with the sulfur. Therefore, the S–Br distance is 0.299 Å longer than the corresponding one in reagent **90**. Apparently, the lower electrophilicity of N1 in the pyrrolidinyl moiety, as compared to the phthalimide, results in a less accessible and possibly more diffuse anti-bonding (S1–N1) orbital. This might foreshadow a less reactive reagent.

3.2 Comparison of the reagents and optimization of sulfenylation conditions

To begin with, the reactivity of the synthesized thioimidazolium reagents was examined by electrophilic sulfenylation of phenyl pyrrole with **91**, which led to the cationic sulfide **97** (Table 5). Initial studies revealed the high impact of the workup protocol on the yield of the reaction.

The initially attempted purification of the crude product applying repetitive column chromatography resulted in low yields (34%) of the highly hydroscopic chloride salt **97**·Cl. This purification problem could be overcome by anion exchange of the chloride anion before the column chromatography. Thus, after evaporation of the acetonitrile under reduced pressure, the residue was dissolved in DCM and washed with aqueous $NaSbF_6$ solution. In this respect, replacing of the chloride with hexafluoroantimonate enabled the isolation of pure and non-hydroscopic **97**·SbF_6 in acceptable yields (66%) after flash column chromatography (fcc). Hexafluoroantimonate demonstrated superiority over other anions such as hexafluorophosphate which yielded the corresponding salt in a moderate 53% yield. The obtained **97**·SbF_6 is air stable and could be stored for several weeks under ambient conditions without any observed decomposition.

Table 5: Screening of different counteranions through the work up.

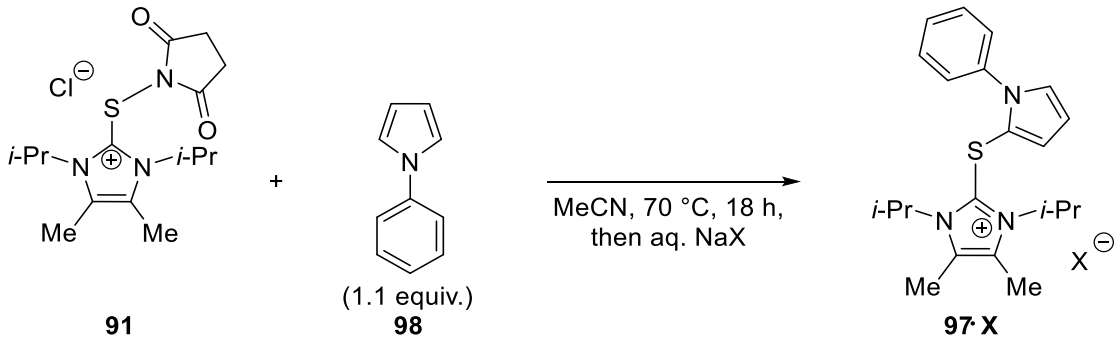

91 **98** **97·X**

Entry	NaX	Isolated **97**·X	Comment
1		34 % (X =Cl)	Multiple fcc; impure, hydroscopic product
2	$NaPF_6$	53 % (X = PF_6)	
3	$NaSbF_6$	66 % (X = SbF_6)	

Hereinafter, the influence of the electron-withdrawing group was investigated by the reaction of the reagents **90**, **91** and **92** with a slight excess of *N*-phenylpyrrole (Table 6). In this regard, the pyrrolidinone-derived reagent **92** gave the desired cationic sulfide **99** in the lowest yield

(30%), presumably due to the weaker electron-withdrawing character of the pyrrolidone moiety compared to the other reagents. Due to the more pronounced electron-withdrawing properties of the phthalimide residue than of pyrrolidine, reagent **90** demonstrated enhanced reactivity in the sulfenylation reaction (yield 50%, Entry 1).

Unfortunately, purification of the desired product from the phthalimide by-product using flash column chromatography (fcc) was not possible. However, the pure antimonate salt was obtained after two subsequent fcc´s.

As expected, the succinimide-based reagents gave the highest yields of compound **99** (Entries 2&3). The predicted lower coordinating hexafluoroantimonate derivative reagent **93** showed a higher reactivity in comparison to the chloride analogue **91**. Additionally, it could be demonstrated that the *in situ* formation of reagent **91** from **78** and NCS did not significantly reduce the yield (Entry 5). This enables the sulfenylation of electron-rich arenes in a one pot reaction from easy to handle starting materials.

Table 6: Evaluation of reactivity for the synthesized reagents in the sulfenylation of *N*-phenylpyrrole.

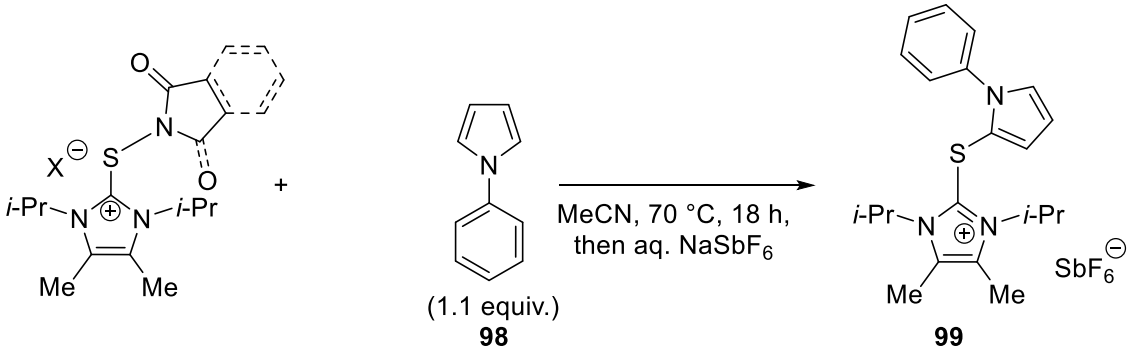

Entry	reagent	EWG	X	Isolated Yield
1	**90**	Phthalimide	Br	50%[a]
2	**91**	Succinimide	Cl	66%
3	**93**	Succinimide	SbF_6	85%
4	**92**	Pyrrolidinone	Br	30%
5	*In situ* formed **91**	Succinimide	Cl	65%

[a]: Isolated **99** was contaminated with phthalimide.

In connection with the discovered possibility of obtaining sulfenylating reagent **91** by oxidation of **78** with NCS *in situ*, several other oxidants were also screened (Table 7). However, NCS turned out to be the only viable oxidant from the tested ones. *N*-Bromosuccinimide led to the formation of an inseparable mixture of different regiomers of **99** whereas *N*-iodosuccinimide

was not reactive enough, as *N*-phenylpyrrole (**98**) was reisolated almost quantitatively. The higher reactivity of *N*-chlorosaccharine resulted in the formation of a complex mixture of **99** with several unidentified side-products.

Table 7: Screening of different oxidants for the *in situ* formation of succinimide-derived reagents.

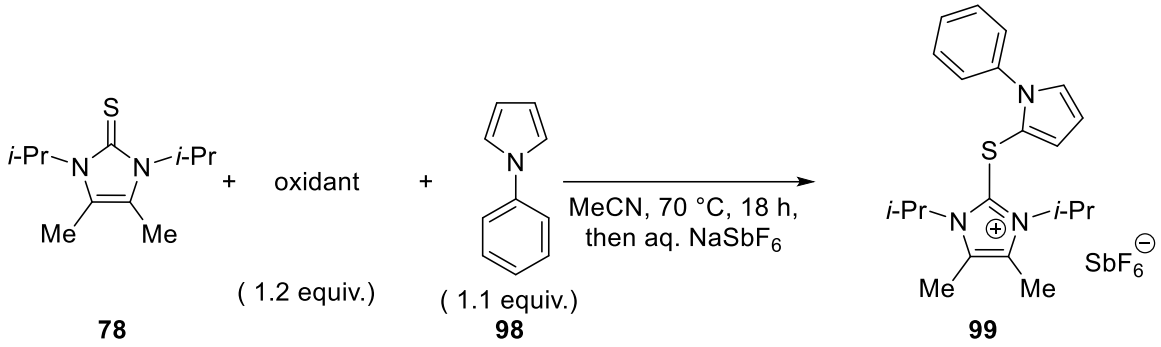

Entry	Oxidant	Isolated yield	Comment
1	*N*-Chlorosuccinimide	65%	
2	*N*-Bromosuccinimide	n.d.	Formation of regiomers
3	*N*-Iodosuccinimide	0%	
4	*N*-Chlorosaccharine	n.d.	Complex mixture
5	none	0%	

Further screening of the reaction conditions revealed no significant influence of polar solvent in the functionalization of 2-phenyl-1-methylindole, since the reaction gave high yields in both acetonitrile and DCE (Table 8, Entries 1 & 2). In toluene the reaction resulted in low yield, probably due to the low solubility of the reagent (Entry 3). As acetonitrile is known to be less toxic, more environmentally friendly and does not tend to undergo substitution reaction with strong nucleophiles; it was the solvent of choice.[264]

Decreasing the reaction temperature resulted in very low yields of compound **100** (Entry 4). Instead, increasing the reaction concentration by factor eight resulted only in a slightly decreased yield (Entry 5). Furthermore, the transformation was sensitive to water, as the addition of small amounts of water significantly lowers the yield (Entry 6). To exclude a radical reaction pathway, equimolar amounts of TEMPO were added to the reaction mixture (Entry 7).

Table 8: Screening of solvents, temperatures and additives.

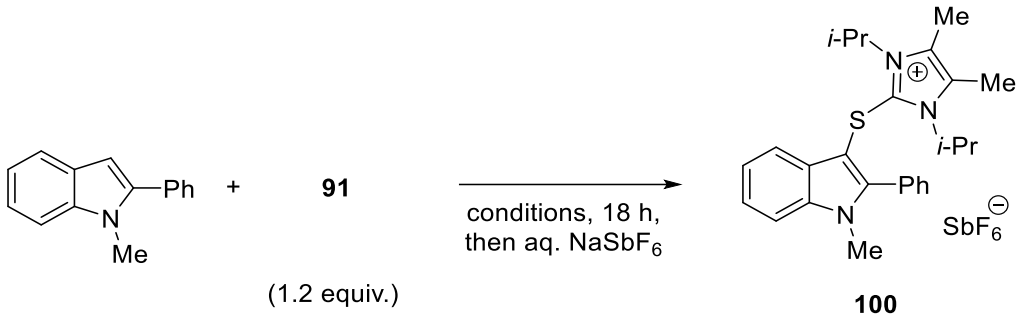

Entry	Solvent	T	c /M	Additives	Yield
1	DCE	70°C	0.1	-	71%
2	MeCN	70°C	0.1	-	72%
3	Tol	70°C	0.1	-	5%
4	MeCN	rt	0.1	-	15%
5	MeCN	70°C	0.8	-	65%
6	MeCN	70°C	0.1	2 equiv. H_2O	47%
7	MeCN	70°C	0.1	1 equiv. TEMPO	47%

Since significant amounts of **100** (47%) were still isolated, although the yield dropped, an electrophilic aromatic substitution (S_EAr) mechanism (see Scheme 82) is proposed for the reaction in analogy to the literature known electrophilic sulfenylation reagents (compare Chapter 1.4.2.3).

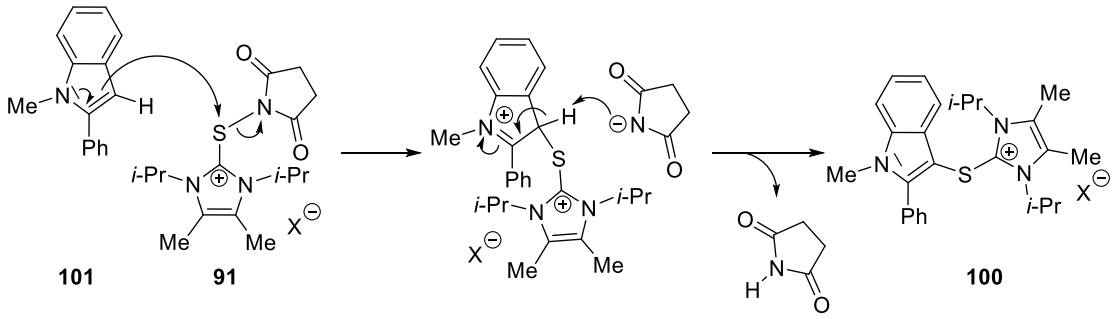

Scheme 82: Proposed mechanism for the sulfenylation of indole **101** with reagent **91**.

3.3 Evaluation of backbone

After appropriate reaction conditions for the imidazole-derived reagents (**91**) have been determined, the influence of the sulfur-containing backbone on the yield of the sulfenylation of *N*-phenylpyrrole was investigated by screening different thiourea derivatives. The latter were *in situ* oxidized with *N*-chlorosuccinimide and tested in the sulfenylation reaction of *N*-phenylpyrrole affording the cationic sulfide of the general form **102** (Scheme 83).

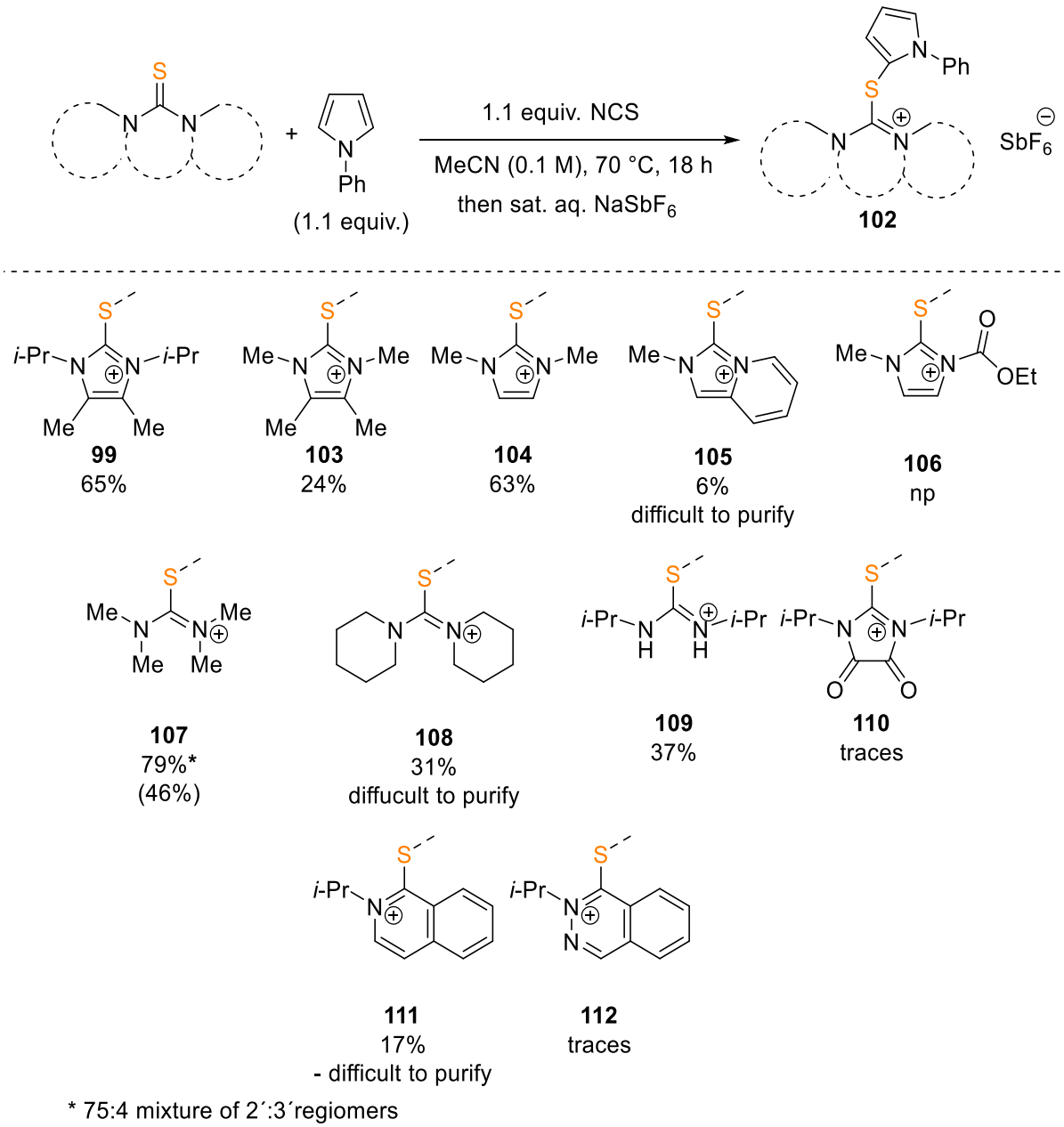

Scheme 83: Screening of different sulfur-containing backbones for the sulfenylation of *N*-phenylpyrrole resulting in cationic sulfides of the general structure **102**.

The reaction proceeded with different alkyl substituted imidazole-2-thione derivatives affording cationic sulfides **99**, **103**, **104** and **105**; the highest yield of 65% was obtained with 1,3-

diisopropyl-4,5-dimethyl-imidazole-2-thione (**78**). The replacement of the methyl group at the nitrogen atom in the imidazolethione fragment by the ethoxycarbonyl group, as well as the oxidation of the imidazole-2-thione, did not lead to the formation of the desired cationic sulfides **106** and **110**, respectively.

In contrast to this, acyclic thiourea derivatives were reactive enough for the sulfenylation of *N*-phenylpyrrole. Unfortunately, the high reactivity, especially of tetramethylthiourea-derived sulfenylation reagent, led to a low selectivity of the sulfenylation, as a 75:4 mixture of the 2'- and 3'-sulfenylated regioisomers **107a** and **107b** was obtained. Both compounds could be separated by repetitive flash column chromatography affording the desired 2'-substituted product **107a** in the yield of 46%. The connectivities in the regioisomers were confirmed by X-ray crystallography of suitable single crystals obtained by slow evaporation of a DCM solution of the mixture of both compounds (Figure 19).

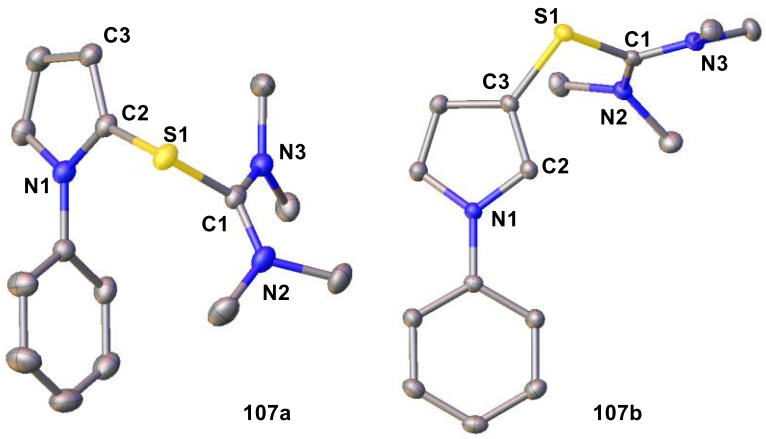

Figure 19: Solid state structure of regio-isomers **107a** and **107b**. Thermal ellipsoids at 50% probability level; hydrogen atoms, anions and solvents are omitted for clarity.

Other tested thiourea derivatives gave the corresponding cationic sulfide **109** and **108** in only moderate yields of 31% and 37%, respectively (Scheme 83).

The utilization of isoquinolinethione as a sulfur precursor resulted in formation of **111** in moderate yield; however, isolation of the product in acceptable purity appeared to be impossible after several attempts. With phthalazinethione as a starting material, only traces of the desired salt **112** were obtained. In general, the yields of the reaction may be affected by solubility effects during the isolation, as some cationic sulfides were highly polar and tend to stick on the silica gel during the flash column chromatography. Since the selectivity and reactivity were in an optimal agreement for the case of 1,3-diisopropyl-4,5-dimethylimidazole-2-thione (**78**) as a sulfur-containing backbone, this sulfur precursor will be used in the next steps. In the solid state the corresponding cationic sulfide **99** shows a C1–S1–C2 bond angle of 100.5° and a dihedral angle φ(N1;C1;S1;C2) of 117.3° (Figure 20). As expected, the S1–C1 bond was elongated from 1.690(5) Å in the imidazole-2-thione to 1.75495(9) Å in **99**.[265]

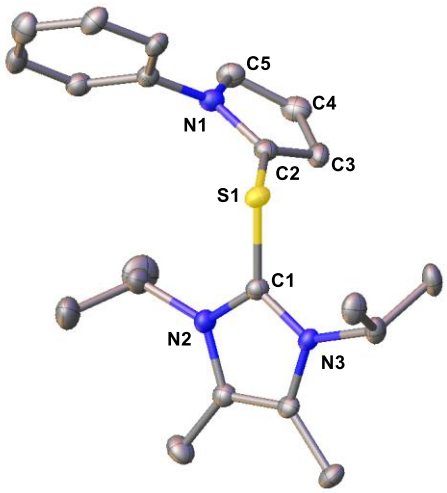

Figure 20: Solid state structure of **99** Thermal ellipsoids at 50% probability level, hydrogen atoms and anions are omitted for clarity.

Furthermore, the connectivity in cationic sulfides **103** – **104**, **92** and **111** was confirmed by X-ray diffraction analysis (for crystal data see Chapter 5.8). As expected, the sulfur-carbon bond of all utilized backbones was elongated and ranged between 1.7868(16) Å and 1.7461(16) Å (see Scheme 84). This is a direct consequence of the reduction of the bonding order in the corresponding bond between sulfur and carbon and refers to the average length of these carbon-sulfur single bond of [1.751(17) Å].[266]

It can be assumed that long sulfur carbon bonds (*e. g.* in **111** & **108**) tend to be weaker and can probably be partially hydrolyzed on the acidic silica gel upon the flash column chromatography, as the cationic sulfides were isolated in lower yields of 17% and 31%, respectively.

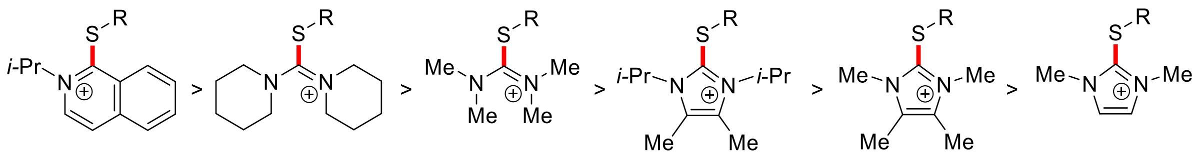

111 1.7868(16) Å; **108** 1.774(4) Å; **107a** 1.7705(15) Å; **99** 1.7495(9) Å; **103** 1.747(2) Å; **104** 1.7461(16) Å

Scheme 84: Bond length of the sulfur-carbon bonds in the cationic sulfides of the general structure 102. R equals to 2-*N*-phenylpyrrolyl residue.

3.4 Scope and limitation of reagent for the synthesis of thioimidazolium intermediates

Having the optimized reaction conditions for the functionalization of *N*-phenylpyrrole and reagents **93** and **91** in hand, further heterocyclic arene derivatives were targeted by the sulfenylation reaction (Scheme 85). Apart of pyrrole derivatives **113** and **99**, several other *N*-heterocyclic arenes like indoles **114** to **118** and carbazole **119** derivatives were also obtained in good to excellent yields. In most cases, even the less reactive succinylthiolimidazolium chloride **91** gave products in excellent yields as well. Among less functionalized nucleophiles, the method tolerated several functionalities such as unprotected indole NH (products **115**, **117**, **118**), hydroxyl- (**115**), carboxylic (**117**) and ester groups (**118**). Upon sulfenylation of indole-2-carboxylic acid, the cationic product **117** was obtained as the corresponding imidazolium chloride salt, which directly precipitated from the reaction mixture. Only electron-poor *N*-heterocyclic arenes like pyrazole and imidazole[1,2-*a*]pyridine derivatives were not sulfenylated by this protocol.

Additionally, some (benzo)thiazoles reacted with the more reactive reagent **93** in the expected fashion to give the corresponding cationic sulfides **122** and **123** in 61% and 90% yields, respectively. Unfortunately, *O*-heterocyclic systems were not reactive enough and could not sufficiently be functionalized, as only traces of the products **126** to **128** were obtained.

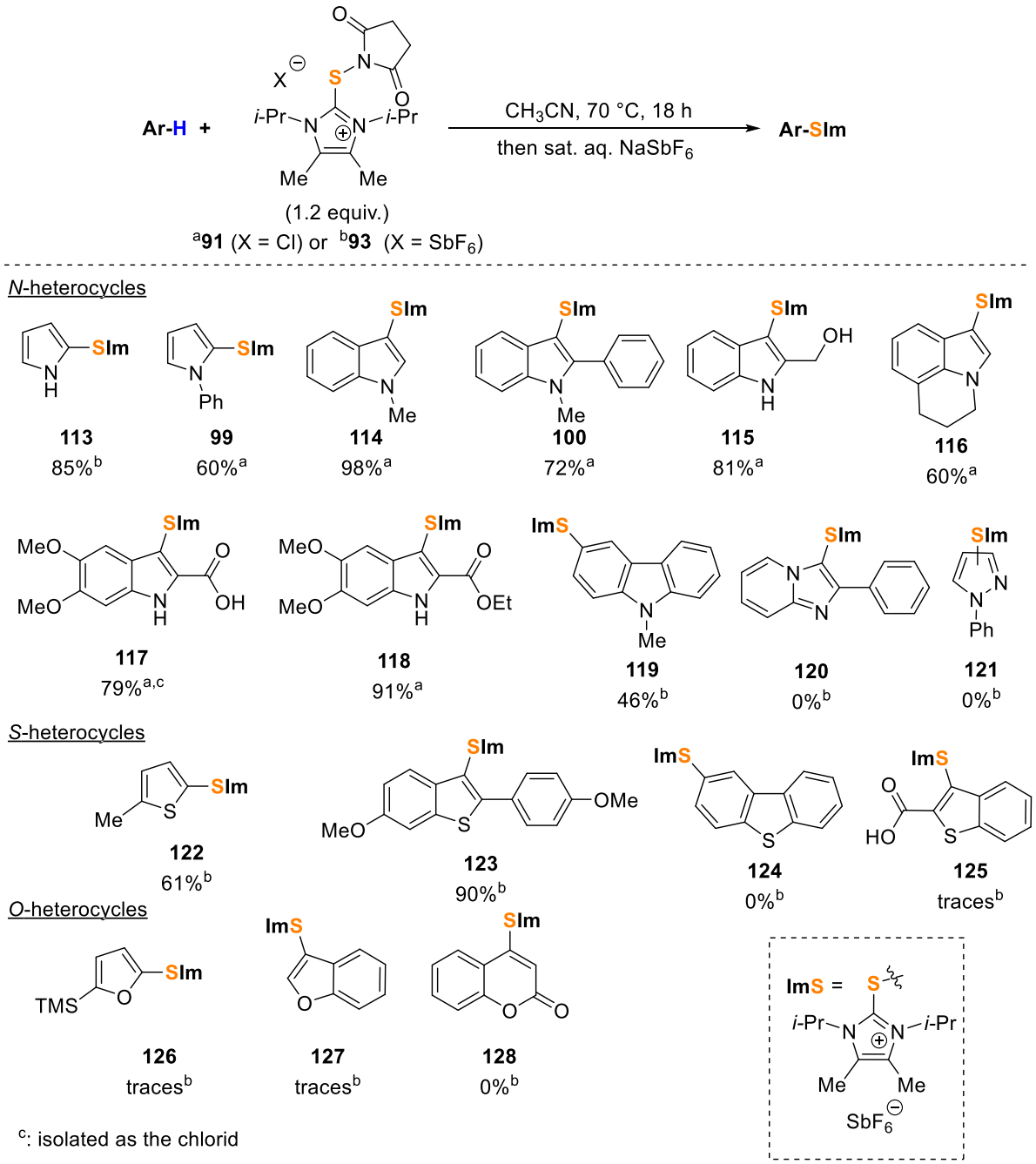

Scheme 85: Scope of the sulfenylation reaction with different heteroarenes-based nucleophiles.

To verify the connectivity in the cationic sulfides, single crystals suitable for X-Ray diffraction of selected representative products were obtained by slow diffusion of hexane, heptane or diethyl ether into saturated solutions in DCM. The solid state structures of various cationic sulfides are presented in Figure 21. All structural motives have a common angular geometry around the imidazole sulfur atom which varies between 102.59(8)° for **123** and 105.0(3)° for **100**. Additionally, no short contacts between the hexafluoroantimonate anion and the imidazolium sulfur atoms were observed, presumably because the antimonate is far less Lewis basic than the bromide or chloride anion. The S–$C_{imidazolium}$ bond length varied between 1.759(4) Å in **113** and 1.7463(8) Å in **116**. The average bond length was slightly shorter than the S–$C_{heteroaryl}$ bond with a length varying between 1.7712(15) Å in **123** and 1.750(5) Å in **113**.

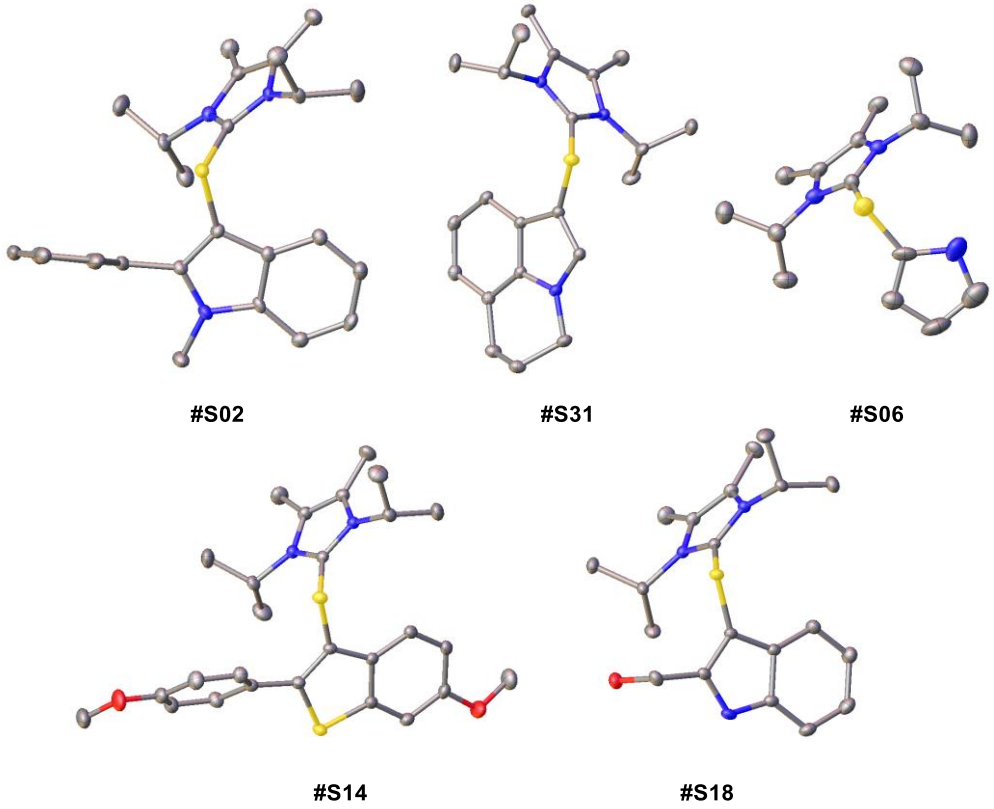

Figure 21: Crystal structures of cationic sulfides of different indole, pyrrole and benzothiophene derivatives. Thermal ellipsoids at 50% probability level; hydrogen atoms, anions and solvents are omitted for clarity.

Interestingly, apart from heterocyclic arenes, also electron-rich aromatics were sulfenylated by reagents **93** and **91** (Scheme 86). Especially, mono- and di-*N*-methylated methylanilines showed high reactivity furnishing compounds **130** and **129** in 43% and 91% yield, respectively. Furthermore, also unprotected and benzyl-protected anilines also gave the corresponding cationic sulfides **131** and **132** in up to 52% yield. Unfortunately, all attempts to sulfenylate *N*-phenylacetamide failed, probably due to the deactivating effect of the attached acetylamide group and the resulting lower nucleophilicity of the arene core. 1,8-Bis(dimethylamino)naphthalene was functionalized affording **136** in yield of 46%. Interestingly, apart from the desired *para*-functionalized product, also minor traces of the corresponding *ortho*-sulfenylated product crystalized from a saturated dichloromethane solution of the crude product (see chapter 5.8.3).

Electron-donating substituents on the aniline core reduced the selectivity of the reaction, as *meta*-methylaniline was sulfenylated in both *ortho* and *para* position (ratio *o*:*p* = 28:72). The product distribution was determined by NMR spectroscopy and was in agreement with those observed in the solid state (compare crystal structure in Chapter 5.8.3). Attempts to increase the selectivity of the reaction employing lower temperature (40 °C) and elongating reaction times up to 24 h failed.

Di- and trimethoxybenzene gave the corresponding sulfides **137** and **138** in good to excellent yields as well. In case of the less electron-rich dimethoxy benzene, the more active reagent **93** has to be used, whereas the utilization of **91** gave only traces of the desired product **137**. In contrast to that, additional electron-withdrawing functionalities in the substrate such as a nitrile group on the aniline core or the acetylation of the aniline amine group strongly inhibited the formation of **135** or **133**, respectively.

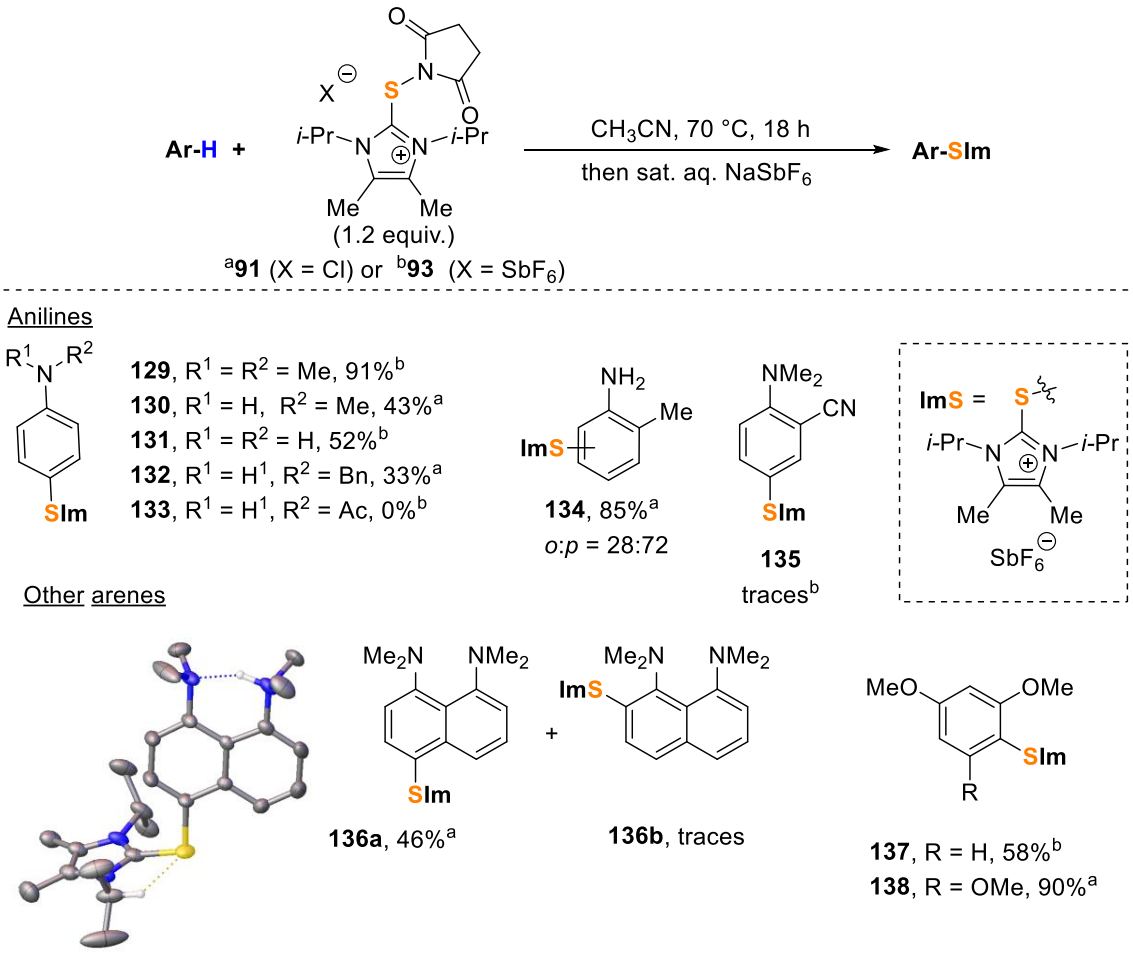

Scheme 86: Reaction scope of the sulfenylation reaction with different arene-based nucleophiles; For crystal structure of **136**: Thermal ellipsoids at 50% probability level; hydrogen atoms, anions and solvents are omitted for clarity.

As most of the obtained imidazolium salts are highly crystalline compounds, single crystal suitable for X-ray analysis of aniline derivatives **129** and **132** as well as methoxybenzenes **137** and **138** were obtained to confirm the expected connectivity (see Figure 22).

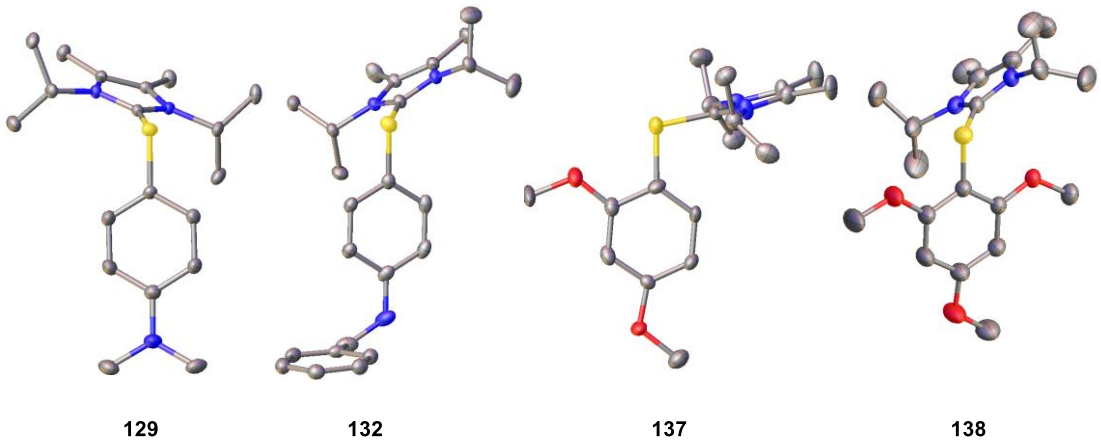

Figure 22: Crystal structure of cationic sulfides from arene derivatives. Thermal ellipsoids at 50% probability level; hydrogen atoms, anions and solvents are omitted for clarity.

Unfortunately, all attempts to synthesize cationic sulfides from methoxybenzenes **140** – **145** derivatives as well as from phenol **143** failed, as these arenes appeared to be not electron-rich enough (Scheme 87). This still remains the major limitation of the sulfenylation protocol and explains also, why triazole derivative **144** and ethynylbenzene (**145**) were not reactive applying the developed methodology.

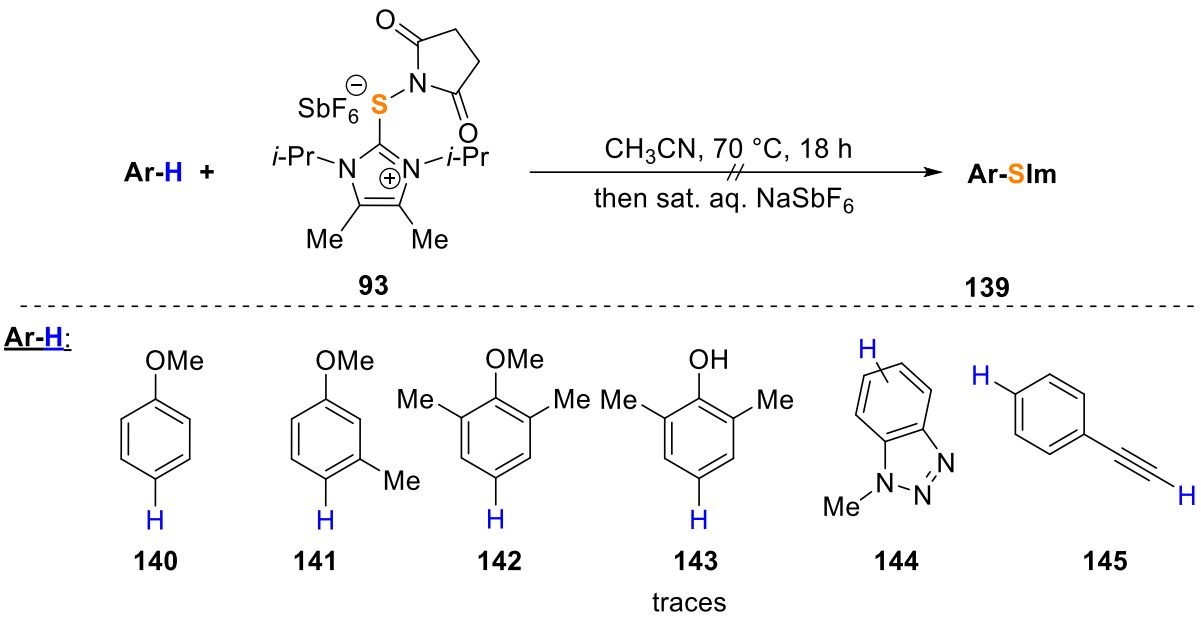

Scheme 87: Attempted synthesis of cationic sulfides from miscellaneous less electron-rich arenes.

As indicator of the high chemical stability of the obtained air-stable cationic sulfides can be used the fact that in all cases no formation of symmetrical diarylsulfide was observed as a side product. Even the intended treatment of **137** with *N*,*N*-dimetylaniline under elevated conditions like extensive heating over elongated times in the presence of cesium carbonate as a base did not result in the formation of diaryl sulfides **146** (Scheme 88). Instead, **137** was nearly quantitatively reisolated.

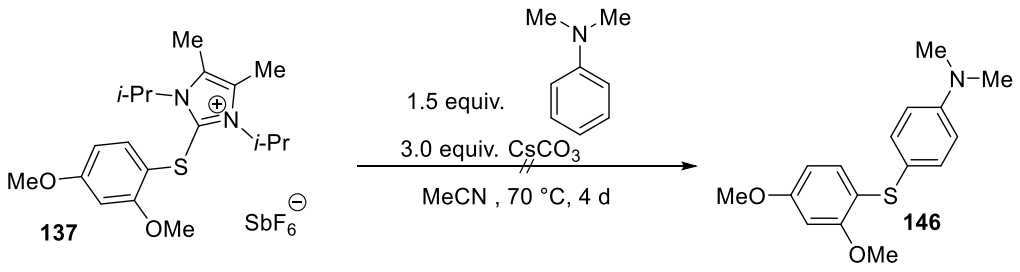

Scheme 88: Stability test of **137** under harsh conditions.

To expand the scope of **93** for the functionalization of aniline derivatives, the core structure of the AZD4407 (**147**) was targeted (Scheme 89). The aryl thioether AZD4407 was of high pharmaceutical interest since it can inhibit the 5-lipoxygenase which makes it a potent candidate for the treatment of a variety of inflammatory conditions such as chronic obstructive pulmonary disease (COPD) and asthma.[267] The strategy to obtain core structure **148** based on the initial sulfenylation of 2-indolone (**150**). It was expected that the *para* to the nitrogen position is the most reactive one in **150**, wherefore salt **149** should be the envisaged product. Surprisingly, the sulfenylation of **150** led to compound **151** in high yields of 84%. This can be rationalized by the keto-enol tautomerism of **150** giving also 1-hydroxyindole as a potential tautomer. To enable the sulfenylation of the arene ring, the introduction of a sterically demanding TBDMS-protecting group was envisaged. The silylation proceeded quantitatively following a modified protocol of E. Merifield and coworker.[267] Unfortunately, the sulfenylation of 152 gave a sluggish reaction and also resulted in the formation of **151** in low yields of 18%.

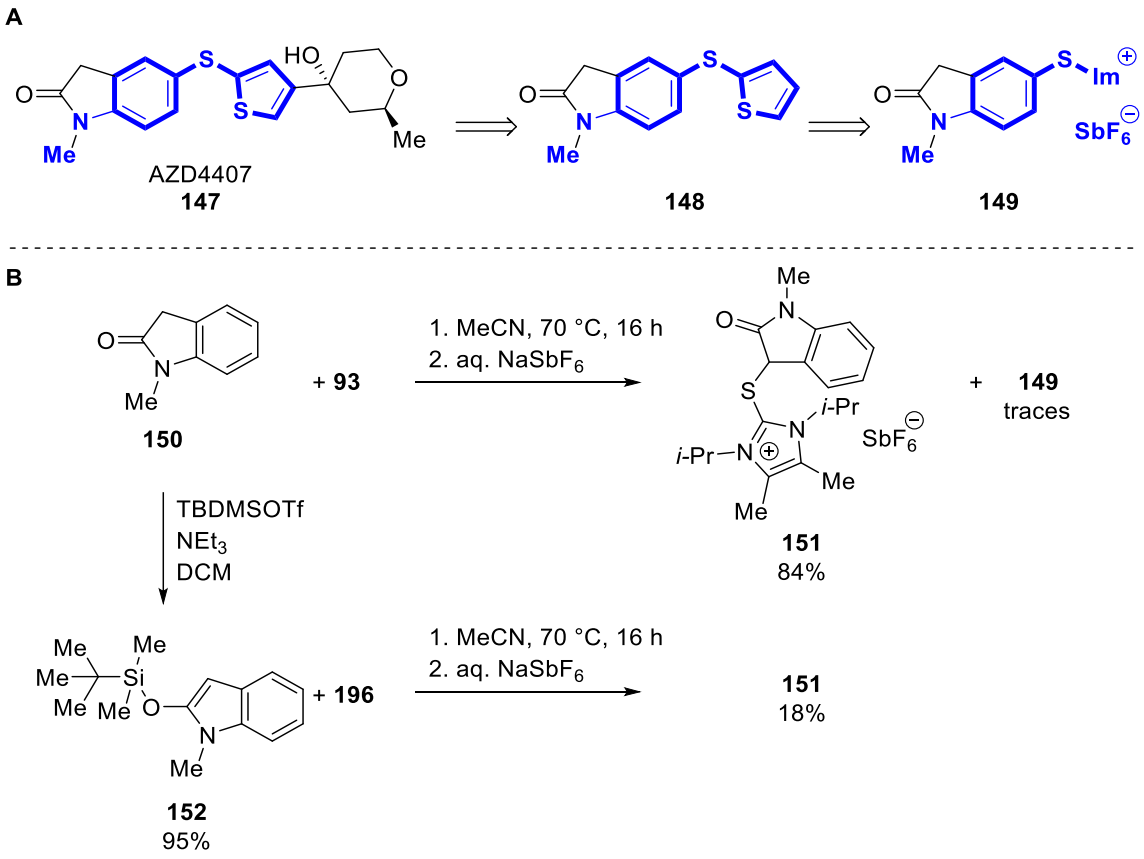

Scheme 89: Attempted synthesis of potential key intermediate **149** for an alternative synthetic approach to **147**.

3.5 Synthesis of arylsulfides

3.5.1 Screening for appropriate nucleophiles

Having established a selective protocol for the synthesis of the cationic imidazolium-derived intermediates **99**, several different nucleophiles were screened for their ability to attack the sulfur atom under formation of a new sulfur-carbon bond and release of the imidazole *N*-heterocyclic carbene (Scheme 90). Weak nucleophiles as enamines were not able to react in a desired manner to give access to iminium species **153.** Also, deprotonated 1,3-dicarbonyl compounds, phosphorus ylides and TMS-protected enolates were not reactive enough to give the desired sulfides **154**, **155** and **156**, respectively. All attempts resulted in formations of complex reaction mixtures. Only unreacted starting material **99** was re-isolated in most cases.

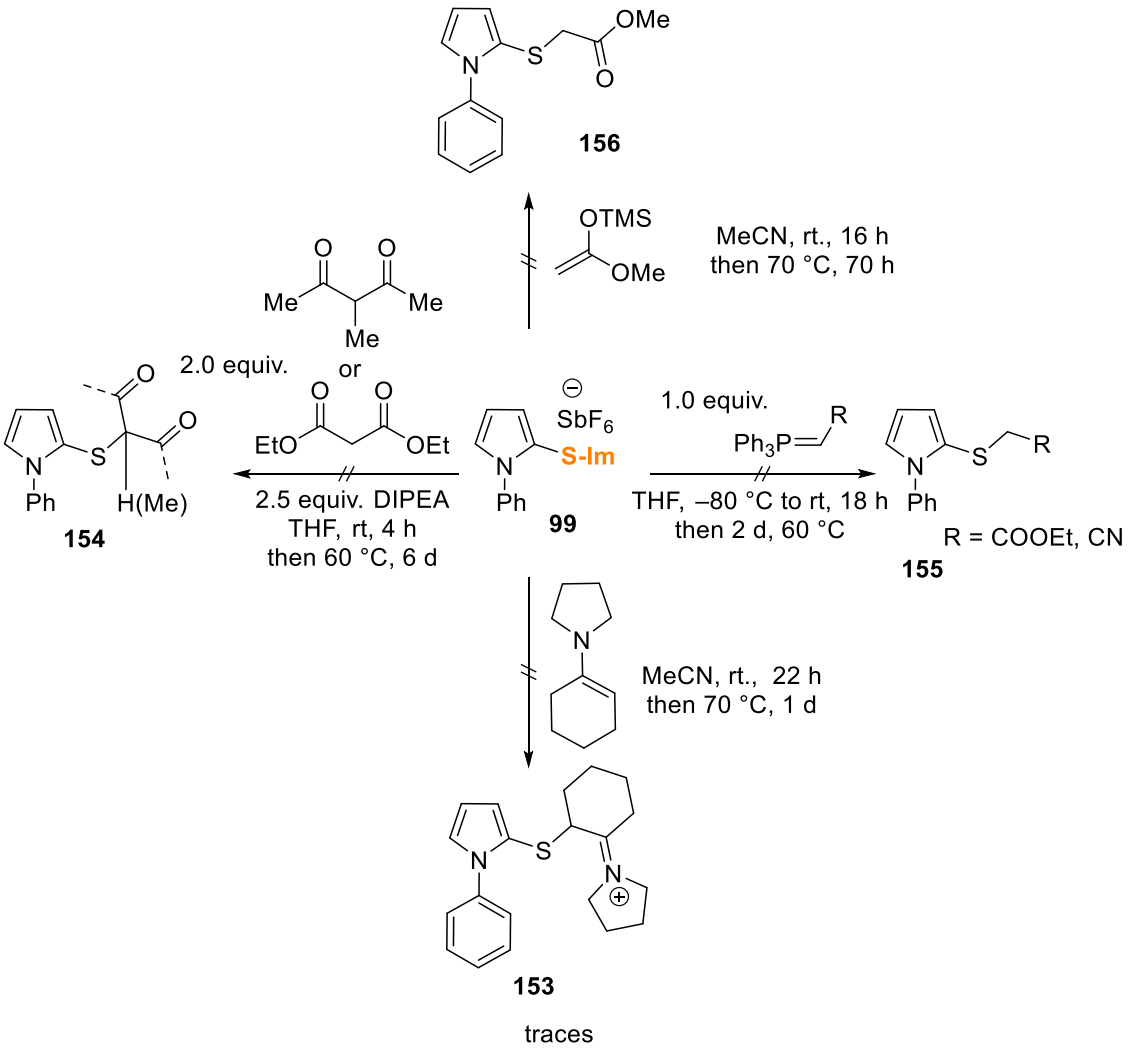

Scheme 90: Exploration for the identification of a suitable nucleophile for the formation of arylsulfides.

Afterwards easy accessible harder nucleophiles like organometallic compounds were tested (Table 9). In this regard, organocupprate which was prepared from *Rieke* copper and *para*-

bromoanisol gave only traces of arylsulfide **157** (Table 9, Entry 1).[268] Also the corresponding zincate obtained by transmetallation of *para*-methoxyphenylmagnesium bromide with an excess of zinc bromide gave only minor yields of **157** (Table 9, Entry 2).

As in the former thioalkynylation protocol of the Alcarazo group (see Chapter 2.1.1), Grignard reagents were found to be suitable nucleophiles enabling the synthesis of the desired unsymmetrical thioethers.[246] Luckily, from model substrate **99** the desired thioether **157** was obtained in excellent yields (94%).

Table 9: Screening of different organometallic reagents.

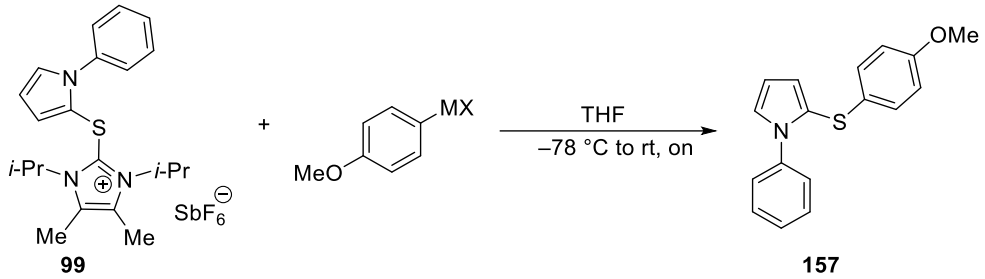

Entry	MX	Yield of **157**
1	CuBr (5.0 equiv.)	Traces
2	ZnBr (1.5 equiv.)	2%
3	MgBr (1.5 equiv.)	94%

Further screening of reaction conditions revealed that in other cases e.g. aniline adduct **129**, bigger amounts of Grignard were needed to achieve high-yielding reactions (Table 10). The *in situ* formation of a turbo-Grignard by addition of LiCl did not result in increased yields (compare Table 10, Entries 2&4).[269] However, slow warming up the reaction mixture overnight resulted in better yields compared to immediately removing of the cooling bath after the addition of the Grignard reagent (compare Table 10, Entries 1&2).

Table 10: Optimization of reaction conditions for **129**

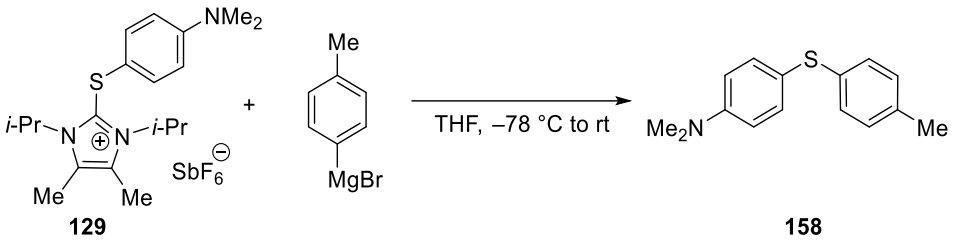

Entry	RMgBr	c /M	Additives	Conditions	Yield of **158**
1	1.4 equiv.	0.1	-	Fast warm up	25%
2	1.5 equiv.	0.1	-	Slow warm up	36%
3	2.9 equiv.	0.1	-	Slow warm up	75%
4	1.5 equiv.	0.1	5 equiv. LiCl	Slow warm up	43%

To confirm the release of the carbene as a leaving group in the reaction, equimolar amounts of selenium powder were successively added after the reaction was finished (Scheme 91). The formation of selenium urea **159** was confirmed by detecting a mass of the corresponding selenourea with *m*/*z* of 260.0789 upon mass spectrometry.

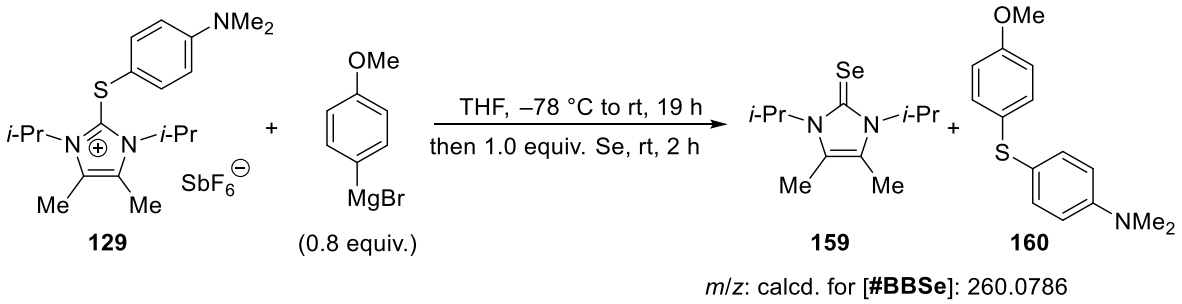

Scheme 91: Trapping of the liberated free imidazole carbene with selenium powder under formation of seleno urea **159**.

3.5.2 Scope, applications and limitations

After Grignard reagents were found to be the best nucleophiles for the synthesis of diaryl sulfides from cationic imidazolium sulfides, as shown in the previous Chapter 3.5.1 for **99** and **129**, a library of 28 diaryl sulfides was synthesized (Scheme 92). The concentration of the utilized Grignard reagents was determined by titration before usage following established protocols.[270] For less reactive reagents and reactants, an excess of up to 2.9 equivalents of the organomagnesium reagent was used. In cases of cationic imidazolium sulfides possessed

protic functional groups like carboxylic acids, additional equivalents of the organometallic nucleophile were added (e. g. **87**).

Studies revealed that more electron-rich und therefore more nucleophilic Grignard reagents gave higher yields of the desired aryl sulfides. Thus, *para*-methoxyphenylmagnesium bromide afforded arylsulfide **161** in 94% yield, whereas the utilization of corresponding fluoro- and cyano-containing Grignards resulted in formation of **162** and **163** in 67% and 78% yield, respectively.

With the optimized reaction conditions in hand also more sophisticated diaryl sulfides with menthol (**165** and **187**) or sugar (**169**) motifs were accessible in yields of 89%, 51% and 53%, respectively. For the introduction of *para*-cyanophenyl (**163**) and bromopyridyl (**172**) motifs, the applied Grignard reagents were obtained by a LiCl-mediated Br/Mg exchange reaction, as reported by the group of Knochel and coworkers.[271]

In other cases, e. g. for the synthesis of benzothiazole- (**170**), dichloropyridine- (**173**) and quinolone-containing (**166**) thioethers, Grignard reagents were prepared by deprotonation of the corresponding heterocycle with 2,2,6,6-tetramethylpiperidinylmagnesium chloride in the presence of lithium chloride (TMPMgCl LiCl) following the protocol of Knochel and coworkers.[272] In case of the furylpyrrolyl sulfide 167 it could be shown that also lithiumorganic reagents can be utilized as nucleophiles. In contrast to the observation of the group of N. Kuhn who reported the nucleophilic substitution of SMe^- at the C2 atom of the imidazolium motif of 2-(methylthio)imidazolium salts with methyl lithium, the utilized furyllithium organyl selectively substituted the NHC under formation of the desired aryl sulfide **167**.[273]

However, different metalalkynyl reagents (metal = Mg, Zn, Li) were not reactive enough to form alkyne sulfides **177**, and sterically demanding Grignard reagents (e. g. mesitylmagnesium bromide) gave only traces of the desired product **178**. Unfortunately, the utilization of thiophenyl- and allylmagnesium bromide resulted in complex reaction mixtures.

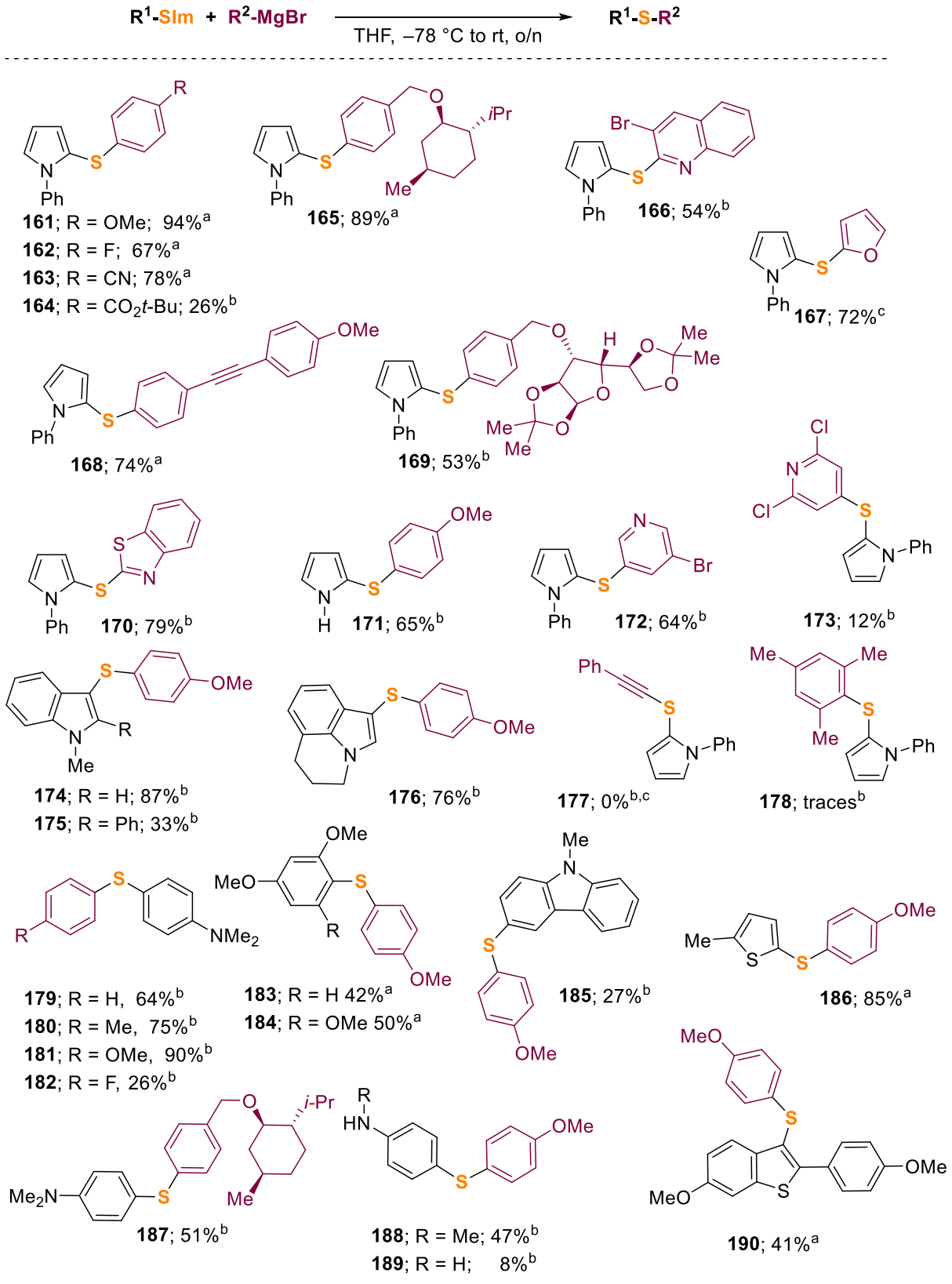

a: 1.5 equiv. RMgBr; b: 2.9 equiv. RMgBr; c:1.5 equiv. Li-R;

Scheme 92: Scope of diaryl sulfides.

In several cases (compounds **168**, **87**, **175**, **170**, **163** and **162**) X-ray crystallography confirmed the expected connectivity of the obtained sulfides. The representative crystal structure of **168** & **87** can be seen in Figure 23.

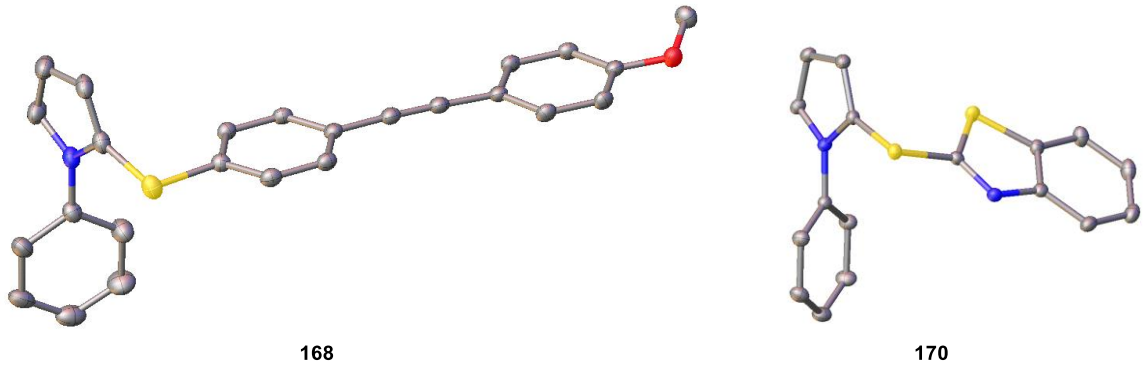

Figure 23: Molecular structure of compound of **168** and **170** Non-acidic hydrogen atoms and solvent molecules are omitted for clarity. Thermal ellipsoids are drawn at 50% probability level.

After several diaryl sulfides were successfully synthesized it could be shown, that alkyl aryl and alkenyl aryl sulfides were also accessible by the developed methodology with yields up to 93% (Scheme 93). From the synthetic point of view, the introduction of alkenyl groups as in compounds **193**, **195**, **196** and **200** is of immense interest, because they are potential precursors for the formation of new C=C double bonds by alkene metathesis reaction.[80] Additionally, double bonds can be functionalized by bromination[274], epoxidation[275], aziridination[276] and other chemical transformations[277] to allow the selective introduction of new functional groups into a structure. As already discussed above in the case of diaryl sulfide synthesis, also lithiumorganic nucleophiles like *sec*- or *tert*-butyllithium can be utilized for the synthesis of the desired alkyl aryl sulfide **197** and **192**.

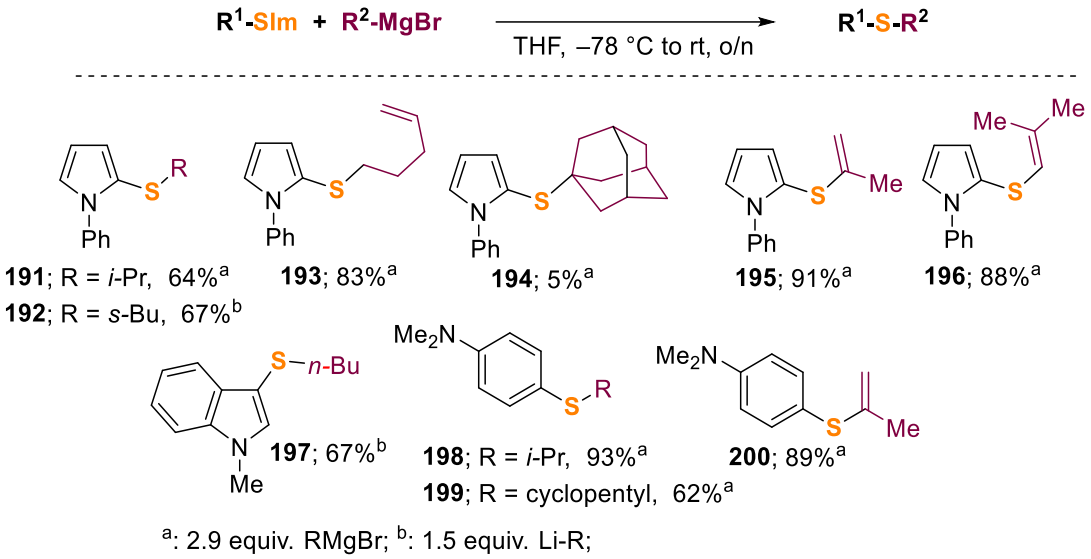

Scheme 93: Scope of alkyl and alkenyl aryl sulfides.

In addition to the mono-sulfenylations of *N*-phenylpyrrole resulting in thioethers **161** to **164** already described above (see Scheme 92), also the twofold sulfenylated species **88** was accessible by stepwise transformation of **161** with an overall yield of 61% (Scheme 94).

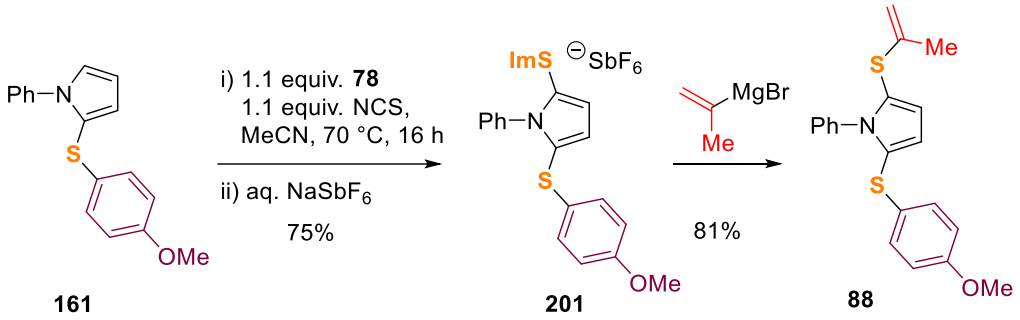

Scheme 94: Synthesis of twofold sulfenylated *N*-phenylpyrrole **88** via imidazolium salt **201**.

Having the established protocol for the sulfenylation of arenes and heteroarenes in hand, the potential of the methodology was demonstrated in the synthesis of the compound **87**, which is the precursor of the compound **151** (Scheme 95, **A**). Studies of R. Silvestri *et al.* have shown that **151** is a potent inhibitor of tubulin assembly and therefore a potential candidate for the treatment of cancer.[11,12] Upon sulfenylation of the indole derivative **203**, the corresponding imidazolium chloride **117** precipitated from the reaction mixture and was obtained in good yield of 79%, as already shown in Scheme 85. Subsequent reaction of **117** with an excess of phenylmagnesium bromide gave access to precursor **87**, whereas lowering the quantity of Grignard reagent to 3.5 equivalents decreased the yield significantly to 35% (Scheme 95, **B**).

Attempts to obtain the tubulin inhibitor **151** starting from ethyl ester **204** failed, since the reaction of nearly quantitatively isolated intermediate **118** with Grignard reagent resulted in the formation of several by-products, most probably due to the reaction of the ester functionality with the Grignard reagent. Noteworthy, the sulfenylation of **190** with an overall yield of 49% starting is superior to the sulfenylation step in the work of R. Silvestri cited above, who reported a lower yield of 35% for the sulfenylation of **204** utilizing *N*-thiophenylsuccinimide and equimolar amounts of boron trifluoride diethyl etherate.[11]

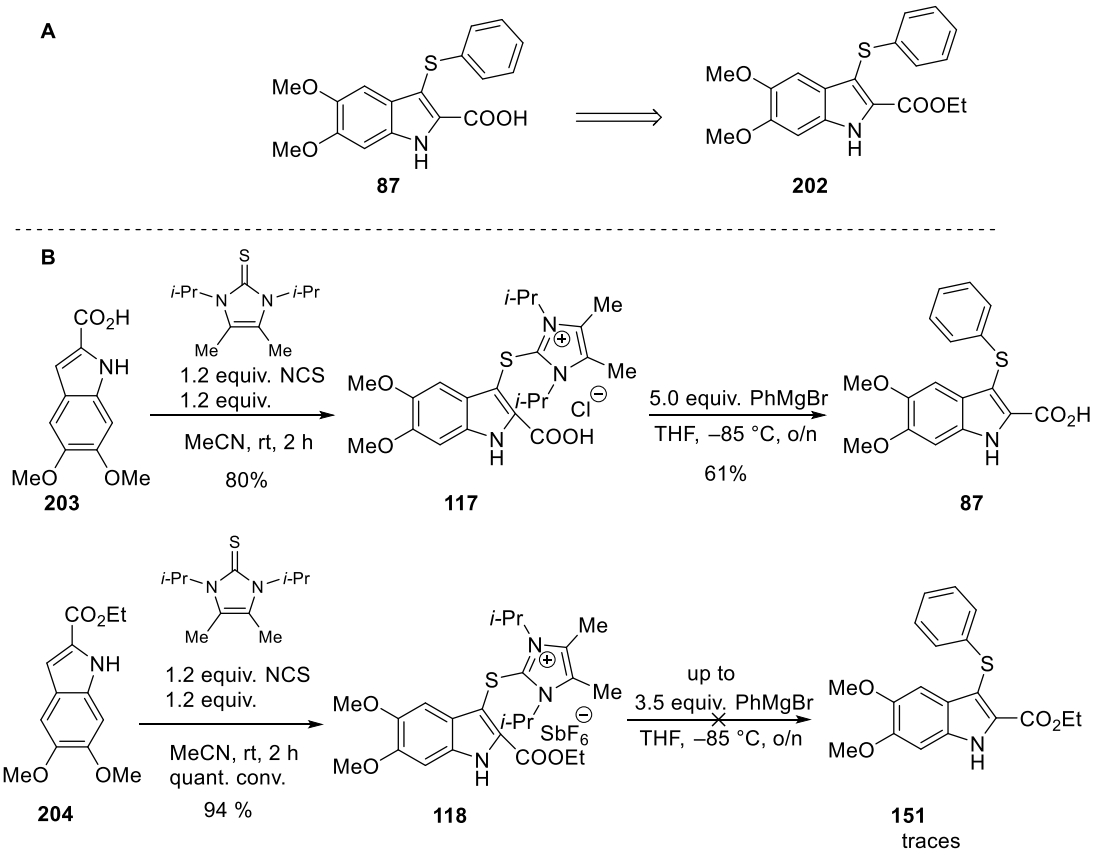

Scheme 95: A: Approach to potent inhibitor of tubulin assembly **151** by esterfication of precursor **87**; B: Preparation of precursor **1141** and attempted synthesis of **151**.

The connectivity of the obtained imidazolium salts **117**, **118** and of compound **87** was verified by X-ray diffraction of single crystals (Figure 24).

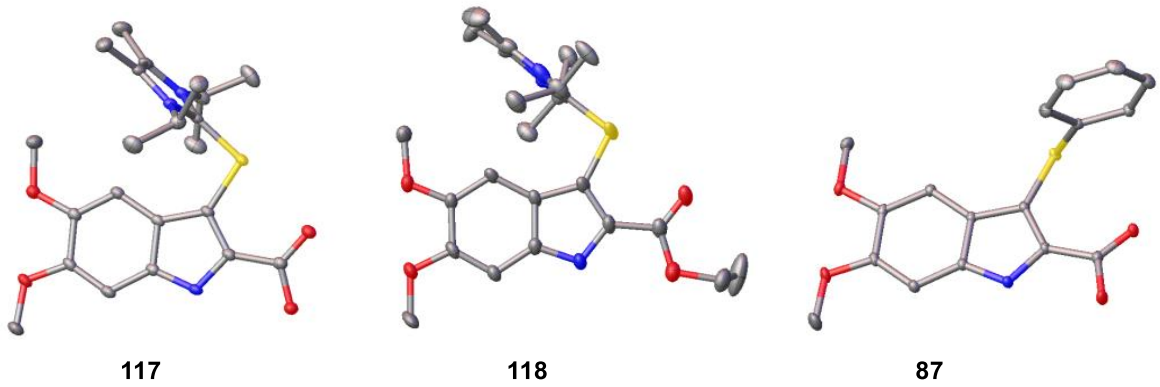

Figure 24: Molecular structure of imidazolium salts **117** and **118** and precursor **87** in the crystal. Non-acidic hydrogen atoms, anions and solvent molecules are omitted for clarity. Thermal ellipsoids are drawn at 50% probability level.

3.6 Investigations towards triazole-based reagents

Since the release of the imidazole-derived NHC carbene is the key step in the formation of diaryl sulfides (compare Scheme 91), it was envisaged that changing from the imidazole-based backbone to the 1,3,4-triazole analogue might enable the utilization of softer nucleophiles like zincates.

When the imidazolium cation **205** is considered as an adduct **206** of an imidazole NHC carbene and a $^{+}$SR fragment, the utilization of a 1,3,4-triazole NHC carbene adduct **207** should led to a weaker sulfur-carbon bond (Scheme 96). This is assumed since 1,3,4-triazole carbenes exhibit weaker σ-donor abilities based on Huynh´s electronic parameter (HEP) than their imidazole-derived counterparts.[278]

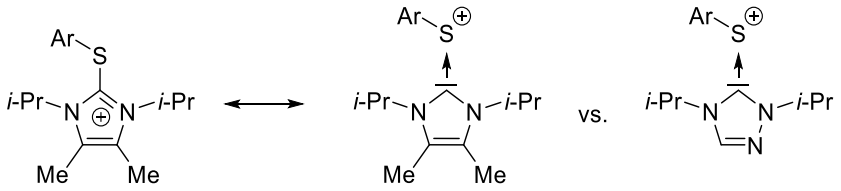

205 **206** **207**

Scheme 96: Mesomeric structures of imidazolium salt as covalent form (**205**) or adduct of σ-donating NHC carbene and cationic sulfide fragment $^{+}$SR (**206**)**:** comparison with envisaged 1,3,4-triazole carbene adduct **207**.

3.6.1 Synthesis of cationic triazolium intermediates

As the activation of imidazole-2-thione **78** via *in situ* oxidation with NCS was a well-established protocol, triazole-3-thione **209** was also oxidized with equimolar amount of NCS in the presence of different (hetero)arenes in DCM at room temperature (Scheme 97). After a subsequent anion exchange with a sodium hexafluoroantimonate solution, the triazolium salts **210** and **211** were purified by flash column chromatography. The yield of the sulfenylation of *N*-phenylpyrrole **98** (64%) was nearly equal to those of sulfenylation with the imidazolium chloride-based reagent **91** (60%).

Interestingly, 1,3-dimethoxybenzene (**208**) is known as a weaker nucleophile than pyrrole derivatives, as reported by the group of H. Mayr and co-workers.[279] Despite this, the triazolium salt **211** was obtained in moderate yield even when the counterion in the *in situ* formed triazolium-derived sulfenylation reagent was a chloride anion. In contrast to this, the imidazolium chloride-derived reagent **91** gave only traces of the desired product, wherefore the more reactive imidazolium hexafluoroantimonate-derived reagent **93** was used.

Nevertheless, the sulfenylation of very weak nucleophiles like 2,6-dimethylanisole (**212**) was not successful, as only traces of the corresponding triazolium salt **213** have been obtained.

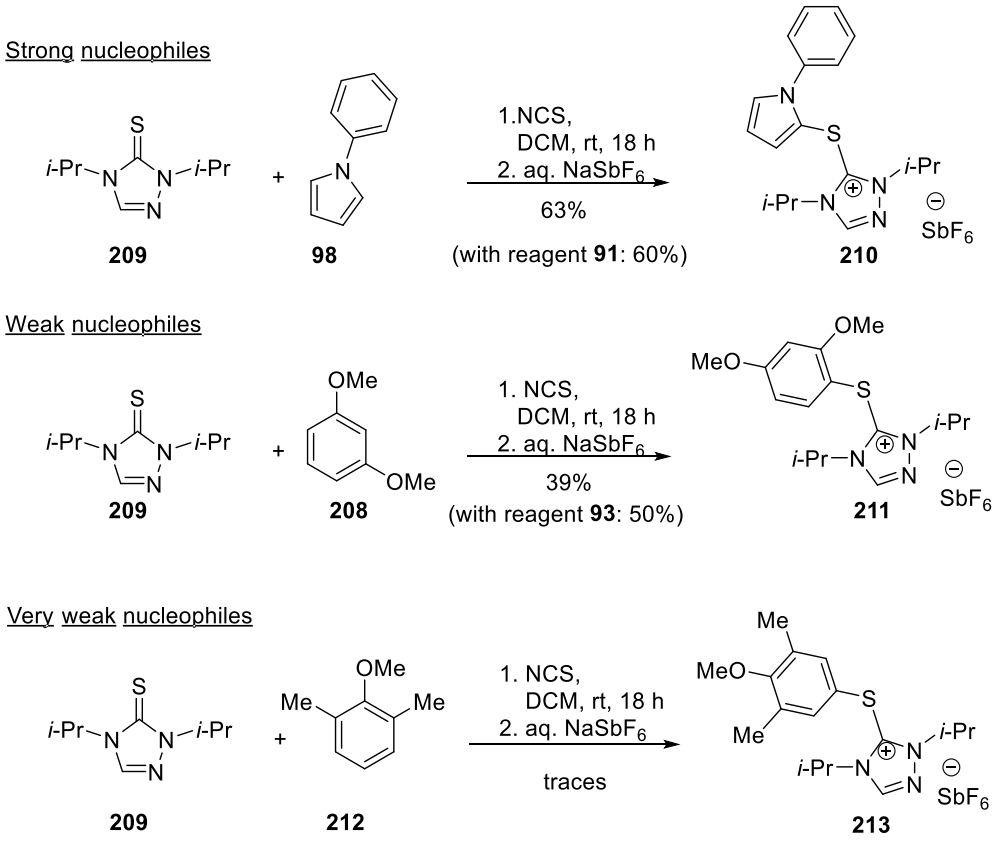

Scheme 97: Synthesis of triazolium salts **210** and **211**.

The expected structural connectivity of triazolium salt **210** was confirmed by X-Ray diffraction experiments of suitable single crystals (Figure 25). Similarly to the imidazolium salt **99**, the structure of the triazolium salt **210** shows an angular geometry around the sulfur atom S1 and almost the same C1–S1 bond length of 1.752(3) Å, as compared to 1.7495(9) Å in **99**.

Therefore, a similar reactivity towards Grignard reagents of both imidazolium and triazolium salts **99** and **210** might be expected.

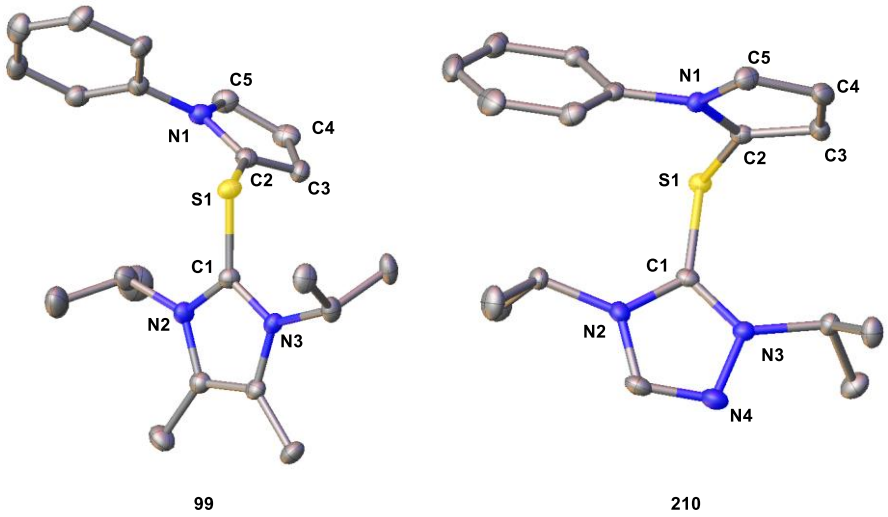

Figure 25: Structures of imidazolium (**99**) and triazolium (**210**) salts in the crystals. Hydrogen atoms, anions and solvent molecules are omitted for clarity. Thermal ellipsoids are drawn at 50% probability level.

3.6.2 Reactivity of triazolium intermediates

With the adduct of *N*-phenylpyrrole **210** in hand, its ability to form aryl sulfides with Grignard reagents or zinc organyls was tested (Scheme 98). As expected, the reaction of triazolium salt **210** with *para*-methoxyphenylmagnesium bromide resulted in the formation of the desired aryl sulfide **161** in comparable yield (83%) as reaction of the imidazolium analogue **99** (92%). Unfortunately, organozincates appeared to be still not strong enough as nucleophiles to release the 1,3,4-triazole carbene, as the reaction of **210** with (4-methoxyphenyl)zinc bromide gave only small amounts (4%) of the aryl sulfide **161**.

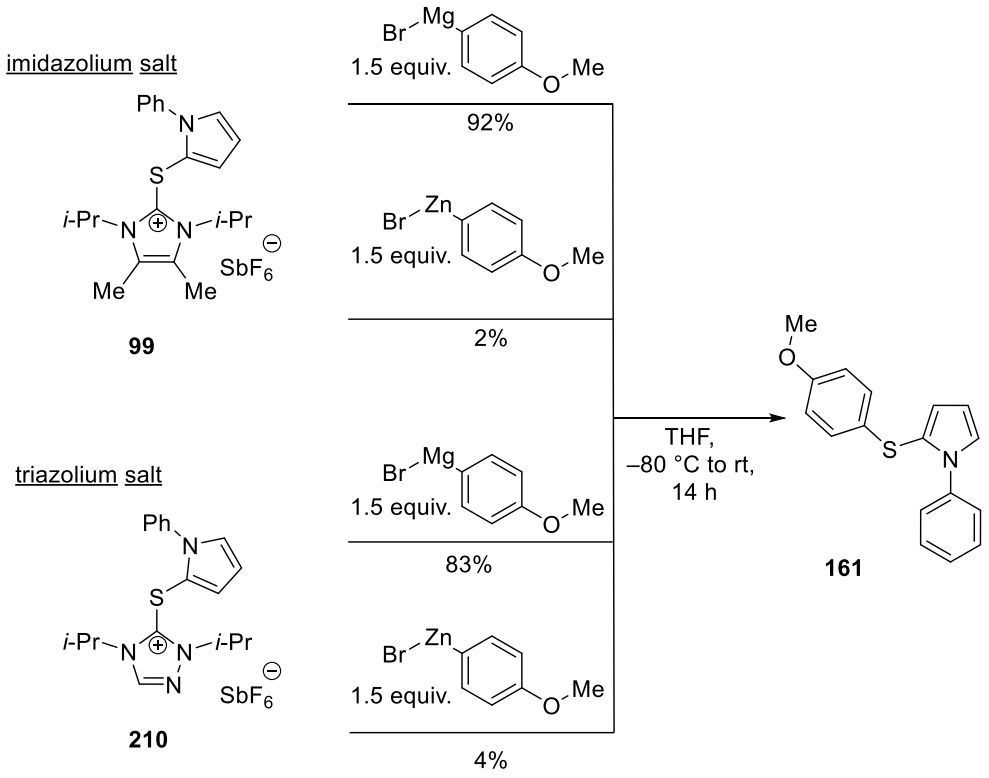

Scheme 98: Comparison of the reactivities of imidazolium and triazolium salt **99** and **210** in the reaction with metalorganic reagents.

In cases where less nucleophilic magnesium organyls like (4-fluorophenyl)magnesium bromide were used, the triazolium salt **210** did not show any advantage over the imidazolium analogue **99** (Scheme 99).

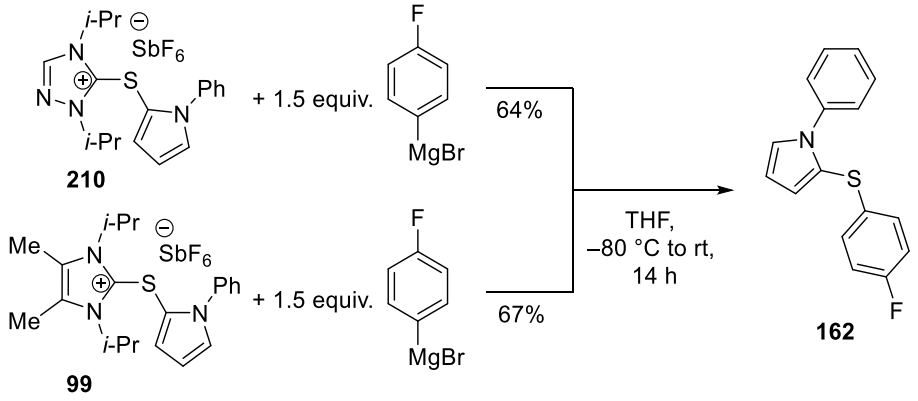

Scheme 99: Synthesis of arylsulfide **162** from triazolium (**210**) and imidazolium (**99**) salts.

All in all, the change from the imidazole backbone **78** to a 1,3,4-triazole-derived backbone **209** in the sulfenylation reagent did not result in significant reactivity benefits of the corresponding salts, as they also require strong nucleophiles as Grignard reagents for the formation of arylsulfides under release of the 1,3,4-triazole carbene.

Small advantages of the triazole-based sulfenylation protocol, like lowering the reaction temperature for the sulfenylation step of (hetero)arenes from 70 °C to rt, do not legitimate the change of the backbone, as the well-established imidazole-2-thione **78** is readily accessible by simple condensation of acetoine with diisopropylthiourea,[280] whereas triazole thione **209** requires a multistep synthesis from cheap commercially available starting materials.[281]

3.7 Extension of the synthetic protocol towards the preparation of unsymmetrical diarylselenides

After the successful evaluation of the developed protocol for the synthesis of several aryl sulfides, it was envisaged to extend the method to the preparation of diaryl selenides. Diaryl selenides have attracted great attention in recent years, because they are known to catalyze important transformations like, for example, the chloroamidation of alkenes with nitriles utilizing *N*-chlorosuccinimide (NCS) as a halogen source.[282] Additionally, diaryl selenides have been employed in the functionalization of alkynes e. g. in trifluoromethylthiolation reactions.[283] Further diaryl selenides show antitubulin and anti-Alzheimer activities as well as they are active 5-lipoxygenase inhibitors, too.[284]

To obtain the selenium analogue of sulfenylation reagent **91**, selenourea **159**, prepared according to published by N. Kuhn *et al*.[285] protocol, was oxidized with NCS in acetonitrile (Scheme 100). The isolated reagent **214** was obtained quantitatively as light orange solid and could react with electron-rich (hetero)arenes to give access to the cationic selenides **215** to **217** in good yields. In contrast to the cationic sulfide intermediates, compound **215** to **217** were only moderately stable at air and needed to be stored for longer times at –20°C. Presumably, the isolated cationic selenoether tend to get oxidized more rapidly, as they afford selenones faster than sulfones are formed from sulfides.[286] Fortunately, studies revealed that succinylselenoimidazolium chloride **214** does not need to be prepared and isolated in advance, as it could also be formed *in situ* from **159** and NCS in the presence of the arenes.

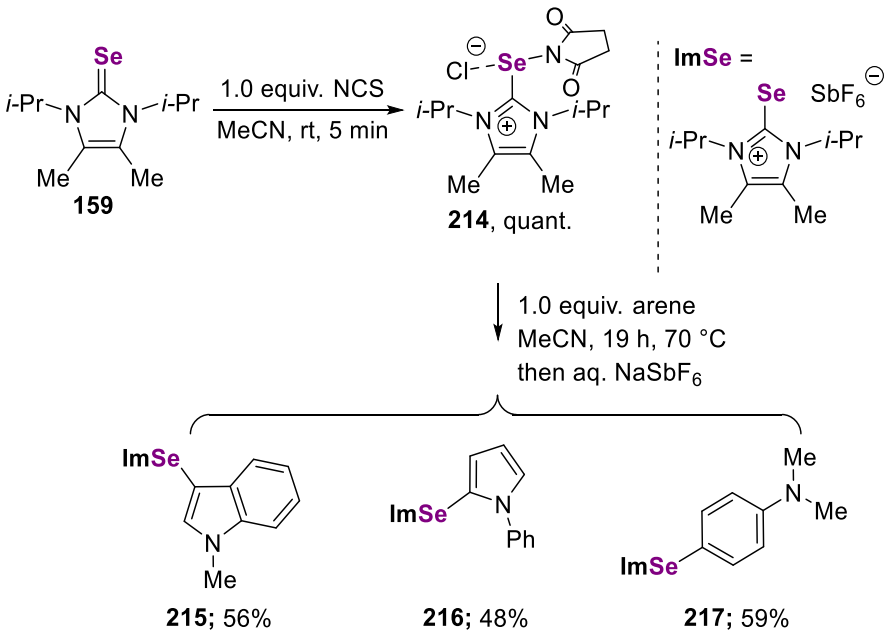

Scheme 100: Synthesis of selenylation reagent **214** and scope of the electrophilic C-H sulfenylation of different electron-rich (hetero)arenes.

To proof the expected connectivity in this completely new compound class, single crystals for X-ray analysis of **217** were obtained by slow diffusion of diethyl ether into a dichloromethane solution of the compound.

As expected, the selenium-carbon bonds of **217** are significant longer [Se1–C1, 1.896(3) Å; Se1–C2, 1.914(4) Å] than the corresponding sulfur-carbon bonds [S1–C1, 1.751(3) Å; S1–C2, 1.775(3) Å] of the isostructural **129** and are in agreement with typical single bond length between those elements (Se–C, 1.970 Å) (Figure 26).[266] The selenium-centered angle C2−Se1−C1 of 99.8(2)° is smaller than the observed sulfur-centered one C2−S1−C1 in **129** [103.3(3)°]. This can be explained by the decreased tendency of heavier atoms towards hybridization in a group.

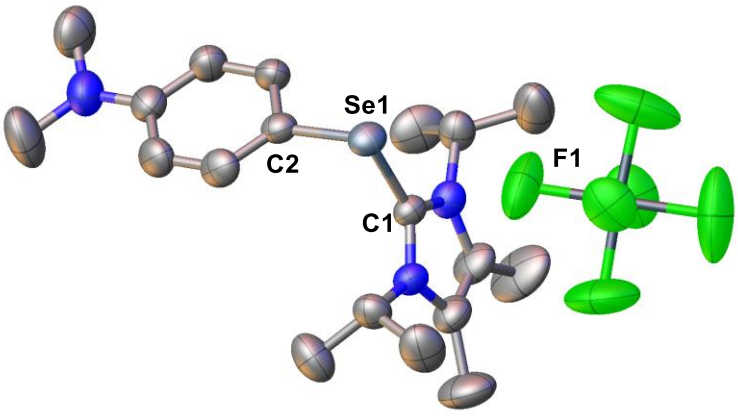

Figure 26: Molecular structure of compound **217**. Hydrogen atoms and solvent molecules (DCM) are omitted for clarity. Thermal ellipsoids are drawn at 50% probability level.

The strong interaction between the hexafluoroantimonate and the cationic selenide in **217** can also be visualized with the Hirshfeld surfaces of **217** (See Figure 27, **A**).[287] The contact between the fluorine atom F1 of the hexafluoroantimonate and the Se1 in compound **217** is 1.025 Å shorter than the shortest sulfur-fluorine contact in **129** where no significant interaction between S–F is observable (See Figure 27, **B**). In contrast to **217**, the cationic sulfide in **129** exhibits close contacts between the *iso*-propyl groups and the SbF_6. Apart from crystal packing forces, the short Se–F contact can be rationalized as a chalcogenic interaction in which the F donates electron density into the sigma-hole of the cationic selenium center. This is in agreement with the nearly linear F1–Se1–C2 geometry of 165.6°.[257]

The selenium center is more polarizable; therefore, it has a more pronounced sigma hole than in the sulfur compound. This might be the reason why the sulfur compound is not “electrophilic” enough to exhibit such interactions with the poor donor hexafluoroantimonate. Such kind of sigma hole interaction of selenium compounds have been recently discussed in literature for nitrogen donors.[288] A similar chalcogen-fluoride interaction is not observed in case of the sulfur analogue **129**, hence the larger S–F distance. Considering the molecular orbitals, the σ* of the Se1–C2 is more diffuse than the S1–C2 bond which is in line with the observable reactivity of the imidazolium moiety as a leaving group.

The stronger chalcogen-fluoride-interaction are also in line with the calculated Mulliken charge, calculated on B3LYP(6-311++g(d,p)) level, whereas the charge of the chalcogen atoms in **129** (+0.33) is lower than in 217 (+0.42).

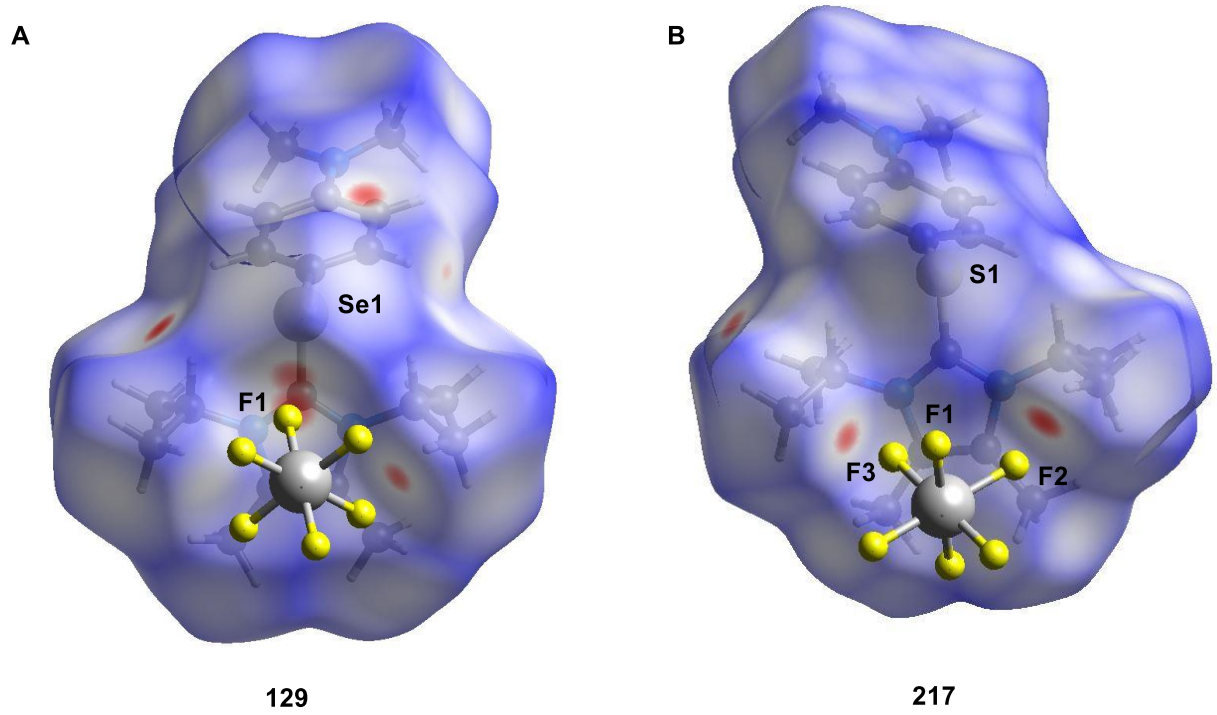

Figure 27: Hirshfeld surfaces of cationic sulfide **129** and of its selenium analogue **217**.

Gratifyingly and as expected, the cationic selenides **215** to **217** undergo reactions with aryl and alkenyl Grignard reagents in the same fashion as the cationic sulfides (compare Chapter 3.5). This gives access to selenides 218–**221** in good yields (Scheme 101). Compared to previously reported protocols of the group of A. L. Braga, no diselenide precursors and harsh conditions like elevated temperature (110 °C) or additional electrochemical equipment were necessary for the synthesis of these kind of electron-rich selenides.[289]

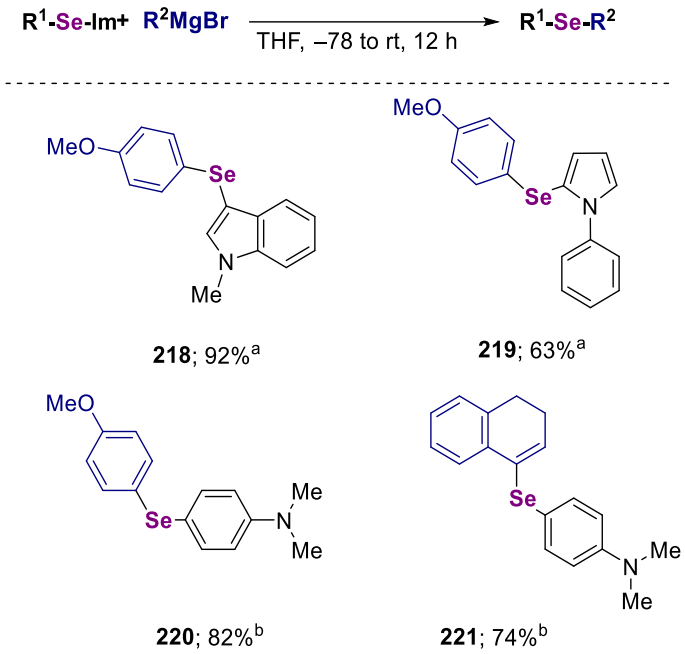

a: 1.5 equiv. R^2MgBr; b: 2.9 equiv. R^2MgBr

Scheme 101: Scope of aryl selenides.

Further attempts to expand the developed methodology to tellurides have not been attempted because of the toxicity of these compound class.[290]

3.8 Investigation towards a one-step synthesis of imidazolyl thioethers

After several diarylsulfides and selenides were successfully prepared, the synthesis of imidazole-containing aryl sulfides became a target of further research, since such sulfides show manifold applications in medicinal chemistry (Scheme 102). E. g. imidazolyl-sulfenylated aniline **222** shows a high pharmaceutical potential as a drug for the treatment of mycobacterium diseases,[291] and indole derivative **223** bearing an imidazolylsulfide moiety may have application in the treatment of prostaglandin D2-mediated diseases.[292]

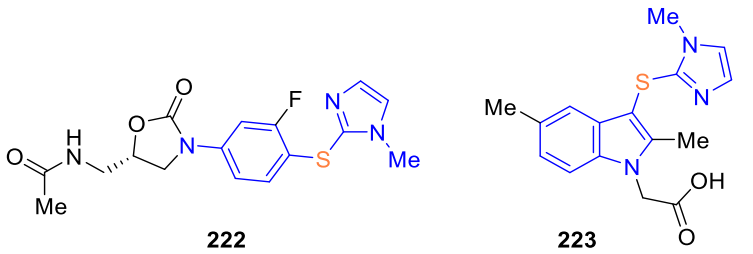

Scheme 102: Pharmaceutically active imidazolyl-sulfenylated arenes.

Traditionally, these imidazolyl sulfides of general structure **226** are mainly prepared by nucleophilic aromatic substitution of 2-chloroimidazoles **224** with arylthiols **225** (Scheme 103).[293] This can be challenging in cases of complex target molecules, as one building block has to be a free thiol **225**.

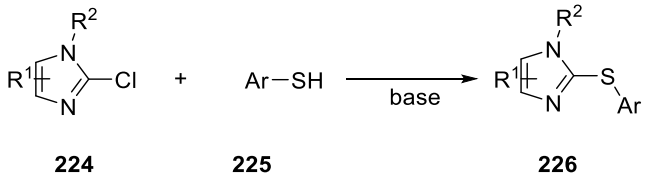

Scheme 103: Classical synthetic route to imidazolyl aryl sulfides **226**.

Following the procedure presented in Chapter 3.5, the synthesis of imidazolyl sulfide would require a two-step synthesis starting with the sulfenylation of arene **227** followed by utilization of imidazole Grignard reagent **229** to obtain the target structure **226** (Scheme 104).

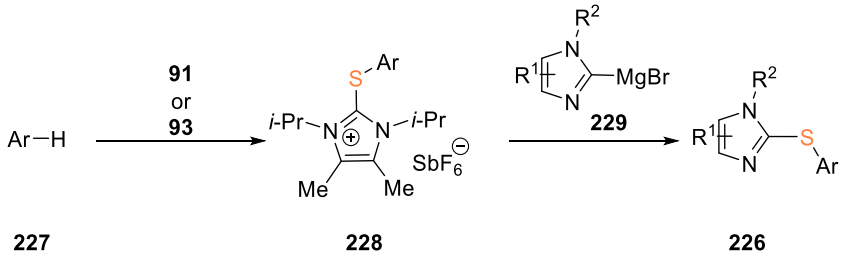

Scheme 104: Envisaged synthesis of imidazole-containing aryl sulfides **226** by the newly presented approach.

During the initial screening of different thiourea backbones (see Chapter 3.3, Scheme 83) it was found that Carbimazole **230**, the prodrug for Thiamazole (an antithyroid agent to treat hyperthyroidism[294]), did not give the envisaged cationic sulfide intermediate **106**. However, upon closer inspection, it turned out that the imidazolyl thioether **231** was formed in good yield of 82% (Scheme 105, **A**) as a white solid after purification (see Experimental Section). The formation of aryl sulfide **231** can be rationalized via the dealkoxycarbonylation of cationic sulfide intermediate **106** at elevated temperatures in the presence of residual water (see Scheme 105, **B**). The final decarboxylation step in the proposed mechanism might be accelerated due to the activation of the carboxyl group by the cationic imidazolium fragment.

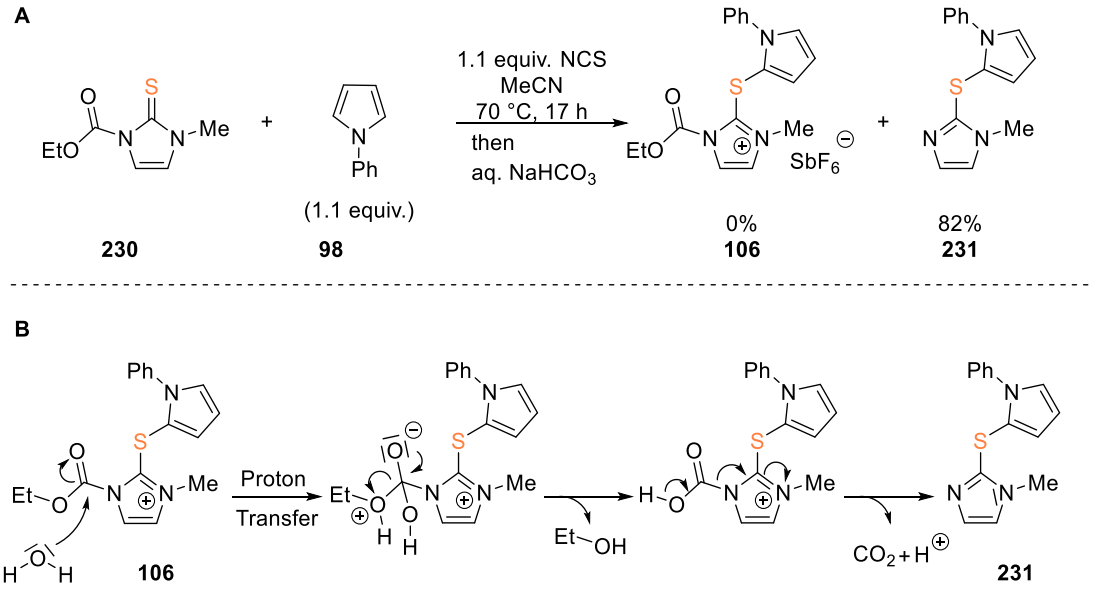

Scheme 105: **A**: Synthesis of imidazolyl sulfide **231**; **B**: Proposed mechanism of the decarboxylation of **106** to **231**.

In line with this observation, heating induced and silica gel-mediated dealkoxycarbonylation reactions of α-monosubstituted β-keto- and α-cyanoesters, have been recently reported by the group of M. Jaramillo-Gómez.[295] Since the unexpected reactivity of imidazole-2-thione **230** gave access to **231**, the generality of this methodology was tested with further arenes and heteroarenes as nucleophiles.

3.8.1 Synthesis and characterization of reagent 232

To investigate the mode of action of this serendipity-based observation and for the better understanding the mechanism of this transformation, the proposed intermediate reactive species **232** of the above discussed sulfenylation was synthesized by oxidizing carbamazole (**230**) with equimolar amounts of NCS in acetonitrile (Scheme 106). Since the obtained air sensitive yellow precipitate was insoluble in common solvents such as DCM, DCE and acetonitrile, the identity of reagent **232** was confirmed by X-ray crystallography.

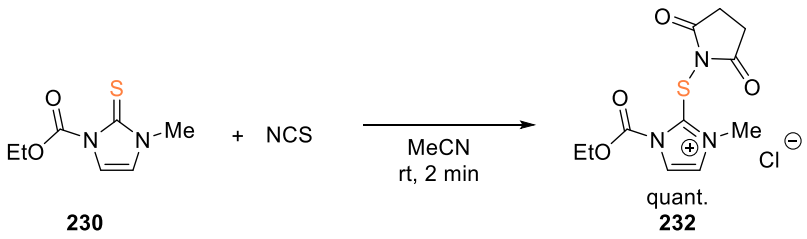

Scheme 106: Synthesis of sulfenylating reagent **232**.

Suitable single crystal for X-ray diffraction experiments of the poorly soluble sulfenylating reagent **232** were prepared by layering a solution of NCS in DCM over a Carbimazole **230** solution. By slow diffusion twinned crystals of **232** were obtained. The interaction of the positively polarized sulfur atom S1 and the nearest chloride anion Cl1 results in an average S1–Cl1 distance of 3.084 Å which is shorter than the sum of the atomic van-der-Waals-radii (3.55 Å) (Figure 28).[296] Similarly to sulfenylation reagent **91**, the structure of reagent **232** shows a short N1–S1 distance of 1.7184(17) Å which correlates to a single bond and a C1-S1-N1 angular of 98.26(8)°.

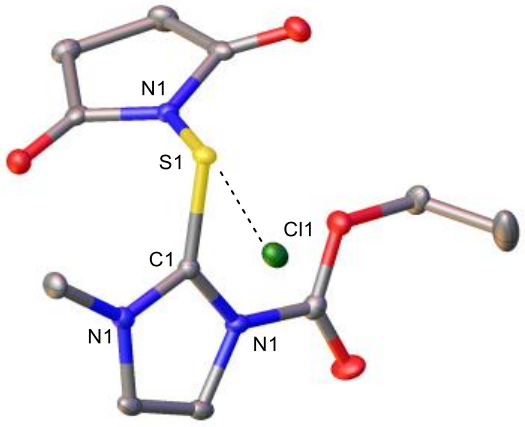

Figure 28: Molecular structure of **232** in the crystal. Hydrogen atoms and solvent molecules (DCM) are omitted for clarity. Thermal ellipsoids are drawn at 50% probability level.

3.8.2 Scope, limitation and application

The generality of this imidazolyl-drived sulfenylation was tested by the reaction with different electron-rich (hetero)arenes as nucleophiles (Scheme 107). *N*-Containing heterocycles like *N*-phenylpyrrole, substituted indole derivatives as well as lilolidine were transformed into the corresponding imidazolyl sulfides **231**, **233**, **234** and **235**, respectively, in moderate to good yields of up to 89%. Even the sulfenylation of ethyl 5,6-dimethoxyindole-2-carboxylate gave thioether **236** in good yield of 60%. Remarkably, also arenes with electron-donating substituents like aniline, *N*,*N*-dimethylaniline and trimethoxybenzene were sulfenylated affording **238**, **237** and **239**, respectively, in moderate to good yields. Additionally, the antipruritic and first-generation antihistamine Phenbenzamine, which is utilized in the treatment of hay fever, asthma and urticarial,[297] was functionalized affording **86** in moderate yields of 31%. Contrary to this, the sulfenylation of methylaniline resulted in the formation an inseparable mixture of the desired thioether **240A** and the corresponding cationic intermediate (**240B**). The **240A/240B** ratio remained unchanged even after prolonged heating of the mixture in MeCN solution. Surprisingly, the sulfenylation of pyrrole gave solely the corresponding cationic intermediate **241**.

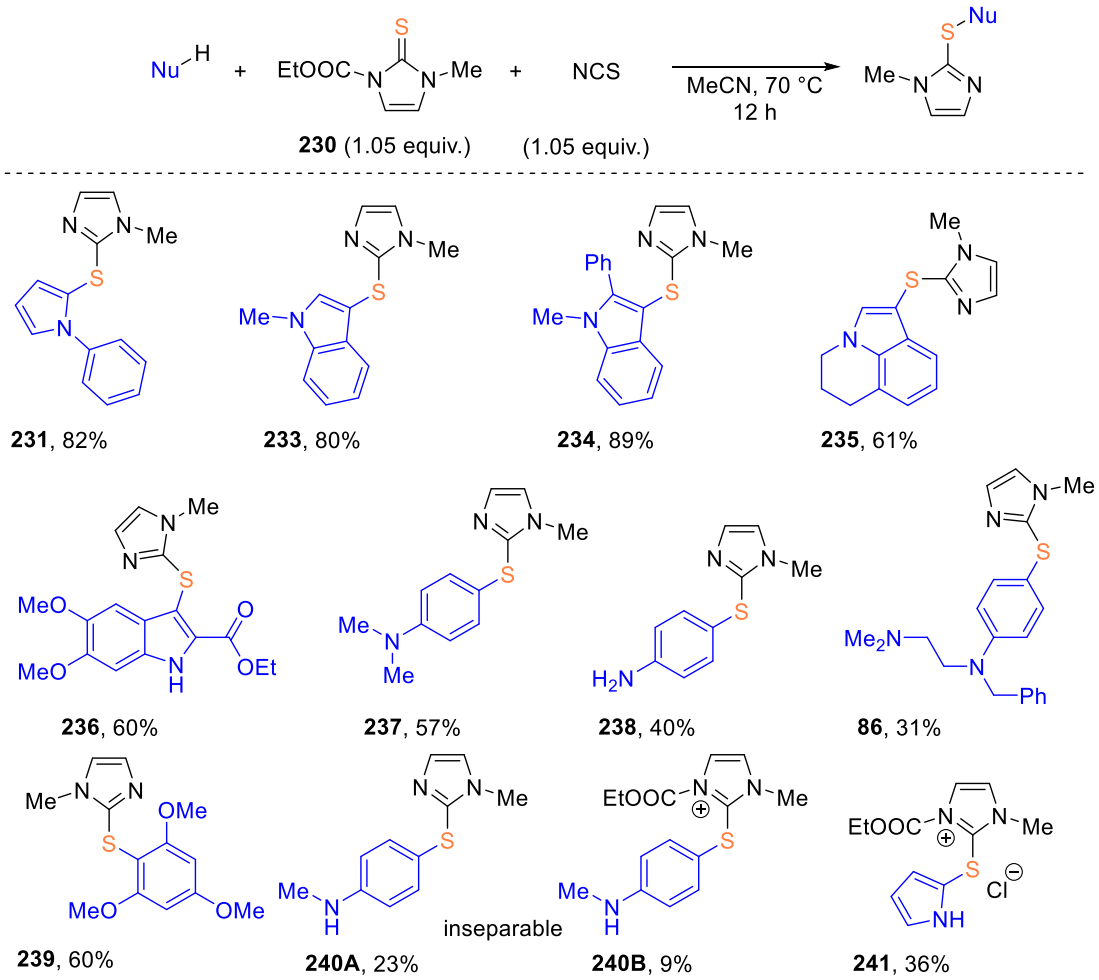

Scheme 107: Scope of the -sulfenylation with *in situ* generated reagent **232**.

The structural identity of selected products was verified by X-ray diffraction experiments. Suitable single crystals were grown by slow evaporation of saturated solutions of either the compounds or crude reaction products in DCM. The molecular structures are presented in Figure 29. The average C–S–C angle of the crystalized species ranged between 100.68(5)° for **237** and 103.89(9)° for **235** and is therefore bigger than the carbon-sulfur-nitrogen angle of the reagent **232** [98.26(8)°].

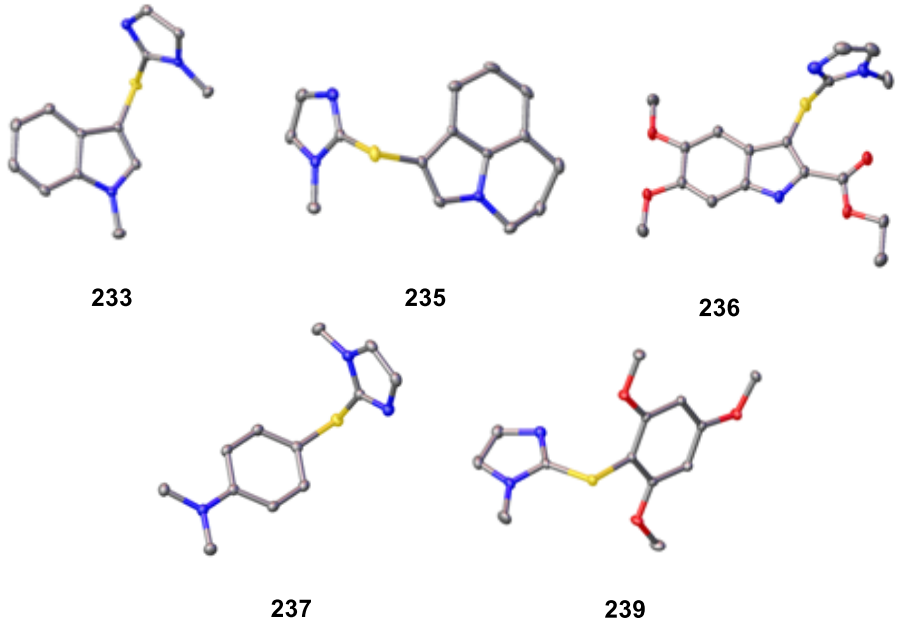

Figure 29: Molecular structures of the imidazolyl sulfenylated derivatives **233**, **235**, **236**, **237**, **239** in the crystals. Hydrogen atoms and solvent molecules (DCM) are omitted for clarity. Thermal ellipsoids are drawn at 50% probability level.

In contrast, the sulfenylated products from less activated arenes like dimethoxybenzene (**242**), less electron-rich heterocycles like benzothiophene derivative (**245**) and targets with carboxyl and hydroxyl functionalities (**244** & **243**) were not accessible by the protocol and only obtained in traces (Scheme 108). An insufficient electron density on the arenes remains still the main limitation of the protocol.

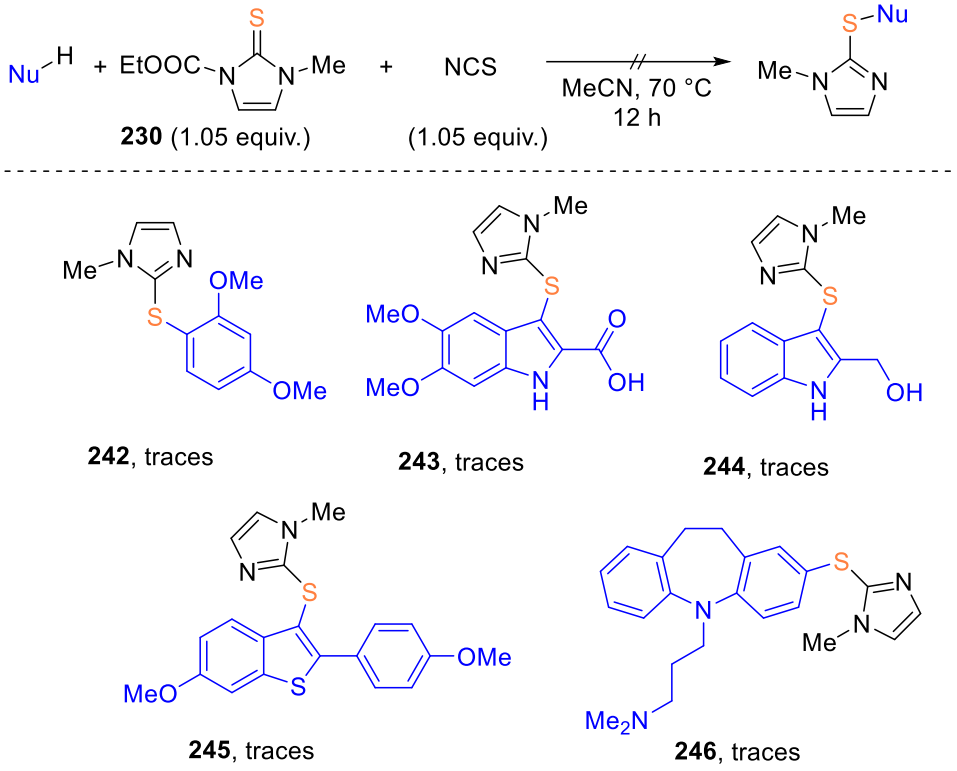

Scheme 108: Attempted sulfenylation reaction of highly functionalized and electron-poor targets.

To verify the necessity of the carbamatester functionality in the Carbimazole-derived reagent **232**, a control experiment with Thiamazole **247** as a sulfur-containing reactant was conducted (Scheme 109). The observation that only traces of the desired product **237** were obtained by this reaction as well as the previously discussed formation of the cationic intermediate **240B** and **241** support the hypothesis that **232** acts as the reactive reagent, even when the exact mode of the subsequent decarboxylation is still unknown.

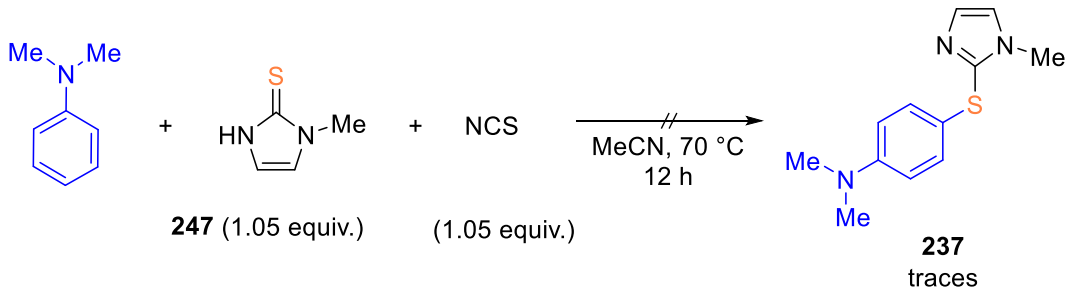

Scheme 109: Control experiment towards the formation of **237**.

3.8.3 Investigation towards the extension of the protocol to benzimidazolyl-, triazolyl- and benzoxazolylthioether

After the successful evaluation of the developed protocol for the synthesis of several imidazolyl arylsulfides with reagent **232**, it was envisaged to extend the method to the preparation of further heterocyclic sulfides. For this purpose, benzoxazole-2-thione **250**, benzimidazole-2-thione **251**and 1,2,4-triazole-3-thione **252** look to be suitable precursors for the synthesis of aryl sulfides of the general structure **249** (Scheme 110).

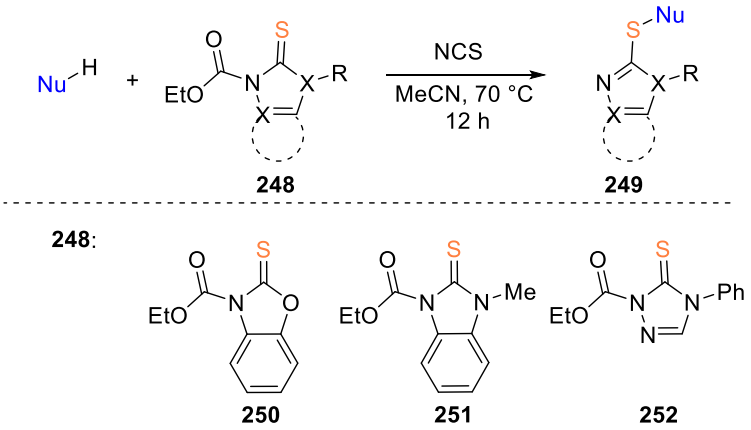

Scheme 110: Envisaged sulfur-containing precursors **250** – **252** for the synthesis of aryl sulfides of general structure **249**.

Imidazole-2-thione- (**251**) and benzoxazole-2-thione-derived (**250**) precursors were accessible by reaction of the corresponding and commercially available benzimidazole-2-thione (**253**) and 2-mercaptobenzoxazole (**254**), respectively, with ethyl chloroformate following a modified protocol of S. Dove *et al*. (Scheme 111).[298] The desired ethyl carbamates were obtained in moderate yields of 33% and 45%, respectively. Since the spectroscopical analysis of the obtained compounds did not allow the differentiation between the conceivable *S*- and the desired *N*-protection of the utilized starting materials, single crystals suitable for X-ray diffraction experiments of compound **250** were grown by slow evaporation of its saturated DCM solution. The molecular structure verified the expected connectivity of the addressed constitutional isomer.

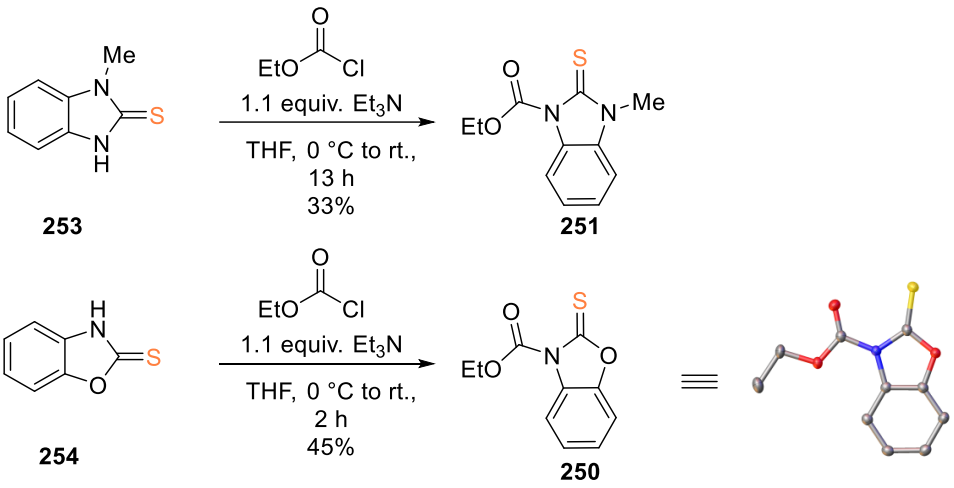

Scheme 111: Synthesis of compound **251** and **250**. Crystal structure of **250**: Hydrogen atoms and solvent molecules are omitted for clarity and thermal ellipsoids are drawn at 50% probability level.

4-Phenyl-1,2,4-triazole-3-thione (**252**) was synthesized according to a modified protocol of M. K. Bharty, N. K. Singh *et. al.*[299] starting with the formation of 1-formyl-4-phenyl-3-thiosemicarbazide (**257**) from phenyl isothiocyanate (**255**) and formic acid hydrazide (**256**) (Scheme 112). The obtained semicarbazide **257** was cyclized under basic conditions to give 4-phenyl-1,2,4-triazole-3-thione (**258**) in acceptable yield of 47% over two steps. Subsequent formation of the desired ethyl carbamate functionality by reaction of triazole **258** with ethyl chloroformate gave the desired 1,2,4-triazole-3-thione **252** in moderate yield of 57%.

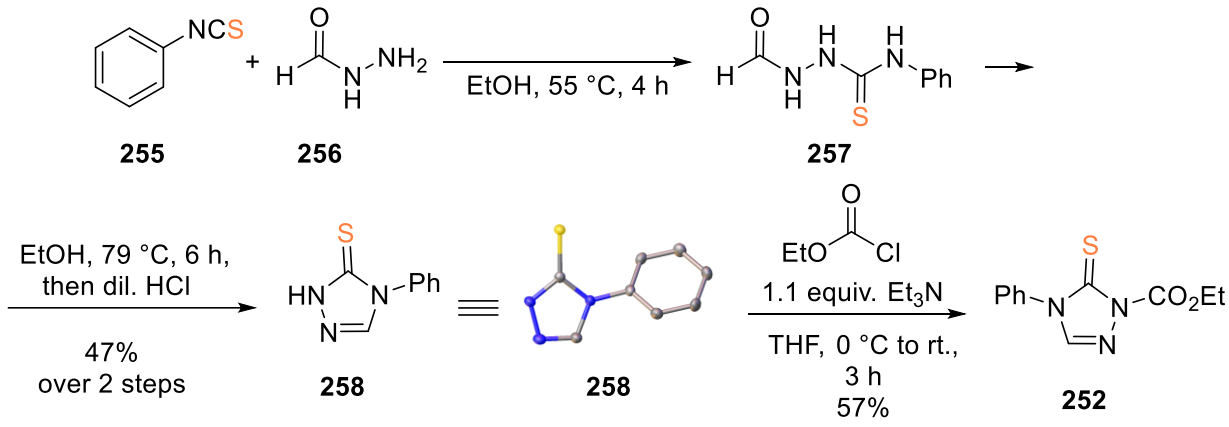

Scheme 112: Synthesis of compound **252**.

Having the sulfur-containing precursors **250** – **252** in hand, the sulfenylation of dimethylaniline was attempted to proof the transferability of the method from simple imidazolyl sulfides (see Chapter 3.8.2) to further heterocycles. In all cases, the sulfur-containing precursors were *in situ* oxidized with NCS.

Unfortunately, only small amounts of the desired thioether **259** and **260** were obtained from complex reaction mixtures by purification with flash column chromatography (Scheme 113). Both compounds were strongly tailing on during the purification attempts, either because of low solubility or decomposition caused by silica gel. For analytical purposes, an additional HPLC separation was necessary. In the case of 1,2,4-triazole, only traces of aryl sulfide **261** were detectable by mass spectrometry, but neither significant amounts of pure product nor residual starting materials were obtained. The sulfenylations of *N*-phenylpyrrole (**98**) gave only traces of benzoxazolyl thioether **262** and minor yields of triazolyl derivative **263**. Due to disappointing initial results, no further sulfenylation attempts with other nucleophiles were performed.

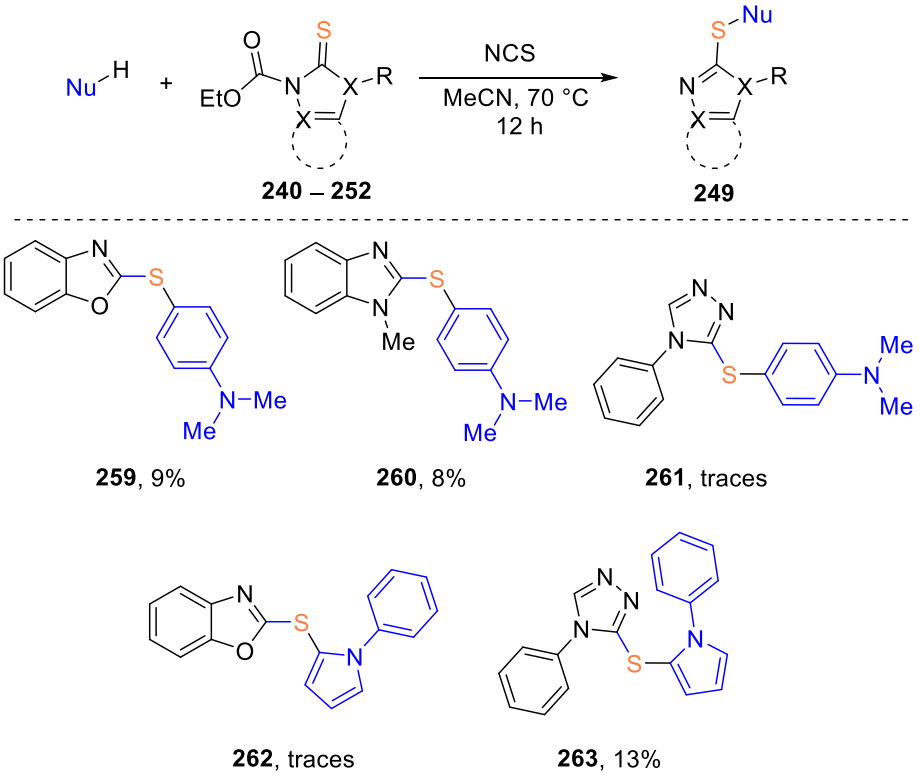

Scheme 113: Attempted sulfenylations of dimethylaniline and *N*-phenylpyrrole with sulfenylating reagents **250** – **252**.

3.9 Investigation towards potential sulfonthioamidation reagents

After the potential of imidazole-2-thione-based sulfenylation reagents was extensively studied and evaluated, reagents of the general structure **264** were synthesized and their reactivity towards the formation of different *N*-(alky/arylthio)sulfonamides **265** was investigated (Scheme 114). As the known cationic intermediate **248** can be considered as a CS^+ synthon, the general structure **264** is envisaged to act as a NS^+ synthon.

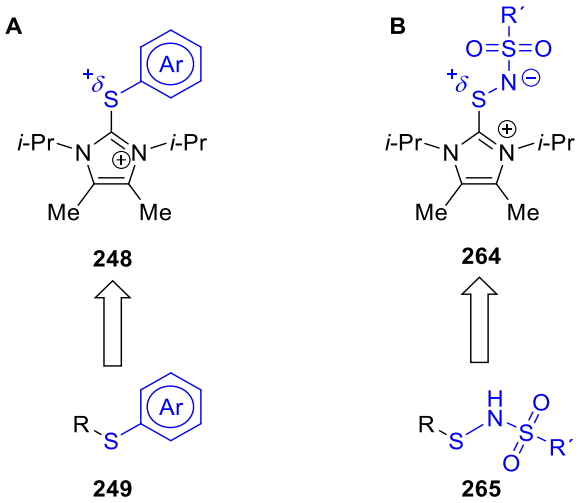

Scheme 114: Concept of a potential reagent **264** for the synthesis of *N*-(alky/arylthio)-*p*-tosylsulfonamides **265**.

These sulfonamides are of synthetic value. Thus, *N*-trifluoromethylthiosulfonamide **266** can be used for the α-trifluoromethylthiolation of simple ketones/aldehydes[300] and arenes[301] or for the chelation-assisted palladium-catalyzed trifluoromethylthiolation of C–H bonds[302] (Figure 30). The cyclic sulfenamide **267** is a valuable reagent as well, as it can be used as highly reactive synthon possessing electrophilic sulfur and nucleophilic nitrogen atoms. It can be applied for the synthesis of different *S*,*N*-heterocyclic scaffolds which have various applications in medicinal chemistry.[303] Since only a small number of these *N*-(alky/arylthio)toxylsulfonamides are known in literature they may hold distinct properties as pharmaceutical relevant compounds.

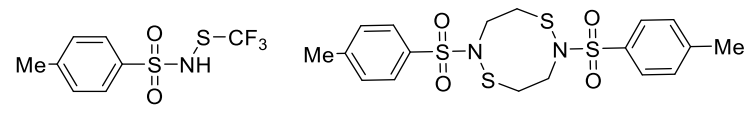

Figure 30: Applications of different alkylthio-*p*-tosylsulfonamides.

3.9.1 Synthesis of imidazole-derived sulfonthioamidation reagent 269

To start with, imidazole thione **78** was brominated with equimolar amounts of bromine resulting in the quantitative formation of dibromide **79** according to the published procedure[242] (Scheme 115; see also Scheme 76). Afterwards, **79** was treated with *p*-toluenesulfonamide (**268**) in the presence of DIPEA. After washing the reaction mixture with water to remove the additionally formed ammonium bromide salt, the reagent **269** was obtained in good yield of 86%

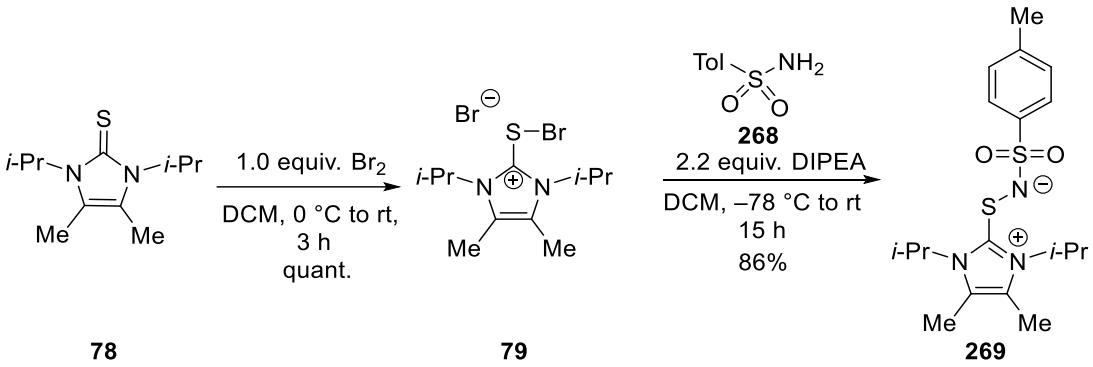

Scheme 115: Synthesis of the reagent **269**.

To get insights into the binding situation of compound **269** and to verify its identity, single crystals suitable for X-ray diffraction experiments were obtained by slow evaporation of a saturated DCM solution of **269**. As expected, **269** exhibits an angular geometry in the solid state structure with an C1–S1–N1 angle of 107.43(4)°and a narrow dihedral angle Φ(N1;C1;S1;N3) of 59.5° (Figure 31), Noteworthy, the angle is significant smaller than the dihedral angle of the sulfenylation reagent **91** (81.8°). Apart of packing effects this can be rationalized by the attractive interaction between the negatively charged nitrogen N3 (Mulliken charge: –1.1), which is more negative compared to that one of free *p*-toluenesulfonamide (–0.58), and the positively charged imidazolium nitrogen N1 (Mulliken charge: +0.68).[304] With the bond lengths of 1.7528(9) Å the for the S1–N3 bond and with 1.5944(8) Å for the S1–N3 bond. Both N–S bonds exhibits typical characteristics of corresponding single bonds [S–N: 1.710(19) and O_2S–N: 1.600(0.012) Å, respectively].[266]

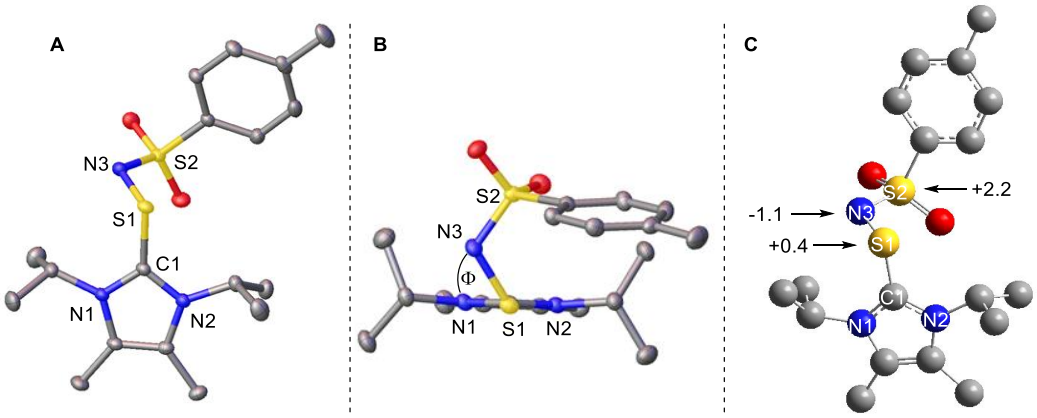

Figure 31: Crystal structure of compound **269** (side view **A** and top view **B**). Hydrogen atoms and solvent molecules are omitted for clarity and thermal ellipsoids are drawn at 50% probability level. **C**: Mulliken charges of compound **269** after optimization with DFT on b3lyp/311-g(d,p) level.

The significant negative charge on N3 resulted in highfield shifted ^{15}N-signal of –283.4 ppm in compound **269**.

3.9.2 Investigation towards reaction of 269 with different nucleophiles

Furthermore, the ability of different nucleophiles to release the imidazole NHC-carbene under the generation of *N*-[(hetero)arylthio]-*p*-tosylsulfonamides was investigated. No transfer of the thiosulfinimide or the *p*-toluenesulfonamide groups of **269** was observed in the initial attempts with electron-rich (hetero)arenes as nucleophiles (Scheme 116). Neither methylindole **270** nor dimethylaniline (**272**) led to the formation of the corresponding coupling products **271** and **273**, respectively, whereas the utilized (hetero)arenes were nearly quantitatively reisolated. In both cases only traces of the already known cationic sulfide **114** and **129** were isolated (compare Chapter 3.4).

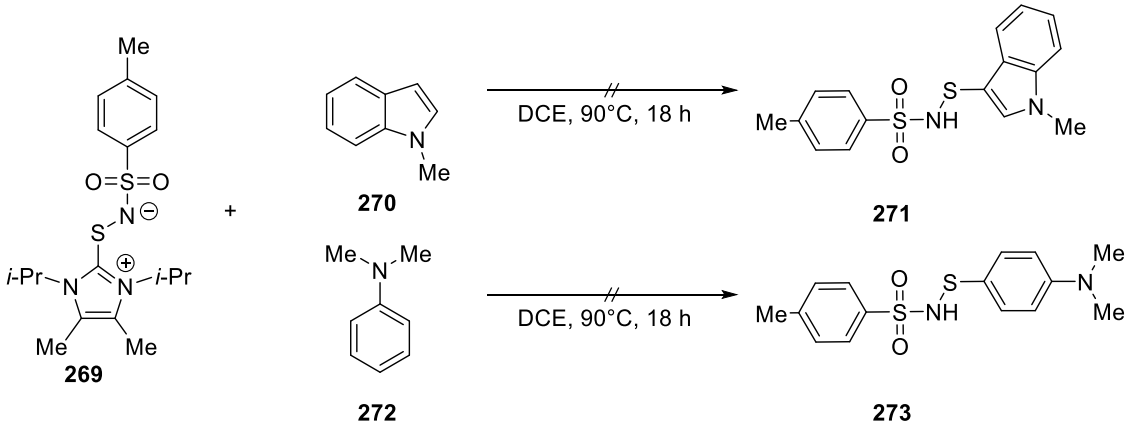

Scheme 116: Attempted thiosulfinimation of *N*-methylindole (**270**) and dimethylaniline (**272**).

The reaction with stronger nucleophiles like Grignards reagents may be more promising, as the latter gave good results with the previously discussed sulfenylation reagents (see Scheme 92). Surprisingly, the reaction of **269** with cyclopentylmagnesium bromide (**274**) resulted in the formation of different products (Table 11). In addition to the desired *N*-(cyclopentylthio)sulfonamide (**275**), *p*-toluenesulfonamide (**268**) and cationic sulfide **277** were formed. This indicates that compound **269** react via two different reaction pathways. In pathway A, the carbene acts as a leaving group leading to the formation of the envisaged product **275** in 20% yield (Entry 1), whereas in pathway B the *p*-toluenesulfonamide (**268**, $TosNH_2$) serves as leaving group furnishing species **277** as the product. Increasing the amount of Grignard reagent slightly favored the formation of toxylsulfonamide **275**, while addition of over stoichiometric quantity of LiCl for the complexation of nitrogen in the tosyl moiety showed no effect on the formation of **275** (Entries 2 & 3). In contrast to this, lowering the concentration of the reagents by factor four was non-beneficial, as the yield of **275** dropped to 12% (Entry 4).

Table 11: Optimization of the reaction conditions for the formation of 275.

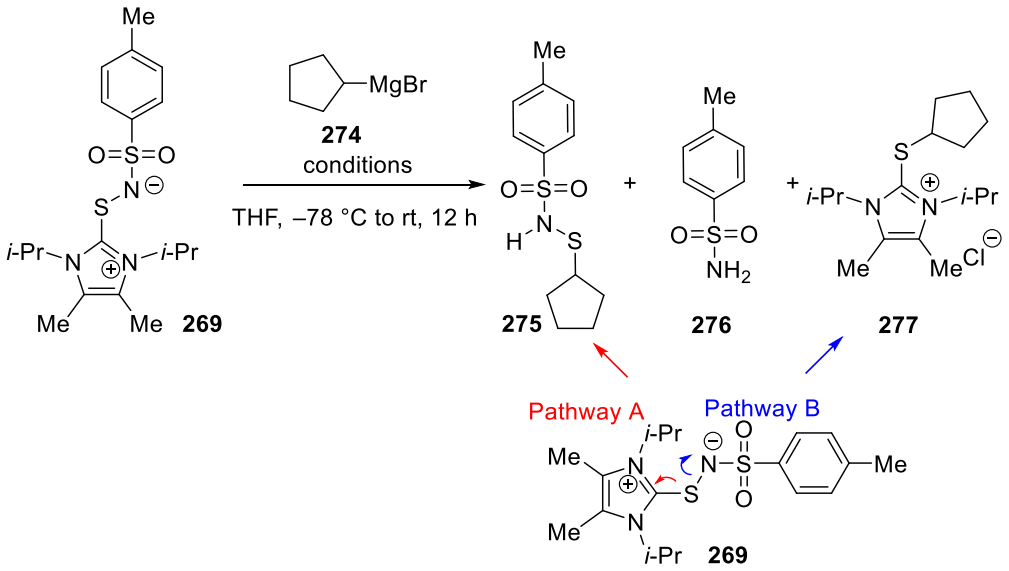

Entry	Equiv. **269**	c[**269**] /M	**275**	**268**	**269**
1	1.5	0.13	20%	27%	11%
2	3.0	0.13	31%	38%	19%
3	3.0 + 6 equiv. LiCl	0.13	31%	50%	27%
4	3.0	0.03	12%	54%	11%

To investigate if the reaction pathway A can be favored by thermodynamic control, the reaction temperature and time were varied (Table 12). When the reaction was continuously stirred at

–77 °C for two days and subsequently quenched with an aqueous ammonium chloride solution, **275** was obtained in 25% yield. Additionally, unreacted **269** was isolated in 7% yield. Increasing the temperature to –35°C significantly affect the outcome of the reaction (Entry 2). When the reaction was run at room temperature, pathway B was strongly favored, as nearly the quantitative amounts of the released *p*-toluenesulfonamide (**268**) have been isolated.

Table 12: Further optimization of the reaction conditions for the formation of **275**.

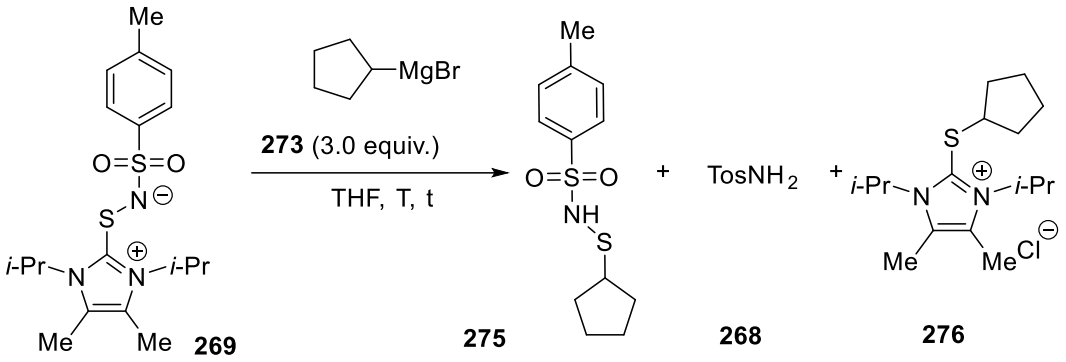

269 **275** **268** **276**

Entry	T	t	**275**	**268**	**269**
1	–77°C	2 d	25%	10%	7%
2	–35°C	2 d	39%	10%	nb
3	rt	1 d	0%	91%	0%

As a preliminary conclusion, three equivalents of Grignard reagent and a reaction temperature of –78 °C to rt over 12 h turned out to be the best possible reaction conditions.

To verify the structural identity of the previously unknown sulfonamide **275**, crystals suitable for X-ray diffraction experiments were grown by slow evaporation of a saturated solution in DCM of either the compound or the crude reaction product. The solid state structure of **275** is depicted in Figure 32.

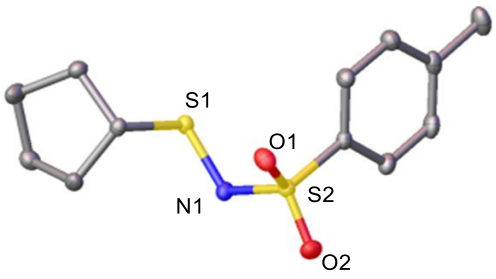

Figure 32: Structure of compound **275** in the crystal. Hydrogen atoms are omitted for clarity and thermal ellipsoids are drawn at 50% probability level.

After partial optimization of the reaction conditions for the sulfenylation reagent **269** using cyclopentylmagnesium bromide, **269** was treated with further strong nucleophiles to test the generality of the reaction (Scheme 117). Unfortunately, employment of neither *para*-methoxybenzyl Grignard reagent (**277**) nor isopropylmagnesium bromide (**280**) nor phenylethynyl-derived Jocić-Normant reagent **283** resulted in formation of noteworthy amounts of the envisaged coupling products **278**, **281** and **284**, respectively (Scheme 117 **A** to **C**). Instead, major amounts of *p*-toluenesulfonamide (**268**) and cationic species **279** and **282** were obtained indicating that the reactions proceeded mainly along pathway B. When slightly over-stoichiometric amounts of *n*-butyllithium (**285**) are utilized as nucleophiles, solely sulfonamide **268** was isolated from a complex product mixture (Scheme 117 **D**).

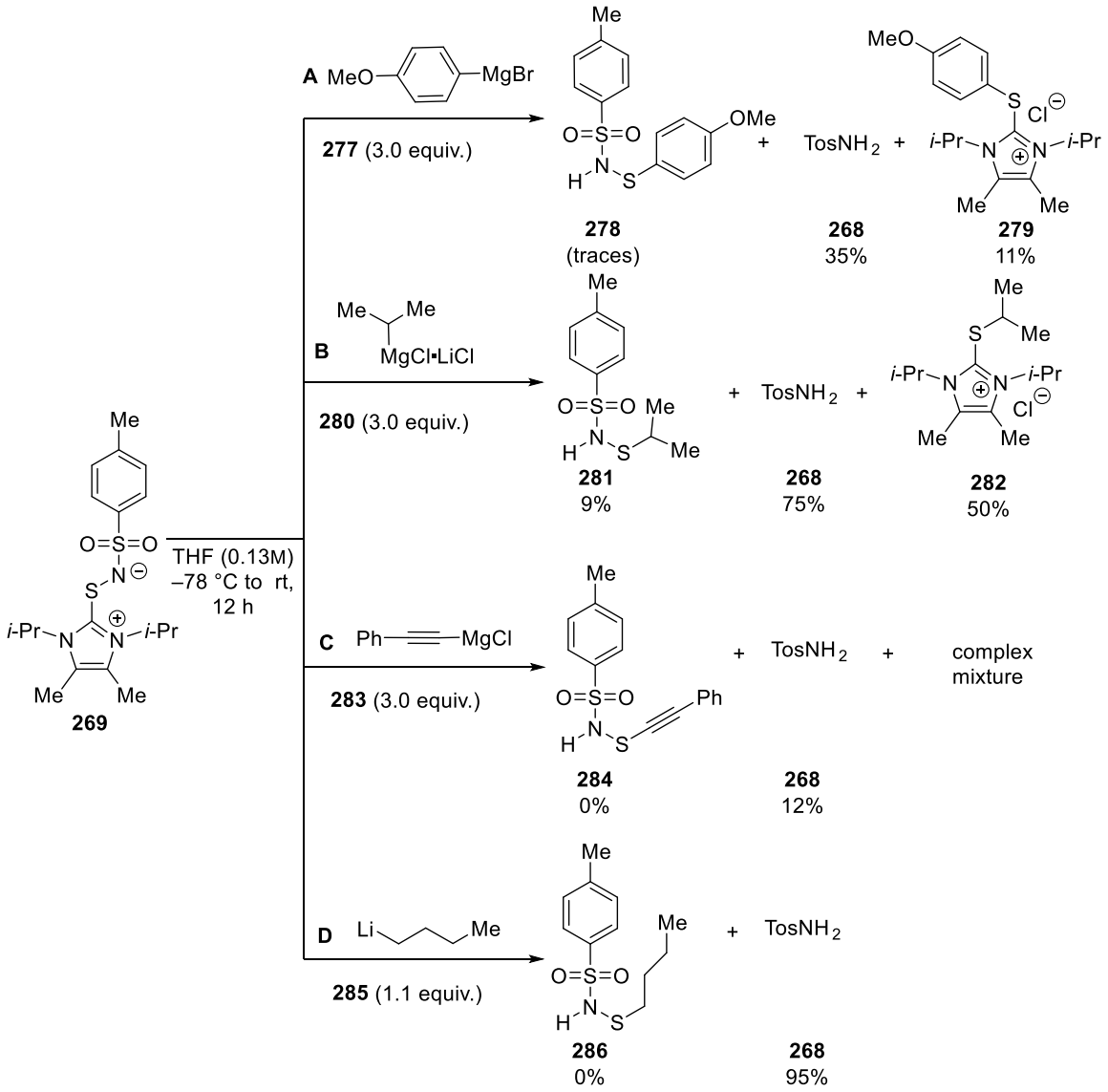

Scheme 117: Attempted scope of the thiosulfinimide transfer reagent **269**.

3.9.3 Synthesis and evaluation of triazole-derived sulfonthioamidation reagent

As discussed above (compare Chapter 3.6), the change of the sulfur-containing backbone from an imidazole to a triazole motif led to slightly better sulfenylation abilities, triazole reagent **288** was synthetically targeted. Therefore, the triazole-derived reagent **288** was obtained as a white foam from brominated 2,4-diisopropyl-1,2,4-triazole-3-thione **287** in the presence of *p*-toluenesulfonamide (**268**) under basic conditions in good yields of 82% (Scheme 118).

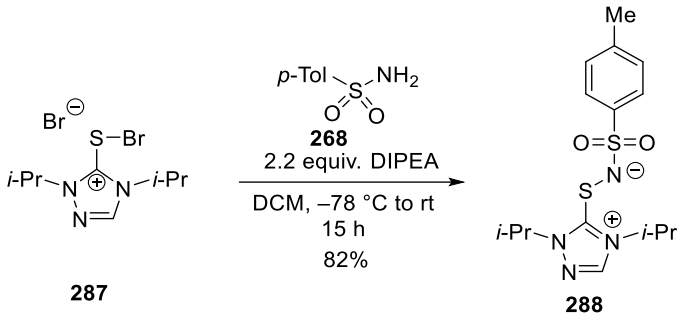

Scheme 118: Synthesis of 1,2,4-triazole-derived reagent **288**.

Unfortunately, only diaryl sulfide **289** was isolated in the reaction of **288** with magnesium organyl **277** (Scheme 119). Nevertheless, cyclopentylmagnesium bromide (**274**) gave the desired product **275** in moderate yield of 24%, only slightly reduced as compared to the efficacy of reagent **269** (25% yield, Table 12).

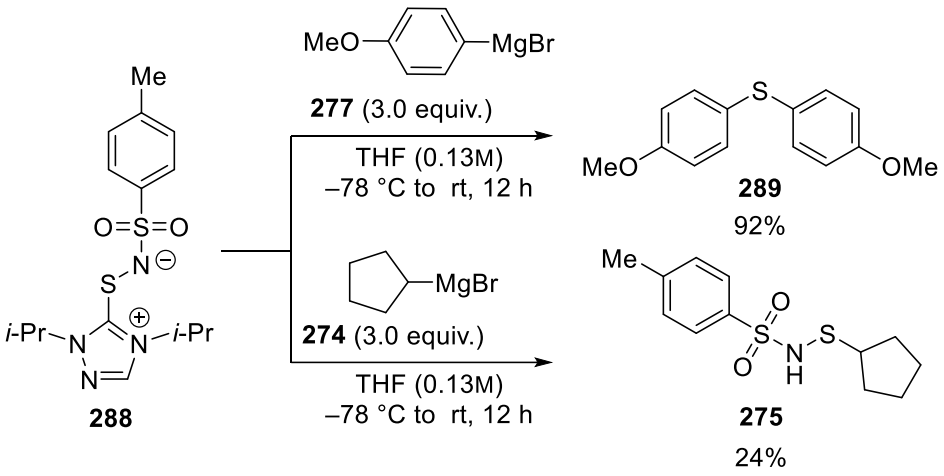

Scheme 119: Reactivity of 1,2,4-triazole-derived reagent **288**.

Since the entire potential of the synthesized sulfonthioamidation reagents has not been fully investigated, yet further studies on the reactivity of the reagents **269** and **288** will be carried out in the nearest future. Potentially, the change of the sulfur-containing platform from an imidazoline-2-thione-based one towards a dibenzothiophene-derived backbone could overcome these limitations or allow the transfer of a nitrogen-containing fragment, since

dibenzothiophenes are extremely versatile platforms for transfer reagents, as recently presented by the Alcarazo group.[241,261,262,305]

4 Summary

In the presented thesis, a highly modular protocol for the transition metal-free preparation of diaryl and alkyl aryl sulfides was accomplished as a significant contribution to the area of sulfide synthesis. For this purpose, the imidazole-2-thione-derived sulfenylation reagents **290** X^- were developed. It was shown that their versatile reactivity allowed the initial activation of several unfunctionalized (hetero)arenes. Additionally, the protocol demonstrated a high functional group tolerance (Scheme 120). Hereby, the influence of the sulfur-containing thiourea backbone as well as the effect of the electron-withdrawing *N*-succinimidyl moiety in the reagents was studied. In a consecutive step, metal organyls were identified as suitable nucleophiles for the synthesis of aryl sulfides from the cationic intermediate **291** which were isolated in moderate to excellent yields.

The presented reagent can be considered as a synthetic equivalent of a $[S]^2$ synthon which undergoes a double electrophilic attack. Noteworthy, the herein developed protocols allow the sequential twofold sulfenylation of electron-rich heterocycles like *N*-phenylpyrrole. In addition, several cationic intermediates **291** were crystallized and analyzed by X-ray crystallography to verify their molecular connectivity. The general methodology was further extended toward the synthesis of unsymmetrical aryl selenides.

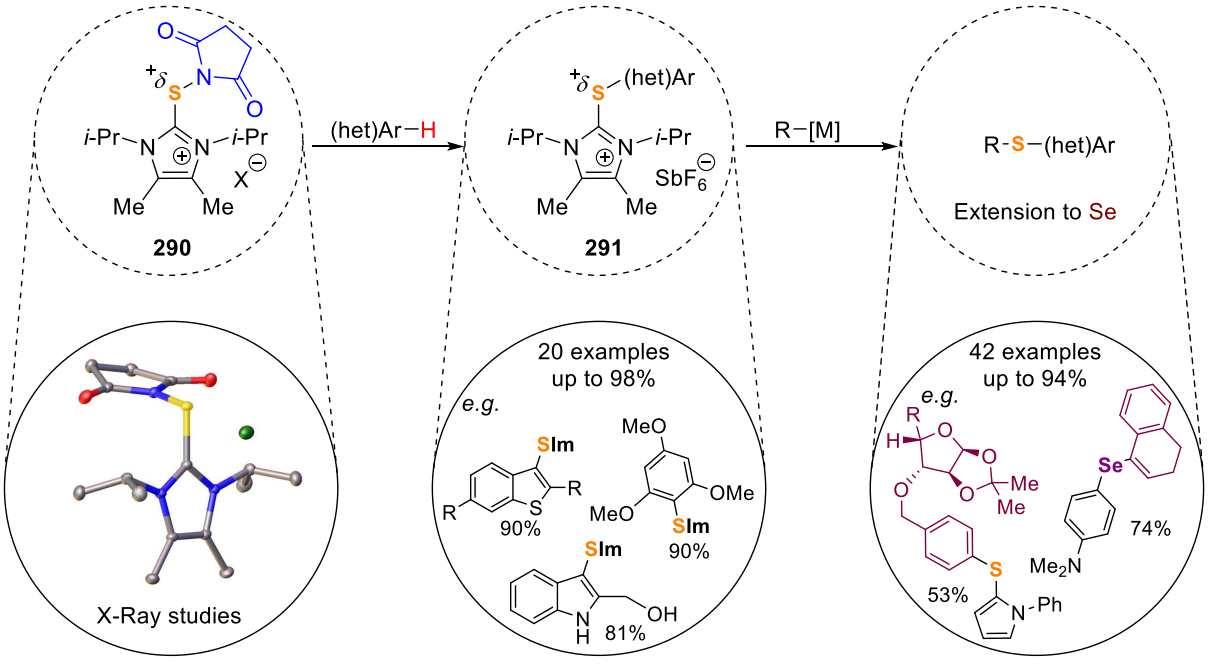

Scheme 120: Elaborated imidazolium-based reagents **290** for the synthesis of aryl sulfides and aryl selenides.

Based on these results, an efficient single step protocol for the synthesis of imidazolyl and further heterocyclic thioethers was elaborated. With this, further diheteroaryl sulfides were synthesized in yields of up to 82% from the *in situ* formed reagents **292** (Scheme 121).

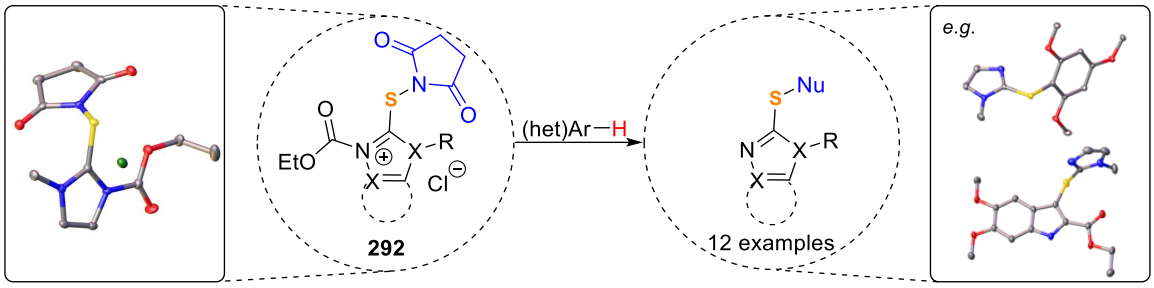

Scheme 121: Investigations towards the synthesis and application of (hetero)aryl-sulfenylating reagent **292**.

Additionally, different reagents of the general structure **293** were synthesized, and their connectivity was verified by X-ray crystallography experiments (Scheme 122). Furthermore, their reactivity with electro rich arenes was investigated. Finally, the reagents were successfully utilized in the reaction with metal organyl compounds in the formation of the scarce structure motif **265**.

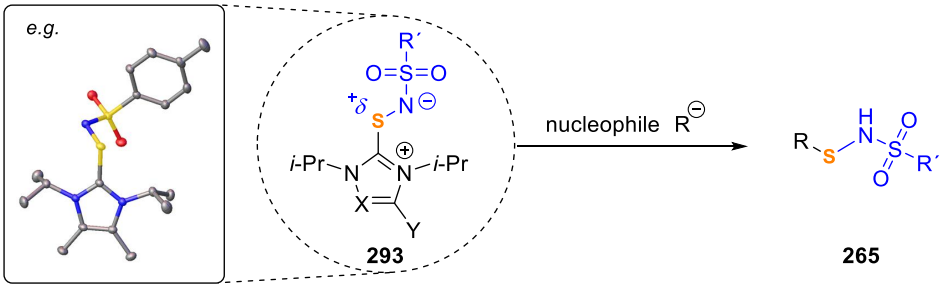

Scheme 122: Research on the synthesis and use of thioimidazolium-based reagent **293**.

5 Experimental

5.1 General considerations

All anhydrous solvents were obtained from a solvent purification system MBSPS7 from MBraun. All reactions were carried out under nitrogen atmosphere unless otherwise stated. IR: JASCO FT-4100 spectrometer, wavelengths in cm^{-1}. Microwave: Biotage Initatior. MS (EI): AccuTOF (Jeol) (70 eV). ESIMS: ESI-HRMS: micrOTOF (Bruker) and maXis (Bruker). GC-MS: Reactions were monitored by GC-MS on Agilent Technologies 7820A gas chromatography system coupled with an Agilent Technologies5977 E MSD EI-MS detector.

NMR: Spectra were recorded on Bruker AV 500, 400 or DPX 300 spectrometers; ^{1}H and ^{13}C chemical shifts (δ) are given in ppm relative to TMS, coupling constants (*J*) in Hz. The solvent signals were used as references and the chemical shifts converted to the TMS scale. All flash column chromatography were performed using a Biotage One automated column chromatography system on CHROMABOND® Flash BT, 15g (or 25g) SiOH 40-63 µm from Macherey-Nagel. Thin-layer chromatography (TLC) analysis was performed using POLYGRAM® SIL G/UV_{254} TLC plates from Macherey-Nagel and visualized by UV irradiation and/or phosphomolybdic acid staining. All commercially available compounds (Acros, ABCR, Alfa Aesar, Aldrich, Fluorochem, TCI) were used as received; other compounds were prepared accordingly to the published procedures. The concentration of Grignard reagents and other metal organic compounds was determined before each experiment using the titration protocol of P. Knochel *et al*.[1]

Crystal structure analysis: Data collection was performed on a Bruker D8 Venture four-circle-diffractometer from Bruker AXS GmbH; used detector: Photon II from Bruker AXS GmbH; used X-ray sources: microfocus IµS Cu/Mo from Incoatec GmbH with mirror optics HELIOS and single-hole collimator from Bruker AXS GmbH.
Used programs: APEX3 Suite (v2017.3-0) and therein integrated programs SAINT (Integration) und SADABS (Absorption correction) from Bruker AXS GmbH; structure solution

[1] A. Krasovskiy, P. Knochel, *Synthesis* **2006**, 890–891.

was done with SHELXT, refinement with SHELXS[2]; OLEX2 was used for data finalization.[3]
Special Utilities: SMZ1270 stereomicroscope from Nikon Metrology GmbH was used for sample preparation; crystals were mounted on MicroMounts or MicroLoops from MiTeGen; for sensitive samples the X-TEMP 2[4] System was used for picking of crystals; crystals were cooled to given temperature with Cryostream 800 from Oxford Cryosystems.
For clarity hydrogen atoms were removed from the Figures and Tables presented below. The numberings in the Figures do not follow that recommended by IUPAC. Ellipsoids are shown at 50% probability level.

Hirshfeld analysis plots were obtained by analyzing the obtained crystallographic data with CrystalExplorer17.[306]

[2] Both: G. M. Sheldrick, *Acta Cryst*. **2008**, *A64*, 112–122.
[3] O .V. Dolomanov, L. J. Bourhis, R. J Gildea, J. A. K. Howard, H. Puschmann, *J. Appl. Cryst*. **2009**, *42*, 339–341.
[4] T. Kottke, D. Stalke, J. Appl. Cryst. **1993**, 26, 615–619.

5.2 Reactions towards the synthesis of sulfides

5.2.1 Synthesis of backbones and reagents

1,3-Dimethyl-1,3-dihydro-2*H*-imidazole-2-thione (**294**)[5]

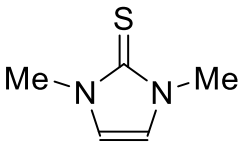

The reaction was carried out under ambient conditions. 1-Methyl-1*H*-imidazole (5.40 g, 5.20 mL, 65.8 mmol, 1.00 equiv.) was dissolved in EtOAc (75 mL). Methyl iodide (9.34 g, 4.10 mL, 65.8 mmol, 1.00 equiv.) was added dropwise. The solution was stirred for 2 h at rt and the obtained white precipitate was filtered off and dried under reduced pressure to obtain 1,3-dimethyl-1*H*-imidazol-3-ium iodide as a white powder (14.6 g, 65.2 mmol, 99%). The white powder was subsequently dissolved in dry MeOH (75 mL); sulfur (2.24 g, 70.0 mmol) and potassium carbonate (7.60 g, 55.0 mmol) were added, and the suspension was stirred at 65 °C for 20 h. The hot brown solution was filtered through a *Celite*® pad. The pad was washed with MeOH (20 mL), and the combined organic phases were cooled to 4 °C for 17 h. The white crystals were filtered off and recrystallized from hot MeOH (75 mL) to give **294** as a white powder (2.33 g, 18.2 mmol, 28% over two steps

^{1}H NMR (300 MHz, d^6-DMSO) δ = 3.45 (s, 6H), 7.11 (s, 2H). HRMS: *m*/*z* calcd. for $C_5H_9N_2S^+$ $[M+H]^+$ = 129.0481; found = 129.0485. The data are in line with the previously published ones.[6]

[5] **294** was synthesized applying a modified procedure of G. Roy *et al.*: M. Banerjee, R. Karri, K. Singh Rawat, K. Muthuvel, B. Pathak, G. Roy, *Angew. Chem. Int. Ed*. **2015**, *54*, 9323–9327.

[6] F. Freeman, J. W. Ziller, H. N. Po, M. C. Keindl, *J. Am. Chem. Soc.* **1988**, *110,* 2586–2591.

1,3,4,5-Tetramethyl-1,3-dihydro-2*H*-imidazole-2-thione (**95**)

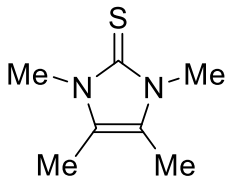

The reaction was carried out without *Schlenk*-techniques. To a stirred solution of 1,3-dimethyl-2-thiourea (8.28 g, 79.5 mmol, 1.00 equiv.) in 1-hexanol (85 mL) was added acetoin (7.00 g, 6.9 mL, 79.5 mmol, 1.00 equiv.). The reaction mixture was stirred at 160 °C for 16 h and cooled down to 4 °C for 18 h. The white solid was filtered off and washed with ice-cold ethanol (3 × 20 mL). **95**[7] was isolated as a white solid (4.00 g, 25.6 mmol, 32%).

^{1}H NMR (300 MHz, $CDCl_3$ ppm) δ = 2.08 (d, *J* = 0.5 Hz, 6H), 3.55 (d, *J* = 0.5 Hz, 6H). HRMS: *m*/*z* calcd. for $C_7H_{12}N_2S^+$ $[M]^+$ = 156.0721; found = 156.0724. The data are in line with the previously published ones.[6,7]

1,3-Diisopropyl-4,5-dimethyl-2(3*H*)-imidazolethione (**78**)[8]

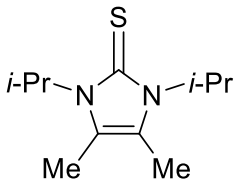

The reaction was carried out without *Schlenk*-techniques. To a stirred solution of 1,3-di(isopropyl)-2-thiourea (38.0 g, 237.1 mmol, 1.00 equiv.) in 1-hexanol (150 mL) was added acetoin (20.9 g, 20.7 mL, 237.2 mmol, 1.00 equiv.). The reaction mixture was stirred at 160 °C for 16 h and cooled down to 4°C for 18 h. The white solid was filtered off and washed with ice-cold ethanol (3 × 20 mL). After recrystallizing from hot 1-hexanol (50 mL), **78** was isolated as a white solid (22.9 g, 107.8 mmol, 45%).

^{1}H NMR (300 MHz, $CDCl_3$ ppm) δ = 1.25 (d, *J* = 7.1 Hz, 12H), 2.00 (d, 6H), 5.49 (s, 6H). ^{13}C NMR (75 MHz, $CDCl_3$, ppm) δ = 10.1, 20.4, 49.0, 121.2, 159.4. IR (neat, cm^{-1}): 2974.3, 2935.9, 1464.9, 1412.3, 1368.5, 1336.4, 1206.1, 1138.8, 1105.3, 1089.3, 980.1, 906.4, 806.6, 759.1, 552.8. HRMS: *m*/*z* calcd. for $C_{11}H_{21}N_2S^+$ $[M+H]^+$ = 213.1420; found = 213.1426. The data are in line with the previously published ones.[6,7]

---

[7] The protocol of M. Alcarazo *et al.* was applied: G. Talavera, J. Peña, M. Alcarazo, *J. Am. Chem. Soc*. **2015**, *27*, 8704–8707.

[8] Employing the protocol of N. Kuhn *et al.*: N. Kuhn, T. Kratz, *Synthesis* **1993**, 561–562.

2-(Bromothio)-1,3,4,5-tetramethyl-1*H*-imidazol-3-ium Bromide (**96**)

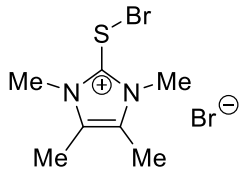

Thiourea **95** (2.00 g, 12.8 mmol, 1.00 equiv.) was dissolved in DCM (18 mL) and the obtained solution was cooled to 0°C. Bromine (2.05 g, 656 µL, 12.8 mmol, 1.00 equiv.) was added dropwise, and the brown suspension was allowed to warm up to rt. After 3 h, all volatiles were removed *in vacuo* and **96**[9] was obtained as an orange solid (4.05 g, 12.8 mmol, 100%).

^{1}H NMR (300 MHz, $CDCl_3$ ppm) δ = 2.28 (s, 6H), 3.82 (s, 6H). The data are in line with the previously published ones.[6]

2-(Bromothio)-1,3-diisopropyl-4,5-dimethyl-1*H*-imidazol-3-ium Bromide (**79**)

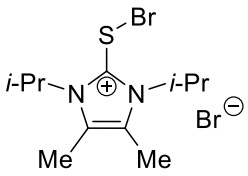

Thiourea **78** (8.63 g, 40.6 mmol, 1.00 equiv.) was dissolved in DCM (42 mL) and the obtained solution was cooled to 0°C. Bromine (6.49 g, 2.08 mL, 40.6 mmol, 1.00 equiv.) was added dropwise, and the brown suspension was allowed to warm up to rt. After 3 h all volatiles were removed *in vacuo* and **79**[10] was obtained as an orange solid (15.1 g, 40.6 mmol, 100%).

^{1}H NMR (300 MHz, $CDCl_3$ ppm) δ = 1.67 (d, *J* = 7.1 Hz, 12H), 2.37 (s, 6H), 5.66 (quint, *J* = 7.1 Hz, 2H). The data are in line with the previously published ones.[6]

[9] The protocol of M. Alcarazo *et al.* was applied: G. Talavera, J. Peña, M. Alcarazo, *J. Am. Chem. Soc*. **2015**, *27*, 8704–8707.

[10] The protocol of M. Alcarazo *et al.* was applied: G. Talavera, J. Peña, M. Alcarazo, *J. Am. Chem. Soc*. **2015**, *27*, 8704–8707.

2-[(2,5-Dioxopyrrolidin-1-yl)thio]-1,3-diisopropyl-4,5-dimethyl-1*H*-imidazol-3-ium Chloride (**91**):

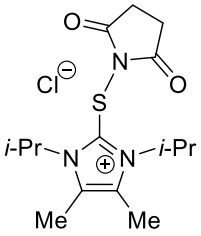

Thiourea **78** (212 mg, 1.00 mmol, 1.00 equiv.) and *N*-chlorosuccinimide (134 mg, 1.00 mmol, 1.00 equiv.) were dissolved in 1,2-DCE (10 mL). The obtained yellow solution was stirred at rt for two hours. The solvent was removed *in vacuo*, and product **91** was isolated as a light yellow solid (346 mg, 1.00 mmol, 100%).

^{1}H NMR (300 MHz, CD_2Cl_2 ppm) δ = 1.62 (d, *J* = 7.0 Hz, 12H), 2.39 (s, 6H), 2.78 (s, 4H), 6.20 (hept, *J* = 7.1 Hz, 2H). ^{13}C NMR (75 MHz, CD_2Cl_2, ppm) δ = 11.2, 21.5, 29.3, 44.5, 54.6, 130.4, 177.0. IR (neat, cm^{-1}): 2971.8, 2941.9, 1773.2, 1714.4, 1610.3, 1470.5, 1445.4, 1422.2, 1391.4, 1372.1, 1346.1, 1287.3, 1250.6, 1216.9, 1179.3, 1161.9, 1132.0, 1113.7, 1092.5, 1010.5, 943.0, 906.4, 869.7, 820.6, 802.2, 752.1, 664.4, 644.1, 575.6, 544.8. HRMS: *m*/*z* calcd. for $C_{15}H_{24}N_3O_2S^+$ $[M–Cl]^+$ = 310.1584; found = 310.1584.

2-[(2,5-Dioxopyrrolidin-1-yl)thio]-1,3-diisopropyl-4,5-dimethyl-1*H*-imidazol-3-ium Hexafluoroantimonate (**93**)**:**

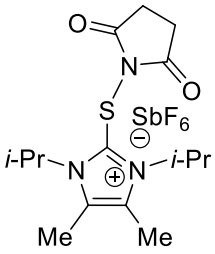

Thiourea **78** (1.06 g, 5.00 mmol, 1.00 equiv.) and *N*-chlorosuccinimide (667 mg, 5.00 mmol, 1.00 equiv.) were dissolved in MeCN (50 mL). The obtained yellow solution was stirred at rt for 5 min. Sodium hexafluoroantimonate (1.94 g, 7.5 mmol, 1.50 equiv.) was added, and the yellow suspension was stirred at rt for 5 h. The solvent was removed *in vacuo*, and the residual yellow solid was extracted with DCM (4 × 50 mL). The organic phases were combined and the solvent was removed *in vacuo.* The title compound **93** was isolated as a yellow solid (2.51 g, 4.60 mmol, 92%).

^{1}H NMR (300 MHz, CD_2Cl_2 ppm) δ = 1.57 (d, *J* = 7.2 Hz, 12H), 2.41 (s, 6H), 2.85 (s, 6 H), 6.23 (sept, *J* = 7.2 Hz, 2H). ^{13}C NMR (126 MHz, CD_2Cl_2, ppm) δ = 11.2, 21.6, 29.3, 55.1, 132.9, 133.5, 176.7.IR (neat, cm^{-1}): 2993.9, 1736.6, 1597.7, 1458.9, 1421.3, 1397.2, 1376.0, 1291.1, 1270.9, 1236.1, 1215.9, 1131.0, 1092.5, 1004.7, 819.6, 749.2, 568.9, 541.9, 516.8. HRMS: *m*/*z* calcd. for $C_{15}H_{24}N_3O_2S^+$ $[M–SbF_6]^+$ = 310.1584; found = 310.1584.

2-[(2,5-Dioxopyrrolidin-1-yl)thio]-1,3-diisopropyl-4,5-dimethyl-1*H*-imidazol-3-ium Bromide (**295**):

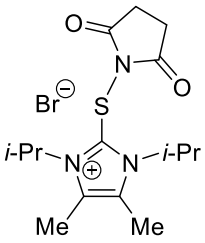

78 (21.2 mg, 100 µmol, 1.00 equiv.) and *N*-bromosuccinimide (17.8 mg, 100 µmol, 1.00 equiv.) were dissolved in DCM (2 mL). The obtained yellow solution was stirred at rt for two hours. The solvent was removed *in vacuo*, and product **295** was isolated as a light yellow solid (39.0 mg, 100 µmol, 100%).

^{1}H NMR (300 MHz, CD_2Cl_2 ppm) δ = 1.62 (d, *J* = 7.0 Hz, 12H), 2.39 (s, 6H), 2.82 (s, 4H), 6.17 (hept, *J* = 7.0 Hz, 2H). ^{13}C NMR (75 MHz, CD_2Cl_2, ppm) δ = 11.3, 21.5, 29.4, 54.7, 131.0, 138.1, 176.9. IR (neat, cm^{-1}): 2971.8, 2939.0, 1717.3, 1445.4, 1422.2, 1391.4, 1299.8, 1280.5, 1246.8, 1232.3, 1219.8, 1159.0, 1139.7, 1132.0, 1092.5, 1009.6, 818.6, 729.9, 696.2, 649.9, 574.7, 502.4. HRMS: *m*/*z* calcd. for $C_{15}H_{24}N_3O_2S^+$ $[M–Br]^+$ = 310.1584; found = 310.1583.

2-[(1,3-Dioxoisoindolin-2-yl)thio]-1,3-diisopropyl-4,5-dimethyl-1*H*-imidazol-3-ium Bromide (**90**)

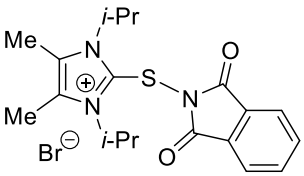

Compound **79** (1.42 g, 3.82 mmol, 1.00 equiv.) and potassium phthalimide (742 mg, 4.01 mmol, 1.05 equiv.) were dissolved in MeCN (50 mL). The orange solution became yellow. The reaction mixture was stirred at rt for two hours, the white precipitate was filtered off and the MeCN was removed *in vacuo*. Product **90** was isolated as a yellow solid (800 mg, 1.82 mmol, 48%).

^{1}H NMR (300 MHz, $CDCl_3$ ppm) δ = 1.51 – 1.82 (bs, 12H), 2.35 (s, 6H), 6.34 (d, *J* = 7.1 Hz, 2H), 7.75 – 7.81 (m, 2H), 7.80 – 7.89 (m, 2H). ^{13}C NMR (101 MHz, $CDCl_3$, ppm) δ = 2.0, 10.9, 54.3, 124.3, 129.9, 131.4, 135.3, 139.6, 167.3. IR (neat, cm^{-1}): 1719, 1584, 1448, 1406, 1370, 1338, 1282, 1268, 1252, 1213, 1173, 1140, 1089, 1054, 1011, 952, 904, 865, 800, 751, 709, 698, 626, 547, 501. HRMS: *m*/*z* calcd. for $C_{19}H_{24}N_3O_2S^+$ $[M–Br]^+$ = 358.1584; found = 358.1579.

1,3,4,5-Tetramethyl-2-[(2-oxopyrrolidin-1-yl)thio]-1*H*-imidazol-3-ium Bromide (**94**)

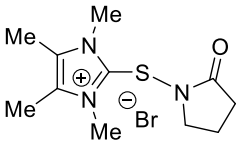

Dibromide **96** (458 mg, 1.45 mmol, 1.00 equiv.) was dissolved in MeCN (80 mL). A solution of 1-(trimethylsilyl)pyrrolidin-2-one (342 mg, 348 µL, 2.17 mmol, 1.50 equiv.) in MeCN (5 mL) was added dropwise over a period of 10 min. The obtained yellow solution was stirred at rt for 1.5 h. The solution was

concentrated under reduced pressure to a volume of ca 3 mL. Under vigorous stirring, Et_2O (20 mL) was added, and the resulting white suspension was sonicated in an ultrasonic bath for 2 min. Solvents were removed by filtration, and the obtained white powder was washed with Et_2O (20 mL). After removing the solvent by filtration, the product was dried *in vacuo.* **94** was isolated as a grey solid (428 mg, 1.34 mmol, 92%).

^{1}H NMR (300 MHz, $CDCl_3$ ppm) δ = 2.05 – 2.22 (m, 2H), 2.35 (s, 6H), 2.40 (dd, *J* = 8.6, 7.4 Hz, 2H), 3.85 (t, *J* = 7.0 Hz, 2H), 4.11 (s, 6H). ^{13}C NMR (101 MHz, $CDCl_3$, ppm) δ = 10.1, 19.2, 29.3, 35.2, 52.3, 130.4, 138.5, 177.8. IR (neat, cm^{-1}): 3403.7, 2949.6, 1707.7, 1623.8, 1497.5, 1433.8, 1366.3, 1283.4, 1243.9, 1213.0, 1120.4, 1105.0, 1011.5, 947.8, 854.3, 778.1, 638.3, 546.7. HRMS: *m*/*z* calcd. for $C_{11}H_{18}N_3OS^+$ $[M–Br]^+$ = 240.1165; found = 240.1163.

1,3-Diisopropyl-4,5-dimethyl-2-[(2-oxopyrrolidin-1-yl)thio]-1*H*-imidazol-3-ium Bromide (**92**)

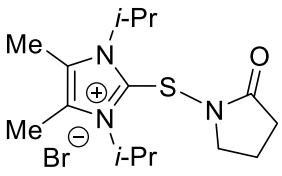

Dibromide **79** (934 mg, 2.51 mmol, 1.00 equiv.) was dissolved in MeCN (90 mL). A solution of 1-(trimethylsilyl)pyrrolidin-2-one (592 mg, 602 µL, 3.76 mmol, 1.50 equiv.) in MeCN (5 mL) was added dropwise over a period of 10 min. The obtained yellow solution was stirred at rt for 1.5 h. All volatiles were removed under reduced pressure, and the obtained yellow foam was washed with Et_2O (3 × 15 mL) under sonication in an ultrasonic for 2 min each time until a fine powder was obtained. After removing the solvent by filtration, the product was dried *in vacuo.* Product **92** was isolated as a grey solid (901 mg, 2.39 mmol, 95%).

^{1}H NMR (300 MHz, CD_3CN ppm) δ = 1.56 (d, *J* = 7.1 Hz, 12H), 1.98 – 2.09 (m, 2H), 2.24 – 2.33 (m, 2H), 2.40 (s, 6H), 3.54 – 3.67 (m, 2H), 5.77 (hept, *J* = 7.1 Hz, 2H). ^{13}C NMR (75 MHz, CD_3CN, ppm) δ = 11.0, 19.6, 21.2, 29.8, 52.3, 54.4, 131.7, 137.6, 178.2. IR (neat, cm^{-1}): 2967.9, 1691.3, 1618.0, 1424.2, 1369.2, 1244.8, 1220.7, 1118.5, 1025.9, 942.1, 907.3, 805.1, 757.9, 693.3, 546.7. HRMS: *m*/*z* calcd. for $C_{15}H_{26}N_3OS^+$ $[M–Br]^+$ = 296.1791; found = 296.1790.

2-[(1,1-Dioxido-3-oxobenzo[*d*]isothiazol-2(3*H*)-yl)thio]-1,3-diisopropyl-4,5-dimethyl-1*H*-imidazol-3-ium Chloride (**296**)

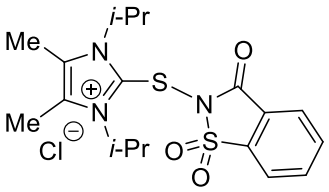

Compound **78** (21.2 mg, 100 µmol, 1.00 equiv.) and *N*-chlorosaccharin (21.8 mg, 100 µmol, 1.00 equiv.) were dissolved in DCM (2 mL). The obtained yellow orange solution was stirred at rt for 1.5 h. All volatiles were removed under reduced pressure, and the product **296** was obtained as a light yellow powder (43.0 mg, 100 µmol, 100%).

^{1}H NMR (400 MHz, CD_2Cl_2 ppm) δ = 1.65 (d, *J* = 7.0 Hz, 12H), 2.40 (s, 6H), 5.88 (hept, *J* = 7.0 Hz, 2H), 7.76 – 7.86 (m, 3H), 7.96 – 7.99 (m, 1H). ^{13}C NMR (101 MHz, CD_2Cl_2, ppm) δ = 11.1, 21.2, 54.4, 54.5, 121.3, 125.6, 129.3, 130.1, 134.5, 135.2, 140.2, 162.4.IR (neat, cm^{-1}): 2982.4, 2938.0, 2553.3, 1727.9, 1607.4, 1448.3, 1425.1, 1393.3, 1373.1, 1322.0, 1283.4, 1241.0, 1218.8, 1175.4, 1159.0, 1110.8, 1047.2, 975.8, 943.0, 892.9, 793.6, 753.1, 729.9, 702.0, 675.0, 624.8, 590.1, 562.1, 534.2, 511.0. HRMS: *m*/*z* calcd. for $C_{18}H_{24}N_3O_3S_2^+$ $[M–Cl]^+$ = 394.1254; found = 394.1247.

5.2.2 Screening of different backbones

General protocol GP1

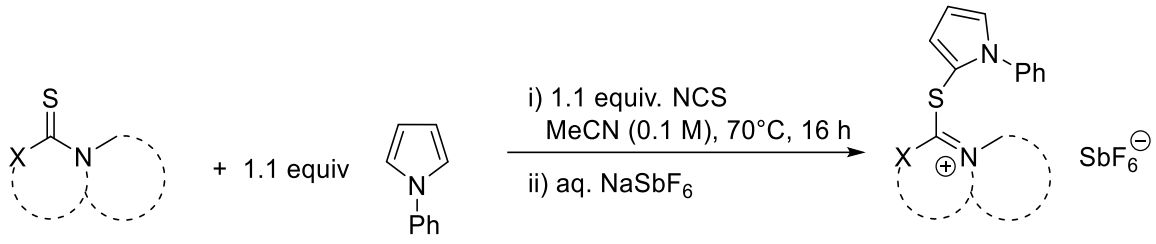

297 **298**

Scheme 123: Preliminary screening of different backbones **297.**

Backbone **297** (1.00 mmol, 1.00 equiv.), *N*-chlorosuccinimide (147 mg, 1.10 mmol, 1.10 equiv.) and phenylpyrrole (158 mg, 1.10 mmol, 1.10 equiv.) were dissolved in MeCN (10 mL). The yellow solution was stirred for 10 min at rt and then at 70 °C for 16 h. The resulting orange brown reaction mixture was allowed to cool down to rt, and all volatiles were removed under reduced pressure. The residual orange oil was dissolved in DCM (10 mL) and washed with sat. aq. $NaSbF_6$ (10 mL) for 3 min. The organic layer was dried over $MgSO_4$ and concentrated *in vacuo*.

2-Isopropyl-1-[(1-phenyl-1H-pyrrol-2-yl)thio]isoquinolin-2-ium Hexafluoroantimonate (**111**):

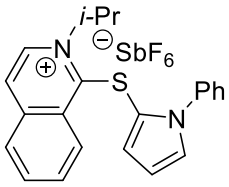

After threefold column chromatography (DCM:MeOH), product **111** was obtained as an orange solid (99.1 mg, 171 µmol, 17%) according to GP1; however, with a purity of 80%. Fortunately, the identity of compound was confirmed by X-Ray crystal structure analysis.

^{1}H NMR (300 MHz, CD_2Cl_2 ppm) δ = 1.41 (d, *J* = 6.7 Hz, 6H), 5.97 (hept, *J* = 6.7 Hz, 1H), 6.44 (dd, *J* = 3.9, 3.0 Hz, 1H), 6.86 – 6.95 (m, 3H), 7.02 (dd, *J* = 3.0, 1.8 Hz, 1H), 7.04 – 7.11 (m, 2H), 7.30 – 7.39 (m, 1H), 7.82 (ddd, *J* = 8.4, 6.1, 2.1 Hz, 1H), 8.00 – 8.09 (m, 2H), 8.26 (q, *J* = 7.0 Hz, 2H), 8.65 (dd, *J* = 8.8, 0.9 Hz, 1H). ^{13}C NMR (101 MHz, CD_2Cl_2, ppm) δ = 23.3, 62.6, 111.7, 121.5, 121.9, 127.0, 127.6, 128.5, 129.2, 129.4, 130.0, 130.5, 130.6, 131.1, 132.4, 132.5, 137.4, 137.5, 138.3. IR (neat, cm^{-1}): 1711.5, 1644.0, 1620.9, 1595.8, 1550.6, 1497.5, 1458.9, 1431.9, 1374.0, 1321.0, 1265.1, 1230.4, 1172.5, 1155.2, 1133.9, 1086.7, 1055.8, 1037.5, 1009.6, 877.5, 823.5, 755.0, 735.7, 697.1, 649.9, 567.9, 514.9. HRMS: *m*/*z* calcd. for $C_{22}H_{21}N_2S^+$ $[M–SbF_6]^+$ = 345.1420; found = 345.1420.

2-Isopropyl-1-[(1-phenyl-1*H*-pyrrol-2-yl)thio]phthalazin-2-ium Hexafluoroantimonate (**112**):

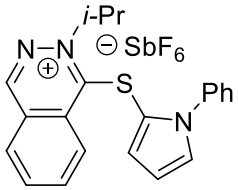

In our hands, it was not possible to isolate pure **112**.

HRMS: *m*/*z* calcd. for $C_{21}H_{20}N_3S^+$ $[M–SbF_6]^+$ = 346.1372; found = 346.1368.

2-Methyl-3-[(1-phenyl-1*H*-pyrrol-2-yl)thio]imidazo[1,5-*a*]pyridin-2-ium hexafluoroantimonate (**105**):

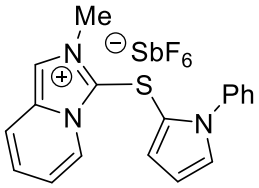

In our hands, it was not possible to isolate **105**.

HRMS: *m*/*z* calcd. for $C_{18}H_{16}N_3S^+$ $[M–SbF_6]^+$ = 306.1059; found = 306.1060.

1-{[(1-Phenyl-1*H*-pyrrol-2-yl)thio](piperidin-1-yl)methylene}piperidin-1-ium Hexafluoroantimonate (**108**):

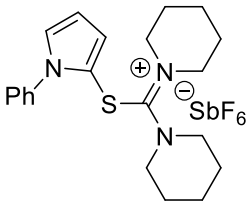

After threefold column chromatography (DCM:MeOH), **108** was obtained as an orange solid (180.7 mg, 306.1 µmol, 31%) according to GP1 with a purity of 90%. However, the identity of compound was confirmed by X-ray crystal structure analysis.

^{1}H NMR (300 MHz, CD_2Cl_2 ppm) δ = 1.43 – 1.51 (m, 8H), 1.58 – 1.67 (m, 2H), 1.75 – 1.81 (m, 2H), 3.38 – 3.44 (m, 8H), 6.48 (dd, *J* = 3.9, 2.9 Hz, 1H), 6.82 (dd, *J* = 3.9, 1.7 Hz, 1H), 7.20 (dd, *J* = 2.9, 1.7 Hz, 1H), 7.27 – 7.33 (m, 2H), 7.49 – 7.61 (m, 3H). ^{13}C NMR (126 MHz, CD_2Cl_2, ppm) δ = 23.6, 26.5, 54.7, 111.7, 112.0, 123.1, 126.8, 129.1, 129.6, 130.3, 138.4, 173.3. IR (neat, cm^{-1}): 2947.7, 1596.8, 1571.7, 1497.5, 1443.5, 1428.0, 1395.2, 1364.4, 1320.0, 1285.3, 1270.9, 1252.5, 1210.1, 1164.8, 1133.9, 1114.7, 1090.5, 1039.4, 1005.7, 950.7, 912.2, 853.3, 789.7, 768.5, 742.5, 696.2, 649.9, 564.1, 509.1. HRMS: *m*/*z* calcd. for $C_{21}H_{28}N_3S^+$ $[M–SbF_6]^+$ = 354.1998; found = 354.1993.

1,3-Dimethyl-2-[(1-phenyl-1*H*-pyrrol-2-yl)thio]-1*H*-imidazol-3-ium Hexafluoroantimonate (**104**):

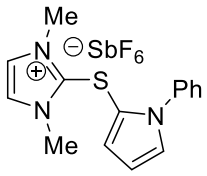

Compound **104** was prepared according to GP1, purified by column chromatography (DCM:MeOH) and obtained as a white solid (321.1 mg, 634.4 µmol, 63%).

^{1}H NMR (300 MHz, CD_2Cl_2 ppm) δ = 3.45 (s, 6H), 6.41 (dd, *J* = 3.9, 3.0 Hz, 1H), 6.96 (dd, *J* = 3.9, 1.7 Hz, 1H), 7.11 (dd, *J* = 3.9, 1.7 Hz, 1H), 7.17 – 7.22 (m, 2H), 7.24 (s, 2H), 7.49 – 7.61 (m, 3H). ^{13}C NMR (126 MHz, CD_2Cl_2, ppm) δ = 36.8, 109.7, 111.0, 123.7, 125.1, 127.6, 130.0, 130.1, 130.4, 138.7. IR (neat, cm^{-1}): 3144.4, 1596.8, 1566.9, 1509.0, 1499.4, 1458.9, 1433.8, 1412.6, 1328.7, 1237.1, 1164.8, 1088.6, 1045.2, 931.5, 799.4, 757.9, 742.5, 725.1, 699.1, 684.6, 650.9, 625.8, 519.7. HRMS: *m*/*z* calcd. for $C_{15}H_{16}N_3S^+$ $[M–SbF_6]^+$ = 270.1059; found = 270.1056.

(*Z*)-1,3-Diisopropyl-2-(1-phenyl-1*H*-pyrrol-2-yl)isothiouronium Hexafluoroantimonate (**109**):

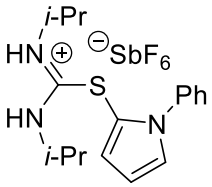

Compound **109** was prepared according to GP1, purified by column chromatography (DCM:MeOH) and obtained as a white solid (200.5 mg, 373.3 µmol, 37%).

^{1}H NMR (600 MHz, CD_2Cl_2 ppm) δ = 1.13 (d, *J* = 6.4 Hz, 6H), 1.23 (d, *J* = 6.5 Hz, 6H), 3.80 – 3.99 (m, 2H), 5.28 – 5.32 (m, 1H), 6.60 (dd, *J* = 3.9, 2.9 Hz, 1H), 6.90 (d, *J* = 8.3 Hz, 1H), 7.04 (dd, *J* = 3.9, 1.7 Hz, 1H), 7.23 (dd, *J* = 7.9, 1.7 Hz, 2H), 7.41 (dd, *J* = 3.0, 1.7 Hz, 1H), 7.50 – 7.57 (m, 3H). ^{13}C NMR (126 MHz, CD_2Cl_2, ppm) δ = 22.1, 22.3, 47.5, 50.2, 106.1, 112.5, 126.6, 126.7, 129.8, 130.1, 132.2, 137.8, 164.5. IR (neat, cm^{-1}): 1708.6, 1618.0, 1513.8, 1497.5, 1466.6, 1432.9, 1392.4, 1375.0, 1319.1, 1159.0, 1039.4, 745.4, 694.2, 653.8, 549.6. HRMS: *m*/*z* calcd. for $C_{17}H_{24}N_3S^+$ $[M–SbF_6]^+$ = 302.1685; found = 302.1680.

1,3,4,5-Tetramethyl-2-[(1-phenyl-1*H*-pyrrol-2-yl)thio]-1*H*-imidazol-3-ium hexafluoroantimonate (**103**):

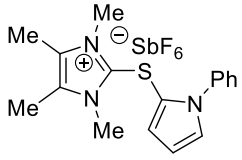

Compound **109** was prepared according to GP1, purified by column chromatography (DCM:MeOH) and obtained as a white solid (128.6 mg, 240.7 µmol, 24%).

^{1}H NMR (300 MHz, CD_2Cl_2 ppm) δ = 2.16 (s, 6H), 3.33 (s, 6H), 6.38 (dd, *J* = 3.9, 3.0 Hz, 1H), 6.92 (dd, *J* = 3.8, 1.8 Hz, 1H), 7.07 (dd, *J* = 3.0, 1.8 Hz, 1H), 7.23 (dd, *J* = 5.6, 4.1 Hz, 2H),

7.50 – 7.58 (m, 3H). ^{13}C NMR (126 MHz, CD_2Cl_2, ppm) δ = 9.6, 33.5, 110.8, 111.4, 122.9, 127.7, 129.6, 129.7, 129.8, 130.2, 136.3, 138.9. HRMS: *m*/*z* calcd. for $C_{17}H_{20}N_3S^+$ $[M–SbF_6]^+$ = 298.1372; found = 298.1373.

1,3-Diisopropyl-4,5-dimethyl-2-[(1-phenyl-1*H*-pyrrol-2-yl)thio]-1*H*-imidazol-3-ium Hexafluoroantimonate (**99**):

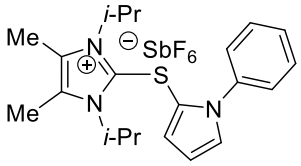

Compound **99** was prepared according to GP1, purified by column chromatography (DCM:MeOH) and obtained as a white solid (383 mg, 648.8 µmol, 65%).

^{1}H NMR (300 MHz, CD_2Cl_2 ppm) δ = 1.34 (d, *J* = 7.1 Hz, 12H), 2.29 (s, 6H), 5.00 (hept, *J* = 7.1 Hz, 2H), 6.40 (dd, *J* = 3.9, 3.0 Hz, 1H), 6.68 (dd, *J* = 3.9, 1.7 Hz, 1H), 7.13 (dd, *J* = 3.0, 1.8 Hz, 1H), 7.33 – 7.39 (m, 2H), 7.49 – 7.62 (m, 3H). ^{13}C NMR (101 MHz, CD_2Cl_2, ppm) δ = 10.8, 21.3, 53.8, 111.7, 112.6, 121.9, 126.5, 128.9, 129.4, 130.4, 130.5, 135.8, 138.7. IR (neat, cm^{-}): 2993.9, 1495.5, 1455.0, 1436.7, 1413.6, 1376.9, 1319.1, 1207.2, 1136.8, 1109.8, 1086.7, 1038.5, 767.5, 725.1, 700.0, 654.7, 615.2, 602.6, 571.8, 559.3. HRMS: *m*/*z* calcd. for $C_{21}H_{28}N_3S^+$ $[M–SbF_6]^+$ = 354.1998; found = 354.2000; calcd. for SbF_6^- $[M]^-$ = 234.8948; found = 234.8951.

1,1,3,3-Tetramethyl-2-(1-phenyl-1*H*-pyrrol-2-yl)isothiouronium hexafluoroantimonate (**107a**) and **1,1,3,3-tetramethyl-2-(1-phenyl-1*H*-pyrrol-3-yl)isothiouronium hexafluoro-antimonate** (**107b**):

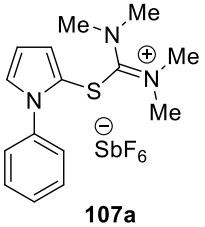

107a
main product

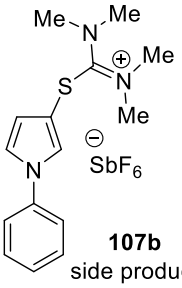

107b
side product

After column chromatography (DCM:MeOH) of a crude product prepared according to GP1, a mixture of **107a** (380 mg, 744.8 µmol, 75%)[11] and **107b** (21 mg, 4.1 µmol, 4%) was obtained as a pale yellow solid.

For **107**: ^{1}H NMR (300 MHz, CD_2Cl_2 ppm) δ = 2.95 (s, 12H), 6.46 (dd, *J* = 3.0, 3.9 Hz, 1H), 6.84 (dd, *J* = 1.9, 3.9 Hz, 1H), 7.19 (dd, *J* = 1.9, 3.0 Hz, 1H), 7.29 (dd, *J* = 1.9, 8.5 Hz, 2H), 7.51 – 7.61 (m, 3H). ^{13}C NMR (75 MHz, $CDCl_3$, ppm) δ = 43.9, 111.3, 111.5, 122.6, 126.8, 129.1, 129.8, 130.3, 138.4, 175.6. IR (neat, cm^{-1}): 1596, 1497, 1457, 1436, 1390, 1320, 1255, 1166, 1111, 868, 773, 738, 703, 649, 616, 605. HRMS: *m*/*z* calcd. for $C_{15}H_{20}N_3S^+$ $[M–SbF_6]^+$ = 274.1372; found = 274.1372; calcd. for SbF_6^- $[M]^-$ = 234.8948; found = 234.8950.

For **107**: ^{1}H NMR (300 MHz, CD_2Cl_2 ppm) δ = 3.22 (s, 12H), 6.41 (dd, *J* = 1.8, 3.1 Hz, 1H), 7.23 (dd, *J* = 2.4, 3.1 Hz, 1H), 7.32 – 7.38 (m, 1H), 7.40 – 7.50 (m, 5H).

[11] To remove residual traces of **107b**, the main product was purified by column chromatography (DCM:MeOH) for the second time affording **107a** as a yellow solid (235 mg, 460.1 µmol, 46%). Crystals of **107a** and **107b** were obtained by slow evaporation of the solutions of the pale yellow solids in DCM.

5.2.3 Synthesis of arylthioimidazolium salts

Optimization of the synthesis of arylthioimidazolium salts

1. Effect of the counterion on the reactivity of **91** and **93**

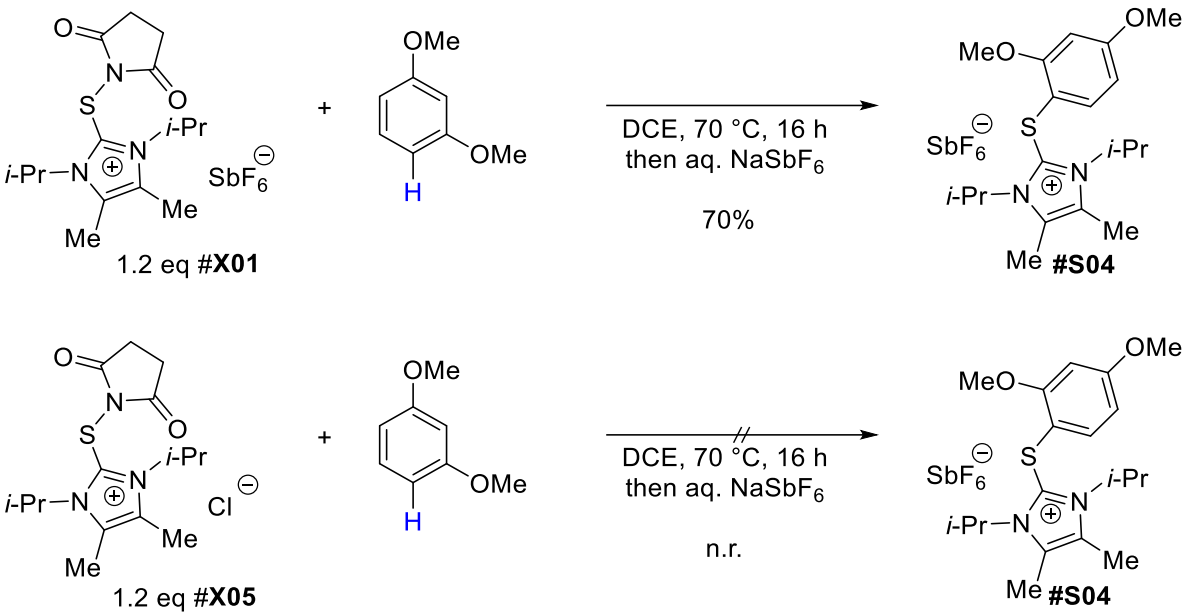

Scheme 124: Effect of the counterion on the reactivity of **91** and **93.**

General protocol GP2

A dry *Schlenk* flask was charged with **91** or **93**, (1.65 mmol, 1.20 equiv.) and 1,3-dimethoxybenzene (190 mg, 181 µL, 1.37 mmol, 1.00 equiv.). 1,2-DCE (0.1 M) was added, and the mixture was stirred at the indicated temperature for the indicated time. The reaction mixture was allowed to reach rt and then washed with sat. aq. $NaSbF_6$ (10 mL) for 5 min. The organic layer was dried over $MgSO_4$ and concentrated *in vacuo.* The crude product was purified by column chromatography (DCM:MeOH).

2. Effect of solvents, concentrations and additives on the formation of arylthioimidazolium salt **100**

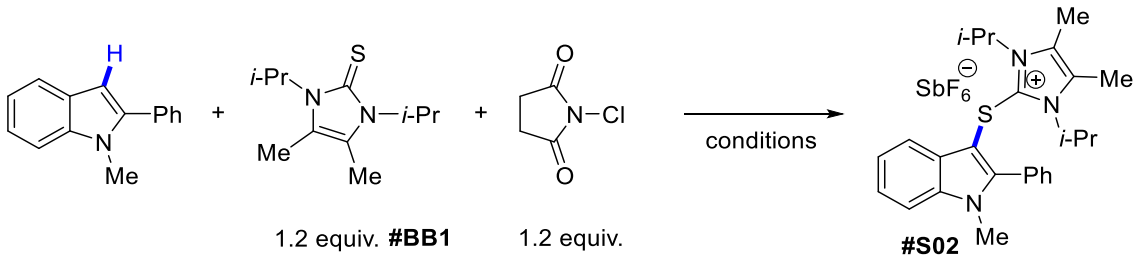

Scheme 125: Formation of arylthioimidazolium salt **100** applying *in situ* generated **91.**

General protocol GP3

A dry *Schlenk* flask was charged with imidazolthione **78** (127 mg, 600 µmol, 1.20 equiv.), *N*-chlorosuccinimide (80.1 mg, 600 µmol, 1.20 equiv.) and 1-methyl-2-phenylindole (104 mg, 500 µmol, 1.00 equiv.). MeCN (6 mL) was added, and the solution was stirred for 10 min at rt. and then at the indicated temperature for the indicated time. The orange brown solution was allowed to cool down to rt and all volatiles were removed under reduced pressure. The obtained orange oil was dissolved in DCM (5 mL) and washed with sat. aq. $NaSbF_6$ solution (5 mL) for 4 min. In case of 1,2-DCE as a solvent, the reaction mixture was directly washed with aq. $NaSbF_6$ solution without evaporation of DCE. The organic layer was dried over $MgSO_4$ and concentrated *in vacuo*. After column chromatography (DCM:MeOH), the arylthioimidazolium salt **100** was obtained as a yellow foam.

Table 13: Effect of solvents, concentrations and additives on the formation of arylthioimidazolium salt **100**.

Entry	Solvent	T	c /M	Additives	Yield
1	1,2-DCE	70°C	0.1	-	71%
2	MeCN	70°C	0.1	-	72%
3	MeCN	rt	0.1	-	15%
4	MeCN	70°C	0.8	-	65%
5	MeCN	70°C	0.1	2 equiv. H_2O	47%
6	MeCN	70°C	0.1	1 equiv. TEMPO	47%

Notes:

- In Entry 6, 3-chloro-1-methyl-2-phenylindole was isolated as a side product (yield: 29%).

- There was no difference in yields if **91** was prepared either *in situ* from imidazolthione **78** and *N*-chlorosuccinimide or synthesized beforehand.

- In cases of high reactivity of the (hetero)arenes towards **91**, the latter was not used to maintain the maximum possible stepwise efficiency of the protocol.

- In case of DCE as a solvent (Table 13, Entry 1), activation of DCE was observed to give 2-[(2-chloroethyl)thio]-1,3-diisopropyl-4,5-dimethyl-1*H*-imidazol-3-ium hexafluoroantimonate as a side-product, ^{1}H NMR spectrum of which is presented below in Figure 33.

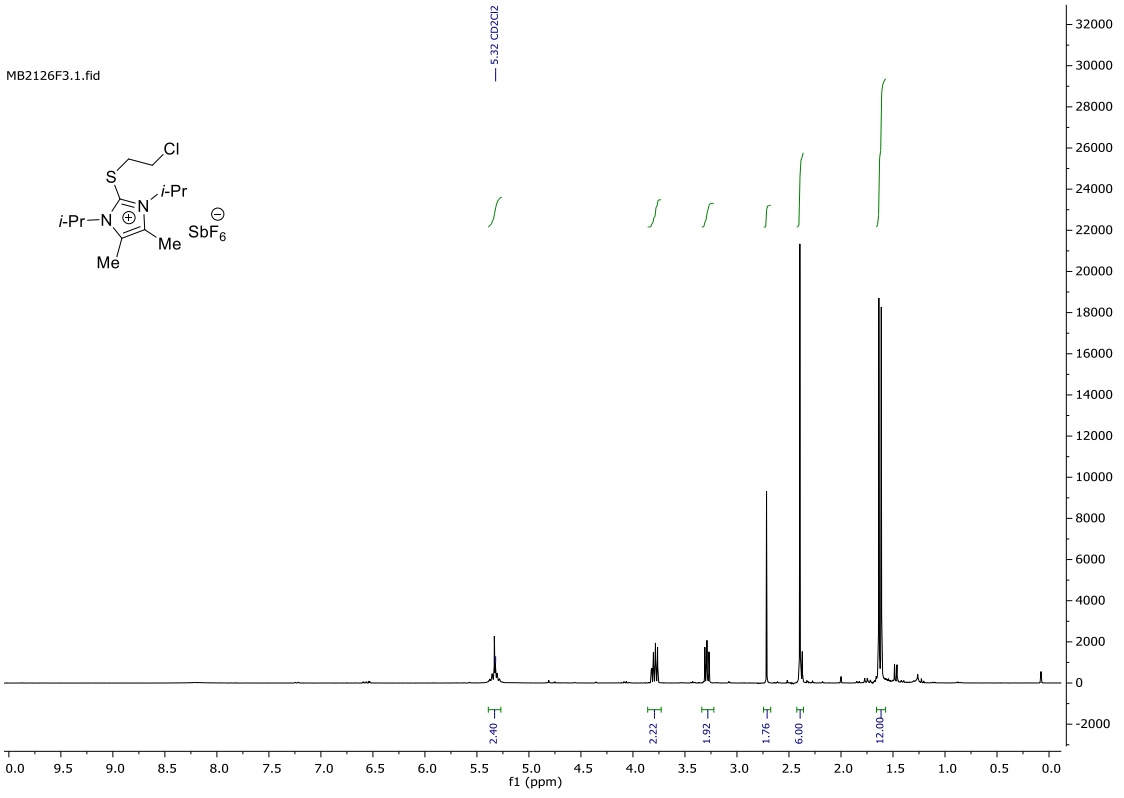

Figure 33: ^{1}H NMR spectrum of the by-formed 2-[(2-chloroethyl)thio]-1,3-diisopropyl-4,5-dimethyl-1*H*-imidazol-3-ium hexafluoroantimonate.

2-[(1*H*-Pyrrol-2-yl)thio]-1,3-diisopropyl-4,5-dimethyl-1*H*-imidazol-3-ium Hexafluoroantimonate (113):

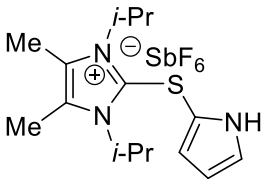

Product **113** was prepared according to modified GP2. A solution of compound **93** (262 mg, 480 µmol, 1.19 equiv.) in MeCN (4 mL) was stirred for 10 min at rt. Pyrrole (27 mg, 402 µmol, 1.00 equiv.) was added, and the yellow solution was stirred at 70 °C for 16 h. The reaction mixture was allowed to cool down to rt, and all volatiles were removed under reduced pressure. The obtained orange oil was dissolved in DCM (4 mL) and washed with sat. aq. $NaSbF_6$ (4 mL) for 5 min. The organic layer was dried over $MgSO_4$ and concentrated *in vacuo*. After column chromatography (DCM:MeOH), compound **113** was obtained as a yellow foam (175 mg, 340 µmol, 85%).

^{1}H NMR (300 MHz, CD_2Cl_2 ppm) δ = 1.54 (d, *J* = 7.2 Hz, 12H), 2.34 (s, 6H), 5.50 (hept, *J* = 7.2 Hz, 2H), 6.20 – 6.26 (m, 1H), 6.46 – 6.52 (m, 1H), 6.95 – 7.03 (m, 1H), 9.37 (s, 1H). ^{13}C NMR (126 MHz, CD_2Cl_2, ppm) δ = 10.9, 21.4, 109.3, 111.4, 118.9, 124.8, 130.3, 136.2. IR (neat, cm^{-1}): 3181.0, 2716.2, 1772.3, 1715.4, 1620.9, 1602.6, 1376.9, 1070.3, 1051.0, 713.5, 648.9, 607.5, 547.7, 533.2, 506.2. HRMS: *m/z* calcd. for $C_{15}H_{24}N_3S^+$ $[M–SbF_6]^+$ = 278.1685; found = 278.1686; calcd. for SbF_6^- $[M]^-$ = 234.8948; found = 234.8951.

1,3-Diisopropyl-4,5-dimethyl-2-[(1-methyl-1*H*-indol-3-yl)thio]-1*H*-imidazol-3-ium Hexafluoroantimonate (114):

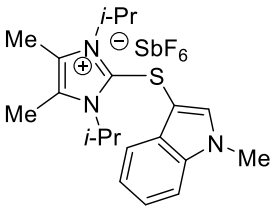

According to GP3, compound **78** (212 mg, 1.00 mmol, 1.20 equiv.) and *N*-chlorosuccinimide (134 mg, 1.00 mmol, 1.20 equiv.) were dissolved in MeCN (10 mL) and stirred for 10 min at rt. 1-Methylindole (107 µL, 109 mg, 831 µmol, 1.00 equiv.) was added, and the yellow solution was stirred at 70 °C for 16 h. The orange brown reaction mixture was allowed to cool down to rt, and all volatiles were removed under reduced pressure. The obtained orange oil was dissolved in DCM (10 mL) and washed with sat. aq. $NaSbF_6$ (10 mL) for 3 min. The organic layer was dried over $MgSO_4$ and concentrated *in vacuo*. After column chromatography (DCM:MeOH), compound **114** was obtained as a yellow foam (361 mg, 624 µmol, 75%).

^{1}H NMR (300 MHz, CD_2Cl_2 ppm) δ = 1.48 (d, *J* = 7.1 Hz, 12H), 2.33 (s, 6H), 3.84 (s, 3H), 5.54 – 5.66 (m, 2H), 7.27 – 7.39 (m, 2H), 7.40 (s, 1H), 7.43 – 7.47 (m, 1H), 7.61 – 7.66 (m, 1H). ^{13}C NMR (75 MHz, CD_2Cl_2, ppm) δ = 10.8, 21.3, 33.9, 53.6, 95.6, 111.4, 118.3, 122.2, 123.9, 128.8, 130.1, 135.8, 137.6, 138.0. IR (neat, cm^{-1}): 2988.2, 2363.3, 1620.9, 1457.9, 1416.5,

1376.0, 1243.9, 1112.7, 737.6, 656.6, 630.6, 541.9. HRMS: *m*/*z* calcd. for $C_{20}H_{28}N_3S^+$ [M–SbF_6]$^+$ = 342.1998; found = 342.1999; calcd. for SbF_6^- [M]$^-$ = 234.8948; found = 234.8952.

1,3-Diisopropyl-4,5-dimethyl-2-[(1-methyl-2-phenyl-1*H*-indol-3-yl)thio]-1*H*-imidazol-3-ium Hexafluoroantimonate (**100**)**:**

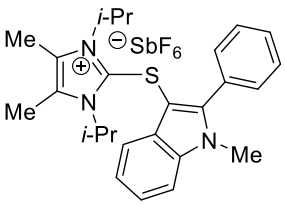

According to GP3, compound **78** (255 mg, 1.20 mmol, 1.20 equiv.) and *N*-chlorosuccinimide (160 mg, 1.20 mmol, 1.20 equiv.) were dissolved in MeCN (10 mL) and stirred for 10 min at rt. 1-Methyl-2-phenylindole (207 mg, 1.00 mmol, 1.00 equiv.) was added, and the yellow solution was stirred at 70 °C for 16 h. The orange brown reaction mixture was allowed to cool down to rt, and all volatiles were removed under reduced pressure. The residual orange oil was dissolved in DCM (10 mL) and washed with sat. aq. $NaSbF_6$ (10 mL) for 4 min. The organic layer was dried over $MgSO_4$ and concentrated *in vacuo*. After column chromatography (DCM:MeOH), compound **100** was obtained as a yellow foam (471 mg, 720 µmol, 72%).

^{1}H NMR (400 MHz, CD_2Cl_2 ppm) δ = 1.22 (d, *J* = 7.1 Hz, 12H), 2.26 (s, 6H), 3.68 (s, 3H), 5.12 (hept, *J* = 7.1 Hz, 2H), 7.34 (t, *J* = 7.6 Hz, 1H), 7.38 – 7.45 (m, 3H), 7.54 (dd, *J* = 18.7, 8.0 Hz, 2H), 7.60 – 7.66 (m, 3H). ^{13}C NMR (126 MHz, CD_2Cl_2, ppm) δ = 11.0, 21.2, 32.5, 53.7, 94.8, 111.6, 118.1, 122.8, 124.4, 128.7, 129.6, 129.7, 129.9, 130.8, 131.1, 137.9, 138.2, 146.9. IR (neat, cm^{-1}): 2993.9, 2941.9, 1693.2, 1621.8, 1464.7, 1445.4, 1427.1, 1396.2, 1377.9, 1338.4, 1294.0, 1236.1, 1217.8, 1157.1, 1134.9, 1111.8, 1020.2, 803.2, 745.4, 709.7, 649.9, 550.6. HRMS: *m*/*z* calcd. for $C_{26}H_{32}N_3S^+$ [M–SbF_6]$^+$ = 418.2311; found = 418.2310; calcd. for SbF_6^- [M]$^-$ = 234.8948; found = 234.8952.

2-{[2-(Hydroxymethyl)-1*H*-indol-3-yl]thio}-1,3-diisopropyl-4,5-dimethyl-1*H*-imidazol-3-ium Hexafluoroantimonate (**115**)**:**

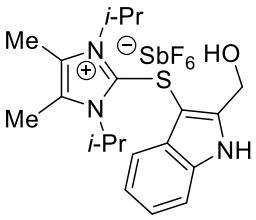

According to GP3, compound **78** (212 mg, 1.00 mmol, 1.20 equiv.), *N*-chlorosuccinimide (134 mg, 1.00 mmol, 1.20 equiv.) and (1*H*-indol-2-yl)methanol (123 mg, 836 µmol, 1.00 equiv.) were dissolved in MeCN (10 mL). The clear red solution was stirred for 16 h at 70 °C. The dark red reaction mixture was allowed to cool down to rt, and all volatiles were removed under reduced pressure. The obtained red solid was dissolved in DCM (10 mL) and washed with sat. aq. $NaSbF_6$ (10 mL) for 5 min. The organic layer was dried over $MgSO_4$ and concentrated *in vacuo*. After column chromatography (DCM:MeOH), compound **115** was obtained as a black foam (403 mg, 678 µmol, 81%).

^{1}H NMR (600 MHz, CD_2Cl_2 ppm) δ = 1.38 (d, *J* = 7.1 Hz, 12H), 2.31 (s, 6H), 4.91 (s, 2H), 5.39 – 5.46 (m, 2H), 7.23 – 7.31 (m, 2H), 7.46 – 7.48 (m, 1H), 7.50 (d, *J* = 8.1 Hz, 2H), 9.45 (s, 1H). ^{13}C NMR (126 MHz, CD_2Cl_2, ppm) δ = 11.0, 21.2, 53.7, 56.8, 93.7, 113.2, 117.5, 122.4, 124.1, 128.9, 129.9, 135.7, 137.9, 144.0. IR (neat, cm^{-1}): 3392.2, 2983.3, 1708.6, 1618.9, 1448.3, 1422.2, 1395.2, 1376.0, 1344.1, 1326.8, 1293.0, 1268.9, 1230.4, 1215.9, 1190.8, 1173.5, 1151.3, 1138.8, 1112.7, 1074.2, 1029.8, 1009.6, 749.2, 651.8, 589.1, 567.0, 546.7. HRMS: *m*/*z* calcd. for $C_{20}H_{28}N_3OS^+$ $[M–SbF_6]^+$ = 358.1948; found = 358.1953; calcd. for SbF_6^- $[M]^-$ = 234.8948; found = 234.8951.

3-[(1,3-Diisopropyl-4,5-dimethyl-1*H*-imidazol-3-ium-2-yl)thio]-5,6-dimethoxy-1*H*-indol-1-ium-2-carboxylate Chloride (**117**)**:**

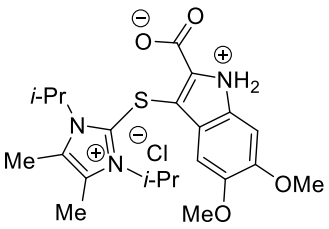

According to GP3, compound **78** (140 mg, 659 µmol, 1.10 equiv.), *N*-chlorosuccinimide (88.1 mg, 660 µmol, 1.10 equiv.) and 5,6-dimethoxy-1*H*-indole-2-carboxylic acid (133 mg, 601 µmol, 1.00 equiv.) were dissolved in MeCN (7.5 mL) and stirred for 24 h at rt. The formed grey precipitate was washed with MeCN (3 × 2 mL) and dried *in vacuo*. Compound **117** was obtained as a white powder (223 mg, 476 µmol, 79%).

^{1}H NMR (400 MHz, CD_2Cl_2 ppm) δ = 1.35 (d, *J* = 7.1 Hz, 12H), 2.34 (s, 6H), 3.21 (s, 2H), 3.85 (d, *J* = 1.3 Hz, 3H), 3.91 (d, *J* = 1.0 Hz, 3H), 5.32 – 5.39 (m, 2H), 6.75 (s, 1H), 7.05 (d, *J* = 1.8 Hz, 1H). ^{13}C NMR (126 MHz, CD_2Cl_2, ppm) δ = 11.1, 21.3, 56.6, 56.8, 95.9, 98.9, 102.5, 121.9, 127.7, 129.7, 131.5, 138.4, 148.4, 151.4, 161.3. IR (neat, cm^{-1}): 3255.3, 1667.2, 1632.4, 1620.9, 1513.8, 1447.3, 1425.1, 1403.9, 1394.3, 1375.0, 1272.8, 1251.6, 1206.3, 1178.3, 1153.2, 1111.8, 1004.7, 849.5, 719.3, 582.4, 564.1. HRMS: *m*/*z* calcd. for $C_{22}H_{30}N_3O_4S^+$ $[M–Cl]^+$ = 432.1952; found = 432.1947.

2-([(2-(Ethoxycarbonyl)-5,6-dimethoxy-1*H*-indol-3-yl)thio]-1,3-diisopropyl-4,5-dimethyl-1*H*-imidazol-3-ium Hexafluoroantimonate (**118**)**:**

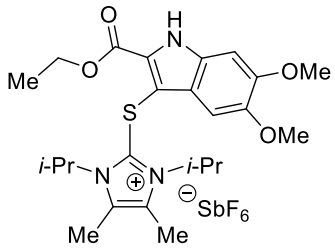

According to GP3, compound **78** (153 mg, 720 µmol, 1.20 equiv.), *N*-chlorosuccinimide (96.1 mg, 720 µmol, 1.20 equiv.) and ethyl 5,6-dimethoxy-1*H*-indole-2-carboxylate (150 mg, 602 µmol, 1.00 equiv.) were dissolved in MeCN (7.5 mL) and stirred for 24 h at rt. All volatiles were removed under reduced pressure. The obtained brown solid was dissolved in DCM (7.5 mL) and washed with sat. aq. $NaSbF_6$ (7.5 mL) for 5 min. The organic layer was dried over $MgSO_4$ and concentrated *in vacuo*. After column chromatography (DCM:MeOH), compound **118** was obtained as a brown foam (392 mg, 563 µmol, 94%).

^{1}H NMR (400 MHz, CD_2Cl_2 ppm) δ = 1.36 – 1.41 (m, 16H), 2.37 (s, 6H), 3.83 (s, 3H), 3.89 (s, 3H), 4.35 (q, *J* = 7.2 Hz, 2H), 5.33 – 5.39 (m, 2H), 6.56 (s, 1H), 7.05 (s, 1H). ^{13}C NMR (101 MHz, CD_2Cl_2, ppm) δ = 11.0, 14.6, 21.3, 54.1, 56.6, 56.7, 62.2, 95.6, 98.8, 104.6, 121.4, 126.0, 130.1, 131.3, 137.4, 148.7, 152.0, 159.7. IR (neat, cm^{-1}): 3415.3, 2357.6, 1696.1, 1514.8, 1454.1, 1341.2, 1263.1, 1241.0, 1209.1, 1180.2, 1157.1, 1112.7, 1032.7, 1019.2, 1003.8, 832.1, 652.8, 593.0, 564.1. HRMS: *m*/*z* calcd. for $C_{24}H_{34}N_3O_4S^+$ $[M–SbF_6]^+$ = 460.2265; found = 460.2266; calcd. for SbF_6^- $[M]^-$ = 234.8948; found = 234.8950.

2-[(5,6-Dihydro-4*H*-pyrrolo[3,2,1-*ij*]quinolin-1-yl)thio]-1,3-diisopropyl-4,5-dimethyl-1*H*-imidazol-3-ium Hexafluoroantimonate (**116**)**:**

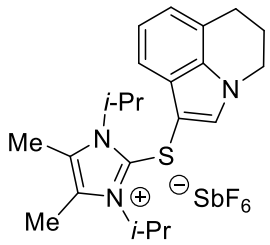

According to GP3, **78** (255 mg, 1.20 mmol, 1.20 equiv.) and *N*-chlorosuccinimide (160 mg, 1.20 mmol, 1.20 equiv.) were dissolved in MeCN (5 mL) and stirred for 10 min at rt. Lilolidine (157 mg, 1.00 mmol, 1.00 equiv.) was added, and the purple solution was stirred at 70 °C for 16 h. The orange reaction mixture was allowed to cool down to rt and all volatiles were removed under reduced pressure. The obtained orange oil was dissolved in DCM (9.0 mL) and washed with sat. aq. $NaSbF_6$ (10 mL) for 3 min. The organic layer was dried over $MgSO_4$ and concentrated *in vacuo*. After column chromatography (DCM:MeOH), compound **116** was obtained as a yellow foam (361 mg, 597 µmol, 60%).

^{1}H NMR (300 MHz, CD_2Cl_2 ppm) δ = 1.49 (d, *J* = 7.1 Hz, 12H), 2.15 – 2.27 (m, 2H), 2.33 (s, 6H), 2.99 (t, *J* = 6.1 Hz, 2H), 4.15 – 4.24 (m, 2H), 5.53 – 5.76 (m, 2H), 7.03 (dd, *J* = 7.2, 1.0 Hz, 1H), 7.18 (dd, *J* = 8.0, 7.1 Hz, 1H), 7.41 (dd, *J* = 8.1, 0.9 Hz, 1H), 7.43 (s, 1H). ^{13}C NMR (126 MHz, CD_2Cl_2, ppm) δ = 10.8, 21.4, 23.3, 24.9, 45.4, 53.7, 95.1, 115.5, 120.7, 122.6, 124.1,

126.6, 129.9, 133.1, 134.8, 138.2. IR (neat, cm^{-1}): 2940.9, 1619.9, 1505.2, 1466.6, 1448.3, 1382.7, 1324.9, 1246.8, 1218.8, 1167.7, 1134.9, 1109.8, 1033.7, 906.4, 827.3, 785.9, 750.2, 652.8, 600.7, 567.9. HRMS: *m*/*z* calcd. for $C_{22}H_{30}N_3S^+$ $[M–SbF_6]^+$ = 368.2155; found = 368.2160; calcd. for SbF_6^- $[M]^-$ = 234.8948; found = 234.8951.

1,3-Diisopropyl-2-{[6-methoxy-2-(4-methoxyphenyl)benzo[*b*]thiophen-3-yl]thio}-4,5-dimethyl-1*H*-imidazol-3-ium Hexafluoroantimonate (**123**)**:**

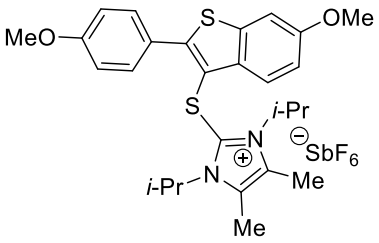

Product **123** was prepared according to modified GP2. Compound **93** (255 mg, 467 µmol, 1.20 equiv.) was dissolved in MeCN (10 mL) and stirred for 10 min at rt. 6-Methoxy-2-(4-methoxyphenyl)benzo[*b*]thiophene (105 mg, 388 µmol, 1.00 equiv.) was added, and the yellow solution was stirred at 70 °C for 16 h. The yellow reaction mixture was allowed to cool down to rt and all volatiles were removed under reduced pressure. The residual orange oil was dissolved in DCM (5 mL) and washed with sat. aq. $NaSbF_6$ (10 mL) for 5 min. The organic layer was dried over $MgSO_4$ and concentrated *in vacuo*. After column chromatography (DCM:MeOH), **123** was obtained as a yellow foam (250 mg, 350 µmol, 90%).

^{1}H NMR (300 MHz, CD_2Cl_2 ppm) δ = 1.28 (d, *J* = 7.1 Hz, 12H), 2.27 (s, 6H), 3.88 (s, 3H), 3.89 (s, 3H), 5.06 (hept, *J* = 7.1 Hz, 2H), 7.05 – 7.11 (m, 2H), 7.11 – 7.15 (m, 1H), 7.37 (d, *J* = 2.3 Hz, 1H), 7.45 (d, *J* = 8.9 Hz, 1H), 7.49 – 7.54 (m, 2H). ^{13}C NMR (75 MHz, CD_2Cl_2, ppm) δ = 10.9, 21.0, 53.9, 56.1, 56.3, 106.2, 112.1, 115.2, 116.3, 122.4, 124.4, 130.7, 131.7, 133.2, 135.9, 140.1, 149.2, 159.0, 161.7. IR (neat, cm^{-1}): 2939.0, 1604.5, 1529.3, 1477.2, 1461.8, 1439.6, 1421.3, 1397.2, 1377.9, 1299.8, 1290.1, 1247.7, 1214.9, 1176.4, 1111.8, 1062.6, 1029.8, 957.5, 849.5, 837.9, 805.1, 766.6, 734.7, 710.6, 651.8, 606.5, 586.3, 562.1, 546.7, 536.1. HRMS: *m*/*z* calcd. for $C_{27}H_{33}N_2O_2S_2^+$ $[M–SbF_6]^+$ = 481.1978; found = 481.1980; calcd. for SbF_6^- $[M]^-$ = 234.8948; found = 234.8950.

1,3-Diisopropyl-4,5-dimethyl-2-[(5-methylthiophen-2-yl)thio]-1*H*-imidazol-3-ium Hexafluoroantimonate (**122**)**:**

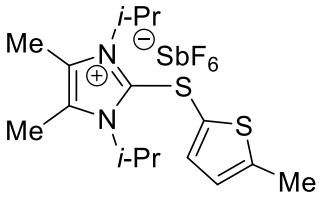

According to modified GP2, compound **93** (120 mg, 220 µmol, 1.20 equiv.) was dissolved in MeCN (1.5 mL) and stirred for 10 min at rt. 2-Methylthiophene (18 mg, 17.6 µL, 183 µmol, 1.0 equiv.) was added, and the yellow solution was stirred at 70 °C for 16 h. The dark brown reaction mixture was allowed to cool down to rt and all volatiles were removed under reduced pressure. The residual orange oil was dissolved in DCM

(2 mL) and washed with sat. aq. $NaSbF_6$ (3 mL) for 5 min. The organic layer was dried over $MgSO_4$ and concentrated *in vacuo*. After column chromatography (DCM:MeOH), compound **122** was obtained as a yellow foam (61.2 mg, 112 µmol, 61%).

^{1}H NMR (300 MHz, CD_2Cl_2 ppm) δ = 1.58 (d, *J* = 7.1 Hz, 12H), 2.39 (s, 6H), 2.47 (d, J = 1.1 Hz, 3H), 5.48 (hept, *J* = 7.1 Hz, 2H), 6.76 – 6.79 (m, 1H), 7.23 (d, *J* = 3.7 Hz, 1H). ^{13}C NMR (75 MHz, CD_2Cl_2, ppm) δ = 10.9, 16.1, 21.4, 54.1, 121.7, 127.4, 131.0, 137.2, 149.2. IR (neat, cm^{-1}): 1422.2, 1396.2, 1376.9, 1217.8, 1137.8, 1112.7, 1092.5, 1070.3, 953.6, 803.2, 711.6, 652.8, 603.6, 567.9, 518.8. HRMS: *m*/*z* calcd. for $C_{16}H_{25}N_2S_2^+$ $[M–SbF_6]^+$ = 309.1454; found = 309.1454; calcd. for SbF_6^- $[M]^-$ = 234.8948; found = 234.8950.

2-{[4-(Dimethylamino)phenyl]thio}-1,3-diisopropyl-4,5-dimethyl-1*H*-imidazol-3-ium Hexafluoroantimonate (**129**)**:**

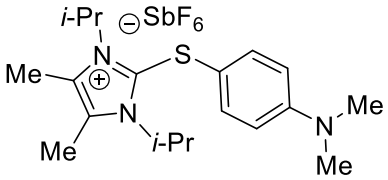

According to modified GP2, compound **93** (157 mg, 287 µmol, 1.20 equiv.) was dissolved in MeCN (3 mL) and stirred for 10 min at rt. Dimetylaniline (**272**, 30.3 µL, 29 mg, 239 µmol, 1.00 equiv.) was added, and the yellow solution was stirred at 70 °C for 16 h. The dark blue reaction mixture was allowed to cool down to rt, and all volatiles were removed under reduced pressure. The residual dark blue oil was dissolved in DCM (3 mL) and washed with sat. aq. $NaSbF_6$ (3 mL) for 5 min. The organic layer was dried over $MgSO_4$ and concentrated *in vacuo*. After column chromatography (DCM:MeOH), compound **129** was obtained as a blue foam (123 mg, 216 µmol, 90%).

^{1}H NMR (300 MHz, CD_2Cl_2 ppm) δ = 1.51 (d, *J* = 7.1 Hz, 12H), 2.38 (s, 6H), 2.96 (s, 6H), 5.35 – 5.50 (m, 2H), 6.64 – 6.70 (m, 2H), 7.15 – 7.22 (m, 2H). ^{13}C NMR (126 MHz, CD_2Cl_2, ppm) δ = 10.9, 21.5, 40.5, 53.9, 112.4, 113.9, 130.4, 133.4, 137.6, 152.0. IR (neat, cm^{-1}): 2939.9, 1595.8, 1505.2, 1469.5, 1444.4, 1426.1, 1393.3, 1373.1, 1359.6, 1218.8, 1197.6, 1171.5, 1140.7, 1112.7, 946.9, 809.0, 653.8, 607.5, 516.8. HRMS: *m*/*z* calcd. for $C_{19}H_{30}N_3S^+$ $[M–SbF_6]^+$ = 332.2155; found = 332.2155; calcd. for SbF_6^- $[M]^-$ = 234.8948; found = 234.8950.

2-{[4,5-Bis(dimethylamino)naphthalen-1-yl]thio}-1,3-diisopropyl-4,5-dimethyl-1*H*-imidazol-3-ium Hexafluoroantimonate (**136**)**:**

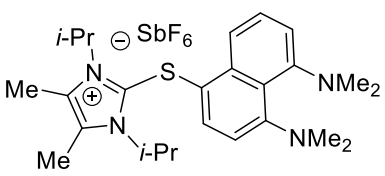

According to modified GP2, compound **93** (600.8 mg, 1.1 mmol, 1.10 equiv.) and 1,8-bis(dimethylamino)-naphthalene (214.3 mg, 1.00 mmol, 1.00 equiv.) were dissolved in MeCN (10 mL), and the deep red solution was stirred for 16 h. All volatiles were removed under reduced pressure. The residual dark green

oil was dissolved in DCM (10 mL) and washed with sat. aq. $NaSbF_6$ (10 mL) for 5 min. The organic layer was dried over $MgSO_4$ and concentrated *in vacuo*. After column chromatography (DCM:MeOH), **136** was obtained as a yellow solid (301.2 mg, 455.3 µmol, 46%).

^{1}H NMR (300 MHz, CD_2Cl_2 ppm) δ = 1.55 (d, *J* = 7.1 Hz, 12H), 2.50 (s, 6H), 3.14 (d, *J* = 2.7 Hz, 6H), 3.18 (d, *J* = 2.5 Hz, 6H), 5.11 (hept, *J* = 7.0 Hz, 2H), 6.93 (d, *J* = 8.2 Hz, 1H), 7.80 – 8.01 (m, 3H), 8.35 (dd, *J* = 7.8, 1.8 Hz, 1H). ^{13}C NMR (101 MHz, CD_2Cl_2, ppm) δ = 11.1, 21.5, 27.3, 47.0, 47.0, 120.2, 122.7, 123.5, 125.2, 126.5, 129.5, 132.1, 132.2, 133.4, 144.2, 145.4. IR (neat, cm^{-1}): 1462.7, 1403.9, 1377.9. 1262.2. 1214.9. 1196.6. 1170.6. 1136.8. 1109.8. 1015.3. 837.9. 807.1. 766.6. 652.8. 588.2. HRMS: *m*/*z* calcd. for $C_{25}H_{37}N_4S^+$ $[M–SbF_6]^+$ = 425.2733; found = 425.2734; calcd. for SbF_6^- $[M]^-$ = 234.8948; found = 234.8952.

2-[(4-Aminophenyl)thio]-1,3-diisopropyl-4,5-dimethyl-1*H*-imidazol-3-ium Hexafluoro-antimonate (**131**)**:**

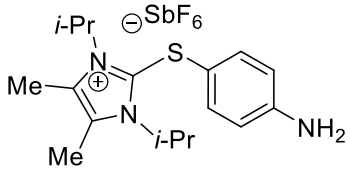

According to modified GP2, compound **93** (150 mg, 275 µmol, 1.22 equiv.) was dissolved in MeCN (5 mL) and stirred for 10 min at rt. Aniline (21 µL, 21 mg, 225 µmol, 1.00 equiv.) was added, and the yellow solution was stirred at 70 °C for 16 h. The yellow reaction mixture was allowed to cool down to rt and all volatiles were removed under reduced pressure. The residual yellow oil was dissolved in DCM (3 mL) and washed with sat. aq. $NaSbF_6$ (3 mL) for 5 min. The organic layer was dried over $MgSO_4$ and concentrated *in vacuo*. After twofold column chromatography (DCM:MeOH), compound **137** was obtained as a yellow oil (63.7 mg, 118 µmol, 52%)[12].

[12] After the first chromatographic purification, the yield was approximated 81%. Unfortunately, the isolated fraction was contaminated with residual succinimide which was removed by the second column chromatography.

^{1}H NMR (300 MHz, CD_2Cl_2 ppm) δ = 1.49 (d, *J* = 7.1 Hz, 12H), 2.37 (s, 6H), 4.12 (s, 2H), 5.35 (sept, *J* = 7.1 Hz, 2 H), 6.69 (m, 2H), 7.09 (m, 2H). ^{13}C NMR (75 MHz, CD_2Cl_2, ppm) δ = 10.8, 21.3, 53.8, 115.2, 116.8, 130.5, 133.4, 137.1, 149.6. IR (neat, cm^{-1}): 3506, 3407, 2984, 2945, 1620, 1595, 1500, 1415, 1305, 835, 655, 530. HRMS: *m*/*z* calcd. for $C_{17}H_{26}N_3S^+$ $[M–SbF_6]^+$ = 304.1851; found = 304.1842; calcd. for SbF_6^- $[M]^-$ = 234.8948; found = 234.8948.

1,3-Diisopropyl-4,5-dimethyl-2-{[4-(methylamino)phenyl]thio}-1*H*-imidazol-3-ium Hexafluoroantimonate (**130**)**:**

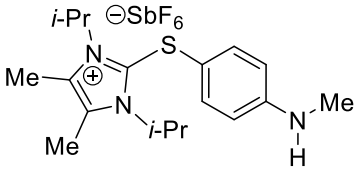

According to GP3, compound **78** (255 mg, 1.20 mmol, 1.20 equiv.), *N*-chlorosuccinimide (160 mg, 1.20 mmol, 1.20 equiv.) and *N*-methylaniline (107 mg, 108 µL, 1.00 mmol, 1.00 equiv.) were dissolved in MeCN (10 mL). The yellow solution was stirred at rt for 16 h. All volatiles were removed under reduced pressure. The residual yellow oil was dissolved in DCM (10 mL) and washed with sat. aq. $NaSbF_6$ (10 mL) for 5 min. The organic layer was dried over $MgSO_4$ and concentrated *in vacuo*. After column chromatography (DCM:MeOH), compound **130** was obtained as a white foam (240 mg, 433 µmol, 43%).

^{1}H NMR (300 MHz, CD_2Cl_2 ppm) δ = 1.50 (d, *J* = 7.1 Hz, 12H), 2.37 (s, 6H), 2.80 (s, 3H), 4.29 (s, 1H), 5.33 – 5.46 (m, 2H), 6.57 – 6.64 (m, 2H), 7.10 – 7.17 (m, 2H). ^{13}C NMR (101 MHz, CD_2Cl_2, ppm) δ = 10.7, 21.3, 30.5, 53.7, 114.1, 130.4, 133.7, 151.6. IR (neat, cm^{-1}): 3437.5, 2988.2, 1596.8, 1509.0, 1448.3, 1421.3, 1397.2, 1376.9, 1326.8, 1215.9, 1186.0, 1111.8, 822.5, 752.1, 570.8, 545.8, 523.6. HRMS: *m*/*z* calcd. for $C_{18}H_{28}N_3S^+$ $[M–SbF_6]^+$ = 318.1998; found = 318.2003; calcd. for SbF_6^- $[M]^-$ = 234.8948; found = 234.8948.

2-[(2,4-Dimethoxyphenyl)thio]-1,3-diisopropyl-4,5-dimethyl-1*H*-imidazol-3-ium Hexafluoroantimonate (**137**)**:**

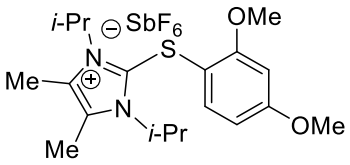

According to modified GP2, compound **93** (901 mg, 1.65 mmol, 1.20 equiv.) was dissolved in MeCN (12 mL) and stirred for 10 min at rt. 1,3-Dimethoxybenzene (190 mg, 180.1 µL, 1.375 mmol, 1.00 equiv.) was added, and the yellow solution was stirred at 70 °C for 16 h. The yellow solution was allowed to cool down to rt and all volatiles were removed under reduced pressure. The residual yellow oil was dissolved in DCM (15 mL) and washed with sat. aq. $NaSbF_6$ (15 mL) for 5 min. The organic layer was dried over $MgSO_4$ and concentrated *in vacuo*. After column chromatography (DCM:MeOH), compound **137** was obtained as a white solid (465 mg, 794.5 µmol, 58%).

^{1}H NMR (300 MHz, CD_2Cl_2 ppm) δ = 1.48 (d, *J* = 7.1 Hz, 12H), 2.38 (s, 6H), 3.82 (s, 3H), 3.83 (s, 3H), 5.39 (hept, *J* = 7.1 Hz, 2H), 6.52 – 6.61 (m, 2H), 7.24 (d, *J* = 8.6 Hz, 1H). ^{13}C NMR (126 MHz, CD_2Cl_2, ppm) δ = 11.0, 21.5, 54.0, 56.4, 57.0, 100.5, 107.5, 130.6, 134.4, 136.6, 159.9, 163.8. IR (neat, cm^{-1}): 2944.8, 2357.6, 1602.6, 1590.0, 1487.8, 1454.1, 1436.7, 1415.5, 1314.3, 1286.3, 1210.1, 1159.0, 1115.6, 1074.2, 1033.7, 828.3, 798.4, 653.8. HRMS: *m*/*z* calcd. for $C_{19}H_{29}N_2O_2S^+$ $[M–SbF_6]^+$ = 349.1944; found = 349.1947; calcd. for SbF_6^- $[M]^-$ = 234.8948; found = 234.8948.

1,3-Diisopropyl-4,5-dimethyl-2-[(2,4,6-trimethoxyphenyl)thio]-1*H*-imidazol-3-ium Hexafluoroantimonate (**138**)**:**

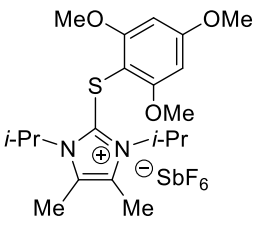

According to GP3, compound **78** (510 mg, 2.40 mmol, 1.20 equiv.), *N*-chlorosuccinimide (320 mg, 2.40 mmol, 1.20 equiv.) and 1,3,5-trimethoxybenzene (336 mg, 2.00 mmol, 1.00 equiv.) were dissolved in dry MeCN (20 mL). The red solution was stirred at 70 °C for 16 h. The dark red reaction mixture was allowed to cool down to rt and all volatiles were removed under reduced pressure. The residual yellow oil was dissolved in DCM (20 mL) and washed with sat. aq. $NaSbF_6$ (20 mL) for 5 min. The organic layer was dried over $MgSO_4$ and concentrated *in vacuo*. After column chromatography (DCM:MeOH), compound **138** was obtained as a yellow solid (1.09 g, 1.77 mmol, 89%).

^{1}H NMR (400 MHz, CD_2Cl_2 ppm) δ = 1.44 (d, *J* = 7.1 Hz, 12H), 2.34 (s, 6H), 3.84 (s, 3H), 3.86 (s, 6H), 5.50 (hept, *J* = 7.1 Hz, 2H), 6.21 (s, 2H). ^{13}C NMR (101 MHz, CD_2Cl_2, ppm) δ = 10.9, 21.4, 53.4, 56.3, 57.1, 92.2, 94.5, 129.8, 138.3, 161.7, 164.8. IR (neat, cm^{-1}): 2978.5, 2942.8, 1582.3, 1455.0, 1412.6, 1374.0, 1339.3, 1231.3, 1204.3, 1187.0, 1160.9, 1122.4, 1092.5, 1026.9, 949.8, 915.1, 808.0, 756.0, 651.8, 633.5, 546.7, 518.8. HRMS: *m*/*z* calcd. for $C_{20}H_{31}N_2O_3S^+$ $[M–SbF_6]^+$ = 379.2050; found = 379.2051; calcd. for SbF_6^- $[M]^-$ = 234.8948; found = 234.8950.

1,3-Diisopropyl-2-[{5-[(4-methoxyphenyl)thio]-1-phenyl-1*H*-pyrrol-2-yl}thio]-4,5-dimethyl-1*H*-imidazol-3-ium Hexafluoroantimonate (**201**)**:**

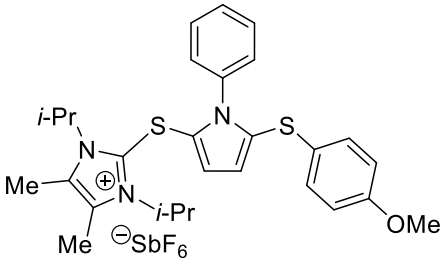

According to GP3, compound **78** (219 mg, 1.03 mmol, 1.00 equiv.), *N*-chlorosuccinimide (138 mg, 1.03 mmol, 1.00 equiv.) and 2-[(4-methoxyphenyl)thio]-1-phenyl-1*H*-pyrrole (290 mg, 1.03 mmol, 1.00 equiv.) were dissolved in dry MeCN (10 mL). The yellow solution was stirred at 70 °C for 17 h. The orange reaction mixture was allowed

to cool down to rt and all volatiles were removed under reduced pressure. The residual yellow oil was dissolved in DCM (10 mL) and washed with sat. aq. $NaSbF_6$ (10 mL) for 5 min. The organic layer was dried over $MgSO_4$ and concentrated *in vacuo*. The almost pure crude product of **201** was obtained as a yellow solid (560 mg, 769 mmol, 75%). An analytical sample was obtained by column chromatography (DCM:MeOH) of a small aliquot of the crude product.

^{1}H NMR (300 MHz, CD_3CN ppm) δ = 1.32 (d, *J* = 7.1 Hz, 12H), 2.28 (s, 6H), 3.73 (s, 3H), 4.89 (hept, *J* = 7.0 Hz, 2H), 6.56 (d, *J* = 4.0 Hz, 1H), 6.70 (d, *J* = 3.9 Hz, 1H), 6.76 (d, *J* = 8.8 Hz, 2H), 6.89 (d, *J* = 8.9 Hz, 2H), 7.05 – 7.11 (m, 2H), 7.43 – 7.59 (m, 3H). ^{13}C NMR (101 MHz, CD_2Cl_2, ppm) δ = 10.7, 21.1, 54.0, 56.0, 115.7, 120.5, 127.2, 127.6, 128.9, 129.7, 130.2, 130.6, 131.1, 131.6, 137.3, 160.1. IR (neat, cm^{-1}): 2992.0, 2942.8, 1615.1, 1599.7, 1568.8, 1519.6, 1461.8, 1422.2, 1403.0, 1377.9, 1342.2, 1320.0, 1266.0, 1216.9, 1196.6, 1170.6, 1139.7, 1109.8, 1054.9, 1014.4, 986.4, 898.7, 838.9, 828.3, 810.0, 766.6, 742.5, 651.8, 588.2, 569.9, 526.5, 517.8, 507.2. HRMS: *m/z* calcd. for $C_{28}H_{34}N_3OS_2^+$ $[M–SbF_6]^+$ = 492.2138; found = 492.2141.

2-[(4-Amino-3-methylphenyl)thio]-1,3-diisopropyl-4,5-dimethyl-1*H*-imidazol-3-ium Hexafluoroantimonate (**134A**) and **2-[(2-Amino-3-methylphenyl)thio]-1,3-diisopropyl-4,5-dimethyl-1*H*-imidazol-3-ium Hexafluoroantimonate** (**134B**)**:**

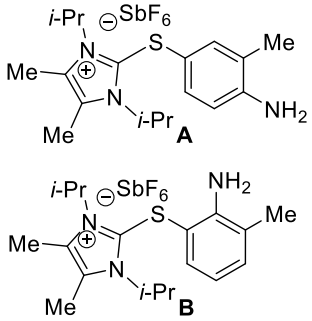

According to GP3, compound **78** (234 mg, 1.10 mmol, 1.10 equiv.), *N*-chlorosuccinimide (147 mg, 1.10 mmol, 1.10 equiv.) and *o*-toluidine (106.6 µL, 107 mg, 1.00 mmol, 1.00 equiv.) were dissolved in dry MeCN (10 mL). The orange solution was stirred at 70 °C for 16 h. The orange reaction mixture was allowed to cool down to rt and all volatiles were removed under reduced pressure. The residual yellow oil was dissolved in DCM (10 mL) and washed with sat. aq. $NaSbF_6$ (10 mL) for 5 min. The organic layer was dried over $MgSO_4$ and concentrated *in vacuo*. After column chromatography (DCM:MeOH), product **134** was obtained as a white solid (470 mg, 848 µmol, 85%) as a mixture of regiomers. The ratio of **134A : 134A B** was 72 : 28, as determined by the integration of the methyl groups in the methylaniline moiety of **134**. Repetitive chromatography (DCM:MeOH) as well as further attempts to separate regiomers by HPLC were not successful. Decreasing the reaction temperature to ambient resulted in a lower yield of 63% after 24 h stirring with a similar ratio of the regiomers **A** and **B**. However, the identity of the compound **134A** and **134B** was confirmed by X-Ray structure analysis of a single crystal. The ratio **A**:**B** in the solid state was essentially identical to their ratio in the solution (76:24).

^{1}H NMR (300 MHz, CD_2Cl_2 ppm) δ = 1.43 – 1.54 (m, A&B, 12H), 2.13 (s, A, 2.28H), 2.21 (s, B, 0.77H), 2.38 (s, A&B, 6H), 4.01 (s, A, 1.38H), 4.41 (s, B, 0.47H), 5.23 (hept, B, *J* = 7.1 Hz, 0.52H), 5.34 – 5.47 (hept, A, *J* = 7.1 Hz, 1.20H), 6.66 – 6.75 (m, A&B, 1.28H), 6.95 – 7.04 (m, A&B, 1.49H), 7.11 (d, B, *J* = 7.0 Hz, 0.24H). IR (neat, cm^{-1}): 1699.0, 1587.1, 1376.9, 1343.2, 1237.1, 1167.7, 1107.9, 1025.0, 907.3, 807.1, 755.0, 652.8. HRMS: *m*/*z* calcd. for $C_{18}H_{28}N_3S_2^+$ $[M–SbF_6]^+$ = 318.1998; found = 318.1997; calcd. for SbF_6^- $[M]^-$ = 234.8948; found = 234.8950.

2-{[4-(Benzylamino)phenyl]thio}-1,3-diisopropyl-4,5-dimethyl-1*H*-imidazol-3-ium Hexafluoroantimonate (**132**):

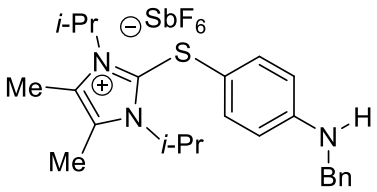

According to modified GP3, compound **78** (1.06 g, 5.00 mmol, 1.00 equiv.), *N*-chlorosuccinimide (668 mg, 5.00 mmol, 1.00 equiv.) and *N*-benzylaniline (1.01 g, 5.50 mmol, 1.10 equiv.) were dissolved in DCE (40 mL). The yellow solution was stirred at 70 °C for 16 h. After the yellow reaction mixture was cooled to rt, it was washed with sat. aq. $NaSbF_6$ (50 mL) for 1 min. The organic layer was dried over $MgSO_4$ and concentrated *in vacuo*. After twofold repetitive column chromatography (DCM:MeOH), **132** was obtained as a yellow solid (1,14 g, 1.82 µmol, 33%)[13].

^{1}H NMR (300 MHz, CD_2Cl_2 ppm) δ = 1.50 (d, *J* = 7.4 Hz, 12H), 2.37 (s, 6H), 4.35 (d, *J* = 6.6 Hz, 2H), 4.72 (bs, 1H), 5.35 (sept, *J* = 7.4 Hz, 2H), 6.65 (m, 2H), 7.12 (m, 2H), 7.23-7.39 (m, 5H). ^{13}C NMR (75 MHz, CD_2Cl_2, ppm) δ = 10.7, 21.3, 47.9, 53.7, 114.0, 114.8, 127.7, 127.8, 129.1, 130.4, 133.6, 137.3, 139.1, 150.2. IR (neat, cm^{-1}): 3423, 2985, 1594, 1441, 1420, 1107, 821, 737, 648, 522. HRMS: *m*/*z* calcd. for $C_{24}H_{32}N_3S^+$ $[M–SbF_6]^+$ = 394.2311; found = 394.2316; calcd. for SbF_6^- $[M]^-$ = 234.8948; found = 234.8949.

[13] After the first chromatographic purification, the NMR yield was 82% (based on ^{1}H NMR spectrum), but some residual succinimide still presented and was removed by the second column chromatography.

1,3-Diisopropyl-4,5-dimethyl-2-[(9-methyl-9*H*-carbazol-3-yl)thio]-1*H*-imidazol-3-ium Hexafluoroantimonate (**119**):

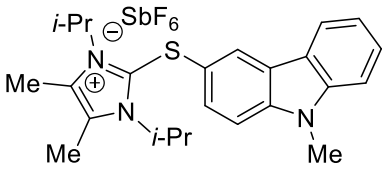

According to GP2, compound **93** (131 mg, 240 µmol, 1.20 equiv.) and 9-methylcarbazole (36.1 mg, 199 µmol, 1.00 equiv.) were dissolved in anhydrous DCE (2.5 mL), and the obtained green solution was stirred at 70 °C for 16 h until complete conversion. The reaction mixture was cooled to rt and washed with sat. aq. $NaSbF_6$ (6 mL) for one minute. The aq. phase was re-extracted with DCM (3 × 10 mL). Combined organic phases were dried over magnesium sulfate, and the solvents were removed *in vacuo*. After column chromatography (DCM:MeOH), **119** was obtained as a blue solid (58.0 mg, 92.3 µmol, 46%).[14]

^{1}H NMR (300 MHz, CD_2Cl_2 ppm) δ = 1.53 (d, *J* = 7.1 Hz, 12H), 2.44 (s, 6H), 3.87 (s, 3 H), 5.51 (s, 2H), 7.30 (td, *J* = 1.0, 8.0 Hz, 1H), 7.38 (dd, *J* = 1.9, 8.6 Hz, 1H), 7.47 (dt, *J* = 0.9, 8.2 Hz, 1H), 7.51 (d, *J* = 8.6 Hz, 1H), 7.55 (td, *J* = 1.2, 8.3 Hz, 1H), 8.09 (dt, *J* = 1.2, 8.0 Hz, 1H), 8.12 (d, *J* = 1.9 Hz, 1H). ^{13}C NMR (75 MHz, CD_2Cl_2, ppm) δ = 11.1, 21.5, 29.9, 44.8, 109.8, 111.4, 113.8, 117.9, 120.5, 121.0, 121.9, 124.0, 124.8, 127.7, 128.6, 130.7, 141.8, 142.2. IR (neat, cm^{-1}): 3404, 2971, 2926, 2856, 1616, 1598, 1458, 1418, 1373, 1249, 1111, 744, 658, 626. HRMS: *m*/*z* calcd. for $C_{24}H_{30}N_3S^+$ $[M–SbF_6]^+$ = 392.2155; found = 392.2165; calcd. for SbF_6^- $[M]^-$ = 234.8948; found = 234.8950.

[14] Due to an essential amount of residual succinimide (0.2 equiv.) in the product, its purification by chromatography was repeated six times until a pure compound was obtained as a blue solid (19.0 mg, 30 µmol, 15%).

2-[(4-Aminophenyl)thio]-1,3,4,5-tetramethyl-1*H*-imidazol-3-ium Hexafluoroantimonate (**299**):

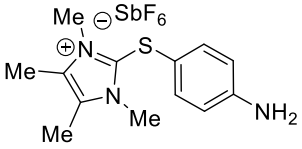

According to modified GP3, *N*-chlorosuccinimide (133.5 mg, 1.00 mmol, 1.20 equiv.) and compound **95** (156 mg, 1.00 mmol, 1.20 equiv.) were dissolved in anhydrous DCE (10 mL). Aniline (75.3 µL, 77.6 mg, 833 µmol, 1.00 equiv.) was added dropwise. The obtained yellow solution was stirred at 70 °C for 18 h. The brown reaction mixture was cooled to rt and washed with sat. aq. $NaSbF_6$ solution. The aq. phase was re-extracted with DCM (3 × 20 mL). The combined organic phases were dried over magnesium sulfate, and the solvents were removed *in vacuo*. The residual brown oily liquid was purified by column chromatography with DCM as the eluent with a 0–10 %-MeOH gradient. The desired compound was obtained as a brown solid (218 mg, 450 µmol, 54%).

^{1}H NMR (300 MHz, CD_2Cl_2, ppm) δ = 2.28 (s, 6H), 3.82 (s, 6H), 4.11 (bs, 2H), 6.69 (d, *J* = 8.7 Hz, 2H), 7.12 (d, *J* = 8.7 Hz, 2H). ^{13}C NMR (75 MHz, CD_2Cl_2, ppm) δ = 9.8, 34.3, 113.5, 116.7, 130.1, 134.47, 138.6, 149.7. IR (neat, cm^{-1}) = 3494, 3402, 3391, 1627, 1618, 1595, 1498, 1303, 1183, 834, 648, 523. MS (ESI): *m*/*z* (negative mode, %): calculated: 234.9 (100) [$^{121}SbF_6$]$^-$, 236.9 (75) [$^{123}SbF_6$]$^-$, found: 234.9 (100) [$^{121}SbF_6$]$^-$, 236.9 (75) [$^{123}SbF_6$]$^-$. HRMS (ESI): *m*/*z* calc. for $C_{13}H_{18}N_3S^+$ [M–SbF_6]$^+$ =: 248.1216; found: 248.1224 (100).

1,3-Diisopropyl-4,5-dimethyl-2-[(1-methyl-2-oxoindolin-3-yl)thio]-1*H*-imidazol-3-ium Hexafluoroantimonate (**151**):

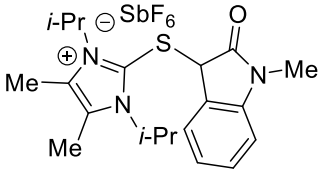

According to modified GP2, compound **93** (65.5 mg, 120 µmol, 1.00 equiv.) and *N*-methylindolin-2-one (17.7 mg, 120 µmol, 1.00 equiv.) were dissolved in anhydrous MeCN (2.0 mL) and the obtained yellow solution was stirred at 70 °C for 16 h until full conversion. The reaction mixture was cooled to rt and ~~was~~ washed with sat. aq. $NaSbF_6$ (6 mL) for one minute. The aq. phase was re-extracted with DCM (3 × 10 mL). The combined organic phases were dried over magnesium sulfate, and the solvents were removed *in vacuo*. After column chromatography (DCM:MeOH), **151** was obtained as a red solid (60.0 mg, 101 µmol, 84%).

^{1}H NMR (400 MHz, CD_2Cl_2 ppm) δ = 1.59 (t, *J* = 6.6 Hz, 12H), 2.44 (s, 6H), 3.19 (s, 3H), 4.74 (s, 1H), 5.35 (sept, *J* = 7.4 Hz, 2H), 6.98 (d, *J* = 7.9 Hz, 1H), 7.21 (td, *J* = 7.6, 1.0 Hz, 1H), 7.47 (tt, *J* = 7.4, 1.0 Hz, 2H). ^{13}C NMR (75 MHz, CD_2Cl_2, ppm) δ = 11.2, 21.5, 21.5, 27.1, 48.3, 110.2, 122.2, 124.4, 125.8, 131.7, 131.8, 144.8, 171.5. IR (neat, cm^{-1}): 2980.6, 1772.2, 1708.7,

1611.6, 1492.3, 1470.9, 1418.5, 1372.1, 1344.0, 1295.2, 1191.1, 1122.7, 1091.6, 819.1, 766.3, 653.5. HRMS: *m*/*z* calcd. for $C_{20}H_{28}N_3OS^+$ [M–SbF_6]$^+$ = 358,1948; found = 358.1977; calcd. for SbF_6^- [M]$^-$ = 234.8948; found = 234.8950.

5.2.4 Synthesis of aryltriazolium salts

5-{[2-(Ethoxycarbonyl)-5,6-dimethoxy-1*H*-indol-3-yl]thio}-1,4-diisopropyl-1*H*-1,2,4-triazol-4-ium Hexafluoroantimonate (**300**):

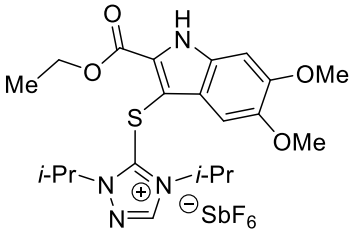

According to GP2, triazole-3-thione **209** (92.6 mg, 500 µmol, 1.00 equiv.), *N*-chlorosuccinimide (66.8 mg, 500 µmol, 1.00 equiv.) and ethyl 5,6-dimethoxy-1*H*-indole-2-carboxylate (131 mg, 525 µmol, 1.05 equiv.) were dissolved in DCM (5.0 mL) and stirred at rt for 17 h. The orange reaction mixture was washed with sat. aq. $NaSbF_6$ (3.5 mL) for 5 min. The organic layer was dried over $MgSO_4$ and concentrated *in vacuo*. After column chromatography (DCM:MeOH), **300** was obtained as a brown foam (222 mg, 332 µmol, 66%).

^{1}H NMR (400 MHz, CD_2Cl_2 ppm) δ = 1.31 – 1.38 (m, 9H), 1.47 (d, *J* = 6.8 Hz, 6H), 3.93 (s, 3H), 3.95 (s, 3H), 4.31 (q, *J* = 7.1 Hz, 2H), 4.93 (d, *J* = 7.0 Hz, 2H), 7.06 (s, 1H), 7.13 (s, 1H), 8.49 (s, 1H), 9.76 (s, 1H). ^{13}C NMR (126 MHz, CD_2Cl_2, ppm) δ = 14.5, 21.7, 22.8, 56.3, 56.7, 56.9, 62.5, 95.6, 98.8, 99.5, 122.9, 127.0, 130.9, 141.8, 147.7, 149.4, 152.4, 159.4. IR (neat, cm^{-1}): 3349.7, 2968.9, 1714.4, 1518.7, 1490.7, 1458.9, 1444.4, 1405.9, 1374.0, 1344.1, 1332.6, 1269.9, 1246.8, 1206.3, 1192.8, 1179.3, 1158.0, 1115.6, 1054.9, 1024.0, 1011.5, 1000.9, 857.2, 830.2, 773.3, 740.5, 658.6, 642.2, 581.4, 558.3. HRMS: *m*/*z* calcd. for $C_{21}H_{29}N_4O_4S^+$ [M–SbF_6]$^+$ = 433.1904; found = 433.1904.

1,4-Diisopropyl-5-[(1-phenyl-1*H*-pyrrol-2-yl)thio]-1*H*-1,2,4-triazol-4-ium Hexafluoroantimonate (**210**):

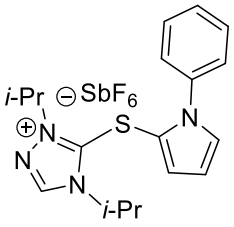

According to GP2, triazole-3-thione **209** (185 mg, 1.00 mmol, 1.00 equiv.), *N*-chlorosuccinimide (133.5 mg, 1.00 mmol, 1.00 equiv.) and phenyl pyrrole (150 mg, 1.05 mmol, 1.05 equiv.) were dissolved in DCM (5.0 mL) and stirred at rt for 17 h. The yellow reaction mixture was washed with sat. aq. $NaSbF_6$ (7.0 mL) for 5 min. The organic layer was dried over $MgSO_4$ and concentrated *in vacuo*. After column chromatography (DCM:MeOH), **210** was obtained as a white solid (362 mg, 643 µmol, 63%).

^{1}H NMR (400 MHz, CD_2Cl_2 ppm) δ = 1.28 (d, *J* = 6.7 Hz, 6H), 1.33 (d, *J* = 6.7 Hz, 6H), 4.32

(hept, *J* = 6.7 Hz, 1H), 4.69 (hept, *J* = 6.7 Hz, 1H), 6.48 (dd, *J* = 4.0, 3.0 Hz, 1H), 7.03 (dd, *J* = 3.9, 1.7 Hz, 1H), 7.19 (dd, *J* = 2.9, 1.7 Hz, 1H), 7.22 – 7.26 (m, 2H), 7.52 – 7.57 (m, 3H), 8.42 (s, 1H). ^{13}C NMR (126 MHz, CD_2Cl_2, ppm) δ = 22.0, 22.8, 53.4, 56.3, 107.6, 112.0, 124.9, 127.1, 130.0, 130.5, 130.9, 138.3, 142.3, 145.3. IR (neat, cm^{-1}): 3154.0, 2988.2, 2360.4, 1709.6, 1597.7, 1524.5, 1499.4, 1460.8, 1438.6, 1405.9, 1392.4, 1380.8, 1372.1, 1346.1, 1326.8, 1299.8, 1203.4, 1178.3, 1147.4, 1136.8, 1094.4, 1079.9, 1054.9, 1042.3, 1013.4, 883.2, 858.2, 777.2, 730.9, 702.9, 684.6, 675.0, 651.8, 617.1, 605.5, 583.4, 571.8, 561.2, 504.3. HRMS: *m*/*z* calcd. for $C_{18}H_{23}N_4S^+$ $[M–SbF_6]^+$ = 327.1638; found = 327.1643; calcd. for SbF_6^- $[M]^-$ = 234.8948; found = 234.8956.

5-[(2,4-Dimethoxyphenyl)thio]-1,4-diisopropyl-1*H*-1,2,4-triazol-4-ium Hexafluoroantimonate (**211**):

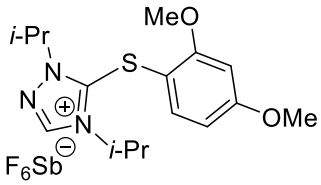

According to GP3, triazole-3-thione **209** (92.6 mg, 500 µmol, 1.00 equiv.), *N*-chlorosuccinimide (66.8 mg, 500 µmol, 1.00 equiv.) and 1,3-dimethoxybenzene (65.4 µL, 69 mg, 500 µmol, 1.00 equiv.) were dissolved in MeCN (5.0 mL) and stirred for 17 h at 70 °C. All volatiles were removed under reduced pressure, and the residual yellow solid was dissolved in DCM (5 mL) and washed with sat. aq. $NaSbF_6$ (3.0 mL) for 5 min. The organic layer was dried over $MgSO_4$ and concentrated *in vacuo*. After column chromatography (DCM:MeOH), **211** was obtained as a colourless oil (110 mg, 197 µmol, 39%).

^{1}H NMR (600 MHz, CD_2Cl_2 ppm) δ = 1.43 (d, *J* = 6.7 Hz, 6H), 1.52 (d, *J* = 6.9 Hz, 6H), 3.77 (s, 3H), 3.85 (s, 3H), 4.96 (d, *J* = 6.9 Hz, 1H), 5.14 (d, *J* = 6.7 Hz, 1H), 6.54 (d, *J* = 2.6 Hz, 1H), 6.66 (dd, *J* = 8.7, 2.6 Hz, 1H), 7.64 (d, *J* = 8.7 Hz, 1H), 8.59 (s, 1H). ^{13}C NMR (126 MHz, CD_2Cl_2, ppm) δ = 21.9, 22.8, 30.3, 56.3, 56.5, 57.2, 100.7, 102.6, 108.0, 137.1, 142.5, 147.0, 160.7, 165.2. IR (neat, cm^{-1}): 1599.7, 1577.5, 1526.4, 1487.8, 1459.8, 1403.0, 1376.0, 1304.6, 1288.2, 1208.2, 1182.2, 1161.9, 1144.5, 1068.4, 1023.1, 829.2, 656.6, 591.1, 530.3. HRMS: *m*/*z* calcd. for $C_{16}H_{24}N_3O_2S^+$ $[M–SbF_6]^+$ = 322.1584; found = 322.1578.

5.2.5 Synthesis of unymmetrical sulfides

Optimization of the synthesis of unsymmetrical sulfides

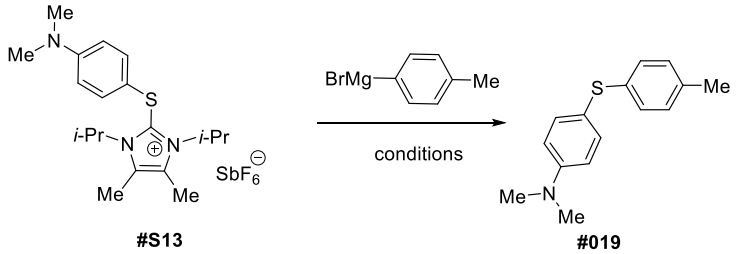

Scheme 126: Formation of unsymmetrical sulfides from thioimidazolium salts and Grignard reagents**.**

General protocol GP4

A dry Schlenk flask was charged with thioimidazolium intermediate **129** (49.0 mg, 86.3 µmol, 1.00 equiv.) was dissolved in anhydrous THF (1.5 mL) and cooled to -78 °C, if not otherwise indicated. Pre-titrated *p*-tolylmagnesium-bromide solution was added dropwise to the violet suspension, and the reaction mixture was allowed to warm up under indicated conditions. The dark brown suspension was quenched with sat. NH_4Cl (5 mL), stirred for 5 min and extracted with DCM (4 × 20 mL). The combined organic phases were dried over $MgSO_4$, concentrated *in vacuo* and purified by column chromatography (DCM:MeOH) to obtain **158** as a colorless oil.

Table 14: Screening of conditions for synthesis of **158**.

Entry	RMgBr	c /M	Additives	Conditions	Yield
1	1.4 equiv.	0.1	-	Fast warm up	25%
2	1.5 equiv.	0.1	-	Slow warm up	36%
3	2.9 equiv.	0.1	-	Slow warm up	75%
4	1.5 equiv.	0.8	5 equiv. LiCl	Slow warm up	43%
5	2.9 equiv.	0.1	5 equiv. LiCl	Slow warm up	71%
6	2.9 equiv.	0.5	5 equiv. LiCl	Slow warm up	66%

Note:

- The addition of LiCl (Entries 4–6), the concentration (Entries 4 *vs*.5) as well as the duration of the warm-up phase (Entries 1 *vs*.3) have a strong influence on the yield of the reactions.

- The amount of Grignard used in the reaction (Entries 2 *vs*.3) did affect the yield. For compound **129** the preparation of further thioethers was performed with 2.9 equiv. Grignard.

In cases of less reactive Grignard´s even higher amounts were used. On the other hand, already 1.5 equiv. of Grignard gave acceptable yields with compound **99**.

Capture of the free carbene by selenium

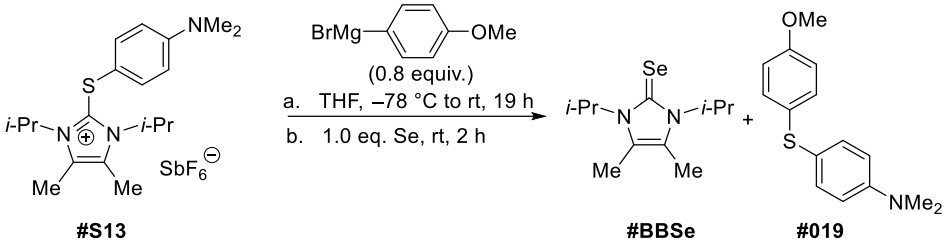

Scheme 127: Formation of 2-selenoimidazoline **159** from thioimidazolium intermediate **129.**

General protocol GP5

A dry Schlenk flask was charged with thioimidazolium intermediate **129** (212 mg, 373 µmol) was dissolved in THF (2.0 mL) and cooled to -78 °C. *para*-Methoxyphenylmagnesium bromide solution (0.5M in THF, 597 µL, 294 µmol, 0.79 equiv.) was added dropwise to the violet suspension and the solution was allowed to warm up overnight. Selenium (29.5 mg, 0.373 mmol) was added to the white suspension, and the mixture was stirred for at rt for 2 h. GC-MS & HRMS confirmed the formation of 2-selenoimidazoline **159** (Figure 34). HRMS: *m*/*z* calcd. for $C_{11}H_{20}N_2Se$ [M]: 260.0792; found: 260.0789.

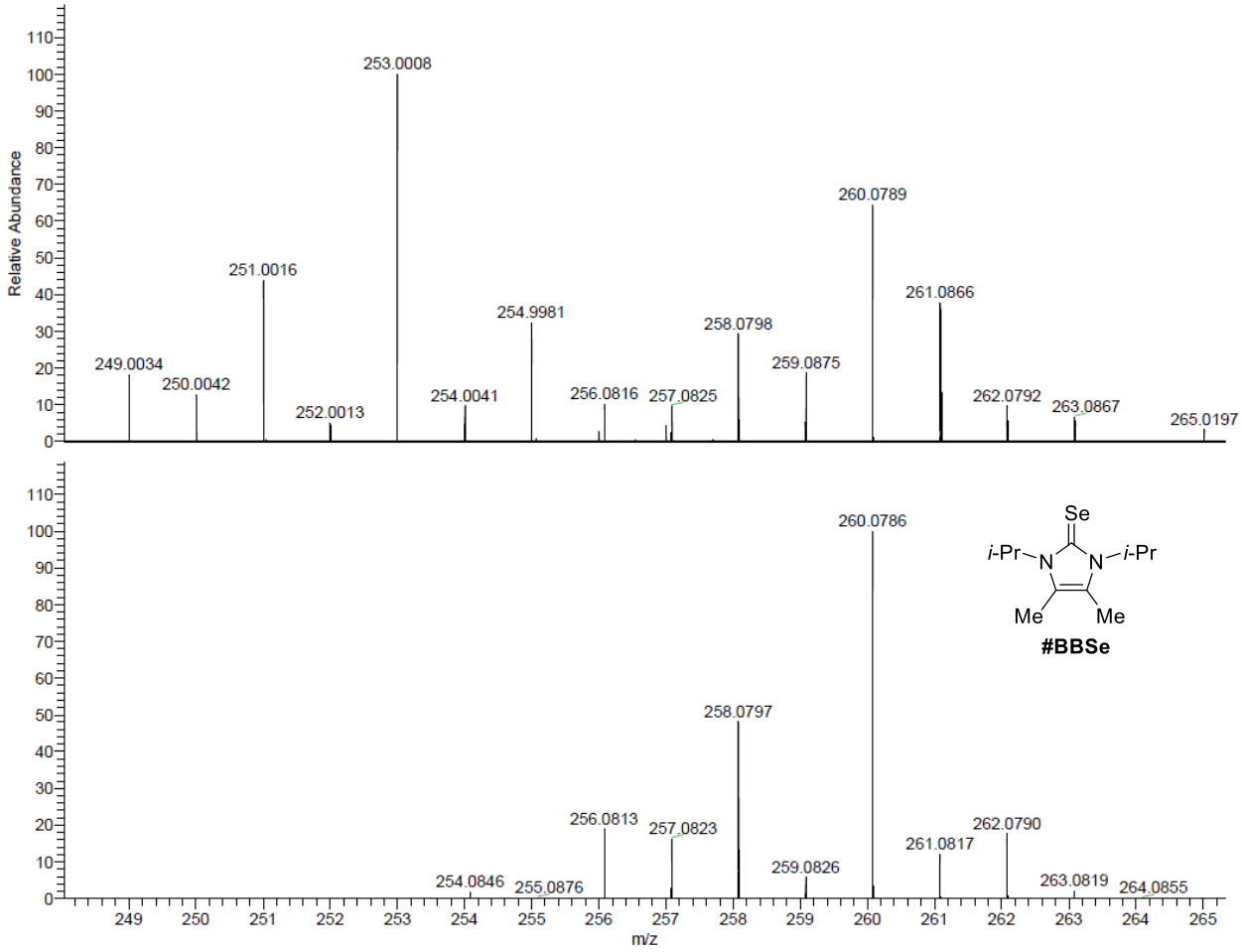

Figure 34: Formation of 2-selenoimidazoline **159**, as confirmed by GC-MS & HRMS.

Synthesis of substrates for Grignard preparation

1-Bromo-4-[{[(1*R*,2*S*,5*R*)-2-isopropyl-5-methylcyclohexyl]oxy}methyl]benzene (**301**):[15]

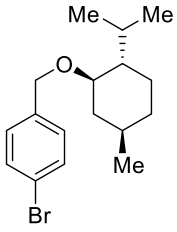

A solution of L-menthol (8.78 g, 56.2 mmol, 1.49 equiv.) in anhydrous THF (40 mL) and added dropwise to a stirred suspension of NaH (1.52 g, 63,3 mmol, 1.68 equiv.) in THF (90 mL). After cessation of the gas evolution, 4-bromobenzyl bromide (9.39 g, 37.6 mmol, 1.00 equiv.) was added dropwise, and the suspension was heated under reflux for 90 min. Afterwards, the suspension was allow to reach rt, and the reaction was carefully quenched with water (100 mL). The mixture was extracted with Et_2O (3 × 90 mL); the combined ethereal extracts were dried over $MgSO_4$ and concentrated *in vacuo*. The obtained oil was purified by column chromatography (hexane:EtOAc). Compound **301** was obtained as a white solid (9.30 g, 28.6 mmol, 76%).

^{1}H NMR (400 MHz, $CDCl_3$ ppm) δ = 0.74 (d, *J* = 6.9 Hz, 3H), 0.85 – 1.01 (m, 9H), 1.26 – 1.44 (m, 2H), 1.61 – 1.71 (m, 2H), 2.14 – 2.21 (m, 1H), 2.28 (heptd, *J* = 7.0, 2.9 Hz, 1H), 3.17 (td, *J* = 10.6, 4.2 Hz, 1H), 4.35 (d, *J* = 11.7 Hz, 1H), 4.61 (d, *J* = 11.8 Hz, 1H), 7.20 – 7.25 (m, 2H), 7.44 – 7.48 (m, 2H). ^{13}C NMR (101 MHz, $CDCl_3$, ppm) δ = 16.3, 21.1, 22.5, 23.4, 25.7, 31.7, 34.7, 40.4, 48.4, 69.7, 79.1, 121.3, 129.5, 131.5, 138.3. IR (neat, cm^{-1}): 2955.4, 2946.7, 2919.7, 2867.6, 2843.5, 1486.8, 1456.0, 1447.3, 1386.6, 1342.2, 1109.8, 1095.4, 1086.7, 1075.1, 1052.9, 1043.3, 1010.5, 994.1, 804.2, 559.3. HRMS: *m*/*z* calcd. for $C_{17}H_{25}BrO^+$ $[M]^+$ = 324.1089; found = 324.1092. The data are identical to the previously published ones.[14]

[15] Compound **301** was synthesis according a modified protocol of E. Nakamura *et al.*: K. Harano, R. M. Gorgoll, E. Nakamura, *Chem. Commun*. **2013**, *49*, 7629–7631.

(3*aR*,5*R*,6*R*,6*aR*)-6-[(4-Bromobenzyl)oxy]-5-[(*R*)-2,2-dimethyl-1,3-dioxolan-4-yl]-2,2-dimethyltetrahydrofuro[2,3-*d*][1,3]dioxole (302)[16]:

A solution of diacetone-D-glucose (3.12 g, 12.0 mmol, 1.50 equiv.) in anhydrous THF (35 mL)

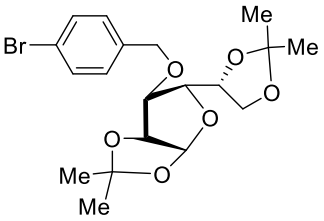

was added dropwise to a stirred suspension of NaH (336 mg, 14.0 mmol, 1.75 equiv.) in THF (15 mL). After the gas evolution ceased, *n*-BuN_4I (3.25 g, 8.80 mmol, 1.10 equiv.) was added. Afterwards, 4-bromobenzyl bromide (2.00 g, 8.00 mmol, 1.00 equiv.) was added dropwise. The suspension stirred for an additional 12 h, the reaction was carefully quenched with water (50 mL). The reaction mixture was extracted with EtOAc (4 × 100 mL); the combined extracts were dried over $MgSO_4$ and concentrated *in vacuo*. The residual oil was purified by column chromatography on (100 g of silica gel, hexane:EtOAc). Compound **302** was obtained as a colorless oil (2.00 g, 4.66 mmol, 58%).

^{1}H NMR (400 MHz, $CDCl_3$ ppm) δ = 1.31 (s, 3H), 1.37 (s, 3H), 1.42 (s, 3H), 1.49 (s, 3H), 3.97 – 4.03 (m, 2H), 4.09 – 4.14 (m, 2H), 4.30 – 4.37 (m, 1H), 4.55 – 4.68 (m, 3H), 5.89 (d, *J* = 3.7 Hz, 1H), 7.21 – 7.25 (m, 2H), 7.44 – 7.49 (m, 2H). ^{13}C NMR (75 MHz, $CDCl_3$, ppm) δ = 25.6, 26.4, 27.0, 67.7, 71.8, 72.6, 81.5, 82.0, 82.8, 105.4, 109.2, 112.0, 121.9, 129.4, 131.7, 136.8. IR (neat, cm^{-1}): 2964.1, 1384.6, 1376.9, 1370.2, 1256.4, 1233.3, 1213.0, 1165.8, 1153.2, 1122.4, 1084.8, 1062.6, 1046.2, 1036.6, 1007.6, 973.9, 967.1, 945.9, 886.1, 862.0, 843.7, 807.1, 638.3, 565.0, 508.2. The data are identical to the previously published ones.[16]

[16] Compound **302** was synthesis according a modified protocol of H.-J. Yang: *Chem. Lett*. **2006**, *35,* 1000–1001.

2-[(*tert*-Butyldimethylsilyl)oxy]-1-methyl-1*H*-indole (**152**):[17]

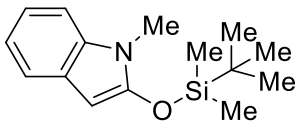

1-Methylindolin-2-one (750 mg, 5.10 mmol, 1.00 equiv.) was dissolved in DCM (52 mL) and cooled to 0°C. Dry trimethylamine (1.86 g, 2.56 mL, 18.4 mmol, 3.60 equiv.) was added dropwise to the light yellow solution, and the reaction mixture became dark orange. After stirring for 15 min, *tert*-butyldimethylsilyl trifluoromethanesulfonate (2.09 g, 1.82 mL, 9.17 mmol, 1.80 equiv.) was added dropwise. The solution was allowed to warm up to rt and stirred for an additional 2.5 h. After quenching the reaction with MeOH (2.5 mL), all volatiles were removed *in vacuo* and the obtained brown oil was extracted with dry pentane (4 × 10 mL). Extracts were combined, and the solvent was removed *in vacuo* to give pure **152** as a light brown solid (1.12 g, 4.28 mmol, 84%).

^{1}H NMR (400 MHz, CD_2Cl_2 ppm) δ = 0.32 (s, 6H), 1.04 (s, 9H), 3.53 (s, 3H), 5.55 (s, 1H), 6.95 – 7.06 (m, 2H), 7.13 (d, *J* = 7.2 Hz, 1H), 7.32 – 7.37 (m, 1H). ^{13}C NMR (126 MHz, CD_2Cl_2, ppm) δ = –3.2, 26.0, 26.5, 36.3, 108.4, 122.5, 124.6, 125.2, 128.2, 145.9, 175.1. IR (neat, cm^{-1}): 3058.5, 2950.6, 2928.4, 2883.1, 2856.1, 1717.3, 1614.1, 1577.5, 1550.5, 1468.5, 1459.8, 1437.7, 1397.2, 1364.4, 1333.5, 1312.3, 1254.5, 1235.2, 1193.7, 1160.9, 1143.6, 1126.2, 1091.5, 1013.4, 935.3, 913.1, 879.4, 837.9, 824.4, 810.9, 783.9, 768.5, 752.1, 733.8, 709.7, 679.8, 650.9, 617.1, 591.1. HRMS: *m*/*z* calcd. for $C_{15}H_{23}NOSi^+$ $[M]^+$ = 261.1549; found = 261.1545. The data are identical to the previously published ones.[17]

[17] Compound **152** was synthesis according a modified protocol of E. Merifield *et al*.: M.-L. Alcaraz, S. Atkinson, P. Cornwall, A. C. Foster, D. M. Gill, L. A. Humphries, P. S. Keegan, R. Kemp, E. Merifield, R. A. Nixon, A. J. Noble, D. O'Beirne, Z. M. Patel, J. Perkins, P. Rowan, P. Sadler, J. T. Singleton, J. Tornos, A. J. Watts, I. A. Woodland, *Org. Process Res. Dev.* **2005**, *9*, 555–569.

.

(Furan-2-yl)trimethylsilane (**303**):[18]

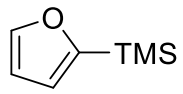

n-BuLi (17.2 mL, 1.6 M in hexane, 27.5 mmol, 1.00 equiv.) was added dropwise to a stirred solution of furane (2.00 mL, 1.87 g, 27.5 mmol, 1.00 equiv.) in dry diethylether (9 mL) at 0 °C within 10 min. The cooling bath was removed and the mixture was stirred for 4 h at rt. After cooling the reaction micture to 0 °C, TMSCl (3.8 mL, 3.26 g, 30.0 mmol, 1.09 equiv.) was dropwise added and the mixture was stirred at 0 °C for 1 h. The reaction was quenched with water (20 mL), phases were separated and the aq. layer was extracted with diethylether (20 mL). The combined organic phases were dried over $MgSO_4$ and the solvents were slowly removed under reduced pressure. **303** could be isolated as a colorless oil (2.56 g, 18.3 mmol, 66%) by careful distillation (b. p. 65 °C/110 mbar).

^{1}H NMR (600 MHz, $CDCl_3$ ppm) δ = 0.27 (s, 9H), 6.38 (dd, *J* = 3.2, 1.6 Hz, 1H), 6.62 (dd, *J* = 3.2, 0.6 Hz, 1H), 7.65 (dd, *J* = 1.7, 0.6 Hz, 1H). ^{13}C NMR (126 MHz, CD_2Cl_2, ppm) δ = –1.3, 109.4, 119.5, 146.6, 160.3. IR (neat, cm^{-1}): 1552.4, 1456.0, 1249.6, 1202.4, 1106.0, 1004.7, 901.6, 836.0, 755.0, 740.5, 697.1, 629.6, 594.9. HRMS: *m*/*z* calcd. for $C_7H_{12}OSi^+$ $[M]^+$ = 140.0657; found = 140.0660. The data are identical to the previously published ones.[18]

[18] Compound **303** was synthesis according to the modified protocol of G. Lefèvre, T. Cantat *et al*.: X. Frogneux, N. von Wolff, P. Thuéry, G. Lefèvre, T. Cantat*, Chem. Eur. J*. **2016**, *22*, 2930–2934.

Synthesis of aryl sulfides with for Grignard reagents

2-[(4-Methoxyphenyl)thio]-1-phenyl-1*H*-pyrrole (**161**)**:**

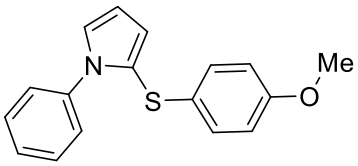

According to GP4, imidazolium salt **99** (60.2 mg, 102.0 µmol, 1.00 equiv.) was dissolved in anhydrous THF (1.0 mL) and cooled to -70 °C. Methoxyphenylmagnesium bromide (0.5M in THF, 306 µL, 153 µmol, 1.50 equiv.) was added dropwise, and the reaction mixture was allowed to warm up to 10 °C over a period of 14 h affording the orange solution. The reaction was quenched with sat. NH_4Cl (5 mL), stirred for 5 min and extracted with DCM (3 × 20 mL). The combined organic phases were dried over $MgSO_4$, concentrated *in vacuo* and purified by column chromatography (hexane:EtOAc) affording **161** as a white solid (26.9 mg, 95.6 µmol, 94%).

The similar reaction with the triazole salt **210** gave **161** in a yield of 83% on a 120 µmol reaction scale.

^{1}H NMR (300 MHz, $CDCl_3$, ppm) δ = 3.74 (s, 3H), 6.35 (dd, *J* = 3.6, 3.0 Hz, 1H), 6.69 – 6.72 (m, 1H), 6.71 (d, *J* = 8.9 Hz, 2H), 6.92 (d, *J* = 8.9 Hz, 2H), 7.03 (dd, *J* = 3.0, 1.8 Hz, 1H), 7.20 – 7.25 (m, 2H), 7.30 – 7.38 (m, 3H). ^{13}C NMR (75 MHz, $CDCl_3$, ppm) δ = 55.5, 109.5, 114.6, 120.5, 126.2, 126.7, 127.5, 128.7, 129.3, 129.4, 139.7, 158.3. IR (neat, cm^{-1}): 2958.3, 2828.1, 2359.5, 1596.8, 1487.8, 1455.0, 1449.2, 1433.8, 1393.3, 1322.0, 1291.1, 1240.0, 1204.3, 1180.2, 1171.5, 1161.9, 1137.8, 1105.0, 1087.7, 1074.2, 1029.8, 1002.8, 962.3, 820.6, 808.0, 795.5, 761.7, 724.1, 692.3, 650.9, 636.4, 619.0, 604.6, 562.1. HRMS: *m*/*z* calcd. for $C_{17}H_{15}NOS^+$ $[M]^+$ = 281.0874; found = 281.0871.

2-[(4-Fluorophenyl)thio]-1-phenyl-1*H*-pyrrole (**162**):

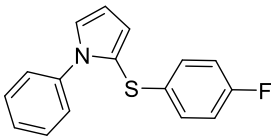

According to GP4, imidazolium salt **99** (94.4 mg, 160 µmol, 1.00 equiv.) was dissolved in THF (1.0 mL) and cooled to -78 °C. 4-Fluorophenylmagnesium bromide solution (1.0M in THF, 240 µL, 240 µmol, 1.50 equiv.) was added dropwise to the colorless solution, and the reaction mixture was allowed to warm up overnight furnishing the yellowish white suspension. The reaction was quenched with sat. NH_4Cl (5 mL), stirred for 5 min and extracted with DCM (3 × 20 mL). The combined organic phases were dried over $MgSO_4$, concentrated *in vacuo* and purified by column chromatography (hexane:DCM) to obtain sulfide **162** as a white solid (28.8 mg, 107 µmol, 67%).

^{1}H NMR (300 MHz, $CDCl_3$, ppm) δ = 6.39 (dd, *J* = 3.6, 3.0 Hz, 1H), 6.74 (dd, *J* = 3.6, 1.8 Hz, 1H), 6.82 – 6.95 (m, 5H), 7.07 (dd, *J* = 3.0, 1.8 Hz, 1H), 7.19 – 7.24 (m, 2H), 7.31 – 7.35 (m, 2H). ^{13}C NMR (126 MHz, $CDCl_3$, ppm) δ = 109.6, 115.9 (d, $J_{C\text{-}F}$ = 22.0 Hz), 119.2, 121.1, 126.5, 126.6, 127.6, 128.6 (d, $J_{C\text{-}F}$ = 7.9 Hz), 128.7, 133.9, 133.9, 139.4, 161.2 (d, $J_{C\text{-}F}$ = 244.5 Hz). ^{19}F NMR (282 MHz, $CDCl_3$, ppm) δ = –117.3. IR (neat, cm^{-1}): 3047.9, 2360.4, 1586.2, 1486.8, 1433.8, 1394.3, 1317.1, 1215.9, 1156.1, 1133.9, 1087.7, 1033.7, 1009.6, 821.5, 806.1, 762.7,749.2, 729.9, 722.2, 692.3, 648.9, 617.1, 603.6, 561.2, 507.2. HRMS: *m*/*z* calcd. for $C_{16}H_{12}FNS^+$ $[M]^+$ = 269.0674; found = 269.0671.

4-[1-Phenyl-1*H*-pyrrol-2-yl)thio]benzonitrile (**163**):

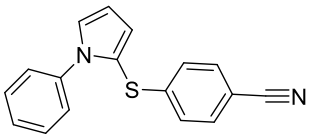

According to GP4, imidazolium salt **99** (45.5 mg, 77.0 µmol, 1.00 equiv.) was dissolved in THF (1.0 mL) and cooled to -40 °C. Nitrilphenylmagnesium chloride•LiCl solution [19] (1.20M in THF, 97 µL, 116 µmol, 1.50 equiv.) was added dropwise to the stirred white suspension, and the reaction mixture was allowed to warm up overnight affording the dark red solution. The reaction was quenched with sat. NH_4Cl (5 mL), stirred for 5 min and extracted with DCM (3 × 20 mL). The combined organic phases were dried over $MgSO_4$, concentrated *in vacuo* and purified by column chromatography (hexane:DCM) affording compound **163** as a colorless oil (16.5 mg, 59.7 µmol, 78%).

^{1}H NMR (300 MHz, $CDCl_3$, ppm) δ = 6.44 (dd, *J* = 3.7, 3.0 Hz, 1H), 6.76 (dd, *J* = 3.7, 1.8 Hz, 1H), 6.92 – 6.96 (m, 2H), 7.15 (dd, *J* = 3.0, 1.8 Hz, 1H), 7.17 – 7.21 (m, 2H), 7.30 – 7.36 (m, 3H), 7.38 – 7.42 (m, 2H). ^{13}C NMR (126 MHz, $CDCl_3$, ppm) δ = 108.4, 110.2, 115.8, 118.9, 122.3, 125.5, 126.3, 127.5, 127.9, 128.9, 132.3, 139.0, 147.1. IR (neat, cm^{-1}): 3047.9, 2224.5, 1590.0, 1497.5, 1482.0, 1455.0, 1433.8, 1394.3, 1319.1, 1138.8, 1077.0, 1035.6, 1014.4, 961.3, 912.2, 819.6, 762.7, 728.0, 692.3, 645.1, 620.0, 606.5, 582.4, 560.2, 541.9. HRMS: *m*/*z* calcd. for $C_{17}H_{12}N_2S^+$ $[M]^+$ = 276.0721; found = 276.0716.

---

[19] The nitrilphenylmagnesium chlorid • LiCl solution was prepared following the well-elaborated protocol of P. Knochel *et al.*: A. Krasovskiy, P. Knochel, *Angew. Chem. Int. Ed*. **2004**, *43*, 3333–3336.

***tert*-Butyl 4-[(1-Phenyl-1*H*-pyrrol-2-yl)thio]benzoate** (**164**):

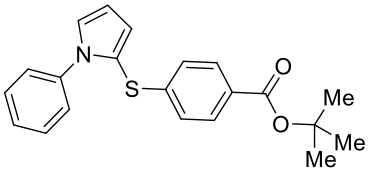

According to GP4, imidazolium salt **99** (72.6 mg, 123 µmol, 1.00 equiv.) was dissolved in THF (1.0 mL) and cooled to -60 °C. 4-(*tert*-butoxycarbonyl)phenylmagnesium bromide solution [20] (0.164M in THF, 2.18 mL, 357 µmol, 2.90 equiv.) was added dropwise to the clear solution and the reaction mixture was allowed to warm up overnight furnishing the dark orange solution. The reaction was quenched with sat. NH_4Cl (5 mL), stirred for 5 min and extracted with DCM (3 × 20 mL). The combined organic phases were dried over $MgSO_4$, concentrated *in vacuo* and purified by two subsequent column chromatographies (hexane:DCM) affording sulfide **164** as a colorless oil (11.4 mg, 32.4 µmol, 26%).

^{1}H NMR (600 MHz, $CDCl_3$, ppm) δ = 1.56 (s, 9H), 6.42 (dd, *J* = 3.7, 3.0 Hz, 1H), 6.76 (dd, *J* = 3.7, 1.8 Hz, 1H), 6.90 – 6.95 (m, 2H), 7.13 (dd, *J* = 3.0, 1.8 Hz, 1H), 7.20 – 7.22 (m, 2H), 7.28 – 7.34 (m, 3H), 7.75 – 7.79 (m, 2H). ^{13}C NMR (126 MHz, $CDCl_3$, ppm) δ = 28.4, 81.0, 110.0, 117.0, 122.0, 124.8, 126.3, 127.1, 127.7, 128.8, 129.8, 139.3, 145.8, 165.5. IR (neat, cm^{-1}): 2977.6, 2928.4, 1706.7, 1590.0, 1498.4, 1456.0, 1434.8, 1392.4, 1366.3, 1318.1, 1305.6, 1290.1, 1254.5, 1161.9, 1138.8, 1117.5, 1106.9, 1089.6, 1034.6, 1012.4, 960.4, 846.6, 758.9, 724.1, 690.4, 620.0, 509.1. HRMS: *m*/*z* calcd. for $C_{21}H_{22}NO_2S^+$ $[M+H]^+$ = 352.1366; found = 352.1364.

4-[(4-Methoxyphenyl)thio]-*N*-methylaniline (**188**):

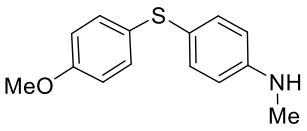

According to GP4, imidazolium salt **130** (89.8 mg, 162 µmol, 1.00 equiv.) was dissolved in THF (1.0 mL) and cooled to -78 °C. Methoxyphenylmagnesium bromide (0.50M in THF, 939 µL, 470 µmol, 2.90 equiv.) was added dropwise to the stirred white suspension, and the reaction mixture was allowed to warm up overnight furnishing an orange solution. The reaction was

[20] 4-(*tert*-butoxycarbonyl)phenylmagnesium bromide solution was prepared following the TMPMgCl deprotonation protocol of P. Knochel *et al.*: A. Krasovskiy, V. Krasovskaya, P. Knochel, *Angew. Chem. Int. Ed*. **2006**, *45*, 2958–2961.

quenched with sat. NH_4Cl (5 mL), stirred for 5 min and extracted with DCM (3 × 20 mL). The combined organic phases were dried over $MgSO_4$, concentrated *in vacuo* and purified by column chromatography (hexane:DCM) affording sulfide **188** as a white solid (18.8 mg, 76.6 µmol, 47%).

^{1}H NMR (300 MHz, $CDCl_3$, ppm) δ = 2.84 (s, 3H), 3.77 (s, 3H), 6.56 – 6.62 (m, 2H), 6.77 – 6.84 (m, 2H), 7.17 – 7.22 (m, 2H), 7.24 – 7.30 (m, 3H). ^{13}C NMR (75 MHz, $CDCl_3$, ppm) δ = 31.0, 55.5, 113.6, 114.8, 131.2, 134.4. IR (neat, cm^{-1}): 1604.5, 1496.5, 1437.7, 1273.8, 1246.8, 1182.2, 1039.4, 1011.5, 823.5, 809.0, 781.0, 551.5, 514.9. HRMS: *m/z* calcd. for $C_{14}H_{15}NOS^+$ $[M]^+$ = 245.0874; found = 245.0877.

4-[(4-Methoxyphenyl)thio]aniline (**189**):

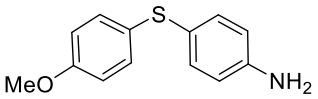

According to GP4, imidazolium salt **131** (118.9 mg, 220 µmol, 1.00 equiv.) was dissolved in THF (1.0 mL) and cooled to -78 °C. Methoxyphenylmagnesium bromide (0.50M in THF, 1.28 mL, 640 µmol, 2.90 equiv.) was added dropwise to the stirred white suspension, and the reaction mixture was allowed to warm up overnight affording the brown solution. The reaction was quenched with sat. NH_4Cl (5 mL), stirred for 5 min and extracted with DCM (3 × 20 mL). The combined organic phases were dried over $MgSO_4$, concentrated *in vacuo* and purified by column chromatography (hexane:DCM) furnishing sulfide **189** as a white solid (3.9 mg, 17 µmol, 8%).

^{1}H NMR (300 MHz, CD_2Cl_2, ppm) δ = 3.76 (s, 3H), 3.80 (s, 2H), 6.59 – 6.65 (m, 2H), 6.78 – 6.84 (m, 2H), 7.16 – 7.23 (m, 4H). ^{13}C NMR (128 MHz, CD_2Cl_2, ppm) δ = 55.9, 115.1, 116.0, 123.6, 129.4, 131.9, 134.5, 147.2, 159.1. IR (neat, cm^{-1}): 3372.9, 3312.1, 3205.1, 2921.6, 1631.5, 1589.1, 1571.7, 1488.8, 1461.8, 1452.1, 1438.6, 1425.1, 1278.6, 1260.3, 1245.8, 1171.5, 1119.5, 1100.2, 1083.8, 1025.0, 1005.7, 818.6, 795.5, 754.0, 723.2, 695.2, 646.0, 635.4, 622.9, 523.6, 504.3. HRMS: *m/z* calcd. for $C_{13}H_{14}NOS^+$ $[M+H]^+$ = 232.0791; found = 232.0789.

2-{[4-({[(1*R*,2*S*,5*R*)-2-Isopropyl-5-methylcyclohexyl]oxy}methyl)phenyl]thio}-1-phenyl-1*H*-pyrrole (**165**):

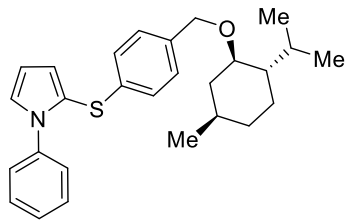

According to GP4, imidazolium salt **99** (94.4 mg, 160 µmol, 1.00 equiv.) was dissolved in THF (1.0 mL) and cooled to -78 °C. 4-(Mentholoxymethyl)phenylmagnesium bromide (0.36M, 667 µL, 240 µmol, 1.50 equiv.)[21] was added dropwise, and the was allowed to warm up overnight affording the orange solution. The reaction was quenched with sat. NH_4Cl (5 mL), stirred for 5 min and extracted with DCM (3 × 20 mL). The combined organic phases were dried over $MgSO_4$, concentrated *in vacuo* and purified by column chromatography (Hexane:DCM) furnishing sulfide **165** as a colourless oil (60.1 mg, 143 µmol, 89%).

^{1}H NMR (400 MHz, $CDCl_3$, ppm) δ = 0.69 (d, *J* = 6.9 Hz, 3H), 0.82 – 1.01 (m, 9H), 1.22 – 1.40 (m, 2H), 1.56 – 1.70 (m, 2H), 2.12 – 2.19 (m, 1H), 2.20 – 2.31 (m, 1H), 3.13 (td, *J* = 10.5, 4.1 Hz, 1H), 4.30 (d, *J* = 11.4 Hz, 1H), 4.56 (d, *J* = 11.4 Hz, 1H), 6.39 (t, *J* = 3.3 Hz, 1H), 6.71 – 6.76 (m, 1H), 6.90 – 6.95 (m, 2H), 7.06 – 7.12 (m, 1H), 7.16 (d, *J* = 8.2 Hz, 2H), 7.20 – 7.25 (m, 2H), 7.27 – 7.36 (m, 3H). ^{13}C NMR (101 MHz, $CDCl_3$, ppm) δ = 16.2, 21.1, 22.5, 23.4, 25.6, 31.7, 34.7, 40.4, 48.4, 70.1, 78.8, 109.7, 118.5, 121.6, 126.1, 126.4, 126.6, 127.5, 128.6, 128.8, 136.4, 138.6, 139.6. IR (neat, cm^{-1}): 2951.5, 2917.8, 2865.7, 1597.7, 1498.4, 1455.0, 1433.8, 1319.1, 1105.0, 1085.7, 1073.2, 1052.9, 1035.6, 1015.3, 834.1, 804.2, 759.8, 721.2, 692.3, 508.2. HRMS: *m/z* calcd. for $C_{27}H_{33}NOS^+$ $[M]^+$ = 419.2283; found = 419.2275.

[21] Prepared from **301** in accordance with procedure published by H. Ess, L. Kürti *et al*.: H. Gao, Z. Zhou, D.-H. Kwon, J. Coombs, S. Jones, N. E. Behnke, D. H. Ess, L. Kürti, *Nat. Chem*. **2017**, *9*, 681–688. $BrCH_2CH_2Br$ was used to initiate the formation of the Grignard.

3-[(4-Methoxyphenyl)thio]-9-methyl-9*H*-carbazole (185):

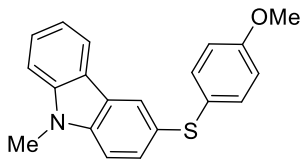

According to GP4, imidazolium salt **119** (38.5 mg, 61.2 µmol, 1.00 equiv.) was dissolved in THF (1.0 mL) and cooled to -78 °C. Methoxyphenylmagnesium bromide (0.5M in THF, 354 µL, 177 µmol, 2.89 equiv.) was added dropwise, and the reaction mixture was allowed to warm up overnight affording the brown solution. The reaction was quenched with sat. NH_4Cl (5 mL), stirred for 5 min and extracted with DCM (3 × 20 mL). The combined organic phases were dried over $MgSO_4$, concentrated *in vacuo* and purified by column chromatography (hexane:DCM) to obtain sulfide **185** as a white solid (5.3 mg, 16.5 µmol, 27%).

^{1}H NMR (400 MHz, CD_2Cl_2, ppm) δ = 3.77 (s, 3H), 3.78 (s, 3H), 6.81 – 6.84 (m, 2H), 6.86 – 6.90 (m, 2H), 7.26 – 7.35 (m, 4H), 7.37 (d, *J* = 8.6 Hz, 1H), 7.52 (dd, *J* = 8.5, 1.8 Hz, 1H), 8.08 (dd, *J* = 1.8, 0.6 Hz, 1H). ^{13}C NMR (126 MHz, CD_2Cl_2, ppm) δ = 55.6, 55.9, 110.1, 115.0, 115.1, 115.2, 123.4, 124.9, 126.1, 128.9, 129.6, 130.9, 132.6, 137.1, 137.7, 141.2, 159.4, 160.6. IR (neat, cm^{-1}): 1591.0, 1571.7, 1512.9, 1487.8, 1457.9, 1428.0, 1389.5, 1319.1, 1285.3, 1241.0, 1199.5, 1171.5, 1123.3, 1101.2, 1085.7, 1072.2, 1029.8, 1003.8, 949.8, 819.6, 789.7, 760.8, 720.3, 692.3, 630.6, 617.1, 594.9, 546.7, 513.0. HRMS: *m/z* calcd. for $C_{20}H_{17}NOS^+$ $[M]^+$ = 319.1031; found = 319.1020.

2-(Furan-2-ylthio)-1-phenyl-1*H*-pyrrole (**167**):

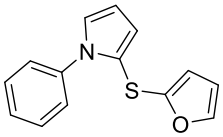

According to modified GP4, imidazolium salt **99** (177 mg, 300 µmol, 1.00 equiv.) was dissolved in THF (1.5 mL) and cooled to -78 °C. Furan-2-yllithium[22] (0.35M in Et_2O/THF, 1.29 mL, 452 µmol, 1.50 equiv.) was added dropwise to the clear solution, and the reaction mixture was allowed to warm up overnight furnishing an orange suspension. The reaction was quenched with sat. NH_4Cl (5 mL), stirred for 5 min and extracted with DCM (3 × 20 mL). The combined organic phases were dried over

[22] Prepared according to the protocol of G. Lefèvre, T. Cantat *et al.*: X. Frogneux, N. von Wolff, P. Thuéry, G. Lefèvre, T. Cantat, *Chem. Eur. J*. **2016**, *22*, 2930–2930.

$MgSO_4$, concentrated *in vacuo* and purified by repeated twofold column chromatography (DCM:MeOH & hexane:DCM) affording sulfide **167** as a light yellow oil (52.0 mg, 215.4 µmol, 72%).

^{1}H NMR (500 MHz, CD_2Cl_2, ppm) δ = 6.07 (dd, *J* = 3.3, 0.9 Hz, 1H), 6.23 – 6.28 (m, 2H), 6.63 (dd, *J* = 3.7, 1.8 Hz, 1H), 6.97 (dd, *J* = 3.0, 1.8 Hz, 1H), 7.33 – 7.37 (m, 3H), 7.39 – 7.49 (m, 3H). ^{13}C NMR (126 MHz, CD_2Cl_2, ppm) δ = 109.7, 111.9, 115.5, 119.6, 119.7, 126.5, 127.4, 128.1, 129.3, 140.0, 145.4, 146.0. IR (neat, cm^{-1}): 1715.4, 1596.8, 1497.5, 1456.0, 1434.8, 1391.4, 1367.3, 1319.1, 1213.0, 1205.3, 1151.3, 1135.9, 1110.8, 1086.7, 1073.2, 1058.7, 1034.6, 1003.8, 957.5, 905.4, 880.3, 761.7, 720.3, 692.3, 655.7, 633.5, 615.2, 595.9, 557.3. HRMS: *m*/*z* calcd. for $C_{14}H_{11}NNaOS^+$ $[M+Na]^+$ = 264.0454; found = 264.0462.

2-{[4-({[(3*aR*,5*R*,6*R*,6*a**R*)-5-[(*R*)-2,2-Dimethyl-1,3-dioxolan-4-yl]-2,2-dimethyltetrahydro-furo[2,3-*d*][1,3]dioxol-6-yl]oxy}methyl)phenyl]thio}-1-phenyl-1*H*-pyrrole** (**169**):

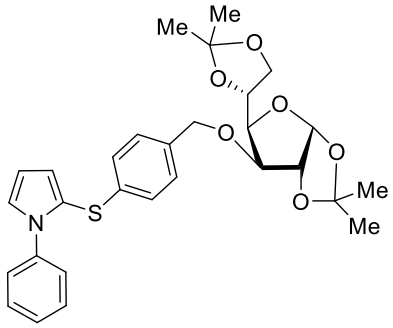

According to modified GP4, imidazolium salt **99** (183 mg, 310 µmol, 1.00 equiv.) was dissolved in THF (1.3 mL) and cooled to -78 °C. The linked fructose-derived Grignard reagent[23] solution (0.70M in THF, 1.28 mL, 896 µmol, 2.89 equiv.) was added dropwise to the clear solution, and the reaction mixture was allowed to warm up overnight affording the brown solution. The reaction was quenched with sat. NH_4Cl (5 mL), stirred for 5 min and extracted with DCM (3 × 20 mL). The combined organic phases were dried over $MgSO_4$, concentrated *in vacuo* and purified by repetitive twofold column chromatography (DCM:MeOH) affording sulfide **169** as a white solid (86.9 mg, 164 µmol, 53%).

[23] The linked fructose-derived magnesium bromide solution was prepared from the corresponding arylbromide **302** and Mg tuning following the protocol of H. Ess, L. Kürti *et al*.: H. Gao, Z. Zhou, D.-H. Kwon, J. Coombs, S. Jones, N. E. Behnke, D. H. Ess, L. Kürti, *Nat. Chem*. **2017**, *9*, 681–688.

^{1}H NMR (300 MHz, $CDCl_3$, ppm) δ = 1.30 (s, 3H), 1.34 – 1.36 (m, 3H), 1.41 – 1.42 (m, 3H), 1.49 (s, 3H), 3.95 – 4.01 (m, 2H), 4.09 (s, 2H), 4.28 – 4.35 (m, 1H), 4.50 – 4.57 (m, 3H), 5.87 (d, *J* = 3.7 Hz, 1H), 6.40 (dd, *J* = 3.6, 3.0 Hz, 1H), 6.73 (dd, *J* = 3.6, 1.8 Hz, 1H), 6.89 – 6.93 (m, 2H), 7.09 (dd, *J* = 3.0, 1.8 Hz, 1H), 7.12 – 7.16 (m, 2H), 7.20 – 7.25 (m, 2H), 7.26 (s, 3H). ^{13}C NMR (126 MHz, $CDCl_3$, ppm) δ = 25.7, 26.5, 27.0, 27.1, 67.6, 72.1, 72.6, 81.3, 81.4, 81.7, 105.4, 109.1, 109.7, 111.9, 118.4, 121.4, 126.1, 126.4, 126.6, 127.5, 128.3, 128.7, 134.8, 139.1, 139.4. IR (neat, cm^{-1}): 2985.3, 2934.2, 2890.8, 1498.4, 1455.0, 1435.7, 1379.8, 1371.1, 1349.0, 1320.0, 1251.6, 1211.1, 1163.8, 1121.4, 1069.3, 1014.4, 960.4, 942.1, 884.2, 845.6, 802.2, 763.7, 733.8, 696.2, 636.4, 605.5, 535.2, 510.1. HRMS: *m*/*z* calcd. for $C_{29}H_{34}NO_6S^+$ $[M+H]^+$ = 524.2101; found = 524.2085.

3-Bromo-2-[(1-phenyl-1*H*-pyrrol-2-yl)thio]quinoline (**166**):

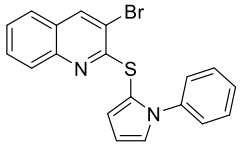

According to GP4, imidazolium salt **99** (116.9 mg, 198 µmol, 1.00 equiv.) was dissolved in THF (1.0 mL) and cooled to -30 °C. 3-(Bromoquinolin-2-yl)magnesium bromide solution[24] (0.36M in THF, 1.52 mL, 547 µmol, 2.76 equiv.) was added dropwise to the clear solution, and the reaction mixture was allowed to warm up overnight furnishing the dark brown solution. The reaction was quenched with sat. NH_4Cl (5 mL), stirred for 5 min and extracted with DCM (3 × 20 mL). The combined organic phases were dried over $MgSO_4$, concentrated *in vacuo* and purified by column chromatography (hexane:DCM) affording sulfide **166** as a white solid (40.8 mg, 107 µmol, 54%).

^{1}H NMR (600 MHz, $CDCl_3$, ppm) δ = 6.48 (dd, *J* = 3.6, 3.0 Hz, 1H), 6.76 (dd, *J* = 3.7, 1.8 Hz, 1H), 7.16 – 7.26 (m, 3H), 7.39 – 7.44 (m, 3H), 7.56 – 7.61 (m, 2H), 7.71 – 7.74 (m, 1H), 8.06 (s, 1H). ^{13}C NMR (126 MHz, $CDCl_3$, ppm) δ = 109.8, 114.9, 116.5, 121.2, 126.1, 126.4, 126.5, 127.1, 127.2, 127.3, 128.4, 128.6, 129.7, 137.9, 139.9, 146.7, 159.2. IR (neat, cm^{-1}): 3053.7, 1540.8, 1494.6, 1484.9, 1365.4, 1321.0, 1143.6, 1133.0, 1110.8, 1090.5, 1035.6, 953.6, 906.4,

[24] 3-Bromoquinolin-2-yl magnesium bromide solution was prepared following the TMPMgCl deprotonation protocol of P. Knochel *et al.*: A. Krasovskiy, V. Krasovskaya, P. Knochel, *Angew. Chem. Int. Ed*. **2006**, *45*, 2958–2961.

877.5, 863.0, 768.5, 748.2, 719.3, 693.3, 688.5, 675.9, 648.9, 600.7, 522.6. HRMS: *m*/*z* calcd. for $C_{19}H_{13}BrN_2S^+$ $[M]^+$ = 379.9983; found = 379.9983.

2-({4-[(4-Methoxyphenyl)ethynyl]phenyl}thio)-1-phenyl-1*H*-pyrrole (**168**):

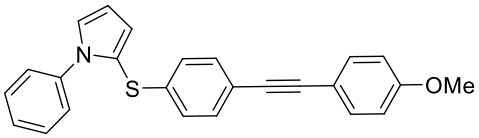

According to GP4, imidazolium salt **99** (183 mg, 310 µmol, 1.00 equiv.) was dissolved in THF (1.5 mL) and cooled to -78 °C. 4-[(4-Methoxyphenyl)ethynyl]phenyl-magnesium bromide solution[25] (0.45M in THF, 1.03 mL, 464 µmol, 1.50 equiv.) was added dropwise to the clear solution, and the reaction mixture was allowed to warm up overnight furnishing the brown solution. The reaction was quenched with sat. NH_4Cl (5 mL), stirred for 5 min and extracted with DCM (3 × 20 mL). The combined organic phases were dried over $MgSO_4$, concentrated *in vacuo* and purified by column chromatography (hexane:DCM) affording sulfide **168** as a white solid (86.9 mg, 228 µmol, 74%).

^{1}H NMR (600 MHz, $CDCl_3$, ppm) δ = 3.82 (s, 3H), 6.43 (dd, *J* = 3.7, 2.9 Hz, 1H), 6.78 (dd, *J* = 3.7, 1.8 Hz, 1H), 6.86 – 6.92 (m, 4H), 7.12 (dd, *J* = 3.0, 1.8 Hz, 1H), 7.21 – 7.24 (m, 2H), 7.30 – 7.35 (m, 5H), 7.42 – 7.48 (m, 2H). ^{13}C NMR (126 MHz, $CDCl_3$, ppm) δ = 55.5, 87.9, 89.6, 109.8, 114.1, 115.4, 117.7, 120.4, 121.7, 125.7, 126.4, 126.8, 127.6, 128.7, 131.8, 133.0, 139.4, 139.8, 159.6. IR (neat, cm^{-1}): 1603.5, 1509.0, 1497.5, 1456.0, 1435.7, 1396.2, 1319.1, 1286.3, 1243.9, 1179.3, 1171.5, 1137.8, 1106.0, 1030.8, 1010.5, 819.6, 762.7, 728.0, 694.2, 621.0, 569.9, 538.0, 518.8. HRMS: *m*/*z* calcd. for $C_{25}H_{19}NOS^+$ $[M]^+$ = 381.1187; found = 381.1186.

[25] The aryl magnesium bromide solution was prepared starting from 1-bromo-4-(4-methoxyphenyl) ethynylbenzene following the Br-Mg-exchange protocol published by P. Knochel *et al.*: A. Krasovskiy, P. Knochel, *Angew. Chem. Int. Ed*. **2004**, *43*, 3333–3336. The Br-Mg-exchange was completed after 19 h at rt.

2-[(1-Phenyl-1*H*-pyrrol-2-yl)thio]benzo[*d*]thiazole (**170**):

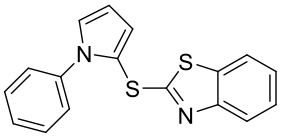

According to GP4, imidazolium salt **99** (99.2 mg, 168 µmol, 1.00 equiv.) was dissolved in THF (1.3 mL) and cooled to -78 °C. (Benzo[*d*]thiazol-2-yl)-magnesium bromide solution (0.318M in THF, 1.54 mL, 487 µmol, 2.90 equiv.) was added dropwise to the clear solution, and the reaction mixture was allowed to warm up overnight furnishing the dark brown solution. The reaction was quenched with sat. NH_4Cl (5 mL), stirred for 5 min and extracted with DCM (3 × 20 mL). The combined organic phases were dried over $MgSO_4$, concentrated *in vacuo* and purified by column chromatographiy (hexane:DCM) affording sulfide **170** as a white solid (40,9 mg, 132.6 µmol, 79%).

^{1}H NMR (300 MHz, CD_3CN ppm) δ = 6.50 (dd, *J* = 3.8, 3.0 Hz, 1H), 6.93 (dd, *J* = 3.8, 1.8 Hz, 1H), 7.24 – 7.34 (m, 2H), 7.35 – 7.44 (m, 7H), 7.70 – 7.75 (m, 1H), 7.76 – 7.80 (m, 1H). ^{13}C NMR (126 MHz, CD_3CN, ppm) δ = 111.3, 116.0, 122.3, 122.5, 123.8, 125.3, 127.2, 127.5, 129.1, 129.6, 129.9, 136.3, 139.7, 155.1, 173.2. IR (neat, cm^{-1}): 3053.7, 2924.5, 1591.0, 1494.6, 1463.7, 1454.1, 1428.0, 1389.5, 1319.1, 1237.1, 1140.7, 1078.0, 1068.4, 1000.9, 958.4, 916.0, 764.6, 754.0, 726.1, 720.3, 691.4, 672.1, 617.1. HRMS: *m*/*z* calcd. for $C_{17}H_{12}N_2S_2^+$ $[M]^+$ = 308.0442; found = 308.0449.

2,6-Dichloro-4-[(1-phenyl-1*H*-pyrrol-2-yl)thio]pyridine (**173**):

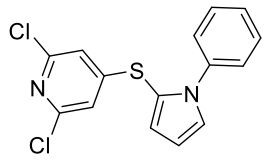

According to GP4, imidazolium salt **99** (79.7 mg, 135 µmol, 1.00 equiv.) was dissolved in THF (1.0 mL) and cooled to -78 °C. 2,6-Dichloropyridin-4-yl magnesium bromide solution[26] (0.43M in THF, 908 µL, 390 µmol, 2.90 equiv.) was added dropwise to the stirred clear solution, and the reaction mixture was allowed to warm up overnight furnishing the dark brown solution. The reaction was quenched with sat. NH_4Cl (5 mL), stirred for 5 min and extracted with DCM (3 × 20 mL). The combined organic phases were dried over $MgSO_4$, concentrated *in vacuo* and purified by column chromatography (hexane:DCM) affording sulfide **173** as a white solid (5.1 mg, 15.8 µmol, 12%).

^{1}H NMR (400 MHz, $CDCl_3$, ppm) δ = 6.47 (dd, *J* = 3.7, 3.0 Hz, 1H), 6.68 (s, 2H), 6.78 (dd, *J* = 3.7, 1.8 Hz, 1H), 7.19 (dd, *J* = 3.0, 1.8 Hz, 1H), 7.20 – 7.24 (m, 2H), 7.33 – 7.41 (m, 3H). ^{13}C NMR (101 MHz, $CDCl_3$, ppm) δ = 110.7, 113.1, 118.2, 122.9, 126.3, 128.3, 128.3, 129.2, 138.8, 150.5, 157.7. IR (neat, cm^{-1}): 3059.5, 1716.3, 1596.8, 1551.5, 1521.6, 1495.5, 1455.0, 1433.8, 1392.4, 1355.7, 1318.1, 1260.3, 1233.3, 1208.2, 1161.9, 1139.7, 1079.9, 1035.6, 1002.8, 979.7, 961.3, 844.7, 804.2, 760.8, 727.0, 692.3, 620.0, 606.5, 553.5, 513.9. HRMS: *m/z* calcd. for $C_{15}H_{10}Cl_2N_2S^+$ $[M]^+$ = 319.9942; found = 319.9944.

3-Bromo-5-[(1-phenyl-1*H*-pyrrol-2-yl)thio]pyridine (**172**):

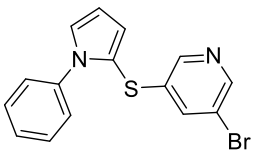

According to GP4, imidazolium salt **99** (105.7 mg, 179 µmol, 1.00 equiv.) was dissolved in THF (1.3 mL) and cooled to -78 °C. 5-Bromopyridin-3-yl-magnesium bromide (1.23M in THF, 420 µL, 517 µmol, 2.90 equiv.) was added dropwise to the stirred clear solution, and the reaction mixture was allowed to warm

[26] 2,6-Dichloropyridin-4-yl magnesium bromide solution was prepared following the TMPMgCl deprotonation protocol of P. Knochel *et al.*: A. Krasovskiy, V. Krasovskaya, P. Knochel, *Angew. Chem. Int. Ed*. **2006**, *45*, 2958–2961.

up overnight furnishing the dark brown solution. The reaction was quenched with sat. NH_4Cl (5 mL), stirred for 5 min and extracted with DCM (3 × 20 mL). The combined organic phases were dried over $MgSO_4$, concentrated *in vacuo* and purified by column chromatography (hexane:DCM) affording sulfide **172** as a colorless oil (38.0 mg, 114,6 µmol, 64%).

^{1}H NMR (300 MHz, $CDCl_3$, ppm) δ = 6.39 – 6.43 (m, 1H), 6.77 (ddd, *J* = 3.7, 1.8, 0.3 Hz, 1H), 7.12 (ddd, *J* = 3.0, 1.8, 0.3 Hz, 1H), 7.19 – 7.23 (m, 2H), 7.29 (td, *J* = 2.0, 0.3 Hz, 1H), 7.32 – 7.40 (m, 3H), 8.02 (s, 1H), 8.32 (s, 1H). ^{13}C NMR (126 MHz, $CDCl_3$, ppm) δ = 110.2, 115.6, 122.0, 126.5, 127.5, 128.0, 128.9, 136.2, 139.0, 144.9, 147.1. IR (neat, cm^{-1}): 3006.5, 2950.6, 2843.5, 1540.8, 1408.7, 1369.2, 1311.4, 1106.0, 1084.8, 1060.7, 1004.7, 982.6, 950.7, 874.6, 752.1, 685.6, 645.1. HRMS: *m*/*z* calcd. for $C_{15}H_{11}BrN_2S^+$ $[M]^+$ = 329.9826; found = 329.9821.

2-[(4-Methoxyphenyl)thio]-1*H*-pyrrole (**171**):

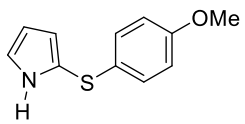

According to GP4, imidazolium salt **113** (90.0 mg, 175 µmol, 1.00 equiv.) was suspended in THF (1.0 mL) and cooled to -78 °C. Methoxyphenylmagnesium bromide (0.50M solution in THF, 1.02 mL, 510 µmol, 2.91 equiv.) was added dropwise to the stirred white suspension, and the reaction mixture was allowed to warm up overnight furnishing the brown suspension. The reaction was quenched with sat. NH_4Cl (5 mL), stirred for 5 min and extracted with DCM (3 × 20 mL). The combined organic phases were dried over $MgSO_4$, concentrated *in vacuo* and purified by column chromatography (hexane:DCM) affording sulfide **171** as a white solid (23.2 mg, 113 µmol, 65%).

^{1}H NMR (300 MHz, $CDCl_3$, ppm) δ = 3.76 (s, 3H), 6.28 (ddd, *J* = 3.4, 2.5 Hz, 1H), 6.54 (ddd, *J* = 3.4, 2.5, 1.5 Hz, 1H), 6.76 – 6.85 (m, 2H), 6.86 – 6.93 (m, 1H), 7.05 – 7.12 (m, 2H), 8.26 (s, 1H). ^{13}C NMR (75 MHz, $CDCl_3$, ppm) δ = 55.5, 110.4, 114.8, 117.7, 117.8, 121.5, 128.9, 129.3, 158.4. IR (neat, cm^{-1}): 3366.1, 2939.0, 2835.8, 1590.0, 1573.6, 1489.7, 1460.8, 1439.6, 1404.9, 1284.4, 1236.1, 1173.5, 1107.9, 1087.7, 1074.2, 1024.0, 1006.7, 928.6, 819.6, 794.5, 724.1, 655.7, 636.4, 621.9, 518.8. HRMS: *m*/*z* calcd. for $C_{11}H_{12}NOS^+$ $[M+H]^+$ = 206.0634; found = 206.0630.

3-[(4-Methoxyphenyl)thio]-1-methyl-1*H*-indole (**157**):

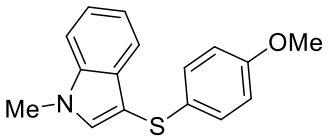

According to GP4, imidazolium salt **114** (37.0 mg, 63.9 µmol, 1.00 equiv.) was dissolved in THF (1.0 mL) and cooled to -80 °C. Methoxyphenylmagnesium bromide (0.5M solution in THF, 371 µL, 185.5 µmol, 2.90 equiv.) was added dropwise, and the reaction mixture was allowed to warm up to 10 °C over a period of 14 h furnishing the dark brown solution. The reaction was quenched with sat. NH_4Cl (5 mL), stirred for 5 min and extracted with DCM (3 × 20 mL). The combined organic phases were dried over $MgSO_4$, concentrated *in vacuo* and purified by column chromatography (hexane:EtOAc) affording sulfide **157** as a white solid (15.0 mg, 55.6 µmol, 87%).

^{1}H NMR (400 MHz, $CDCl_3$, ppm) δ = 3.73 (s, 3H), 3.83 (s, 3H), 6.69 – 6.78 (m, 2H), 7.09 – 7.17 (m, 2H), 7.13 – 7.20 (m, 1H), 7.25 – 7.33 (m, 1H), 7.32 (s, 1H), 7.36 (d, *J* = 8.1 Hz, 1H), 7.63 (d, *J* = 8.0 Hz, 1H). ^{13}C NMR (126 MHz, $CDCl_3$, ppm) δ = 33.3, 55.5, 102.6, 109.7, 114.5, 119.8, 120.4, 122.5, 128.5, 129.8, 130.1, 134.5, 137.5, 157.8. IR (neat, cm^{-1}): 2934.2, 2831.0, 1591.9, 1571.7, 1509.0, 1488.8, 1457.9, 1439.6, 1420.3, 1353.8, 1332.6, 1315.2, 1284.4, 1237.1, 1171.5, 1154.2, 1125.3, 1110.8, 1088.6, 1027.9, 1007.6, 819.6, 795.5, 765.6, 738.6, 637.4, 623.9, 610.4, 513.0. HRMS: *m/z* calcd. for $C_{16}H_{15}NOS^+$ $[M]^+$ = 269.0869; found = 269.0873.

3-[(4-Methoxyphenyl)thio]-1-methyl-2-phenyl-1*H*-indole (**175**):

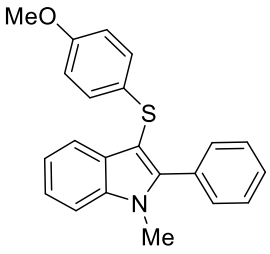

According to GP4, imidazolium salt **100** (45.8 mg, 70.0 µmol, 1.00 equiv.) was suspended in THF (1.0 mL) and cooled to -70 °C. Methoxyphenylmagnesium bromide (0.5M solution in THF, 406 µL, 203 µmol, 2.90 equiv.) was added dropwise, and the reaction mixture was allowed to warm up to 10 °C over a period of 14 h furnishing the orange solution. The reaction was quenched with sat. NH_4Cl (5 mL), stirred for 5 min and extracted with DCM (3 × 20 mL). The combined organic phases were dried over $MgSO_4$, concentrated *in vacuo* and purified by column chromatography (hexane:EtOAc) to obtain **175** as a white solid (8.0 mg, 23.2 µmol, 33%).

^{1}H NMR (600 MHz, $CDCl_3$, ppm) δ = 3.72 (s, 3H), 3.72 (s, 3H), 6.69 – 6.73 (m, 2H), 6.99 – 7.03 (m, 2H), 7.15 – 7.22 (m, 1H), 7.28 – 7.33 (m, 1H), 7.39 – 7.49 (m, 6H), 7.66 – 7.69 (m, 1H). ^{13}C NMR (126 MHz, $CDCl_3$, ppm) δ = 31.9, 55.5, 101.5, 109.8, 114.3, 114.5, 119.9, 120.9, 122.8, 127.8, 128.1, 128.3, 128.7, 129.9, 130.8, 137.6, 145.5, 157.5. IR (neat, cm^{-1}): 2921.6, 2852.2, 1489.7, 1459.8, 1435.7, 1378.9, 1285.3, 1276.6, 1238.1, 1176.4, 1033.7, 1024.0,

1010.5, 824.4, 814.8, 797.4, 737.6, 697.1, 620.0, 550.6, 506.2. HRMS: *m*/*z* calcd. for $C_{22}H_{19}NOS^+$ [M]$^+$ = 345.1182; found = 345.1187.

5,6-Dimethoxy-3-(phenylthio)-1*H*-indole-2-carboxylic acid (**87**):

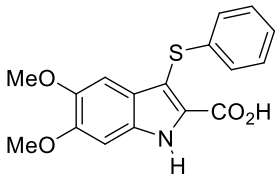

According to GP4, imidazolium salt **117** (98.2 mg, 209.8 µmol, 1.00 equiv.) was suspended in THF (1.0 mL) and cooled to -78 °C. Phenylmagnesium bromide (0.84M solution in THF, 1.25 mL, 1.05 mmol, 5.00 equiv.) was added dropwise to the stirred white suspension, and the reaction mixture was allowed to warm up overnight affording the yellow solution. The reaction was quenched with sat. NH_4Cl (5 mL), stirred for 5 min and extracted with DCM (3 × 20 mL). The combined organic phases were dried over $MgSO_4$, concentrated *in vacuo* and purified by column chromatography (DCM:MeOH) furnishing sulfide **87** as a white solid (42.2 mg, 128 µmol, 61%).

^{1}H NMR (400 MHz, CD_2Cl_2, ppm) δ = 3.77 (s, 3H), 3.89 (s, 3H), 6.92 (d, *J* = 2.6 Hz, 2H), 7.16 – 7.29 (m, 5H), 9.53 (s, 2H). ^{13}C NMR (126 MHz, $CDCl_3$, ppm) δ = 56.3, 56.4, 94.5, 100.9, 108.0, 123.0, 126.7, 127.5, 128.5, 129.4, 131.7, 135.4, 147.8, 151.6, 161.5. IR (neat, cm^{-1}): 2920.7, 1671.0, 1632.4, 1579.4, 1508.1, 1476.2, 1461.8, 1437.7, 1258.3, 1227.5, 1205.3, 1172.5, 1149.4, 1085.7, 1049.1, 1021.1, 1003.8, 913.1, 836.0, 797.4, 734.7, 688.5, 663.4, 561.2. HRMS: *m*/*z* calcd. for $C_{17}H_{15}NNaO_4S^+$ [M+Na]$^+$ = 352.0614; found = 352.0610.

1-[(4-Methoxyphenyl)thio]-5,6-dihydro-4*H*-pyrrolo[3,2,1-*ij*]quinoline (**176**):

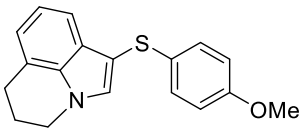

According to GP4, imidazolium salt **116** (175 mg, 290 µmol, 1.00 equiv.) was dissolved in THF (3.0 mL) and cooled to -78 °C. Methoxyphenylmagnesium bromide solution (0.50M in THF, 1.68 mL, 840 µmol, 4.80 equiv.) was added dropwise to the stirred clear solution, and the obtained orange reaction mixture was allowed to warm up overnight furnishing the red solution. The reaction was quenched with sat. NH_4Cl (5 mL), stirred for 5 min and extracted with DCM (3 × 20 mL). The combined organic phases were dried over $MgSO_4$, concentrated *in vacuo* and purified by column chromatography (hexane:DCM) affording sulfide **176** as a white solid (65.1 mg, 220 µmol, 76%).

^{1}H NMR (300 MHz, CD_2Cl_2 ppm) δ 2.20 – 2.31 (m, 2H), 3.00 (dd, *J* = 6.7, 5.5 Hz, 2H), 3.72 (s, 3H), 4.13 – 4.27 (m, 2H), 6.72 – 6.75 (m, 2H), 6.93 – 7.04 (m, 2H), 7.11 – 7.15 (m, 2H), 7.30 – 7.36 (m, 2H). ^{13}C NMR (126 MHz, CD_2Cl_2, ppm) δ = 23.5, 25.1, 45.0, 55.8, 102.5, 114.8, 117.1, 119.8, 121.1, 123.0, 127.7, 129.1, 130.6, 132.3, 135.4, 158.3. IR (neat, cm^{-1}): 2931.3,

1591.0, 1489.7, 1459.8, 1438.6, 1378.9, 1362.5, 1322.9, 1284.4, 1240.0, 1173.5, 1162.9, 1153.2, 1103.1, 1029.8, 957.5, 821.5, 777.2, 748.2, 608.4, 517.8. HRMS: *m*/*z* calcd. for $C_{18}H_{18}NOS^+$ $[M+H]^+$ = 296.1104; found = 296.1094.

2-[(4-Methoxyphenyl)thio]-5-methylthiophene (**186**):

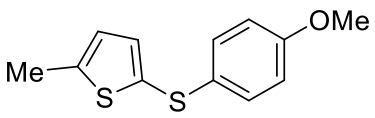

According to GP4, imidazolium salt **122** (66.0 mg, 121 µmol, 1.00 equiv.) was dissolved in THF (1.0 mL) and cooled to -78 °C. Methoxyphenylmagnesium bromide (0.5M solution in THF, 363 µL, 181.5 µmol, 1.50 equiv.) was added dropwise to the brown suspension, and the reaction mixture was allowed to warm up overnight furnishing the orange solution. The reaction was quenched with sat. NH_4Cl (5 mL), stirred for 5 min and extracted with DCM (3 × 20 mL). The combined organic phases were dried over $MgSO_4$, concentrated *in vacuo* and purified by column chromatography (DCM:MeOH) affording sulfide **186** as a colorless oil (24.3 mg, 102.8 µmol, 85%).

^{1}H NMR (400 MHz, $CDCl_3$, ppm) δ = 2.46 (d, *J* = 1.1 Hz, 3H), 3.77 (s, 3H), 6.67 (dt, *J* = 3.5, 1.1 Hz, 1H), 6.79 – 6.85 (m, 2H), 7.05 (d, *J* = 3.5 Hz, 1H), 7.24 – 7.28 (m, 2H). ^{13}C NMR (126 MHz, $CDCl_3$, ppm) δ = 15.9, 55.5, 114.7, 125.9, 129.1, 130.6, 130.7, 134.9, 145.3, 158.8. IR (neat, cm^{-1}): 2916.8, 2831.0, 1591.9, 1572.7, 1489.7, 1458.9, 1438.6, 1285.3, 1241.0, 1212.0, 1171.5, 1160.0, 1104.0, 1064.5, 1029.8, 1005.7, 952.7, 821.5, 793.6, 637.4, 624.8, 566.0, 528.4. HRMS: *m*/*z* calcd. for $C_{12}H_{12}OS_2^+$ $[M]^+$ = 236.0324; found = 236.0324.

6-Methoxy-2-(4-methoxyphenyl)-3-[(4-methoxyphenyl)thio]benzo[*b*]thiophene (**190**):

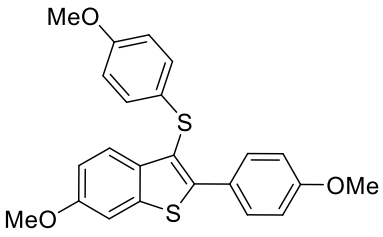

According to GP4, imidazolium salt **123** (50.2 mg, 69.9 µmol, 1.00 equiv.) was dissolved in THF (1.0 mL) and cooled to -78 °C. Methoxyphenylmagnesium bromide (0.5M solution in THF, 210 µL, 105 µmol, 1.50 equiv.) was added dropwise to the light yellow suspension, and the reaction mixture was allowed to warm up overnight affording the white suspension. The reaction was quenched with sat. NH_4Cl (5 mL), stirred for 5 min and extracted with DCM (3 × 20 mL). The combined organic phases were dried over $MgSO_4$, concentrated *in vacuo* and purified by column chromatography (hexane:DCM) furnishing sulfide **190** as a white solid (11.7 mg, 28.6 µmol, 41%).

^{1}H NMR (300 MHz, $CDCl_3$, ppm) δ = 3.72 (s, 3H), 3.84 (s, 3H), 3.87 (s, 3H), 6.71 – 6.76 (m, 2H), 6.93 – 7.05 (m, 5H), 7.29 – 7.32 (m, 1H), 7.61 – 7.70 (m, 3H). ^{13}C NMR (126 MHz, $CDCl_3$, ppm) δ = 55.5, 55.5, 55.8, 105.0, 114.0, 114.8, 114.8, 118.4, 124.5, 126.2, 128.2, 128.5, 131.0, 135.2, 137.4, 139.4, 146.1, 157.9, 160.0. IR (neat, cm^{-1}): 2934.2, 2832.0, 1602.6, 1571.7,

1557.2, 1523.5, 1489.7, 1470.5, 1435.7, 1402.0, 1298.8, 1285.3, 1112.7, 1061.6, 985.4, 904.5, 819.6, 803.2, 765.6, 730.9, 647.0, 636.4, 621.0, 584.3, 560.2, 511.0. HRMS: *m*/*z* calcd. for $C_{23}H_{20}O_3S_2^+$ $[M]^+$ = 408.0848; found = 408.0854.

***N,N*-Dimethyl-4-(phenylthio)anilin**e (**179**):

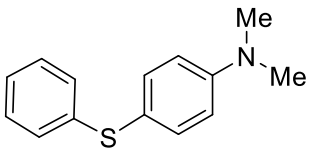

According to GP4, imidazolium salt **129** (55.0 mg, 96.7 µmol, 1.00 equiv.) was dissolved in THF (1.5 mL) and cooled to -78 °C. Phenylmagnesium bromide solution (0.92M in THF, 300 µL, 276 µmol, 2.85 equiv.) was added dropwise to the violet suspension, and the reaction mixture was allowed to warm up overnight affording the dark brown suspension. The reaction was quenched with sat. NH_4Cl (5 mL), stirred for 5 min and extracted with DCM (3 × 20 mL). The combined organic phases were dried over $MgSO_4$, concentrated *in vacuo* and purified by column chromatography (DCM:MeOH) furnishing sulfide **179** as a colorless oil (14.2 mg, 61.9 µmol, 64%).

^{1}H NMR (300 MHz, $CDCl_3$, ppm) δ = 3.00 (s, 6H), 6.69 – 6.75 (m, 2H), 7.05 – 7.13 (m, 3H), 7.14 – 7.25 (m, 2H), 7.38 – 7.42 (m, 2H). ^{13}C NMR (75 MHz, $CDCl_3$, ppm) δ = 40.5, 113.1, 117.6, 125.1, 127.0, 128.9, 136.3, 140.4, 150.8. IR (neat, cm^{-1}): 2885.0, 1677.8, 1591.9, 1550.5, 1504.2, 1475.3, 1438.6, 1354.7, 1314.3, 1260.3, 1223.6, 1192.8, 1167.7, 1129.1, 1100.2, 1084.8, 1062.6, 1023.1, 998.0, 944.0, 906.4, 810.9, 764.6, 735.7, 688.5, 644.1, 621.0, 610.4, 594.0, 527.4. HRMS: *m*/*z* calcd. for $C_{14}H_{16}NS^+$ $[M+H]^+$ = 230.0998; found = 230.0999.

***N,N*-Dimethyl-4-(*p*-tolylthio)aniline** (**158**):

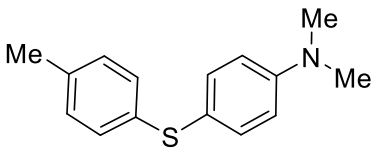

According to GP4, imidazolium salt **129** (49.0 mg, 86.2 µmol, 1.00 equiv.) was dissolved in THF (1.5 mL) and cooled to -78 °C. *p*-Tolylmagnesium bromide solution (0.92M in THF, 272 µL, 250 µmol, 2.90 equiv.) was added dropwise to the violet suspension, and the reaction mixture was allowed to warm up overnight giving the dark brown suspension. The reaction was quenched with sat. NH_4Cl (5 mL), stirred for 5 min and extracted with DCM (4 × 20 mL). The combined organic phases were dried over $MgSO_4$, concentrated *in vacuo* and purified by column chromatography (DCM:MeOH) affording sulfide **158** as a colorless oil (15.8 mg, 64.9 µmol, 75%)

^{1}H NMR (300 MHz, $CDCl_3$, ppm) δ = 2.29 (s, 3H), 2.98 (s, 6H), 6.66 – 6.74 (m, 2H), 7.00 –

7.09 (m, 4H), 7.34 – 7.40 (m, 2H).[27]

4-[(4-Methoxyphenyl)thio]-*N,N*-dimethylaniline (**160**):

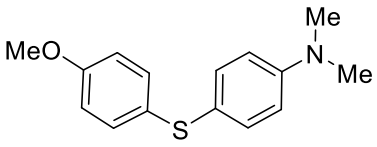

According to GP4, imidazolium salt **129** (104.6 mg, 184 µmol, 1.00 equiv.) and LiCl (39.0 mg, 920 µmol, 5.00 equiv.) were dissolved in THF (1.5 mL) and cooled to -78 °C. 4-Methoxyphenylmagnesium bromide solution (0.50M in THF, 1.07 mL, 535 µmol, 2.91 equiv.) was added dropwise to the violet suspension, and the reaction mixture was allowed to warm up overnight affording the yellow suspension. The reaction was quenched with sat. NH_4Cl (5 mL), stirred for 5 min and extracted with DCM (3 × 20 mL). The combined organic phases were dried over $MgSO_4$, concentrated *in vacuo* and purified by column chromatography (DCM:MeOH) furnishing sulfide **160** as a white solid (43.1 mg, 166 µmol, 90%).

^{1}H NMR (300 MHz, $CDCl_3$, ppm) δ = 2.86 (s, 6H), 3.67 (s, 3H), 6.53 – 6.61 (m, 2H), 6.67 – 6.73 (m, 2H), 7.06 – 7.13 (m, 2H), 7.18 – 7.27 (m, 2H). ^{13}C NMR (75 MHz, $CDCl_3$, ppm) δ = 40.5, 55.4, 113.1, 114.7, 120.6, 129.7, 131.0, 134.4, 137.4, 150.2, 158.4. IR (neat, cm^{-1}): 2855.1, 1590.0, 1487.8, 1453.1, 1356.7, 1280.5, 1230.4, 1193.7, 1028.8, 808.0, 628.7, 523.6, 504.3. HRMS: *m*/*z* calcd. for $C_{15}H_{17}NOS^+$ $[M]^+$ = 259.1025; found = 259.1024.

4-{[4-({[(1*R*,2*S*,5*R*)-2-Isopropyl-5-methylcyclohexyl]oxy}methyl)phenyl]thio}-*N,N*-dimethylaniline (**187**):

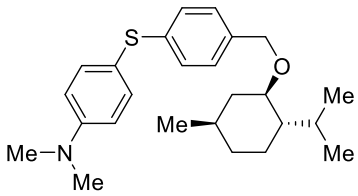

According to GP4, imidazolium salt **129** (75.0 mg, 131.9 µmol, 1.00 equiv.) was dissolved in THF (1.0 mL) and cooled to -78 °C. 4-(Mentholoxymethyl)phenylmagnesium bromide[28]

[27] ^{1}H NMR spectrum was in agreement with the data published by R. K. Peddinti *et al.*: S. K. R. Parumala, R. K. Peddinti, *Green Chem*. **2015**, *17*, 4068–4073.

[28] Prepared from **301** in accordance with the procedure published by H. Ess, L. Kürti *et al*.: H. Gao, Z. Zhou, D.-H. Kwon, J. Coombs, S. Jones, N. E. Behnke, D. H. Ess, L. Kürti, *Nat. Chem*. **2017**, *9*, 681–689. $BrCH_2CH_2Br$ was used to initiate the formation of the Grignard

solution (0.404M in THF, 948 µL, 382.9 µmol, 2.90 equiv.) was added dropwise to the violet solution, and the reaction mixture was allowed to warm up overnight furnishing the orange suspension. The reaction was quenched with sat. NH_4Cl (5 mL), stirred for 5 min and extracted with DCM (3 × 20 mL). The combined organic phases were dried over $MgSO_4$, concentrated *in vacuo* and purified by column chromatography (hexane:DCM) affording sulfide **187** as a white solid (26.8 mg, 67.4 µmol, 51%).

^{1}H NMR (300 MHz, $CDCl_3$, ppm) δ = 0.71 (d, *J* = 6.9 Hz, 3H), 0.86 – 1.01 (m, 9H), 1.22 – 1.44 (m, 2H), 1.64 (ddt, *J* = 12.6, 9.7, 3.2 Hz, 2H), 2.17 (dtd, *J* = 12.2, 3.8, 1.9 Hz, 1H), 2.27 (hd, *J* = 7.0, 2.8 Hz, 1H), 2.99 (s, 6H), 3.14 (td, *J* = 10.6, 4.2 Hz, 1H), 4.32 (d, *J* = 11.4 Hz, 1H), 4.58 (d, *J* = 11.4 Hz, 1H), 6.67 – 6.73 (m, 2H), 7.08 – 7.13 (m, 2H), 7.17 – 7.22 (m, 2H), 7.34 – 7.40 (m, 2H). ^{13}C NMR (126 MHz, $CDCl_3$, ppm) δ = 16.3, 21.2, 22.6, 23.5, 25.7, 31.8, 34.8, 40.5, 40.5, 48.5, 77.2, 78.8, 113.1, 118.1, 127.3, 128.4, 135.8, 136.2, 139.1, 150.6. IR (neat, cm^{-1}): 2949.6, 2916.8, 2864.7, 1592.9, 1505.2, 1490.7, 1444.4, 1355.7, 1223.6, 1192.8, 1168.7, 1103.1, 1081.9, 1066.4, 1014.4, 944.9, 806.1, 655.7, 528.4. HRMS: *m*/*z* calcd. for $C_{25}H_{35}NOS^+$ $[M]^+$ = 397.2434; found = 397.2436.

(2,4-Dimethoxyphenyl)(4-methoxyphenyl)sulfane (**184**):

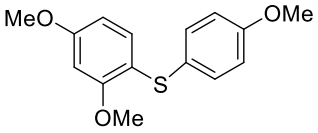

According to GP4, imidazolium salt **137** (70.2 mg, 119.9 µmol, 1.00 equiv.) was dissolved in THF (1.0 mL) and cooled to -78 °C. Methoxyphenylmagnesium bromide (0.50M in THF, 360 µL, 180 µmol, 1.50 equiv.) was added dropwise to the stirred white suspension, and the reaction mixture was allowed to warm up overnight giving the brown suspension. The reaction was quenched with sat. NH_4Cl (5 mL), stirred for 5 min and extracted with DCM (3 × 20 mL). The combined organic phases were dried over $MgSO_4$, concentrated *in vacuo* and purified by column chromatography (hexane:DCM) affording sulfide **184** as a white solid (16.5 mg, 59.7 µmol, 50%).

^{1}H NMR (400 MHz, $CDCl_3$, ppm) δ = 3.79 (s, 3H), 3.80 (s, 3H), 3.84 (s, 3H), 6.40 – 6.46 (m, 1H), 6.49 (d, *J* = 2.6 Hz, 1H), 6.82 – 6.86 (m, 2H), 7.08 (dd, *J* = 8.5, 1.0 Hz, 1H), 7.25 – 7.30 (m, 2H). ^{13}C NMR (126 MHz, $CDCl_3$, ppm) δ = 55.5, 55.6, 56.1, 99.2, 105.3, 114.8, 115.9, 126.4, 132.7, 133.4, 158.8, 158.9, 160.7. IR (neat, cm^{-1}): 2937.1, 2832.9, 1589.1, 1572.7, 1489.7, 1458.9, 1435.7, 1409.7, 1299.8, 1279.5, 1240.0, 1206.3, 1170.6, 1159.0, 1102.1, 1007.6, 933.4, 917.0, 820.6, 793.6, 634.5, 621.9, 518.8. HRMS: *m*/*z* calcd. for $C_{15}H_{16}O_3S^+$ $[M]^+$ = 276.0815; found = 276.0825.

2-(Isopropylthio)-1-phenyl-1*H*-pyrrole (**191**):

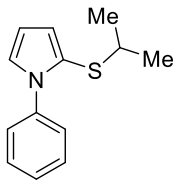

According to GP4, imidazolium salt **99** (135.7 mg, 230 µmol, 1.00 equiv.) was dissolved in THF (1.0 mL) and cooled to -78 °C. Isopropylmagnesium chloride solution (1.30M in THF, 513 µL, 667 µmol, 2.90 equiv.) was added dropwise to the clear solution, and the reaction mixture was allowed to warm up overnight furnishing the yellow solution. The reaction was quenched with sat. NH_4Cl (5 mL), stirred for 5 min and extracted with DCM (3 × 20 mL). The combined organic phases were dried over $MgSO_4$, concentrated *in vacuo* and purified by column chromatography (hexane:DCM) affording sulfide **191** as a colorless oil (32.0 mg, 147 µmol, 64%).

^{1}H NMR (300 MHz, $CDCl_3$, ppm) δ = 1.02 (d, *J* = 6.7 Hz, 6H), 2.72 (hept, *J* = 6.7 Hz, 1H), 6.29 (dd, *J* = 3.5, 2.9 Hz, 1H), 6.54 (dd, *J* = 3.6, 1.8 Hz, 1H), 7.00 (dd, *J* = 2.9, 1.8 Hz, 1H), 7.32 – 7.49 (m, 5H). ^{13}C NMR (126 MHz, $CDCl_3$, ppm) δ = 23.1, 40.5, 108.9, 120.1, 121.6, 125.6, 126.8, 127.2, 128.7, 140.1. IR (neat, cm^{-1}): 2958.3, 2920.7, 2858.0, 1596.8, 1497.5, 1455.0, 1431.9, 1363.4, 1319.1, 1237.1, 1153.2, 1133.0, 1088.6, 1073.2, 1050.1, 1033.7, 959.4, 760.8, 718.4, 616.1, 606.5, 559.3, 505.3. HRMS: *m*/*z* calcd. for $C_{13}H_{15}NS^+$ $[M]^+$ = 217.0920; found = 217.0923.

2-(2-Butylthio)-1-phenyl-1H-pyrrole (**192**):

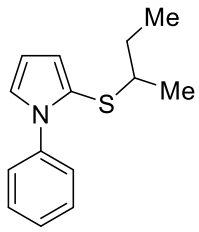

According to modified GP4, imidazolium salt **99** (218.4 mg, 370 µmol, 1.00 equiv.) was dissolved in THF (1.5 mL) and cooled to -78 °C. *sec*-Buthyllithium (1.50M in cyclohexane, 396 µL, 594 µmol, 1.61 equiv.) was added dropwise to the clear solution, and the reaction mixture was allowed to warm up overnight furnishing the dark brown solution. The reaction was quenched with sat. NH_4Cl (5 mL), stirred for 5 min and extracted with DCM (3 × 20 mL). The combined organic phases were dried over $MgSO_4$, concentrated *in vacuo* and purified by column chromatography (hexane:DCM) affording sulfide **192** as a light yellow oil (57.2 mg, 247.2 µmol, 67%).

^{1}H NMR (600 MHz, $CDCl_3$, ppm) δ = 0.75 (t, *J* = 7.4 Hz, 3H), 0.99 (d, *J* = 6.8 Hz, 3H), 1.22 – 1.29 (m, 1H), 1.30 – 1.40 (m, 1H), 2.43 – 2.51 (m, 1H), 6.28 (dd, *J* = 3.6, 2.9 Hz, 1H), 6.54 (dd, *J* = 3.6, 1.8 Hz, 1H), 7.00 (dd, *J* = 3.0, 1.8 Hz, 1H), 7.34 – 7.41 (m, 3H), 7.42 – 7.46 (m, 2H). ^{13}C NMR (126 MHz, $CDCl_3$, ppm) δ = 11.5, 20.6, 29.4, 47.3, 108.9, 120.2, 121.3, 125.5, 126.9, 127.2, 128.6, 140.1. IR (neat, cm^{-1}): 2961.2, 2919.7, 1596.8, 1514.8, 1497.5, 1455.0, 1431.9, 1374.0, 1319.1, 1133.0, 1088.6, 1072.2, 1034.6, 958.4, 796.5, 760.8, 717.4, 692.3, 621.0, 606.5, 559.3, 503.3. HRMS: *m*/*z* calcd. for $C_{14}H_{17}NOS^+$ $[M]^+$ = 231.1076; found = 231.1088.

2-(Pent-4-en-1-ylthio)-1-phenyl-1*H*-pyrrole (**193**):

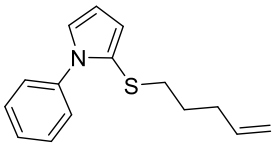

According to GP4, imidazolium salt **99** (76.7 mg, 130 µmol, 1.00 equiv.) was dissolved in THF (1.3 mL) and cooled to -78 °C. 4-Pentenylmagnesium bromide solution (1.80M in Et_2O, 209 µL, 376 µmol, 2.89 equiv.) was added dropwise to the clear solution, and the reaction mixture was allowed to warm up overnight furnishing the grey suspension. The reaction was quenched with sat. NH_4Cl (5 mL), stirred for 5 min and extracted with DCM (3 × 20 mL). The combined organic phases were dried over $MgSO_4$, concentrated *in vacuo* and purified by column chromatography (hexane:DCM) affording sulfide **193** as a colorless oil (26.3 mg, 108 µmol, 83%).

^{1}H NMR (300 MHz, CD_2Cl_2 ppm) δ = 1.44 (p, *J* = 7.3 Hz, 2H), 1.92 – 2.02 (m, 2H), 2.38 (d, *J* = 7.1 Hz, 2H), 4.87 – 4.89 (m, 1H), 4.91 – 4.95 (m, 1H), 5.67 (ddt, *J* = 15.9, 10.7, 6.7 Hz, 1H), 6.26 (dd, *J* = 3.6, 3.0 Hz, 1H), 6.49 (dd, *J* = 3.6, 1.8 Hz, 1H), 6.98 (dd, *J* = 3.0, 1.8 Hz, 1H), 7.34 – 7.51 (m, 5H). ^{13}C NMR (126 MHz, CD_2Cl_2, ppm) δ = 28.9, 32.8, 37.2, 109.4, 115.2, 119.2, 122.5, 125.7, 127.0, 127.7, 129.1, 138.3, 140.4. IR (neat, cm^{-1}): 2926.4, 1718.3, 1639.2, 1596.8, 1515.8, 1497.5, 1455.0, 1432.9, 1393.3, 1319.1, 1295.0, 1272.8, 1257.4, 1205.3, 1173.5, 1133.0, 1088.6, 1073.2, 1033.7, 999.9, 990.3, 957.5, 910.2, 879.4, 823.5,796.5, 760.8, 717.4, 692.3, 660.5, 641.2, 619.0, 605.5, 575.6, 556.4, 533.2. HRMS: *m*/*z* calcd. for $C_{15}H_{18}NS^+$ $[M+H]^+$ = 244.1154; found = 244.1157.

1-Phenyl-2-(prop-1-en-2-ylthio)-1*H*-pyrrole (**195**):

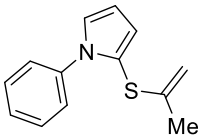

According to GP4, imidazolium salt **99** (79.1 mg, 134 µmol, 1.00 equiv.) was dissolved in THF (1.0 mL) and cooled to -78 °C. Isopropenylmagnesium bromide solution (0.5M in THF, 772 µL, 386 µmol, 2.88 equiv.) was added dropwise to the colorless solution, and the reaction mixture was allowed to warm up overnight furnishing the orange solution. The reaction was quenched with sat. NH_4Cl (5 mL), stirred for 5 min and extracted with DCM (3 × 20 mL). The combined organic phases were dried over $MgSO_4$, concentrated *in vacuo* and purified by column chromatography (DCM:MeOH) affording sulfide **195** as a colorless oil (26.2 mg, 121.6 µmol, 91%).

^{1}H NMR (300 MHz, $CDCl_3$, ppm) δ = 1.77 – 1.81 (m, 3H), 4.47 – 4.49 (m, 1H), 4.87 – 4.90 (m, 1H), 6.34 (dd, *J* = 3.6, 2.9 Hz, 1H), 6.63 (dd, *J* = 3.6, 1.8 Hz, 1H), 7.06 (dd, *J* = 3.0, 1.8 Hz, 1H), 7.32 – 7.45 (m, 5H). ^{13}C NMR (126 MHz, $CDCl_3$, ppm) δ = 22.2, 108.7, 109.5, 118.7, 121.1, 126.1, 127.4, 128.7, 139.7, 143.3. IR (neat, cm^{-1}): 2955.4, 1595.8, 1488.8, 1456.0, 1448.3, 1432.9, 1393.3, 1320.0, 1290.1, 1240.0, 1204.3, 1180.2, 1171.5, 1160.9, 1136.8,

1105.0, 1086.7, 1028.8, 1002.8, 820.6, 808.0, 794.5, 760.8, 725.1, 691.4, 649.9, 635.4, 619.0, 561.2, 509.1. HRMS: *m*/*z* calcd. for $C_{13}H_{13}NS^+$ $[M]^+$ = 215.0763; found = 215.0767.

2-[(2-Methylprop-1-en-1-yl)thio]-1-phenyl-1*H*-pyrrole (**196**):

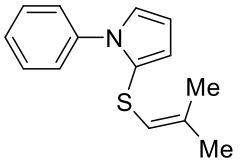

According to GP4, imidazolium salt **99** (96.8 mg, 163.9 µmol, 1.00 equiv.) was dissolved in THF (1.0 mL) and cooled to -78 °C. 2-Methyl-1-propenylmagnesium bromide solution (0.5M in THF, 951 µL, 475.5 µmol, 2.90 equiv.) was added dropwise to the colorless solution, and the reaction mixture was allowed to warm up overnight furnishing the yellow solution. The reaction was quenched with sat. NH_4Cl (5 mL), stirred for 5 min and extracted with DCM (3 × 20 mL). The combined organic phases were dried over $MgSO_4$, concentrated *in vacuo* and purified by column chromatography (hexane:DCM) affording sulfide **196** as a colorless oil (33.2 mg, 144.7 µmol, 88%).

^{1}H NMR (400 MHz, $CDCl_3$, ppm) δ = 1.64 (dd, *J* = 1.2, 0.5 Hz, 3H), 1.66 – 1.69 (m, 3H), 5.55 – 5.58 (m, 1H), 6.30 (dd, *J* = 3.6, 3.0 Hz, 1H), 6.53 (dd, *J* = 3.6, 1.8 Hz, 1H), 6.98 (dd, *J* = 2.9, 1.8 Hz, 1H), 7.33 – 7.48 (m, 5H). ^{13}C NMR (126 MHz, $CDCl_3$, ppm) δ = 19.3, 25.1, 109.2, 117.4, 119.4, 122.3, 125.1, 126.6, 127.2, 128.7, 134.9, 139.8. IR (neat, cm^{-1}): 2909.1, 1596.8, 1498.4, 1454.1, 1433.8, 1371.1, 1319.1, 1298.8, 1133.0, 1087.7, 1072.2, 1059.7, 1033.7, 959.4, 798.4, 759.8, 716.4, 692.3, 664.4, 619.0, 605.5, 558.3, 504.3. HRMS: *m*/*z* calcd. for $C_{14}H_{16}NS^+$ $[M+H]^+$ = 230.0998; found = 230.0995.

3-(*n*-Butylthio)-1-methyl-1*H*-indole (**197**):

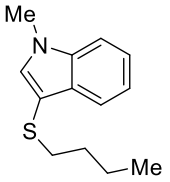

According to modified GP4, imidazolium salt **114** (49.2 mg, 85.1 µmol, 1.00 equiv.) was dissolved in THF (1.3 mL) and cooled to -78 °C. *n*-Buthyllithium (1.23M in hexane, 104 µL, 127.9 µmol, 1.50 equiv.) was added dropwise to the clear solution, and the reaction mixture was allowed to warm up overnight furnishing the orange solution. The reaction was quenched with sat. NH_4Cl (5 mL), stirred for 5 min and extracted with DCM (3 × 20 mL). The combined organic phases were dried over $MgSO_4$, concentrated *in vacuo* and purified by column chromatography (hexane:DCM) affording sulfide **197** as a colorless oil (12.0 mg, 54.7 µmol, 64%).

^{1}H NMR (300 MHz, CD_2Cl_2 ppm) δ = 0.79 (t, 3H), 1.25 – 1.34 (m, 2H), 1.45 – 1.57 (m, 2H), 2.59 – 2.69 (m, 2H), 3.34 (s, 3H), 7.13 – 7.37 (m, 4H), 7.71 (ddd, *J* = 7.6, 1.5, 0.8 Hz, 1H). ^{13}C NMR (126 MHz, CD_2Cl_2, ppm) δ = 14.1, 22.3, 32.6, 33.4, 37.0, 104.4, 110.1, 119.7, 120.2, 122.5, 130.6, 134.4, 137.8. IR (neat, cm^{-1}): 3056.6, 2916.8, 1511.9, 1487.8, 1476.2, 1461.8,

1419.4, 1328.7, 1315.2, 1241.0, 1204.3, 1152.3, 1133.0, 1100.2, 1077.0, 1012.4, 883.2, 761.7, 734.7, 709.7, 572.8. HRMS: *m*/*z* calcd. for $C_{13}H_{18}NS^+$ $[M+H]^+$ = 220.1154; found = 220.1151.

4-(Isopropylthio)-*N,N*-dimethylaniline (**198**):

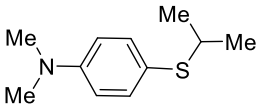

According to GP4, imidazolium salt **129** (45.4 mg, 79.9 µmol, 1.00 equiv.) was dissolved in THF (1.0 mL) and cooled to -78 °C. Isopropylmagnesium chloride solution (1.3M in THF, 178 µL, 231.4 µmol, 2.90 equiv.) was added dropwise to the stirred violet suspension, and the reaction mixture was allowed to warm up overnight furnishing the colorless solution. The reaction was quenched with sat. NH_4Cl (5 mL), stirred for 5 min and extracted with DCM (3 × 20 mL). The combined organic phases were dried over $MgSO_4$, concentrated *in vacuo* and purified by column chromatography (hexane:DCM) affording sulfide **198** as a colorless oil (14.6 mg, 74.7 µmol, 93%).

^{1}H NMR (400 MHz, $CDCl_3$, ppm) δ = 1.23 (d, *J* = 6.7 Hz, 6H), 2.96 (s, 6H), 3.11 (hept, *J* = 6.7 Hz, 1H), 6.60 – 6.72 (m, 2H), 7.30 – 7.42 (m, 2H). ^{13}C NMR (126 MHz, $CDCl_3$, ppm) δ = 23.4, 40.0, 40.6, 112.6, 119.8, 136.1, 150.2. IR (neat, cm^{-1}): 2956.3, 2921.6, 2859.9, 1591.9, 1502.3, 1442.5, 1349.9, 1223.6, 1192.8, 1166.7, 1153.2, 1130.1, 1100.2, 1059.7, 1049.1, 944.9, 810.9, 524.5. HRMS: *m*/*z* calcd. for $C_{11}H_{17}NS^+$ $[M]^+$ = 195.1076; found = 195.1089.

4-(Cyclopentylthio)-*N,N*-dimethylaniline (**182**):

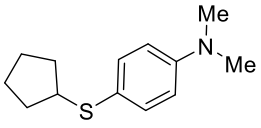

According to modified GP4, imidazolium salt **129** (76.7 mg, 134.9 µmol, 1.00 equiv.) and LiCl (28.6 mg, 676 µmol, 5.00 equiv.) were dissolved in THF (1.5 mL) and cooled to -78 °C. Cyclopentyl-magnesium bromide solution (2.0M in THF, 196 µL, 392 µmol, 2.90 equiv.) was added dropwise to the stirred violet suspension, and the reaction mixture was allowed to warm up overnight furnishing the brown suspension. The reaction was quenched with sat. NH_4Cl (5 mL), stirred for 5 min and extracted with DCM (4 × 20 mL). The combined organic phases were dried over $MgSO_4$, concentrated *in vacuo* and purified by column chromatography (DCM:MeOH) affording sulfide **182** as a colorless oil (18.5 mg, 83.5 µmol, 62%).

^{1}H NMR (300 MHz, $CDCl_3$, ppm) δ = 1.50 – 1.64 (m, 4H), 1.69 – 1.81 (m, 2H), 1.84 – 2.01 (m, 2H), 2.95 (s, 6H), 3.29 – 3.41 (m, 1H), 6.60 – 6.70 (m, 2H), 7.32 – 7.39 (m, 2H). ^{13}C NMR (75 MHz, $CDCl_3$, ppm) δ = 24.7, 33.5, 40.6, 48.8, 112.8, 121.3, 135.1, 150.1. IR (neat, cm^{-1}): 2951.5, 2799,2, 1592,9, 1502,3, 1442,5, 1349,9, 1222,6, 1191,8, 1166,7, 944,9, 810, 524,5. HRMS: *m*/*z* calcd. for $C_{13}H_{20}NS^+$ $[M+H]^+$ = 222.1311; found = 222.1317.

4-[(4-Fluorophenyl)thio]-*N,N*-dimethylaniline (**182**):

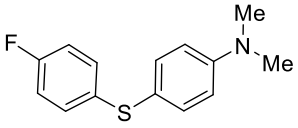

According to GP4, imidazolium salt, **129** (108 mg, 190 µmol, 1.00 equiv.) was dissolved in THF (1.0 mL) and cooled to -78 °C. 4-Fluorophenylmagnesium-bromide solution (1.0M in THF, 551 µL, 551 µmol, 2.90 equiv.) was added dropwise to the stirred violet suspension, and the reaction mixture was allowed to warm up overnight furnishing the white suspension. The reaction was quenched with sat. NH_4Cl (5 mL), stirred for 5 min and extracted with DCM (3 × 20 mL). The combined organic phases were dried over $MgSO_4$, concentrated *in vacuo* and purified by column chromatography (hexane:DCM) affording sulfide **182** as a white solid (12.2 mg, 49.3 µmol, 26%).

^{1}H NMR (300 MHz, $CDCl_3$, ppm) δ = 2.99 (s, 6H), 6.65 – 6.74 (m, 2H), 6.88 – 6.96 (m, 2H), 7.07 – 7.18 (m, 2H), 7.30 – 7.41 (m, 2H). ^{13}C NMR (126 MHz, $CDCl_3$, ppm) δ = 40.5, 113.1, 115.9 (d, $J_{C\text{-}F}$ = 21.9 Hz), 118.4, 129.5 (d, $J_{C\text{-}F}$ = 7.7 Hz), 135.0, 135.6, 150.6, 161.2 (d, $J_{C\text{-}F}$ = 244.1 Hz). ^{19}F NMR (282 MHz, $CDCl_3$, ppm) δ = –117.3. IR (neat, cm^{-1}): 2892.7, 1587.1, 1552.4, 1503.2, 1484.9, 1443.5, 1393.3, 1349.0, 1261.2, 1208.2, 1196.6, 1169.6, 1154.2, 1091.5, 1080.9, 1063.6, 1010.5, 943.0, 825.4, 814.8, 802.2, 765.6, 637.4, 623.9, 612.3, 526.5. HRMS: *m*/*z* calcd. for $C_{14}H_{14}NFS^+$ $[M]^+$ = 247.0825; found = 247.0835.

***N,N*-Dimethyl-4-(prop-1-en-2-ylthio)aniline** (**200**):

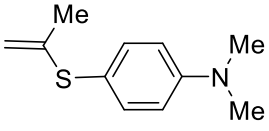

According to GP4, imidazolium salt **129** (108.5 mg, 190.9 µmol, 1.00 equiv.) was dissolved in THF (1.0 mL) and cooled to -78 °C. Isopropenylmagnesium bromide solution (0.50M in THF, 1.11 mL, 555 µmol, 2.91 equiv.) was added dropwise to the violet suspension, and the reaction mixture was allowed to warm up overnight furnishing the yellowish white suspension. The reaction suspension was quenched with sat. NH_4Cl (5 mL), stirred for 5 min and extracted with DCM (3 × 20 mL). The combined organic phases were dried over $MgSO_4$, concentrated *in vacuo* and purified by column chromatography (hexane:DCM) affording sulfide **200** as a white solid (32.9 mg, 170.1 µmol, 89%).

^{1}H NMR (300 MHz, $CDCl_3$, ppm) δ = 1.96 (dd, *J* = 1.4, 0.8 Hz, 3H), 2.98 (s, 6H), 4.57 (s, 1H), 4.93 (q, *J* = 1.4 Hz, 1H), 6.63 – 6.73 (m, 2H), 7.31 – 7.39 (m, 2H). ^{13}C NMR (75 MHz, $CDCl_3$, ppm) δ = 22.8, 40.4, 108.4, 112.8, 117.3, 136.4, 144.0, 150.8. IR (neat, cm^{-1}): 2913.9, 1593.9, 1550.5, 1505.2, 1481.1, 1443.5, 1355.7, 1315.2, 1288.2, 1224.6, 1188.9, 1168.7, 1129.1, 1101.2, 1062.6, 1000.9, 845.9, 921.8, 853.3, 812.8, 765.6, 716.4, 616.4, 557.3, 527.4. HRMS:

m/*z* calcd. for $C_{11}H_{15}NS^+$ [M]$^+$ = 193.0920; found = 193.0920.

2-{[(1*s*,3*s*)-Adamantan-1-yl]thio}-1-phenyl-1*H*-pyrrole (**194**):

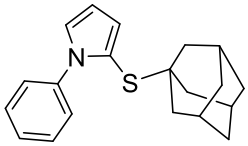

According to GP4, imidazolium salt **99** (207 mg, 350.6 µmol, 1.00 equiv.) was dissolved in THF (1.0 mL) and cooled to -78 °C. Under stirring, adamantylmagnesium bromide solution (2.0M in THF, 510 µL, 1.02 mmol, 2.91 equiv.) was added dropwise to the colourless solution, and the reaction mixture was allowed to warm up overnight furnishing the yellow solution. The reaction was quenched with sat. NH_4Cl (5 mL), stirred for 5 min and extracted with DCM (3 × 20 mL). The combined organic phases were dried over $MgSO_4$, concentrated *in vacuo* and purified first by column chromatography (hexane:DCM), then by preparative HPLC (YMX PVA-Sil, 4.6 × 250 mm, 5µm; gradient hexane:DCM from 100:0 to 60:40) affording sulfide **194** as a white solid (5.4 mg, 17.5 µmol, 5%).

^{1}H NMR (400 MHz, $CDCl_3$, ppm) δ = 1.45 – 1.60 (m, 12H), 1.85 – 1.90 (m, 3H), 6.28 (dd, *J* = 3.6, 3.0 Hz, 1H), 6.51 (dd, *J* = 3.6, 1.8 Hz, 1H), 7.04 (dd, *J* = 3.0, 1.8 Hz, 1H), 7.32 – 7.37 (m, 3H), 7.39 – 7.47 (m, 2H). ^{13}C NMR (126 MHz, CD_2Cl_2, ppm) δ = 30.7, 36.6, 43.9, 50.0, 105.2, 109.1, 122.2, 126.5, 127.3, 127.6, 128.8. IR (neat, cm^{-1}): 2925.5, 1591.0, 1489.7, 1458.9, 1438.6, 1378.9, 1338.4, 1322.9, 1284.4, 1239.0, 1161.9, 1102.1, 1028.8, 955.6, 818.6, 776.2, 746.3, 635.4, 621.9, 607.5, 513.0. HRMS: *m*/*z* calcd. for $C_{20}H_{24}NS^+$ [M+H]$^+$ = 310.1624; found = 310.1623.

(4-Methoxyphenyl)(2,4,6-trimethoxyphenyl)sulfane (**184**):

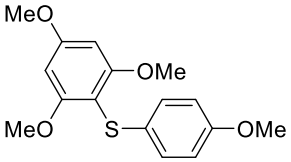

According to GP4, imidazolium salt **138** (949 mg, 1.54 mmol, 1.00 equiv.) was dissolved in THF (8.0 mL) and cooled to -78 °C. Methoxyphenylmagnesium bromide (0.35M in THF, 6.61 mL, 2.31 mmol, 1.50 equiv.) was added dropwise to the stirred white suspension, and the reaction mixture was allowed to warm up overnight furnishing the brown solution. The reaction was quenched with sat. NH_4Cl (15 mL), stirred for 5 min and extracted with DCM (2 × 25 mL). The combined organic phases were dried over $MgSO_4$, concentrated *in vacuo* and purified by column chromatography (hexane:DCM) furnishing sulfide **184** as a white solid (200 mg, 652.7 µmol, 42%).

^{1}H NMR (300 MHz, CD_2Cl_2, ppm) δ = 3.73 (s, 3H), 3.80 (s, 6H), 3.85 (s, 3H), 6.22 (s, 2H), 6.66 – 6.82 (m, 2H), 7.03 (d, *J* = 8.9 Hz, 2H). ^{13}C NMR (101 MHz, CD_2Cl_2, ppm) δ = 55.8, 55.9, 56.7, 91.7, 100.8, 114.8, 128.8, 130.1, 158.1, 162.9, 163.3. IR (neat, cm^{-1}): 2939.0, 2833.9,

1580.4, 1491.7, 1468.5, 1449.2, 1409.7, 1334.5, 1285.3, 1242.9, 1222.6, 1205.3, 1178.3, 1160.9, 1116.6, 1027.9, 953.6, 916.0, 812.8, 782.0, 679.8, 660.5, 633.5, 621.9, 520.7. HRMS: *m*/*z* calcd. for $C_{16}H_{18}NaO_4S^+$ $[M+Na]^+$ = 329.0818; found = 329.0823.

2-[(4-Methoxyphenyl)thio]-1-phenyl-5-(prop-1-en-2-ylthio)-1*H*-pyrrole (**88**):

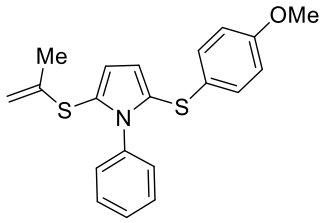

According to GP4, imidazolium salt **201** (200 mg, 274.5 µmol, 1.00 equiv.) was dissolved in THF (6.0 mL) and cooled to -78 °C. Under stirring, isopropenylmagnesium bromide solution (0.50M in THF, 1.59 mL, 795 µmol, 2.90 equiv.) was added dropwise to the suspension, and the reaction mixture was allowed to warm up overnight furnishing the yellow suspension solution. The reaction was quenched with sat. NH_4Cl (5 mL), stirred for 5 min and extracted with DCM (3 × 20 mL). The combined organic phases were dried over $MgSO_4$, concentrated *in vacuo* and purified by column chromatography (hexane:DCM) giving sulfide **88** as a white solid (78.1 mg, 221 µmol, 81%).

^{1}H NMR (300 MHz, $CDCl_3$, ppm) δ = 1.76 (s, 3H), 3.75 (s, 3H), 4.50 (d, *J* = 0.8 Hz, 1H), 4.84 – 4.90 (m, 1H), 6.65 (d, *J* = 3.7 Hz, 1H), 6.68 – 6.75 (m, 3H), 6.87 – 6.95 (m, 2H), 7.00 – 7.06 (m, 2H), 7.26 – 7.42 (m, 3H). ^{13}C NMR (126 MHz, CD_3Cl, ppm) δ = 22.3, 55.4, 109.3, 114.5, 118.6, 119.7, 123.3, 126.0, 127.8, 128.0, 128.2, 128.9, 130.3, 137.5, 142.4, 158.5. IR (neat, cm^{-1}): 1706.7, 1618.9, 1450.2, 1423.2, 1376.0, 1326.8, 1293.0, 1215.9, 1175.4, 1111.8, 1074.2, 1029.8, 906.4, 822.5, 749.2, 652.8, 545.8. HRMS: *m*/*z* calcd. for $C_{20}H_{20}NOS_2^+$ $[M+H]^+$ = 354.0981; found = 354.0979.

5.3 Reactions towards the synthesis of selenides

5.3.1 Synthesis of arylselenoimidazolium salts

2-[(2,5-Dioxopyrrolidin-1-yl)selanyl]-1,3-diisopropyl-4,5-dimethyl-1*H*-imidazol-3-ium Chloride (**214**):

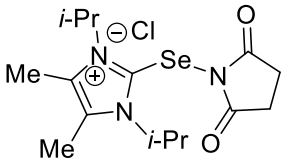

2-Selenoimidazoline (**159**) (75.0 mg, 0.289 mmol, 1.00 equiv.) and *N*-chlorosuccinimide (38.6 mg, 0.289 mmol, 1.00 equiv.) were dissolved in MeCN (2 mL) and the mixture was stirred for 5 min at r.t. Removal of the solvents *in vacuo* afforded **214** as a light yellow solid (114 mg, 0.290 mmol, quantitative).

^{1}H NMR (400 MHz, CD_2Cl_2 ppm) δ = 1.48 – 1.70 (m, 12 H), 2.36 (s, 6H), 2.61 (s, 4H), 6.03 (hept, *J* = 7.0 Hz, 2H). ^{13}C NMR (101 MHz, CD_2Cl_2, ppm) δ = 10.9, 21.3, 30.1, 56.1, 129.0, 142.8, 180.6. IR (neat, cm^{-1}): 2176.4, 2037.9, 2029.8, 1983.1, 1969.1, 1707.6, 1594.4, 1511.3, 1360.4, 1178.3, 670.9, 658.5, 634.7, 624.1. HRMS: *m*/*z* calcd. for $C_{15}H_{24}N_3O_2Se^+$ $[M–Cl]^+$ = 358.1028; found: 358.1031.

1,3-Diisopropyl-4,5-dimethyl-2-[(1-methyl-1*H*-indol-3-yl)selanyl]-1*H*-imidazol-3-ium Hexafluoroantimonate (**215**):

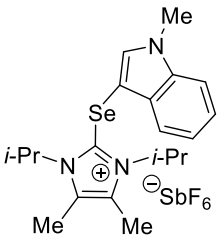

According to GP3, 2-selenoimidazoline (**159**) (180 mg, 694 µmol), *N*-chlorosuccinimide (92.7 mg, 694 µmol) and *N*-methylindole (89 µL, 91 mg, 694 µmol, 1.00 equiv.) were dissolved in MeCN (5.0 mL) and stirred at 70 °C for 19 h. All volatiles were removed *in vacuo*; the residual red solid was dissolved in DCM (5 mL) and washed with sat. aq. $NaSbF_6$ (3.0 mL) for 5 min. The organic layer was dried over $MgSO_4$ and concentrated *in vacuo*. After column chromatography (DCM:MeOH), product **215** was obtained as a yellow foam (244 mg, 390 µmol, 56%).

^{1}H NMR (300 MHz, CD_2Cl_2 ppm) δ = 1.47 (d, J = 7.1 Hz, 12H), 2.32 (s, 6H), 3.85 (s, 3H), 5.63 (s, 2H), 7.26 – 7.38 (m, 2H), 7.41 – 7.46 (m, 2H), 7.59 – 7.64 (m, 1H). ^{13}C NMR (75 MHz, CD_2Cl_2, ppm) δ = 10.9, 21.4, 33.9, 55.2, 92.2, 111.2, 119.1, 122.1, 123.8, 129.7, 130.5, 136.9, 137.7. IR (neat, cm^{-1}): 2964.1, 2923.6, 2901.4, 1432.9, 1398.1, 1384.6, 1358.6, 1344.1, 1323.9, 1229.4, 1197.6, 1161.9, 1144.5, 1121.4, 1090.5, 944.9, 759.8, 601.7, 584.3, 530.3. HRMS: *m*/*z* calcd. for $C_{20}H_{28}N_3Se^+$ $[M–SbF_6]^+$ = 390.1443; found = 390.1461; *m*/*z* calcd. for SbF_6^- $[M]^-$ = 234.8948; found = 234.8957.

1,3-Diisopropyl-4,5-dimethyl-2-[(1-phenyl-1*H*-pyrrol-2-yl)selanyl]-1*H*-imidazol-3-ium Hexafluoroantimonate (**216**):

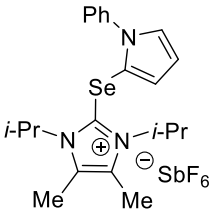

According to GP3, 2-selenoimidazoline **159** (180 mg, 694 µmol, 1.00 equiv.), *N*-chlorosuccinimide (92.7 mg, 694 µmol, 1.00 equiv.) and 1-phenylpyrrole (99.4 mg, 694 µmol, 1.00 equiv.) were dissolved in MeCN (5.0 mL) and stirred at 70 °C for 19 h. All volatiles were removed under reduced pressure; the yellow solid was dissolved in DCM (7.0 mL) and washed with sat. aq. $NaSbF_6$ (7.0 mL) for 5 min. The organic layer was dried over $MgSO_4$ and concentrated *in vacuo*. After column chromatography (DCM:MeOH), product **216** was obtained as an yellow solid (212 mg, 332.7 µmol, 48%).

^{1}H NMR (300 MHz, CD_2Cl_2 ppm) δ 1.32 (d, *J* = 7.1 Hz, 12H), 2.29 (s, 6H), 5.02 (hept, *J* = 7.1 Hz, 2H), 6.41 (dd, *J* = 3.8, 3.0 Hz, 1H), 6.74 (dd, *J* = 3.8, 1.8 Hz, 1H), 7.13 (dd, *J* = 3.0, 1.7 Hz, 1H), 7.30 – 7.35 (m, 2H), 7.48 – 7.60 (m, 3H). ^{13}C NMR (75 MHz, CD_2Cl_2, ppm) δ = 10.8, 21.3, 55.2, 109.6, 111.9, 123.6, 126.6, 129.0, 129.2, 130.2, 130.8, 139.5. IR (neat, cm^{-1}): 3089.4, 3032.5, 2961.2, 2903.3, 1767.4, 1747.2, 1605.4, 1509.0, 1438.6, 1404.9, 1383.7, 1333.5, 1304.6, 1234.2, 1194.7, 1147.4, 1133.0, 1121.4, 1098.3, 1081.9, 914.1, 756.0, 716.4, 709.7, 618.1, 584.3. HRMS: *m*/*z* calcd. for $C_{21}H_{28}N_3Se$ $[M–SbF_6]^+$ = 402.1443, found = 402.1456; calcd. for SbF_6^- $[M]^-$ = 234.8948; found = 234.8954.

2-{[4-(Dimethylamino)phenyl]selanyl}-1,3-diisopropyl-4,5-dimethyl-1*H*-imidazol-3-ium Hexafluoroantimonate (**217**):

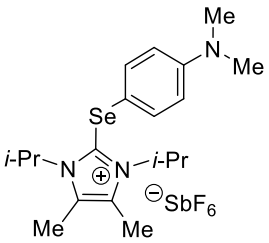

According to GP3, 2-selenoimidazoline **159** (427 mg, 1.65 mmol, 1.00 equiv.), *N*-chlorosuccinimide (220 mg, 1.65 mmol, 1.00 equiv.) and dimethylaniline (209 µL, 200 mg, 1.65 mmol, 1.00 equiv.) were dissolved in MeCN (8.0 mL) and stirred at 70 °C for 19 h. All volatiles were removed under reduced pressure, the yellow residual solid was dissolved in DCM (15 mL) and washed with sat. aq. $NaSbF_6$ (15 mL) for 5 min. The organic layer was dried over $MgSO_4$ and concentrated *in vacuo*. After column chromatography (DCM:MeOH), product **217** was obtained as an orange solid (602 mg, 979 µmol, 59%).

^{1}H NMR (300 MHz, CD_2Cl_2 ppm) δ = 1.32 (d, *J* = 7.1 Hz, 12H), 2.36 (s, 6H), 2.96 (s, 6H), 5.47 (s, 2H), 6.65 (d, *J* = 8.9 Hz, 2H), 7.34 (d, *J* = 8.9 Hz, 2H). ^{13}C NMR (101 MHz, CD_2Cl_2, ppm) δ = 10.9, 21.5, 40.4, 55.2, 109.4, 114.0, 130.7, 136.0, 152.1. IR (neat, cm^{-1}): 2984.3, 2942.8, 2886.9, 2815.6, 1715.4, 1618.9, 1590.0, 1508.1, 1463.7, 1445.4, 1417.4, 1363.4, 1331.6, 1318.1, 1264.1, 1216.9, 1197.6, 1173.5, 1137.8, 1111.8, 1076.1, 1067.4, 991.2, 952.7, 944.9,

906.4, 814.8, 750.2, 737.6, 710.6, 652.8, 582.4, 570.8, 542.9, 523.6. HRMS: *m*/*z* calcd. for $C_{19}H_{30}N_3Se$ $[M–SbF_6]^+$ = 380.1600, found = 380.1595; calcd. for SbF_6^- $[M]^-$ = 234.8948; found = 234.8957.

5.3.2 Synthesis of unsymmetrical selenides

3-[(4-Methoxyphenyl)selanyl]-1-methyl-1*H*-indole (**218**):

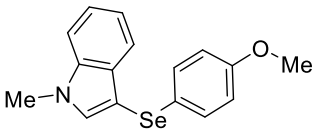

According to GP4, imidazolium salt **215** (225 mg, 360 µmol, 1.00 equiv.) was dissolved in THF (2.0 mL) and cooled to -78 °C. Under stirring, methoxyphenylmagnesium bromide (0.5M in THF, 1.08 mL, 540 µmol, 1.50 equiv.) was added dropwise to the white suspension, and the obtained yellow suspension was allowed to warm up overnight furnishing the orange solution. The reaction was quenched with sat. NH_4Cl (5 mL), stirred for 5 min and extracted with DCM (3 × 20 mL). The combined organic phases were dried over $MgSO_4$, concentrated *in vacuo* and purified by column chromatography (hexane:DCM) to obtain **218** as a white solid (104.6 mg, 331 µmol, 92%).

^{1}H NMR (300 MHz, CD_2Cl_2 ppm) δ = 3.71 (s, 3H), 3.83 (s, 3H), 6.71 (d, *J* = 8.8 Hz, 2H), 7.14 (ddd, *J* = 8.0, 7.0, 1.1 Hz, 1H), 7.23 – 7.29 (m, 3H), 7.35 (s, 1H), 7.36 – 7.41 (m, 1H), 7.59 (d, *J* = 8.0 Hz, 1H). ^{13}C NMR (101 MHz, CD_2Cl_2, ppm) δ = 33.5, 55.8, 97.8, 110.2, 115.2, 120.6, 120.7, 122.8, 124.2, 131.0, 131.9, 135.8, 138.1, 159.1. ^{77}Se NMR (76 MHz, CD_2Cl_2 ppm) δ = 196.9. IR (neat, cm^{-1}): 2939.0, 1597.7, 1577.5, 1496.5, 1280.5, 1157.1, 1117.5, 1016.3, 831.2, 818.6, 810.0, 795.5, 575.6, 518.8. HRMS: *m*/*z* calcd. for $C_{16}H_{16}NOSe^+$ $[M+H]^+$ = 318.0392; found = 318.0388.

2-[(4-Methoxyphenyl)selanyl]-1-phenyl-1*H*-pyrrole (**219**):

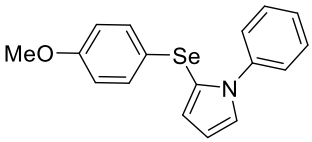

According to GP4, imidazolium salt **216** (127 mg, 199.3 µmol, 1.00 equiv.) was dissolved in THF (2.0 mL) and cooled to -78 °C. Methoxyphenylmagnesium bromide (0.5M in THF, 600 µL, 300 µmol, 1.50 equiv.) was added dropwise to the stirred colorless solution, and the obtained dark brown solution was allowed to warm up overnight furnishing the yellow solution. The reaction was quenched with sat. NH_4Cl (5 mL), stirred for 5 min and extracted with DCM (3 × 20 mL). The combined organic phases were dried over $MgSO_4$, concentrated *in vacuo* and purified by column chromatography (hexane:DCM) to obtain **219** as a colourless oil (41.5 mg, 126 µmol, 63%).

^{1}H NMR (300 MHz, CD_2Cl_2 ppm) δ = 3.74 (s, 3H), 6.33 (dd, *J* = 3.6, 2.9 Hz, 1H), 6.66 (dd, *J* =

3.6, 1.8 Hz, 1H), 6.72 (d, *J* = 8.8 Hz, 2H), 7.02 – 7.09 (m, 3H), 7.18 – 7.23 (m, 2H), 7.31 – 7.39 (m, 3H). ^{13}C NMR (101 MHz, CD_2Cl_2, ppm) δ 55.8, 110.3, 115.3, 116.4, 120.9, 121.9, 124.0, 126.7, 127.3, 128.0, 129.1, 130.2, 132.4, 141.0, 159.4. ^{77}Se NMR (76 MHz, CD_2Cl_2 ppm) δ = 262.4. IR (neat, cm^{-1}): 3049.9, 2978.5, 2943.8, 2914.9, 1577.5, 1470.5, 1444.4, 1396.2, 1305.6, 1207.2, 1094.4, 1079.0, 1010.5, 794.5, 776.2, 745.4, 703.9, 610.4. HRMS: *m*/*z* calcd. for $C_{17}H_{16}NOSe^+$ $[M+H]^+$ = 330.0392; found = 330.0387.

4-[(4-Methoxyphenyl)selanyl]-*N,N*-dimethylaniline (**220**):

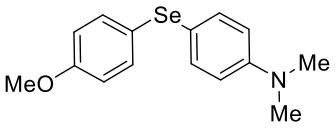

According to GP4, imidazolium salt **217** (215 mg, 349 µmol, 1.00 equiv.) was dissolved in THF (2.0 mL) and cooled to -78 °C. Methoxyphenylmagnesium bromide (0.5M in THF, 2.03 mL, 1.02 mmol, 2.92 equiv.) was added dropwise to the white suspension, and the obtained light yellow suspension was allowed to warm up overnight furnishing the yellow solution. The reaction was quenched with sat. NH_4Cl (5 mL), stirred for 5 min and extracted with DCM (3 × 20 mL). The combined organic phases were dried over $MgSO_4$, concentrated *in vacuo* and purified by column chromatography (hexane:DCM) to obtain **220** as a white solid (87.2 mg, 284.7 µmol, 82%).

^{1}H NMR (300 MHz, $CDCl_3$ ppm) δ = 2.95 (s, 6H), 3.77 (s, 3H), 6.64 (d, *J* = 8.8 Hz, 2H), 6.78 (d, *J* = 8.8 Hz, 2H), 7.33 (d, *J* = 8.8 Hz, 2H), 7.41 (d, *J* = 8.8 Hz, 2H). ^{13}C NMR (75 MHz, $CDCl_3$, ppm) δ = δ 40.5, 55.4, 113.4, 115.0, 116.0, 123.7, 133.3, 135.7, 150.3, 158.9. ^{77}Se NMR (MHz, CD_2Cl_2 ppm) δ = 380.0. IR (neat, cm^{-1}): 2950.6, 2917.8, 2864.7, 1592.9, 1505.2, 1490.7, 1444.4, 1356.7, 1193.7, 1102.1, 1082.8, 1068.4, 1015.3, 807.1, 529.4. HRMS: *m*/*z* calcd. for $C_{15}H_{18}NOSe^+$ $[M+H]^+$ = 308.05488; found = 308.0541.

4-[(3,4-Dihydronaphthalen-1-yl)selanyl]-*N,N*-dimethylaniline (**221**):

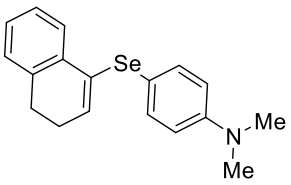

According to GP4, imidazolium salt **217** (33 mg, 53.6 µmol, 1.0 equiv.) was dissolved in THF (1.0 mL) and cooled to -78 °C. (3,4-Dihydronaphthalen-1-yl)magnesium bromide (0.4M in THF, 200 µL, 80 µmol, 1.49 equiv.) was added dropwise to the white suspension, and the obtained light yellow suspension was allowed to warm up overnight furnishing the yellow solution. The reaction was quenched with sat. NH_4Cl (5 mL), stirred for 5 min and extracted with DCM (3 × 20 mL). The combined organic phases were dried over $MgSO_4$, concentrated *in vacuo* and purified by column chromatography (hexane:DCM) to obtain product **221** as a white solid (13.0 mg, 39.6 µmol, 74%).

^{1}H NMR (300 MHz, CD_2Cl_2 ppm) δ = 2.27–2.36 (m, 2H), 2.78 (t, *J*=8.0 Hz, 2H), 2.93 (s, 6H), 6.20 (t, *J*=4.7 Hz, 1H), 6.61–6.68 (m, 2H), 7.09–7.20 (m, 3H), 7.35–7.43 (m, 2H), 7.50–7.59 (m, 1H). ^{13}C NMR (126 MHz, CD_2Cl_2, ppm) δ = 28.5, 40.7, 113.6, 114.3, 126.3, 126.9, 127.8, 127.9, 130.8, 133.0, 134.8, 135.8, 136.9, 150.7. ^{77}Se NMR (MHz, $CDCl_3$ ppm) δ = 345.8. IR (neat, cm^{-1}): 1587.9, 1503.1, 1480.8, 1446.4, 1424.7, 1358.3, 1315.3, 1277.0, 1260.8, 1228.0, 1195.6, 1170.2, 1083.5, 1066.3, 1043.2, 1029.5, 1015.7, 953.6, 935.7, 809.3, 779.0, 758.0, 729.7, 690.9. HRMS: *m/z* calcd. for $C_{18}H_{20}NSe^{+}$ $[M+H]^{+}$ = 330.0756; found: 330.0750.

5.4 Reaction towards the synthesis of imidazole-, benzimidazole-, triazole- and benzoxazole-thioether

5.4.1 Synthesis of imidazole-thioethers

General protocol GP6

A dry *Schlenk* flask was charged with imidazolthione **78** (127 mg, 600 µmol, 1.20 equiv.), *N*-chlorosuccinimide (80.1 mg, 600 µmol, 1.20 equiv.) and 1-methyl-2-phenylindole (104 mg, 500 µmol, 1.00 equiv.). MeCN (6 mL) was added, and the solution was stirred for 10 min at rt. and then at the indicated temperature for the indicated time. The orange brown solution was allowed to cool down to rt and all volatiles were removed under reduced pressure. The obtained orange oil was dissolved in DCM (5 mL) and washed with sat. aq. $NaSbF_6$ solution (5 mL) for 4 min. In case of 1,2-DCE as a solvent, the reaction mixture was directly washed with aq. $NaSbF_6$ solution without evaporation of DCE. The organic layer was dried over $MgSO_4$ and concentrated *in vacuo*. After column chromatography (DCM:MeOH), the arylthioimidazolium salt **100** was obtained as a yellow foam.

***N,N*-Dimethyl-4-[(1-methyl-1H-imidazol-2-yl)thio]aniline** (**237**), **General protocol GP6**:

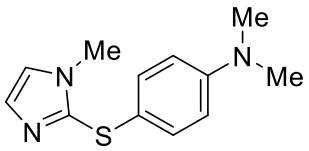

In a dry *Schlenk* flask, carbimazole (186 mg, 1.00 mmol, 1.05 equiv.), *N*-chlorosuccinimide (133.5 mg, 1.00 mmol, 1.05 equiv.) and *N,N*-dimethylaniline (115.4 mg, 121 µL, 952 µmol, 1.00 equiv.) were dissolved in MeCN (10.0 mL) and stirred at 70 °C for 12 h. All volatiles were removed *in vacuo*; the residual violet oil was dissolved in DCM (10 mL) and washed with sat. aq. $NaHCO_3$ (10 mL) for 2 min. The organic layer was dried over $MgSO_4$ and concentrated *in vacuo*. After column chromatography (DCM:MeOH) and purification by HPLC (CH_3CN:H_2O; 40:60, 10 min → 100:0 over 15 min), sulfide **237** was obtained as an orange solid (126 mg, 540 µmol, 57%).

^{1}H NMR (300 MHz, CD_3CN) δ = 2.90 (s, 6H)), 3.63 (s, 3H), 6.64 – 6.72 (m, 2H), 6.95 (d, *J* = 1.3 Hz, 1H), 7.09 (d, *J* = 1.2 Hz, 1H), 7.17 – 7.24 (m, 2H)ppm. ^{13}C NMR (126 MHz, CD_3CN) δ = 34.3, 40.5, 111.1, 113.9, 119.1, 124.7, 129.8, 133.3, 151.4 ppm. IR (neat, cm^{-1}): 3111.5, 3091.6, 2947.0, 2888.7, 2819.2, 1874.7, 1772.3, 1762.0, 1709.8, 1604.6, 1545.0, 1511.1, 1479.0, 1444.7, 1406.3, 1365.2, 1339.8, 1315.1, 1281.0, 1228.7, 1191.5, 1154.9, 1120.5, 1096.7, 1080.8, 1059.3, 1041.1, 998.6, 947.7, 931.9, 915.5, 865.3, 804.4, 784.8, 716.6, 683.3, 643.5, 632.7, 611.7, 520.7. ESI-MS: *m/z* calcd. for $C_{12}H_{16}N_3S^+$ $[M+H]^+$ = 234.1059; found = 234.1064.

1-Methyl-2-[(1-phenyl-1*H*-pyrrol-2-yl)thio]-1*H*-imidazole (**231**):

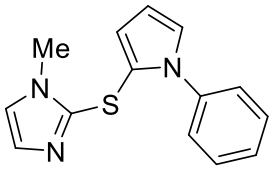

According to GP6, carbimazole (186 mg, 1.00 mmol, 1.05 equiv.), *N*-chlorosuccinimide (133.5 mg, 1.00 mmol, 1.05 equiv.) and *N*-phenylpyrrole (136 mg, 950 µmol, 1.00 equiv.) were dissolved in MeCN (10.0 mL) and stirred at 70 °C for 12 h. All volatiles were removed *in vacuo*; the residue yellow oil was dissolved in DCM (10 mL) and washed with sat. aq. $NaHCO_3$ (10 mL) for 2 min. The organic layer was dried over $MgSO_4$ and concentrated *in vacuo*. After column chromatography (DCM:MeOH), sulfide **231** was obtained as an orange solid (199 mg, 779 µmol, 82%).

^{1}H NMR (300 MHz, CD_3Cl) δ = 3.27 ppm (s, 3H), 6.29 (dd, *J* = 3.7, 2.9 Hz, 1H), 6.72 (dd, *J* = 3.7, 1.8 Hz, 1H), 6.77 (d, *J* = 1.2 Hz, 1H), 6.95 (dd, *J* = 3.0, 1.8 Hz, 1H), 6.97 (d, *J* = 1.2 Hz, 1H), 7.23 – 7.33 (m, 2H), 7.33 – 7.47 (m, 3H). ^{13}C NMR (75 MHz, CD_3Cl) δ = 33.3, 109.7, 118.0, 119.9, 122.4, 127.0, 127.8, 128.8, 129.7, 139.6, 140.5 ppm. IR (neat, cm^{-1}): 3103.3, 3065.1, 2982.0, 2942.5, 2258.8, 1771.3, 1740.7, 1708.7, 1597.1, 1579.0, 1498.2, 1455.2, 1435.9, 1410.6, 1390.7, 1366.5, 1340.1, 1318.0, 1277.8, 1241.9, 1206.1, 1184.5, 1145.6, 1121.6, 1076.5, 1036.3, 1012.7, 1003.9, 985.9, 958.5, 913.5, 878.1, 838.2, 763.1, 724.0, 694.0, 629.9, 618.5, 606.7, 583.9, 558.6, 530.0, 504.5. ESI-MS: *m*/*z* calcd. for $C_{14}H_{14}N_3S^+$ $[M+H]^+$ = 256.0903; found = 256.0908.

1-**Methyl-3-[(1-methyl-1*H*-imidazol-2-yl)thio]-1*H*-indole** (**233**):

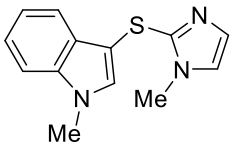

According to GP6, carbimazole (186 mg, 1.00 mmol, 1.05 equiv.), *N*-chlorosuccinimide (133.5 mg, 1.00 mmol, 1.05 equiv.) and *N*-methylindole (125 mg, 119 µL, 952 µmol, 1.00 equiv.) were dissolved in MeCN (10.0 mL) and stirred for 12 h at 70 °C. All volatiles were removed *in vacuo*; the residual yellow oil was dissolved in DCM (10 mL) and washed with sat. aq. $NaHCO_3$ (10 mL) for 2 min. The organic layer was dried over $MgSO_4$ and concentrated *in vacuo*. After column chromatography (DCM:MeOH) and purification by HPLC (CH_3CN:H_2O; 60:40 → 100:0 over 20 min), sulfide **233** was obtained as a yellow oil (190 mg, 781 µmol, 82%).

^{1}H NMR (300 MHz, CD_3CN) δ = 3.70 (s, 3H), 3.76 (s, 3H), 6.86 (d, *J* = 1.3 Hz, 1H), 6.97 (d, *J* = 1.3 Hz, 1H), 7.14 (ddd, *J* = 8.0, 7.0, 1.1 Hz, 1H), 7.23 (ddd, *J* = 8.2, 7.0, 1.3 Hz, 1H), 7.34 – 7.42 (m, 1H), 7.45 (s, 1H), 7.67 – 7.74 (m, 1H). ^{13}C NMR (101 MHz, CD_3CN) δ = 33.5, 34.4, 100.8, 111.1, 120.0, 121.1, 124.1, 129.4, 130.2, 135.2, 138.1, 141.3 ppm. IR (neat, cm^{-1}): 3110.1, 3091.3, 1710.9, 1648.5, 1610.5, 1575.6, 1556.4, 1508.0, 1481.8, 1454.0, 1412.1, 1369.6, 1354.8, 1335.7, 1320.8, 1283.3, 1241.5, 1177.4, 1152.6, 1126.1, 1110.8, 1088.6,

1046.7, 1009.6, 970.1, 919.3, 853.0, 825.0, 773.4, 767.3, 751.1, 732.3, 696.8, 689.6, 633.1, 605.0, 583.6, 574.0, 543.4, 533.8, 502.1. ESI-MS: *m*/*z* calcd. for $C_{13}H_{14}N_3S^+$ $[M+H]^+$ = 244.0903; found = 244.0911.

1-Methyl-3-[(1-methyl-1*H*-imidazol-2-yl)thio)-2-phenyl-1*H*-indole (**234**):

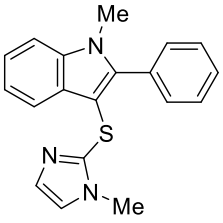

According to GP6, carbimazole (186 mg, 1.00 mmol, 1.05 equiv.), *N*-chlorosuccinimide (133.5 mg, 1.00 mmol, 1.05 equiv.) and *N*-methyl-2-phenylindole (197 mg, 950 µmol, 1.00 equiv.) were dissolved in MeCN (10.0 mL) and stirred at 70 °C for 12 h. All volatiles were removed *in vacuo*; the residual yellow oil was dissolved in DCM (10 mL) and washed with sat. aq. $NaHCO_3$ (10 mL) for 2 min. The organic layer was dried over $MgSO_4$ and concentrated *in vacuo*. After column chromatography (DCM:MeOH) and purification by HPLC (CH_3CN:H_2O; 50:50 → 100:0 over 25 min), sulfide **234** was obtained as a yellow oil (271 mg, 848 µmol, 89%).

^{1}H NMR (400 MHz, CD_3CN) δ = 3.34 (s, 3H)), 3.63 (s, 3H), 6.82 (d, *J* = 1.3 Hz, 1H), 6.90 (d, *J* = 1.3 Hz, 1H), 7.16 (ddd, *J* = 7.9, 7.0, 1.0 Hz, 1H), 7.27 (ddd, *J* = 8.3, 7.1, 1.2 Hz, 1H), 7.41 – 7.44 (m, 1H), 7.50 – 7.60 (m, 5H), 7.72 (dt, *J* = 7.9, 1.0 Hz, 1H) ppm. ^{13}C NMR (101 MHz, CD_3CN) δ = 32.2, 33.9, 100.2, 111.2, 120.2, 121.5, 123.7, 129.4, 130.3, 131.5, 132.0, 138.2, 141.9, 145.6 ppm. IR (neat, cm^{-1}): 3044.5, 2932.3, 2912.1, 1766.5, 1697.5, 1603.9, 1589.1, 1571.0, 1507.0, 1470.8, 1463.4, 1455.6, 1442.7, 1428.0, 1409.0, 1383.1, 1365.3, 1337.7, 1314.7, 1275.6, 1239.9, 1220.0, 1157.5, 1132.5, 1122.0, 1108.4, 1075.7, 1055.7, 1039.6, 1020.6, 1012.0, 981.1, 969.3, 925.1, 913.0, 850.4, 842.1, 832.8, 802.1, 765.9, 745.7, 707.6, 694.1, 681.7, 632.3, 621.1, 591.8, 577.6, 510.3. ESI-MS: *m*/*z* calcd. for $C_{19}H_{18}N_3S^+$ $[M+H]^+$ = 320.1216; found = 320.1211.

Ethyl 5,6-Dimethoxy-3-[(1-methyl-1*H*-imidazol-2-yl)thio]-1*H*-indole-2-carboxylate (**236**):

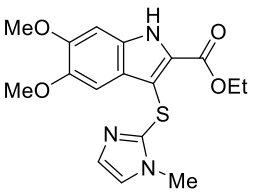

According to GP6, carbimazole (186 mg, 1.00 mmol, 1.052 equiv.), *N*-chlorosuccinimide (133.5 mg, 1.00 mmol, 1.052 equiv.) and ethyl-5,6-dimethoxy-1*H*-indole-2-carboxylate (237 mg, 950.8 µmol, 1.00 equiv.) were dissolved in MeCN (10.0 mL) and stirred at 70 °C for 12 h. All volatiles were removed *in vacuo*; the residual yellow oil was dissolved in DCM (10 mL) and washed with sat. aq. $NaHCO_3$ (10 mL) for 3 min. The organic layer was dried over $MgSO_4$ and concentrated *in vacuo*. After column chromatography (DCM:MeOH) and purification by HPLC (CH_3CN:H_2O; 40:60, 10 min → 100:0 over 15 min), sulfide **236** was obtained yellow solid (207 mg, 572.7 µmol, 60%).

^{1}H NMR (400 MHz, CD_2Cl_2) δ = 1.11 – 1.66 (m, 3H), 3.59 (t, J = 5.2 Hz, 3H), 3.67 (t, J = 5.1 Hz, 3H), 3.76 (t, J = 5.2 Hz, 3H), 4.14 – 4.52 (m, 2H), 6.41 (t, J = 5.1 Hz, 1H), 6.67 (t, J = 5.1 Hz, 1H), 6.96 – 7.23 (m, 2H), 9.85 (s, 1H) ppm. ^{13}C NMR (101 MHz, CD_2Cl_2) δ = 14.7, 34.3, 56.3, 61.3, 94.6, 100.9, 110.3, 121.8, 123.6, 124.7, 129.7, 131.9, 140.2, 146.8, 150.8, 161.1 ppm. IR (neat, cm^{-1}): 3311.4, 3104.6, 2960.1, 2931.4, 2904.3, 2833.0, 1692.7, 1631.5, 1576.6, 1507.2, 1455.9, 1440.7, 1409.4, 1377.5, 1338.3, 1272.8, 1247.7 1203.6, 1175.0, 1151.1, 1124.3, 1093.9, 1034.0, 1018.7, 1004.6, 923.0, 863.7, 821.5, 770.6, 734.4, 694.5, 686.0, 655.3, 625.2, 614.2, 592.6, 564.7, 528.8, 508.1. ESI-MS: *m*/*z* calcd. for $C_{17}H_{20}N_3O_4S^+$ $[M+H]^+$ = 362.1169; found = 362.1175.

1-Methyl-2-[(2,4,6-trimethoxyphenyl)thio]-1*H*-imidazole (**239**):

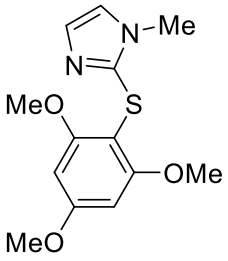

According to GP6, carbimazole (186 mg, 1.00 mmol, 1.05 equiv.), *N*-chlorosuccinimide (133.5 mg, 1.00 mmol, 1.05 equiv.) and 1,3,5-trimethoxybenzene (160 mg, 951.3 µmol, 1.00 equiv.) were dissolved in MeCN (10.0 mL) and stirred at 70 °C for 24 h. All volatiles were removed *in vacuo*; the residual brown oil was dissolved in DCM (10 mL) and washed with sat. aq. $NaHCO_3$ (10 mL) for 3 min. The organic layer was dried over $MgSO_4$ and concentrated *in vacuo*. After column chromatography (DCM:MeOH), sulfide **239** was obtained as a colorless solid (160 mg, 570.7 µmol, 60%).

^{1}H NMR (400 MHz, CD_3CN) δ = 3.68 (s, 3H), 3.75 (s, 6H), 3.80 (s, 3H), 6.22 (s, 2H), 6.81 (s, 1H), 6.97 (s, 1H) ppm. ^{13}C NMR (101 MHz, CD_3CN) δ = 30.4, 34.1, 56.2, 56.9, 92.4, 123.4, 129.4, 162.3, 163.5 ppm. IR (neat, cm^{-1}): 3121.7, 3101.3, 2975.4, 2944.0, 2839.5, 1772.5, 1708.3 1581.7, 1505.0, 1452.1, 1434.9, 1411.6, 1369.6, 1334.4, 1278.7, 1230.8, 1207.3, 1186.6, 1162.1, 1118.3, 1087.7, 1035.1, 951.0, 915.3, 849.9, 809.7, 759.5, 729.8, 718.6, 681.1, 662.0, 635.3, 584.3, 516.0. ESI-MS: *m*/*z* calcd. for $C_{13}H_{17}N_2O_3S^+$ $[M+H]^+$ = 281.0954; found = 281.0962.

4-[(1-Methyl-1*H*-imidazol-2-yl)thio]aniline (**238**):

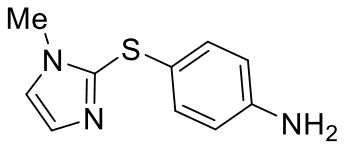

According to GP6, carbimazole (186 mg, 1.00 mmol, 1.05 equiv.), *N*-chlorosuccinimide (133.5 mg, 1.00 mmol, 1.05 equiv.) and aniline (86 µL, 88.7 mg, 952 µmol, 1.00 equiv.) were dissolved in MeCN (10.0 mL) and stirred at 70 °C for 24 h. All volatiles were removed *in vacuo*; the residual red oil was dissolved in DCM (10 mL) and washed with sat. aq. $NaHCO_3$ (10 mL) for 3 min. The organic layer was dried over $MgSO_4$ and concentrated *in vacuo*. After column chromatography (DCM:MeOH) and purification by HPLC (CH_3CN:H_2O; 40:60, 10 min → 80:20 over 20 min), aniline **238** was obtained as a yellow oil (78.2 mg, 381 µmol, 40%).

^{1}H NMR (300 MHz, CD_3CN) δ = 3.62 (d, J = 0.7 Hz, 3H)), 4.28 (s, 2H), 6.54 – 6.62 (m, 2H), 6.96 (d, J = 1.2 Hz, 1H), 7.05 – 7.14 (m, 3H) ppm. ^{13}C NMR (101 MHz, CD_3CN) δ = 34.3, 49.9, 116.0, 124.7, 129.9, 133.4, 141.0, 149.1 ppm. IR (neat, cm^{-1}): 3228.1, 3169.2, 3088.6, 3026.1, 2978.7, 2964.2, 2927.0, 1771.1, 1704.6, 1596.5, 1579.1, 1537.7, 1496.9, 1475.1, 1455.0, 1402.1, 1365.0, 1350.7, 1342.8, 1315.4, 1294.3, 1279.7, 1225.8, 1182.1, 1158.0, 1124.3, 1095.2, 1057.8, 1011.6, 934.1, 921.0, 841.4, 823.7, 764.0, 734.7, 712.0, 690.9, 685.7, 674.6, 638.1, 556.0, 527.9. ESI-MS: *m*/*z* calcd. For $C_{10}H_{12}N_3S^+$ $[M+H]^+$ = 206.0746; found = 206.0749.

1-[(1-Methyl-1*H*-imidazol-2-yl)thio]-5,6-dihydro-4*H*-pyrrolo[3,2,1-*ij*]quinoline (**235**):

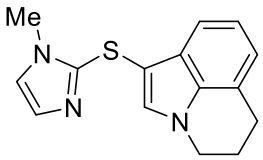

According to GP6, carbimazole (186 mg, 1.00 mmol, 1.05 equiv.), *N*-chlorosuccinimide (133.5 mg, 1.00 mmol, 1.05 equiv.) and Lilolidine (148 mg, 952 µmol, 1.00 equiv.) were dissolved in MeCN (10.0 mL) and stirred at 70 °C for 24 h. All volatiles were removed *in vacuo*; the residual yellow oil was dissolved in DCM (10 mL) and washed with sat. aq. $NaHCO_3$ (10 mL) for 3 min. The organic layer was dried over $MgSO_4$ and concentrated *in vacuo*. After column chromatography (DCM:MeOH) and purification by HPLC (CH_3CN:H_2O; 60:40 → 100:0 over 20 min), sulfide **235** was obtained as a yellow oil (157 mg, 583 µmol, 61%).

^{1}H NMR (400 MHz, CD_3CN) δ = 2. 10 – 2.20 (m, 2H)), 2.82 – 2.95 (m, 2H), 3.70 (s, 3H), 4.06 – 4.15 (m, 2H), 6.85 (d, J = 1.2 Hz, 1H), 6.91 (dd, J = 7.1, 1.0 Hz, 1H), 6.97 (d, J = 1.3 Hz, 1H), 7.01 (dd, J = 8.0, 7.1 Hz, 1H), 7.43 (dd, J = 8.0, 0.9 Hz, 1H), 7.43 (s, 1H) ppm. ^{13}C NMR (75 MHz, CD_3CN) δ = 23.5, 25.0, 34.4, 45.0, 100.7, 117.3, 120.2, 121.6, 123.8, 124.1, 127.9, 129.4, 132.4, 135.4, 141.6 ppm. IR (neat, cm^{-1}): 3103.3, 3091.6, 2955.0, 2929.7, 1650.7, 1500.1, 1471.9, 1447.6, 1438.3 1427.5, 1411.8, 1383.3, 1365.2, 1336.2, 1322.1,

1309.8, 1281.2, 1248.0, 1180.1, 1165.7, 1121.7, 1083.0, 1067.6, 1033.3, 955.1, 914.0, 831.7, 777.1, 750.9, 699.9, 685.6, 673.1, 636.3, 601.0, 526.6, 504.1. ESI-MS: *m*/*z* calcd. *for* $C_{15}H_{16}N_3S^+$ $[M+H]^+$ = 270.1059; found = 270.1061.

2-[(1*H*-Pyrrol-2-yl)thio]-3-(ethoxycarbonyl)-1-methyl-1*H*-imidazol-3-ium Chloride (**241**):

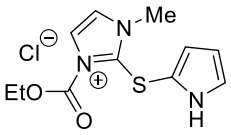

According to GP6, carbimazole (186 mg, 1.00 mmol, 1.05 equiv.), *N*-chlorosuccinimide (133.5 mg, 1.00 mmol, 1.05 equiv.) and pyrrole (63.9 mg, 66.1 µL, 952 µmol, 1.00 equiv.) were dissolved in MeCN (10.0 mL) and stirred at 70 °C for 24 h. All volatiles were removed *in vacuo*; the residual black oil was dissolved in DCM (10 mL) and washed with sat. aq. $NaHCO_3$ (10 mL) for 3 min. The organic layer was dried over $MgSO_4$ and concentrated *in vacuo*. After column chromatography (DCM:MeOH) and purification by HPLC (CH_3CN:H_2O; 40:60, 10 min → 80:20 over 20 min), sulfide **241** was obtained as a yellow solid (98.8 mg, 343 µmol, 36%).

^{1}H NMR (300 MHz, CD_3CN) δ = 1.37 (td, *J* = 7.1, 0.8 Hz, 3H)), 3.64 (d, *J* = 0.7 Hz, 3H), 4.33 – 4.47 (m, 2H), 5.36 – 5.46 (m, 1H), 6.15 (td, *J* = 3.4, 0.8 Hz, 1H), 7.05 (d, *J* = 1.2 Hz, 1H), 7.21 (d, *J* = 1.2 Hz, 1H), 7.26 – 7.36 (m, 1H) ppm. ^{13}C NMR (75 MHz, CD_3CN) δ = 14.4, 34.2, 65.0, 112.9, 114.3, 123.0, 125.6, 130.5, 138.1, 151.2 ppm. IR (neat, cm^{-1}): 3107.1, 2980.3, 2940.2, 1737.7, 1538.4, 1507.9, 1453.0, 1399.9, 1369.2, 1319.6, 1297.4, 1279.4, 1243.9, 1208.0, 1192.8, 1161.1, 1147.5, 1121.7, 1093.3, 1054.1, 1014.0, 989.9, 926.5, 914.2, 878.2, 864.3, 832.0, 792.7, 764.1, 712.2, 696.2, 686.7, 612.9, 592.0, 573.4, 528.3, 504.0. ESI-MS: *m*/*z* calcd. for $C_{11}H_{14}N_3O_2S^+$ $[M–Cl]^+$ = 252.0801; found = 252.0804.

***N*^{1}-Benzyl-*N*^{2},*N*^{2}-dimethyl-*N*^{1}-{4-[(1-methyl-1*H*-imidazol-2-yl)thio]phenyl}ethane-1,2-diamine** (**86**):

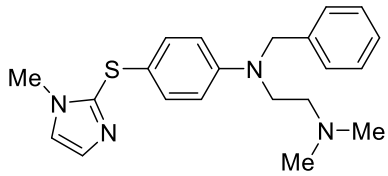

According to GP6, phenbenzamine hydrochloride (145 mg, 500 µmmol, 1.00 equiv.), *N*-chlorosuccinimide (70 mg, 524 µmol, 1.05 equiv.) and carbimazole (98 mg, 526 µmol, 1.05 equiv.) were dissolved in MeCN (5 mL). The yellow solution was stirred at 70 °C for 24 h All volatiles were removed under reduced pressure, the residual yellow oil was dissolved in DCM (3 mL) and washed with a sat. $NaHCO_3$ solution (5 mL). The precipitate was purified by column chromatography (DCM:MeOH). Sulfide **86** was obtained as a white solid (57 mg, 155.5 µmol, 31%).

^{1}H NMR (300 MHz, CD_3CN) δ = 2.26 (s, 6H)), 2.51 (t, *J* = 7.1 Hz, 2H), 3.51 (t, *J* = 7.1 Hz, 2H), 3.62 (s, 3H), 4.52 (s, 2H), 6.59 (d, *J* = 8.9 Hz, 2H), 6.92 (s, 1H), 7.05 (s, 1H), 7.12 – 7.32 (m, 7H) ppm. ^{13}C NMR (101 MHz, $CDCl_3$) δ = 33.9, 45.9, 49.5, 54.7, 56.3, 112.8, 118.1, 123.0, 126.5, 127.0, 128.7, 129.6, 133.0, 138.3, 141.0, 148.2 ppm. IR (neat, cm^{-1}): 2940.9, 2767.4, 1592.9, 1500.3, 1451.2, 1393.3, 1353.8, 1278.6, 1237.1, 1196.6, 1148.4, 1119.5, 1097.3, 1077.0, 1040.4, 1027.9, 952.7, 912.2, 808.0, 728.0, 694.2, 524.5. ESI-MS: *m*/*z* calcd. for $C_{21}H_{27}N_4S^+$ $[M+H]^+$ = 367.1951, found = 367.1953.

5.4.2 Synthesis of sulfur-containing precursors

4-Phenyl-2,4-dihydro-3*H*-1,2,4-triazole-3-thione (**258**):

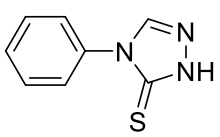

Compound **258** was synthesized according to the modified protocol of M. K. Bharty, N. K. Singh *et al.*[299] Formyl hydrazine (900.8 mg, 15.0 mmol, 1.00 equiv.) was dissolved in EtOH (30 mL). Phenyl isocyanate (1.86 mL, 2.03 g, 17.0 mmol, 1.13 equiv.) was added, and the solution was stirred at 65 °C for 4 h. The solid precipitate was washed with H_2O (10 mL) and Et_2O (10 mL) and dried *in vacuo*. The obtained solid was dissolved in EtOH (30 mL) and NaOH (0.75 g, 18.75 mmol, 1.25 equiv.) was added. The resulting solution was stirred at 78 °C for 12 h. After cooling, aq. HCl (1M, 30 mL, 30 mmol, 2.0 equiv.) was added; the obtained white precipitate was filtered off, washed with water, dried *in vacuo* and finally recrystallized from a mixture of MeOH:$CHCl_3$ (50:50). Sulfide **258** was obtained as a white solid (1.263 g, 7.11 mmol, 47%).

^{1}H NMR (300 MHz, $CDCl_3$) δ = 7.42 – 7.69 (m, 5H), 7.93 (s, 1H), 11.22 (s, 1H) ppm. ^{13}C NMR (101 MHz, $CDCl_3$) δ = 125.7, 129.8, 133.8, 141.0, 167.6 ppm. IR (neat, cm^{-1}): 1556.3, 1498.4, 1484.9, 1456.0, 1373.1, 1327.7, 1298.8, 1280.5, 1242.9, 1154.2, 1076.1, 940.1, 840.8, 767.5, 689.4, 675.9, 570.8. ESI-MS: *m*/*z* calcd. for $C_8H_8N_3S^+$ $[M+H]^+$ = 178.0433; found = 178.0436. Remark: Two signals in the ^{13}C NMR-spectrum overlapped each other.

Ethyl 2-Thioxobenzo[*d*]oxazole-3(2*H*)-carboxylate (**250**):

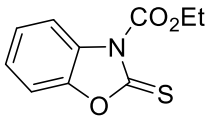

Compound **250** was synthesized using the modified protocol of S. Dove *et al.*[298] 2-Mercaptobenzoxazole (1.50 g, 9.92 mmol, 1.00 equiv.) was dissolved in dry THF (15 mL); Et_3N (1.51 mL, 1.095 g, 10.82 mmol, 1.09 equiv.) was added and the solution was cooled to 0 °C. A solution of ethyl chloroformate (945 µL, 1.08 g, 9.93 mmol, 1.00 equiv.) in THF (15 mL) was added dropwise, the reaction mixture was stirred for an additional 2 h, then allowed to warm up to rt. All volatile were removed *in vacuo*. The residual white precipitate was dissolved and extracted ~~two times~~ with EtOAc (2 × 25 mL). The combined organic phases were washed with H_2O (2 × 15 mL) and dried over $MgSO_4$; the solvent was removed under reduced pressure. The obtained crude product was purified by column chromatography (DCM:MeOH) affording compound **250** as a white solid (1.00 g, 4.48 mmol, 45%).

^{1}H NMR (400 MHz, $CDCl_3$) δ = 1.53 (t, *J* = 7.1 Hz, 3H), 4.61 (q, *J* = 7.2 Hz, 2H), 7.28 – 7.36 (m, 3H), 7.73 – 7.78 (m, 1H) ppm. ^{13}C NMR (101 MHz, $CDCl_3$) δ = 14.3, 65.3, 110.2, 115.2, 125.4, 126.0, 129.3, 146.4, 149.9, 177.0 ppm. IR (neat, cm^{-1}): 1775.2, 1306.5, 1271.8, 1238.1, 1210.1, 1158.0, 1140.7, 1090.5, 1055.8, 1011.5, 934.3, 828.3, 762.7, 749.2, 652.8, 628.7. ESI-MS: *m*/*z* calcd. for $C_{10}H_{10}NO_3S^+$ $[M+H]^+$ = 224.0376; found = 224.0380.

Ethyl 3-Methyl-2-thioxo-2,3-dihydro-1*H*-benzo[*d*]imidazole-1-carboxylate (**251**):

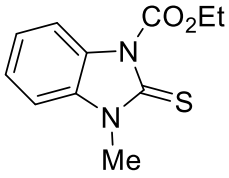

Compound **251** was synthesized employing the modified protocol of S. Dove *et al.*[295] The solution of 1-methyl-1*H*-benzimidazole-2-thiol (492 mg, 3.00 mmol, 1.00 equiv.) in dry THF (5 mL) was cooled to 0 °C. Under stirring, NEt_3 (806 µl, 585 mg, 5.78 mmol, 1.93 equiv.) was added dropwise followed by a solution of ethyl chloroformate (286 µL, 325.6 mg, 3.00 mmol, 1.00 equiv.) in THF (5 mL). The suspension was allowed to warm up to rt within 1 h and stirred for an additional 12 h. The reaction was quenched with EtOH (1 mL). After removing all volatile compounds *in vacuo,* the obtained white precipitate was dissolved in EtOAc (50 mL); the extract was washed with H_2O (15 mL). After drying and concentrating the organic phase, the obtained white solid was purified by column chromatography (DCM:MeOH). Product **251** was obtained as a white solid (344 mg, 1.46 mmol, 49%, literature: 32%).

^{1}H NMR (300 MHz, $CDCl_3$) δ = 1.53 (t, *J* = 7.1 Hz, 3H)), 3.76 (s, 3H), 4.60 (q, *J* = 7.1 Hz, 2H), 7.10 – 7.18 (m, 1H), 7.27 – 7.37 (m, 2H), 7.83 – 7.90, (m, 1H) ppm. ^{13}C NMR (101 MHz, $CDCl_3$) δ = 14.4, 31.3, 64.6, 108.9, 114.8, 124.1, 125.2, 129.7, 132.8, 150.7, 170.0 ppm. IR

(neat, cm^{-1}): 1715.4, 1440.6, 1384.6, 1360.5, 1335.5, 1311.4, 1285.3, 1250.6, 1177.3, 1150.3, 1091.5, 1019.2, 759.8, 739.6, 557.3. ESI-MS: *m/z* calcd. for $C_{11}H_{13}N_2O_2S^+$ $[M+H]^+$ = 237.0692; found = 237.0696.

Ethyl 4-Phenyl-5-thioxo-4,5-dihydro-1*H*-1,2,4-triazole-1-carboxylate (**252**):

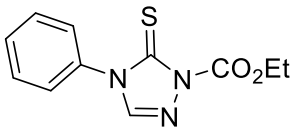

Compound **252** was synthesized in modified protocol of S. Dove *et al.*[295] The solution of compound **258** (531.7 mg, 3.00 mmol, 1.00 equiv.) in dry THF (5 mL) was cooled to 0 °C. Under stirring, NEt_3 (808 µL, 587 mg, 5.8 mmol, 1.93 equiv.) was added dropwise followed by a solution of ethyl chloroformate (286 µL, 326 mg, 3.00 mmol, 1.00 equiv.) in THF (5 mL). The suspension was allowed to warm up to rt within 1 h and stirred for an additional 2 h. The reaction was quenched with EtOH (1 mL). After removing the volatiles *in vacuo,* the residual white precipitate was dissolved in EtOAc (50 mL) and washed with H_2O (15 mL). The organic phase was dried and concentrated under reduced pressure; the obtained white crude product was purified by column chromatography (DCM:MeOH) affording **252** as a white solid (425 mg, 1.70 mmol, 57%).

^1H NMR (300 MHz, $CDCl_3$) δ = 1.50 (t, *J* = 7.1 Hz, 3H), 4.58 (q, *J* = 7.2 Hz, 2H), 7.46 – 7.62 (m, 5H), 7.90 (s, 1H) ppm. ^{13}C NMR (101 MHz, $CDCl_3$) δ =14.3, 65.3, 126.4, 129.9, 130.1, 133.7, 140.6, 148.6, 169.2 ppm. IR (neat, cm^{-1}): 1772.3, 1553.4, 1366.3, 1336.4, 1316.2, 1242.9, 1216.9, 1171.5, 1044.3, 1014.4, 953.6, 892.9, 841.8, 757.9, 741.5, 690.4, 594.9, 585.3. ESI-MS: *m/z* calcd. for $C_{11}H_{12}N_3O_2S^+$ $[M+H]^+$ = 250.0645; found = 250.0651. The analytical data were identical to the previously published ones.[29]

[29] M. Wujec, M. Pitucha, M. Dobosz, U. Kosikowska, A. Malm*, Acta Polon. Pharm*. **2003**, *60*, 451 – 456.

5.4.3 Synthesis of benzimidazole-, triazole- and benzoxazole-thioethers

4-(Benzo[*d*]oxazol-2-ylthio)-*N,N*-dimethylaniline (**259**):

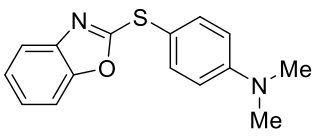

According to GP6, compound **250** (223 mg, 1.00 mmol, 1.05 equiv.) and *N*-chlorosuccinimide (134 mg, 1.00 mmol, 1.00 equiv.) were dissolved in MeCN (10 mL). *N,N*-dimethylaniline (117 µL, 122 mg, 1.00 mmol, 1.00 equiv.) was added dropwise to the yellow solution. The reaction mixture was stirred for 12 h at 70 °C. After cooling, all volatiles were removed under reduced pressure; the green oil was dissolved in DCM (3 mL) and washed with a sat. $NaHCO_3$ solution (10 mL), dried and evaporated. The residual precipitate was purified by column chromatography (DCM:MeOH) and subsequent preparative HPLC (MeCN:H_2O; 20:80, 20 min). Sulfide **259** was obtained as a white solid (24 mg, 89 µmol, 9%).

^{1}H NMR (400 MHz, CD_3CN) δ = 2.96 (s, 6H)), 6.71 – 6.80 (m, 2H), 7.19 – 7.28 (m, 2H), 7.39 – 7.44 (m, 1H), 7.44 – 7.50 (m, 3H) ppm. ^{13}C NMR (126 MHz, CD_3CN) δ = 40.4, 110.9, 113.7, 119.3, 125.1, 125.4, 137.6, 143.0, 152.8, 152.9, 166.4 ppm. IR (neat, cm^{-1}): 1589.1, 1504.2, 1486.8, 1446.4, 1368.2, 1235.2, 1193.7, 1133.0, 1118.5, 1087.7, 995.1, 948.8, 918.9, 803.2, 754.0, 738.6, 710.6, 621.0, 529.4. ESI-MS: *m/z* calcd. for $C_{15}H_{15}N_2OS^+$ $[M+H]^+$ = 271.0900, found = 271.0892.
Two signals in the ^{13}C NMR spectrum overlapped each other.

***N,N*-Dimethyl-4-[(4-phenyl-4*H*-1,2,4-triazol-3-yl)thio]aniline** (**261**):

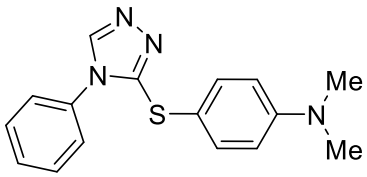

According to GP6, compound **252** (125 mg, 500 µmol, 1.00 equiv.) and *N*-chlorosuccinimide (67 mg, 500 µmol, 1.00 equiv.) were dissolved in MeCN (5 mL). *N,N*-Dimethylaniline (63 µL, 60.6 mg, 500 µmol, 1.00 equiv.) was added dropwise to the green solution; the reaction mixture was stirred for 24 h at ambient temperature, than at 70 °C for another 24 h. After cooling, all volatiles were removed under reduced pressure, the obtained blue oil was dissolved in DCM (3 mL) and washed with a sat. $NaHCO_3$ solution (5 mL). After drying and evaporation of the solvent, the attempted purification of the residual solid by column chromatography (DCM:MeOH) was performed. NMR analysis of the crude product indicated the formation of traces of **261**.

ESI-MS: *m/z* calcd. for $C_{16}H_{17}N_4S^+$ $[M+H]^+$ = 297.1168; found = 297.1168.

***N*,*N*-Dimethyl-4-[(1-methyl-1*H*-benzo[*d*]imidazol-2-yl)thio]aniline** (**260**):

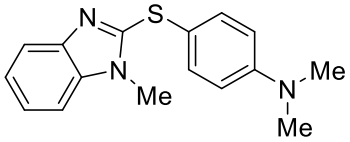

According to GP6, compound **251** (118 mg, 500 µmol, 1equiv.) and *N*-chlorosuccinimide (67 mg, 500 µmol, 1.00 equiv.) were dissolved in MeCN (5 mL). *N*,*N*-dimethylaniline (63 µL, 60.6 mg, 500 µmol, 1.00 equiv.) was added dropwise to the yellow solution. The reaction mixture was stirred at 70 °C for 12 h. After cooling, all volatiles were removed under reduced pressure; the obtained green oil was dissolved in DCM (3 mL) and washed with a sat. $NaHCO_3$ solution (5 mL). After drying and evaporation of the solvent, the residual solid was purified by column chromatography (DCM:MeOH) and subsequent preparative HPLC (MeCN:H_2O; 60:40 → 100:0 over 10 min). Sulfide **260** was obtained as white solid (11 mg, 39 µmol, 8%).

^{1}H NMR (400 MHz, $CDCl_3$) δ = 2.96 (s, 6H)), 3.74 (s, 3H), 6.64 – 6.69 (m, 2H), 7.18 – 7.25 (m, 3H), 7.40 – 7.45 (m, 2H), 7.69 – 7.72 (m, 1H) ppm. ^{13}C NMR (101 MHz, $CDCl_3$) δ = 30.8, 40.4, 109.0, 113.2, 114.8, 119.6, 122.1, 122.6, 134.7, 136.8, 143.3, 150.8, 151.1 ppm. IR (neat, cm^{-1}): 1594.8, 1507.1, 1467.6, 1439.6, 1409.7, 1361.5, 1323.9, 1276.6, 1225.5, 1189.9, 1093.4, 1063.6, 807.1, 765.6, 756.0, 742.5, 729.9, 680.7, 516.8. ESI-MS: *m*/*z* calcd. for $C_{16}H_{17}N_3S^+$ $[M+H]^+$ = 284.1216; found = 284.1220.

2-[(1-Phenyl-1*H*-pyrrol-2-yl)thio]benzo[*d*]oxazole (**262**):

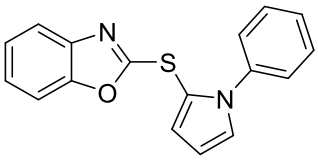

According to GP6, compound **251** (112 mg, 500 µmol, 1.00 equiv.), *N*-chlorosuccinimide (67 mg, 500 µmol, 1.00 equiv.) and 1-phenylpyrrole (72 mg, 500 µmol, 1.00 equiv.) were dissolved in MeCN (5 mL). The brown reaction mixture was stirred at 70 °C for 24 h. After cooling, all volatiles were removed under reduced pressure; the obtained brown solid was dissolved in DCM (3 mL) and washed with a sat. $NaHCO_3$ solution (5 mL). After drying and evaporation of the solvent, the residual solid was purified by column chromatography (DCM:MeOH). Unfortunately, **262** was obtained in minor amounts and low purity.

ESI-MS: *m*/*z* calcd. for $C_{17}H_{13}N_2OS^+$ $[M+H]^+$ = 293.0743, found = 293.0532.

1-Phenyl-5-[(1-phenyl-1*H*-pyrrol-2-yl)thio]-1*H*-1,2,4-triazole (**263**):

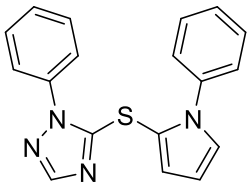

According to GP6, compound **252** (100 mg, 400 µmol, 1.00 equiv.), *N*-chlorosuccinimide (54 mg, 400 µmol, 1.00 equiv.) and 1-phenylpyrrole (57.2 mg, 400 µmol, 1.00 equiv.) were dissolved in MeCN (4 mL). The brown reaction mixture was stirred at 70 °C for 24 h. After cooling, all volatiles were removed under reduced pressure; the obtained brown oil was dissolved in DCM (3 mL) and washed with a sat. $NaHCO_3$ solution (4mL). The precipitate was purified with column chromatography (DCM:MeOH) and subsequent preparative HPLC (MeCN:H_2O; 60:40, 7 min → 65:35 over 3 min; 100:0, 2 min). **263** was obtained as a brown solid (17 mg, 52 µmol, 13%).

^{1}H NMR (300 MHz, CD_3CN) δ = 6.28 (t, *J* = 3.0, 1H)), 6.54 (dd, *J* = 3.8, 1.8 Hz, 1H), 7.01 (dd, *J* = 3.0, 1.8 Hz, 1H), 7.09 – 7.17 m, 2H), 7.27 – 7.50 (m, 8H), 8.18 (s, 1H) ppm. ^{13}C NMR (101 MHz, $CDCl_3$) δ = 110.0, 113.0, 121.0, 126.0, 127.0, 127.0, 128.0, 129.0, 130.0, 130.0, 133.0, 139.0, 145.0 ppm. IR (neat, cm^{-1}): 1595.8, 1497.5, 1435.7, 1417.4, 1392.4, 1319.1, 1267.0, 1159.0, 1139.7, 1086.7, 1074.2, 1036.6, 1005.7, 760.8, 726.1, 691.4, 656.6, 618.1, 549.6. ESI-MS: *m*/*z* calcd. for $C_{18}H_{15}N_4S^+$ $[M+H]^+$ = 319.1012; found = 319.1009.
Remark: Two signals in the ^{13}C-NMR-spectrum overlapped each other.

5.5 Tosylamide- and 1,3-diketone-derived reagents

5.5.1 Synthesis of reagents

2-[(1,3-Diisopropyl-4,5-dimethyl-1,3-dihydro-2*H*-imidazol-2-ylidene)-λ⁴-sulfaneylidene]-1,3-diphenylpropane-1,3-dione (**304**):

The information presented below is included for the sake of completeness of data but are not discussed in this thesis.

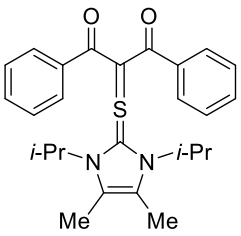

1,3-Diphenyl-1,3-propanedione (112 mg, 500 µmol, 1.00 equiv.) was dissolved in dry MeCN (5.0 mL). DIPEA (261 µL, 194 mg, 1.50 mmol, 3.00 equiv.) was added dropwise, and the clear solution was stirred for 20 min at rt. Dibromide **79** (241 mg, 648 µmol, 1.30 equiv.) was added to the solution. After the orange solid was completely dissolved within 5 min, the yellow solution was stirred for an additional 2 h. Solvents were removed under reduced pressure, the residual yellow oil was dissolved in DCM (4.0 mL) and washed with water (20 mL) for 2 min to remove residual ammonium salts. The organic layer was dried over $MgSO_4$ and concentrated *in vacuo*. The obtained yellow oil was purified by column chromatography (DCM:MeOH) affording product **304** as a light yellow oil (166 mg, 382 µmol, 76%).

^{1}H NMR (300 MHz, CD_2Cl_2, ppm) δ = 1.57 (d, *J* = 7.1 Hz, 12H), 2.30 (s, 6H), 6.00 (q, *J* = 7.0 Hz, 2H), 6.87 – 7.01 (m, 6H), 7.14 – 7.23 (m, 4H). ^{13}C NMR (75 MHz, CD_2Cl_2, ppm) δ =10.7, 21.0, 49.7, 113.0, 128.9, 129.0, 129.3, 130.0, 130.9, 132.8, 133.9, 136.5, 157.6, 191.7. IR (neat, cm^{-1}) = 2916.8, 1589.1, 1487.8, 1400.1, 1376.9, 1321.0, 1291.1, 1180.2, 1134.9, 1076.1, 1064.5, 1031.7, 815.7, 803.2, 703.9, 649.9, 637.4, 579.5, 519.7. HRMS: *m*/*z* calcd. for $C_{26}H_{31}N_2O_2S$ $[M+H]^+$ = 435.2101; found = 435.2108.

2-[(1,3-Diisopropyl-4,5-dimethyl-1,3-dihydro-2*H*-imidazol-2-ylidene)-λ⁴-sulfaneylidene]-1-phenylbutane-1,3-dione (**305**):

The information presented below is included for the sake of completeness of data but are not discussed in this thesis.

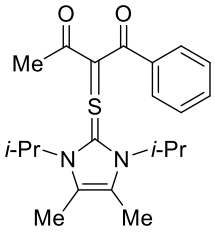

1-Phenyl-1,3-butanedione (81.1 mg, 500 µmol, 1.00 equiv.) was dissolved in dry MeCN (5.0 mL). DIPEA (261 µL, 194 mg, 1.50 mmol, 3.00 equiv.) was dropwise added and the clear solution was stirred for 20 min at rt. Dibromide **79** (242 mg, 650 µmol, 1.30 equiv.) was added to the solution. After the orange solid was completely dissolved within 5 min, the dark pink reaction mixture was stirred for an additional 2 h. Solvents were removed under reduced pressure, the

residual pink solid was dissolved in DCM (4.0 mL) and washed with water (20 mL) for 2 min to remove residual ammonium salts. The organic layer was dried over $MgSO_4$ and concentrated *in vacuo*. The obtained light violette oil was purified by column chromatography (DCM:MeOH) affording product **305** as a light yellow oil (120 mg, 322 µmol, 64%).

^{1}H NMR (300 MHz, $CDCl_3$, ppm) δ = 1.42 (d, *J* = 7.1 Hz, 12H), 1.88 (s, 3H), 2.19 (s, 6H), 5.55 (h, *J* = 7.0 Hz, 2H), 7.21 – 7.25 (m, 3H), 7.29 – 7.34 (m, 2H). ^{13}C NMR (101 MHz, $CDCl_3$, ppm) δ = 10.5, 21.3, 29.8, 52.1, 98.4, 126.5, 127.3, 127.7, 128.4, 144.6, 145.2, 189.8, 190.5. IR (neat, cm^{-1}) = 1729.8, 1609.3, 1593.9, 1467.6, 1432.9, 1396.2, 1367.3, 1329.7, 1268.0, 1168.7, 1146.5, 1096.3, 1066.4, 1032.7, 954.6, 845.6, 798.4, 770.4, 674.0, 601.7, 572.8. HRMS: *m*/*z* calcd. for $C_{21}H_{28}N_2NaO_2S^+$ $[M+Na]^+$ = 395.1764; found = 395.1764.

[(1,3-Diisopropyl-4,5-dimethyl-1*H*-imidazol-3-ium-2-yl)thio](tosyl)amide (**269**):

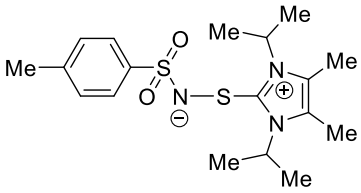

Dibromide **79** (744 mg, 2.00 mmol, 1.00 equiv.) and *p*-toluenesulfonamide (342 mg, 2.00 mmol, 1.00 equiv.) were dissolved in dry DCM (20 mL) and cooled to –78 °C. Under vigorous stirring, DIPEA (766 µL, 569 mg, 4.40 mmol, 2.20 equiv.) was added dropwise to the obtained orange gel. The clear colorless reaction mixture was stirred for 15 min at –78 `C, then allowed to warm up to rt within 60 min and stirred with water (12 mL) for 1 min. The organic phase was subsequently filtered through $MgSO_4$ and all volatiles were removed *in vacuo*. Product **269** was obtained as a white foam (660 mg, 1.73 mmol, 86%).

^{1}H NMR (300 MHz, CD_2Cl_2, ppm) δ = 1.58 (d, *J* = 7.1 Hz, 12H), 2.32 (s, 6H), 2.38 (s, 3H), 5.58 (hept, *J* = 7.0 Hz, 2H), 7.18 – 7.24 (m, 2H), 7.61 – 7.69 (m, 2H). ^{13}C NMR (75 MHz, CD_2Cl_2, ppm) δ = 10.8, 21.6, 21.6, 52.9, 127.4, 127.8, 129.2, 140.8, 143.0. ^{15}N NMR (51 MHz, CD_2Cl_2, ppm) δ = –185.9, –283.4. IR (neat, cm^{-1}) = 2975.6, 1447.3, 1391.4, 1370.2, 1258.3, 1129.1, 1087.7, 913.1, 813.8, 729.9, 708.7, 644.1, 565.0, 553.5. HRMS: *m*/*z* calcd. for $C_{21}H_{28}N_3O_2S_2$ $[M+H]^+$ = 382.1617; found = 382.1620.

[(1,3-Diisopropyl-4,5-dimethyl-1*H*-imidazol-3-ium-2-yl)thio][(trifluoromethyl)sulfonyl]-amide (**306**):

The information presented below is included for the sake of completeness of data but are not discussed in this thesis.

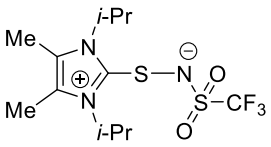

Dibromide **79** (186 mg, 500 µmol, 1.00 equiv.) and trifluoromethanesulfonamide (75 mg, 500 µmol, 1.00 equiv.) were dissolved in dry DCM (5 mL) and cooled to –78 °C. Under vigorous stirring, DIPEA (191 µL, 142 mg, 1.10 mmol, 2.20 equiv.) was added dropwise to the obtained orange gel. The clear colorless reaction mixture was stirred for 15 min at –78 `C, then allowed to warm up to rt within 60 min and stirred with water (12 mL) for 1 min. The organic phase was subsequently filtered through $MgSO_4$ and all volatiles were removed *in vacuo*. Product **306** was obtained as a white foam (140 mg, 389.5 µmol, 78%).

^{1}H NMR (300 MHz, CD_2Cl_2, ppm) δ = 1.59 (d, *J* = 7.0 Hz, 12H), 2.35 (d, *J* = 0.6 Hz, 6H), 5.65 (p, *J* = 7.0 Hz, 2H). ^{13}C NMR (75 MHz, CD_2Cl_2, ppm) δ = 10.8, 21.5, 53.5, 115.5, 119.8, 124.2, 128.5, 128.9, 145.5. ^{15}N NMR (51 MHz, CD_2Cl_2, ppm) δ = -183.3, -294.3. ^{19}F NMR (282 MHz, CD_2Cl_2, ppm) δ = -77.2. IR (neat, cm^{-1}) = 2991.1, 2252.4, 1449.2, 1376.0, 1294.0, 1208.2, 1157.1, 1037.5, 973.9, 918.9, 837.0, 753.1, 615.2, 567.0. HRMS: *m*/*z* calcd. for $C_{12}H_{21}N_3F_3O_2S_2^+$ $[M+H]^+$ = 360.1022; found = 360.1018.

[(1,4-Diisopropyl-1*H*-1,2,4-triazol-4-ium-5-yl)thio](tosyl)amide (**288**):

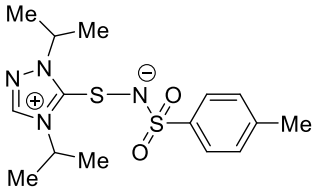

Brominated 2,4-diisopropyl-1,2,4-triazole-3-thione **287** [5-(bromothio)-1,4-diisopropyl-1*H*-1,2,4-triazol-4-ium bromide, 173 mg, 501 µmol, 1.00 equiv.] and *p*-toluenesulfonamide (324 mg, 2.00 mmol, 1.00 equiv.) were dissolved in dry DCM (5 mL) and cooled to –78 °C. Under vigorous stirring, DIPEA (200 µL, 149 mg, 1.150 mmol, 2.30 equiv.) was added dropwise to the obtained orange gel. The clear colorless reaction mixture was stirred for 15 min at –78 `C, then allowed to warm up to rt within 60 min and stirred with water (12 mL) for 1 min. The organic phase was subsequently filtered through $MgSO_4$ and all volatiles were removed *in vacuo*. Product **288** was obtained as a white foam (145 mg, 409 µmol, 82%).

^{1}H NMR (400 MHz, CD_2Cl_2, ppm) δ = 1.40 – 1.63 (m, 12H), 2.38 (s, 3H), 5.22 – 5.29 (m, 2H), 7.09 – 7.34 (m, 2H), 7.65 (d, *J* = 8.2 Hz, 2H), 8.20 (s, 1H). ^{13}C NMR (126 MHz, CD_2Cl_2, ppm) δ = 21.8, 22.7, 51.8, 54.7, 127.4, 129.3, 141.1, 141.4, 141.6, 155.7. IR (neat, cm^{-1}) = 1524.5, 1474.3, 1462.7, 1403.0, 1380.8, 1367.3, 1302.7, 1264.1, 1214.0, 1178.3, 1133.9, 1107.9,

1081.9, 1042.3, 1012.4, 902.5, 813.8, 736.7, 667.3, 648.0, 596.9, 567.0, 552.5. HRMS: *m/z* calcd. for $C_{15}H_{23}N_4O_2S_2^+$ $[M+H]^+$ = 355.1257; found = 355.1260.

5.5.2 Reactivity of reagents

(**4-Methoxyphenyl)(phenyl)methanone** (**307**):

The information presented below is included for the sake of completeness of data but are not discussed in this thesis.

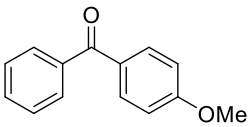

Sulfaneylidene **304** (80.0 mg, 184 µmol, 1.00 equiv.) was dissolved in dry THF (1.5 mL) and cooled to –78 °C. 4-Methoxyphenylmagnesium bromide solution (0.50M in THF, 644 µL, 322 µmol, 1.75 equiv.) was added dropwise, and the reaction was allowed to warm up to 10 °C over a period of 14 affording the yellow solution. The reaction was quenched with sat. NH_4Cl (5 mL), stirred for 5 min and extracted with DCM (2 × 20 mL). The combined organic phases were dried over $MgSO_4$, concentrated *in vacuo* and purified by column chromatography (DCM:MeOH) furnishing benzophenone **307** as a colorless oil (17.9 mg, 84.3 µmol, 46%).

^{1}H NMR (300 MHz, CD_2Cl_2, ppm) δ = 3.89 (s, 3H), 6.95 – 7.03 (m, 2H), 7.44 – 7.53 (m, 2H), 7.54 – 7.65 (m, 1H), 7.70 – 7.77 (m, 2H), 7.77 – 7.85 (m, 2H). ^{13}C NMR (75 MHz, CD_2Cl_2, ppm) δ =56.1, 114.1, 128.7, 130.1, 130.7, 132.4, 132.9, 138.9, 163.8, 195.6. IR (neat, cm^{-1}) 1646.9, 1594.8, 1505.2, 1456.0, 1444.4, 1317.1, 1279.5, 1258.3, 1180.2, 1168.7, 1149.4, 1111.8, 1073.2, 1021.1, 999.9, 954.6, 936.3, 917.0, 841.8, 791.6, 738.6, 693.3, 676.9, 632.5, 597.8, 564.1, 512.0. HRMS: *m/z* calcd. for $C_{28}H_{24}NaO_4^+$ $[2M+Na]^+$ = 447.1567; found = 447.1563.

1-(4-Methoxyphenyl)ethan-1-one (**308**):

The information presented below is included for the sake of completeness of data but are not discussed in this thesis.

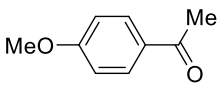

Sulfaneylidene **305** (80.0 mg, 214.7 µmol, 1.00 equiv.) was dissolved in dry THF (1.5 mL) and cooled to –78 °C. 4-Methoxyphenylmagnesium bromide solution (0.50M in THF, 644 µL, 322 µmol, 1.50 equiv.) was added dropwise, and the reaction was allowed to warm up to 10 °C over a period of 14 affording the yellow solution. The reaction was quenched with sat. NH_4Cl (5 mL), stirred for 5 min and extracted with DCM (2 × 20 mL). The combined organic phases were dried over $MgSO_4$, concentrated *in vacuo* and purified by column chromatography (DCM:MeOH) furnishing acetophenone **308** as a colorless oi (17.9 mg, 119.1 µmol, 55%).

^{1}H NMR (300 MHz, $CDCl_3$, ppm) δ = 2.56 (s, 3H), 3.87 (s, 3H), 6.93 (d, *J* = 9.0 Hz, 2H), 7.94 (d, *J* = 9.0 Hz, 2H). ^{13}C NMR (75 MHz, $CDCl_3$, ppm) δ =26.5, 55.6, 113.8, 130.7, 163.6, 196.9. IR (neat, cm^{-1}) = 1665.2, 1595.8, 1573.6, 1506.1, 1460.8, 1415.5, 1355.7, 1309.4, 1273.8, 1246.8, 1169.6, 1110.8, 1074.2, 1019.2, 953.6, 829.2, 817.7, 805.1, 590.1, 575.6. HRMS: *m*/*z* calcd. for $C_9H_{10}O_2^+$ $[M]^+$ = 150.0675; found = 150.0678.

***N*-(Cyclopentylthio)-4-methylbenzenesulfonamide** (**275**):

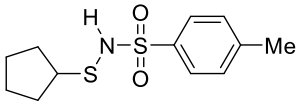

Compound **269** (100.0 mg, 262 µmol, 1.00 equiv.) was dissolved in dry THF (2.0 mL) and cooled to –35 °C. Cyclopentylmagnesium bromide solution (2.00M in THF, 394 µL, 788 µmol, 3.00 equiv.) was added dropwise, and the reaction mixture was stirred for 2 d at –35°C, then allowed to warm up to 10 °C over 2 h furnishing the yellow solution. The reaction was quenched with sat. NH_4Cl (5 mL), stirred for 5 min and extracted with DCM (2 × 20 mL). The combined organic phases were dried over $MgSO_4$, concentrated *in vacuo* and purified by column chromatography (DCM:MeOH) affording **275** as a colorless oil (27.5 mg, 101 µmol, 39%).

^{1}H NMR (300 MHz, CD_2Cl_2, ppm) δ = 1.41 – 1.74 (m, 6H), 1.77 – 1.92 (m, 2H), 2.43 (s, 3H), 3.41 – 3.54 (m, 1H), 5.88 (s, 1H), 7.27 – 7.41 (m, 2H), 7.77 (d, *J* = 8.3 Hz, 2H). ^{13}C NMR (126 MHz, CD_2Cl_2, ppm) δ =21.9, 25.3, 31.0, 50.6, 128.0, 130.1, 137.0, 144.7. IR (neat, cm^{-1}) = 3268.8, 2957.3, 1596.8, 1445.4, 1363.4, 1291.1, 1155.2, 1088.6, 1020.2, 849.5, 809.0, 660.5, 559.3, 541.9. HRMS: *m*/*z* calcd. for $C_{12}H_{18}NO_2S_2^+$ $[M+H]^+$ = 272.0773; found = 272.0777.

***N*-(Isopropylthio)-4-methylbenzenesulfonamide** (**281**) and **1,3-Diisopropyl-2-(isopropylthio)-4,5-dimethyl-1*H*-imidazol-3-ium Chloride** (**282**):

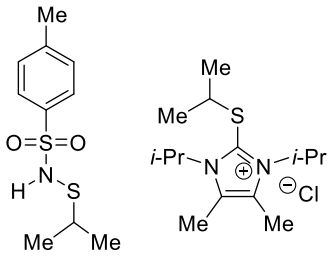

281 **282**

Compound **269** (71.0 mg, 186 µmol, 1.00 equiv.) was dissolved in dry THF (1.0 mL) and cooled to –78 °C. *iso*-Propylmagnesium bromide solution (1.30M in THF, 220 µL, 286 µmol, 1.54 equiv.) was added dropwise, and the reaction mixture was allowed to warm up rt over 21 h furnishing the red solution. The reaction was quenched with sat. NH_4Cl (5 mL), stirred for 5 min and extracted with DCM (2 × 20 mL). The combined organic phases were dried over $MgSO_4$, concentrated *in vacuo* and purified by column chromatography (DCM:MeOH) affording products **281** as a colorless oil (4.0 mg, 16.3 µmol, 9%) and **282** as a white solid (26.9 mg, 92.4 µmol, 50%).

Product **281**:

^{1}H NMR (300 MHz, CD_2Cl_2, ppm) δ 1.17 (d, *J* = 6.7 Hz, 6H), 2.43 (s, 3H), 3.18 (hept, *J* = 6.7 Hz, 1H), 5.76 (s, 1H), 7.29 – 7.38 (m, 2H), 7.68 – 7.84 (m, 2H). ^{13}C NMR (126 MHz, CD_2Cl_2, ppm) δ =20.5, 21.9, 41.8, 128.0, 130.1, 136.9, 144.7. IR (neat, cm^{-1}) = 1750.1, 1678.7, 1604.5, 1456.0, 1303.6, 1217.8, 1181.2, 1093.4, 1011.5, 914.1, 838.9, 802.2, 753.1, 702.9, 666.3, 597.8. HRMS: *m*/*z* calcd. for $C_{10}H_{16}NO_2S_2^+$ $[M+H]^+$ = 246.0617; found 246.0617.

Product **282**:

^{1}H NMR (300 MHz, CD_2Cl_2, ppm) δ 1.33 (d, *J* = 6.7 Hz, 6H), 1.59 (d, *J* = 7.1 Hz, 12H), 2.43 (s, 6H), 3.45 (hept, *J* = 6.7 Hz, 1H), 5.19 – 5.46 (m, 2H). ^{13}C NMR (126 MHz, CD_2Cl_2, ppm) δ =11.3, 21.8, 23.7, 44.8, 131.0, 137.0. IR (neat, cm^{-1}) = 3102.9, 1710.6, 1595.8, 1497.5, 1455.0, 1433.8, 1409.7, 1392.4, 1319.1, 1277.6, 1206.3, 1155.2, 1134.9, 1119.5, 1075.1, 1035.6, 1001.8, 957.5, 912.2, 879.4, 760.8, 722.2, 693.3, 636.4, 617.1, 605.5, 558.3. HRMS: *m*/*z* calcd. for $C_{14}H_{27}N_2S^+$ $[M]^+$ = 255.1889; found = 255.1893.

***N*-(2,4-Dinitrophenyl)-4-methylbenzenesulfonamide** (**309**):

The information presented below is included for the sake of completeness of data but are not discussed in this thesis.

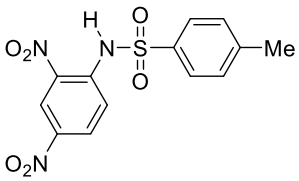

Compound **269** (95.4 mg, 250 µmol, 1.00 equiv.) was dissolved in dry MeCN (5.0 mL). A solution of 1-fluoro-2,4-dinitrobenzene (46.5 mg, 250 µmol, 1.00 equiv.) in MeCN (2.0 mL) was added dropwise to the yellow solution. After stirring the reaction mixture at 70 °C for 16 h, the orange solution was concentrated *in vacuo* and purified by column chromatography (DCM:MeOH) to afford **309** as a yellow solid (23.9 mg, 70.8 µmol, 28%).

^{1}H NMR (400 MHz, CD_3CN, ppm) δ = 2.33 – 2.53 (m, 3H), 7.41 (dd, *J* = 8.6, 0.7 Hz, 2H), 7.84 – 7.88 (m, 1H), 7.89 – 7.93 (m, 2H), 8.36 (dd, *J* = 9.3, 2.7 Hz, 1H), 8.89 (d, *J* = 2.7 Hz, 1H), 10.07 (s, 1H). ^{13}C NMR (126 MHz, CD_2Cl_2, ppm) δ =21.9, 25.3, 31.0, 50.6, 128.0, 130.1, 137.0, 144.7. IR (neat, cm^{-1}) = 2925.5, 1619.9, 1594.8, 1539.9, 1518.7, 1489.7, 1424.2, 1394.3, 1345.1, 1326.8, 1300.8, 1277.6, 1219.8, 1187.0, 1168.7, 1141.7, 1083.8, 1064.5, 1039.4, 930.5, 914.1, 885.2, 838.9, 813.8, 763.7, 739.6, 711.6, 702.0, 652.8, 610.4, 588.2, 544.8, 528.4, 505.3. HRMS: *m*/*z* calcd. for $C_{13}H_{11}N_3NaO_6S^+$ $[M+Na]^+$ = 360.0261; found = 60.0258.

5.6 Reactions towards the synthesis of aryldisulfides

The information presented in this Subchapter is included for the sake of completeness of data but are not discussed in this thesis.

5.6.1 Synthesis of cationic tetramethylthiourea salts

2-[4-(Dimethylamino)phenyl]-1,1,3,3-tetramethylisothiouronium Hexafluoroantimonate (**310**):

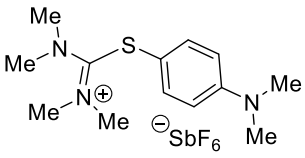

Tetramethylthiourea (159 mg, 1.20 mmol, 1.20 equiv.) and *N*-chlorosuccinimide (160 mg, 1.20 mmol, 1.20 equiv.) were dissolved in DCE (10 mL). Dimethylaniline (127 µL, 121 mg, 1.00 mmol, 1.00 equiv.) was added dropwise, and the yellow reaction mixture was stirred for 17 h at 70 °C, then cooled to rt and washed with aq. $NaSbF_6$ (7.0 mL) for 5 min. The aq. phase was re-extracted with DCM (3 × 10 mL), the combined organic phases were dried over $MgSO_4$ and concentrated *in vacuo*. After column chromatography (DCM:MeOH), the salt **310** was obtained as a white solid (268 mg, 549 µmol, 55%).

^{1}H NMR (300 MHz, $CDCl_3$ ppm) δ = 2.97 (s, 6H), 3.17 (s, 12H), 6.67 (d, *J* = 9.0 Hz, 2H), 7.23 (d, *J* = 9.0 Hz, 2H). ^{13}C NMR (75 MHz, $CDCl_3$, ppm) δ = 40.1, 44.0, 110.6, 113.4, 134.0, 151.4, 176.7. IR (neat, cm^{-1}): 3451.0, 2896.5, 1589.1, 1512.8, 1440.9, 1397.0, 1362.3, 1253.6, 1201.8, 1149.5, 1103.4, 826.3, 810.8, 530.7, 507.7. HRMS: *m*/*z* calcd. for $C_{13}H_{22}N_3S^+$ [M–SbF_6]$^+$ = 252.1529; found = 252.1531; calcd. for SbF_6^- [M]$^-$ = 234.8948; found = 234.8950.

Additional information:

- To optimize the yield of compound **310**, this reaction was repeated several times under different conditions varying solvent, temperature and time, as presented in Table 15.
- If the reaction was done in MeCN as a solvent, the anion exchange was performed in a different way: The solution was cooled, and sodium hexafluoroantimonate (776 mg, 3.0 mmol, 3.0 equiv.) was added. The suspension was stirred for 15 min, ~~and~~ then the white solid was filtered off and was washed with DCM (3 × 10 mL). The solvent was removed *in vacuo*. Thereafter, the purification by column chromatography has been performed.

Table 15: Screening of conditions for the synthesis of **310**.

Reaction	Solvent	Temperature [°C]	Time [h]	Yield [%]
1	DCE	70	16	12
2	DCM	30	18	40
3	MeCN	70	24	67
4	DCE	70	16	55

***N*-[(Dimethylamino)(phenylamino)methylene]-*N*-methylmethanaminium Hexafluoroantimonate** (**311**):

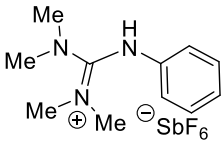

Tetramethylthiourea (159 mg, 1.20 mmol, 1.20 equiv.) and *N*-chlorosuccinimide (160 mg, 1.20 mmol, 1.20 equiv.) were dissolved in MeCN (10 mL). Aniline (90 µL, 93 mg, 1.00 mmol, 1.00 equiv.) was added dropwise, and the yellow reaction mixture was stirred at 70 °C for 2 h affording the violet solution. The latter was cooled to rt, $NaSbF_6$ (776 mg, 3.00 mmol, 3.00 equiv.) was added, and the suspension was stirred for 15 min. The organic layer was filtered off, dried over $MgSO_4$ and concentrated *in vacuo*. After column chromatography (DCM:MeOH), product **311** was obtained as a red solid (273 mg, 638 mmol, 64%).[30]

^{1}H NMR (300 MHz, CD_2Cl_2 ppm) δ = 2.95 (s, 12H), 6.98 (d, 3 = 8.0 Hz, 2H), 7.23 (t, *J* = 8.0 Hz, 1H), 7.41 (t, *J* = 8.0 Hz, 2H), 7.51 (s, 1 H). ^{13}C NMR (75 MHz, CD_2Cl_2, ppm) δ = 40.6, 121.2, 126.4, 130.6, 138.9, 158.9. IR (neat, cm^{-1}): 3356.0, 3161.9, 3070.7, 2948.6, 1770.5, 1704.3, 1626.8, 1597.1, 1557.1, 1402.9, 1355.0, 1293.6, 1168.7, 848.5, 821.1, 749.3, 653.0, 640.1, 556.6. HRMS: *m*/*z* calcd. for $C_{11}H_{18}N_3$ $[M–SbF_6]^+$ = 192.1495; found = 192.1496.

1,1,3,3-Tetramethyl-2-[4-(methylamino)phenyl]isothiouronium Hexafluoroantimonate (**312**):

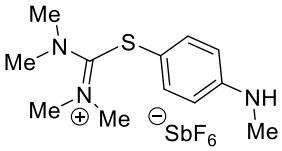

Tetramethylthiourea (159 mg, 1.20 mmol, 1.20 equiv.) and *N*-chlorosuccinimide (160 mg, 1.20 mmol, 1.20 equiv.) were dissolved in MeCN (10 mL). *N*-Methylaniline (108 µL, 107 mg, 1.00 mmol, 1.00 equiv.) was added dropwise, and the yellow reaction mixture was stirred for 17 h at 70 °C furnishing the violet solution. The latter was cooled to rt, $NaSbF_6$ (776 mg, 3.00 mmol, 3.00 equiv.) was added and the suspension was stirred for 15 min. The organic

[30] It was not possible to separate residual succinimide from the desired product after twofold repetitive column chromatography, as indicated by the singlets at 2.70 ppm and at 3.02 ppm in the ^{1}H NMR spectrum as well as the signals at 30.1 ppm and 179.0 ppm in the ^{13}C NMR spectrum. The vibration of the carbonyl group is visible at 1770 cm^{-1} and 1704 cm^{-1} in the IR spectrum.

layer was filtered of, dried over $MgSO_4$ and concentrated *in vacuo*. After column chromatography (DCM:MeOH), compound **312** was obtained as a yellow oil (268 mg, 565 µmol, 57%) with 85% purity.[31]

^{1}H NMR (300 MHz, CD_2Cl_2 ppm) δ = 2.84 (d, *J* = 5.2 Hz, 3 H), 3.16 (s, 12 H), 4.34 (s, 1 H), 6.66 (d, *J* = 9.4 Hz, 2 H), 7.19 (d, *J* = 9.4 Hz, 2 H). ^{13}C NMR (75 MHz, CD_2Cl_2, ppm) δ = 30.5, 44.4, 111.0, 114.2, 134.7, 151.9, 178.1. IR (neat, cm^{-1}): 3441.1, 2936.0, 2890.6, 2827.0, 1593.7, 1509.5, 1401.9, 1390.1, 1329.0, 1258.9, 1111.0, 823.2, 650.7. HRMS: *m*/*z* calcd. for $C_{12}H_{20}N_3S^+$ $[M–SbF_6]^+$ = 238.1372; found = 238.1381.

2-[4-(Benzylamino)phenyl]-1,1,3,3-tetramethylisothiouronium Hexafluoroantimonate (**313**):

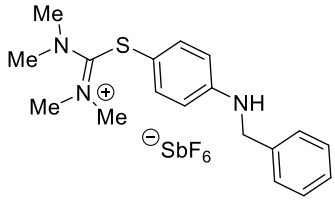

Tetramethylthiourea (159 mg, 1.20 mmol, 1.20 equiv.), *N*-chlorosuccinimide (160 mg, 1.20 mmol, 1.20 equiv.) and *N*-benzylaniline (183 mg, 1.00 mmol, 1.00 equiv.) were dissolved in MeCN (10 mL). The yellow reaction mixture was stirred at 70 °C for 19 h. Solvents were removed, and the residue was pre-purified by a column chromatography on a short column with DCM as the eluent and a 0–10% gradient of MeOH. The obtained product was dissolved in DCM (10 mL) and washed with aq. $NaSbF_6$ solution (10 mL). After drying and evaporation of the solvent, compound **313** was obtained as a yellow solid (128 mg, 233 µmol, 23%).

^{1}H NMR (300 MHz, CD_3CN ppm) δ = 3.08 (s, 12H), 4.36 (bs, 2H), 5.51 (bs, 1H), 6.69 (d, *J* = 8.7 Hz, 2H), 7.19 (d, *J*

= 8.7 Hz, 2H), 7.22 – 7.33 (m, 1H), 7.22 – 7.33 (m, 4H). ^{13}C NMR (126 MHz, CD_3CN, ppm) δ = 44.4, 47.6, 112.4, 114.8, 127.9, 128.1, 129.4, 134.9, 140.0, 151.2, 177.4. IR (neat, cm^{-1}): 3415.0, 3034.5, 2948.4, 2854.8, 1595.5, 1503.0, 1466.3, 1452.6, 1401.1, 1390.1, 1326.0,

[31] Spectroscopically pure product (120.5 mg, 254 µmol, 25% yield) was obtained after repetitive twofold column chromatography.

1255.5, 1167.7, 1111.7, 825.1, 752.5, 652.5. HRMS: *m*/*z* calcd. for $C_{18}H_{24}N_3S^+$ $[M–SbF_6]^+$ = 314.1685; found = 314.1685.

1,1,3,3-Tetramethyl-2-(1-methyl-1*H*-indol-3-yl)isothiouronium Hexafluoroantimonate (**314**):

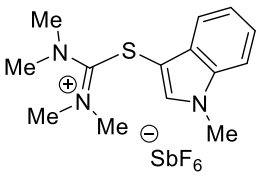

Tetramethylthiourea (132 mg, 1.00 mmol, 1.20 equiv.) and *N*-chlorosuccinimide (134 mg, 1.00 mmol, 1.20 equiv.) were dissolved in DCE (8 mL). *N*-Methylindole (107 µL, 109 mg, 833 µmol, 1.00 equiv.) were added, and the yellow solution was stirred for 18 h at 70 °C. The dark brown solution was allowed to reach rt and washed with aq. $NaSbF_6$ solution (647 mg, 2.50 mmol, 3.00 equiv. in 10 mL H_2O). The organic layer was dried over $MgSO_4$, concentrated *in vacuo* and the obtained crude product was purified by column chromatography with DCM as the eluent and a 0–10% gradient of MeOH. Compound **314** was obtained as a brown solid (300 mg, 602 µmol, 72%).

^{1}H NMR (300 MHz, CD_2Cl_2, ppm) δ = 3.19 (d, *J* = 0.9 Hz, 12H), 3.88 (d, *J* = 0.9 Hz, 3H), 7.25 – 7.32 (m, 1H), 7.36 (ddt, *J* = 8.2, 7.0, 1.3 Hz, 1H), 7.42 – 7.50 (m, 2H), 7.56 (s, 1H). ^{13}C NMR (75 MHz, CD_2Cl_2, ppm) δ = 34.0, 44.3, 93.8, 111.4, 118.0, 122.4, 124.0, 128.2, 135.8, 137.8, 177.9. IR (neat, cm^{-1}): 1686.4, 1591.0, 1506.1, 1467.6, 1445.4, 1399.1, 1368.2, 1294.0, 1257.4, 1227.5, 1197.6, 1167.7, 1107.9, 1061.6, 944.0, 872.6, 814.8, 649.9, 523.6. HRMS: *m*/*z* calcd. for $C_{14}H_{20}N_3S^+$ $[M–SbF_6]^+$ = 262.1372; found = 262.1378.

1,1,3,3-Tetramethyl-2-(1-methyl-2-phenyl-1H-indol-3-yl)isothiouronium hexafluoroantimonate (**315**):

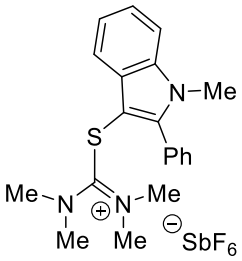

Tetramethylthiourea (159 mg, 1.20 mmol, 1.20 equiv.), *N*-chlorosuccinimide (160 mg, 1.20 mmol, 1.20 equiv.) and *N*-Methyl-2-phenylindole (207 mg, 1.00 mmol, 1.00 equiv.) were dissolved in DCE (10 mL). The yellow solution was stirred at 70 °C for 15 h. The orange reaction mixture was allowed to reach rt and washed with a solution of $NaSbF_6$ (777 mg, 3.00 mmol, 3.00 equiv.) in H_2O (10 mL). The organic layer was dried over $MgSO_4$ and concentrated *in vacuo*. The crude product was purified by column chromatography with DCM as the eluent with a 0–10% gradient of MeOH. Compound **315** was obtained as a white solid (331 mg, 575 µmol, 58%).

^{1}H NMR (300 MHz, CD_2Cl_2, ppm) δ = 2.97 (s, 12H), 3.73 (s, 3H), 7.31 – 7.45 (m, 4H), 7.50 – 7.57 (m, 2H), 7.58 – 7.67 (m, 3H). ^{13}C NMR (126 MHz, CD_2Cl_2, ppm) δ = 32.5, 44.3, 93.9,

111.6, 118.0, 123.0, 124.4, 127.8, 129.3, 129.7, 130.7, 130.8, 137.9, 146.2, 177.9. IR (neat, cm^{-1}): 1702.8, 1597.7, 1499.4, 1466.6, 1445.4, 1399.1, 1382.7, 1336.4, 1259.3, 1237.1, 1205.3, 1165.8, 1134.9, 1104.0, 1080.9, 1057.8, 1023.1, 871.7, 801.3, 761.7, 749.2, 703.9, 651.8, 574.7, 549.6. HRMS: *m*/*z* calcd. for $C_{20}H_{24}N_3S^+$ $[M–SbF_6]^+$ = 338.1685; found = 338.1685.

5.6.2 Synthesis of thiols and disulfides

4,4'-Disulfanediylbis(*N*,*N*-dimethylaniline) (**316**):

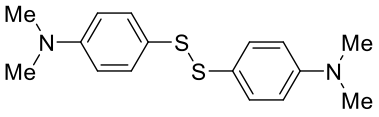

Compound **310** (195 mg, 399 µmol, 1.00 equiv.) was added to a solution of methylamine (9.8M in MeOH, 4.32 mL, 42.30 mmol, 106 equiv.). The reaction mixture was stirred for 10 min at rt until no starting material was detectable by TLC. The solvent was removed *in vacuo* at 100–200 mbar. The product was purified by column chromatography with DCM as the eluent with a 0–10% gradient of MeOH affording the yellow oily liquid which, according to ^{1}H NMR spectrum, was essentially a 1:2.5 mixture of the thiol and the disulfide. Exposing the product to air for several days lead to the formation of pure **316** (43.4 mg, 143 µmol, 62%)

^{1}H NMR (300 MHz, $CDCl_3$ ppm) δ = 2.98 (s, 12H), 6.63 (d, *J* = 9.0 Hz, 4H), 7.27 (d, *J* = 9.0 Hz, 2H), 7.36 (d, *J* = 9.0 Hz, 2H). ^{13}C NMR (75 MHz, $CDCl_3$, ppm) δ = 40.4, 112.6, 123.5, 134.3, 150.8. IR (neat, cm^{-1}): 2891.6, 2799.1, 1591.9, 1504.0, 1443.1, 1357.4, 1226.7, 1193.6, 1168.4, 1094.8, 945.4, 811.5, 521.5. HRMS: *m*/*z* calcd. for $C_{16}H_{21}N_2S_2^+$ $[M+H]^+$ = 305.1141; found = 305.1143.

4-(Methylamino)benzenethiol (**317a**) and **4,4'-Disulfanediylbis(*N*-methylaniline)** (**317b**):

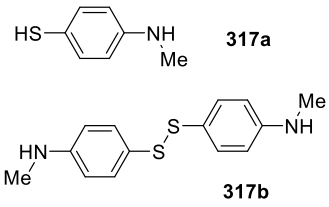

Compound **312** (192 mg, 406 µmol, 1.00 equiv.) was added to a solution of methylamine (9.8M in MeOH, 4.50 mL, 44.1 mmol, 108.6 equiv.). The reaction mixture was stirred for 10 min at rt until no starting material was detectable by TLC. The solvent was removed *in vacuo* at 100–200 mbar. The product was purified by column chromatography with DCM as the eluent with a 0–10% gradient of MeOH. The thiol **317a** (4.2 mg, 30 µmol, 7.4%) and the disulfide **317b** (46.2 mg, 167 µmol, 83%) were isolated both as yellow oily liquids.

Compound **317a:**

^{1}H NMR (300 MHz, $CDCl_3$ ppm) δ = 2.81 (s, 3H), 3.30 (s, 1H), 3.74 (s, 1H), 6.52 (d, *J* = 8.9 Hz, 2H), 7.21 (d, *J* = 8.9 Hz, 2H). ^{13}C NMR (75 MHz, $CDCl_3$, ppm) δ = 31.0, 113.2, 114.4,

133.5, 148.6. IR (neat, cm^{-1}): 3408.0, 2932.8, 2888.2, 2810.8, 1591.8, 1498.0, 1316.3, 1291.6, 1259.7, 1179.9, 1154.9, 1091.5, 1059.0, 812.9, 513.2. HRMS: *m*/*z* calcd. for $C_7H_{10}NS^+$ $[M+H]^+$ = 140.0528; found = 140.0534.

Compound **317b**

^1H NMR (300 MHz, $CDCl_3$ ppm) δ = 2.84 (s, 6H), 3.87 (s, 2H), 6.53 (d, *J* = 8.9 Hz, 4H), 7.29 (d, *J* = 8.9 Hz, 4H). ^{13}C NMR (75 MHz, $CDCl_3$, ppm) δ = 30.6, 112.7, 124.4, 134.6, 149.9. IR (neat, cm^{-1}): 3390.1, 3364.0, 2915.4, 2880.5, 2818.0, 1587.8, 1505.8, 1324.3, 1265.4, 1177.5, 1088.0, 813.0, 521.3. HRMS: *m*/*z* calcd. for $C_{14}H_{17}N_2^+S_2$ $[M+H]^+$ = 277.0828; found = 277.0824.

4,4'-Disulfanediylbis(*N*-benzylaniline) (**318**):

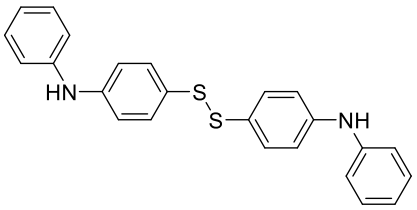

Compound **313** (132 mg, 240 µmol, 1.00 equiv.) was added to the solution of methylamine (9.8M in MeOH, 4.19 mL, 41 mmol, 170 equiv.). The reaction mixture was stirred for 10 min at rt until no starting material was detectable by TLC. The solvent was removed *in vacuo* at 100–200 mbar. The product was purified by column chromatography with DCM as the eluent with a 0–10% gradient of MeOH. The disulfide **318** was isolated as a yellow oily solid (44.1 mg, 103 µmol, 86%).

^1H NMR (300 MHz, $CDCl_3$ ppm) δ = 4.12 (s, 2H), 4.32 (d, *J* = 4.8 Hz, 4H), 6.55 (d, *J* = 9.0 Hz, 4H), 7.19 (d, *J* = 9.0 Hz, 2H), 7.28 (d, *J* = 9.0 Hz, 4H), 7.31 – 7.39 (m, 8H). ^{13}C NMR (75 MHz, $CDCl_3$, ppm) δ = 48.4, 113.7, 115.0, 127.5, 128.8, 133.4, 134.4, 139.2, 148.7. IR (neat, cm^{-1}): 3380.3, 3027.0, 2924.7, 2849.4, 1665.9, 1618.9, 1592.8, 1493.0, 1471.1, 1452.7, 1323.2, 1291.1, 1176.9, 1088.6, 818.8, 734.8, 698.4, 516.6. HRMS: *m*/*z* calcd. for $C_{26}H_{24}N_2NaS_2^+$ $[M+Na]^+$ = 451.1273; found = 451.1268.

1-Phenyl-2-[(1-phenyl-4,5-dihydro-1*H*-pyrrol-2-yl)disulfaneyl]-1*H*-pyrrole (**319**):

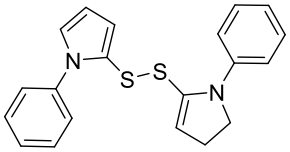

Compound **107a** (92.7 mg, 182 µmol, 1.00 equiv.) was added to a solution of methylamine (9.8M in MeOH, 2.02 mL, 19.8 mmol, 109 equiv.). The reaction mixture was stirred for 10 min at rt until no starting material was detectable by TLC. The solvent was removed *in vacuo* at 100–200 mbar. The product was purified by column chromatography with DCM as the eluent with a 0–10% gradient of MeOH. Compound **319** was isolated as a brown oil (17.4 mg, 49.8 µmol, 55%).

^1H NMR (300 MHz, CD_2Cl_2 ppm) δ = 2.93 (ddd, *J* = 0.7, 4.4, 18.3 Hz, 1H), 3.24 (dd, *J* = 7.8, 18.1 Hz, 1H), 3.36 – 3.45 (m, 1H), 3.74 (ddd, *J* = 0.7, 4.0, 11.8 Hz, 1H), 4.11 (dd, *J* = 6.8, 11.8

Hz, 1H), 6.31 (dd, *J* = 2.9, 3.6 Hz, 1H), 6.64 (dd, *J* = 1.9, 3.8 Hz, 1H), 7.06 (dd, *J* = 2.1, 3.2 Hz, 1H), 7.27 – 7.50 (m, 10H). ^{13}C NMR (75 MHz, $CDCl_3$, ppm) δ = 42.8, 52.2, 64.0, 110.0, 122.0, 125.7, 127.3, 127.4, 128.2, 128.3, 129.5, 129.5, 140.0. IR (neat, cm^{-1}): 3104.6, 3044.4, 2919.8, 1596.5, 1496.6, 1430.1, 1387.1, 1317.7, 1137.6, 1087.1, 1072.7, 1035.2, 759.5, 721.7, 690.1, 617.0, 605.7, 557.5. HRMS: *m*/*z* calcd. for $C_{20}H_{19}N_2S_2^+$ $[M+H]^+$ = 351.0984; found = 351.0980.

4,4'-Disulfanediyldianiline (**320**):

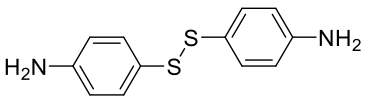

Compound **131** (100 mg, 185 μmol, 1.00 equiv.) was added to a solution of methylamine (9.8M in MeOH, 2.05 mL, 20.1 mmol, 108.6 equiv.). The red reaction mixture was stirred for 22 h at rt and then the solvent was removed in vacuo (100–200 mbar). The product was purified by column chromatography with DCM as the eluent with a 0–10% gradient of MeOH. Compound **320** was obtained as a yellow solid (1.5 mg, 6.0 μmol, 6.5%).

^{1}H NMR (300 MHz, CD_2Cl_2 ppm) δ =3.71 (s, 4H), 6.63 (d, *J* = 8.8 Hz, 4H), 7.15 (d, *J* = 8.8 Hz, 4H). ^{13}C NMR (75 MHz, CD_2Cl_2, ppm) δ = 116.0, 126.0, 131.3, 145.9. IR (neat, cm^{-1}): 2975.9, 2393.5, 2817.3, 1591.7, 1506.1, 1489.6, 1446.8, 1360.8, 1195.1, 801.0, 653.1, 527.3. HRMS: *m*/*z* calcd. for $C_6H_7NS^+$ $[M–C_6H_6NS+H]^+$ = 125.0294; found = 125.0291.

9-Methyl-9*H*-carbazole-3-thiol (**321**):

Compound **119** (118 mg, 188 μmol, 1.00 equiv.) was added to a solution of methylamine (9.8M in MeOH, 2.09 mL, 21.3 mmol, 100 equiv.). The yellow reaction mixture was stirred for 18 h at rt and then the solvent was removed in vacuo (100–200 mbar). The product was purified by column chromatography with DCM as the eluent with a 0–10% gradient of MeOH and obtained as a yellow solid. According to ^{1}H NMR spectrum, it consisted from thiol **321b** (7.3 mg, 34.1 μmol, 18%) and disulfide **321a** (16.7 mg, 39.3 μmol, 42%). After exposure of the product to air for one week the ratio **321a**:**321b** did not change. Further separation attempts were not successful.

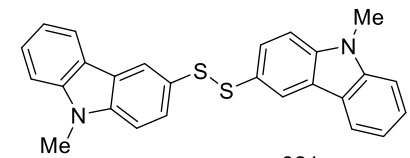

321a

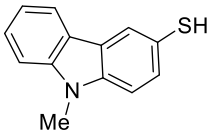

321b

^{1}H NMR (300 MHz, CD_2Cl_2, ppm) δ =3.82 (s, 2.7H, A), 3.86 (s, 0.3H, B), 7.21 (td, *J* = 1.0, 8.1 Hz, 1H), 7.32 – 7.53 (m, 3H), 7.62 (dd, *J* = 2.0, 8.4 Hz, 1H), 7.99 (dd, *J* = 1.0, 7.8 Hz, 1H), 8.10 (dd, *J* = 0.7, 1.8 Hz, 0.3H, B), 8.24 (dd, *J* = 0.7, 1.8 Hz, 0.7H, A). ^{13}C NMR (75 MHz, CD_2Cl_2, ppm) δ = 29.7, 109.2 (B), 109.4 (A), 109.7 (B), 109.7 (A), 119.5 (B), 119.9 (A), 120.9 (B), 120.9

(A), 121.6 (B), 122.7 (B), 123.9 (B), 125.0 (A), 126.6 (B), 126.8 (A), 127.4, 128.0 (B), 130.4 (A), 141.7 (A), 142.0 (A). IR (neat, cm^{-1}): 3048.8, 2924.8, 1586.8, 1474.0, 1456.1, 1420.6, 1268.0, 1243.8, 1210.1, 797.1, 742.5, 724.2, 597.4, 580.1, 563.6. HRMS of **321a**: *m*/*z* calcd. for $C_{26}H_{20}N_2S_2^+$ $[M]^+$ = 424.1062; found = 424.1060.

5.7 Dibenzothiophene studies

The following information is included for the sake of completeness of data but are not discussed in this thesis.

[5,2':8',5''-Terdibenzo[*b*,*d*]thiophene]-5,5''-diium Ditriflate (**322**):

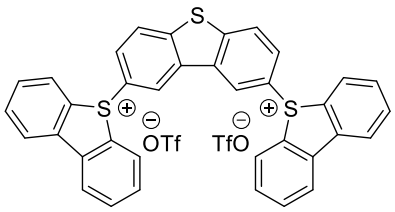

A solution of dibenzothiophene sulfoxide (300 mg, 1.50 mmol, 3.00 equiv.) in dry DCM (15 mL) was cooled to –50°C. Under stirring, a solution of triflic anhydride (252 µL, 423 mg, 1.50 mmol, 3.00 equiv.) in dry DCM (2 mL) was added dropwise over 7 min, and the orange suspension was stirred at –50°C for 4 h. A solution of 1-(trimethylsilyl)pyrrolidine (262 µL, 215 mg, 1.50 mmol, 3.00 equiv.) in dry DCN (2.0 mL) was added dropwise over 10 min. The obtained orange reaction mixture was allowed to reach –20°C within 60 min and stirred for an additional 17 h at this temperature. The white solid was filtered off and washed initially with dry DCM (2.0 mL) at –20°C, then with dry Et_2O (4 × 20 mL) and dry pentane (20 mL). The solid was dissolved in DCM (20 mL) and washed with water (10 mL). The organic layer was dried over $MgSO_4$ and concentrated *in vacuo* to obtain **322** as a white solid (101.9 mg, 120 µmol, 24%).

^{1}H NMR (400 MHz, CD_2Cl_2, ppm) δ = 7.45 (dd, *J* = 8.7, 2.0 Hz, 2H), 7.74 (td, *J* = 7.9, 1.1 Hz, 4H), 8.00 (td, *J* = 7.7, 1.0 Hz, 4H), 8.10 (d, *J* = 8.1 Hz, 4H), 8.16 (d, *J* = 8.7 Hz, 2H), 8.41 (dd, *J* = 7.9, 1.1 Hz, 4H), 8.75 (d, *J* = 2.0 Hz, 2H). ^{13}C NMR (101 MHz, CD_3CN, ppm) δ = 123.3, 124.8, 126.7, 126.7, 127.7, 128.1, 131.8, 132.0, 134.7, 135.4, 139.6, 147.0. ^{19}F NMR (282 MHz, CD_3CN, ppm) δ = –78.8. IR (neat, cm^{-}1) = 3358.4, 3112.5, 3050.8, 2995.9, 2920.7, 2867.6, 2854.1, 2826.2, 1928.5, 1893.8, 1644.0, 1598.7, 1537.0, 1517.7, 1478.2, 1457.9, 1441.5, 1426.1, 1376.0, 1346.1, 1309.4, 1263.1, 1222.6, 1152.3, 1124.3, 1104.0, 1065.5, 1024.0, 986.4, 944.0, 869.7, 857.2, 805.1, 778.1, 763.7, 740.5, 711.6, 702.0, 661.5, 636.4, 613.3, 571.8, 552.5, 540.0, 531.3, 516.8. HRMS: *m*/*z* calcd. for $C_{36}H_{22}S_2^{2+}$ $[M–2OTf]^{2+}$ = 275.0436; found = 275.0437.

1-(5*H*-Dibenzo[*b*,*d*]thiophen-5-ium-5-yl)-4-(dimethylamino)pyridin-1-ium Ditriflate (**323**):

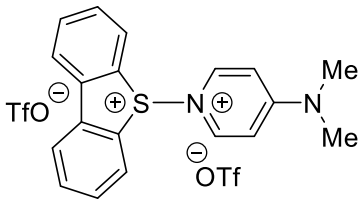

A solution of dibenzothiophene sulfoxide (300 mg, 1.50 mmol, 3.00 equiv.) in dry DCM (30 mL) was cooled to –42°C. Under stirring, a solution of triflic anhydride (239 µL, 402 mg, 1.42 mmol, 0.95 equiv.) in dry DCM (2 mL) was added dropwise over 10 min, and the orange suspension was stirred at –42°C for

6 h. A solution of DMAP (192 mg, 1.57 mmol, 1.05 equiv.) in dry DCM (7.0 mL) was added dropwise over 10 min. The obtained light orange suspension was stirred at –42°C for 15 h. The cryostat was switched off, all volatiles were removed under high vacuum over a period of 2 h and the residual orange solid ~~residue~~ was dried for an additional hour under high vacuum. Dry DCM (12 mL) was added, and the suspension was sonicated in an ultrasound bath for 1 min. The orange solution was filtered off and the residual yellow solid was washed again with dry DCM (12 mL). The precipitate was filtered off and dried for 1 h under high vacuum affording product **323** (202 mg, 334 µmol, 24%) as a yellow solid. Compound **323** is extremely moisture sensitive and was stored at –20°C.

^{1}H NMR (300 MHz, CD_3CN, ppm) δ = 3.27 (s, 6H), 6.91 (d, *J* = 7.9 Hz, 2H), 7.79 (t, *J* = 7.8 Hz, 2H), 7.90 (d, *J* = 8.1 Hz, 2H), 8.07 (d, *J* = 7.8 Hz, 2H), 8.33 (t, *J* = 8.1 Hz, 4H). ^{13}C NMR (101 MHz, CD_3CN, ppm) δ = 42.3, 111.8, 126.6, 130.1, 131.5, 133.7, 139.3, 140.5, 141.6, 158.5. ^{19}F NMR (282 MHz, CD_3CN, ppm) δ = -79.3. IR (neat, cm^{-1}) = 3266.8, 3093.3, 1645.0, 1565.9, 1444.4, 1403.9, 1270.9, 1214.0, 1171.5, 1147.4, 1059.7, 1025.0, 998.0, 943.0, 863.0, 833.1, 799.4, 780.1, 758.9, 710.6, 632.5, 587.2, 572.8, 510.1. HRMS: Neither EI-spectrometry, nor ESI-spectrometry under anhydrous condition were able to detect the product in gas phase.

2-(5H-Dibenzo[*b*,*d*]thiophen-5-ium-5-yl)-1,3-diisopropyl-4,5-dimethyl-1*H*-imidazol-3-ium Ditriflate (**324**):

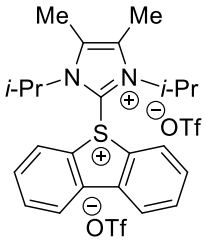

To the yellow stirred suspension of the salt **323** (139 mg, 230 µmol, 1.00 equiv.) in dry THF (5.0 mL), a solution of 1,3-diisopropyl-4,5-dimethylimidazol carbene (**81**) (45.6 mg, 253 µmol, 1.10 equiv.) in dry THF (3.0 mL) was added dropwise at –45 °C. The yellow reaction mixture was allowed to warm up to –20 °C over a period of 1 h. After stirring for an additional 30 min, the obtained white precipitate was filtered off, washed with dry THF (3.0 mL) and dried *in vacuo*. Compound **324** (30.9 mg, 46.6 µmol, 20%) was isolated as a white solid. ^{1}H NMR (400 MHz, CD_3CN, ppm) δ = 0.82 (d, *J* = 7.0 Hz, 5H), 1.96 (d, *J* = 7.0 Hz, 5H), 2.39 (s, 3H), 2.54 (s, 3H), 3.41 (hept, *J* = 7.0 Hz, 1H), 5.53 (d, *J* = 7.0 Hz, 1H), 7.79 – 7.98 (m, 2H), 8.02 – 8.15 (m, 2H), 8.24 (d, *J* = 8.3 Hz, 2H), 8.46 (d, *J* = 7.9 Hz, 2H). ^{13}C NMR (101 MHz, CD_3CN, ppm) δ = 11.3, 12.0, 19.0, 22.9, 54.5, 56.9, 123.7, 126.7, 127.3, 130.3, 133.5, 137.3, 140.1, 140.1, 140.6. ^{19}F NMR (282 MHz, CD_3CN, ppm) δ = –79.3. IR (neat, cm^{-1}) = 1587.1, 1484.0, 1450.2, 1404.9, 1380.8, 1248.7, 1222.6, 1148.4, 1090.5, 1026.9, 899.6, 799.4, 753.1, 702.0, 634.5, 572.8, 508.2. HRMS: *m*/*z* calcd. for $C_{24}H_{28}F_3N_2O_3S_2^-$ $[M–OTf]^+$ = 513.1488; found = 513.1482.

5-(3,4-Dimethoxyphenyl)-5*H*-dibenzo[*b*,*d*]thiophen-5-ium Triflate (**325**):

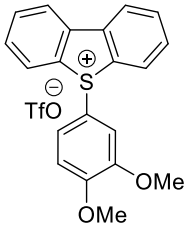

To the stirred suspension of the salt **323** (25.0 mg, 41.3 µmol, 1.00 equiv.) in dry DCM (2.0 mL), a solution of 1,2-dimethoxybenzene (6.9 mg, 49.9 µmol, 1.2 equiv.) in dry DCM (1.0 mL) was added dropwise at –40 °C. The reaction mixture was stirred at –40 °C for 23 h affording the dark blue suspension. The latter was allowed to warm up to rt, stirred for an additional 2 h and directly purified by column chromatography (DCM:MeOH), affording **325** as light yellow solid (5.0 mg, 10.6 µmol, 26%).

^{1}H NMR (400 MHz, CD_3CN, ppm) δ = 3.67 (s, 3H), 3.86 (s, 3H), 6.87 (s, 1H), 7.08 (dd, *J* = 8.8, 1.8 Hz, 1H), 7.25 (dd, *J* = 8.8, 2.4 Hz, 1H), 7.67 – 7.77 (m, 2H), 7.94 (t, *J* = 7.6 Hz, 2H), 8.02 (d, *J* = 8.1 Hz, 2H), 8.33 (d, *J* = 7.6 Hz, 2H). ^{13}C NMR (126 MHz, CD_3CN, ppm) δ = 57.0, 57.1, 112.9, 114.1, 125.5, 126.6, 128.7, 132.6, 133.3, 135.3, 140.1. ^{19}F NMR (282 MHz, CD_3CN, ppm) δ = -79.4. IR (neat, cm^{-1}) = 2917.8, 2359.5, 1586.2, 1508.1, 1449.2, 1340.3, 1260.3, 1224.6, 1147.4, 1086.7, 1029.8, 1013.4, 807.1, 756.9, 705.8, 637.4, 572.8, 516.8. HRMS: *m*/*z* calcd. for $C_{20}H_{17}O_2S^+$ $[M–OTf]^+$ = 321.0944; found 321.0949.

5-(1-Methyl-1*H*-indol-3-yl)-5*H*-dibenzo[*b*,*d*]thiophen-5-ium Triflate (**326**):

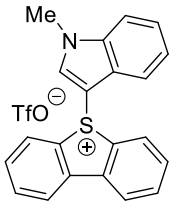

To the stirred suspension of the salt **323** (50.0 mg, 82.7 µmol, 1.00 equiv.) in dry DCM (2.5 mL), a solution of methylindole (12.7 µL, 13.0 mg, 99.1 µmol, 1.20 equiv.) in dry DCM (1.0 mL) was added dropwise at – 40 °C. The reaction mixture was stirred at this temperature for an additional 23 h affording the white suspension. The latter was allowed to warm up to rt, stirred for 2 h more and directly purified by column chromatography (DCM:MeOH) affording **326** as a white solid (6.0 mg, 12.9 µmol, 16%).

^{1}H NMR (400 MHz, CD_3CN, ppm) δ 3.97 (s, 3H), 6.21 (d, *J* = 8.1 Hz, 1H), 6.90 (t, *J* = 7.7 Hz, 1H), 7.29 (t, *J* = 7.8 Hz, 1H), 7.58 (d, *J* = 8.4 Hz, 1H), 7.68 (t, *J* = 7.8 Hz, 2H), 7.87 – 8.00 (m, 4H), 8.39 (d, *J* = 7.8 Hz, 2H), 8.48 (s, 1H). ^{13}C NMR (126 MHz, CD_3CN, ppm) δ = 35.0, 113.4, 118.0, 124.2, 125.2, 125.6, 128.2, 132.4, 135.0, 139.8, 143.3 ^{19}F NMR (282 MHz, CD_3CN, ppm) δ = –79.3. IR (neat, cm^{-1}) = 1577.5, 1518.7, 1483.0, 1452.1, 1421.3, 1381.7, 1261.2, 1223.6, 1157.1, 1132.0, 1055.8, 1029.8, 976.8, 758.9, 744.4, 708.7, 636.4, 594.0, 572.8, 559.3, 516.8. HRMS: *m*/*z* calcd. for $C_{21}H_{16}NS^+$ $[M–OTf]^+$ = 314.0998; found 314.0996.

1,3-Diisopropyl-4,5-dimethyl-1*H*-imidazol-3-ium-2-ide (**81**):

Carbene **81** was synthesized following a modified protocol of M. S. Sanford *et al.*[307]

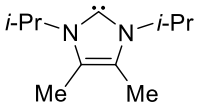

Potassium (1.49 g, 38.2 mmol, 2,50 equiv.) was placed in a three-neck flask and washed with dry pentane (2 × 10 mL) to remove residual mineral oil. Afterwards, dry THF (90 mL) was added followed by 1,3-diisopropyl-4,5-dimethyl-2(3*H*)-imidazolethione (**78**) (3.23 g, 15.2 mmol, 1.00 equiv.). The reaction mixture was vigorously stirred at 84 °C for 4 h. The resulting blue suspension was allowed to cool down to rt and filtered through a pad of *Celite*®. All volatiles were removed under reduced pressure and pure **81** (2.11 g, 11.6 mmol, 77%) was isolated as a white solid, which was kept at –20 °C.

^{1}H NMR (300 MHz, C_6D_6, ppm) δ 1.51 (d, *J* = 6.5 Hz, 12H), 1.73 (s, 6H), 3.95 (hept, *J* = 6.6 Hz, 2H).

Spectral properties were identically to those reported in the literature.[307]

2-(2-Bromophenyl)pyridine (**327**):

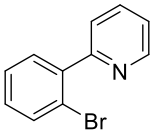

327 was synthesized following a modified protocol of A. Togni *et al.*[308]

N-Bromosuccinimide (979 mg, 5.50 mmol, 1.10 equiv.) and palladium(II) acetate (202 mg, 900 µmol, 16 mol%) were dissolved in dry MeCN (25 mL). A solution of 2-phenylpyridine (715 µL, 776 mg, 5.00 mmol, 1.00 equiv.) in MeCN (2 mL) was added dropwise, and the suspension was stirred at 100°C for 48 h. The orange reaction mixture was allowed to reach rt, and the orange solution was filtered off. The residual white solid was washed with MeCN (10 mL), and the combined organic phases were dried over $MgSO_4$. All volatiles were removed under reduced pressure, and the obtained orange oil was purified by column chromatography (cyclohexane:EtOAc). Compound **327** was isolated as a slightly yellow oil (737 mg, 3.15 mmol, 63%).

^{1}H NMR (300 MHz, $CDCl_3$, ppm) δ = 7.22 – 7.34 (m, 2H), 7.41 (td, *J* = 7.5, 1.2 Hz, 1H), 7.54 (dd, *J* = 7.7, 1.8 Hz, 1H), 7.60 (d, *J* = 7.9 Hz, 1H), 7.68 (dd, *J* = 8.0, 1.2 Hz, 1H), 7.77 (d, *J* = 1.8 Hz, 1H), 8.72 (d, *J* = 4.9 Hz, 1H). ^{13}C NMR (126 MHz, $CDCl_3$, ppm) δ = 122.6, 124.9, 127.7, 129.8, 131.6, 133.4, 135.9, 149.6. IR (neat, cm^{-1}) = 1591.0, 1582.3, 1566.9, 1480.1, 1457.0, 1437.7, 1418.4, 1299.8, 1149.4, 1093.4, 1077.0, 1046.2, 1025.9, 1015.3, 989.3, 789.7, 745.4, 666.3, 632.5, 614.2, 555.4, 527.4. HRMS: *m*/*z* calcd. for $C_{11}H_9NBr$ $[M+H]^+$ = 233.9913; found 233.9912.

2-[2-(Trimethylsilyl)phenyl]pyridine (**328**):

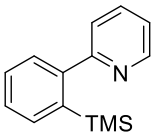

Compound **327** (520 mg, 2.22 mmol, 1.00 equiv.) was dissolved in dry THF (20 mL) and cooled to –78 °C. *sec*-Buthyllithium (1.4M in THF, 2.38 mL, 3.33 mmol, 1.50 equiv.) was added dropwise within 5 min. After 25 min, no **327** was detectable by GC-MS. TMSCl (761 µL, 652 mg, 6.00 mmol, 2.70 equiv.) was added dropwise within 5 min. The dark red solution was allowed to warm up to –15°C within 1 h. After an additional stirring for 24 h, sat. NH_4Cl solution (10 mL) was added to the white suspension. The phases were separated, and the aqueous layer was extracted with Et_2O (2 × 20 mL). The combined organic phases were dried over $MgSO_4$ and all volatiles were removed under reduced pressure. The obtained crude product was purified by column chromatography (cyclohexane:EtOAc) to obtain **328** as colorless oil (490 mg, 2.15 mmol, 97%).

^{1}H NMR (400 MHz, $CDCl_3$ ppm) δ = 0.08 (s, 9H), 7.23 – 7.29 (m, 1H), 7.37 – 7.52 (m, 4H), 7.69 – 7.77 (m, 2H), 8.64 (ddd, *J* = 4.9, 1.8, 1.0 Hz, 1H). ^{13}C NMR (101 MHz, $CDCl_3$, ppm) δ = 1.0, 122.1, 123.1, 127.6, 128.7, 128.9, 135.6, 136.5, 139.5, 147.2, 148.6, 161.5. IR (neat, cm^{-1}) = 1586.2, 1568.8, 1557.2, 1477.2, 1466.6, 1424.2, 1241.9, 1150.3, 1123.3, 1101.2, 1021.1, 833.1, 798.4, 767.5, 746.3, 727.0, 680.7, 634.5, 622.9, 615.2, 557.3. HRMS: *m*/*z* calcd. for $C_{14}H_{18}NSi^+$ $[M+H]^+$ = 228.1203; found 228.1203.

Note:

Attempts to perform a Br-Mg exchange using *i*-PrMgBr (1.30 equiv.) in dry Et_2O at –78°C were not successful. GC-MS analysis of the reaction mixture indicated no metalation of **327**.

5.8 Crystal structures

5.8.1 Structure of reagents

Structure 91

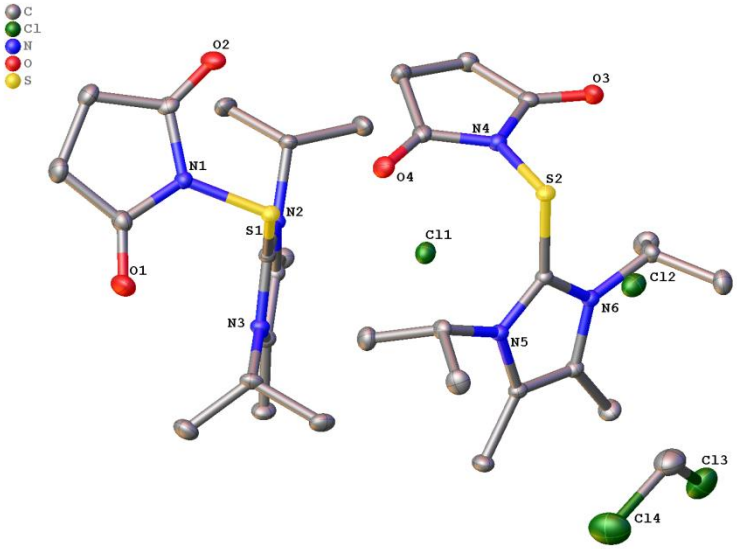

Figure S1: Asymmetric unit of **91**.

CSD code	1843380
Empirical formula	$C_{31}H_{50}Cl_4N_6O_4S_2$
Formula weight	776.69
Temperature/K	100(2)
Crystal system	triclinic
Space group	P-1
a/Å	9.2375(7)
b/Å	12.5810(12)
c/Å	16.6226(17)
α/°	94.204(4)
β/°	90.453(3)
γ/°	102.479(3)
Volume/Å^3	1880.6(3)
Z	2
ρ_{calc}g/cm^3	1.372
μ/mm^{-1}	0.469
F(000)	820.0
Crystal size/mm^3	0.284 × 0.177 × 0.05
Radiation	MoKα (λ = 0.71073)
2Θ range for data collection/°	4.284 to 63.122
Index ranges	-13 ≤ h ≤ 13, -18 ≤ k ≤ 18, -24 ≤ l ≤ 24
Reflections collected	73341
Independent reflections	12576 [R_{int} = 0.0317, R_{sigma} = 0.0221]
Data/restraints/parameters	12576/0/436
Goodness-of-fit on F^2	1.038
Final R indexes [I>=2σ (I)]	R_1 = 0.0304, wR_2 = 0.0748
Final R indexes [all data]	R_1 = 0.0366, wR_2 = 0.0785
Largest diff. peak/hole / e Å^{-3}	0.58/-0.65

Structure 94

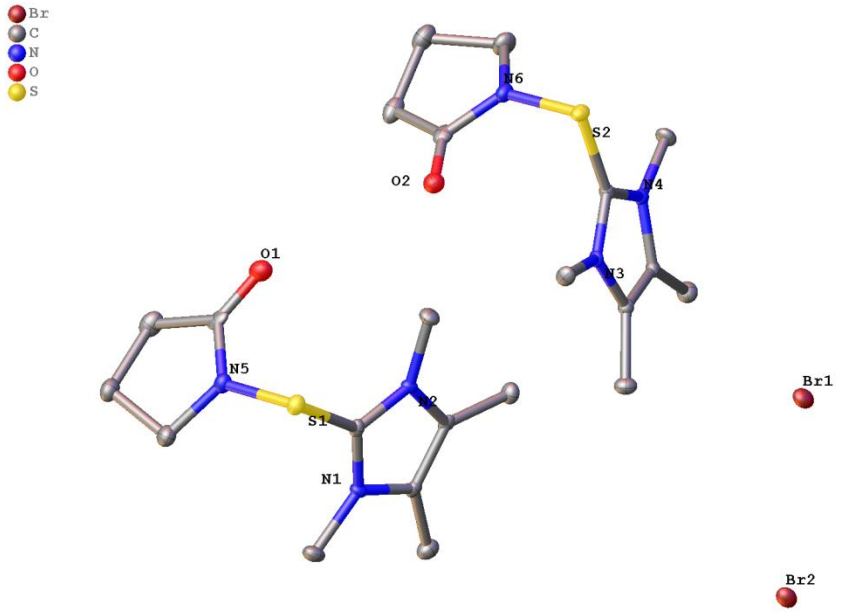

Figure S2: Asymmetric unit of **94**.

Empirical formula	$C_{11}H_{18}BrN_3OS$
Formula weight	320.25
Temperature/K	106(2)
Crystal system	monoclinic
Space group	$P2_1$
a/Å	7.4262(2)
b/Å	11.3331(3)
c/Å	16.0948(5)
α/°	90
β/°	100.078(2)
γ/°	90
Volume/Å^3	1333.67(7)
Z	4
ρ_{calc}g/cm^3	1.595
μ/mm^{-1}	3.228
F(000)	656.0
Crystal size/mm^3	0.233 × 0.232 × 0.110
Radiation	MoKα (λ = 0.71073)
2Θ range for data collection/°	4.42 to 61.14
Index ranges	-10 ≤ h ≤ 10, -16 ≤ k ≤ 16, -23 ≤ l ≤ 23
Reflections collected	42209
Independent reflections	8187 [R_{int} = 0.0748, R_{sigma} = 0.0646]
Data/restraints/parameters	8187/1/316
Goodness-of-fit on F^2	1.009
Final R indexes [I>=2σ (I)]	R_1 = 0.0342, wR_2 = 0.0478
Final R indexes [all data]	R_1 = 0.0582, wR_2 = 0.0526
Largest diff. peak/hole / e Å^{-3}	0.40/-0.48
Flack parameter	0.359(6)

Structure 90

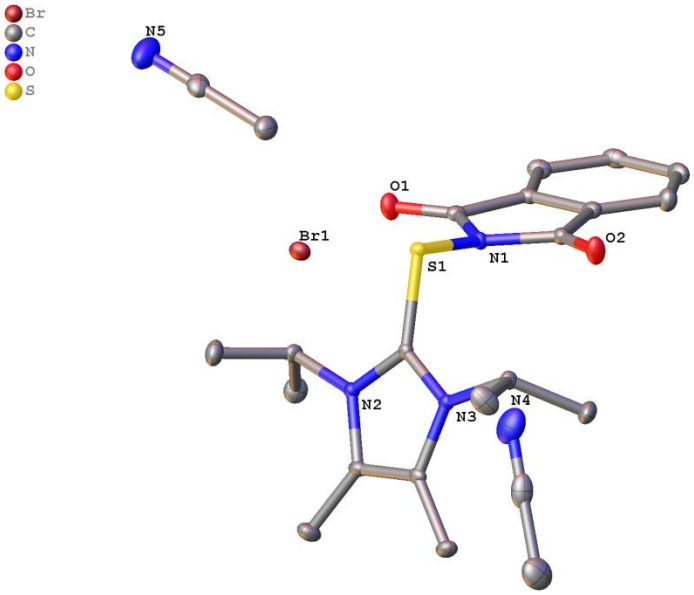

Figure S3: Asymmetric unit of **90** containing two MeCN molecules.

The short S1-Br1 distance of 3.177Å indicates a strong interaction between the cationic sulfide and the anion.

Empirical formula	$C_{23}H_{30}BrN_5O_2S$
Formula weight	520.49
Temperature/K	104(2)
Crystal system	orthorhombic
Space group	Pbca
a/Å	11.6964(6)
b/Å	20.2093(10)
c/Å	20.8590(10)
α/°	90
β/°	90
γ/°	90
Volume/Å^3	4930.6(4)
Z	8
ρ_{calc}g/cm^3	1.402
μ/mm^{-1}	1.781
F(000)	2160.0
Crystal size/mm^3	0.222 × 0.219 × 0.092
Radiation	MoKα (λ = 0.71073)
2Θ range for data collection/°	4.03 to 61.016
Index ranges	-16 ≤ h ≤ 16, -28 ≤ k ≤ 28, -29 ≤ l ≤ 29
Reflections collected	279010
Independent reflections	7531 [R_{int} = 0.1299, R_{sigma} = 0.0313]
Data/restraints/parameters	7531/0/297
Goodness-of-fit on F^2	1.045
Final R indexes [I>=2σ (I)]	R_1 = 0.0351, wR_2 = 0.0576
Final R indexes [all data]	R_1 = 0.0593, wR_2 = 0.0640
Largest diff. peak/hole / e Å^{-3}	0.41/-0.41

5.8.2 Structure of backbone derivatives

Structure 107b

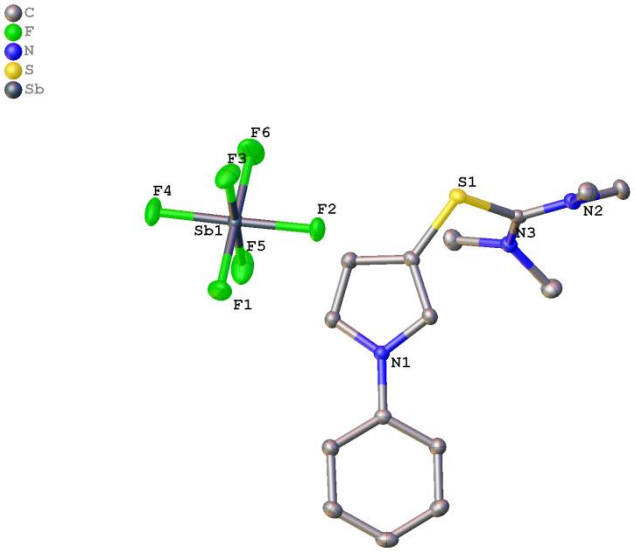

Figure S4: Asymmetric unit of **107b**.

Empirical formula	$C_{15}H_{20}F_6N_3SSb$
Formula weight	510.15
Temperature/K	120(2)
Crystal system	monoclinic
Space group	$P2_1/n$
a/Å	8.6111(3)
b/Å	17.8265(7)
c/Å	12.2312(5)
α/°	90
β/°	94.297(2)
γ/°	90
Volume/Å^3	1872.28(12)
Z	4
ρ_{calc}g/cm^3	1.810
μ/mm^{-1}	1.646
F(000)	1008.0
Crystal size/mm^3	0.2 × 0.1 × 0.05
Radiation	MoKα (λ = 0.71073)
2Θ range for data collection/°	5.266 to 59.998
Index ranges	-11 ≤ h ≤ 12, -25 ≤ k ≤ 25, -17 ≤ l ≤ 17
Reflections collected	58949
Independent reflections	5425 [R_{int} = 0.0339, R_{sigma} = 0.0158]
Data/restraints/parameters	5425/0/239
Goodness-of-fit on F^2	1.074
Final R indexes [I>=2σ (I)]	R_1 = 0.0179, wR_2 = 0.0396
Final R indexes [all data]	R_1 = 0.0225, wR_2 = 0.0435
Largest diff. peak/hole / e Å^{-3}	0.40/-0.60

Structure 107a

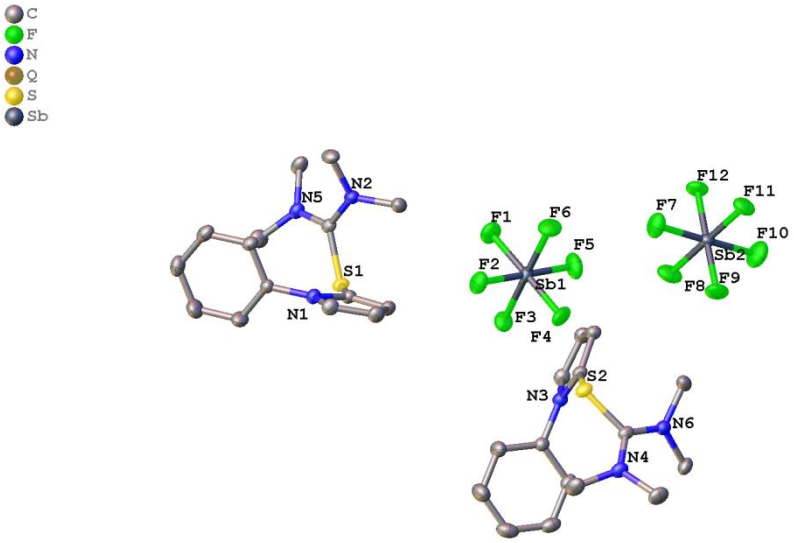

Figure S5: Asymmetric unit of **107a**.

Empirical formula	$C_{15}H_{20}F_6N_3SSb$
Formula weight	510.15
Temperature/K	120(2)
Crystal system	monoclinic
Space group	$P2_1/c$
a/Å	16.7471(6)
b/Å	11.4907(4)
c/Å	20.3725(7)
α/°	90
β/°	99.8340(10)
γ/°	90
Volume/Å^3	3862.8(2)
Z	8
ρ_{calc}g/cm^3	1.754
μ/mm^{-1}	1.596
F(000)	2016.0
Crystal size/mm^3	0.404 × 0.218 × 0.15
Radiation	MoKα (λ = 0.71073)
2Θ range for data collection/°	4.058 to 66.328
Index ranges	-25 ≤ h ≤ 25, -17 ≤ k ≤ 17, -31 ≤ l ≤ 31
Reflections collected	198418
Independent reflections	14734 [R_{int} = 0.0372, R_{sigma} = 0.0161]
Data/restraints/parameters	14734/0/477
Goodness-of-fit on F^2	0.917
Final R indexes [I>=2σ (I)]	R_1 = 0.0273, wR_2 = 0.0793
Final R indexes [all data]	R_1 = 0.0391, wR_2 = 0.0999
Largest diff. peak/hole / e Å^{-3}	1.17/-2.67

Structure 310

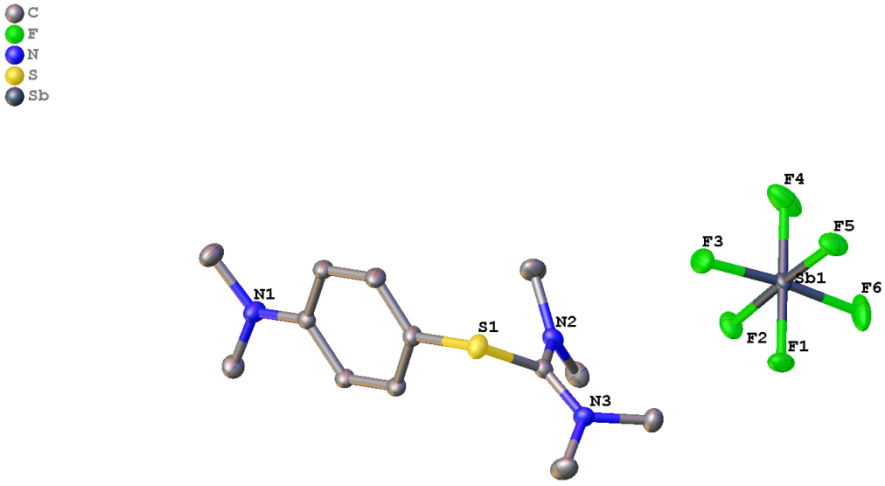

Figure S6: Asymmetric unit of **310**.

Empirical formula	$C_{13}H_{22}F_6N_3SSb$
Formula weight	488.14
Temperature/K	120(2)
Crystal system	triclinic
Space group	P-1
a/Å	8.6347(4)
b/Å	10.4132(6)
c/Å	11.7499(6)
α/°	109.832(2)
β/°	95.488(2)
γ/°	109.583(2)
Volume/Å^3	909.85(8)
Z	2
ρ_{calc}g/cm^3	1.782
μ/mm^{-1}	1.689
F(000)	484.0
Crystal size/mm^3	0.146 × 0.121 × 0.095
Radiation	MoKα (λ = 0.71073)
2Θ range for data collection/°	4.522 to 72.904
Index ranges	-14 ≤ h ≤ 14, -17 ≤ k ≤ 17, -19 ≤ l ≤ 19
Reflections collected	71029
Independent reflections	8893 [R_{int} = 0.0353, R_{sigma} = 0.0215]
Data/restraints/parameters	8893/0/223
Goodness-of-fit on F^2	1.354
Final R indexes [I>=2σ (I)]	R_1 = 0.0245, wR_2 = 0.0722
Final R indexes [all data]	R_1 = 0.0331, wR_2 = 0.0967
Largest diff. peak/hole / e Å^{-3}	1.24/-1.52

Structure 111

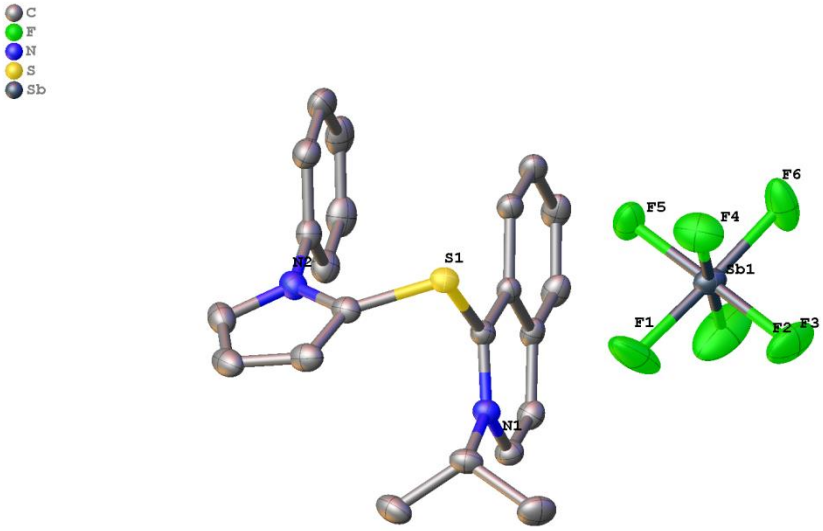

Figure S7: Asymmetric unit of **111.**

Empirical formula	$C_{22}H_{21}F_6N_2SSb$
Formula weight	581.22
Temperature/K	100(2)
Crystal system	monoclinic
Space group	$P2_1/n$
a/Å	15.2643(5)
b/Å	9.7130(3)
c/Å	15.4112(5)
α/°	90
β/°	103.5930(10)
γ/°	90
Volume/Å^3	2220.90(12)
Z	4
ρ_{calc}g/cm^3	1.738
μ/mm^{-1}	1.399
F(000)	1152.0
Crystal size/mm^3	0.304 × 0.304 × 0.056
Radiation	MoKα (λ = 0.71073)
2Θ range for data collection/°	4.998 to 65.172
Index ranges	-23 ≤ h ≤ 19, -14 ≤ k ≤ 14, -23 ≤ l ≤ 22
Reflections collected	28007
Independent reflections	8089 [R_{int} = 0.0203, R_{sigma} = 0.0208]
Data/restraints/parameters	8089/0/292
Goodness-of-fit on F^2	1.035
Final R indexes [I>=2σ (I)]	R_1 = 0.0314, wR_2 = 0.0763
Final R indexes [all data]	R_1 = 0.0359, wR_2 = 0.0795
Largest diff. peak/hole / e Å^{-3}	1.50/-1.24

Structure 112

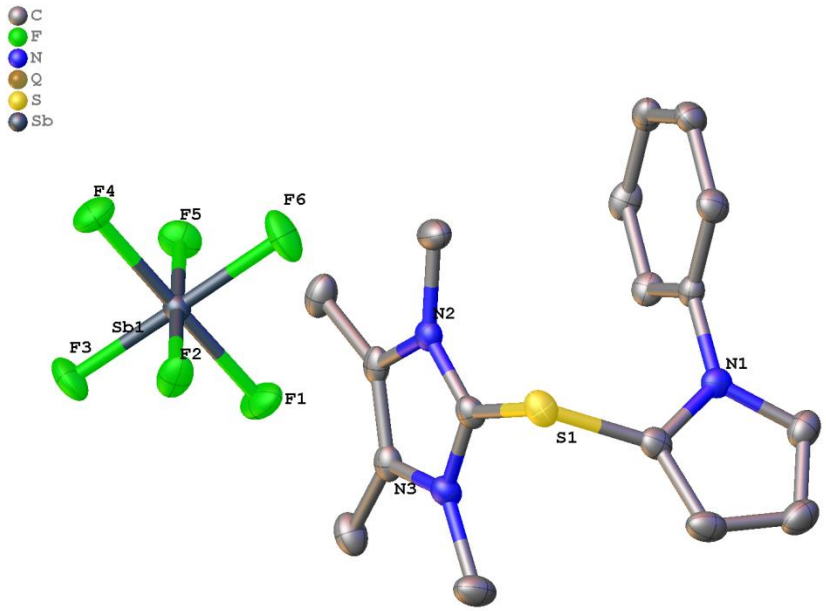

Figure S8: Asymmetric unit of **112.**

Empirical formula	CHNFSSb
Formula weight	199.84
Temperature/K	100(2)
Crystal system	monoclinic
Space group	$P2_1/c$
a/Å	12.2043(5)
b/Å	9.1873(4)
c/Å	18.8925(10)
α/°	90
β/°	105.750(2)
γ/°	90
Volume/Å^3	2038.78(16)
Z	19
ρ_{calc}g/cm^3	3.093
μ/mm^{-1}	6.743
F(000)	1710.0
Crystal size/mm^3	0.210 × 0.300 × 0.150
Radiation	MoKα (λ = 0.71073)
2Θ range for data collection/°	4.48 to 56.654
Index ranges	-16 ≤ h ≤ 16, -12 ≤ k ≤ 12, -25 ≤ l ≤ 23
Reflections collected	36353
Independent reflections	5079 [R_{int} = 0.0463, R_{sigma} = 0.0266]
Data/restraints/parameters	5079/0/257
Goodness-of-fit on F^2	1.066
Final R indexes [I>=2σ (I)]	R_1 = 0.0217, wR_2 = 0.0428
Final R indexes [all data]	R_1 = 0.0307, wR_2 = 0.0464
Largest diff. peak/hole / e Å^{-3}	0.68/-0.47

Structure 104

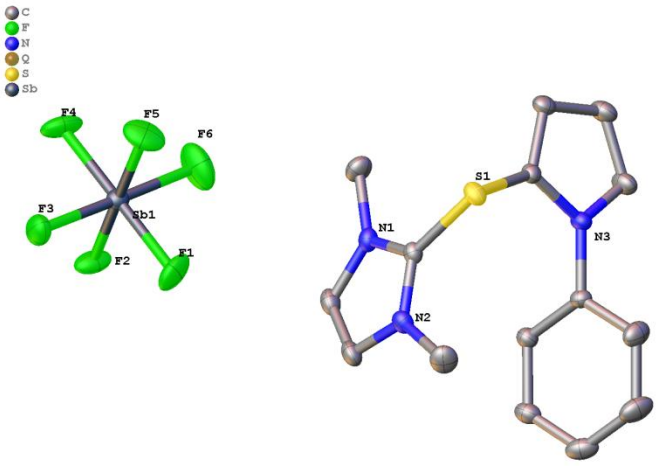

Figure S9: Asymmetric unit of **104.**

Empirical formula	CHNFSSb
Formula weight	199.84
Temperature/K	100(2)
Crystal system	monoclinic
Space group	$P2_1/c$
a/Å	8.8256(4)
b/Å	17.4237(7)
c/Å	11.9860(5)
α/°	90
β/°	92.419(2)
γ/°	90
Volume/Å^3	1841.50(14)
Z	17
ρ_{calc}g/cm^3	3.063
μ/mm^{-1}	6.679
F(000)	1530.0
Crystal size/mm^3	0.454 × 0.297 × 0.21
Radiation	MoKα (λ = 0.71073)
2Θ range for data collection/°	4.128 to 61.092
Index ranges	-12 ≤ h ≤ 12, -24 ≤ k ≤ 24, -17 ≤ l ≤ 17
Reflections collected	56424
Independent reflections	5612 [R_{int} = 0.0437, R_{sigma} = 0.0185]
Data/restraints/parameters	5612/0/237
Goodness-of-fit on F^2	1.089
Final R indexes [I>=2σ (I)]	R_1 = 0.0227, wR_2 = 0.0475
Final R indexes [all data]	R_1 = 0.0272, wR_2 = 0.0495
Largest diff. peak/hole / e Å^{-3}	0.53/-0.77

Structure 108

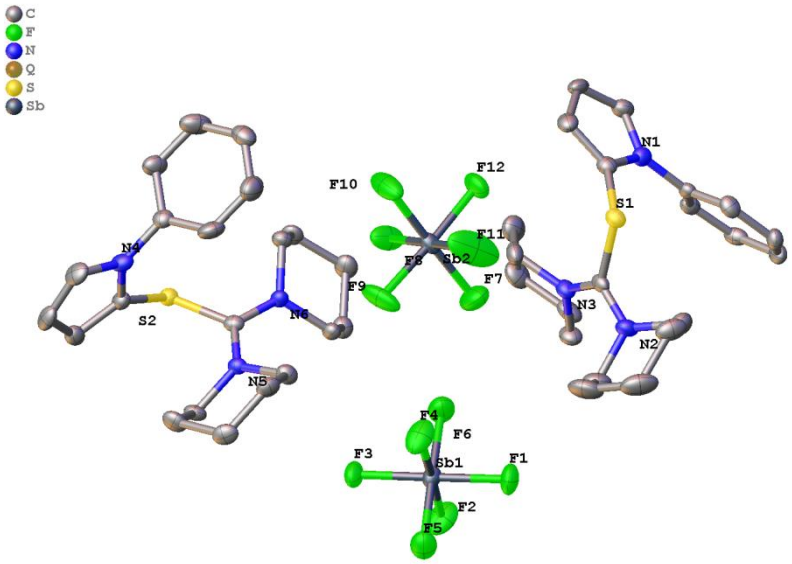

Figure S10: Asymmetric unit of **108**.

The crystal was poorly diffracting and decomposes on the loop over time. Therefore, the completeness of the data set is low (90%). Attempts to grow bigger crystals and repeating of the diffraction experiment have not been successful.

Empirical formula	CHNFSSb
Formula weight	199.84
Temperature/K	100(2)
Crystal system	triclinic
Space group	P-1
a/Å	10.8894(5)
b/Å	11.1177(4)
c/Å	22.5424(9)
α/°	91.8960(10)
β/°	100.3580(10)
γ/°	117.1570(10)
Volume/Å^3	2367.90(17)
Z	22
ρ_{calc}g/cm^3	3.083
μ/mm^{-1}	6.722
F(000)	1980.0
Crystal size/mm^3	0.099 × 0.132 × .0.241
Radiation	MoKα (λ = 0.71073)
2Θ range for data collection/°	4.154 to 48.81
Index ranges	-12 ≤ h ≤ 12, -11 ≤ k ≤ 12, -23 ≤ l ≤ 26
Reflections collected	12766
Independent reflections	7014 [R_{int} = 0.0295, R_{sigma} = 0.0469]
Data/restraints/parameters	7014/0/577
Goodness-of-fit on F^2	1.031
Final R indexes [I>=2σ (I)]	R_1 = 0.0330, wR_2 = 0.0813
Final R indexes [all data]	R_1 = 0.0408, wR_2 = 0.0877
Largest diff. peak/hole / e Å^{-3}	0.89/-0.72

5.8.3 Structure of arylthioimidazolium salts

Structure 113

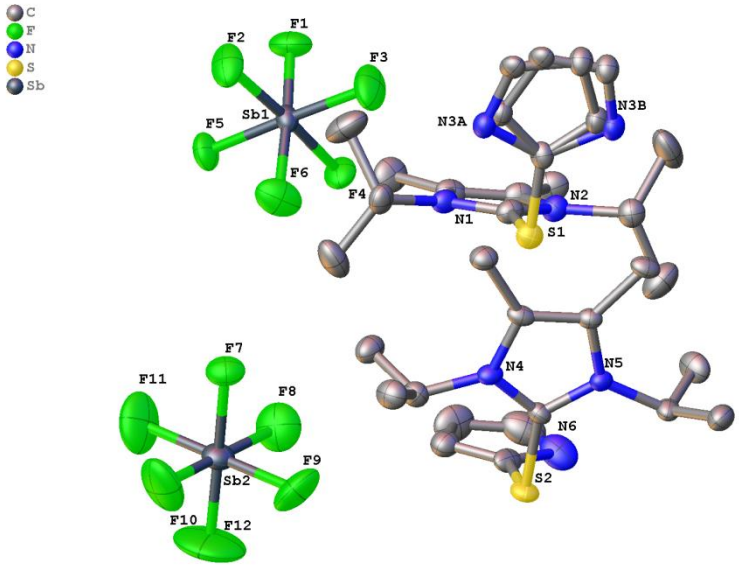

Figure S11: Asymmetric unit of **113.**

The pyrrole ring in one of the two molecules disordered about two positions. They were refined with distance restraints and restraints for the anisotropic displacement parameters. The occupancy of the minor position including N3A was refined to 0.46525.

CSD code	1842214
Empirical formula	$C_{15}H_{23}F_6N_3SSb$
Formula weight	513.17
Temperature/K	100(2)
Crystal system	triclinic
Space group	P-1
a/Å	10.6342(8)
b/Å	13.9433(11)
c/Å	15.3612(12)
α/°	80.585(3)
β/°	69.903(3)
γ/°	67.620(3)
Volume/Å^3	1976.5(3)
Z	4
ρ_{calc}g/cm^3	1.725
μ/mm^{-1}	1.560
F(000)	1020.0
Crystal size/mm^3	0.458 × 0.218 × 0.118
Radiation	MoKα (λ = 0.71073)
2Θ range for data collection/°	5.964 to 56
Index ranges	-12 ≤ h ≤ 14, -17 ≤ k ≤ 18, 0 ≤ l ≤ 20
Reflections collected	9134
Independent reflections	9134 [R_{sigma} = 0.0418]
Data/restraints/parameters	9134/20/495
Goodness-of-fit on F^2	1.061
Final R indexes [I>=2σ (I)]	R_1 = 0.0454, wR_2 = 0.1160
Final R indexes [all data]	R_1 = 0.0470, wR_2 = 0.1174
Largest diff. peak/hole / e Å^{-3}	1.84/-1.94

Structure 114

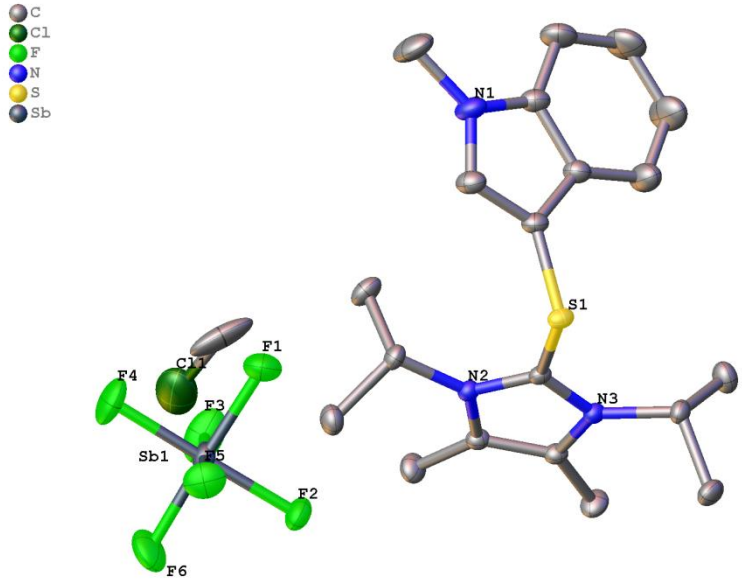

Figure S12: Asymmetric unit of **114** including a molecule dichloromethane.

CSD code	1842208
Empirical formula	$C_{21}H_{30}ClF_6N_3SSb$
Formula weight	627.74
Temperature/K	100(2)
Crystal system	triclinic
Space group	P-1
a/Å	8.6895(7)
b/Å	10.6326(8)
c/Å	14.2624(12)
α/°	103.338(3)
β/°	102.901(3)
γ/°	92.570(3)
Volume/Å^3	1243.36(17)
Z	2
ρ_{calc}g/cm^3	1.677
μ/mm^{-1}	1.361
F(000)	630.0
Crystal size/mm^3	0.448 × 0.32 × 0.028
Radiation	MoKα (λ = 0.71073)
2Θ range for data collection/°	4.346 to 59.198
Index ranges	-12 ≤ h ≤ 12, -14 ≤ k ≤ 14, -19 ≤ l ≤ 19
Reflections collected	42400
Independent reflections	6985 [R_{int} = 0.0206, R_{sigma} = 0.0146]
Data/restraints/parameters	6985/0/305
Goodness-of-fit on F^2	1.058
Final R indexes [I>=2σ (I)]	R_1 = 0.0291, wR_2 = 0.0808
Final R indexes [all data]	R_1 = 0.0298, wR_2 = 0.0815
Largest diff. peak/hole / e Å^{-3}	1.13/-1.94

Structure 99

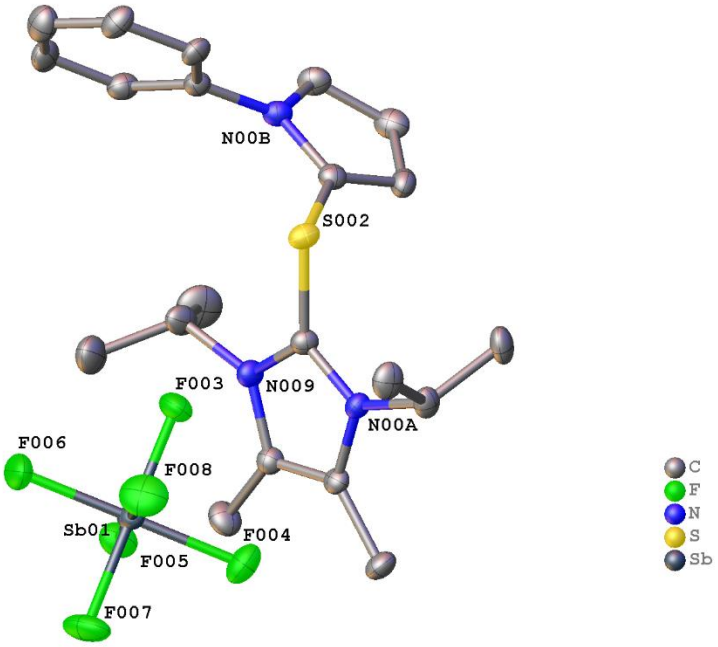

Figure S13: Asymmetric unit of **99**.

Empirical formula	$C_{21}H_{29}F_6N_3SSb$
Formula weight	591.28
Temperature/K	100.
Crystal system	monoclinic
Space group	$P2_1/n$
a/Å	10.4709(4)
b/Å	22.2447(7)
c/Å	10.8000(4)
α/°	90
β/°	99.9630(10)
γ/°	90
Volume/Å^3	2477.62(15)
Z	4
ρ_{calc}g/cm^3	1.585
μ/mm^{-1}	1.256
F(000)	1188.0
Crystal size/mm^3	? × ? × ?
Radiation	MoKα (λ = 0.71073)
2Θ range for data collection/°	5.004 to 59.28
Index ranges	-14 ≤ h ≤ 13, -26 ≤ k ≤ 29, -14 ≤ l ≤ 14
Reflections collected	16803
Independent reflections	5563 [R_{int} = 0.0381, R_{sigma} = 0.0393]
Data/restraints/parameters	5563/0/295
Goodness-of-fit on F^2	1.210
Final R indexes [I>=2σ (I)]	R_1 = 0.0279, wR_2 = 0.0791
Final R indexes [all data]	R_1 = 0.0375, wR_2 = 0.1069
Largest diff. peak/hole / e Å^{-3}	0.83/-1.18

Structure 100

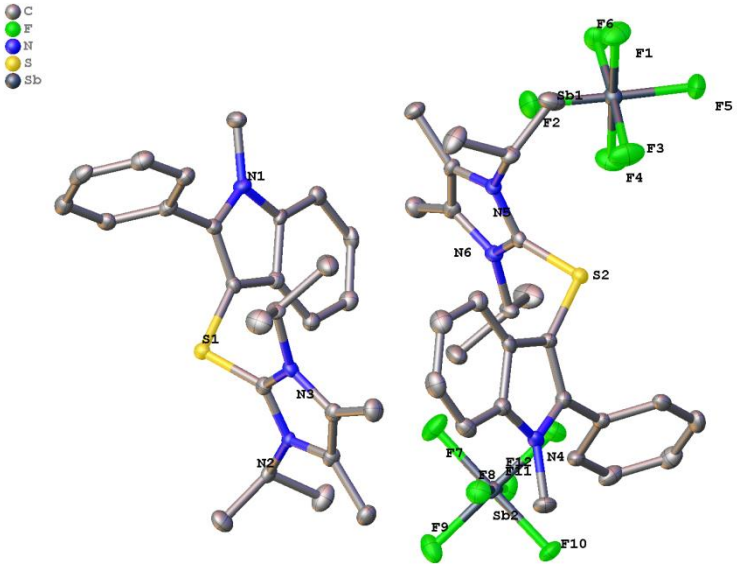

Figure S14: Asymmetric unit of **100**.

CSD code	1842198
Empirical formula	$C_{26}H_{32}F_6N_3SSb$
Formula weight	654.35
Temperature/K	100(2)
Crystal system	orthorhombic
Space group	P n a 2_1
a/Å	16.992(3)
b/Å	14.219(2)
c/Å	22.529(3)
α/°	90
β/°	90
γ/°	90
Volume/Å^3	5443.4(14)
Z	8
ρ_{calc}g/cm^3	1.597
μ/mm^{-1}	1.152
F(000)	2640
Crystal size/mm^3	0.19 × 0.100 × 0.060
Radiation	MoKα (λ = 0.71073)
2Θ range for data collection/°	3.106 to 28.283
Index ranges	-22 ≤ h ≤ 22, -18 ≤ k ≤ 18, -30 ≤ l ≤ 30
Reflections collected	121075
Independent reflections	13511 [R_{int} = 0.1455; R_{sigma} = 0.0807]
Data/restraints/parameters	13511/1/682
Goodness-of-fit on F^2	1.058
Final R indexes [I>=2σ (I)]	R_1 = 0.0434, wR_2 = 0.0913
Final R indexes [all data]	R_1 = 0.0564, wR_2 = 0.0973
Largest diff. peak/hole / e Å^{-3}	1.066/-0.734

Structure 115

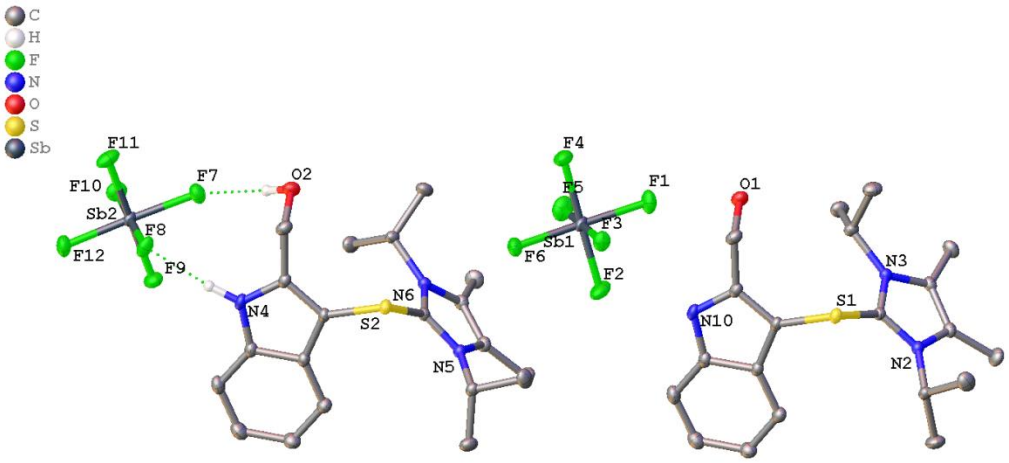

Figure S15: Asymmetric unit of **115**.

Both molecules in the asymmetric unit of 115 exhibited hydrogen bonds between the OH/NH and the flour atom of the anion. For clarity, the interaction is only shown once in Figure S15. The hydrogen bond between F7 and O2 leads to an elongation of the Sb2-F7 which results in a bond length of 1.8846(7)Å. In case of Sb2-F8, elongated by the NH, the bond length is 1.8923(7)Å. Both bonds are significant longer than the average axial Sb-F bonds of both anions (1.8718[7]Å).

CSD code	1842205
Empirical formula	$C_{20}H_{28}F_6N_3OSSb$
Formula weight	594.26
Temperature/K	100(2)
Crystal system	triclinic
Space group	P-1
a/Å	11.3916(4)
b/Å	12.0591(5)
c/Å	18.7226(7)
α/°	79.9640(10)
β/°	77.9580(10)
γ/°	70.4490(10)
Volume/Å^3	2355.08(16)
Z	4
ρ_{calc}g/cm^3	1.676
μ/mm^{-1}	1.325
F(000)	1192.0
Crystal size/mm^3	0.279 × 0.272 × 0.169
Radiation	MoKα (λ = 0.71073)
2Θ range for data collection/°	4.382 to 63.022
Index ranges	-15 ≤ h ≤ 16, -17 ≤ k ≤ 17, -27 ≤ l ≤ 27
Reflections collected	38257
Independent reflections	15617 [R_{int} = 0.0144, R_{sigma} = 0.0178]
Data/restraints/parameters	15617/4/601
Goodness-of-fit on F^2	1.063
Final R indexes [I>=2σ (I)]	R_1 = 0.0177, wR_2 = 0.0439
Final R indexes [all data]	R_1 = 0.0192, wR_2 = 0.0447
Largest diff. peak/hole / e Å^{-3}	0.47/-0.55

Structure 117

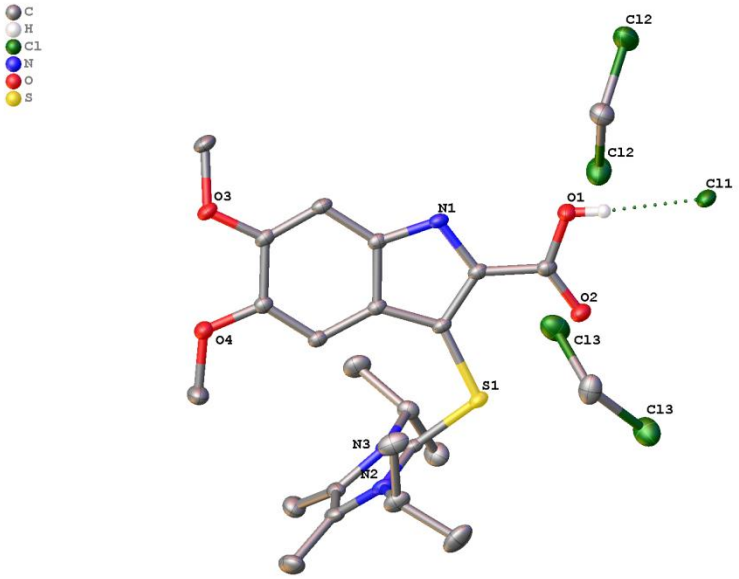

Figure S16: Asymmetric unit of **117** containing two dichloromethane molecules.

117 shows hydrogen bond interaction between the COOH (O1) and the chloride (Cl1). The distance between O1 and Cl1 is 2.97575(13)Å.

CSD code	1842207
Empirical formula	$C_{23}H_{32}Cl_3N_3O_4S$
Formula weight	552.92
Temperature/K	100(2)
Crystal system	monoclinic
Space group	C2/c
a/Å	18.565(4)
b/Å	24.465(5)
c/Å	12.017(3)
α/°	90
β/°	101.886(6)
γ/°	90
Volume/Å^3	5341.1(19)
Z	8
ρ_{calc}g/cm^3	1.375
μ/mm^{-1}	0.455
F(000)	2320.0
Crystal size/mm^3	0.135 × 0.068 × 0.022
Radiation	MoKα (λ = 0.71073)
2Θ range for data collection/°	4.484 to 59.236
Index ranges	-25 ≤ h ≤ 25, -34 ≤ k ≤ 34, -15 ≤ l ≤ 16
Reflections collected	41385
Independent reflections	7530 [R_{int} = 0.0378, R_{sigma} = 0.0284]
Data/restraints/parameters	7530/0/322
Goodness-of-fit on F^2	1.055
Final R indexes [I>=2σ (I)]	R_1 = 0.0355, wR_2 = 0.0838
Final R indexes [all data]	R_1 = 0.0466, wR_2 = 0.0901
Largest diff. peak/hole / e Å^{-3}	0.54/-0.43

Structure 118

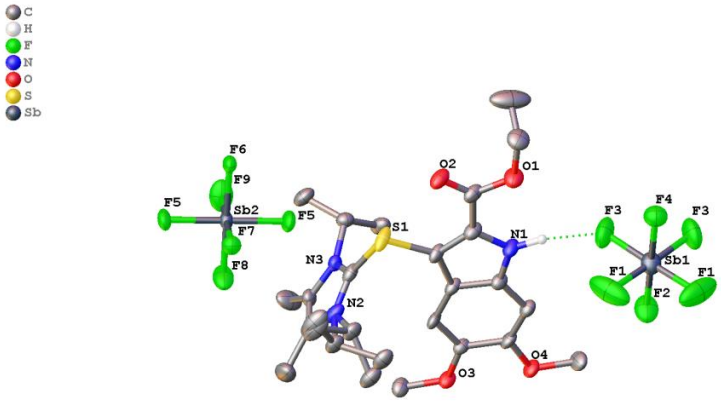

Figure S17: Asymmetric unit of **118**.

The ethyl residue attached to O1 is disordered resulting in big ADPs of the carbon atoms. The hydrogen bond between N1 and F3 results in N1-F3 distance of 2.939 Å as well as in an elongation of the Sb1-F3-bond (1.879(3)Å) compared to the average of the other Sb-F-bonds (1.867Å). The disorder of the isopropyl group attached to N2 was disordered about two positions. They were refined with distance restraints and restraints for the anisotropic displacement parameters. The occupancy of the minor position refined to 0.447(15). Due to disordered solvent molecule contribution to the calculated structure factors. PLATON SQUEEZE[309] was used to take this observation into account. The intensity of the highest unassigned peak decreased from 5.9 e Å^{-3} to 3.1 e Å^{-3}.

CSD code	1742205
Empirical formula	$C_{24}H_{34}F_6N_3O_4SSb$
Formula weight	696.35
Temperature/K	100(2)
Crystal system	orthorhombic
Space group	Pnma
a/Å	8.3908(15)
b/Å	25.698(4)
c/Å	27.710(4)
α/°	90
β/°	90
γ/°	90
Volume/Å^3	5975.1(17)
Z	8
ρ_{calc}g/cm^3	1.548
μ/mm^{-1}	1.064
F(000)	2816.0
Crystal size/mm^3	0.2 × 0.067 × 0.064
Radiation	MoKα (λ = 0.71073)
2Θ range for data collection/°	4.324 to 59.28
Index ranges	-11 ≤ h ≤ 11, -35 ≤ k ≤ 34, -38 ≤ l ≤ 38
Reflections collected	42615
Independent reflections	8592 [R_{int} = 0.0386, R_{sigma} = 0.0315]
Data/restraints/parameters	8592/1/394
Goodness-of-fit on F^2	1.180
Final R indexes [I>=2σ (I)]	R_1 = 0.0704, wR_2 = 0.1503
Final R indexes [all data]	R_1 = 0.0829, wR_2 = 0.1557
Largest diff. peak/hole / e Å^{-3}	3.08/-3.30

Structure 129

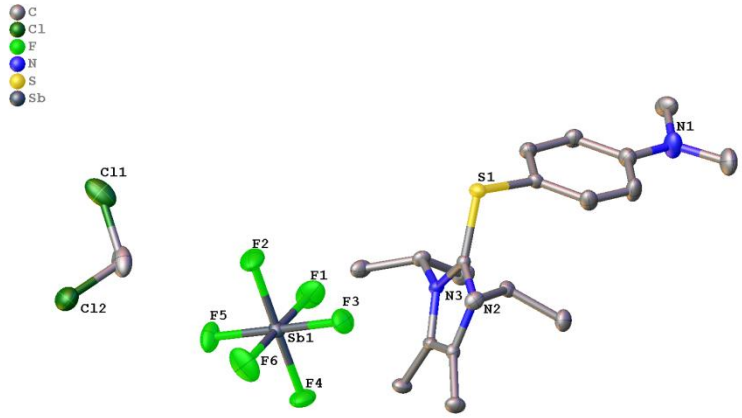

Figure S18: Asymmetric unit of **129** including one molecule dichloromethane.

CSD code	1842200
Empirical formula	$C_{20}H_{32}Cl_2F_6N_3SSb$
Formula weight	653.19
Temperature/K	100(2)
Crystal system	monoclinic
Space group	$P2_1/c$
a/Å	8.5286(3)
b/Å	10.6320(5)
c/Å	28.8881(13)
α/°	90
β/°	93.371(2)
γ/°	90
Volume/Å^3	2614.93(19)
Z	4
ρ_{calc}g/cm^3	1.659
μ/mm^{-1}	1.396
F(000)	1312.0
Crystal size/mm^3	0.281 × 0.186 × 0.062
Radiation	MoKα (λ = 0.71073)
2Θ range for data collection/°	4.76 to 60
Index ranges	-10 ≤ h ≤ 11, -12 ≤ k ≤ 14, -40 ≤ l ≤ 35
Reflections collected	18803
Independent reflections	7580 [R_{int} = 0.0331, R_{sigma} = 0.0436]
Data/restraints/parameters	7580/0/306
Goodness-of-fit on F^2	1.269
Final R indexes [I>=2σ (I)]	R_1 = 0.0494, wR_2 = 0.0952
Final R indexes [all data]	R_1 = 0.0616, wR_2 = 0.1001
Largest diff. peak/hole / e Å^{-3}	1.44/-1.26

Structure 123

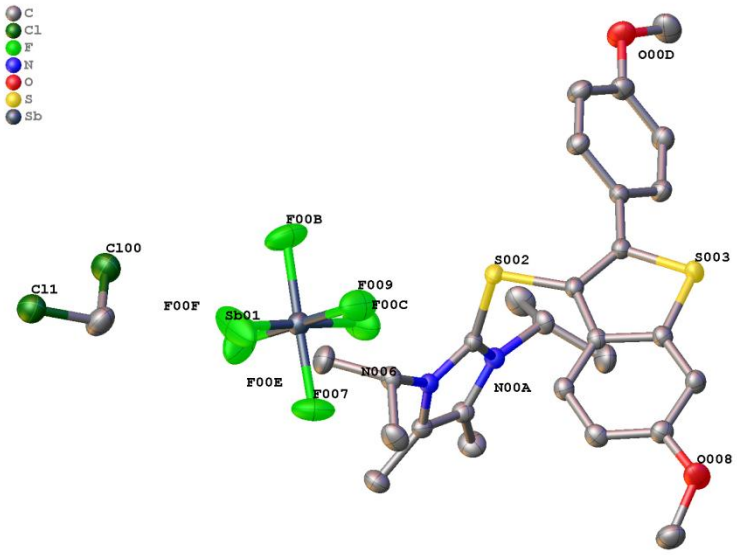

Figure S19: Asymmetric unit of **123** including one molecule dichloromethane.

CSD code	1842199
Empirical formula	$C_{28}H_{35}Cl_2F_6N_2O_2S_2Sb$
Formula weight	802.35
Temperature/K	150(2)
Crystal system	monoclinic
Space group	$P2_1/c$
a/Å	9.7036(11)
b/Å	26.893(3)
c/Å	12.5997(13)
α/°	90
β/°	93.073(4)
γ/°	90
Volume/Å^3	3283.2(6)
Z	4
ρ_{calc}g/cm^3	1.623
μ/mm^{-1}	1.194
F(000)	1616.0
Crystal size/mm^3	0.299 × 0.220 × .0.174
Radiation	MoKα (λ = 0.71073)
2Θ range for data collection/°	4.434 to 63.192
Index ranges	-14 ≤ h ≤ 14, -39 ≤ k ≤ 39, -18 ≤ l ≤ 15
Reflections collected	164305
Independent reflections	10998 [R_{int} = 0.0355, R_{sigma} = 0.0156]
Data/restraints/parameters	10998/0/396
Goodness-of-fit on F^2	1.062
Final R indexes [I>=2σ (I)]	R_1 = 0.0318, wR_2 = 0.0749
Final R indexes [all data]	R_1 = 0.0401, wR_2 = 0.0806
Largest diff. peak/hole / e Å^{-3}	0.63/-1.27

Structure 130

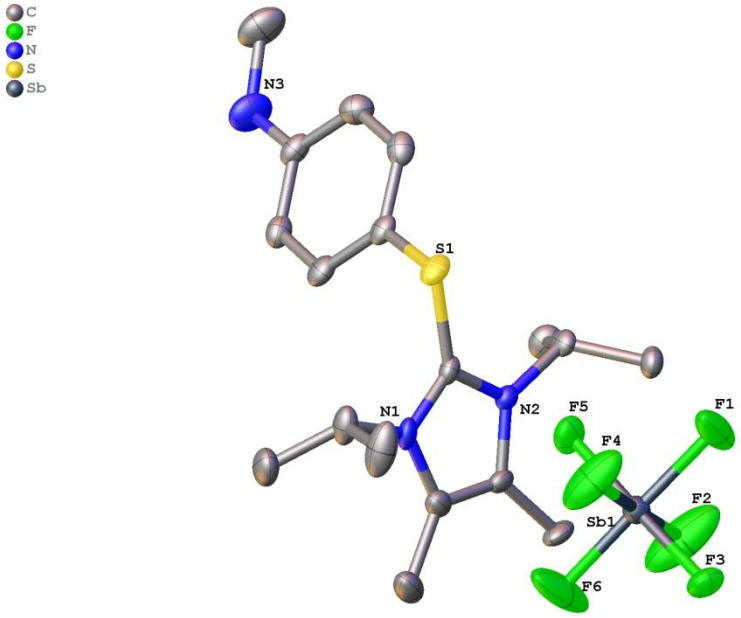

Figure S20: Asymmetric unit of **130**.

CSD code	1842204
Empirical formula	$C_{18}H_{27}F_6N_3SSb$
Formula weight	553.23
Temperature/K	100(2)
Crystal system	monoclinic
Space group	$P2_1/n$
a/Å	8.4731(6)
b/Å	12.5408(6)
c/Å	21.0842(15)
α/°	90
β/°	92.469(2)
γ/°	90
Volume/Å^3	2238.3(2)
Z	4
ρ_{calc}g/cm^3	1.642
μ/mm^{-1}	1.384
F(000)	1108.0
Crystal size/mm^3	0.202 × 0.197 × 0.096
Radiation	MoKα (λ = 0.71073)
2Θ range for data collection/°	5.05 to 59.13
Index ranges	-11 ≤ h ≤ 11, -17 ≤ k ≤ 17, -29 ≤ l ≤ 29
Reflections collected	34568
Independent reflections	6272 [R_{int} = 0.0256, R_{sigma} = 0.0191]
Data/restraints/parameters	6272/0/269
Goodness-of-fit on F^2	1.276
Final R indexes [I>=2σ (I)]	R_1 = 0.0525, wR_2 = 0.1074
Final R indexes [all data]	R_1 = 0.0545, wR_2 = 0.1083
Largest diff. peak/hole / e Å^{-3}	1.86/-1.18

Structure 116

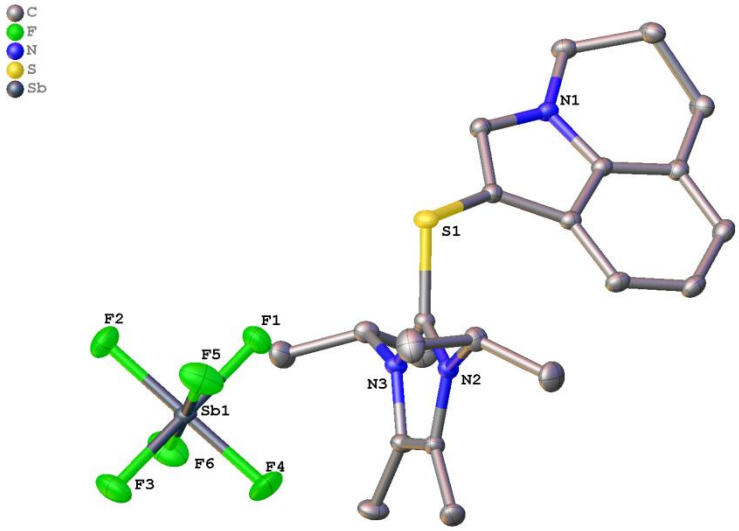

Figure S21: Asymmetric unit of **116**.

CSD code	1842213
Empirical formula	$C_{22}H_{30}F_6N_3SSb$
Formula weight	604.30
Temperature/K	100(2)
Crystal system	monoclinic
Space group	$P2_1/n$
a/Å	8.3461(2)
b/Å	12.7053(4)
c/Å	22.9335(7)
α/°	90
β/°	90.1370(10)
γ/°	90
Volume/Å^3	2431.85(12)
Z	4
ρ_{calc}g/cm^3	1.651
μ/mm^{-1}	1.282
F(000)	1216.0
Crystal size/mm^3	0.291 × 0.169 × 0.096
Radiation	MoKα (λ = 0.71073)
2Θ range for data collection/°	5.19 to 70.092
Index ranges	-13 ≤ h ≤ 13, -20 ≤ k ≤ 20, -37 ≤ l ≤ 37
Reflections collected	47413
Independent reflections	10652 [R_{int} = 0.0166, R_{sigma} = 0.0138]
Data/restraints/parameters	10652/0/305
Goodness-of-fit on F^2	1.055
Final R indexes [I>=2σ (I)]	R_1 = 0.0187, wR_2 = 0.0474
Final R indexes [all data]	R_1 = 0.0195, wR_2 = 0.0479
Largest diff. peak/hole / e Å^{-3}	0.94/-0.88

Structure 134

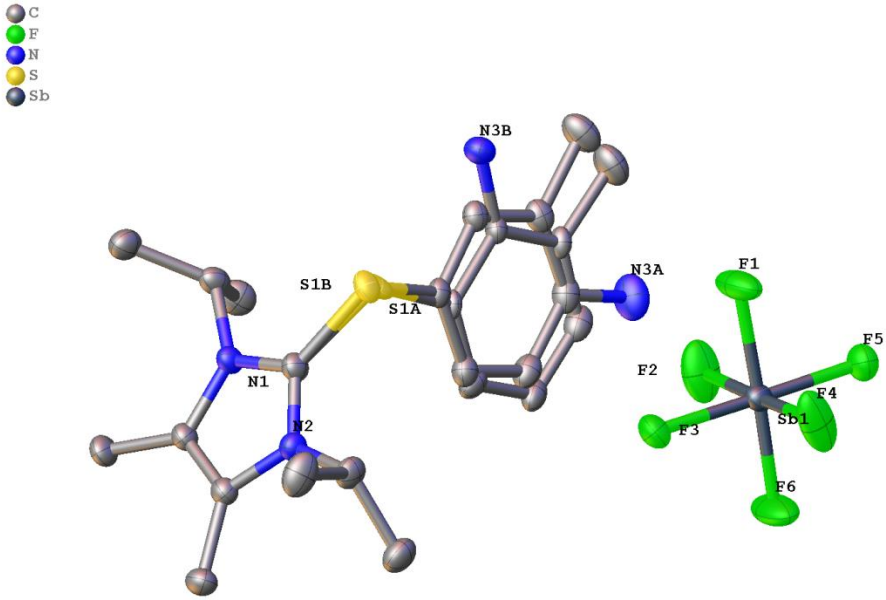

Figure S22: Asymmetric unit of **134**.

The methyl-aniline substituent is disordered about two positions. They were refined with distance restraints and restraints for the anisotropic displacement parameters. The occupancy of the minor position including N3B was refined to 0.24085

Empirical formula	$C_{18}H_{28}F_6N_3SSb$
Formula weight	554.24
Temperature/K	100(2)
Crystal system	monoclinic
Space group	$P2_1/n$
a/Å	8.5751(3)
b/Å	11.8860(5)
c/Å	21.7274(8)
α/°	90
β/°	92.4020(10)
γ/°	90
Volume/Å^3	2212.59(15)
Z	4
ρ_{calc}g/cm^3	1.664
μ/mm^{-1}	1.400
F(000)	1112.0
Crystal size/mm^3	0.534 × 0.487 × 0.249
Radiation	MoKα (λ = 0.71073)
2Θ range for data collection/°	5.038 to 61.076
Index ranges	-12 ≤ h ≤ 11, -16 ≤ k ≤ 16, -29 ≤ l ≤ 31
Reflections collected	50462
Independent reflections	6723 [R_{int} = 0.0237, R_{sigma} = 0.0150]
Data/restraints/parameters	6723/99/354
Goodness-of-fit on F^2	1.128
Final R indexes [I>=2σ (I)]	R_1 = 0.0224, wR_2 = 0.0521
Final R indexes [all data]	R_1 = 0.0228, wR_2 = 0.0524
Largest diff. peak/hole / e Å^{-3}	1.01/-1.20

Structure 329

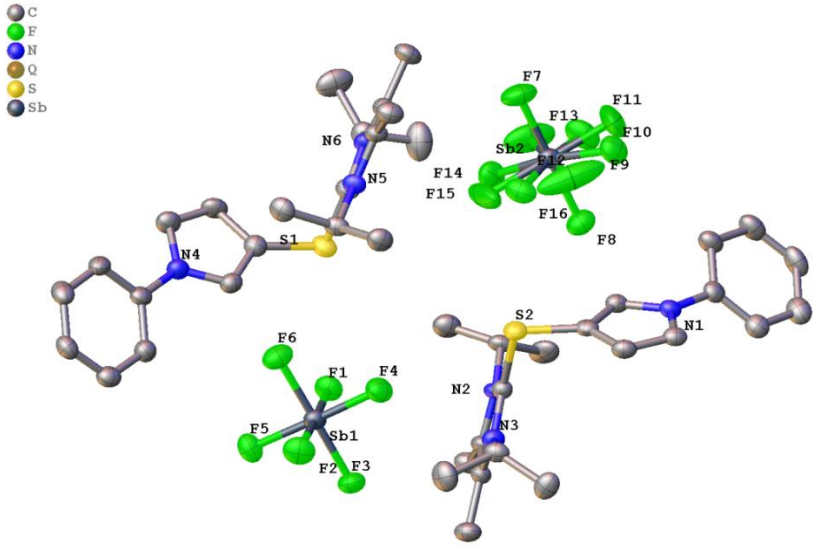

Figure S23: Asymmetric unit of **329**.

Due to the low scattering properties of the obtained crystal the R_{int} is high. It was not possible to measure the same crystal a second time with longer exposure times. One of the SbF_6 anion is disordered by rotation of the F7-F8 axis. The overlapping anions were refined and restraints for the anisotropic displacement parameters. The occupancy of the minor position was refined to 0.13156 (F10, F12, F14, F16.)

Empirical formula	$C_{21}H_{28}F_6N_3SSb$
Formula weight	590.27
Temperature/K	100(2)
Crystal system	monoclinic
Space group	$P2_1/n$
a/Å	13.2399(8)
b/Å	27.0374(15)
c/Å	13.7406(8)
α/°	90
β/°	100.178(2)
γ/°	90
Volume/Å^3	4841.4(5)
Z	8
ρ_{calc}g/cm^3	1.620
μ/mm^{-1}	1.285
F(000)	2368.0
Crystal size/mm^3	0.222 × 0.214 × 0.064
Radiation	MoKα (λ = 0.71073)
2Θ range for data collection/°	4.26 to 52.824
Index ranges	-16 ≤ h ≤ 16, -33 ≤ k ≤ 33, -17 ≤ l ≤ 17
Reflections collected	125907
Independent reflections	9920 [R_{int} = 0.1615, R_{sigma} = 0.0612]
Data/restraints/parameters	9920/67/626
Goodness-of-fit on F^2	1.041
Final R indexes [I>=2σ (I)]	R_1 = 0.0524, wR_2 = 0.0930
Final R indexes [all data]	R_1 = 0.0890, wR_2 = 0.1089
Largest diff. peak/hole / e Å^{-3}	1.21/-0.89

Structure 99

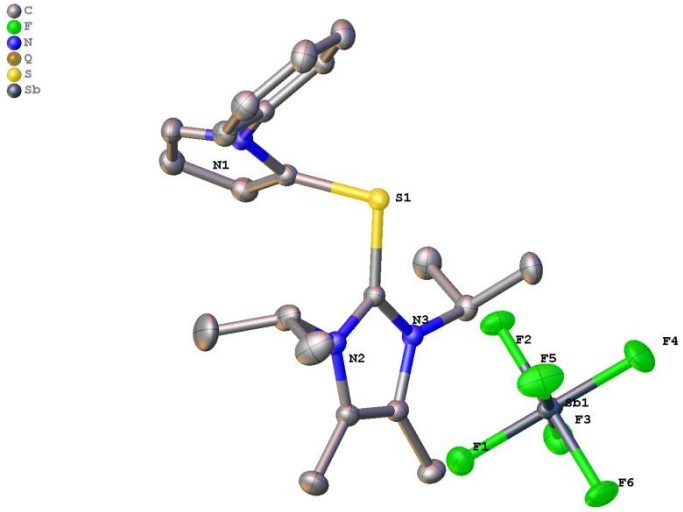

Figure S24: Asymmetric unit of **99**.

Empirical formula	$C_{21}H_{28}F_6N_3SSb$
Formula weight	590.27
Temperature/K	100(2)
Crystal system	monoclinic
Space group	$P2_1/n$
a/Å	10.4709(4)
b/Å	22.2447(7)
c/Å	10.8000(4)
α/°	90
β/°	99.9630(10)
γ/°	90
Volume/Å^3	2477.62(15)
Z	4
ρ_{calc}g/cm^3	1.582
μ/mm^{-1}	1.256
F(000)	1184.0
Crystal size/mm^3	0.385 × 0.342 × 0.116
Radiation	MoKα (λ = 0.71073)
2Θ range for data collection/°	4.244 to 80.636
Index ranges	-19 ≤ h ≤ 19, -40 ≤ k ≤ 40, -19 ≤ l ≤ 19
Reflections collected	151537
Independent reflections	15581 [R_{int} = 0.0333, R_{sigma} = 0.0165]
Data/restraints/parameters	15581/0/295
Goodness-of-fit on F^2	1.031
Final R indexes [I>=2σ (I)]	R_1 = 0.0249, wR_2 = 0.0579
Final R indexes [all data]	R_1 = 0.0302, wR_2 = 0.0611
Largest diff. peak/hole / e Å^{-3}	1.78/-2.09

Structure 138

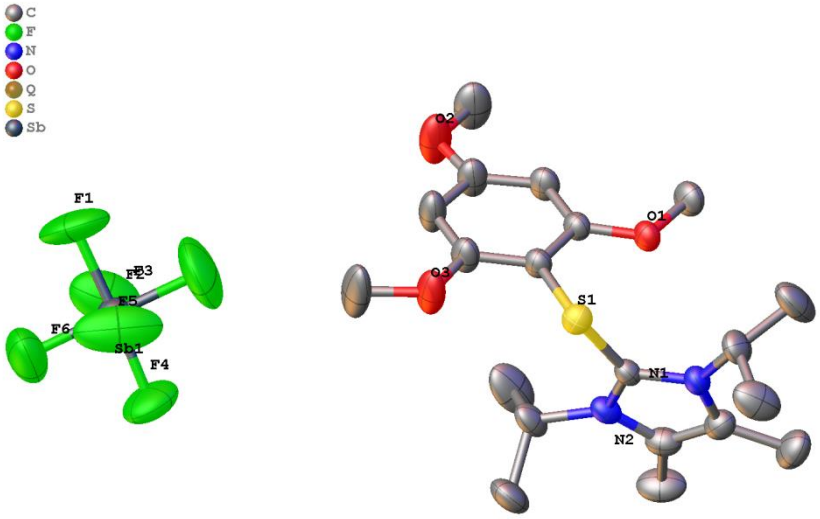

Figure S25: Asymmetric unit of **138**.

Due to a phase transition of the crystal at lower temperatures data collection had to be carried out at an elevated temperature of 200 K causing increased thermal movement.

Empirical formula	$CNOFS_2SbH_{0.13}$
Formula weight	247.02
Temperature/K	200(2)
Crystal system	triclinic
Space group	P-1
a/Å	8.0772(3)
b/Å	9.5091(3)
c/Å	17.2074(7)
α/°	80.5930(10)
β/°	84.2550(10)
γ/°	82.0220(10)
Volume/$Å^3$	1287.19(8)
Z	8
$\rho_{calc}g/cm^3$	2.549
μ/mm^{-1}	4.847
F(000)	905.0
Crystal size/mm^3	0.256 × 0.174 × 0.12
Radiation	MoKα (λ = 0.71073)
2Θ range for data collection/°	4.376 to 61.104
Index ranges	-11 ≤ h ≤ 11, -13 ≤ k ≤ 13, -24 ≤ l ≤ 24
Reflections collected	137499
Independent reflections	7879 [R_{int} = 0.0253, R_{sigma} = 0.0126]
Data/restraints/parameters	7879/0/307
Goodness-of-fit on F^2	1.177
Final R indexes [I>=2σ (I)]	R_1 = 0.0403, wR_2 = 0.1237
Final R indexes [all data]	R_1 = 0.0465, wR_2 = 0.1416
Largest diff. peak/hole / e $Å^{-3}$	1.60/-1.33

Structure 132

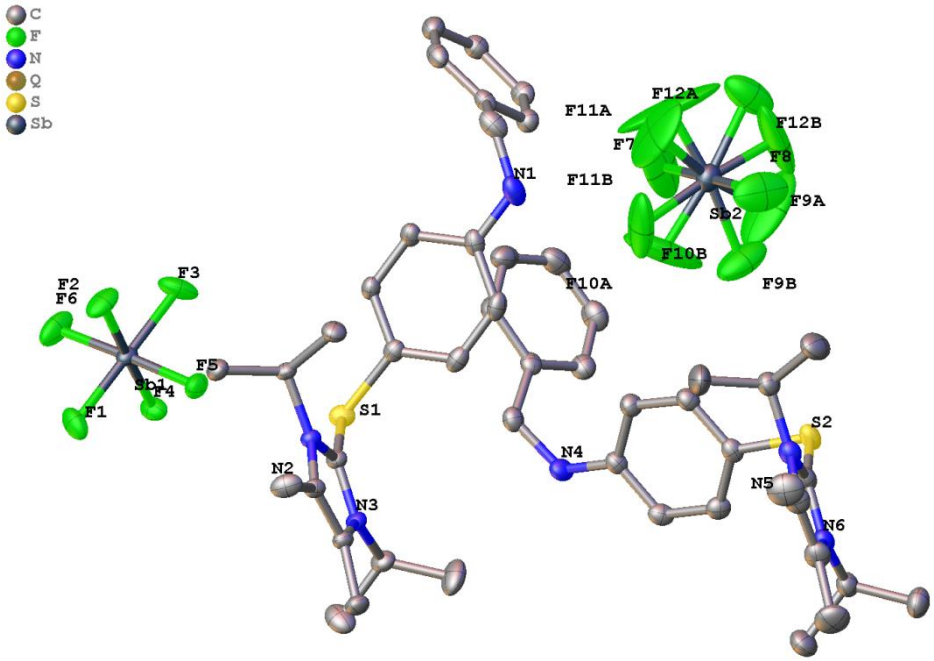

Figure S26: Asymmetric unit of **132**.

One hexafluoroantimonate anion is disordered about two positions. It is refined with distance restraints. The occupancy of the minor position (F9B to F12B) is refined to 0.49162.

Empirical formula	$C_{24}H_{32}F_6N_3SSb$
Formula weight	630.33
Temperature/K	100(2)
Crystal system	triclinic
Space group	P-1
a/Å	8.8424(4)
b/Å	11.2732(8)
c/Å	27.7533(19)
α/°	79.465(2)
β/°	84.329(2)
γ/°	89.118(2)
Volume/Å^3	2706.6(3)
Z	4
ρ_{calc}g/cm^3	1.547
μ/mm^{-1}	1.155
F(000)	1272.0
Crystal size/mm^3	0.43 × 0.2 × 0.076
Radiation	MoKα (λ = 0.71073)
2Θ range for data collection/°	4.214 to 62.898
Index ranges	-12 ≤ h ≤ 12, -16 ≤ k ≤ 16, -40 ≤ l ≤ 40
Reflections collected	92745
Independent reflections	17894 [R_{int} = 0.0397, R_{sigma} = 0.0304]
Data/restraints/parameters	17894/119/687
Goodness-of-fit on F^2	1.036
Final R indexes [I>=2σ (I)]	R_1 = 0.0353, wR_2 = 0.0816
Final R indexes [all data]	R_1 = 0.0398, wR_2 = 0.0844
Largest diff. peak/hole / e Å^{-3}	2.26/-1.93

Structure 136-SP

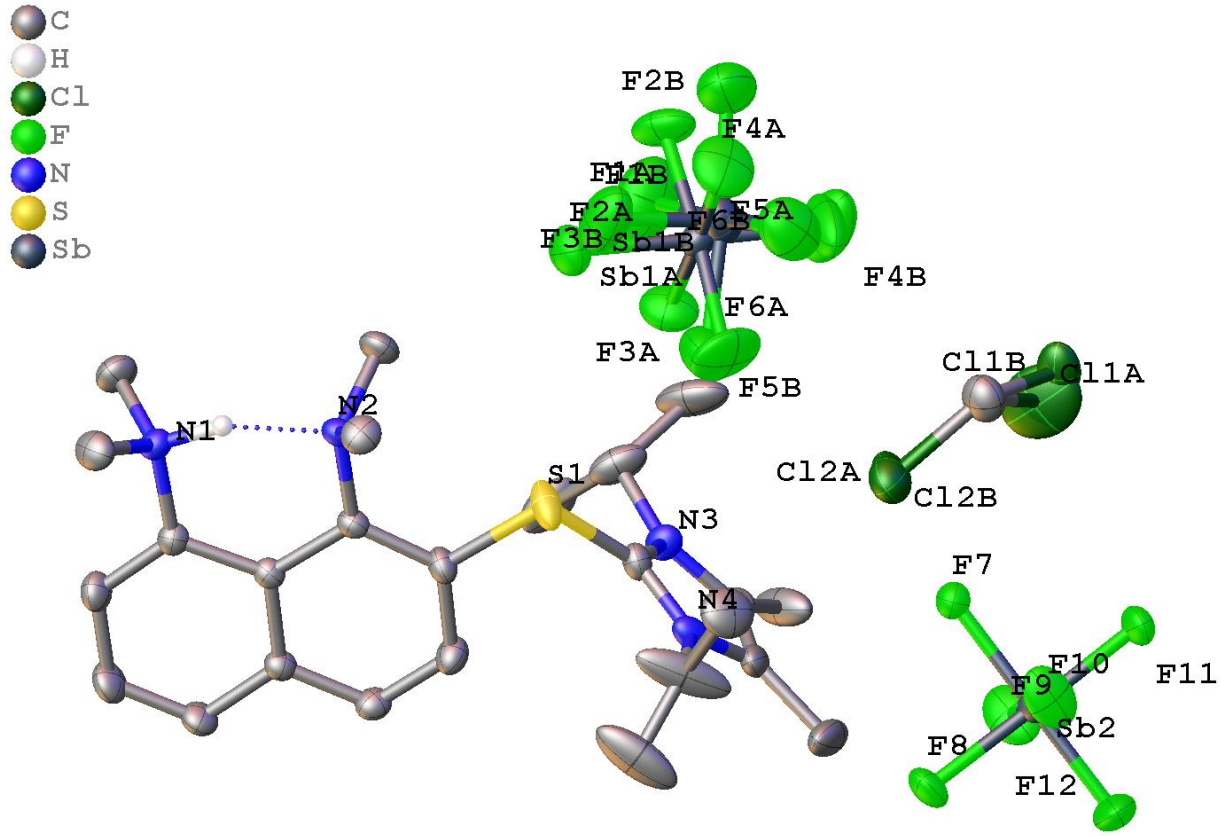

Figure S27: Asymmetric unit of **136-SP**.

One of the two SbF_6 anions is disordered about two positions. It is refined with distance restraints and some of the anisotropic displacement parameters are constrained to be the same. The occupancy of the minor position refined to 0.185. The enclosed dichloromethane is disordered about two positions. The occupancy of the minor position refined to 0.498(18). A bridged hydrogen bond between N4 and N2 is observable.

Empirical formula	$C_{26}H_{40}Cl_2F_{12}N_4SSb_2$
Formula weight	983.08
Temperature/K	100(2)
Crystal system	orthorhombic
Space group	Pbca
a/Å	17.5297(10)
b/Å	13.1456(6)
c/Å	31.3247(18)
α/°	90
β/°	90
γ/°	90
Volume/Å^3	7218.4(7)
Z	8
ρ_{calc}g/cm^3	1.809
μ/mm^{-1}	1.790
F(000)	3872.0
Crystal size/mm^3	0.601 × 0.266 × 0.076
Radiation	MoKα (λ = 0.71073)
2Θ range for data collection/°	4.648 to 59.224
Index ranges	-24 ≤ h ≤ 20, -18 ≤ k ≤ 16, -41 ≤ l ≤ 43
Reflections collected	56715
Independent reflections	10102 [R_{int} = 0.0300, R_{sigma} = 0.0219]
Data/restraints/parameters	10102/121/521
Goodness-of-fit on F^2	1.033
Final R indexes [I>=2σ (I)]	R_1 = 0.0375, wR_2 = 0.0818
Final R indexes [all data]	R_1 = 0.0441, wR_2 = 0.0854
Largest diff. peak/hole / e Å^{-3}	1.82/-0.81

Structure 136

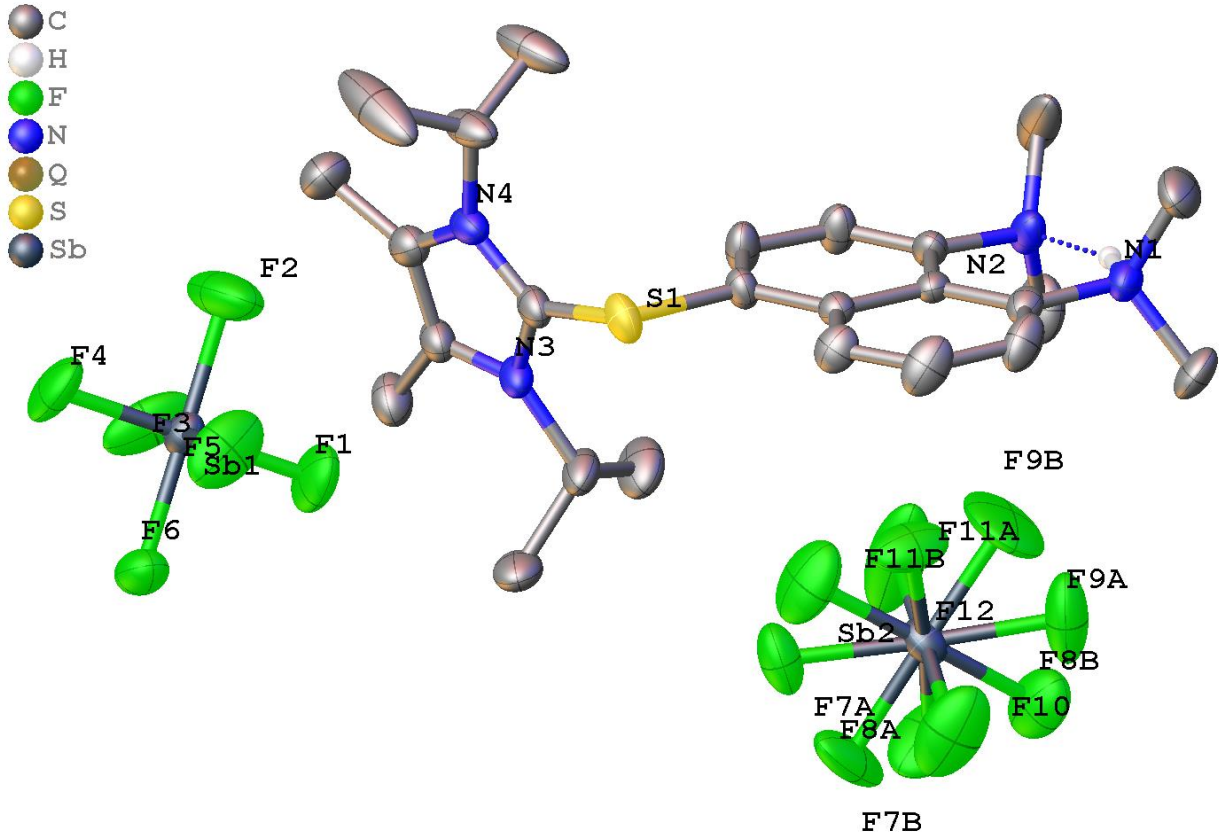

Figure S28: Asymmetric unit of **136**.

One of the two SbF_6 anions is disordered about two positions. The occupancy of the minor position refined to 0.185. The enclosed dichloromethane is disordered about two positions. The occupancy of the minor position refined to 0.46695. A bridged hydrogen bond between N1 and N2 is observable. **136** crystalized twin, following the twin-law TWIN -1 0 0 0 -1 0 0 0 -1 2. The model was refined with BASF 0.159.

Empirical formula	$C_{25}H_{38}F_{12}N_4SSb_2$
Formula weight	898.15
Temperature/K	100(2)
Crystal system	orthorhombic
Space group	$Pca2_1$
a/Å	17.2749(8)
b/Å	7.9258(3)
c/Å	24.4029(11)
α/°	90
β/°	90
γ/°	90
Volume/Å^3	3341.2(3)
Z	4
ρ_{calc}g/cm^3	1.785
μ/mm^{-1}	1.769
F(000)	1768.0
Crystal size/mm^3	0.511 × 0.311 × 0.256
Radiation	MoKα (λ = 0.71073)
2Θ range for data collection/°	4.716 to 59.23
Index ranges	-23 ≤ h ≤ 23, -10 ≤ k ≤ 9, -32 ≤ l ≤ 33
Reflections collected	52887
Independent reflections	9307 [R_{int} = 0.0213, R_{sigma} = 0.0156]
Data/restraints/parameters	9307/1/445
Goodness-of-fit on F^2	1.035
Final R indexes [I>=2σ (I)]	R_1 = 0.0238, wR_2 = 0.0601
Final R indexes [all data]	R_1 = 0.0243, wR_2 = 0.0605
Largest diff. peak/hole / e Å^{-3}	1.15/-0.68
Flack parameter	0.159(18)

5.8.4 Structure of thioethers

Structure of 170

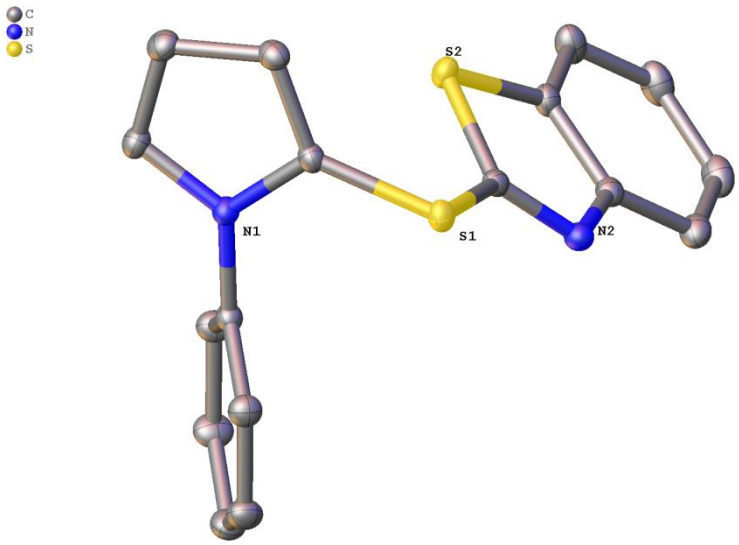

Figure S29: Asymmetric unit of **170**.

CSD code	1842212
Empirical formula	$C_{17}H_{12}N_2S_2$
Formula weight	308.41
Temperature/K	100(2)
Crystal system	monoclinic
Space group	$P2_1/n$
a/Å	12.9549(12)
b/Å	5.7904(6)
c/Å	19.3714(18)
α/°	90
β/°	97.300(4)
γ/°	90
Volume/Å^3	1441.3(2)
Z	4
ρ_{calc}g/cm^3	1.421
μ/mm^{-1}	0.362
F(000)	640.0
Crystal size/mm^3	0.293 × 0.21 × 0.035
Radiation	MoKα (λ = 0.71073)
2Θ range for data collection/°	6.342 to 61.012
Index ranges	-18 ≤ h ≤ 16, -8 ≤ k ≤ 8, -27 ≤ l ≤ 27
Reflections collected	26393
Independent reflections	4386 [R_{int} = 0.0204, R_{sigma} = 0.0150]
Data/restraints/parameters	4386/0/190
Goodness-of-fit on F^2	1.059
Final R indexes [I>=2σ (I)]	R_1 = 0.0268, wR_2 = 0.0726
Final R indexes [all data]	R_1 = 0.0282, wR_2 = 0.0738
Largest diff. peak/hole / e Å^{-3}	0.45/-0.27

Structure 87

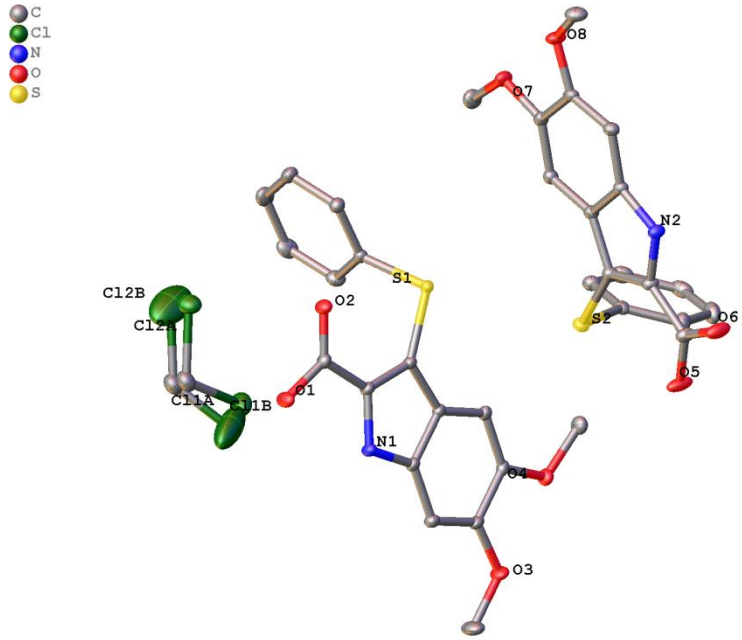

Figure S30: Asymmetric unit of **87**with one highly disordered dichloromethane molecule.

The dichloromethane molecule was disordered about two positions. The occupancy of the minor position refined to 0.084(3).

CSD code	1842203
Empirical formula	$C_{35}H_{32}Cl_2N_2O_8S_2$
Formula weight	743.64
Temperature/K	100(2)
Crystal system	triclinic
Space group	P-1
a/Å	11.0578(8)
b/Å	11.8434(9)
c/Å	13.5784(8)
α/°	87.855(2)
β/°	81.169(3)
γ/°	71.873(2)
Volume/Å^3	1669.9(2)
Z	2
ρ_{calc}g/cm^3	1.479
μ/mm^{-1}	0.376
F(000)	772.0
Crystal size/mm^3	0.394 × 0.158 × 0.054
Radiation	MoKα (λ = 0.71073)
2Θ range for data collection/°	4.438 to 59.202
Index ranges	-15 ≤ h ≤ 15, -16 ≤ k ≤ 16, -18 ≤ l ≤ 18
Reflections collected	52316
Independent reflections	9391 [R_{int} = 0.0202, R_{sigma} = 0.0165]
Data/restraints/parameters	9391/21/478
Goodness-of-fit on F^2	1.033
Final R indexes [I>=2σ (I)]	R_1 = 0.0285, wR_2 = 0.0751
Final R indexes [all data]	R_1 = 0.0299, wR_2 = 0.0761
Largest diff. peak/hole / e Å^{-3}	0.48/-0.40

Structure 168

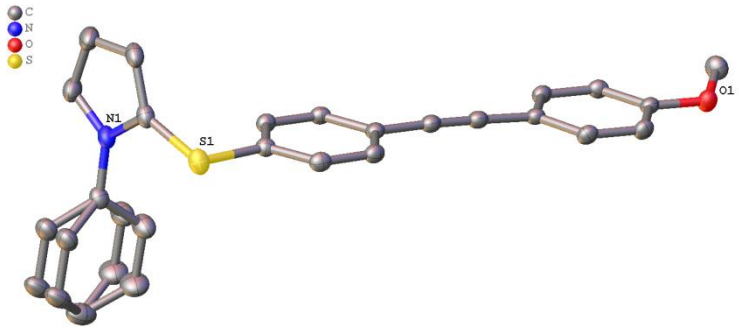

Figure S31: Asymmetric unit of **168**.

The phenyl rings of the 1-phenylpyrrole are disordered about two positions. They were refined with a fitted hexagon as free rotating group (C24B[C23,C22B,C21B,C20,C25B]) and restraints for the anisotropic displacement parameters. The occupancy of the minor position was refined to 0.068(3).

CSD code	1842201
Empirical formula	$C_{25}H_{19}NOS$
Formula weight	381.47
Temperature/K	100(2)
Crystal system	monoclinic
Space group	$P2_1$
a/Å	5.9190(8)
b/Å	7.7752(8)
c/Å	21.527(2)
α/°	90
β/°	95.175(5)
γ/°	90
Volume/Å^3	986.6(2)
Z	2
ρ_{calc}g/cm^3	1.284
μ/mm^{-1}	0.179
F(000)	400.0
Crystal size/mm^3	0.37 × 0.325 × 0.052
Radiation	MoKα (λ = 0.71073)
2Θ range for data collection/°	5.574 to 63.09
Index ranges	-8 ≤ h ≤ 8, -11 ≤ k ≤ 11, -31 ≤ l ≤ 31
Reflections collected	38446
Independent reflections	6609 [R_{int} = 0.0260, R_{sigma} = 0.0194]
Data/restraints/parameters	6609/1/255
Goodness-of-fit on F^2	1.070
Final R indexes [I>=2σ (I)]	R_1 = 0.0314, wR_2 = 0.0840
Final R indexes [all data]	R_1 = 0.0331, wR_2 = 0.0855
Largest diff. peak/hole / e Å^{-3}	0.33/-0.21
Flack parameter	-0.005(11)

Structure 163

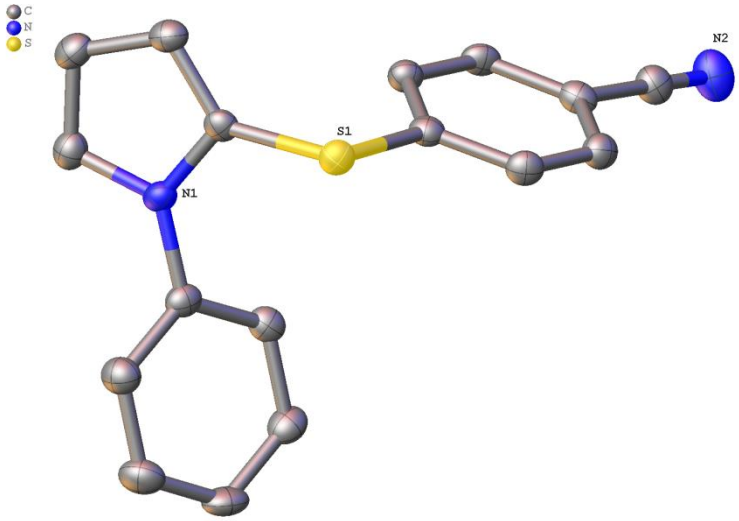

Figure S32: Asymmetric unit of **163**.

The completeness of the dataset is low (88%) due to very low scattering abilities of the crystal especially at higher angles when each frame was recorded with a frame time of 100s.

CSD code	1842209
Empirical formula	$C_{17}H_{12}N_2S$
Formula weight	276.35
Temperature/K	100(2)
Crystal system	monoclinic
Space group	$P2_1/n$
a/Å	14.139(3)
b/Å	6.0096(12)
c/Å	16.475(4)
α/°	90
β/°	90.480(6)
γ/°	90
Volume/Å^3	1399.8(5)
Z	4
ρ_{calc}g/cm^3	1.311
μ/mm^{-1}	0.221
F(000)	576.0
Crystal size/mm^3	0.256 × 0.085 × 0.035
Radiation	MoKα (λ = 0.71073)
2Θ range for data collection/°	4.946 to 53.996
Index ranges	-18 ≤ h ≤ 17, -7 ≤ k ≤ 5, -21 ≤ l ≤ 21
Reflections collected	5768
Independent reflections	2666 [R_{int} = 0.0348, R_{sigma} = 0.0556]
Data/restraints/parameters	2666/0/181
Goodness-of-fit on F^2	1.013
Final R indexes [I>=2σ (I)]	R_1 = 0.0458, wR_2 = 0.1068
Final R indexes [all data]	R_1 = 0.0722, wR_2 = 0.1196
Largest diff. peak/hole / e Å^{-3}	0.32/-0.27

Structure 162

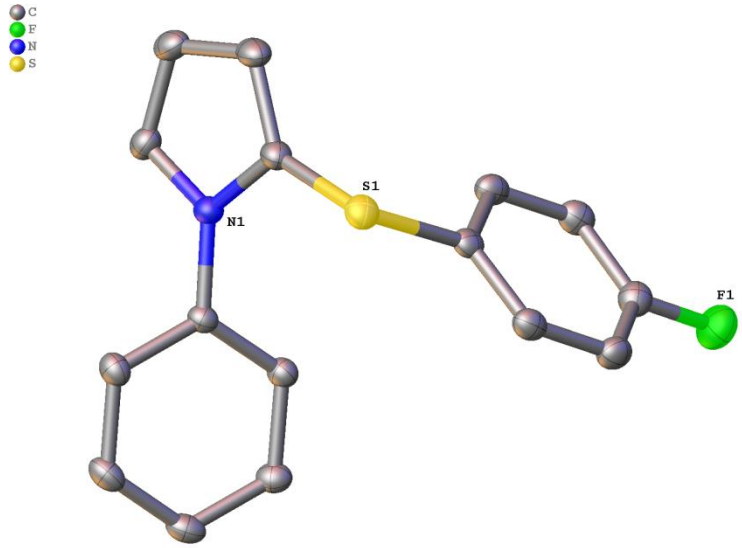

Figure S33: Asymmetric unit of **162**.

CSD code	1842211
Empirical formula	$C_{16}H_{12}FNS$
Formula weight	269.33
Temperature/K	100(2)
Crystal system	triclinic
Space group	P-1
a/Å	9.0400(6)
b/Å	9.3397(7)
c/Å	9.4356(5)
α/°	112.285(2)
β/°	101.900(2)
γ/°	106.502(2)
Volume/Å^3	661.07(8)
Z	2
ρ_{calc}g/cm^3	1.353
μ/mm^{-1}	0.240
F(000)	280.0
Crystal size/mm^3	0.317 × 0.304 × 0.224
Radiation	MoKα (λ = 0.71073)
2Θ range for data collection/°	4.988 to 61.05
Index ranges	-12 ≤ h ≤ 12, -13 ≤ k ≤ 13, -13 ≤ l ≤ 13
Reflections collected	20832
Independent reflections	4030 [R_{int} = 0.0195, R_{sigma} = 0.0153]
Data/restraints/parameters	4030/0/172
Goodness-of-fit on F^2	1.033
Final R indexes [I>=2σ (I)]	R_1 = 0.0312, wR_2 = 0.0830
Final R indexes [all data]	R_1 = 0.0328, wR_2 = 0.0844
Largest diff. peak/hole / e Å^{-3}	0.40/-0.24

5.8.5 Structure of aryltriazolium salts

Structure 210

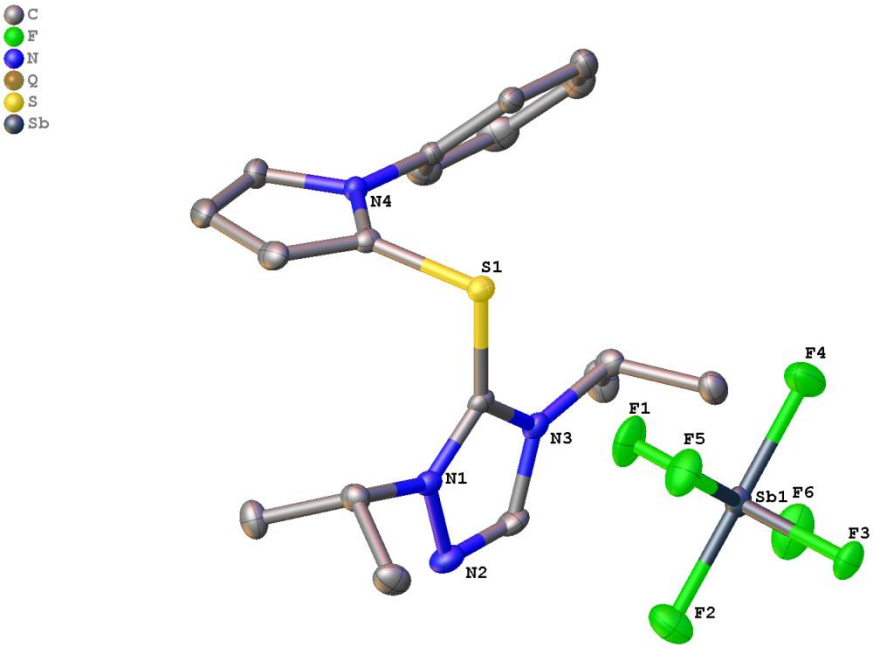

Figure S34: Asymmetric unit of **210**.

Empirical formula	$C_{18}H_{23}F_6N_4SSb$
Formula weight	563.21
Temperature/K	100(2)
Crystal system	tetragonal
Space group	$P4_1$
a/Å	8.5569(4)
b/Å	8.5569(4)
c/Å	30.0518(13)
α/°	90
β/°	90
γ/°	90
Volume/Å^3	2200.4(2)
Z	4
ρ_{calc}g/cm^3	1.700
μ/mm^{-1}	1.411
F(000)	1120.0
Crystal size/mm^3	0.448 × 0.399 × 0.064
Radiation	MoKα (λ = 0.71073)
2Θ range for data collection/°	4.76 to 59.16
Index ranges	-11 ≤ h ≤ 11, -11 ≤ k ≤ 11, -41 ≤ l ≤ 41
Reflections collected	21863
Independent reflections	6160 [R_{int} = 0.0386, R_{sigma} = 0.0368]
Data/restraints/parameters	6160/1/275
Goodness-of-fit on F^2	1.090
Final R indexes [I>=2σ (I)]	R_1 = 0.0194, wR_2 = 0.0459
Final R indexes [all data]	R_1 = 0.0197, wR_2 = 0.0461
Largest diff. peak/hole / e Å^{-3}	0.27/-0.49
Flack parameter	0.009(8)

Structure 300

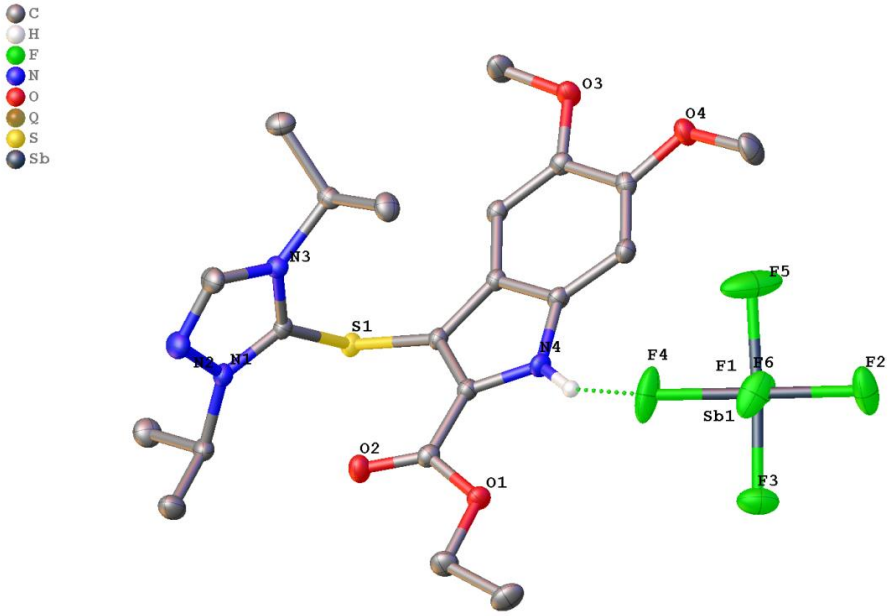

Figure S35: Asymmetric unit of **300**.

The hydrogen bond between N4 and F4 results in N4-F4 distance of 2.860 Å as well as in an elongation of the Sb1-F4-bond (1.888(1)Å) compared to the average of the other Sb-F-bonds (1.864Å).

Empirical formula	$C_{21}H_{29}F_6N_4O_4SSb$
Formula weight	669.29
Temperature/K	100(2)
Crystal system	monoclinic
Space group	$P2_1/c$
a/Å	10.9060(9)
b/Å	11.8738(12)
c/Å	20.949(2)
α/°	90
β/°	99.768(3)
γ/°	90
Volume/Å^3	2673.5(4)
Z	4
ρ_{calc}g/cm^3	1.663
μ/mm^{-1}	1.186
F(000)	1344.0
Crystal size/mm^3	0.288 × 0.059 × 0.048
Radiation	MoKα (λ = 0.71073)
2Θ range for data collection/°	4.986 to 63.098
Index ranges	-16 ≤ h ≤ 15, -17 ≤ k ≤ 17, -30 ≤ l ≤ 30
Reflections collected	54251
Independent reflections	8930 [R_{int} = 0.0234, R_{sigma} = 0.0162]
Data/restraints/parameters	8930/1/344
Goodness-of-fit on F^2	1.145
Final R indexes [I>=2σ (I)]	R_1 = 0.0249, wR_2 = 0.0562
Final R indexes [all data]	R_1 = 0.0275, wR_2 = 0.0573
Largest diff. peak/hole / e Å^{-3}	1.08/-0.91

5.8.6 Additional structures

Structure 301

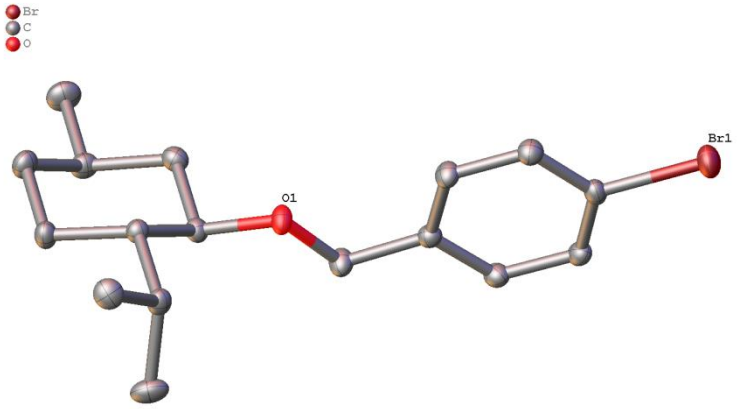

Figure S36: Asymmetric unit of **301**.

CSD code	1843380
Empirical formula	$C_{17}H_{25}BrO$
Formula weight	325.28
Temperature/K	99.99
Crystal system	orthorhombic
Space group	$P2_12_12_1$
a/Å	6.3330(2)
b/Å	7.9935(3)
c/Å	31.5153(12)
α/°	90
β/°	90
γ/°	90
Volume/Å^3	1595.39(10)
Z	4
ρ_{calc}g/cm^3	1.354
μ/mm^{-1}	2.568
F(000)	680.0
Crystal size/mm^3	0.483 × 0.445 × 0.25
Radiation	MoKα (λ = 0.71073)
2Θ range for data collection/°	5.17 to 65.17
Index ranges	-9 ≤ h ≤ 9, -12 ≤ k ≤ 12, -47 ≤ l ≤ 46
Reflections collected	21580
Independent reflections	5807 [R_{int} = 0.0233, R_{sigma} = 0.0222]
Data/restraints/parameters	5807/0/175
Goodness-of-fit on F^2	1.050
Final R indexes [I>=2σ (I)]	R_1 = 0.0230, wR_2 = 0.0516
Final R indexes [all data]	R_1 = 0.0255, wR_2 = 0.0524
Largest diff. peak/hole / e Å^{-3}	0.34/-0.39
Flack parameter	0.004(2)

Structure 330

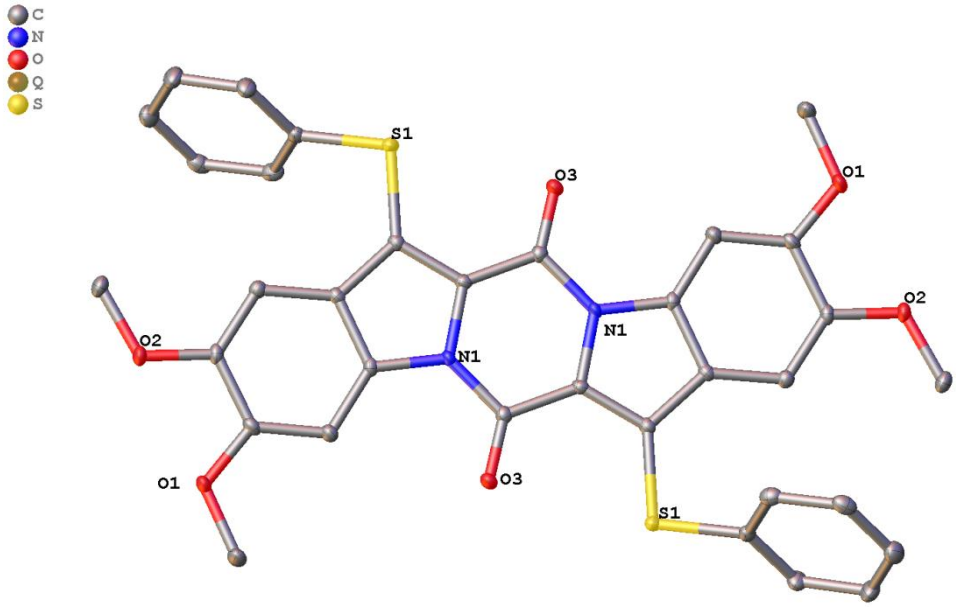

Figure S37: Two asymmetric unit of **330** generated by symmetry element [2-X,1-Y,1-Z].

Empirical formula	$C_{34}H_{26}N_2O_6S_2$
Formula weight	622.69
Temperature/K	100(2)
Crystal system	monoclinic
Space group	$P2_1/c$
a/Å	6.0491(3)
b/Å	19.1171(9)
c/Å	12.1059(5)
α/°	90
β/°	99.251(2)
γ/°	90
Volume/Å^3	1381.73(11)
Z	2
ρ_{calc}g/cm^3	1.497
μ/mm^{-1}	0.247
F(000)	648.0
Crystal size/mm^3	? × ? × ?
Radiation	MoKα (λ = 0.71073)
2Θ range for data collection/°	5.458 to 54.276
Index ranges	-7 ≤ h ≤ 7, -24 ≤ k ≤ 24, -15 ≤ l ≤ 15
Reflections collected	40746
Independent reflections	3064 [R_{int} = 0.0337, R_{sigma} = 0.0148]
Data/restraints/parameters	3064/0/201
Goodness-of-fit on F^2	1.083
Final R indexes [I>=2σ (I)]	R_1 = 0.0347, wR_2 = 0.0816
Final R indexes [all data]	R_1 = 0.0385, wR_2 = 0.0836
1Largest diff. peak/hole / e Å^{-3}	0.34/-0.28

5.8.7 Structure of arylselenoimidazolium salts

Structure 217

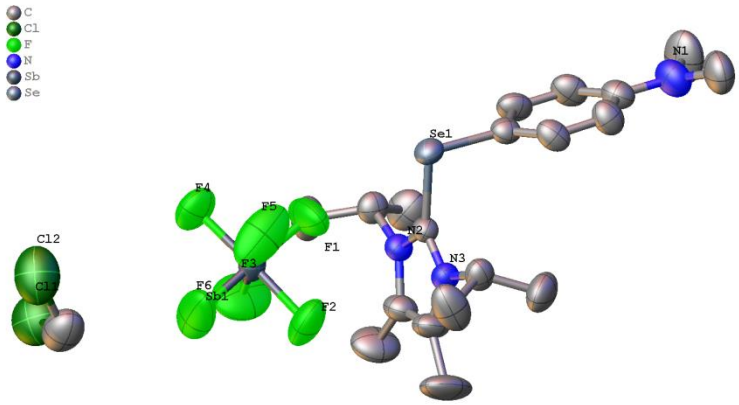

Figure S38: Asymmetric unit of **217** containing one dichloromethane molecule.

CSD code	1844013
Empirical formula	$C_{20}H_{32}Cl_2F_6N_3SbSe$
Formula weight	700.09
Temperature/K	150(2)
Crystal system	orthorhombic
Space group	$P2_12_12_1$
a/Å	9.2925(4)
b/Å	10.8514(5)
c/Å	27.7046(13)
α/°	90
β/°	90
γ/°	90
Volume/Å^3	2793.6(2)
Z	4
ρ_{calc}g/cm^3	1.665
μ/mm^{-1}	2.535
F(000)	1384.0
Crystal size/mm^3	0.643 × 0.456 × 0.088
Radiation	MoKα (λ = 0.71073)
2Θ range for data collection/°	4.032 to 59.32
Index ranges	-12 ≤ h ≤ 12, -14 ≤ k ≤ 15, -38 ≤ l ≤ 38
Reflections collected	52383
Independent reflections	7868 [R_{int} = 0.0374, R_{sigma} = 0.0248]
Data/restraints/parameters	7868/0/307
Goodness-of-fit on F^2	1.065
Final R indexes [I>=2σ (I)]	R_1 = 0.0346, wR_2 = 0.0975
Final R indexes [all data]	R_1 = 0.0365, wR_2 = 0.0989
Largest diff. peak/hole / e Å^{-3}	0.81/-0.93
Flack parameter	0.435(14)

5.8.8 Structure of imidazolthioether

Structure 232

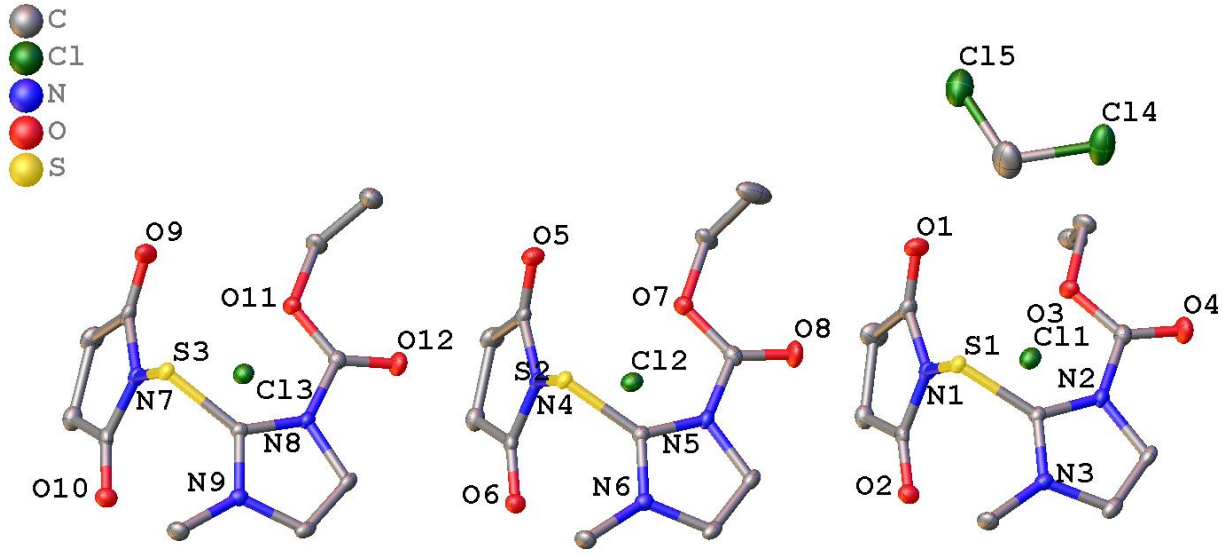

Figure S39: Asymmetric unit of **232** containing one molecule dichloromethane.

232 crystalized as a twin. The interaction of the positive polarized sulfur atom and the nearest chloride anion result in an average distance between S-Cl is 3.084Å. [Summe(v.-d.-Waals):3.55Å][296].

Empirical formula	$C_{34}H_{44}Cl_5N_9O_{12}S_3$
Formula weight	1044.21
Temperature/K	100(2)
Crystal system	triclinic
Space group	P-1
a/Å	11.205(3)
b/Å	14.007(3)
c/Å	16.650(3)
α/°	67.291(5)
β/°	89.525(7)
γ/°	71.495(7)
Volume/Å^3	2266.5(8)
Z	2
ρ_{calc}g/cm^3	1.530
μ/mm^{-1}	0.527
F(000)	1080.0
Crystal size/mm^3	0.317 × 0.188 × 0.058
Radiation	MoKα (λ = 0.71073)
2Θ range for data collection/°	4.404 to 57.296
Index ranges	-15 ≤ h ≤ 15, -17 ≤ k ≤ 18, 0 ≤ l ≤ 22
Reflections collected	11527
Independent reflections	11527 [R_{int} = ?, R_{sigma} = 0.0213]
Data/restraints/parameters	11527/0/575
Goodness-of-fit on F^2	1.060
Final R indexes [I>=2σ (I)]	R_1 = 0.0307, wR_2 = 0.0739
Final R indexes [all data]	R_1 = 0.0343, wR_2 = 0.0761
Largest diff. peak/hole / e Å^{-3}	0.90/-0.64

Structure 237

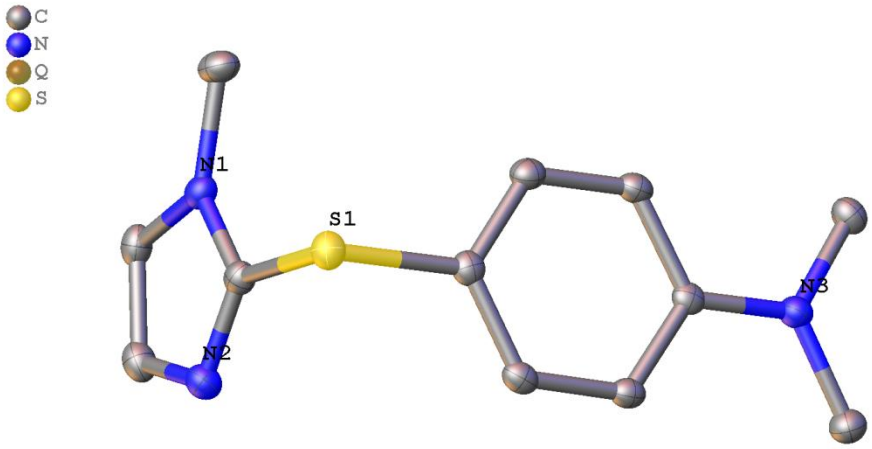

Figure S40: Asymmetric unit of **237**.

Empirical formula	$C_{12}H_{15}N_3S$
Formula weight	233.33
Temperature/K	100(2)
Crystal system	monoclinic
Space group	$P2_1/c$
a/Å	13.6491(10)
b/Å	7.4013(5)
c/Å	11.4104(6)
α/°	90
β/°	92.807(3)
γ/°	90
Volume/Å^3	1151.31(13)
Z	4
ρ_{calc}g/cm^3	1.346
μ/mm^{-1}	0.256
F(000)	496.0
Crystal size/mm^3	0.396 × 0.255 × 0.088
Radiation	MoKα (λ = 0.71073)
2Θ range for data collection/°	5.976 to 59.172
Index ranges	-18 ≤ h ≤ 18, -10 ≤ k ≤ 10, -15 ≤ l ≤ 14
Reflections collected	24847
Independent reflections	3198 [R_{int} = 0.0226, R_{sigma} = 0.0134]
Data/restraints/parameters	3198/0/148
Goodness-of-fit on F^2	1.041
Final R indexes [I>=2σ (I)]	R_1 = 0.0292, wR_2 = 0.0789
Final R indexes [all data]	R_1 = 0.0314, wR_2 = 0.0810
Largest diff. peak/hole / e Å^{-3}	0.40/-0.25

Structure 235

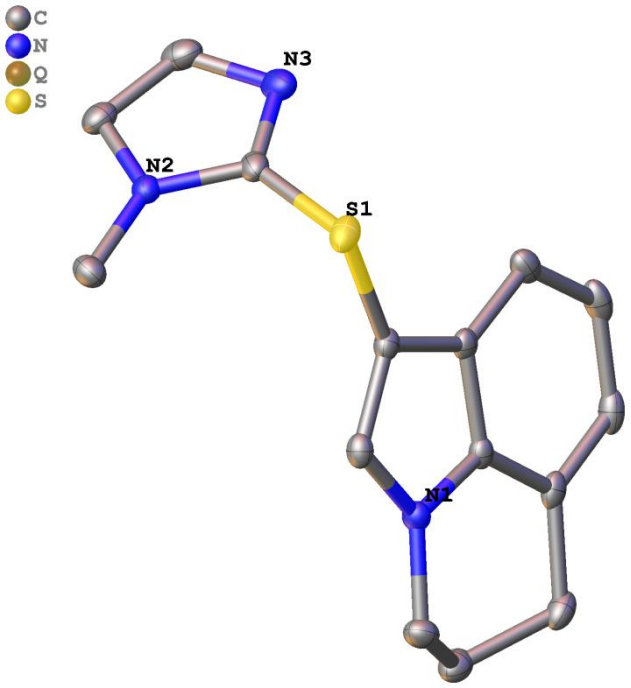

Figure S41: Asymmetric unit of **235**.

Empirical formula	$C_{15}H_{15}N_3S$
Formula weight	269.36
Temperature/K	100(2)
Crystal system	monoclinic
Space group	$P2_1/c$
a/Å	11.5161(16)
b/Å	9.7152(15)
c/Å	11.8038(14)
α/°	90
β/°	102.249(5)
γ/°	90
Volume/Å^3	1290.6(3)
Z	4
ρ_{calc}g/cm^3	1.386
μ/mm^{-1}	0.239
F(000)	568.0
Crystal size/mm^3	0.476 × 0.42 × 0.108
Radiation	MoKα (λ = 0.71073)
2Θ range for data collection/°	5.482 to 59.204
Index ranges	-15 ≤ h ≤ 15, -13 ≤ k ≤ 13, -16 ≤ l ≤ 15
Reflections collected	17877
Independent reflections	3590 [R_{int} = 0.0284, R_{sigma} = 0.0214]
Data/restraints/parameters	3590/0/173
Goodness-of-fit on F^2	1.039
Final R indexes [I>=2σ (I)]	R_1 = 0.0311, wR_2 = 0.0787
Final R indexes [all data]	R_1 = 0.0346, wR_2 = 0.0817
Largest diff. peak/hole / e Å^{-3}	0.39/-0.32

Structure 234 NHS

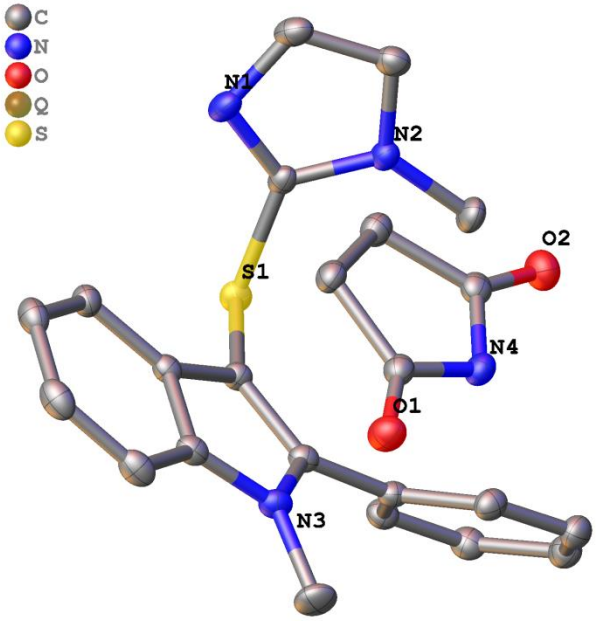

Figure S42: Asymmetric unit of **234 NHS**.

Empirical formula	$C_{23}H_{22}N_4O_2S$
Formula weight	418.50
Temperature/K	100(2)
Crystal system	monoclinic
Space group	$P2_1/c$
a/Å	13.7652(14)
b/Å	8.3479(7)
c/Å	17.6642(18)
α/°	90
β/°	97.550(3)
γ/°	90
Volume/Å^3	2012.2(3)
Z	4
ρ_{calc}g/cm^3	1.381
μ/mm^{-1}	0.190
F(000)	880.0
Crystal size/mm^3	0.667 × 0.345 × 0.254
Radiation	MoKα (λ = 0.71073)
2Θ range for data collection/°	4.652 to 61.06
Index ranges	-19 ≤ h ≤ 19, -11 ≤ k ≤ 11, -24 ≤ l ≤ 25
Reflections collected	51129
Independent reflections	6120 [R_{int} = 0.0249, R_{sigma} = 0.0154]
Data/restraints/parameters	6120/0/276
Goodness-of-fit on F^2	1.065
Final R indexes [I>=2σ (I)]	R_1 = 0.0338, wR_2 = 0.0928
Final R indexes [all data]	R_1 = 0.0355, wR_2 = 0.0942
Largest diff. peak/hole / e Å^{-3}	0.42/-0.28

Structure 239

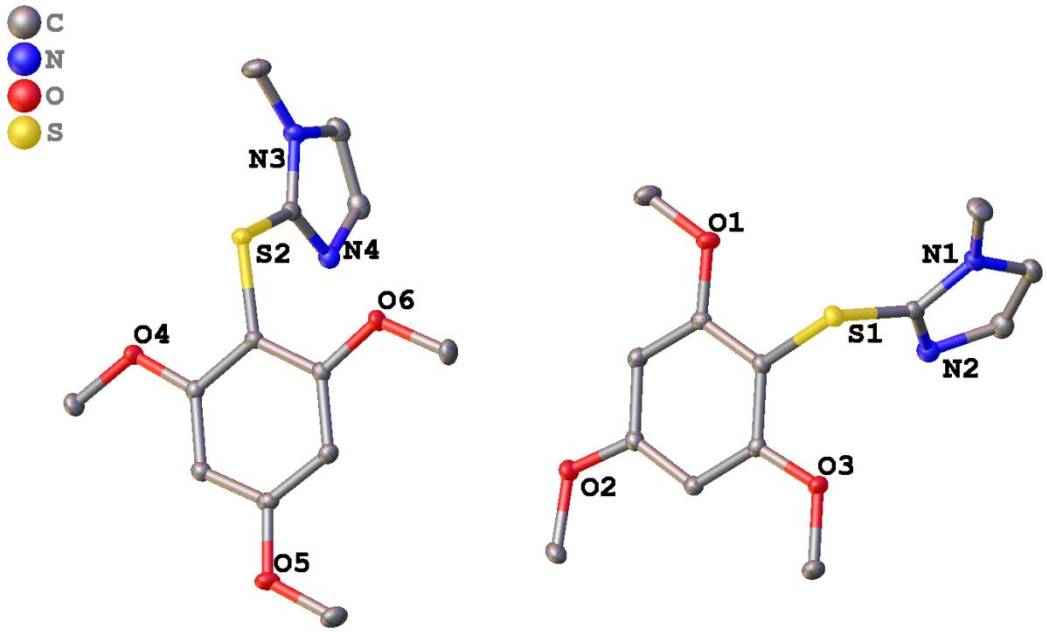

Figure S43: Asymmetric unit of **239**.

Empirical formula	$C_{13}H_{16}N_2O_3S$
Formula weight	280.34
Temperature/K	100(2)
Crystal system	triclinic
Space group	P-1
a/Å	7.9206(5)
b/Å	12.8647(8)
c/Å	14.0093(8)
α/°	69.954(2)
β/°	88.577(2)
γ/°	82.141(2)
Volume/Å^3	1328.05(14)
Z	4
ρ_{calc}g/cm^3	1.402
μ/mm^{-1}	0.249
F(000)	592.0
Crystal size/mm^3	0.406 × 0.269 × 0.231
Radiation	MoKα (λ = 0.71073)
2Θ range for data collection/°	5.194 to 57.46
Index ranges	-10 ≤ h ≤ 10, -17 ≤ k ≤ 17, -18 ≤ l ≤ 18
Reflections collected	44288
Independent reflections	6864 [R_{int} = 0.0190, R_{sigma} = 0.0133]
Data/restraints/parameters	6864/0/351
Goodness-of-fit on F^2	1.043
Final R indexes [I>=2σ (I)]	R_1 = 0.0267, wR_2 = 0.0724
Final R indexes [all data]	R_1 = 0.0277, wR_2 = 0.0732
Largest diff. peak/hole / e Å^{-3}	0.42/-0.27

Structure 233

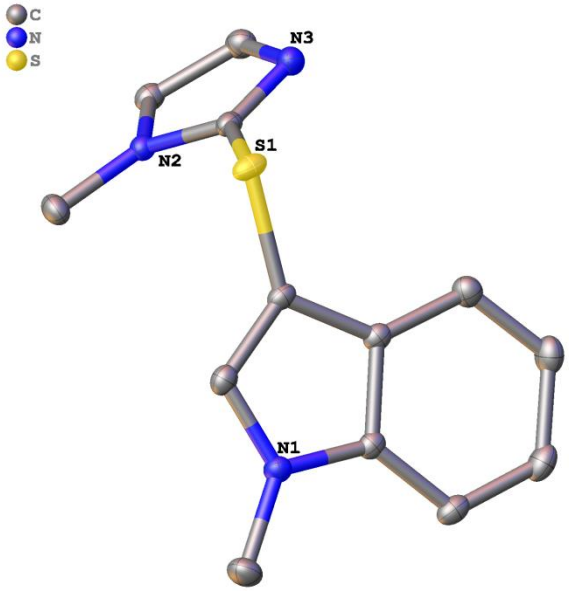

Figure S44: Asymmetric unit of **233**.

Empirical formula	$C_{13}H_{13}N_3S$
Formula weight	243.32
Temperature/K	100
Crystal system	monoclinic
Space group	$P2_1/c$
a/Å	10.9446(3)
b/Å	10.4950(3)
c/Å	11.1756(3)
α/°	90
β/°	114.0750(10)
γ/°	90
Volume/Å^3	1172.01(6)
Z	4
ρ_{calc}g/cm^3	1.379
μ/mm^{-1}	0.255
F(000)	512.0
Crystal size/mm^3	0.337 × 0.283 × 0.102
Radiation	MoKα (λ = 0.71073)
2Θ range for data collection/°	5.63 to 61.052
Index ranges	-15 ≤ h ≤ 15, -14 ≤ k ≤ 15, -15 ≤ l ≤ 15
Reflections collected	41743
Independent reflections	3572 [R_{int} = 0.0199, R_{sigma} = 0.0114]
Data/restraints/parameters	3572/0/156
Goodness-of-fit on F^2	1.058
Final R indexes [I>=2σ (I)]	R_1 = 0.0287, wR_2 = 0.0757
Final R indexes [all data]	R_1 = 0.0297, wR_2 = 0.0765
Largest diff. peak/hole / e Å^{-3}	0.47/-0.25

5.8.9 Structure of other heterocyclic backbones

Structure 258

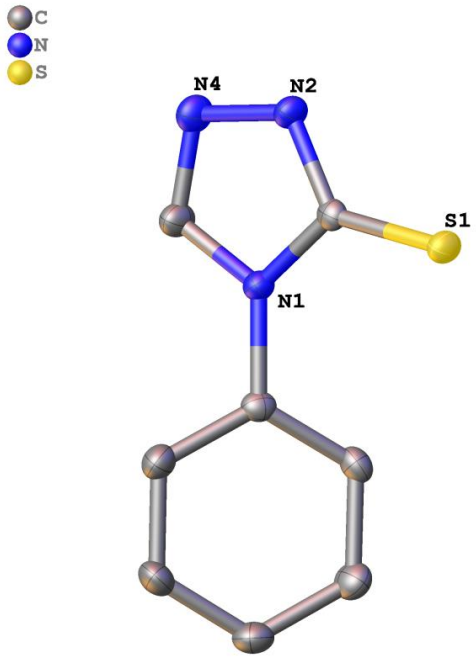

Figure S45: Asymmetric unit of **258**.

258 forms hydrogen bond bridged dimers in the solid state between N1H and S2 which is accessible by the symmetry operation [-1+X,3/2-Y,1/2+Z].

Empirical formula	$C_8H_7N_3S$
Formula weight	177.23
Temperature/K	100(2)
Crystal system	monoclinic
Space group	$P2_1/c$
a/Å	6.0142(6)
b/Å	14.1041(11)
c/Å	10.1918(8)
α/°	90
β/°	98.841(3)
γ/°	90
Volume/Å^3	854.25(13)
Z	4
ρ_{calc}g/cm^3	1.378
μ/mm^{-1}	0.322
F(000)	368.0
Crystal size/mm^3	0.277 × 0.084 × 0.073
Radiation	MoKα (λ = 0.71073)
2Θ range for data collection/°	4.97 to 52.778
Index ranges	-7 ≤ h ≤ 7, -15 ≤ k ≤ 17, -12 ≤ l ≤ 12
Reflections collected	5371
Independent reflections	1717 [R_{int} = 0.0701, R_{sigma} = 0.0705]
Data/restraints/parameters	1717/0/137
Goodness-of-fit on F^2	1.091
Final R indexes [I>=2σ (I)]	R_1 = 0.0478, wR_2 = 0.0854
Final R indexes [all data]	R_1 = 0.0724, wR_2 = 0.0979
Largest diff. peak/hole / e Å^{-3}	0.26/-0.33

5.8.10 Structure of tetramethylthiourea adducts

The following structures are included for the sake of completeness of data but are not discussed in this thesis.

Structure 315

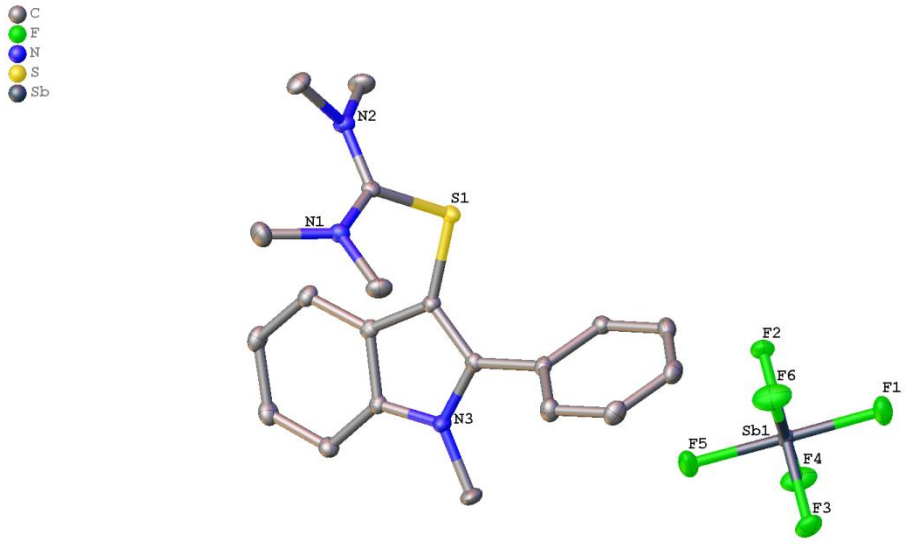

Figure S46: Asymmetric unit of **315.**

Empirical formula	$C_{20}H_{24}F_6N_3SSb$
Formula weight	574.23
Temperature/K	100(2)
Crystal system	monoclinic
Space group	$P2_1/n$
a/Å	10.9954(4)
b/Å	15.1752(5)
c/Å	14.1479(5)
α/°	90
β/°	107.5950(10)
γ/°	90
Volume/Å^3	2250.24(14)
Z	4
ρ_{calc}g/cm^3	1.695
μ/mm^{-1}	1.380
F(000)	1144.0
Crystal size/mm^3	0.155 × 0.087 × 0.073
Radiation	MoKα (λ = 0.71073)
2Θ range for data collection/°	4.724 to 61.164
Index ranges	-15 ≤ h ≤ 15, -21 ≤ k ≤ 21, -20 ≤ l ≤ 20
Reflections collected	94108
Independent reflections	6920 [R_{int} = 0.0318, R_{sigma} = 0.0132]
Data/restraints/parameters	6920/0/285
Goodness-of-fit on F^2	0.746
Final R indexes [I>=2σ (I)]	R_1 = 0.0191, wR_2 = 0.0777
Final R indexes [all data]	R_1 = 0.0228, wR_2 = 0.0844
Largest diff. peak/hole / e Å^{-3}	0.45/-0.64

5.8.11 Struture of further reagents and products

Structure 269

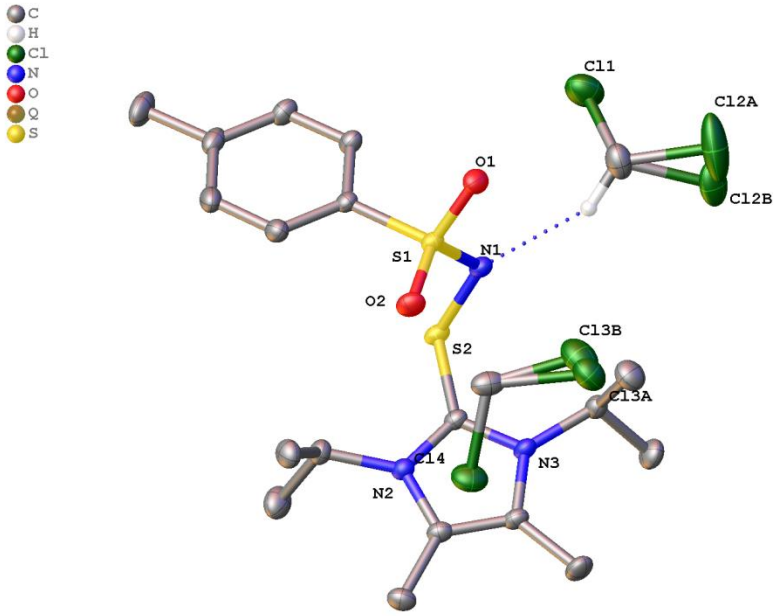

Figure S47: Asymmetric unit of **269** containing two dichloromethane molecules**.**

The distance of N1 and the C19 of the nearest dichloromethane molecule of 3.075Å indicates N-HC interactions of the switterionic compound **269** and the dichloromethane. Both dichloromethane molecules are disordered about two positions. They are refined with some restrained anisotropic displacement parameters. The occupancies of the minor positions are refined to 0.08997 (Cl12B) and 0.32382 (Cl13B), respectively.

Empirical formula	$C_{20}H_{31}Cl_4N_3O_2S_2$
Formula weight	551.40
Temperature/K	100(2)
Crystal system	triclinic
Space group	P-1
a/Å	9.8104(5)
b/Å	10.3280(6)
c/Å	14.4043(8)
α/°	101.815(2)
β/°	106.662(2)
γ/°	94.336(2)
Volume/Å^3	1354.46(13)
Z	2
ρ_{calc}g/cm^3	1.352
μ/mm^{-1}	0.613
F(000)	576.0
Crystal size/mm^3	0.418 × 0.236 × 0.161
Radiation	MoKα (λ = 0.71073)
2Θ range for data collection/°	4.466 to 63.11
Index ranges	-14 ≤ h ≤ 14, -15 ≤ k ≤ 15, -21 ≤ l ≤ 21
Reflections collected	49416
Independent reflections	9042 [R_{int} = 0.0230, R_{sigma} = 0.0198]
Data/restraints/parameters	9042/24/307
Goodness-of-fit on F^2	1.033
Final R indexes [I>=2σ (I)]	R_1 = 0.0304, wR_2 = 0.0818
Final R indexes [all data]	R_1 = 0.0322, wR_2 = 0.0831
Largest diff. peak/hole / e Å^{-3}	0.77/-0.72

Structure 275

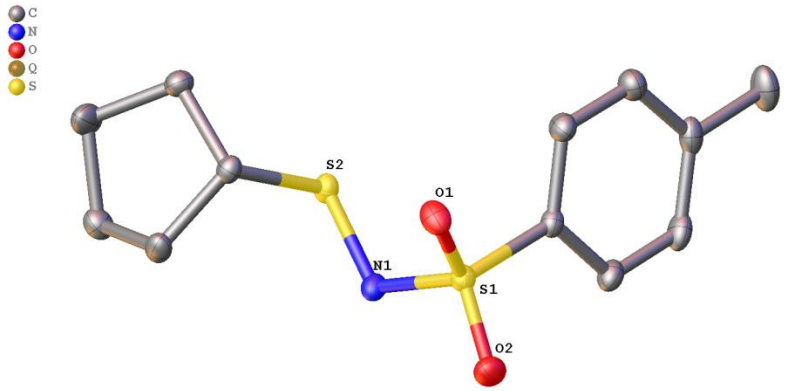

Figure S 48: Asymmetric unit of **275**.

Empirical formula	$C_{12}H_{17}NO_2S_2$
Formula weight	271.38
Temperature/K	100(2)
Crystal system	monoclinic
Space group	$P2_1/n$
a/Å	5.0837(10)
b/Å	19.708(4)
c/Å	13.403(2)
α/°	90
β/°	100.063(5)
γ/°	90
Volume/Å^3	1322.2(4)
Z	4
ρ_{calc}g/cm^3	1.363
μ/mm^{-1}	0.392
F(000)	576.0
Crystal size/mm^3	0.413 × 0.066 × 0.038
Radiation	MoKα (λ = 0.71073)
2Θ range for data collection/°	5.16 to 63.006
Index ranges	-7 ≤ h ≤ 7, -28 ≤ k ≤ 28, -19 ≤ l ≤ 17
Reflections collected	29571
Independent reflections	4394 [R_{int} = 0.0256, R_{sigma} = 0.0167]
Data/restraints/parameters	4394/0/159
Goodness-of-fit on F^2	1.058
Final R indexes [I>=2σ (I)]	R_1 = 0.0278, wR_2 = 0.0761
Final R indexes [all data]	R_1 = 0.0311, wR_2 = 0.0784
Largest diff. peak/hole / e Å^{-3}	0.45/-0.32

Structure 306

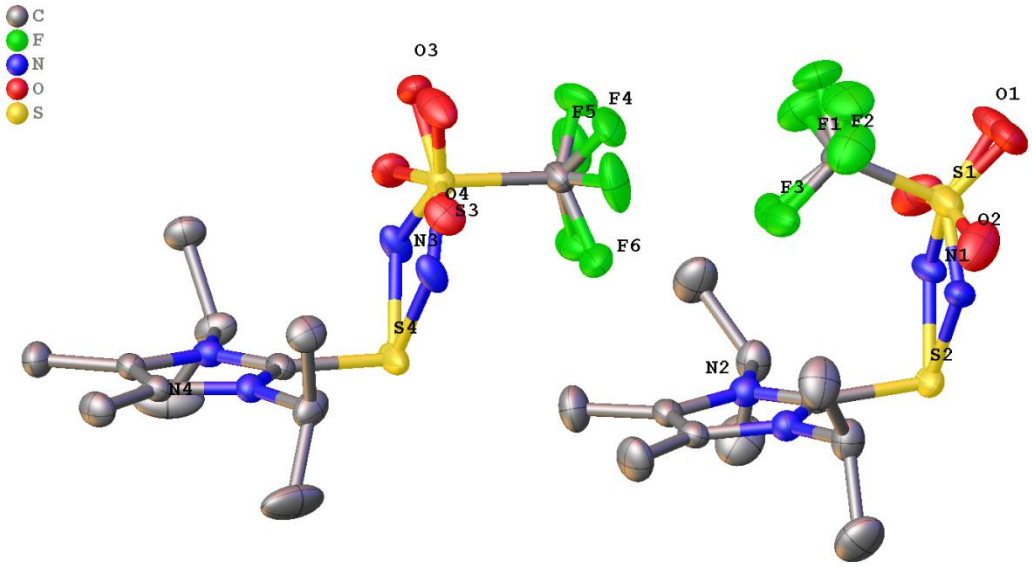

Figure S49: Asymmetric unit of **306** after symmetry operation [+X,1/2-Y,+Z]**.**

306 lays on a mirror plane located through S1, S2 and S4. The TfN-group is disordered about two positions over the mirror plane.

Empirical formula	$C_{12}H_{20}F_3N_3O_2S_2$
Formula weight	359.43
Temperature/K	100(2)
Crystal system	orthorhombic
Space group	Pnma
a/Å	21.4772(9)
b/Å	15.1570(8)
c/Å	9.9949(5)
α/°	90
β/°	90
γ/°	90
Volume/Å^3	3253.6(3)
Z	8
ρ_{calc}g/cm^3	1.468
μ/mm^{-1}	0.367
F(000)	1504.0
Crystal size/mm^3	0.432 × 0.134 × 0.104
Radiation	MoKα (λ = 0.71073)
2Θ range for data collection/°	4.494 to 61.024
Index ranges	-30 ≤ h ≤ 30, -21 ≤ k ≤ 21, -14 ≤ l ≤ 14
Reflections collected	54470
Independent reflections	5118 [R_{int} = 0.0377, R_{sigma} = 0.0176]
Data/restraints/parameters	5118/0/271
Goodness-of-fit on F^2	1.045
Final R indexes [I>=2σ (I)]	R_1 = 0.0491, wR_2 = 0.1129
Final R indexes [all data]	R_1 = 0.0589, wR_2 = 0.1204
Largest diff. peak/hole / e Å^{-3}	1.01/-1.10

Structure 309

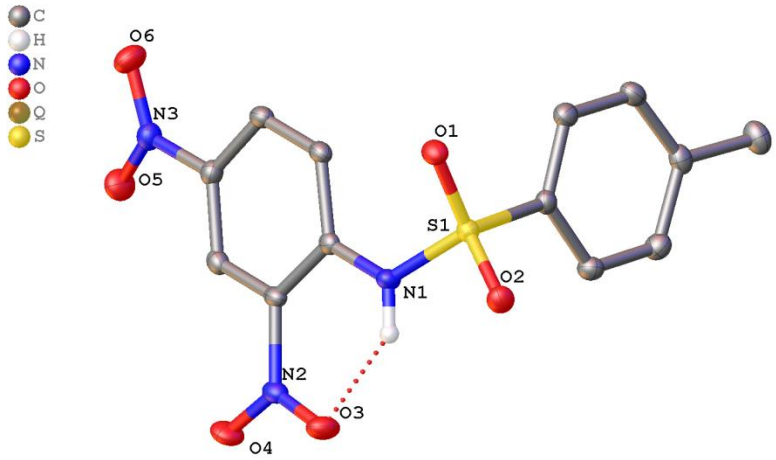

Figure S50: Asymmetric unit of **309**.

The hydrogen bond between N1 and O3 results in N1-O3 distance of 2.599 Å.

Empirical formula	$C_{13}H_{11}N_3O_6S$
Formula weight	337.31
Temperature/K	100(2)
Crystal system	monoclinic
Space group	$P2_1/c$
a/Å	7.9828(15)
b/Å	16.640(3)
c/Å	10.691(3)
α/°	90
β/°	98.939(12)
γ/°	90
Volume/Å^3	1402.9(5)
Z	4
ρ_{calc}g/cm^3	1.597
μ/mm^{-1}	0.269
F(000)	696.0
Crystal size/mm^3	0.268 × 0.072 × 0.036
Radiation	MoKα (λ = 0.71073)
2Θ range for data collection/°	5.166 to 57.388
Index ranges	-10 ≤ h ≤ 10, -22 ≤ k ≤ 22, -14 ≤ l ≤ 12
Reflections collected	20454
Independent reflections	3618 [R_{int} = 0.0308, R_{sigma} = 0.0218]
Data/restraints/parameters	3618/0/212
Goodness-of-fit on F^2	1.055
Final R indexes [I>=2σ (I)]	R_1 = 0.0326, wR_2 = 0.0787
Final R indexes [all data]	R_1 = 0.0373, wR_2 = 0.0814
Largest diff. peak/hole / e Å^{-3}	0.38/-0.47

5.8.12 Studies of dibenzothiophene-based structure

The following structures are included for the sake of completeness of data but are not discussed in this thesis.

Structure 323

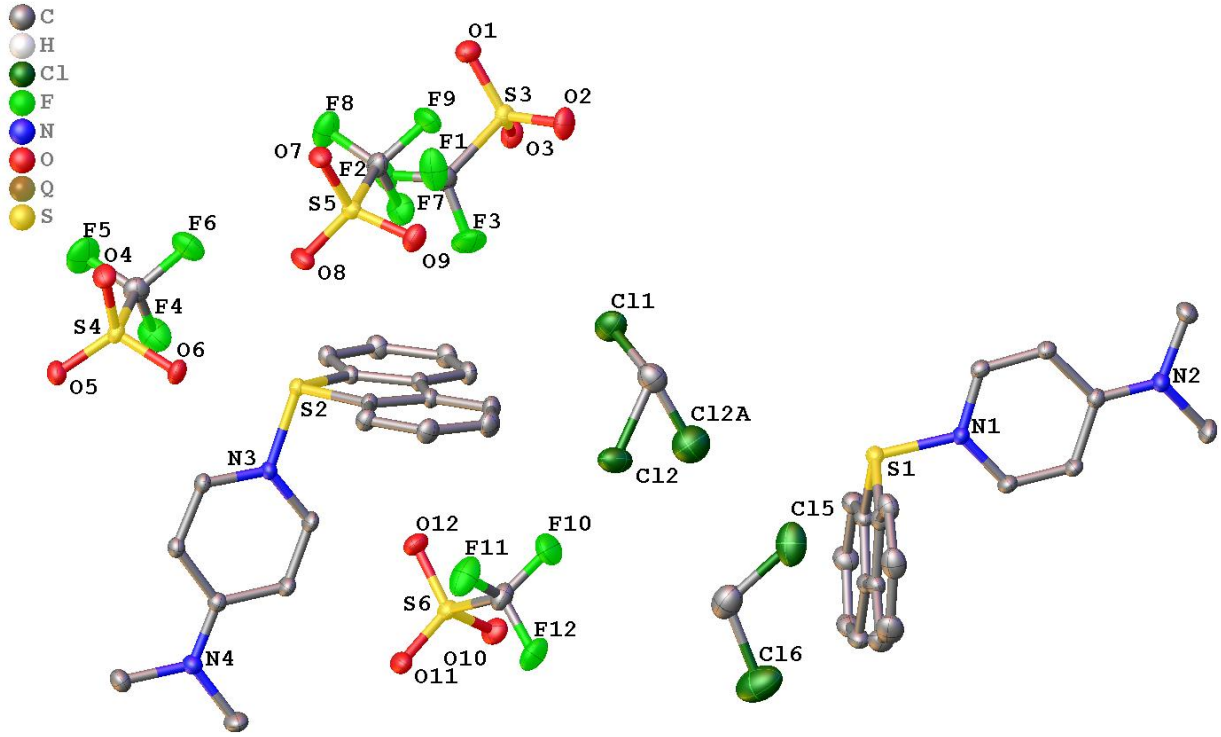

Figure S51: Asymmetric unit of **323** containing four dichloromethane molecules. Two dichloromethane molecules are emitted for clarity.

Two of the four dichloromethane molecules in the asymmetric unit are disordered about two positions. and are emitted in Figure S51. They are is refined with distance restraints and some of the anisotropic displacement parameters are constrained to be the same.

Empirical formula	$C_{23}H_{22.01}Cl_{4.01}F_6N_2O_6S_3$
Formula weight	774.68
Temperature/K	100(2)
Crystal system	triclinic
Space group	P-1
a/Å	12.4396(18)
b/Å	16.799(2)
c/Å	17.184(3)
α/°	103.843(6)
β/°	102.712(5)
γ/°	106.394(7)
Volume/Å^3	3181.5(8)
Z	4
ρ_{calc}g/cm^3	1.617
μ/mm^{-1}	0.646
F(000)	1569.0
Crystal size/mm^3	0.735 × 0.141 × 0.1
Radiation	MoKα (λ = 0.71073)
2Θ range for data collection/°	4.824 to 61.104
Index ranges	-15 ≤ h ≤ 17, -24 ≤ k ≤ 22, -24 ≤ l ≤ 24
Reflections collected	64517
Independent reflections	19403 [R_{int} = 0.0264, R_{sigma} = 0.0281]
Data/restraints/parameters	19403/49/874
Goodness-of-fit on F^2	1.025
Final R indexes [I>=2σ (I)]	R_1 = 0.0403, wR_2 = 0.1062
Final R indexes [all data]	R_1 = 0.0487, wR_2 = 0.1117
Largest diff. peak/hole / e Å^{-3}	1.21/-0.81

5.9 NMR spectra

NMR-Spektren

Synthesis of backbones and reagents

^{1}H NMR (300 MHz, $CDCl_3$) **78**

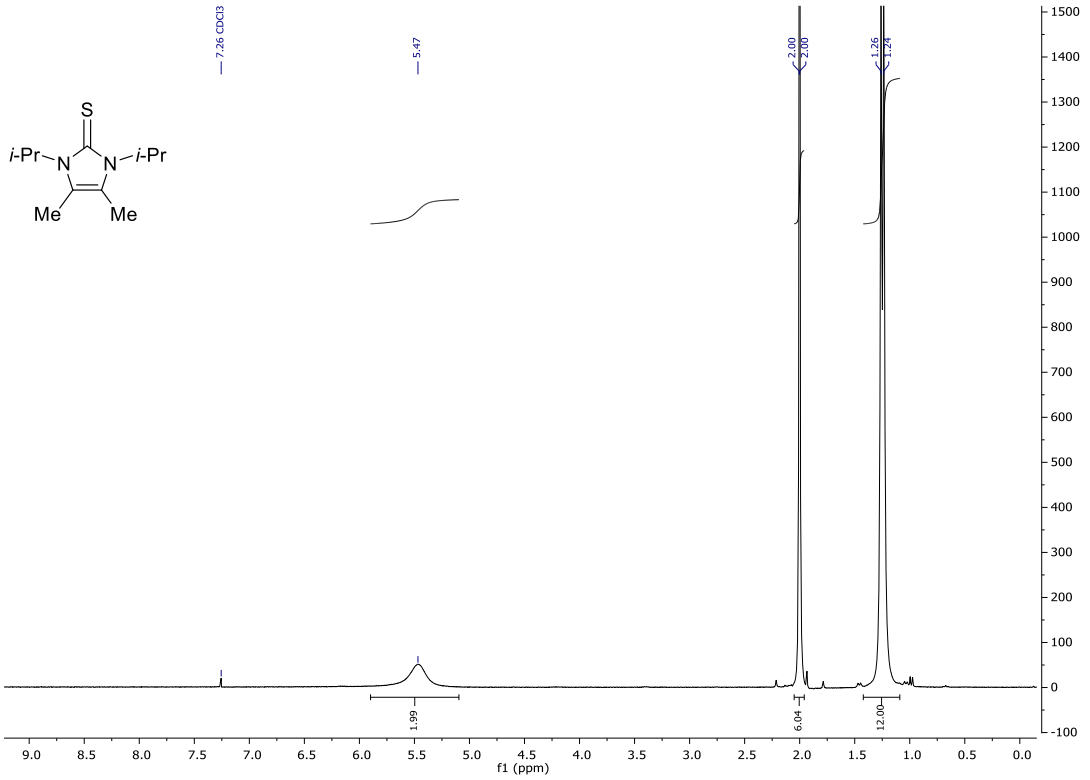

^{13}C NMR (75 MHz, $CDCl_3$) **78**

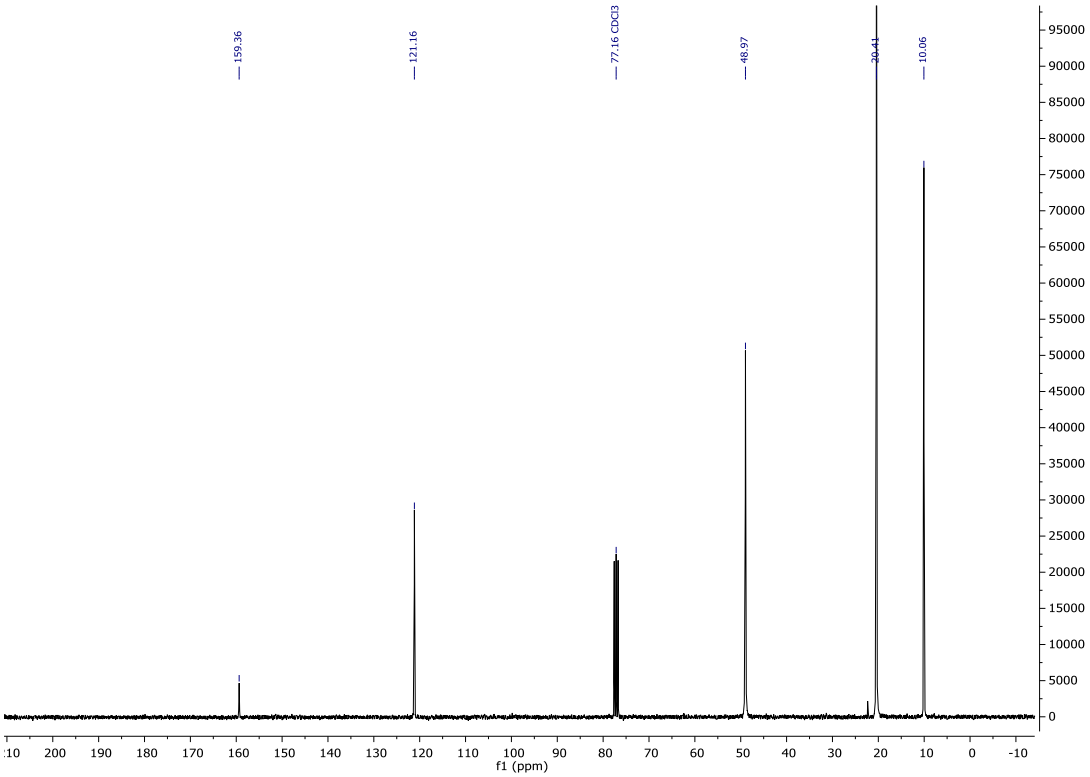

^{1}H NMR (300 MHz, $CDCl_3$) **95**

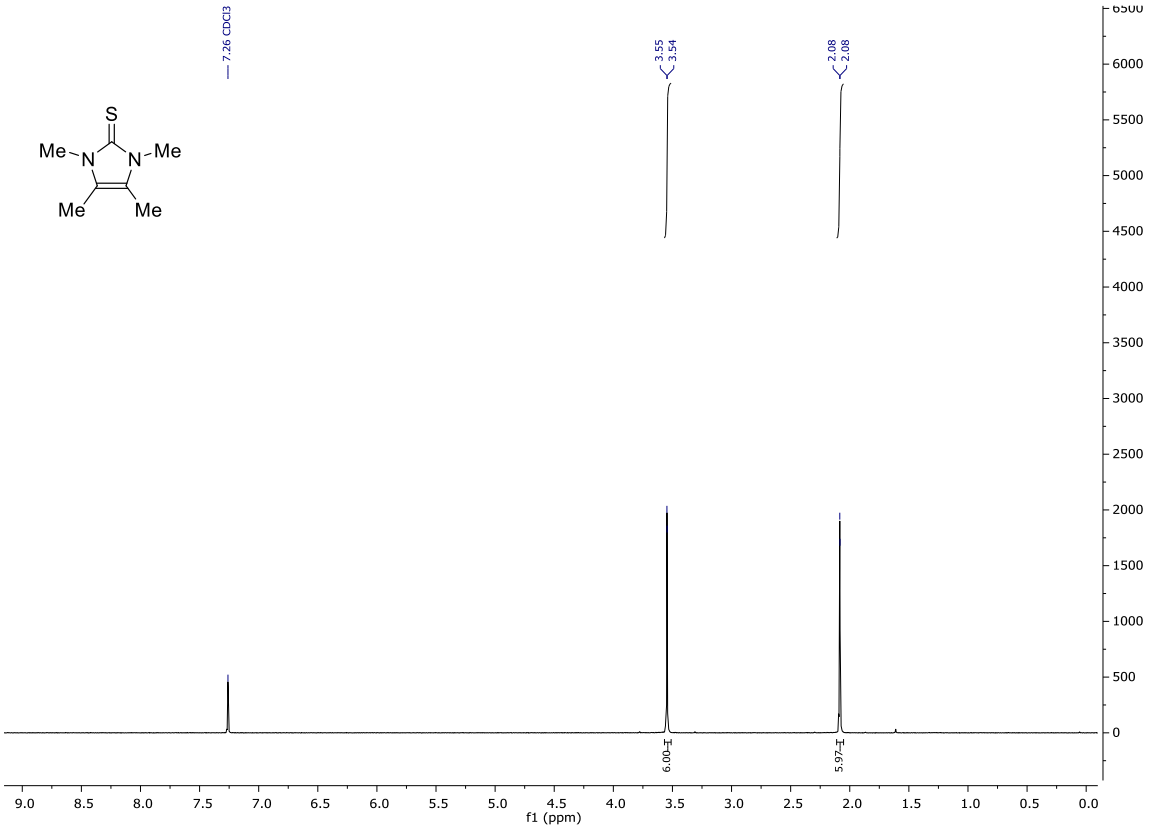

^{1}H NMR (300 MHz, CD_2Cl_2) **91**

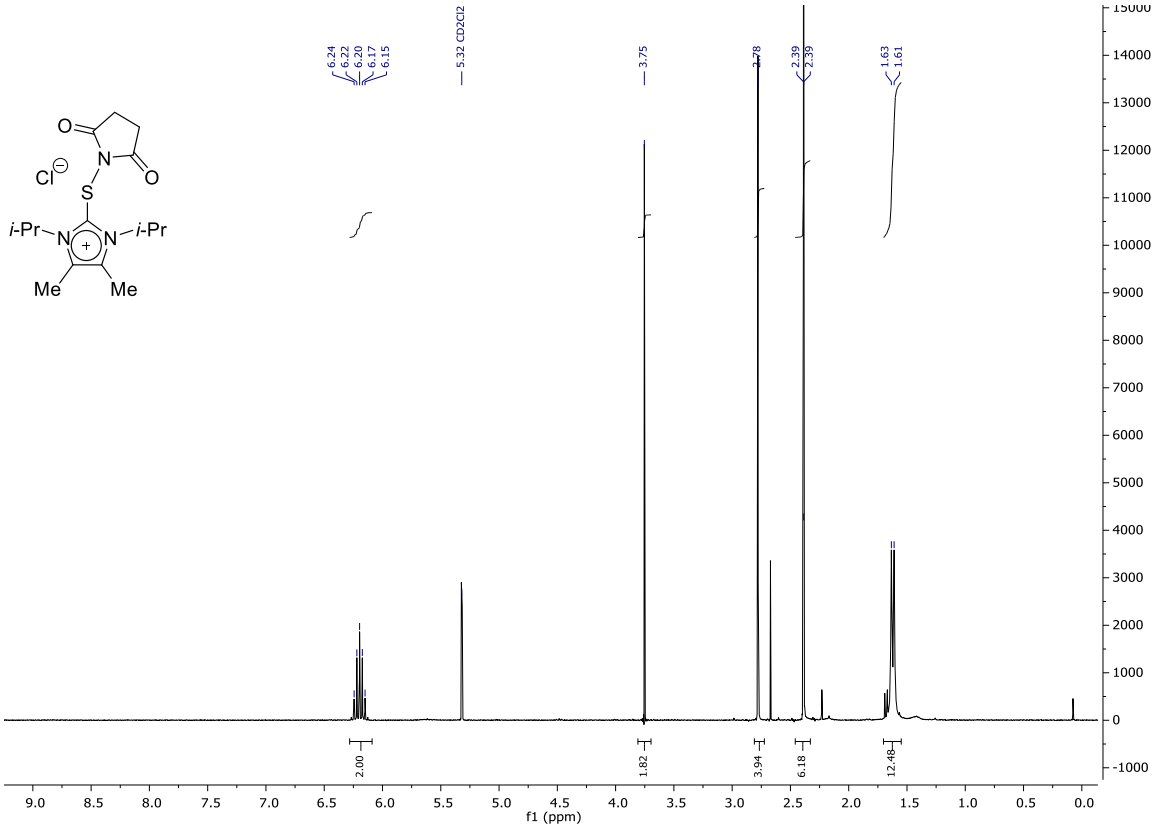

^{13}C NMR (75 MHz, CD_2Cl_2) **91**

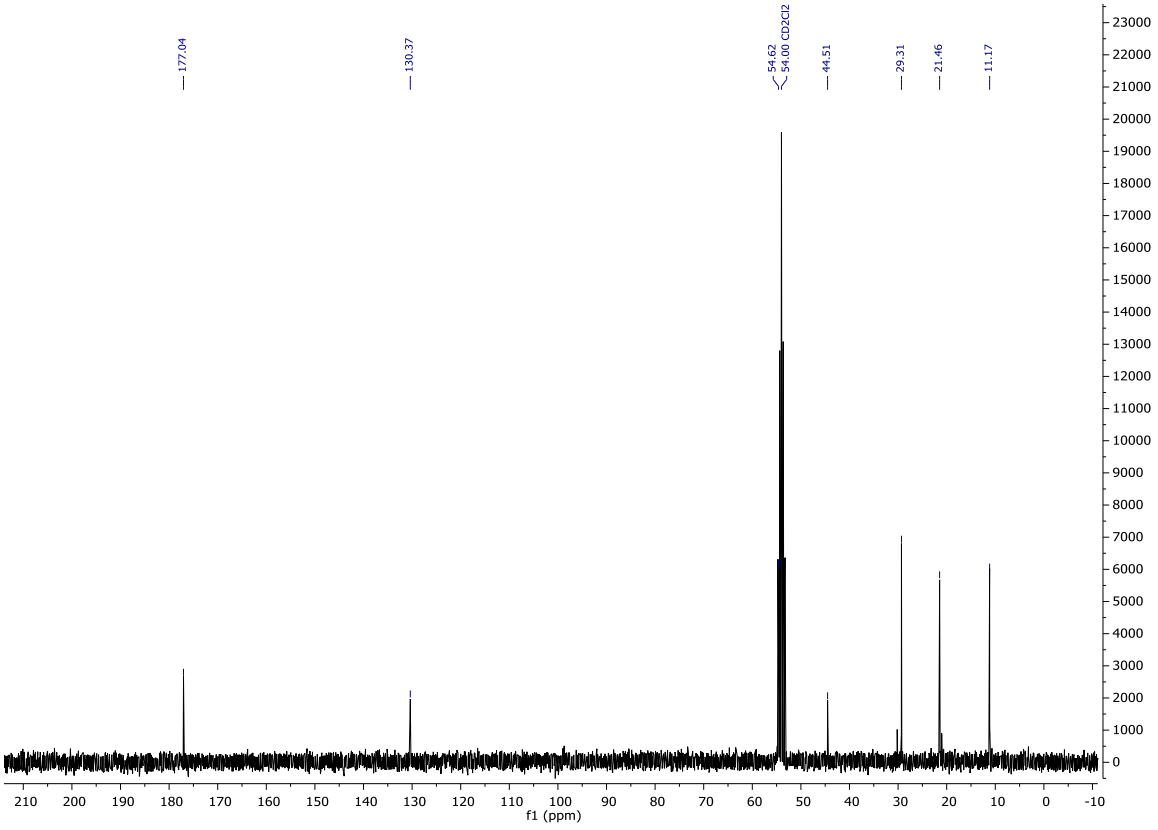

^{1}H NMR (300 MHz, CD_2Cl_2) **93**

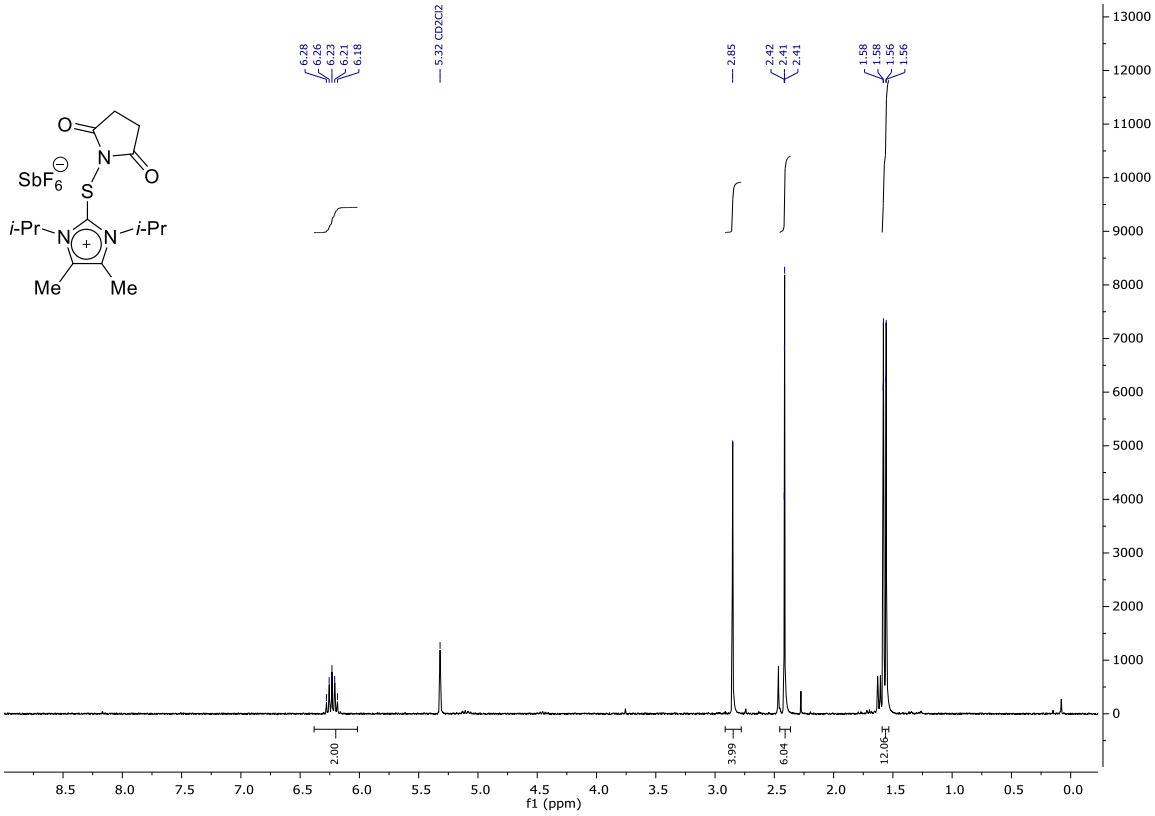

^{13}C NMR (126 MHz, CD_2Cl_2) **93**

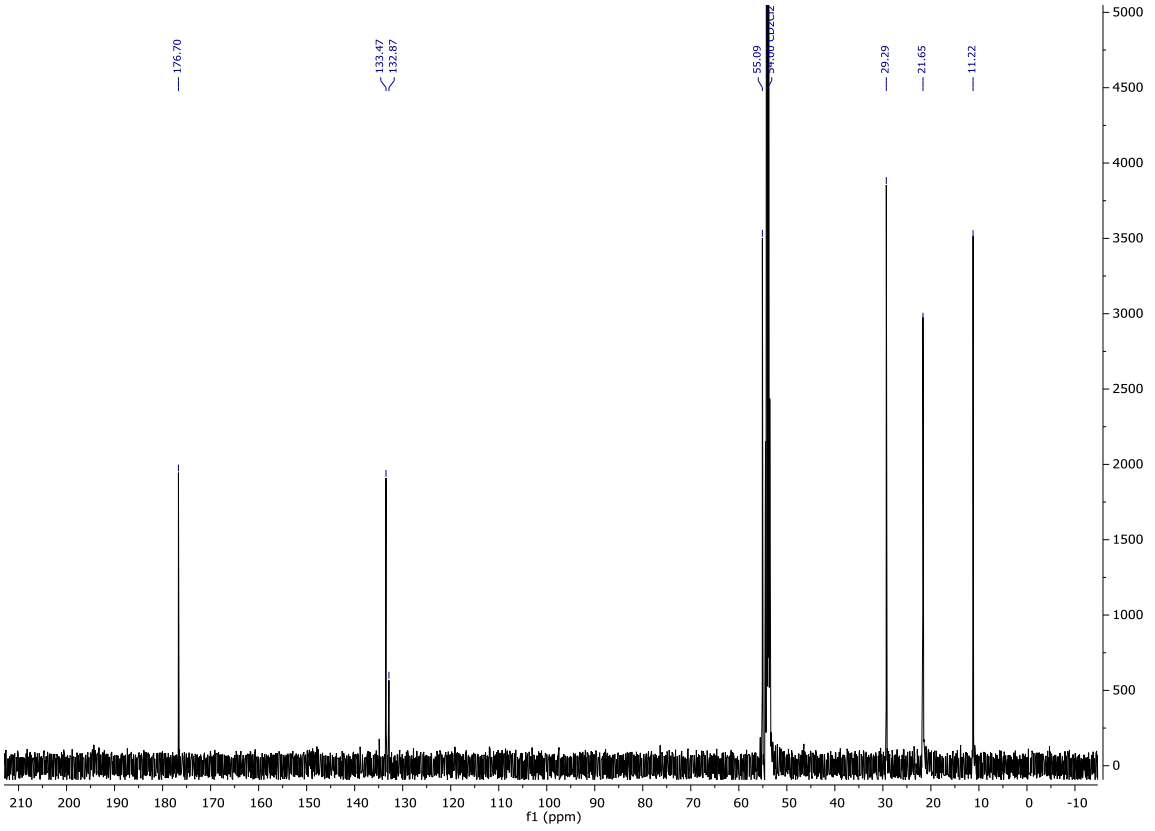

^{1}H NMR (300 MHz, CD_2Cl_2) **295**

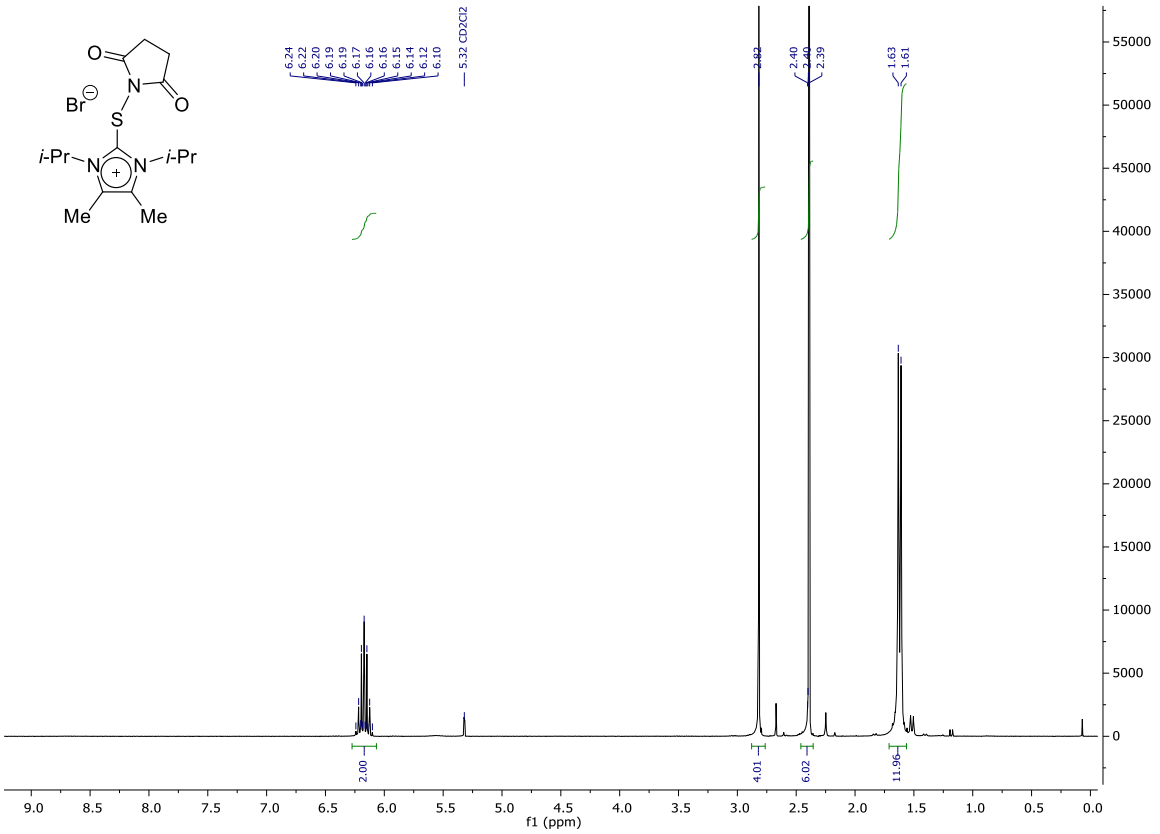

^{13}C NMR (75 MHz, CD_2Cl_2) **295**

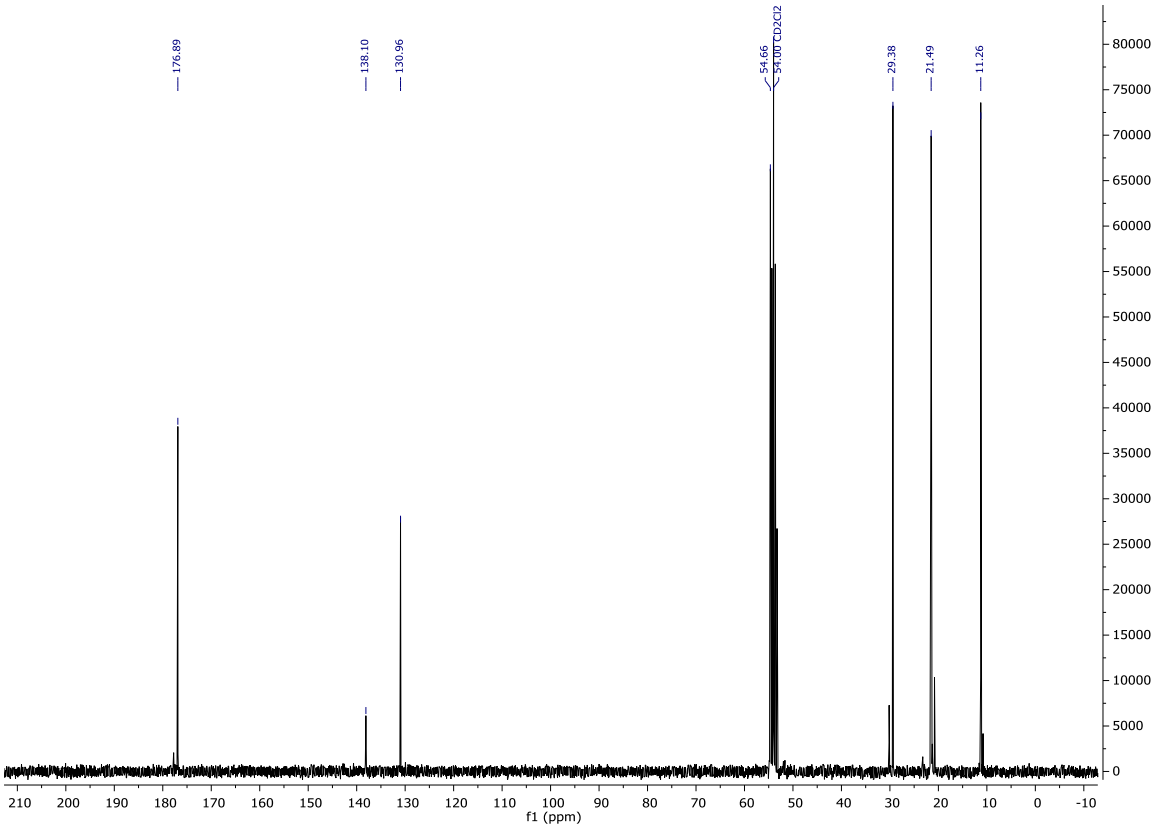

^{1}H NMR (300 MHz, CD_3CN) **92**

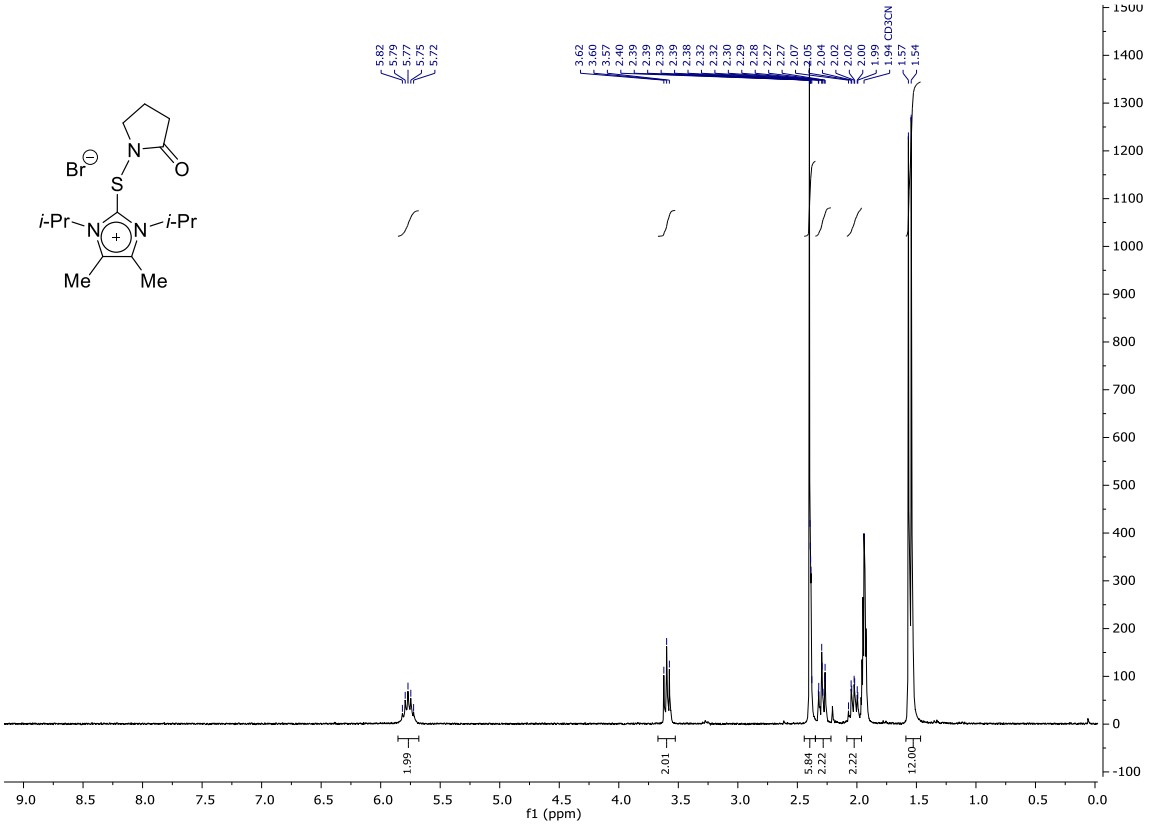

^{13}C NMR (75 MHz, CD_3CN) **92**

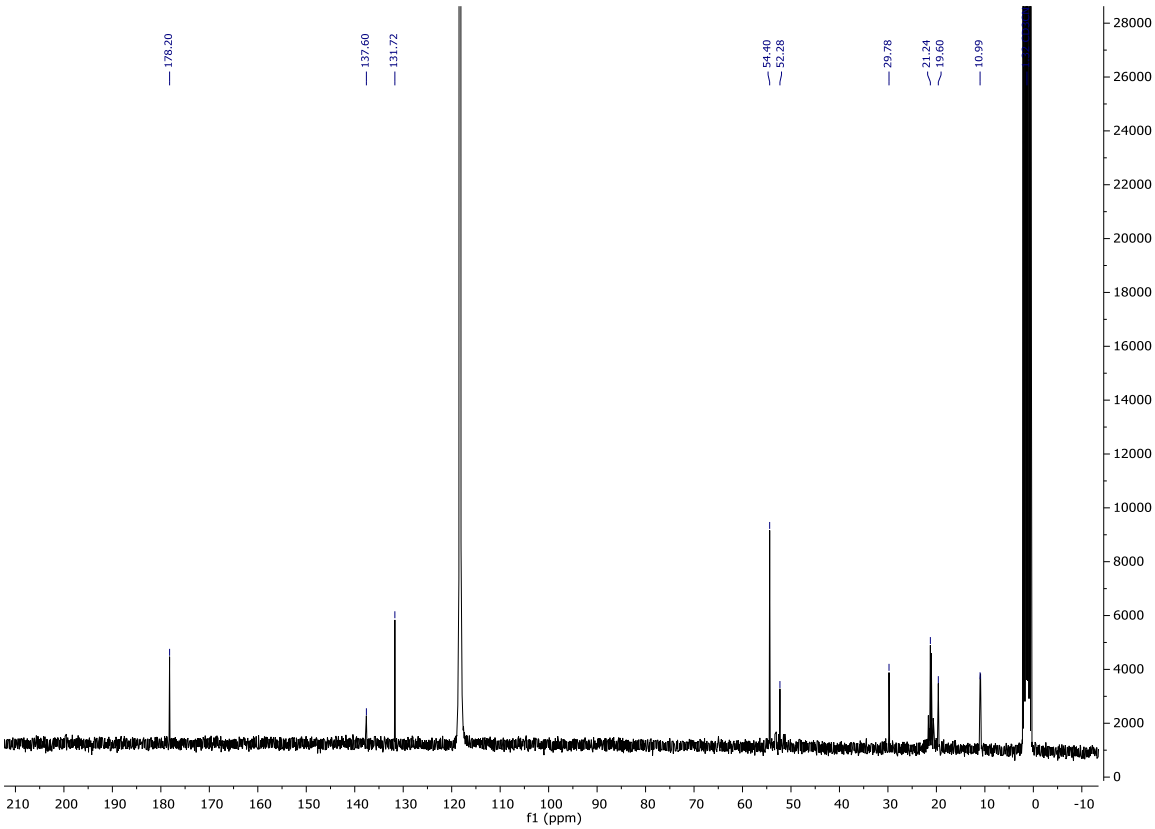

^{1}H NMR (300 MHz, $CDCl_3$) **94**

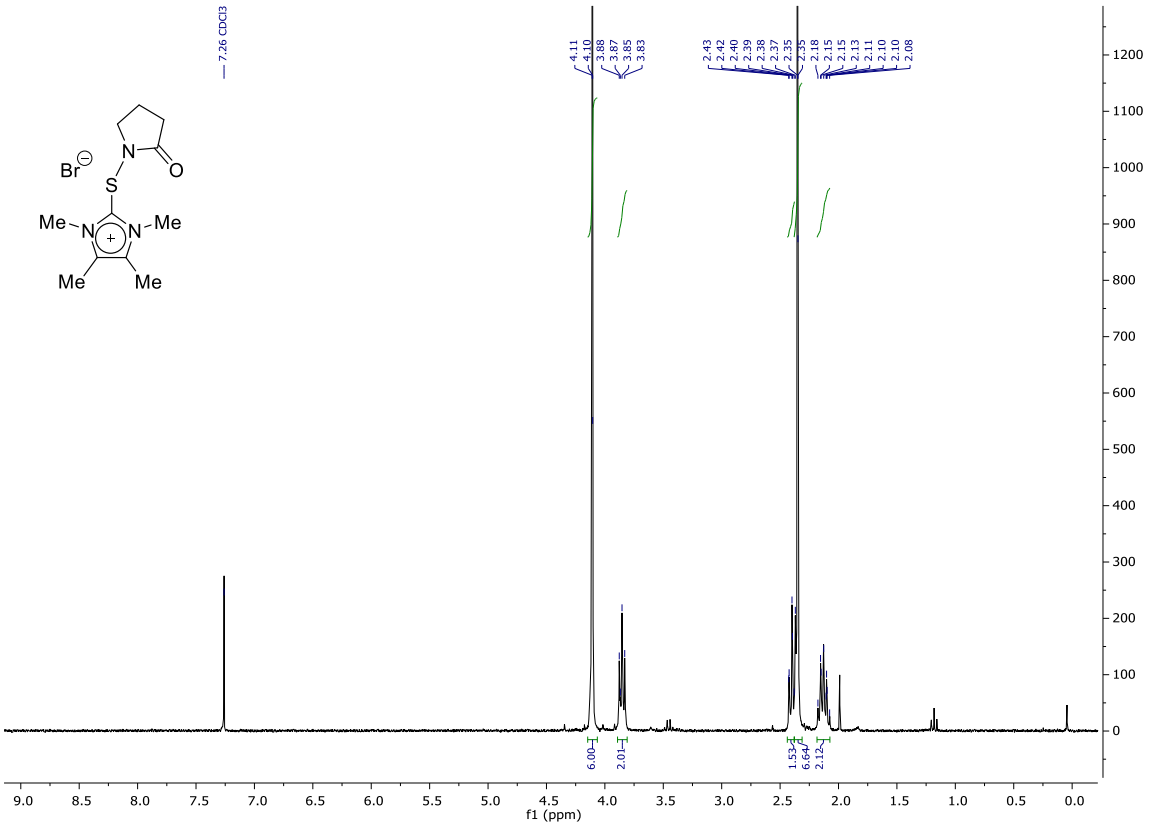

^{13}C NMR (75 MHz, CD_3CN) **94**

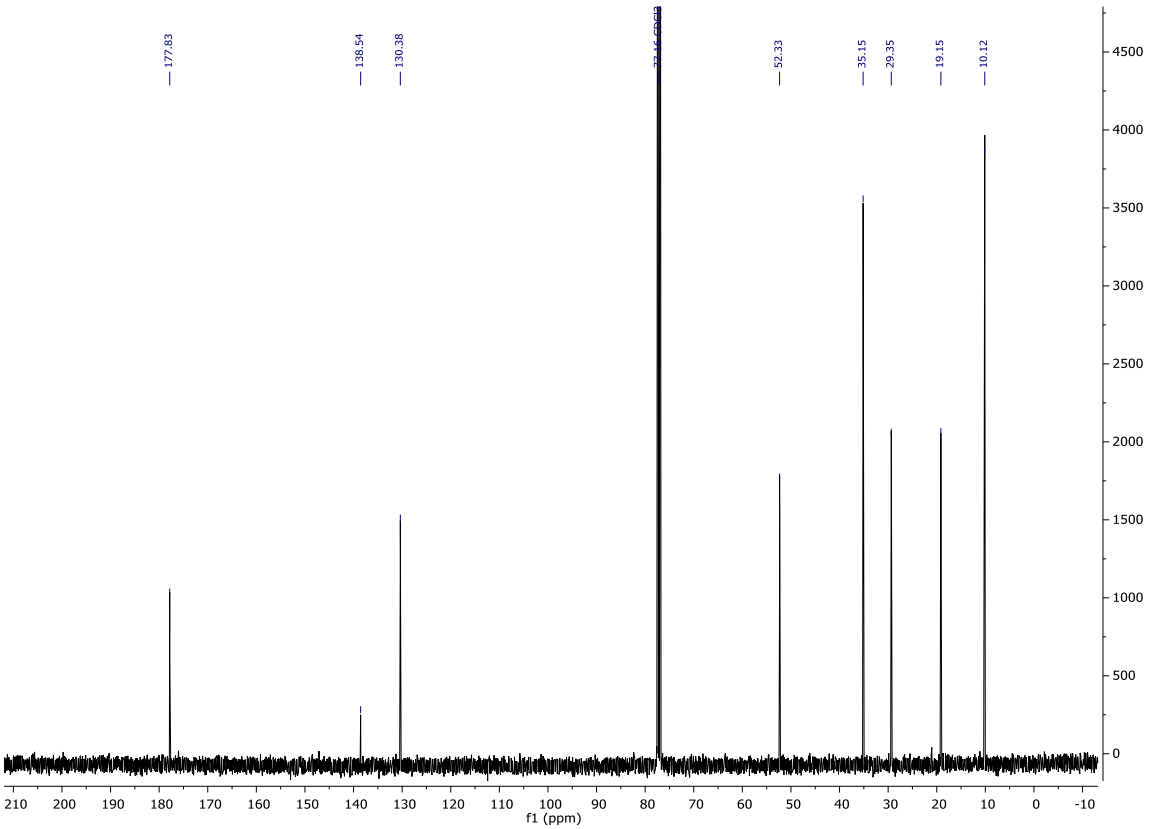

^{1}H NMR (300 MHz, $CDCl_3$) **90**

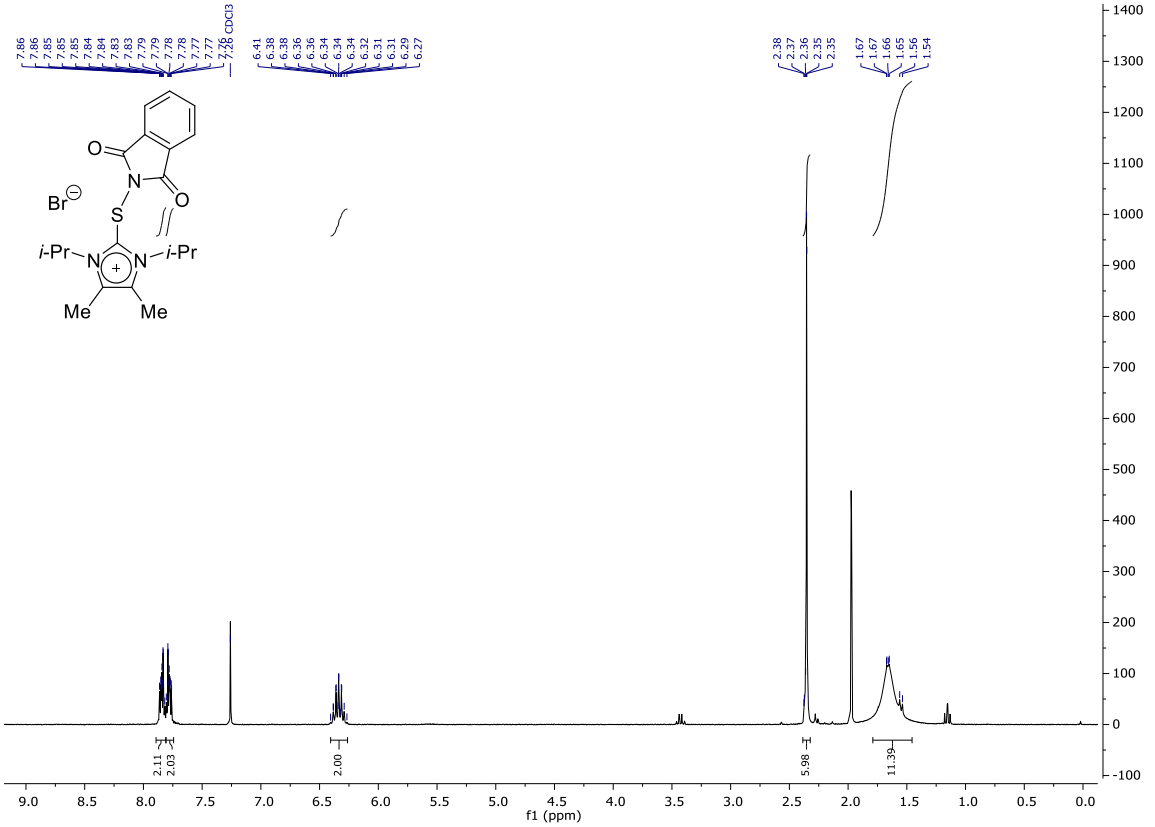

^{13}C NMR (75 MHz, $CDCl_3$) **90**

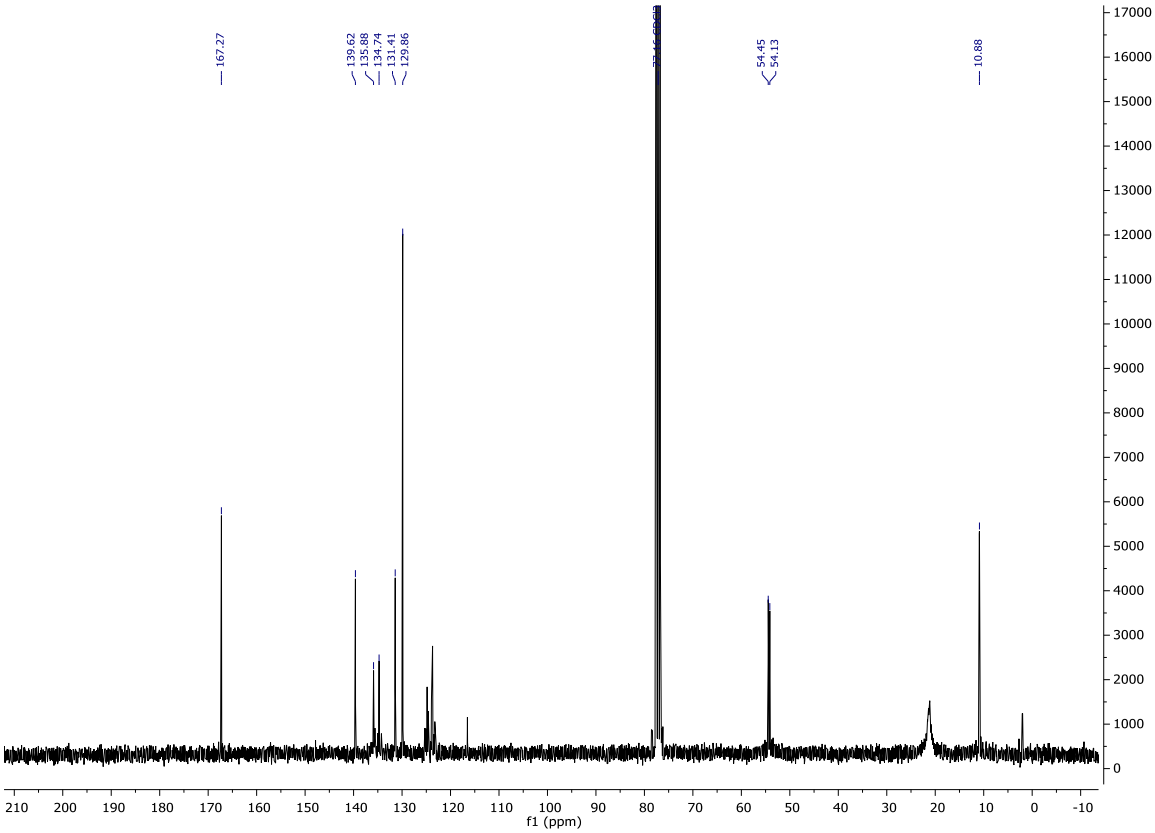

^{1}H NMR (400 MHz, CD_2Cl_2) **296**

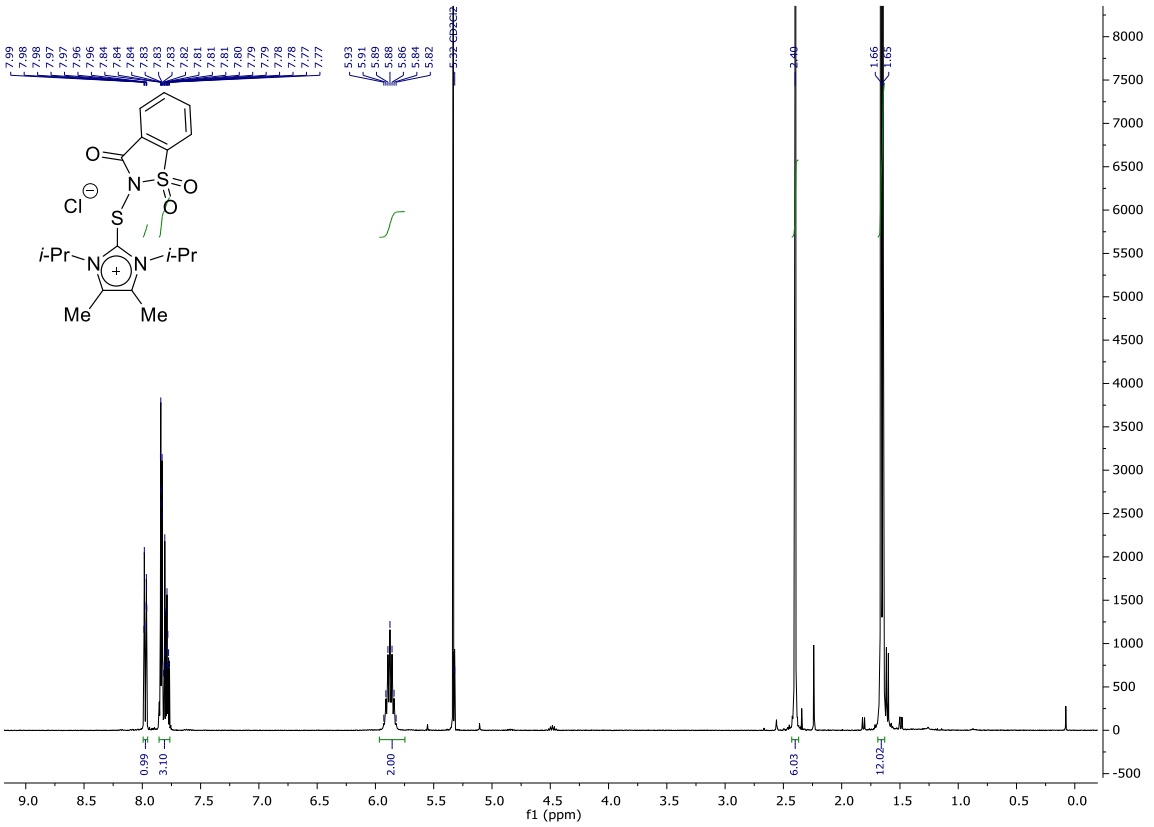

^{13}C NMR (101 MHz, CD_2Cl_2) **296**

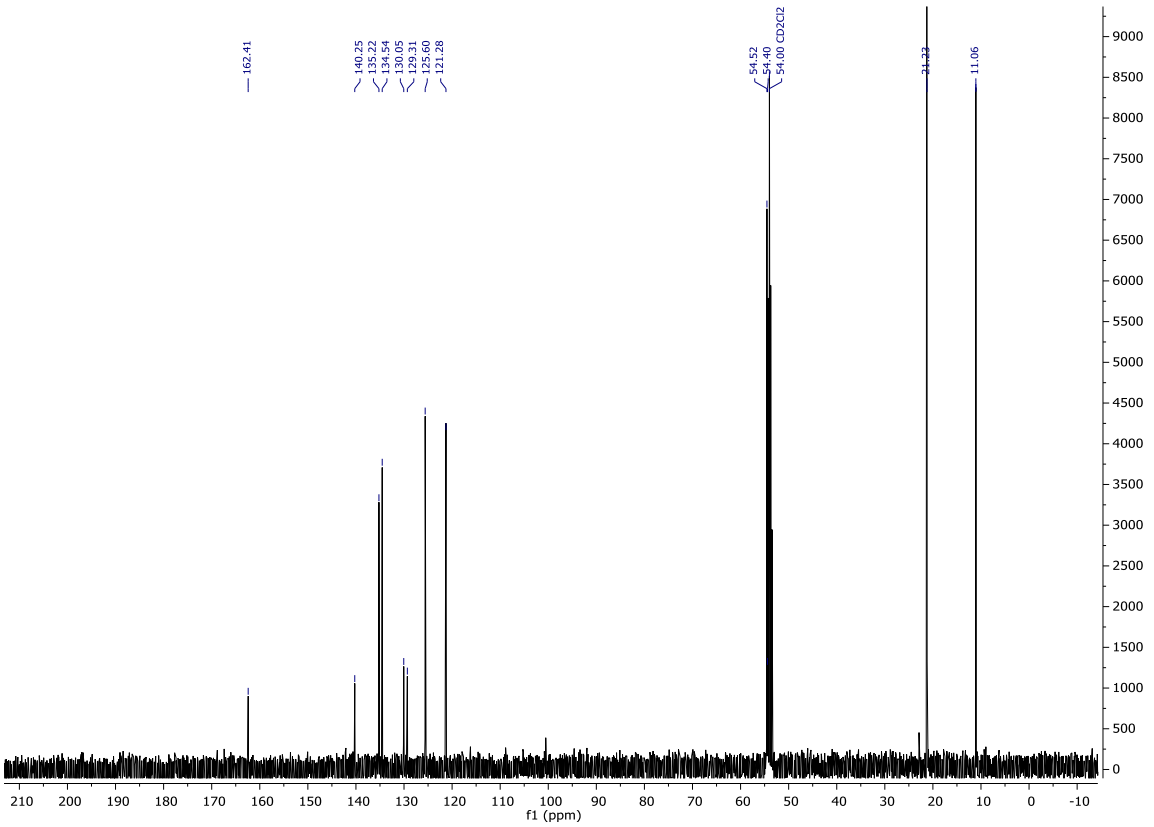

^{1}H NMR (300 MHz, $CDCl_3$) **96**

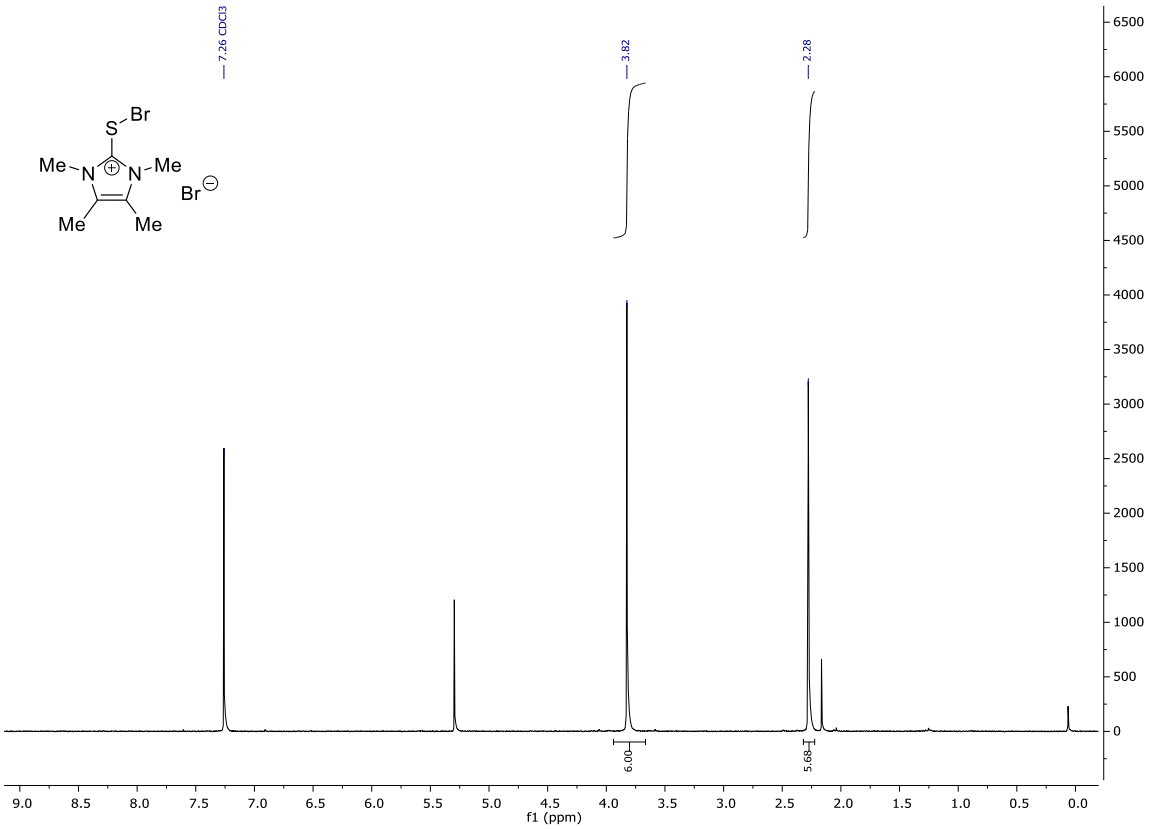

Screening of different backbones

^{1}H NMR (400 MHz, CD_2Cl_2) **111**

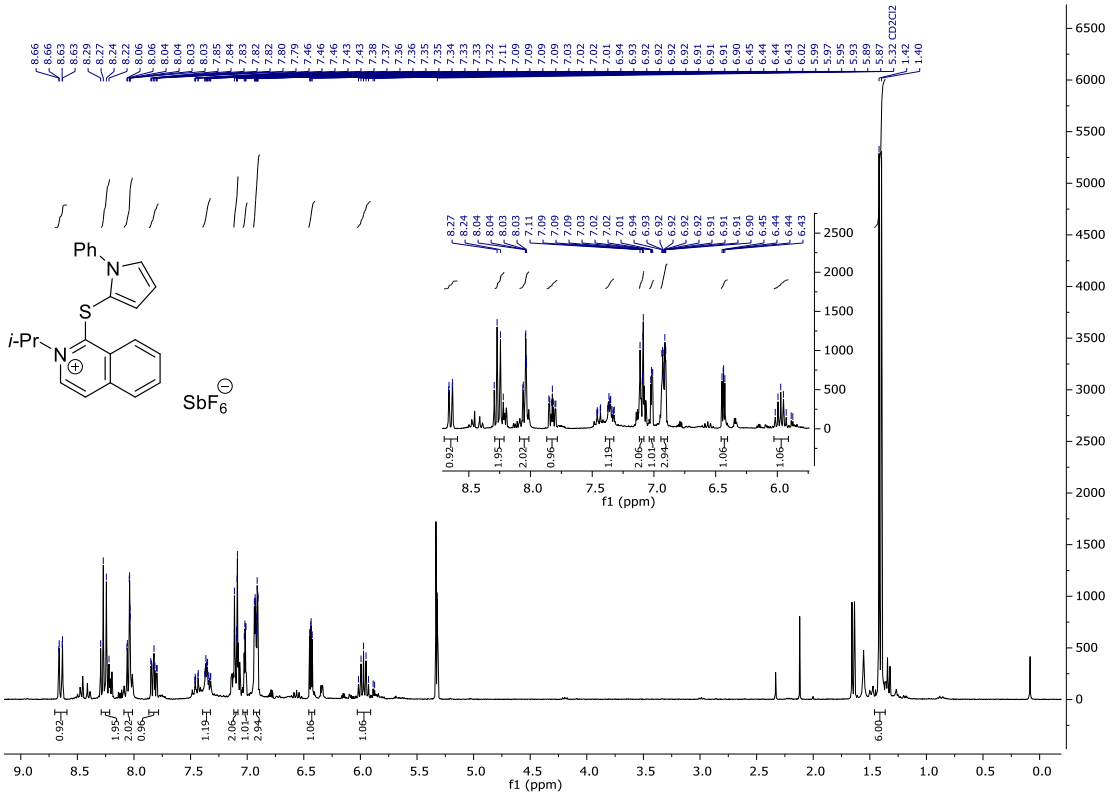

^{13}C NMR (101 MHz, CD_2Cl_2) **111**

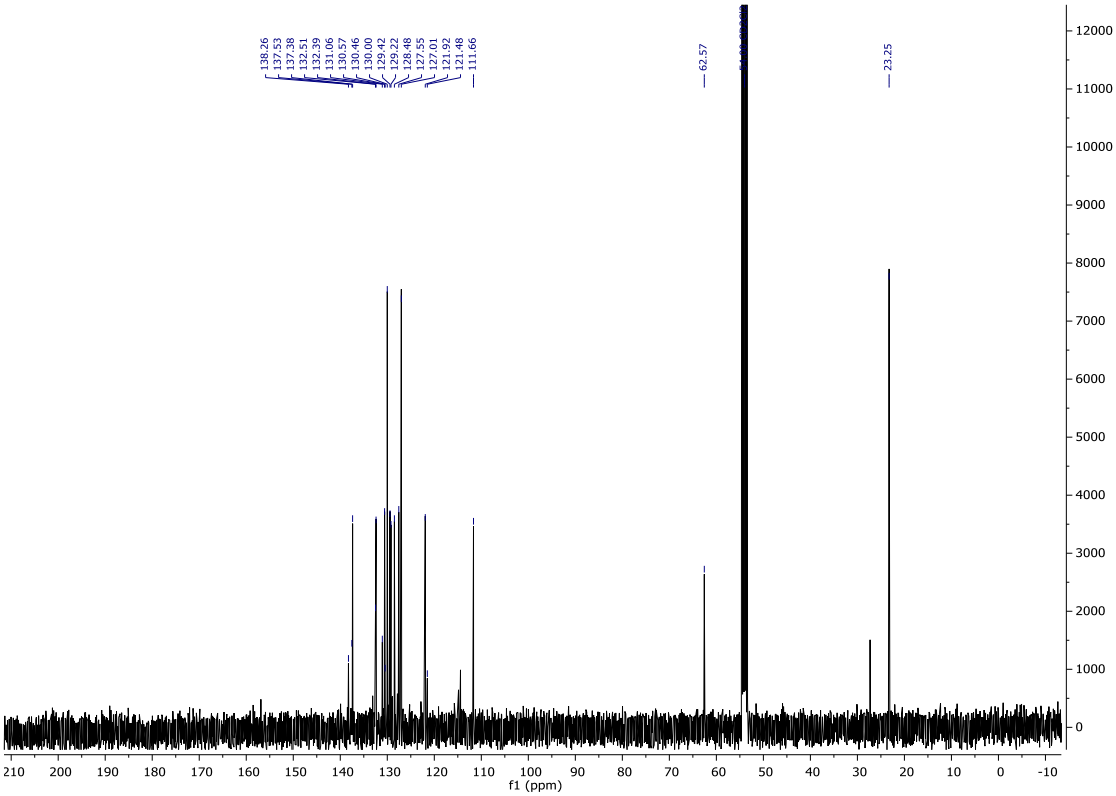

^{1}H NMR (300 MHz, CD_2Cl_2) **108**

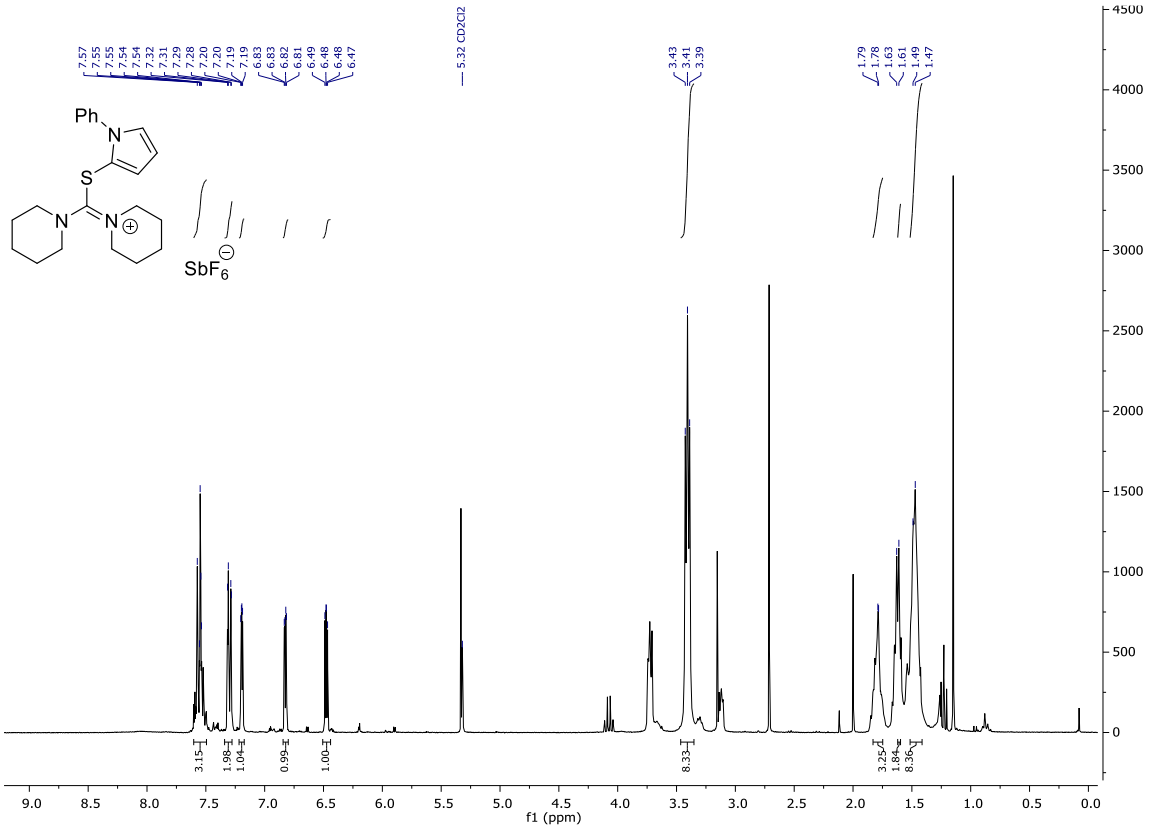

^{13}C NMR (126 MHz, CD_2Cl_2) **108**

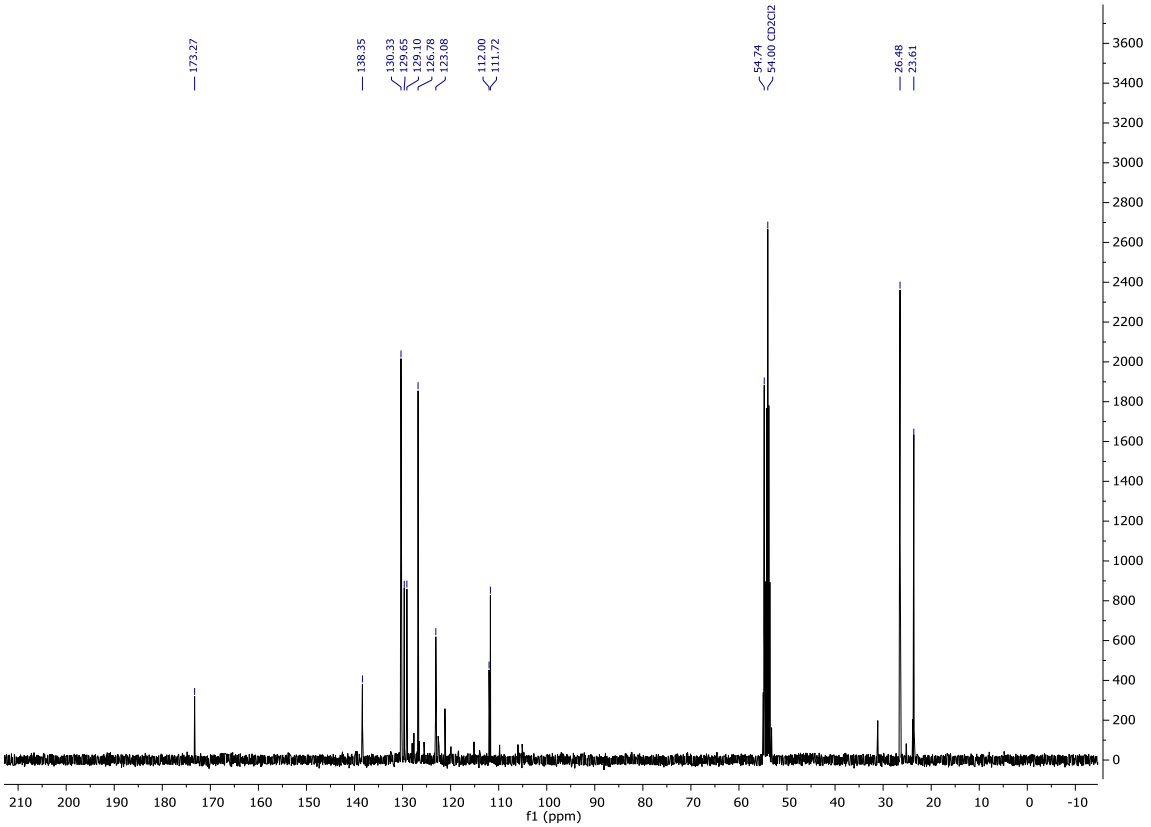

^{1}H NMR (300 MHz, CD_2Cl_2) **104**

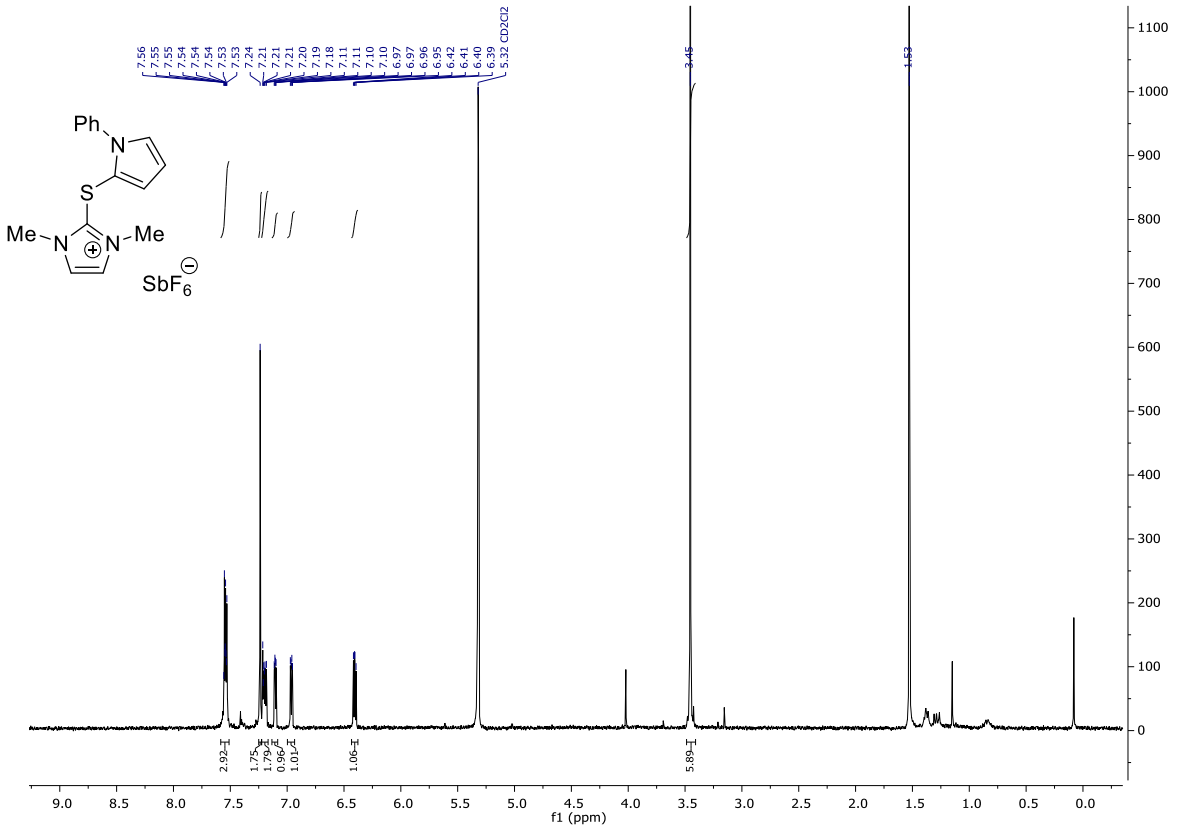

^{13}C NMR (126 MHz, CD_2Cl_2) **104**

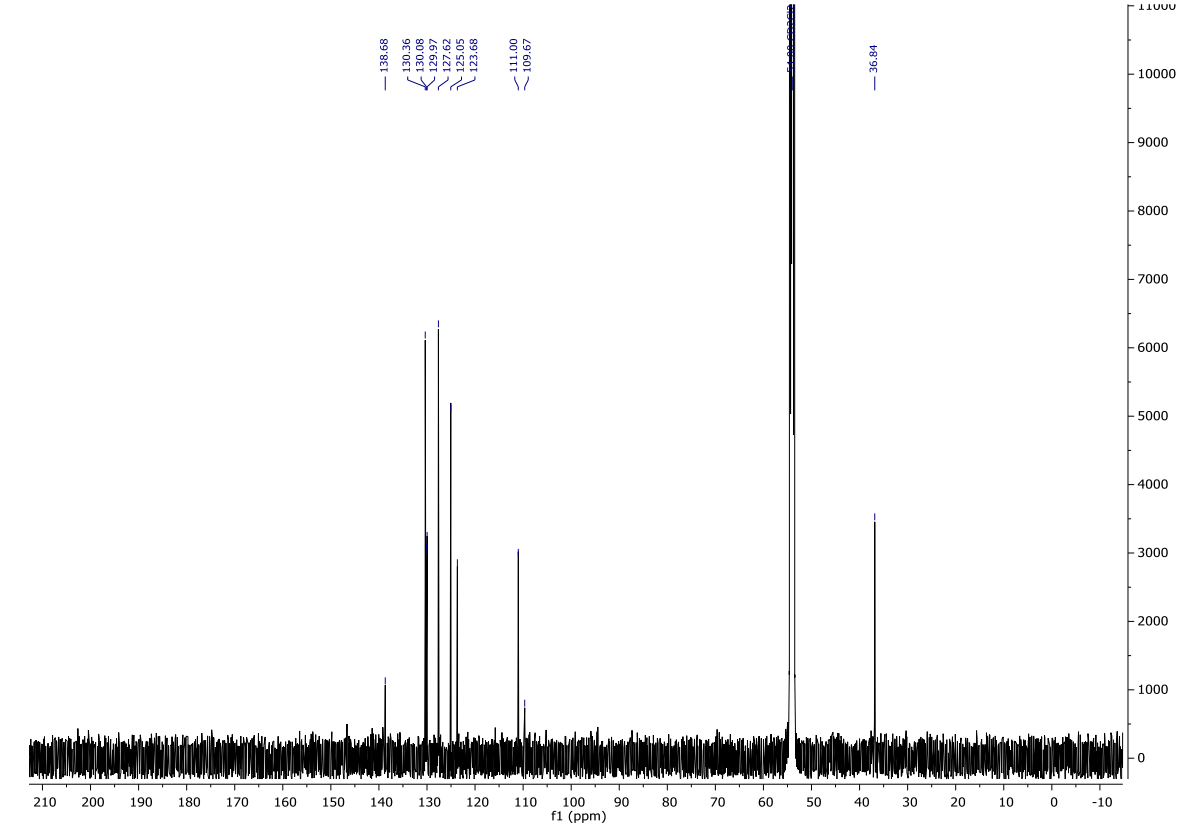

^{1}H NMR (300 MHz, CD_2Cl_2) **109**

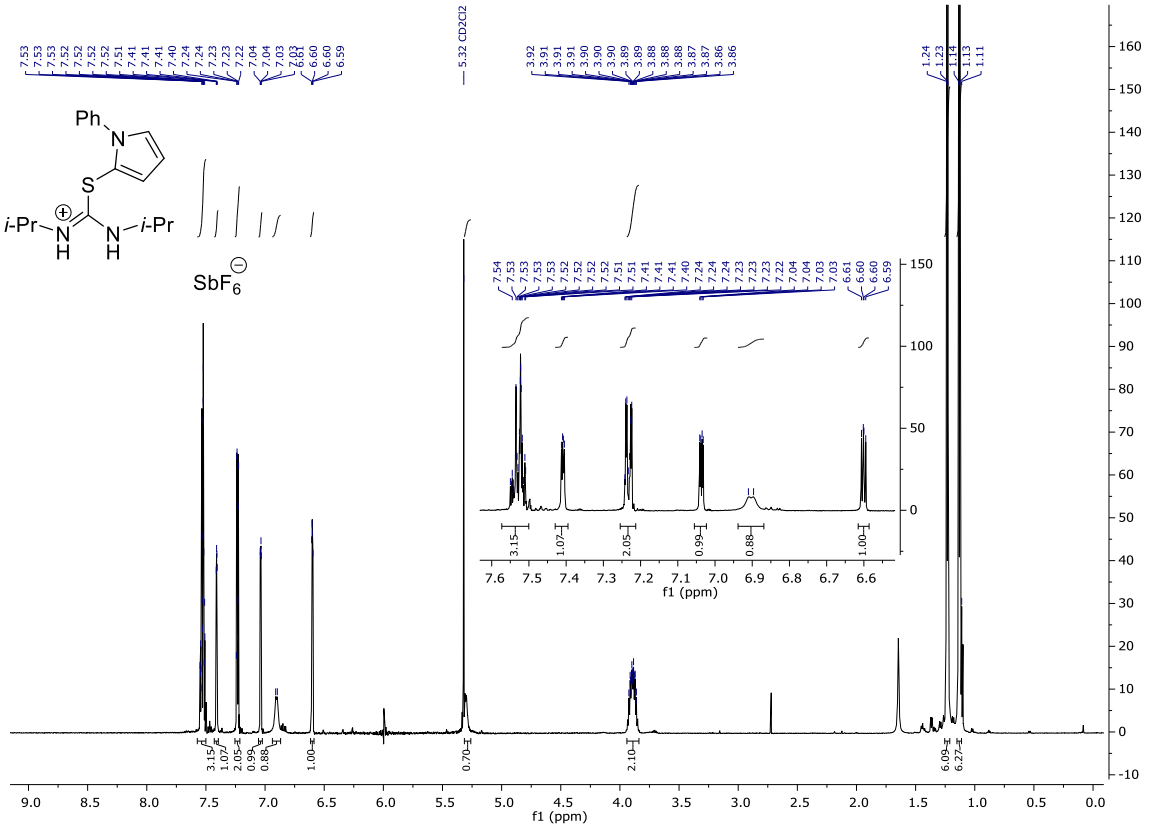

^{13}C NMR (126 MHz, CD_2Cl_2) **109**

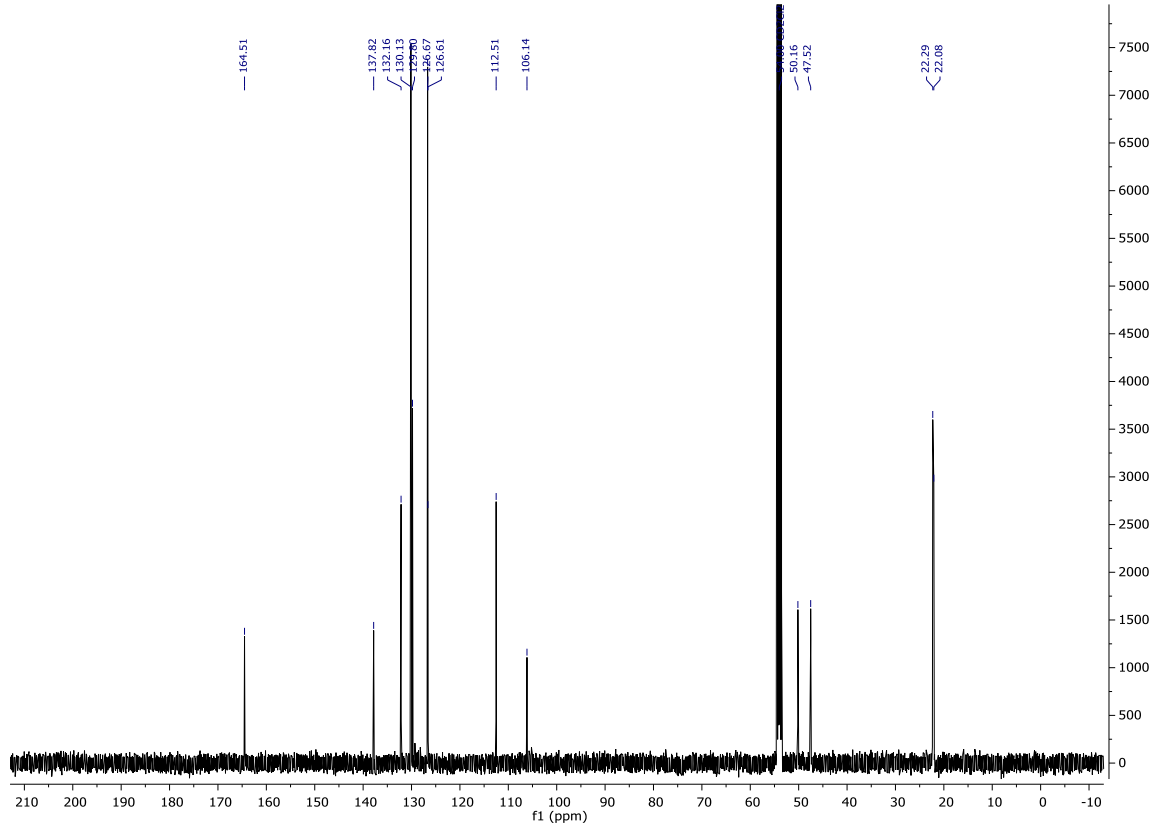

^{1}H NMR (300 MHz, CD_2Cl_2) **103**

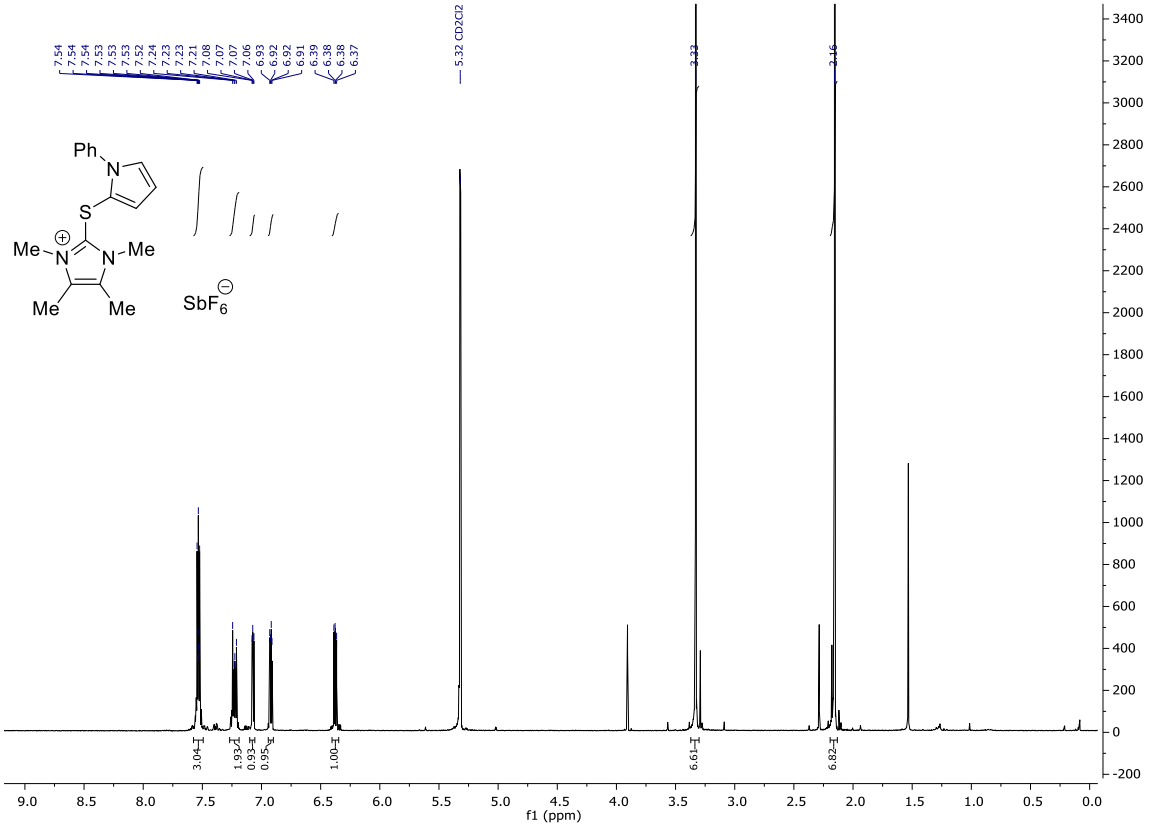

^{13}C NMR (126 MHz, CD_2Cl_2) **103**

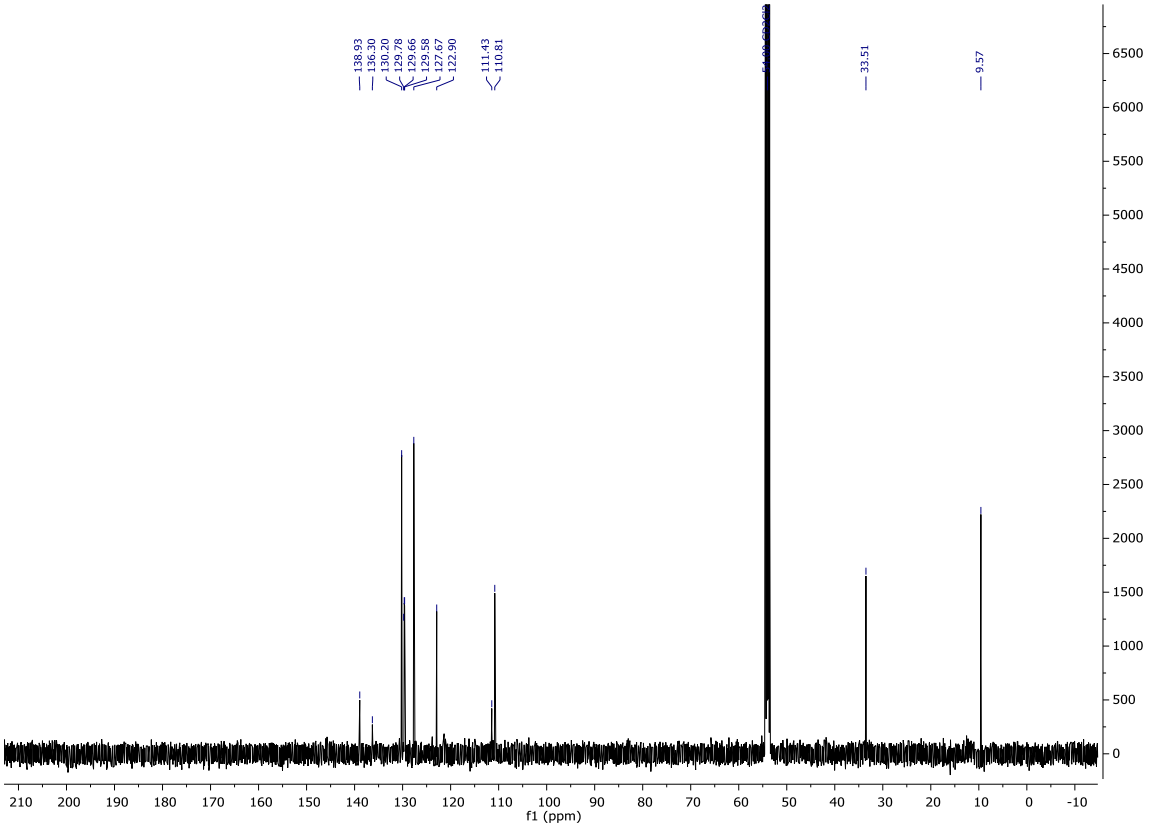

^{1}H NMR (300 MHz, CD_2Cl_2) **107a**

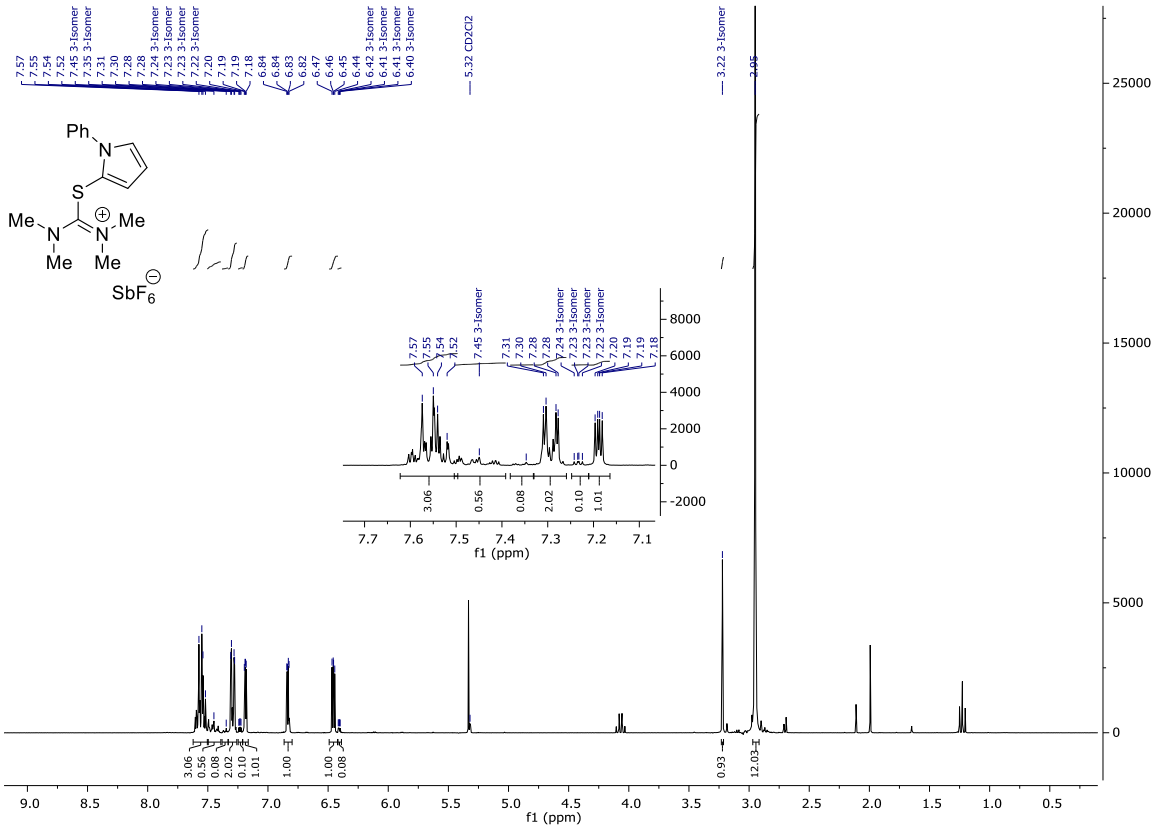

^{13}C NMR (75 MHz, CD_2Cl_2) **107a**

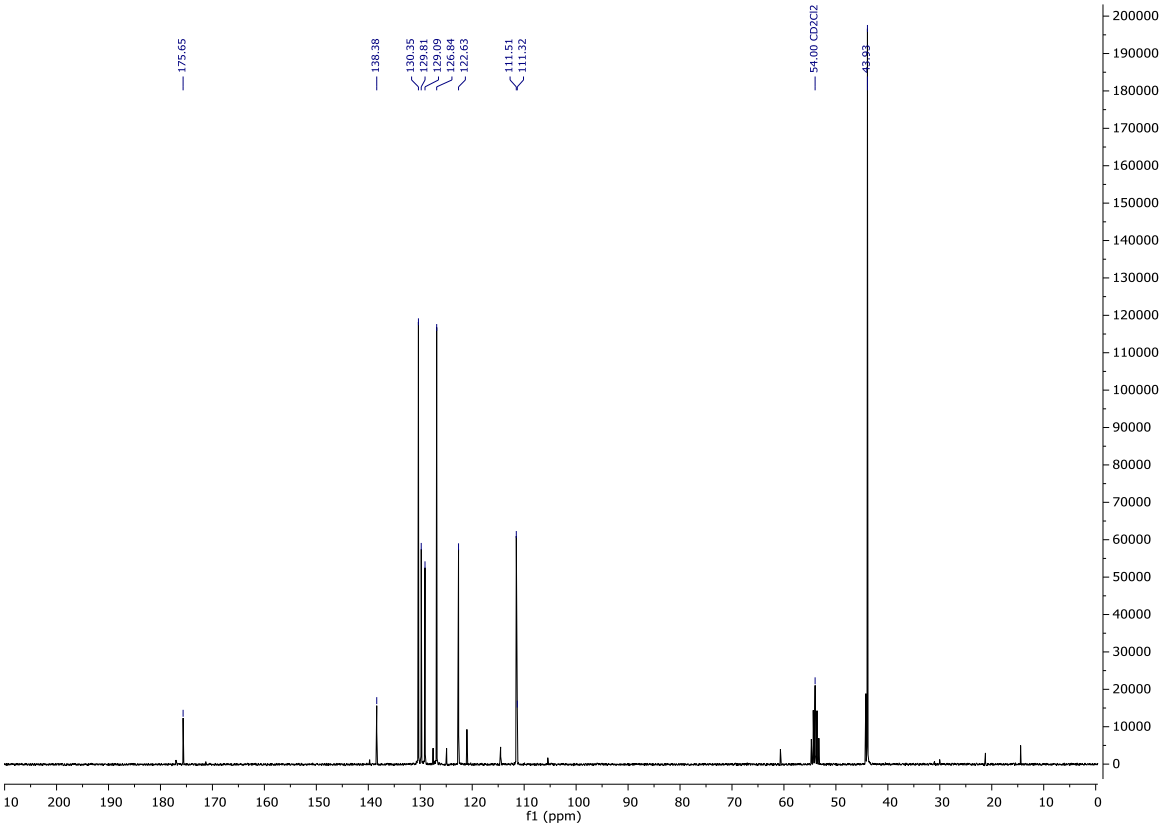

Synthesis of arylthiazolium salts

^{1}H NMR (300 MHz, CD_2Cl_2) **113**

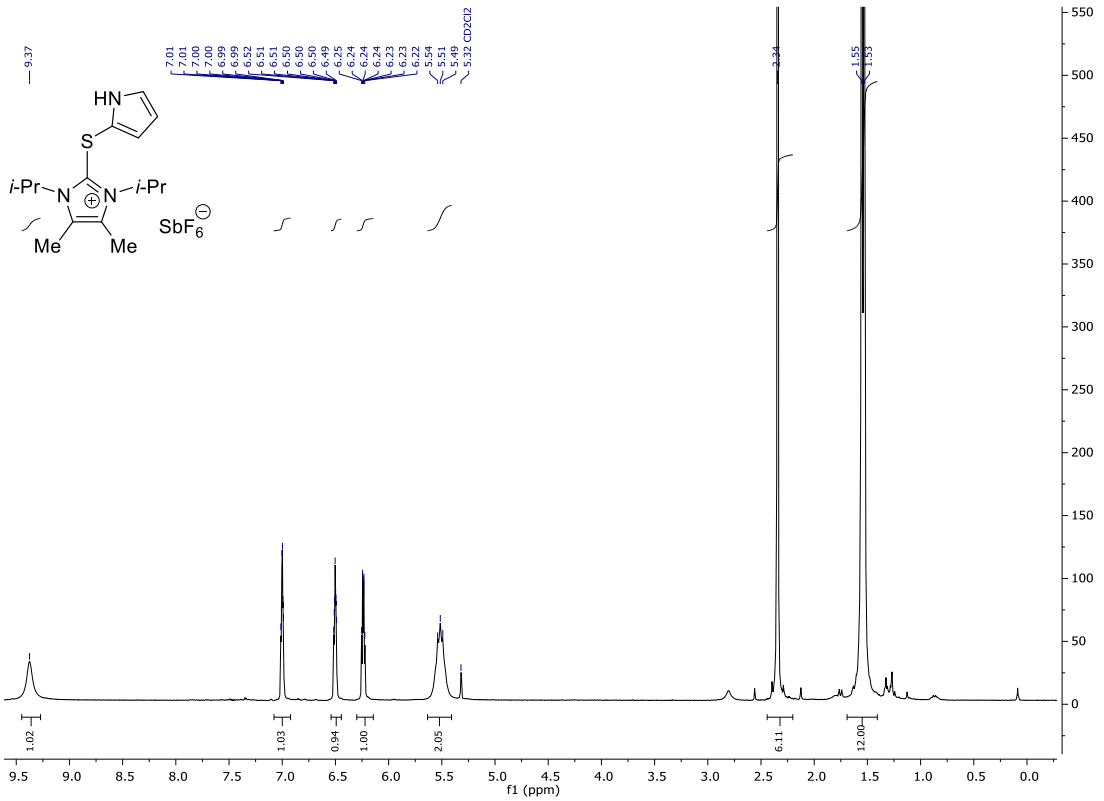

^{13}C NMR (126 MHz, CD_2Cl_2) **113**

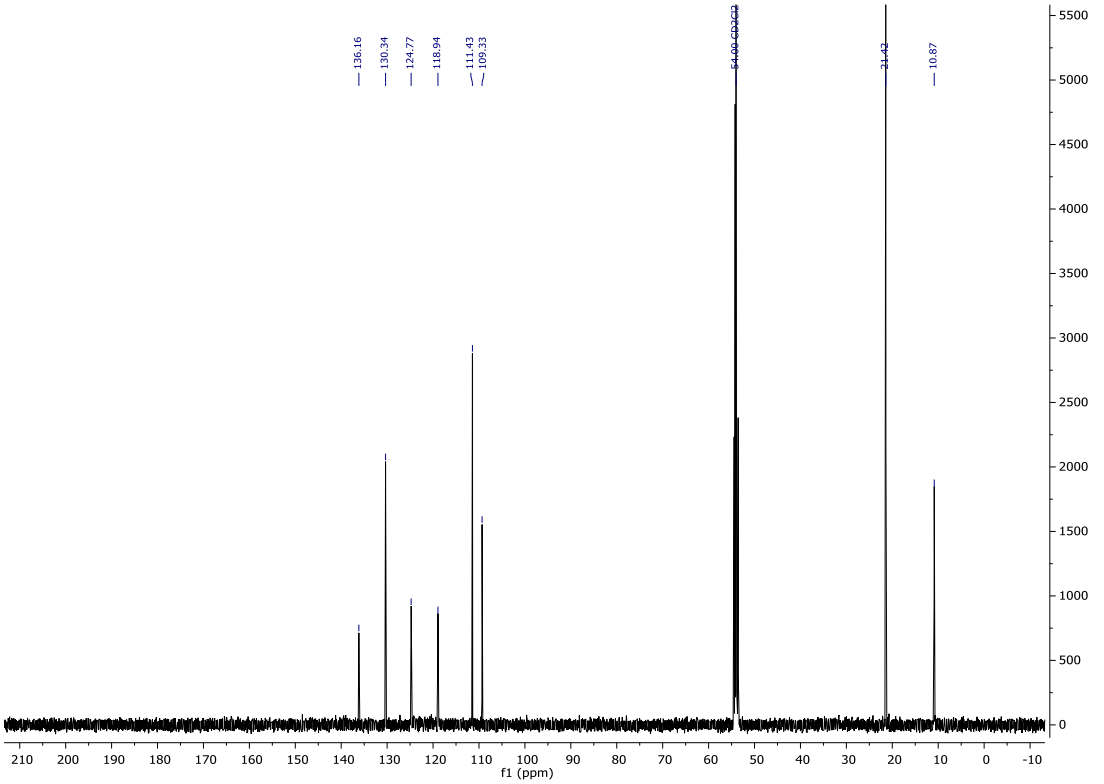

^{1}H NMR (300 MHz, CD_2Cl_2) **99**

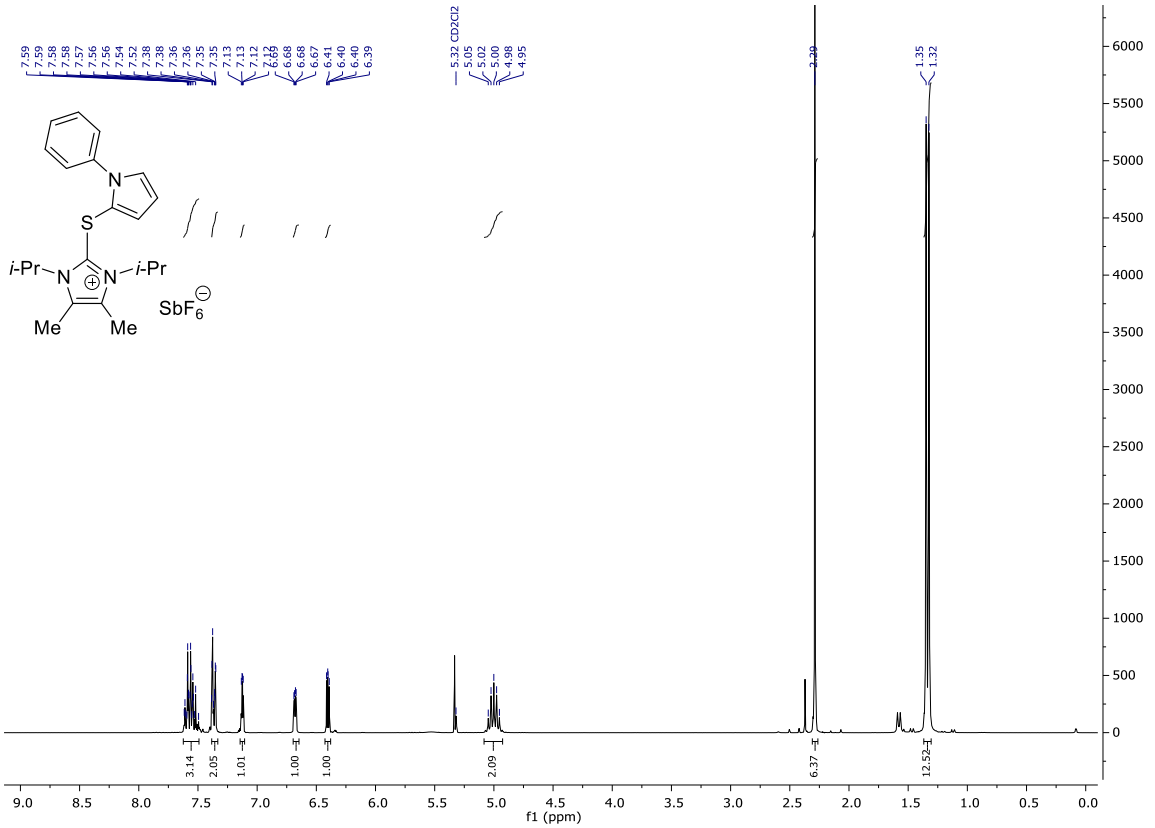

^{13}C NMR (101 MHz, CD_2Cl_2) **99**

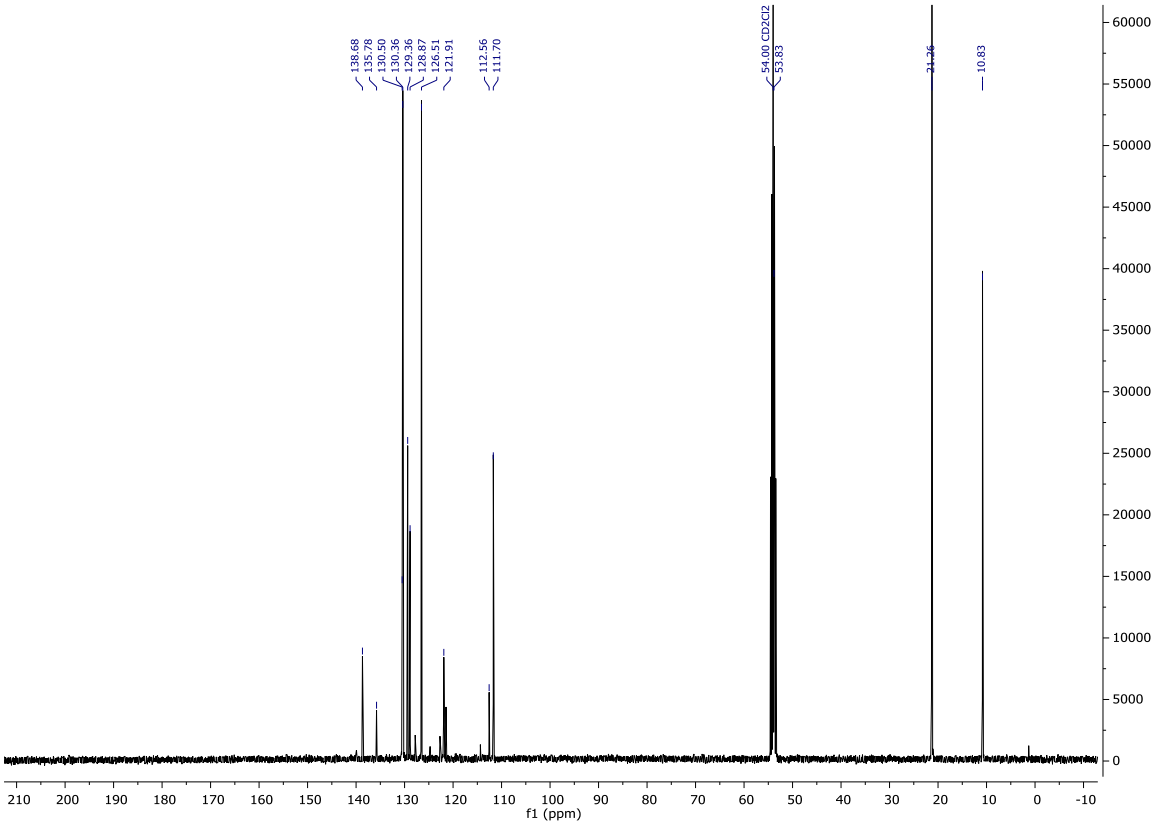

^{1}H NMR (300 MHz, CD_2Cl_2) **114**

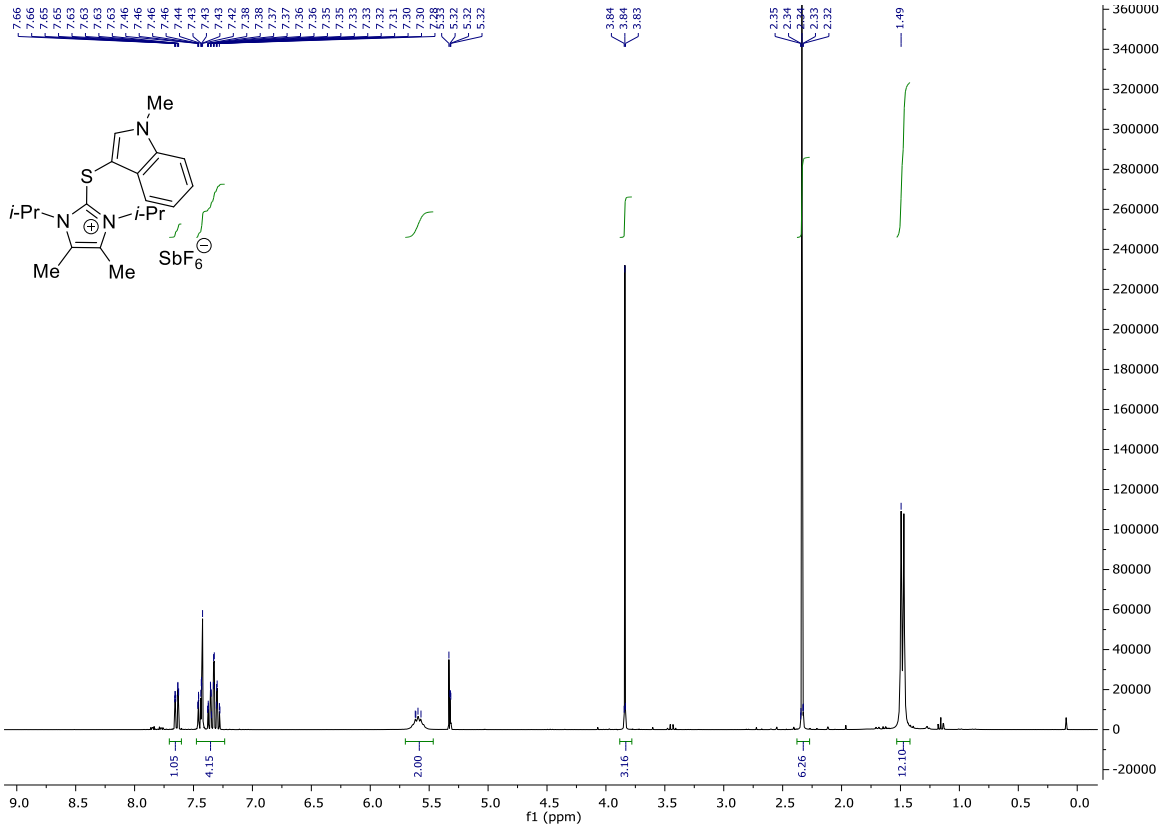

^{13}C NMR (75 MHz, CD_2Cl_2) **114**

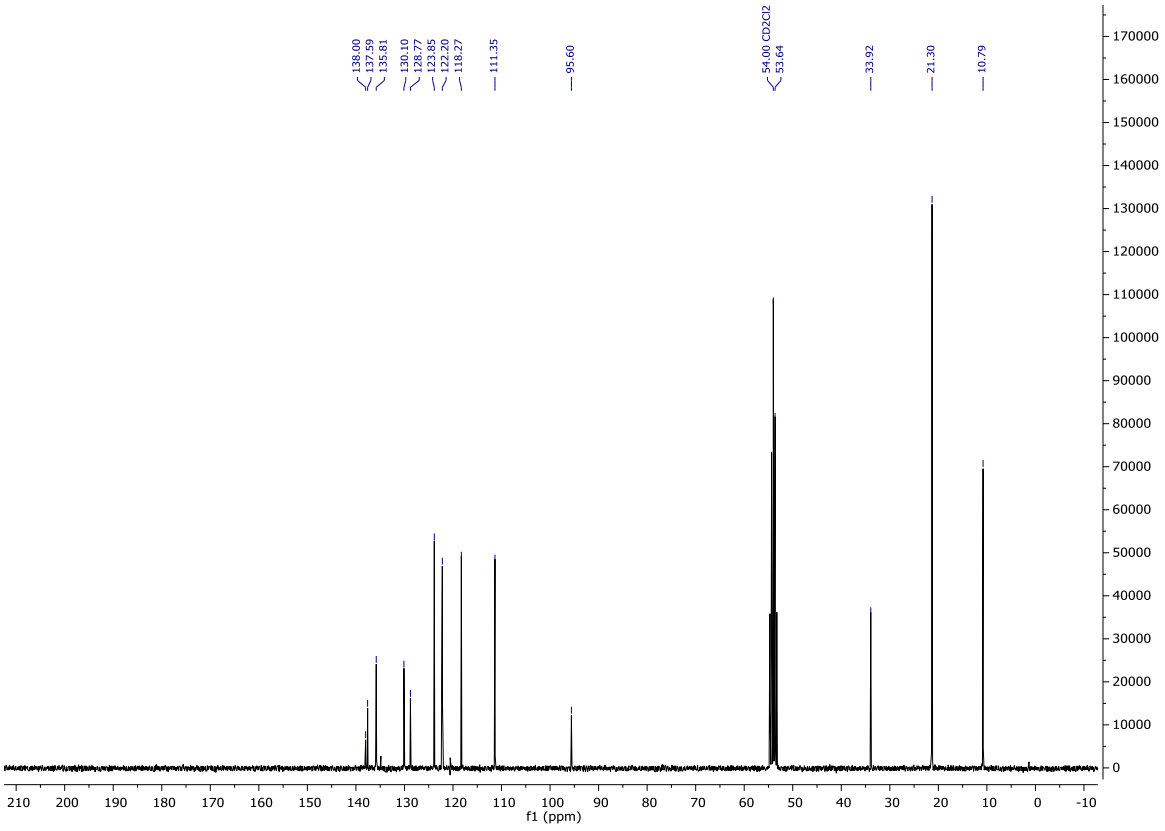

^{1}H NMR (400 MHz, CD_2Cl_2) **100**

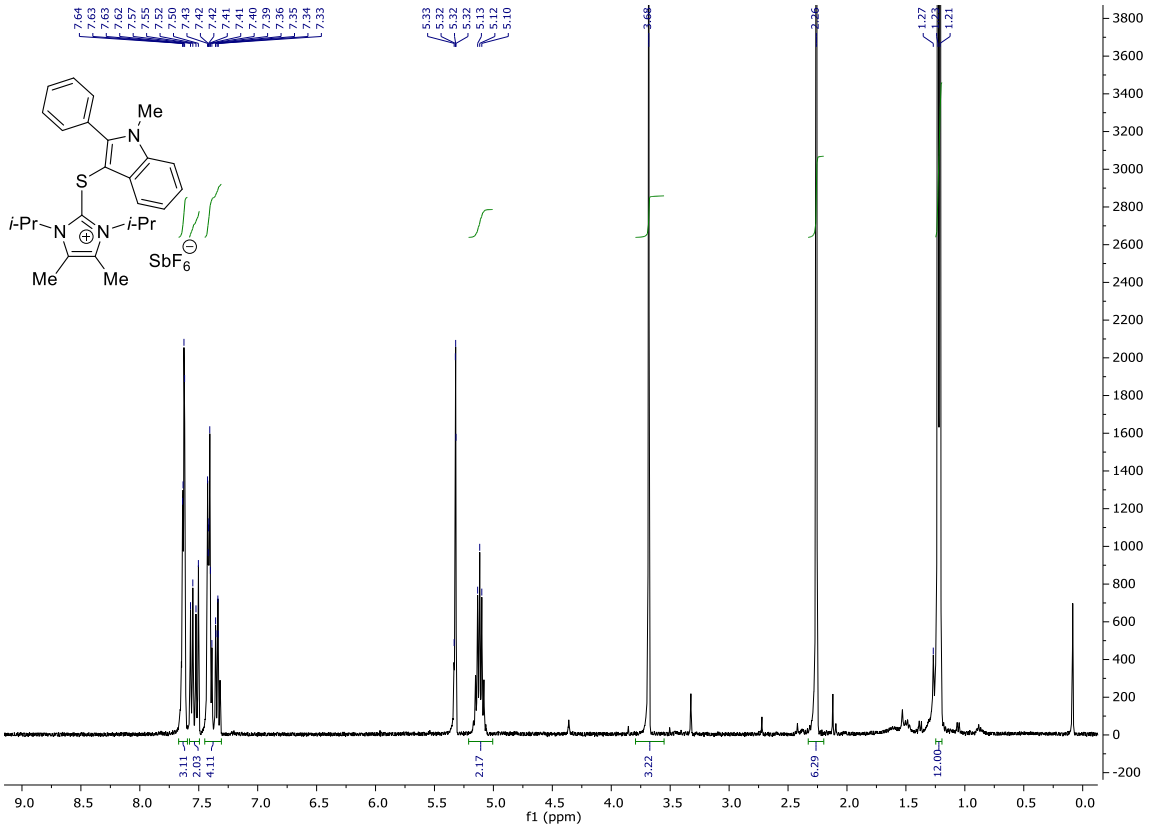

^{13}C NMR (126 MHz, CD_2Cl_2) **100**

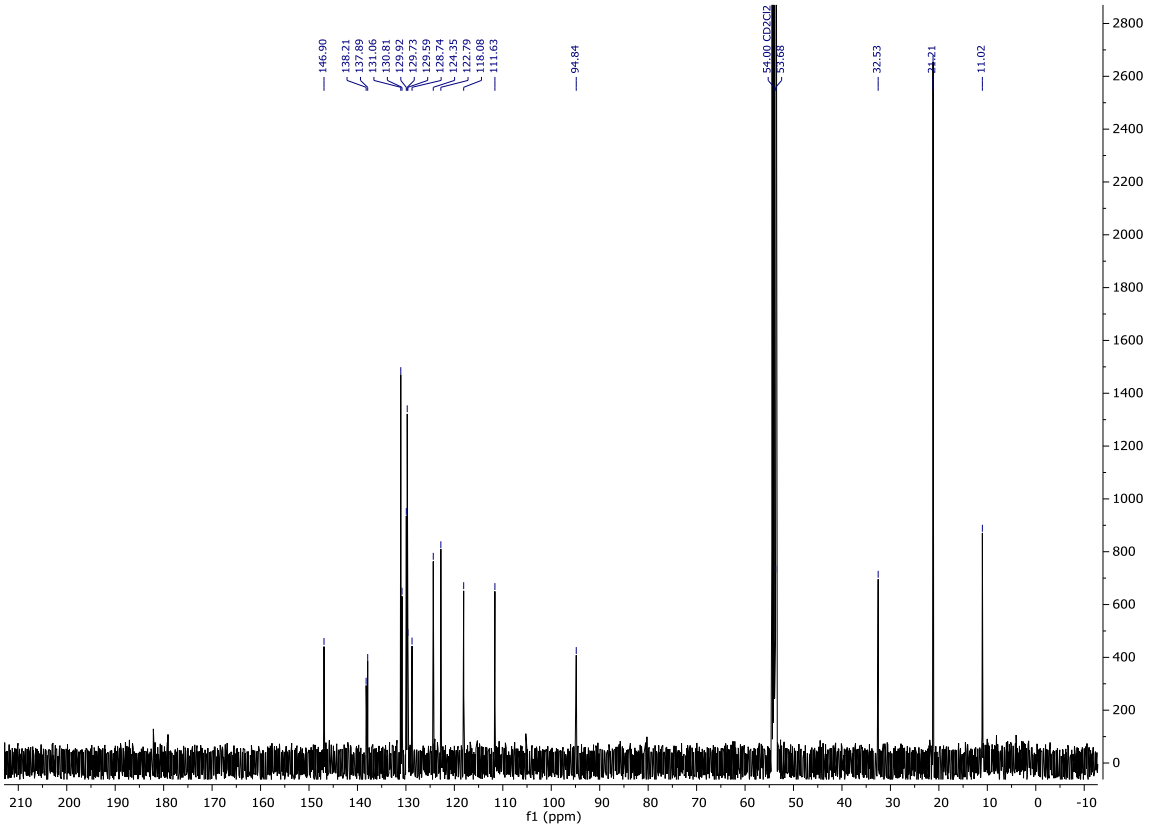

^{1}H NMR (600 MHz, CD_2Cl_2) **115**

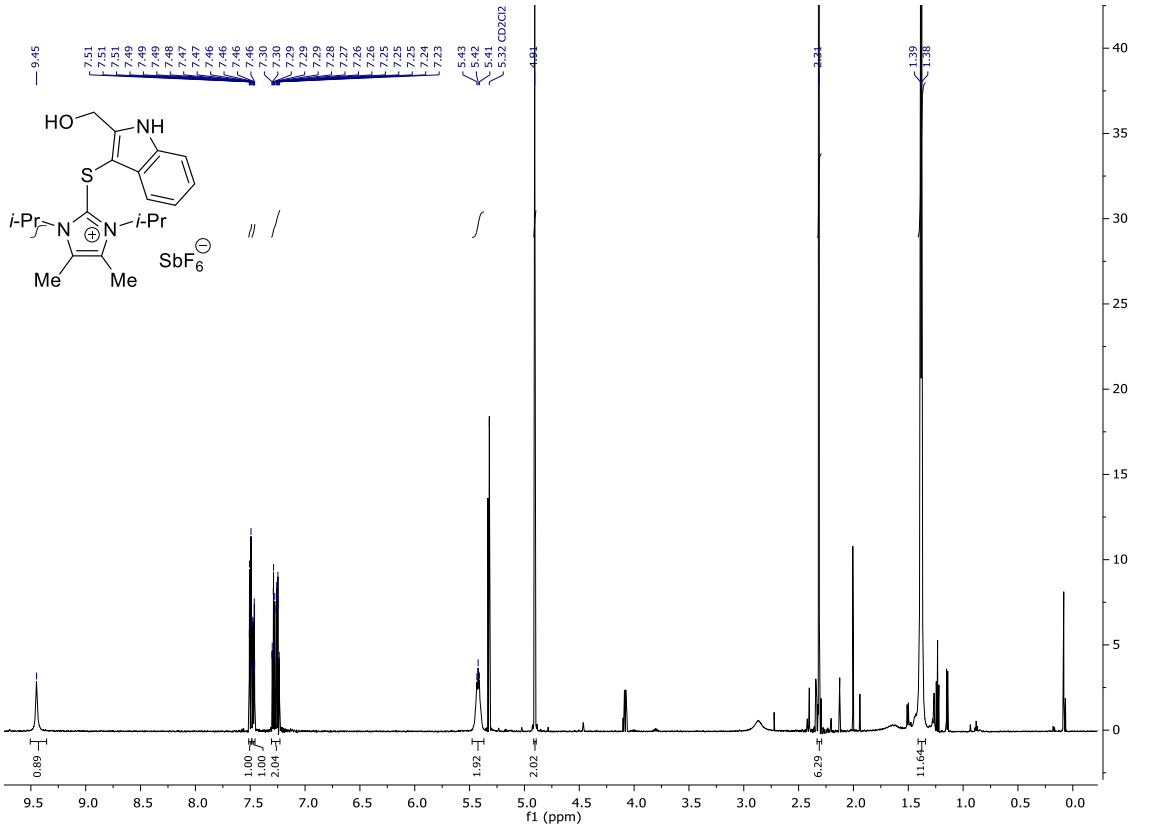

^{13}C NMR (126 MHz, CD_2Cl_2) **115**

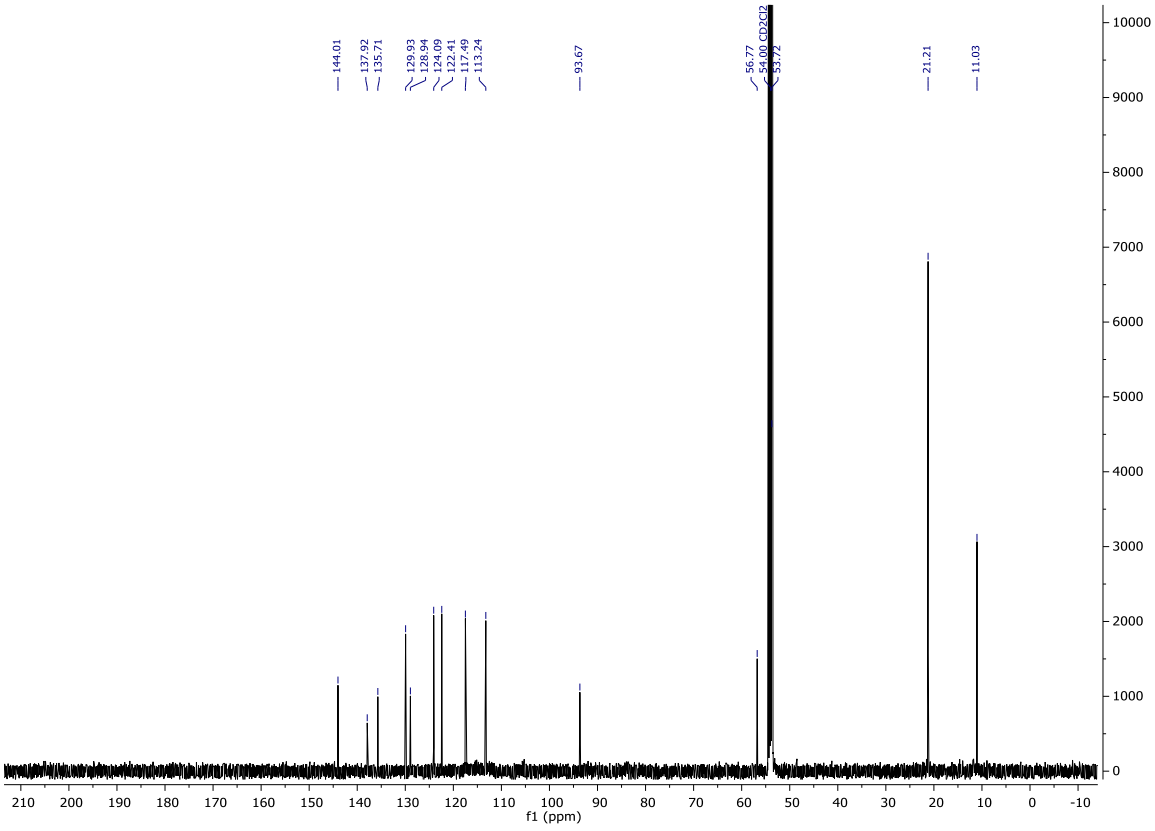

^{1}H NMR (400 MHz, CD_2Cl_2) **117**

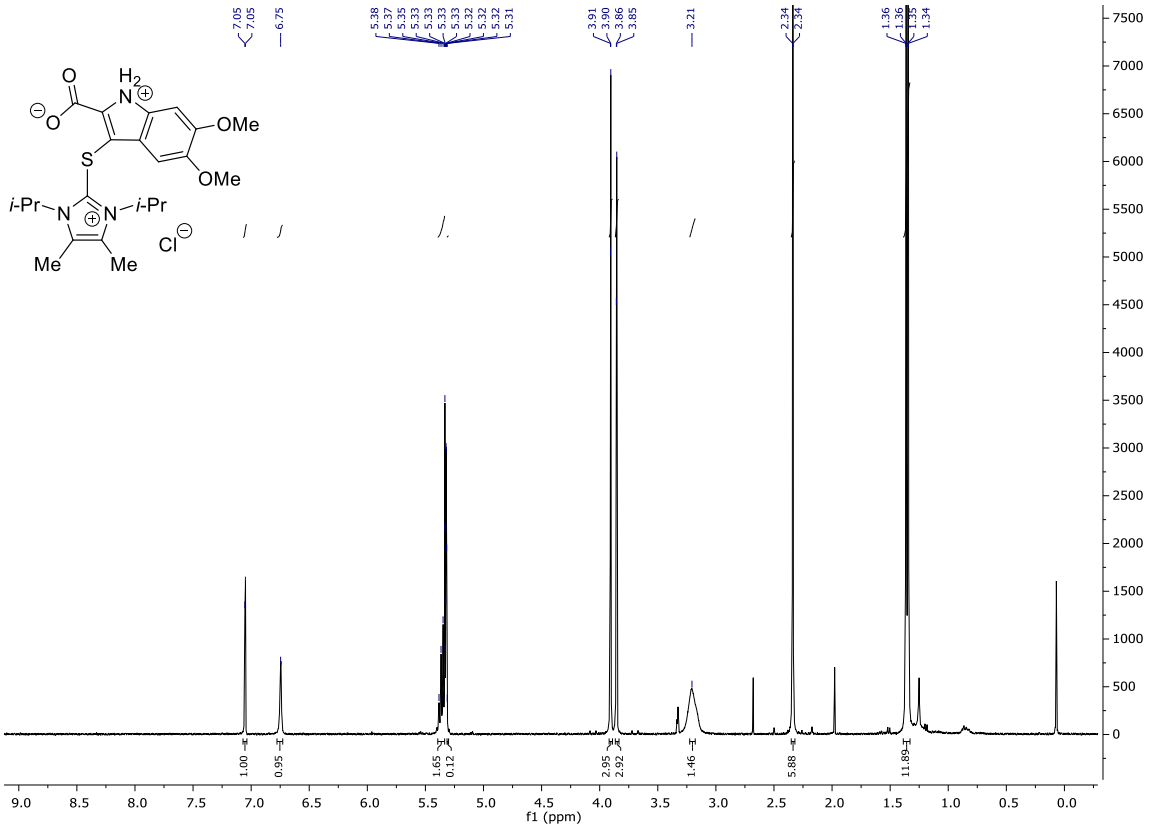

^{13}C NMR (126 MHz, CD_2Cl_2) **117**

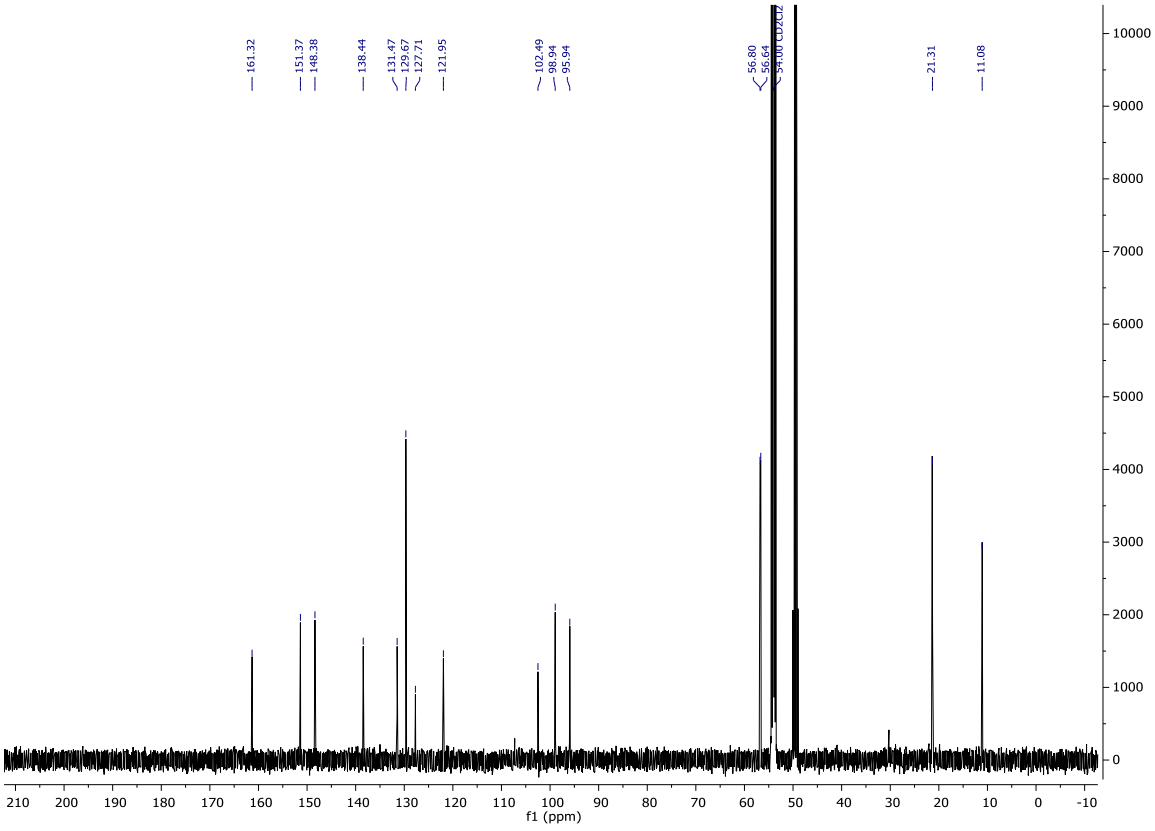

^{1}H NMR (400 MHz, CD_2Cl_2) **118**

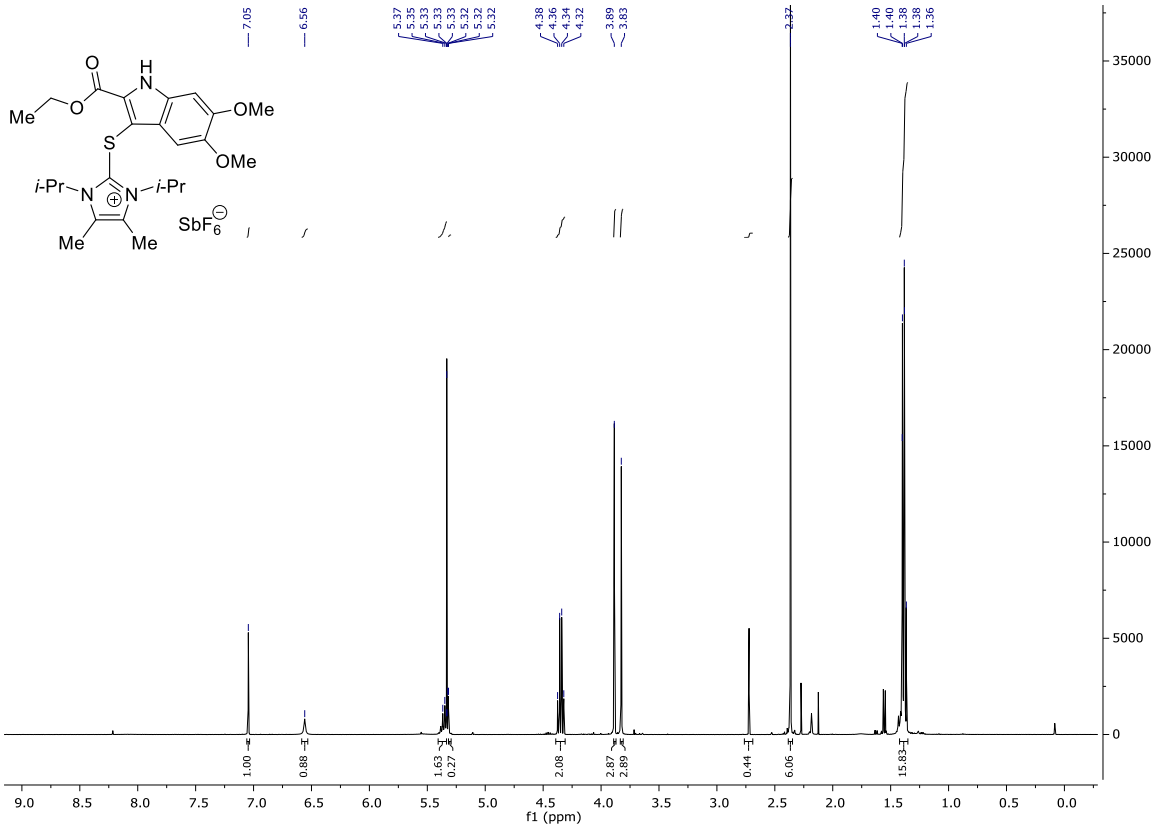

^{13}C NMR (101 MHz, CD_2Cl_2) **118**

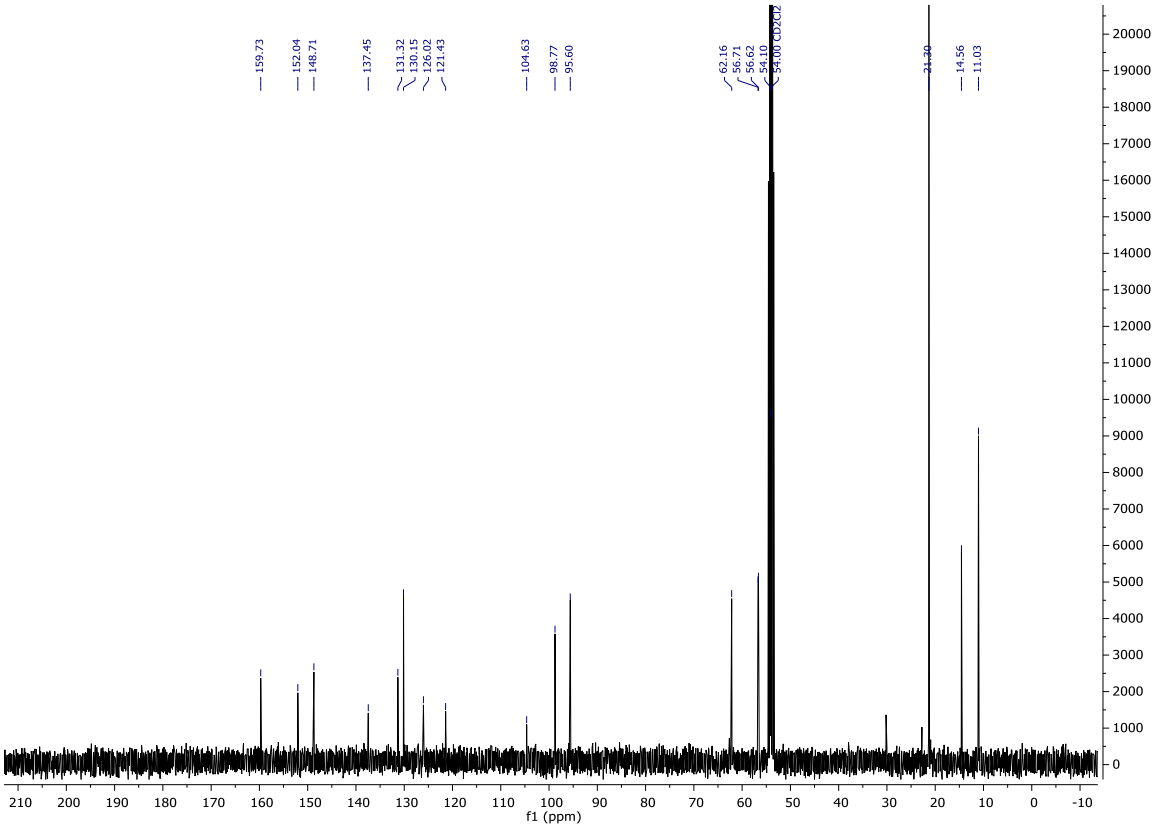

^{1}H NMR (300 MHz, CD_2Cl_2) **116**

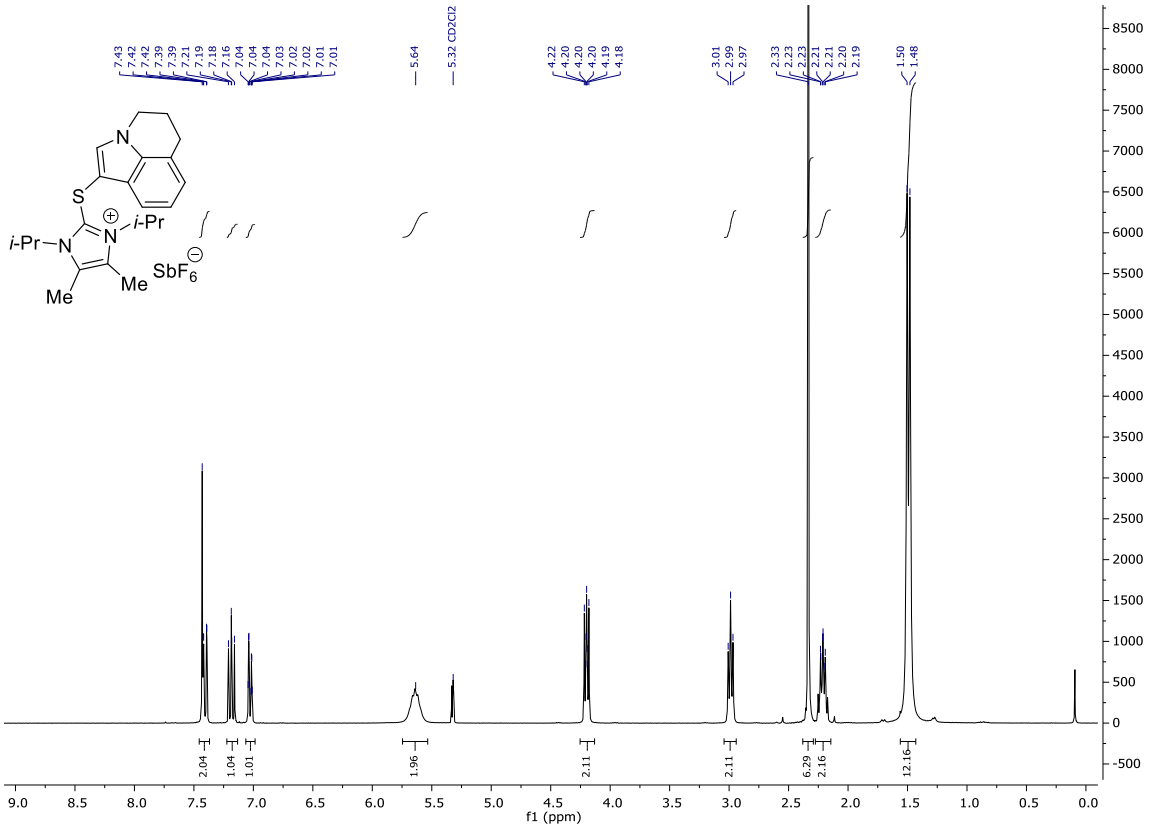

^{13}C NMR (126 MHz, CD_2Cl_2) **116**

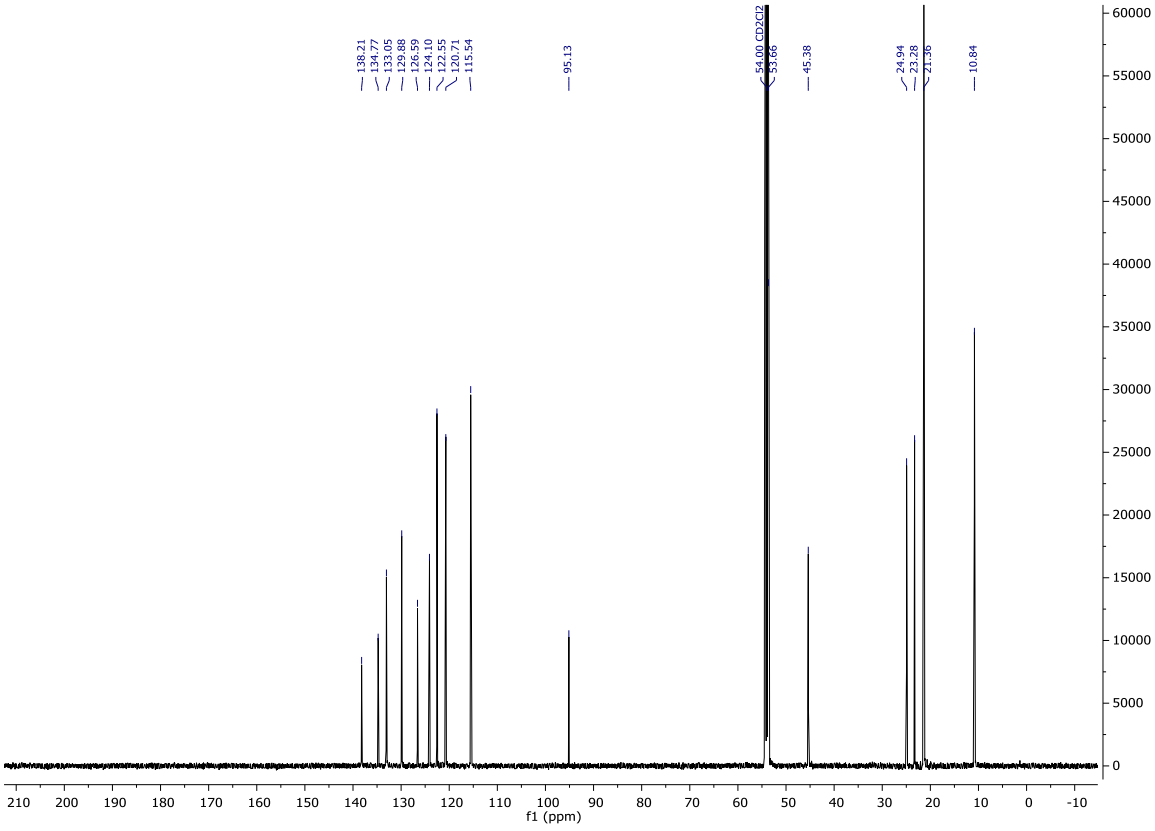

^{1}H NMR (300 MHz, CD_2Cl_2) **122**

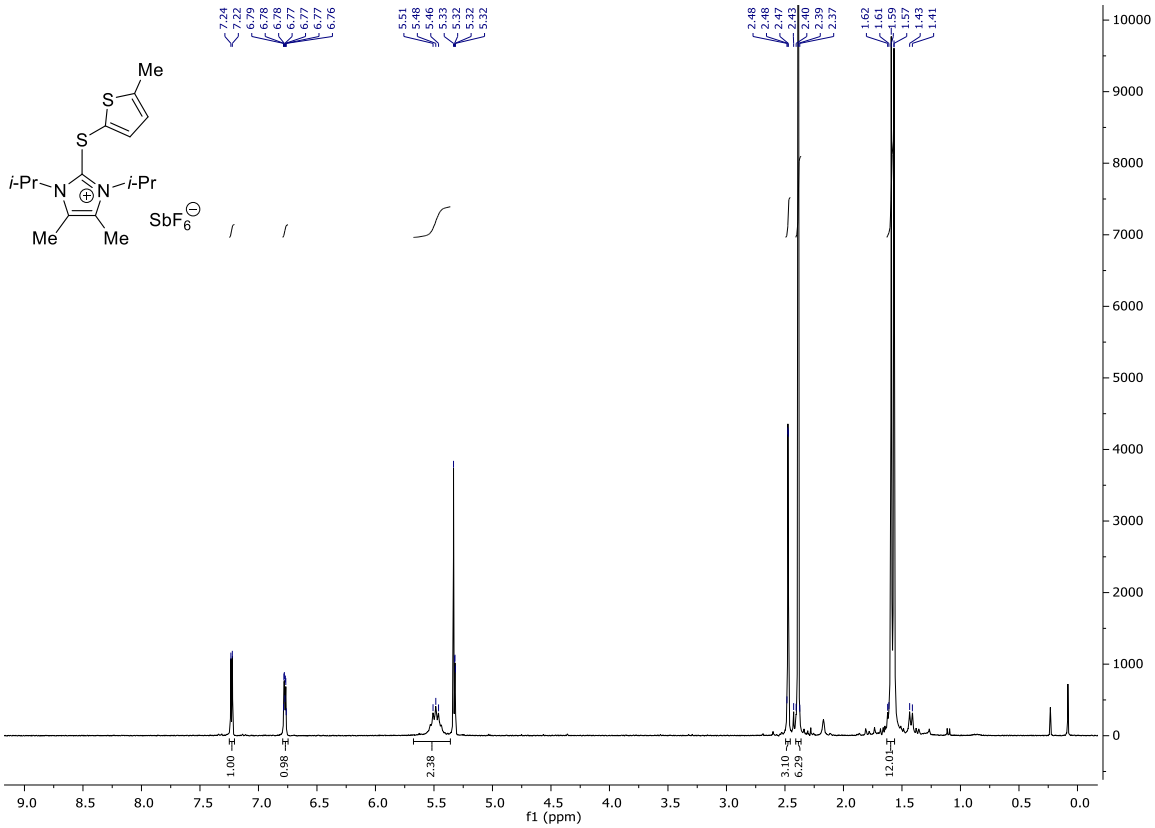

^{13}C NMR (75 MHz, CD_2Cl_2) **122**

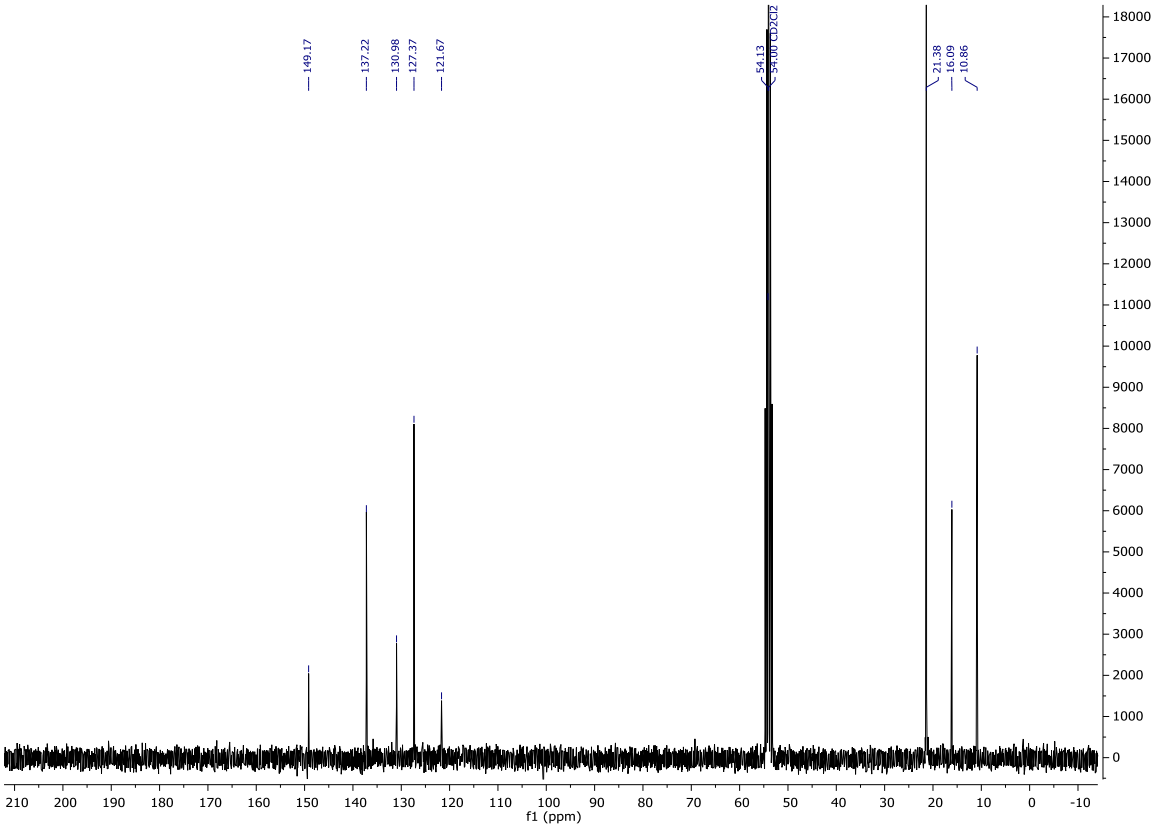

^{1}H NMR (300 MHz, CD_2Cl_2) **123**

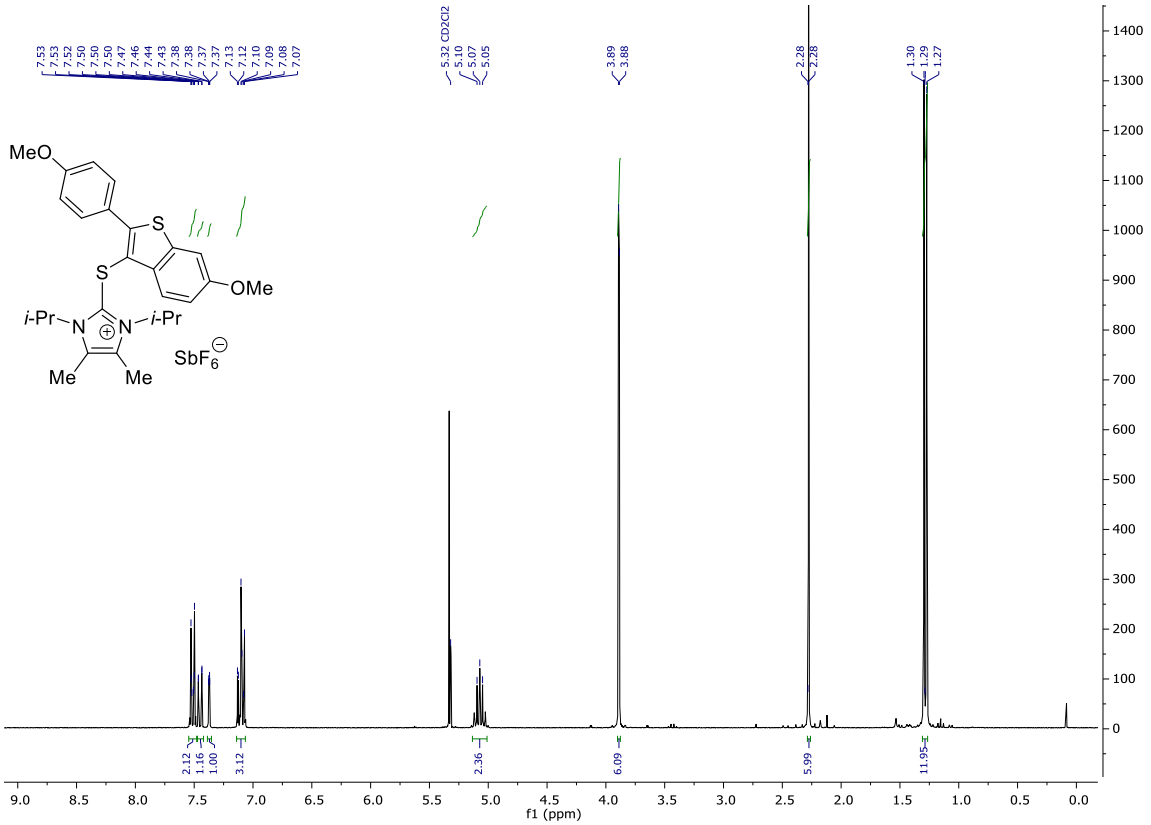

^{13}C NMR (126 MHz, CD_2Cl_2) **123**

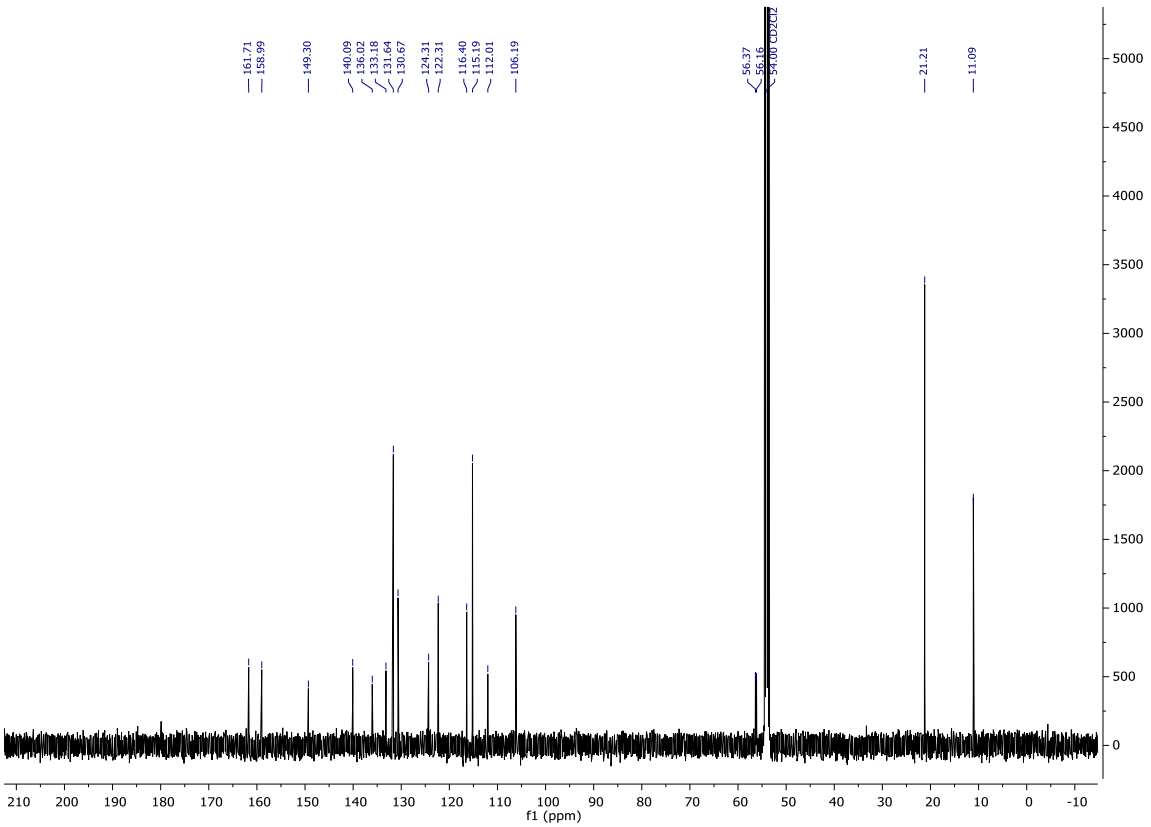

^{1}H NMR (300 MHz, CD_2Cl_2) **129**

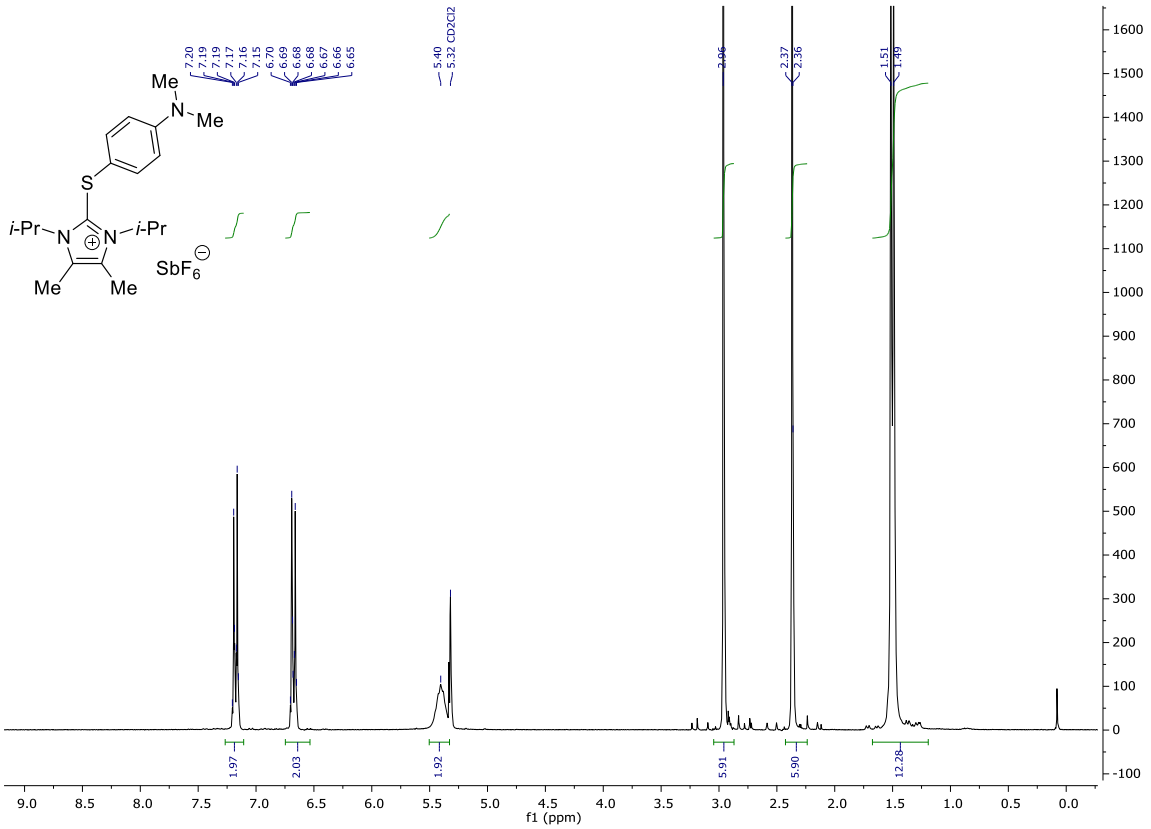

^{13}C NMR (126 MHz, CD_2Cl_2) **129**

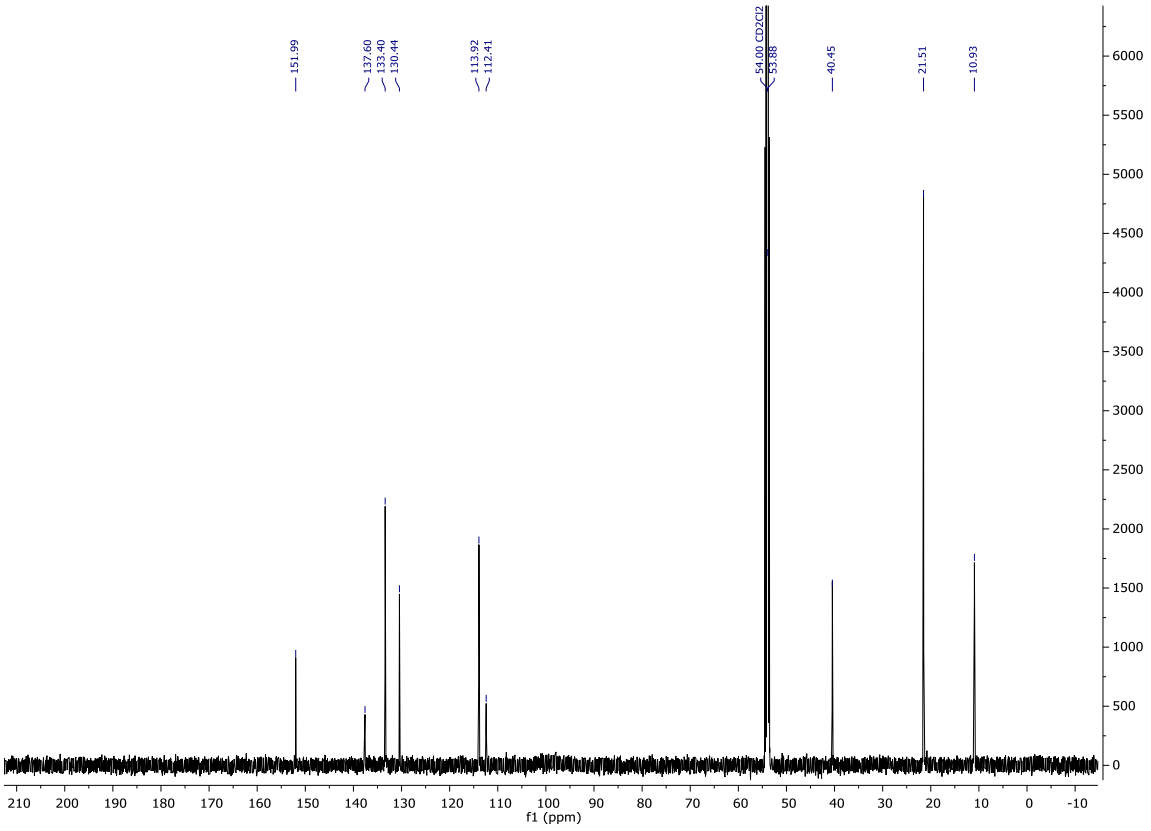

^{1}H NMR (300 MHz, CD_2Cl_2) **119**

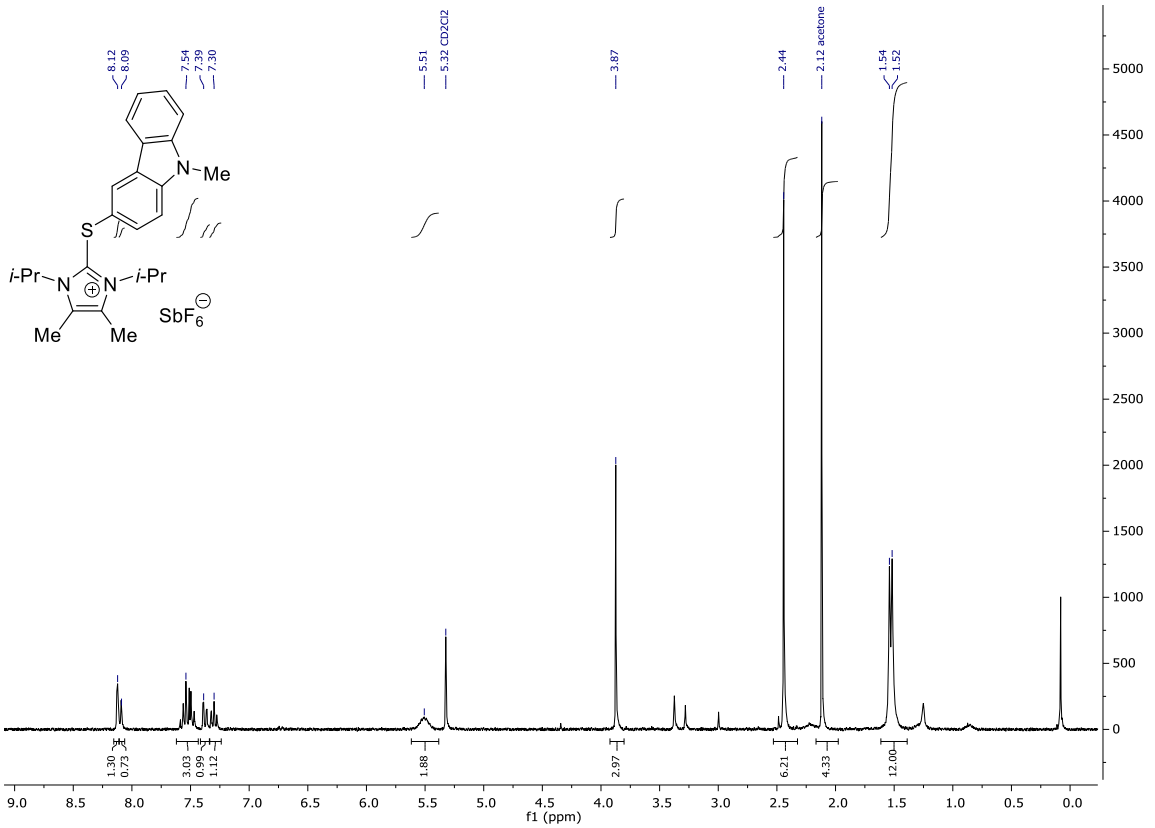

^{13}C NMR (75 MHz, CD_2Cl_2) **119**

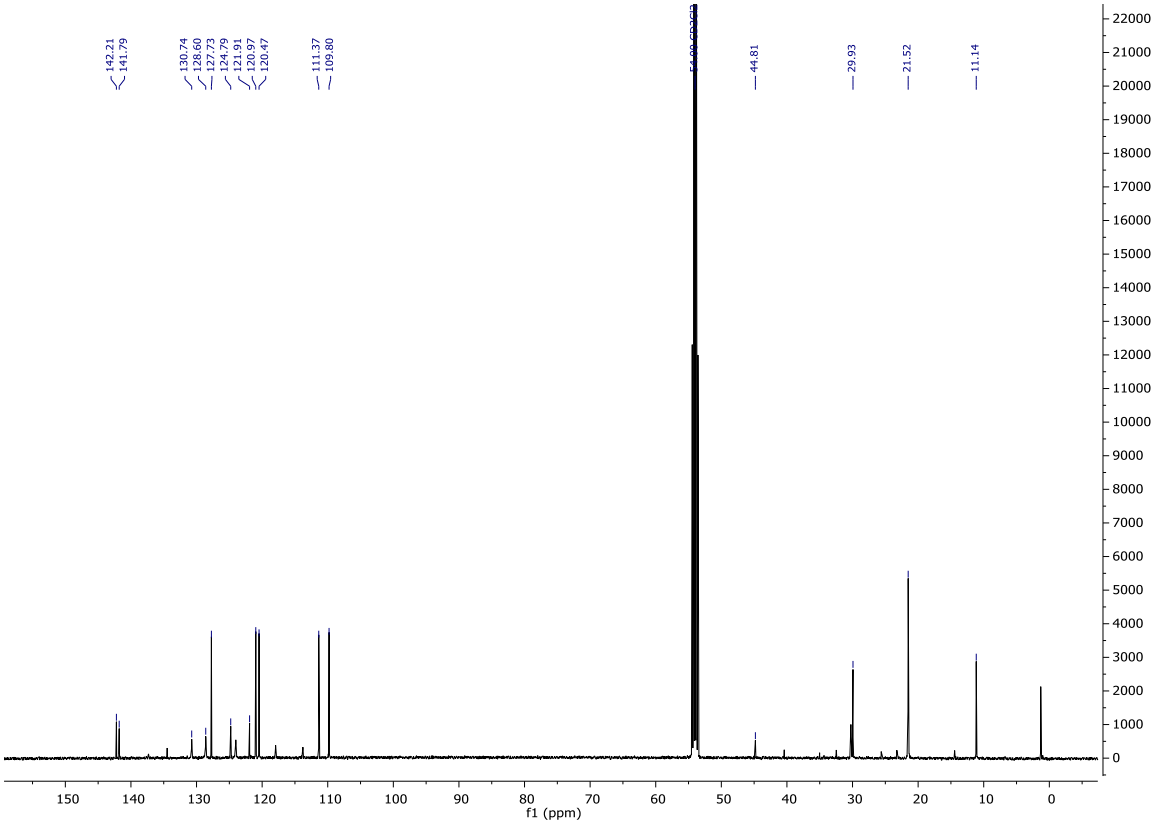

^{1}H NMR (300 MHz, CD_2Cl_2) **132**

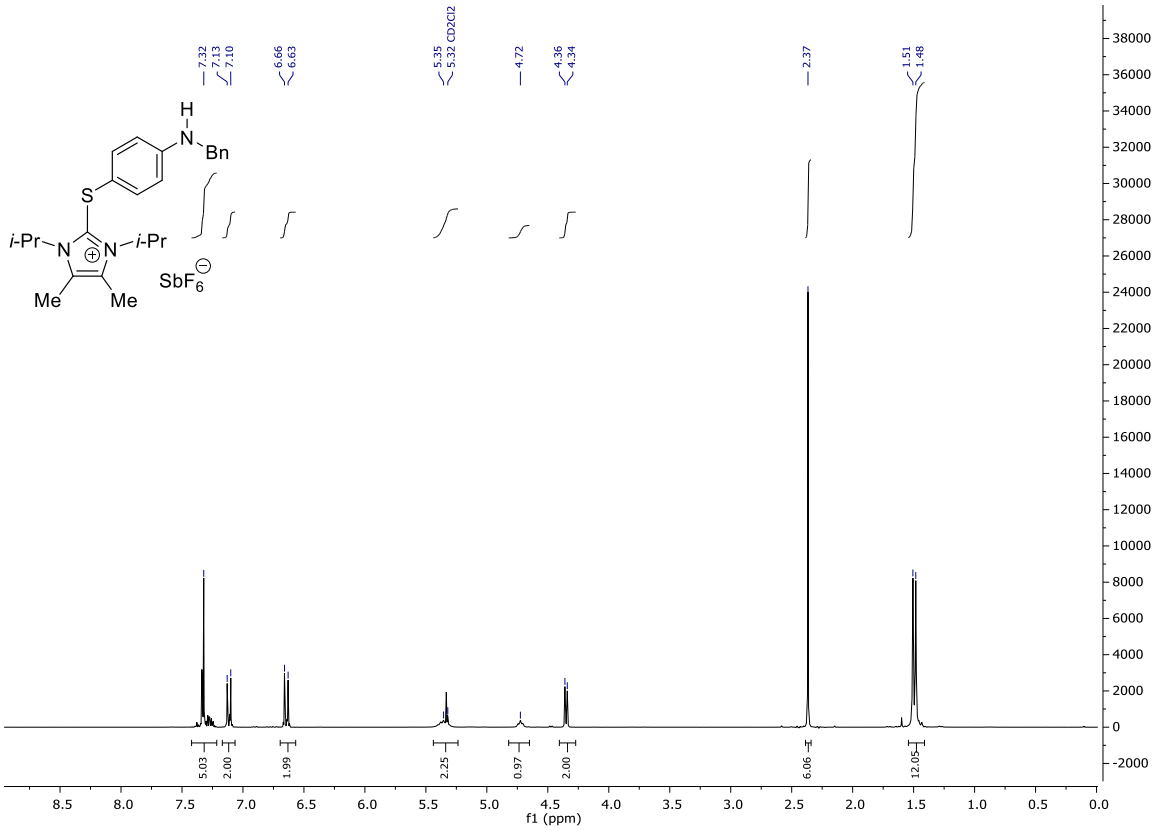

^{13}C NMR (75 MHz, CD_2Cl_2) **132**

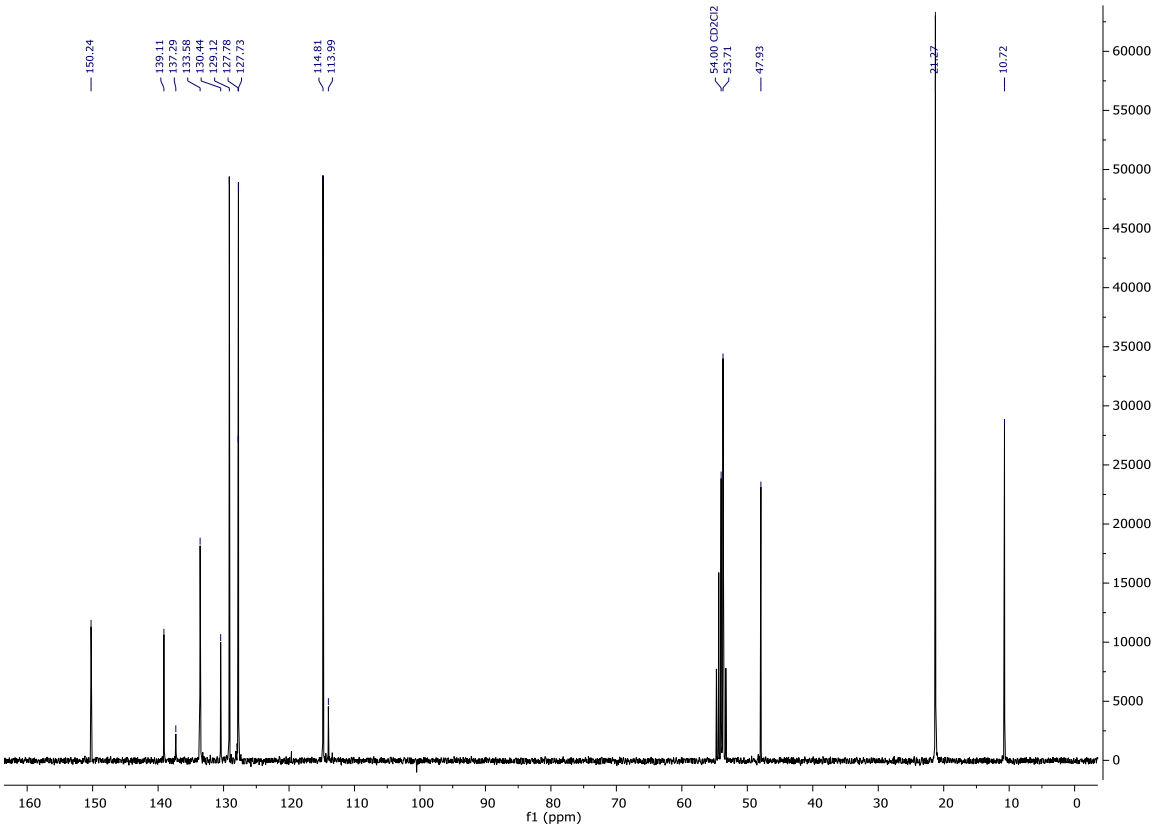

^{1}H NMR (300 MHz, CD_2Cl_2) **131**

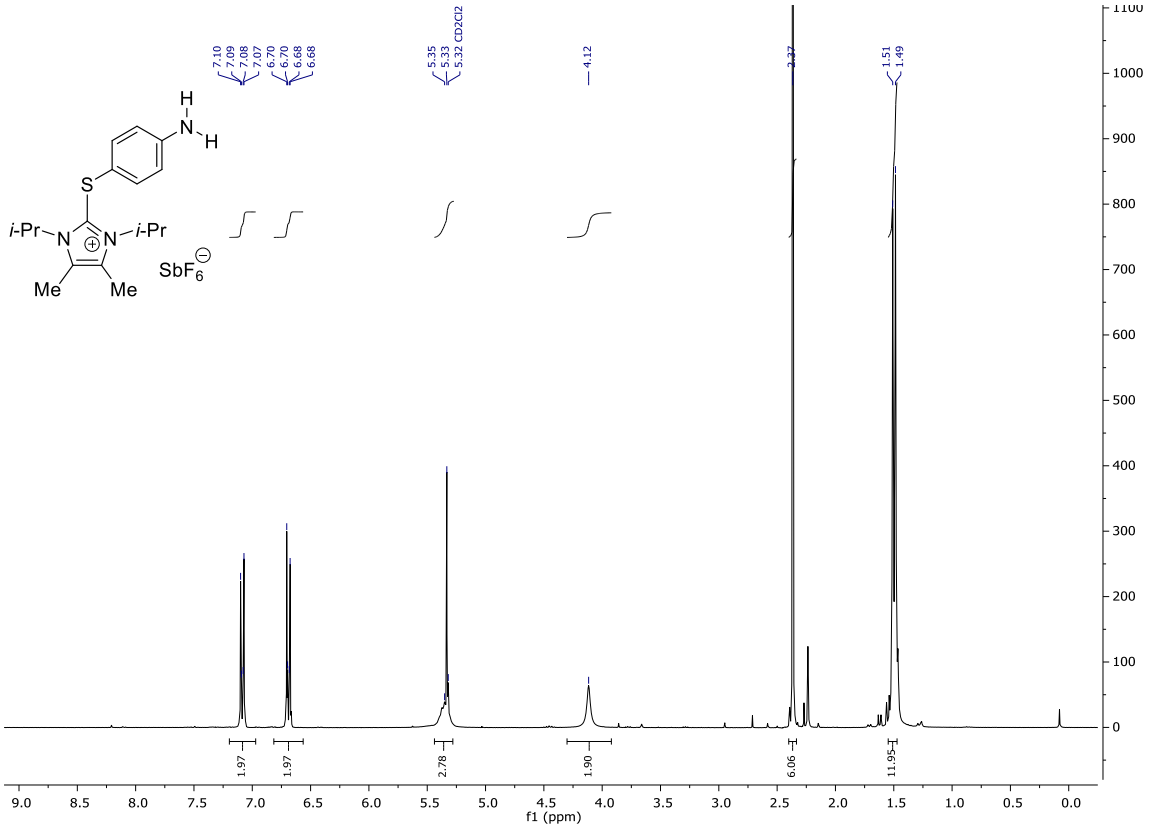

^{13}C NMR (75 MHz, CD_2Cl_2) **131**

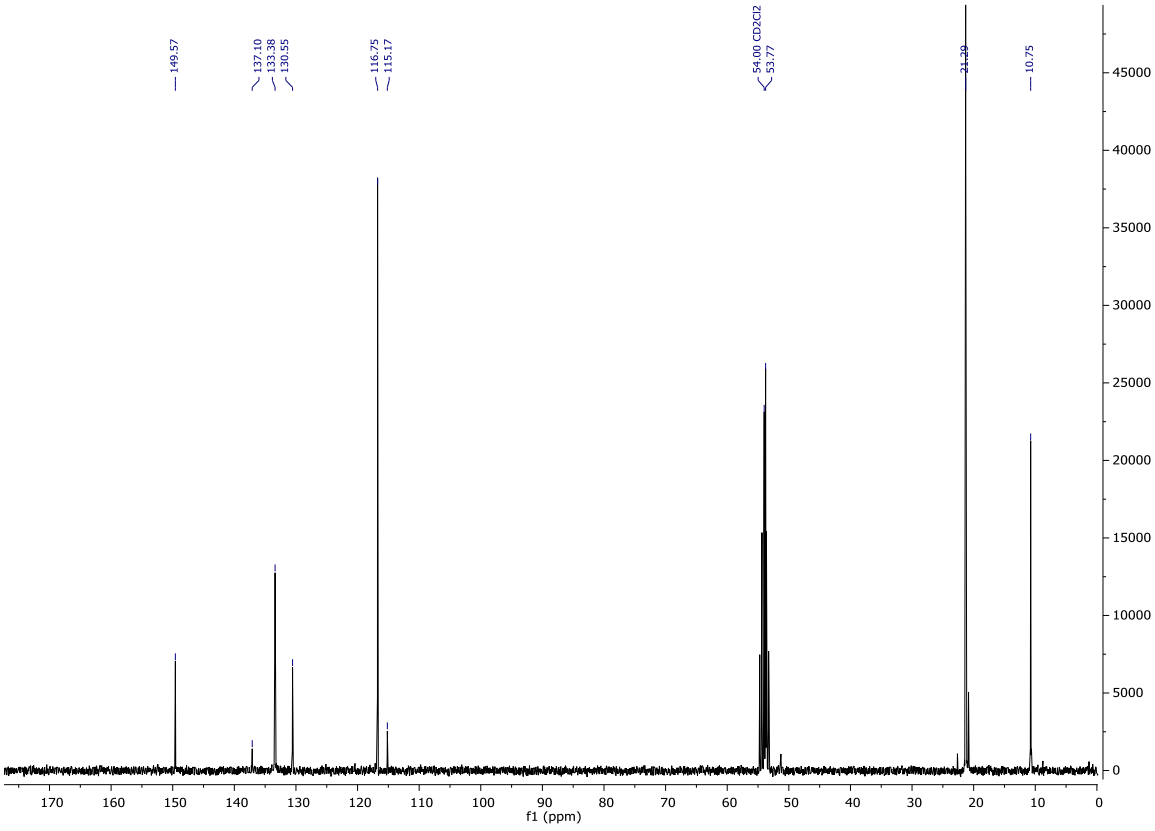

^{1}H NMR (300 MHz, CD_2Cl_2) **130**

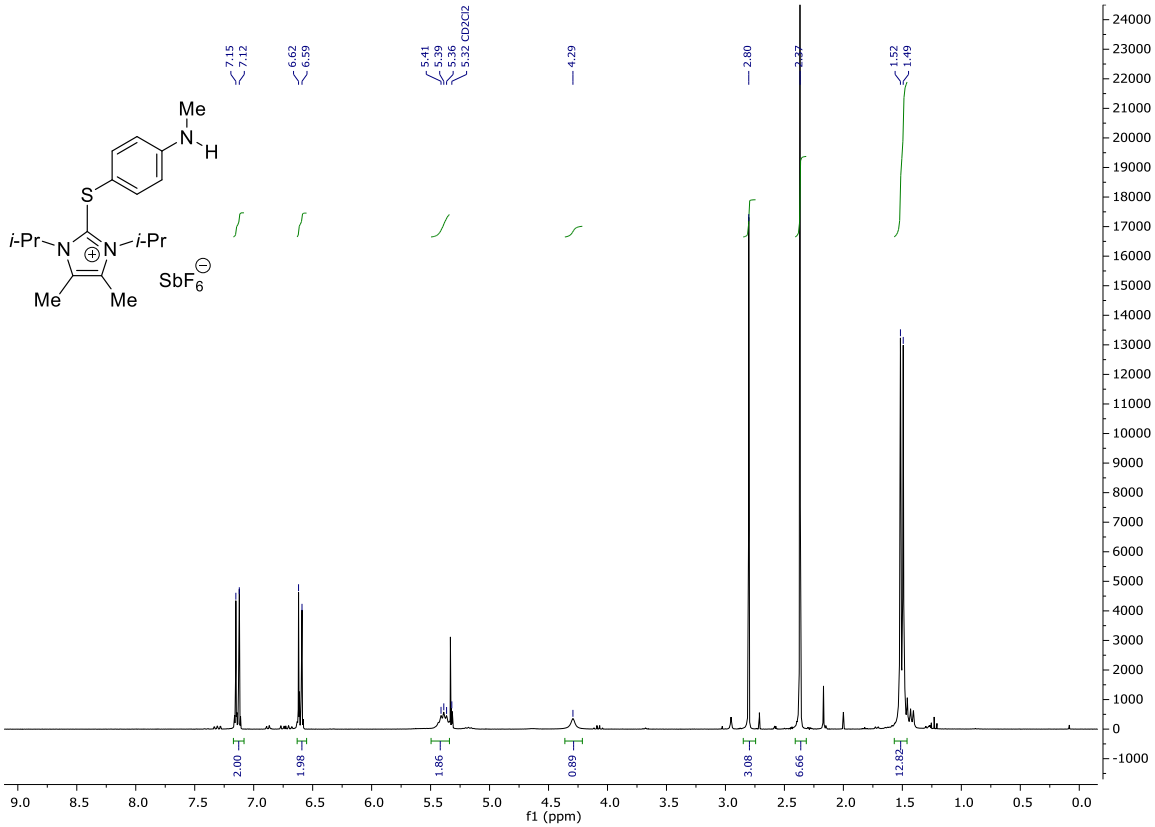

^{13}C NMR (101 MHz, CD_2Cl_2) **130**

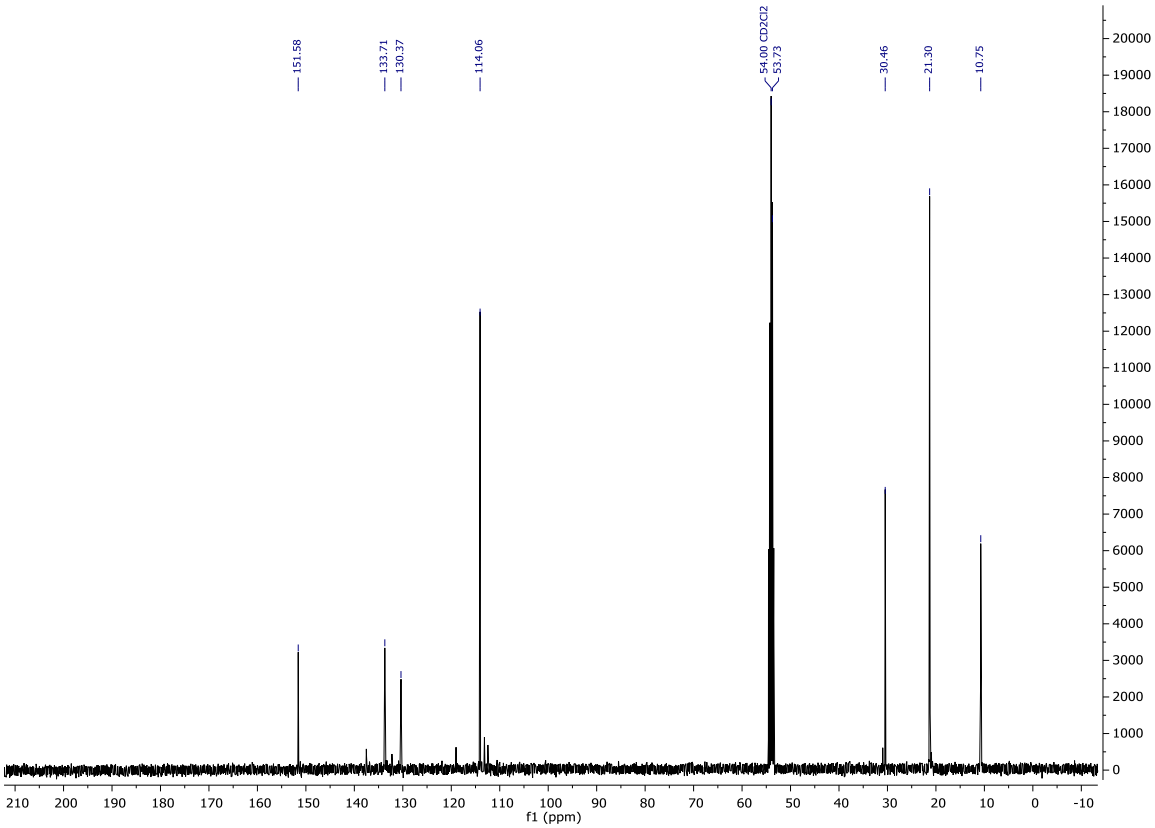

^{1}H NMR (300 MHz, CD_2Cl_2) **137**

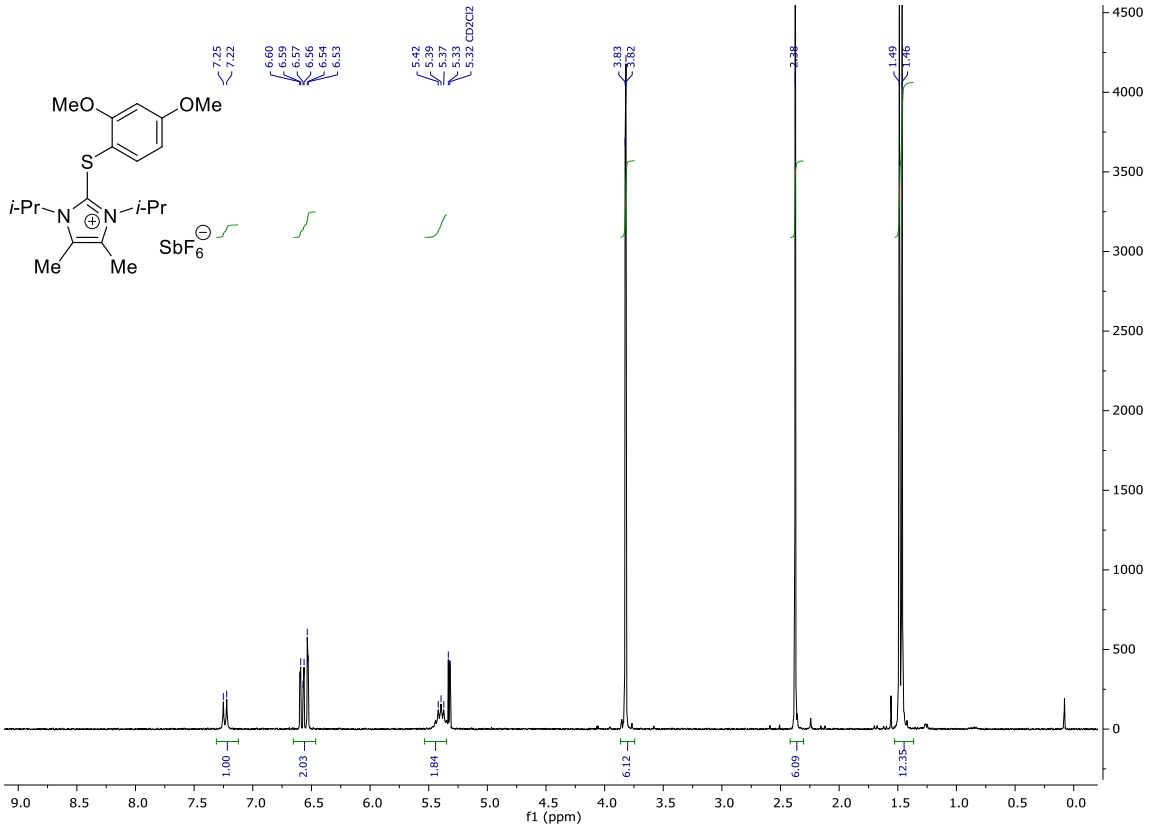

^{13}C NMR (126 MHz, CD_2Cl_2) **17**

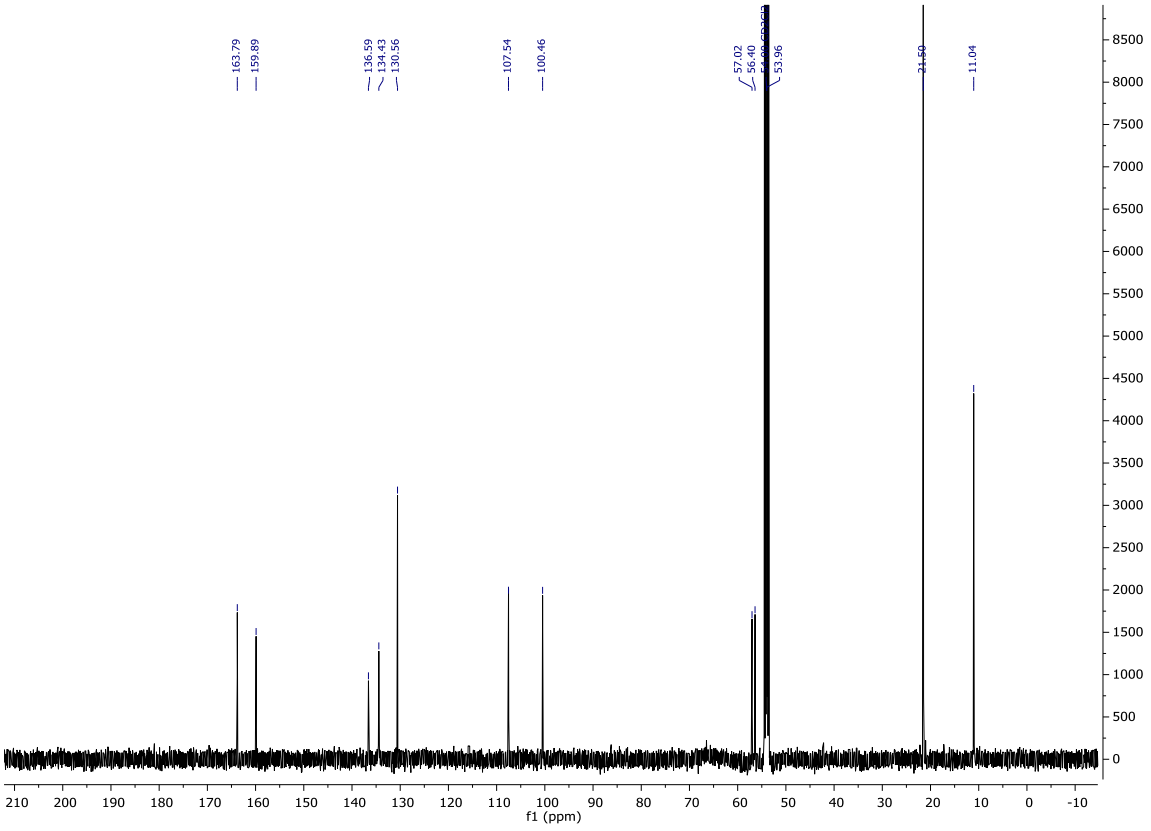

^{1}H NMR (300 MHz, CD_2Cl_2) **136**

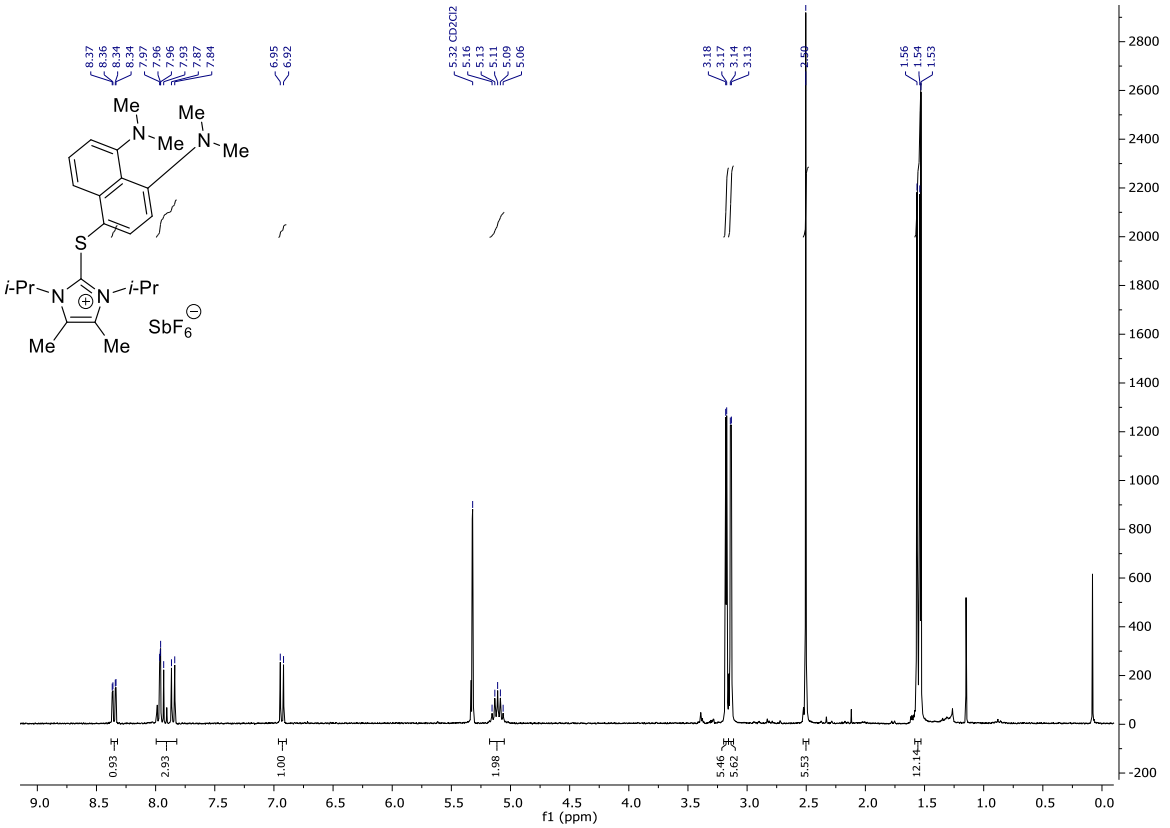

^{13}C NMR (101 MHz, CD_2Cl_2) **136**

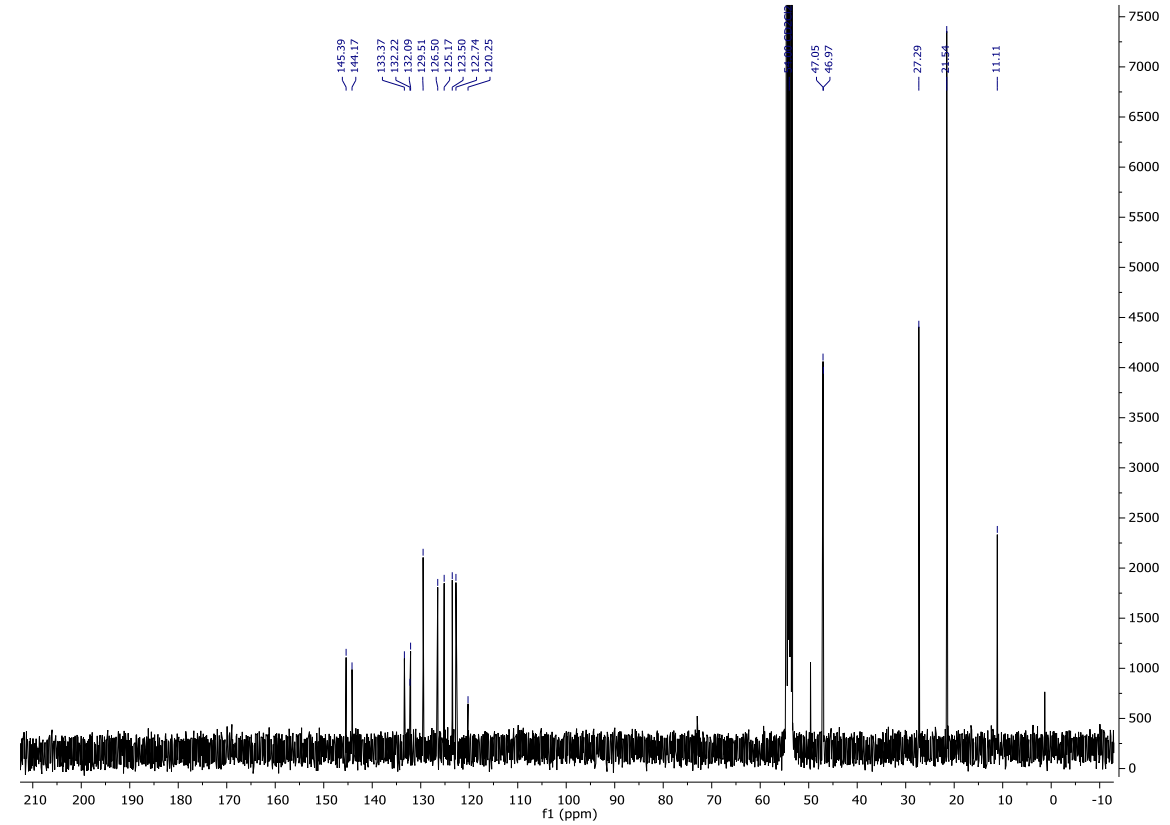

^{1}H NMR (400 MHz, CD_2Cl_2) **138**

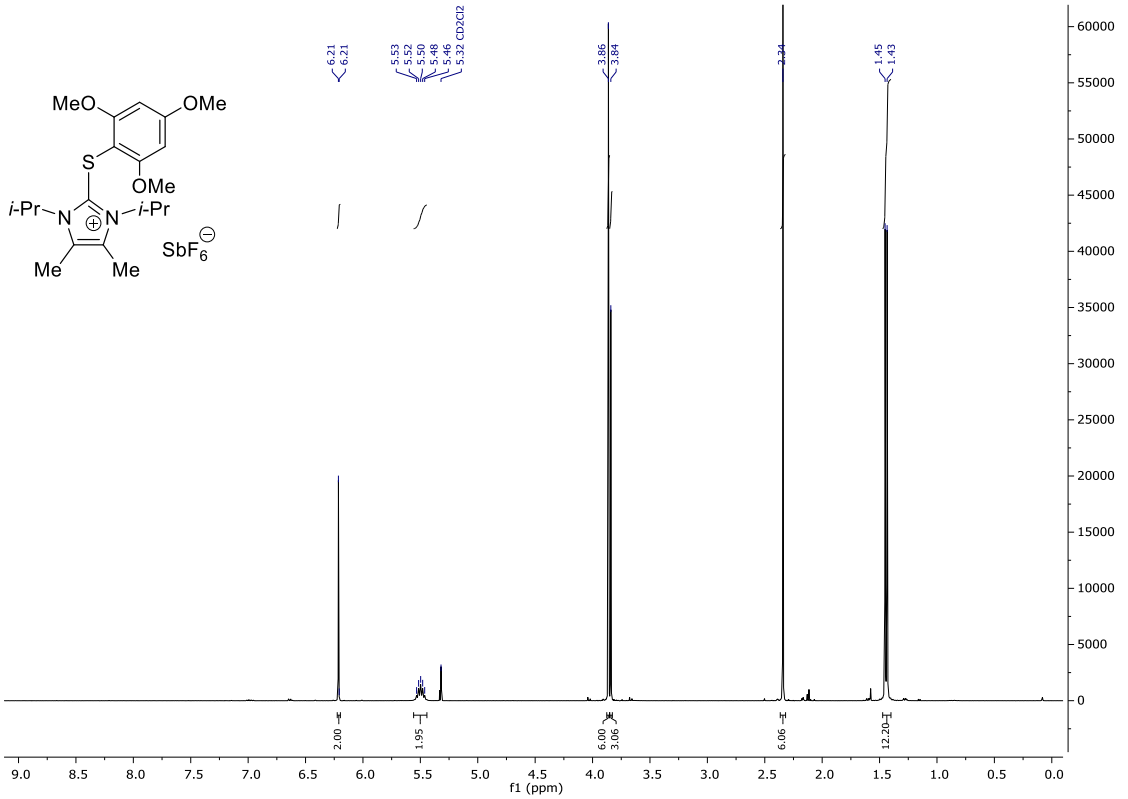

^{13}C NMR (101 MHz, CD_2Cl_2) **138**

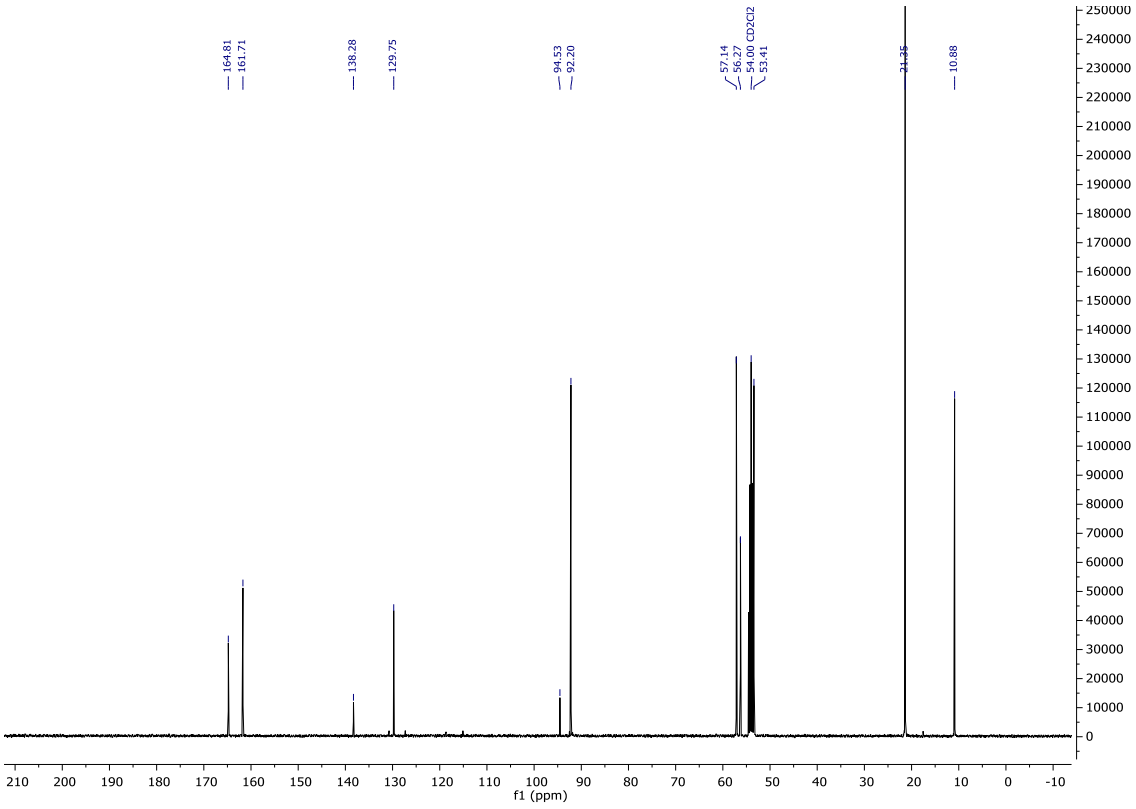

^{1}H NMR (300 MHz, CD_3CN) **201**

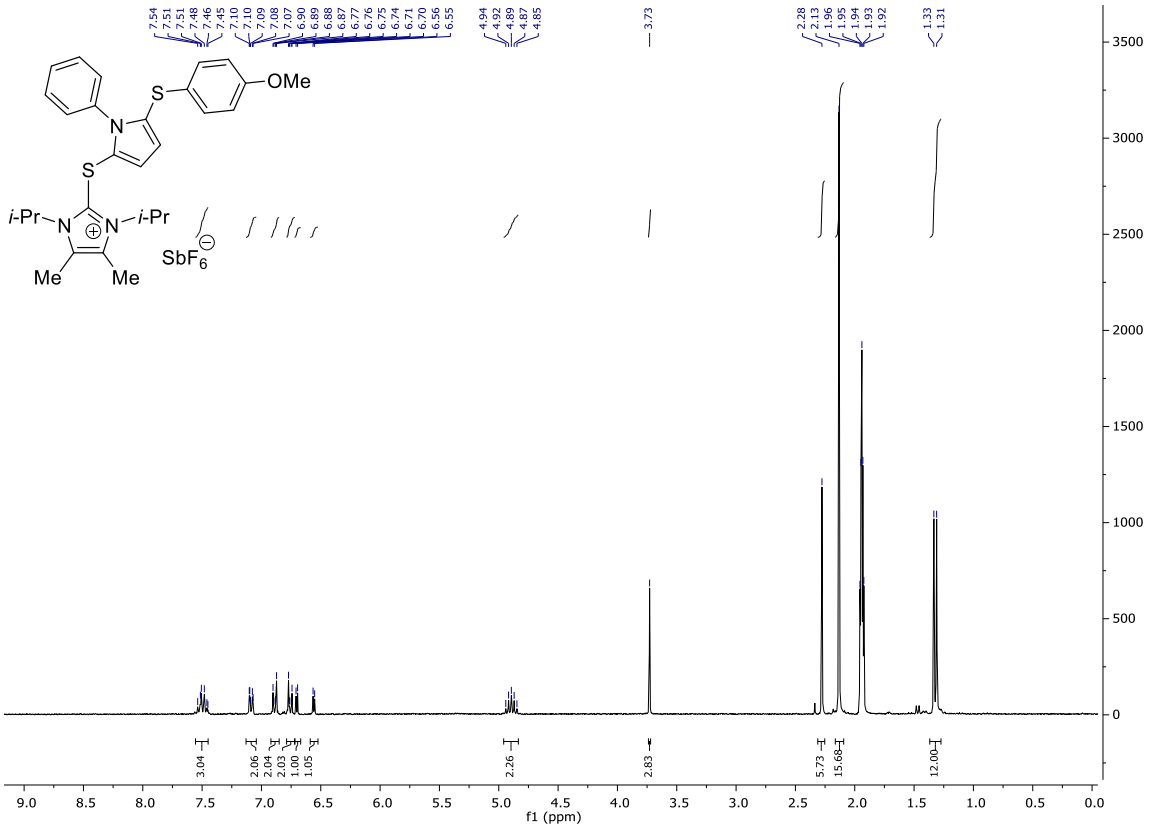

^{13}C NMR (126 MHz, CD_3CN) **201**

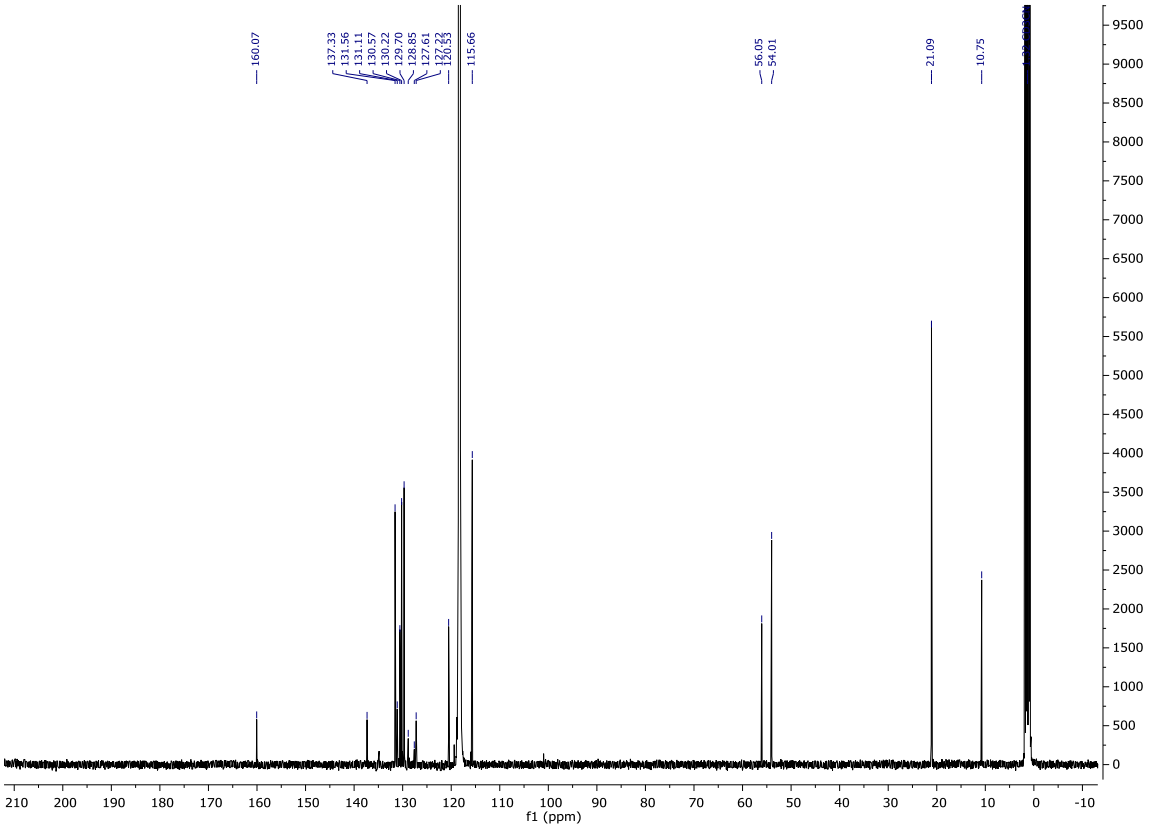

^{1}H NMR (300 MHz, CD_2Cl_2) **201**

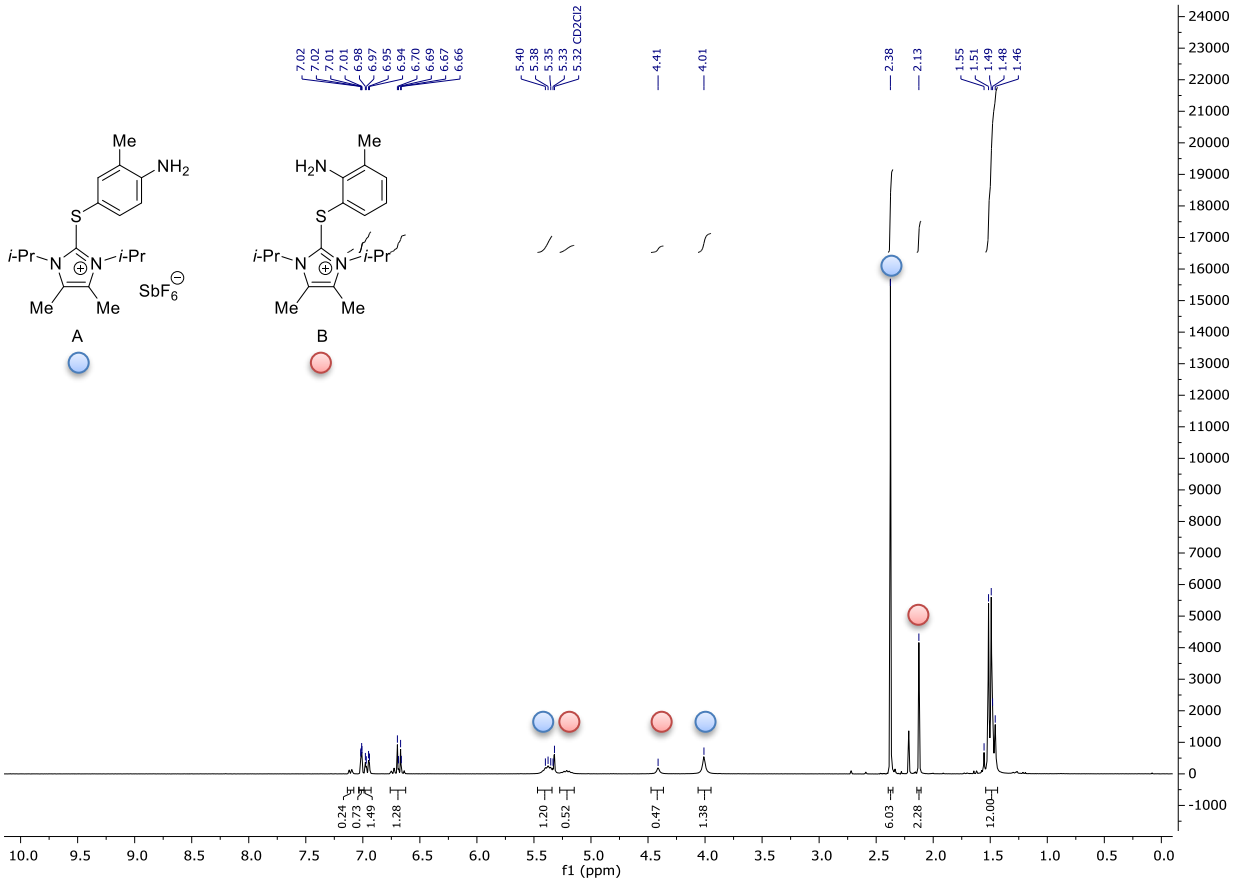

^{1}H NMR (300 MHz, CD_2Cl_2) **299**

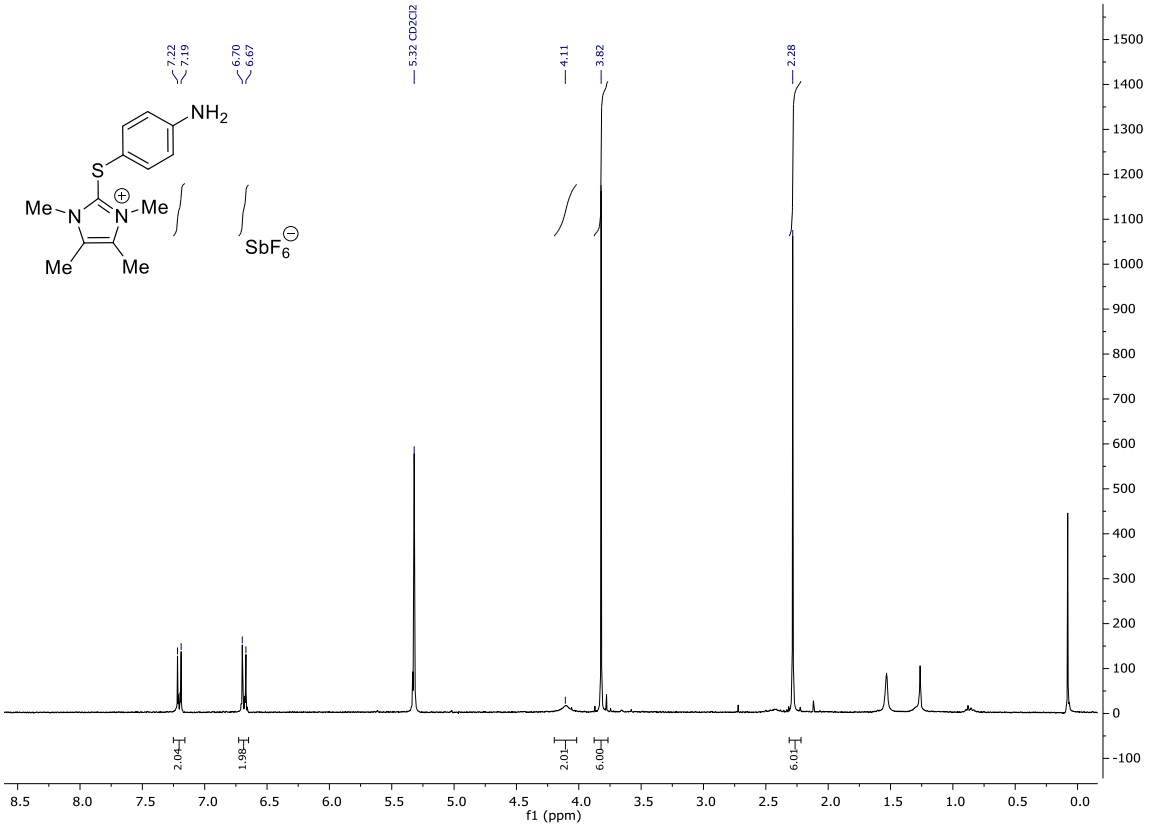

^{13}C NMR (75 MHz, CD_2Cl_2) **299**

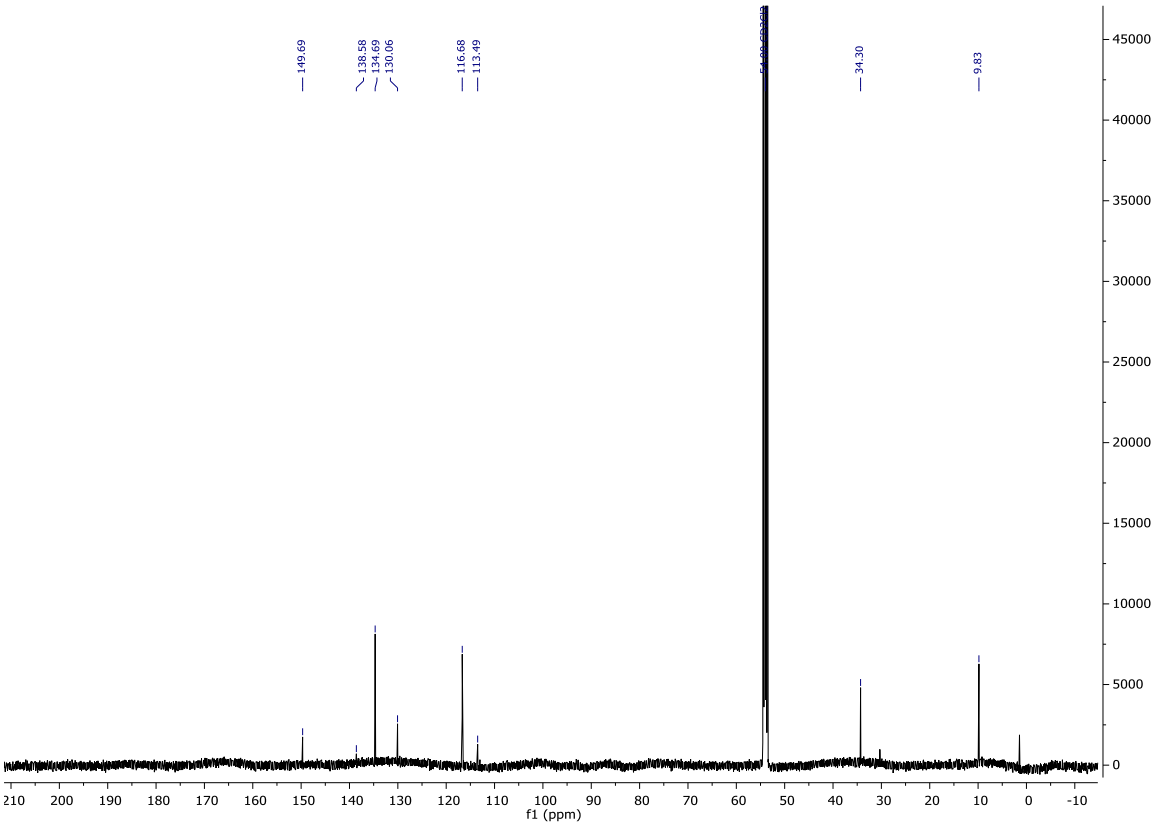

^{1}H NMR (400 MHz, CD_2Cl_2) **151**

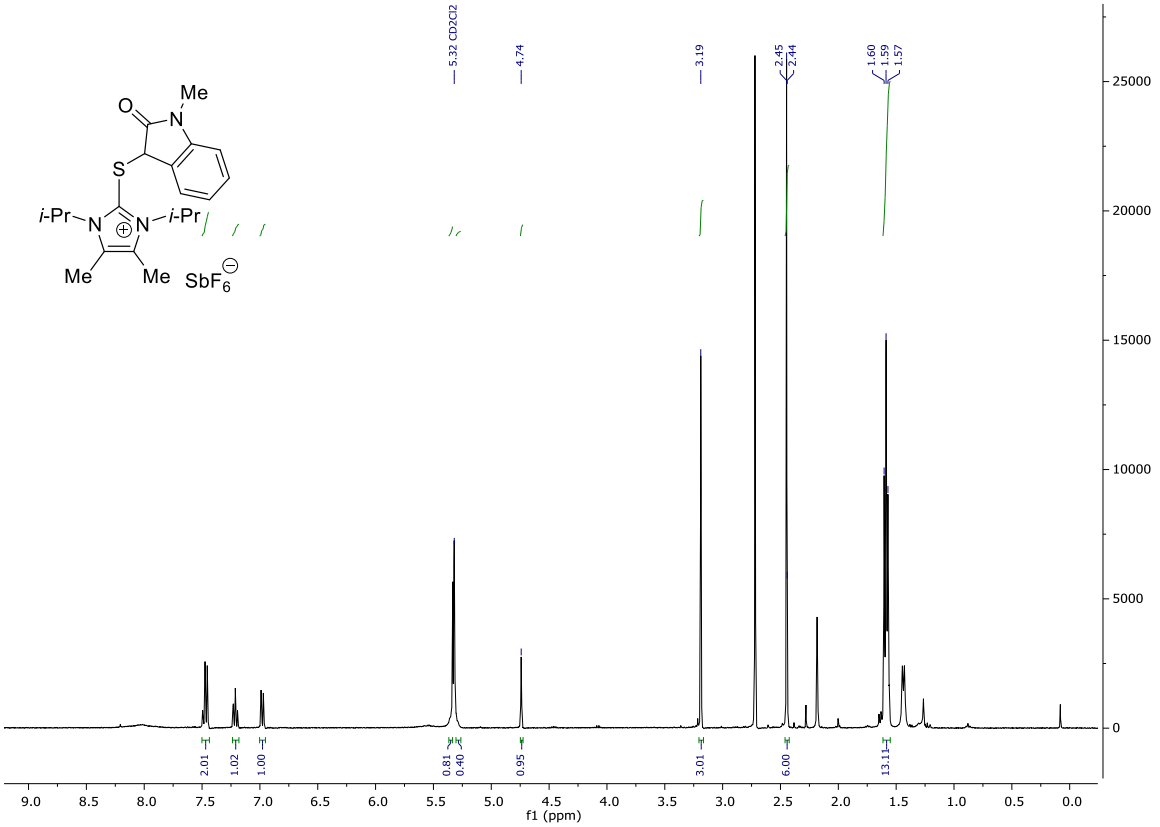

^{13}C NMR (75 MHz, CD_2Cl_2) **151**

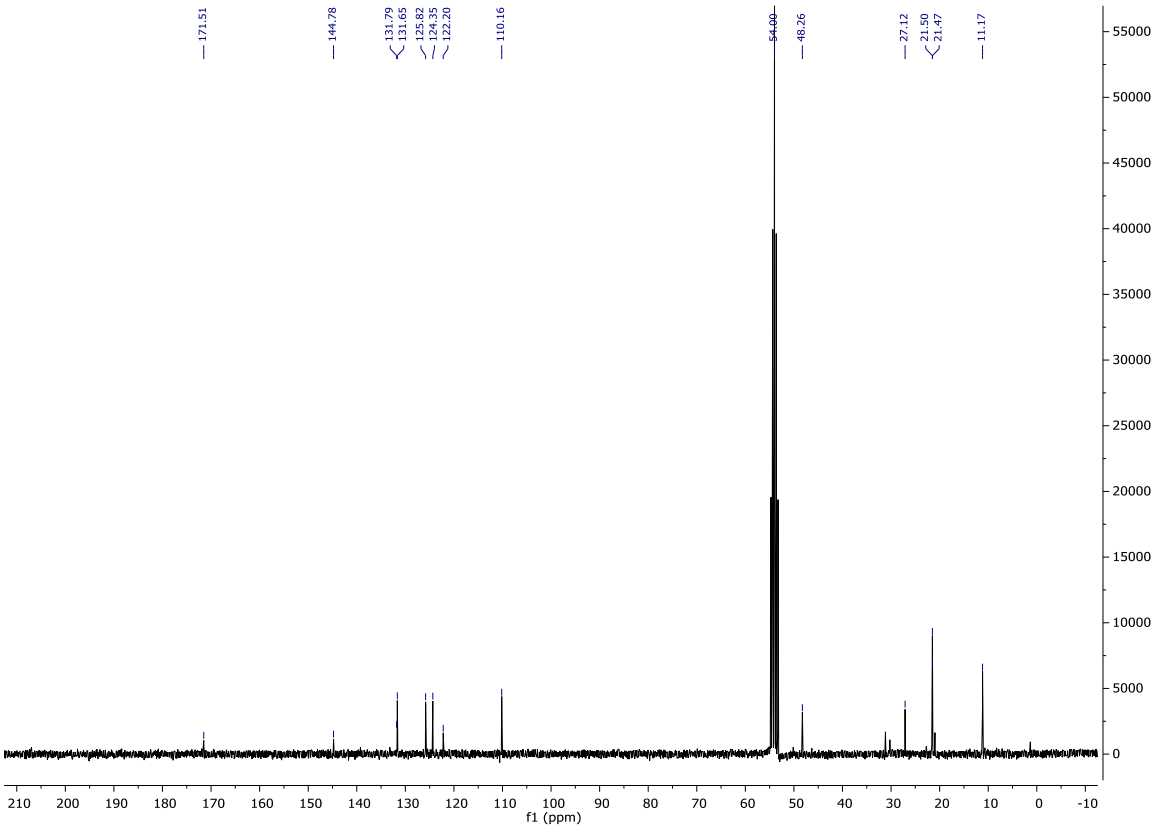

Synthesis of aryltriazolium salts

^{1}H NMR (400 MHz, CD_2Cl_2) **300**

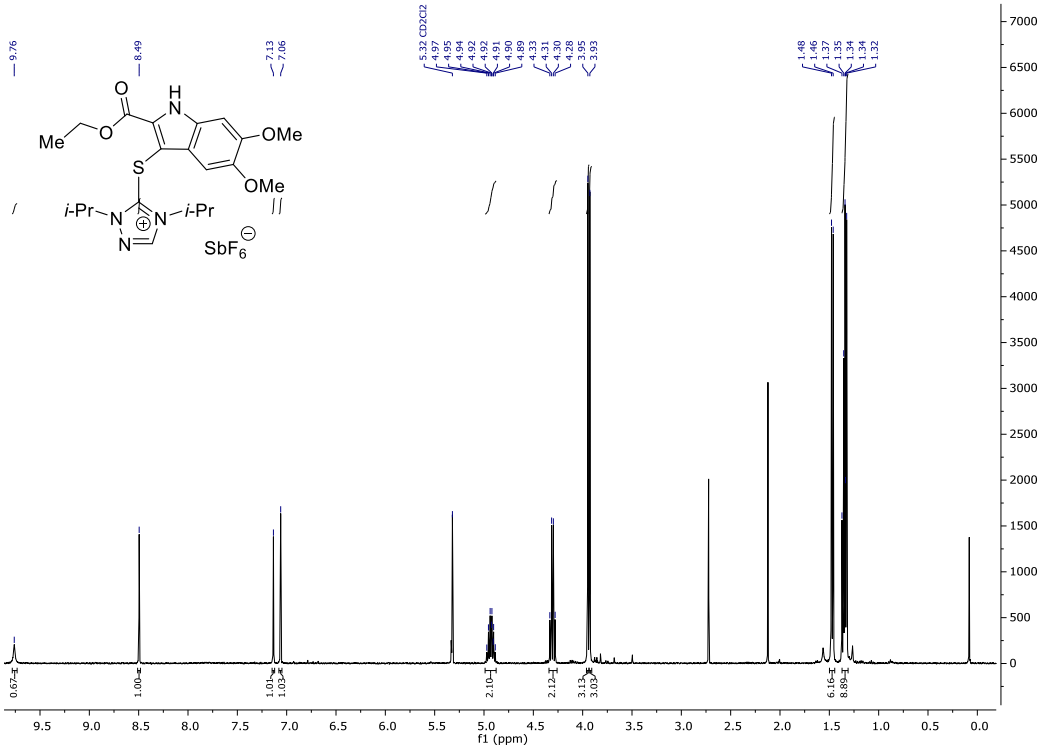

^{13}C NMR (101 MHz, CD_2Cl_2) **300**

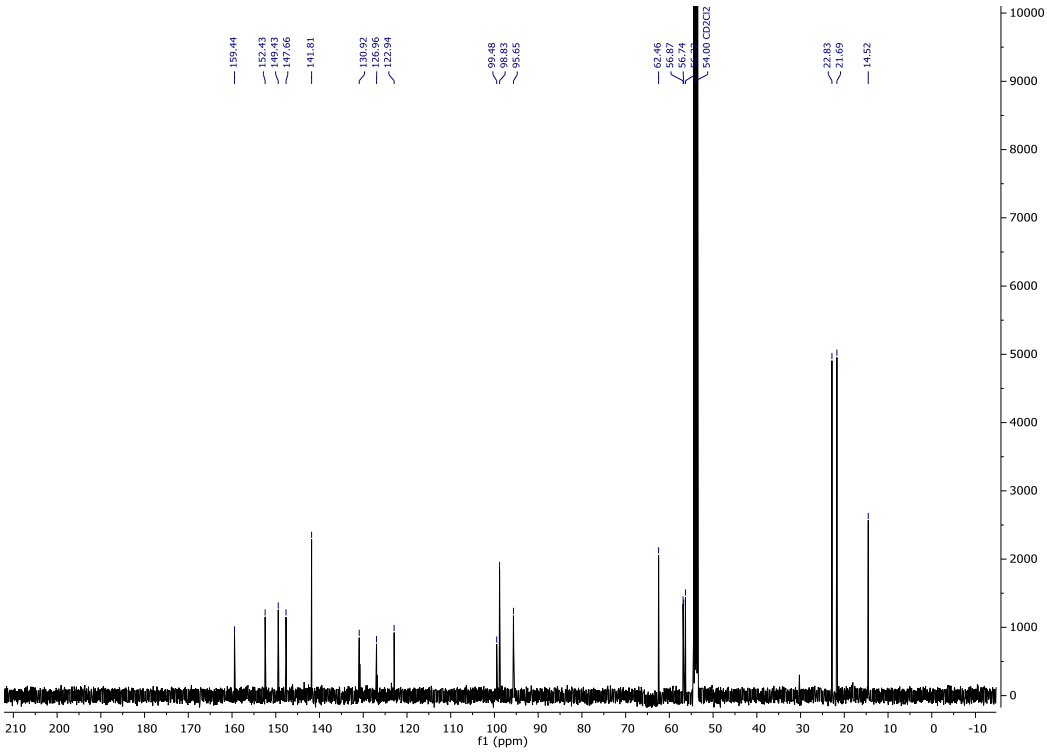

^{1}H NMR (400 MHz, CD_2Cl_2) **105**

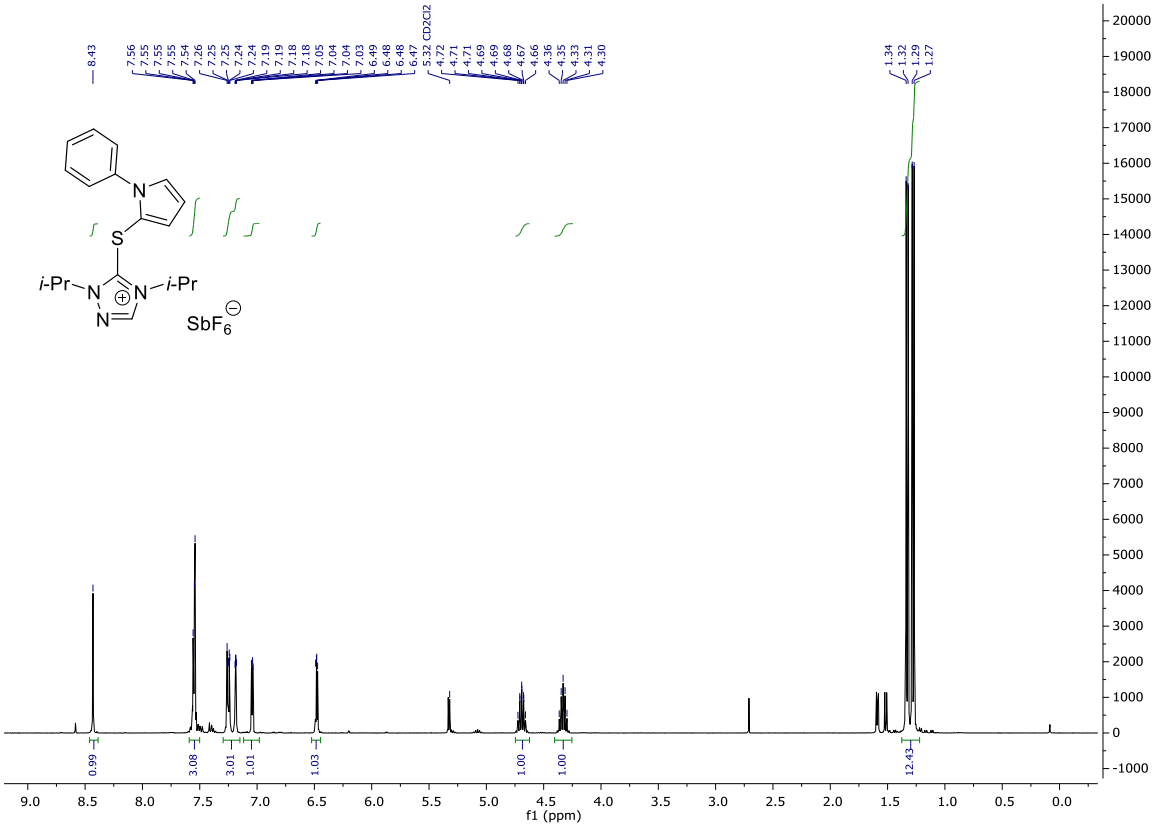

^{13}C NMR (101 MHz, CD_2Cl_2) **105**

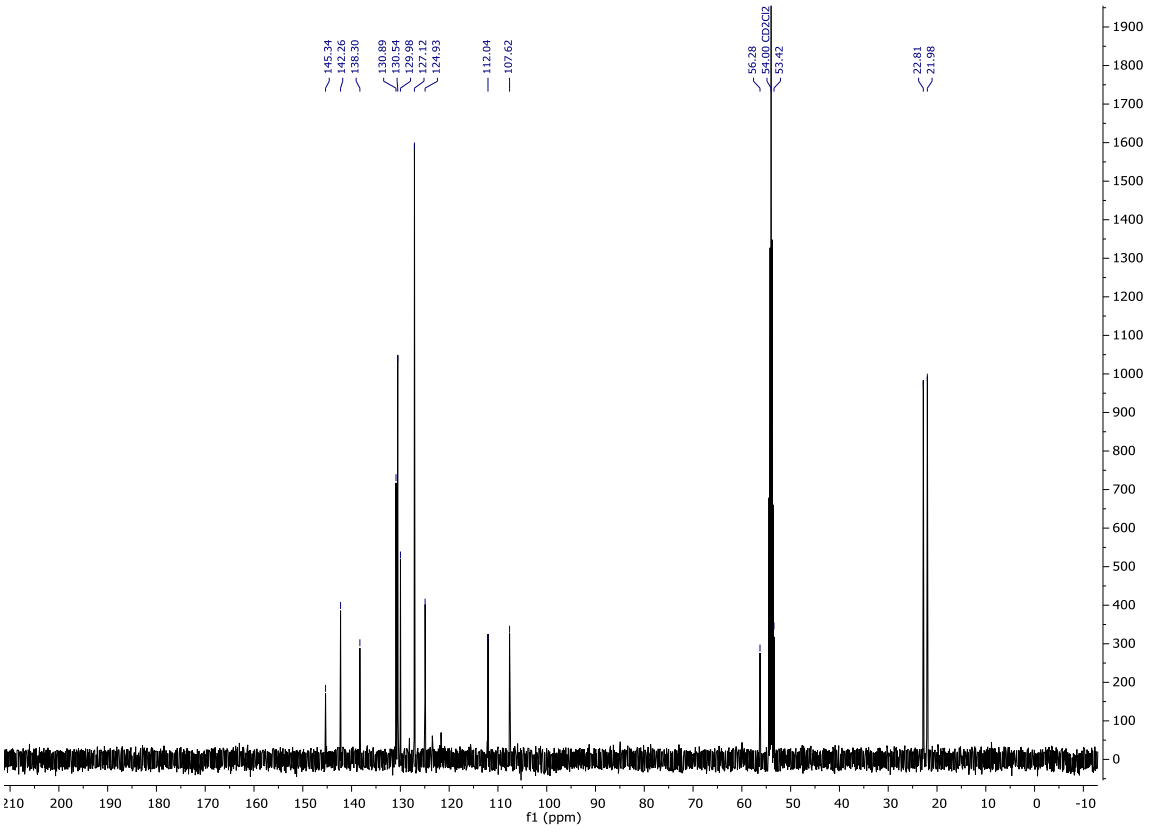

^{1}H NMR (400 MHz, CD_2Cl_2) **211**

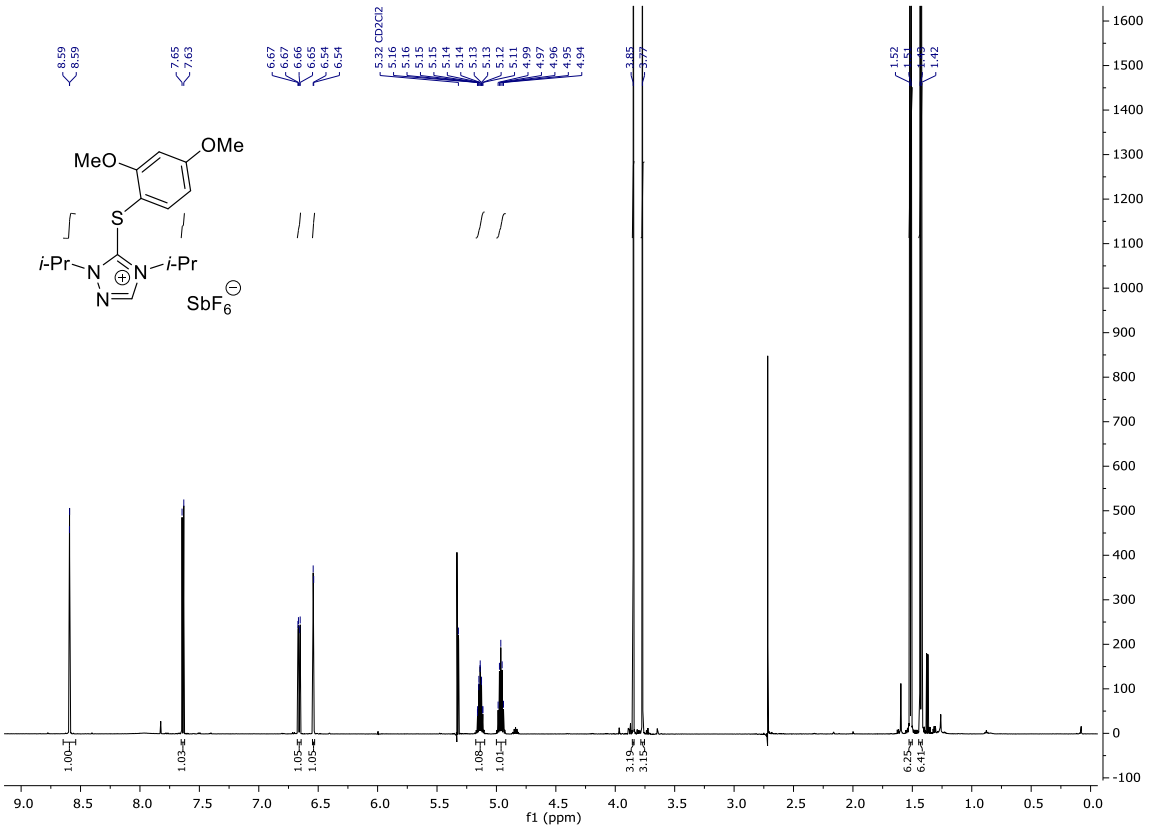

^{13}C NMR (126 MHz, CD_2Cl_2) **211**

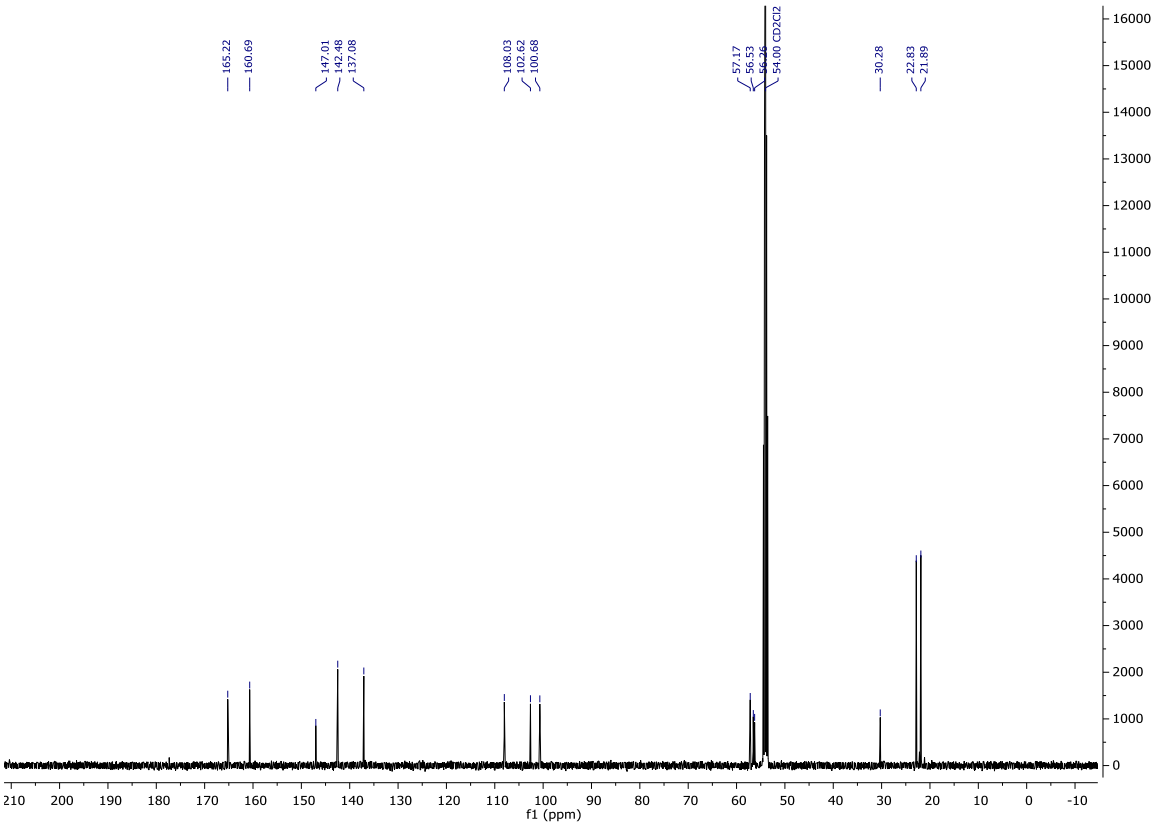

Synthesis of ansymmetrical sulfides

^{1}H NMR (400 MHz, $CDCl_3$) **301**

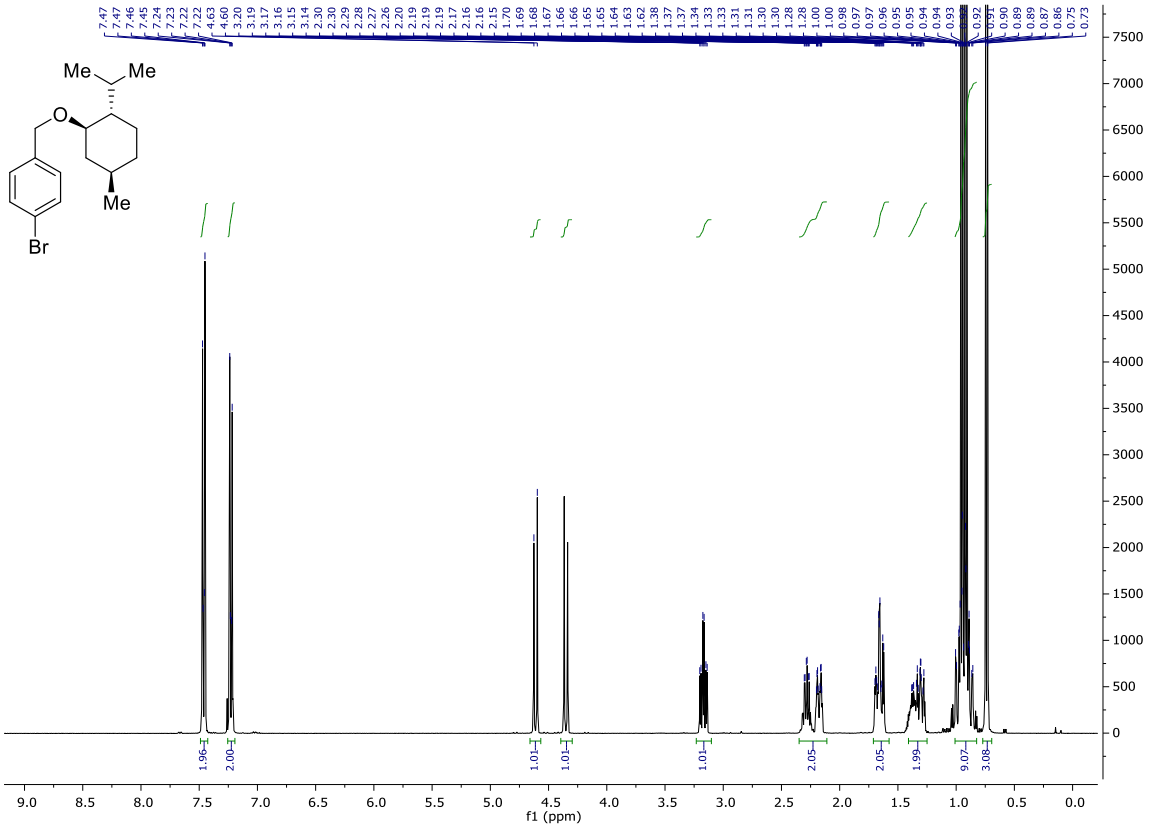

^{13}C NMR (101 MHz, $CDCl_3$) **301**

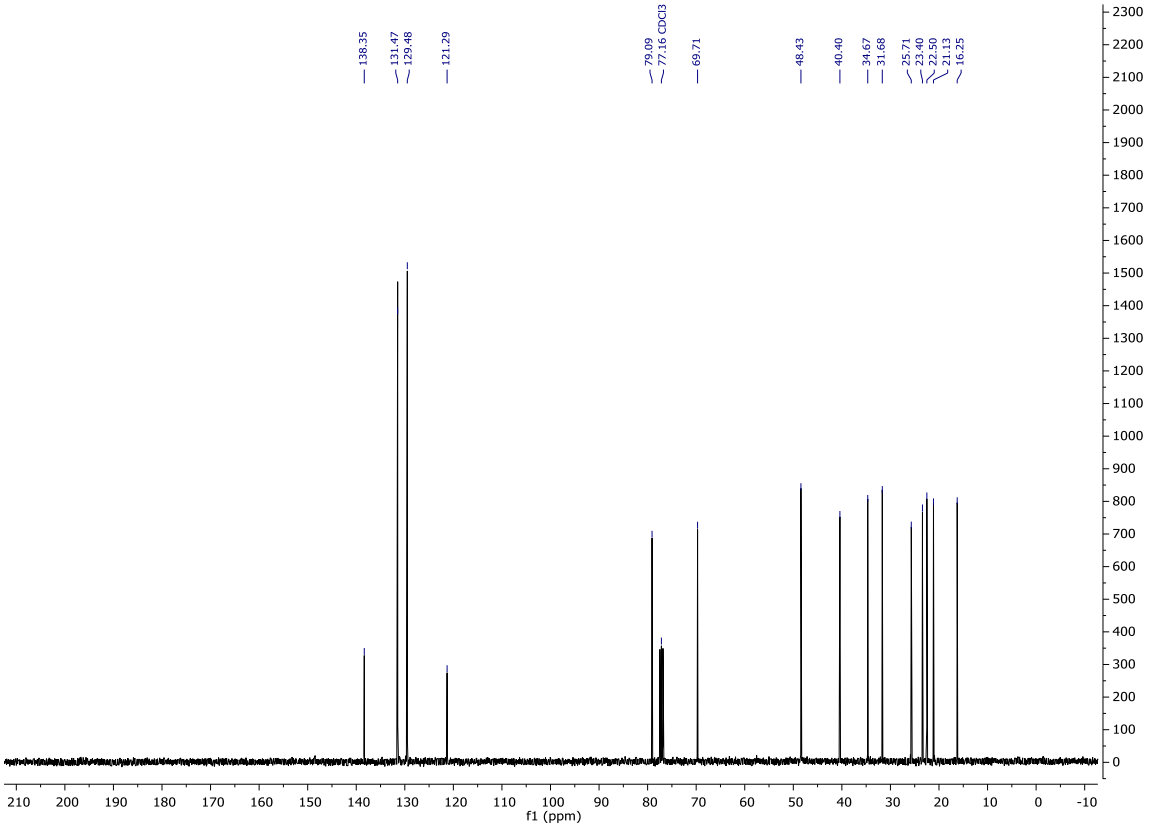

^{1}H NMR (400 MHz, $CDCl_3$) **302**

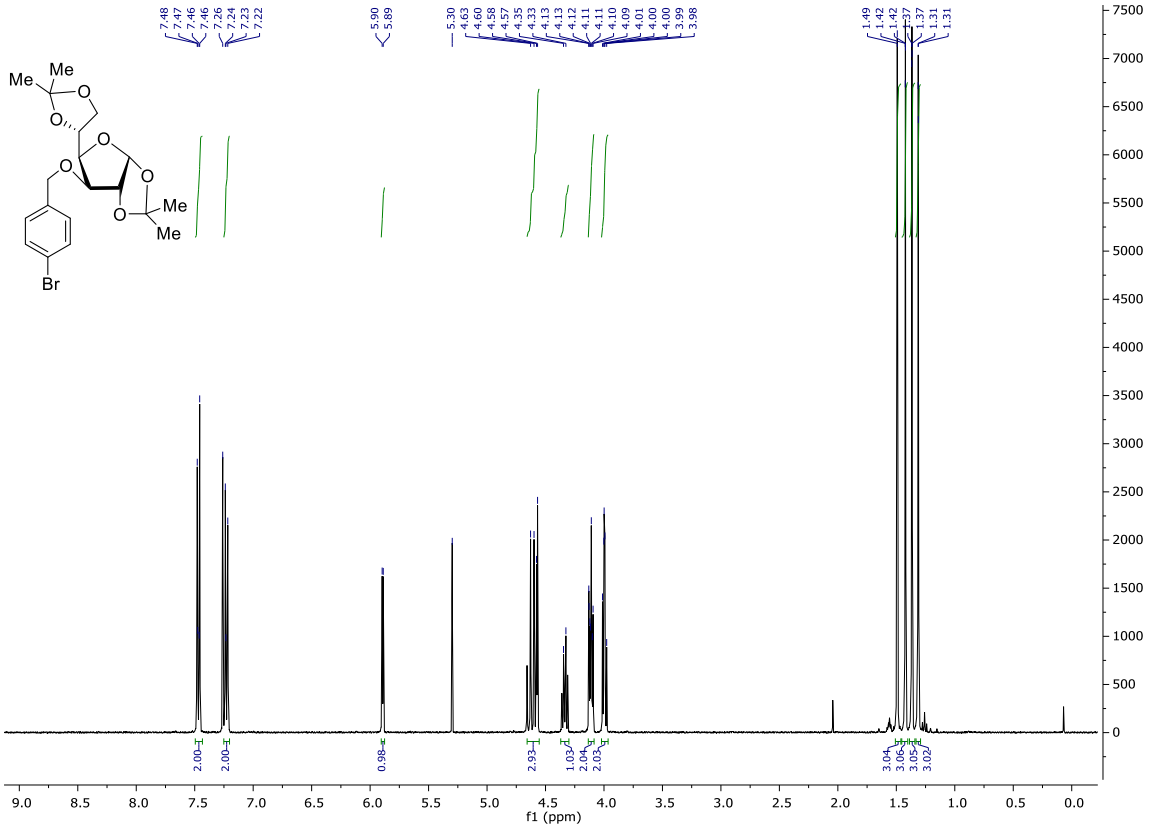

^{13}C NMR (75 MHz, $CDCl_3$) **302**

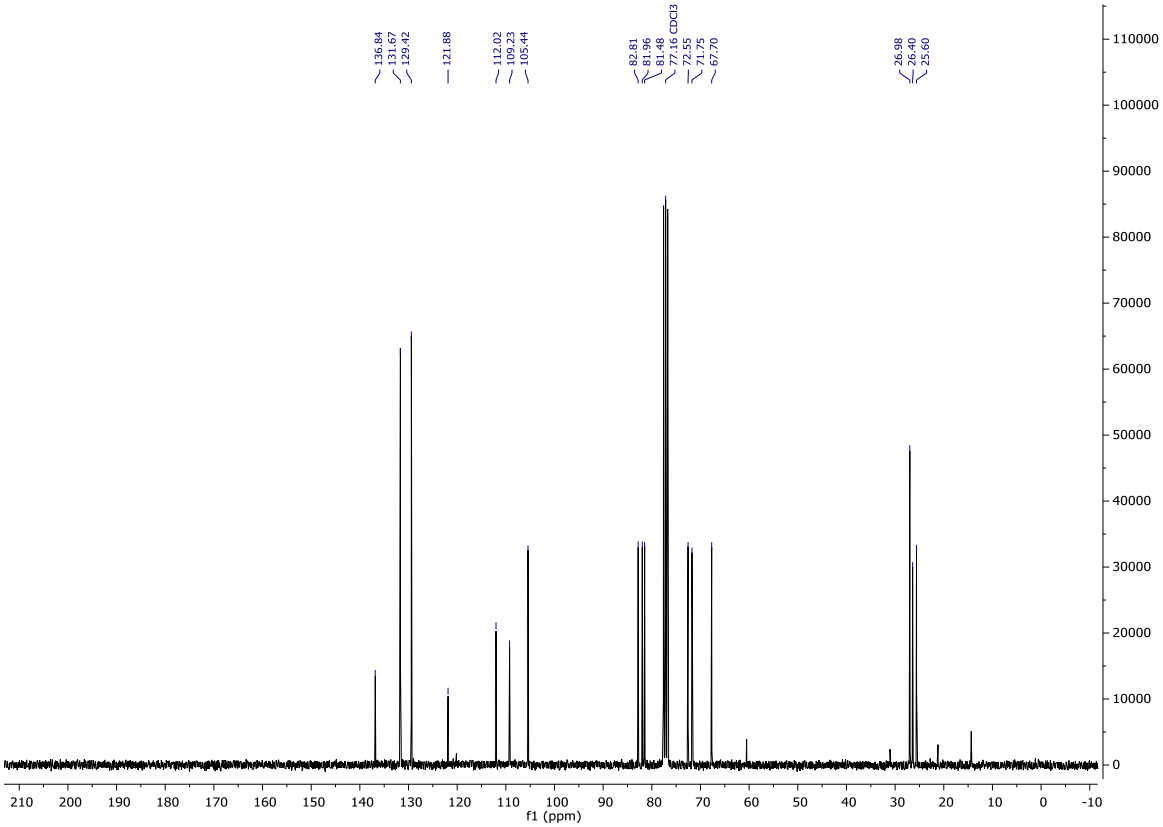

^{1}H NMR (600 MHz, $CDCl_3$) **303**

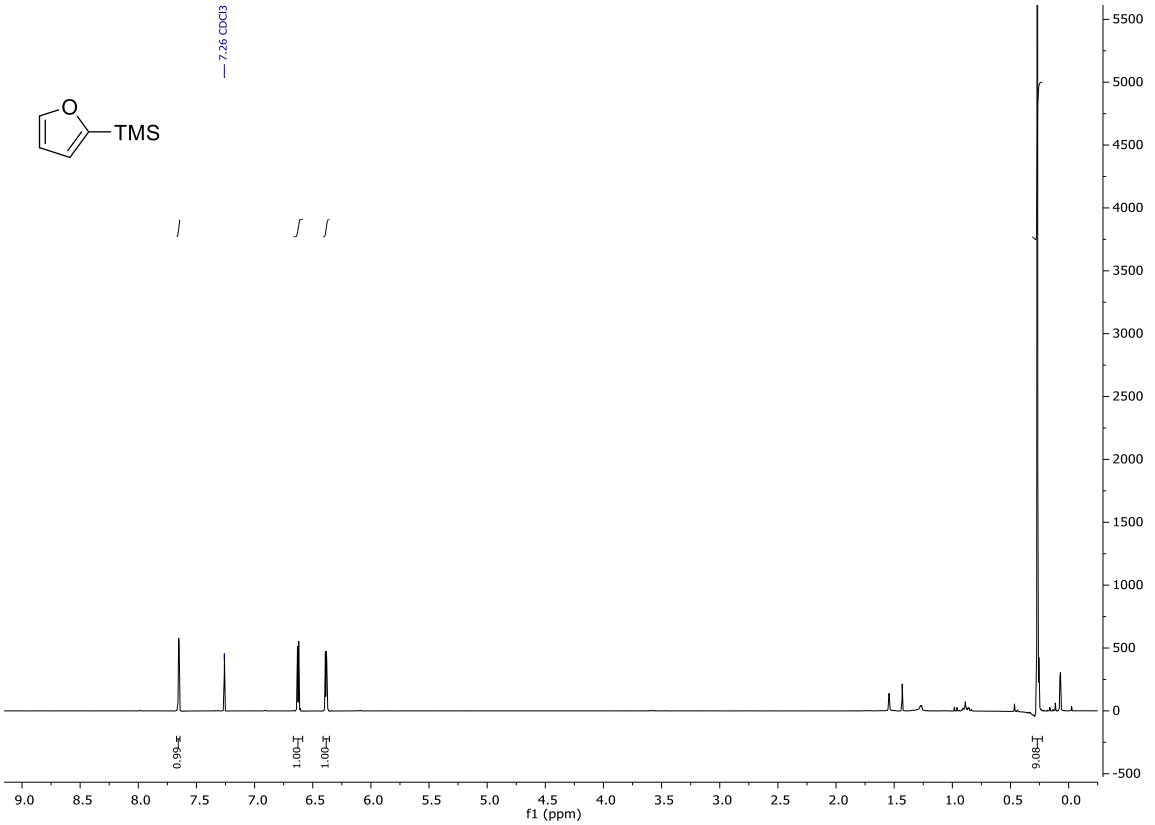

^{13}C NMR (126 MHz, $CDCl_3$) **303**

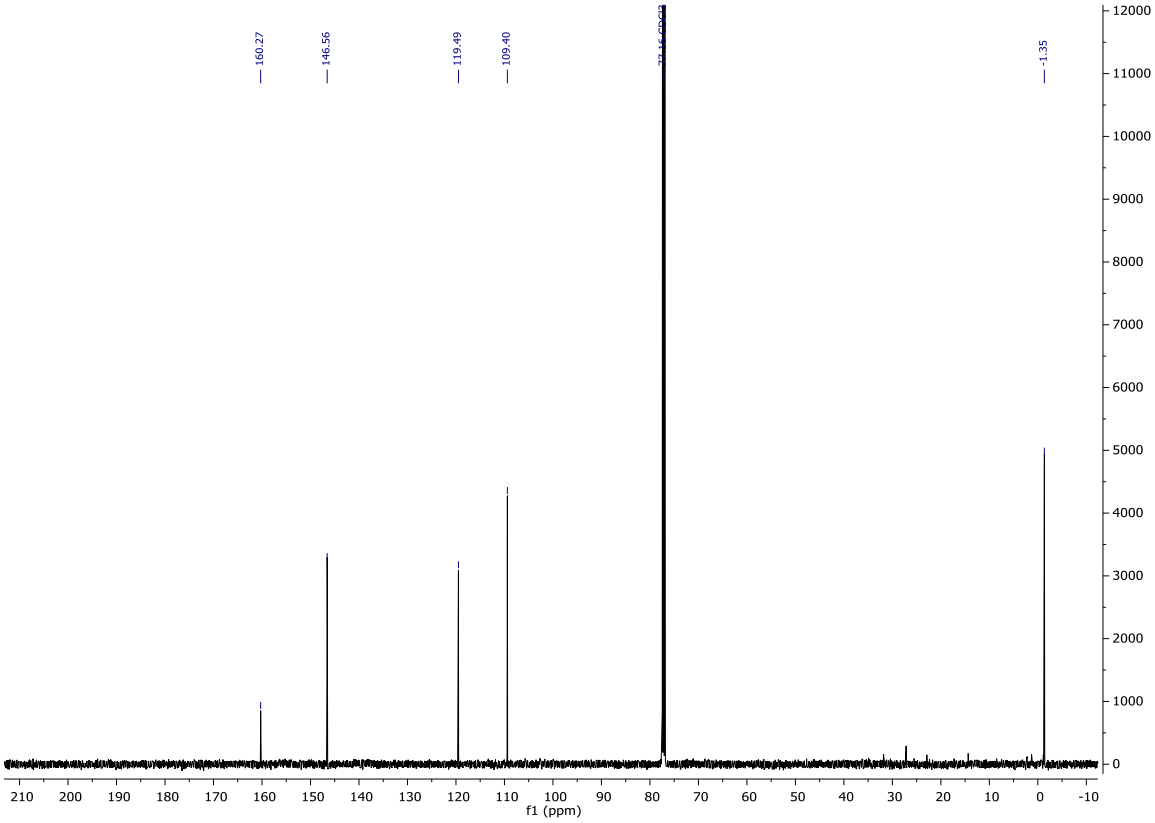

^{1}H NMR (300 MHz, $CDCl_3$) **161**

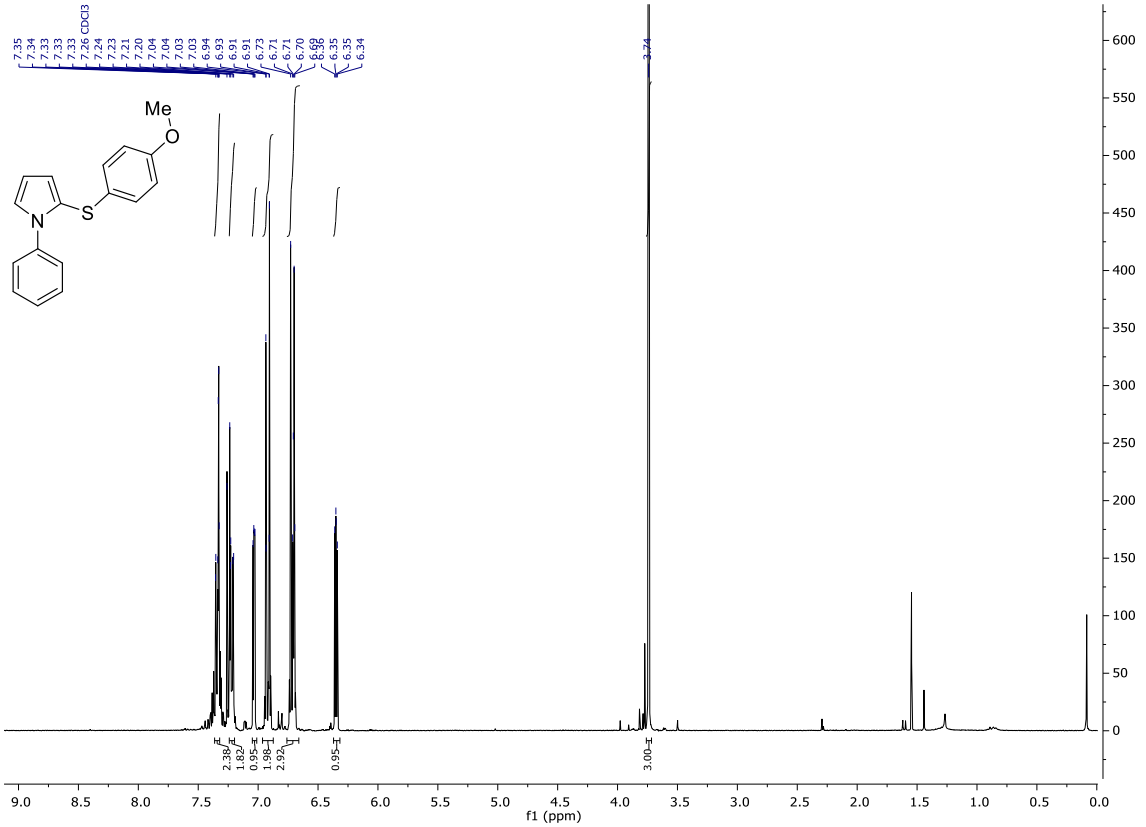

^{13}C NMR (75 MHz, $CDCl_3$) **161**

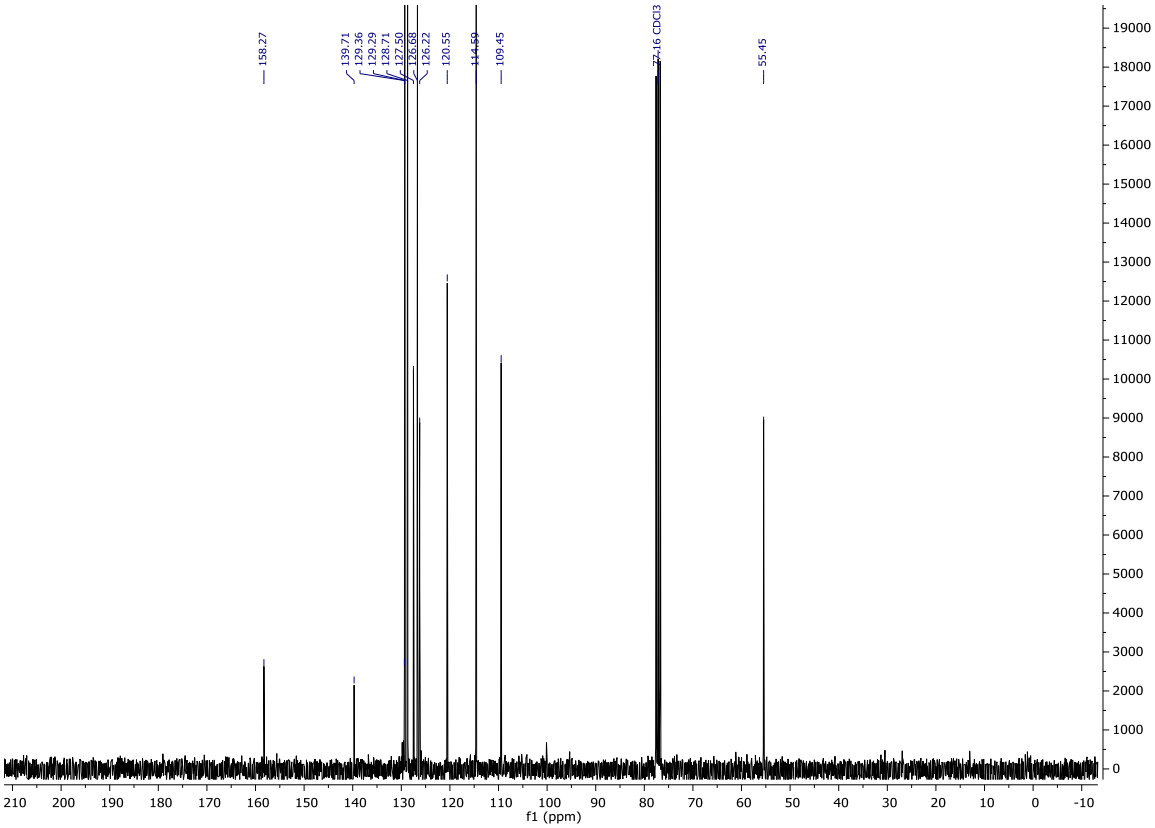

^{1}H NMR (300 MHz, $CDCl_3$) **162**

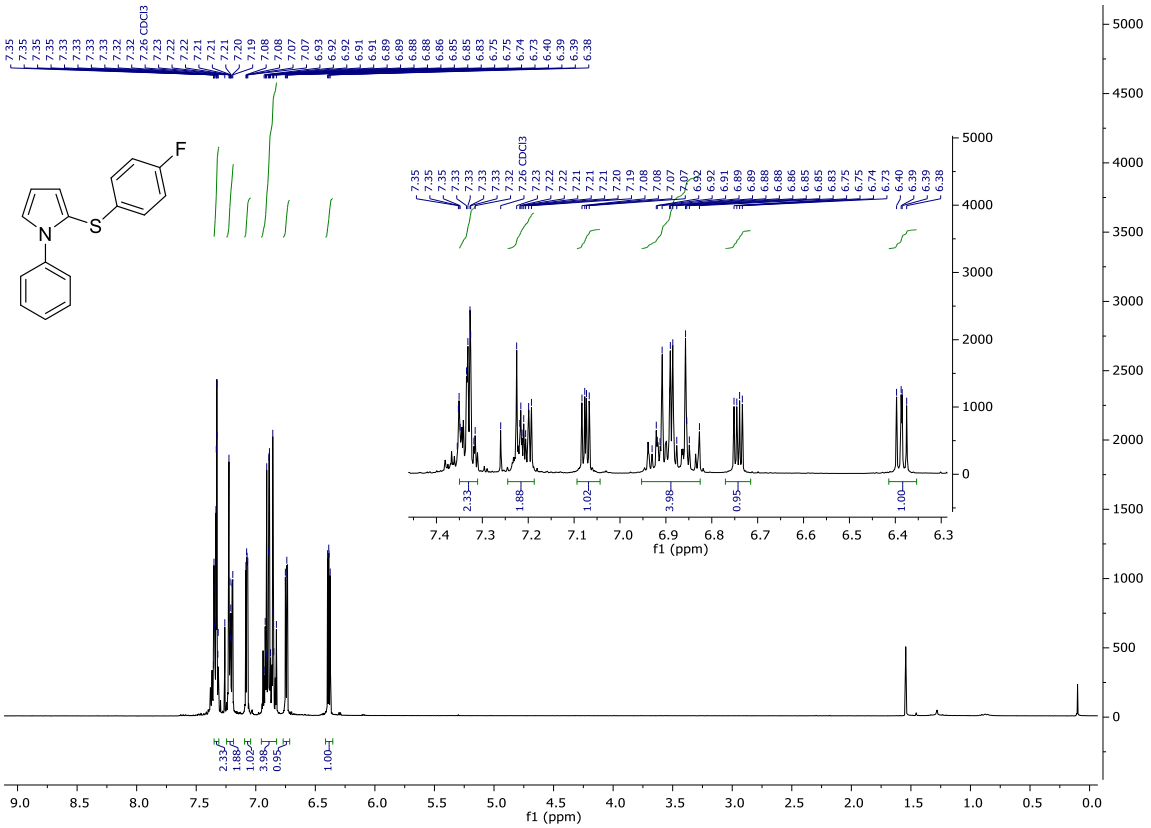

^{13}C NMR (126 MHz, $CDCl_3$) **162**

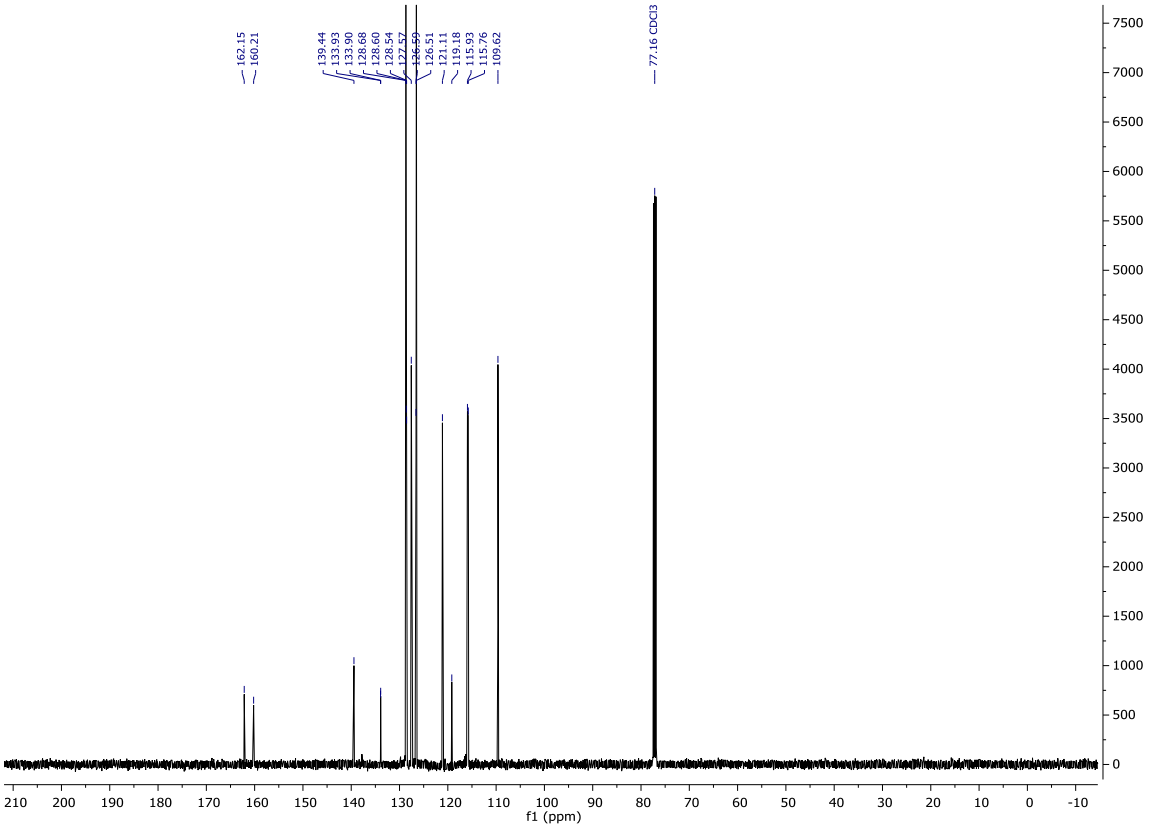

^{19}F NMR (282 MHz, $CDCl_3$) **19**

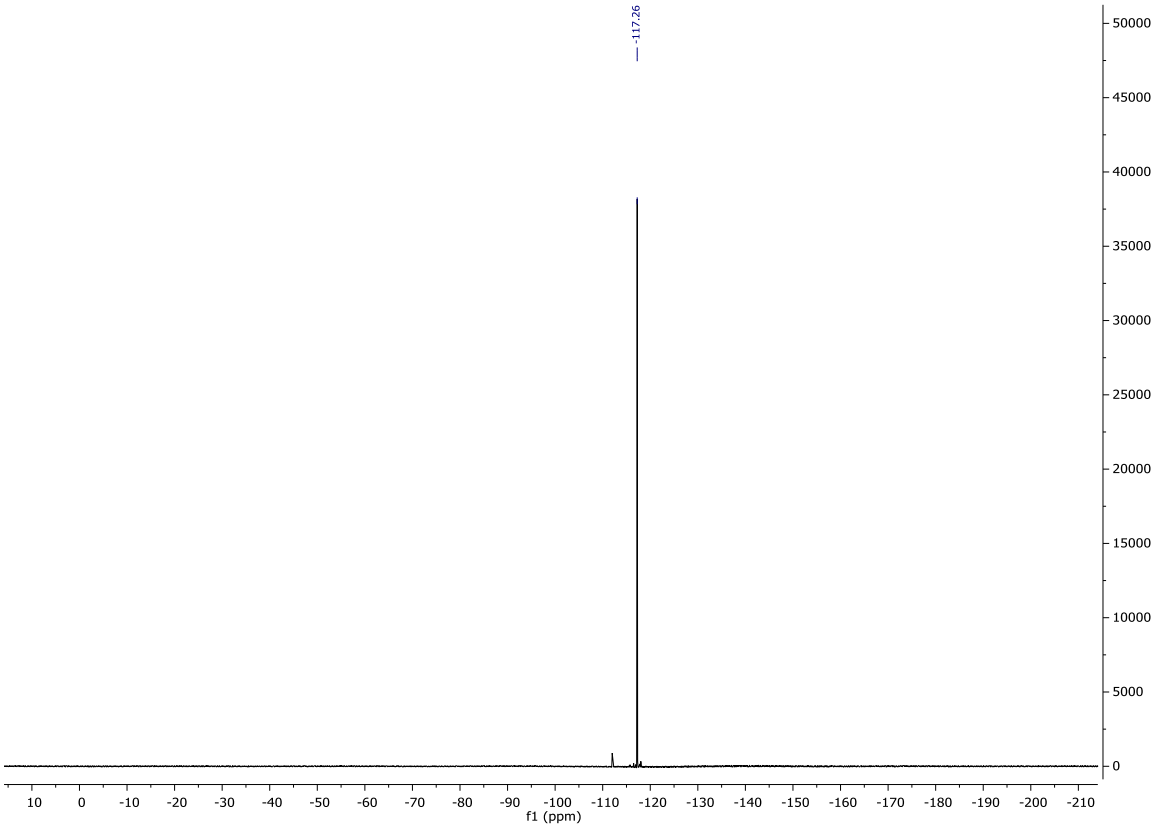

^{1}H NMR (300 MHz, $CDCl_3$) **163**

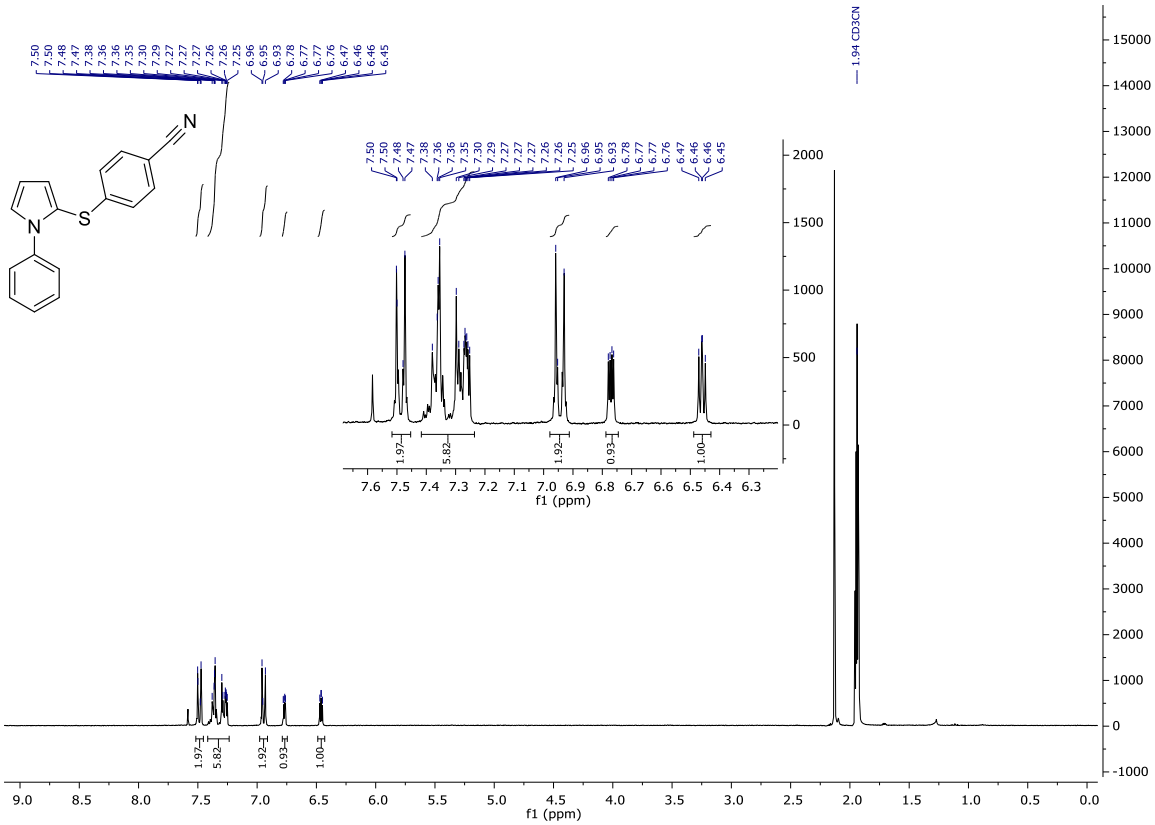

^{13}C NMR (126 MHz, $CDCl_3$) **163**

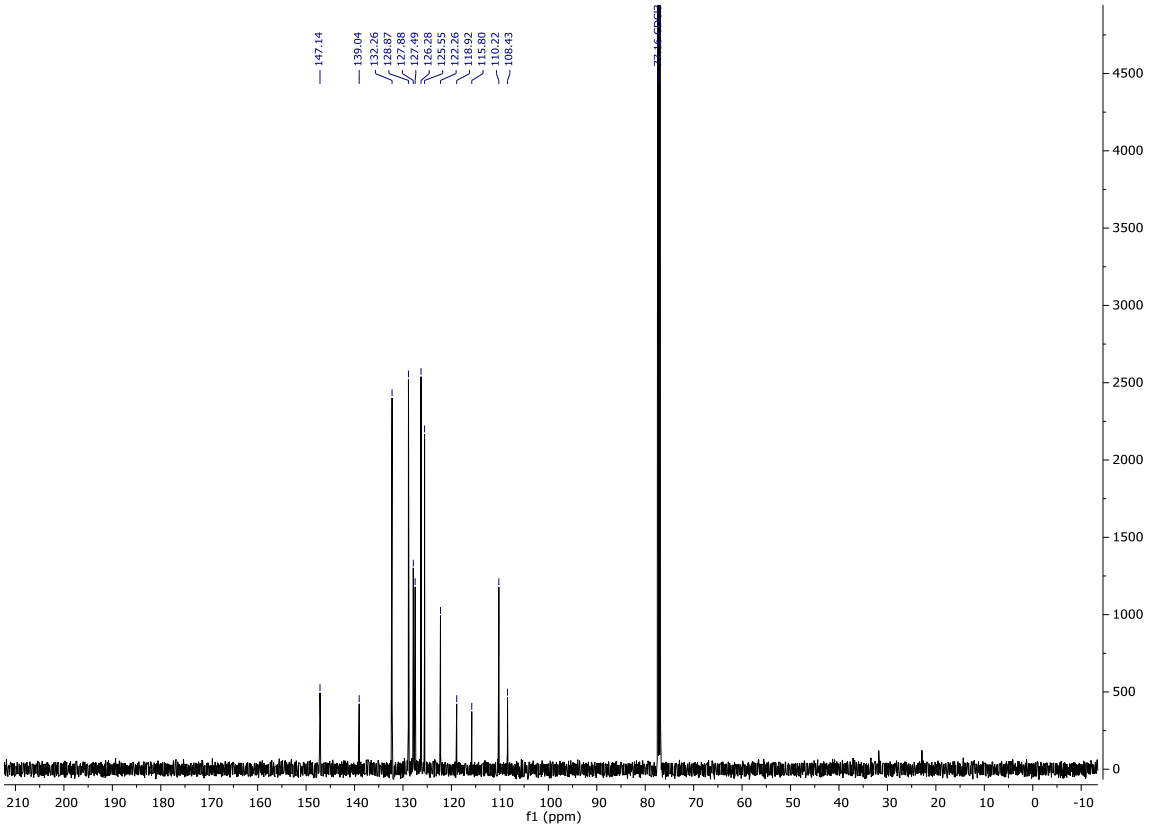

^{1}H NMR (600 MHz, $CDCl_3$) **164**

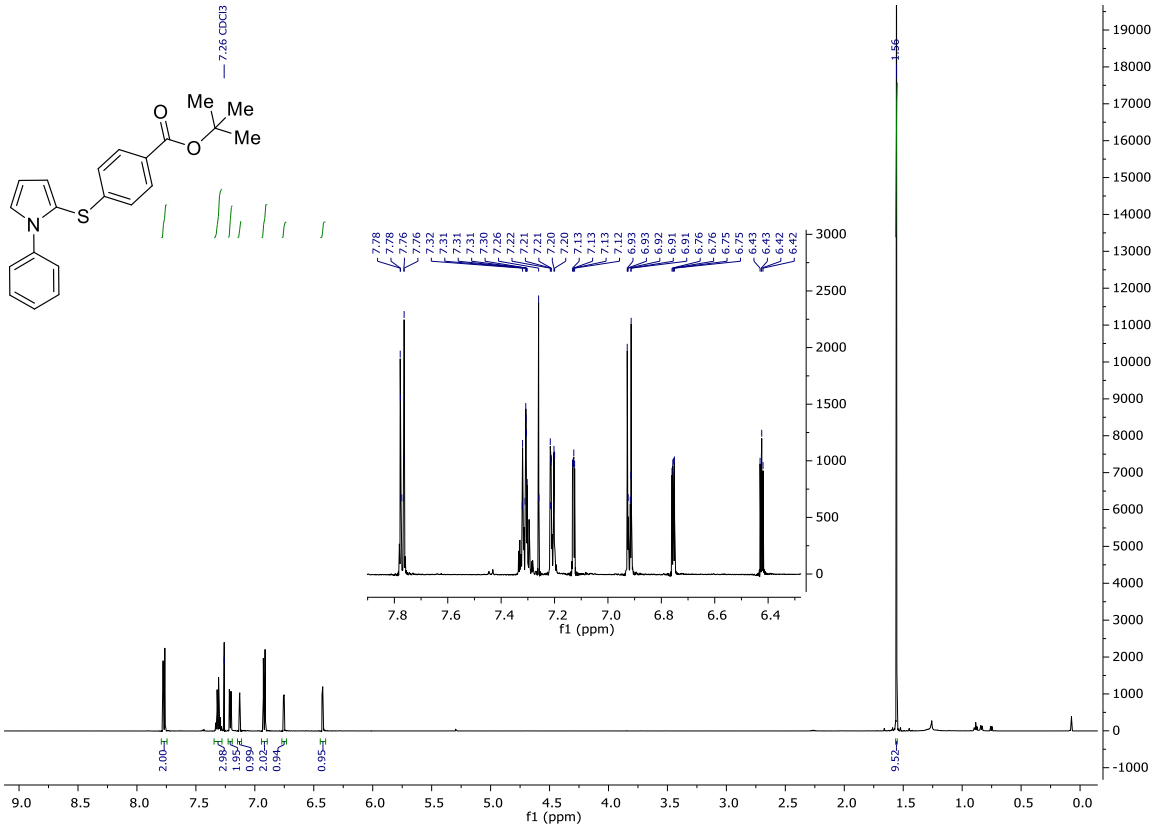

^{13}C NMR (126 MHz, $CDCl_3$) **164**

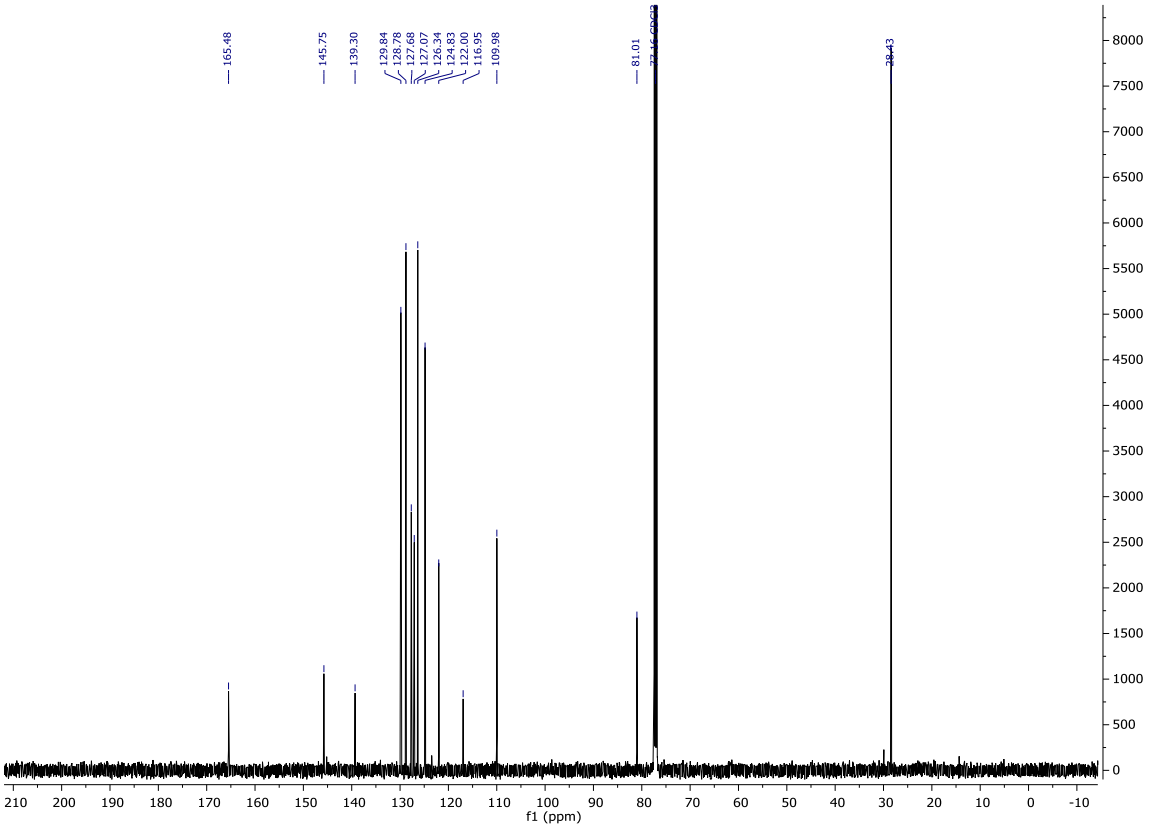

^{1}H NMR (400 MHz, $CDCl_3$) **165**

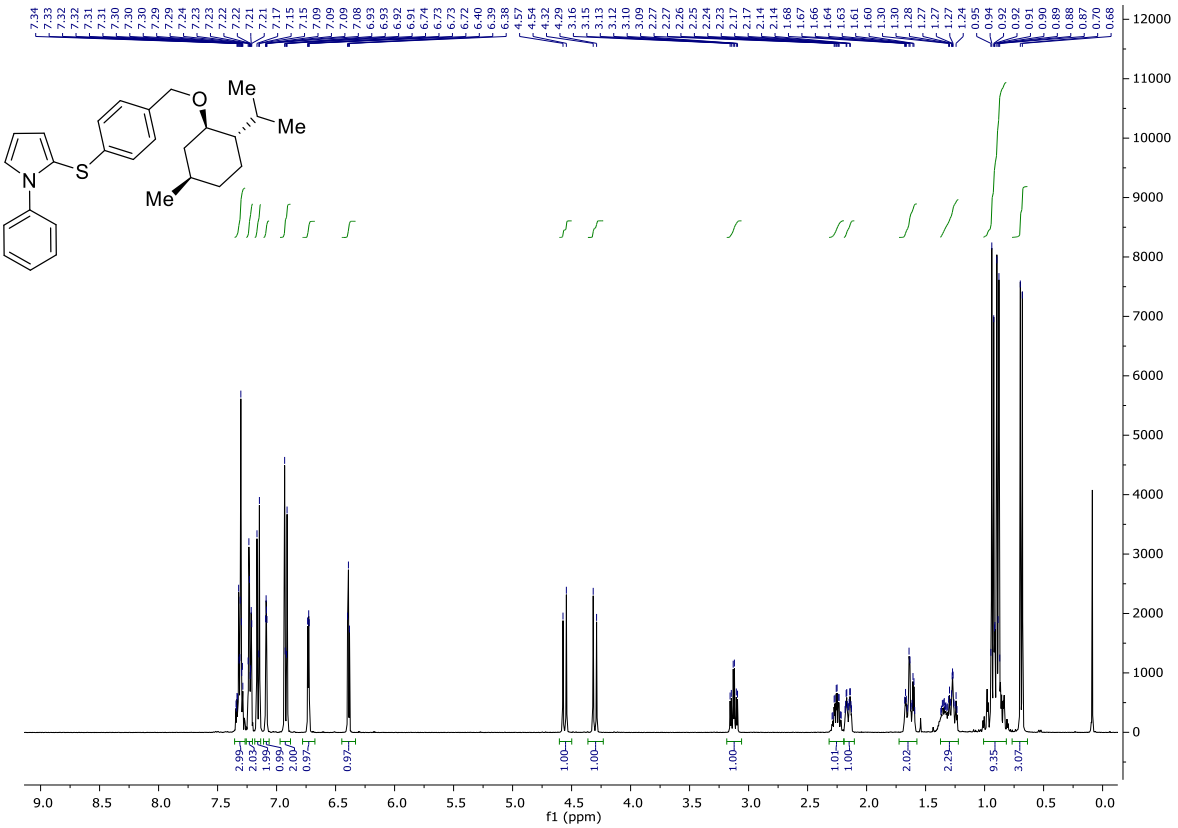

^{13}C NMR (101 MHz, $CDCl_3$) **165**

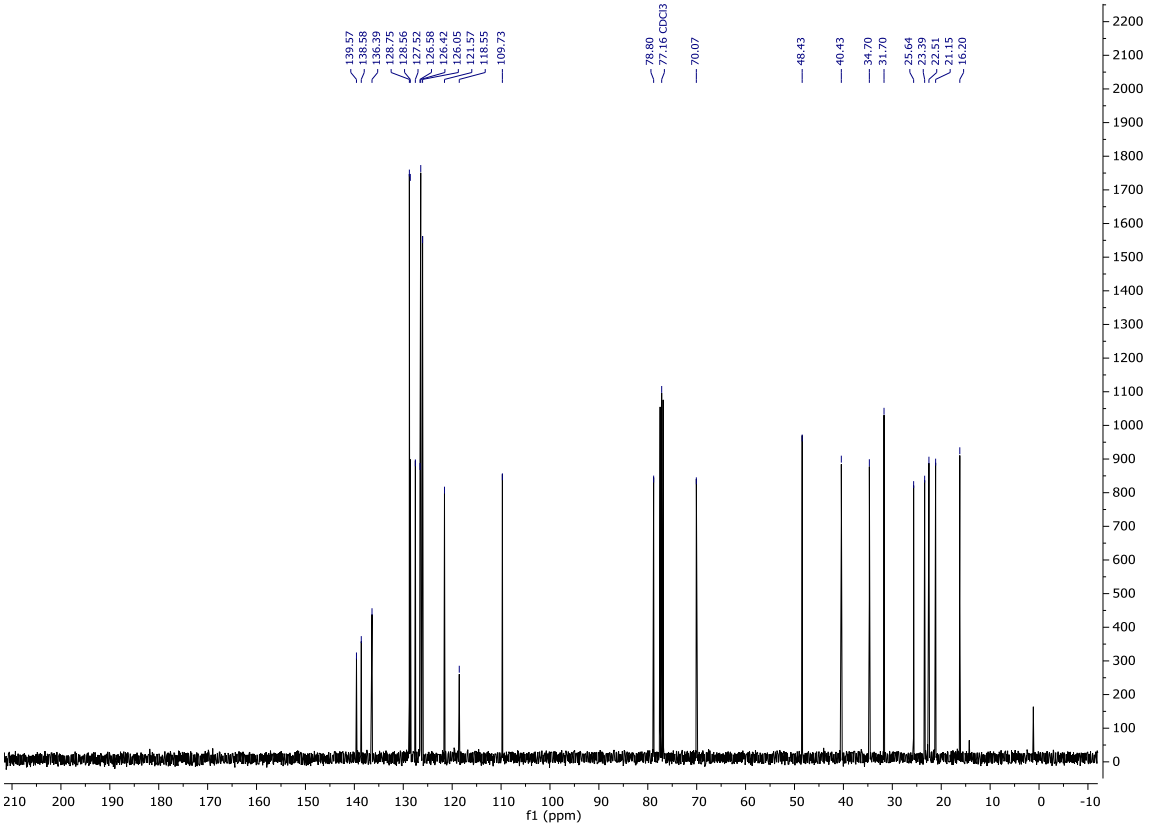

^{1}H NMR (600 MHz, CD_2Cl_2) **167**

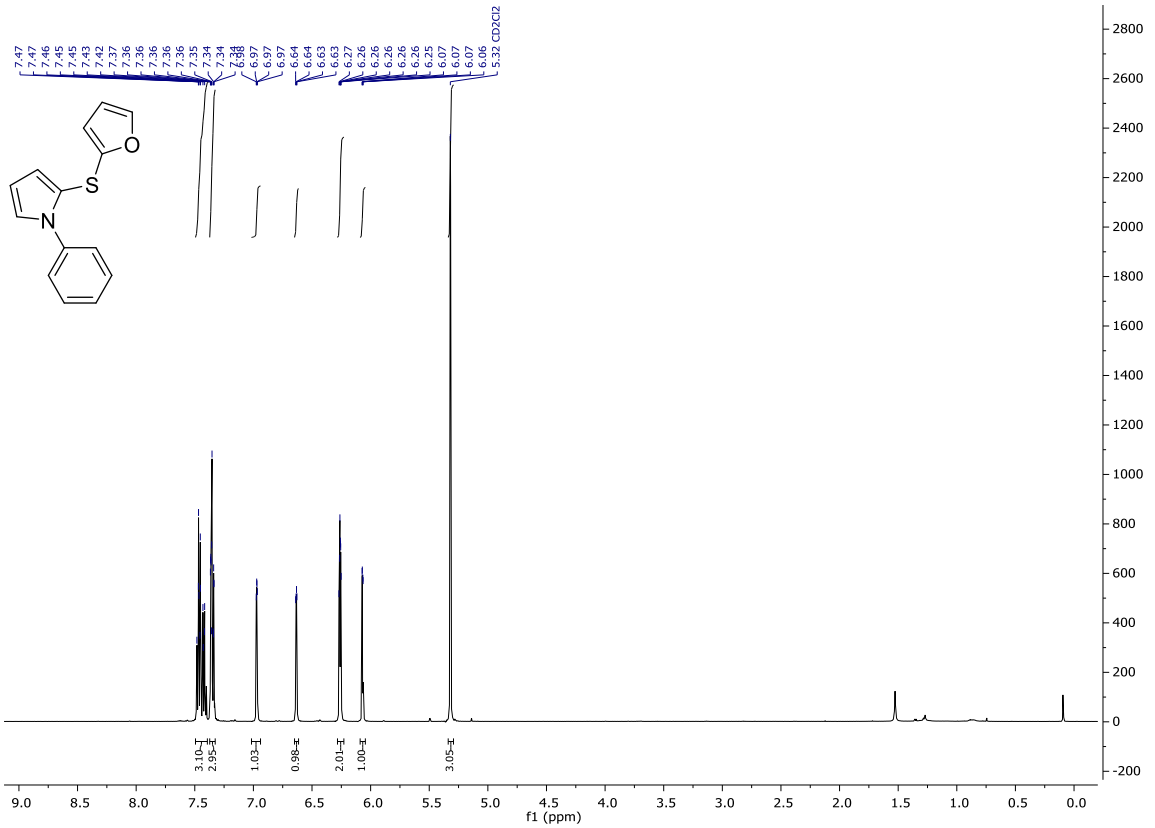

^{13}C NMR (126 MHz, CD_2Cl_2) **167**

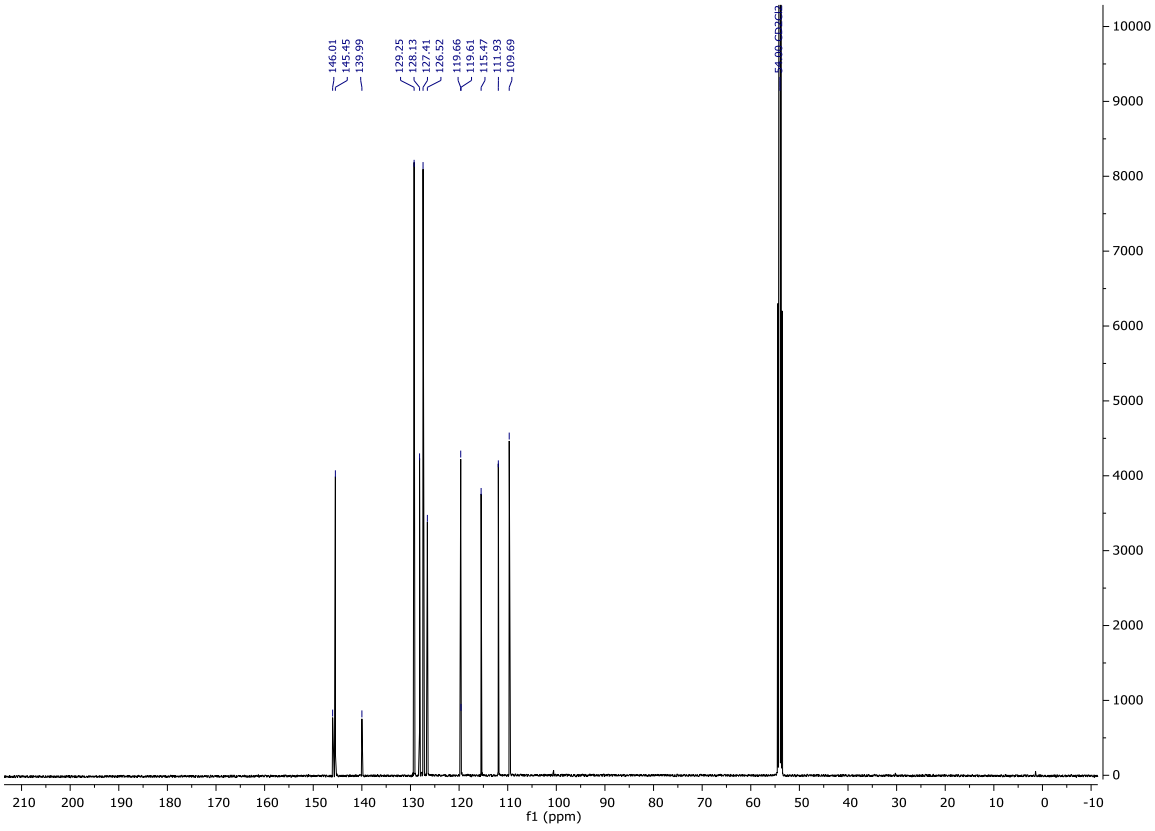

^{1}H NMR (300 MHz, $CDCl_3$) **169**

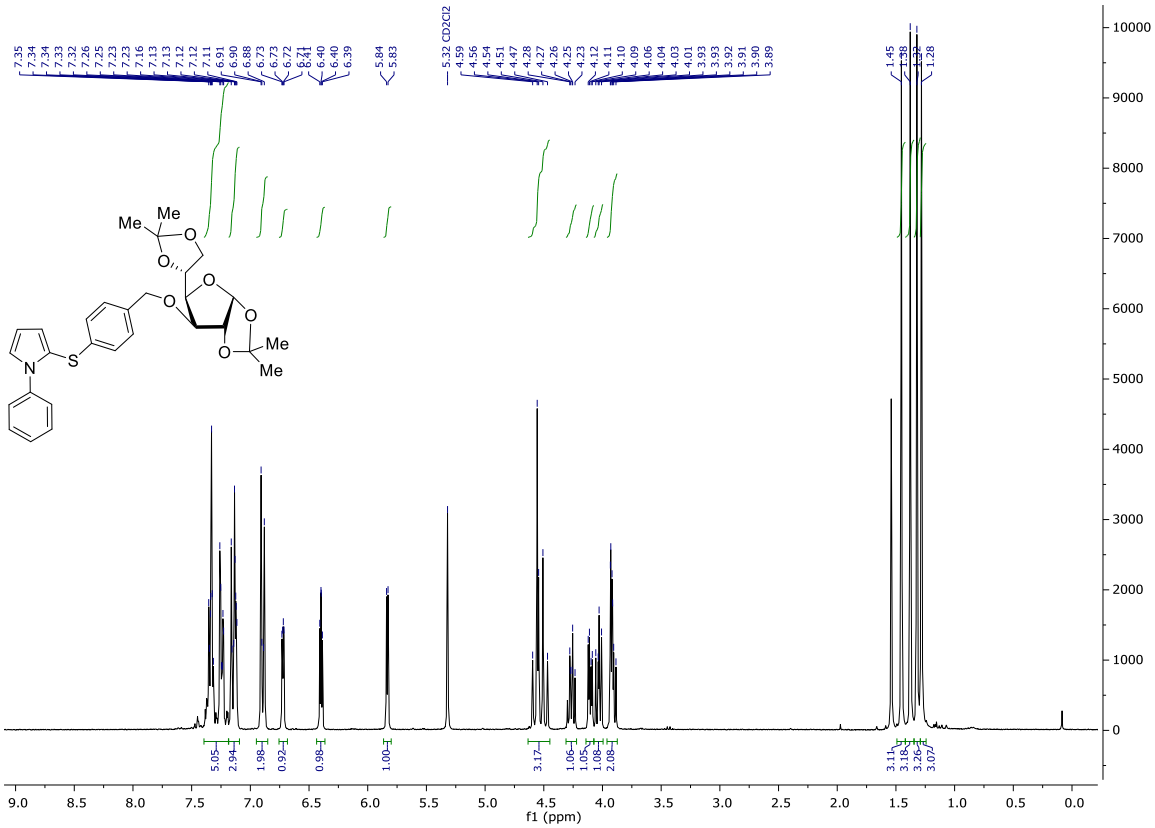

^{13}C NMR (126 MHz, $CDCl_3$) **169**

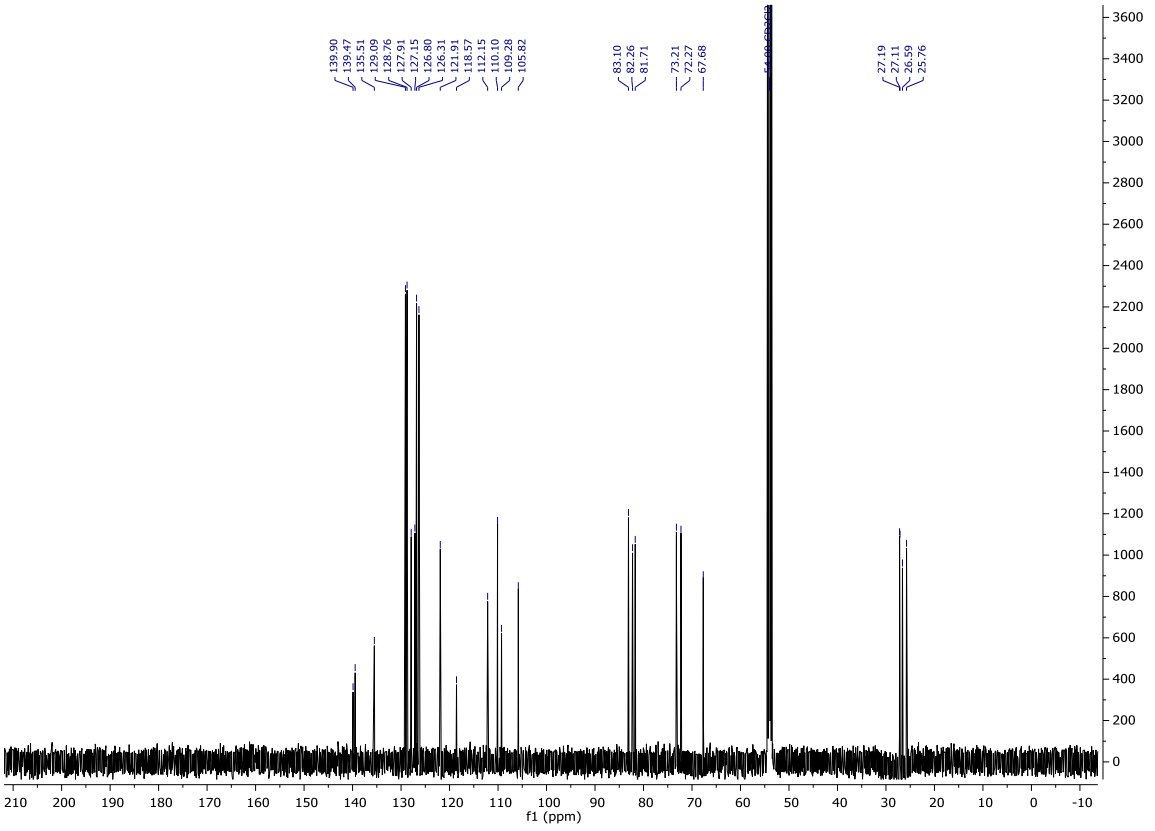

^{1}H NMR (600 MHz, $CDCl_3$) **166**

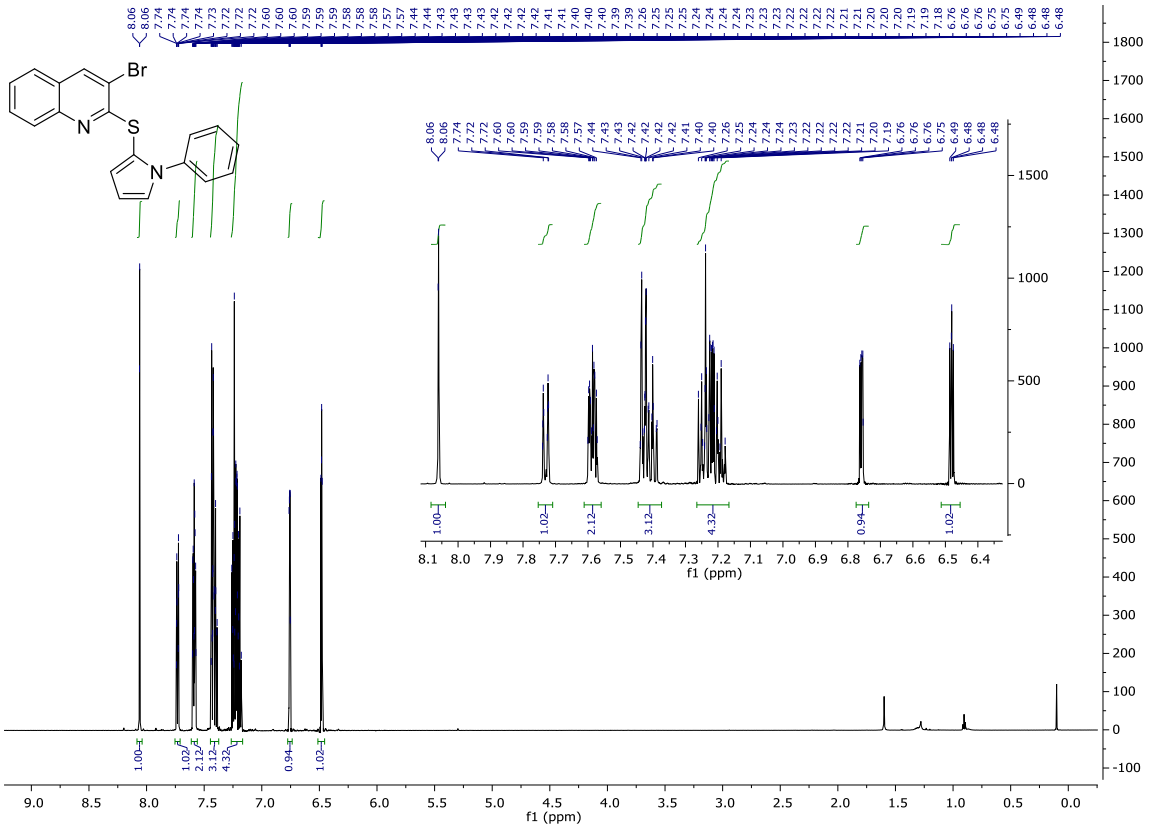

^{13}C NMR (126 MHz, $CDCl_3$) **166**

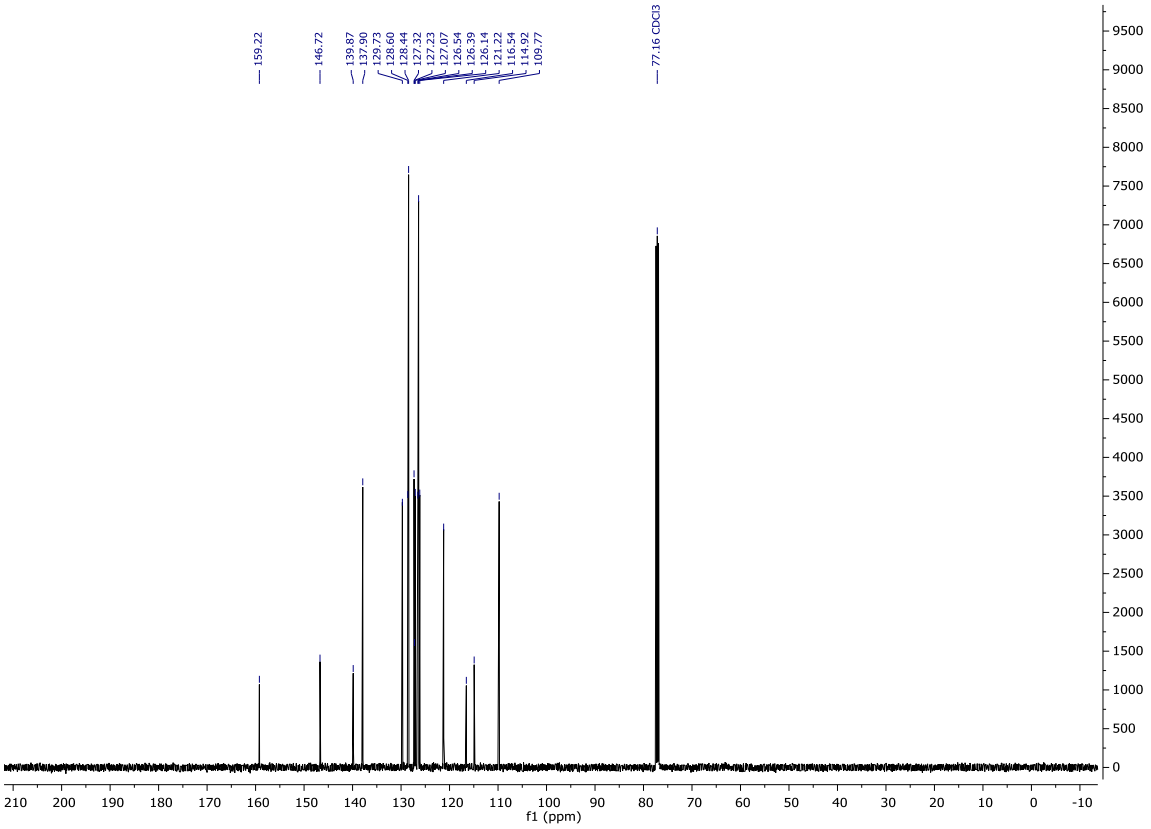

^{1}H NMR (600 MHz, $CDCl_3$) **168**

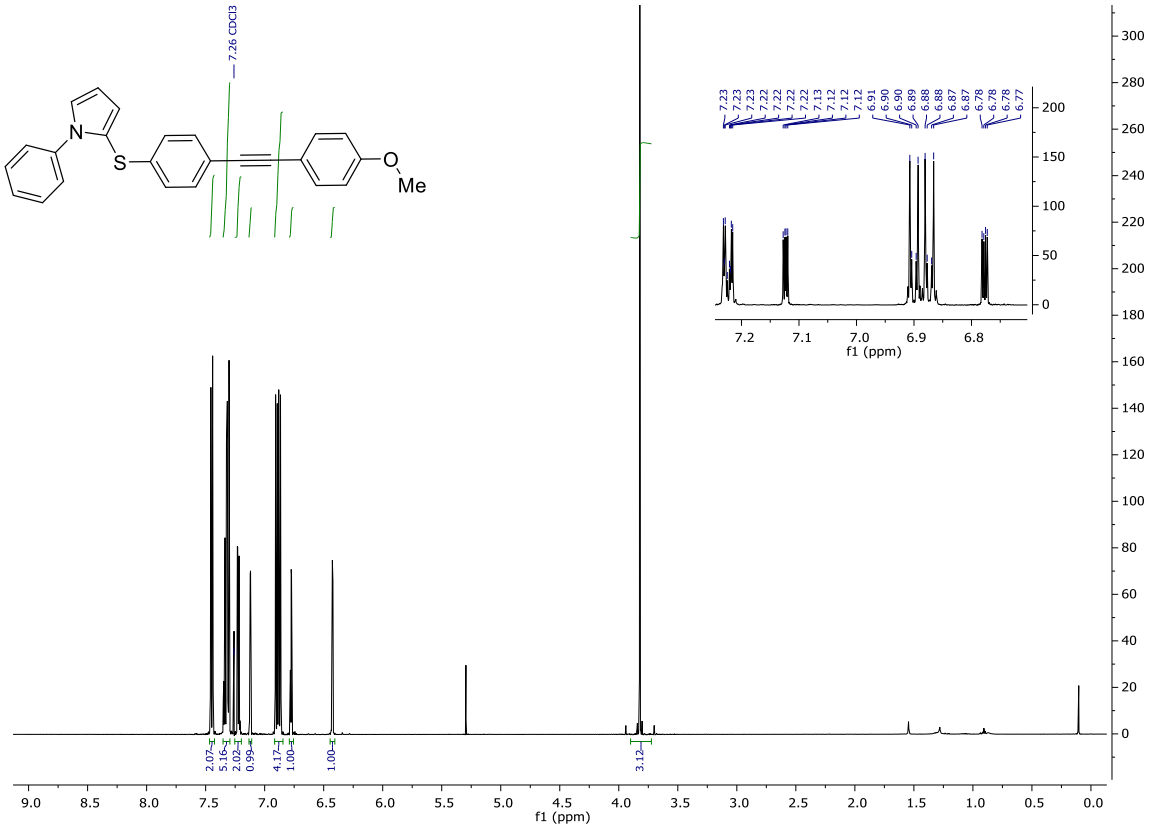

^{13}C NMR (126 MHz, $CDCl_3$) **168**

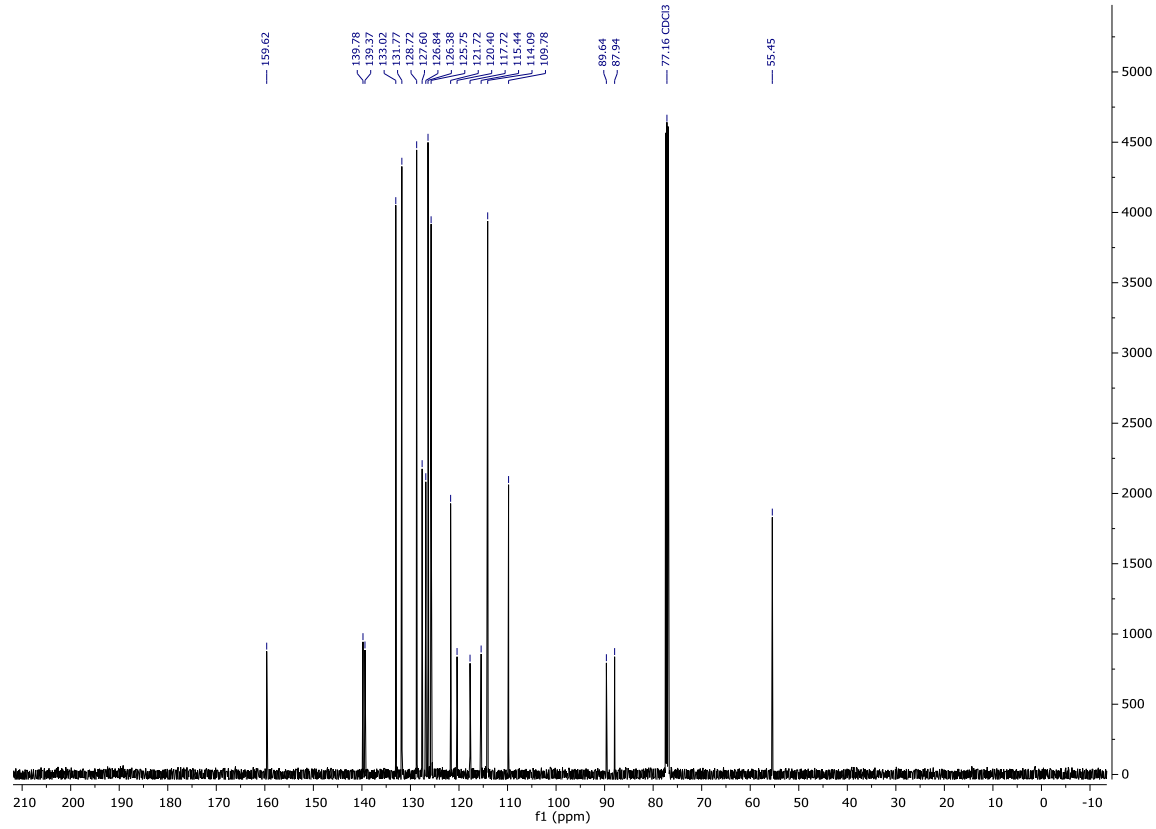

^{1}H NMR (300 MHz, CD_3CN) **170**

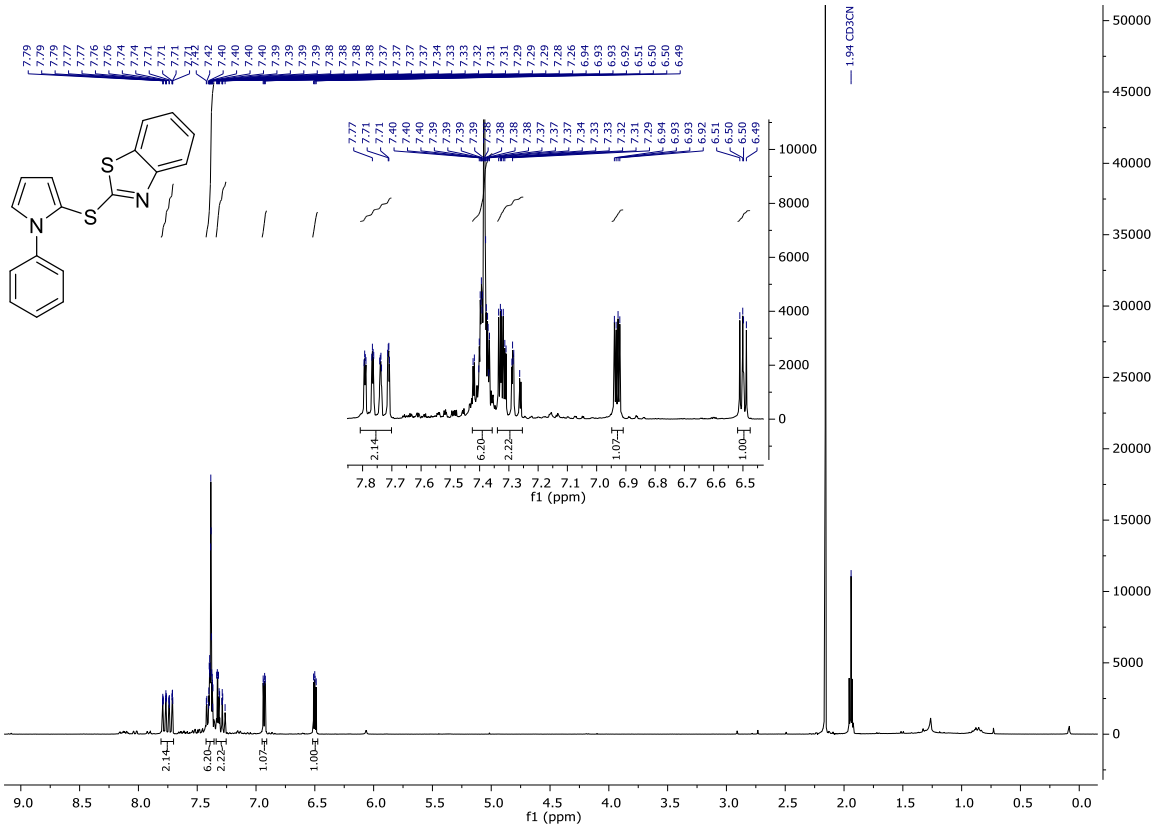

^{13}C NMR (126 MHz, CD_3CN) **170**

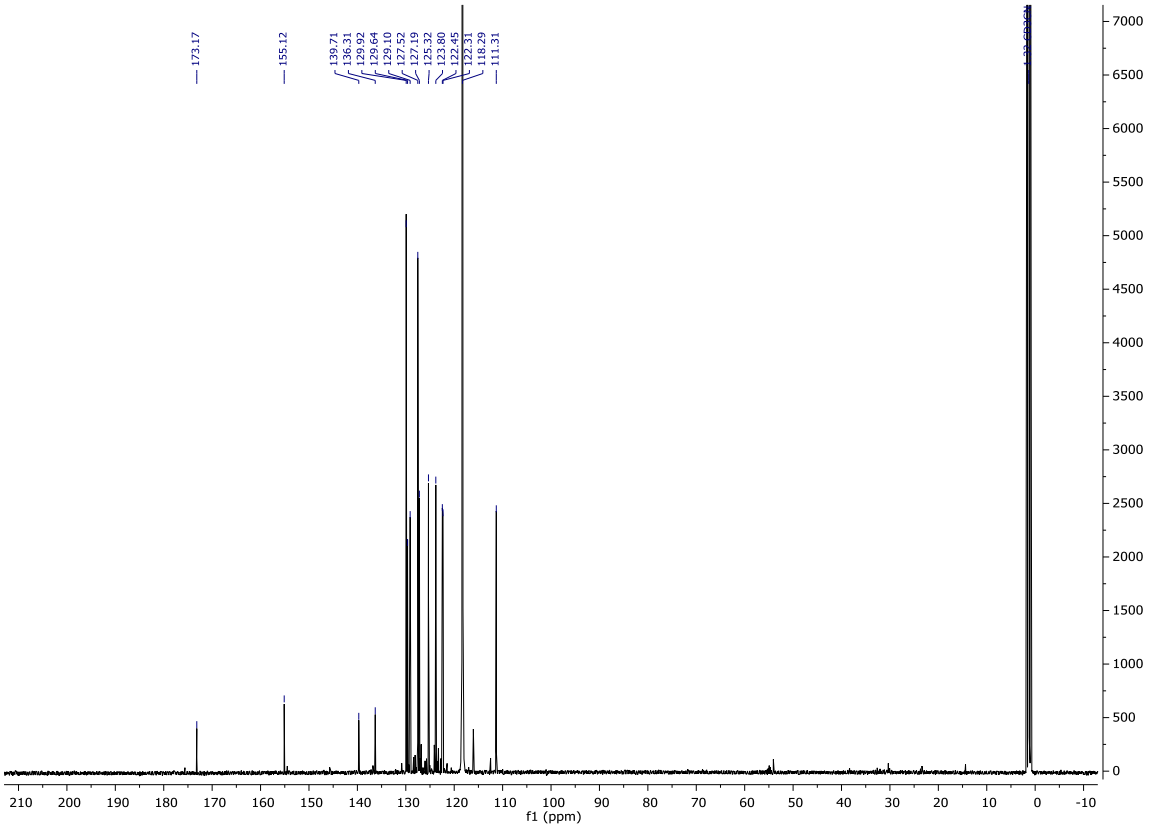

^{1}H NMR (300 MHz, $CDCl_3$) **172**

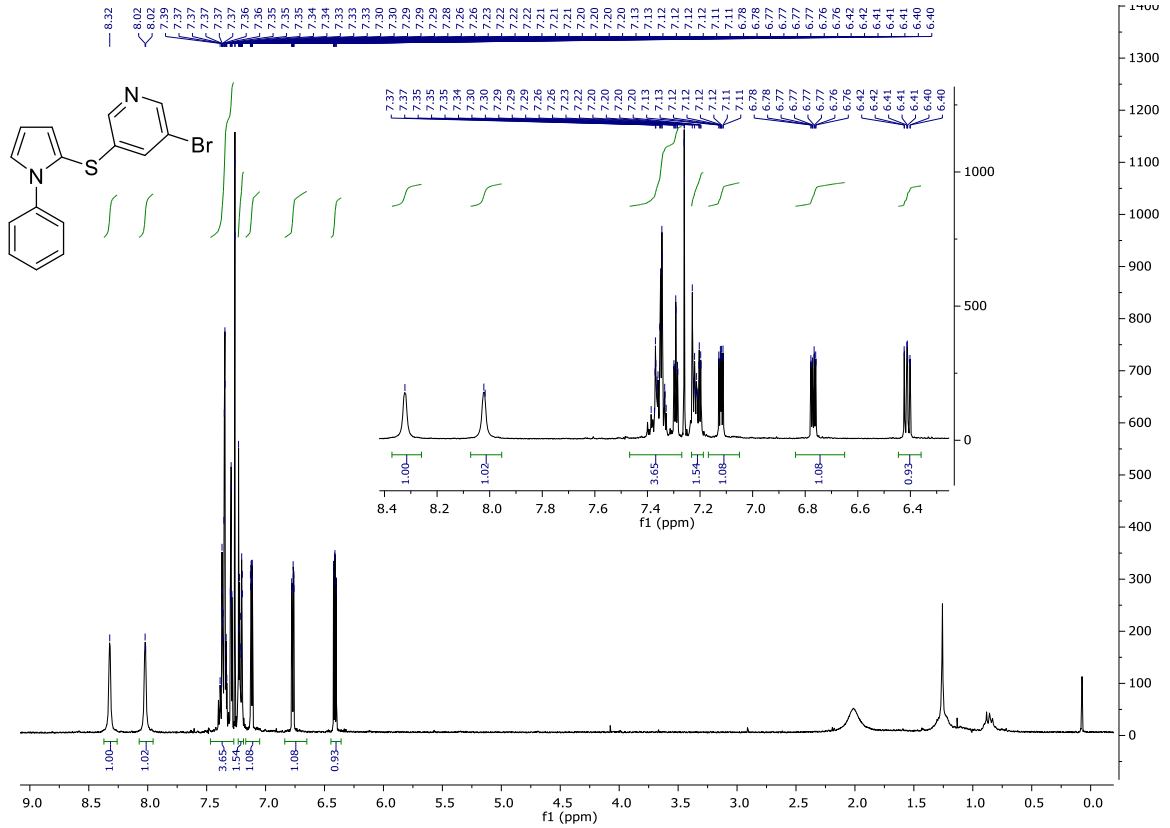

^{13}C NMR (126 MHz, $CDCl_3$) **172**

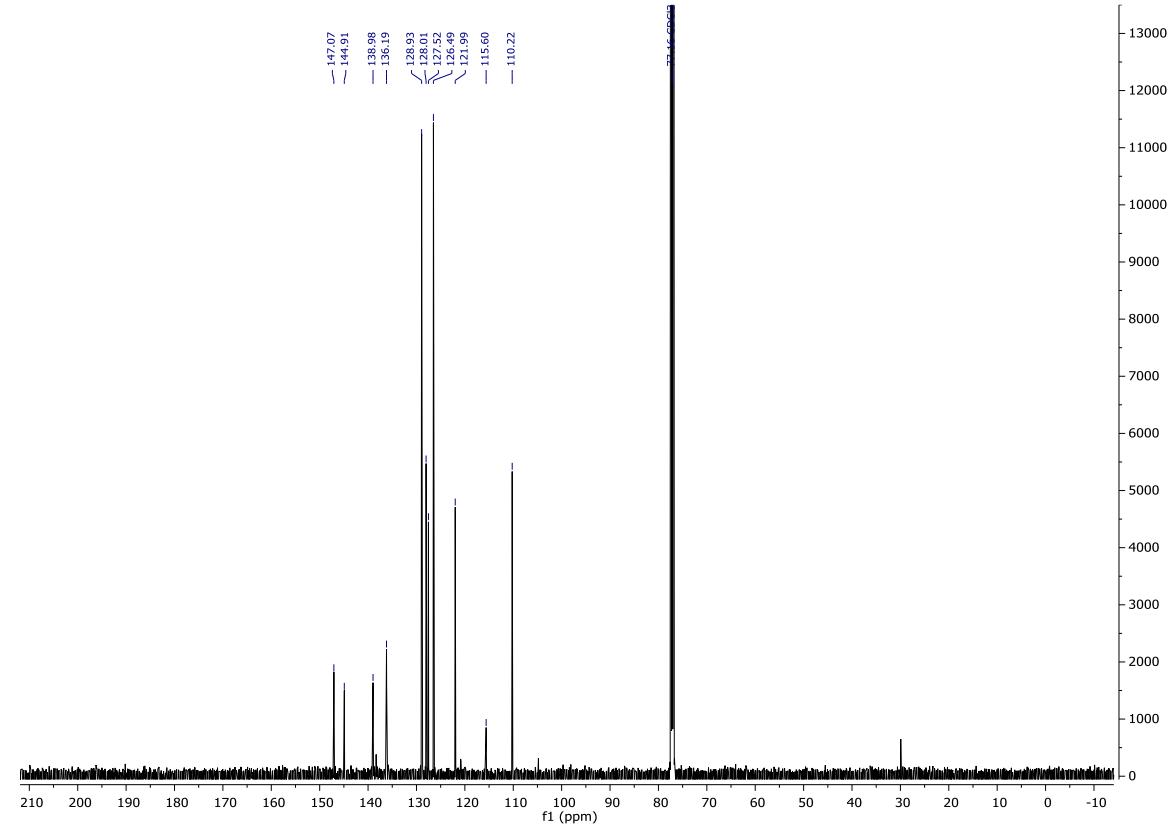

^{1}H NMR (300 MHz, $CDCl_3$) **171**

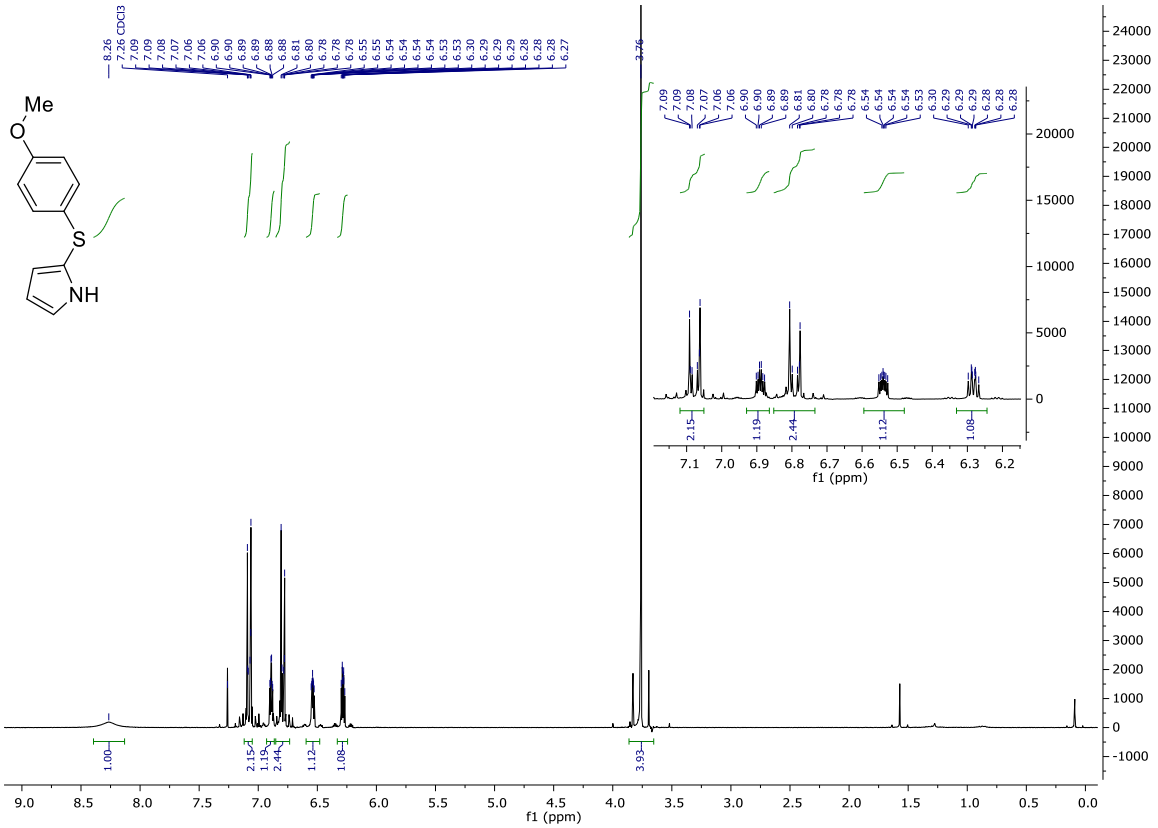

^{13}C NMR (75 MHz, $CDCl_3$) **171**

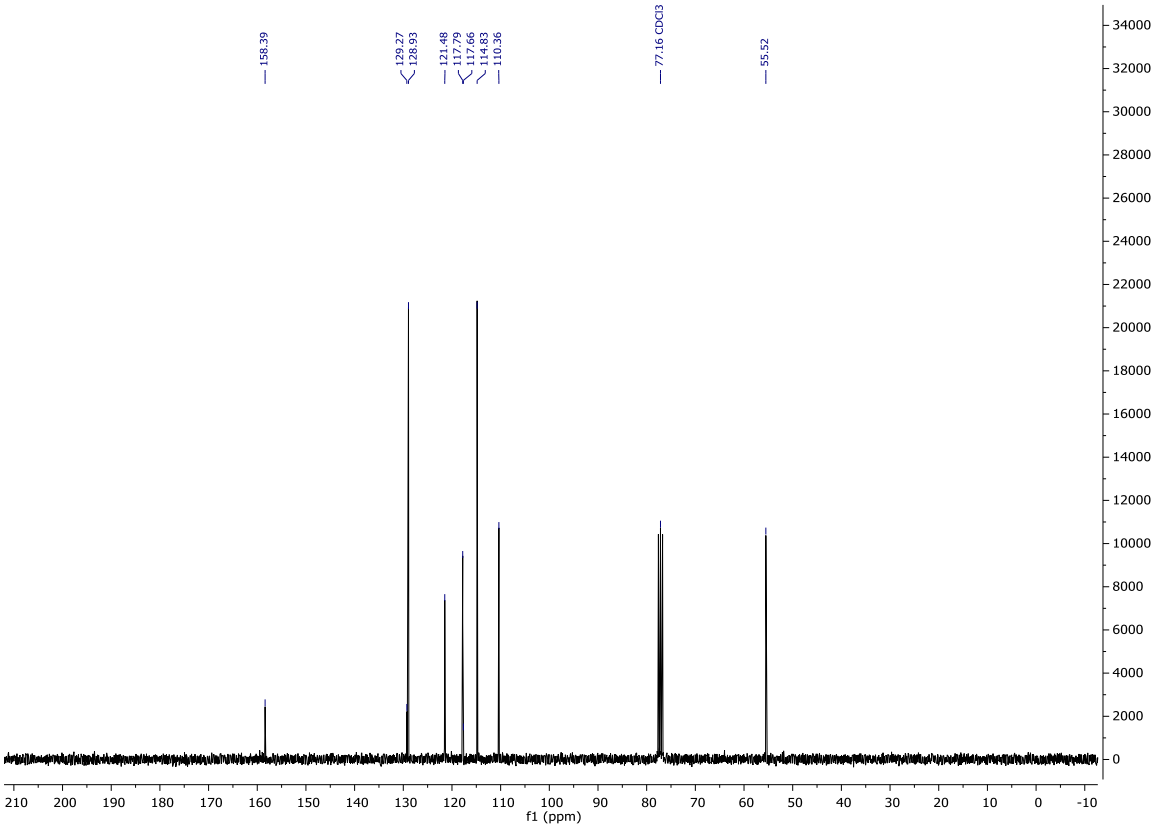

^{1}H NMR (400 MHz, $CDCl_3$) **157**

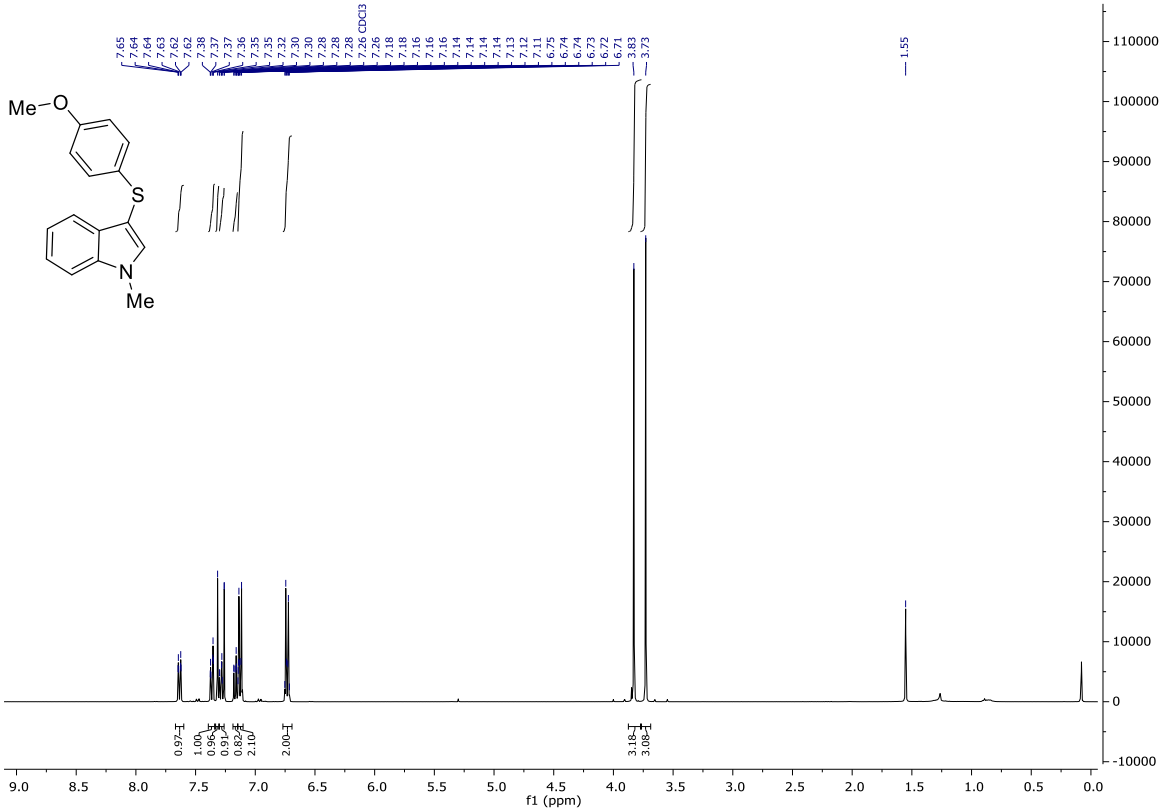

^{13}C NMR (126 MHz, $CDCl_3$) **157**

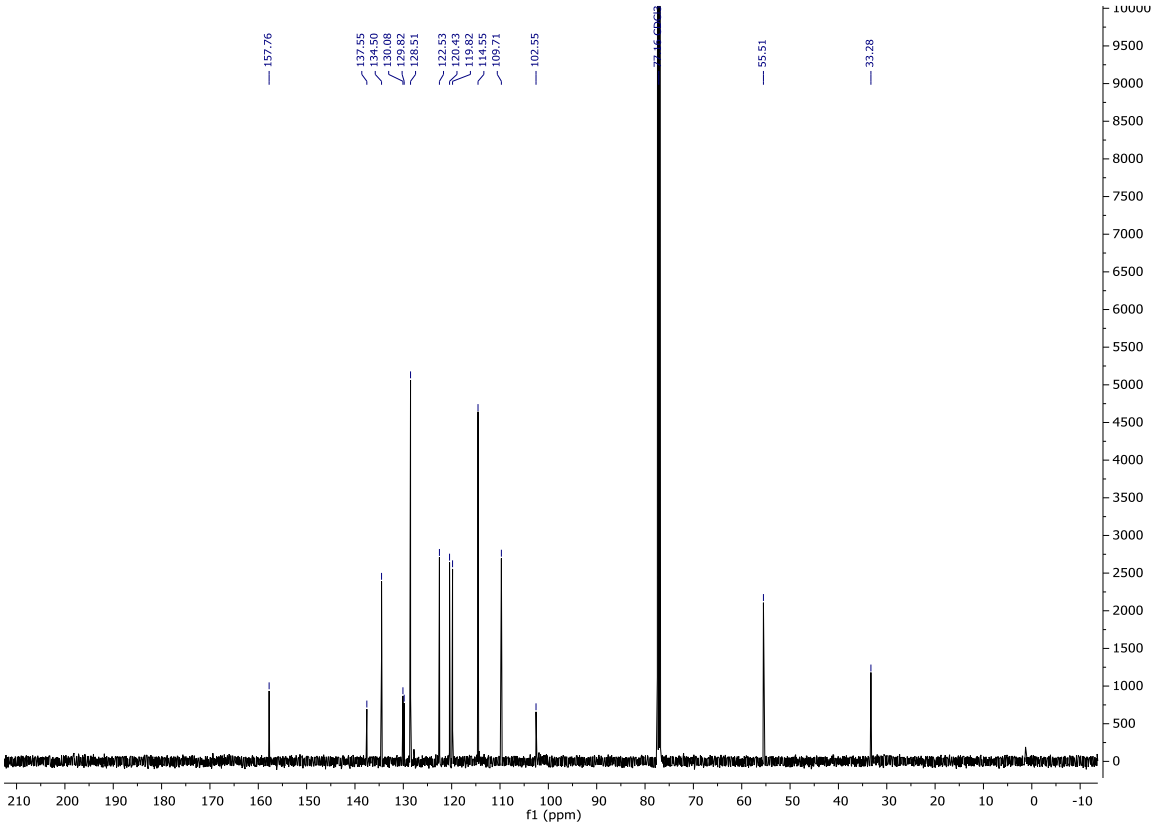

^{1}H NMR (600 MHz, CD_3CN) **175**

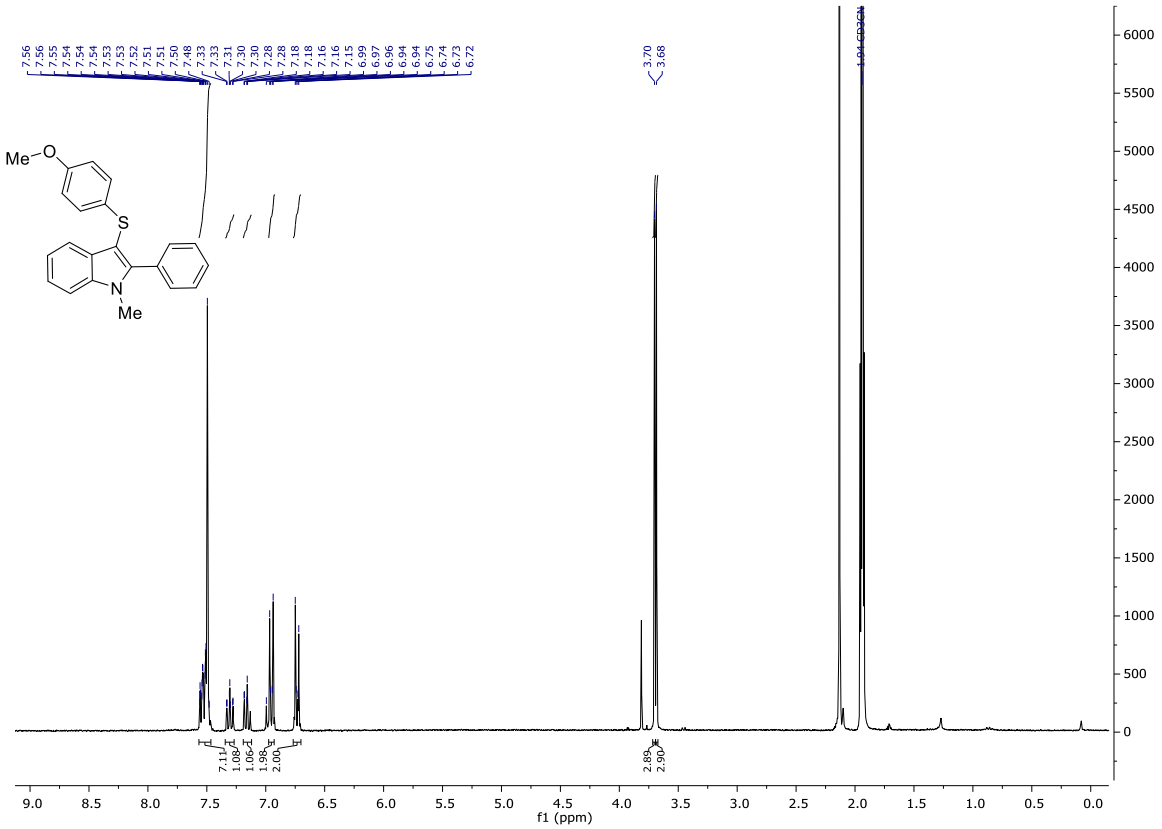

^{13}C NMR (126 MHz, $CDCl_3$) **175**

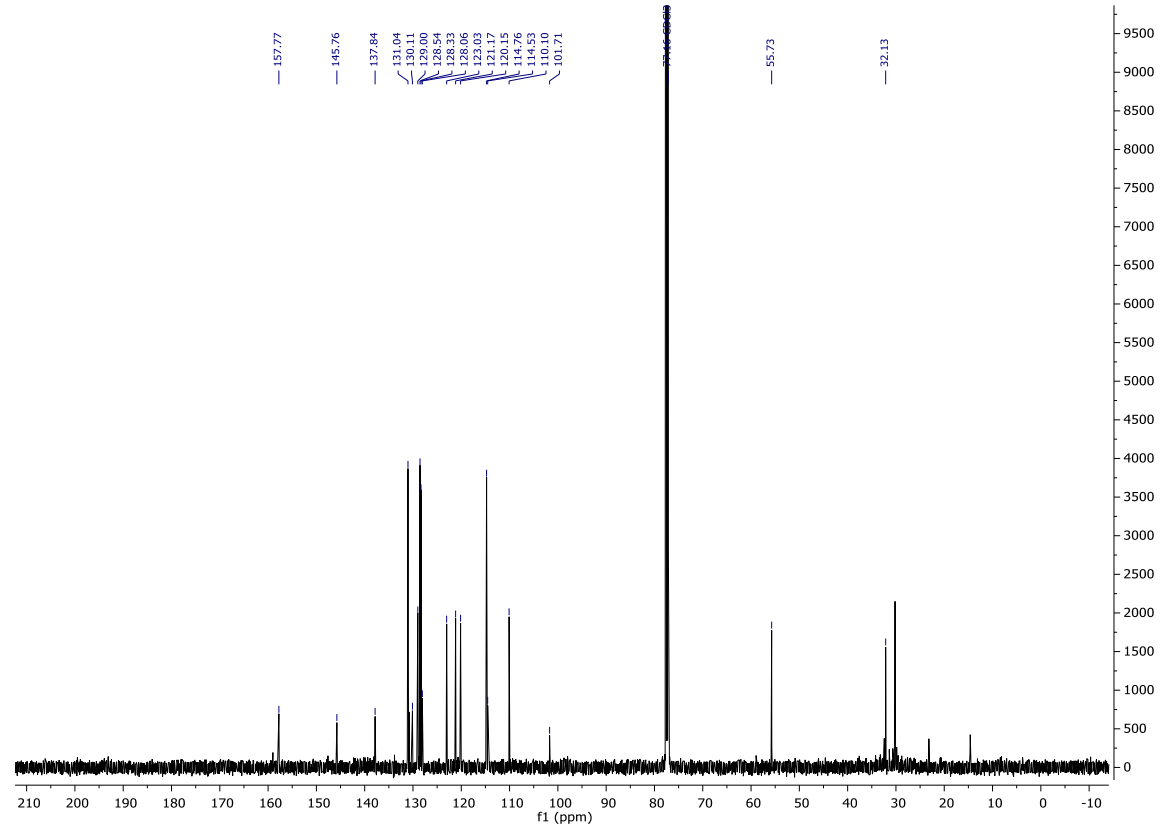

^{1}H NMR (400 MHz, CD_2Cl_2) **87**

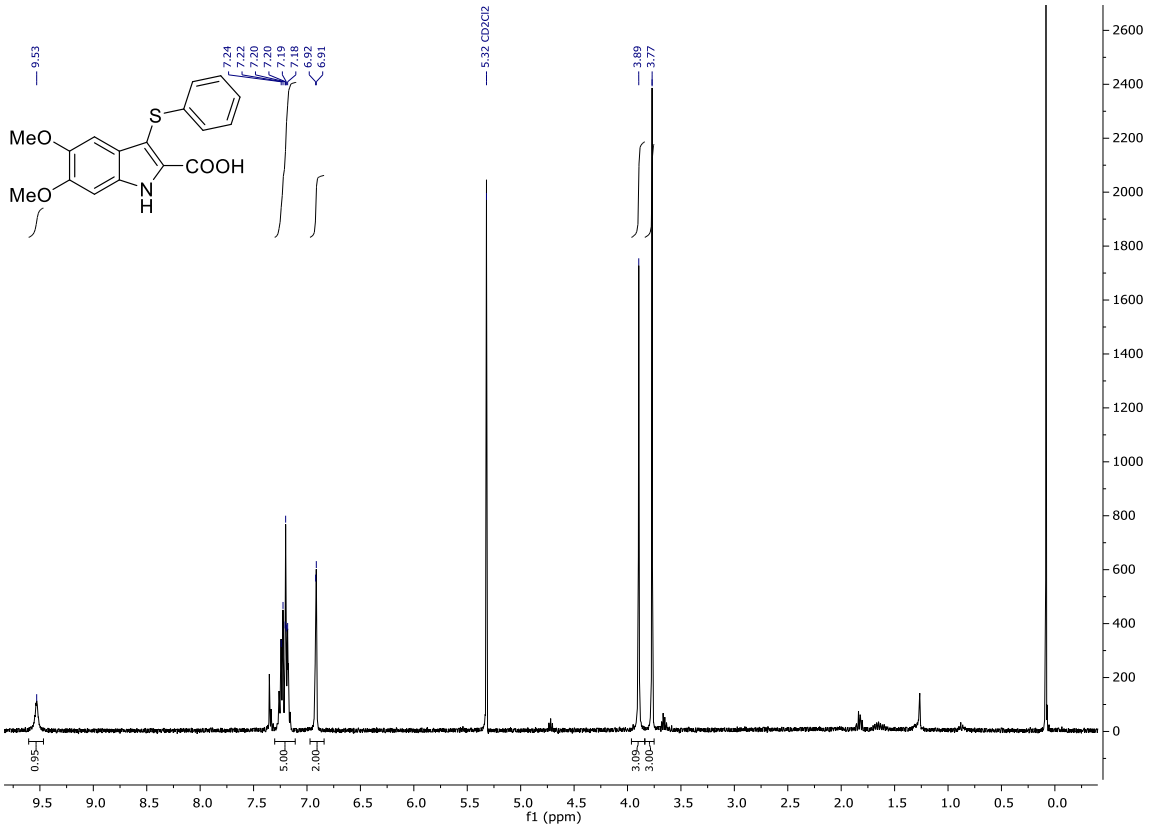

^{13}C NMR (126 MHz, CD_2Cl_2) **87**

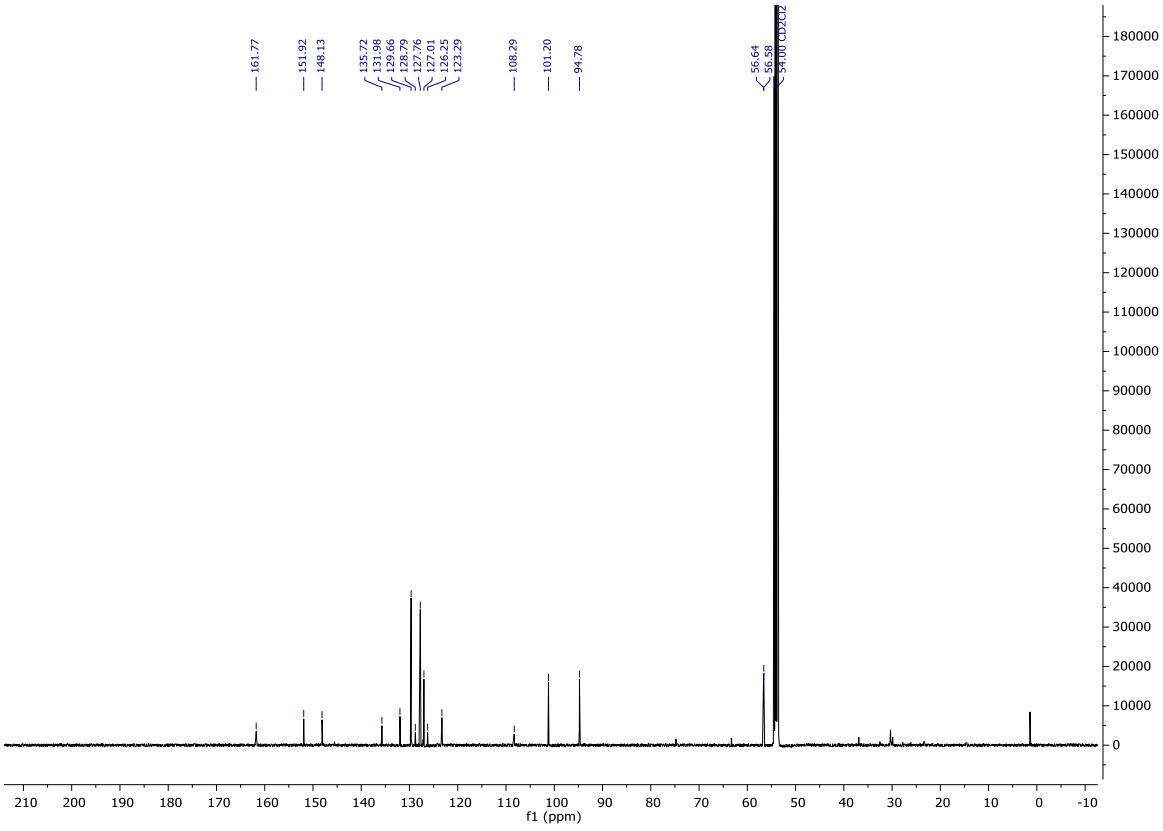

^{1}H NMR (300 MHz, CD_2Cl_2) **176**

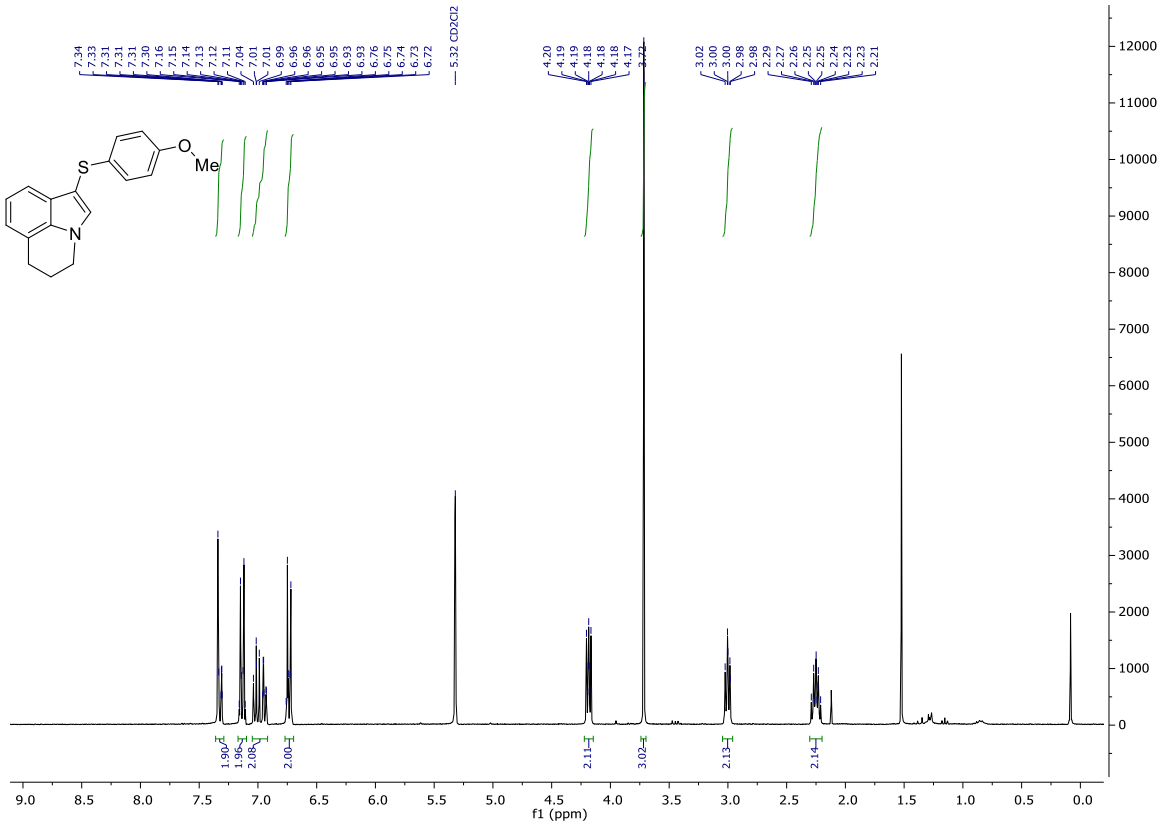

^{13}C NMR (126 MHz, CD_2Cl_2) **176**

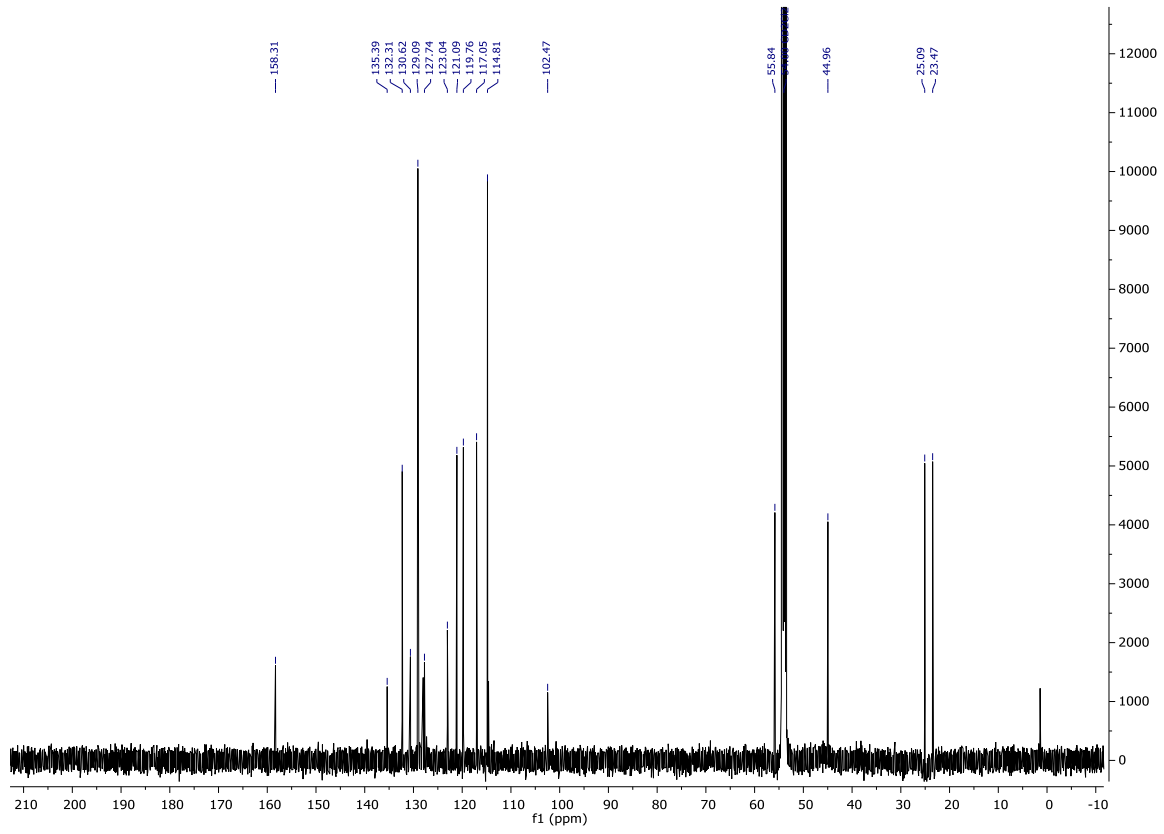

^{1}H NMR (400 MHz, $CDCl_3$) **186**

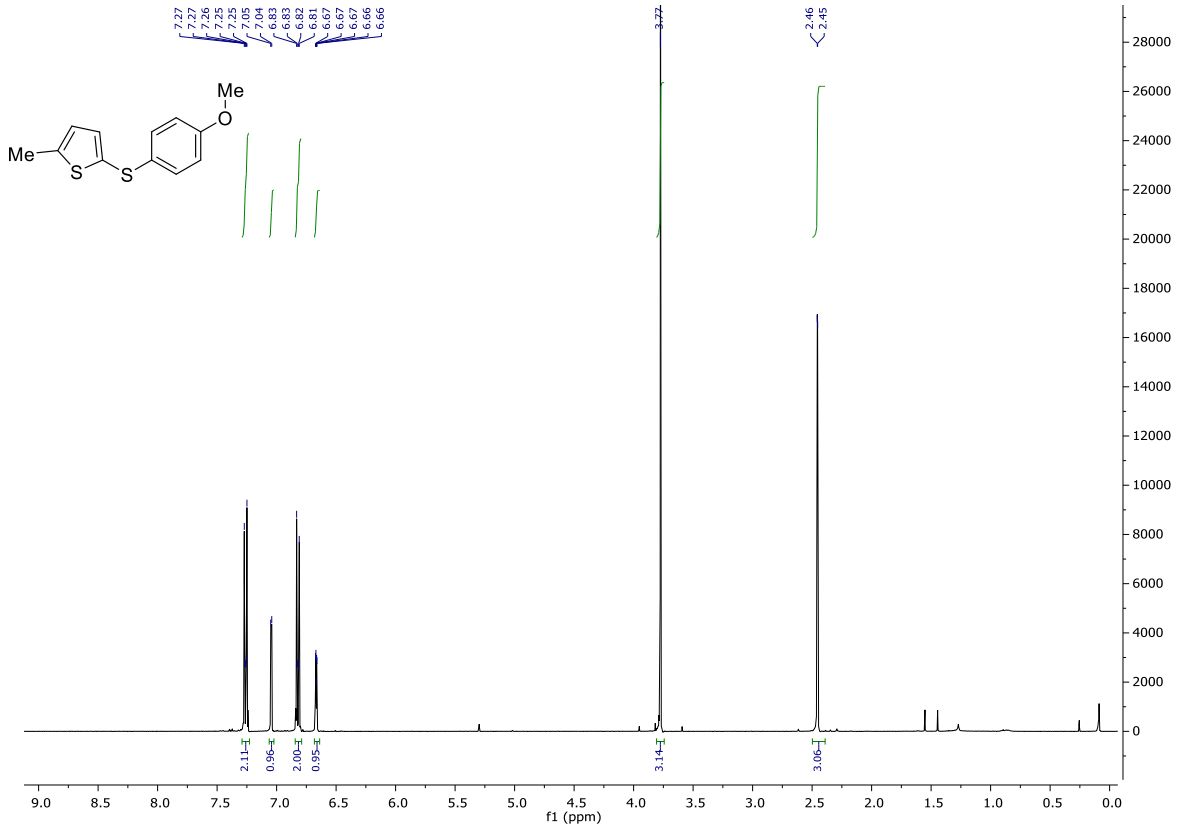

^{13}C NMR (126 MHz, $CDCl_3$) **186**

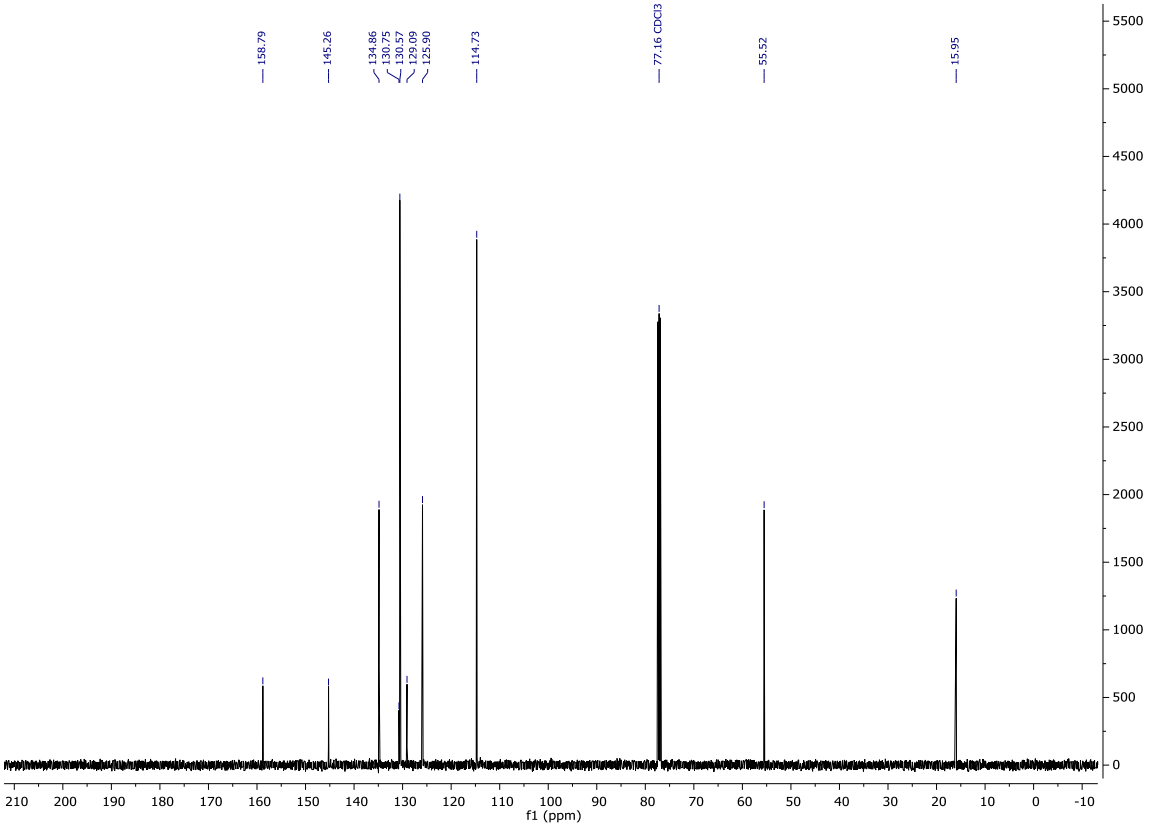

^{1}H NMR (300 MHz, $CDCl_3$) **190**

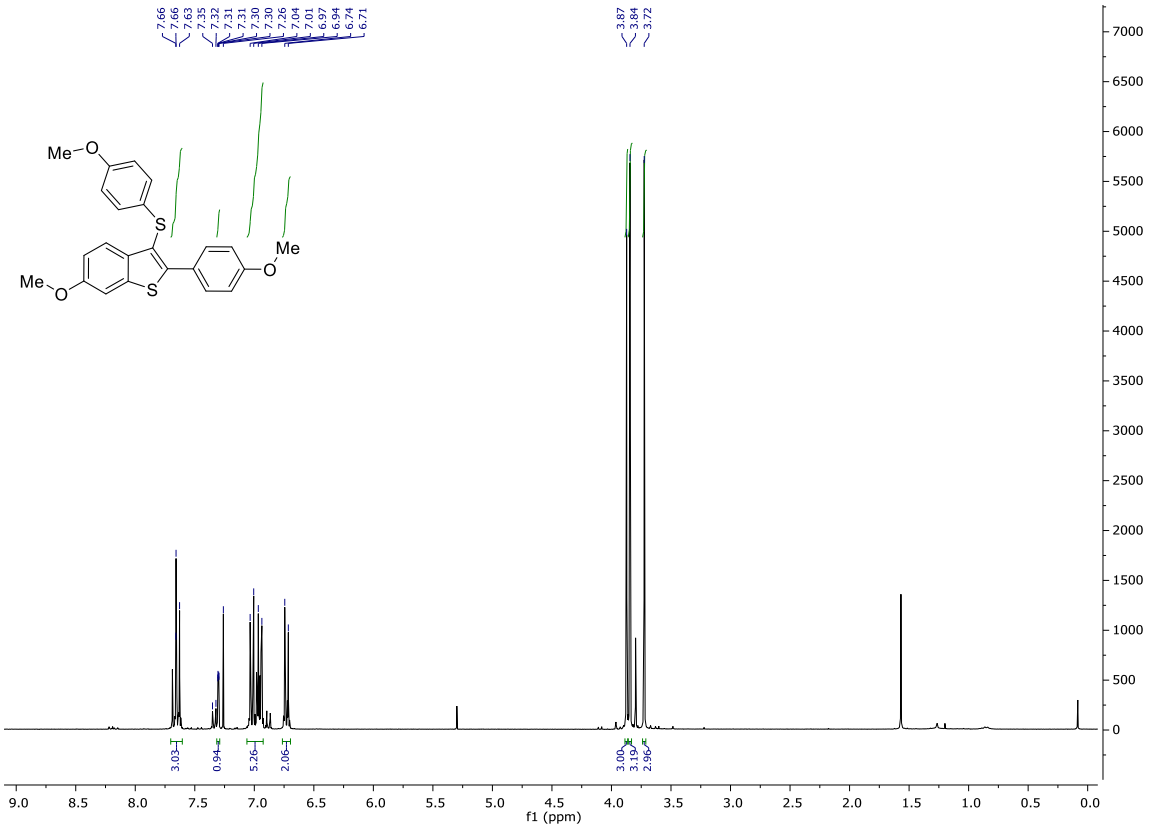

^{13}C NMR (126 MHz, $CDCl_3$) **190**

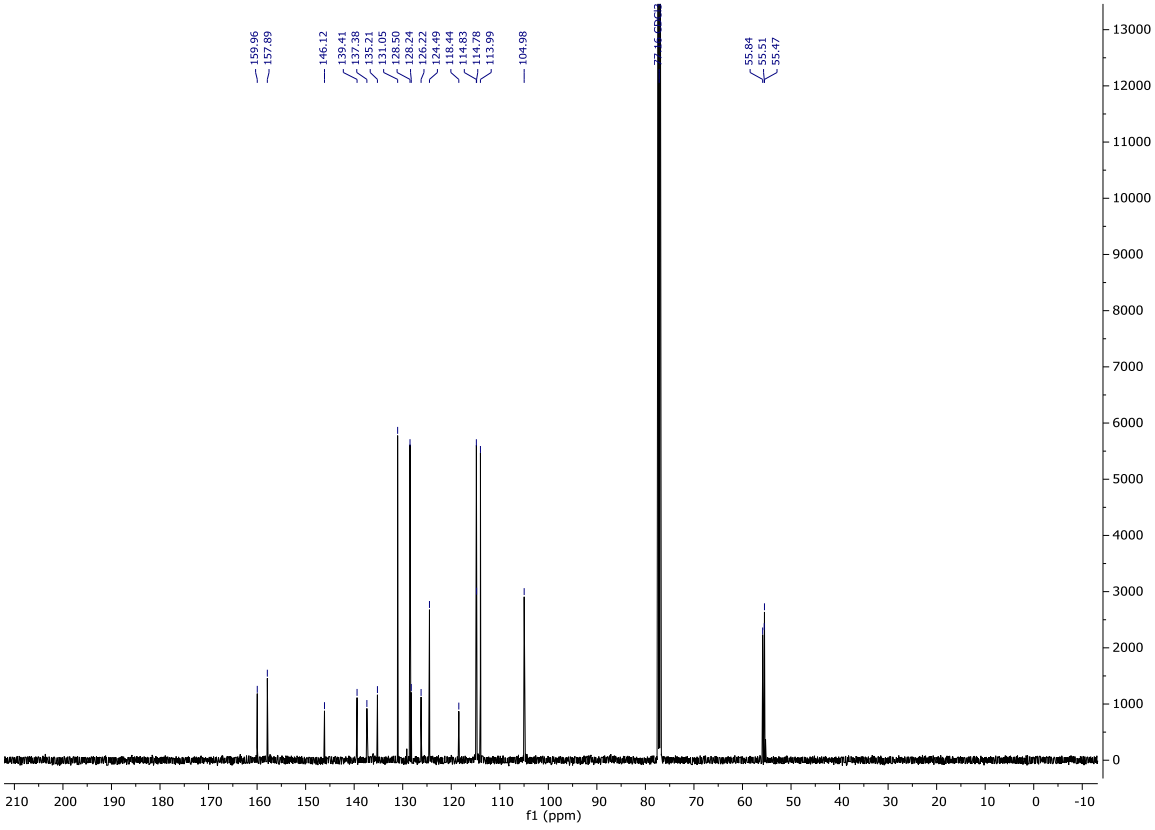

^{1}H NMR (300 MHz, $CDCl_3$) **179**

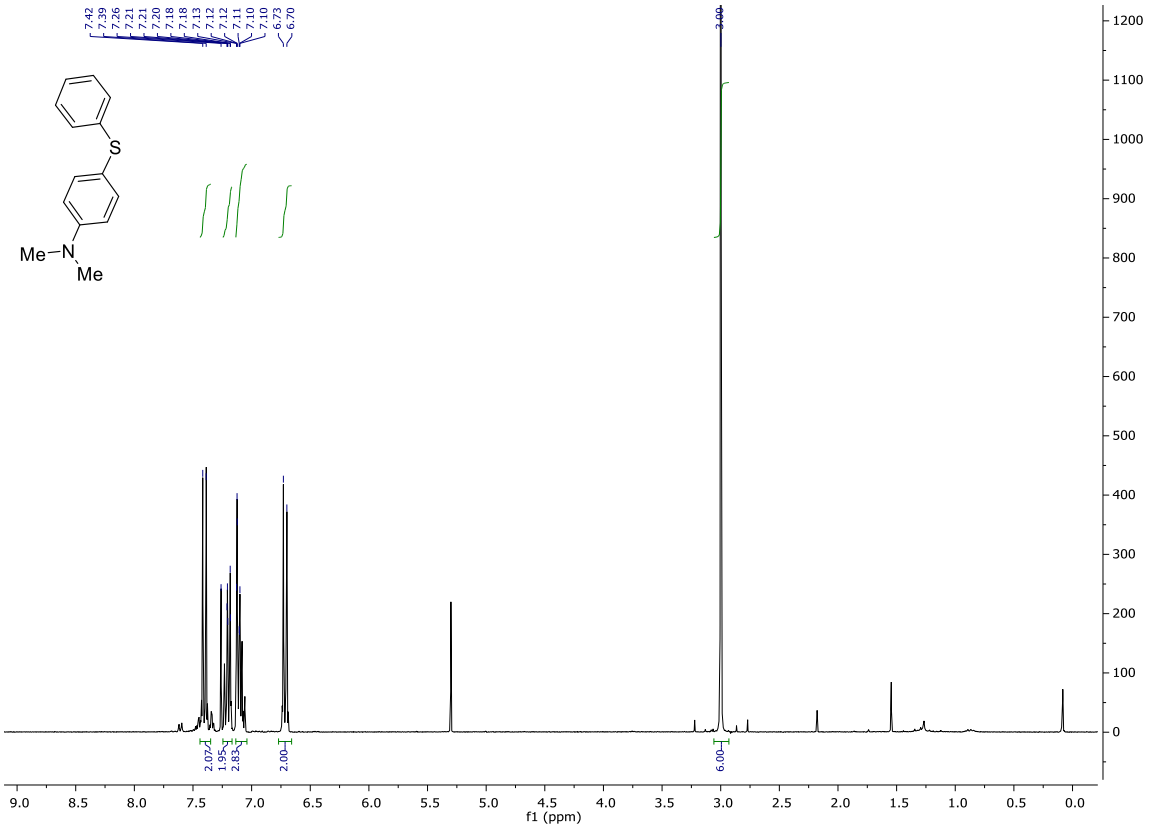

^{13}C NMR (75 MHz, $CDCl_3$) **179**

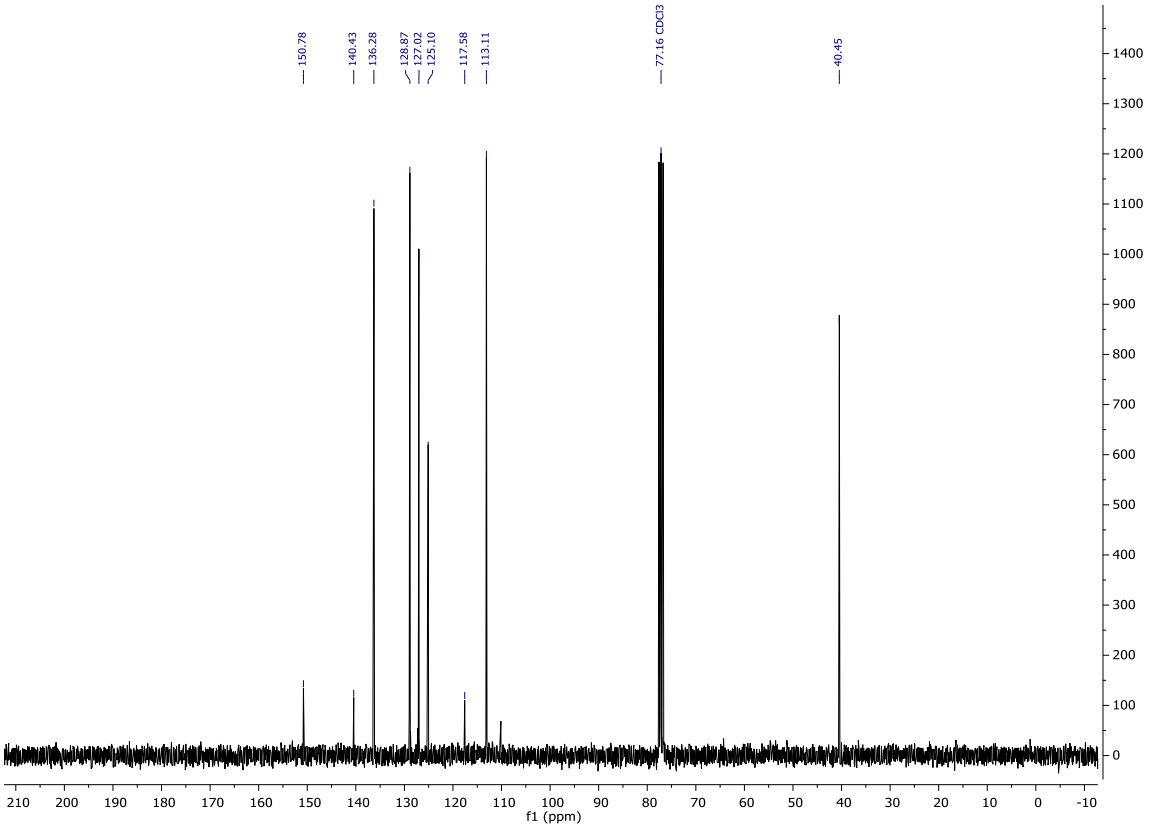

^{1}H NMR (300 MHz, $CDCl_3$) **158**

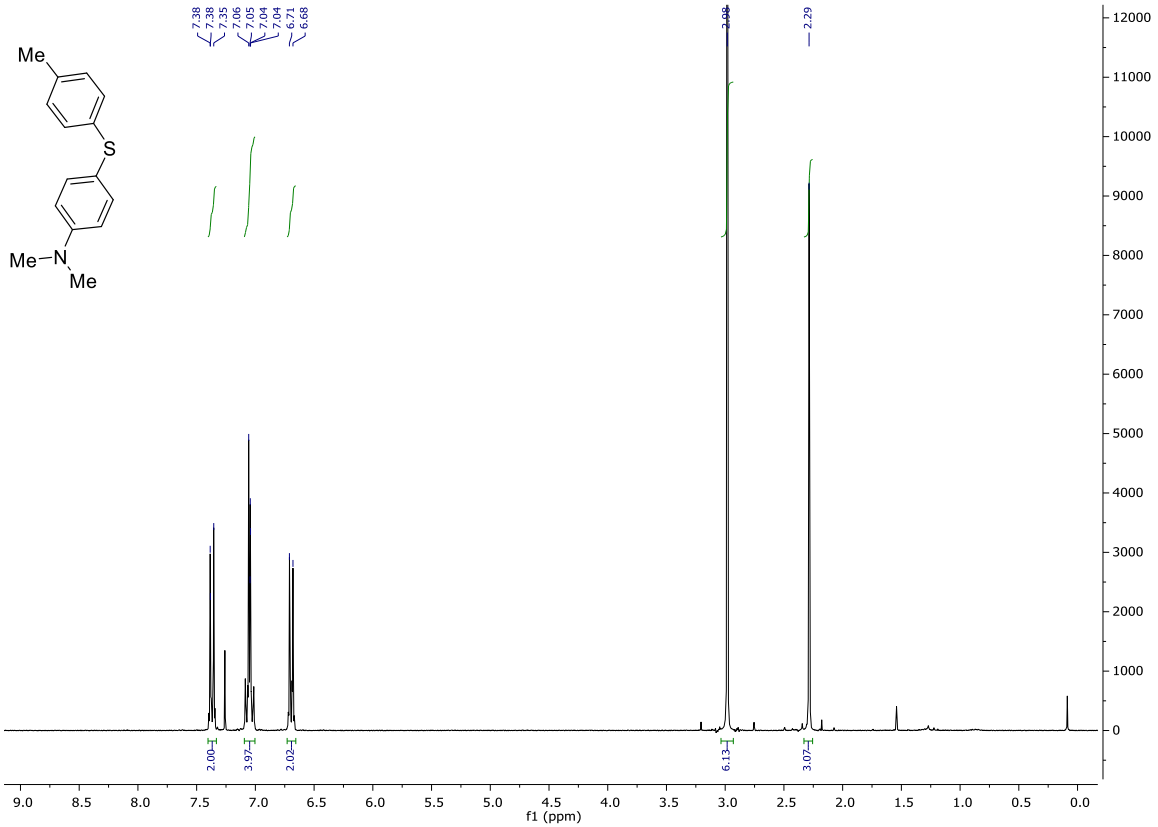

^{1}H NMR (300 MHz, $CDCl_3$) **160**

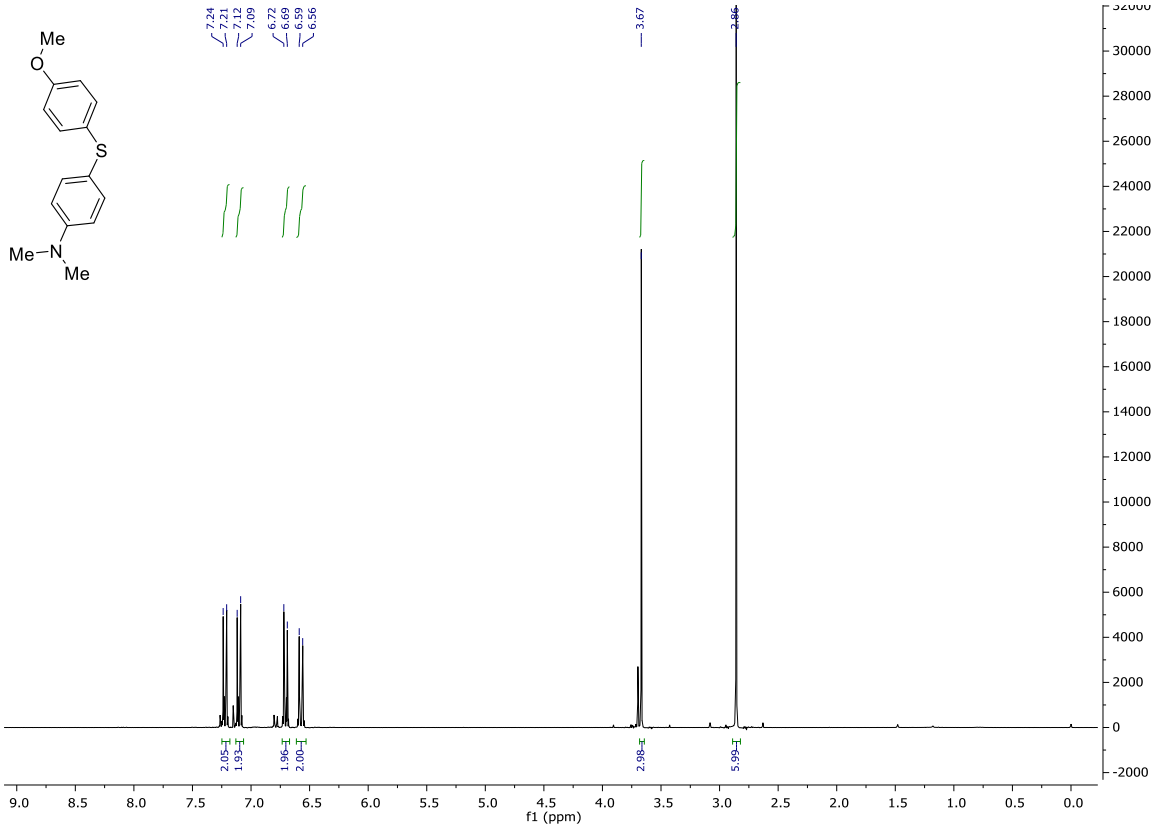

^{13}C NMR (75 MHz, $CDCl_3$) **160**

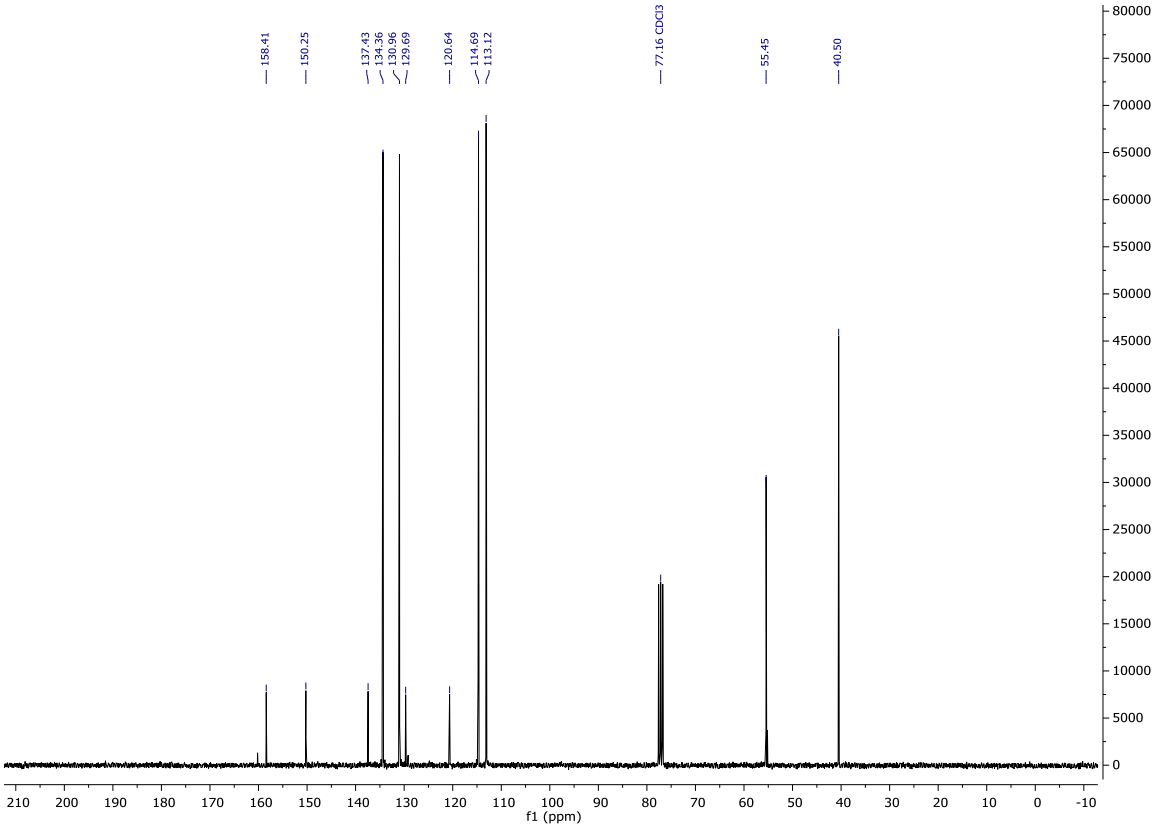

^{1}H NMR (300 MHz, $CDCl_3$) **187**

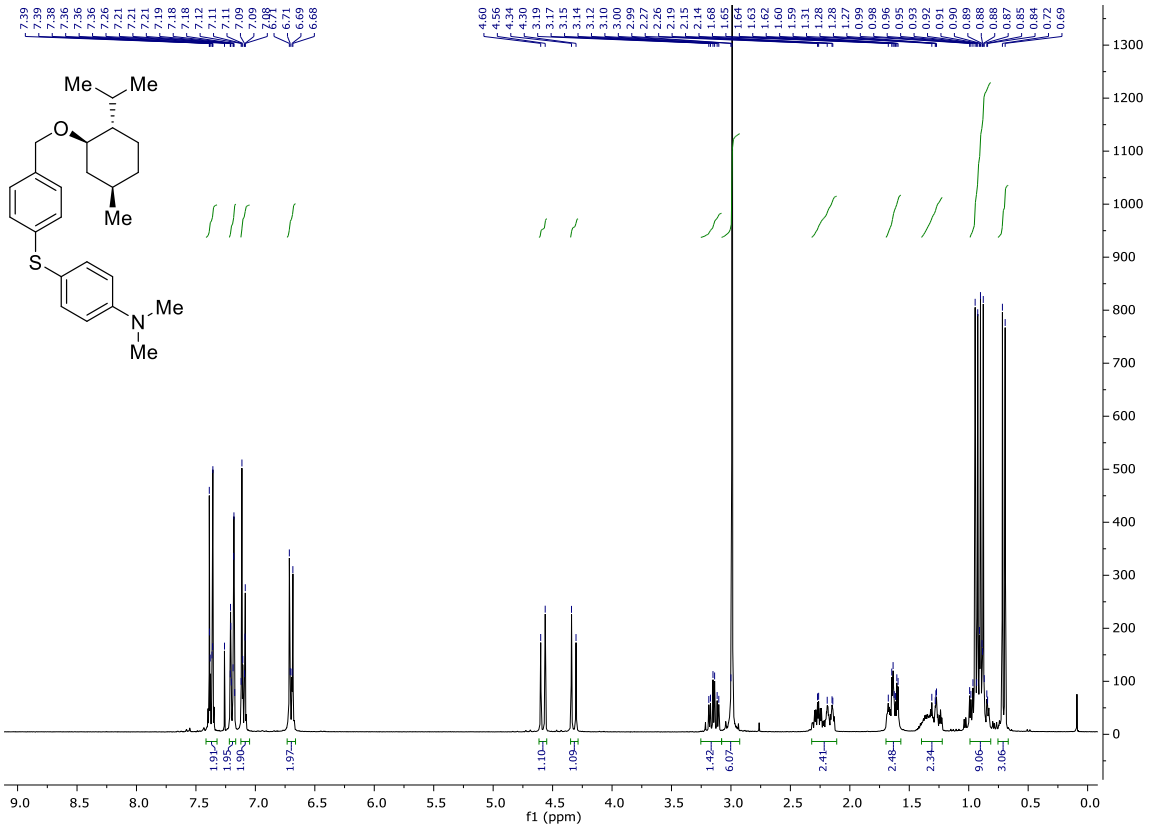

^{13}C NMR (126 MHz, $CDCl_3$) **187**

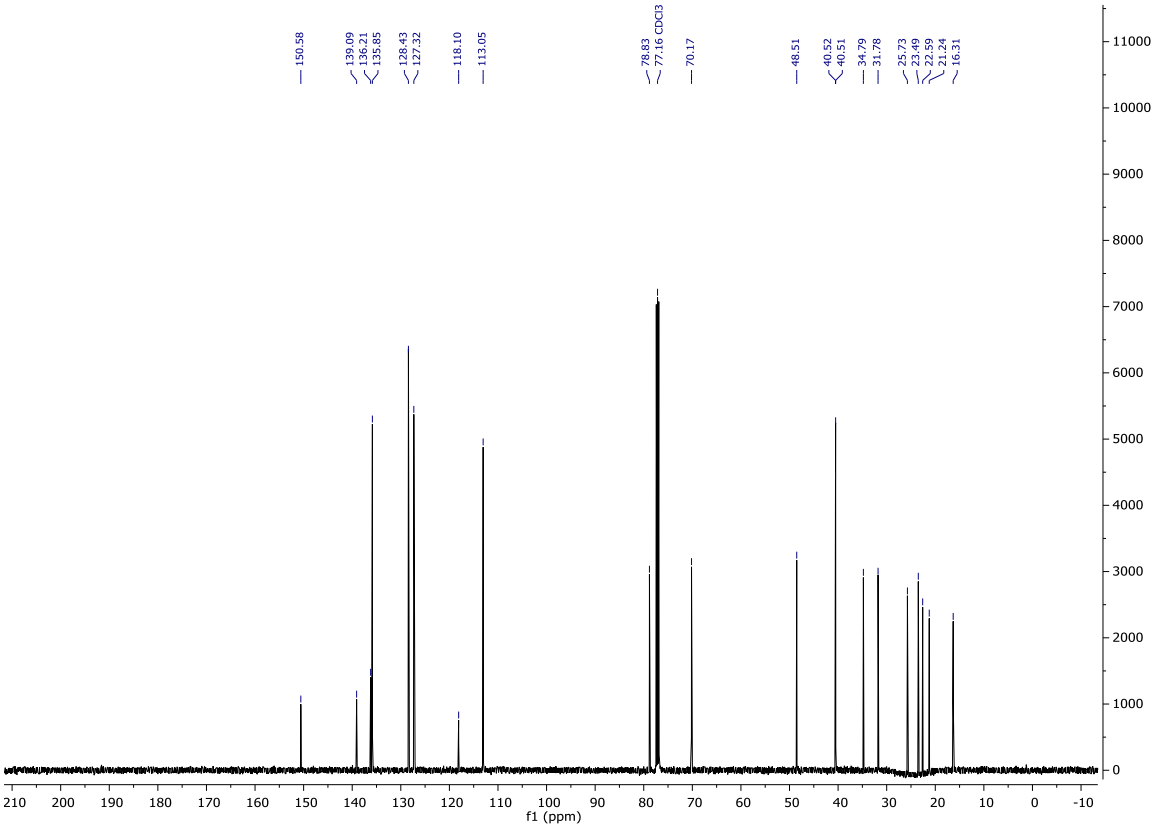

^{1}H NMR (400 MHz, $CDCl_3$) **184**

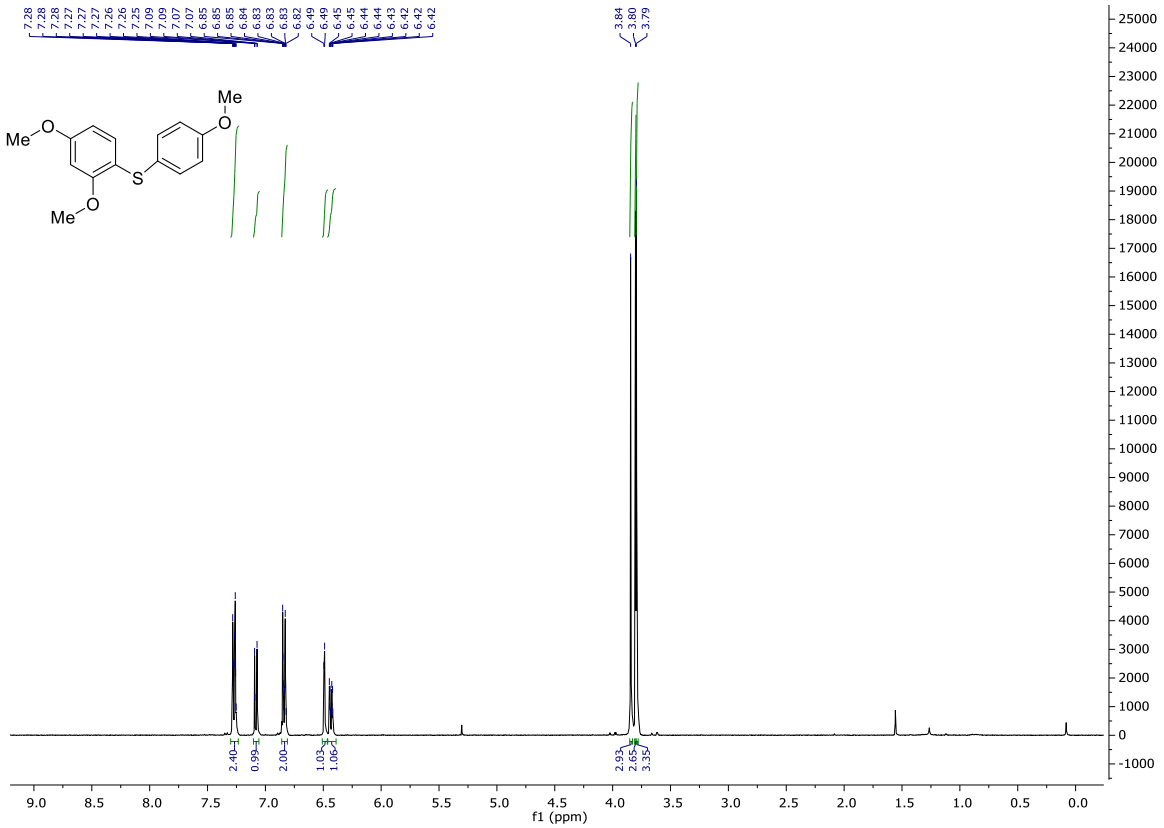

^{13}C NMR (126 MHz, $CDCl_3$) **184**

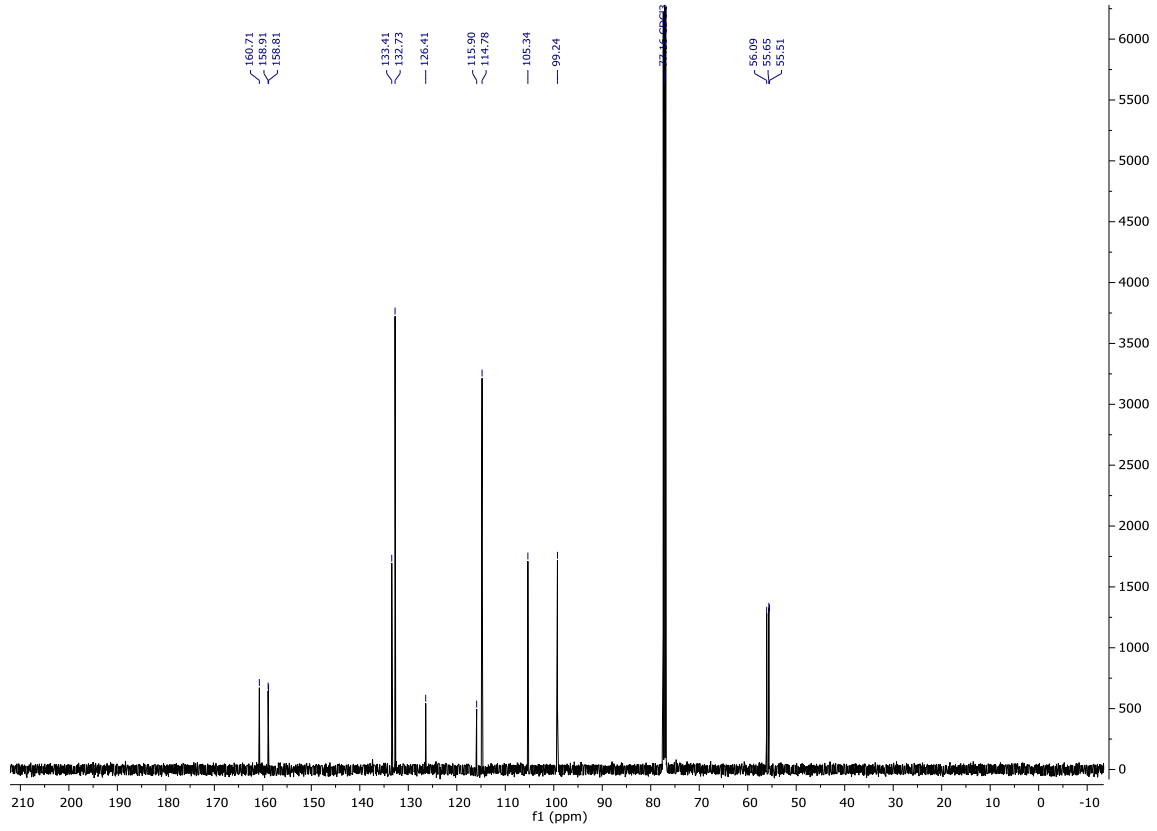

^{1}H NMR (300 MHz, $CDCl_3$) **191**

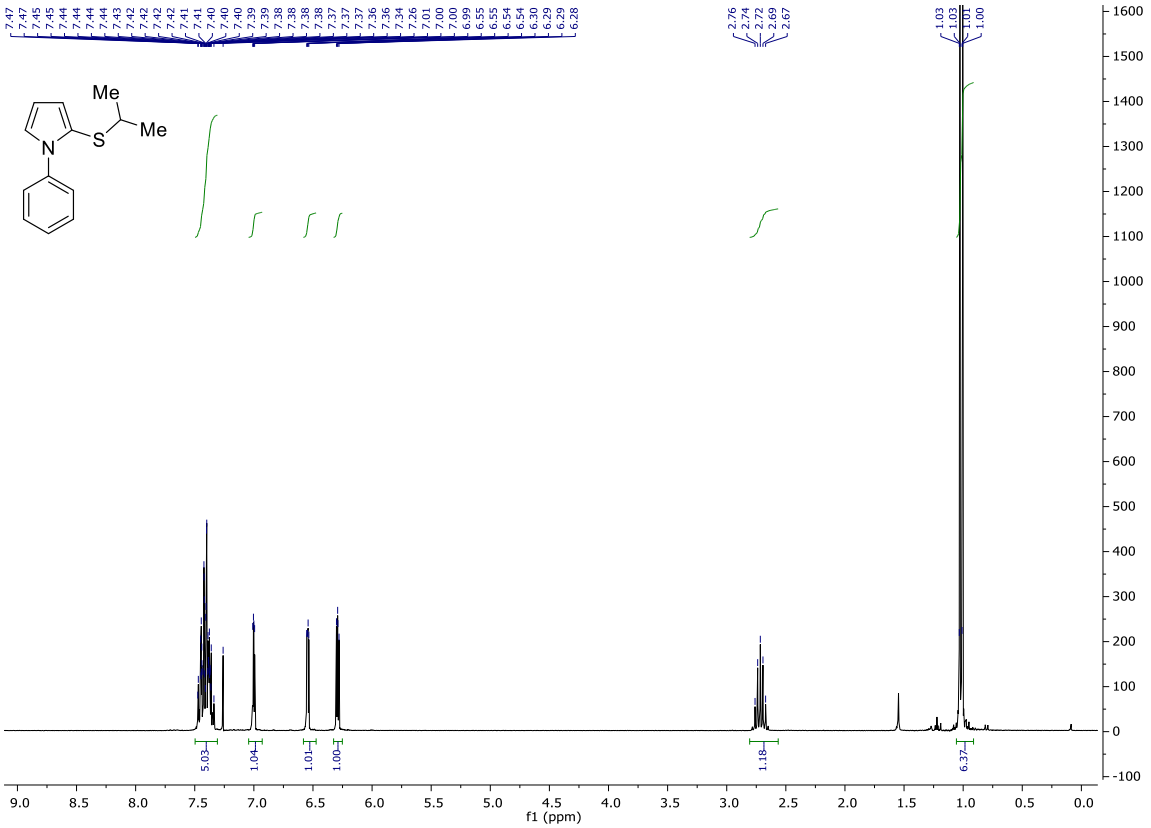

^{13}C NMR (126 MHz, $CDCl_3$) **191**

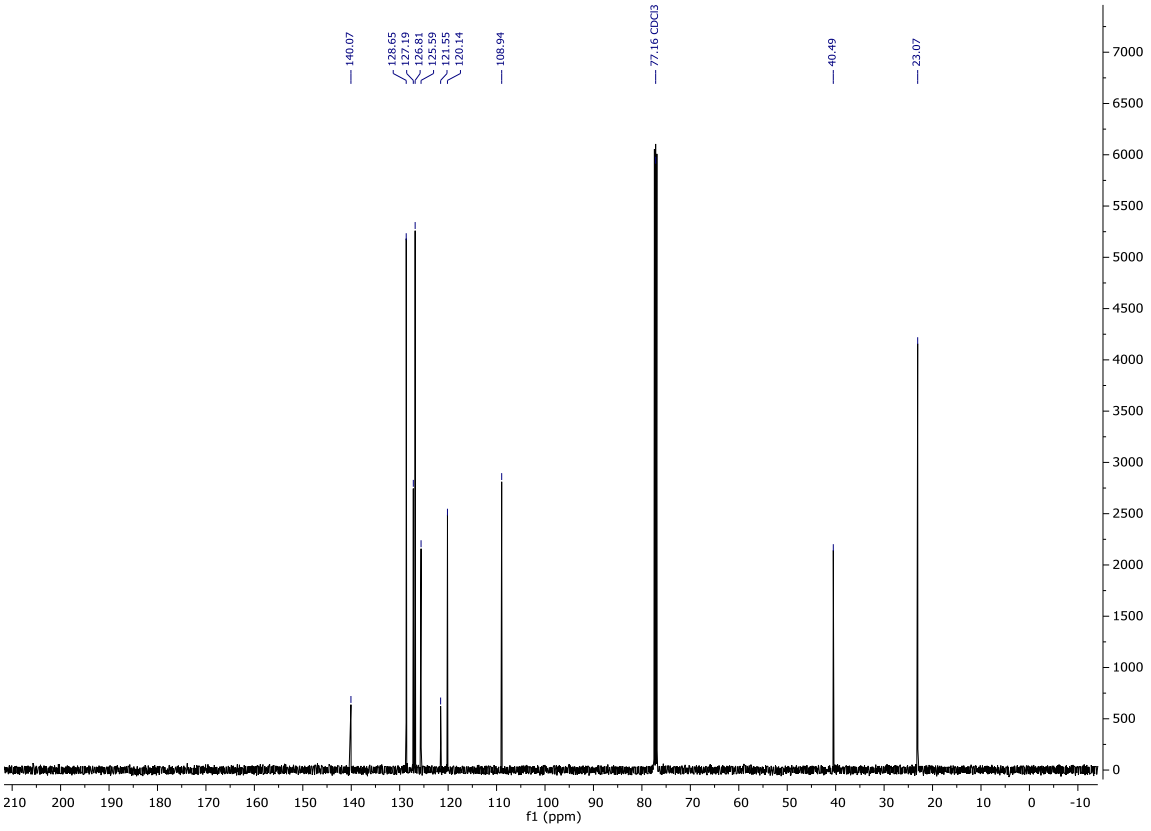

^{1}H NMR (600 MHz, $CDCl_3$) **192**

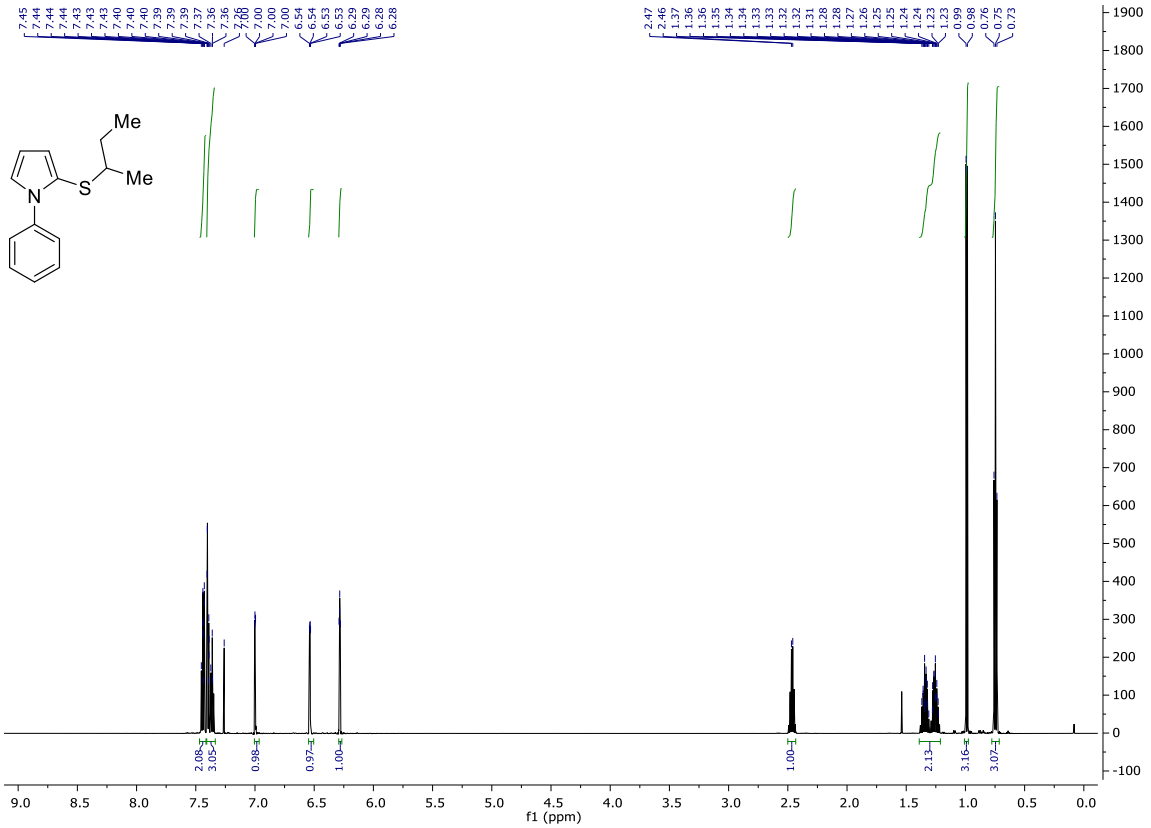

^{13}C NMR (126 MHz, $CDCl_3$) **192**

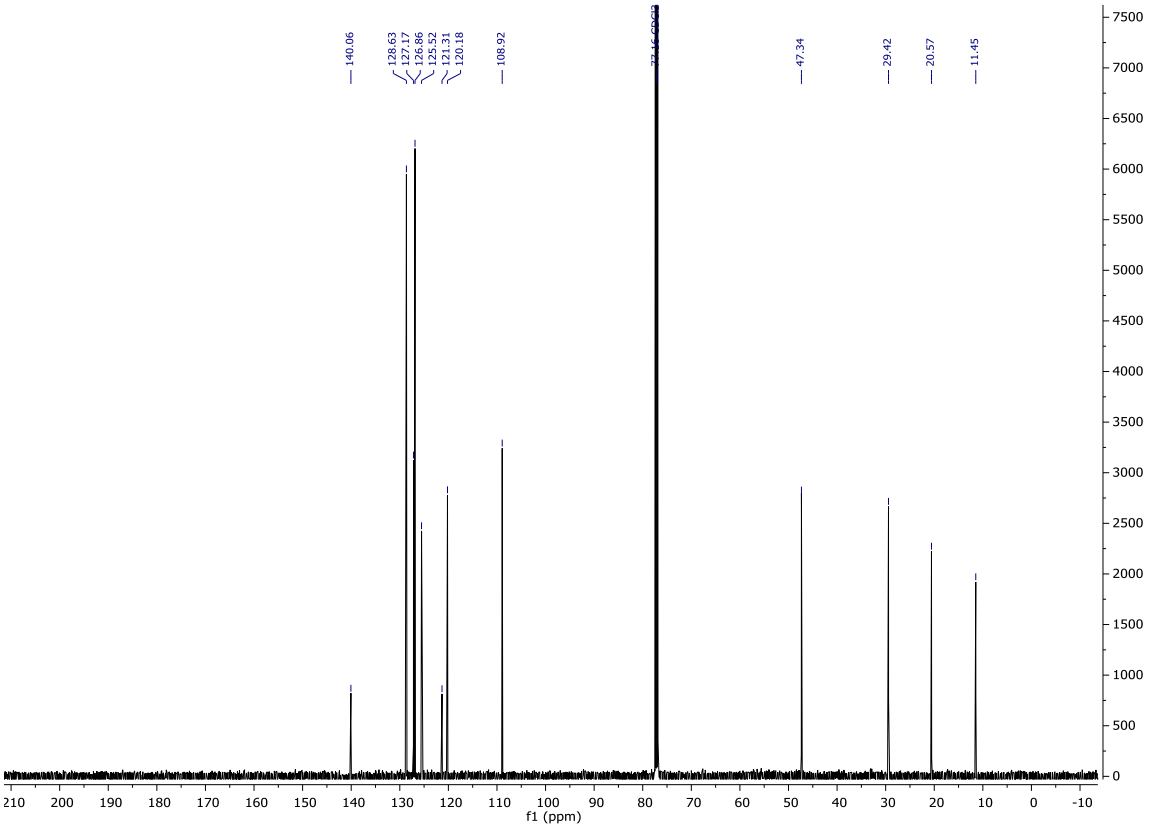

^{1}H NMR (300 MHz, CD_2Cl_2) **193**

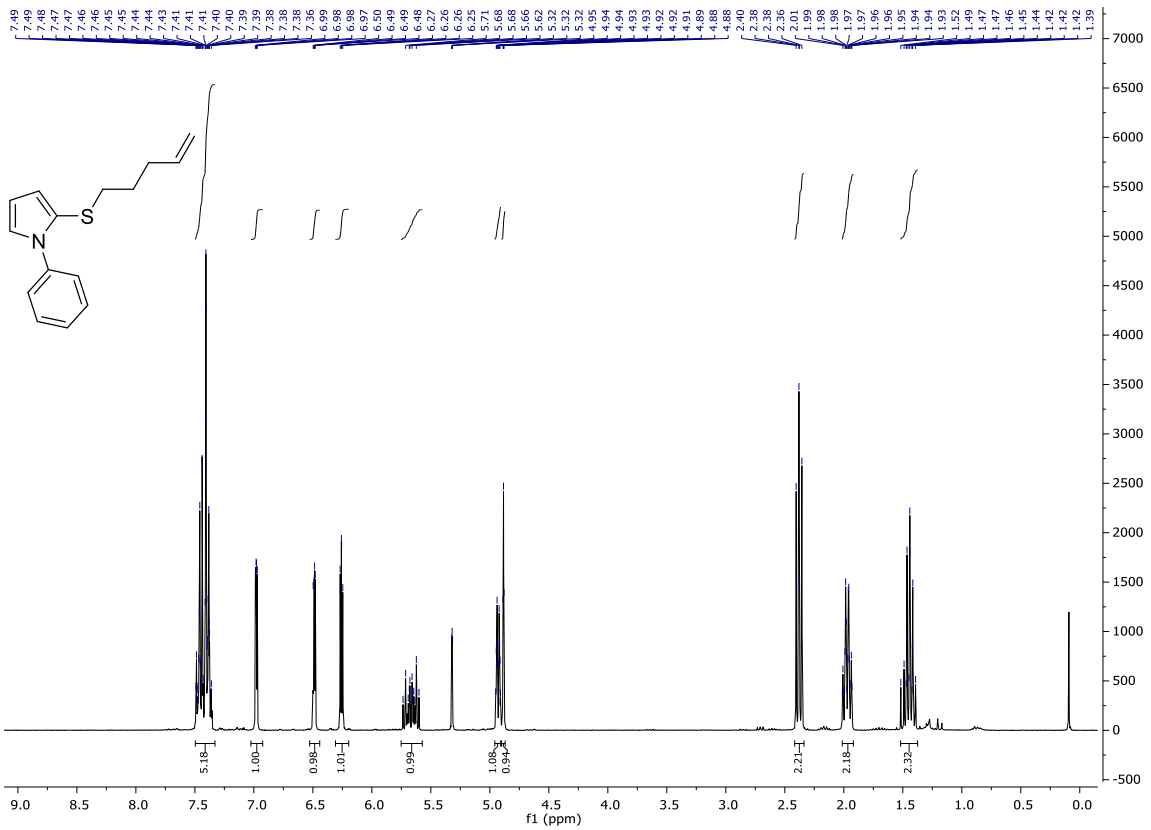

^{13}C NMR (126 MHz, CD_2Cl_2) **193**

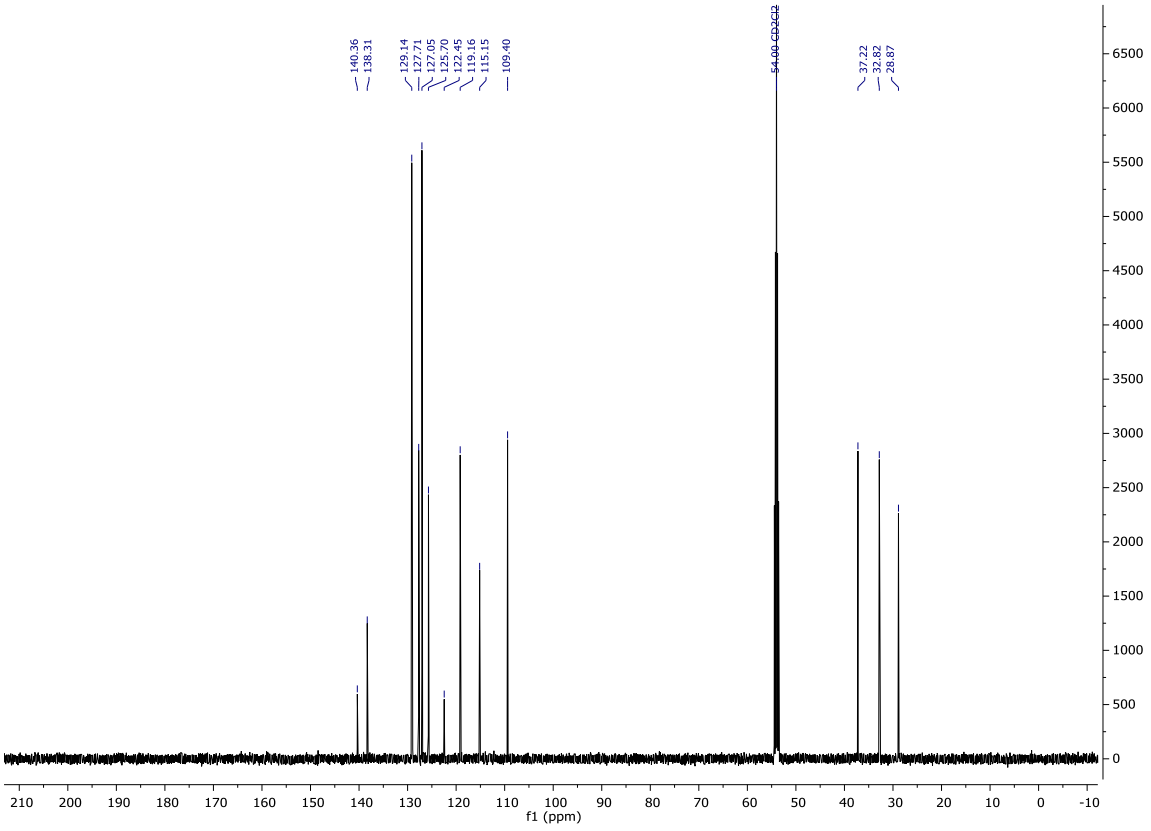

^{1}H NMR (300 MHz, $CDCl_3$) **195**

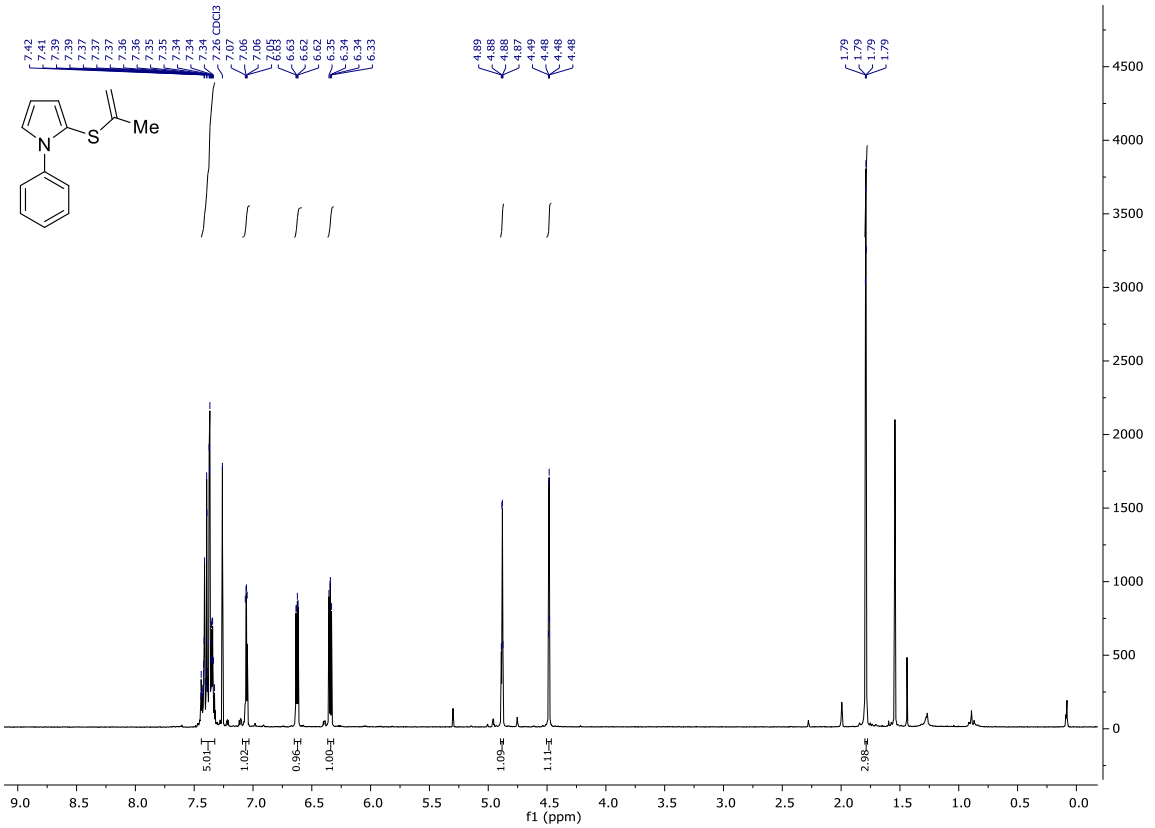

^{13}C NMR (126 MHz, $CDCl_3$) **195**

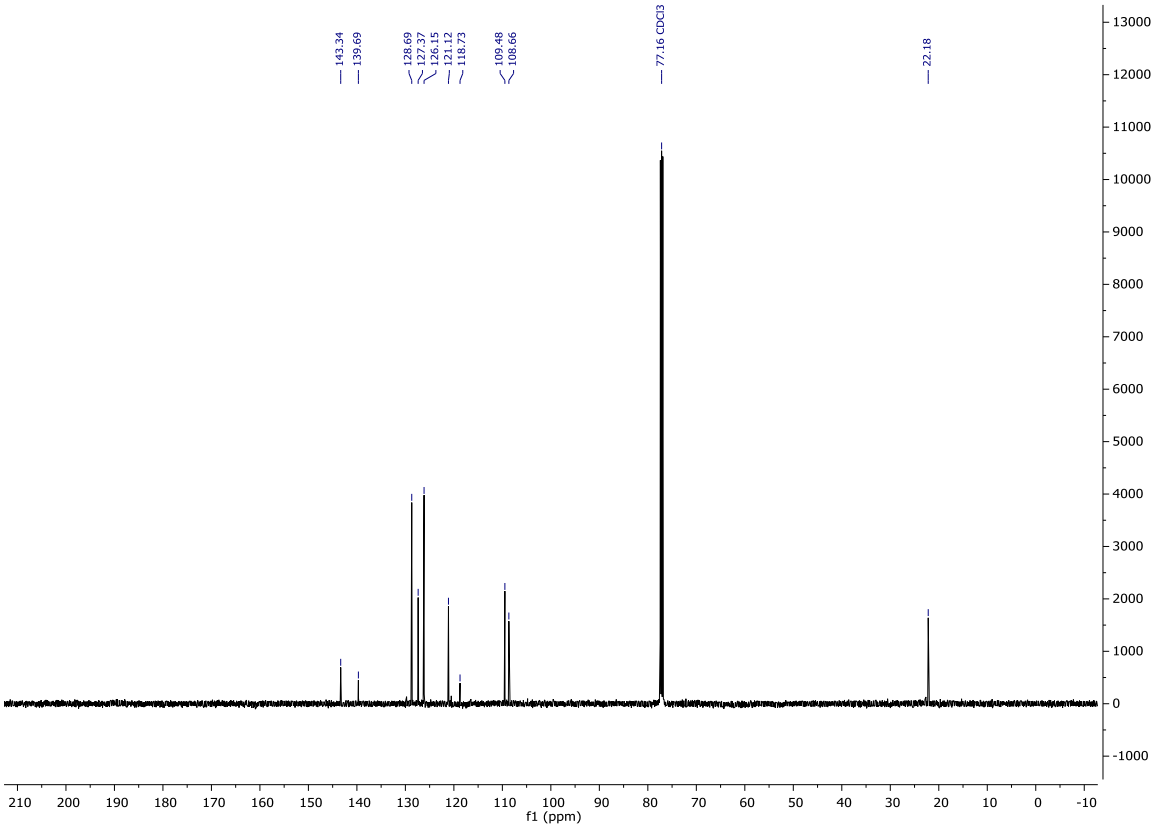

^{1}H NMR (400 MHz, $CDCl_3$) **196**

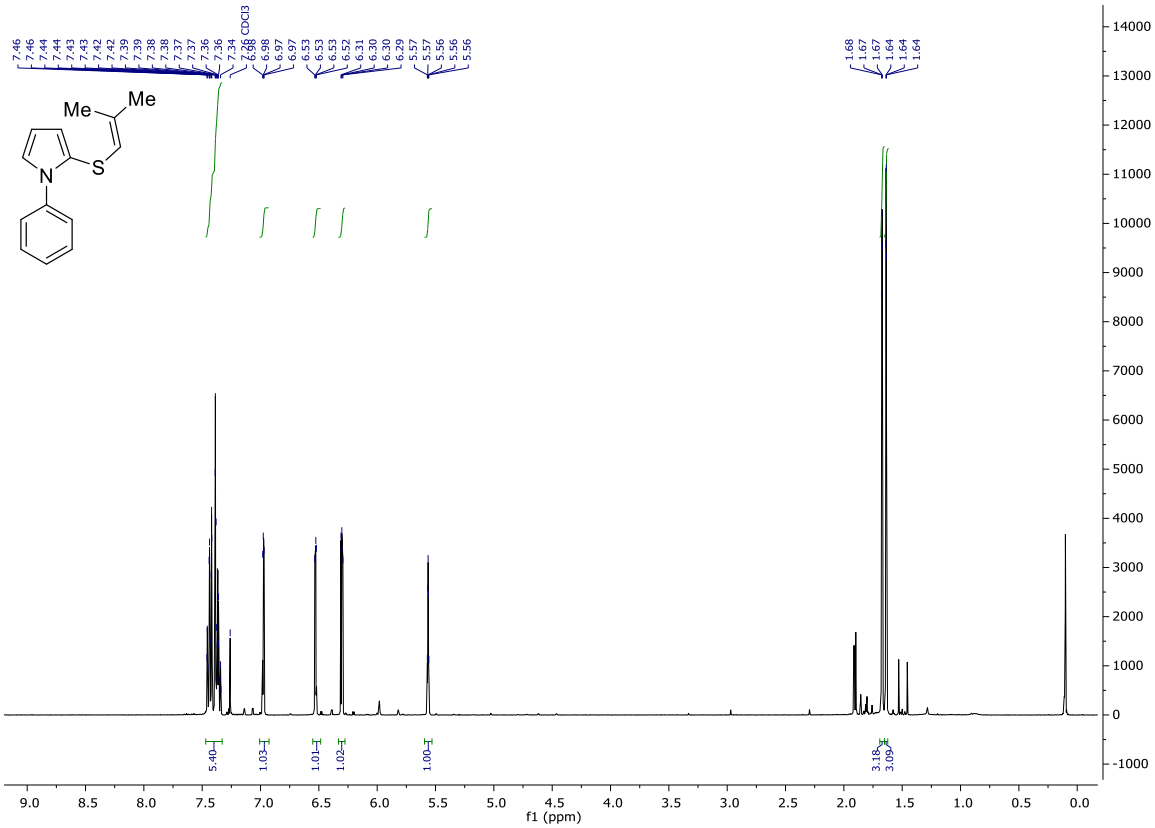

^{13}C NMR (126 MHz, $CDCl_3$) **196**

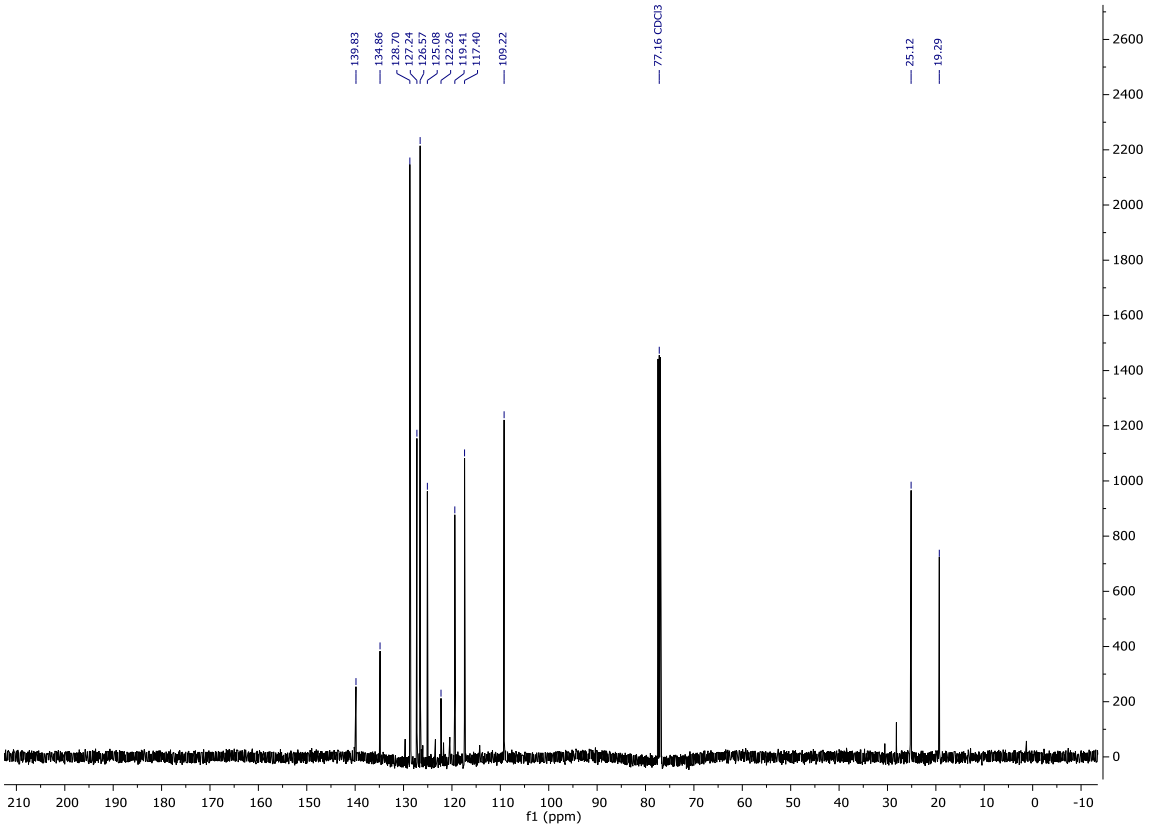

^{1}H NMR (300 MHz, CD_2Cl_2) **197**

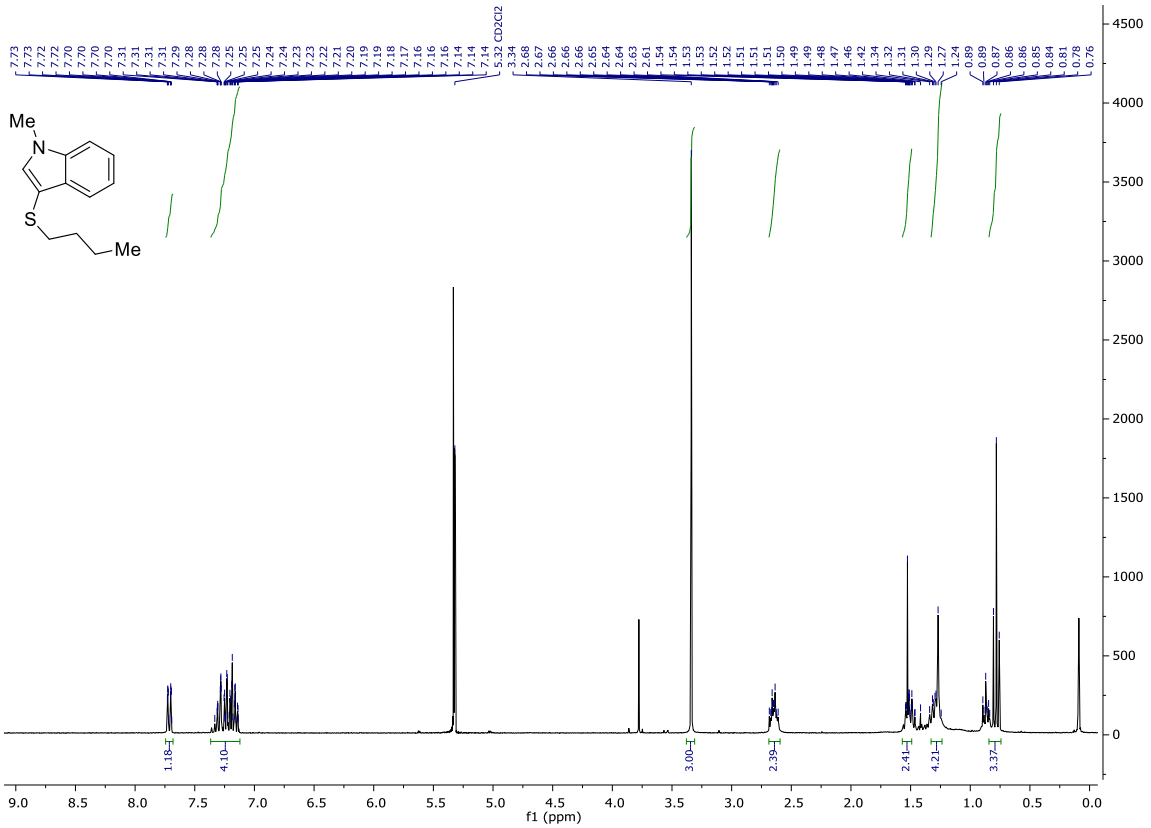

^{13}C NMR (126 MHz, CD_2Cl_2) **197**

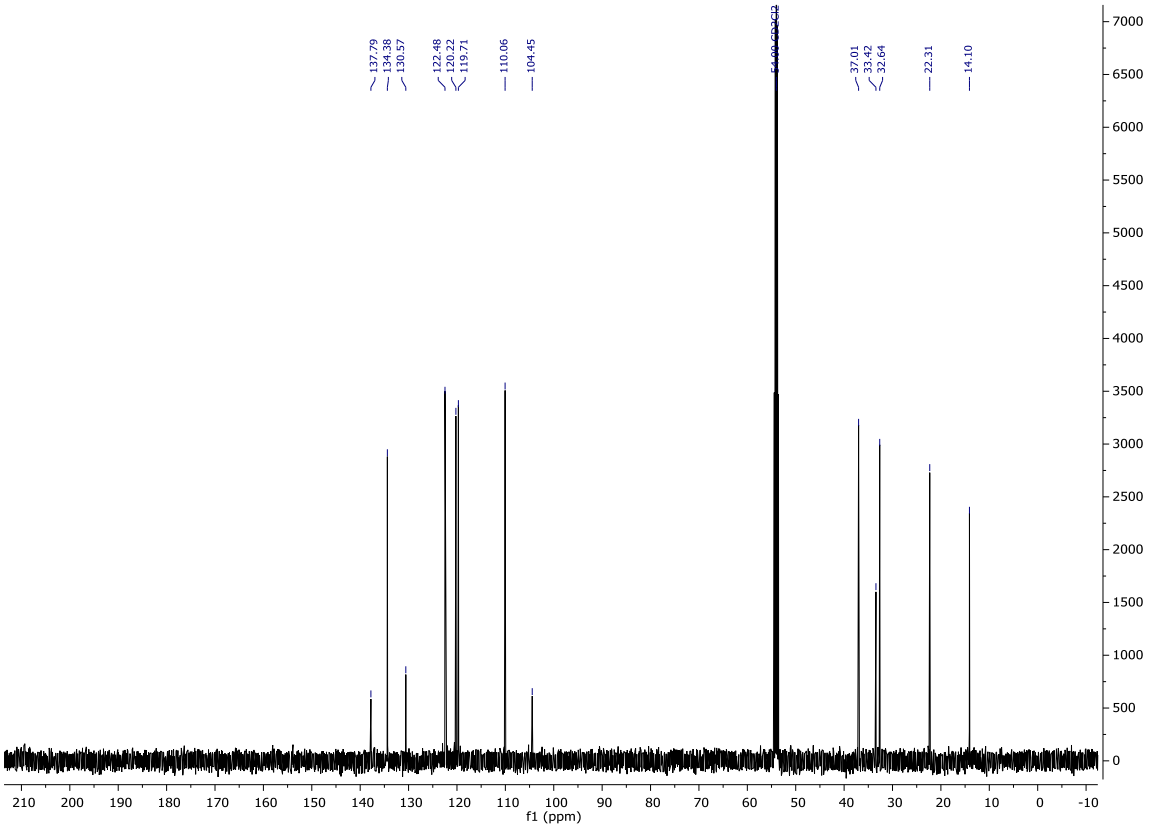

^{1}H NMR (400 MHz, $CDCl_3$) **198**

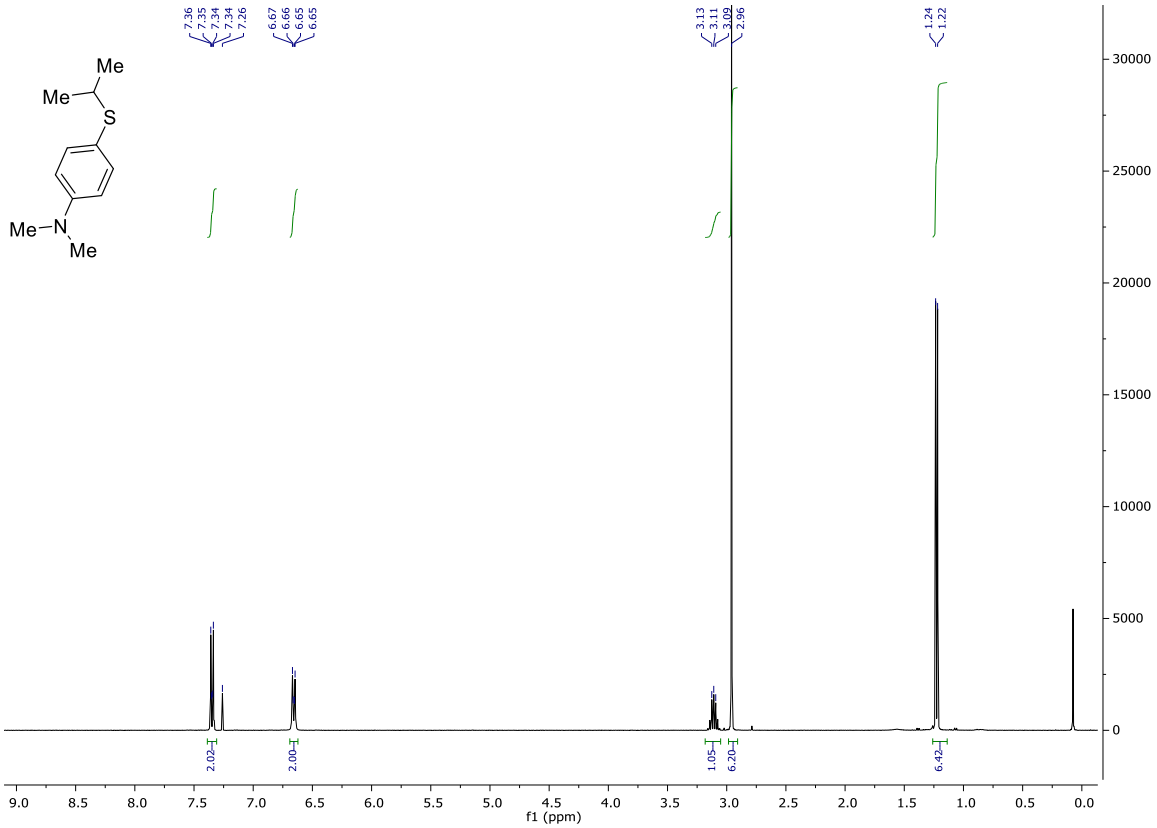

^{13}C NMR (126 MHz, $CDCl_3$) **198**

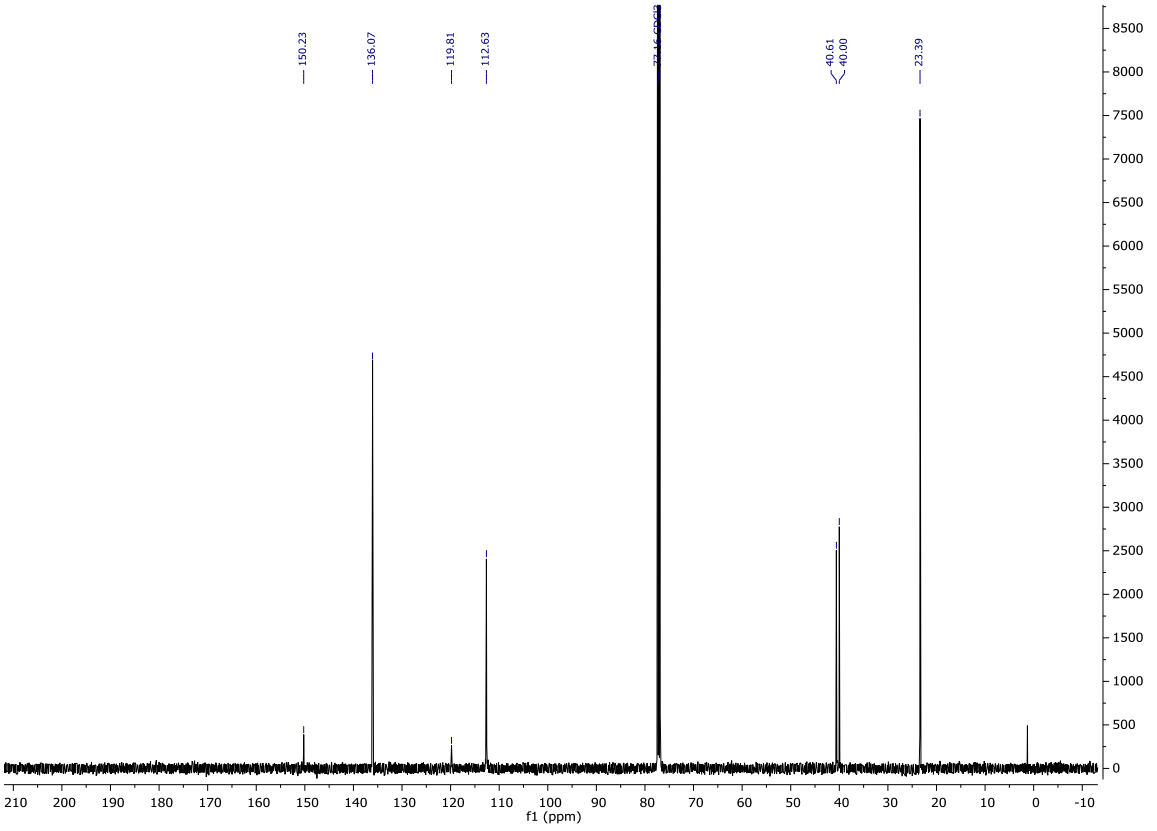

^{1}H NMR (300 MHz, $CDCl_3$) **182**

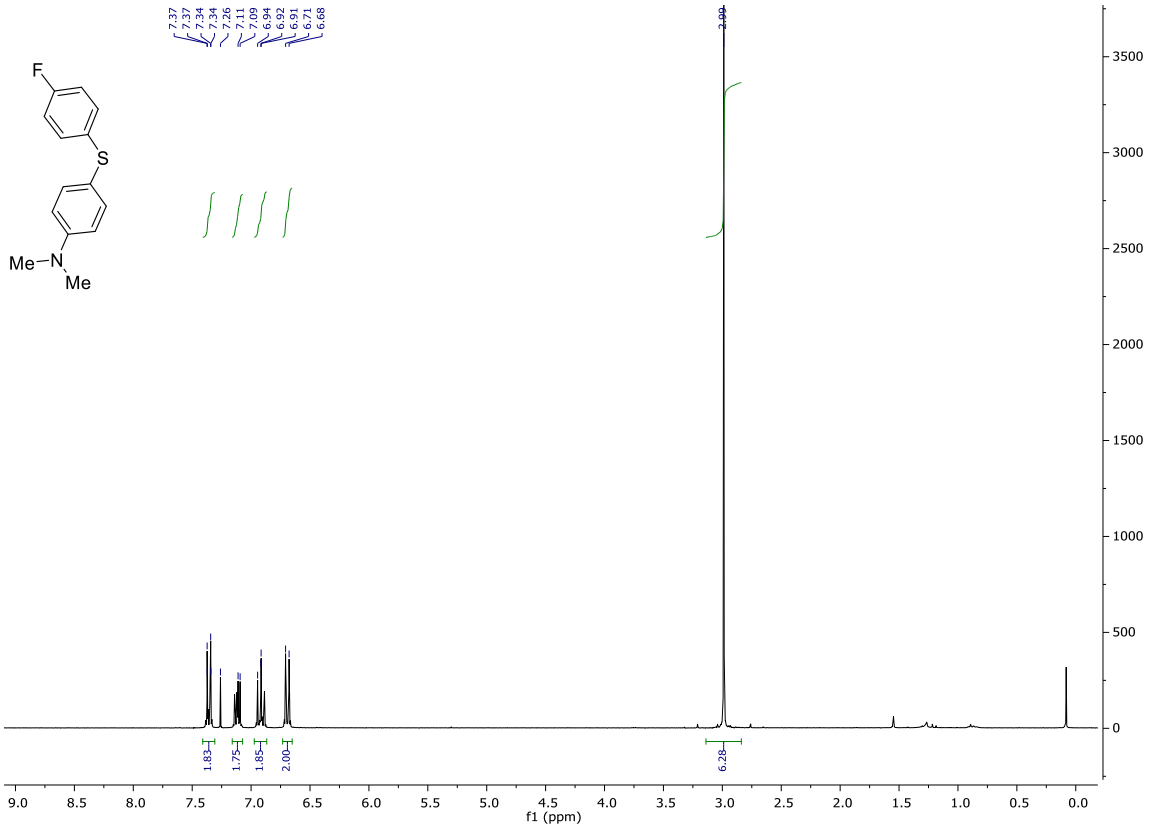

^{13}C NMR (126 MHz, $CDCl_3$) **182**

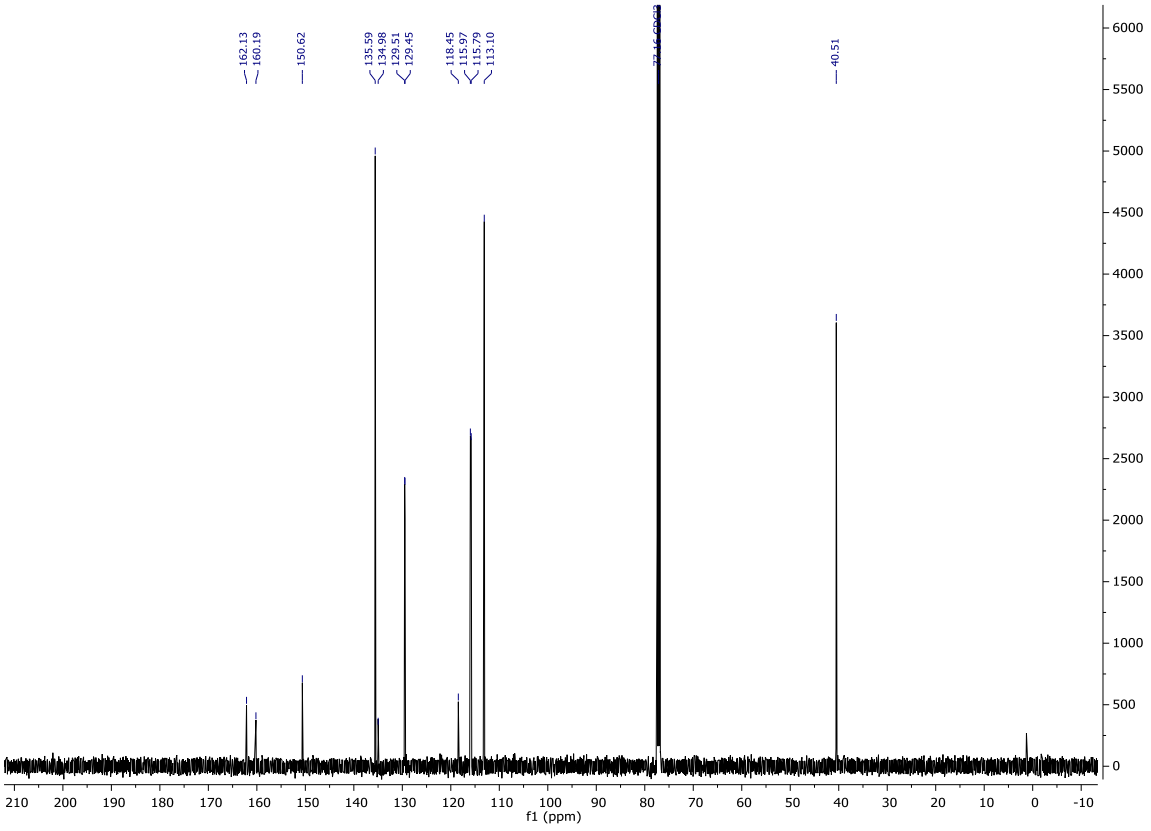

^{19}F NMR (282 MHz, $CDCl_3$) **182**

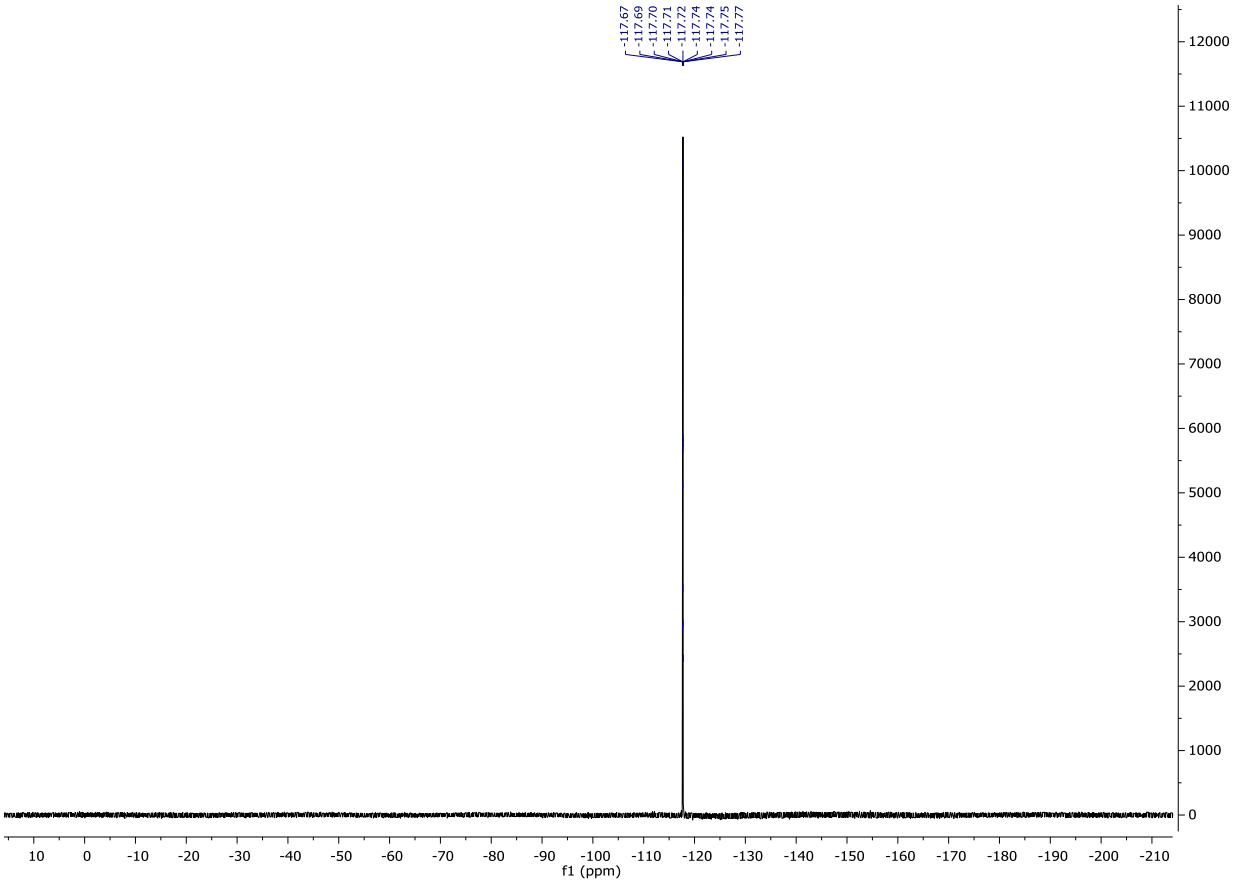

^{1}H NMR (300 MHz, $CDCl_3$) **182**

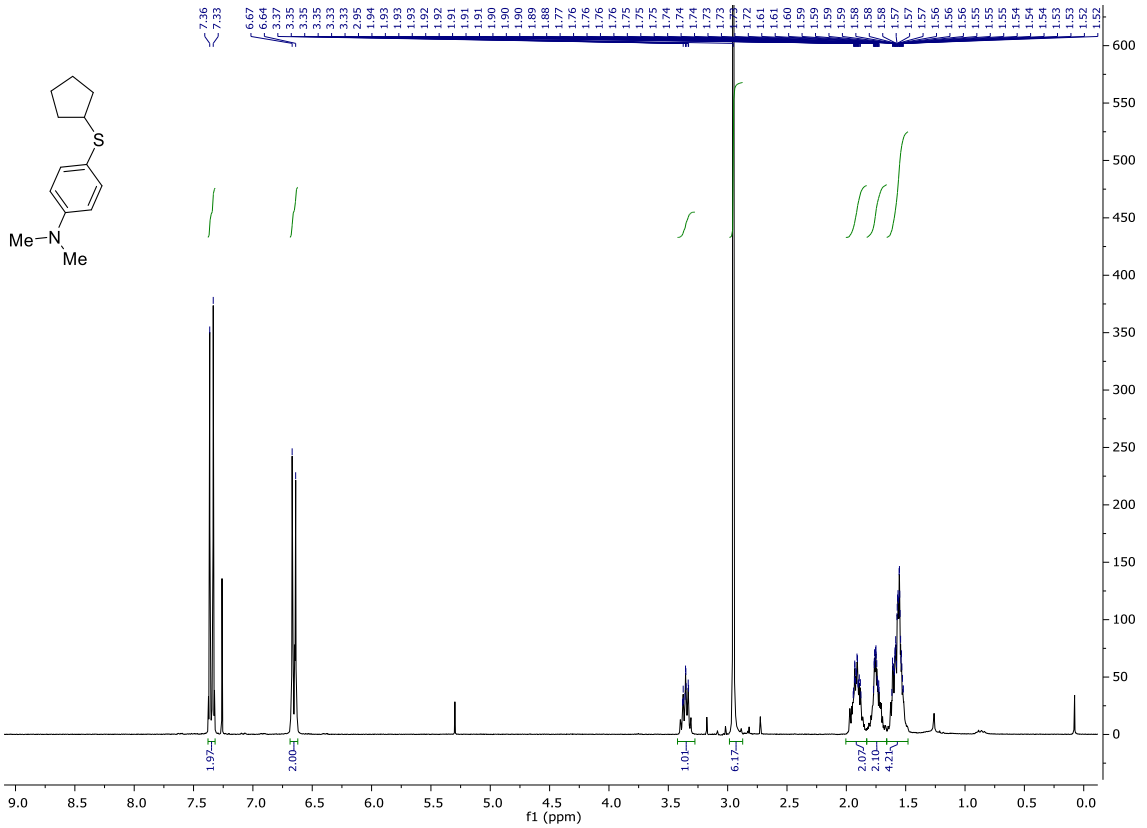

^{13}C NMR (75 MHz, $CDCl_3$) **182**

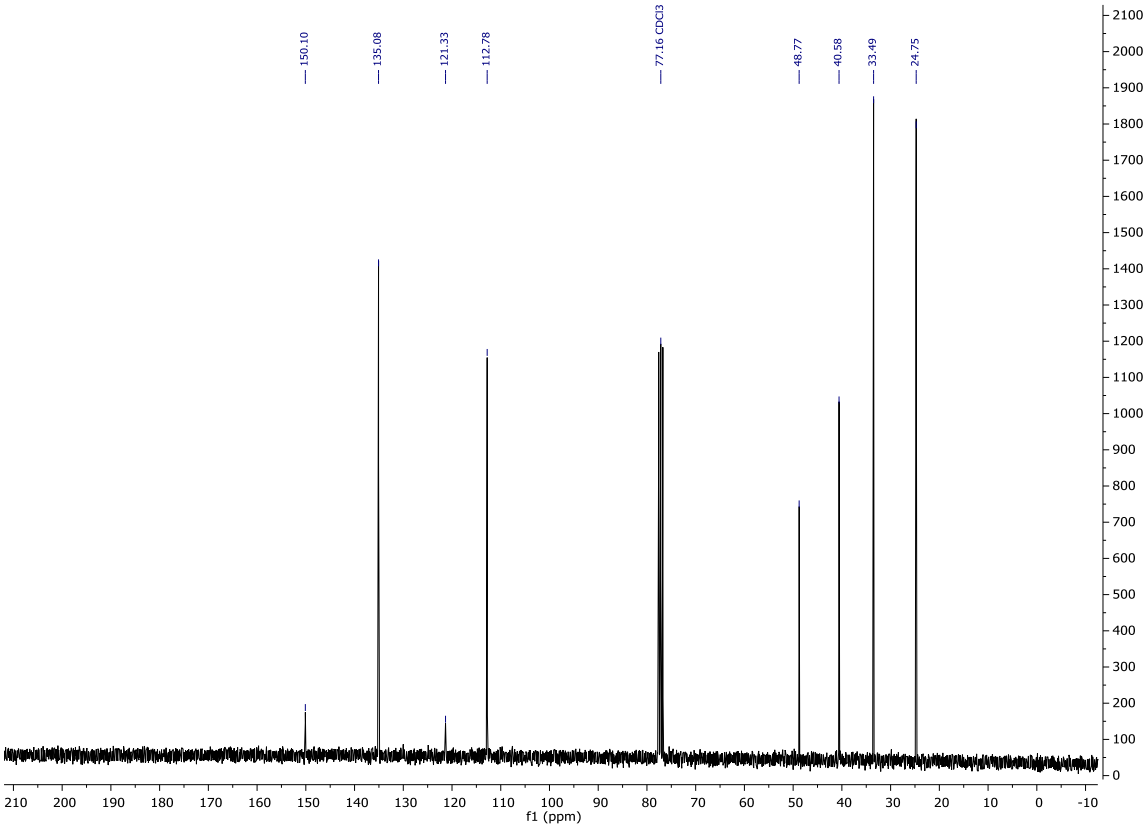

^{1}H NMR (300 MHz, $CDCl_3$) **200**

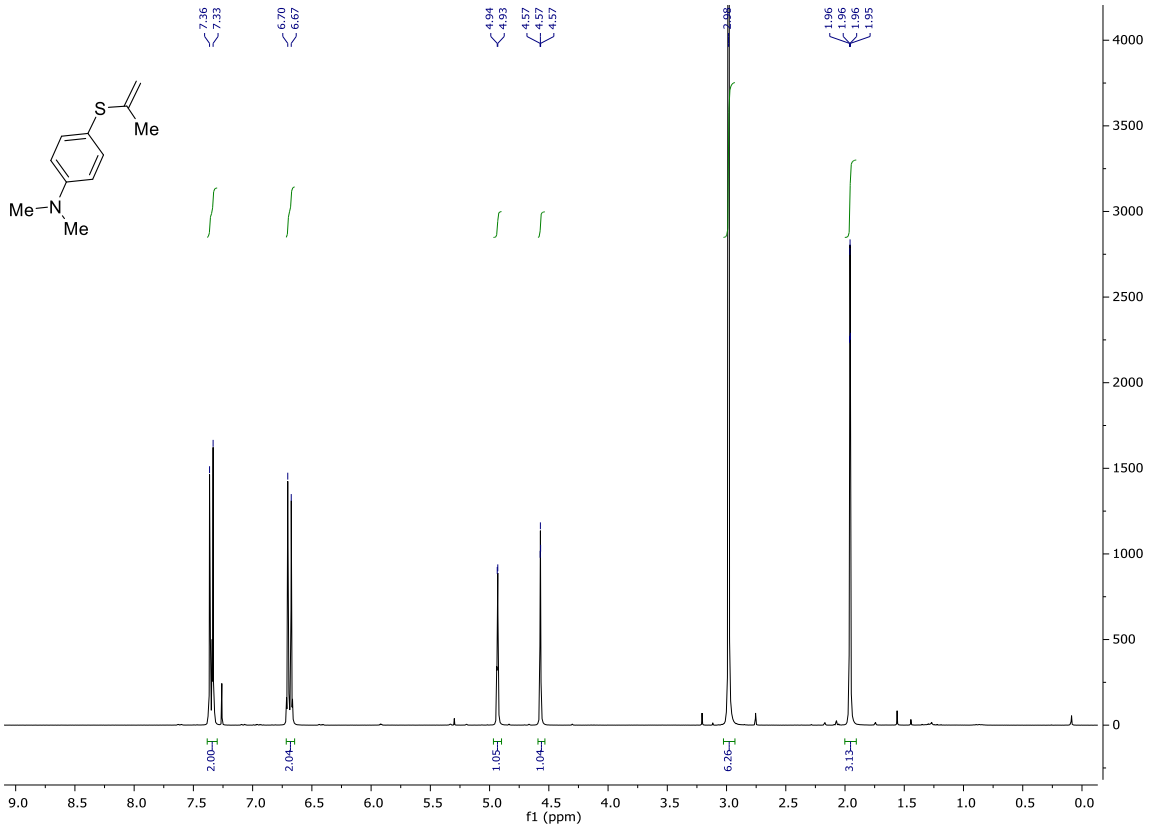

^{13}C NMR (75 MHz, $CDCl_3$) **200**

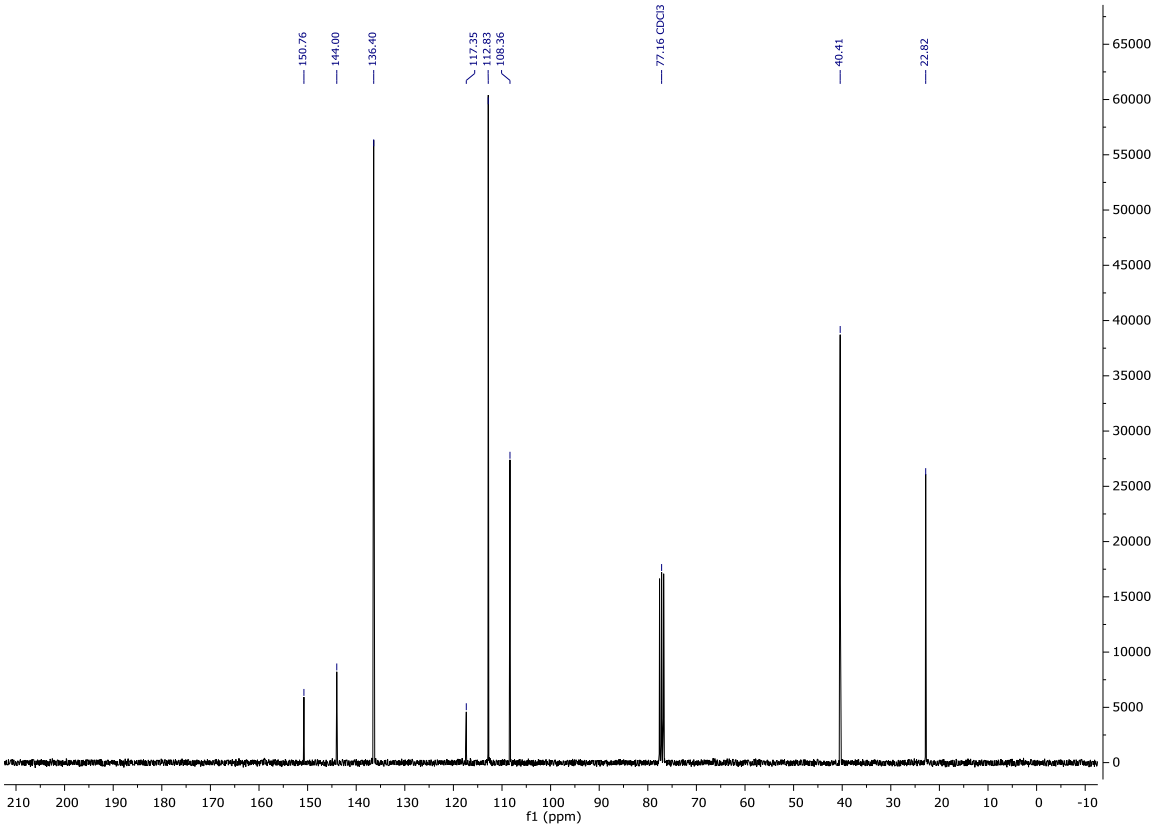

^{1}H NMR (400 MHz, $CDCl_3$) **194**

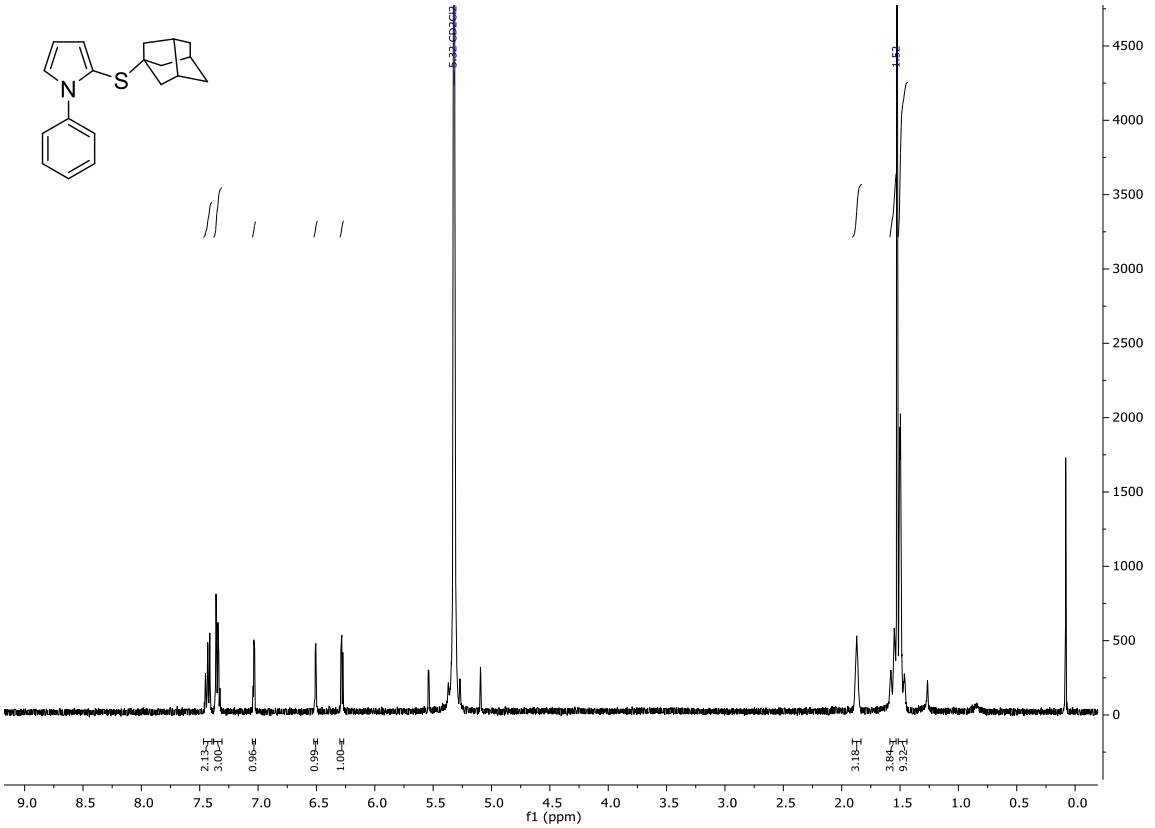

^{13}C NMR (126 MHz, $CDCl_{23}$) **194**

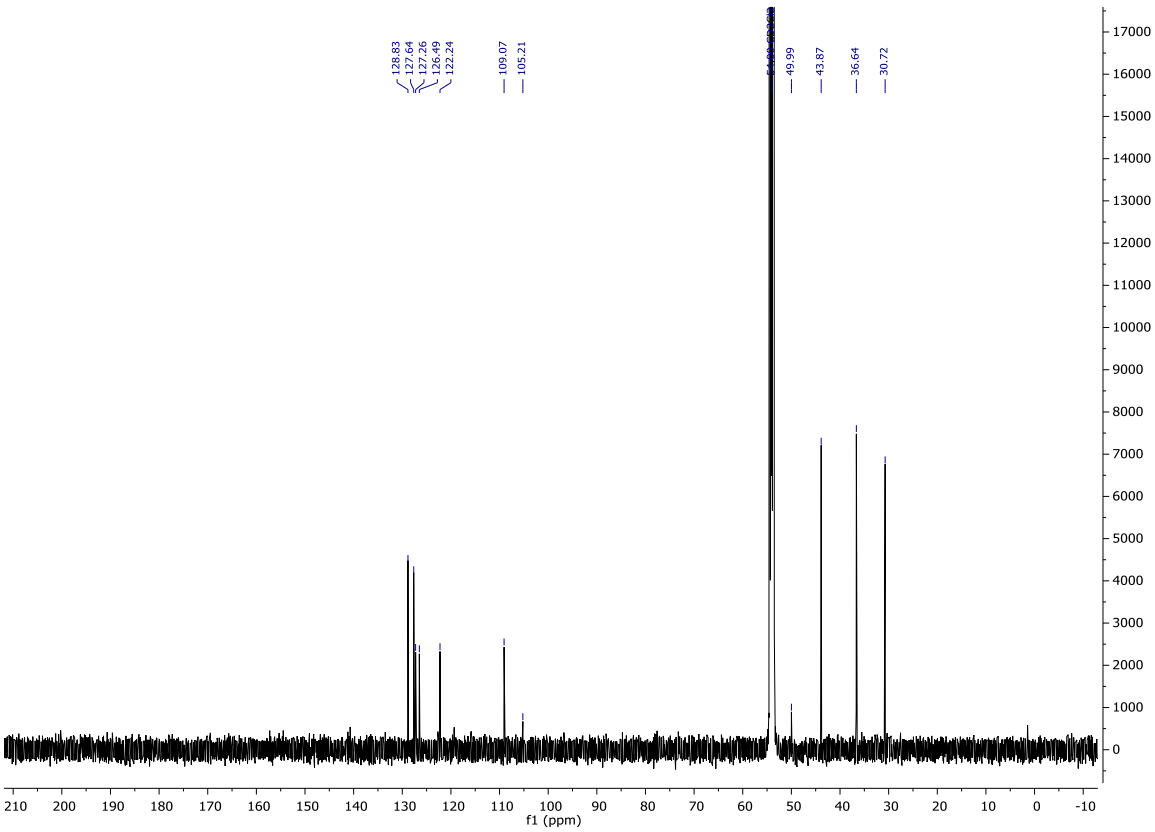

^{1}H NMR (400 MHz, $CDCl_3$) **173**

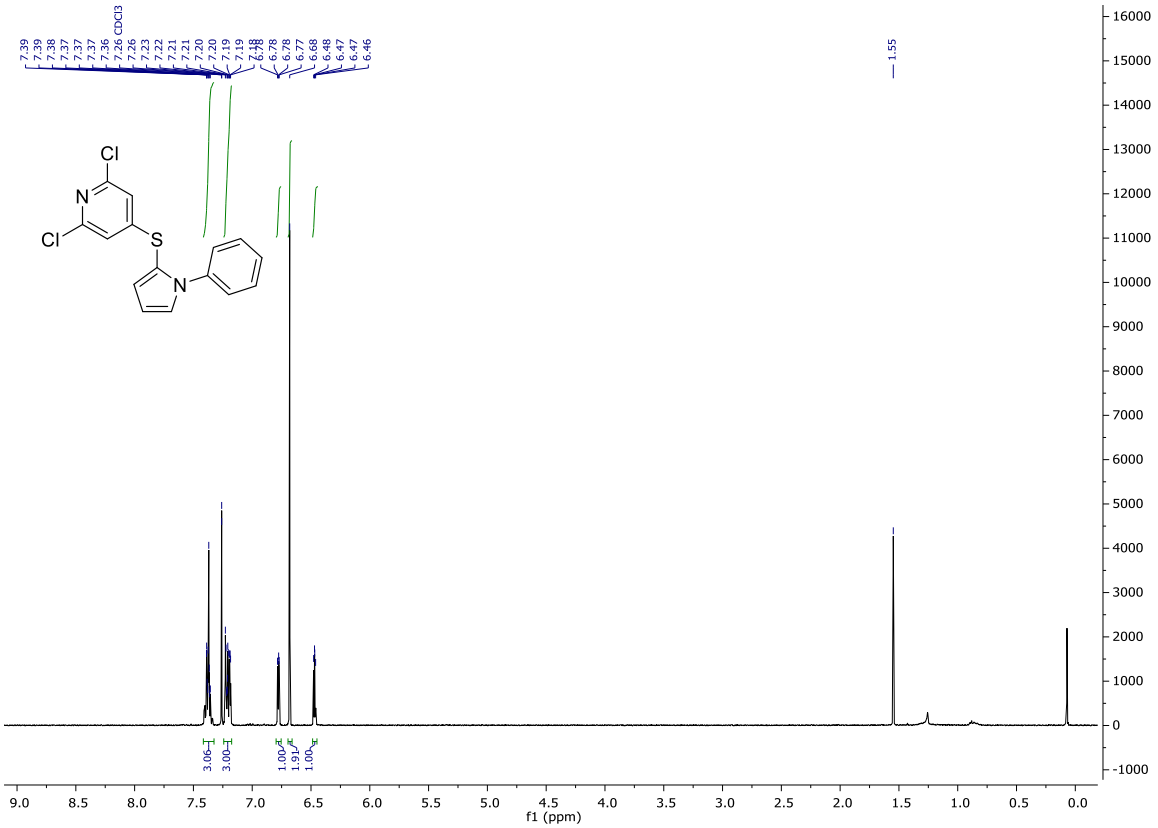

^{13}C NMR (101 MHz, $CDCl_3$) **173**

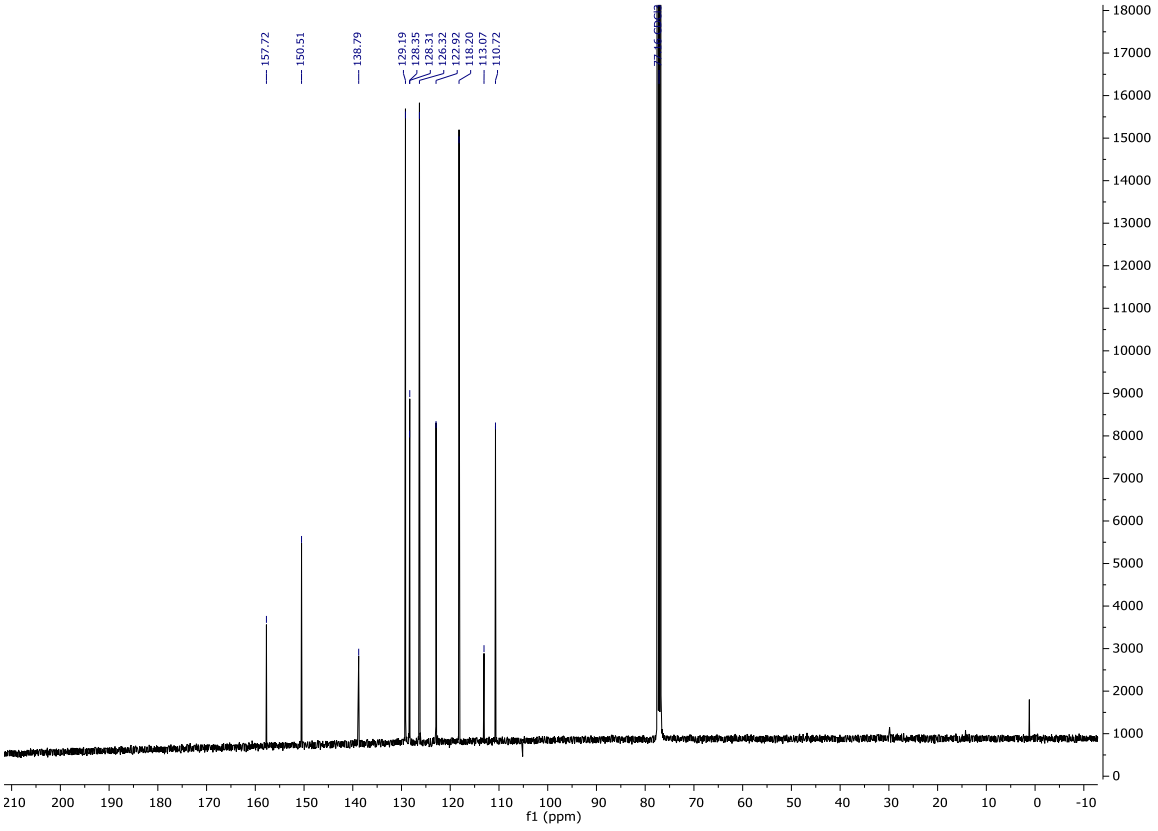

^{1}H NMR (300 MHz, CD_2Cl_2) **184**

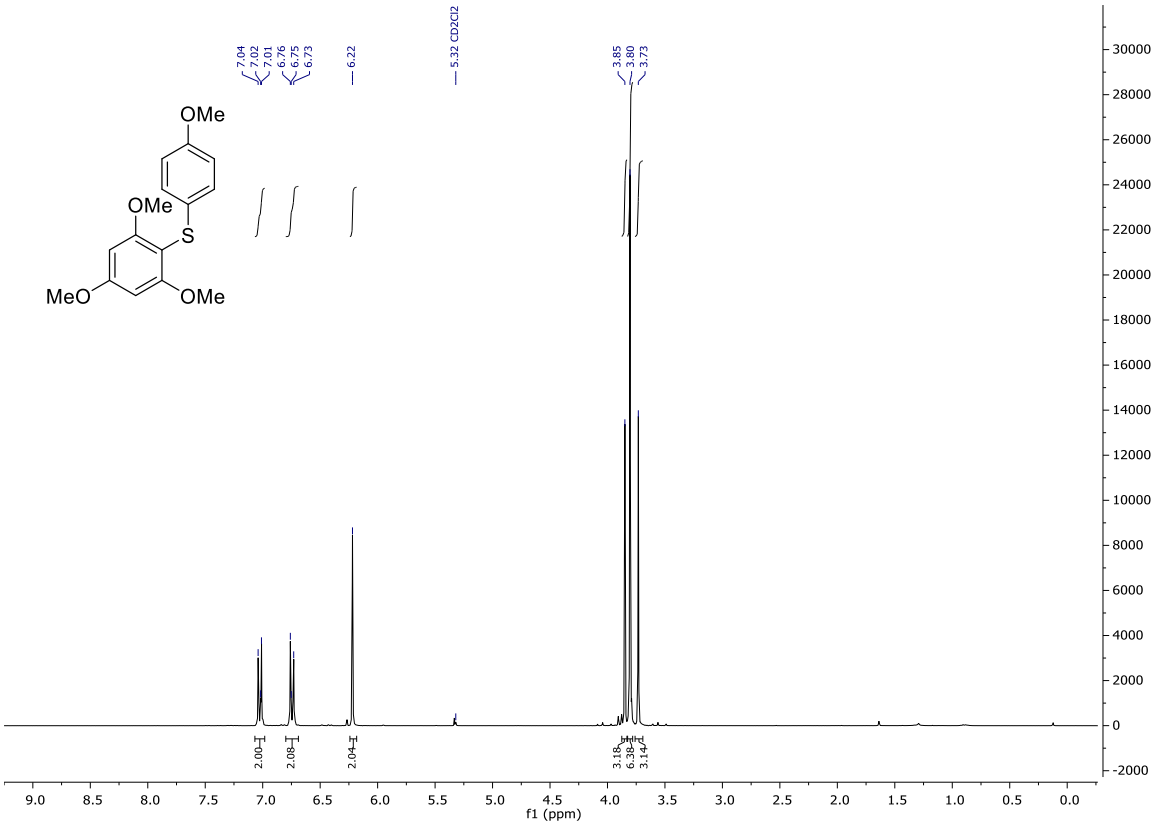

^{13}C NMR (101 MHz, CD_2Cl_2) **184**

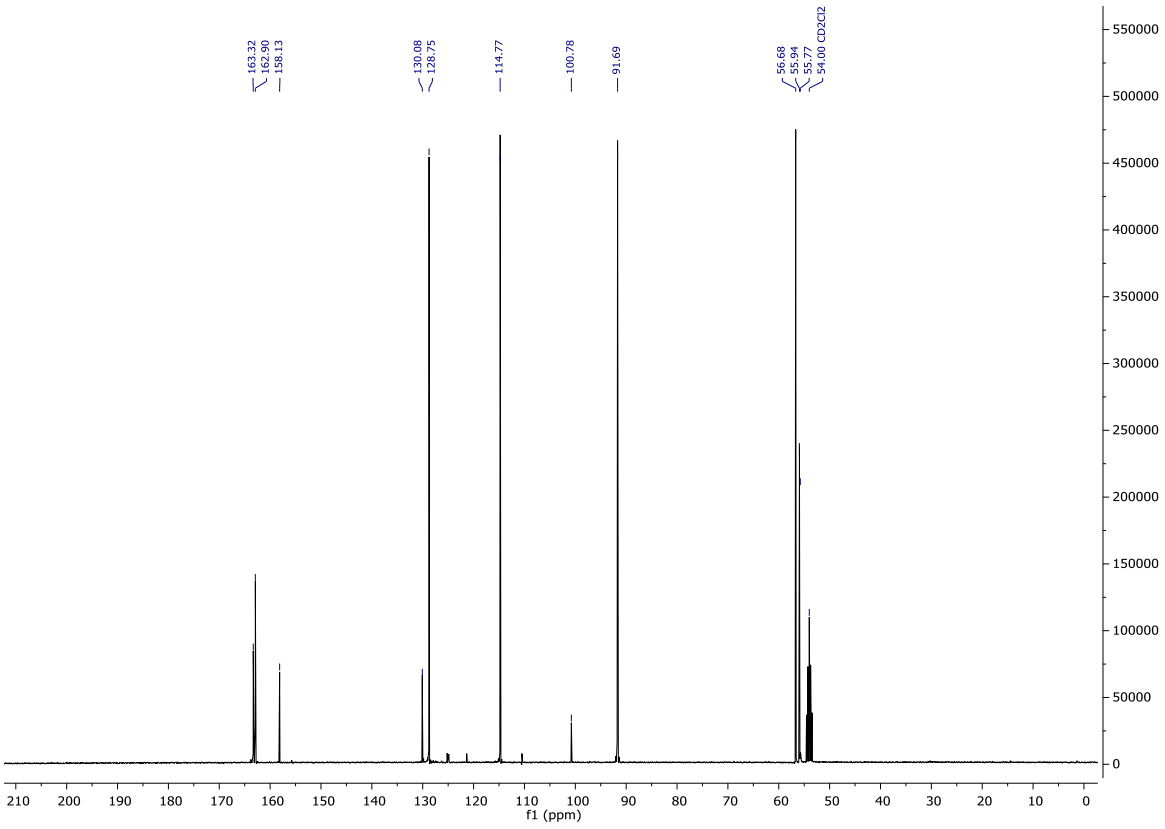

^{1}H NMR (300 MHz, $CDCl_3$) **88**

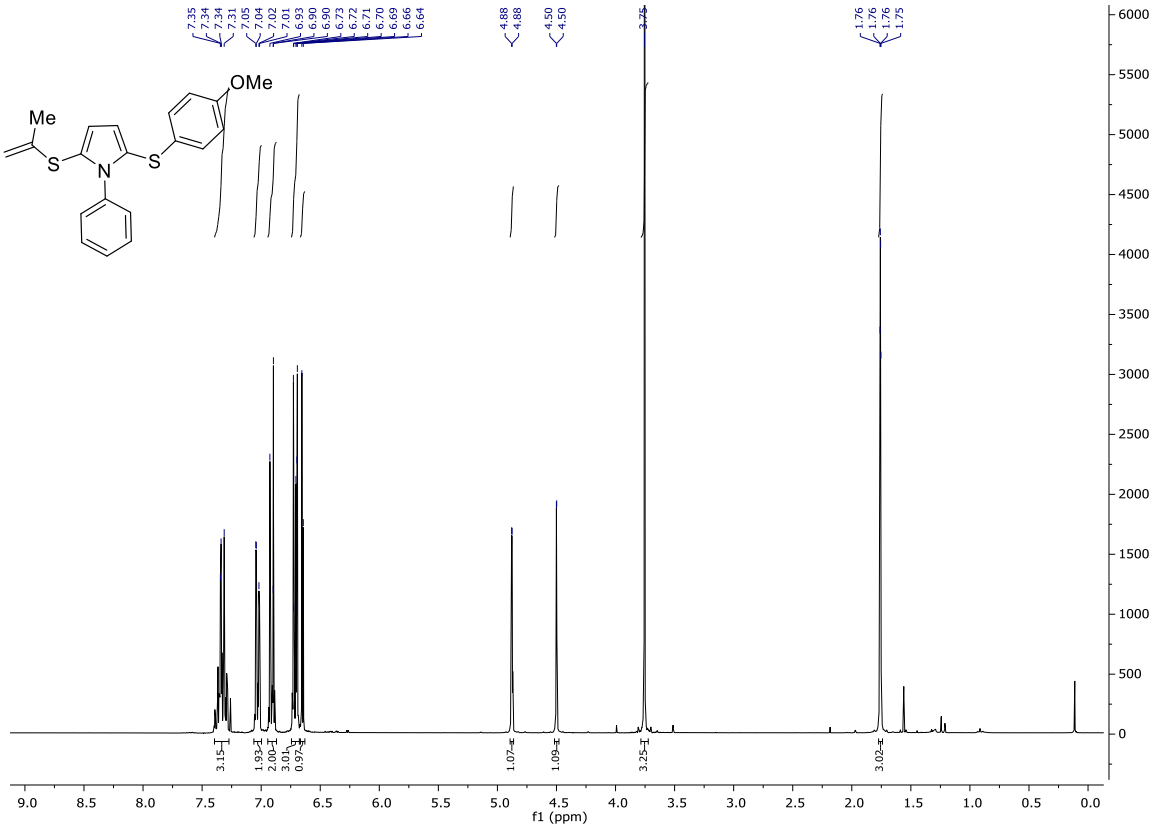

^{13}C NMR (101 MHz, CD_2Cl_2) **88**

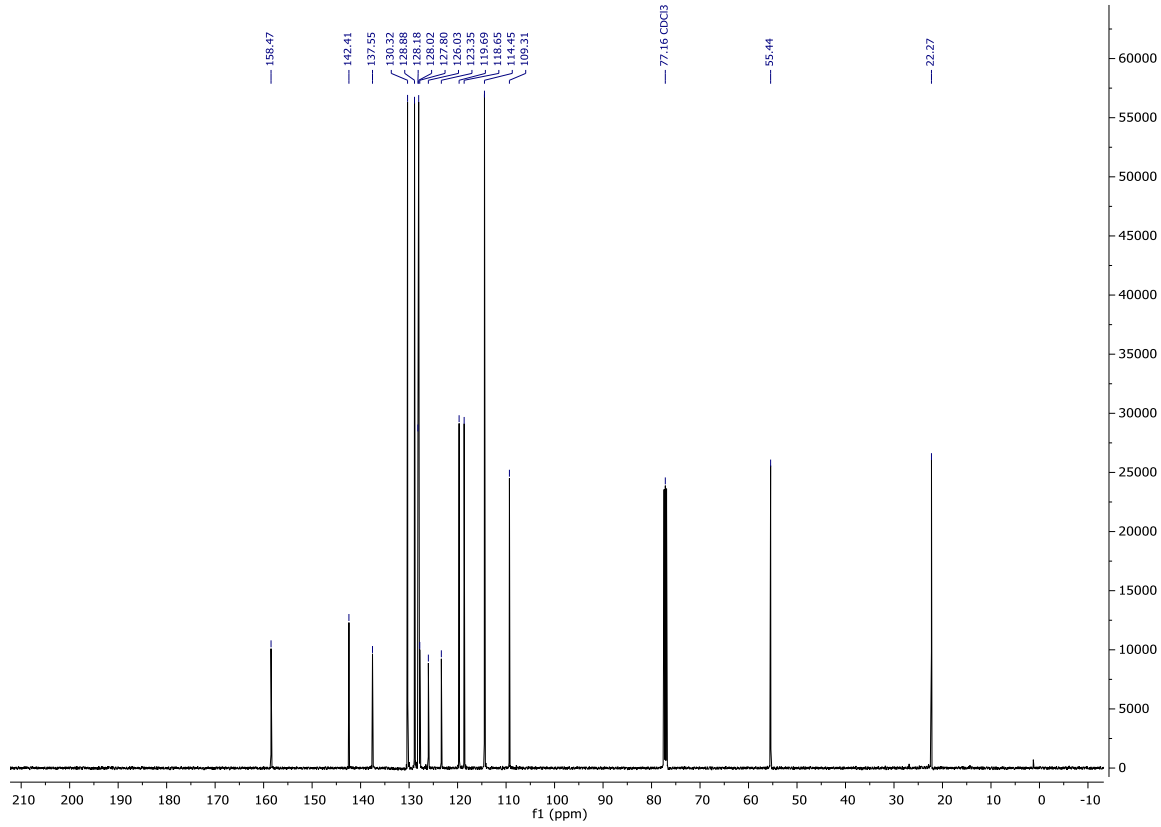

^{1}H NMR (400 MHz, $CDCl_3$) **86**

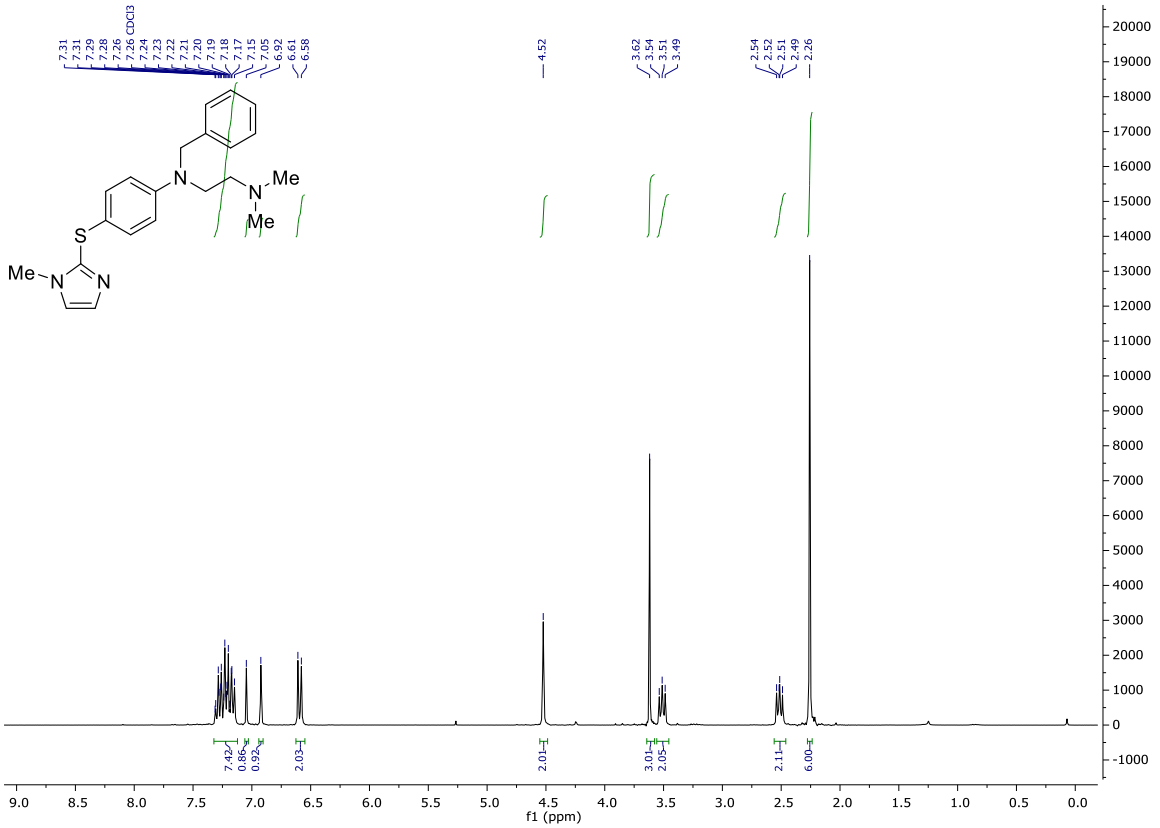

^{13}C NMR (101 MHz, $CDCl_3$) **86**

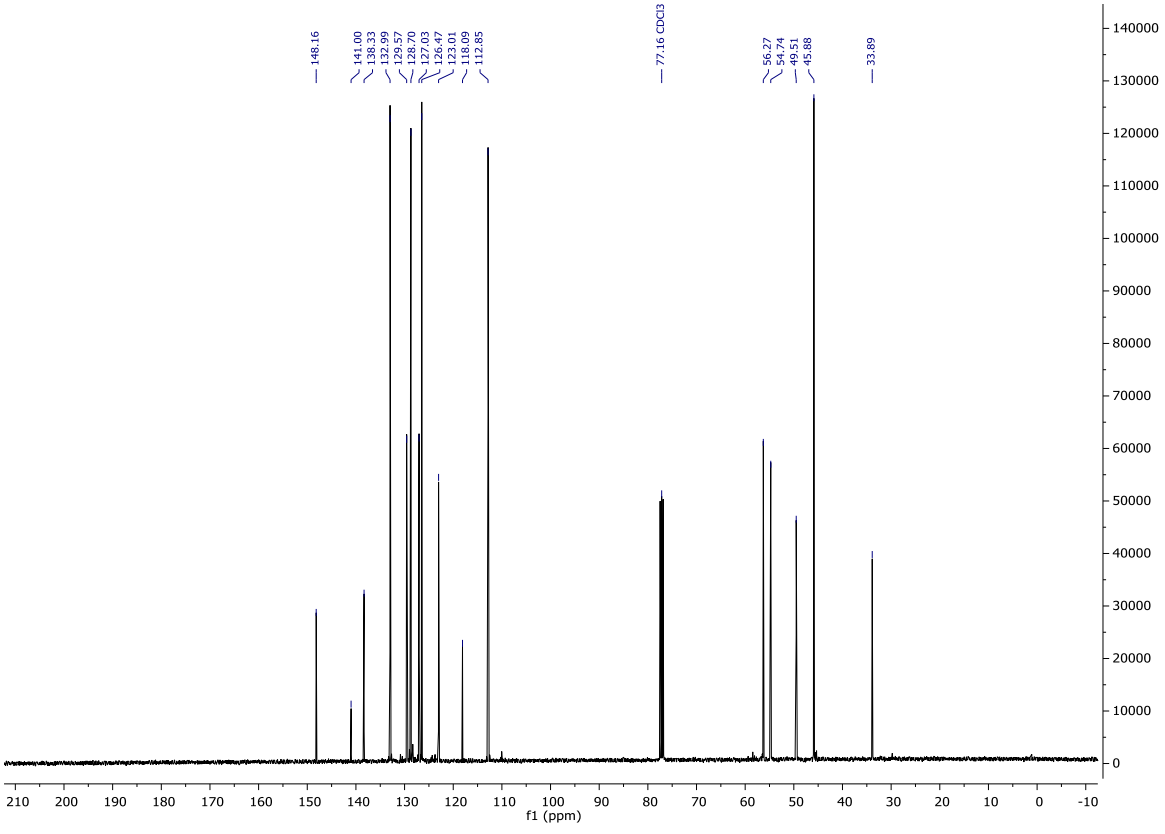

Synthesis of arylselenoimidazolium salts

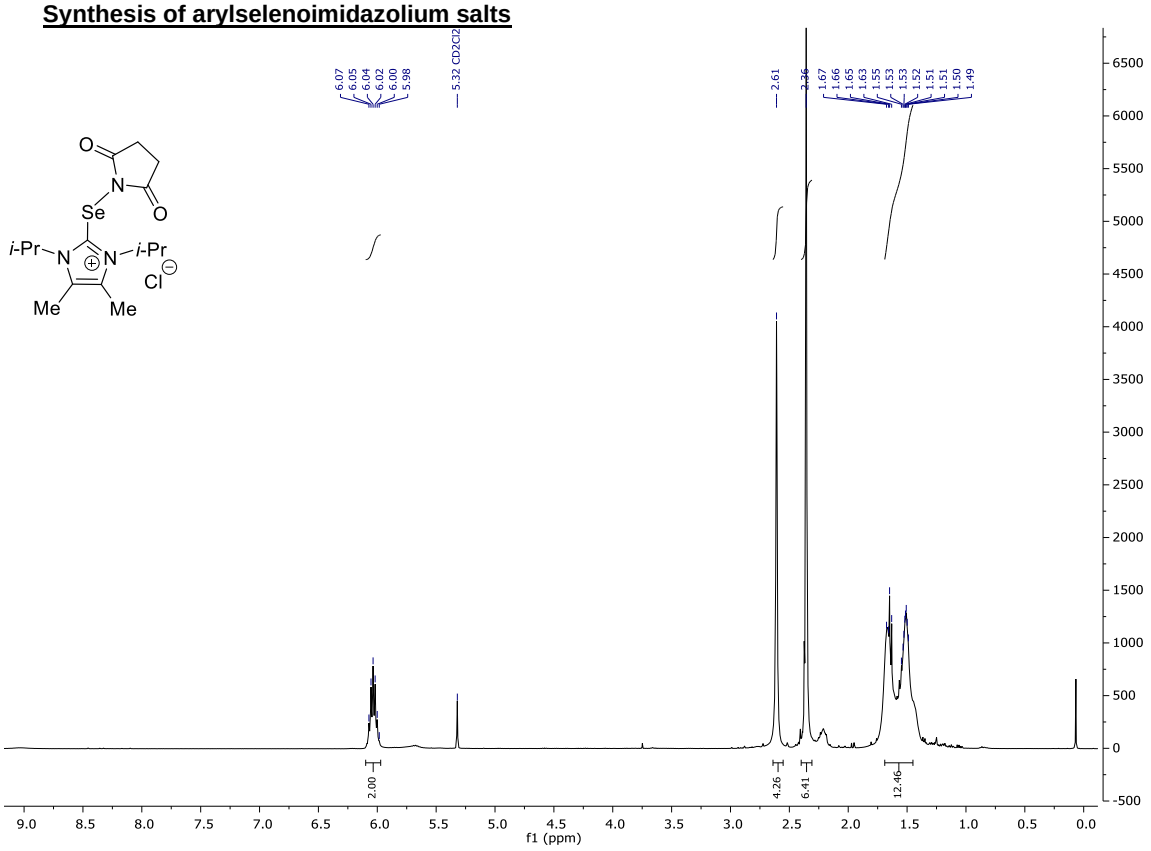

^{13}C NMR (101 MHz, CD_2Cl_2) **214**

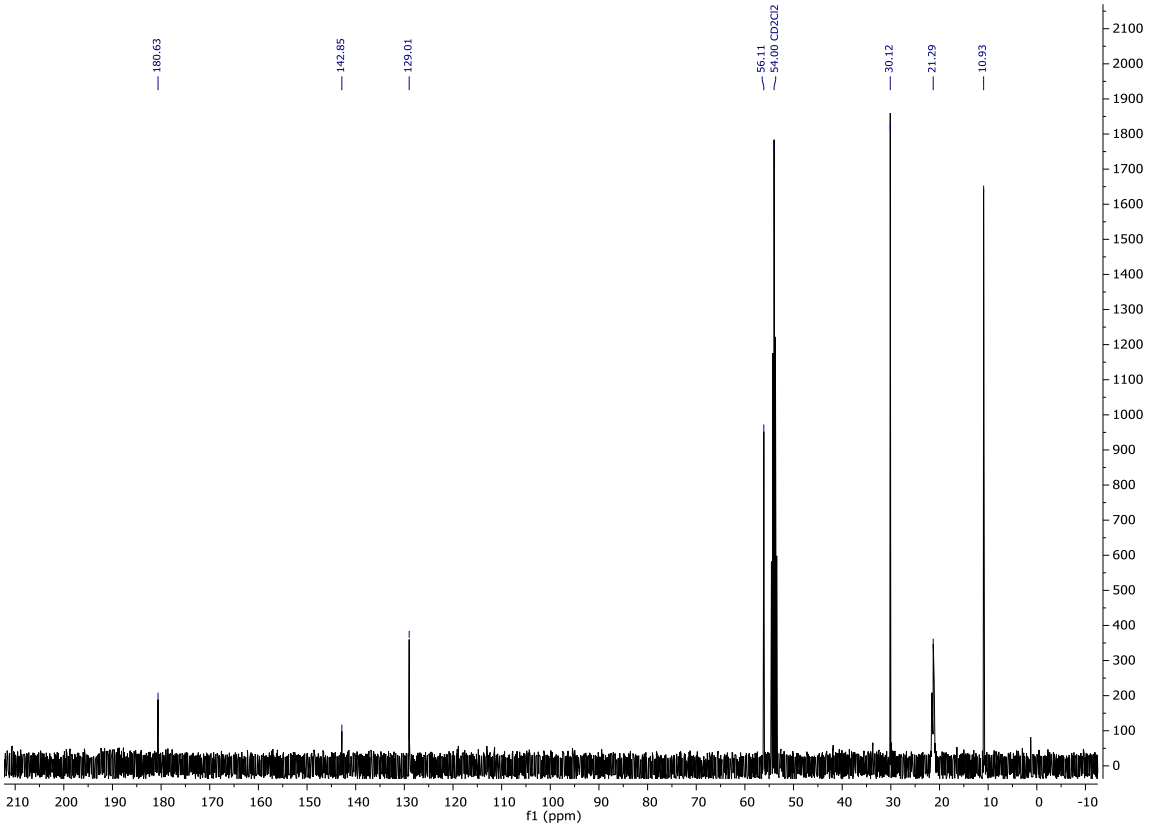

^{1}H NMR (300 MHz, CD_2Cl_2) **215**

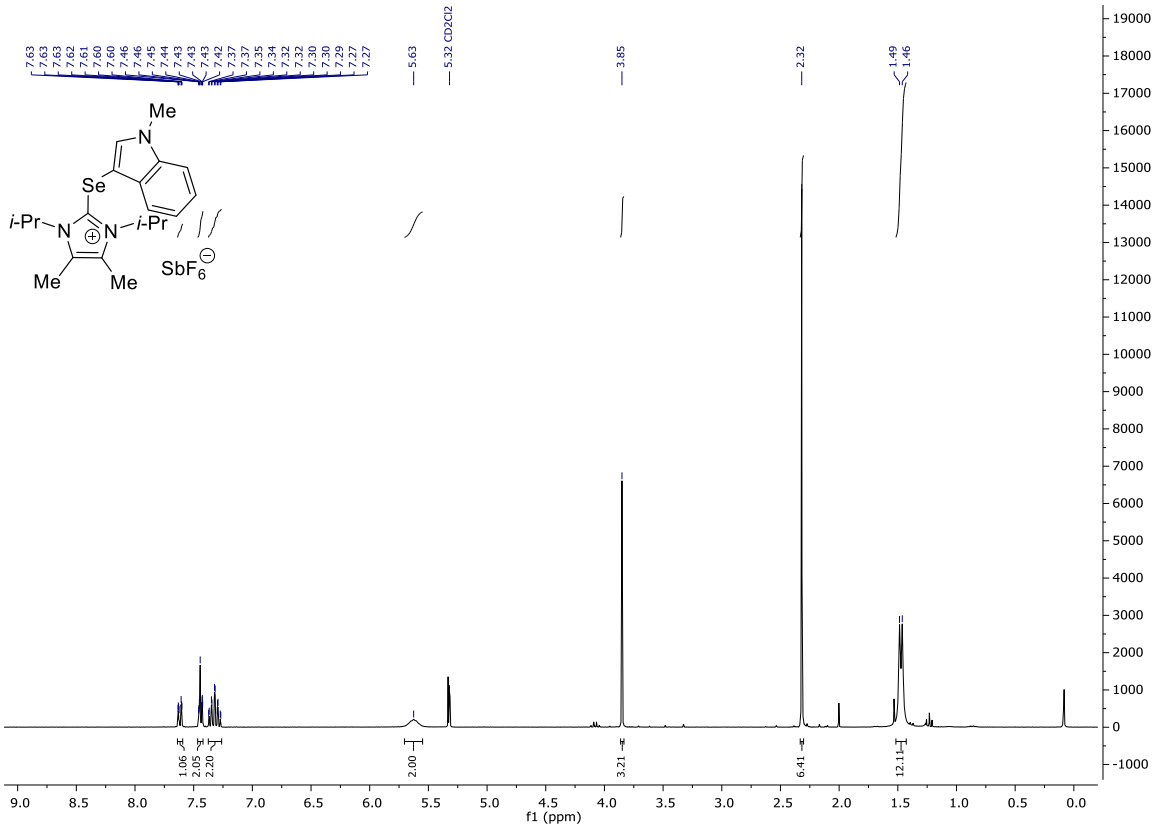

^{13}C NMR (75 MHz, CD_2Cl_2) **215**

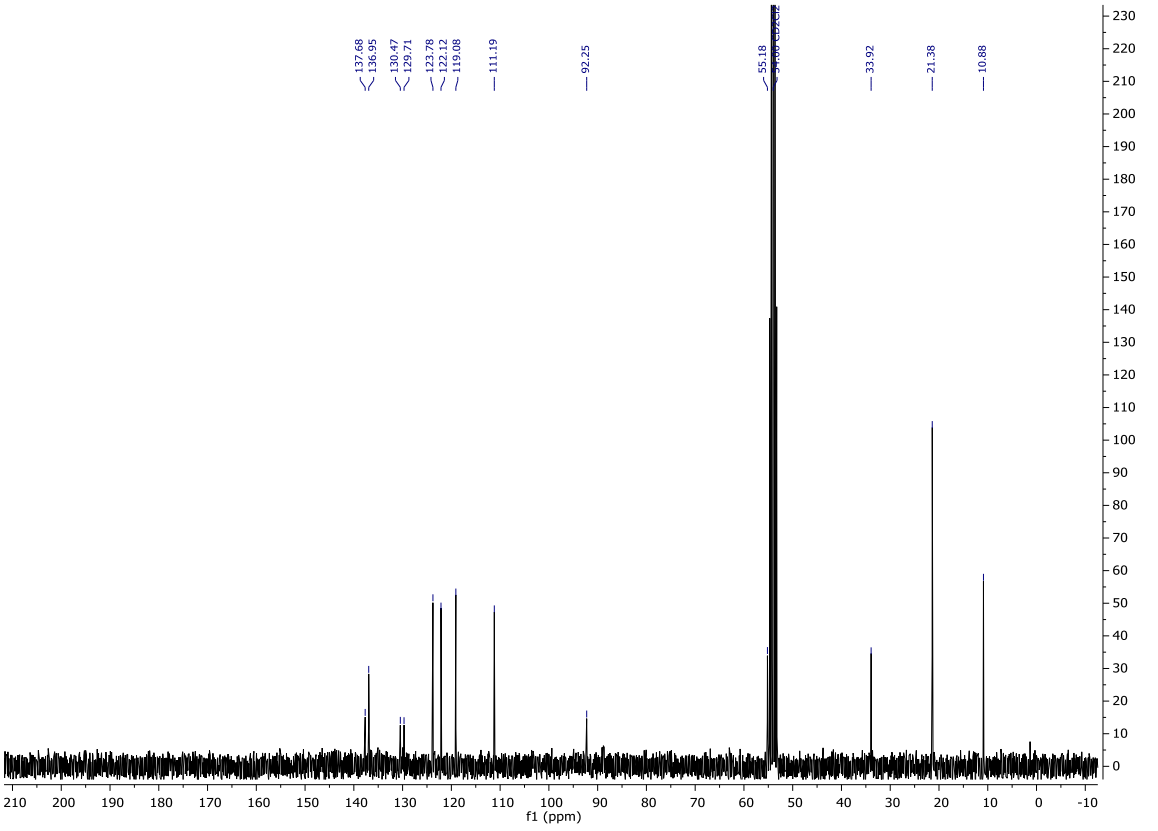

^{1}H NMR (300 MHz, CD_2Cl_2) **216**

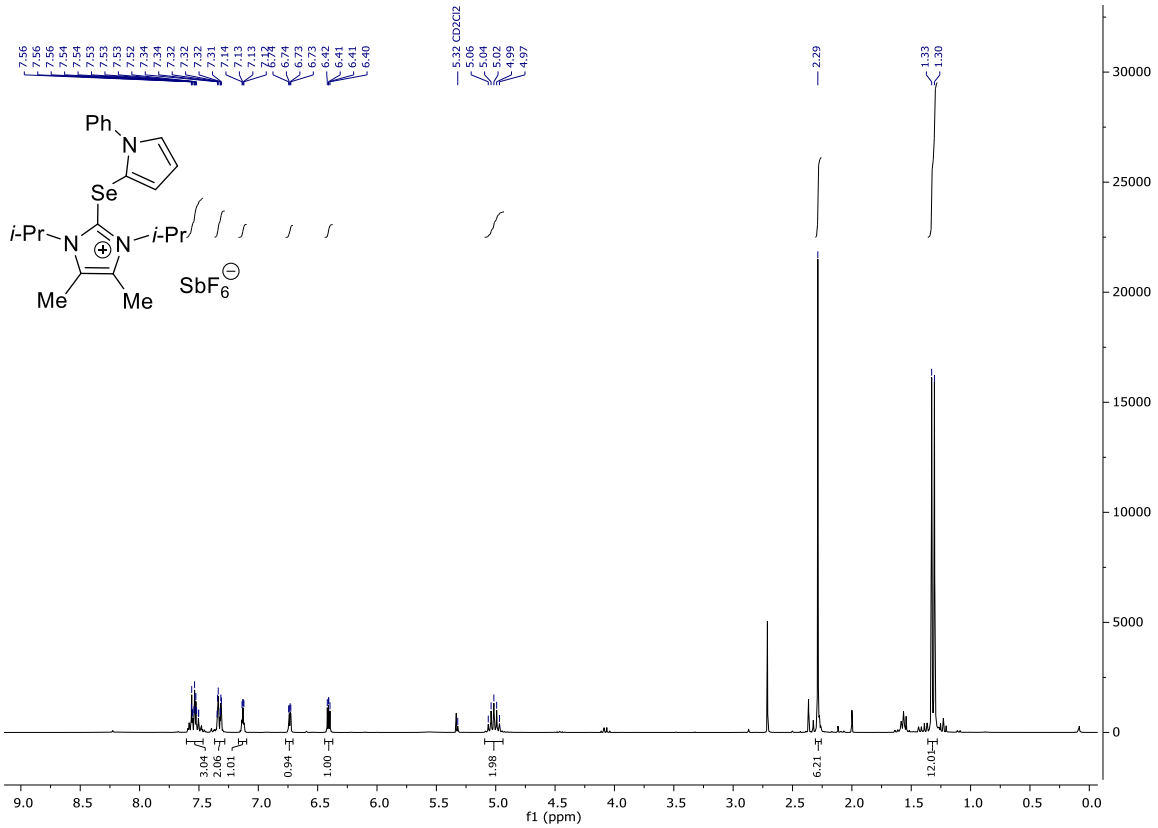

^{13}C NMR (75 MHz, CD_2Cl_2) **216**

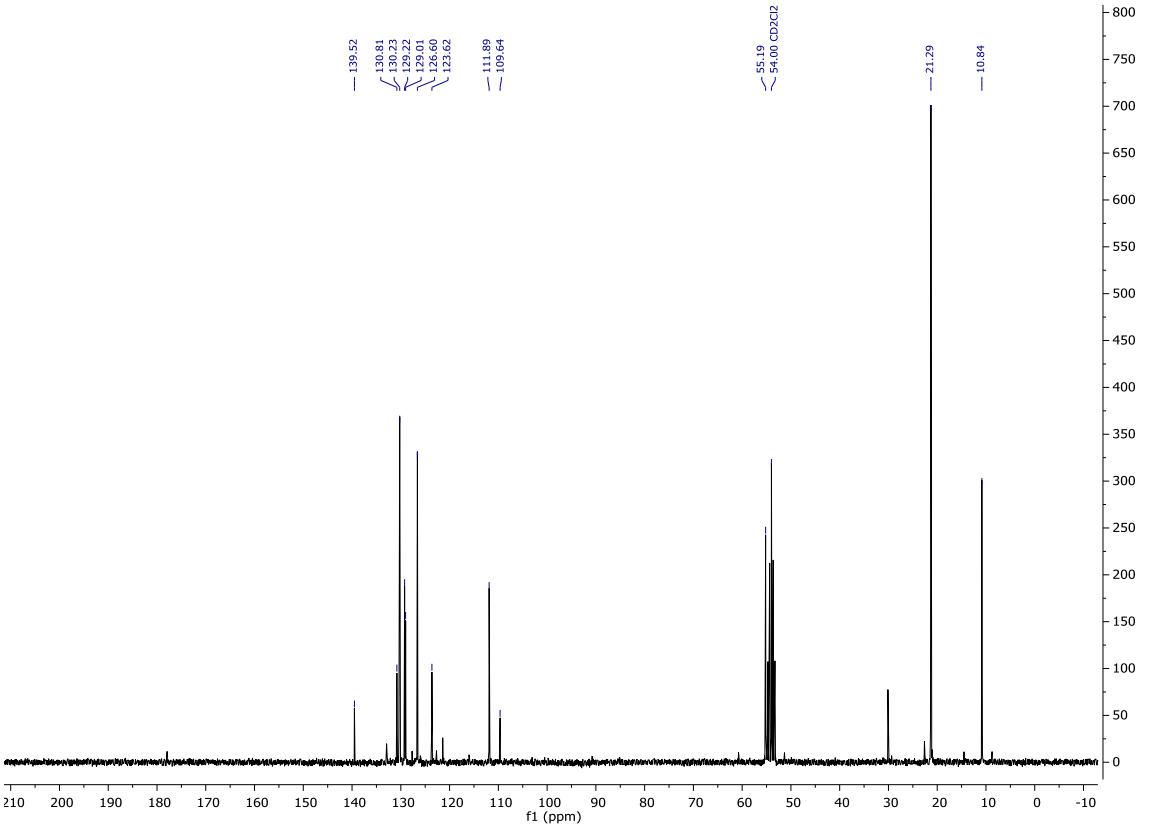

^{1}H NMR (300 MHz, CD_2Cl_2) **217**

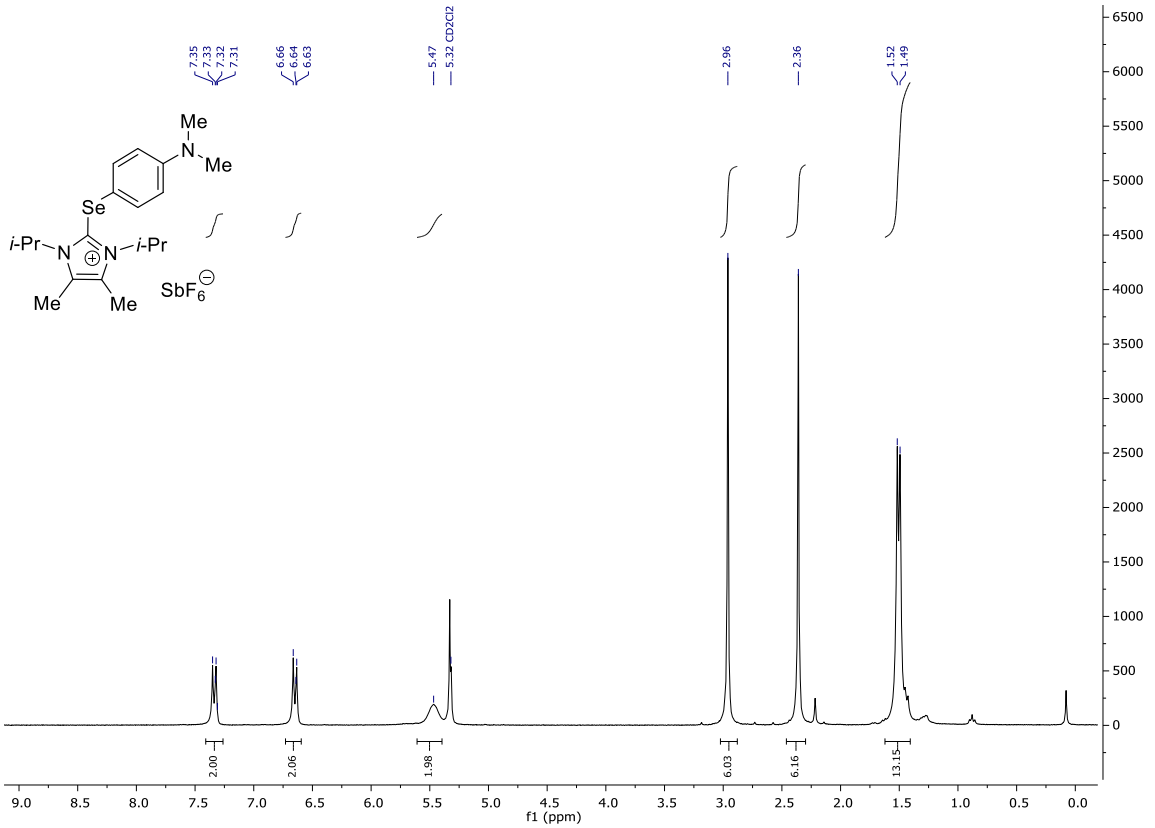

^{13}C NMR (101 MHz, CD_2Cl_2) **217**

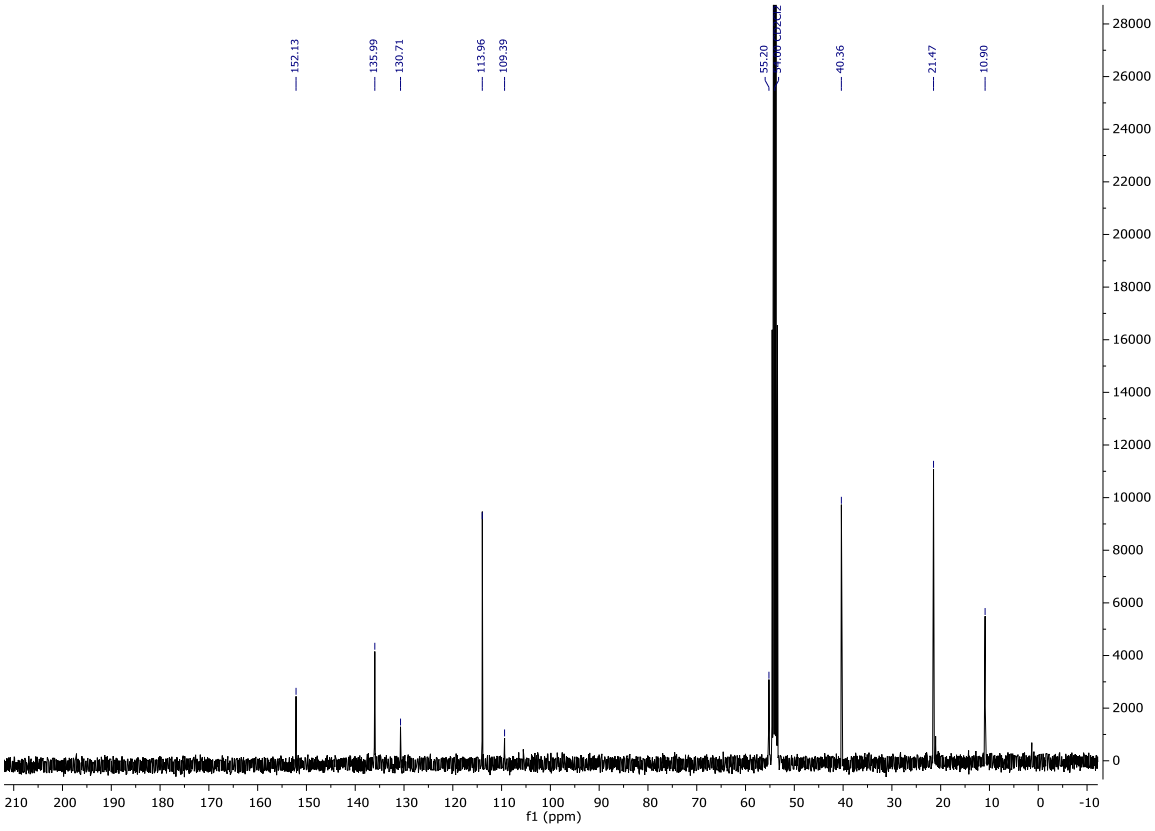

Synthesis of unsymmetrical selenides

^{1}H NMR (300 MHz, CD_2Cl_2) **218**

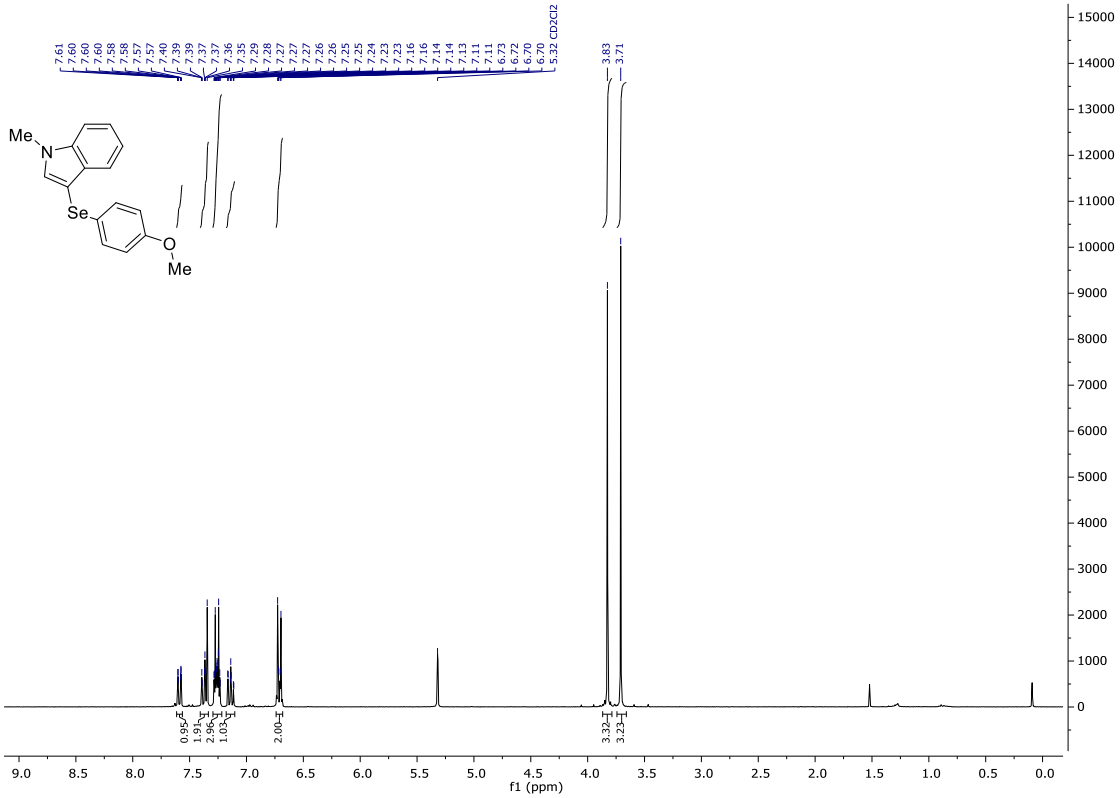

^{13}C NMR (101 MHz, CD_2Cl_2) **218**

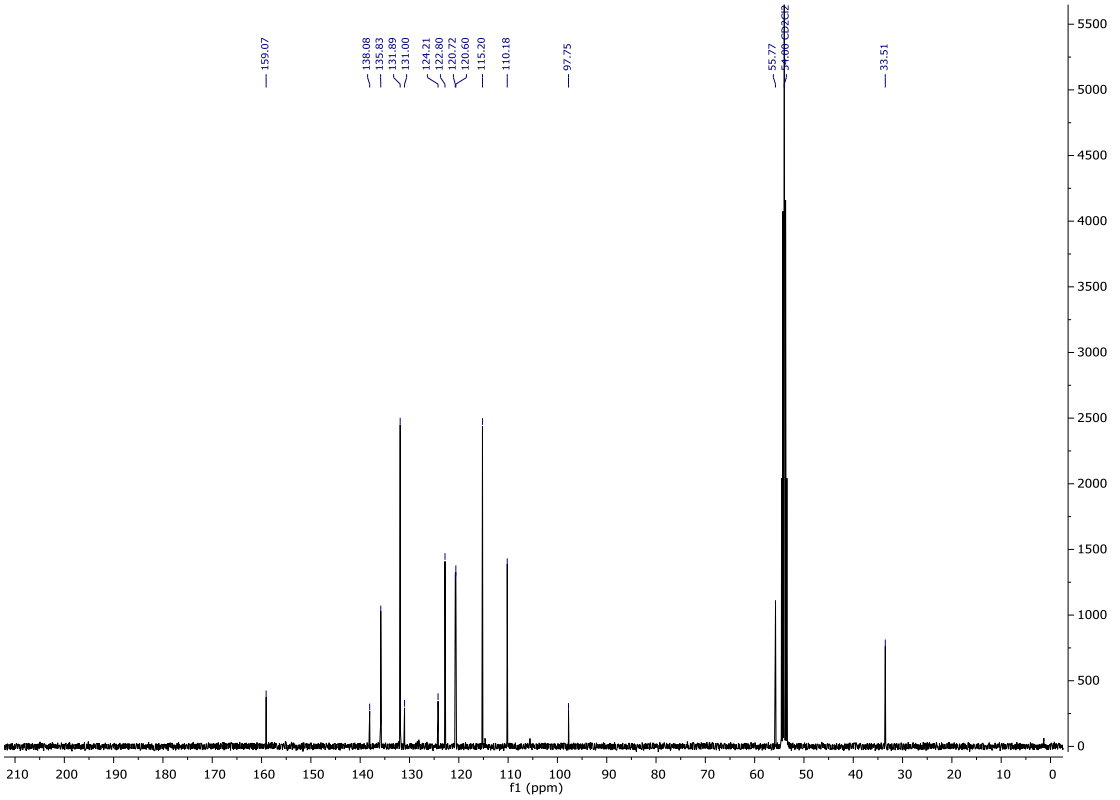

^{77}Se NMR (76 MHz, CD_2Cl_2 ppm) **218**

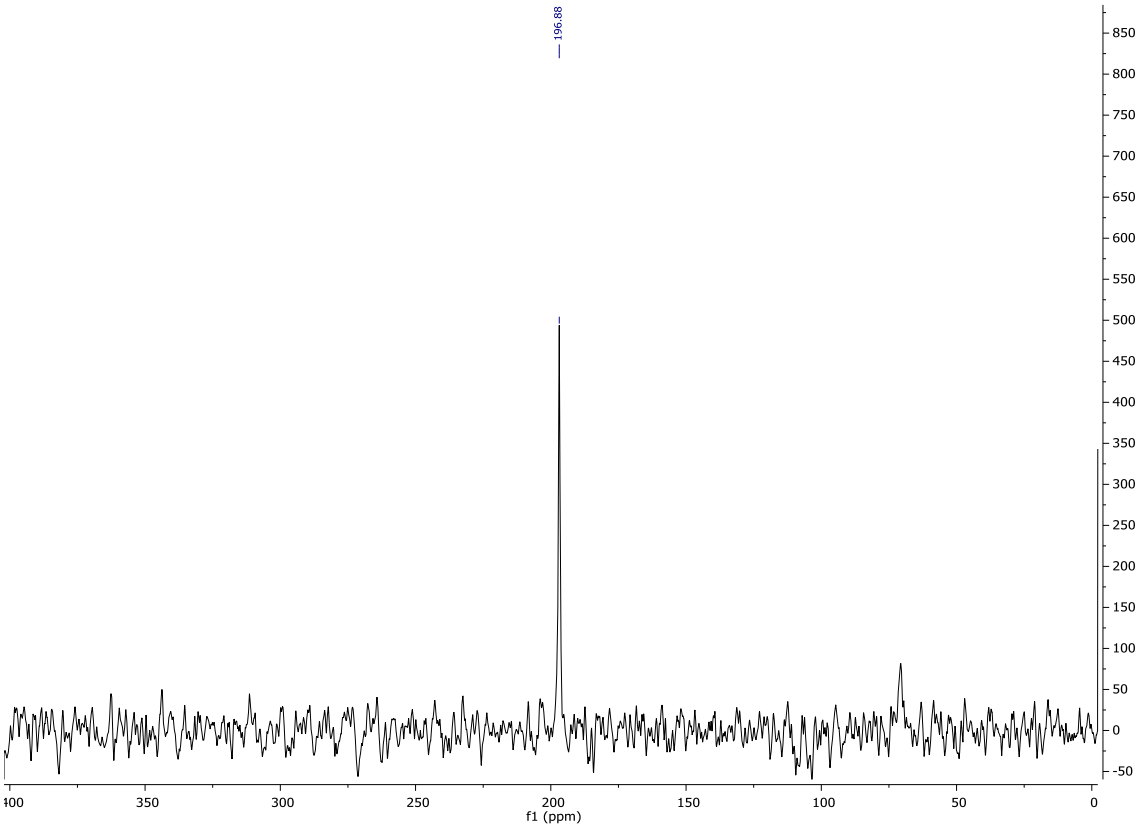

^{1}H NMR (300 MHz, CD_2Cl_2) **219**

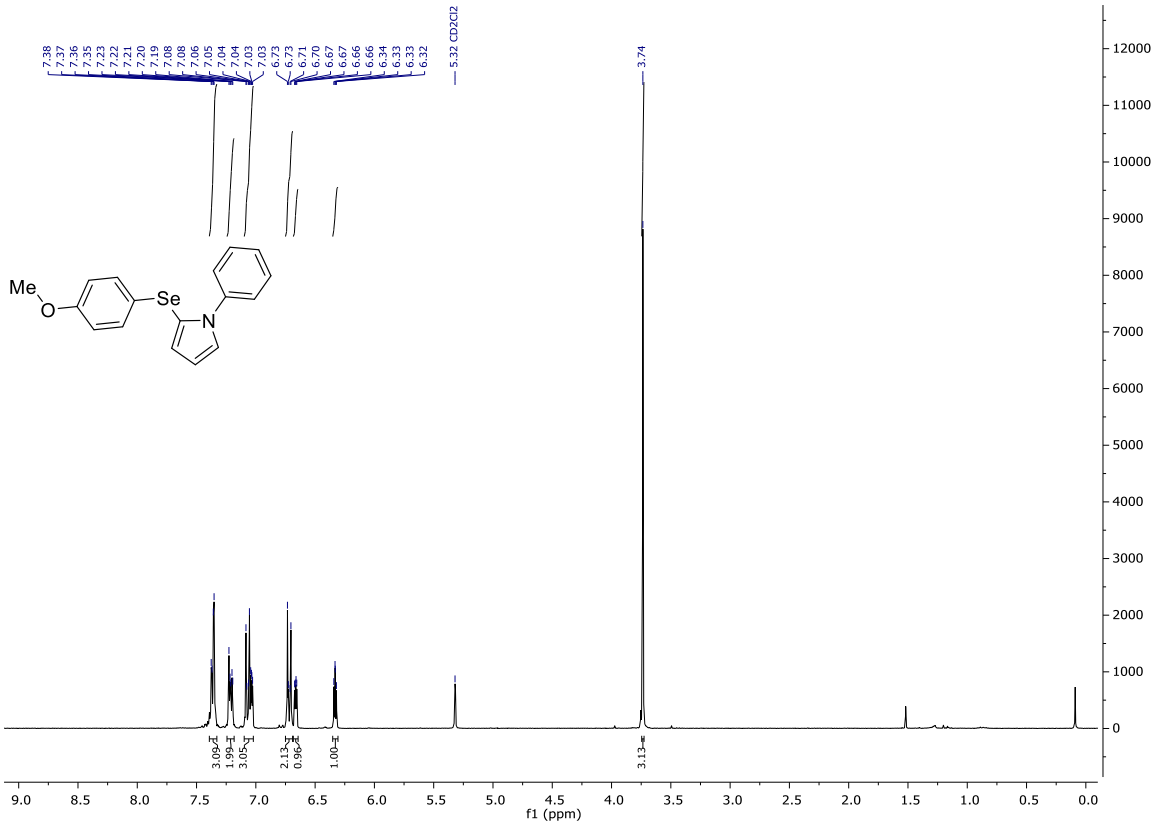

^{13}C NMR (101 MHz, CD_2Cl_2) **219**

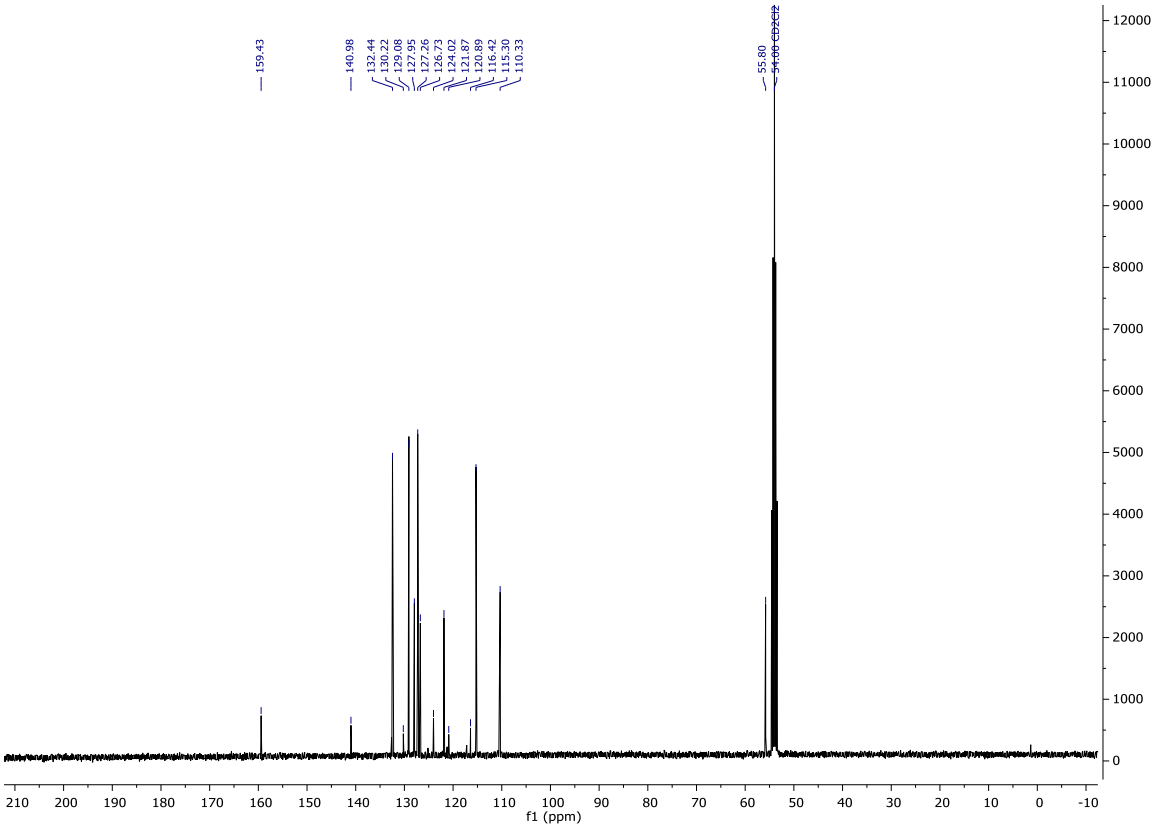

^{77}Se NMR (76 MHz, CD_2Cl_2 ppm) **219**

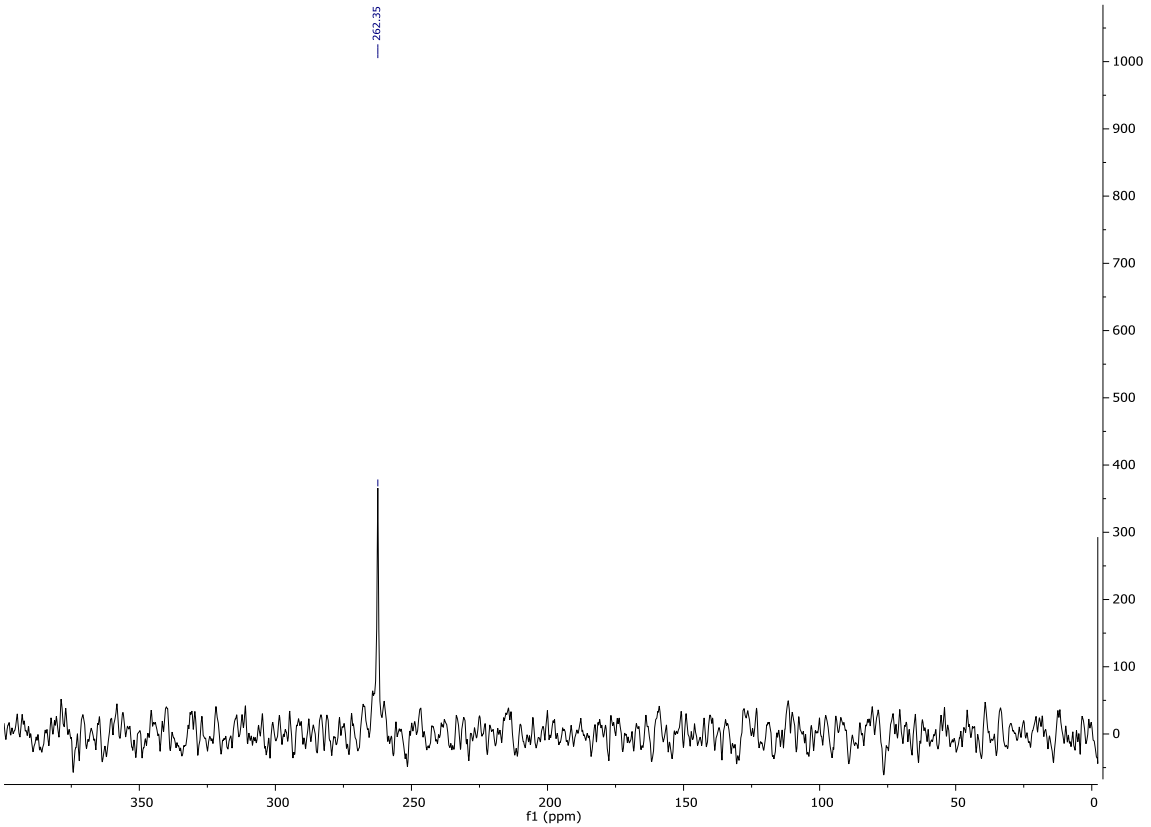

^{1}H NMR (300 MHz, $CDCl_3$) **220**

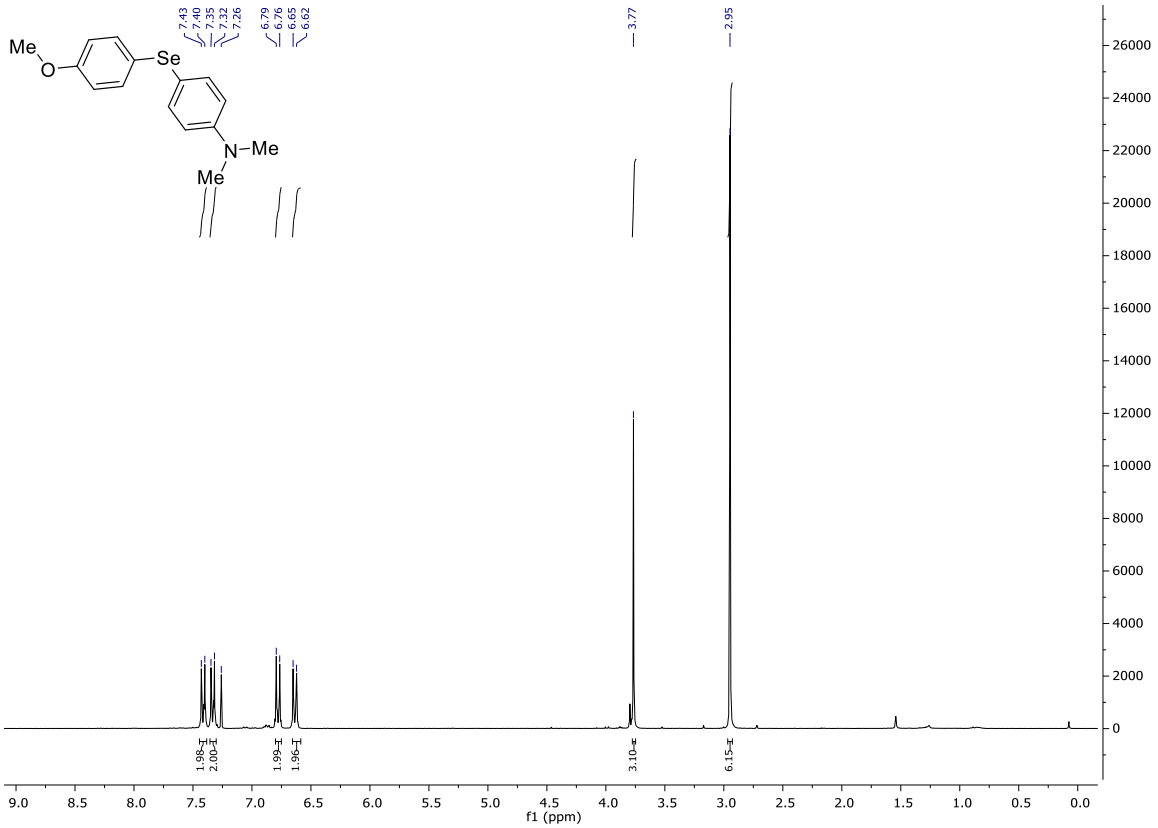

^{13}C NMR (75 MHz, CD_2Cl_2) **220**

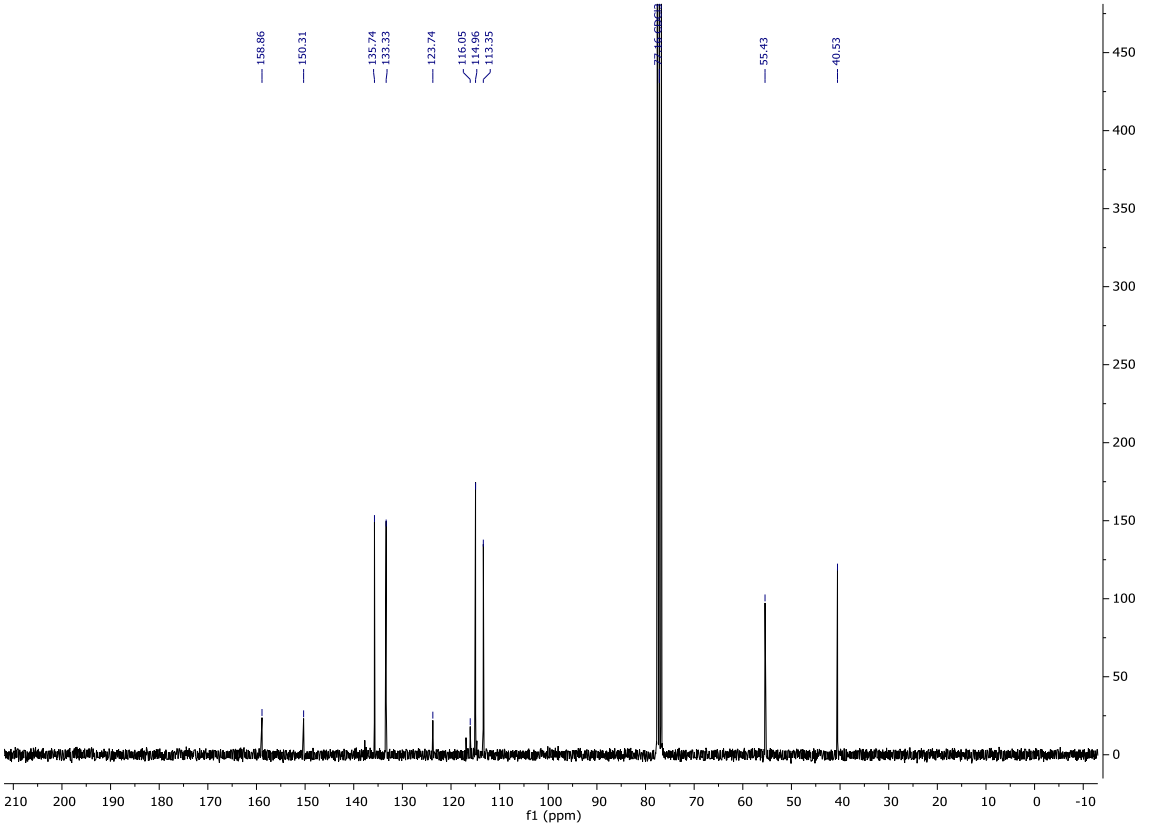

^{77}Se NMR (MHz, $CDCl_3$ ppm) **220**

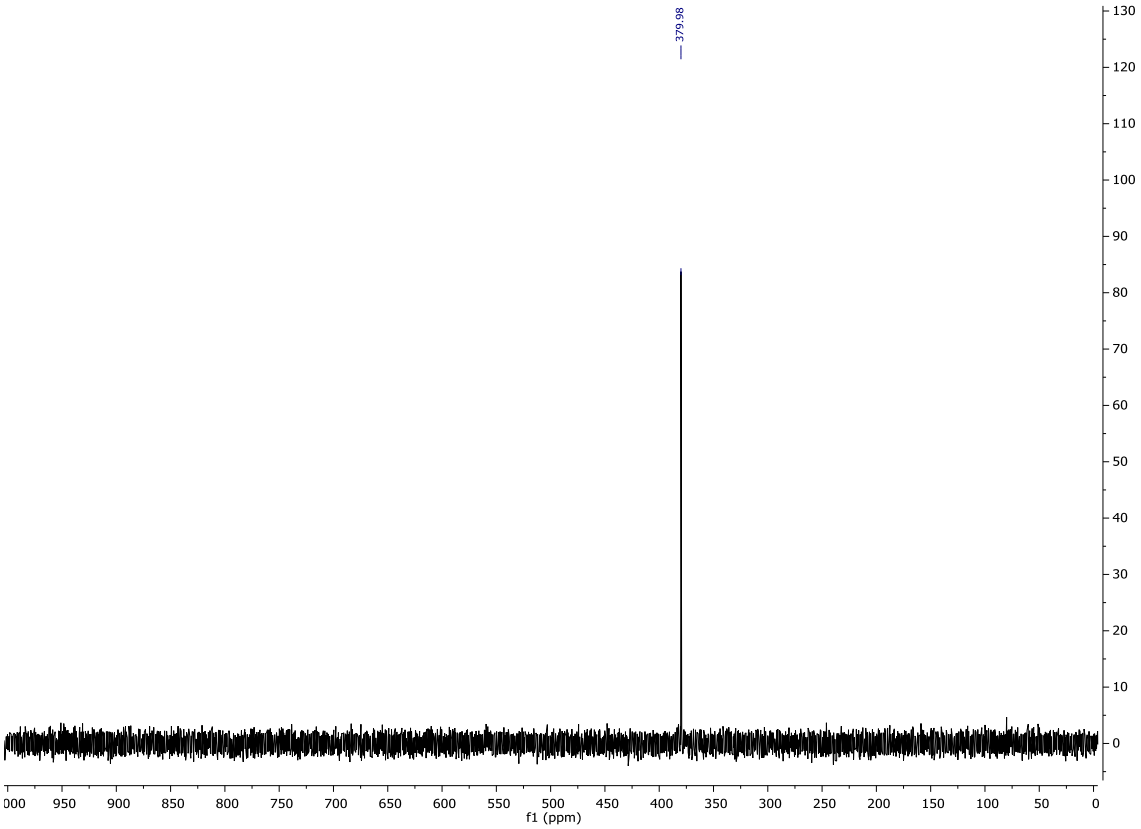

^{1}H NMR (300 MHz, CD_2Cl_2) **221**

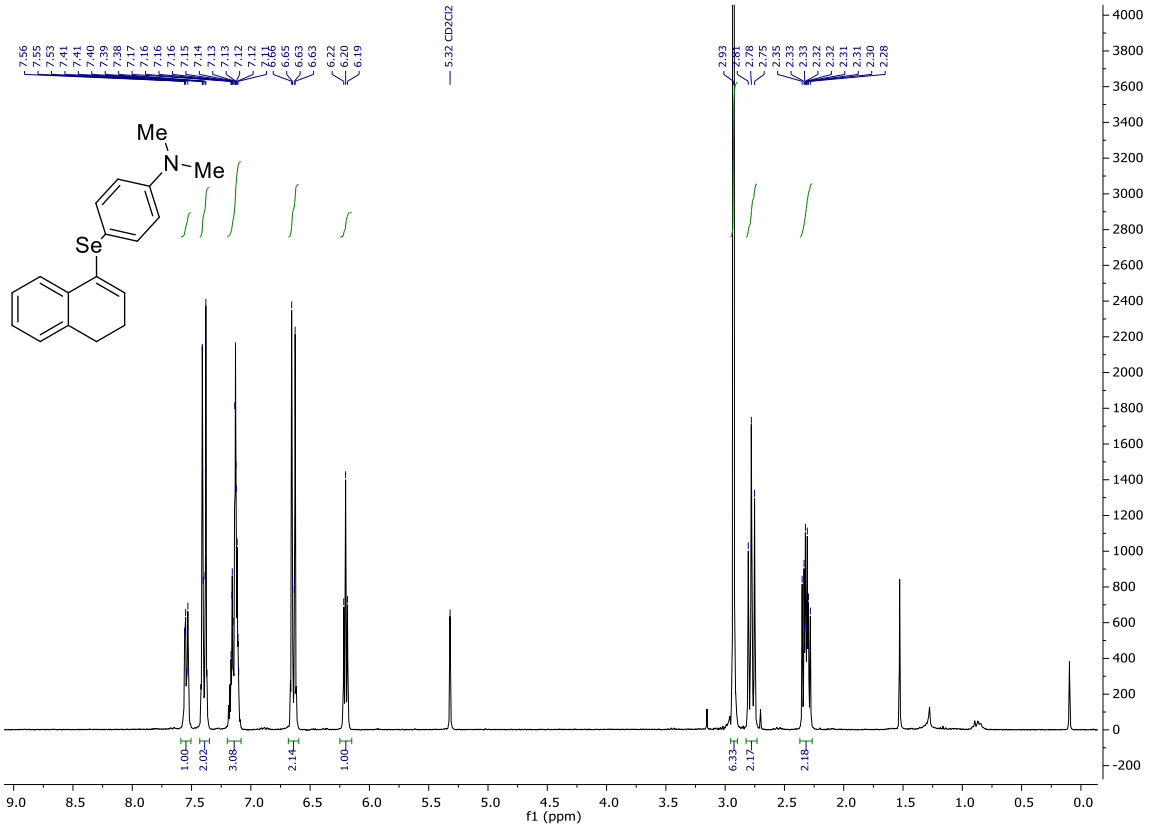

^{13}C NMR (126 MHz, CD_2Cl_2) **221**

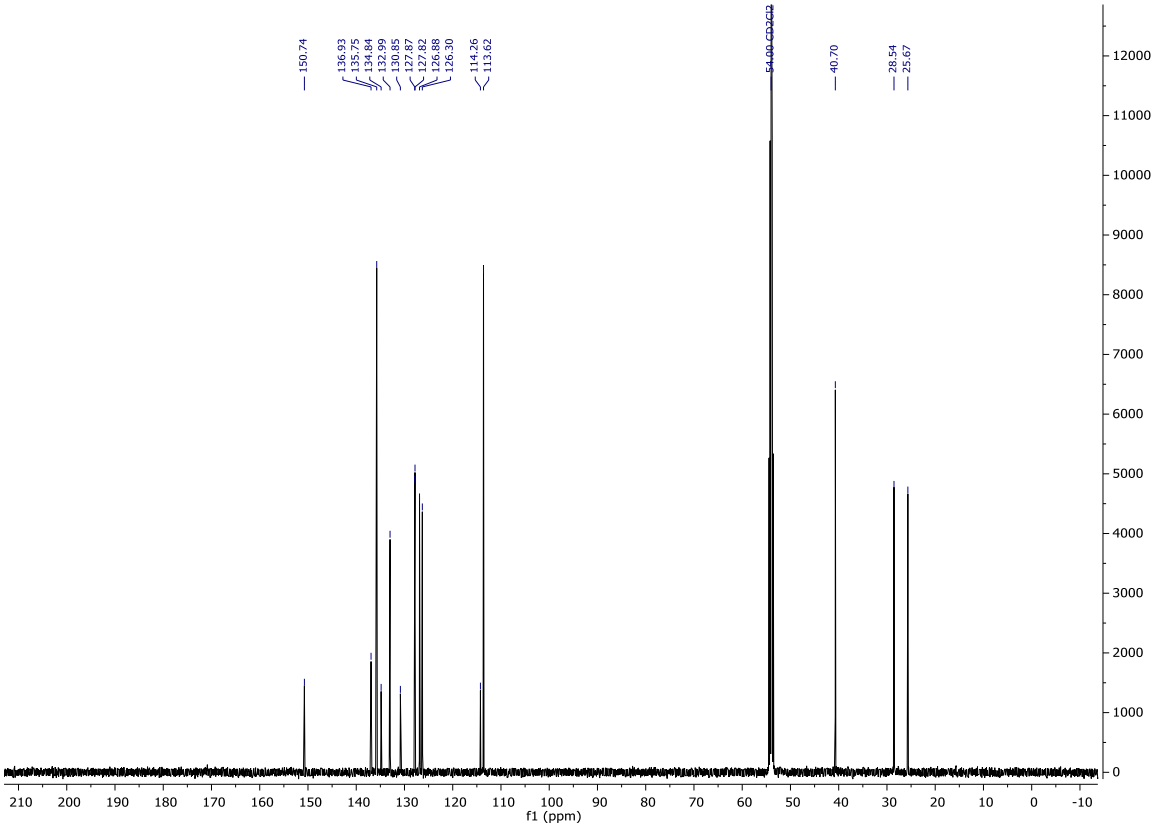

^{77}Se NMR (76 MHz, CD_2Cl_2) **221**

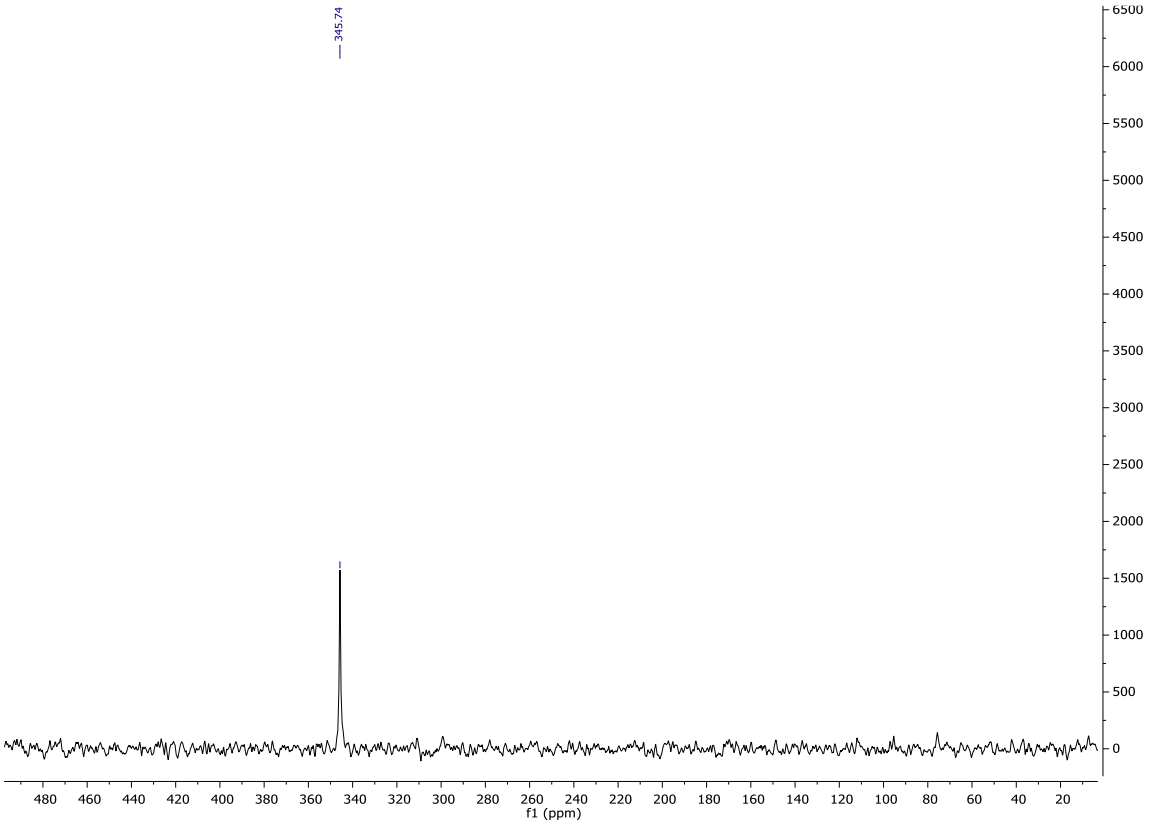

Synthesis of imidazole thioether

^{1}H NMR (400 MHz, $CDCl_3$) **231**

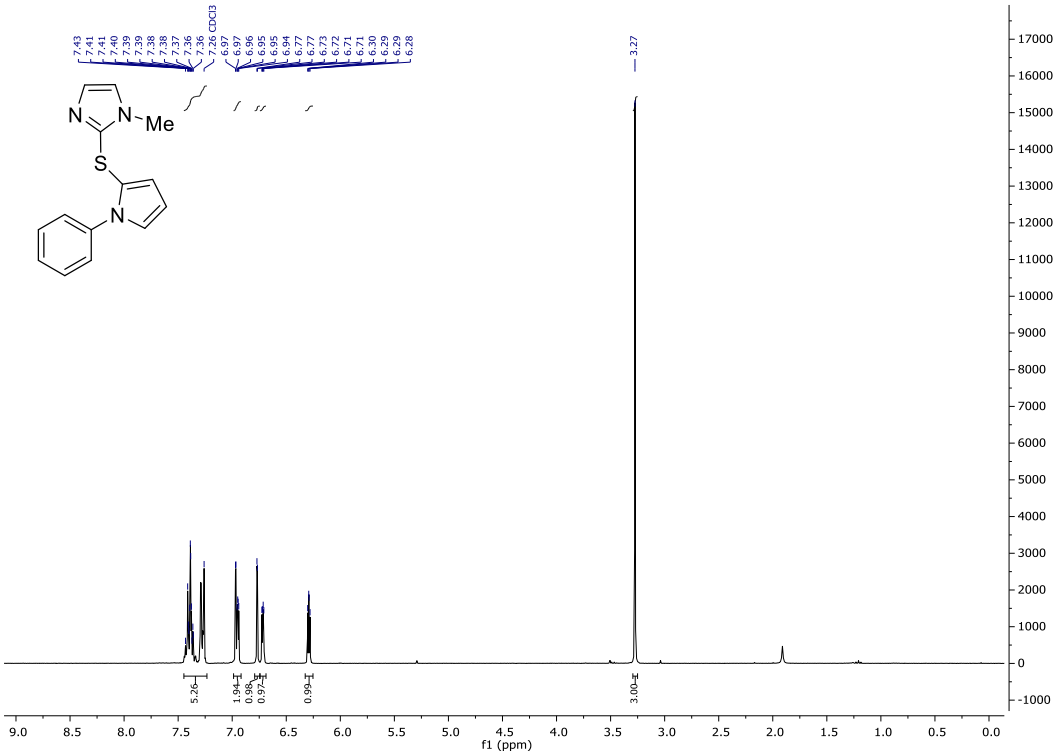

^{13}C NMR (126 MHz, $CDCl_3$) **231**

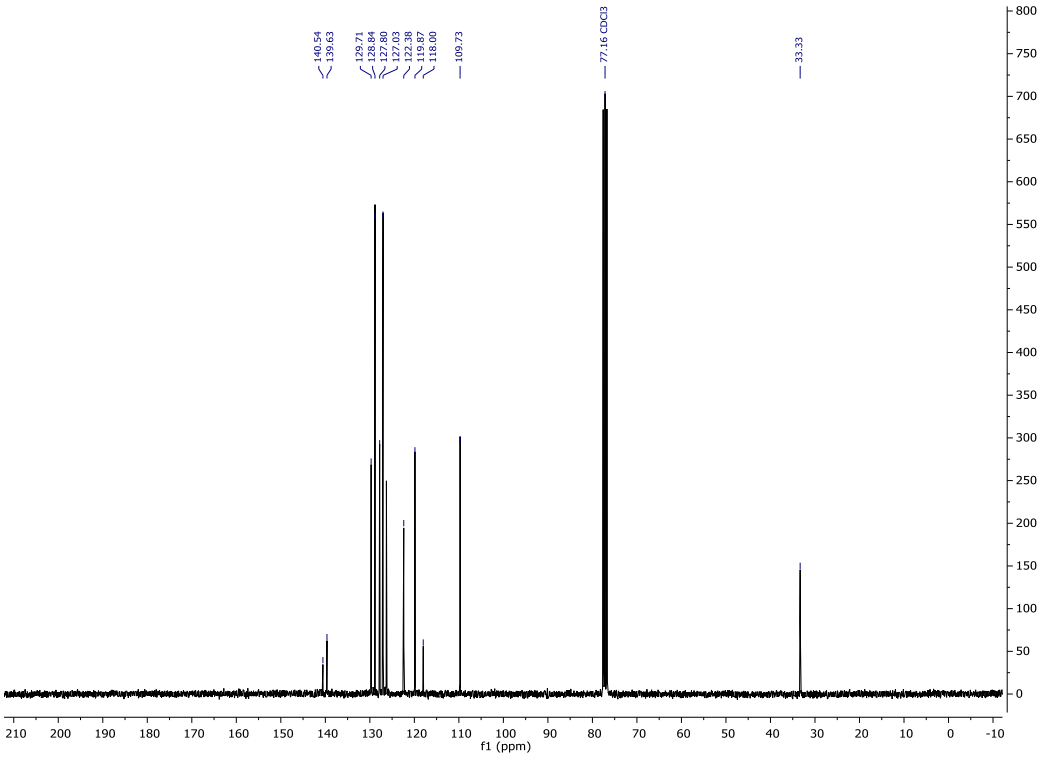

^{1}H NMR (400 MHz, CD_3CN) **237**

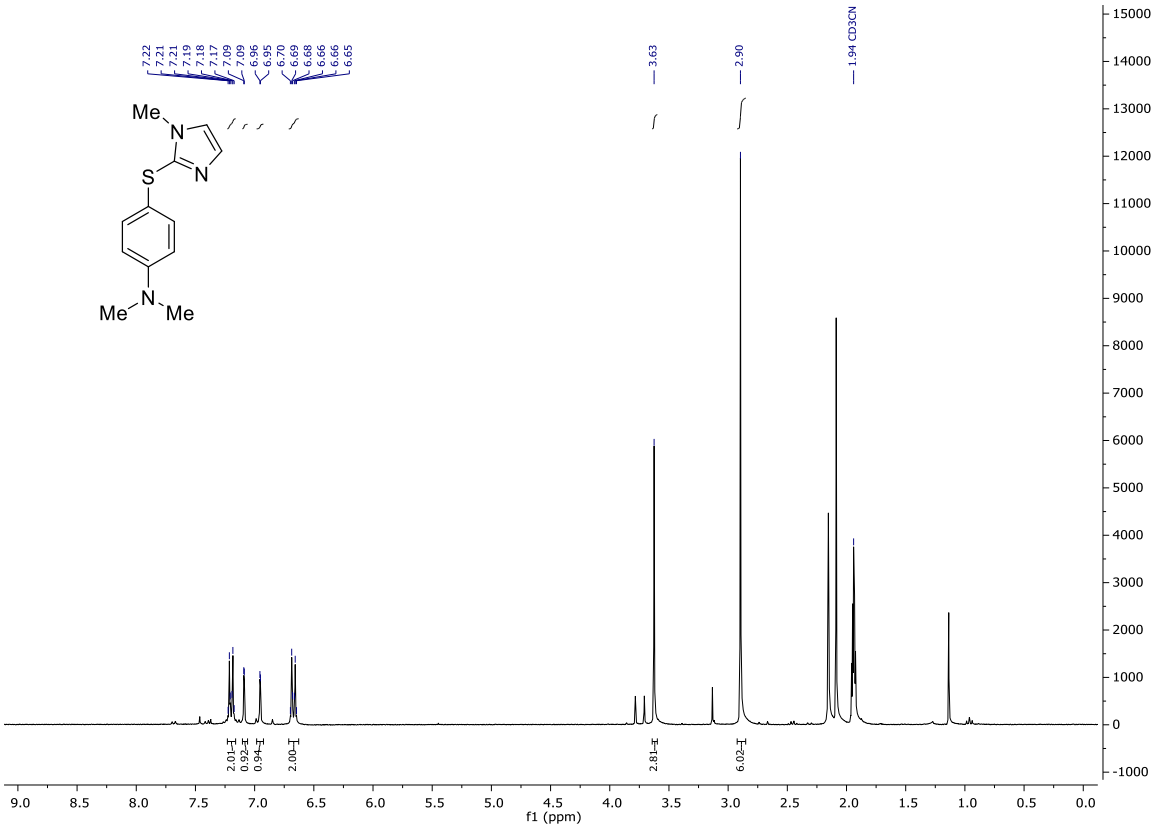

^{13}C NMR (126 MHz, CD_3CN) **237**

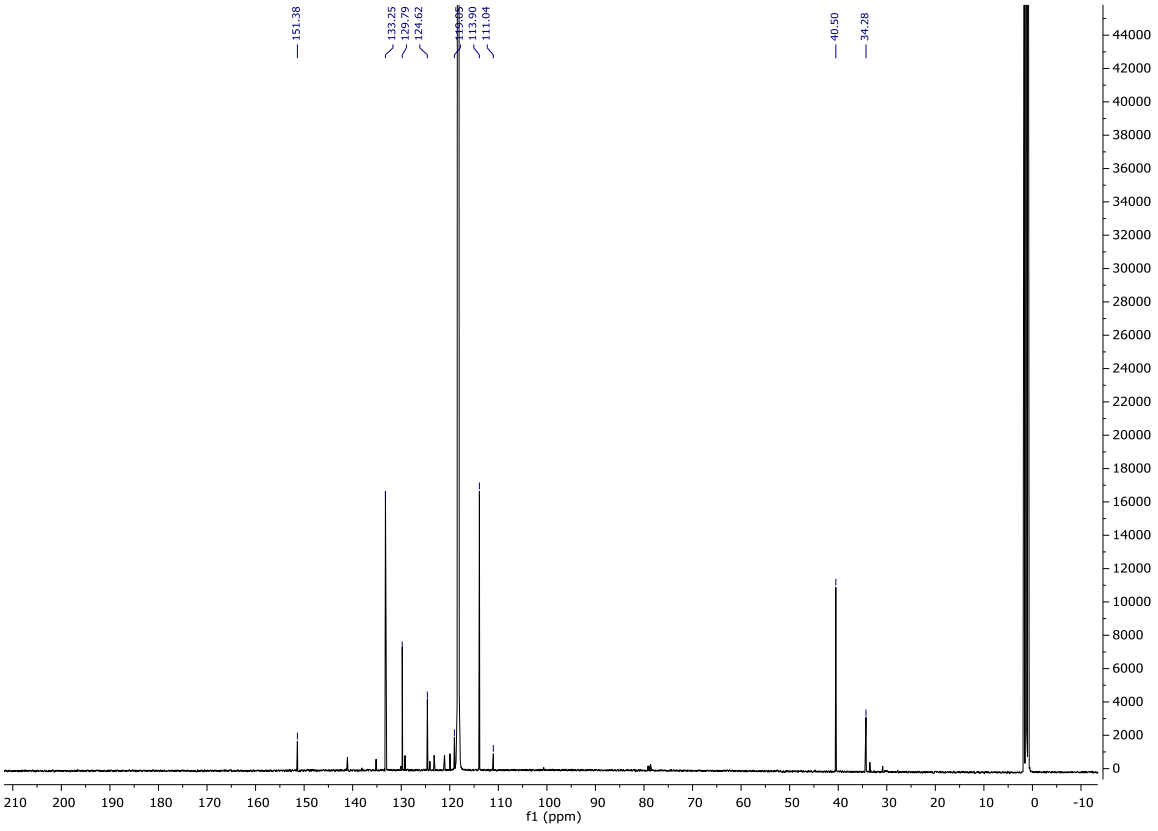

^{1}H NMR (400 MHz, CD_3CN) **233**

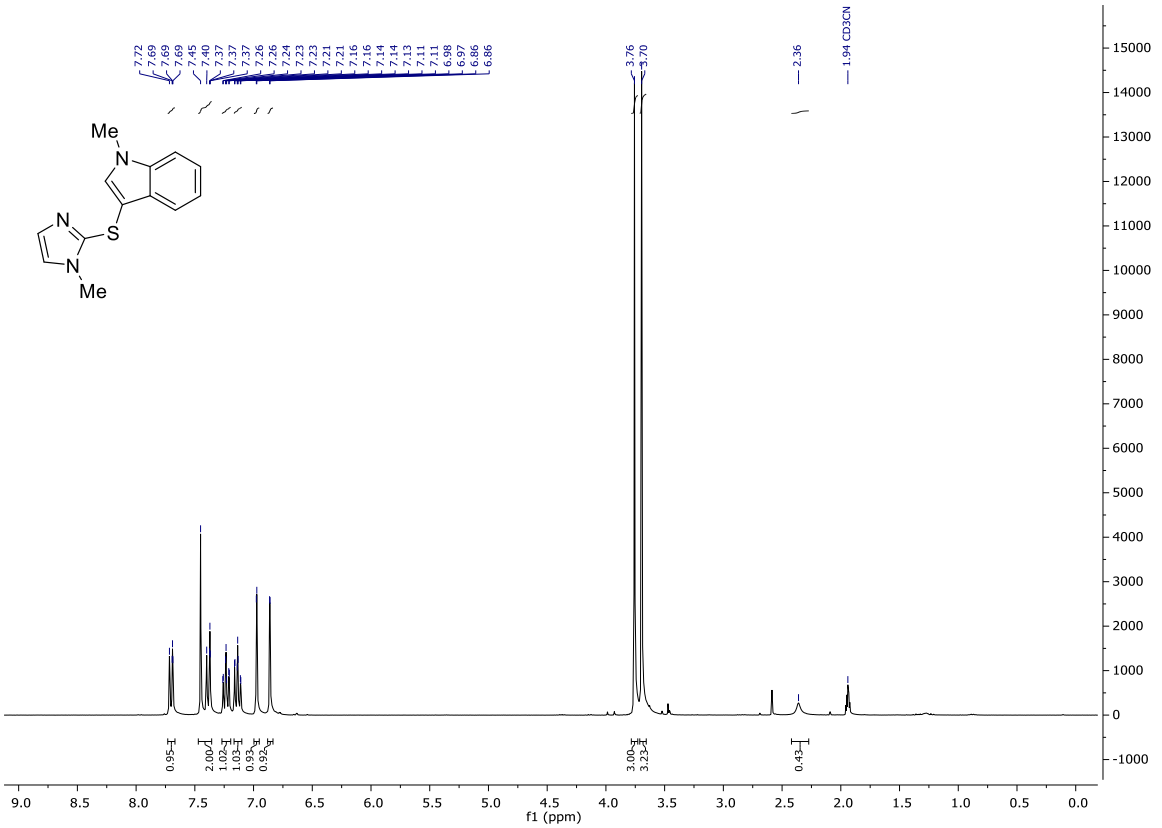

^{13}C NMR (126 MHz, CD_3CN) **233**

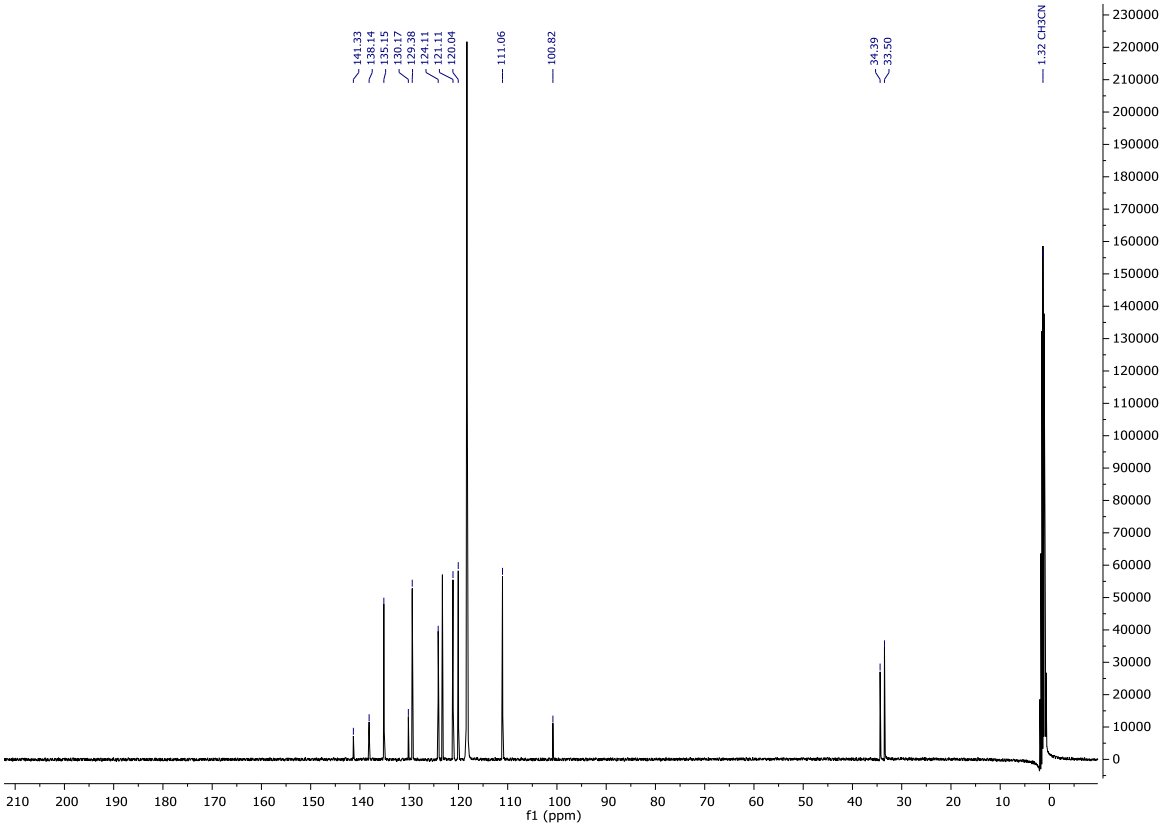

^{1}H NMR (400 MHz, CD_3CN) **234**

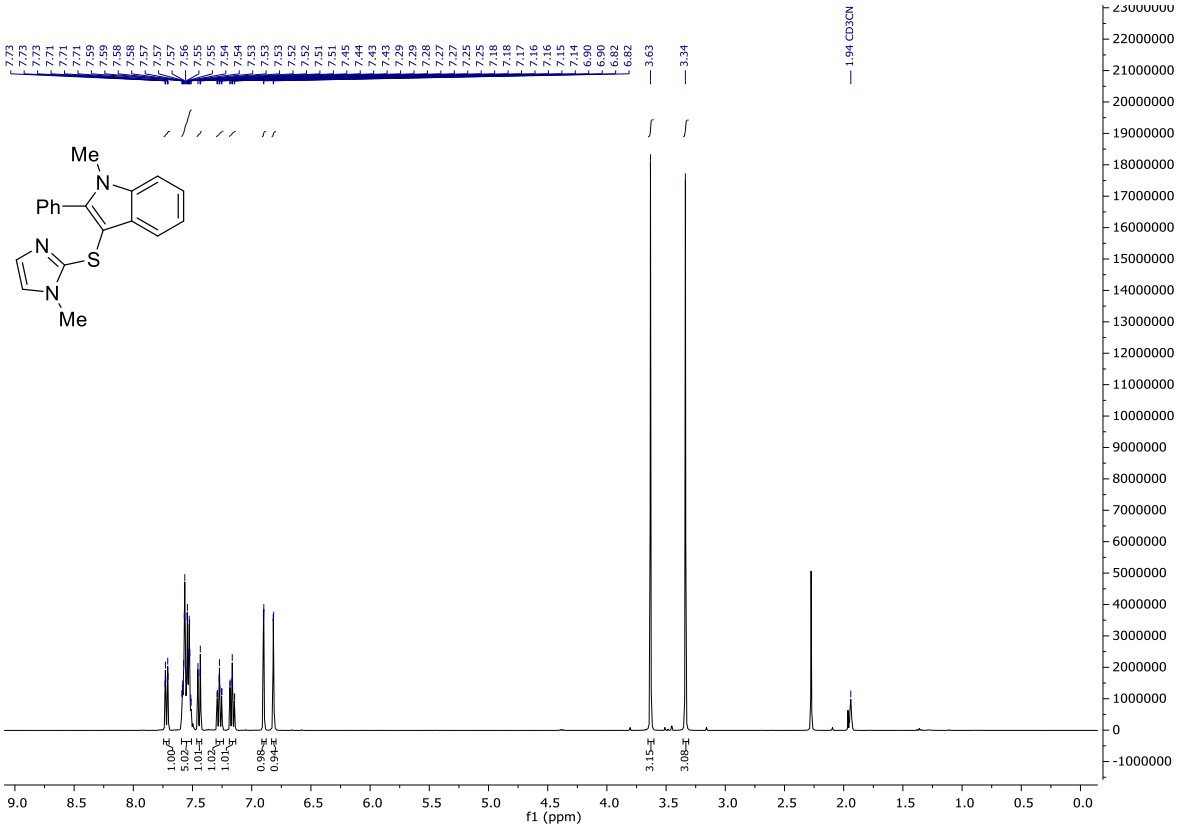

^{13}C NMR (126 MHz, CD_3CN) **234**

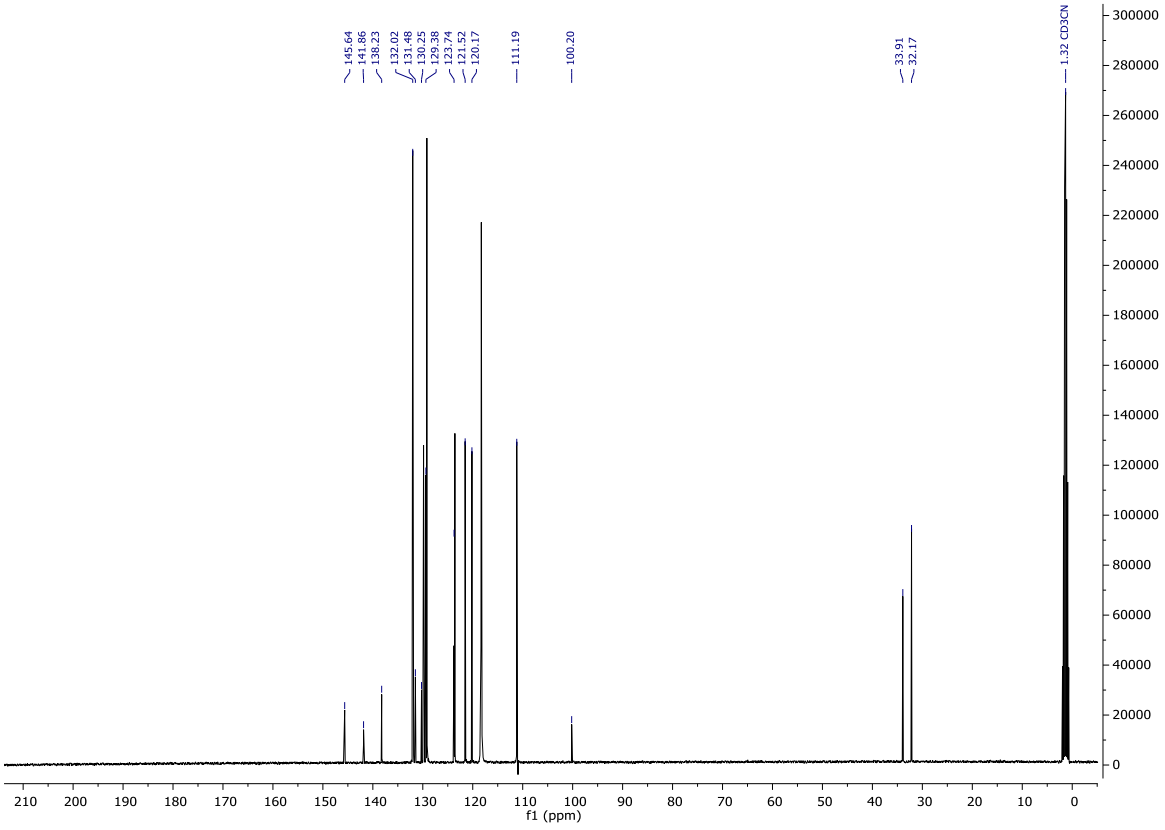

^{1}H NMR (400 MHz, CD_2Cl_2) **236**

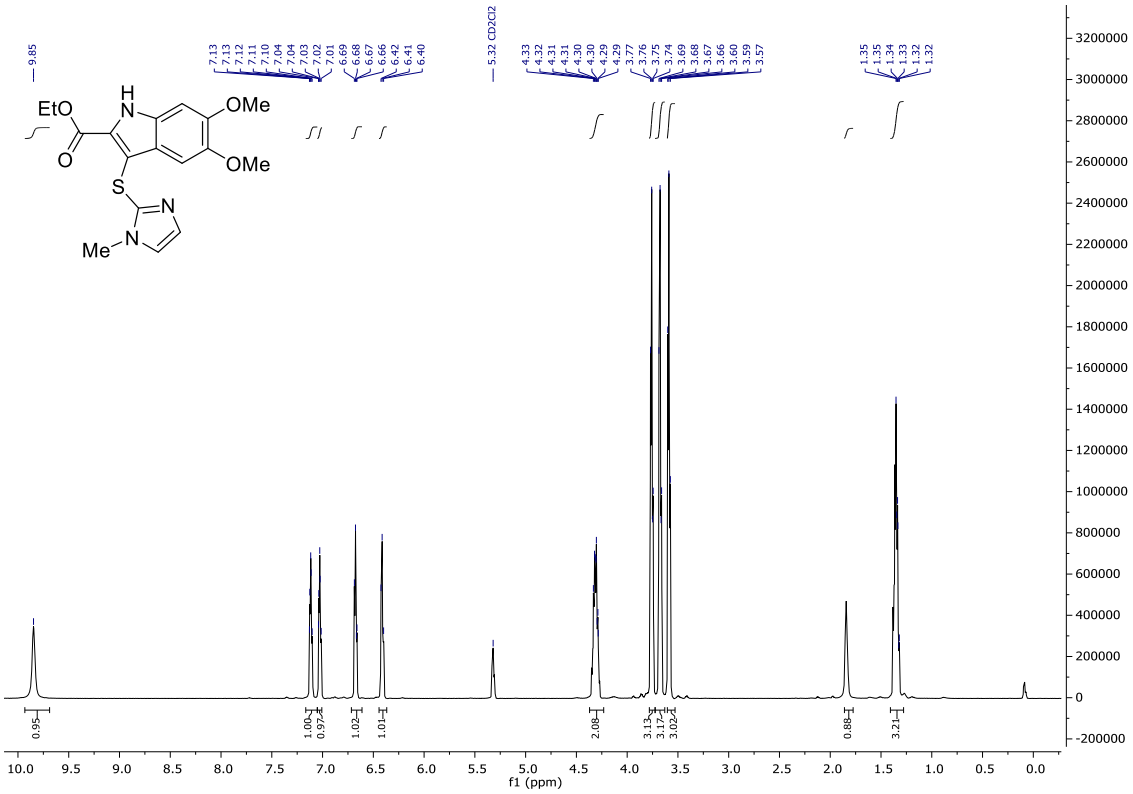

^{13}C NMR (126 MHz, CD_2Cl_2) **236**

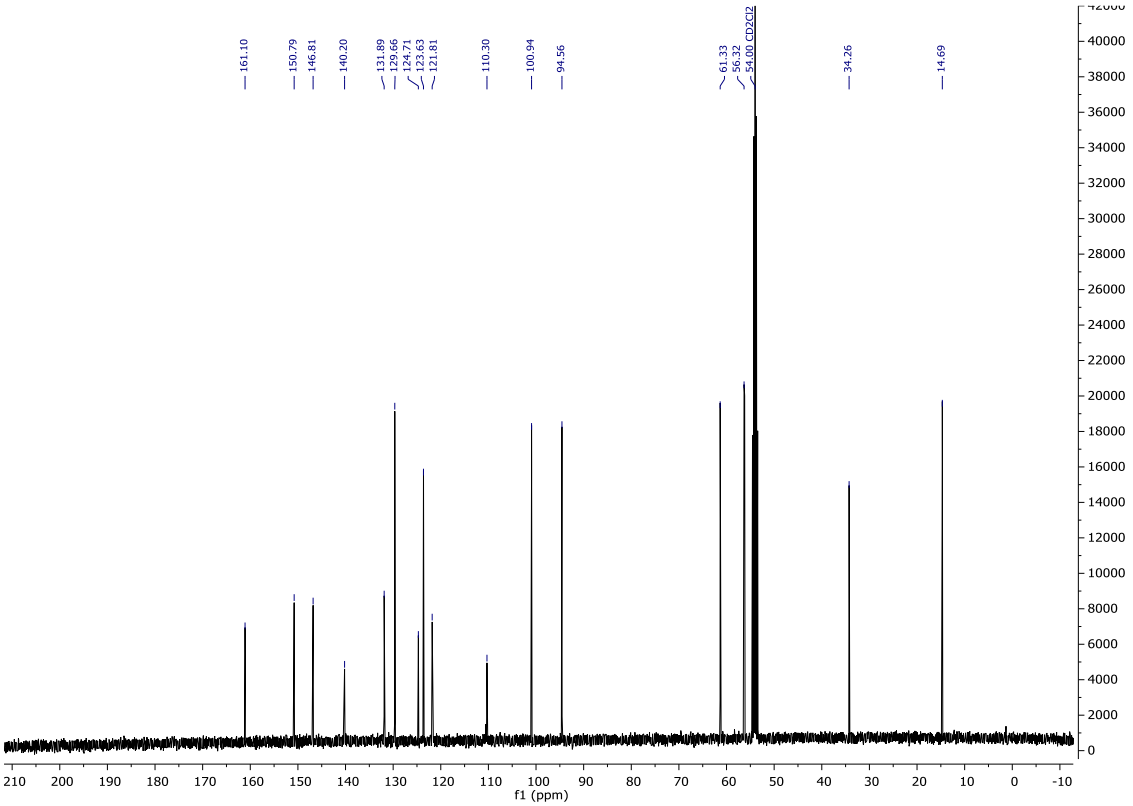

^{1}H NMR (400 MHz, CD_3CN) **240**

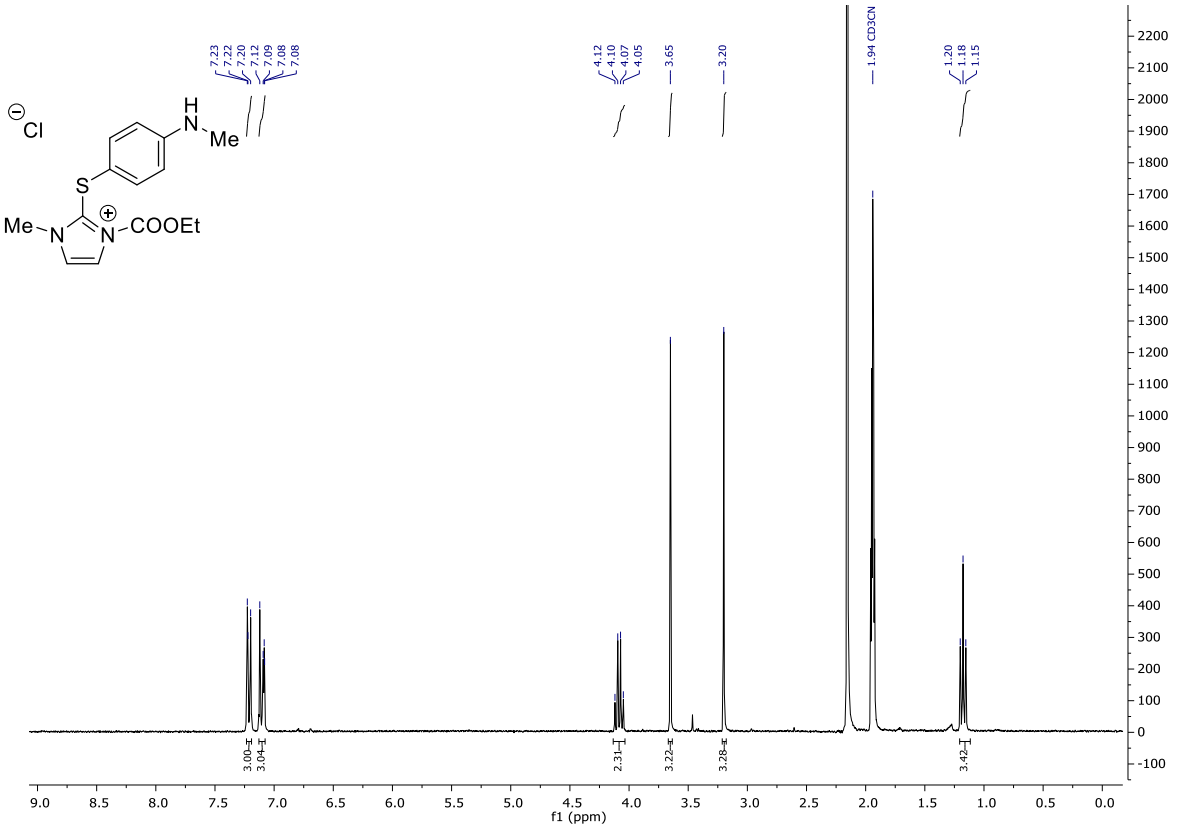

^{13}C NMR (126 MHz, CD_3CN) **240**

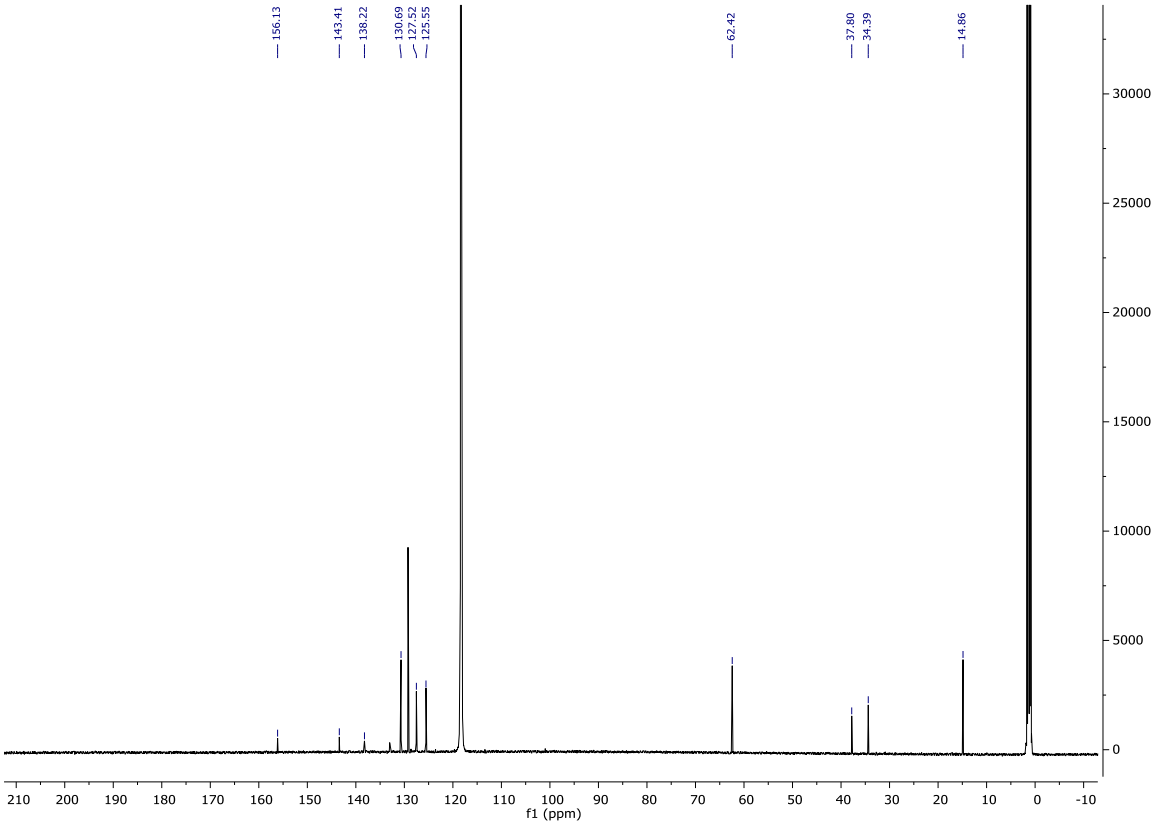

^{1}H NMR (400 MHz, CD_3CN) **239**

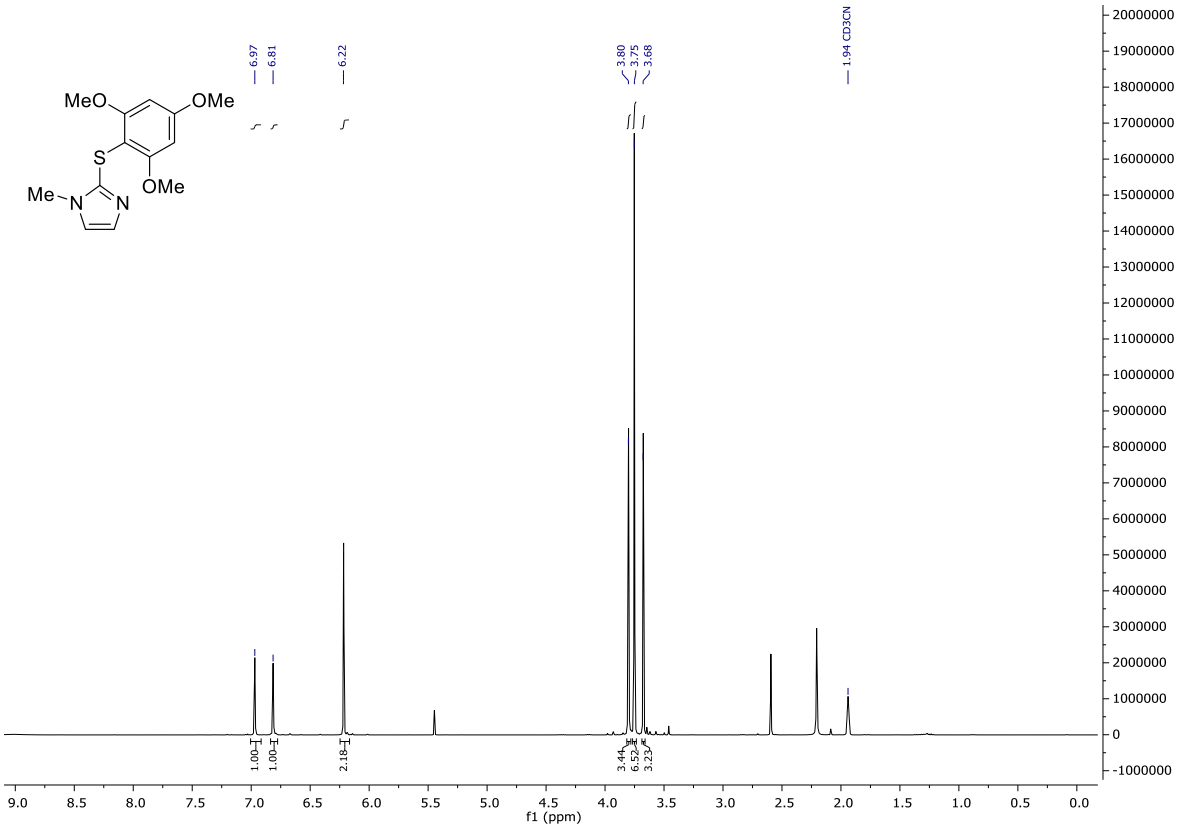

^{13}C NMR (126 MHz, CD_3CN) **239**

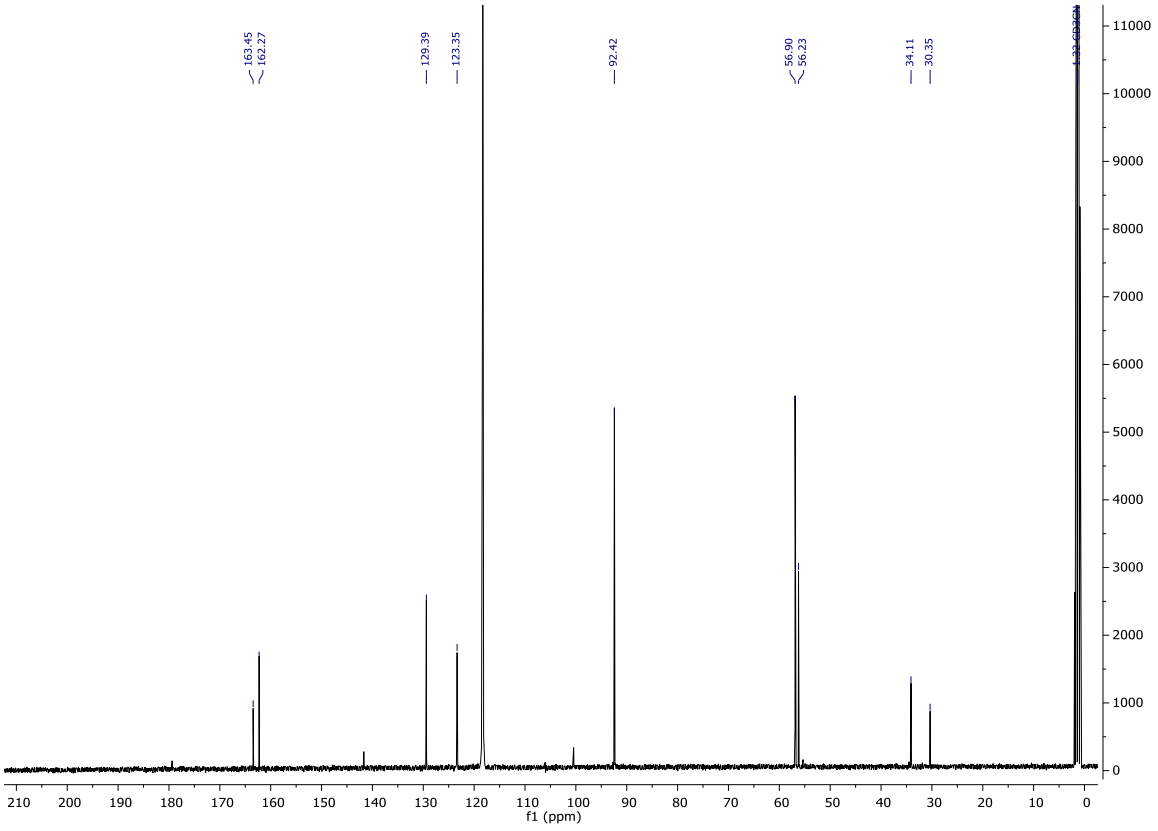

^{1}H NMR (400 MHz, CD_3CN) **238**

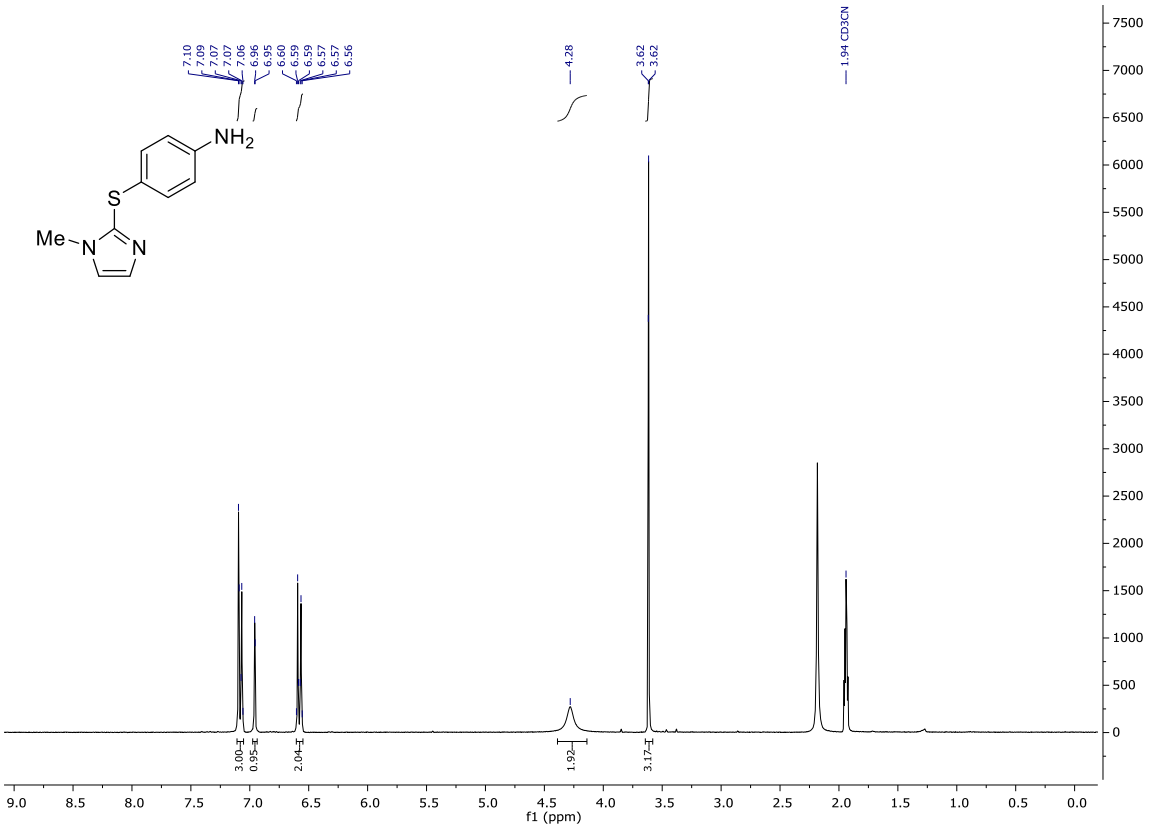

^{13}C NMR (126 MHz, CD_3CN) **238**

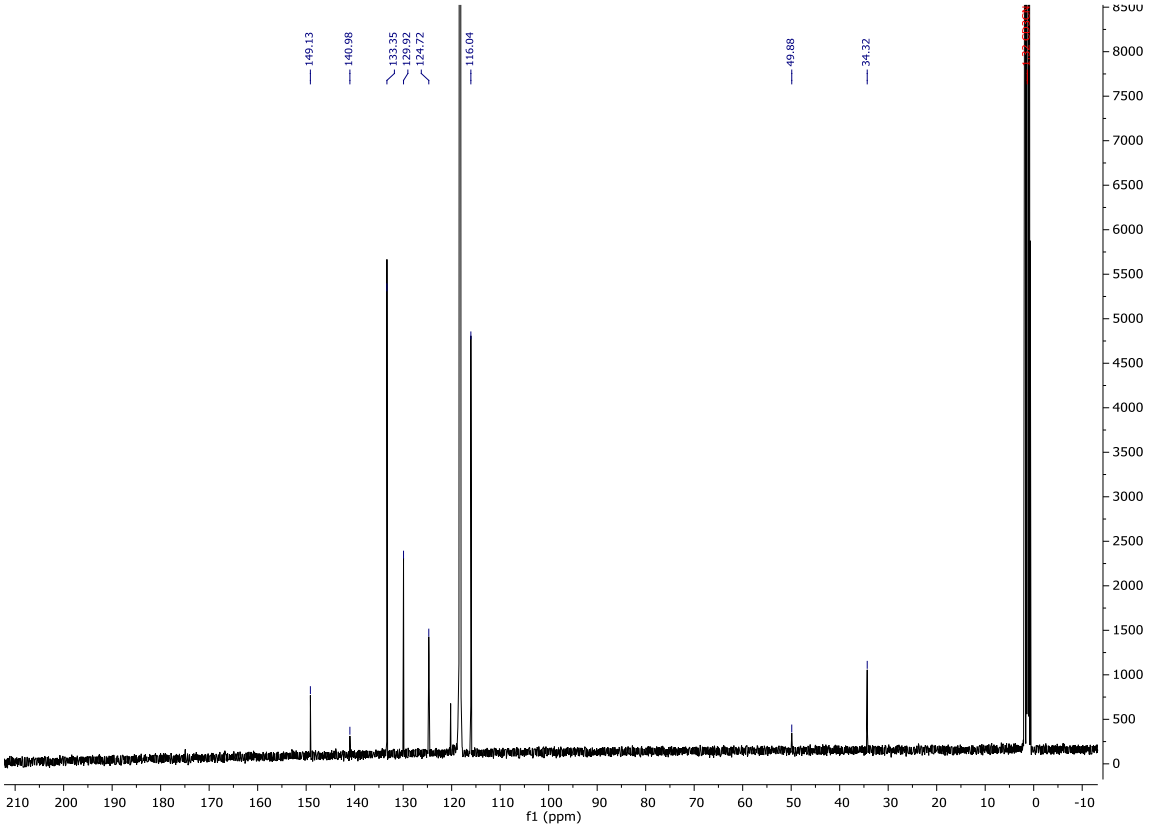

^{1}H NMR (400 MHz, CD_3CN) **235**

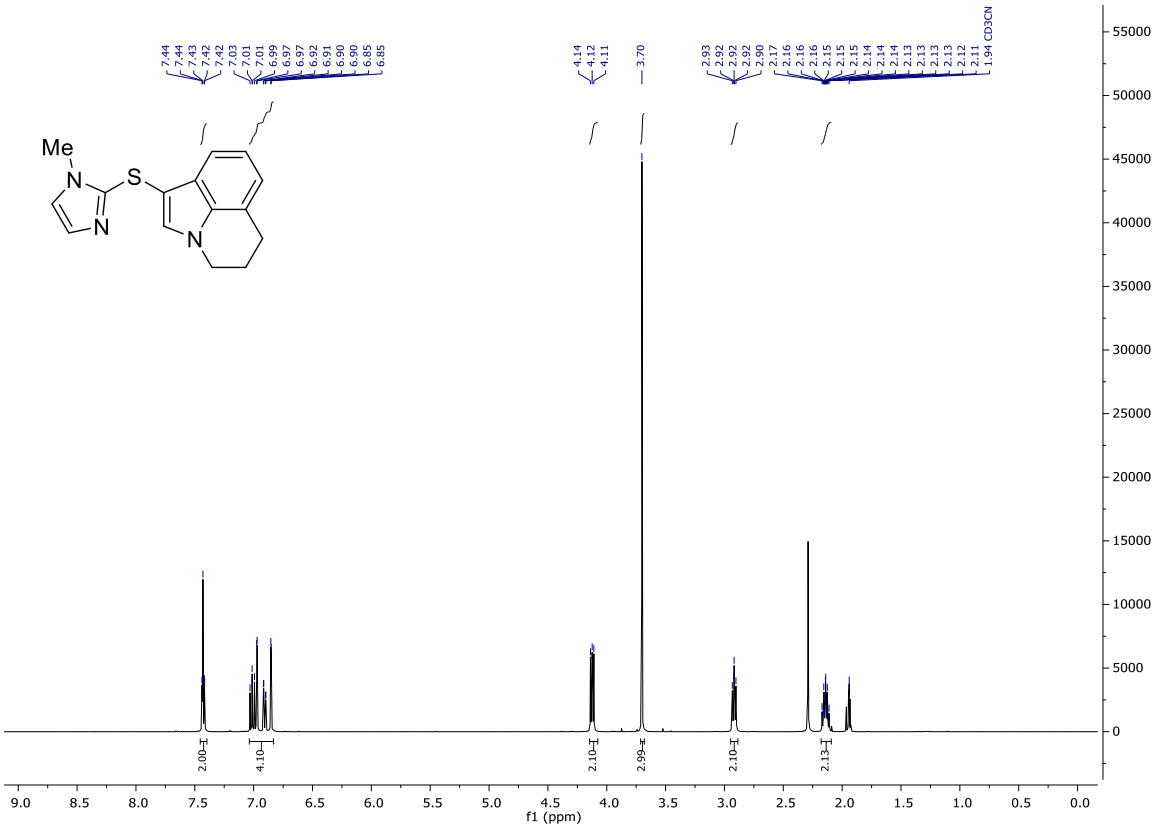

^{13}C NMR (126 MHz, CD_3CN) **235**

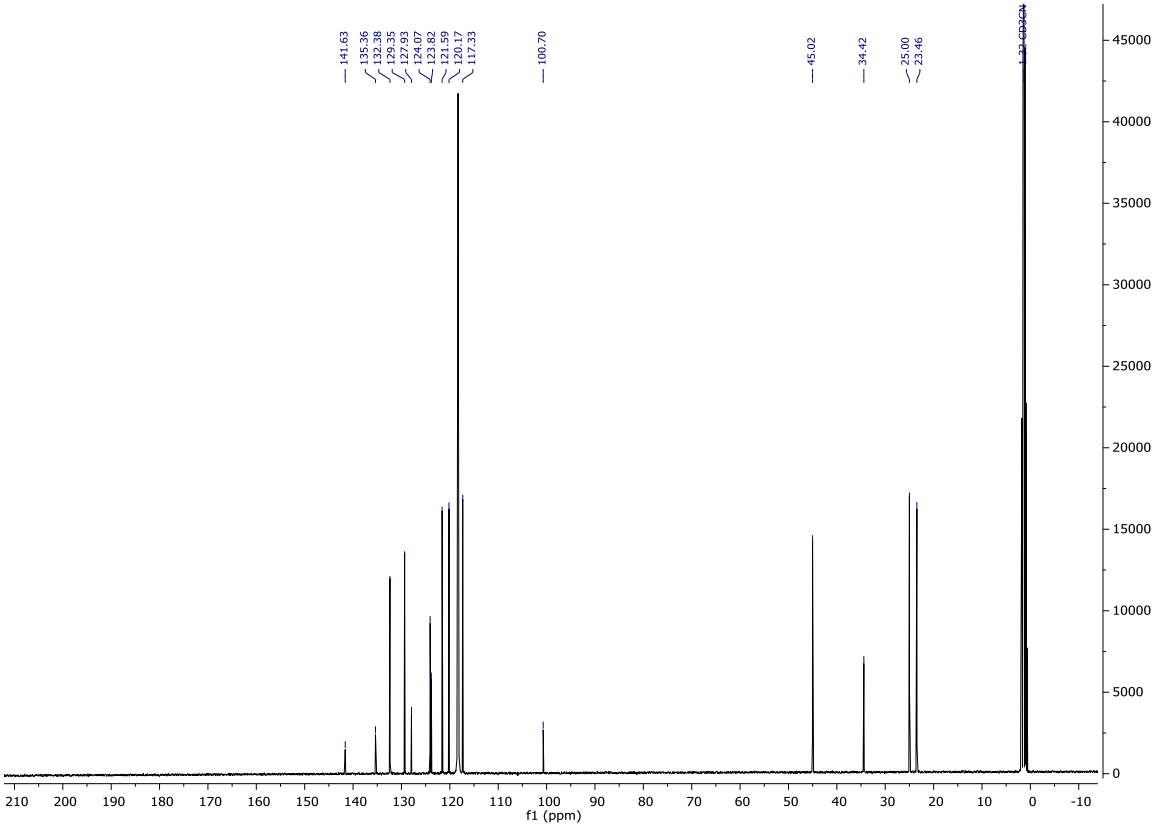

^{1}H NMR (400 MHz, CD_3CN) **241**

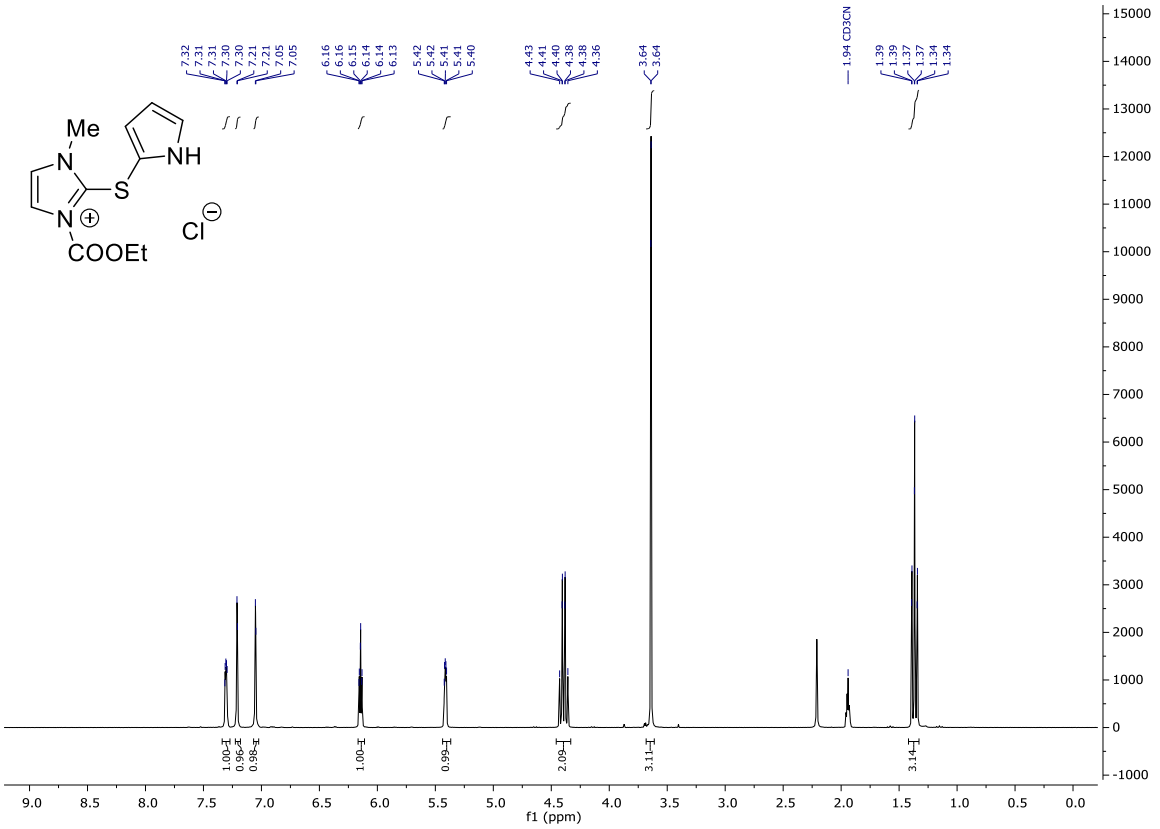

^{13}C NMR (126 MHz, CD_3CN) **241**

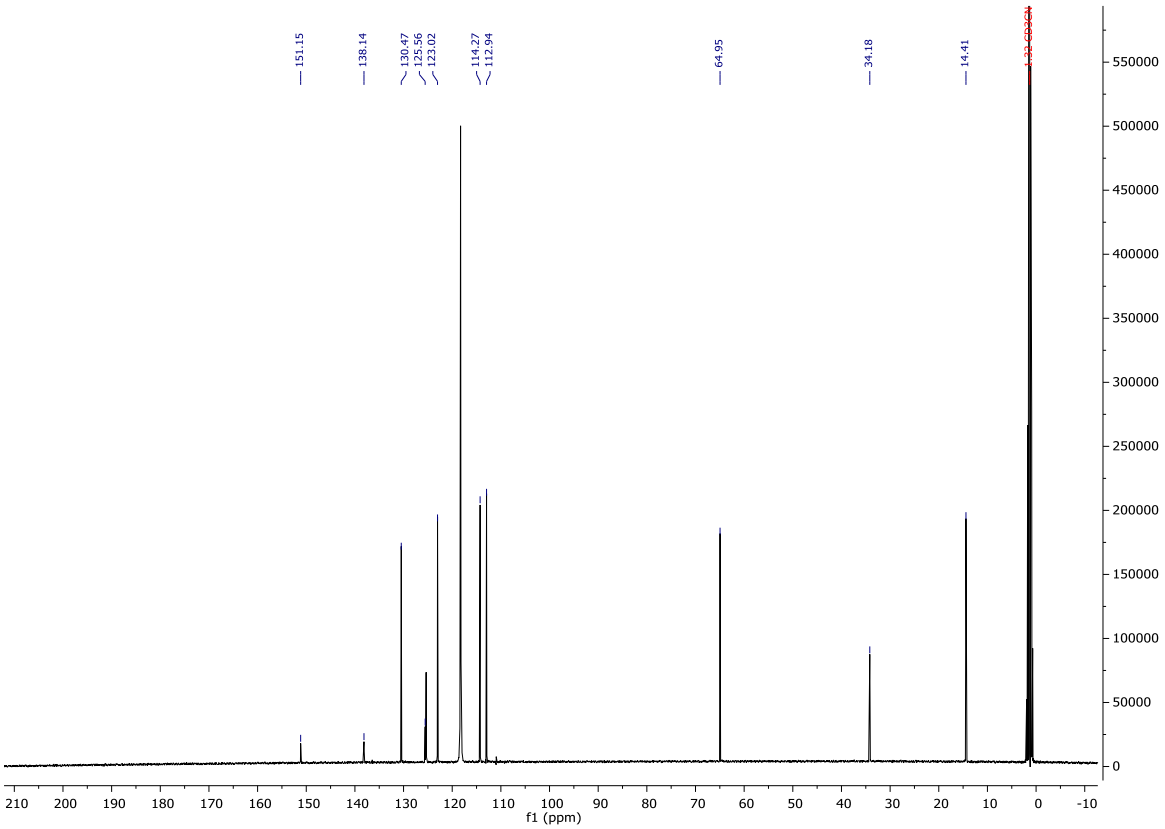

Synthesis of sulfur containing precursors

^{1}H NMR (300 MHz, $CDCl_3$) **258**

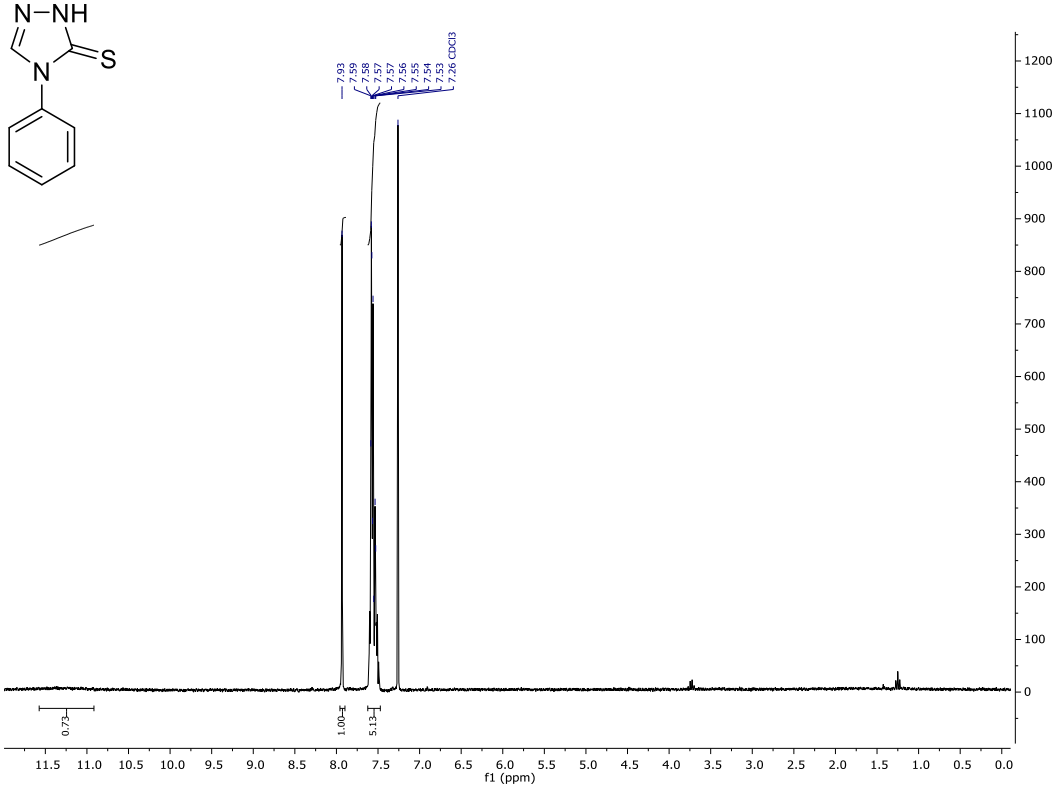

^{13}C NMR (101 MHz, $CDCl_3$) **258**

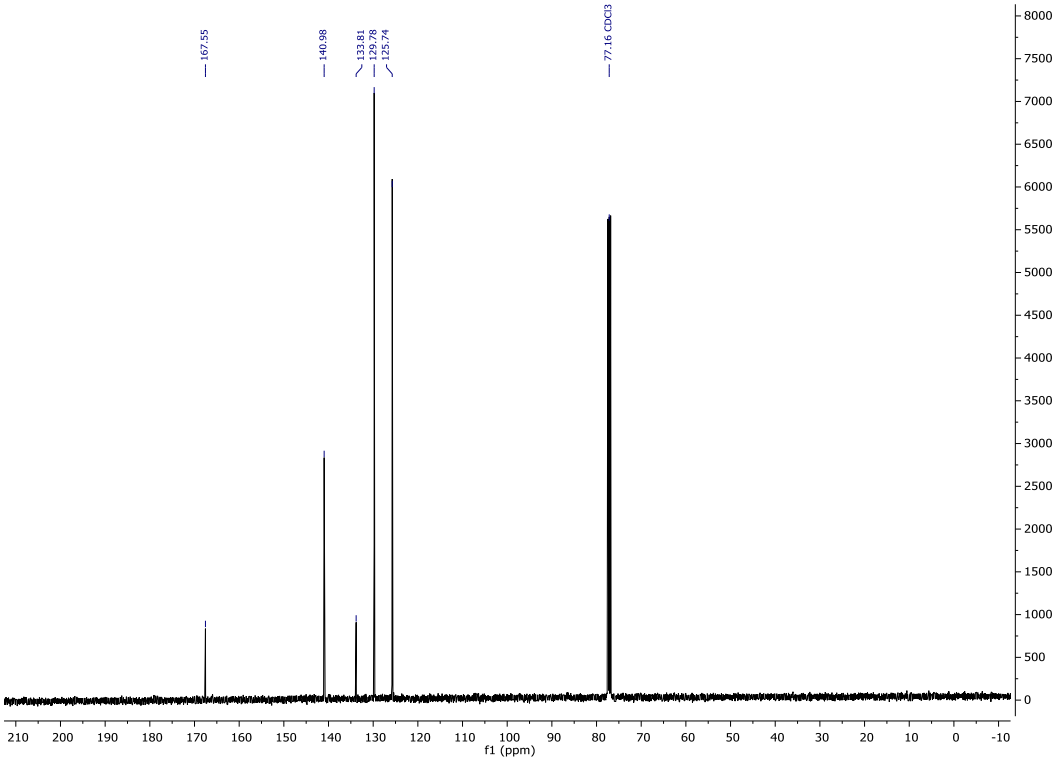

^{1}H NMR (400 MHz, $CDCl_3$) **250**

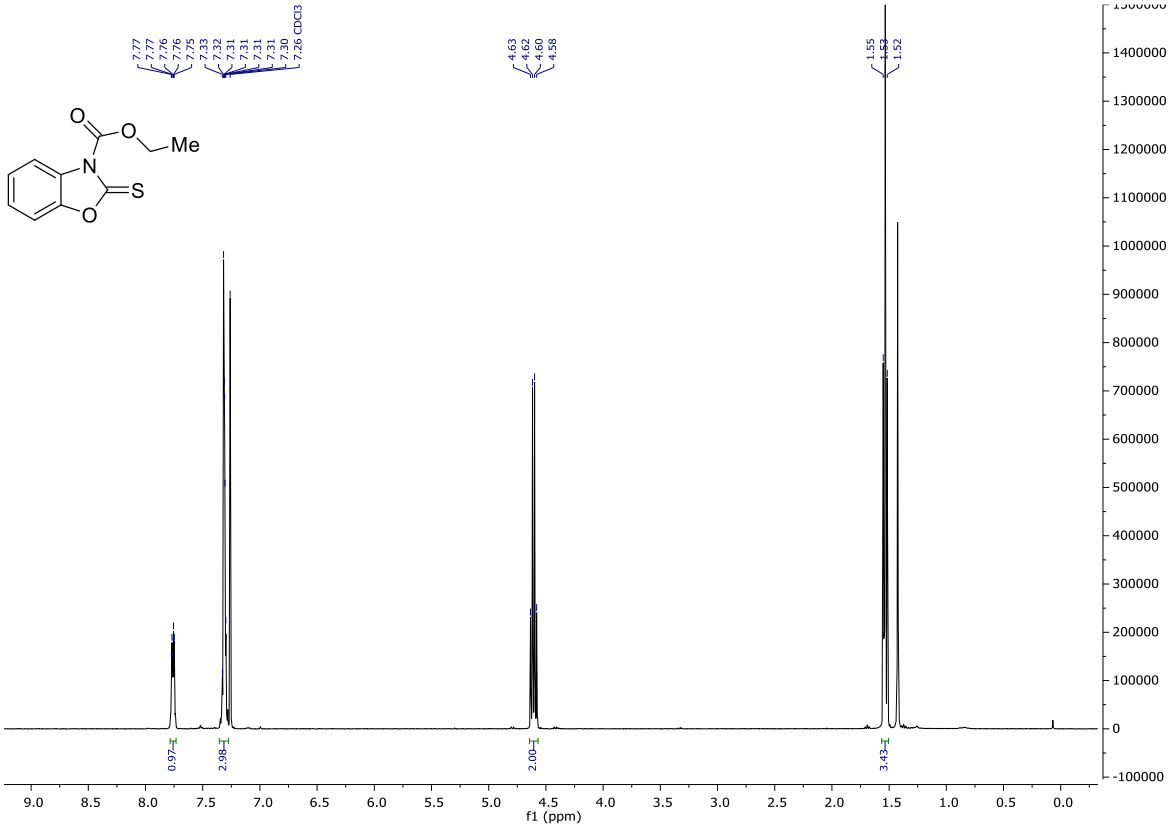

^{13}C NMR (101 MHz, $CDCl_3$) **250**

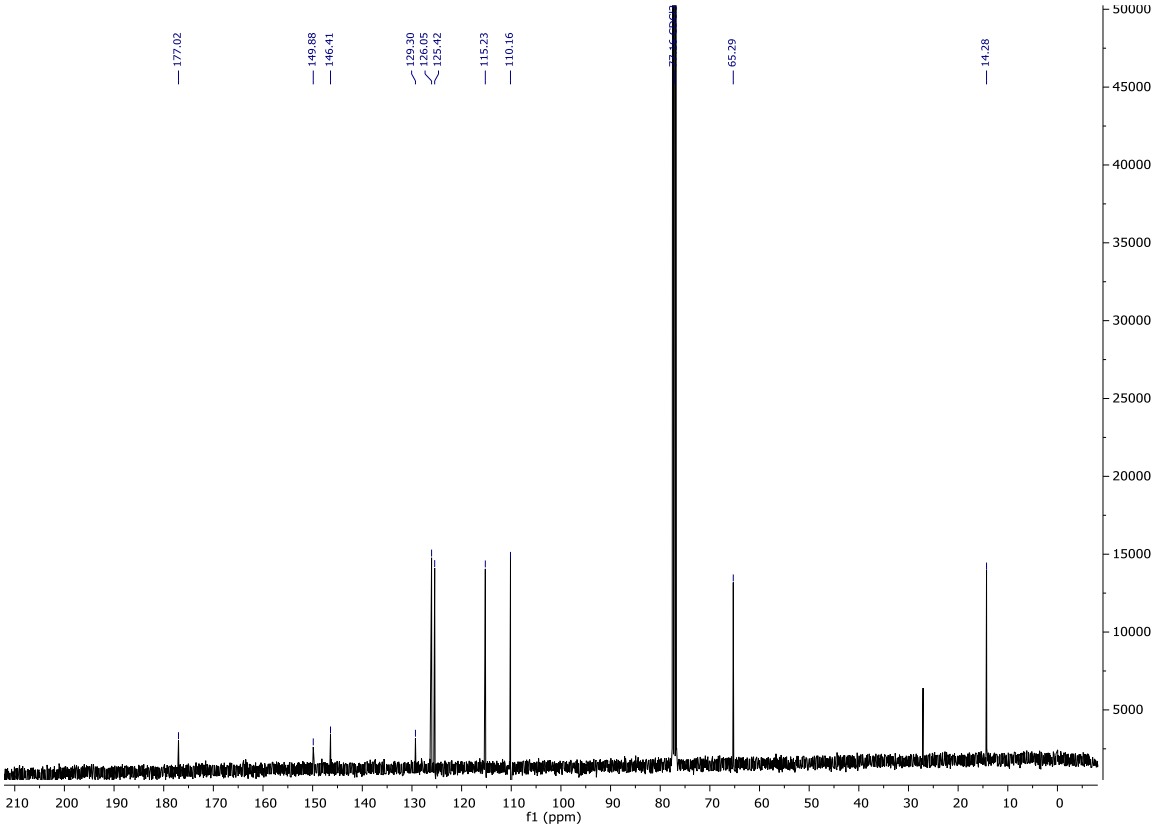

^{1}H NMR (300 MHz, $CDCl_3$) **251**

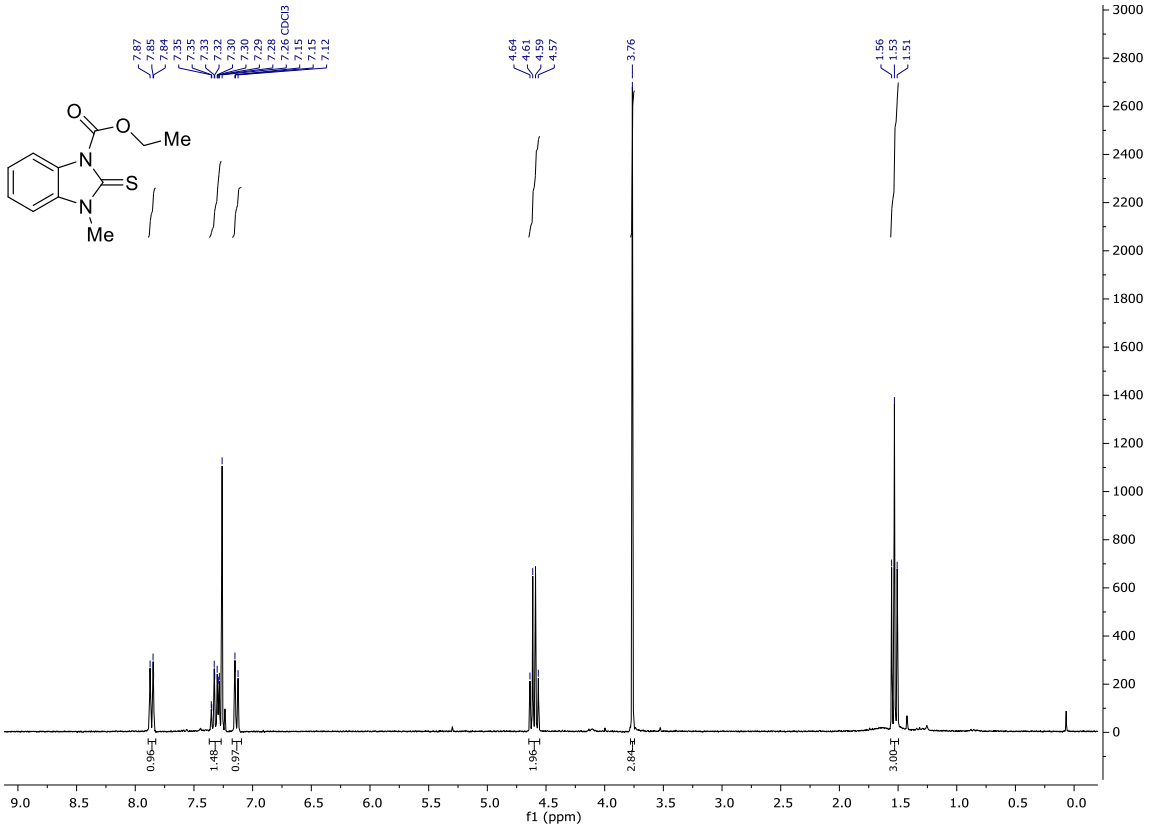

^{13}C NMR (101 MHz, $CDCl_3$) **251**

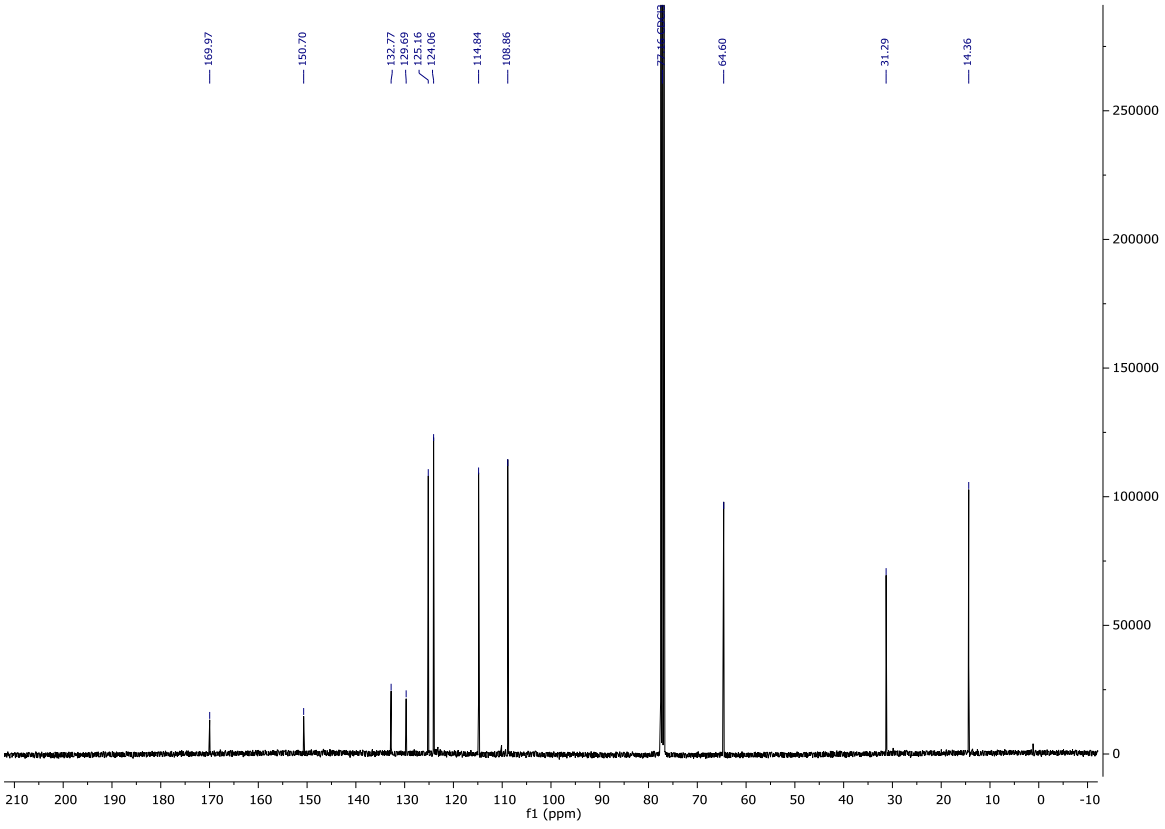

^{1}H NMR (300 MHz, $CDCl_3$) **252**

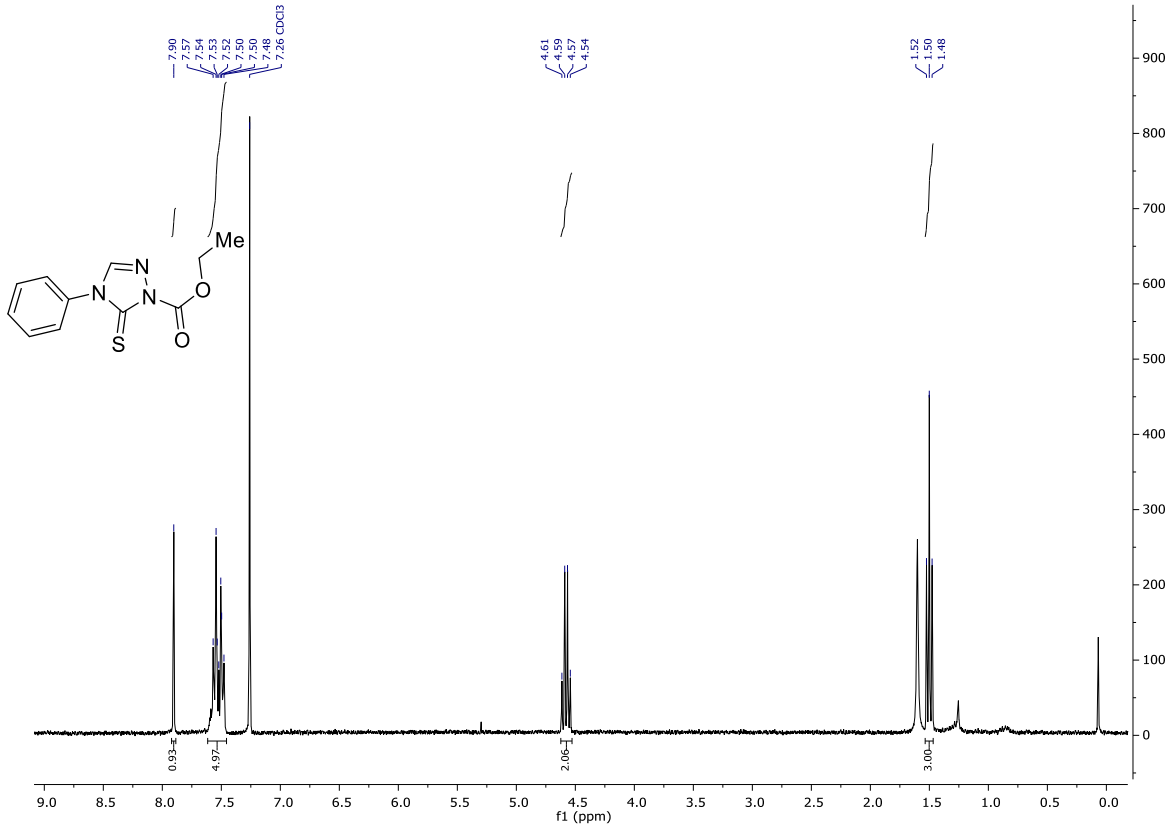

^{13}C NMR (101 MHz, $CDCl_3$) **252**

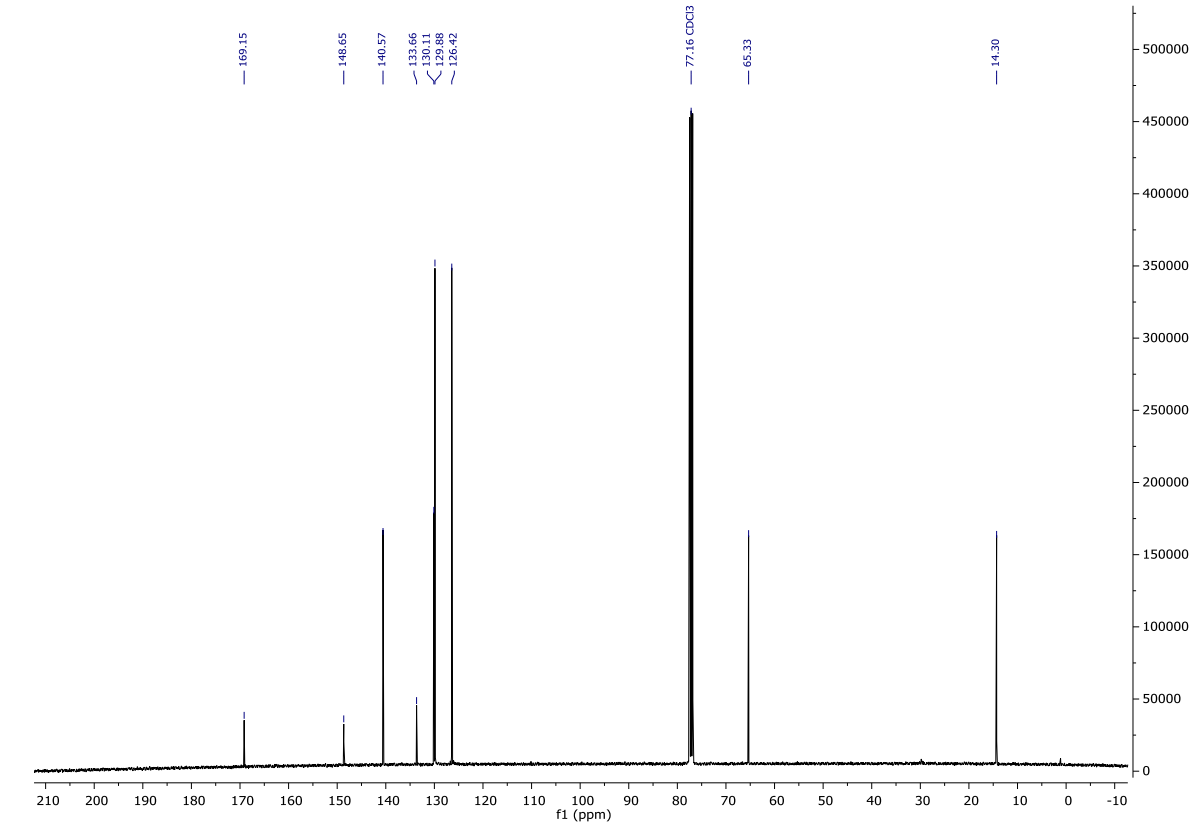

^{1}H NMR (400 MHz, CD_3CN) **259**

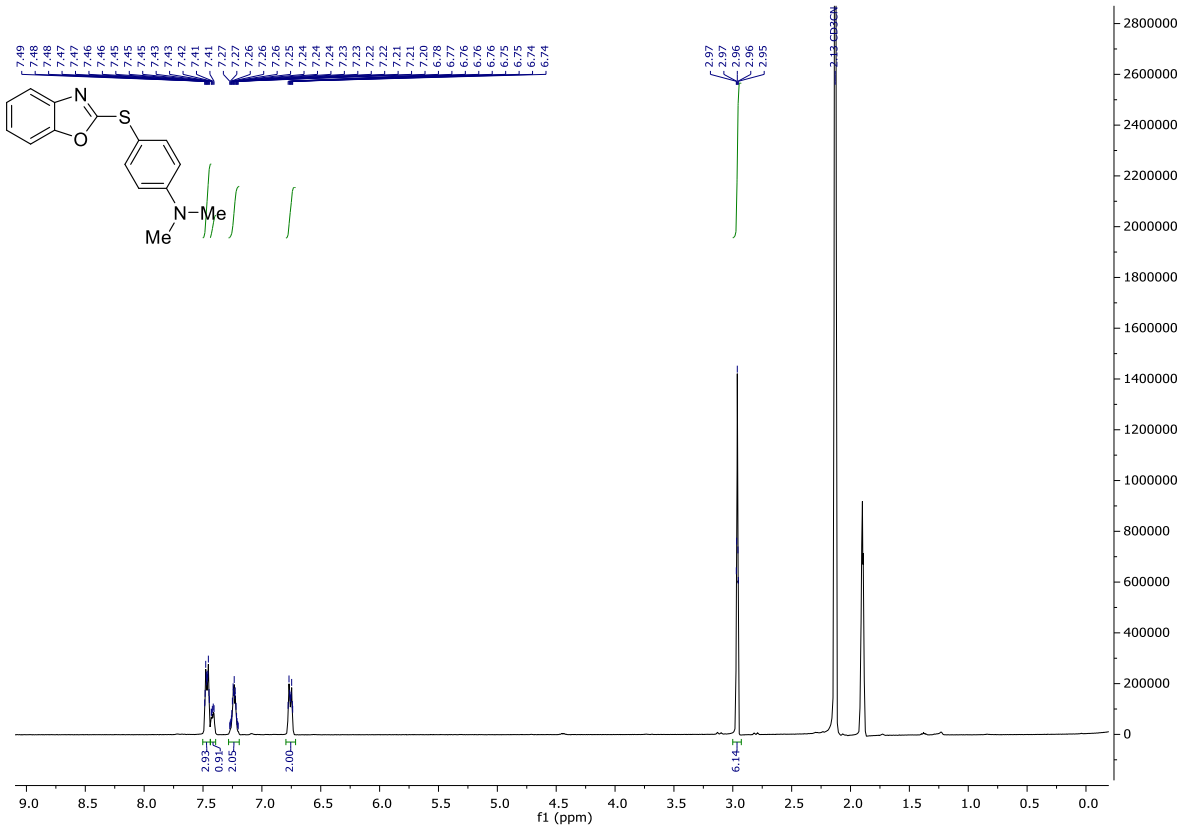

^{13}C NMR (101 MHz, $CDCl_3$) **259**

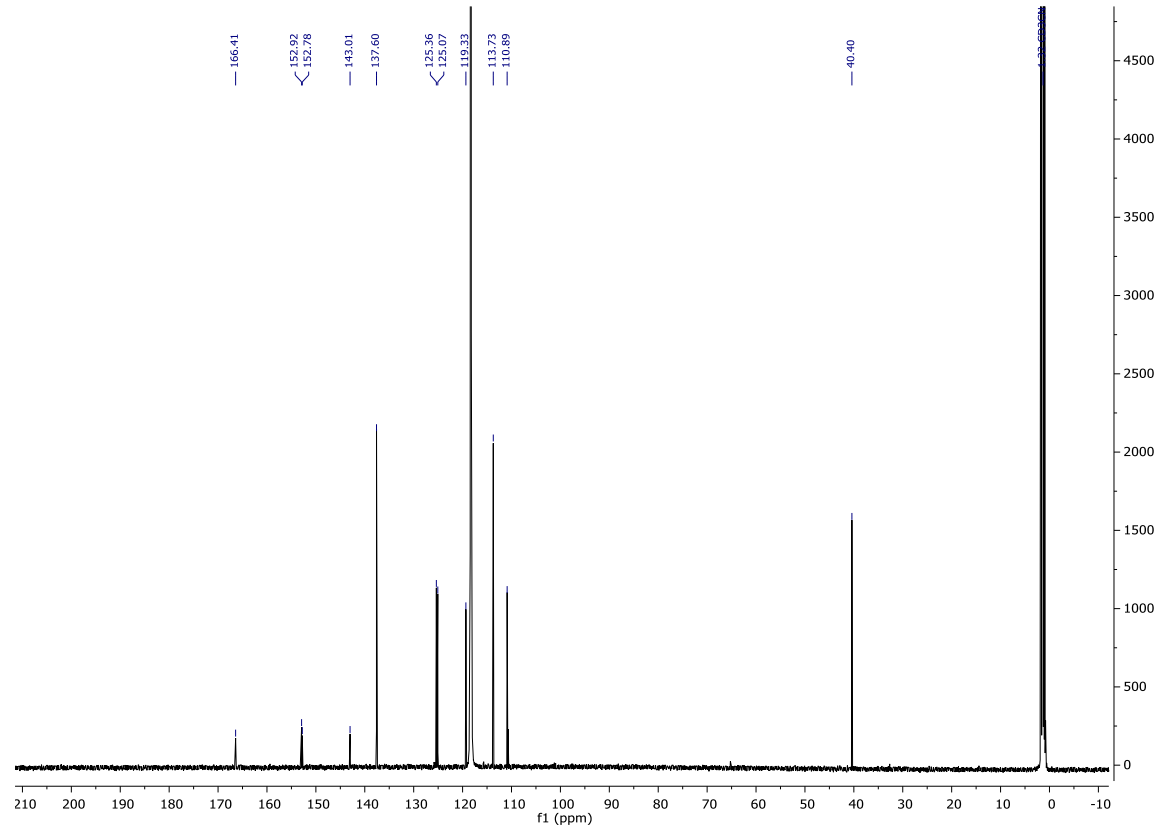

^{1}H NMR (400 MHz, $CDCl_3$) **260**

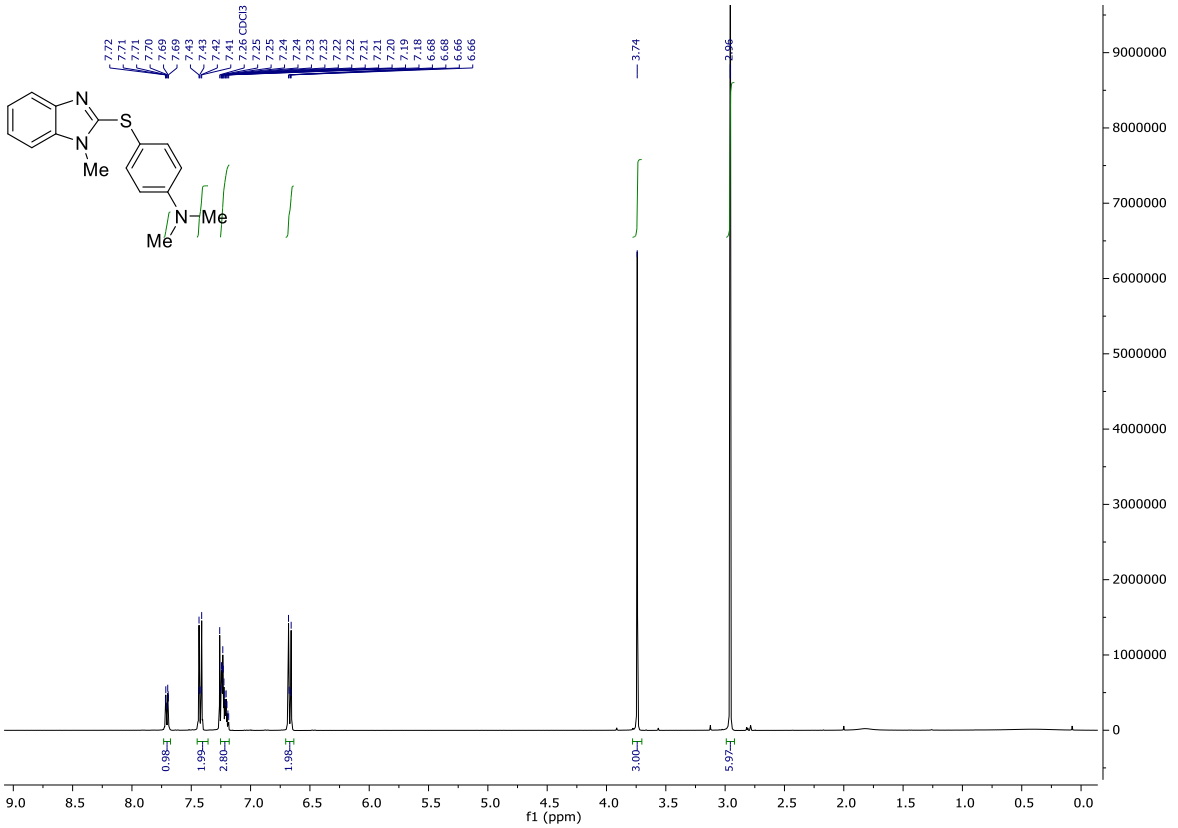

^{13}C NMR (101 MHz, $CDCl_3$) **260**

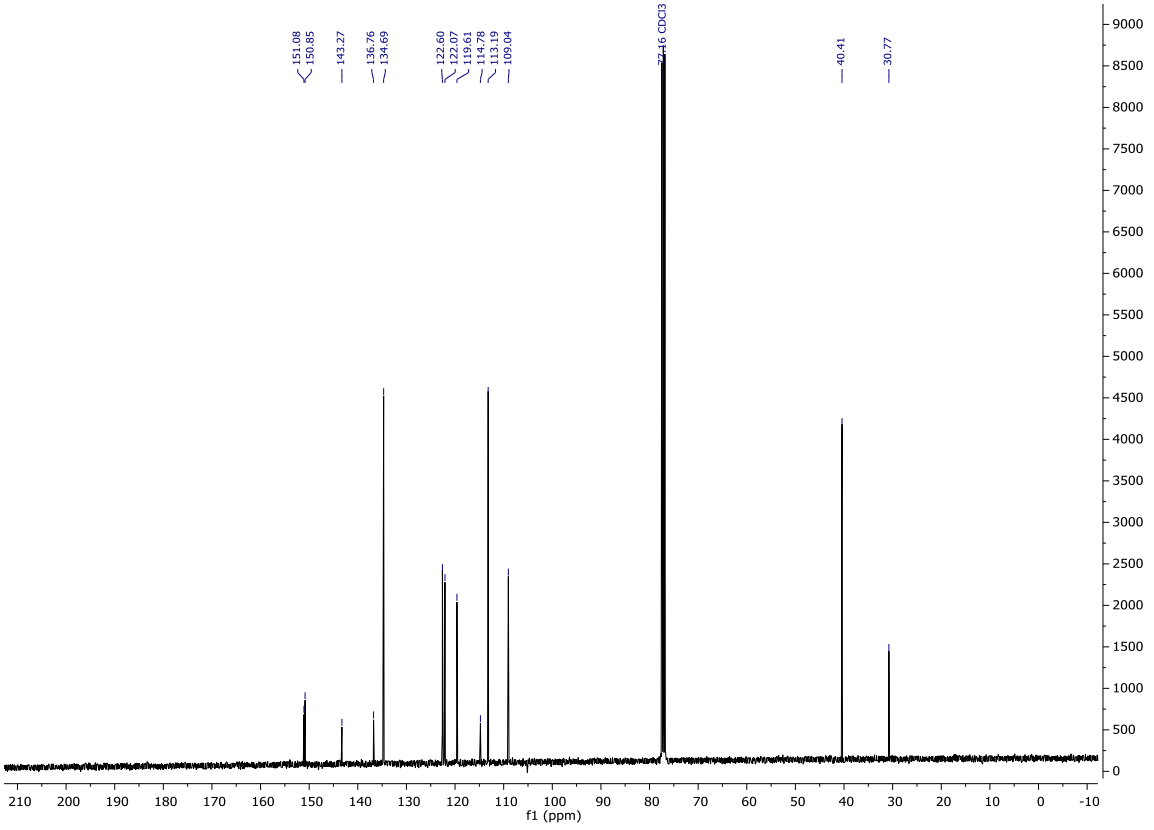

^{1}H NMR (400 MHz, CD_3CN) **263**

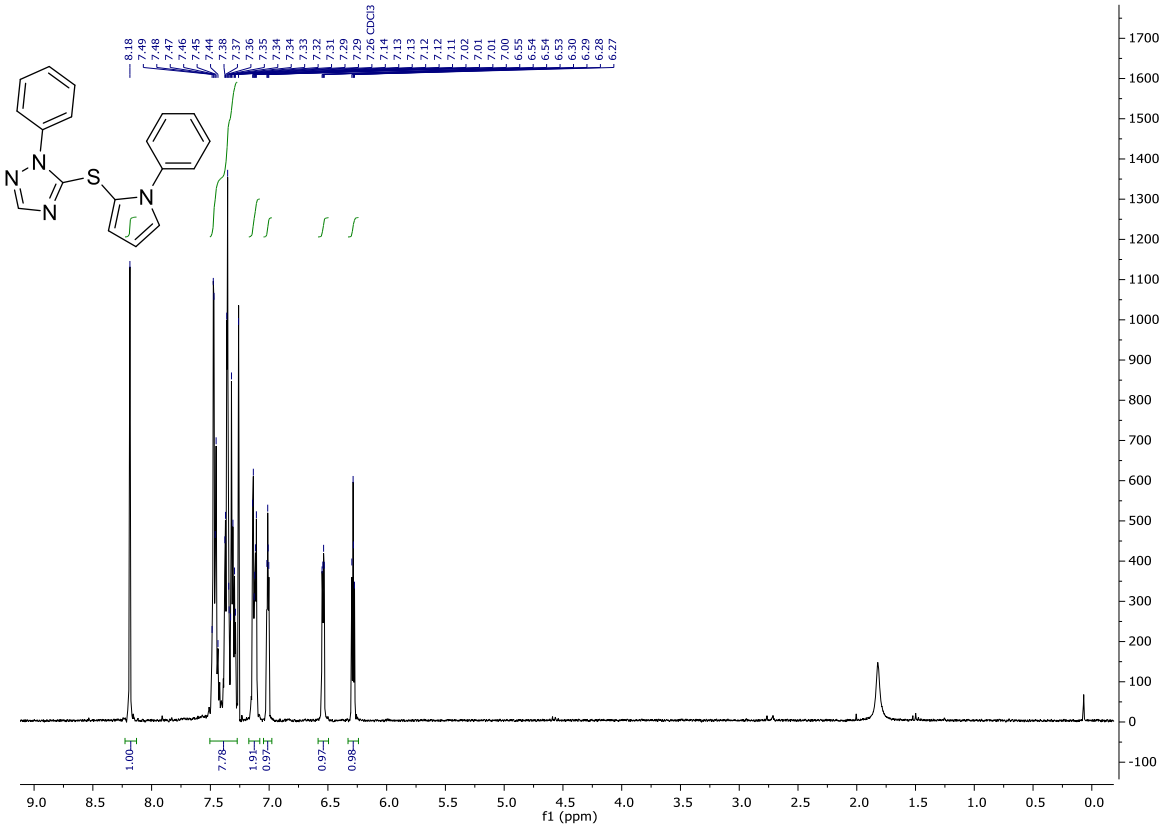

^{13}C NMR (101 MHz, $CDCl_3$) **263**

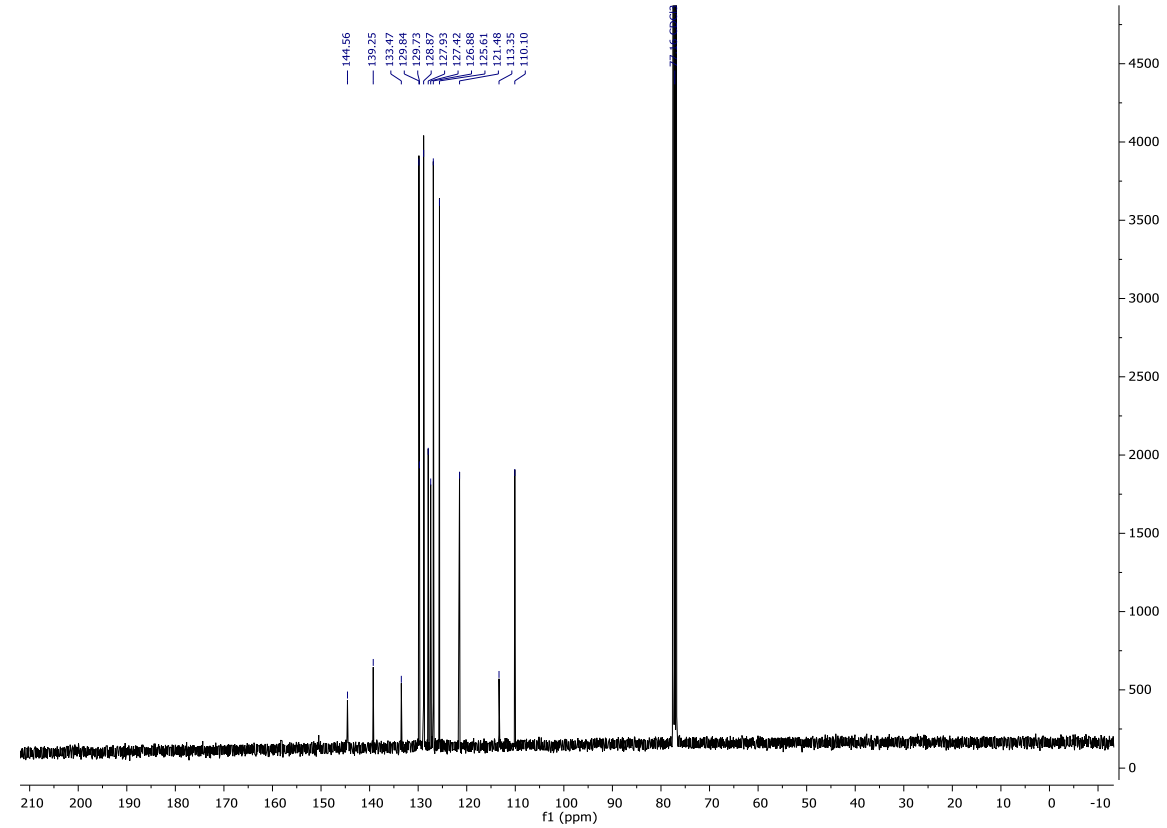

Synthesis of tetramethyl thiourea salts

^{1}H NMR (300 MHz, $CDCl_3$) **310**

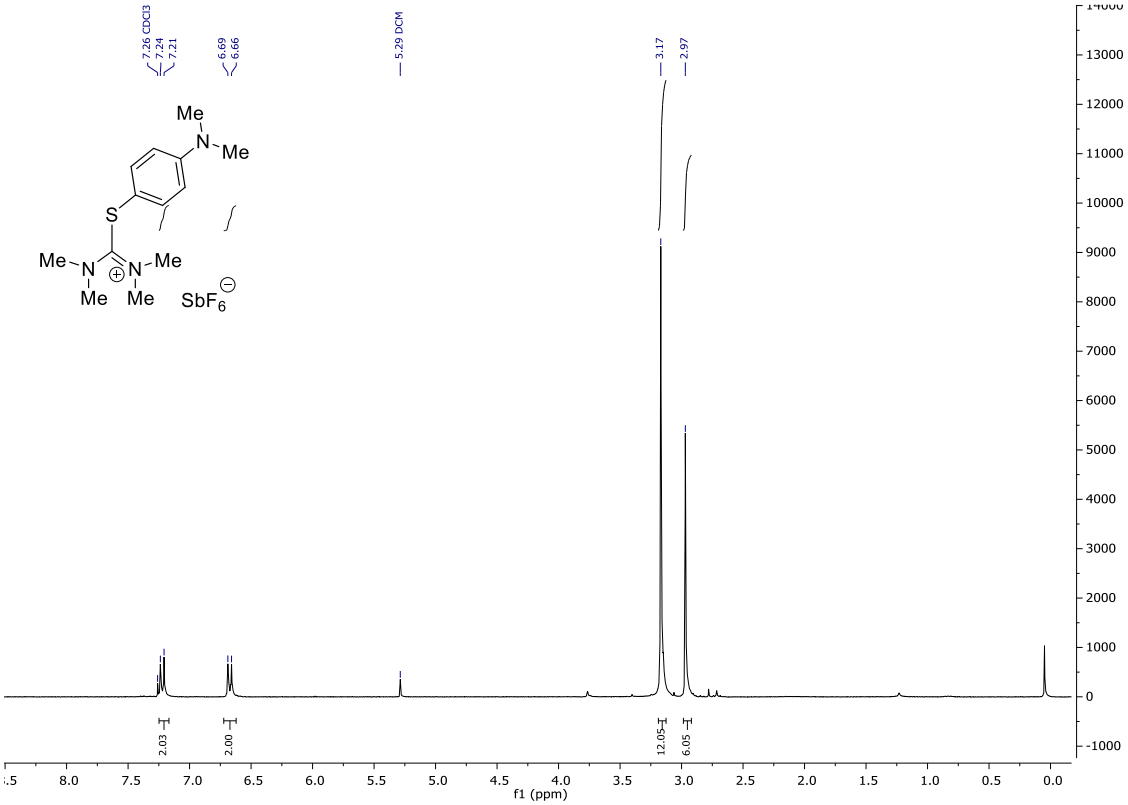

^{13}C NMR (75 MHz, $CDCl_3$) **310**

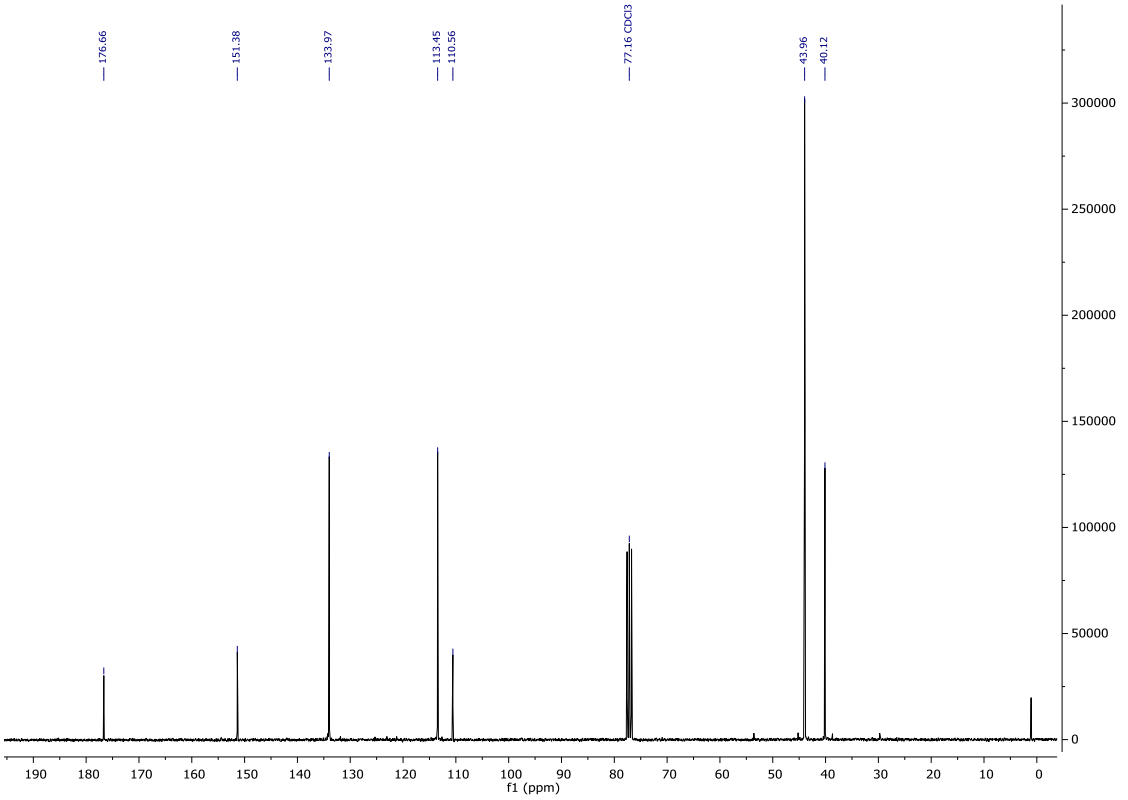

^{1}H NMR (300 MHz, CD_2Cl_2) **311**

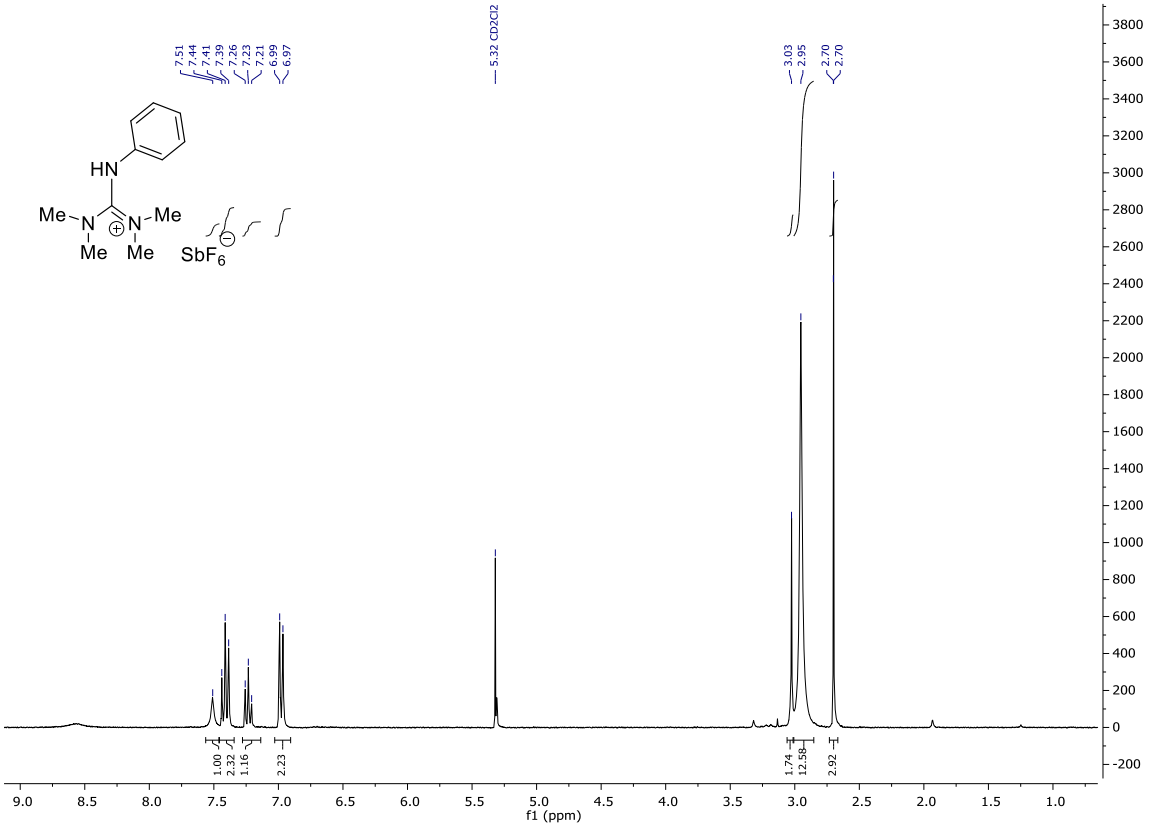

^{13}C NMR (75 MHz, CD_2Cl_2) **311**

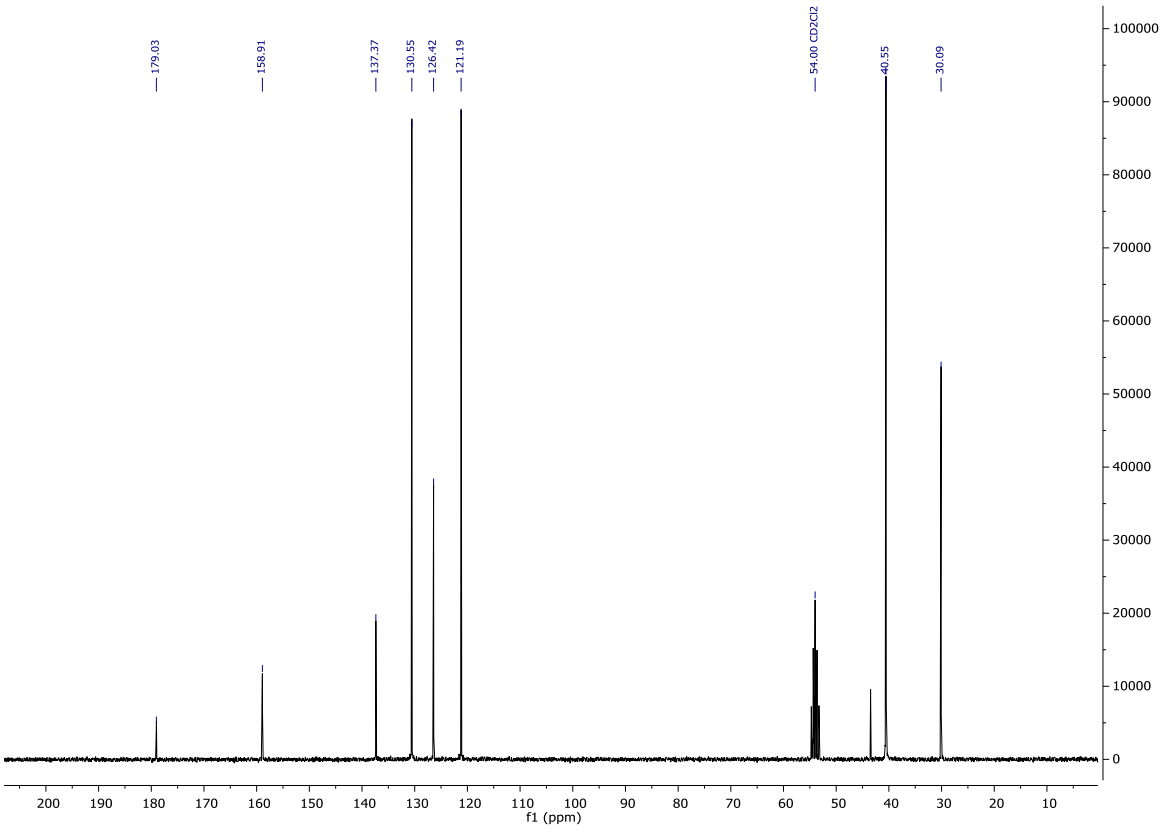

^{1}H NMR (300 MHz, CD_2Cl_2) **312**

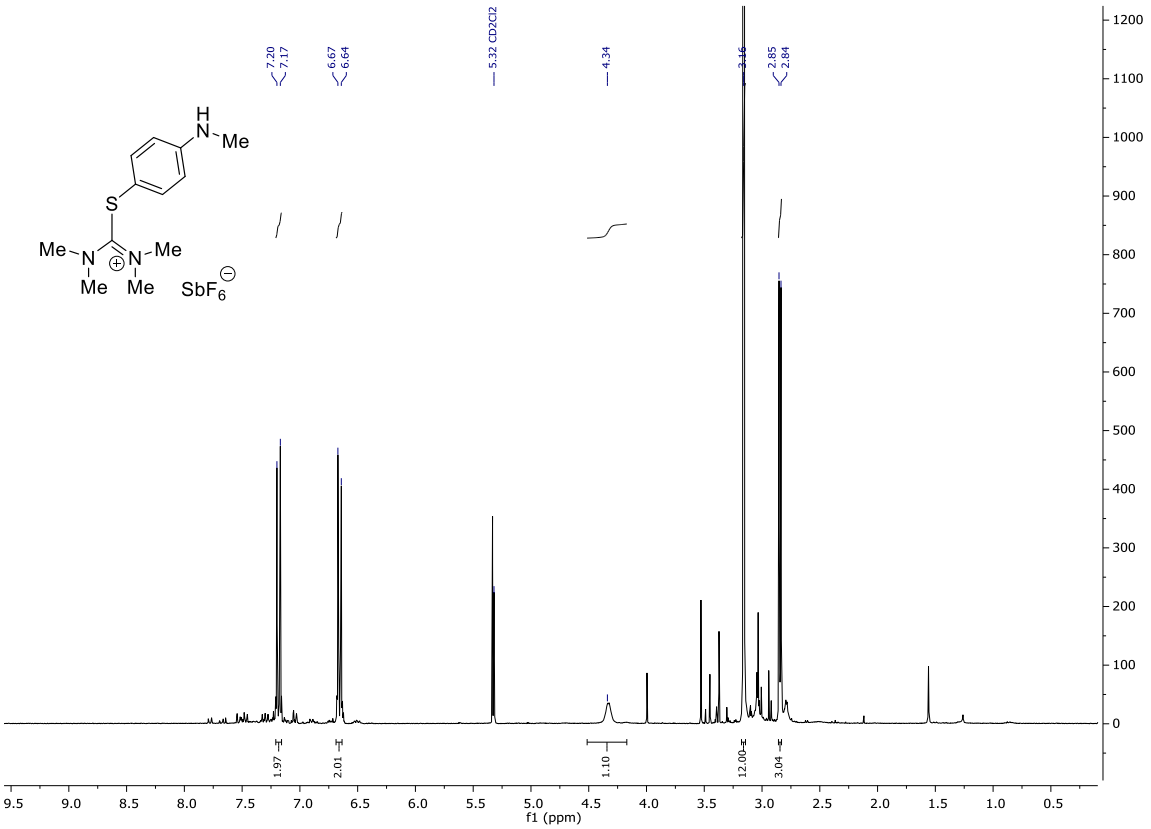

^{13}C NMR (75 MHz, CD_2Cl_2) **312**

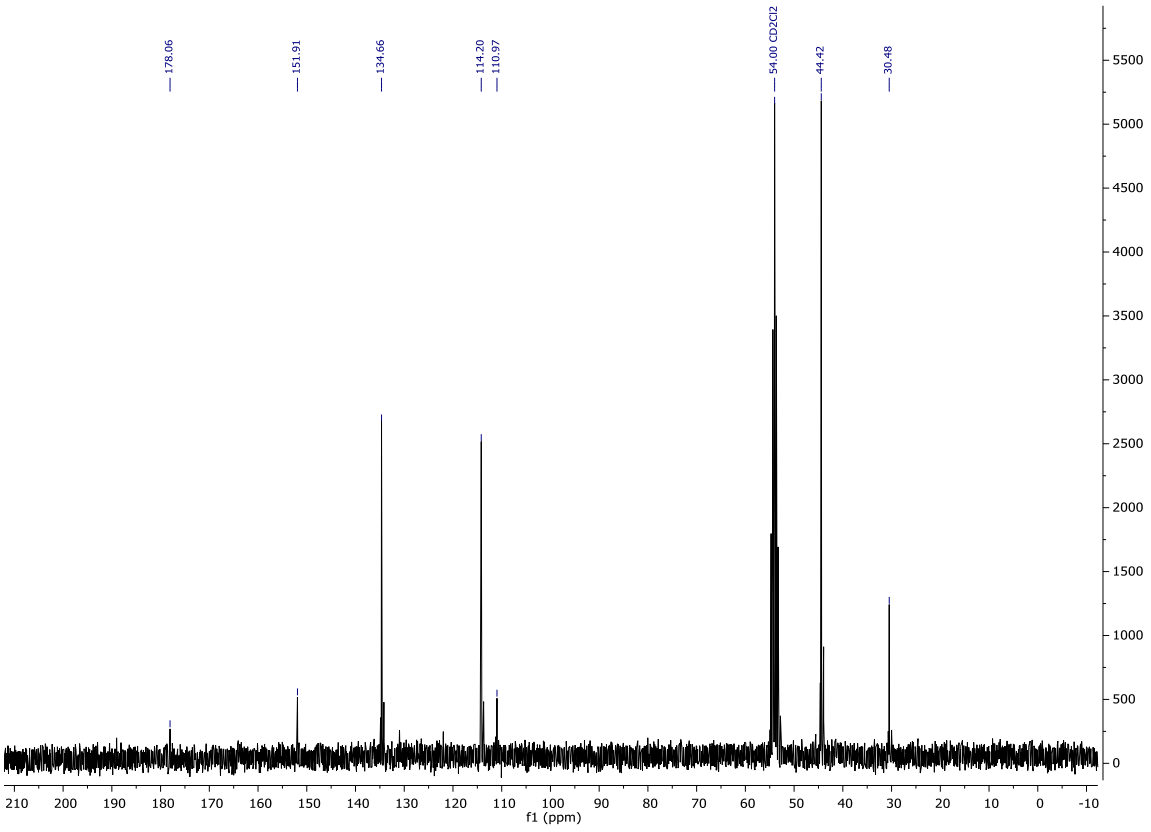

^{1}H NMR (300 MHz, CD_3CN) **313**

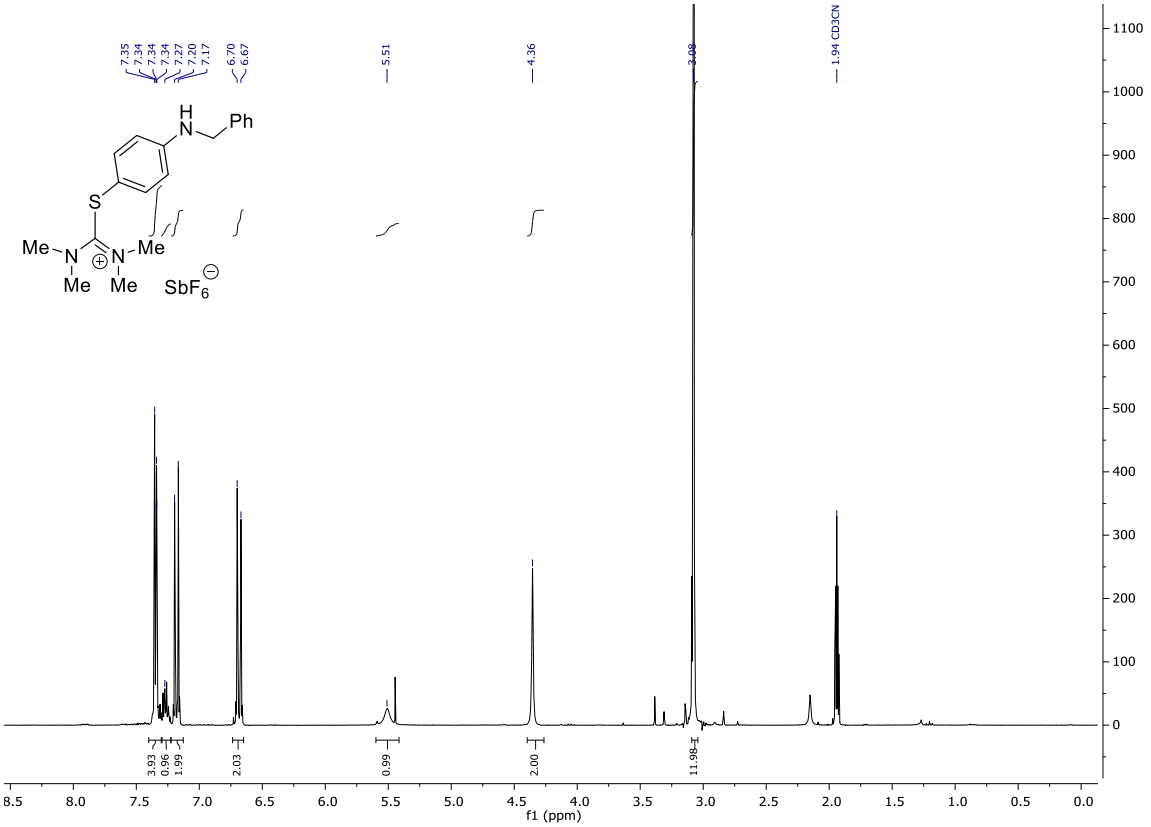

^{13}C NMR (126 MHz, CD_3CN) **313**

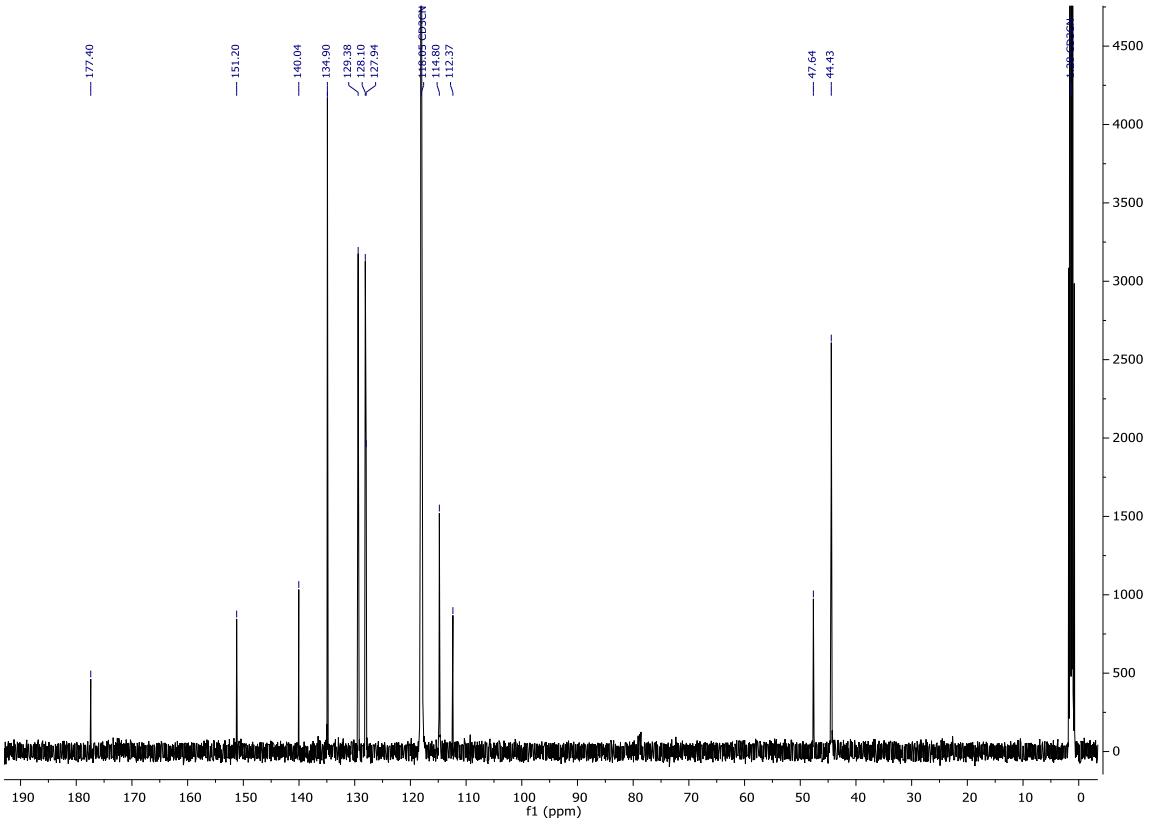

^{1}H NMR (300 MHz, CD_2Cl_2) **107a**

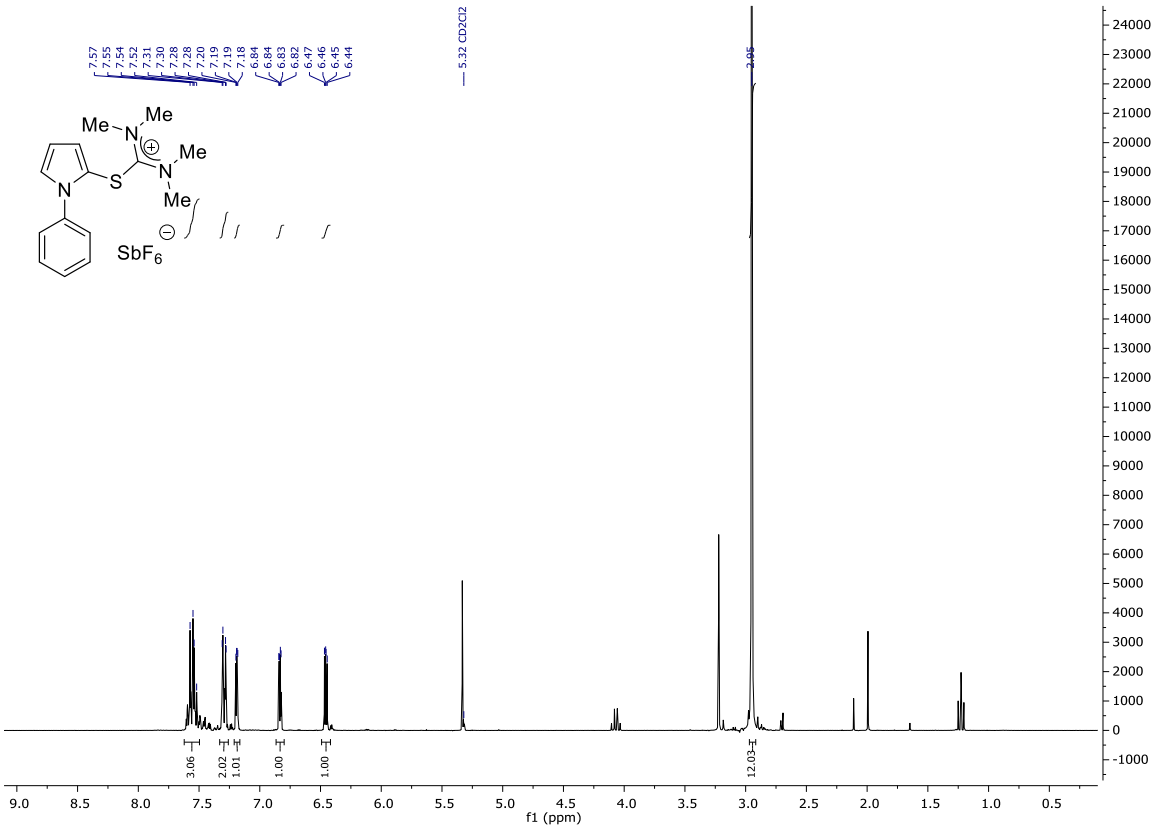

^{13}C NMR (75 MHz, CD_2Cl_2) **107a**

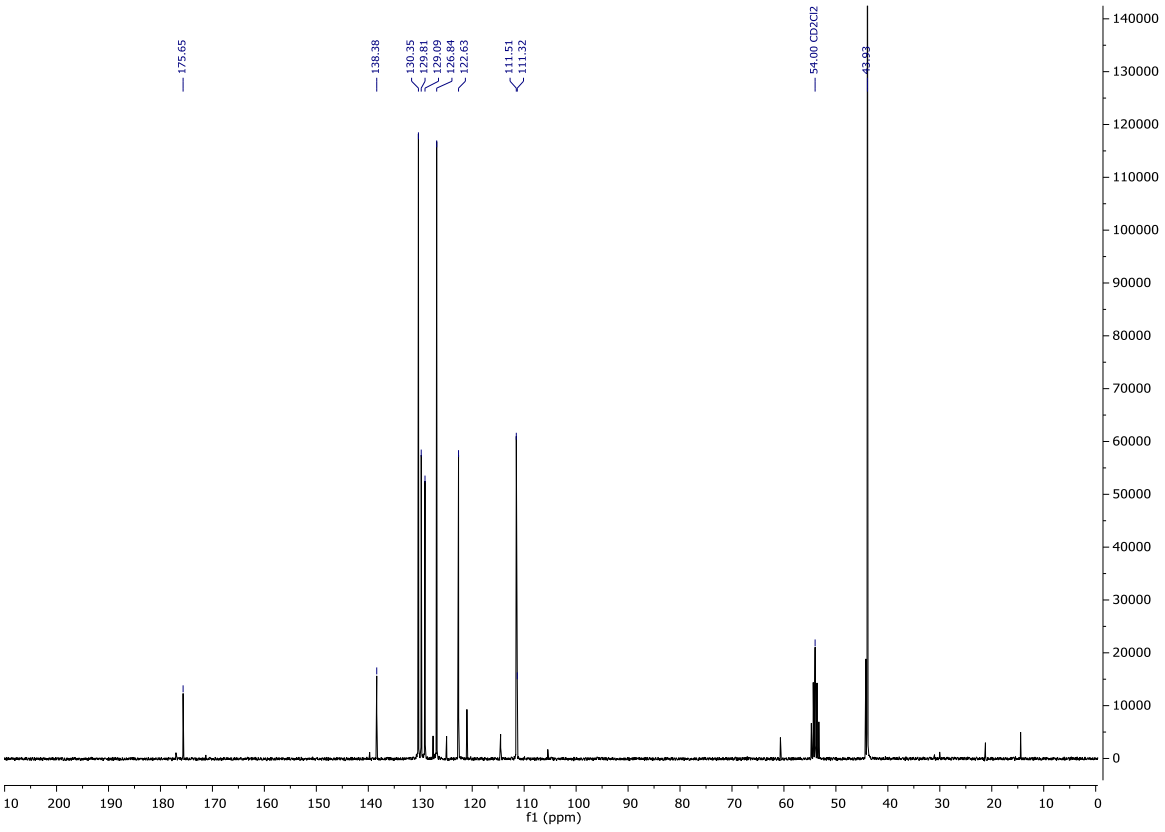

^{1}H NMR (300 MHz, CD_2Cl_2) **314**

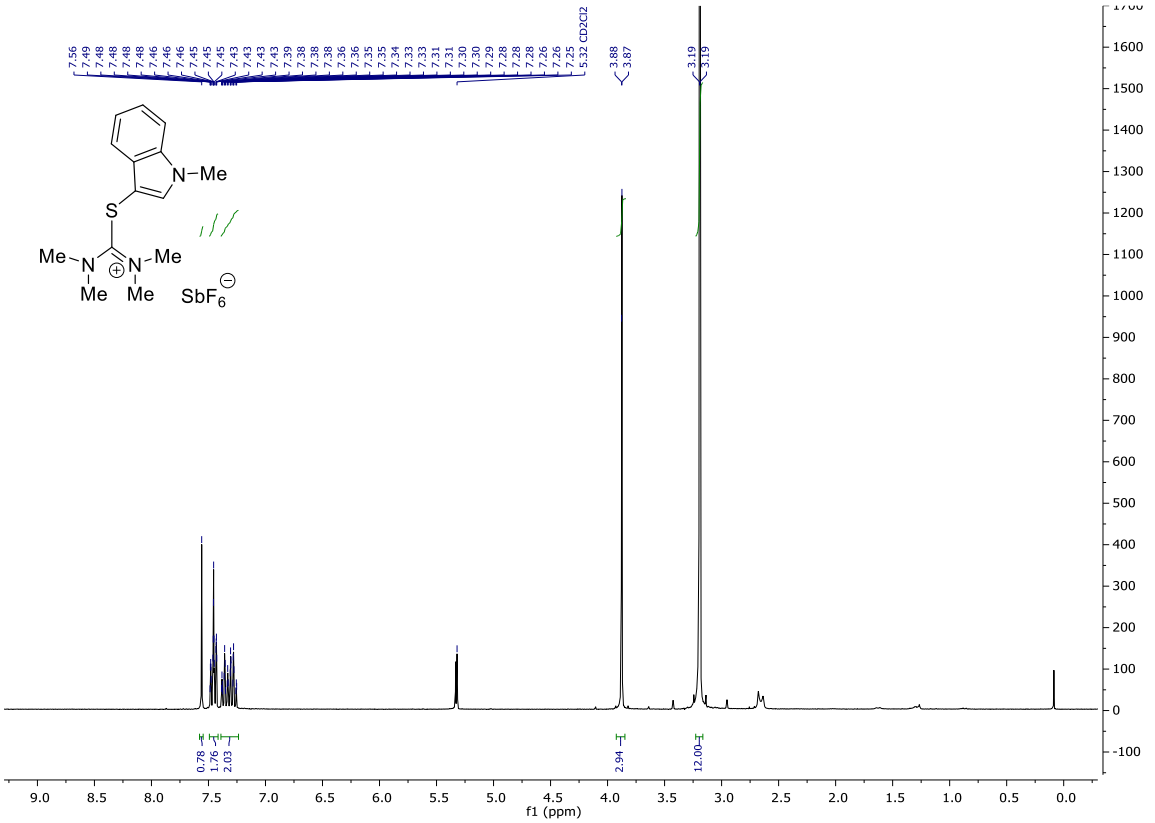

^{13}C NMR (75 MHz, CD_2Cl_2) **314**

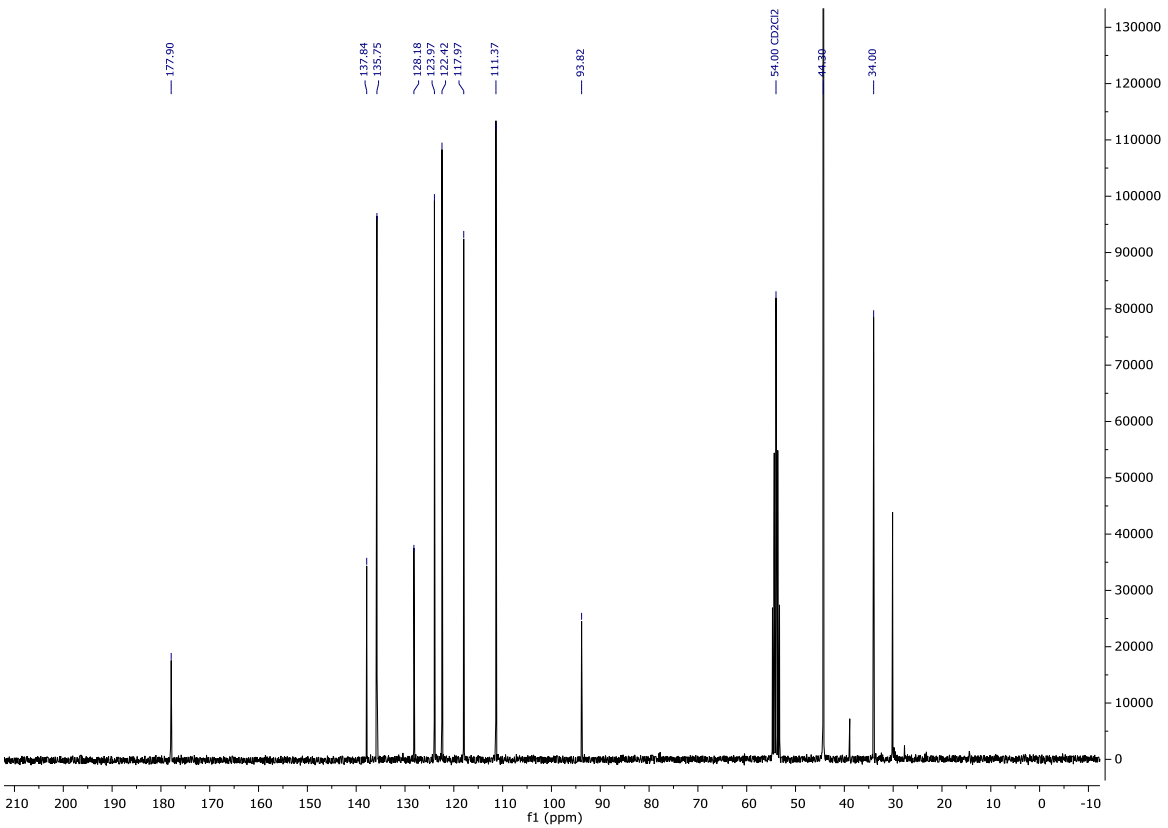

^{1}H NMR (300 MHz, CD_2Cl_2) **315**

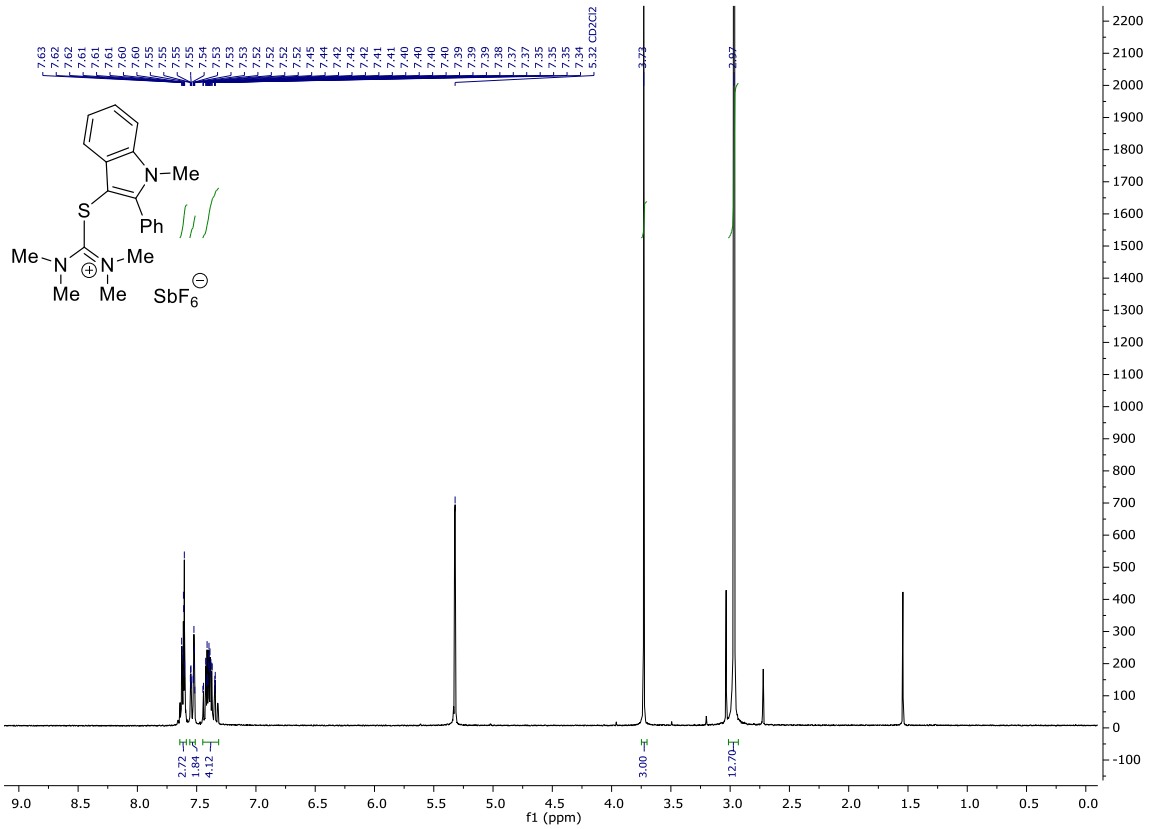

^{13}C NMR (75 MHz, CD_2Cl_2) **315**

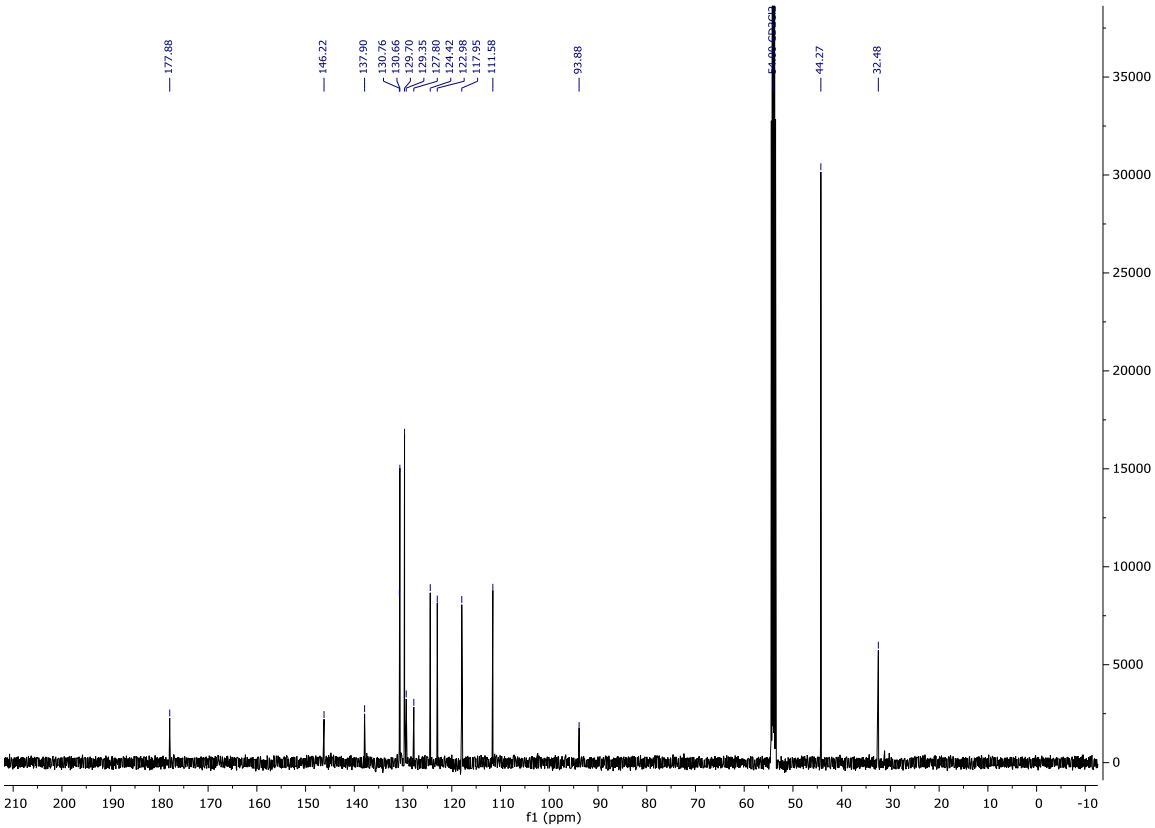

Synthesis of thiols and disulfides

^{1}H NMR (300 MHz, $CDCl_3$) **316**

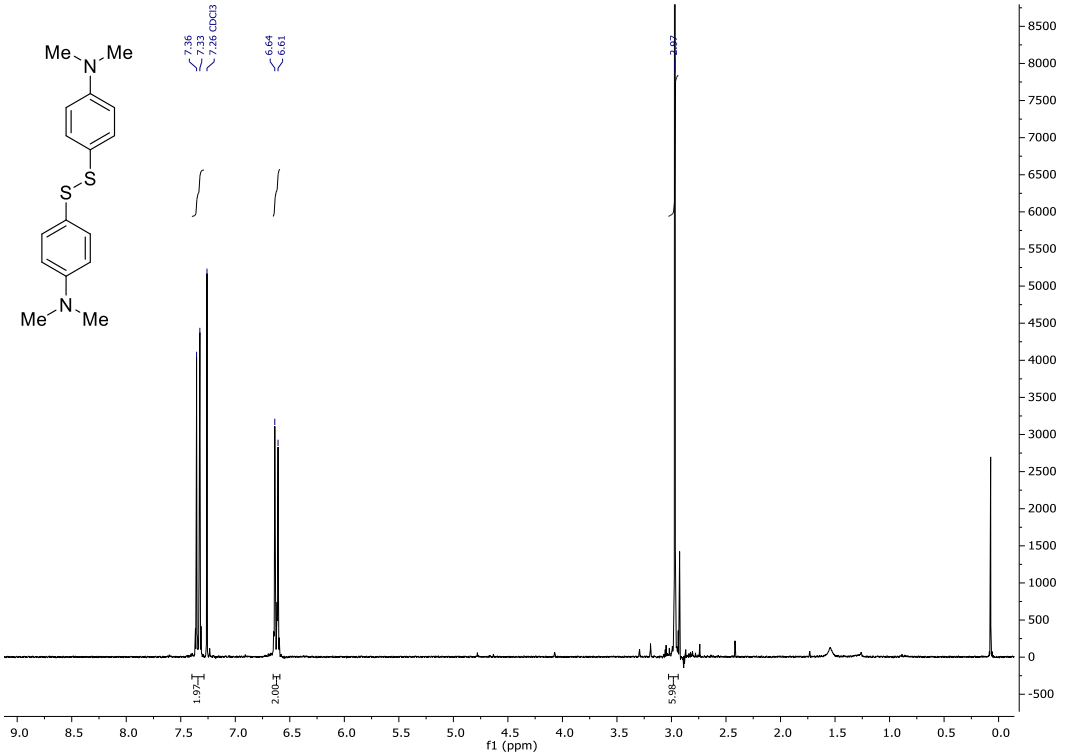

^{13}C NMR (75 MHz, $CDCl_3$) **316**

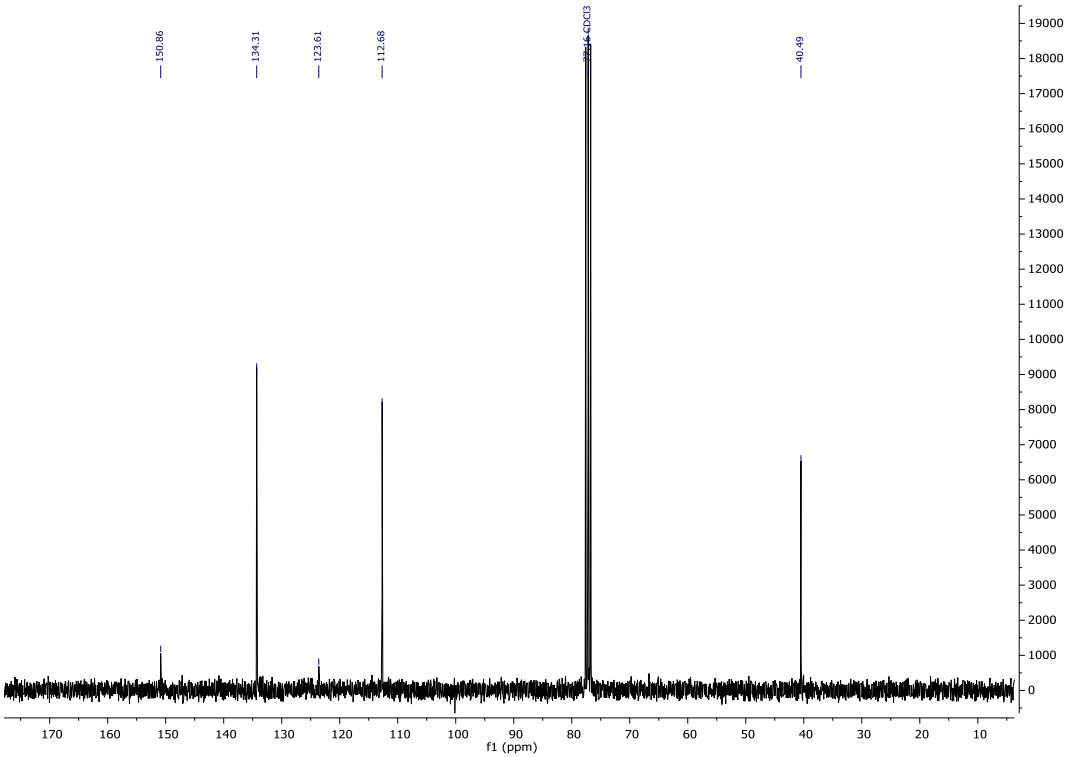

^{1}H NMR (300 MHz, $CDCl_3$) **317a**

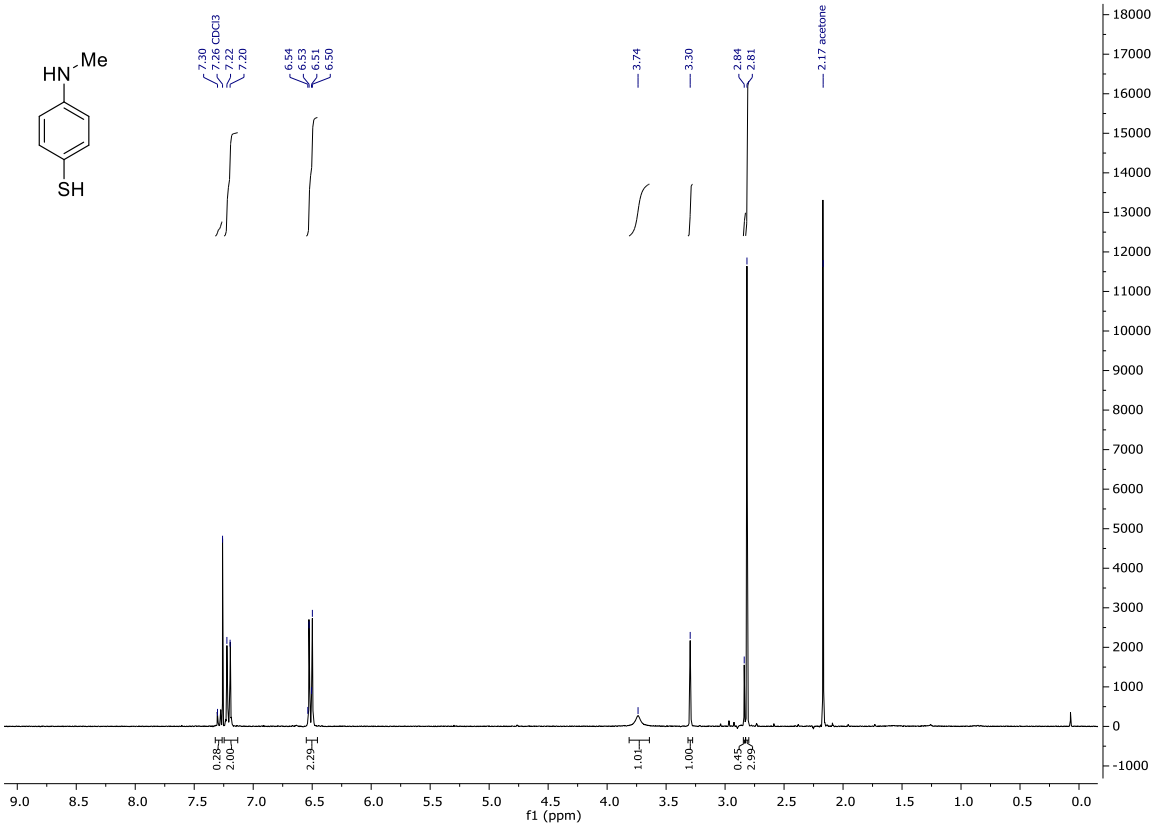

^{13}C NMR (75 MHz, $CDCl_3$) **317a**

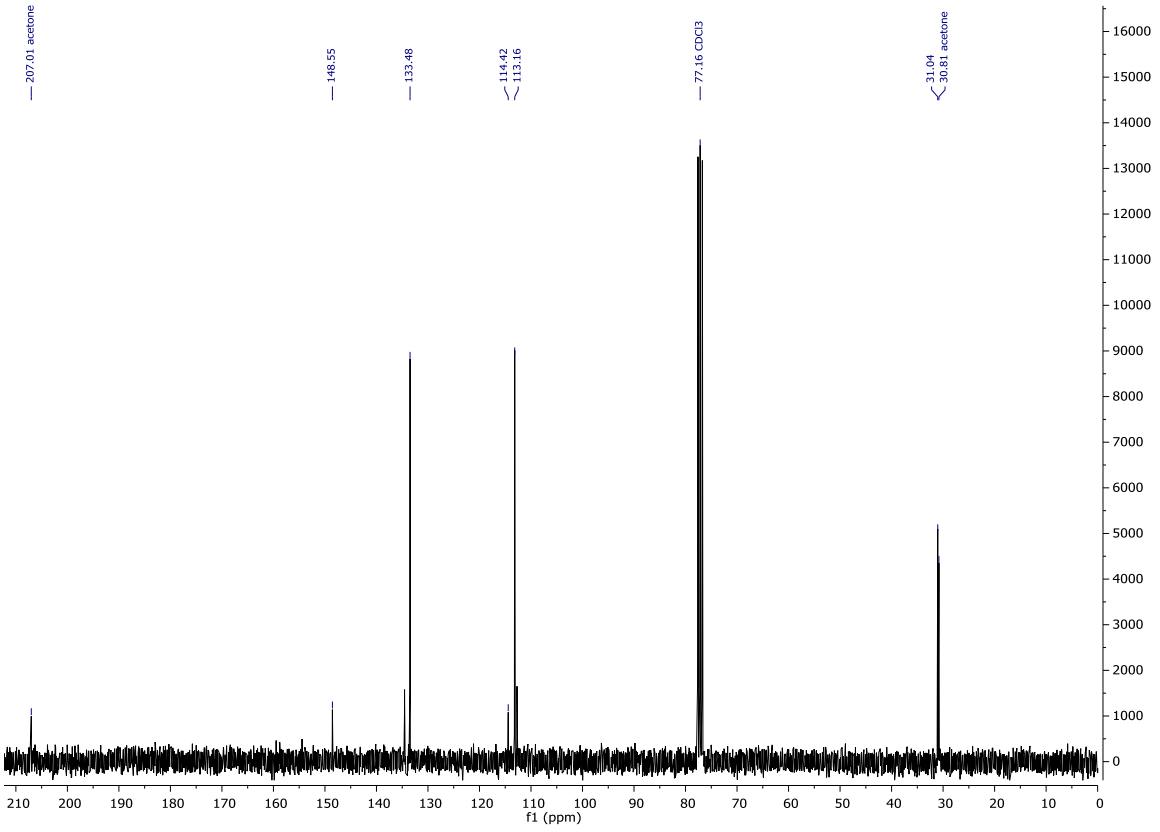

^{1}H NMR (300 MHz, CD_2Cl_2) **317b**

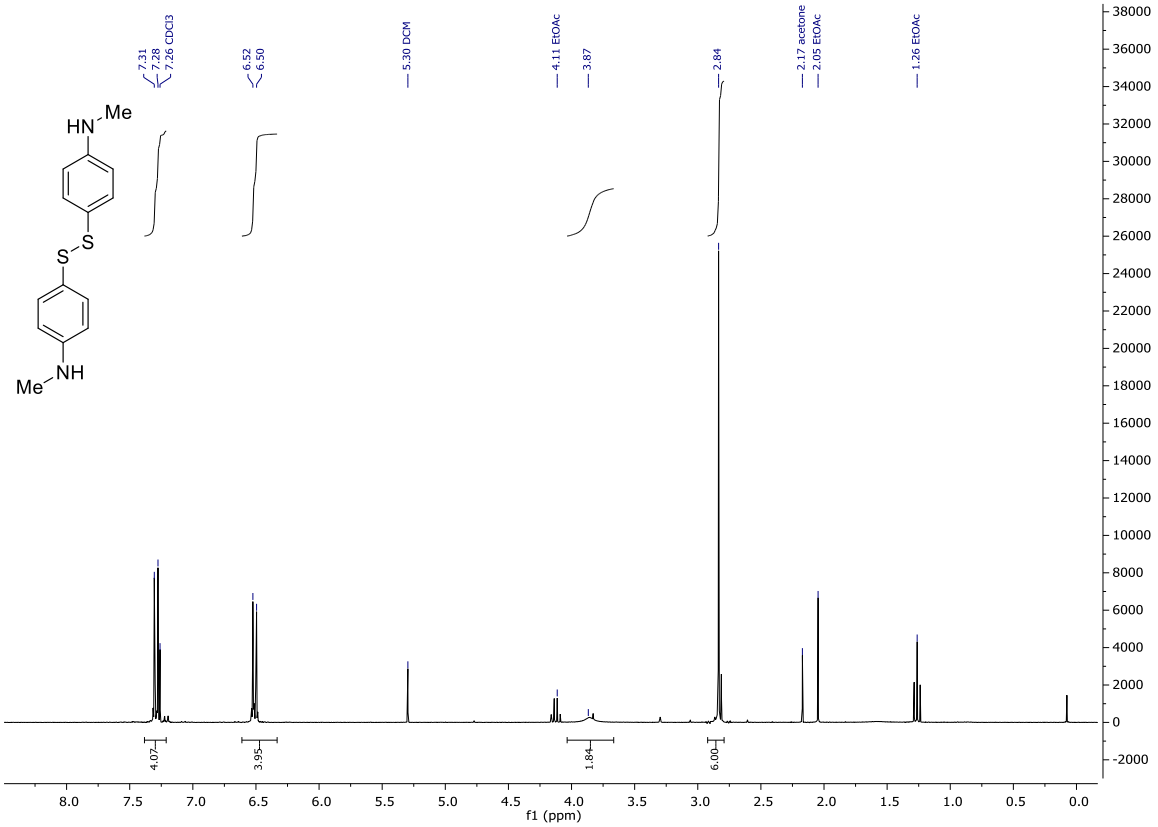

^{13}C NMR (75 MHz, CD_2Cl_2) **317b**

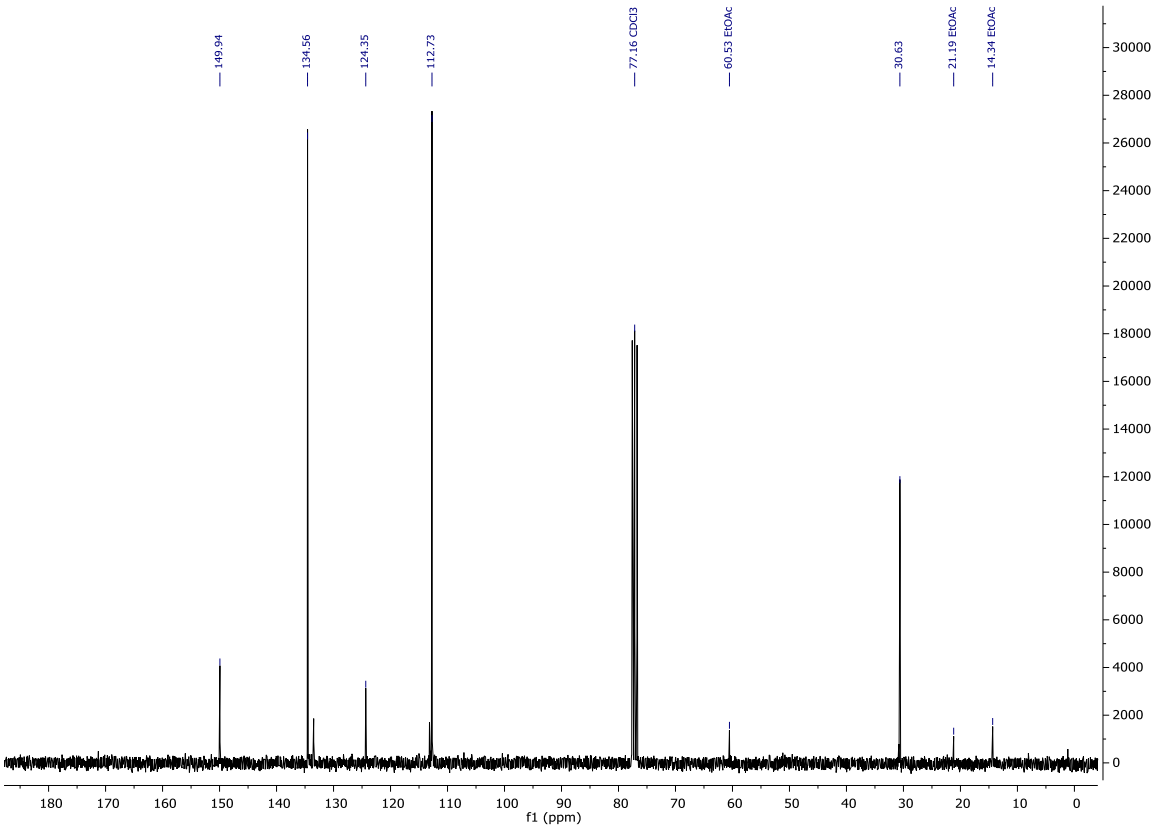

^{1}H NMR (300 MHz, $CDCl_3$) **318**

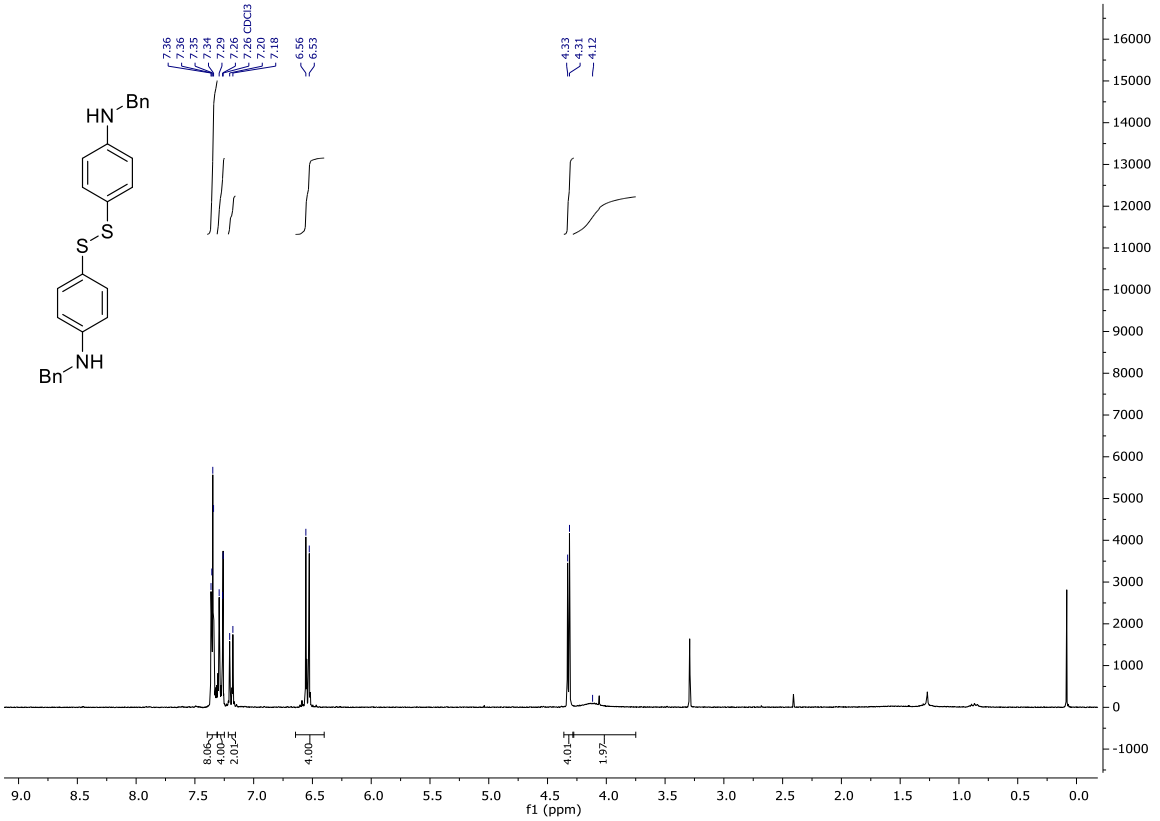

^{13}C NMR (75 MHz, $CDCl_3$) **318**

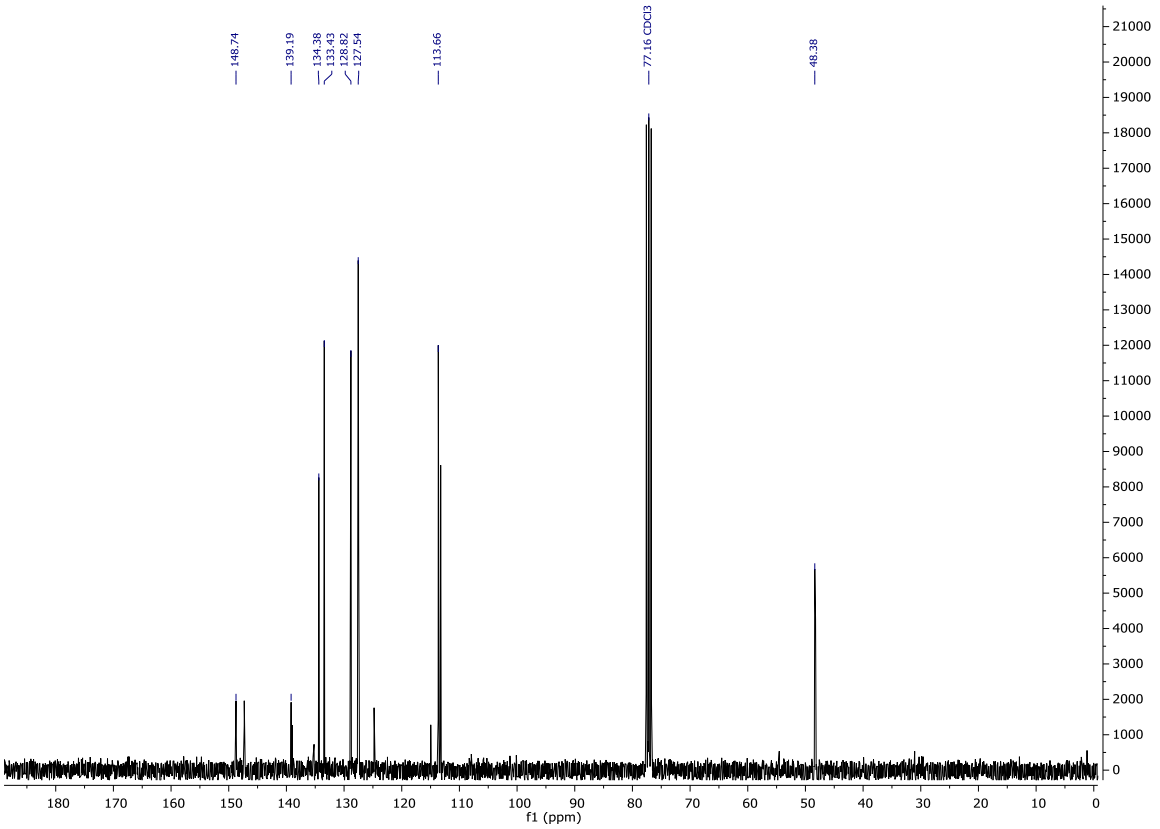

^{1}H NMR (300 MHz, CD_2Cl_2) **319**

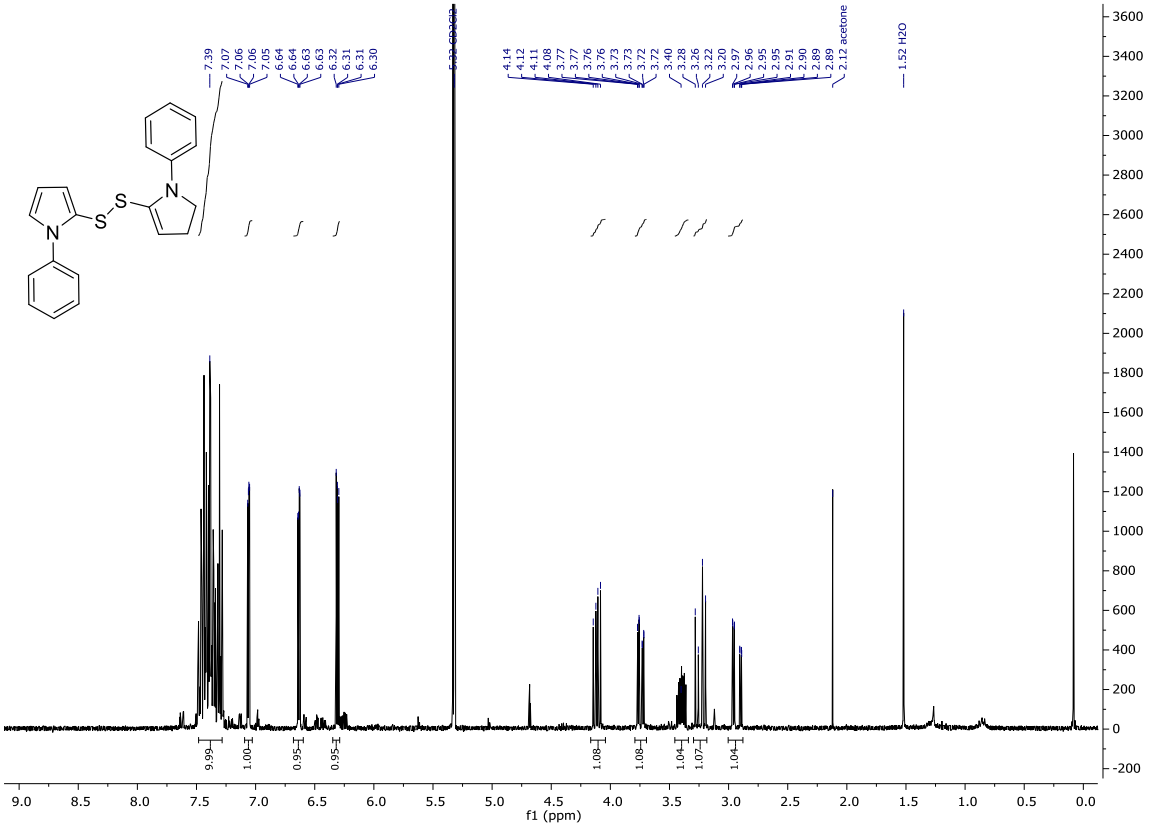

^{13}C NMR (75 MHz, CD_2Cl_2) **319**

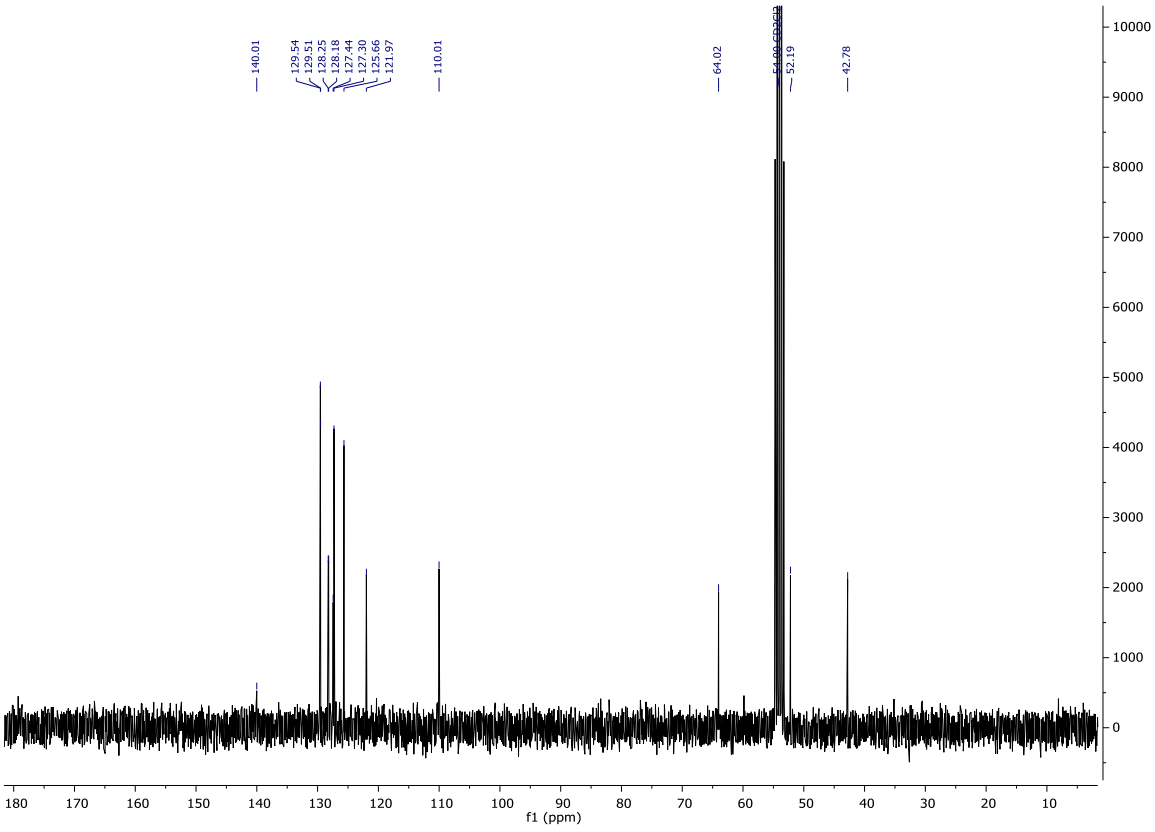

^{1}H NMR (300 MHz, CD_2Cl_2) **320**

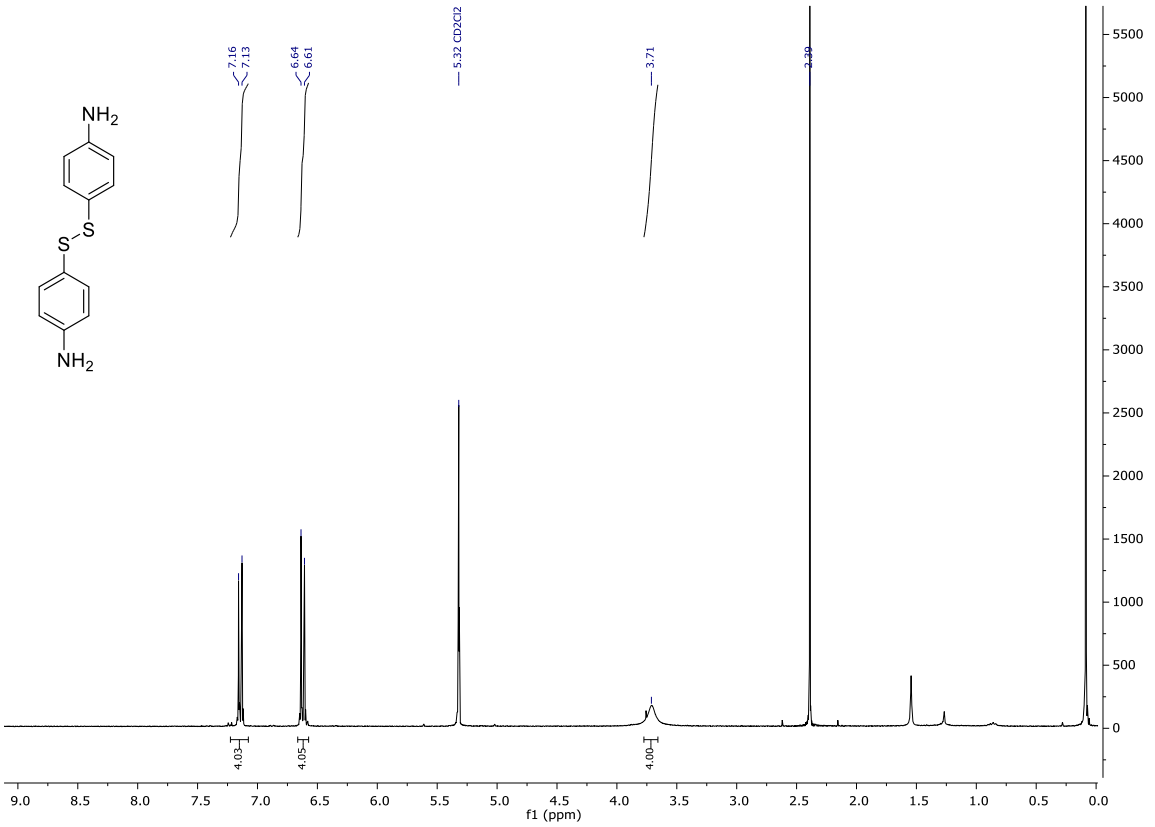

^{13}C NMR (75 MHz, CD_2Cl_2) **320**

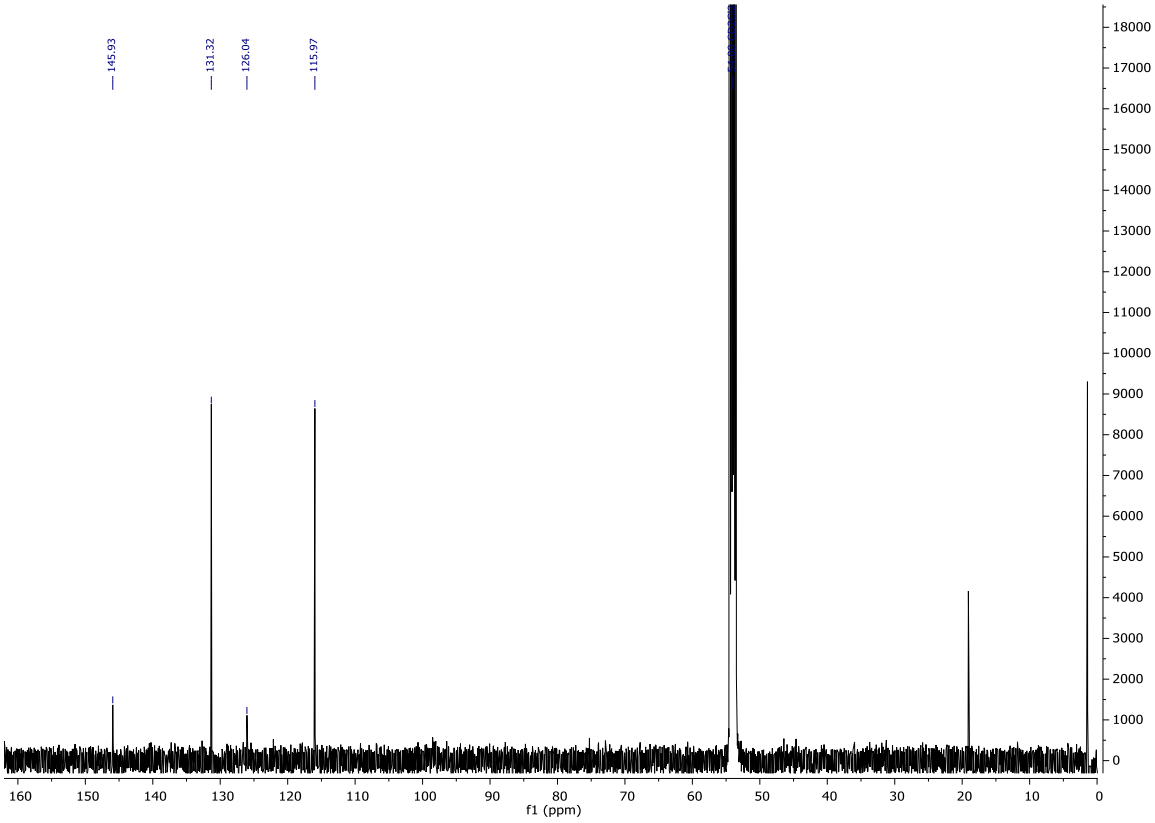

^{1}H NMR (300 MHz, CD_2Cl_2) **321**

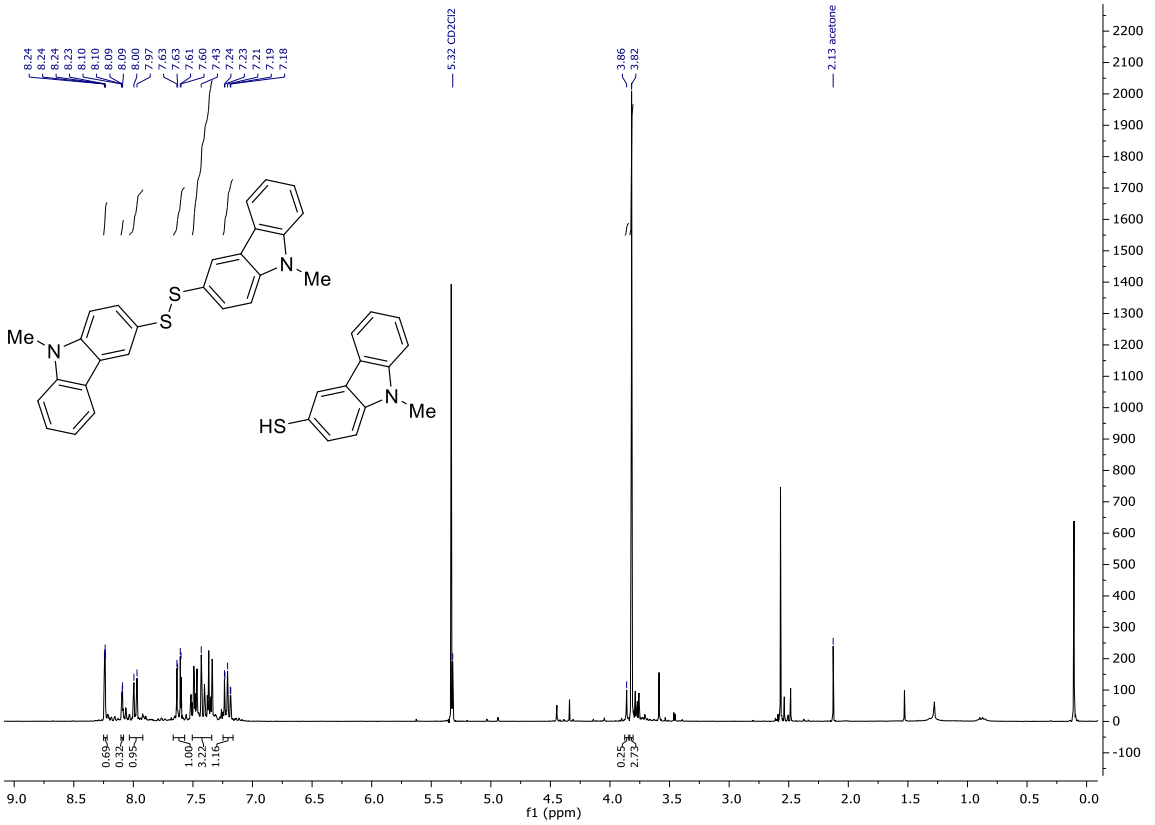

^{13}C NMR (75 MHz, CD_2Cl_2) **321**

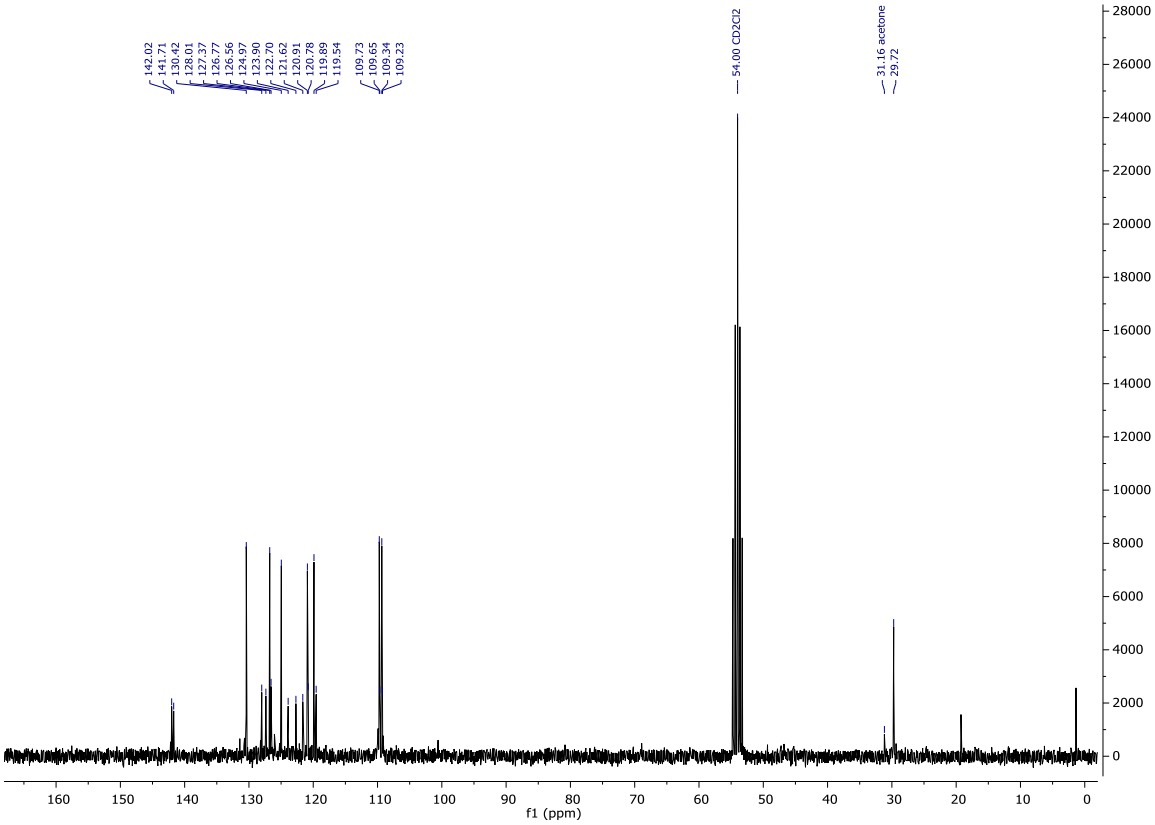

Dibenzothiophene studies

^{1}H NMR (400 MHz, CD_3CN) **304**

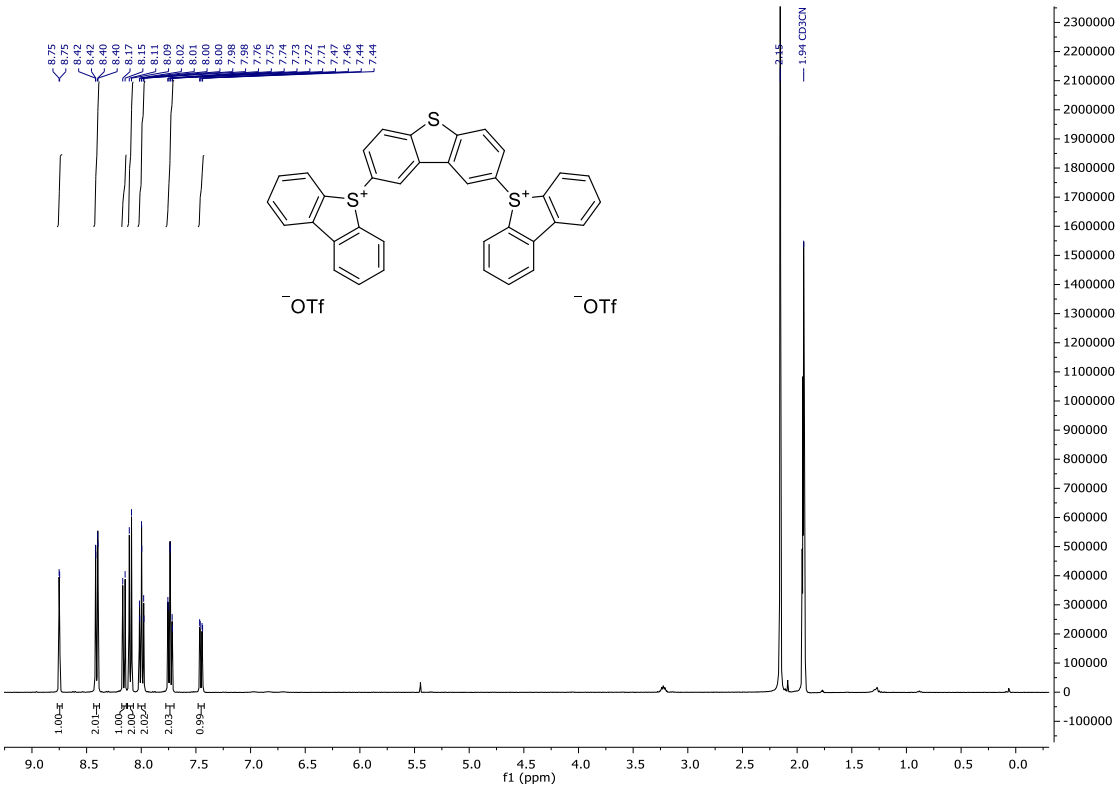

^{13}C NMR (101 MHz, CD_3CN) **304**

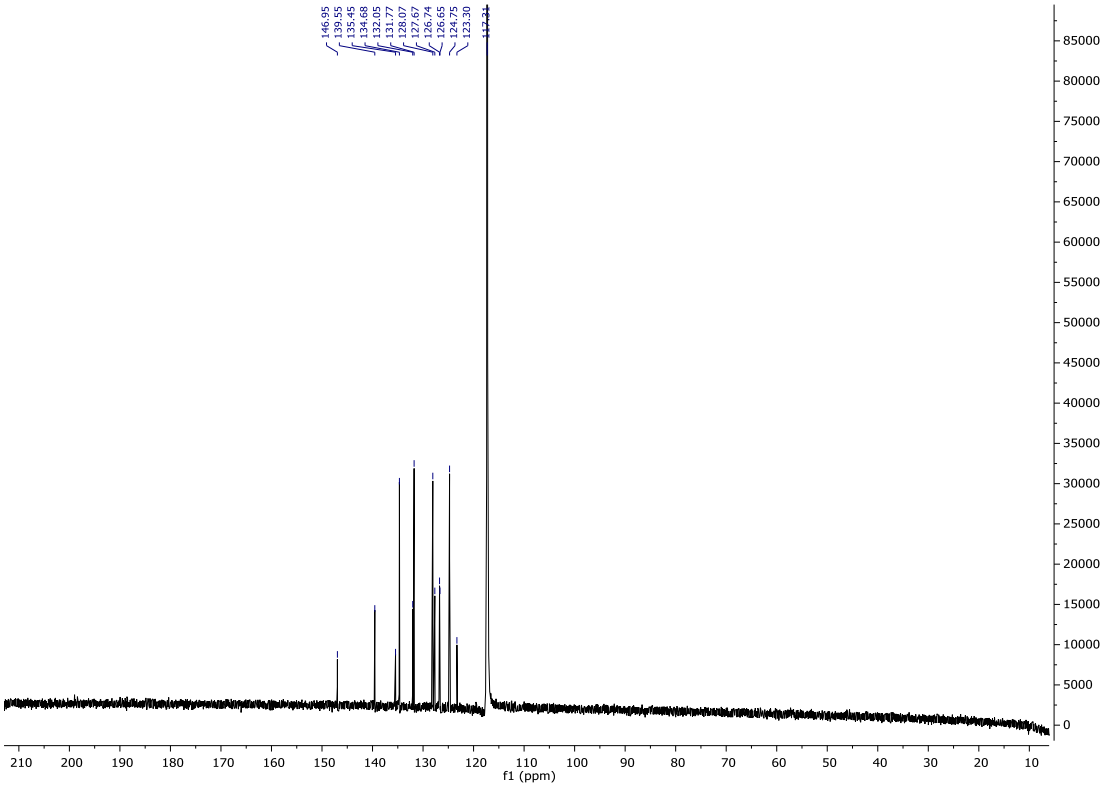

^{19}F NMR (282 MHz CD_3CN) **304**

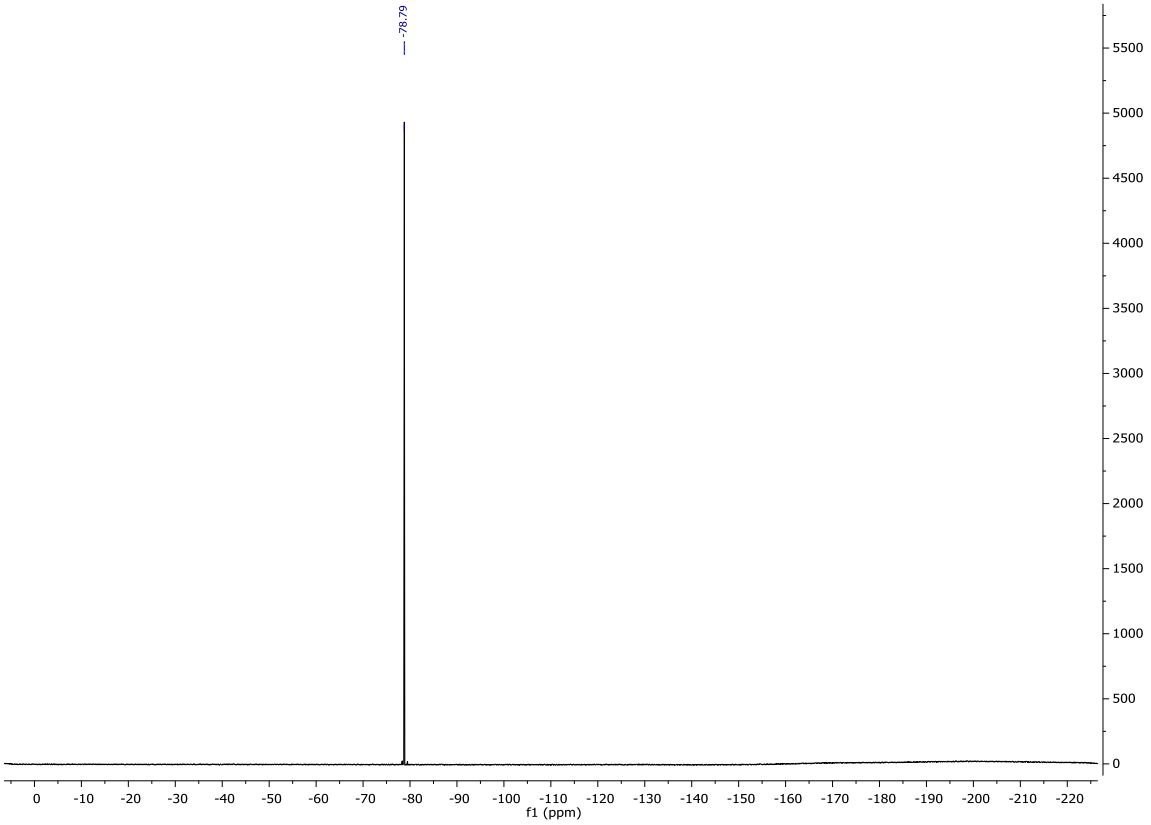

^{1}H NMR (300 MHz, CD_3CN) **323**

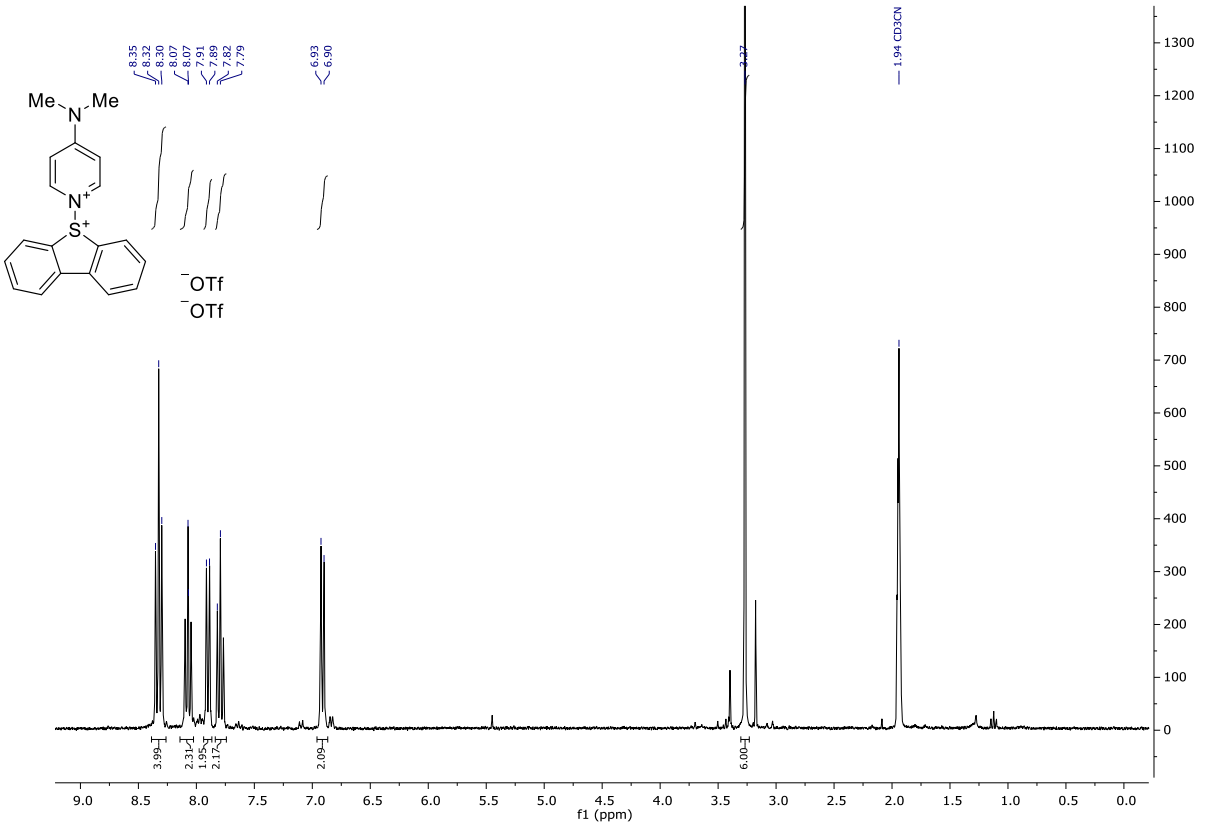

^{13}C NMR (101 MHz, CD_2Cl_2) **323**

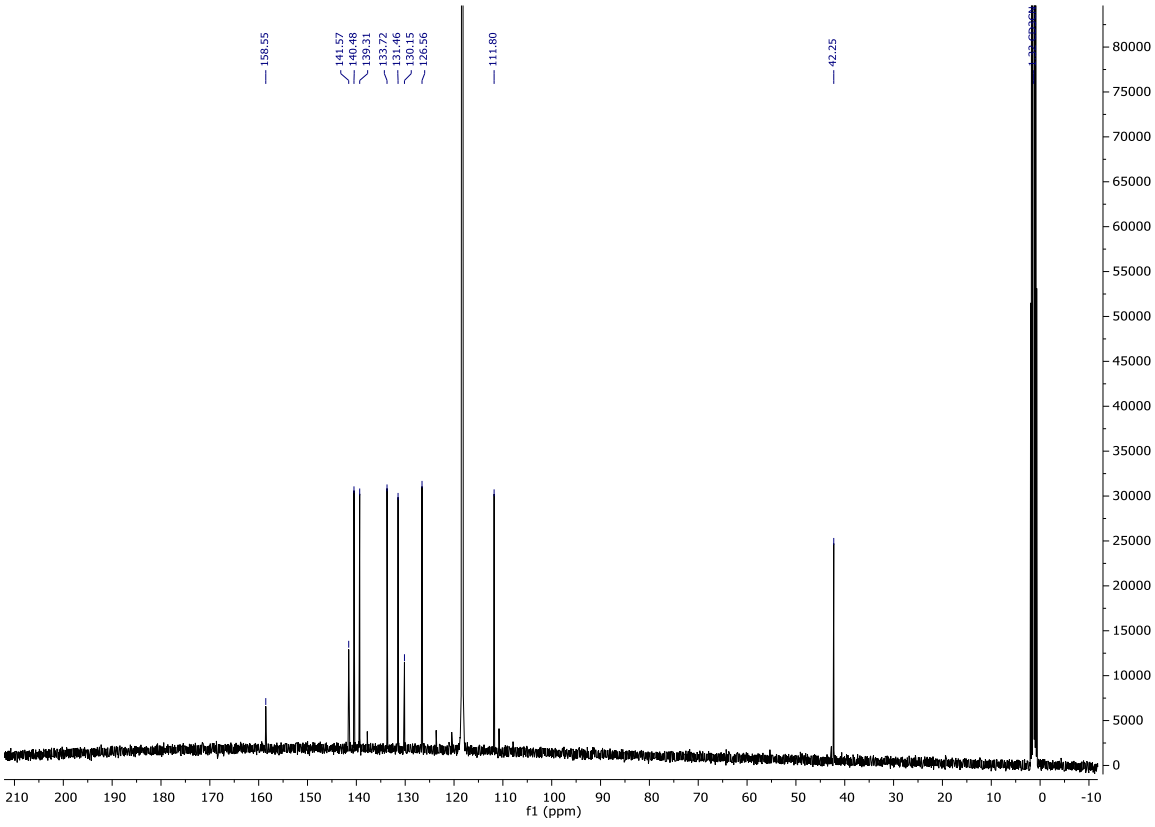

^{19}F NMR (282 MHz CD_3CN) **323**

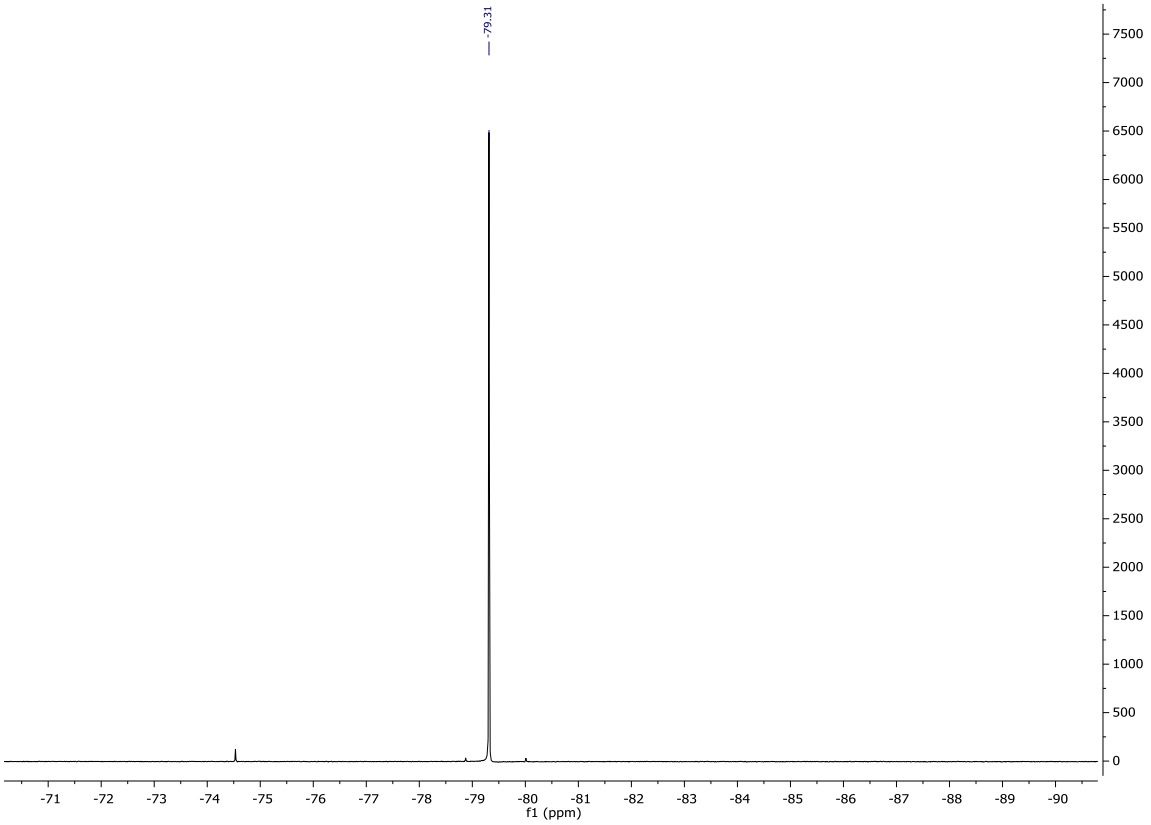

^{1}H NMR (400 MHz, CD_3CN) **324**

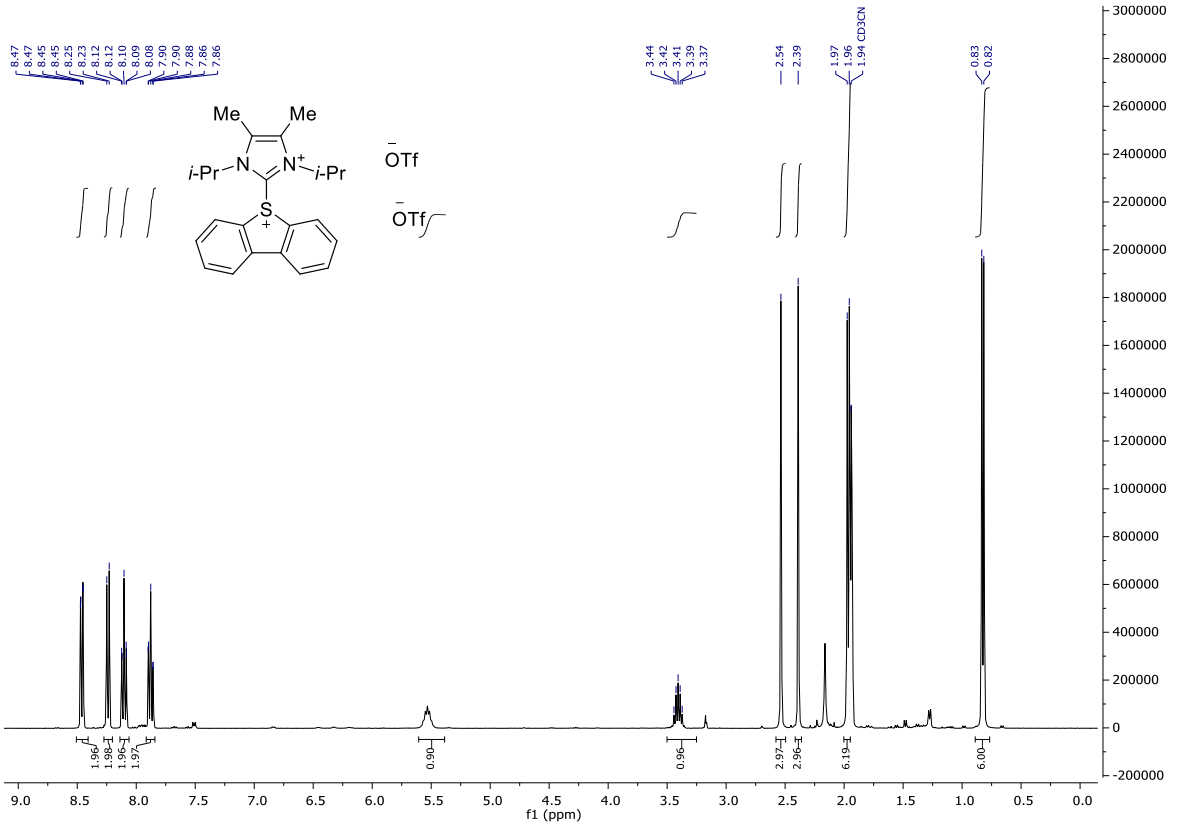

^{13}C NMR (126 MHz, CD_3CN) **324**

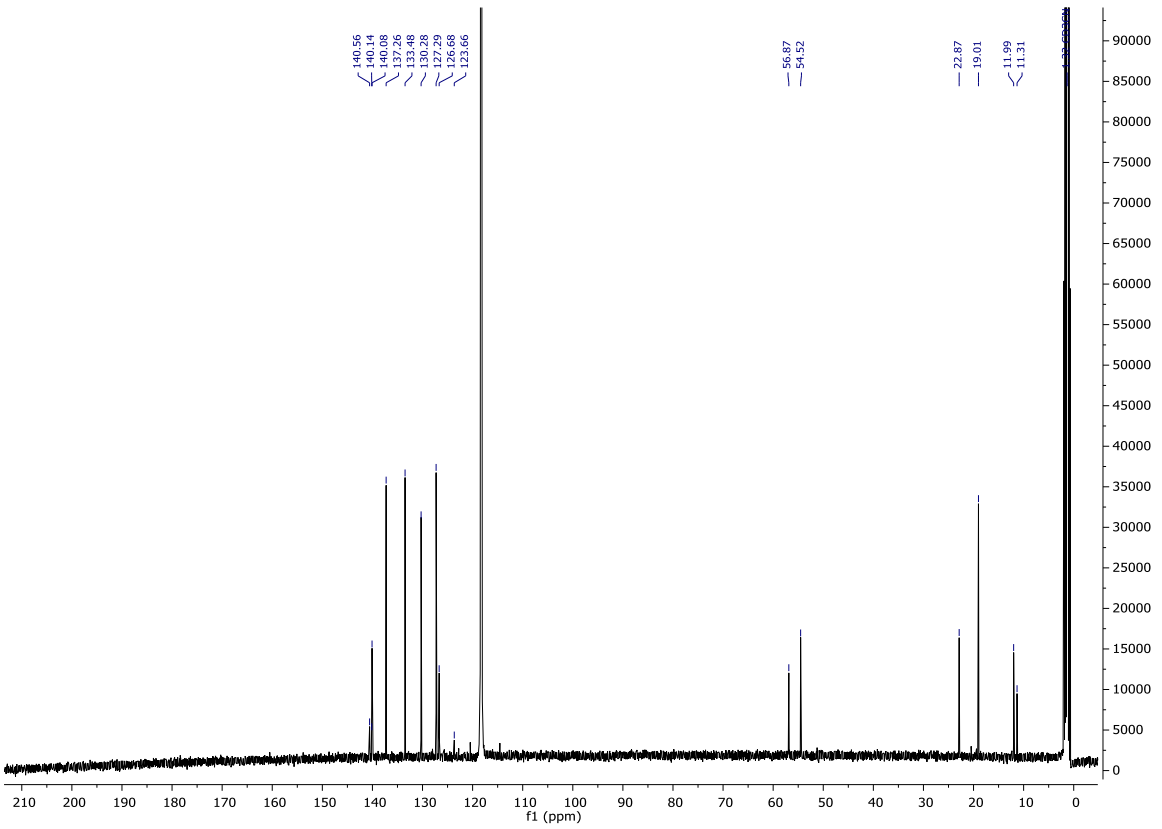

^{19}F NMR (282 MHz CD_3CN) **324**

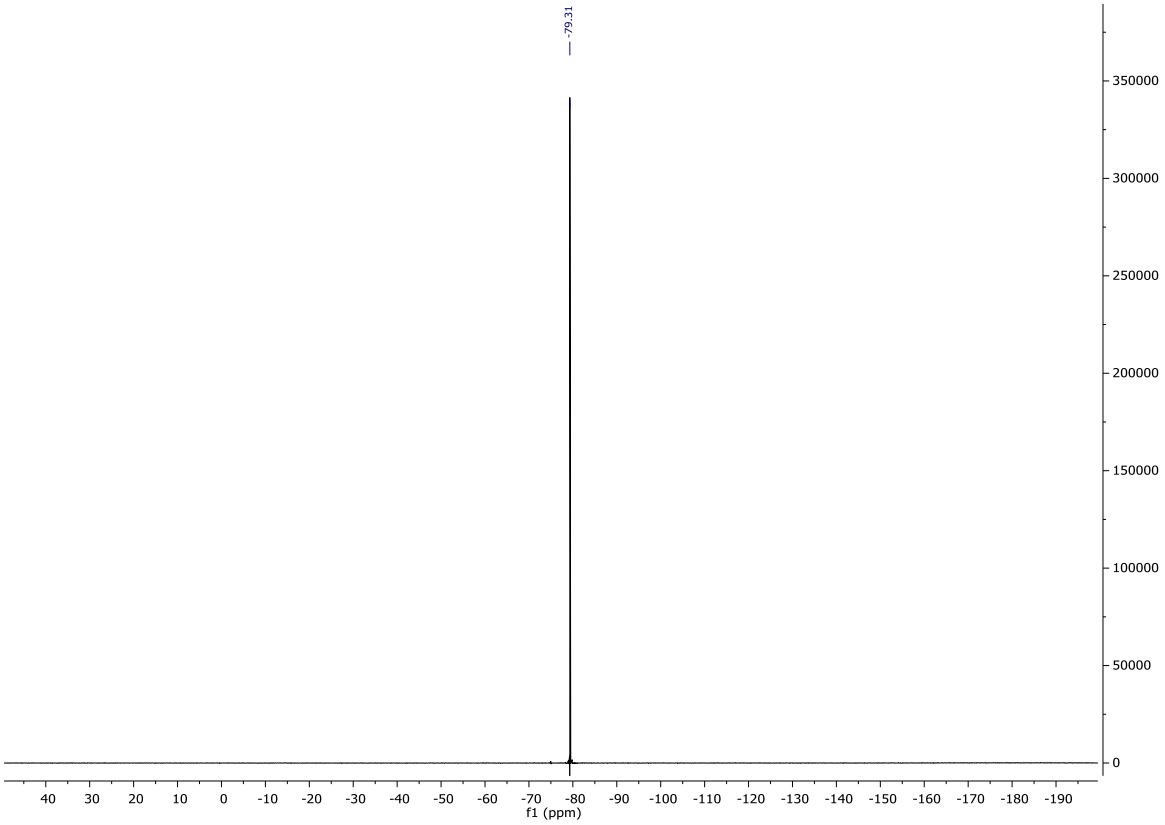

COSY ^{1}H-^{1}H-NMR (400 MHz, CD_3CN) **324**

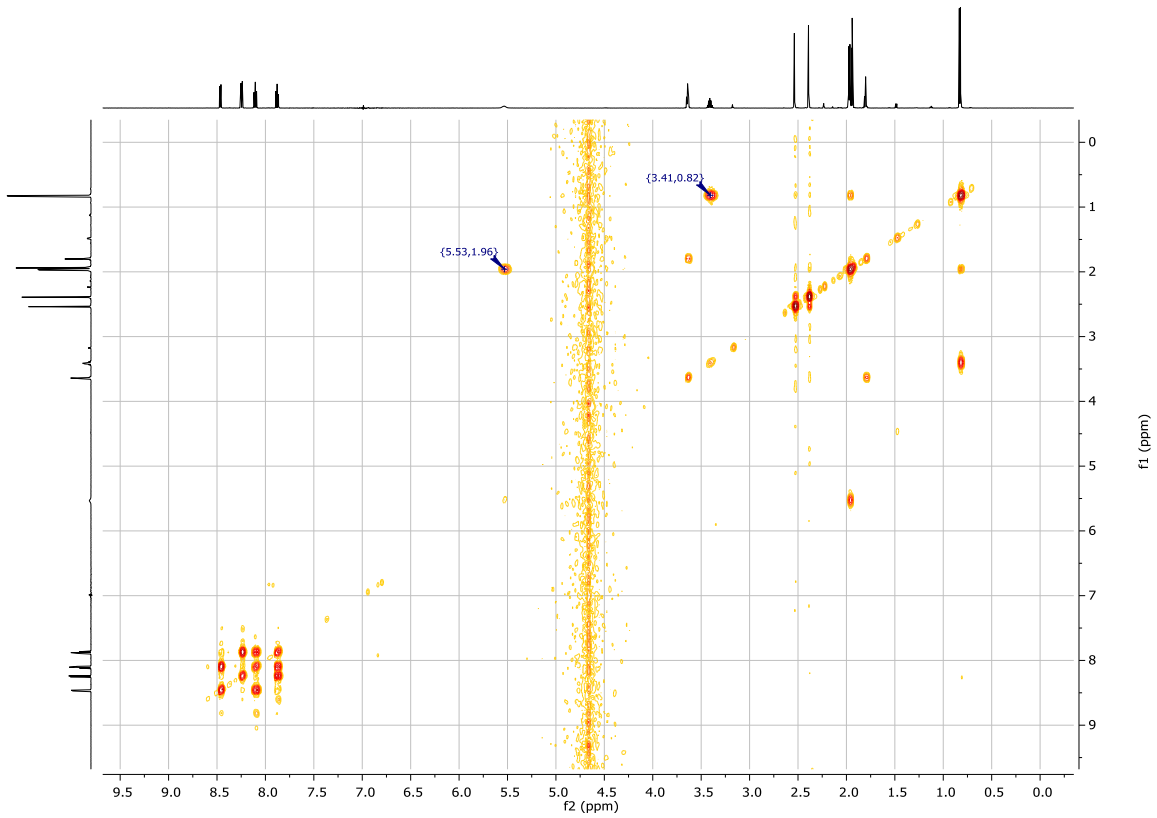

NOESY ^{1}H-^{1}H-NMR (400 MHz, CD_3CN) **324**

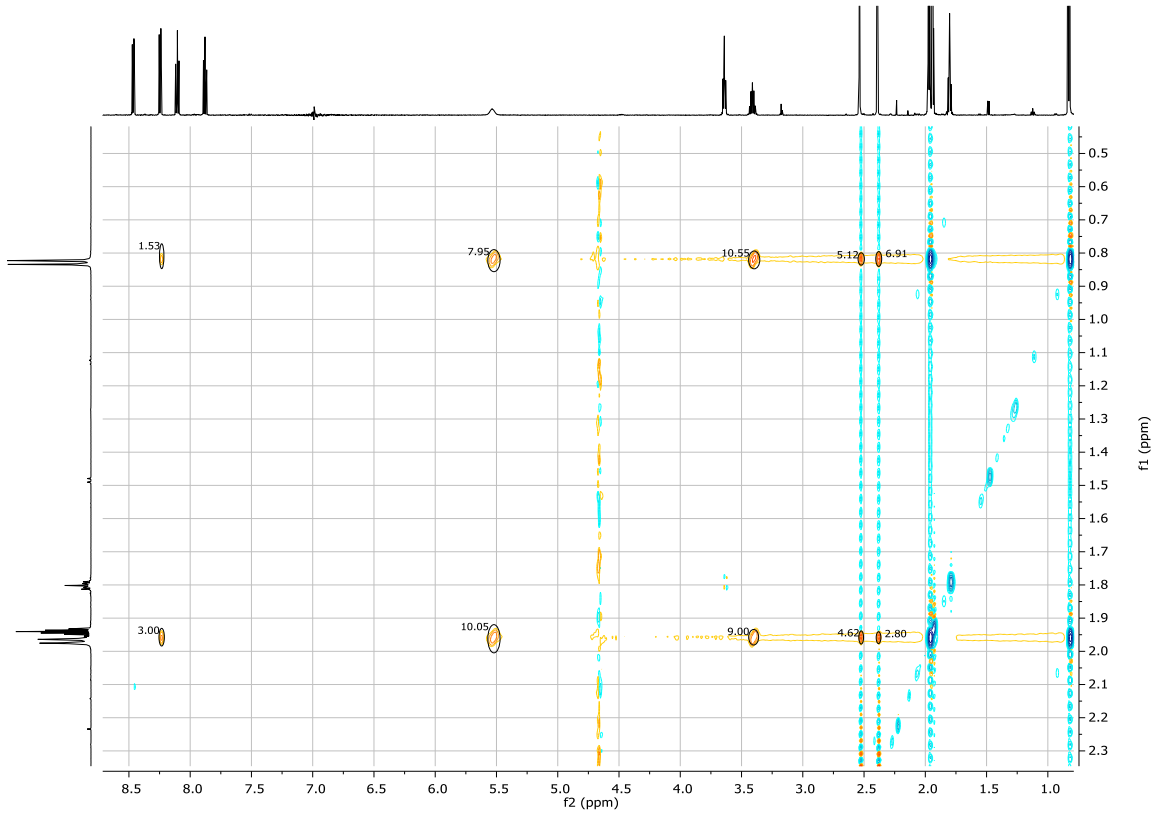

^{1}H NMR (400 MHz, CD_2Cl_2) **325**

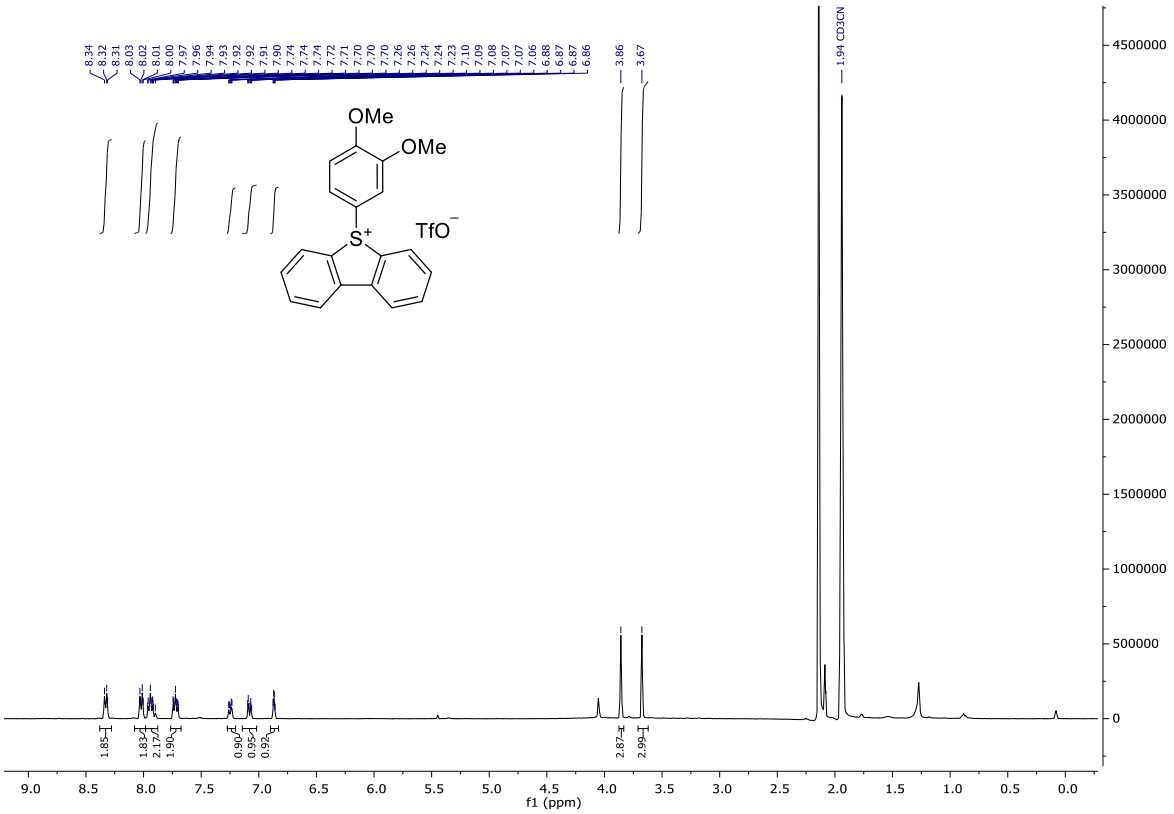

^{13}C NMR (126 MHz, $CDCl_3$) **325**

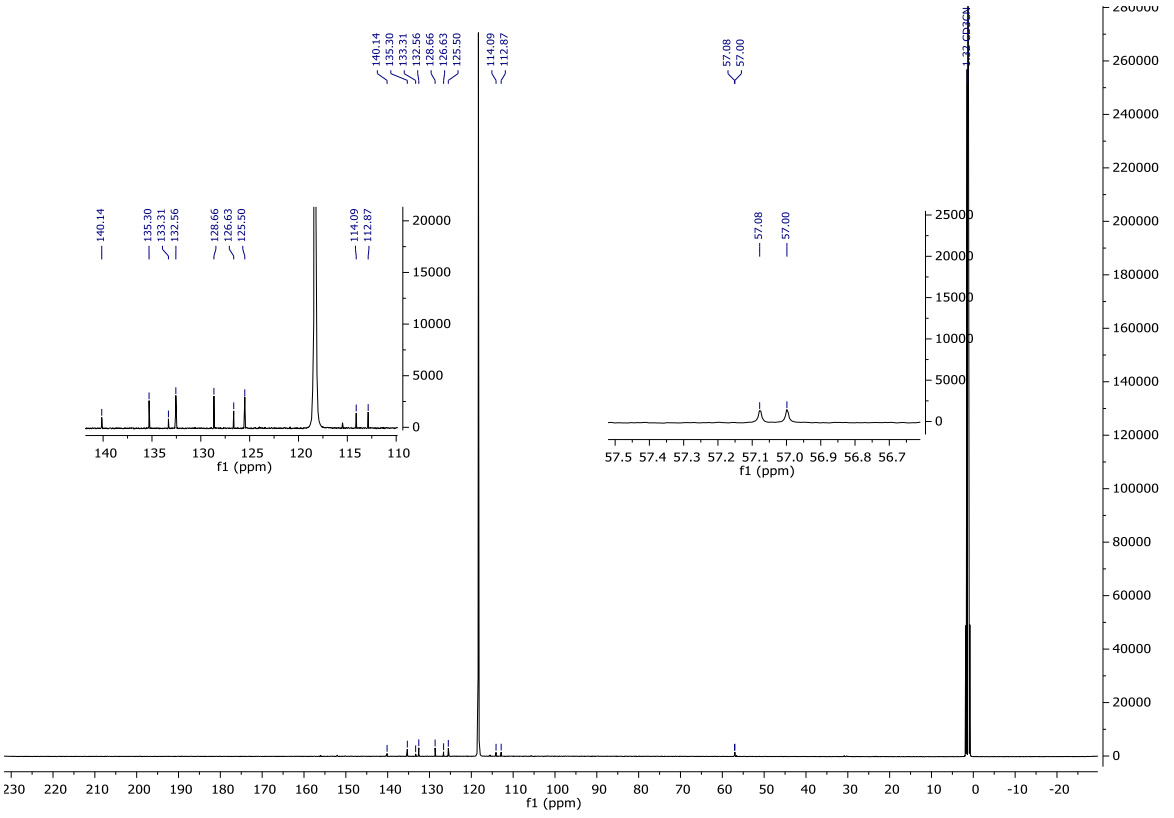

^{19}F NMR (282 MHz, CD_3CN) **325**

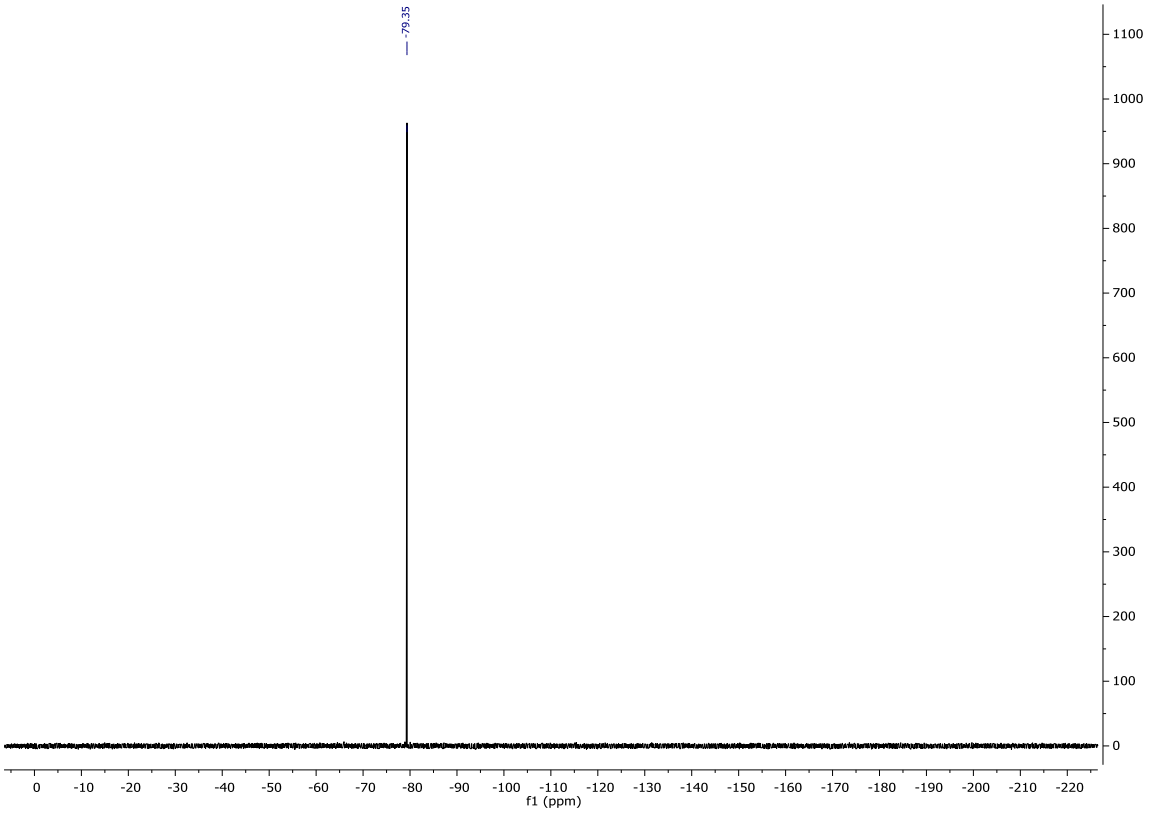

^{1}H NMR (300 MHz, CD_3CN) **326**

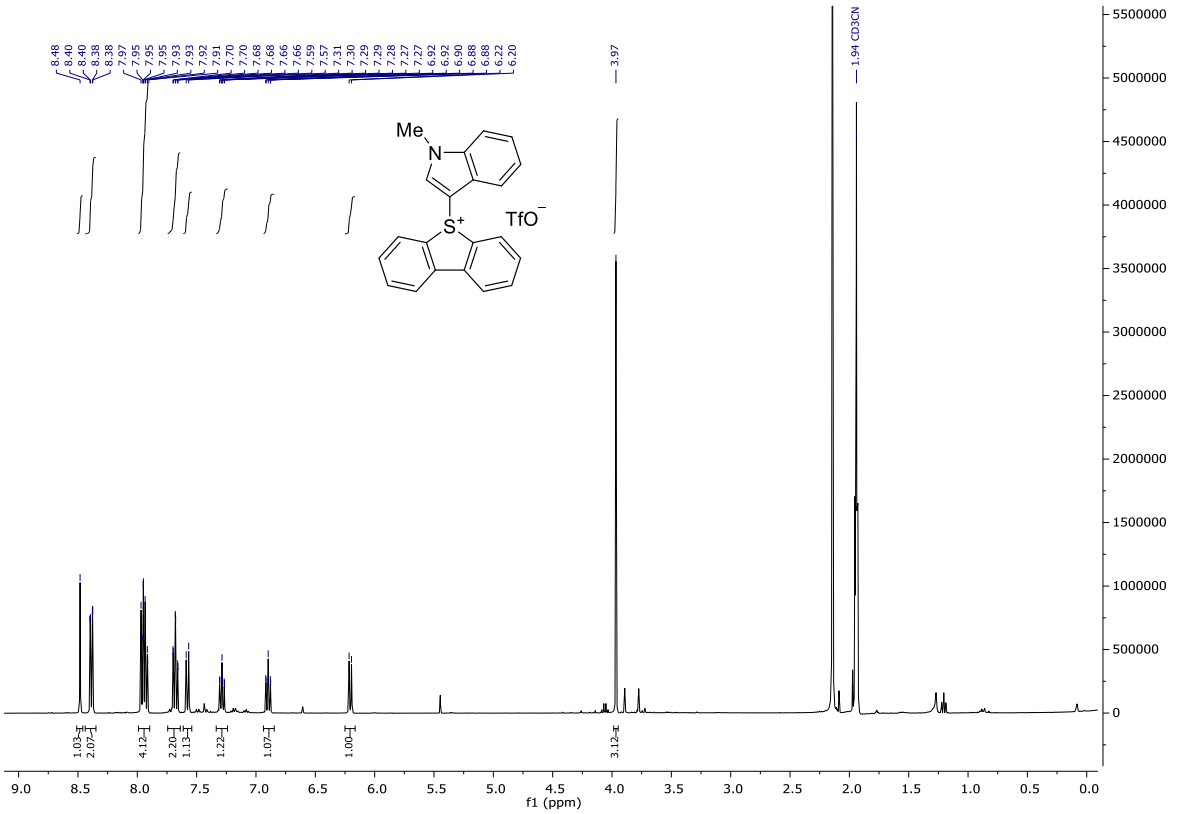

^{13}C NMR (126 MHz, CD_3CN) **326**

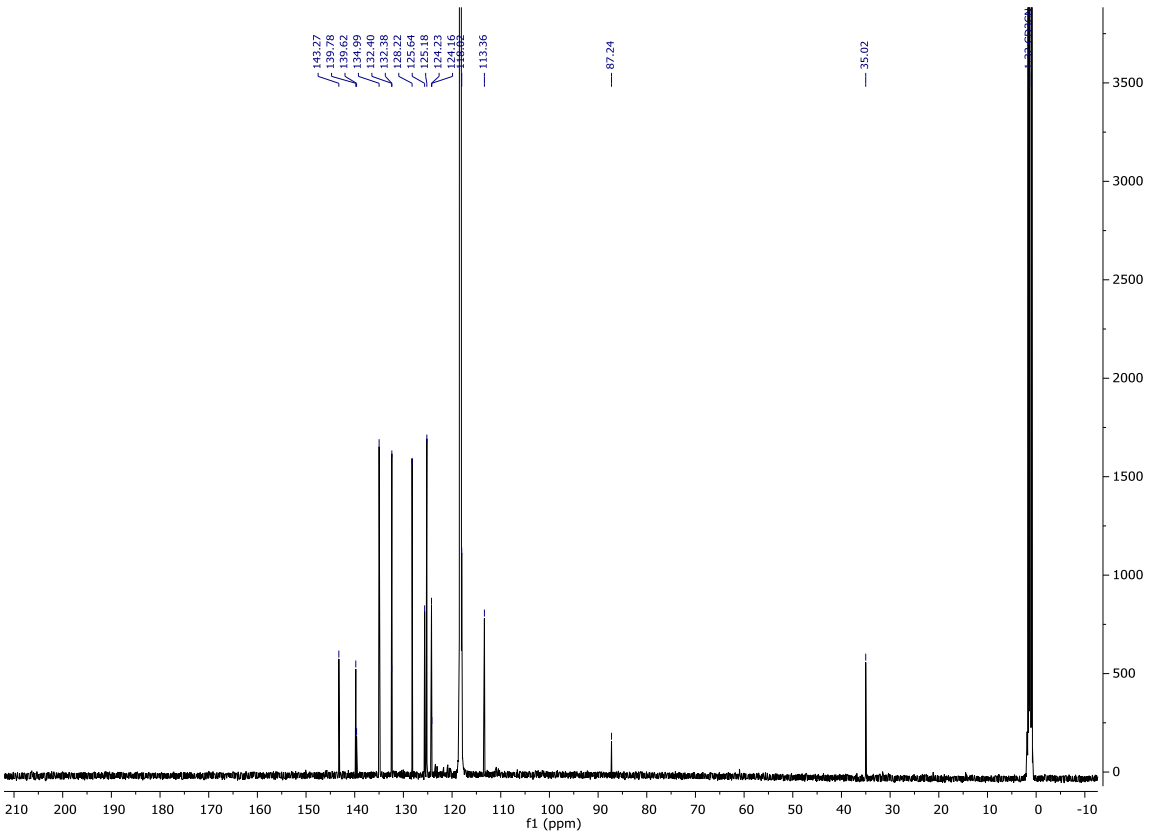

^{19}F NMR (282 MHz, CD_3CN) **326**

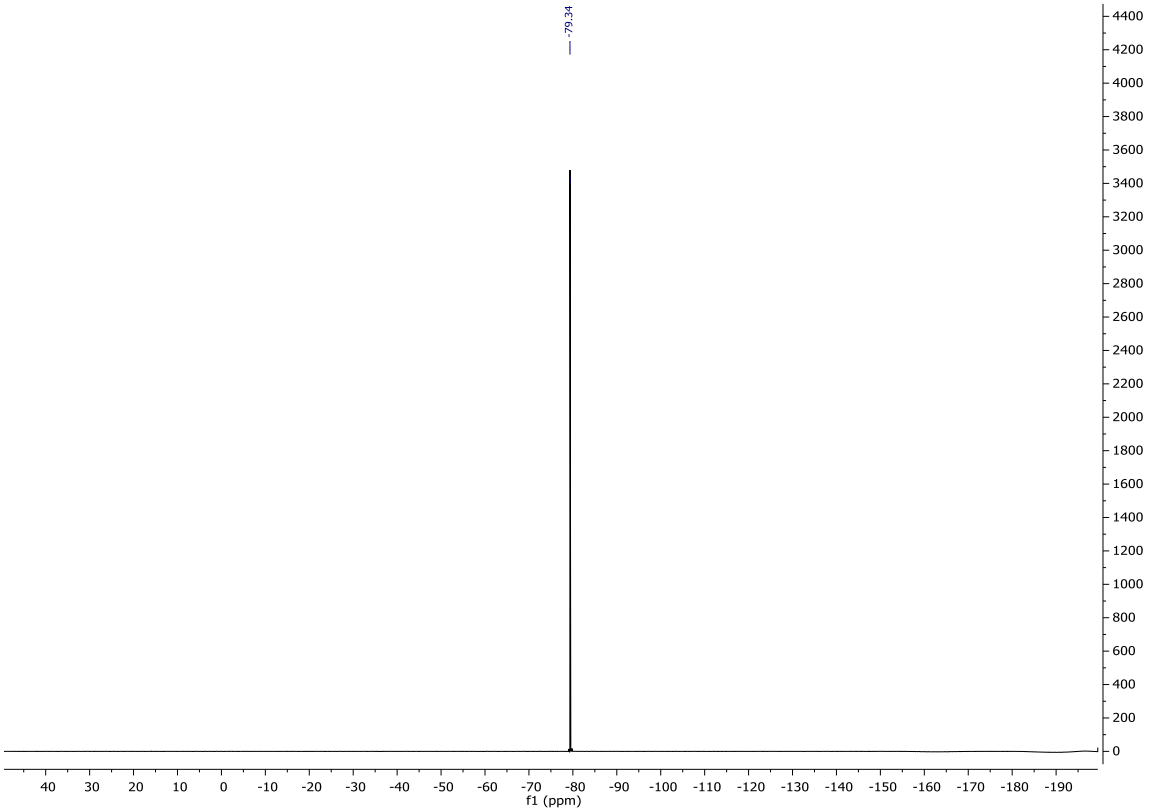

^{1}H NMR (300 MHz, C_6D_6,) **81**

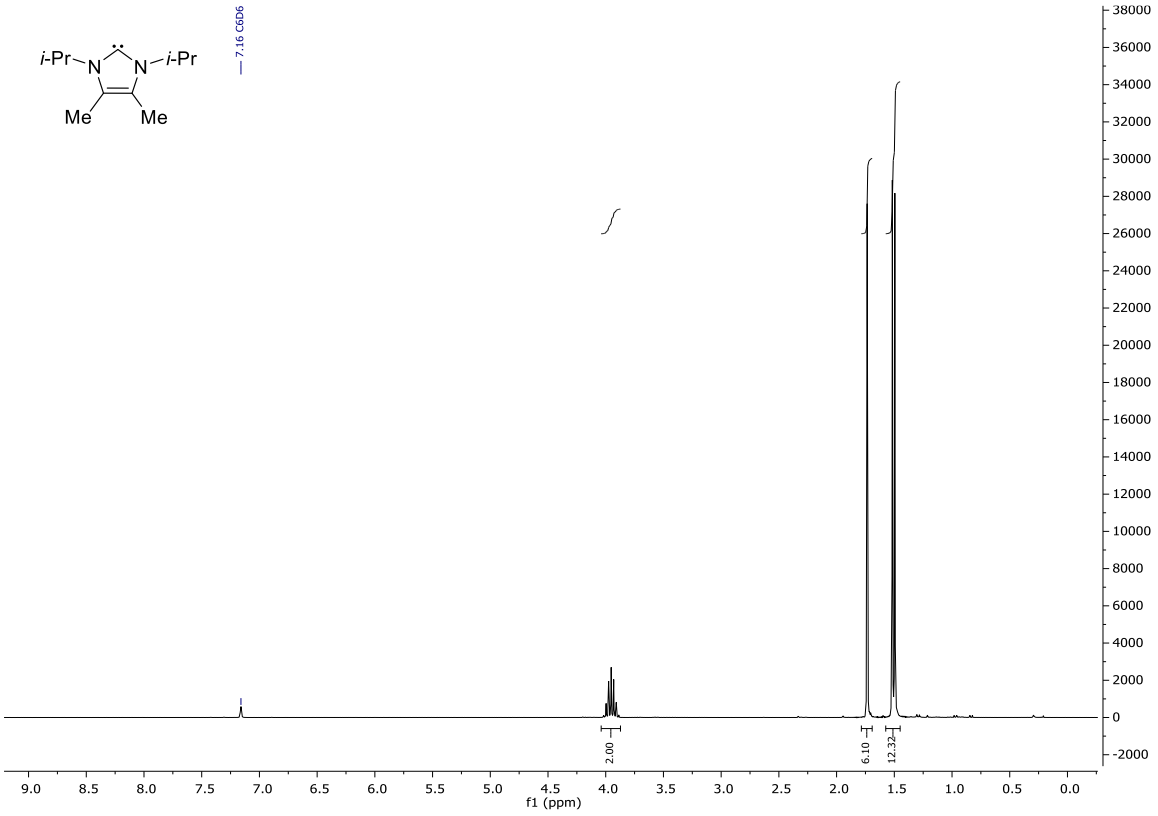

^{1}H NMR (400 MHz, $CDCl_3$) **327**

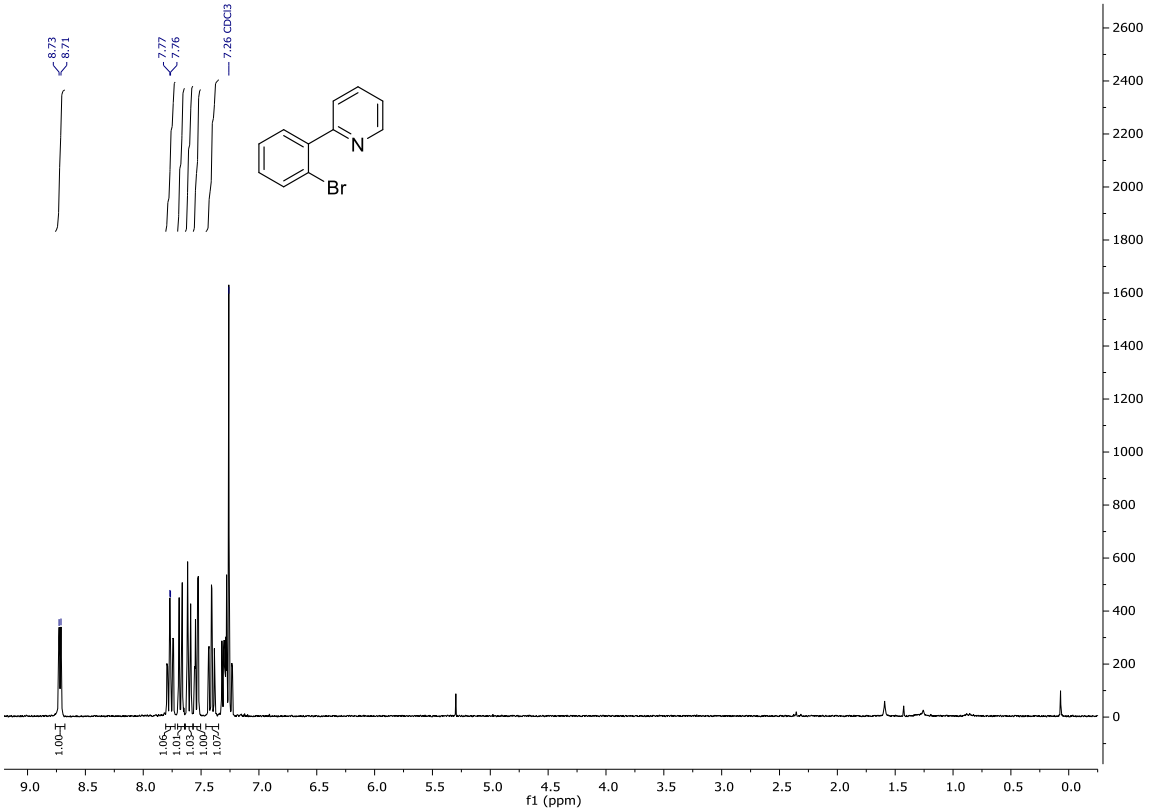

^{13}C NMR (101 MHz, $CDCl_3$) **327**

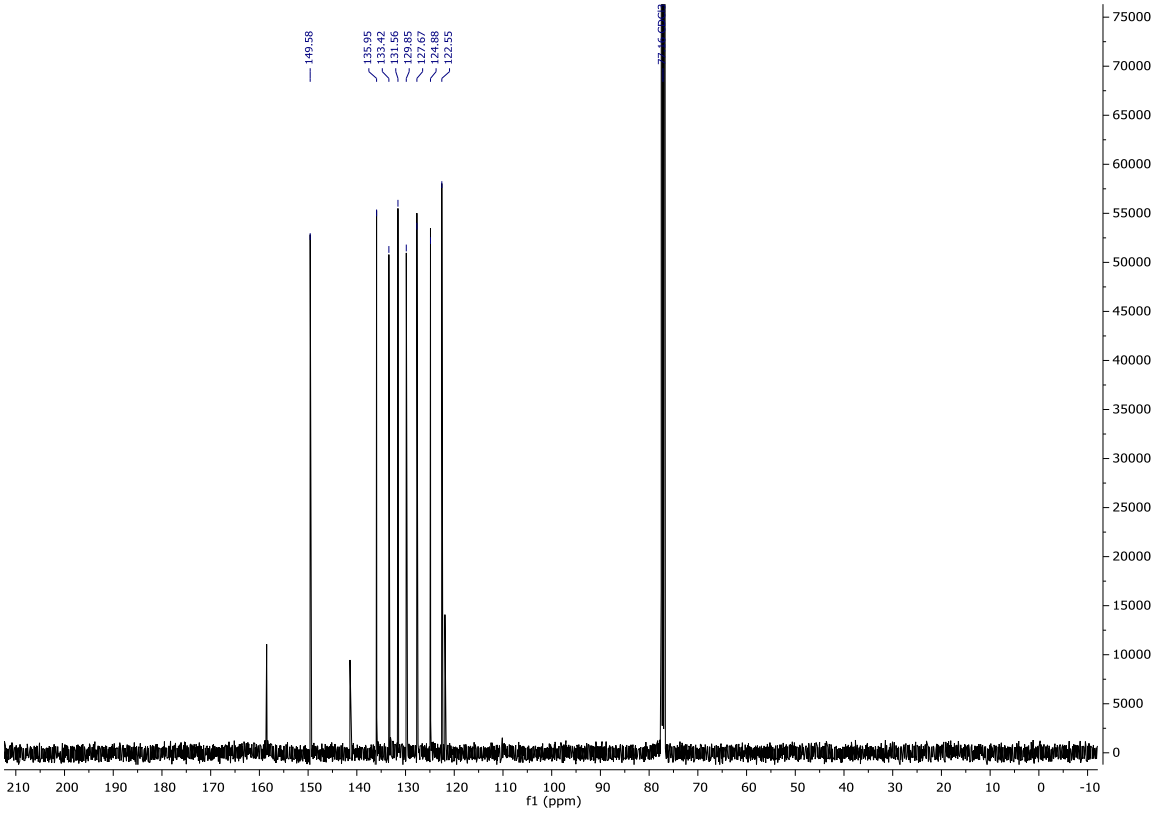

^{1}H NMR (400 MHz, CD_2Cl_2) **328**

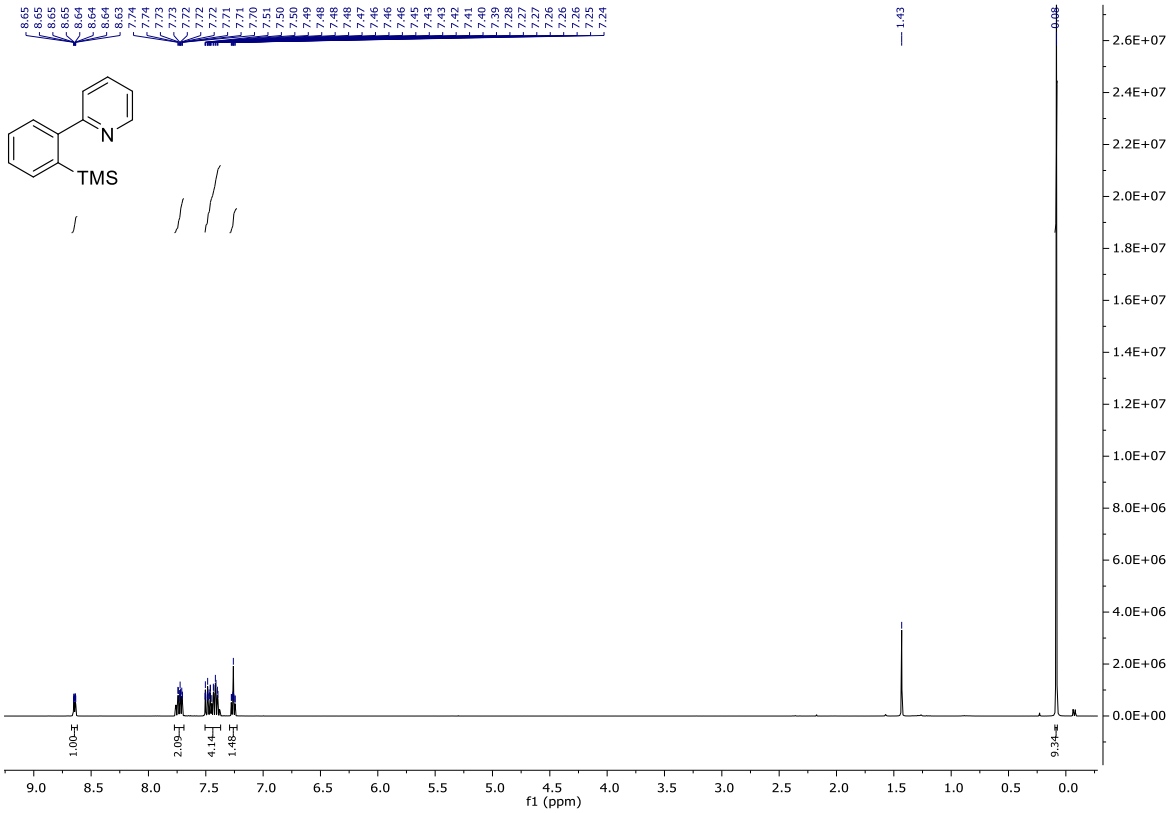

^{1}H NMR (101 MHz, $CDCl_3$) **328**

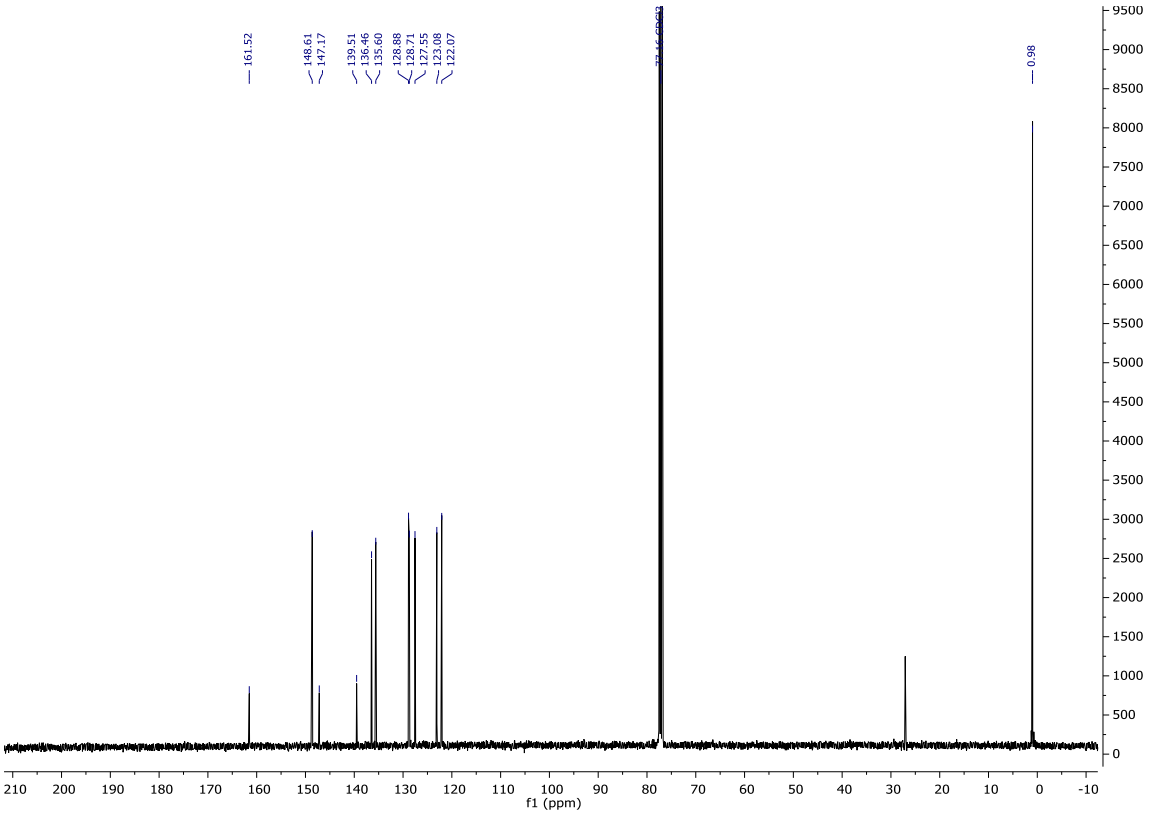

6 Bibliography

[1] C. Allègre, G. Manhès, É. Lewin, *Earth and Planetary Science Letters* **2001**, *185*, 49.

[2] A. F. Holleman, E. Wiberg, N. Wiberg, *Lehrbuch der anorganischen Chemie*, De Gruyter, Berlin, **2007**.

[3] Agarwal Chemical Industries, can be found under https://4.imimg.com/data4/TS/IY/MY-24139470/sulphur-powder-250x250.jpg, **2020**.

[4] Values obtained from the CSD data base version 5.38 including the update from 18.11.2018 using program Conquest 1.19, Mercury 4.1.0 and Mogul 1.8.1 by evaluation of the distribution of ∢(C-E-C) (E = O or S) in diaryl species under exclusion of charge R3E-species as well as (thio)esters.

[5] a) J. T. Mattiza, V. J. Meyer, H. Duddeck, *Magnetic resonance in chemistry : MRC* **2010**, *48*, 192; b) R. G. Pearson, *J. Am. Chem. Soc.* **1963**, *85*, 3533.

[6] M. Feng, B. Tang, S. H. Liang, X. Jiang, *CTMC* **2016**, *16*, 1200.

[7] E. A. Ilardi, E. Vitaku, J. T. Njardarson, *Journal of medicinal chemistry* **2014**, *57*, 2832.

[8] S. Bourdoulous, K. Denis, L. Le Guennec, WO 2019008141 A1, **2019**.

[9] J. Brent, K. Burkhart, P. Dargan, B. Hatten, B. Megarbane, R. Palmer, *Critical care toxicology*, Springer International Publishing, Switzerland, **2016**.

[10] J. Dumas, D. Brittelli, J. Chen, B. Dixon, H. Hatoum-Mokdad, G. König, R. Sibley, J. Witowsky, S. Wong, *Bioorganic & medicinal chemistry letters* **1999**, *9*, 2531.

[11] G. de Martino, M. C. Edler, G. La Regina, A. Coluccia, M. C. Barbera, D. Barrow, R. I. Nicholson, G. Chiosis, A. Brancale, E. Hamel et al., *Journal of medicinal chemistry* **2006**, *49*, 947.

[12] S.-y. Liao, T.-f. Miao, J.-c. Chen, H.-l. Lu, K.-c. Zheng, *Chinese Journal of Chemical Physics* **2009**, *22*, 473.

[13] Z. Diamant, M. C. Timmers, H. van der Veen, B. S. Friedman, M. D. Smet, M. Depré, D. Hilliard, E. H. Bel, P. J. Sterk, *Journal of Allergy and Clinical Immunology* **1995**, *95*, 42.

[14] S. S. Khandekar, D. R. Gentry, G. S. van Aller, P. Warren, H. Xiang, C. Silverman, M. L. Doyle, P. A. Chambers, A. K. Konstantinidis, M. Brandt et al., *The Journal of biological chemistry* **2001**, *276*, 30024.

[15] John J. Acton, Peter T. Meinke, Harold B. Wood, Regina M. Black, WO2004019869A2, **2003**.

[16] P. Sarver, M. Acker, J. T. Bagdanoff, Z. Chen, Y.-N. Chen, H. Chan, B. Firestone, M. Fodor, J. Fortanet, H. Hao et al., *Journal of medicinal chemistry* **2019**, *62*, 1793.

[17] G. Liu, J. T. Link, Z. Pei, E. B. Reilly, S. Leitza, B. Nguyen, K. C. Marsh, G. F. Okasinski, T. W. von Geldern, M. Ormes et al., *J. Med. Chem.* **2000**, *43*, 4025.

[18] S. Parveen, M. O. F. Khan, S. E. Austin, S. L. Croft, V. Yardley, P. Rock, K. T. Douglas, *Journal of medicinal chemistry* **2005**, *48*, 8087.

[19] a) C. Hansch, A. Leo, *Substituent constants for correlation analysis in chemistry and biology*, Wiley, New York (Chichester etc.), **1979**; b) H. Kubinyi, *QSAR : Hansch analysis and related approaches*, VCH, Weinheim, New York, **1993**.

[20] J. F. Giudicelli, C. Richer, A. Berdeaux, *British journal of clinical pharmacology* **1976**, *3*, 113.

[21] T. Silverstone, J. Fincham, J. Plumley, *British journal of clinical pharmacology* **1979**, *7*, 353.

[22] M. Diaferia, F. Veronesi, G. Morganti, L. Nisoli, D. P. Fioretti, *Parasitology research* **2013**, *112 Suppl 1*, 163.

[23] a) X. T. Liang, X. D. Xu, Z. P. Zhang, H. E. Gu, W. X. Wang, *Sci. Sin* **1977**, *20*, 106; b) L. Sun, S. Zhang, X. Hu, J. Jin, Z. Li, *Future medicinal chemistry* **2019**, *11*, 2877.

[24] R. Wang, M. R. Seyedsayamdost, *Org. Lett.* **2017**, *19*, 5138.

[25] S. Gomi, S. Amano, E. Sato, S. Miyadoh, Y. Kodama, *J. Antibiot.* **1994**, *47*, 1385.

[26] A. Martinez, P. Usan, M. Medina, E. Garsia Palomero, J. Perez Baz, R. I. Fernandez Medarde, L. M. Canedo Hernandez, F. Romero Millan, A. Castro Morena, M. Alonso Cascon et al., WO/2007/017146.

[27] a) U. Zschieschang, H. Klauk, *J. Mater. Chem. C* **2019**, *7*, 5522; b) Q. Meng, H. Dong, W. Hu, D. Zhu, *J. Mater. Chem.* **2011**, *21*, 11708.

[28] U. Kraft, K. Takimiya, M. J. Kang, R. Rödel, F. Letzkus, J. N. Burghartz, E. Weber, H. Klauk, *Organic Electronics* **2016**, *35*, 33.

[29] K. Takimiya, H. Ebata, K. Sakamoto, T. Izawa, T. Otsubo, Y. Kunugi, *J. Am. Chem. Soc.* **2006**, *128*, 12604.

[30] H. Usta, D. Kim, R. Ozdemir, Y. Zorlu, S. Kim, M. C. Ruiz Delgado, A. Harbuzaru, S. Kim, G. Demirel, J. Hong et al., *Chem. Mater.* **2019**.

[31] N. Spassky, *Phosphorus, Sulfur, and Silicon and the Related Elements* **1993**, *74*, 71.

[32] A. S. Rahate, K. R. Nemade, S. A. Waghuley, *Reviews in Chemical Engineering* **2013**, *29*.

[33] N. H. Park, G. D. P. Gomes, M. Fevre, G. O. Jones, I. V. Alabugin, J. L. Hedrick, *Nature communications* **2017**, *8*, 166.

[34] P. Zuo, A. Tcharkhtchi, M. Shirinbayan, J. Fitoussi, F. Bakir, *Macromol. Mater. Eng.* **2019**, *304*, 1800686.

[35] A. Shockravi, S. Mehdipour-Ataei, E. Abouzari-Lotf, A. Yousefi, *European Polymer Journal* **2006**, *42*, 133.

[36] A. Kausar, S. Zulfiqar, M. I. Sarwar, *Polymer Reviews* **2014**, *54*, 185.

[37] H. Mutlu, E. B. Ceper, X. Li, J. Yang, W. Dong, M. M. Ozmen, P. Theato, *Macromolecular rapid communications* **2019**, *40*, e1800650.

[38] X.-Y. Liu, Y.-L. Zhang, X. Fei, L.-S. Liao, J. Fan, *Chemistry (Weinheim an der Bergstrasse, Germany)* **2019**, *25*, 4501.

[39] H. Wu, W. Chi, G. Baryshnikov, B. Wu, Y. Gong, D. Zheng, X. Li, Y. Zhao, X. Liu, H. Ågren et al., *Angewandte Chemie (International ed. in English)* **2019**, *58*, 4328.

[40] G. J. Dawson, C. G. Frost, C. J. Martin, J. M.J. Williams, S. J. Coote, *Tetrahedron Letters* **1993**, *34*, 7793.

[41] S.-L. You, Y.-G. Zhou, X.-L. Hou, L.-X. Dai, *Chem. Commun.* **1998**, 2765.

[42] O. García Mancheño, J. Priego, S. Cabrera, R. Gómez Arrayás, T. Llamas, J. C. Carretero, *J. Org. Chem.* **2003**, *68*, 3679.

[43] a) S. Cabrera, O. García Mancheño, R. Gómez Arrayás, I. Alonso, P. Mauleón, J. C. Carretero, *Pure and Applied Chemistry* **2006**, *78*, 257; b) S. Cabrera, R. Gómez Arrayás, I. Alonso, J. C. Carretero, *J. Am. Chem. Soc.* **2005**, *127*, 17938.

[44] O. García Mancheño, R. Gómez Arrayás, J. C. Carretero, *J. Am. Chem. Soc.* **2004**, *126*, 456.

[45] P. Dubey, S. Gupta, A. K. Singh, *Organometallics* **2019**.

[46] K. Naksomboon, C. Valderas, M. Gómez-Martínez, Y. Álvarez-Casao, M. Á. Fernández-Ibáñez, *ACS Catal.* **2017**, *7*, 6342.

[47] Y. Álvarez-Casao, M. Á. Fernández-Ibáñez, *Eur. J. Org. Chem.* **2019**, *2019*, 1842.

[48] X. Zhou, S. Malakar, T. Zhou, S. Murugesan, C. Huang, T. J. Emge, K. Krogh-Jespersen, A. S. Goldman, *ACS Catal.* **2019**, *9*, 4072.

[49] a) K. Yu, W. Sommer, J.?M. Richardson, M. Weck, C.?W. Jones, *Adv. Synth. Catal.* **2005**, *347*, 161; b) D. E. Bergbreiter, P. L. Osburn, Y.-S. Liu, *J. Am. Chem. Soc.* **1999**, *121*, 9531.

[50] a) H. Pellissier, *Chiral sulfur ligands*. *Asymmetric catalysis / Hélène Pellissier*, Royal Society of Chemistry, Cambridge, **2009**; b) M. Mellah, A. Voituriez, E. Schulz, *Chem. Rev.* **2007**, *107*, 5133.

[51] Q. Cao, J. Luo, X. Zhao, *Angewandte Chemie (International ed. in English)* **2019**, *58*, 1315.

[52] Z. He, F. Song, H. Sun, Y. Huang, *Journal of the American Chemical Society* **2018**, *140*, 2693.

[53] a) C. Märcker, *Ann. Chem. Pharm.* **1865**, *136*, 75; b) J. Voss, *Journal of Sulfur Chemistry* **2009**, *30*, 167.

[54] a) G. W. Gokel, H. M. Gerdes, D. M. Dishong, *J. Org. Chem.* **1980**, *45*, 3634; b) S. T. Purrington, A. G. Glenn, *Organic Preparations and Procedures International* **2009**, *17*, 227; c) A. Shaabani, P. Mirzaei, S. Naderi, D. G. Lee, *Tetrahedron* **2004**, *60*, 11415.

[55] B. Maleki, S. Hemmati, A. Sedrpoushan, S. S. Ashrafi, H. Veisi, *RSC Adv.* **2014**, *4*, 40505.

[56] A. Shaabani, M. Behnam, A. H. Rezayan, *Catalysis Communications* **2009**, *10*, 1074.

[57] A. MAGGIOLO, E. A. BLAIR in *Advances in Chemistry*, American Chemical Society, 1155 Sixteenth St., N.W. Washington 6, D.C., **1959**, pp. 200–201.

[58] B. M. Trost, D. P. Curran, *Tetrahedron Letters* **1981**, *22*, 1287.

[59] M. Kirihara, A. Itou, T. Noguchi, J. Yamamoto, *Synlett* **2010**, *2010*, 1557.

[60] K. Sato, M. Hyodo, M. Aoki, X.-Q. Zheng, R. Noyori, *Tetrahedron* **2001**, *57*, 2469.

[61] O. Bortolini, F. Di Furia, G. Modena, R. Seraglia, *J. Org. Chem.* **1985**, *50*, 2688.

[62] S. Yamazaki, *BCSJ* **1996**, *69*, 2955.

[63] S. Hussain, S. K. Bharadwaj, R. Pandey, M. K. Chaudhuri, *Eur. J. Org. Chem.* **2009**, *2009*, 3319.

[64] S. Doherty, J. G. Knight, M. A. Carroll, J. R. Ellison, S. J. Hobson, S. Stevens, C. Hardacre, P. Goodrich, *Green Chem.* **2015**, *17*, 1559.

[65] E. Voutyritsa, I. Triandafillidi, C. Kokotos, *Synthesis* **2017**, *49*, 917.

[66] M. Jereb, *Green Chem.* **2012**, *14*, 3047.

[67] R. J. Griffin, A. Henderson, N. J. Curtin, A. Echalier, J. A. Endicott, I. R. Hardcastle, D. R. Newell, M. E. M. Noble, L.-Z. Wang, B. T. Golding, *J. Am. Chem. Soc.* **2006**, *128*, 6012.

[68] L. Xu, J. Cheng, M. L. Trudell, *J. Org. Chem.* **2003**, *68*, 5388.

[69] M. Khodaei, K. Bahrami, A. Karimi, *Synthesis* **2008**, *2008*, 1682.

[70] M. H. Ali, G. J. Bohnert, *Synthesis* **1998**, *1998*, 1238.

[71] B. M. Trost, M. Rao, *Angewandte Chemie (International ed. in English)* **2015**, *54*, 5026.

[72] S. Nishiguchi, T. Izumi, T. Kouno, J. Sukegawa, L. Ilies, E. Nakamura, *ACS Catal.* **2018**, *8*, 9738.

[73] Y. K. Bong, S. Song, J. Nazor, M. Vogel, M. Widegren, D. Smith, S. J. Collier, R. Wilson, S. M. Palanivel, K. Narayanaswamy et al., *The Journal of organic chemistry* **2018**, *83*, 7453.

[74] R. V. Kupwade, *Journal of Chemical Reviews* **2019**, *1*, 99.

[75] Y. Uetake, T. Niwa, T. Hosoya, *Organic letters* **2016**, *18*, 2758.

[76] J. Yang, J. Xiao, T. Chen, S.-F. Yin, L.-B. Han, *Chemical communications (Cambridge, England)* **2016**, *52*, 12233.

[77] T. Sugahara, K. Murakami, H. Yorimitsu, A. Osuka, *Angew. Chem. Int. Ed.* **2014**, *53*, 9329.

[78] M. Tobisu, T. Shimasaki, N. Chatani, *Chem. Lett.* **2009**, *38*, 710.

[79] K. Gao, H. Yorimitsu, A. Osuka, *Eur. J. Org. Chem.* **2015**, *2015*, 2678.

[80] A. Fürstner, *Angewandte Chemie (International ed. in English)* **2013**, *52*, 2794.

[81] J. M. Brown, P. Dixneuf, L. S. Hegedus, *Alkene Metathesis in Organic Synthesis*, Springer Berlin Heidelberg, Berlin/Heidelberg, **1999**.

[82] Z. Lian, B. N. Bhawal, P. Yu, B. Morandi, *Science (New York, N.Y.)* **2017**, *356*, 1059.

[83] L. S. Liebeskind, J. Srogl, *Org. Lett.* **2002**, *4*, 979.

[84] L. S. Liebeskind, J. Srogl, *J. Am. Chem. Soc.* **2000**, *122*, 11260.

[85] M. Klečka, R. Pohl, J. Čejka, M. Hocek, *Organic & biomolecular chemistry* **2013**, *11*, 5189.

[86] V. P. Mehta, A. Sharma, E. van der Eycken, *Adv. Synth. Catal.* **2008**, *350*, 2174.

[87] a) V. P. Mehta, S. G. Modha, E. van der Eycken, *The Journal of organic chemistry* **2009**, *74*, 6870; b) H. Okamura, M. Miura, H. Takei, *Tetrahedron Letters* **1979**, *20*, 43.

[88] A. Metzger, L. Melzig, C. Despotopoulou, P. Knochel, *Org. Lett.* **2009**, *11*, 4228.

[89] J. F. Hooper, R. D. Young, I. Pernik, A. S. Weller, M. C. Willis, *Chem. Sci.* **2013**, *4*, 1568.

[90] a) H.-G. Cheng, H. Chen, Y. Liu, Q. Zhou, *Asian J. Org. Chem.* **2018**, *7*, 490; b) L. Wang, W. He, Z. Yu, *Chemical Society reviews* **2013**, *42*, 599; c) H. Prokopcová, C. O. Kappe, *Angewandte Chemie (International ed. in English)* **2009**, *48*, 2276.

[91] Y. Ma, J. Cammarata, J. Cornella, *Journal of the American Chemical Society* **2019**, *141*, 1918.

[92] F. Zhu, Z.-X. Wang, *Org. Lett.* **2015**, *17*, 1601.

[93] S. G. Modha, V. P. Mehta, E. V. van der Eycken, *Chemical Society reviews* **2013**, *42*, 5042.

[94] X. Wang, Y. Tang, C.-Y. Long, W.-K. Dong, C. Li, X. Xu, W. Zhao, X.-Q. Wang, *Organic letters* **2018**, *20*, 4749.

[95] R. Chamberlin, M. R. Crampton, *J. Chem. Soc., Perkin Trans. 2* **1993**, *72*, 75.

[96] M. Yu, Y. Xie, C. Xie, Y. Zhang, *Organic letters* **2012**, *14*, 2164.

[97] X.-S. Zhang, Q.-L. Zhu, Y.-F. Zhang, Y.-B. Li, Z.-J. Shi, *Chemistry (Weinheim an der Bergstrasse, Germany)* **2013**, *19*, 11898.

[98] P. Villuendas, E. P. Urriolabeitia, *Organic letters* **2015**, *17*, 3178.

[99] B. Xu, W. Liu, C. Kuang, *Eur. J. Org. Chem.* **2014**, *2014*, 2576.

[100] C. N. Kona, Y. Nishii, M. Miura, *Organic letters* **2018**, *20*, 4898.

[101] C. N. Kona, Y. Nishii, M. Miura, *Org. Lett.* **2020**, *22*, 4806.

[102] M. Shigeno, Y. Nishii, T. Satoh, M. Miura, *Asian J. Org. Chem.* **2018**, *7*, 1334.

[103] S. Moon, Y. Nishii, M. Miura, *Organic letters* **2018**.

[104] a) J. Clayden, N. Greeves, S. G. Warren, *Organic chemistry*, Oxford University Press, Oxford, **2012**; b) C. M. Rayner, *Contemp. Org. Synth.* **1995**, *2*, 409.

[105] a) T. Kondo, T.-a. Mitsudo, *Chem. Rev.* **2000**, *100*, 3205; b) I. P. Beletskaya, V. P. Ananikov, *Chemical reviews* **2011**, *111*, 1596; c) C.-F. Lee, Y.-C. Liu, S. S. Badsara, *Chemistry, an Asian journal* **2014**, *9*, 706; d) C. Shen, P. Zhang, Q. Sun, S. Bai, T. S. A. Hor, X. Liu, *Chemical Society reviews* **2015**, *44*, 291.

[106] M. Kosugi, T. Shimizu, T. Migita, *Chem. Lett.* **1978**, *7*, 13.

[107] T. Migita, T. Shimizu, Y. Asami, J.-i. Shiobara, Y. Kato, M. Kosugi, *BCSJ* **1980**, *53*, 1385.

[108] E. Alvaro, J. F. Hartwig, *Journal of the American Chemical Society* **2009**, *131*, 7858.

[109] X. Moreau, J. M. Campagne, G. Meyer, A. Jutand, *Eur. J. Org. Chem.* **2005**, *2005*, 3749.

[110] C. Wang, Z. Zhang, Y. Tu, Y. Li, J. Wu, J. Zhao, *The Journal of organic chemistry* **2018**, *83*, 2389.

[111] Z. Duan, S. Ranjit, P. Zhang, X. Liu, *Chemistry (Weinheim an der Bergstrasse, Germany)* **2009**, *15*, 3666.

[112] J.-M. Becht, C. Le Drian, *The Journal of organic chemistry* **2011**, *76*, 6327.

[113] M. A. Fernández-Rodríguez, Q. Shen, J. F. Hartwig, *J. Am. Chem. Soc.* **2006**, *128*, 2180.

[114] X. Moreau, J.-M. Campagne, *Journal of Organometallic Chemistry* **2003**, *687*, 322.

[115] a) C. C. Eichman, J. P. Stambuli, *The Journal of organic chemistry* **2009**, *74*, 4005; b) G. Bastug, S. P. Nolan, *The Journal of organic chemistry* **2013**, *78*, 9303.

[116] a) T. Scattolin, E. Senol, G. Yin, Q. Guo, F. Schoenebeck, *Angewandte Chemie (International ed. in English)* **2018**, *57*, 12425; b) M. Sayah, M. G. Organ, *Chemistry (Weinheim an der Bergstrasse, Germany)* **2011**, *17*, 11719.

[117] a) M. Murata, S. L. Buchwald, *Tetrahedron* **2004**, *60*, 7397; b) M. A. Fernández-Rodríguez, Q. Shen, J. F. Hartwig, *Chem. Eur. J.* **2006**, *12*, 7782.

[118] N. Zheng, J. C. McWilliams, F. J. Fleitz, J. D. Armstrong, R. P. Volante, *J. Org. Chem.* **1998**, *63*, 9606.

[119] T. Ishiyama, M. Mori, A. Suzuki, N. Miyaura, *Journal of Organometallic Chemistry* **1996**, *525*, 225.

[120] S.-i. Fukuzawa, D. Tanihara, S. Kikuchi, *Synlett* **2006**, 2145.

[121] Z. Qiao, X. Jiang, *Org. Lett.* **2016**, *18*, 1550.

[122] J. Mao, T. Jia, G. Frensch, P. J. Walsh, *Org. Lett.* **2014**, *16*, 5304.

[123] M. A. Fernández-Rodríguez, J. F. Hartwig, *Chemistry (Weinheim an der Bergstrasse, Germany)* **2010**, *16*, 2355.

[124] G. Yin, I. Kalvet, F. Schoenebeck, *Angewandte Chemie (International ed. in English)* **2015**, *54*, 6809.

[125] G. Teverovskiy, D. S. Surry, S. L. Buchwald, *Angewandte Chemie (International ed. in English)* **2011**, *50*, 7312.

[126] a) C. Xu, Q. Shen, *Org. Lett.* **2014**, *16*, 2046; b) M. Iwasaki, M. Iyanaga, Y. Tsuchiya, Y. Nishimura, W. Li, Z. Li, Y. Nishihara, *Chemistry (Weinheim an der Bergstrasse, Germany)* **2014**, *20*, 2459.

[127] S. Vásquez-Céspedes, A. Ferry, L. Candish, F. Glorius, *Angewandte Chemie (International ed. in English)* **2015**, *54*, 5772.

[128] P. Saravanan, P. Anbarasan, *Org. Lett.* **2014**, *16*, 848.

[129] P. Anbarasan, H. Neumann, M. Beller, *Chemical communications (Cambridge, England)* **2011**, *47*, 3233.

[130] H. J. Cristau, B. Chabaud, A. Chêne, H. Christol, *Synthesis* **1981**, 892.

[131] a) O. Baldovino-Pantaleón, S. Hernández-Ortega, D. Morales-Morales, *Adv. Synth. Catal.* **2006**, *348*, 236; b) O. Baldovino-Pantaleón, S. Hernández-Ortega, D. Morales-Morales, *Inorganic Chemistry Communications* **2005**, *8*, 955; c) V. Gómez-Benítez, O. Baldovino-Pantaleón, C. Herrera-Álvarez, R. A. Toscano, D. Morales-Morales, *Tetrahedron Letters* **2006**, *47*, 5059.

[132] X.-B. Xu, J. Liu, J.-J. Zhang, Y.-W. Wang, Y. Peng, *Org. Lett.* **2013**, *15*, 550.

[133] Y. Zhang, K. C. Ngeow, J. Y. Ying, *Organic letters* **2007**, *9*, 3495.

[134] K. D. Jones, D. J. Power, D. Bierer, K. M. Gericke, S. G. Stewart, *Org. Lett.* **2018**, *20*, 208.

[135] V. Percec, J.-Y. Bae, D. H. Hill, *J. Org. Chem.* **1995**, *60*, 6895.

[136] a) P. Guan, C. Cao, Y. Liu, Y. Li, P. He, Q. Chen, G. Liu, Y. Shi, *Tetrahedron Letters* **2012**, *53*, 5987; b) N. P. N. Wellala, H. Guan, *Organic & biomolecular chemistry* **2015**, *13*, 10802.

[137] N. Taniguchi, *J. Org. Chem.* **2004**, *69*, 6904.

[138] R. Sikari, S. Sinha, S. Das, A. Saha, G. Chakraborty, R. Mondal, N. D. Paul, *The Journal of organic chemistry* **2019**, *84*, 4072.

[139] Y. Wang, L. Deng, X. Wang, Z. Wu, Y. Wang, Y. Pan, *ACS Catal.* **2019**, 1630.

[140] D. Liu, H.-X. Ma, P. Fang, T.-S. Mei, *Angewandte Chemie (International ed. in English)* **2019**, *58*, 5033.

[141] Y. Fang, T. Rogge, L. Ackermann, S.-Y. Wang, S.-J. Ji, *Nature communications* **2018**, *9*, 2240.

[142] T. Müller, L. Ackermann, *Chemistry (Weinheim an der Bergstrasse, Germany)* **2016**, *22*, 14151.

[143] C. Palomo, M. Oiarbide, R. López, E. Gómez-Bengoa, *Tetrahedron Letters* **2000**, *41*, 1283.

[144] C. Uyeda, Y. Tan, G. C. Fu, J. C. Peters, *Journal of the American Chemical Society* **2013**, *135*, 9548.

[145] M. W. Johnson, K. I. Hannoun, Y. Tan, G. C. Fu, J. C. Peters, *Chem. Sci.* **2016**, *7*, 4091.

[146] C.-W. Chen, Y.-L. Chen, D. M. Reddy, K. Du, C.-E. Li, B.-H. Shih, Y.-J. Xue, C.-F. Lee, *Chemistry (Weinheim an der Bergstrasse, Germany)* **2017**, *23*, 10087.

[147] E. Sperotto, G. P. M. van Klink, G. van Koten, J. G. de Vries, *Dalton transactions (Cambridge, England : 2003)* **2010**, *39*, 10338.

[148] J. X. Qiao, P. Y. S. Lam in *Boronic acids*. *Preparation and applications in organic synthesis, medicine and materials* (Ed.: D. G. Hall), WILEY-VCH, Weinheim, **2011**, pp. 315–361.

[149] H.-J. Xu, Y.-Q. Zhao, T. Feng, Y.-S. Feng, *The Journal of organic chemistry* **2012**, *77*, 2878.

[150] R. Pluta, P. Nikolaienko, M. Rueping, *Angewandte Chemie (International ed. in English)* **2014**, *53*, 1650.

[151] K. Kang, C. Xu, Q. Shen, *Org. Chem. Front.* **2014**, *1*, 294.

[152] M. Li, J. M. Hoover, *Chemical communications (Cambridge, England)* **2016**, *52*, 8733.

[153] E. Sperotto, G. P. M. van Klink, J. G. de Vries, G. van Koten, *The Journal of organic chemistry* **2008**, *73*, 5625.

[154] a) F. Y. Kwong, S. L. Buchwald, *Org. Lett.* **2002**, *4*, 3517; b) C. G. Bates, R. K. Gujadhur, D. Venkataraman, *Org. Lett.* **2002**, *4*, 2803.

[155] P. S. Herradura, K. A. Pendola, R. K. Guy, *Org. Lett.* **2000**, *2*, 2019.

[156] a) N. Taniguchi, *J. Org. Chem.* **2007**, *72*, 1241; b) N. Taniguchi, *Synlett* **2006**, 1351.

[157] P.-S. Luo, F. Wang, J.-H. Li, R.-Y. Tang, P. Zhong, *Synthesis* **2009**, 921.

[158] J.-H. Cheng, C.-L. Yi, T.-J. Liu, C.-F. Lee, *Chemical communications (Cambridge, England)* **2012**, *48*, 8440.

[159] Z. Qiao, N. Ge, X. Jiang, *Chemical communications (Cambridge, England)* **2015**, *51*, 10295.

[160] S. Yoshida, Y. Sugimura, Y. Hazama, Y. Nishiyama, T. Yano, S. Shimizu, T. Hosoya, *Chemical communications (Cambridge, England)* **2015**, *51*, 16613.

[161] K. Kanemoto, S. Yoshida, T. Hosoya, *Chem. Lett.* **2018**, *47*, 85.

[162] T.-T. Wang, F.-L. Yang, S.-K. Tian, *Adv. Synth. Catal.* **2015**, *357*, 928.

[163] C. Savarin, J. Srogl, L. S. Liebeskind, *Organic letters* **2002**, *4*, 4309.

[164] X. Shao, X. Wang, T. Yang, L. Lu, Q. Shen, *Angewandte Chemie (International ed. in English)* **2013**, *52*, 3457.

[165] a) X. Chen, X.-S. Hao, C. E. Goodhue, J.-Q. Yu, *J. Am. Chem. Soc.* **2006**, *128*, 6790; b) L. Gu, X. Fang, Z. Weng, Y. Song, W. Ma, *Eur. J. Org. Chem.* **2019**, 1825.

[166] S. Zhang, P. Qian, M. Zhang, M. Hu, J. Cheng, *The Journal of organic chemistry* **2010**, *75*, 6732.

[167] a) P. Peng, J. Wang, C. Li, W. Zhu, H. Jiang, H. Liu, *RSC Adv.* **2016**, *6*, 57441; b) Z. Li, J. Hong, X. Zhou, *Tetrahedron* **2011**, *67*, 3690; c) M. Noikham, S. Yotphan, *Eur. J. Org. Chem.* **2019**, 2759; d) D. Alves, R. G. Lara, M. E. Contreira, C. S. Radatz, L. F.B. Duarte, G. Perin, *Tetrahedron Letters* **2012**, *53*, 3364; e) S.-i. Fukuzawa, E. Shimizu, Y. Atsuumi, M. Haga, K. Ogata, *Tetrahedron Letters* **2009**, *50*, 2374; f) A.-X. Zhou, X.-Y. Liu, K. Yang, S.-C. Zhao, Y.-M. Liang, *Organic & biomolecular chemistry* **2011**, *9*, 5456; g) S. Ranjit, R. Lee, D. Heryadi, C. Shen, J.'E. Wu, P. Zhang, K.-W. Huang, X. Liu, *The Journal of organic chemistry* **2011**, *76*, 8999.

[168] I. Bauer, H.-J. Knölker, *Chemical reviews* **2015**, *115*, 3170.

[169] S. L. Buchwald, C. Bolm, *Angewandte Chemie (International ed. in English)* **2009**, *48*, 5586.

[170] J.-R. Wu, C.-H. Lin, C.-F. Lee, *Chemical communications (Cambridge, England)* **2009**, 4450.

[171] K. S. Sindhu, T. G. Abi, G. Mathai, G. Anilkumar, *Polyhedron* **2019**, *158*, 270.

[172] J. Yadav, B. Reddy, Y. Reddy, K. Praneeth, *Synthesis* **2009**, 1520.

[173] X.-L. Fang, R.-Y. Tang, X.-G. Zhang, J.-H. Li, *Synthesis* **2011**, 1099.

[174] J. Sun, Y. Wang, Y. Pan, *Organic & biomolecular chemistry* **2015**, *13*, 3878.

[175] a) M.-T. Lan, W.-Y. Wu, S.-H. Huang, K.-L. Luo, F.-Y. Tsai, *RSC Adv.* **2011**, *1*, 1751; b) Y.-C. Wong, T. T. Jayanth, C.-H. Cheng, *Org. Lett.* **2006**, *8*, 5613.

[176] A. P. Thankachan, K. S. Sindhu, K. K. Krishnan, G. Anilkumar, *RSC Adv.* **2015**, *5*, 32675.

[177] S. Yang, B. Feng, Y. Yang, *The Journal of organic chemistry* **2017**, *82*, 12430.

[178] Y. Yang, W. Hou, L. Qin, J. Du, H. Feng, B. Zhou, Y. Li, *Chemistry (Weinheim an der Bergstrasse, Germany)* **2014**, *20*, 416.

[179] a) M. Arisawa, T. Suzuki, T. Ishikawa, M. Yamaguchi, *Journal of the American Chemical Society* **2008**, *130*, 12214; b) K. Kanemoto, Y. Sugimura, S. Shimizu, S. Yoshida, T. Hosoya, *Chemical communications (Cambridge, England)* **2017**, *53*, 10640.

[180] a) Y.-Q. Zhu, J.-L. He, Y.-X. Niu, H.-Y. Kang, T.-F. Han, H.-Y. Li, *The Journal of organic chemistry* **2018**, *83*, 9958; b) G. Yan, A. J. Borah, L. Wang, *Organic & biomolecular chemistry* **2014**, *12*, 9557.

[181] M. L. Czyz, G. K. Weragoda, R. Monaghan, T. U. Connell, M. Brzozowski, A. D. Scully, J. Burton, D. W. Lupton, A. Polyzos, *Organic & biomolecular chemistry* **2018**, *16*, 1543.

[182] M. Jiang, H. Li, H. Yang, H. Fu, *Angewandte Chemie (International ed. in English)* **2017**, *56*, 874.

[183] E. C. Ashby, *Acc. Chem. Res.* **1988**, *21*, 414.

[184] a) M. Jouffroy, C. B. Kelly, G. A. Molander, *Org. Lett.* **2016**, *18*, 876; b) B. A. Vara, X. Li, S. Berritt, C. R. Walters, E. J. Petersson, G. A. Molander, *Chem. Sci.* **2018**, *9*, 336; c) M. S. Oderinde, M. Frenette, D. W. Robbins, B. Aquila, J. W. Johannes, *Journal of the American Chemical Society* **2016**, *138*, 1760.

[185] A. Wimmer, B. König, *Beilstein journal of organic chemistry* **2018**, *14*, 54.

[186] Committee for Human Medicinal Products, *ICH guideline Q3D (R1) on elemental impurities*, Amesterdam, **2019**.

[187] J. F. Bunnett, R. E. Zahler, *Chem. Rev.* **1951**, *49*, 273.

[188] E. E. Kwan, Y. Zeng, H. A. Besser, E. N. Jacobsen, *Nature chemistry* **2018**, *10*, 917.

[189] a) M. Barbero, I. Degani, N. Diulgheroff, S. Dughera, R. Fochi, M. Migliaccio, *J. Org. Chem.* **2000**, *65*, 5600; b) G. Petrillo, M. Novi, G. Garbarino, D.'e. Carlo, *Tetrahedron* **1986**, *42*, 4007.

[190] Y.-C. Shieh, K. Du, R. S. Basha, Y.-J. Xue, B.-H. Shih, L. Li, C.-F. Lee, *The Journal of organic chemistry* **2019**, *84*, 6223.

[191] L. Bering, L. D'Ottavio, G. Sirvinskaite, A. P. Antonchick, *Chemical communications (Cambridge, England)* **2018**, *54*, 13022.

[192] Z. Huang, D. Zhang, X. Qi, Z. Yan, M. Wang, H. Yan, A. Lei, *Organic letters* **2016**, *18*, 2351.

[193] Y. Li, M. Wang, X. Jiang, *ACS Catal.* **2017**, *7*, 7587.

[194] G. Kibriya, S. Mondal, A. Hajra, *Organic letters* **2018**, *20*, 7740.

[195] B. Liu, C.-H. Lim, G. M. Miyake, *Journal of the American Chemical Society* **2017**, *139*, 13616.

[196] J. F. Bunnett, X. Creary, *J. Org. Chem.* **1974**, *39*, 3173.

[197] R. S. Glass, *Topics in current chemistry (Cham)* **2018**, *376*, 22.

[198] A. M. Wagner, M. S. Sanford, *The Journal of organic chemistry* **2014**, *79*, 2263.

[199] J. A. Campbell, C. A. Broka, L. Gong, K. A.M. Walker, J.-H. Wang, *Tetrahedron Letters* **2004**, *45*, 4073.

[200] J.-H. Cheng, C. Ramesh, H.-L. Kao, Y.-J. Wang, C.-C. Chan, C.-F. Lee, *The Journal of organic chemistry* **2012**, *77*, 10369.

[201] a) P. Thamyongkit, A. D. Bhise, M. Taniguchi, J. S. Lindsey, *J. Org. Chem.* **2006**, *71*, 903; b) G. Campiani, V. Nacci, S. Bechelli, S. M. Ciani, A. Garofalo, I. Fiorini, H. Wikström, P. de Boer, Y. Liao, P. G. Tepper et al., *Journal of medicinal chemistry* **1998**, *41*, 3763.

[202] T. Hostier, V. Ferey, G. Ricci, D. Gomez Pardo, J. Cossy, *Organic letters* **2015**, *17*, 3898.

[203] T. Hostier, V. Ferey, G. Ricci, D. Gomez Pardo, J. Cossy, *Chemical communications (Cambridge, England)* **2015**, *51*, 13898.

[204] C. J. Nalbandian, Z. E. Brown, E. Alvarez, J. L. Gustafson, *Organic letters* **2018**, *20*, 3211.

[205] C. J. Nalbandian, E. M. Miller, S. T. Toenjes, J. L. Gustafson, *Chemical communications (Cambridge, England)* **2017**, *53*, 1494.

[206] H. Tian, H. Yang, C. Zhu, H. Fu, *Adv. Synth. Catal.* **2015**, *357*, 481.

[207] H. Gillis, L. Greene, A. Thompson, *Synlett* **2008**, 112.

[208] S. SUWA, T. SAKAMOTO, Y. KIKUGAWA, *Chem. Pharm. Bull.* **1999**, *47*, 980.

[209] H. Tian, C. Zhu, H. Yang, H. Fu, *Chemical communications (Cambridge, England)* **2014**, *50*, 8875.

[210] E. Marcantoni, R. Cipolletti, L. Marsili, S. Menichetti, R. Properzi, C. Viglianisi, *Eur. J. Org. Chem.* **2013**, *2013*, 132.

[211] C. C. Silveira, S. R. Mendes, L. Wolf, G. M. Martins, *Tetrahedron Letters* **2010**, *51*, 2014.

[212] R. Honeker, J. B. Ernst, F. Glorius, *Chemistry (Weinheim an der Bergstrasse, Germany)* **2015**, *21*, 8047.

[213] D. Zhu, Y. Gu, L. Lu, Q. Shen, *Journal of the American Chemical Society* **2015**, *137*, 10547.

[214] Z. Tao, K. A. Robb, K. Zhao, S. E. Denmark, *Journal of the American Chemical Society* **2018**, *140*, 3569.

[215] J. Yu, C. Gao, Z. Song, H. Yang, H. Fu, *Organic & biomolecular chemistry* **2015**, *13*, 4846.

[216] K. M. Schlosser, A. P. Krasutsky, H. W. Hamilton, J. E. Reed, K. Sexton, *Organic letters* **2004**, *6*, 819.

[217] C. Ravi, D. C. Mohan, S. Adimurthy, *Organic letters* **2014**, *16*, 2978.

[218] P. Hamel, *J. Org. Chem.* **2002**, *67*, 2854.

[219] S. K. R. Parumala, R. K. Peddinti, *Green Chem.* **2015**, *17*, 4068.

[220] W. Ge, Y. Wei, *Green Chem.* **2012**, *14*, 2066.

[221] J. B. Azeredo, M. Godoi, G. M. Martins, C. C. Silveira, A. L. Braga, *The Journal of organic chemistry* **2014**, *79*, 4125.

[222] J. Rafique, S. Saba, M. S. Franco, L. Bettanin, A. R. Schneider, L. T. Silva, A. L. Braga, *Chemistry (Weinheim an der Bergstrasse, Germany)* **2018**, *24*, 4173.

[223] P. Sang, Z. Chen, J. Zou, Y. Zhang, *Green Chem.* **2013**, *15*, 2096.

[224] L.-H. Zou, J. Reball, J. Mottweiler, C. Bolm, *Chemical communications (Cambridge, England)* **2012**, *48*, 11307.

[225] Q. Wu, D. Zhao, X. Qin, J. Lan, J. You, *Chemical communications (Cambridge, England)* **2011**, *47*, 9188.

[226] J. M. Klunder, K. B. Sharpless, *J. Org. Chem.* **1987**, *52*, 2598.

[227] M. Raban, L.-J. Chern, *J. Org. Chem.* **1980**, *45*, 1688.

[228] A. Ghosh, M. Lecomte, S.-H. Kim-Lee, A. T. Radosevich, *Angewandte Chemie (International ed. in English)* **2019**, *58*, 2864.

[229] F.-L. Yang, S.-K. Tian, *Angewandte Chemie (International ed. in English)* **2013**, *52*, 4929.

[230] X. Kang, R. Yan, G. Yu, X. Pang, X. Liu, X. Li, L. Xiang, G. Huang, *The Journal of organic chemistry* **2014**, *79*, 10605.

[231] G. Kumaraswamy, R. Raju, V. Narayanarao, *RSC Adv.* **2015**, *5*, 22718.

[232] X. Zhao, L. Zhang, X. Lu, T. Li, K. Lu, *The Journal of organic chemistry* **2015**, *80*, 2918.

[233] F.-L. Yang, F.-X. Wang, T.-T. Wang, Y.-J. Wang, S.-K. Tian, *Chemical communications (Cambridge, England)* **2014**, *50*, 2111.

[234] H. Qi, T. Zhang, K. Wan, M. Luo, *The Journal of organic chemistry* **2016**, *81*, 4262.

[235] F. Xiao, H. Xie, S. Liu, G.-J. Deng, *Adv. Synth. Catal.* **2014**, *356*, 364.

[236] F. Xiao, S. Chen, J. Tian, H. Huang, Y. Liu, G.-J. Deng, *Green Chem.* **2016**, *18*, 1538.

[237] P. Katrun, S. Hongthong, S. Hlekhlai, M. Pohmakotr, V. Reutrakul, D. Soorukram, T. Jaipetch, C. Kuhakarn, *RSC Adv.* **2014**, *4*, 18933.

[238] C.-R. Liu, L.-H. Ding, *Organic & biomolecular chemistry* **2015**, *13*, 2251.

[239] M. Matsugi, K. Murata, H. Nambu, Y. Kita, *Tetrahedron Letters* **2001**, *42*, 1077.

[240] V. G. Nenaidenko, E. S. Balenkova, *Russian Journal of Organic Chemistry* **2003**, *39*, 291.

[241] S. I. Kozhushkov, M. Alcarazo, *Eur. J. Inorg. Chem.* **2020**, 2486.

[242] J. A. Fernández-Salas, A. P. Pulis, D. J. Procter, *Chemical communications (Cambridge, England)* **2016**, *52*, 12364.

[243] Z. Zhang, P. He, H. Du, J. Xu, P. Li, *The Journal of organic chemistry* **2019**, *84*, 4517.

[244] G. Talavera, J. Peña, M. Alcarazo, *J. Am. Chem. Soc.* **2015**, *137*, 8704.

[245] A. G. Barrado, A. Zieliński, R. Goddard, M. Alcarazo, *Angewandte Chemie (International ed. in English)* **2017**, *56*, 13401.

[246] J. Peña, G. Talavera, B. Waldecker, M. Alcarazo, *Chem. Eur. J.* **2017**, *23*, 75.

[247] T. Ding, L. Jiang, W. Yi, *Organic letters* **2018**, *20*, 170.

[248] S. Nakamura, N. Tsuno, M. Yamashita, I. Kawasaki, S. Ohta, Y. Ohishi, *J. Chem. Soc., Perkin Trans. 1* **2001**, 429.

[249] a) N. Nowrouzi, M. Abbasi, H. Latifi, *Appl. Organometal. Chem.* **2017**, *31*, e3579; b) E. P.L. van der Geer, Q. Li, G. van Koten, R. J.M. Klein Gebbink, B. Hessen, *Inorganica Chimica Acta* **2008**, *361*, 1811.

[250] M. Carla Aragoni, Massimiliano Arca, Francesco Demartin, Francesco A. Devillanova, Alessandra Garau, Francesco Isaia, Francesco Lelj, Vito Lippolis, Gaetano Verani, *Chem. Eur. J.* **2001**, *7*, 3122.

[251] J. Kister, G. Assef, G. Mille, J. Metzger, *Can. J. Chem.* **1979**, *57*, 813.

[252] A. C. Baumruck, D. Tietze, A. Stark, A. A. Tietze, *The Journal of organic chemistry* **2017**, *82*, 7538.

[253] G. Seconi, P. Vivarelli, A. Ricci, *J. Chem. Soc. B* **1970**, *0*, 254.

[254] J. Boström, D. G. Brown, R. J. Young, G. M. Keserü, *Nat Rev Drug Discov* **2018**, *17*, 709.

[255] a) C. Perez, A. M. Barkley-Levenson, B. L. Dick, P. F. Glatt, Y. Martinez, D. Siegel, J. D. Momper, A. A. Palmer, S. M. Cohen, *Journal of medicinal chemistry* **2019**, *62*, 1609; b) H. Cong, L. Xu, Y. Wu, Z. Qu, T. Bian, W. Zhang, C. Xing, C. Zhuang, *Journal of medicinal chemistry* **2019**; c) D. Ma, X. Kang, Y. Gao, J. Zhu, L. Yi, Z. Xi, *Tetrahedron* **2019**, *75*, 888.

[256] N. Burford, A. D. Phillips, H. A. Spinney, K. N. Robertson, T. S. Cameron, R. McDonald, *Inorganic chemistry* **2003**, *42*, 4949.

[257] P. Politzer, J. S. Murray, T. Clark, *Physical chemistry chemical physics : PCCP* **2013**, *15*, 11178.

[258] J. D. Dunitz, *Structure Correlation*, Wiley VCH, **2008**.

[259] N. Wiberg, *Lehrbuch der Anorganischen Chemie*, De Gruyter.

[260] K. T. Mahmudov, M. N. Kopylovich, M. F. C. Guedes da Silva, A. J. L. Pombeiro, *Dalton transactions (Cambridge, England : 2003)* **2017**, *46*, 10121.

[261] K. Kafuta, A. Korzun, M. Böhm, C. Golz, M. Alcarazo, *Angewandte Chemie (International ed. in English)* **2020**, *59*, 1950.

[262] X. Li, C. Golz, M. Alcarazo, *Angewandte Chemie (International ed. in English)* **2019**, *58*, 9496.

[263] B. Waldecker, F. Kraft, C. Golz, M. Alcarazo, *Angewandte Chemie (International ed. in English)* **2018**, *57*, 12538.

[264] D. Prat, J. Hayler, A. Wells, *Green Chem.* **2014**, *16*, 4546.

[265] N. Burford, A. D. Phillips, H. A. Spinney, K. N. Robertson, T. S. Cameron, R. McDonald, *CCDC 218301: Experimental Crystal Structure Determination*, Cambridge Crystallographic Data Centre, **2004**.

[266] F. H. Allen, D. G. Watson, L. Brammer, A. G. Orpen, R. Taylor in *International Tables for Crystallography* (Eds.: E. Prince, H. Fuess, T. Hahn, H. Wondratschek, U. Müller, U. Shmueli, A. Authier, V. Kopský, D. B. Litvin, M. G. Rossmann et al.), International Union of Crystallography, Chester, England, **2006**, pp. 790–811.

[267] M.-L. Alcaraz, S. Atkinson, P. Cornwall, A. C. Foster, D. M. Gill, L. A. Humphries, P. S. Keegan, R. Kemp, E. Merifield, R. A. Nixon et al., *Org. Process Res. Dev.* **2005**, *9*, 555.

[268] R. D. Rieke, T.-C. Wu, D. E. Stinn, R. M. Wehmeyer, *Synthetic Communications* **1989**, *19*, 1833.

[269] R. L.-Y. Bao, R. Zhao, L. Shi, *Chemical communications (Cambridge, England)* **2015**, *51*, 6884.

[270] A. Krasovskiy, P. Knochel, *Synthesis* **2006**, *2006*, 890.

[271] A. Krasovskiy, P. Knochel, *Angewandte Chemie (International ed. in English)* **2004**, *43*, 3333.

[272] A. Krasovskiy, V. Krasovskaya, P. Knochel, *Angewandte Chemie (International ed. in English)* **2006**, *45*, 2958.

[273] N. Kuhn, H. Bohnen, T. Kratz, G. Henkel, *Liebigs Ann. Chem.* **1993**, *1993*, 1149.

[274] M. Eissen, D. Lenoir, *Chemistry (Weinheim an der Bergstrasse, Germany)* **2008**, *14*, 9830.

[275] in *Stereoselective Synthesis 1* (Ed.: de Vries), Georg Thieme Verlag, Stuttgart, **2011**.

[276] D. A. Evans, M. M. Faul, M. T. Bilodeau, *J. Org. Chem.* **1991**, *56*, 6744.

[277] a) B. Marciniec, *Hydrosilylation*. *A comprehensive review on recent advances / Bogdan Marciniec, editor ; contributing authors, Bogdan Marciniec … [et al.]*, Springer, New York, **2009**; b) K. Burgess, M. J. Ohlmeyer, *Chem. Rev.* **1991**, *91*, 1179.

[278] H. V. Huynh, *Chemical reviews* **2018**, *118*, 9457.

[279] H. Mayr, T. Bug, M. F. Gotta, N. Hering, B. Irrgang, B. Janker, B. Kempf, R. Loos, A. R. Ofial, G. Remennikov et al., *J. Am. Chem. Soc.* **2001**, *123*, 9500.

[280] N. Kuhn, T. Kratz, *Synthesis* **1993**, 561.

[281] Jerome Esselborn, *Masterthesis: Synthese und Eigenschaften von neuen aromatischen Thiocyanaten als potentielle elektrophile Cyanidtransferreagenzien*, **2017**.

[282] D. W. Tay, I. T. Tsoi, J. C. Er, G. Y. C. Leung, Y.-Y. Yeung, *Org. Lett.* **2013**, *15*, 1310.

[283] J.-J. Wu, J. Xu, X. Zhao, *Chemistry (Weinheim an der Bergstrasse, Germany)* **2016**, *22*, 15265.

[284] a) L. Engman, D. Stern, H. Frisell, K. Vessman, M. Berglund, B. Ek, C.-M. Andersson, *Bioorganic & Medicinal Chemistry* **1995**, *3*, 1255; b) E. d. A. dos Santos, E. Hamel, R. Bai, J. C. Burnett, C. S. S. Tozatti, D. Bogo, R. T. Perdomo, A. M. M. Antunes, M. M. Marques, M. d. F. C. Matos et al., *Bioorganic & medicinal chemistry letters* **2013**, *23*, 4669; c) J. Rodrigues, S. Saba, A. C. Joussef, J. Rafique, A. L. Braga, *Asian J. Org. Chem.* **2018**, *7*, 1819.

[285] N. Kuhn, G. Henkel, T. Kratz, *Zeitschrift für Naturforschung B* **1993**, *48*, 973.

[286] S. Potash, S. Rozen, *Eur. J. Org. Chem.* **2013**, 5574.

[287] M. A. Spackman, D. Jayatilaka, *CrystEngComm* **2009**, *11*, 19.

[288] J. Lee, L. M. Lee, Z. Arnott, H. Jenkins, J. F. Britten, I. Vargas-Baca, *New J. Chem.* **2018**, *42*, 10555.

[289] a) S. Saba, J. Rafique, A. L. Braga, *Catal. Sci. Technol.* **2016**, *6*, 3087; b) A. G. Meirinho, V. F. Pereira, G. M. Martins, S. Saba, J. Rafique, A. L. Braga, S. R. Mendes, *Eur. J. Org. Chem.* **2019**, 6465.

[290] a) F. Wöhler, *Annalen der Chemie und Pharmacie* **1840**, *35*, 111; b) B. L. Sailer, N. Liles, S. Dickerson, S. Sumners, T. G. Chasteen, *Toxicology in vitro : an international journal published in association with BIBRA* **2004**, *18*, 475; c) R. S. Laitinen, R. Oilunkaniemi in *Encyclopedia of inorganic chemistry* (Ed.: R. B. King), Wiley, Chichester, **2005**; d) R. L. O. R. Cunha, I. E. Gouvea, L. Juliano, *Anais da Academia Brasileira de Ciencias* **2009**, *81*, 393.

[291] F. Que, Y. Wang, WO 2013182070.

[292] Roger Bonnert, Stephen Brough , Tony Cook, Mark Dickinson, Rukhsana Rasul, Hitesh Sanganee, Simon Teague, WO2003101961A1.

[293] a) Todd K. Jones, Neelakandha Mani, WO2005110998A1; b) S. Laufer, G. Wagner, D. Kotschenreuther, *Angew. Chem. Int. Ed.* **2002**, *41*, 2290.

[294] A. D. Toft in *Encyclopedia of endocrine diseases* (Ed.: L. Martini), London, Amsterdam, **2004**, pp. 261–264.

[295] A. Guerrero-Caicedo, D. M. Soto-Martínez, R. Abonia, L. M. Jaramillo-Gómez, *New J. Chem.* **2018**, *42*, 2649.

[296] A. Bondi, *The Journal of Physical Chemistry* **1964**, *68*, 441.

[297] R. S. Vardanyan, V. J. Hruby in *Synthesis of essential drugs* (Eds.: R. S. Vardanyan, V. J. Hruby), Elsevier, Amsterdam, Boston, **2006**, pp. 219–235.

[298] S. Braun, A. Botzki, S. Salmen, C. Textor, G. Bernhardt, S. Dove, A. Buschauer, *European journal of medicinal chemistry* **2011**, *46*, 4419.

[299] R. K. Dani, M. K. Bharty, S. Paswan, S. Singh, N. K. Singh, *Inorganica Chimica Acta* **2014**, *421*, 519.

[300] S. Alazet, E. Ismalaj, Q. Glenadel, D. Le Bars, T. Billard, *Eur. J. Org. Chem.* **2015**, 4607.

[301] Q. Glenadel, S. Alazet, T. Billard, *Journal of Fluorine Chemistry* **2015**, *179*, 89.

[302] A. Kesavan, M. Chaitanya, P. Anbarasan, *Eur. J. Org. Chem.* **2018**, 3276.

[303] T. Javorskis, G. Bagdžiūnas, E. Orentas, *Chemical communications (Cambridge, England)* **2016**, *52*, 4325.

[304] A. Perjéssy, E. Kolehmainen, W. M.F. Fabian, M. Ludwig, K. Laihia, J. Kulhánek, Z. Šusteková, *Sulfur Letters* **2002**, *25*, 71.

[305] B. Waldecker, *Org. Synth.* **2019**, *96*, 258.

[306] C. F. Mackenzie, P. R. Spackman, D. Jayatilaka, M. A. Spackman, *IUCrJ* **2017**, *4*, 575.

[307] S. J. Ryan, S. D. Schimler, D. C. Bland, M. S. Sanford, *Organic letters* **2015**, *17*, 1866.

[308] K. Niedermann, J. M. Welch, R. Koller, J. Cvengroš, N. Santschi, P. Battaglia, A. Togni, *Tetrahedron* **2010**, *66*, 5753.

[309] A. L. Spek, *Acta crystallographica. Section C, Structural chemistry* **2015**, *71*, 9.

7 Acknowledgement

An erster Stelle gilt mein Dank meinem Doktorvater Prof. Dr. Manuel Alcarazo für die Möglichkeit in seiner Arbeitsgruppe meine Promotion durchzuführen zu können. Für sein Vertrauen in meine Arbeit, die Bereitstellung einer exzellenten Forschungsumgebung und die Freiheit mich in vielerlei Hinsicht ausprobieren zu können, bin ich sehr dankbar. Jegliche Erfahrungen, die ich sowohl während des Aufbaus seiner Arbeitsgruppe in Göttingen als auch während meines wissenschaftlichen Tunes mit ihm gesammelt habe, wertschätze ich sehr.

Des Weiteren gilt mein Dank Prof. Dr. Lutz Ackermann für die Übernahme des Zweitgutachtens sowie allen Mitgliedern der Prüfungskommission.

Nicht nur in Göttingen, sondern auch während meiner Zeit am Max-Planck-Institut für Kohlenforschung in Mülheim a. d. Ruhr (09.-11.2016) hatte ich wissenschaftlich inspirierende und persönlich bereichernde Begegnungen. Danke Prof. Dr. Christian W. Lehmann, Dr. Richard Goddard, sowie Jörg Rust, Nils Nöthling, Elke Dreher und Heike Schucht aus der Abteilung für Chemische Kristallographie and Elektronenmikroskopie. Die Arbeit mit euch hat stets Freude gemacht und ich danke euch für die Bereitschaft auch manchmal spät am Abend noch über theoretische Probleme der Kristallografie zu diskutieren.

Um bei der Kristallografie zu bleiben: Danke Dr. Christopher Golz; bei dir wusste ich die frisch aufgebaute Serviceabteilung Kristallografie in guten Händen und habe die weitere Arbeit mit dir sehr genossen. Danke für die Messung meiner Kristalle und den fachlichen Austausch.
Ich danke ebenfalls der Serviceabteilung für Massenspektometrie von Dr. Holm Fraundorf und dem NMR-Service von Dr. Michael John für die zuverlässige und schnelle Messung von unzähligen meiner Proben.

Ebenfalls danke ich Dr. Rainer Oswald für die anregenden quantenchemische Diskurse und den ein oder anderen gesellschaftlichen Gedankenaustausch.

Des Weiteren gilt mein großer Dank allen Mitgliedern und Freunden des Arbeitskreises Alcarazo die mich am Anfang meiner Doktorarbeit kollegial in die Gruppe aufgenommen haben. Hierbei möchte ich vor allem Dr. Kai Averesch, Dr. Alejandro Barrado, Dr. Leo Nicholls, Dr. Javier Peña, Dr. Garazi Talavera, Dr. Hendrik Tinnermann, Dr. Bernd Waldecker, Dr. Yin Zhang und Adam Zielinski für die tollen Gespräche und Aktionen auch im nicht-wissenschaftlichen Kontext danken.

Ein besonderer Dank geht außerdem an Bernd für über drei gemeinsame Laborjahre. Es war großartig mit dir zusammen zu arbeiten, zu erzählen und unzählige Stunden im und außerhalb

des Labors zu verbringen. Danke. Die Mettwochs und Katy Perry Fridays fehlen mir jetzt schon.

Ebenfalls schätze ich alle Kollegen, die ich im Laufe der Jahre kennenlernen durfte, sehr. Danke Martì Recort Fornals, Pablo Redero Garcia, Thierry Hartung, Tim Johannsen, Steve Karreman, Kevin Kafuta, Morwenna Mögel, Christian Rugen, Lukas Schaaf, Kristin Sprenger und Valentina Pelliccioli für die tolle Zeit, das gemeinsame Klettern und die ein oder andere Party.

Auch bin ich dankbar für die Unterstützung von Isabelle Rüter, Nele Treblin, Katharina Wenderoth, Finn Kraft und Marius Deuker. Euch während eurer Bachelorarbeit oder eurem Abteilungspraktikum zu fördern und zu fordern hat mir immer viel Spaß bereitet.

Martina Pretor und Martin Simon möchte ich danken für die technische und infrastrukturelle Unterstützung. Danke, Martin, für die vielen HPLCs und das gemeinsame Schrauben an diversen Geräten. Auch Sabine Schacht danke ich für die Hilfe bei Personalunterlagen, Reisekostenabrechnungen und für die netten Gespräche am Rande.

Für die Diskussion dieses Manuskripts und viele hilfreiche Anmerkungen und Kritiken danke ich Prof. Dr. Manuel Alcarazo, Dr. Sergei I. Kozhushkov, Dr. Christopher Golz, Dr. Bernd Waldecker and Kevin Kafuta.

Ebenfalls möchte ich der Stiftung der deutschen Wirtschaft für ein Klaus Murmann Stipendium danken. Die finanzielle und ideelle Förderung hat mir sehr geholfen, meinen Horizont erweitert, und haben mich ebenfalls zu dem gemacht, der ich heute bin.

Für die Gewährung eines Reisestipendiums zum International Symposium on Catalysis and Fine Chemicals 2018 (C&FC 2018) in Bangkok/Thailand möchte ich der Gesellschaft Deutscher Chemiker (GDCh) danken, ohne die ich dort meine Forschung nicht hätte präsentieren können.

Im fachlichen, als auch außerfachlichen Kontext danke ich den Mitgliedern des JungChemikerForums Göttingen. Danke Nico Graf, Annika Nitsche and Bernd Waldecker. Es war großartig mit euch Symposien zu organisieren und durchzuführen.

Abschließend möchte ich mich bei meinen Familien und Freunden bedanken. Danke, dass ihr stets an mich geglaubt habt, mich unterstützt habt und ihr immer für mich da wart.

Dank gilt vor allem dir, Friederike. Danke, dass ich mit dir schon fast mein halbes Leben durch die Welt, die Freuden und anstrengenden Zeiten und in eine gemeinsame Zukunft gehen darf.